Ken Busch

27th

Annual Conference on Mass Spectrometry and Allied Topics

June 3-June 8, 1979
Seattle, Wa.

THE
TWENTY - SEVENTH
ANNUAL CONFERENCE
ON
MASS SPECTROMETRY
AND ALLIED TOPICS

JUNE 3 - 8, 1979

SEATTLE, WASHINGTON

TABLE OF CONTENTS

		PAGE NO.
1.	Introduction	I
2.	Acknowledgements	II
3.	Proceedings of the 27th Annual Conference	IV
4.	Author Index	757
5.	ASTM Committee E-14 and ASMS Officers	767
6.	Minutes of Annual Business Meeting	768
7.	ASMS Committees and ASTM E-14 Subcommittees	770
8.	Committee and Sub-committee Reports	771
9.	Workshop on "MS and GCMS Components and Accessories"	785
10.	Registration List, 27th Annual Conference	787

PRINTED IN CANADA

INTRODUCTION

In this volume are collected the short or extended abstracts of papers presented at the Twenty-Seventh Annual Conference on Mass Spectrometry and Allied Topics held in Seattle, Wa., June 3 - 8, 1979. It is intended that this volume be distributed only to members of ASMS and non-member registrants at the Conference and, therefore, it should not be considered a publication. It is requested that any future reference to individual reports be cited in the form: author(s), presented at Twenty-Seventh Annual Conference on Mass Spectrometry and Allied Topics, Seattle, Wa., June 3 - 8, 1979.

As I end three years as editor, I would like to thank the contributors for their cooperation in meeting various deadlines. I also am indebted to the members of my research group over the past three years for their assistance in producing and mailing the volumes. For three years Ms. Glen McCourt has carried out, in her usual and cheerful manner, the many and varied tasks necessary to transform the submitted material into book form. Without her efforts the volumes would never have reached you. Such delays as have been encountered are entirely the responsibility of the editor, with some assistance from various postal systems.

A. G. Harrison.

American Society for Mass Spectrometry

President: J. A. McCloskey, Dpt. Biopharmaceutical Sciences, University of Utah, Salt Lake City, Utah 84112.

Vice-President, Programs: B. Munson, Department of Chemistry, University of Delaware, Newark, Delaware 19711.

Vice-President, Arrangements: E. J. Bonelli, Hewlett-Packard, 3200 Hillview, Palo Alto, Ca. 94304.

Secretary: H. M. Fales, National Institute of Health, Bldg. 10, Rm. 7n, Bethesda, Maryland 20014.

Treasurer: M. A. Frisch, IBM, Thomas J. Watson Research Center, Box 218, Yorktown Heights, N. Y. 10598.

Past-President: J. H. Futtrell, Department of Chemistry, University of Utah, Salt Lake City, Utah 84112.

Directors-at-Large: C. C. Fenselau, Department of Pharmacology and Experimental Therapeutics, The John Hopkins University School of Medicine, Baltimore, Maryland 21205.

A. G. Harrison, Department of Chemistry, University of Toronto, Toronto, Canada M5S 1A1.

ACKNOWLEDGEMENTS

The American Society for Mass Spectrometry gratefully acknowledges the support provided by the following corporate members.

BALZERS HIGH VACUUM
C/O DR PHILIP IRVING
8 SAGAMORE PK RD
HUDSON
NH 03051

BELL ASSOCIATES
C/O MR DANIEL ADAMS
2211 SOUTH 19TH AVE
PHOENIX
AZ 85005

COMMERCL TESTING/ENG
C/O MR M L JACOBS
490 ORCHARD ST
GOLDEN
CO 80401

CVC INC
C/O MR DAN STEVENSON
525 LEE ROAD
PO BOX 1886
ROCHESTER
NY 14603

E I DUPONT INSTRUM
C/O DR ED CHAIT
1500 S SHAMROCK
MONROVIA
CA 91016

EXTRANUCLEAR LAB
C/O MICHAEL MCKEOWN
250 ALPHA DRIVE
PO BOX 11512
PITTSBURGH
PA 15238

FINNIGAN CORP
C/O MR MICHAEL STORY
845 W MAUDE
SUNNYVALE
CA 94086

GALILEO ELECTRO-OPTC
C/O MR P W GRAVES
GALILEO PARK
STURBRIDGE
MA 01518

HEWLETT PACKARD
C/O MR HARMON BROWN
1601 CALIFORNIA AV
PALO ALTO
CA 94304

HEYDEN & SON, INC
C/O MR JOEL PACKMAN
247 S 41ST STREET
PHILADELPHIA
PA 19104

INFICON LH INC
C/O MR RUSS CARR
6500 FLY RD
E SYRACUSE
NY

ION INSTRUMENTS INC
C/O MR B A HOPPER
1875 N 105 ST & E AV
PO BOX 51373
TULSA
OK 74116

KEARNS GROUP
C/O MR G L KEARNS
58 BUCKINGHAM DRIVE
STAMFORD
CT 06902

KEITHLEY INSTRUMENTS
C/O MR R J ERDMAN
28775 AURORA RD
CLEVELAND
OH 44139

KOR ISOTOPES INC
C/O JOEL C BRADLEY
DIV ECO-CONTROL INC
56 ROGERS ST
CAMBRIDGE
MA 02142

KRATOS-AEI SCI INST
C/O MR R P FEDCHENKO
3344 NO TORREY PINES
LA JOLLA
CA 92037

LKB INSTRUMENTS
C/O MR R MARTENS
BIODYNAMICS
PO BOX 50100
INDIANAPOLIS
IN 46250

MASSPEC, INC
C/O DR RON D GRIGSBY
PO BOX 9314
COLLEGE STATION
TX 77840

MERCK & CO ISOTOPES
C/O DR S P MANRAO
PO BOX 2000
RAHWAY
NJ 07065

NIH/EPA CHM INFO SYS
C/O DR AL FEIN
2519 FARRINGDON RD
BALTIMORE
MD 21209

NUCLIDE CORPORATION
C/O MR L F HERZOG
642 E COLLEGE AVE
STATE COLLEGE
PA 16801
8C 960

PERNICKA CORP
C/O MR J C PERNICKA
1026 W MAUDE
SUITE 301
SUNNYVALE
CA 94086

RIBER DATA SYSTEMS
C/O DAVID SPARKMAN
1020 CORPORATION WAY
PALO ALTO
CA 94304

SCIEX INC
C/O DR A LOVETT
55 GLENCAMERON RD
SUITE 202
THORNHILL, ONTARIO
CANADA, L3T 1P2

S G E, INC
C/O MR K O MAHLER
2800 LONGHORN BLVD
SUITE 103
AUSTIN
TX 78759

SHRADER ANAL LAB
C/O DR S R SHRADER
3450 LOVETT AVE
DETROIT
MI 48210

STOHLER ISOTOPE INC
C/O MR JACK TURGEL
49 JONES RD
WALTHAM
MA 02154

TEKNIVENT CORP
C/O MR P F BERGER
10712 KAHLMEYER DR
ST LOUIS
MO 63132

UTHE TECHNOLOGY INC
C/O J D BURDEN
325 N MATHILDA AVE
SUNNYVALE
CA 94086

VACUMETRICS INC
C/O MR R DUCET
2261 PALMA DRIVE
VENTURA
CA 93003

VARIAN MAT, USA
C/O DR WOLSTENHOLME
25 HANOVER ROAD
FLORHAM PARK
NJ 07932

Paper No. Page No.

*PL-1 Metabolic Profiling: Automated Analysis of Complex Mixtures from Tissues and Physiological Fluids.
C. C. Sweeley..... 1

*PL-2 Collision Dynamics of Feeble Bonds: Van der Waals Molecules and Solvent Clusters.
D. R. Herschbach..... 21

Fossil/Synthetic Fuels/Pyrolysis

MAMOA-1 Comparison of Separation Efficiencies of Probe Micro distillation/Mass Spectrometry and High Performance Liquid Chromatography.
L. R. Schronk, R. D. Grigsby, and A. R. Hanks..... 21

MAMOA-2 Quantitative Analysis via Computerized Probe Distillation/Field-Ionization Mass Spectrometry.
Q. Grindstaff, C. S. Hwang, T. D. Marriott, P. A. Benson, and S. E. Scheppele..... 22

MAMOA-3 Detection of Heterocyclic Compounds Containing Two Nitrogen Atoms in a Base Fraction Separated from Anthracene Oil.
R. D. Grigsby, L. R. Schronk, Q. Grindstaff, and S. E. Scheppele..... 22

MAMOA-4 Withdrawn

MAMOA-5 Mass Spectral Analysis of Mutagenically Active Subfractions from Coal Liquids.
B. W. Wilson and R. A. Pelroy..... 23

MAMOA-6 Mass Spectrometric Analysis of Nitrogen Heterocycles in Coal Liquefaction Product.
C. E. Schmidt, Z. Przybylski, H. L. Retcofsky, and C. M. White..... 25

MAMOA-7 The Use of Mass Spectrometry in Characterizing Coal- and Petroleum-Derived Materials Relevant to Coking Additives.
M. L. Bennett and A. A. Herod..... 26

MAMOA-8 Coal Liquid Characterization II. Mechanism of Benzyl Ether Pyrolysis.
T. R. Ashe, R. J. Pancirov, and R. H. Schlosberg..... 28

MAMOA-9 Monitoring the Photo-oxidation of Crude Oil by a Gas Chromatography-Mass Spectrometry System: Extracted Ion Current Profiles of Dibenzothiophenes and Their Sulfoxides.
J. R. Patel, S. W. Mascarella, E. B. Overton, and J. L. Laseter..... 29

MAMOA-10 Analysis of Polynuclear Aromatic Hydrocarbons in Coke Oven Effluents.
R. G. Beimer..... 31

*Plenary Lecture

Paper No. Page No.

MAMOA-11 A Comparison of the Composition of Eastern and Western Shale Oil Samples as Determined by Low Electron Energy, Capillary GC-MS-DS.
R. O. Yelton, T. O. Tiernan, M. L. Taylor, V. M. Franchetti, and C. Kinard..... 32

MAMOA-12 GC-High Resolution-MS-C As a Nitrogen Compound Specific Detector.
E. J. Gallegos..... 33

MAMOA-13 Applications of GC/FIMS to Hydrocarbon Analysis.
A. M. Hogg, J. D. Payzant, I. Rubenstein, and O. P. Strausz..... 35

MAMOA-14 The High Temperature Pyrolysis of Aromatic Hydrocarbons.
R. D. Smith..... 37

MAMOA-15 Withdrawn

Field Desorption/High Temperature/Inorganic

MAMOB-1 The Application of Microfabrication Technology to the Construction of Field Emission Ionizers.
C. A. Spindt..... 39

MAMOB-2 Ionization by Proton Attachment.
W. V. Ligon, Jr..... 41

MAMOB-3 Characterization of a Volcano Style Field Ionization Source and Magnetic Sector Mass Spectrometer.
S. E. Buttrill, Jr., G. A. St. John, and C. A. Spindt. 42

MAMOB-4 Characterization of Low Molecular Weight Polymers by Liquid Chromatography-Field Desorption Mass Spectroscopy.
R. P. Lattimer, D. J. Harmon, and K. R. Welch..... 44

MAMOB-5 Electrohydrodynamic Ionization Mass Spectrometry of Organic Salts.
S-T. F. Lai and K. D. Cook..... 46

MAMOB-6 Field Desorption Mass Spectra of Transition Metal Containing Organic Coordinate Complexes.
S. A. Carr, C. E. Costello, B. W. Wilson, C. Orvig, A. Davison, and K. Biemann..... 48

MAMOB-7 Structure Investigation of Higher Molecular Weight Polyether Antibiotics Using Field Desorption Mass Spectrometry.
J. L. Occolowitz and R. L. Hamill..... 50

MAMOB-8 Use of Complete Field Desorption Mass Spectra for Structural Studies in Biological Chemistry.
C. E. Costello, S. A. Carr, N. R. Mancuso, and K. Biemann..... 51

MAMOB-9 Withdrawn

MAMOB-10 Field Desorption of Some Substituted Ammonio-Carboxylates.
T. Keough and A. J. Destefano.....53

MAMOB-11 Rapid Heating Evaporation of $Pb(NO_3)_2$.
T. Radus, H. R. Udseth, and L. Friedman.....55

MAMOB-12 An Electron Bombardment Heated Knudsen Cell Mass Spectrometer.
P. J. Turner and W. D. Unsworth 56

Paper No. Page No.

MAMOB-13 PES of Higher Temperature Vapors.
J. Berkowitz and C. H. Batson..... 58

MAMOB-14 Anodic Behaviour of Uranium (VI) in a Sulfate-Sulfuric Acid System.
R. Newbury, R. Carver, and J. Rego..... 60

MAMOB-15 Withdrawn

Negative Ions

MAMOC-1 Negative Ion Production Using Rydberg Atoms.
R. W. Odom and R. M. Hill..... 61

MAMOC-2 Joint Experimental and Theoretical Study of CO_2^- Potential Energy Surfaces.
R.L.C. Wu, T. O. Tiernan, E. S. Sachs, and D. G. Hopper..... 63

MAMOC-3 Laser Photodetachment of Chlorine Molecular Negative Ions.
R. O. Daubach and J. R. Eyler.....64

MAMOC-4 Negative Ion-Molecule Reactions in Sulfuryl Halides.
R. Robbiani and J. L. Franklin..... 65

MAMOC-5 Withdrawn

MAMOC-6 Thermochemistry and Structure of Molecular Negative Ion NO_3^-
R.L.C. Wu and T. O. Tiernan..... 67

MAMOC-7 Enhancement of Electron Capture Detector Sensitivity to Non-Electron Attaching Compounds Using N_2O Carrier Gas Doping.
M. P. Phillips, P. D. Goldan, R. Sievers, and F. C. Fehsenfeld..... 69

MAMOC-8 The Reaction of 2,3,7,8-Tetrachloro-p-dioxin in an Oxygen Rich Plasma at Atmospheric Pressure.
R. K. Mitchum and G. F. Moler..... 70

MAMOC-9 Withdrawn

MAMOC-10 Withdrawn

MAMOC-11 Advantages of Negative Chemical Ionization-MS for Analysis of Pentafluorobenzyl-Phenyl Ethers.
G. R. Dubay, D. L. Stalling, J. D. Petty, and L. M. Smith..... 71

MAMOC-12 Withdrawn

MAMOC-13 Positive/Negative Chemical Ionization Mass Spectrometry of Mycotoxins.
W. C. Brumley, J.A.G. Roach, P. A. Dreifuss, D. Andrzejewski, and J. A. Sphon..... 73

MAMOC-14 Survey of Chemistry Department Mass Spectrometry Service Facilities in the United States and Canada.
R. D. Minard and F. W. Lampe..... 74

Paper No. Page No.

Pharmacology/Ionization Processes

MAMP-1 GC-MS Determination of Urinary Polyamines During Treatment of Acute Leukemia.
M. D. Denton, B. Finley, and E. J. Norman..... 76

MAMP-2 A GC-PICIMS Stable Isotope Method for the Determination of Sulfadimethoxine in Cattle and Swine Livers and Kidneys at the 0.1 ppm Regulatory Level.
B. J. Hodshon, W. A. Garland, G. Chen, G. Weiss, and A. MacDonald..... 77

MAMP-3 Determination of Prostaglandin Analog TM-PGE$_2$ in Dog Plasma by Combined Capillary Column Gas Chromatography-Negative Ion Chemical Ionization Mass Spectrometry.
B. H. Min, J. Pao, W. A. Garland, and J.A.F. de Silva. 79

MAMP-4 Application of Chromatographic and Mass Spectrometric Techniques to Differentiate Lidocaine from Phencyclidine Metabolites.
S. D. Erk, M. R. Bogdan, R. O. Yelton, and M. L. Taylor..... 81

MAMP-5 Withdrawn

MAMP-6 Analysis of the Enantiomeric Composition of Warfarin in Human Plasma by Chemical Ionization Mass Spectrometry.
W. N. Howald, E. D. Busch, W. F. Trager, K. Motley, and R. A. O'Reilly..... 83

MAMP-7 A GCMS Assay for Phenylalanine Mustard.
S. Pallante, M. Appler, R. Brundrett, R. Menell, O. M. Colvin, and C. Fenselau..... 86

MAMP-8 Mass Spectrometry of Folic Acid Analogues.
R. G. Smith, Y.-M. Wang, J. G. Pegues, D. Farquhar, and T. L. Loo..... 88

MAMP-9 GC-MS-SIM Quantitation of the Antitumor Agent N-(Phosphonacetyl)-L-Aspartic Acid in Human Biological Fluids.
R. J. Bruni, Y. Merrill, A. R. Branfman, J. M. Strong, and T. J. Ervin..... 90

MAMP-10 Characterization of the Glucuronic Acid Conjugates Found During Clofibrate Metabolism.
C. E. Hignite, C. Tschanz, S. Lemons, D. H. Huffman, and D. L. Azarnoff..... 92

MAMP-11 Mass Spectra of Quaternary Ammonium Chlorides.
F. A. Elder, L. J. Bluett, K. M. Maloney, and R.K. Crandall..... 92

MAMP-12 A Study of the Decomposition of Arylazopyrolines.
F. A. Elder and K. M. Maloney..... 93

MAMP-13 Liquid Ionization at Atmospheric Pressure: Cluster Ions from Liquid Produced by Charge Transfer.
M. Tsuchiya, T. Taira, and K. Hiraoka..... 94

MAMP-14 Withdrawn

MAMP-15 Photoelectron Spectroscopy of Phthalocyanine Vapors.
J. Berkowitz..... 96

Paper No. Page No.

MAMP-16 Electron Impact Fragmentation of the Methyl and Ethyl Esters of Formic And Acetic Acids.
R. M. Kiser, P. A. Purdue, and J. D. Tarrant..... 98

MAMP-17 Ionic Structure of Diene Ions.
R. C. Benz and R. C. Dunbar..... 100

MAMP-18 Photodissociation of Protonated Organic Carbonyls.
J. P. Honovich and R. C. Dunbar..... 100

MAMP-19 Autoionization in O_2.
A. Tabche-Fouhaile, I. Nenner, P. M. Guyon, P. Morin, L. F. Ferreira, K. Ito, and K. Kollmann..... 101

MAMP-20 Observation of Highly Excited Vibrational States in Atmospheric Molecules.
R. Stockbauer..... 103

MAMP-21 State-Selected Fragmentation of Nitromethane Ions by Threshold Photoelectron Coindicent Photoion Mass Spectrometry.
M. J. Weiss and G. G. Meisels..... 104

MAMP-22 Mass Spectrometric Measurements of Partial and Total Electron Impact Ionization Cross Section Functions of Rare Gas Atoms and Molecules.
H. Helm, K. Stephan, and T. D. Mark..... 104

MAMP-23 ArF Laser Multiphoton Ionization Mass Spectrometry.
M. Seaver, J. W. Hudgens, J. J. deCorpo, and J. R. Wyatt..... 108

Advances in Gas Chromatography and Gas Chromatography/Mass Spectrometry

MPMOA-1 High Resolution Columns in G.C.-M.S.
C. A. Cramers and P. A. Leclerq..... 110

MPMOA-2 On the $(GC)^2$ in $(GC)^2$-MS.
M. Verzele..... 114

MPMOA-3 Gas Liquid-Solid Chromatography in Environmental and Trace Analysis.
F. Bruner..... 118

MPMOA-4 Environmental and Biomedical Applications of Glass Capillary Gas Chromatography/Mass Spectrometry.
R. L. Foltz, D.C.K. Lin, S. V. Lucas, B. A. Petersen, T. M. Engel, G. A. Jungclaus, F. W. Crow, A. Bjorseth, and B. J. Hidy..... 120

MPMOA-5 Alternatives to High Performance Glass Capillary Gas Chromatography Mass Spectrometry for the Analysis of Complex Samples.
T. M. Harvey..... 120

MPMOA-6 Capillary GC/MS Analysis of Isomer/Homolog Mixtures in Studies of CI-Induced Fragmentation.
W. J. Richter, W. Blum, J. Liehr, and E. Schlumpf..... 121

Paper No. Page No.

Organic Chemistry

MPMOB-1 EI Induced Cyclization of Ortho Substituted Diphenylmethanes.
G. G. Liehr, R. M. Caprioli, A. G. Brenton, and J. H. Beynon..... 121

MPMOB-2 Multiple Labelling in Mass Spectrometry.
T. Gaumann, D. Stahl, and P. Tecon..... 122

MPMOB-3 Effects of Sulfur-for-Oxygen Substitution on EI and FI Mass Spectra of Esters.
G. W. Wood and B. Kiremire..... 124

MPMOB-4 Chemical Ionization Mass Spectrometry of Aryl Substituted Cyclohexenes: Analogy to Solvolysis.
G. Sudhakar Reddy, M. Vairamani, K. G. Das, H. Budzikiewicz, and M. M. Green..... 126

MPMOB-5 Loss of Alkane from Ionized Secondary Alkyl Ethers.
C. E. Hudson, R. D. Lerner, R. Aleman, and D. J. McAdoo..... 129

MPMOB-6 Low Energy Fragmentation of the Major Ions of Cyclohexane by Tandem Quadrupole Mass Spectrometry.
R. A. Yost, R. K. Latven, and C. G. Enke..... 131

MPMOB-7 Application of B/E Linked Scans to the Analysis of Natural Products.
G. A. Warburton, R. McDowell, D. Hazelby, S. Evans, and K. R. Compson..... 133

MPMOB-8 Diagnostic TMS-Containing Ions in the Mass Spectra of Sterol Derivatives.
D. J. Harvey and P. Vouros..... 135

MPMOB-9 Structure and Formation of Gaseous $C_4H_5O^+$ Ions.
J. K. Terlouw..... 136

MPMOB-10 Mass Spectra of the Novel Oxepane Diterpenes from the Mexican Plant Zoapatle (Montanosa Tomentosa): Zoapatanol and Montanol.
C. J. Shaw, M. L. Cotter, R. Chen, R. Kanojia, and M. Wachter..... 138

MPMOB-11 The Stabilities of Unsaturated Carbocations.
D. H. Aue, W. R. Davidson, L. D. Betowski, E. Motell, and M. T. Bowers..... 140

MPMOB-12 Some Aspects of the Unimolecular Decarbonylation Reaction of $C_7H_7O^+$ Cations.
D. H. Russell, D. C. Canada, and E. H. McBay..... 142

MPMOB-13 Stereospecificity and Hidden Hydrogen Migration in the Elimination of Methanol from Cyclic Diesters under Electron Impact.
A. Mandelbaum, R. Bar-Shai, J. Sharvit, and I. Merksammer..... 144

Paper No. Page No.

Ion-Molecule Reactions

MPMOC-1 Theory of the Effect of the Electric Field Inhomogeneity in Ion Cyclotron Resonance Spectrometry.
G. Baykut, K.-M. Chung, K.-P. Wanczek and H. Hartmann..... 145

MPMOC-2 Exact Mass Determination in Ion Cyclotron Resonance Spectrometry.
G. Baykut, K.-M. Chung, K.-P. Wanczek, and H. Hartmann..... 147

MPMOC-3 Electronic Excitation in Symmetric Ion-Atom Collisions.
E. G. Jones..... 149

MPMOC-4 Low Energy Collision Processes in Tandem Quadrupole Mass Spectrometry.
C. G. Enke, J. A. Chakel, and E. J. Darland..... 151

MPMOC-5 Reactions of Methyl Cations with Methyl Silanes.
G. W. Goodloe, E. R. Austin, and F. W. Lampe..... 153

MPMOC-6 A Tandem-Ion Cyclotron Resonance Study of the Reaction of N_2^+ with SO_2.
Y. Nishimura, R. Orth, and J. H. Futrell..... 155

MPMOC-7 Ion-Molecule Reaction Rates Using A Selected Ion Flow Tube.
A. V. Viggiano, F. Howorka, D. I. Albritton, and F. C. Fehsenfeld..... 155

MPMOC-8 Vibrational Energy Dependence of the Reaction $C_2H_4^+ + C_2H_4 \rightarrow C_3H_5^+ + CH_3$
T. Su and M. T. Bowers..... 156

MPMOC-9 Transition State Analysis of Ion-Dipole Capture Dynamics.
W. J. Chesnovich, T. Su, and M. T. Bowers..... 158

MPMOC-10 Intermolecular Forces and Collision Frequencies in Ion Molecule Systems.
F. Celli, G. Weddle, and D. P. Ridge..... 158

MPMOC-11 Ion Clustering Studies Using an Atmospheric Pressure Ionization Source.
W. N. Allen, J. J. Decorpo, F. E. Saalfed, and J. R. Wyatt..... 159

MPMOC-12 Solvation of K^+ and Cl^- by DMSO.
T. F. Magnera, J. Sunner, and P. Kebarle..... 160

MPMOC-13 Ion Cyclotron Resonance Studies of $TiCl_4$ and CH_3TiCl_3 Ion Chemistry with Some Organic Molecules.
J. S. Uppal and R. H. Staley..... 160

MPMOC-14 Ion-Molecule Reactions in Dimethylsulfoxide Studied by High Pressure Photoionization Mass Spectrometry.
J. A. Stone and M. S. Lin..... 161

Paper No. Page No.

Field Desorption/High Temperature/Inorganic Solids

MPMP-1 Photoelectron Spectra of Trinuclear Metal Cluster Complexes.
W. C. Trogler and J. Berkowitz..... 163

MPMP-2 Comparison Between the Photoelectron Spectra of Transition Metal Beta-diketonate Complexes and Their Ionization Efficiency Curves in the Threshold Region.
J. B. Westmore and C. Reichert..... 165

MPMP-3 Improved SIMS Energy Prefilter.
J. R. Wyatt, R. J. Colton, J. D. Ganjei, J. J. DeCorpo, and J. S. Murday..... 167

MPMP-4 The Automation of a SIMS System: Philosophy and Design.
M. A. Frisch..... 169

MPMP-5 Rapid Measurement of Calcium Isotope Ratios Using a New Thermal Ionization Method.
A. L. Yergey..... 170

MPMP-6 A New Automated UF_6-Mass Spectrometer with Molecular Beam Inlet and Multiple Ion Collector.
C. Brunee, B. Laser, H. Rache, and H. Ravens..... 171

MPMP-7 Two Programmable Calculator Programs for Isotope Dilution
E. H. Daughtrey, Jr. and J. K. Bostick, Jr..... 172

MPMP-8 Desorption Mechanisms and Their Relationships to the Apparent Locus of Ion Formation in Field Desorption Mass Spectrometry.
J. F. Holland, B. Soltmann, R. Olinger, and J. Dye..... 174

MPMP-9 The Application of Field Desorption Mass Spectrometry (FDMS) to the Analysis of Lipid Radiolysis Products.
C. Merritt, S. G. Kayser, W. W. Nawar, M. R. Olinger, and J. F. Holland..... 176

MPMP-10 Comparison of Three Methods of Obtaining Metabolic Profiles from Urine.
E. Blaisdell, W. Aberth, A. Sheets, C. Tsao, J. C. Engels, and J. S. MacGuire..... 178

MPMP-11 A Study of the Mechanism of Field Ionization by Conditioned Graphite Filaments.
D.D.J. Allman, P. L. Gutshall, and P. J. Bryant..... 180

MPMP-12 Pulsed Field Desorption Mass Spectrometry.
R. W. Odom and S. E. Butrill, Jr..... 182

MPMP-13 Use of Modified KRATOS/AEI MS-902 for Field Desorption/Collision Induced Dissociation (FD/CID) Mass Spectrometry.
H. Kambara, F. C. Walls, R. McPherron, K. Straub, and A. L. Burlingame..... 184

MPMP-14 Solution Chemistry as a Guide to Selective Surface Reactions on Field Desorption Emitters.
M. M. Bursey, T. L. Youngless, D. F. Fraley, and N.B.H. Henis..... 186

MPMP-15 Coal Terpane Analysis by Methane Chemical Ionization GC/MS.
J. G. Moncur and R. M. Teeter 187

Paper No. Page No.

MPMP-16 Mass Spectrometry of Bitumen Distillates and Related Streams.
I. P. Fisher and H. P. Fischer..... 189

MPMP-17 Calculation of Physical and Chemical Properties of Petroleum Fractions from Mass Spectrometric Compositional Data.
M. P. Hahto..... 191

MPMP-18 Selective Chemical Ionization Reagent Gases for Carcinogens in Synthetic Fuels.
D. M. Schoengold..... 193

MPMP-19 Pyrolysis Mass Spectrometry of Poly (4,4'-Diphenylene Oxide Pyromellitimide).
M. A. Grayson..... 194

MPMP-20 The Characterization of Muscles from Duchenne Muscular Dystrophy Patients Using Pyrolysis Mass Spectrometry.
F. D. Hileman, H.L.C. Meuzelaar, L. H. Wojcik, and J. H. Petajan..... 196

MPMP-21 A Multi-Purpose Thermal MS System and Types of Applications in Industrial Research.
C. Elkins..... 198

MPMP-22 Analysis of Volatile Emissions from Polymers by GC/MS/COM.
J. P. Hoppesch, C. J. Pinson, and V. H. Schneider..... 200

GC/MS

TAMOA-1 Capillary GC/MS of Triglycerides Using EI and CI Techniques.
U. Rapp, G. Dielmann, M. Hohn, and E. Schulte..... 201

TAMOA-2 Rapid Instrumental Techniques for the Analysis of Volatiles in Cereals.
J. B. Stanley, M. G. Legendre, H. P. Dupuy, and W. H. Schuller..... 202

TAMOA-3 Capillary GC/MS Analysis Using A Computer Controlled EI/CI Mass Spectrometer.
E. M. Chait and T. A. Blazer..... 204

TAMOA-4 Elemental Composition Determination in Capillary GC Runs Using Medium Resolution.
U. Rapp, H. Kaufmann, and M. Hohn..... 201

TAMOA-5 Methods of Utilizing a Computer Controlled GC/MS for Improvement of Mass Spectral Data.
R. L. Conrad, R. W. Howard, and C. W. Hull..... 205

TAMOA-6 Quantitative Analysis with GC/MS.
W. L. Budde and J. W. Eichelberger..... 206

TAMOA-7 GC/MS Identification of High Boiling Components from the Direct Process Manufacturer of Chlorosilanes.
G. F. Dudding, W. D. Kray, and A. Ritzer..... 207

TAMOA-8 Applications of Automatic Operation of a Computer Controlled GC/MS to Environmental and Biomedical Analysis.
H. Roden, E. M. Chait, and T. A. Blazer..... 209

Paper No. Page No.

TAMOA9 Identification of the Decomposition Products of $C_{10}H_{21}(OCH_2CH_2)_5OH$.
A. J. Destefano, D. W. Leedy, and R.A.Sanders..... 210

TAMOA10 Automatic Search, Identify, and Quantify Mass Spectral Data File Computer Programme for Priority Pollutant Analysis.
J. F. Ryan, R. A. Novak, and W. A. Farr..... 212

TAMOA11 Involatile Sample Analysis by Dense Gas Chromatography/ Mass Spectrometry.
A. L. Wahrhaftig and L. G. Randall..... 215

Pharmacology

TAMOB1 Phyrolysis Gas Chromatography Chemical Ionization Mass Fragmentography (PGC/CI/MF) to Analyze Choline and Acetylcholine in Picomole Quantities.
J. K. Khandelwal, P.I.A. Szilagyi, and J. P. Green..... 216

TAMOB2 Metabolism of Two PCB Isomers by Rhesus Monkeys.
H. T. Cory, G. D. Daves, R. G. Smith, and W. P. McNulty..... 218

TAMOB3 A comparison of the Analysis for Carbon-13 and Carbon-14 in the Serum of Dogs Following the Intravenous Infusion of Labelled Disodium Dichloromethonediphosphonate.
R. S. Ampulski..... 220

TAMOB4 GC/MS Determination of the Metabolic Pattern of Propanolol.
V. T. Vu and E. P. Abramson..... 222

TAMOB5 Withdrawn

TAMOB6 Use of MS and HPLC in Studies of the in vitro Metabolism of Guthion (Azinphosmethyl) by Mice and Rat Liver Homogenates.
C.-Y. Chen, R. M. Caprioli, and S. D. Murphy..... 224

TAMOB7 2,5-Di-tert-amyl-p-benzoquinone: An Antioxidant Encountered during Analysis of Human Tissues.
B. S. Middleditch, H. B. Hines, F. O. Bastian, and P. R. Middleditch..... 224

TAMOB8 Formation of O- and S-Methylated Products in the Derivitization of 5,5-Disubstituted Hydantoins: Application to the Preparation of ^{18}O Labelled Phenytoin.
J. P. Thenot, A. Hung, T. I. Ruo, and R.DeSagher.. 225

TAMOB9 A GC-MS Assay for Low Levels of Retinoic Acid in Human Blood.
T. C.Chiang..... 226

TAMOB10 Detection of Methadone Metabolites Using Deuterium Labelled Analogs.
F. S. Abbott, G. I. Kang, and R. W. Burton..... 228

TAMOB11 Potential Role of Hydroxypolyenoic Fatty Acids in Humoral Hypercalcemia of Malignant Disease.
W. Hubbard, A. Hough, Jr., A. R. Brash, R. Johnson, and J. A. Oates..... 230

Paper No. Chemical Ionization Page No.

TAMOC1 A Microwave-Discharge Ion Source for Chemical Ionization.
M. W. Siegel..... 232

TAMOC2 Low Pressure CI by FT/MS.
S. Ghaderi, P. S. Kulkarni, R. Spencer, E. Ledford, Jr., C. L. Wilkins, and M. L. Gross..... 235

TAMOC3 Real Time Trace Analysis by Atmospheric Pressure Chemical Ionization: Supplementary Techniques in Molecular Ion Identification.
N. M. Reid, B. A. Thomson, W. R. Davidson, J. B. French, and J. A. Buckley..... 237

TAMOC4 Electron Penetration: Characterization and Application of a Chemical Ionization Source with Coaxial Electron Entrance Aperature and Ion Exit Slit.
A. J. Illies, R. Infante, C. Polley, and G. G. Meisels..... 239

TAMOC5 Fast Radical Reactions Observed by Chemical Ionization Mass Spectrometry.
C. N. McEwen and M. A. Rudat..... 242

TAMOC6 Structural Analysis of Hydrocarbon Radicals Produced in a CI Source Using Collisional Activation Mass Spectrometry.
M. A. Rudat and C. N. McEwen..... 243

TAMOC7 Negative Ion Chemical Ionization Mass Spectrometry of Explosives.
J. Yinon..... 245

TAMOC8 Analysis of Silicones by Chemical Ionization Mass Spectrometry.
H. Grade and W. V. Ligon..... 247

TAMOC9 Ammonia CIMS of 16-membered Ring Macrolide Antibiotics.
M. Suzuki, K. I. Harada, N. Takeda, and A. Tatematsu..... 248

TAMOC10 Mass Spectral Studies on the Molecular Fragmentation and Urinary Metabolism of a New Antiarrhythmic Agent, N-Hexyl-N^4-(isobutyliminobenzyl)-piperazine, USV-G233.
M. O'Hare, R. Biniakewitz, and J. Shroff..... 251

TAMOC11 Direct CI-MS Analysis of Estrogen in Pregnancy Urine.
J.M.L. Mee and B. Halpern..... 252

Paper No. Page No.

Computer Applications,Organic Chemistry

TAMP-1 Selected IOn Recording Data System.
L. K. Barden, R. L. Tate, A. R. Schultz,
S. P. Markey, and J. A. Oliver..... 253

TAMP-2 Data Communication for Computer Assisted Amino Acid Sequence Determination.
R. J. Madden, M. E. Jackson, and R. A. Day..... 255

TAMP-3 A Microcomputer-Based GC-MS Controller.
T. Clem, W. Comstock, and H. M. Fales..... 257

TAMP-4 Data Transfer Between an Incos Data System and a Varian 620L/100 Minicomputer.
W. D. Jamieson, E. W. Dyer, F. G. Mason, and
M. Weiss..... 258

TAMP-5 Improvements to PBM and STIRS for Computer Identification of Unknown Mass Spectra.
I. K. Mun, K. S. Haraki, B. L. Atwater(Fell),
K. J. Bierre, K. Hosokawa, R. Venkataraghavan,
and F. W.McLafferty..... 260

TAMP-6 Withdrawn

TAMP-7 Predicting Mass Spectra: Applications to Structure Education.
A. Lavanchy, N.A.B. Gray, D. H. Smith, and
B. G. Buchanan..... 261

TAMP-8 Advanced Software for a Low Cost GC/MS.
J. Justice..... 263

TAMP-9 Modification of the Dupont 094B Data System for Real Time Capability and Enhanced Post-Run Processing.
J. J. Solomon and L. M. Morin..... 264

TAMP-10 Optimization of Automatic Data Reduction for Qualitative GC/MS Studies.
B. N. Colby, M. E. Rose, and A. E. Rosecrance..... 264

TAMP-11 Withdrawn

TAMP-12 NIH/EPA/MSDC Mass Spectral Search System and Data Base.
D. P. Martinsen and R. S. Heller..... 265

TAMP-13 Comparison of Forward and Reverse Search for The Automatic Processing of GC/MS Data.
D. Rosenthal and W. L. Hargrove..... 266

TAMP-14 Computer Facilitated Complex Mixture Analysis I: Detection and Identification of Co-Eluting Compounds.
M. N. Kan, J. Jugovich, and J. Slayback..... 268

TAMP-15 Computer Facilitated Complex Mixture Analysis II: Rapid and Specific Detection of Organic Compounds by Reverse Library Spectral-Matching.
J. Slayback, J. Jugovich, and M. N. Kan..... 269

TAMP-16 Computer-Controlled MIKES Analysis: A Rapid, Convenient, and Sensitive Method of Detecting Specific Components of Complex Mixtures.
M. Weiss, J. Karnofsky, R. Hass, and D. Harvan.... 270

Paper No. Page No.

TAMP-17 Electron Impact Fragmentation Mechanisms of 2,4,6-Trinitrotoluene (TNT) Derived from Metastable Scanning and Isotopic Labelling.
S. Bulusu and T. Axenrod..... 272

TAMP-18 Applications of a New Interactive Colour Graphics Terminal in Organic GCMS.
T. S. Davis, J. C. Bill, M. J. Wallington, and P. Powers..... 274

TAMP-19 Mass Spectrometry of 3,5-Cyclovitamins D_3.
Z.V.I. Zaretskii..... 275

TAMP-20 Rearrangement of N-Acyl Prostaglandin Carboxamides to Nitriles and Trimethylsilyl Esters.
F. C. Falkner..... 277

TAMP-21 Mass Spectrometric Analysis of Some Benzyltrichloromethylamidines.
R. E. Rhodes, A. G. Zacchei, J. R. Huff, and W. S. Saari..... 279

TAMP-22 Energetic Analysis of a 1,4-Elimination.
D. R. Hilker, and M. L. Gross..... 281

TAMP-23 The Mechanis m of H /D Randomization of the Molecular Ion of Tetralin.
S. M. Arghestani, E. K. Chess, and M. L. Gross.... 283

Chemistry of Ions: Solution and Gas Phase

TPMOA-1 Rates and Mechanisms of Thermal Ion-Molecule Reactions.
J. I. Brauman..... 285

TPMOA-2 Protonic Acid-Base Equilibria: Gas Phase and Solution.
R. W. Taft..... 286

TPMOA-3 Structure and Chemistry of Gaseous Organic Ions Studied by Collisional Activation Mass Spectrometry.
F. W. McLafferty, D. C. McGilvery, and P. J. Todd..... 289

TPMOA-4 Solvation Energies-The Link Between Ionizations in the Gas Phase and Solution.
E. M. Arnett and N. J. Pienta..... 290

TPMOA-5 Ion-Solvent Molecule Clusters in Gas Phase and Ion Solvation in Liquid Solvents.
P. Kebarle..... 294

TPMOA-6 Withdrawn

Paper No. Page No.

Combination of Techniques for Solids Analysis

TPMOB-1 A Comparison of Surface Analytical Techniques.
C. A. Evans, Jr..... 295

TPMOB-2 An ISS-SIMS Study of Sapphire Surfaces and the Silicon/Sapphire Interface.
W. L. Harrington and C. W. Magee..... 298

TPMOB-3 A Quantitative SIMS Analysis of Decalibrated Chromel versus Alumel Thermocouples Using Indexed Sensitivity Factors.
W. H. Christie, R. E. Eby, and T. G. Kollie..... 301

TPMOB-4 Initial Energy Distributions of Secondary (+) Ions from the Sputtering of Metals with 10 KeV Ar^+.
F. G. Satkiewicz..... 303

TPMOB-5 Etching of SiO_2 and Si by a Helium-Fluorine RF Discharge.
M. J. Vasile..... 305

TPMOB-6 Detailed Examination of the Outer Surface by Combined Techniques: SIMS Combined with ISS and SEM.
G. R. Sparrow..... 306

TPMOB-7 A Computerized Data Acquisition System for Quadrupole Secondary Ion Mass Spectroscopy.
B. F. Phillips and N. E. Lares..... 307

TPMOB-8 SIMS Spectra of Steel and Their Analysis by Computer.
M. Baril..... 309

TPMOB-9 Sample Mounting Technique--A Significant Source of Bias in Thermal Ionization Mass Spectrometry.
E. L. Garner and K. A. Brletic..... 312

TPMOB-10 Experiences with a Fully Automatic Thermal Ionization Mass Spectrometer.
R. C. Haines, T. O. Merren, P. J. Turner, and S. Sayyid..... 313

TPMOB-11 Analysis of U and PU Resin Bead Samples with a Single Stage Mass Spectrometer.
D. H. Smith, R. L. Walker, L. K. Bertram, and J. A. Carter..... 315

TPMOB-12 The Diffusion of Trace Metals in Metals and Alloys and Its Applicability to Environmental Assays.
M. E. Koslin and F. A. White..... 317

Paper No. Page No.

Ionization Processes, Ion-Molecule Reactions

TPMOC-1 Threshold Photoelectron-Photoion Coincidence and Photoionization Mass Spectral Study of Cyclopropene.
A. C. Parr and A. J. Jason..... 317

TPMOC-2 Mass Spectra of Organic Compounds in Liquid Phase at Atmospheric Pressure-Liquid Surface Ionization.
M. Tsuchiya and T. Taira..... 320

TPMOC-3 Angular Distributions in Molecular Ion Dissociations Observed by Photoelectron-Photoion Coincidence Spectroscopy.
J.H.D. Eland..... 322

TPMOC-4 Photoionization of Formic Acid: Fragmentation Mechanisms and the Proton Affinity of Carbon Dioxide.
K. E. McCulloh..... 326

TPMOC-5 Laser-Induced Fluorescence as a Probe of Ground State Ions Formed by Electron Impact.
J. Allison, K. Jackson, and R. Zare..... 326

TPMOC-6 Laser Photodissociation of Positive and Negative Ions.
J. Hiller, J. Robeson, and M. L. Vestal..... 328

TPMOC-7 Laser Photodissociation of Chloroethane Molecular Ions.
L. N. Morgenthaler and J. R. Eyler..... 330

TPMOC-8 Laser-Enhanced Ionization of Involatile Samples in Solution.
E. R. Lory and F. W. McLafferty..... 332

TPMOC-9 Photodissociation Spectroscopy of Cycloactadiene Radical Cations.
J. D. Hays and R. C. Dunbar..... 333

TPMOC-10 Ion Focussing Properties of a "Thick" Retardation Lens.
G. L. Merrill, C. A. Calkins, and C. L. Peterson.. 334

TPMOC-11 The Interface of Desorption Chemical Ionization (DCI) in Mass Spectral Ionization Methods.
D. E. Games, J. L. Gower, E. Lewis, U. Rupp, and G. Dielmann..... 336

TPMOC-12 Ion Cyclotron Resonance Study of Reactions of Ions With Atomic Hydrogen.
V. G. Anicich, Z. Karpas, and W. T. Huntress, Jr.. 338

TPMOC-13 Charge and Proton Transfer Reactions of $NH_3^+(v)$ on NH_3: The Effect of Incident Ion Vibrational and Translational Energy on the Reaction Cross Section.
P. T. Murray and T. Baer..... 338

Paper No. Page No.

GC/MS and LC/MS

TPMP-1 A Convenient Method for Analysis of the ^{18}O Content of Water and Phosphate.
T. R. Sharp and R. D. Minard..... 339

TPMP-2 A Method for the Isotopic Analysis of Biosynthetic ^{13}C-Carbon Monoxide by GC/MS.
A. Swanson and M. W. Anders..... 341

TPMP-3 Evaluation of Long-Term Stability in Chromatographic Relative Retention Time and Mass Spectrometric Relative Response Ratios in GC/MS Datafiles.
J. F. Ryan, R. A. Novak, B. J. Dowty, and R. M. Segesta..... 343

TPMP-4 Gas Chromatography and Mass Spectrometry of Nucleic Acid Hydrolysates.
D. L. Smith and J. A. McCloskey..... 345

TPMP-5 Applications of GCMS in Plastics Research and Development.
M. A. Haney..... 347

TPMP-6 Direct Analysis of Mixtures by MIKES.
R. G. Cooks, A. E.Schoen, M. L. Sigsby, S. E. Unger, D. Zakett, V. M. Shaddock, and T. L. Kruger..... 348

TPMP-7 The Mechanics of Capillary Column GC/MS and On-Column Injection.
C. B.Norwood and J. L. Lake..... 349

TPMP-8 Studies of Herbicides and Drugs by Combined LC/MS.
D. E. Games, M. E. Knight, E. Lewis and N. C. Weerasinghe..... 350

TPMP-9 Analysis of Insulation Integrity of Large Electrical Generators Using GC/MS/COM.
J. W. Auld and D.B. Kehoe..... 351

TPMP-10 A Gas Chromatograph/Field Ionization Mass Spectrometer (GC/FIMS) System.
S. E.Young, S. E. Buttrill, Jr., and G. A. St.John. 353

TPMP-11 An Ion Cyclotron Resonance Spectrometer as a Detector For a Gas Chromatograph.
M. T. Nguyen, J. Wronka and D. P. Ridge..... 355

TPMP-12 Design and Testing of a Two-Dimensional Gas Chromatography system for Mass Spectrometry.
R. J. May and W. V. Ligon, Jr..... 356

TPMP-13 A Comparative Evaluation of Quantitative Techniques for Scanning GC/MS Analysis.
A. E. Rosecrance, M. E. Rose, and B. N. Colby..... 357

TPMP-14 Comparison of Packed and Capillary Chromatography for Quantification of Drugs from Biological Samples by GC/FIMS
F. W. Crow and R. L. Foltz..... 357

Paper No. Page No.

TPMP-15 An HPLC-MS Study of Some Polycyclic Aromatic Hydrocarbons, Carbamates, and Hydrazines.
F. L. De Roos, and R. L. Foltz..... 358

TPMP-16 Quantitation of Δ^9-THC, 11-Hydroxy-Δ^9-THC, and 11-Nor-Δ^9-THC-9-Carboxylic Acid from Plasma Using Chemical Ionization Gas Chromatography/Mass Spectrometry.
B. J. Hidy, R. F. Foltz and D. L. Perry..... 360

TPMP-17 Developments of Programs to Improve On-Line Data Computation Capability of Hewlett-Packard (H.P.)5933A Data System Interfaced with H.P. 5930A GC/MS.
J. K. Khandelwal and H. Weinstein..... 362

TPMP-18 The Carrier Effect in GC/MS.
T. A. Blazer..... 362

TPMP-19 Chemical Applications of an LC-MS Interface.
A. Melera..... 363

TPMP-20 Progress in LC/MS Interfacing Based on the DLI Concept.
P. J. Arpino, G. Guiochon, G. Devant, and P. Krien..... 366

TPMP-21 A Combined Data-Blocking, Cross Correlation Peak Detection Method for Computerized GC-Mass Spectrometry.
W. Bryant, M. Trivedi, B. Hinchman, S. Sofranko, and P. Mitachek, Jr. 368

TPMP-22 LC-MS Analysis of Drugs.
J. D. Baty, D. A. Yorke, and B. N. Green.....369

TPMP-23 A Newsletter for Practical Mass Spectroscopy Communication.
W. Hyde..... 369

Pharmacology and Quantitative Biochemistry

WAMOA-1 Characterization of Thioether Conjugates of Acetoaminophen by Field Desorption Mass Spectrometry.
T. A. Baillie, H. Kambara, S. D. Nelson, and Y. Vaishnav..... 370

WAMOA-2 Preparation and GCMS Studies of N-Ethyl Derivatives of Desmethyl Metabolites of Antidepressant and Antipsychotic Drugs.
N. Narasinhachari and R. O. Friedel..... 372

WAMOA-3 Mass Spectrometric Techniques for Determining N-phosphonacetyl-L-Aspartic Acid (PALA) in Serum.
J. Robos, R. Suzuki, E.Rose, and T. Ohnuma..... 374

WAMOA-4 Quantitative Measurements of Indicine-N-Oxide in the Urine and Plasma of Cancer Patients.
J. V. Evans, S. K. Daley, and C. J. Nielsen..... 375

WAMOA-5 Identification of Rat and Human Urinary Metabolites of Placidyl ^{R} (Ethchlorvynol).
M. D. Scamuffa, S. Mueller, J. Wang and J. Machinist..... 379

Paper No. Page No.

WAMOA-6 Characterization of Urinary Metabolites of PGD_2 in the Monkey Using GC/MS.
B. J. Sweetman, C. K. Ellis, and J. A. Oates..... 379

WAMOA-7 5-Methoxytryptamine in Rat Hypothalmus and Human CSF. A Fact or Artifact?
N. Narasimhachari..... 381

WAMOA-8 Mass Spectrometric Analysis of Deuterium Triple-Labelled Blood Lipids.
W. K. Rohwedder, and E. A. Emken..... 383

WAMOA-9 Effects of Sample Storage Time on Precision and Accuracy in Measuring Picomole Quantities of Monamine Metabolites in Plasma by Selected Ion Monitoring.
S. E. Hattox, D. H. Landis, and J. W. Maas..... 385

WAMOA-10 Candidate Definitive Methods for the Determination of Uric Acid and Glucose in Human Serum by Isotope Dilution Mass Spectrometry.
A. Cohen, H. Hertz, R. Schaffer, L. Sniegaski, E. White, V., and M. Welch..... 387

WAMOA-11 Simultaneous GC-MS Assay of Rat Brain 3,4-Dihydroxy-phenylethylene,Glycol (DHPG) and 3-Methoxy-4-hydroxy-phenylethylene Glycol (MHPG).
D. D. Godse and J. J. Warsh..... 389

WAMOA-12 Withdrawn

WAMOA-13 Withdrawn

WAMOA-14 Use of [1-^{13}C] Leucine to Measure Human Whole Body Leucine and Protein Turnover.
D. E. Matthews, K. J. Motil, D. K. Rohrbaugh, J. F. Burke, V. R. Young, and D. M. Bier..... 391

WAMOA-15 Volatile Metal Chelates for Isotope Ratio Analysis of Biomedical Samples.
D. L. Hachey, J.-C. Blais, and P. D. Klein..... 392

WAMOA-16 Applications of FC/CID Mass Spectrometry to Modified Nucleic Acids.
K. M. Straub and A. L. Burlingame..... 394

Analysis of Solid Environmental Samples

WAMOB-1 Analysis and Identification of Microparticles in the Ion Microprobe.
J. Gavrilovic..... 396

WAMOB-2 Ion Microprobe Characterization of Particulate Matter.
C. A. Evans, Jr. and V. R. Deline..... 401

WAMOB-3 Isotope Dilution Mass Spectrometry of Coal and Fly Ash.
D. L. Donohue, J. A. Carter, R. L. Walker, and J. C. Franklin..... 403

Paper No. Page No.

WAMOB-4 Environmental and Isotope Dilution Reference Standards.
P. J. Paulsen..... 402

WAMOB-5 Sample Preparation of Particulates for Multi-Element Examination by Spark Source Mass Spectrography.
M. L. Jacobs and S. L. Sweeney..... 404

WAMOB-6 Elemental Characterization of Fueld and Effluents from Waste-to-Energy Systems by Spark Source Mass Spectrometry.
G. M. Trischan..... 406

WAMOB-7 Comparison of Spark Source Mass Spectrometry with Other Methods in the Analysis of Ambient Air Particulate Samples.
E. H. Daughtery, Jr. and J. K. Bostick, Jr. 410

WAMOB-8 Level 1 Environmental Assessment with the Source Assessment Sampling Train.
F. Briden and J. Dorsey..... 412

WAMOB-9 A Closer Look at the Alchemy of Fire.
L. L. Lamparski, T. J. Nestick, and S. S. Cutie... 415

WAMOB-10 The Analysis of Organic Solids by Metal Ion Attachment in SIMS.
R. G. Cooks, R. J. Day, and S. E. Unger..... 418

WAMOB-11 Hazardous Products from the Combustion of Organochlorine Compounds.
Y. Tondeur, R. G. Dougherty,C. Rappe, and H.-R. Buser..... 419

Reactions of Ions in Solution and Gas Phase

WAMOC-1 The Dissociation Dynamics of Furan Studied by Photoion - Photoelectron Coincidence.
G. D. Willet, T. Baer, and J. J. Butler..... 421

WAMOC-2 Energy Dependent Fragmentation of $C_6H_{12}^{+\cdot}$ Molecular Ions.
A. G. Harrison, N. E. Middlemiss, and Y. H. Li.... 423

WAMOC-3 Isomerizations of Hydrocarbon Molecular Ions.
J. L. Holmes and P. Wolkoff..... 425

WAMOC-4 The Electrocyclic Ring Opening of the Cyclobutene Radical Ion.
D. H. Russell and M. L. Gross..... 427

WAMOC-5 The Decomposition of the 1,3-Butadiene Radical Cation at Discrete Times between 10^{-11} and 10^{-5} Seconds.
D. H. Russell, M. L. Gross, J. van der Greef, and N.M.M. Nibbering..... 428

Paper No. Page No.

WAMOC-6 Proton-Transfer Reactions with Specifically Solvated Ions.
D. Smith, N. G. Adams, and M. J. Henchman..... 429

WAMOC-7 Reactions of Organic Anions in the Gas Phase.
C. H. DePuy, V. M. Bierbaum, R. J. Schmitt, J. J. Grabowski, and G. K. King..... 431

WAMOC-8 Organometallic Ion Chemistry: Parallels Between Gas Phase and Condensed Phase.
R. Freas, K. Kalmbach, J. Wronka, and D. P. Ridge. 433

WAMOC-9 Gas Phase Basicities of Main Group Fluorides and Oxyfluorides.
C. E. Doiron and T. B. McMahon..... 434

WAMOC-10 Spectroscopic Properties of Ions in the Gas Phase and in Solution.
W. D. Reents, Jr. and B. S. Freiser..... 433

WAMOC-11 The Chemistry of Glycine in the Gas Phase: Acidity, Basicity, and Structure.
M. J. Locke, R. L. Hunter, and R. T. McIver..... 436

WAMOC-12 Proton Bound Dimers: Thermochemistry and Applications to Stereochemical Analysis.
T. L. Kruger, G. M. McCluskey, D. Cameron, and R. G. Cooks..... 438

WAMOC-13 Bonding Energies and Resonance Stabilization in Dimer Ions of Polycyclic Aromatics.
M. Meot-Ner (Mautner), E. P. Hunter, and F. H. Field..... 438

WAMOC-14 The Stabilities of Proton Bound Dimers in the Gas Phase.
L. D. Betowski, D. H. Aue, H. M. Webb, and M. T. Bowers..... 439

WAMOC-15 The Hydrogen Deuterium Kinetic Isotope Effect Bridge Between Mass Spectrometry and Electrochemistry.
M. M. Green, G. Mayotte, and L. Meites..... 441

WAMOC-16 Decompositions of Metastable $C_4H_8O^{+\cdot}$ Ions.
D. J. McAdoo, C. E. Hudson, and D. N. Witiak..... 444

Instrumentation

WAMP-1 A Finnigan 4000 MS Integrated Thermal Desorber for Air Sampling Cartridges.
R. Narang, P. P. Dymerski, and J. Knight..... 446

WAMP-2 A Tandem Double-Focusing Mass Spectrometer for CA/MS and MS/MS Studies.
P. J. Todd, D. G. McGilvery, M. A. Baldwin, G. J. Wendel, M. R. Wixom, and F. W. McLafferty... 448

WAMP-3 Quadrupole Ion Store: Characterization and Application.
M. A. Armitage, J. E. Fulford, R. J. Hughes, and R. E. March..... 449

Paper No. Page No.

WAMP-4 Design of a Dense Gas Chromatograph/Mass Spectrometer Instrument for Involatile Sample Analysis.
L. G. Randall and A. L. Wahrhaftig..... 451

WAMP-5 Multiple Ion Detection at 10,000 Resolution.
D. A. Durden..... 453

WAMP-6 A RF-Only Quadrupole Mass Filter.
P. H. Dawson, M. Meunier, and W.-C. Tam..... 455

WAMP-7 A New Approach to Fast Scanning Pyrolysis/Mass Spectrometry.
G. Wells, K. J. Voorhees, and J. H. Futrell..... 457

WAMP08 Wide Band Fast Fourier Transform Ion Cyclotron Resonance.
V. G. Anicich and W. T. Huntress, Jr. 457

WAMP-9 Withdrawn.

WAMP-10 Characteristics and Design of a Fingerprint Field Ionization Mass Spectrometer.
W. Aberth..... 458

WAMP-11 Automated Mass Spectrometer Adjustment for Quadrupole Mass Spectrometers.
M. S. Story and E. L. Markel..... 460

WAMP-12 A Triple Quadrupole Mass Spectrometer for Direct Mixture, Analysis and Structure Elucidation.
R. A. Yost and C. G. Enke..... 461

WAMP-13 Construction Details of a Fourier Transform Mass Spectrometer.
S. Ghaderi, E. B. Ledford, Jr., R. B. Spencer, C. L. Wilkins, and M. L. Gross..... 463

WAMP-14 Microcomputer-Based Fourier Transform Ion Cyclotron Resonance Mass Spectrometer.
R. J. Doyle, Jr., T. J. Buckley, and J. R. Eyler.. 465

WAMP-15 Gas Chromatograph Column Effluent Venting System for the Dupont 490 GCMS.
D. L. Winmill and R. L. Williams..... 467

WAMP-16 Fomblin: A High Molecular Weight Reference Compound.
G. A. Warburton, R. McDowell, and K. R. Compson... 469

WAMP-17 Applications of a New Mass Spectrometer to Quantitative Hydrocarbon Analysis.
G. A. Errock, D. J. Hoy, K. T. Taylor, and K. R. Compson..... 471

WAMP-18 A Review of Recent Developments in Data Acquisition for Time-of-Flight Mass Spectrometers.
K. A. Lincoln.....472

WAMP-19 Positive Ion Composition Measurements in the Stratosphere - Experimental Aspects and Results.
E. Arijs, J. Ingels and D. Nevejans..... 474

Paper No. Page No.

WAMP-20 A New Mass Spectrometer for Hydrocarbon Mixture Analysis.
C. Brunee, H. Rache, H. Ravens, and B. Windel..... 476

WAMP-21 The Effects of High Input Current Pulses upon Channel Electron Multipliers.
E. A. Kurz..... 477

WAMP-22 A Dual Ouput Channeltron.
E. A. Kurz and R. L. Roy..... 479

WAMP-23 Withdrawn

WAMP-24 Multichannel Scaling for Ultra Sensitive Data Acquisition on the Varian MAT731.
W. V. Ligon, Jr..... 481

Biological and Biomedical Applications

RAMOA-1 Biomedical Applications of Steroid Metabolic Profiling by GC/MS.
P. G. Marsh and P. V. Fennessey..... 482

RAMOA-2 Analyses of Organic Acids and Amino Acids in Amniotic Fluid by GC/MS/COM System.
T. Shinka, I. Maruyama, T. Kuhara, I.Matsumoto, K. Kabashima, H. Abe, and T. Kato..... 484

RAMOA-3 The Detection of Biochemical Markers in Disease. The Use of Quantitative GC/MS in the Discovery of New Disorders of Metabolism.
P. V. Fennessey, C. Butler, S. Kibler, G. March, and S. Tjoa..... 486

RAMOA-4 Profiles of Organic Acids in Mouse Brain Homogenates.
S. Yamada, T. Kuhara, I. Matsumoto, and K. InOnaga..... 488

RAMOA-5 Radiogas Chromatography/Mass Spectrometry in Drug Mode-of-Action Studies.
I. M. Campbell, D. L. Doerfler, J. M. Malloy, I. R. McManus, J. D. Nawaral, and E. R. Rosenblum. 490

RAMOA-6 Applications of Glass Capillary Gas Chromatography/ High Resolution Mass Spectrometry to Problem Areas of Urinary Organic Acid Analysis.
S. Lewis and A. L. Burlingame..... 492

RAMOA-7 Analysis of Trace Levels of Organic Compounds using the New Electrooptical Ion Detector Mass Spectrometer (EOID/MS) at JPL.
H. G. Boettger, C. E. Giffen, and R. A. Britten... 494

RAMOA-8 Cf-252 PDMS of Synthetic Gene Fragments.
C. J. McNeal and R. D. Macfarlane..... 495

RAMOA-9 Steroid Analysis Using Chemically Labelled Immunoassay.
F. M. Bockhoff and H. G. Boettger.....496

RAMOA-10 Studies of Chlorophyll A Solvation by ^{252}Cf-PDMS.
J. E. Hunt and R. D. Macfarlane..... 497

Paper No. Page No.

RAMOA-11 In Vivo Study of the Metabolism of Chirally Labelled Valine in Rats.
I. J. Amster, D. J. Aberhart, and K. Tanaka..... 499

Fundamental Aspects

RAMOB-1 Rate of Formation of Ar^+_3.
D. C. Conway..... 501

RAMOB-2 Fragmentation of SO_2^+ Prepared in Selected Internal Energy States.
M. J. Weiss, T.-C. Hsieh, and G. G. Meisels..... 502

RAMOB-3 Dissociative Photoionization.
T. Masuoka and J.A.R. Samson..... 504

RAMOB-4 Stoichiometry of the Reaction of Electrons with $CBrCl_3$ in an Electron Capture Detector.
E. P. Grimsrud and S. H. Kim..... 506

RAMOB-5 Kinetic Shift in Chlorobenzene Fragmentation and the Heat of Formation of the Phenyl Ion.
R. Stockbauer and H. M. Rosenstock..... 508

RAMOB-6 Ionization Energies, Proton and Hydrogen Affinities of Polycyclic Aromatics.
M. Meot-Ner (Mautner), E. P. Hunter, and
F. H. Field..... 509

RAMOB-7 Withdrawn

RAMOB-8 Chemical Accelator Studies of Ion-Molecule Reactions: $X^+ + CH_4$
P. M. Hierl..... 510

RAMOB-9 Kinetic and Internal Energy of H_2S^+ Ions Produced in Thermal Energy Charge Transfer from Xe^+ to H_2S.
G. Mauclaire, R. Derai, S. Fenistein, and
R. Marx..... 512

RAMOB-10 Ion-Molecule Half-Reactions.
C. E. Klots..... 514

RAMOB-11 FT-ICR Study of the Ion Molecule Chemistry of $CpCr(CO)_2NS$ and Related Compounds.
M. Comisarow and G. Parisod.....514

Environmental

RAMOC-1 A GC/MS Study of the Total Fluorescence Method for the Analysis of Polynuclear Aromatic Compounds in Sea Water.
W. D. Jamieson, J. B. Addison, M. D. MacKinnon,
W. J. Cretney, and D. R. Green..... 515

RAMOC-2 Capillary On-Column Injection and GC/MS Analysis of Organic Pollutants in Marine Samples.
C. B. Norwood and J. L. Lake..... 517

Paper No. Page No.

RAMOC-3 Instrumental Approaches to a Master Scheme for Analysis of Organics in Water.
J. Bursey, K. Tomer, L. Sheldon, E. D. Pellizzari, and C. Sparacino..... 518

RAMOC-4 Peak Locator for Environmental Containment Analysis.
L. B. Hansen..... 520

RAMOC-5 Practical Considerations in the Analysis of Complex Industrial Waste Streams.
J. Bouldin, R. Stowe, K. Shewbart, and M. J. McAdams..... 522

RAMOC-6 Glass Capillary GC/MS Analysis of Drinking and Advanced Waste Treatment Water Concentrates.
D.C.K. Lin, R. Foltz, S. Lucas, B. Peterson, and L. Slivon..... 523

RAMOC-7 A Comparative Study of Volatile Halogenated Hydrocarbons in Man and the Environmental Media by GC/MS/COMP.
E. D. Pellizzari, R. A. Zweidinger, R. N. Williams, M. D. Erickson, B. Harris, III, D. S. Smith, K. B. Tomer, and M. Ray..... 524

RAMOC-8 A Quality Controlled Operating Procedure for a General Type Quantitative GC/MS Analysis.
V. L. Warren..... 526

RAMOC-9 GC/MS Verification of Identity of Chlorinated Pesticides and Biphenyls in Municipal Sewage Treatment Plant Sludge.
C. F. Rodriguez, C. P. Nulton, and W. A. McMahon... 528

RAMOC-10 Applications of Recent Mass Spectrometric Techniques to the Analysis of Environmental Samples.
D. J. Harvon, J. R. Hass, and K. L. Busch..... 529

RAMOC-11 GC/MS Analysis of Volatile Purgeable Halogenated Organic Compounds in Human Serum and Adipose Tissue.
C. D. Pfaffenberger..... 531

Environmental and Ion-Molecule Reactions

RAMP-1 The Kinetic Isotopic Fractionation Effect for Carbon and Oxygen in the Reaction CO + OH.
C. M. Stevens, R. Gorse, S. Cohen, S. Durkee, and K. Bielling..... 533

RAMP-2 Quantitation of Individual Organic Compounds in Shale Oil.
L. R. Hilpert, H. S. Hertz, W. E. May, S. N. Chesler, F. R. Guenther, J. M. Brown, and R. M. Parris..... 534

RAMP-3 Withdrawn

RAMP-4 The Determination of Polycyclic Aromatic Hydrocarbons at the ng/L Level in Drinking Water.
F. M. Benoit, G. L. Lebel, and D. T. Williams..... 537

Paper No.		Page No.
RAMP-5	The Analysis of Tetrachlorodibenzodioxin (TCDD) at the Parts-per-Trillion Level. P. A. Lyon, J. O. Lay, D. L. Miller, and M. L. Gross	539
RAMP-6	Heat Degradation of Solar Heat Transfer Fluids. T. R. Henderson, C. R. Clark, T. C. Marshall, R. L. Hanson, and C. H. Hobbs	541
RAMP-7	Ubiquitousness of Long Chain Hydrocarbons and Derivatives in Industrial Waste Waters by G.C.M.S.D.S. R. J. Teece, S. M. Somani, and D. Schaeffer	543
RAMP-8	Measurements of Organic Compounds in Sediment Soils, and Material from Chemical Waste Dumps. J. W. Eichelberger and W. L. Budde	544
RAMP-9	A Unique Scan Circuit For Use in Multiple Ion, GC-High Resolution MS Determination of Picogram Quantities of Chlorodioxins. J. D. Solch, C. D. Miller, R. O. Yelton, M. L. Taylor, and T. O. Tiernan	545
RAMP-10	Determination of Thermal Decomposition Properties of Toxic Organic Wastes. J. A. Mescher and W. A. Rubey	547
RAMP-11	Environmental Applications of Crossed-Beam LC/MS. M. J. McAdams, C. R. Blakley, and M. L. Vestal	548
RAMP-12	Application of Mass Spectrometry to Environmental Problems: The Structure of Aquatic Humic Acid. M.-J. Bobenrieth, J. R. Hass, W.-T. Liao, R. F. Christman, and F. K. Pfaender	550
RAMP-13	Withdrawn	
RAMP-14	High Pressure Negative Ion Mass Spectra of Organo-metallic Compounds. K. L. Busch, N. B.H. Henis, J. R. Hass, and M. M. Bursey	554
RAMP-15	Methane Enhanced Negative Ion Mass Spectra of Organic Nitriles. C. E. Parker, K. L. Busch, D. J. Harvan, J. R. Hass, and M. M. Bursey	556
RAMP-16	Proposed Applications of Fourier Transform Mass Spectrometry. M. L. Gross, S. Ghaderi, E. Ledford, P. S. Kulkarni, and C. L. Wilkins	557
RAMP-17	Temperature Dependence of Momentum Transfer Rate Constants. D. C. Parent and M. T. Bowers	558
RAMP-18	Protonation of Alkenes: Heats of Formation of Alkyl Ions. P. Ausloos and S. G. Lias	559
RAMP-19	Mobilities of CH_5^+, $C_2H_5^+$, $C_3H_5^+$, and $C_3H_7^+$ Ions in Methane Gas. M. Saporoschenko	560

Paper No. Page No.

RAMP-20 Relative Proton Affinities of Some Halobenzenes and Halotoluenes.
D. K. Bohme, J. A. Stone, R. S. Stradling, R. S. Mason, and K. R. Jennings..... 560

RAMP-21 Determination of Proton Affinities by Reactant Ion Monitoring.
V. T. Tran and B. Munson..... 562

RAMP-22 Negative Ion Chemistry of the Vinyl Group.
J. E. Bartmess and R. Hays..... 564

RAMP-23 Ion-Molecule Reactions of Alkynes.
C. Lifshitz, S. Gefen, Y. Gleitman, and U.Shainok. 566

Fundamental Aspects of Processes Relevant to Formation and Reactions of Ions

RPMOA-1 On the Behaviour of Vibrationally-Excited Molecules.
R. A. Marcus..... 568

RPMOA-2 Classical Trajectory Studies of Unimolecular Dynamics.
W. L. Hase..... 572

RPMOA-3 The Role of Electronically Excited States in The Fragmentation of Large Ions.
H. M. Rosenstock..... 575

RPMOA-4 The Statistical Theory and the Decay of State Selected Ions.
T. Baer..... 576

RPMOA-5 Ion Photofragment Spectroscopy.
J. T. Moseley and P. C. Cosby..... 579

RPMOA-6 Energetics and Dynamics of Molecular Ions by Photoionization of Van der Waals Molecules.
S. Ceyer, P. Tiedemann, T. Hirooka, S. Anderson, B. H. Mahan, and Y. T. Lee..... 583

Computer Applications

RPMOB-1 Computer Controlled Mass Spectral Data Acquisition with a Fast New High Dynamic Range Interface.
J. C. Bill, W. E. Morden, P. Powers, and M. J. Wallington..... 587

RPMOB-2 Microprocessor Controlled Sample Heating Current Programmer for Direct Exposure Probes.
R. J. Cotter..... 590

RPMOB-3 Automated Qualitative and Quantitative Analysis of GC/MS Data from Complex Organic Mixtures.
G. I. Ouchi..... 592

RPMOB-4 Simulation of the Quadrupole Mass Filter.
J. E. Campana and P. C. Jurs..... 594

RPMOB-5 Elements of a Cost Effective Mass Spectroscopy Data System.
D. E. Smith and P. L. Warren..... 596

Paper No. Page No.

RPMOB-6 Simulation of Hydrocarbon Mass Spectra.
H. A. Clark and P. C. Jurs..... 598

RPMOB-7 Microcomputer Control of a Mass Spectrometer for Trace Noble Gas Determination.
J. C. Newton, R. G. Bedford, H. R. Brand, R. W. Crawford, and J. R. Elliott..... 599

RPMOB-8 Accurate Mass Measurement Using a Computerized Ion Cyclotron Resonance Mass Spectrometer.
R. L. Hunter and R. T. McIver, Jr. 601

RPMOB-9 Applications of a Multi-User, Multi-Instrument Data System.
P.R.J. Matejcek and W. A. Wolstenholme..... 601

RPMOB-10 A GC-MS-DS to Support Pharmaceutical Research: Practical Design Considerations in View of the Pending Good Laboratory Practices Regulations.
W. Bryant, M. Trivedi, B. Hinchman, S. Sofranko, and P. Mitachek, Jr. 602

RPMOB-11 Computerization of the Hitachi-Perkin Elmer RMH-2 Mass Spectrometer.
D. T. Terwilliger..... 604

RPMOB-12 Automatic Normalization of Mass Abundances in Scanned Mass Spectra.
J. Justice..... 606

RPMOB-13 The Development of Automatic Sampler and Library Search Systems for Computer GC/MS Operation.
H. Roden and R. L. Conrad..... 608

Environmental and LC/MS

RPMOC-1 Identification of Chemical Residues Found in Peanut Butter.
D. L. Heikes..... 609

RPMOC-2 GC/MS Detection of Mammalian Urine.
G. D. Castillo and R. B. Bradicich..... 611

RPMOC-3 Analysis of the Urinary Metabolites of the Carcinogen Acrylonitrile.
Y. Y. Lin and A. E. Ahmed..... 613

RPMOC-4 Identification of Metabolites of Hexazinone by Mass Spectrometry.
R. W. Reiser, I. J. Belasco, and R. C. Rhodes..... 614

RPMOC-5 Withdrawn

RPMOC-6 An On-Line Segmented Flow LC/MS Combination.
B. L. Karger, D. P. Kirby, P. Vouros, R. L. Foltz, and B. Hidy..... 616

RPMOC-7 The Use of Membrane Inlet System for the Determination of Trace Organics in Air.
A. W. Spratley and D. Talbert..... 617

Paper No. Page No.

RPMOC-8 Analysis of Polynuclear Aromatic Hydrocarbons (PAH) in Diesel Exhaust Particulates by GC/MS.
B. A. Petersen, C. C. Chuang, and R. M. Riggin.... 619

RPMOC-9 LC/MS Employing Continuous Sample Preconcentration.
R. G. Christensen, H. S. Hertz, S. Meiselman, and E. White, V 620

RPMOC-10 LC/MS Interface Using Molecular Beam Techniques.
C. R. Blakley, M. J. McAdams, and M. L. Vestal.... 622

RPMOC-11 A New HPLC/MS Interface.
D. A. Yorke, P. Burns, and D. S. Millington..... 624

RPMOC-12 High Efficiency Radially Compressed Liquid Chromatography/Mass Spectrometry (RCLC/MS)--Is it the Answer?
D. Hilker and P. P. Dymerski..... 625

RPMOC-13 Combined LC/MS in Studies of Natural Products.
D. E. Games, C. Eckers, P. Hirter, E. Lewis, and K.R.N. Rao..... 627

Biological and Biochemical Applications

RPMP-1 The Application of Mass Spectrometric Techniques to the Recognition of Organophosphate Pesticide Transformation Products in a Case of Human Poisoning by an Unknown Toxic Agent.
R. L. Harless, G. W. Sovocool, D. E. Bradway, L. H. Wright, E. M. Lores, and L. E. Feige..... 629

RPMP-2 Withdrawn

RPMP-3 Screening of the Inherited Diseases by GC/MS/COM.
I. Matsumoto, T. Shinka, T. Kuhara, S. Haraguchi, N. Hisanaga, T. Mizuno, and Y. Itagaki..... 630

RPMP-4 Analysis of Organic Acids in CSF of Various Neurological Disorders by GC/MS.
M. Yoshida, T. Kuhara, T. Shinka, I. Matsumoto, and S. Kuramoto..... 632

RPMP-5 E.I./C.I./F.I. Mass Spectra of Selected Prostaglandin Derivatives and Analogs.
L. Baczynskj..... 634

RPMP-6 Withdrawn

RPMP-7 Regioselectivity in the Enzymatic Formation of Dihydrodiols of 7,12-Dimethylbenz(a)anthracene.
C.-L.A. Wang, F. B. Daniel, and L. K. Wong..... 636

RPMP-8 Selective Metastable Peak Monitoring.
D. S. Millington, J. A. Smith, and S. J. Gaskell.. 638

RPMP-9 Mass Spectrometry and Reactivity of Chloroalkene Epoxides.
J. J. Solomon, S. A. Kline, S. C. Agarwal, and B. L. Van Duuren..... 639

RPMP-10 A Search for Neuroactive Compounds in the Central Nervous System of Molluscs.
M. J. McCaman..... 640

Paper No. Page No.

RPMP-11 Measurement of Plasma FFA Turnover and Oxidation Using 1-^{13}C-Palmitic Acid.
R. R. Wolfe, J. Evans, C. Mullany, and J. F. Burke..... 640

RPMP-12 Withdrawn

RPMP-13 Performance of a Wide Dynamic Range Mass Spectrometer for Respiratory Studies.
D. J. Marshall and J. Lehr..... 641

RPMP-14 Applications of Isotope Ratio Mass Spectroscopy to Metabolic Study in Burned Children.
D. Rohrbaugh, R. R. Wolfe, C. J. Mullany, J. F. Burke, and V. R.Young..... 643

RPMP-15 Amphetamine Metabolism: Is Phenylacetone Oxime a Necessary Intermediate in Deamination Reactions? A Study by Stable Isotope GC/MS.
J. Wright, P. S. Callery, and J. Gal..... 644

RPMP-16 A Mass Spectral Study of the Perbenzoyl and Bo-Perbenzoyl Derivatives of Various Polyols.
R. M. Thompson and D. A. Cory..... 645

RPMP-17 Ion Plasma Desorption Mass Spectrometry of Sulfhydryl Drug Conjugates.
R. N. Stillwell, J. R. Mitchell, W. G. Stillwell, B. H. Lauterburg, E. C. Horning, and J. G. Nowlin. 645

RPMP-18 In Vitro Formation of Methylthio Metabolites of Naphthalene from Mercapturic Acid Derivatives.
W. G. Stillwell..... 646

RPMP-19 Analysis of Peptides.
L. A. Smith, R. M. Caprioli, and S.-N. Lin..... 647

RPMP-20 GC-MS Analysis of Methylmalonic Acids from Biological Fluids as the Dicyclohexyl Ester.
E. J. Norman, E. K. Berry, and M. D. Denton..... 648

RPMP-21 Identification of a Novel Type of a Glucuronide Conjugate in the Metabolism of Carbazolol.
M. Senn, H. Hindermayr, and K. Koch..... 649

RPMP-22 Measurement of 6-Keto-PGF$_{1\alpha}$ in Biological Media by Selected Ion Monitoring.
M. Claeys, A. Duchateau, C. VAn Hove,and A. G. Herman..... 651

RPMP-23 The Mass Spectra of Bruceolides: A Preliminary Investigation.
M. Baldwin, D. Carter, and F. Darwish..... 654

Paper No. Page No.

Fundamental Aspects of Processes Relevant to Formation and Reactions of Ions

FAMOA-1 Pulsed Molecular Beam Studies of Photodissociation Dynamics.
W. R. Gentry..... 656

FAMOA-2 Unimolecular Reactions and Energy Transfer in Ionic Systems.
M. T. Bowers..... 660

FAMOA-3 Vibrational Energy Transfer in Unimolecular Systems.
M.C. Flowers, D. F. Kelley, F. C. Wolters, and B. S. Rabinovitch.....661

FAMOA-4 Charge Transfer Reactions of Molecular Ions.
T. F. Moran..... 665

FAMOA-5 Beam Studies of Organic Chemi-ionization Reactions.
R. J. Cross, A. Auerbach, L. Lee, and M. Saunders..... 668

Biochemistry

FAMOB-1 Silylation - Mediated Oxidation.
J. A. Kelley..... 672

FAMOB-2 Identification of TMSi Ether C_{26} Bile Alcohol Analogs via Side Chain Fragmentation Patterns.
G. S. Tint, B. Dayal, S. Shefer, and G. Salen..... 674

FAMOB-3 Mass Spectrometry of Labile Organic Solids.
D. L. Turner and D. C. Conway..... 676

FAMOB-4 Mass Spectrometry of Chemically Derivatized Hypothalamic Oligopeptides.
D. M. Desiderio, J. Z. Sabbatini, and J. L. Stein..... 678

FAMOB-5 Polypeptide Sequencing by Mass Spectrometry: New Methodology.
D. F. Hunt, A. M. Buko, J. Ballard, and J. Shabanowitz..... 680

FAMOB-6 Structural Studies of the Non-Host Specific Mycotoxins Associated with Southern Corn Leaf Blight.
D. A. Hoisington, V. Walbot, and M. K. Hoffman.....682

FAMOB-7 Studies in Molecular Species of Glycerophospholipids by a GC-MS System.
K. Saito and K. Satouchi..... 684

FAMOB-8 Identification and Mass Spectrometry of Phytotoxins in Coffea Arabica.
G. R. Waller and C.-H. Chou..... 686

FAMOB-9 Glycoconjugate Structural Studies by Field Desorption Mass Spectrometry.
V. N. Reinhold..... 688

FAMOB-10 CI and EI Mass Spectral Identification of the Urinary Metabolites of Zomepirac.
W. N. Wu, L. E. Weaner, J. Kalbron, P. J. O'Neill, and J. M. Grindel..... 690

Paper No. Page No.

FAMOB-11 Mass Spectrometry of Underivatized Epoxides, Hydroperoxides, Epoxy- and Hydroxy Fatty Acids.
K. Halpaap-Wood, J. Nowlin, G. W. Griffin, M. G. Horning, and E. G. Horning..... 691

FAMOB-12 Techniques for the Structure Elucidation of Modified Nucleosides from tRNA by High Resoltion Mass Spectrometry.
Z. Yamaizumi, S. Nishimura, H. J. Gross, H. Yamamoto, P. F. Crain, and J. A. McCloskey..... 693

FAMOB-13 Mass Spectra of Permethylated Nucleotides.
P. Brown, J. J. Einck, and G. R. Pettit..... 694

FAMOB-14 New Ganglioside Structure of Human Erythrocytes as Analyzed by Mass Spectrometry Combined with Enzymatic Degradation.
M. Powell, K. Watanabe, and S. Hakomori..... 695

FAMOB-15 Sequence Analysis of Carbohydrates by FD/CID Mass Spectrometry.
H. Kambara and A. L. Burlingame..... 697

Instrumental Design

FAMOC-1 A Time-of-Flight Mass Spectrometer for Measurement of Secondary Ion Mass Spectra.
B. T. Chait and K. G. Standing..... 699

FAMOC-2 CID and Mixture Analysis Studies on a Finnigan Triple Stage Quadrupole Mass Spectrometer.
D. F. Hunt, J. Shabanowitz, and A. Giordani..... 701

FAMOC-3 A New Mass Spectrometer for the Study of Field Free Region Ion Chemistry.
D. H. Russell, D. H. Smith, and R. J. Warmack..... 703

FAMOC-4 A General Method for Recording B-E Linked Scan Metastable Ion Spectra.
W. F. Haddon..... 704

FAMOC-5 The Moving-Quadrupole Improvement to Phase-Spectroscopy.
M. W. Siegel..... 705

FAMOC-6 A New High Performance, Medium Resolution Mass Spectrometer - MS80.
D. R. Denne, M. L. Aspinal, K. R. Compson, and W. Henderson..... 707

FAMOC-7 Extending the Capabilities of an APCI-MS System with a Preconcentrator for the Rapid Ultra-Trace Detection of Polychlorobiphenyls and Hexachlorobenzene in the Atmosphere.
B. A. Thompson, D. A. Lane, T. Sakuma, N. M. Reid, J. B. French, E. Quan, and S. Nacson..... 709

FAMOC-8 Transverse Ionization of a Supersonic Molecular Beam: Effects of Space Charge on Mass Spectra and Velocity Measurements.
M. J. Vasile..... 711

FAMOC-9 Analytical Performance of a Fourier Transform Mass Spectrometer.
E. B. Ledford, Jr., R. White, R. B. Spencer, P.S. Kulkarni, S. Ghaderi, C. L. Wilkins, and M. L. Gross..... 712

Paper No. Page No.

FAMOC-10 Fourier Transform Ion Cyclotron Resonance Spectroscopy.
M. Comisarow..... 713

FAMOC-11 Electro-Optical Ion Detection Using Solid State Photo-Diode Array Detectors.
C. E. Giffin, R. Britten, J. Conley, D. Norris, and H. Boettger..... 714

FAMOC-12 Modification of the Finnigan ^{1015}MS for Direct Chemical Ionization of Non-Volatile Organic Compounds.
D. T. Carroll, J. G. Nowlin, F. E. Montgomery, R. N. Stillwell, and E. C. Horning..... 716

FAMOC-13 A Modified Electron Bombardment Source for KRATOS/AEI MS9-MS50 Spectrometers.
G. W. Eigendorf..... 717

FAMOC-14 The Performance of a Simultaneous Ion Detector Using Surface Barrier Diodes.
J. D. Stein and C. L. Peterson..... 719

Chemical Ionization/Environmental Applications

FAMP-1 NIH/EPA Chemical Ionization Mass Spectral Data Base and Search System.
D. P. Marinsen, S. R. Heller, and G.W.A. Milne.... 721

FAMP-2 Negative Ion Chemical Ionization Mass Spectrometry: Reactions of F^- ion.
C. C. Cheng, C. Chang, and T. O. Tiernan..... 722

FAMP-3 Application of Negative Chemical Ionization to GC/MS and LC/MS.
D. P. Beggs and A. Melera..... 724

FAMP-4 Mass Measurement of Negative Ion Chemical Ionization Spectra by Double Beam Mass Spectrometry.
M. L. Aspinal, D. R. Denne, K. R. Compson, and S. Evans..... 726

FAMP-5 Instrumental Aspects of Positive and Negative Ion Chemical Ionization Mass Spectrometry.
G. C. Stafford..... 727

FAMP-6 Negative EC-CI Assays for Norepinephrine Metabolites Use of Hexafluoroacetone to Produce Cyclic Derivatives.
P. A. Blomberg, S. P. Markey, and I. J. Kopin.....729

FAMP-7 The Application of Alternate CI/EI to Extract GC-MS on the MS-25.
K. T. Taylor, J. R. Chapman, C. J. Wakefield, and K. R. Compson..... 731

FAMP-8 Ion-Molecule Reactions in N_2O/CH_4 Mixtures.
C. L. Polley and G. G. Meisels..... 733

Paper No.		Page No.
FAMP-9	Negative Chemical Ionization Analysis of Xenobiotic Chemicals from Milligram Quantities of Human Samples. D. W. Kriehl, M. J. Whitaker, and R. C. Dougherty.	735
FAMP-10	EI Type Mass Spectra Recorded Under CI Conditions. D. F. Hunt and P. J. Gale.....	736
FAMP-11	Ion Molecule Isotope Exchange Reactions: Methodology for Locating Protons in Sample Molecules by CIMS. D. F. Hunt and S. K. Sethi.....	737
FAMP-12	A Flowing Discharge Ion Source for Positive and Negative Ion Mass Spectrometry of Compounds in Air. S. E. Buttrill, Jr.	739
FAMP-13	Characterization of Fossil Fuels by Chemical Ionization Mass Spectrometry. L. W. Sieck.....	741
FAMP-14	Withdrawn	
FAMP-15	Characterization of Underivatized Phenols in Human Urine by HPLC/MS. L. H. Wright and T. R. Edgerton.....	742
FAMP-16	Quantitative Mass Spectrometry of Mirex and Its Degradation Products by Means of High Performance WCOT Column Gas Chromatography/Mass Spectrometry. F. I. Onuska, M. E. Comba, and J. A. Coburn.....	743
FAMP-17	Withdrawn	
FAMP-18	A Direct Sampling Field Ionization Mass Spectrometer System for Detecting Organic Compounds in Air at Sub-PBB Levels. S. E. Buttrill, Jr., and G. A. St. John.....	745
FAMP-19	Metastable Spectra of Polynuclear Aromatic Hydrocarbons by Linked Scan Techniques. B. Shushan and R. K. Boyd.....	747
FAMP-20	Application of Mass Spectrometry to the Quantification of Hydrocarbons in Avian Tissue. M. L. Gay and A. Belisle.....	748
FAMP-21	GC/MS Investigations of the Heterocyclic Aromatic Hydrocarbons Found in the Environment. R. C. Burk, R. C. Lao, and R. S. Thomas.....	749
FAMP-22	Operator Interactive Semiautomatic Processing of Priority Pollutants and Other Specific Compound Analysis. C. E. Rechsteiner, J. L. Stauffer, J. E. Oberholtzer and P. L. Levins.....	751
FAMP-23	Electron Transfer Ionization Mass Spectrometery for Hydrazine. P. Breisacher, P. Mahadevan, and W. A. Hicks.....	753
FAMP-24	Analysis of Base Neutrals by Glass Capillary EI-GC-MS on the Finnigan 3200. R. D. Minard and M. R. Bogdan.....	755

Metabolic Profiling: Automated Analysis of Complex Mixtures From Tissues and Physiological Fluids

Charles C. Sweeley

Department of Biochemistry, Michigan State University, East Lansing, Michigan 48824

SUMMARY

The simultaneous detection and quantitative determination of a very large number of the component metabolites in physiological fluids, and the subsequent comparison of these data with reference values, obtained with supposedly healthy subjects, is a process which has commonly been called "metabolic profiling" analysis. The concept is appealing because it may be possible to detect a large number of diseases by a single procedure, it may provide the possibility of early diagnosis, before there are visible clinical manifestations of illness, and it may enable physicians to more accurately assess the course of treatment.

The analytical requirements for quantitative metabolic profiling seem to be ideally matched by the capabilities of modern combined gas chromatography-mass spectrometry-computer systems. Profiles are generated by repetitive scanning techniques during either packed column or glass capillary column gas chromatography, individual substances are identified by comparison of their mass spectra with those of reference compounds by forward or reverse library search techniques, and statistical methods are employed for analysis of the data. The shortcomings of library searching procedures with complete mass spectra are severe when dealing with poorly resolved mixtures of two or more substances, but can be overcome to a large extent with computer methods which provide "cleaned up" mass spectra of each of the components in the mixture. Alternatively, use can be made of detection algorithms which depend upon the presence of ions in the set of mass spectra that are characteristic and unique for a particular substance. The high correlation in the values for approximately one hundred organic acids in human urine obtained by these two techniques suggests that both approaches can provide reliable analytical profile data.

The concept of automated multicomponent analyses of physiological fluids is probably as old as clinical laboratories. Determination of the levels of metabolites is an important clinical laboratory procedure, which assists the physician in the assessment of the health status of an individual and the proper diagnosis of an abnormal condition. Sophisticated procedures are available for the accurate quantitative determination of individual substances, employing colorimetric tests, chromatography, radioimmunoassays, etc. and most hospital laboratories have autoanalyzers of various kinds that perform a score or more of chemical tests on large numbers of blood and urine samples.

Chromatography was certainly one of the earliest and perhaps most critical of the analytical breakthroughs, which led in the 1940's and 1950's to the development of ion exchange chromatography for the analysis of amino acid profiles in serum and urine, still a popular procedure for the diagnosis of metabolic diseases, particularly among the population of mentally retarded patients. Paper chromatography was also an attractive and popular technique at that time for analyses of many kinds of metabolites.

Roger Williams at the University of Texas was particularly perceptive about the diagnostic importance of multicomponent analysis. His papers in the early 1950's, dealing with the concept of biochemical individuality, were based on the results of a large number of paper chromatographic analyses of a few urinary metabolites and determinations of the taste thresholds of several substances. I would like to quote from one of Roger Williams papers (1), as follows: "It appears that each individual we have studied has exhibited a characteristic pattern of measurements which is distinctive for that individual alone." Williams, who used the term metabolic patterns, employed his methods to examine samples from a variety of subjects, including alcoholics, schizophrenics and residents of mental hospitals and thus laid the foundation for later studies with paper chromatography by Armstrong (2), Dalgleish (3) and others and to subsequent more sophisticated methods.

In the 1960's much work was devoted to the perfection of instrumentation and techniques for the gas chromatographic (GC) separation of various classes of substances. The successful coupling of the gas chromtograph and the mass spectrometer (4,5) made possible the simultaneous separation and identification of abnormal components of complex mixtures from physiological fluids.

In the early 1970's the Hornings outlined procedures for the isolation and analysis of serum and urinary mixtures of several classes of metabolites, such as steroids, sugars and aromatic acids. They were the first to use the term "metabolic profiles," which was coined to describe the composite of biochemical reactions leading to a particular pattern of metabolites (6,7). The Hornings predicted in these classic papers that metabolic profiles would be useful in characterizing normal and pathologic states and were among the first to use mass spectrometry to characterize the mixtures.

In 1971, Jellum et al. (8) reported a screening program for inborn errors of metabolism, involving gas chromatography to separate various classes of substances and mass spectrometry to identify abnormal components with the aid of computerized forward library search techniques. The methodology was designed to provide diagnostic information about known disorders; occasionally new diseases were found by Jellum's group (9) and others such as Goodman et al. (10), Chalmers, Watts and Lawson (11), Hillman et al. (12), Tanaka et al. (13), Gompertz et al. (14), Wilson et al. (15) and others. Altogether some 23 new metabolic diseases have been uncovered by these techniques, raising the number of inborn errors that might be analyzed by GC or GC-MS to at least 50.

Obviously not all of the components of these mixtures can be separated completely from each other with packed GC columns, and several groups have exploited the high resolution of capillary columns for metabolic profiling analyses. Time prevents me from discussing the excellent results that have been obtained with low molecular weight volatiles from urine and expired air by Robinson and Pauling (16), Lee et al. (17), McConnell and Novotny (18) and others, nor work on steroids, especially by Luyten and Rutten (19), Pfaffenberger, Malinak and Horning (20), Shackleton and Honour (21), Leunissen and Thijssen (22), and Ludwig et al. (23), and urinary organic acids by Knights et al. (24), Burlingame et al. (25) and others. It is obvious that the separation of these mixtures on capillary columns is greatly superior to those obtained with packed columns.

Recent work by Molnar and Horvath (26) and others indicates that high pressure liquid chromatography (HPLC) also gives excellent resolution and instruments with HPLC coupled to the mass spectrometer will certainly have to be considered for metabolic profiling work.

Excellent reviews are available on metabolic profiling analysis and other applications of GC-MS in clinical chemistry (27-32).

My own work in this field began about 6 years ago with the premise that the computer could utilize gas chromatographic retention behavior and mass spectral data for the simultaneous identification of all of the constituents of complex mixtures of urinary organic acids and for the estimation of the relative amounts of each of the constituents. Similar ideas have been advanced by Smith et al. (33) for the organic acids fraction, by Nau and Biemann for drugs and oligopeptides (34), and by Sjövall et al. for analyses of steroids (35).

The objectives of our project are as follows:

1. Development of a GC-MS-COM system for qualitative identification and quantitative estimation of the components of complex mixtures from physiological fluids,
2. Evaluation of the method with the organic acids fraction of normal and pathological human urine,
3. Development of statistical tests of significance and reporting methods,
4. Routine use in clinical laboratory diagnoses of inborn errors of metabolism, early diagnosis, and for studies of biochemical mechanisms.

While tests of the system have been performed largely with the organic acids fraction from urine of reference subjects and patients with several kinds of disease, the method itself should be general and therefore useful with any mixture of compounds. The remainder of this presentation will be devoted to the GC methodology used to separate the organic acids, the computer processing algorithms involved in the analysis of GC-MS data, and evaluation of the system with urinary organic acids. Statistical analyses of the data are currently under active investigation by us and in several other laboratories. I shall not be able to discuss the current status of this aspect of the problem.

There are several sources of variation in metabolic profiles, some of which must be minimized so that standard deviations from the mean for a particular group will not be distorted. The effects of diet and drugs certainly cannot be overlooked but samples can be selected so as to minimize the effects of these two variables. Diurnal variations can be controlled in the same way but other cyclic factors such as menstrual cycles are not so easily dealt with. Individuality will obviously expand the standard deviation but hopefully disease can be singled out as a variable with some certainty.

Packed columns were chosen for GC of the urinary organic acids because of scan cycle limitations of our instruments when this project was begun. Even with high resolution columns, however, overlaps may be common. It is clear from the comparative scan data of packed and capillary columns (Fig. 1) that scan cycles of less than 1 second will be necessary for complete resolution of substances separated by only a few seconds. It is likely that even with 100,000 theoretical plates, many of the components of this fraction will be incompletely resolved.

We have used two different computer approaches for the identification and quantitative estimation of urinary organic acids, called MSSMET (36-39) and LIANAL (40), and have developed a complementary technique for the determination of "cleaned-up" spectra of unresolved components and of unknowns, called SVIA (41).

The organic acids are isolated and derivatized by a procedure developed by the Hornings (6,7), Thompson and Markey (42), and Chalmers and Watts (43), involving precipitation of sulfate and phosphate from the sample, stabilization of α-keto acids as their oximes, DEAE-Sephadex purification and trimethylsilylation (39). It is a tedious procedure but proved by these groups and by Fitch et al. (44) to be superior to extraction methods.

Because the computer relies on gas chromatographic behavior as an important component in identification, the GC conditions must be standardized. Hydrocarbons are added to the samples for computer conversion of scan number to retention index, or more properly methylene unit values since temperature programming is used. This part of the procedure was first described by Nau and Biemann (34). MSSMET also uses characteristic ions, selected to distinguish a particular compound from other substances eluted at about the same time.

MSSMET analysis, developed largely by Gates and Young (36), involves a reverse library search (45), in which the library contains the following information for each substance: a retention index, a most characteristic (designate) ion and its intensity per unit of mass, and a set of confirming ions and their relative intensities. The presence of each compound in turn is sought at the scan corresponding to its retention index, plus or minus a window of about 8 or 10 scans. Each found peak is evaluated in terms of its retention index and the relative intensities of the confirming ion set, and correlation coefficients are calculated for each parameter. The computer outputs a record of compounds found and the relative amounts of each. Table

I shows a very small part of a summary record of the mean relative levels of urinary acidic metabolites in supposedly healthy subjects. A typical computer summary contains relative levels of about 120 substances (46). Designate ions and retention indices of unknowns were determined either by manual inspection of mass chromatograms or by the computer program SVIA, which I will describe later. Some of the unknowns were subsequently identified by comparisons of mass spectal data with the Markey collection (47) and the retention indices published by Butts (48) and Petersson (49). These substances and others were also identified by high resolution GC-high resolution MS by Burlingame, Kenyon, Lewis and Meili (25).

Table I

Normalized Analytical Concentration Factors for Urinary Organic Acids

Name[b]	RI[c]	DI[d]	Median	Minimum	Maximum
Methylmalonic	1299	247	1.5	0	20.1
UN14	1336	174	0	0	81.0
UN15(2-methylglyceric)	1341	219	41.4	5.2	102
Phosphoric[h]	1360	299	2930	723	10900
Benzoic	1372	179	31.9	0	58.8
UN16(4-deoxyerythronic)[h]	1377	292	883	445	2530
UN17(4-deoxythreonic)[h]	1393	292	1060	266	1740
Succinic	1408	247	112	0	362
UN18	1413	261	26.0	12.2	38.3

[a] Values are uncorrected concentration factors, normalized to the sum of all but the most intense peaks (46).
[b] Common name is in parentheses.
[c] Retention index on 5% OV-17.
[d] Designate ion used for quantitation by MSSMET (36).

The concentration range, observed in these MSSMET data, is very large. A minimum useful dynamic range of at least 2,000 is necessary for analysis of the urinary organic acids. Many of the substances, found in some but not all urines, were trace constituents whose levels were just at the threshold of instrument sensitivity. An order of magnitude improvement in sensitivity and linear dynamic range would be useful, at least with this biological mixture.

Comparisons were made of the absolute concentrations, normalized to creatinine content, of some of the urinary organic acids with literature values for these substances. The agreement was generally very good (46).

I have chosen three examples of MSSMET results with abnormal urines. The first is a case of alcaptonuria, an inborn error of tyrosine metabolism. In this disorder, deficiency of homogentisic acid oxidase characteristically causes a pronounced elevation in the level of excreted homogentisic acid, which is readily observed in the metabolic profile in Fig. 2. The second example is neuroblastoma, in which a malignancy of neural crest cells causes an overproduction of dopamine or norepinephrine, or both, and is expressed by an elevation of the urinary levels of homovanillic and

vanilmandelic acids (Fig. 3). The abnormal features of the metabolic profile in this case are not nearly as readily deduced by visual inspection of the chromatogram. The third example is juvenile diabetes (Fig. 4). The MSSMET data for significantly different relative levels of some substances in these urines, as compared with mean relative levels in reference subjects, are shown in Table II.

Table II

Normalized MSSMET Values of Selected Organic Acids[1]

Subject	Homo-vanillic	Vanil-mandelic	Caffeic	Homo-gentisic	2-methyl-glyceric	3-deoxy-tetronic	Lactic
Control	157.	421.	0.0	13.7	298.	178.	297.
Neuro-blastoma	241.	1580.	122.	17.3	23.6	78.	146.
Juvenile Diabetes	15.	50.	0.0	0.0	611.	2830.	1960.
Alcaptonuria	0.0	82.	2.	3580.	56.	99.	130.

[1]Statistically distinguishing compounds are underlined.

To summarize, MSSMET has provided reliable identifications, it is performed on some 750 scans with greater speed than forward library search techniques because the search is directed to only small portions of the data set for each compound, the library is readily exported to other laboratories since MSSMET does not rely on reproducibility of an entire mass spectrum in a certain fixed pattern of intensities, and raw data are stored on magnetic tape so that reruns are possible when additional compounds have been added to the library. An obvious disadvantage is that MSSMET is oblivious to the presence of substances that are not in the library - this is a serious shortcoming when the abnormality sought may be the presence of an unusual compound.

To overcome this deficiency, another kind of analysis of the GC-MS data set is necessary. It involves the determination of "cleaned-up" mass spectra from GC-MS data and analysis of their GC peak profiles. Biller and Biemann (50) described an approach in which all mass chromatograms are inspected by the computer for ions which have coincident maximum intensities at the same or adjacent scans. A plot of these m/e values and their intensities was called a reconstructed mass spectrum. It does not deal adequately with situations in which ions of low intensity occur in a peak adjacent to another substance with intense ions at the same m/e value. Dromey *et al*. (51) have described an alternative but similar procedure of analysis, based on the detection of unique mass chromatograms of a substance, derivation from them of a tabular model of the GC peak shape, and use of these models to separate unresolved mass chromatograms into their components. It uses a subset of the ions in the spectra and provides "cleaned-up" spectra with background removed and corrected for time distortions resulting from the finite time required for a scan, during which

sample concentration may change. The third approach (41) was developed in my laboratory by Blaisdell. The program is called SVIA, for singular value and invariant analysis.

Briefly, a GC-MS data matrix consisting of 6 to 12 scans of all masses from m/e 50 to 550 are analyzed by singular value analysis for information about the number of substances in the mixture. Two orthogonal vector bases are obtained, the proper invariant linear combination of which gives "cleaned-up" mass spectra and GC peak profiles. The six highest points of each GC peak profile are fitted by least squares to a fourth degree polynomial in the scan number, providing GC peak maxima to a fraction of a scan. The total process requires a few seconds for each matrix of 6 to 12 scans and hence requires five or ten minutes for an entire run of 750 spectra.

In Fig. 5 the peak maxima and intensities at the maxima are given for 4 components of an unresolved mixture, observed about 5 minutes after injection of the TMSi derivatives of a mixture of urinary organic acids. The peaks were located by SVIA at scans 80.6, 81.3, 82.7 and 84.5. The "cleaned-up" mass spectrum of the component at scan 82.7 was identical with that in the Markey collection (47) of TMSi glycolate, as shown in Fig. 6. The other components were phenol, pyridol, and an unknown. Fig. 7 shows the "cleaned-up" mass spectrum of a hydroxymethylfuroic acid derivative, as compared with the spectrum in the Markey collection (47). Its peak maximum was at a scan later in the run where 8 substances occurred at measurable concentrations. The strong ions of TMSi pyroglutamate at m/e 156, 230 and 258 were completely removed, even though pyroglutamic acid was 2.7 times more concentrated in the urine sample and its peak was only 1.3 scans (5 seconds) away.

Analysis of an entire run by SVIA generated the "cleaned-up" mass spectra of 86 substances, one of which represented less than one ten thousandth of the total level of all constitutents in the mixture. These analyses were used to add data for about 50 unknowns to the MSSMET library.

Finally, I would like to discuss another approach for the automated analysis of a GC-MS data set for the levels of library substances, called LIANAL. It has the advantage over MSSMET that it indicates the maxima and approximate levels of substances that are not in the library. The procedure is illustrated with a region of a run of urinary organic acids that is deceptively simple when inspected as total ion current (Fig. 8). This region, from scan 330 to 365, is about 2.5 minutes long and occurs near the middle of the run. MSSMET analysis of this region with a complete library of knowns and unknowns, determined by the method of SVIA, is illustrated in Fig. 9. As is evident from these mass chromatograms of MSSMET designate ions, approximately 15 compounds are in fact eluted from the GC column in this region. The peaks of m/e 284 and m/e 363 were used in Fig. 1 to illustrate theoretical plate requirements for complete resolution by capillary GC.

LIANAL, conceived and written by Blaisdell (40), is a reverse library search in the sense that use is made of a data matrix of the complete library spectra of compounds with retention indices below and above that of

a scan from the GC-MS data set. Computer least squares methods are used to fit each scan from the data set as a linear combination of the library spectra in the queue. That is, the program solves the least squares problem $D(M,n) = C(K,n)S(M,K)$, where S is the matrix of library spectra in the queue, with up to K components; C is the relative concentration of each substance whose mass spectrum is in the queue; D is the data spectrum and M is the number of masses recorded. The least squares problem was solved by the common normal equation method with double precision inversion of the matrix of coefficients, pivoting with both row and column interchanges (40).

A beautiful aspect of LIANAL is that root mean square values of the residuals of the least squares fits provide a misfit plot of substances whose mass spectra are not in the library. Fig. 10 shows the LIANAL analysis of the same region from scan 330 to 365, using a library of nine commercially available substances with retention indices in this region. The asterisks show the misfit plot, indicating the presence of unknowns at scans 333, 338, 349 and 355. Inspection of the raw data matrix revealed the presence in moderate to high concentrations of eight substances whose spectra were not in the library. The mass spectra of these eight substances were determined by SVIA, as previously described, and were added to the library. Fig. 11 shows a plot of the new LIANAL analysis with the expanded library of sixteen substances. The quality of the GC peak profiles has improved and new peaks appear which reflect the additional library spectra. There is still a residual in the misfit plot at scan 355, which lies directly under the GC peak maximum of substance 6, pyroglutamic acid. Inspection of the library mass spectrum of pyroglutamate revealed that it was of poor quality, corrupted by ions of an unknown contaminant. A new mass spectrum of pyroglutamate was substituted in the library and LIANAL analysis a third time gave a smooth residual plot, except for a minor discrepancy at scan 354 which was the result of a blunder value in the raw data.

Comparison of MSSMET and LIANAL analyses of the same urine samples shows a very high correlation of the results (52). Direct comparison of raw data from the two methods (Table III) is impossible because one method gives a relative concentration derived from the integrated intensity of a single ion, for each substance, over the GC peak and the other method gives the sum of the ion intensities of all ions for a compound at its GC peak maximum. Normalization of the data, as a percent of some added internal standard or to a subset of the total, does not improve the comparability of the data, but the ratios of the MSSMET values for two urines should be exactly the same as the ratios of LIANAL values for the same two urines. Table IV shows these ratios for a few of the substances and indicates a high correlation of the two sets of data.

The levels of urinary acids have been determined in several other laboratories by GC (42,53-57) and GC-MS (44) methods. Comparison of these results with the relative levels obtained by MSSMET and LIANAL is extremely difficult at present, since different procedures were used and most of the

data are reported in terms of relative concentration. Such intralaboratory comparisons of various methodologies are much needed.

Table III

COMPARISON OF TWO METHODS OF LIBRARY SEARCH FOR QUANTITATIVE METABOLIC PROFILE ANALYSIS OF HUMAN URINARY ACIDS.

		RAW VALUES*			
		RUN A		RUN B	
RI	IDENTIFICATION	MSSMET	LIANAL	MSSMET	LIANAL
1078	α-hydroxyisobutyric	0.38	0.27	2.66	2.34
1101	lactic	1.96	3.83	9.99	30.80
1223	UN8	3.98	1.40	91.20	51.00
1349	phosphoric	102.00	39.80	183.00	96.40
1279	levulinic	0.0557	0.0580	0.526	0.70
1436	nicotinic	0.138	0.0428	0.295	0.175
1673	pyroglutamic	34.70	11.80	44.90	27.30
1874	citric	46.20	78.30	39.40	91.50
2040	hydrocaffeic	0.259	0.666	0.515	25.70

*Areas of designate ion intensities over GC peak for MSSMET; sum of ion intensities at GC maxima for LIANAL.

Table IV

COMPARISON OF TWO METHODS OF LIBRARY SEARCH FOR QUANTITATIVE METABOLIC PROFILE ANALYSIS OF HUMAN URINARY ACIDS

		RATIO OF NORMALIZED VALUES*	
RI	IDENTIFICATION	MSSMET	LIANAL
1078	α-hydroxyisobutyric	3.72	3.03
1101	lactic	2.69	2.83
1223	UN8	12.1	12.8
1349	phosphoric	0.95	0.85
1279	levulinic	4.94	4.20
1436	nicotinic	1.13	1.44
1673	pyroglutamic	0.68	0.82
1874	citric	0.45	0.41
2040	hydrocaffeic	1.05	1.36

*Normalized value for Run B divided by that for Run A

In closing, I would like to draw some conclusions about metabolic profiling. First of all, I would be remiss if I didn't at least mention that other attractive methods of analysis are under active investigation. Nonchromatographic procedures such as chemical ionization analysis during temperature programmed elution of direct probe samples have been examined with a single stage mass spectrometer by Issachar and Yinon (58), and preliminary tests of a tandom quadrupole mass spectrometer have been reported by Enke and Yost (59). Similarly, such samples could be analyzed by field ionization, as proposed by Anbar and Aberth (60) and presented in a poster session at this meeting. Cooks has been an advocate of direct analysis of mixed samples by MIKES (61) and, finally, Muezelaar and his colleagues have done elegant work on the analysis of mixtures by pyrolysis mass spectrometry (62). These alternatives will probably have some shortcomings in terms of the concentration range that can be dealt with, but it will be interesting to compare results by these procedures with those that can be achieved with GC-MS procedures for metabolic profiling. I have described two such methods of analysis, MSSMET and LIANAL, that provide quantitative data from mass spectral data. Smith et al. have described a similarly automated procedure (33), based on a series of programs that provides "cleaned-up" spectra, carries out library search on the basis of retention indices and mass spectra with a historical library, and calculates relative concentrations of each found component. By whatever procedure, Stanford's HISLIB program, MSSMET or LIANAL, quantitative metabolic profiling appears to work well and should be applicable to a variety of biomedical problems. The most serious disadvantages at this stage of development are that it is expensive and time consuming. These factors could be alleviated to some extent by the instrument companies, if instruments were designed explicitly for metabolic profiling analysis. Some of the prerequisites of an ideal instrument for metabolic profiling, particularly a linear dynamic range of 5-10,000, are beyond the capabilities of most commercially available systems. Hopefully, modifications could be made to meet this specification with an instrument having a mass range up to about m/e 650, sensitivity down to at least 1 ng using mass chromatography (repetitive scans), resolution of at least 650 (10% valley), insensitivity to high levels of contamination, and a moderate price.

Acknowledgements: I have described several collaborative research projects on metabolic profiling analysis; the results were obtained by an excellent group of colleagues including N. Young, S. Gates, B. Blaisdell, F. Martin, D. DeWitt, J. Andre, N. Dendramis, M. Smisko, J. Harten and C. Aschendel. I am grateful to several clinical colleagues, particularly W. Krivit, D. Bier and R. Hillman, for samples of urine from various patients, to J. Holland for the critical role he has played throughout this work in providing analog and digital expertise for interfaces and computer software, and to D. Byrne for expert assistance in preparing the manuscript. This research has been supported in large part by an NIH grant (RR00480) from the Biotechnology Resources Branch, Division of Research Resources, to the Michigan State

University Mass Spectrometry Facility.

References

1. Williams, R.J. "Individual Metabolic Patterns and Human Disease: An Exploratory Study Utilizing Predominantly Paper Chromatographic Methods," Univ. Texas Publication No. 5109, p. 7, 1951.

2. Armstrong, M.D., Shaw, K.N.F., and Wall, P.E. "The Phenolic Acids of Human Urine," J. Biol. Chem. 218, 293 (1956).

3. Dalgliesh, C.E. "Two-Dimensional Paper Chromatography of Urinary Indoles and Related Substances," Biochem. J. 64, 481 (1956).

4. Watson, J.T., and Biemann, K. "High Resolution Mass Spectra of Compounds Emerging From a Gas Chromatograph," Anal. Chem. 36, 1135 (1964).

5. Ryhage, R. "Use of a Mass Spectrometer as a Detector and Analyzer for Effluents Emerging From High Temperature Gas-Liquid Chromatography Columns," Anal. Chem. 36, 759 (1964).

6. Horning, E.C., and Horning, M.G. "Metabolic Profiles: Gas-Phase Methods for Analysis of Metabolites," Clin. Chem. 17, 802 (1971).

7. Horning, E.C., and Horning, M.G. "Human Metabolic Profiles Obtained by GC and GC/MS," J. Chromatogr. Sci. 9, 129 (1971).

8. Jellum, E., Stokke, O., and Eldjarn, L. "Screening for Metabolic Disorders Using Gas-Liquid Chromatography, Mass Spectrometry, and Computer Technique," Scand. J. Clin. Lab. Invest. 27, 273 (1971).

9. Jellum, E., Kluge, T., Borresen, H.C., Stokke, O., and Eldjarn, L. "Pyroglutamic Aciduria, A New Inborn Error of Metabolism," Scand. J. Clin. Lab. Invest. 26, 327 (1970).

10. Goodman, S.J., Markey, S.P., Moe, P.G., Miles, B.S., and Teng, C.C. "Glutaric Aciduria, A New Disorder of Amino Acid Metabolism," Biochem. Med. 12, 12 (1975).

11. Chalmers, R.A., Lawson, A.M., and Watts, R.W.E. "Studies on the Urinary Acidic Metabolites Excreted by Patients with β-Methylcrotonylglycinuria, Propionicacidemia and Methylmalonicacidemia, Using GLC and MS," Clin. Chim. Acta 52, 43 (1974).

12. Keating, J.P., Feigin, R.D., Tenenbaum, S.M., and Hillman, R.E. "Hyperglycemia with Ketosis Due to a Defect in Isoleucine Metabolism; A Preliminary Report," Pediatrics 50, 890 (1972).

13. Tanaka, K., Budd, M.A., Efron, M.L., and Isselbacher, K.J. "Isovaleric Acidemia, A Genetic Defect of Leucine Metabolism," Proc. Nat. Acad. Sci. U.S. 56, 236 (1966).

14. Gompertz, D., and Draffan, G.H. "Identification of Tiglylglycine in the Urine of a Child with β-Methylcrotonylglycinuria," Clin. Chim. Acta 37, 405 (1972).

15. Wilson, R.W., Wilson, C.M., Gates, S.C., and Higgins, J.V. "α-Ketoadipic Aciduria: A Description of a New Metabolic Error in Lysine-Tryptophan Degradation," Pediatr. Res. 9, 522 (1975).

16. Robinson, A.B., and Pauling, L. "Techniques of Orthomolecular Diagnosis," Clin. Chem. 20, 961 (1974).

17. Lee, K.Y., Nurok, D., and Zlatkis, A. "Combined Headspace and Extraction Technique for Profile Analysis by Capillary Gas Chromatography," J. Chromatogr. 158, 377 (1978).

18. McConnell, M.L., and Novotny, M. "Automated High Resolution Gas Chromatographic System for Recording and Evaluation of Metabolic Profiles," J. Chromatogr. 112, 559 (1975).

19. Luyten, J.A., and Rutten, G.A.F.M. "Analysis of Steroids by High Resolution Gas Liquid Chromatography. Application to Urinary Samples," J. Chromatogr. 91, 393 (1974).

20. Pfaffenberger, C.D., Malinak, L.R., and Horning, E.C. "High Resolution Biomedical Gas Chromatography. Study of Urinary Steroid Metabolite Ratios of Women with Breast Lesions Using Open Tubular Glass Capillary Columns," J. Chromatogr. 158, 313 (1978).

21. Shackleton, C.H.L., and Honour, J.W. "Simultaneous Estimation of Urinary Steroids by Semi-Automated Gas Chromatography. Investigation of Neonatal Infants and Children With Abnormal Steroid Synthesis," Clin. Chem. Acta 69, 267 (1976).

22. Leunissen, W.J.J., and Thijssen, J.H.H. "Quantitative Analysis of Steroid Profiles from Urine by Capillary Gas Chromatography. I. Accuracy and Reproducibility of Sample Preparation," J. Chromatogr. 146, 365 (1978).

23. Ludwig, H., Spiteller, G., Matthaei, D., and Scheler, F. "Profile bei chronischen Erkrankungen. I. Steroid Profil Untersuchungen bei Uramie," J. Chromatogr. 146, 381 (1978).

24. Knights, B.A., Legendre, M., Laseter, J.L., and Storer, J.S. "Use of High Resolution Open Tubular Glass Capillary Columns to Separate Acidic Metabolites in Urine," Clin. Chem. 21, 888 (1975).

25. Burlingame, A.L., Kenyon, C.N., Lewis, S., and Meili, J. "Identification of Urinary Organic Acid Constituents Using High Resolution Gas Chromatography/Real-Time High Resolution Mass Spectrometry," Anal. Chem., in press.

26. Molnar, I., and Horvath, C. "Rapid Separation of Urinary Acids by High Performance Liquid Chromatography," J. Chromatogr. 143, 391 (1977).

27. Scriver, C.R., Clow, C.L., and Lamm, P. "On the Screening, Diagnosis and Investigation of Hereditary Aminoacidopathies," Clin. Biochem. 6, 142 (1973).

28. Lawson, A.M. "The Scope of Mass Spectrometry in Clinical Chemistry," Clin. Chem. 21, 803 (1975).

29. Jellum, E. "Profiling of Human Body Fluids in Healthy and Diseased States Using Gas Chromatography and Mass Spectrometry with Special Reference to Organic Acids," J. Chromatogr.

30. Liebich, H.M. "The Place of Mass Spectrometry in Clinical Chemistry," in Mass Spectrometry and Combined Techniques in Medicine, Clinical Chemistry and Clinical Biochemistry, ed. M. Eggstein and H.M. Liebich, Tubingen, 1977, pp. 1-19.

31. Watts, R.W.E. "Progress in Screening for Inborn Errors of Metabolism," Experientia 34, 143 (1978).

32. Gates, S.C., and Sweeley, C.C. "Quantitative Metabolic Profiling Based on Gas Chromatography," Clin. Chem. 24, 1663 (1978).

33. Smith, D.H., Achenbach, M., Yeager, W.J., Anderson, P.J., Fitch, W.L., and Rindfleisch, T.C. "Quantitative Comparison of Combined Gas Chromatographic/Mass Spectrometric Profiles of Complex Mixtures," Anal. Chem. 49, 1623 (1977).

34. Nau, H., and Biemann, K. "Computer Assisted Assignment of Retention Indices in Gas Chromatography/Mass Spectrometry and Its Application to Mixtures of Biological Origin," Anal. Chem. 46, 426 (1974).

35. Almé, B., Bremmelgaard, A., Sjövall, J., and Thomassen, P. "Analysis of Metabolic Profiles of Bile Acids in Urine Using A Lipophilic Anion Exchanger and Computerized Gas-Liquid Chromatography-Mass Spectrometry," J. Lipid Res. 18, 339 (1977).

36. Sweeley, C.C., Young, N.D., Holland, J.F., and Gates, S.C. "Rapid Computerized Identification of Compounds in Complex Biological Mixtures by Gas Chromatography/Mass Spectrometry," J. Chromatogr. 99, 507 (1974).

37. Sweeley, C.C., Gates, S.C., Thompson, R.H., Harten, J., Dendramis, N., and Holland, J.F. "Techniques for Quantitative Measurements by Mass Spectrometry," in Quantitative Mass Spectrometry in Life Sciences, ed. A.P. DeLeenheer and R.R. Roncucci, Elsevier, Amsterdam, 1977, pp. 29-48.

38. Gates, S.C., Smisko, M., Aschendel, C., Young, N.D., Holland, J.F., and Sweeley, C.C. "Automated Simultaneous Qualitative and Quantitative Analysis of Complex Organic Mixtures with a Gas Chromatography-Mass Spectrometry-Computer System," Anal. Chem. 50, 433 (1978).

39. Gates, S.C., Dendramis, N., and Sweeley, C.C. "Automated Metabolic Profiling of Organic Acids in Human Urine I. Description of Methods," Clin. Chem. 24, 1674 (1978).

40. Blaisdell, B.E., and Sweeley, C.C. "Analysis of Gas Chromatography-Mass Spectrometry Data by Reverse Library Search and the Detection of Substances Not in the Library," J. Chromatogr., in review.

41. Blaisdell, B.E., and Sweeley, C.C. "Determination in Gas Chromatography-Mass Spectrometry Data of Mass Spectra Free of Background and Neighboring Substances Contributions," J. Chromatogr., in review.

42. Thompson, J.A., and Markey, S.P. "Quantitative Metabolic Profiling of Urinary Organic Acids by Gas Chromatography-Mass Spectrometry: Comparison of Isolation Methods," Anal. Chem. 47, 1313 (1975).

43. Chalmers, R.A., and Watts, R.W.E. "The Quantitative Extraction and Gas-Liquid Chromatographic Determination of Organic Acids in Urine," Analyst (London) 97, 958 (1972).

44. Fitch, W.L., Anderson, P.J., and Smith, D.H. "Isolation, Identification and Quantitation of Urinary Organic Acids," J. Chromatogr. 162, 249 (1979).

45. Abramson, F.P. "Automated Identification of Mass Spectra by the Reverse Search," Anal. Chem. 47, 45 (1975).

46. Gates, S.C., Sweeley, C.C., Krivit, W., DeWitt, D., and Blaisdell, B.E. "Automated Metabolic Profiling of Organic Acids in Human Urine. II. Analysis of Urine Samples from "Healthy" Adults, Sick Children, and Children with Neuroblastoma," Clin. Chem. 24, 1680 (1978).

47. Markey, S.P., Urban, W.G., and Levine, S.P. "Mass Spectra of Compounds of Biological Interest,: U.S. Atomic Energy Comm. Rep. No. TID-26553, National Technical Information Service, U.S. Department of Commerce, Springfield, Va.

48. Butts, W.C. "Two-Column Gas Chromatography of Trimethylsilyl Derivatives of Biochemically Significant Compounds," Anal. Biochem. 46, 187 (1972).

49. Petersson, G. "Retention Data in GLC Analysis, Carbohydrate-Related Hydroxy Carboxylic and Dicarboxylic Acids as Trimethylsilyl Derivatives," J. Chromatogr. Sci. 15, 245 (1977).

50. Biller, J.E., and Biemann, K. "Reconstructed Mass Spectra, A Novel Approach for the Utilization of Gas Chromatograph-Mass Spectrometer Data," Analyt. Letters 7, 515 (1974).

51. Dromey, R.G., Stefik, M.J., Rindfleisch, T.C., and Duffield, A.M. "Extraction of Mass Spectra Free of Background and Neighboring Component Contributions from Gas Chromatography/Mass Spectrometry Data," Anal. Chem. 48, 1368 (1976).

52. Blaisdell, B.E., Gates, S.C., Martin, F.E., and Sweeley, C.C. "Comparison of Two Methods of Library Search for the Detection and Determination in the Data Matrix from a GC-MS System of the Substances Present in Complex Mixtures," J. Chromatogr., in review

53. Witten, T.A., Levine, S.P., King, J.O., and Markey, S.P. "Gas Chromatographic-Mass Spectrometric Determination of Urinary Acid Profiles of Normal Young Adults on a Controlled Diet," Clin. Chem. 19, 586 (1973).

54. Björkman, L., McLean, C., and Steen, G. "Organic Acids in Urine from Human Newborns," Clin. Chem. 22, 49 (1976).

55. Chalmers, R.A., Healy, M.J.R., Lawson, A.M., and Watts, R.W.E. "Urinary Organic acids in Man. II. Effects of Individual Variation and Diet on the Urinary Excretion of Acidic Metabolites," Clin. Chem. 22, 1288 (1976).

56. Chalmers, R.A., Healy, M.J.R., Lawson, A.M., Hart, J.T., and Watts, R.W.E. "Urinary Organic Acids in Man. III. Quantitative Ranges and Patterns of Excretion in a Normal Population," Clin. Chem. 22, 1292 (1976).

57. Thompson, J.A., Miles, B.S., and Fennessey, P.V. "Urinary Organic Acids Quantitated by Age Groups in a Healthy Pediatric Population," Clin. Chem. 23, 1734 (1977).

58. Issachar, D., and Yinon, J. "Screening of Organic Acids in Urine by Chemical Ionization Mass Spectrometry," Biomed. Mass Spectrometry 6, 47 (1979).

59. Yost, R., and Enke, C.G. "A Triple Quadrupole Mass Spectrometer for Direct Mixture Analysis and Structure Elucidation," Anal. Chem., in review.

60. Anbar, M., and Aberth, W.H. "Field Ionization Mass Spectrometry: New Tool for the Analytical Chemist," Anal. Chem. 46, 59A (1974).

61. Kondrat, R.W., McCluskey, G.A., and Cooks, R.G. "Multiple Reaction Monitoring in Mass Spectrometry/Mass Spectrometry for Direct Analysis of Complex Mixtures," Anal. Chem. 50, 2017 (1978).

62. Meuzelaar, H.L.C. "Pyrolysis Mass Spectrometry: Prospects for Intralaboratory Standardization," Abstr. 26th Annual Conf. on Mass Spectrometry and Allied Topics, St. Louis, Mo., 1978, p. 29.

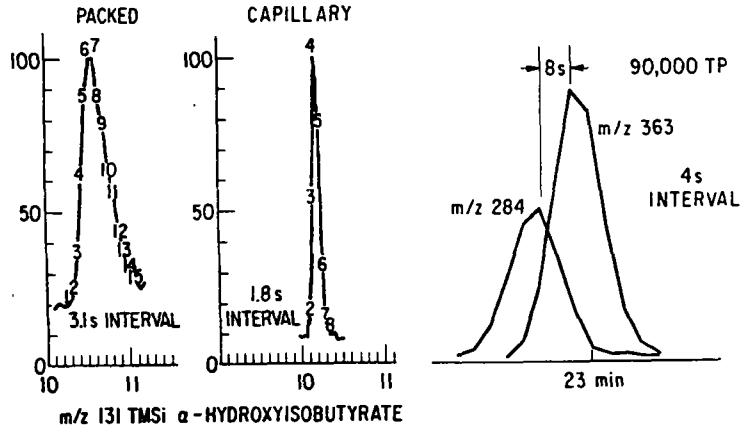


Fig. 1 Comparison of scan cycle and theoretical plate requirements for metabolic profiling by packed column GC-MS versus capillary column GC techniques.

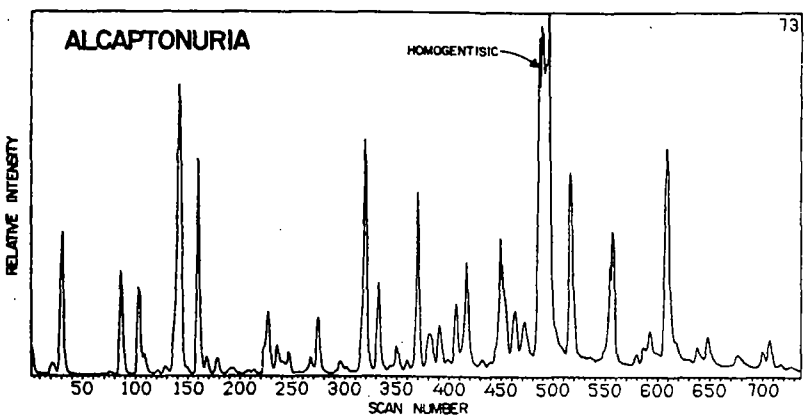


Fig. 2 Metabolic profile of urinary organic acids (TMSi derivatives) from a patient with alcaptonuria.

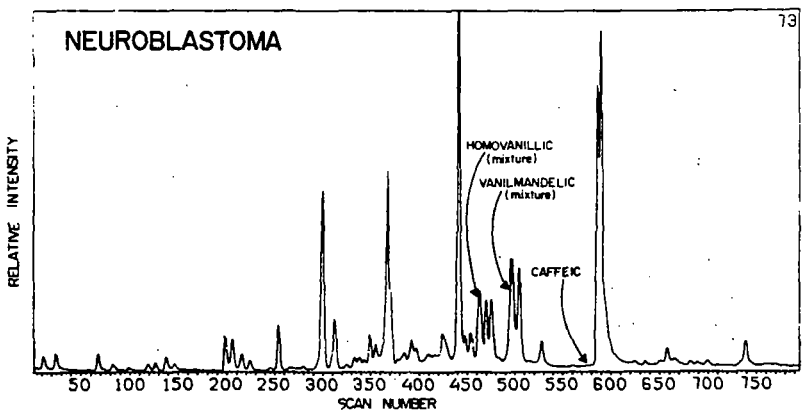


Fig. 3 Metabolic profile of urinary organic acids (TMSi derivatives) from a patient with neuroblastoma.

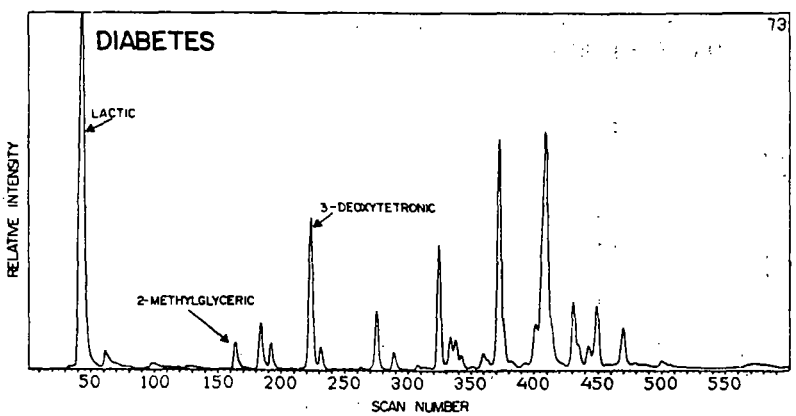


Fig. 4 Metabolic profile of urinary organic acids (TMSi derivatives) from a patient with juvenile diabetes.

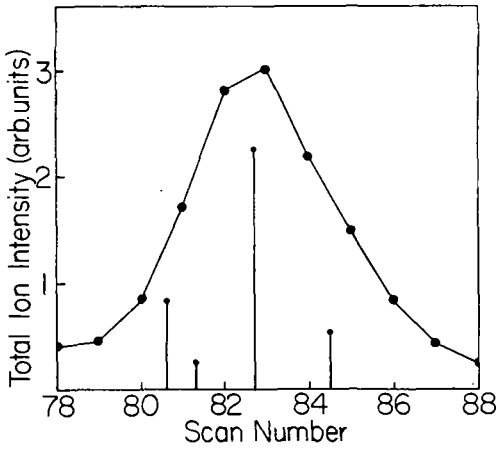


Fig. 5 Total ion intensity of scans 78-88 from a GC-MS run of urinary organic acids (TMSi derivatives), showing exact positions and intensities of four unresolved components (41).

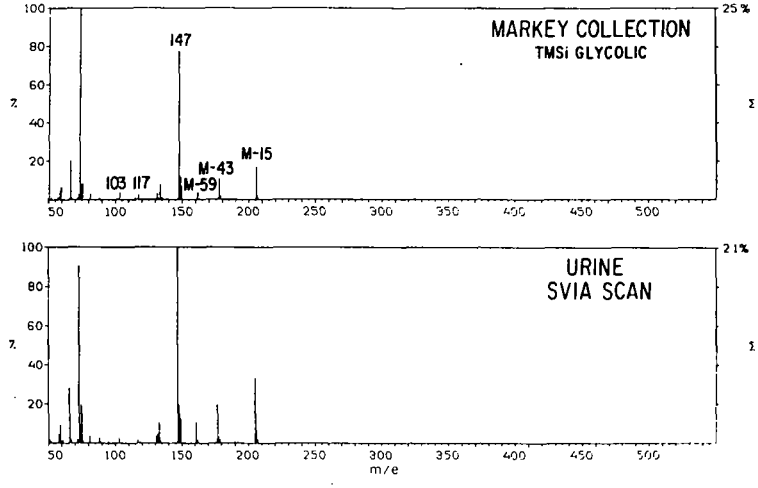


Fig. 6 Comparison of the "cleaned-up" mass spectrum of the component at scan 82.7 (Fig. 5), obtained by the method of SVIA, with the mass spectrum of TMSi glycolate from the Markey collection (47).

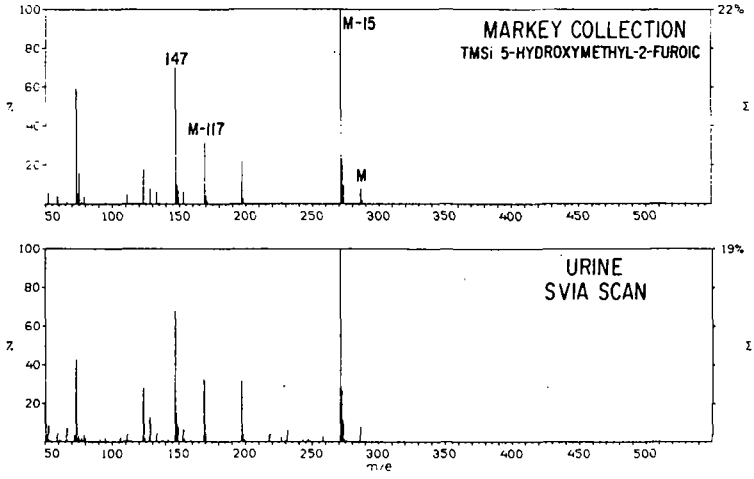


Fig. 7 Comparison of the "cleaned-up" mass spectrum of an unresolved unknown component of urinary organic acids with that of 5-hydroxymethyl-2-furoic acid (TMSi derivative) from the Markey collection (47).

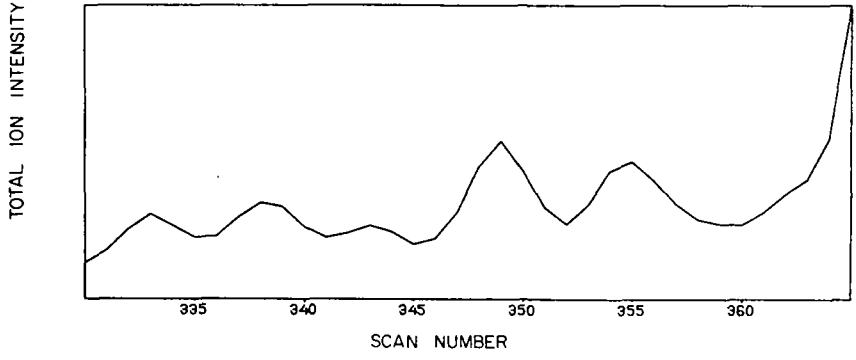


Fig. 8 Total ion intensity plot of a region, from scan 330 to scan 365, of a GC-MS run of urinary organic acids (TMSi derivatives).

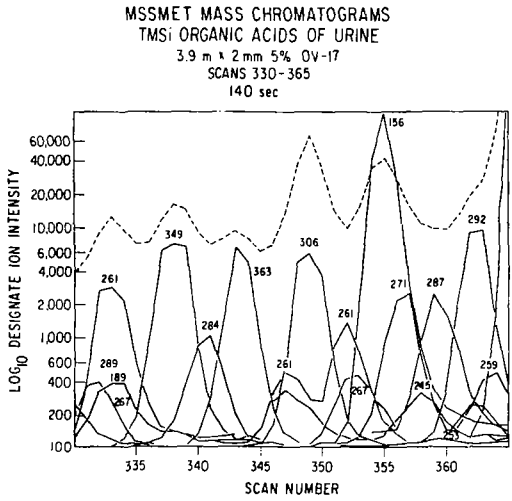


Fig. 9 Mass chromatograms of MSSMET designate ions in a region from scan 330 to scan 365 of a GC-MS run of urinary organic acids (TMSi derivatives).

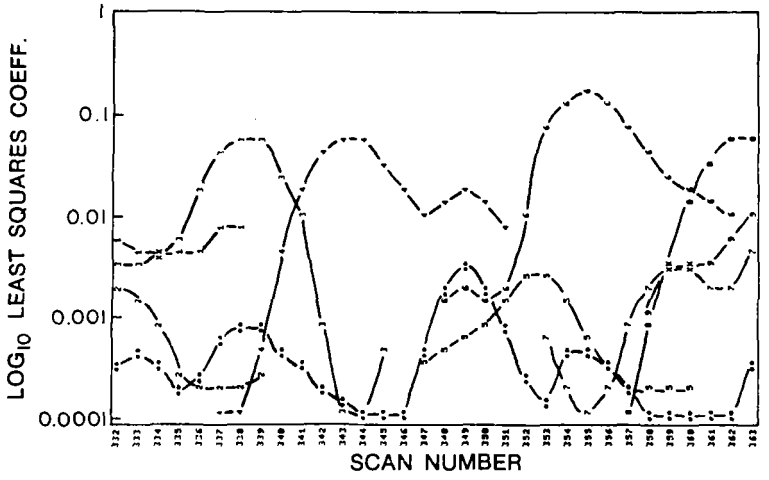


Fig. 10 LIANAL analysis of scans 332 to 363 of a GC-MS run of TMSi urinary organic acids. Above each scan number is plotted the intensities (log scale) of the record numbers of nine library substances and the standard deviations (asterisk plot) of the estimated fit of library substances (40).

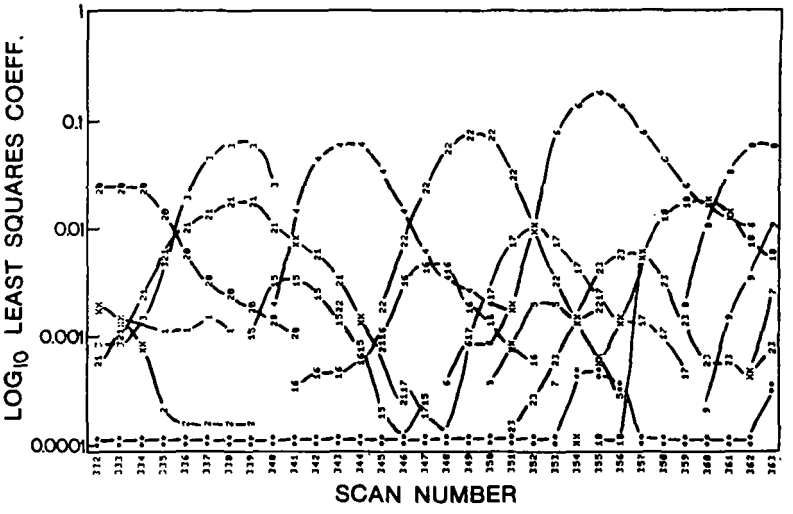


Fig. 11 LIANAL analysis of scans 332 to 363 of a GC-MS run of TMSi urinary organic acids with a library of nine reference substances and eight unknowns, the mass spectra of which were determined by the method of SVIA (comparison with Fig. 10 shows intensity plots of additional compounds and improvement of the asterisk (misfit plot).

PL2 COLLISION DYNAMICS OF FEEBLE BONDS: VAN DER WAALS MOLECULES AND SOLVENT CLUSTERS, DUDLEY R. HERSCHBACH, Dept. of Chem., Harvard Univ., Cambridge, MA 02138

Molecular beam experiments are described which deal with processes akin to liquid-phase reactions, including swapping of molecules between van der Waals clusters, proton transfer, and solvation of ions and electrons. The "solvent clusters" are produced by supersonic expansion through a pinhole nozzle, the reactant or "solute" species is either seeded in the solvent beam or interacts with it as a crossed beam, and the products are detected by mass spectroscopy or laser-induced fluorescence. Among the examples thus far studied are proton transfer reactions; e.g., $HI + (NH_3)_n \rightarrow (NH_4^+I^-)(NH_3)_{n-1}$ with $n = 3 - 13$; this appears to be "driven by solvation" as it is probably energetically forbidden for $n < 2$. Other examples include several electron transfer processes, e.g., $Rb + S_n \rightarrow Rb^+ + S_n^-$, with $S = Cl_2$, SO_2, NO_2, H_2S,...and n up to 8. These processes allow measurement of the electron affinity of S_n as a function of cluster size, under collision conditions which in effect impose a subpicosecond time scale.

MAMOA1 COMPARISON OF SEPARATION EFFICIENCIES OF PROBE MICRODISTILLATION/MASS SPECTROMETRY AND HIGH PERFORMANCE LIQUID CHROMATOGRAPHY, LEONARD R. SCHRONK, RONALD D. GRIGSBY, AND ALAN R. HANKS, Dept. of Biochem. and Biophys., Texas A&M Univ., College Station, TX. 77843

Results are presented to compare the separation efficiency of probe microdistillation/mass spectrometry with that of high performance liquid chromatography on a mixture of model compounds characteristic of nitrogen heterocyclics found in coal. The qualitative and quantitative results from both techniques are compared to each other and to results obtained by a combination of the two methods. Particular attention is focussed on the separation and identification of isomers present in the mixture. A discussion of the applicability of the techniques to the analysis of coal liquids is given.

MAMOA2 QUANTITATIVE ANALYSIS VIA COMPUTERIZED PROBE DISTILLATION/FIELD-IONIZATION MASS SPECTROMETRY, Q. GRINDSTAFF, C. S. HWANG, T. D. MARRIOTT, P. A. BENSON, AND S. E. SCHEPPELE, Dept. of Chem., Oklahoma State University, Stillwater, OK 74074.

The direct introduction probe is ideally suited for the introduction of low volatility and thermally labile compounds into the ion source. Field-ionization mass spectrometry (FI/MS) is an ideal technique for obtaining group-type analyses. Combination of the two techniques requires acquisition of FI/MS as a function of probe temperature. Conventional methods of data acquisition and data reduction preclude routine quantitative analyses using the combined technique. This problem has been circumvented using one computer for the real-time acquisition of probe temperatures and FI/MS and a time-sharing computer for data processing. The accuracy obtained is excellent based upon results for a wide range of samples.

Research supported by the Department of Energy, contract number EX-76-S-01-2537.

MAMOA3 DETECTION OF HETEROCYCLIC COMPOUNDS CONTAINING TWO NITROGEN ATOMS IN A BASE FRACTION SEPARATED FROM ANTHRACENE OIL, R. D. GRIGSBY,[1] L. R. SCHRONK,[1] Q. GRINDSTAFF,[2] And S. E. SCHEPPELE,[2,3] Dept. of Biochem. and Biophys., Texas A&M Univ.,[1] College Station, TX 77843, Dept. of Chem., Oklahoma St. Univ.,[2] Stillwater, OK 74074, and Bartlesville Energy Research Center,[3] Bartlesville, OK 74003

A number of compounds present in a base fraction separated from crude anthracene oil have been found to contain 2 nitrogen atoms. The molecular weights range from about 300 to 400. From high performance liquid chromatography and probe microdistillation/mass spectrometry, the total amount of these components is estimated at 2% by weight in the fraction. High-resolution measurements were made on 2 instruments by introduction with a direct probe and an expansion-volume inlet. The data indicate that the compounds fit into the -30Z series for $C_nH_{2n+z}N_2$ and the -32 series for $C_nH_{2n+z}N_2O$.

MASS SPECTRAL ANALYSIS OF MUTAGENICALLY ACTIVE SUBFRACTIONS FROM COAL LIQUIDS

Bary W. Wilson and Richard A. Pelroy

Departments of Physical Sciences and Biology
Battelle, Pacific Northwest Laboratories
Richland, WA 99352

The solvent refined coal process II (SRC II) is a developing technology, currently in the pilot phase, which produces a liquid fuel. The product discussed here, however, may not necessarily be representative of coal liquefaction fuel products which may eventually be commercially produced using SRC technology. Previous studies have shown that the heavy distillate boiling point cut (HDC) of this fuel is relatively mutagenic compared to petroleum products, other synthetic fuels, complex mixtures, and even some carcinogenic single compounds. Work in this laboratory using fractionation and thin layer chromatography coupled to microbial mutagenesis assays has suggested that primary aromatic amines may be a major contributor to the observed mutagenic activity. Perhaps the most compelling evidence for this conclusion is the loss of mutagenic activity by these materials upon nitrosation. This conclusion is also supported by biochemical evidence based on enzyme activation studies. However, reliable information as to the possible presence and structure of primary aromatic amines in coal and shale derived fossil fuels has not been obtained prior to the work reported here.

Mass spectral analyses were performed on the subfractions of mutagenically active SRC II fractions using both electron impact (EI) and chemical ionization (CI) modes; in the latter, methane was used initially both as the GC carrier and the CI reagent gas. Due to their enhanced chromatographic quality, analyses using a specially prepared SE-52 capillary column were utilized principally to compare GC retention times of various components found in the TLC fractions to those of authentic standards. CI analysis served to confirm molecular ion (M^+) assignments made on the basis of EI spectra.

The methane CI spectra obtained were relatively free from interferences, especially after application of a "background subtract" data system routine, and all compounds reported yielded the characteristic intense $(M+1)^+$ and $(M+29)^+$ ions. Single ion chromatograms were generated for the EI spectra to insure the co-elution of the molecular and major characteristic fragment ions observed in the mass spectra. In most cases, however, the EI spectra, though informative, did not sufficiently differentiate between the primary aromatic amine and the nitrogen heterocycle methyl homolog of the same elemental composition to allow positive identification of the primary amines on the basis of mass spectra alone.

High resolution probe mass spectrometry was particularly useful in confirming the presence of primary amines having two nitrogens such as the amino carbazoles. While confirming the presence of compounds with the proper elemental composition for primary

amines having only one nitrogen, HRMS was of little use in differentiating between these and the corresponding nitrogen heterocycle methyl analogs. Hence, the relative GC retention times of these two types of compounds became of primary importance in their identification as did the use of Argon chemical ionization which enhanced the signal obtained from primary aromatic amines with respect to that of the nitrogen heterocycles.

For the three fractions tested, mutagenic activity was localized in approximately the same TLC regions, with relative mobilities (R_f) ranging from 0.1 to 0.3. GCMS analysis of the TLC regions exhibiting enhanced activity showed that the relative concentrations of primary aromatic amines, as obtained by measuring peak areas of the (M+1) ion in the CI mode, followed essentially the same distribution as the mutagenic activity. Primary aromatic amines identified in the active regions include amino naphthalenes, amino fluorenes, amino carbazoles, amino anthracenes, amino phenanthrenes, amino pyrenes, and amino chrysenes, and their methyl homologs. With the exception of a small amount of amino naphthalene, primary aromatic amines were not found in those TLC regions having undetectable mutagenic activity.

In order to test the premise that primary aromatic amines were important in the mutagenic behavior of the SRC II heavy distillate, a nonmutagenic shale derived crude oil product was analyzed for the presence of such compounds. Figure 1 compares the m/e 143 (M+ for amino naphthalene) and the m/e 193 (M+ for amino anthracene/phenanthrene) traces for SRC II HDC basic fraction and the shale product basic fraction. With the exception of a very small amount of amino naphthalene, no primary aromatic amines were detected in the shale-derived material. In Figure 1, the elution times of the amino anthracene/phenanthrene and the amino naphthalene are indicated by hatched areas in the single ion chromatogram.

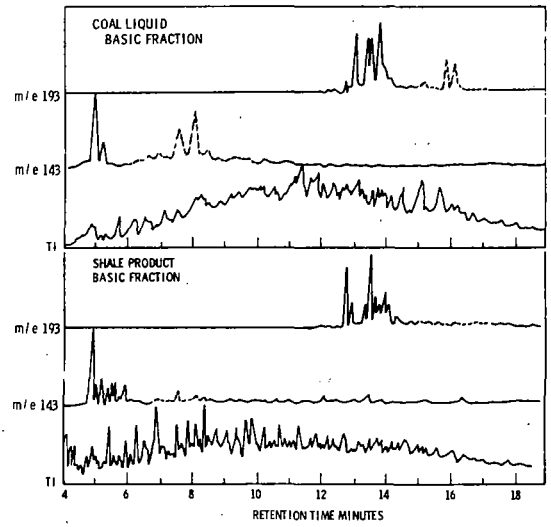


Figure 1

MAM0A6 MASS SPECTROMETRIC ANALYSIS OF NITROGEN HETEROCYCLES IN COAL LIQUEFACTION PRODUCT, C.E.SCHMIDT, Z.PRZYBYLSKI,* H.L.RETCOFSKY AND C.M.WHITE, Pittsburgh Energy Technology Center, 4800 Forbes Ave., Pittsburgh, PA 15213

Nitrogen removal during coal liquefaction most likely proceeds by hydrogenation of the nitrogen-containing ring followed by hydrocracking and subsequent nitrogen elimination in the form of ammonia. Nitrogen bases were separated from coal liquids produced under different process conditions to examine the effect of added catalyst and to investigate the chemistry in the preheater. High resolution mass spectrometry, glass capillary column gas chromatography-mass spectrometry, and gas chromatography with nitrogen specific detection were used to elucidate the nature of nitrogen compounds.

*Visiting scientist from Institute of Petroleum Processing, Krakow, Poland.

THE USE OF MASS SPECTROMETRY IN CHARACTERISING COAL AND PETROLEUM-DERIVED MATERIAL RELEVANT TO COKING ADDITIVES

M.L. Bennett, Broken Hill Prop. Co., Central Research Labs., Shortland, N.S.W., Australia, and
A.A. Herod, National Coal Board, Coal Research Establishment, Stoke Orchard, Cheltenham, Glos., GL52 4RZ, U.K.

Because reserves of prime coking coals are limited, the coal and steel industries in many countries are endeavouring to extend the range of coals which can be used for the production of metallurgical cokes. Many coals when carbonised do not form the fully fused, coherent cokes structure required for blast furnace burden material. The addition of pitches and related materials to such coals, often at quite low levels, can give marked improvements in the abrasion resistance of the resultant cokes. This is believed to be largely due to the additive inducing the plastic phase conditions necessary for a well bonded coke. Solvent refined coals have shown considerable potential as coking additives and are currently being studied in a number of countries.

As part of a study aimed at elucidating the chemical and physical properties required of an effective additive for specific coal blends, three different materials have been heat-treated to temperatures relevant to the plastic stage of coal carbonisation (400-500^{o}C): a high temperature coal tar pitch (AP), of the type commonly used for coal briquetting; a petroleum-derived chemical pitch (CP) and a solvent refined coal (SRC). These materials have many differences in chemical properties, yet they are all effective in improving the properties of coke yielded by certain coal blends. It is relevant, therefore, to try and compare the chemical properties of these materials as they might occur during the plastic phase in coal carbonisation.

The thermal treatment received by a pitch-like additive during carbonisation in a coke oven is clearly difficult to simulate on a laboratory scale for analytical purposes. The most important conditions appear to be a minimum of purge gas, a heating rate relevant to coal-carbonisation and the presence of solid carbonaceous surfaces. For these reasons, techniques such as thermogravimetric analysis or Curie point pyrolysis are considered unsuitable. The Gray-King tar assay apparatus[1] was chosen as the most relevant system readily available and, for this preliminary study, a mixture of pitch or SRC with an isotropic coke was heated at 5^{o}C min^{-1} to a final temperature within the range 400^{o} to 550^{o}C and the residue was rapidly quenched.

Mass spectrometry was used to characterise the more volatile portions of the residues remaining after heat-treatment to 450^{o}C and to compare these with the original pitch or SRC. The analyses were carried out at 10eV in a double beam MS30/DS50 system at a resolution of about 8,000 using the solids injection probe at temperatures up to 350^{o}C.

Comparison of the general features of the MS results indicates that :-

1) The AP residue is similar to the original pitch. It consists predominantly of hydrocarbons; it is highly aromatic and contains a high proportion of unsubstituted components.

2) The CP residue is also similar to the original chemical pitch, as judged by comparison with vacuum distillates of the CP. Over half the intensity of the spectrum observed could be assigned to sulphur compounds, particularly those containing thiophene structures. There were less oxygen and nitrogen compounds, and the hydrocarbons contained fewer rings than in the AP residue. The intensity distributions within nearly all homologous series showed maxima about two carbon atoms higher than those for AP residue and were similar to those found in vacuum distillates of the original pitch. GC/MS confirmed that alkyl substituted dibenzothiophenes and other benzo derivatives were major components in CP distillates.

3) The SRC residue is more complex and includes higher masses than either of the other two residues. It contains more oxygen-containing compounds and perhaps more nitrogen compounds than the AP residue. Over 50% of the intensity of the spectrum was assigned to hydrocarbons. The distribution of hydrocarbon series shows a close similarity to that for the AP residue. The oxygen and nitrogen compounds were also highly aromatic, although a tar fraction collected during heat-treatment was shown by GC/MS to contain significant quantities of phenols. The distribution of intensities within an homologous series showed that alkyl substituted compounds are more common than in the AP residue. However, in the hydrocarbon series the proportion of the first (unsubstituted) members varied from zero to over 50%.

From these MS results and other analyses, it seems likely that heat-treatment of AP and CP pitches up to 450°C under the conditions used caused a gradual but inefficient distillation of typical pitch distillate materials. At 450°C condensation reactions had clearly begun, probably more so in the CP than in the AP pitch, but the medium molecular weight range material (200 to 400) still present in the residue had not undergone significant chemical change. With the SRC, however, significant thermal decomposition has occurred. The compound distribution present is intermediate between that typical of high-temperature coal tar products and those found in coals which have been preheated alone to temperatures near to, and within, the plastic range.

1. "Methods of Analysis of Coal and Coke", Fuel Research Survey Paper No. 44, HMSO, London 1953.

COAL LIQUID CHARACTERIZATION, II. MECHANISM OF BENZYL ETHER PYROLYSIS

T. R. Ashe, R. J. Pancirov, and R. H. Schlosberg

Exxon Research and Engineering Company
Linden, New Jersey 07036

To begin to forge the link of understanding of the thermal behavior of functionalities in coal structures with ultimate product distribution, we have initiated a program of model compound pyrolysis. Since the chief heteroatom both in coal and coal liquids is oxygen, we have looked at the thermal behavior of oxygen-containing organics.

Benzyl ether ($C_{14}H_{14}O$) is a thermally labile compound with functionality such as found in coal precursors, i.e., lignin. Previous workers have shown that in the presence of hydrogen donors such as tetrahydroquinoline, benzyl ether is smoothly and completely converted to toluene and benzyl alcohol.

We shall report our results on the pyrolysis of benzyl ether under carefully controlled simulated liquefaction conditions. Reactions were carried out in a batch autoclave mode using "tubing bombs" in a fluidized sandbath. Reaction temperatures were 450°C and initial pressures of N_2 were approximately 300 psi.

Our data show that at short residence times toluene and benzaldehyde are the major products. At longer reaction times, the benzaldehyde decreases and increased formation of a number of secondary products is observed. Benzaldehyde decomposes to carbon monoxide at a rate equal to or faster than the rate of its formation. Mechanisms to account for these data will be discussed.

In the absence of sufficient hydrogen, growth reactions occur leading to high molecular weight species.

MAM0A9

MONITORING THE PHOTOOXIDATION OF CRUDE OIL BY A GAS CHROMATOGRAPHY-MASS SPECTROMETRY SYSTEM: EXTRACTED ION CURRENT PROFILES OF DIBENZOTHIOPHENES AND THEIR SULFOXIDES

Jayanti R. Patel, S. Wayne Mascarella, Edward B. Overton and John L. Laseter

Center for Bio-Organic Studies, University of New Orleans
New Orleans, Louisiana 70122

INTRODUCTION

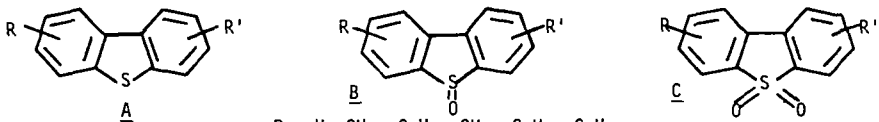
Analytical methods used to detect, monitor and elucidate the photooxidation of crude oil include infrared[1] and ultraviolet[2] spectroscopy. These techniques are suitable for obtaining primary indications of oxygenated products, but can not distinguish single compounds in trace amounts from complex mixtures. High resolution GC-MS is found to be a potential tool for good separation and identification of individual compounds by retention time comparison and mass spectral analyses.

EXPERIMENTAL

GC-MS data were collected using a Varian MAT 311A mass spectrometer interfaced to a Varian SS1ØØ data system. The inlet system consisted of a Varian model 2700 gas chromatograph equipped with glass capillary column coated with SE-52 liquid phase. The photooxidation of crude oil (Arabian medium) in the laboratory was carried out under simulated environmental conditions as previously described[3] for 7 hours. The reaction mixture was separated into organic and aqueous extracts. The organic phase was concentrated and fractionated into hexane, 40% benzene in hexane and methanol fractions. Details of experimental, analytical and instrumental procedures can be found in our previously described work[3].

RESULTS AND DISCUSSION

The analyses of the hexane and the 40% benzene in hexane fractions indicated saturated hydrocarbons and aromatic hydrocarbons, respectively, as anticipated. Since most of the oxidized products are polar in nature, they were expected to elute in the methanol fraction. The GC-MS characterization of the methanol fraction of photooxidized crude oil indicated the presence of sulfur containing heteroaromatic hydrocarbons (A), and their corresponding sulfoxides (B) by mass chromatograms monitored at their molecular ions and major fragment ions. The total ion chromatogram and mass chromatograms monitored at the molecular ions are depicted in Figure 1. Since it is well established[4] that dibenzothiophene-5-oxide loses oxygen upon electron impact, the signals appearing for dibenzothiophenes in the mass spectra of sulfoxides were expected. Representative mass spectra and mass spectral fragmentation patterns for each group of dibenzothiophenes and their sulfoxides were studied. The signals representing the formation of tropyllium type ions for most of the alkylated compounds and the loss of CH_3 group for certain C_2 and C_3 alkylated dibenzothiophenes were observed, but structural confirmation of individual isomers was not possible without reference mass spectral data. The presence of corresponding sulfones (C) of the dibenzothiophenes were detected in trace quantities by molecular ion monitoring.



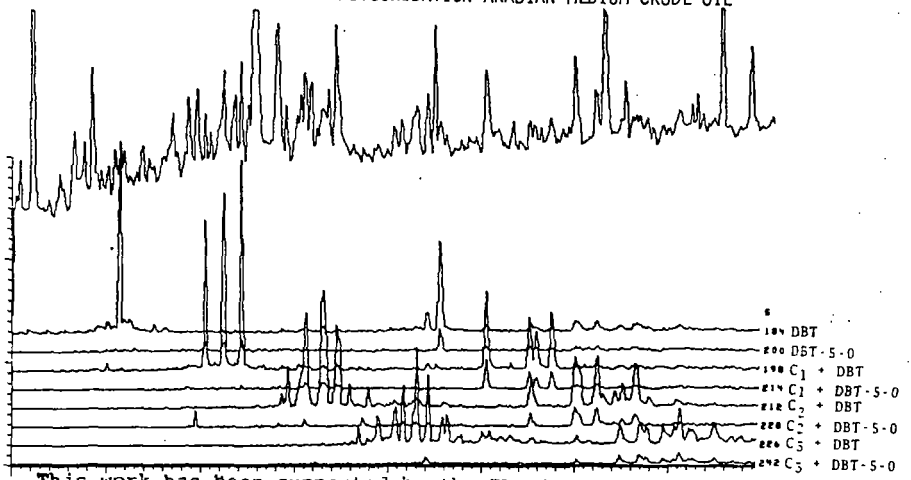
R = H, CH_3, C_2H_5, CH_3, C_3H_7, C_2H_5
R' = H, H , H , CH_3, H , CH_3

Since dibenzothiophenes were eluted in the 40% benzene in hexane fraction, their presence in the methanol fraction was not expected. To gain insight into this anomalous situation, we studied the thermal decomposition of independently[5] synthesized dibenzothiophene-5-oxide in the gas chromatograph[6]. It was found that dibenzothiophene-5-oxide partially decomposed to dibenzothiophene if the temperature of the inlet system was equal to or exceeded 250°C.

Singlet oxygen, a reactive oxidant which is thought to be generated in the environment[7], was formed for the photooxidation of crude oil in this experiment by using molecular oxygen, visible light (tungsten lamp) and perylene, a naturally occurring polycyclic aromatic hydrocarbon, as the photosensitizer[8].

Sulfur containing heteroaromatic petroleum hydrocarbons were found to be very susceptible to an exposure to visible light in the presence of oxygen and photosensitizer. In the case of an actual oil spill, GC-MS monitoring for sulfoxides could be a useful indicator, possibly a quantitative indicator of crude oil weathering . The method discussed here was successfully applied to detect environmentally photooxygenated products in a sample collected from the AMOCO CADIZ oil spill[3]. It has been noted that photooxidation occurring at the surface of the oil films can lead to the production of toxic oxygenated products[9]. The increased toxicity of petroleum hydrocarbons observed following oxidation[10] suggest that photooxidation of spilled oil could increase its toxicity to impacted organisms.

FIGURE 1. THE TOTAL ION CHROMATOGRAM AND SELECTED MASS CHROMATOGRAMS OBTAINED FROM THE METHANOL FRACTION OF PHOTOOXIDATION ARABIAN MEDIUM CRUDE OIL



This work has been supported by the EPA Grant #R804646-01-1 and NOAA Grant #03-78-B01-64.

REFERENCES

1. H.P. Hansen, Marine Chemistry, 3, 183, 1975.
2. J.M. Mjewski and J. O'Brien, Environ. Lett., 7, 145, 1974.
3. a. E.B. Overton, J.R. Patel and J.L. Laseter, in Proceedings of 1979 Oil Spill Conference, EPA, API, USCG, Los Angeles, March 19-22, 1979, 169.
   b. J.R. Patel, E.B. Overton and J.L. Laseter, "Environmental Photooxidation of Dibenzothiophenes Following the Amoco Cadiz Oil Spill," Chemosphere, in press, 1979.
4. S. Meyerson and E.K. Fields, J. Org, Chem., 33, 847, 1968.
5. J. Gilman and D.L. Esmay, J. Am. Chem. Soc. 74, 2021, 1952.
6. G.M. Gurria and G.H. Posner, J. Org. Chem., 38, 2418, 1973.
7. R.A. Zepp, N.L. Wolfe, G.L. Baughman and R.C. Mollis, Nature, 267, 421, 1977.
8. J.R. Patel, G.W. Griffin and J.L. Laseter, "Reaction of Polycyclic Aromatic hydrocarbons with naturally ocurring singlet oxygen: Photooxidation of Phenanthrene" 34th ACS Southwest Regional Meeting, Corpus Cristi, Texas, Nov. 29-Dec.1, 1978, Abstract #27.
9. R.A. Larson, L.L. Hunt and D.W. Blankenship, Environ. Sci. Technol., 11, 492, 1977.
10. a. A. Scheier, D. Gominger, Bull. Environ. Contam. Toxicol., 16, 595, 1976.
    b. J.C. Lacaze and O. Villendon de Naide, Mar. Pollut. Bull., 7, 73, 1976.

Since details of this and related work will be published elsewhere, only a brief discussion appears here.

MAMOA10 ANALYSIS OF POLYNUCLEAR AROMATIC HYDROCARBONS IN COKE OVEN EFFLUENTS, ROBERT G. BEIMER, Dept. of Chem., TRW, One Space Park, 01-2020, Redondo Beach, CA 90278

Polynuclear aromatic hydrocarbons (PAH, also referred to as polycyclic organic matter (POM), are suspected of being serious health hazards since some of the individual compounds are known carcinogens. This class of compounds condense on particulate matter and can be inhaled into the lungs or contacted with the skin. This study was directed at determining the type and amount of PAH compounds emitted from the coking process. Samples were taken in the working area around a coke oven and analyzed by GC/MS. The results reveal significant concentrations of PAH's in the ambient air and some of the species identified are known carcinogens.

A COMPARISON OF THE COMPOSITION OF EASTERN AND WESTERN SHALE OIL SAMPLES AS DETERMINED BY LOW ELECTRON ENERGY, CAPILLARY GC-MS-DS

R. O. Yelton,
T. O. Tiernan and M. L. Taylor

The Brehm Laboratory and Department of Chemistry
Wright State University
Dayton, Ohio 45435

V. M. Franchetti and C. Kinard
Mound Facility, Monsanto Research Corporation
Miamisburg, Ohio 45342

We have investigated the compositions of the paraffin-naphthene fractions of a retorted Eastern (Effingham County, Illinois) and a Western (Parachute Creek) shale sample. The objectives included characterization of the Eastern sample using GC-MS techniques to derive geochemical data. Comparison with the well-characterized and oil-rich Western shale was also made. Additionally, correlation of existing gas chromatographic techniques with mass spectral analysis was desirable to evaluate techniques which are used to characterize these extremely complicated organic mixtures. Samples were run on a Kratos MS-25 GC-MS-DS instrument. The use of low energy electron ionization provided a more efficient means of detecting the C_nH_{2n+2} molecular ions and matching them with chromatographic peaks. Relative distributions and amounts of acyclic, monocyclic and dicyclic components, including various isoprenoid and terpenoid compounds were monitored utilizing computer generated selected ion mass chromatograms.

In general, the Western shale sample contained a higher carbon number acyclic alkane distribution (C_9-C_{28}) than the Eastern sample (C_9-C_{24}). The Eastern sample indicated a higher degree of unresolved components. However, mass chromatograms have shown that these unresolved portions consisted mainly of N-alkylcyclohexanes characterized by their prominent m/e 83 ion. The Western sample also contained amounts of monocyclic species but were successfully resolved chromatographically. This data implies that traditional packed column techniques which determine the paraffin-naphthene as well as pristane-phytane ratios relating to thermal maturity may be misleading.

Tricyclic diterpanes and pentacyclic triterpanes are very important biological markers. These compounds are more commonly found in higher plants, though the hopane series is abundant in bacteria and blue-green algae. Identification of these components in kerogen-derived oils yields information as to the nature of the depositional material and environment. The presence of these cyclic terpanes was confirmed in both samples by m/e 191 chromatograms. The presence of such components was indicated in each sample. However, mass spectra of the two most abundant chromatographic peaks in the Eastern shale oil did not yield sufficient mass spectral information to provide absolute identification of the particular terpane, though a tentative molecular ion of 412 may be indicative of a hopane derived species.

A prominent component peak of the Western shale sample enhanced by a m/e 125 selected ion chromatogram indicating the presence of tetra alkyl substituted isoprenoids, seems to have arisen from a B-carotene precursor (molecular ion 266). The m/e 125 chromatogram in the Eastern sample yielded little information.

Our data indicate compositional differences in the ratios of paraffin naphthene compounds as well as the types and amounts of other biological markers in the two shales. This is not surprising as their geological histories are exceedingly different. Nevertheless, our study has confirmed that some geochemical individuality is maintained through the breakdown of kerogen during the retort process. Samples such as the ones studied, consisting of a complex mixture of organic components are best characterized using GC-MS-DS techniques, rather than relying on gas chromatographic techniques alone.

GC-HIGH RESOLUTION-MS-C AS A NITROGEN COMPOUND SPECIFIC DETECTOR

By Emilio J. Gallegos
Chevron Research Company, Richmond, California 94802

A B S T R A C T

Introduction

Nitrogen compounds in gasoline and in refining processes are considered bad actors, i.e., they are thought to be the cause of gum formation in engine pistons, valves, and rings. They are also known to be catalyst poisons in refining processes. The use of ever-heavier ends of petroleum and, in the near future, the refining of coal and shale oils will tend to increase the importance of isolating and identifying nitrogen components both in the finished product and in the feedstock to the various processes. The method that is described here is an alternative way of nitrogen compound specific detection to that of using NP, thermionic, or alkali flame detectors which use a rhubidium silica glass bead or something similar. These beads, in a plasma, detect specifically organically coupled nitrogen, phosphorus, and sulfur. The mechanims of operation is not that well understood (B. Kolb, et al[1] and D. K. Albert[2]). An alternative way, which is described here, is to look at the CH_2N+ ion and the NO+ ion using medium resolution mass spectroscopy. This will allow detection of all nitrogen-containing compounds with the exception of ammonia.

Figure 1 shows all possible fragment ions at nominal mass m/e 28. These are CO^+, N_2^+, CH_2N^+, $CC^{13}H^{3+}$, and $C_2H_4^+$ at about 5000 resolutions. Any one of these ions can be monitored without interference from the other ions present at that mass.

Figure 2 shows the fragment ions possible after m/e 30. These are NO^+, $C^{13}HO^+$, CH_2O^+, and $C_2H_5^+$. This profile was obtained using a mixture of nitrobenzene and acetone. The question that we might ask next is what sort of sensitivity is possible using these minor fragment ions in the mass spectrum of a variety of nitrogen compounds?, i.e., what is the percent of total ionization of the CH_2N^+ for the various nitrogen-containing compounds?

Nitrogen-containing compounds expected to be found in a gasoline range sample on the average show that CH_2N^+ fragment ions make up 1.5% of the total ionization, but the values vary in this sampling of 21 components from about 30:1 in sensitivity. However, if we throw out the substituted indols, the sensitivity ranges is only 2:1.

The following figures will show that the sensitivity limit using this technique is about 10 ppm:

Figure 3 shows the CH_2N^+ and $C_2H_4^+$ mass chromatograms of a standard 21 nitrogen compound mix. This was done using a squalane-coated 1000-ft capillary column coupled to our high resolution MS-9 mass spectrometer.

Multiple ion detection for specific fragment ions was also done on six coals. An example is shown in Figure 4, a Loveridge carboniferous coal. Specific ions at m/e 28 are the CO^+, CH_2N^+, and the hydrocarbon $C_2H_4^+$. The most interesting results of this probe on the six coals is that the nitrogen-containing moieties are released from the coal at about 100°C earlier than the bulk of the hydrocarbons or the CO-containing components. This should be of interest to processing people.

Conclusions

Obviously a high resolution, i.e., around 500 mass, spectrometer coupled to GC can be used to monitor any combination of elements, such as the CO_2^+, CH_2S^+ for sulfur compounds which has been done,[3] dinitrogen compounds, or any elemental combination which can be separated at low mass. So this system is a multielement specific detector.

References

1. Kolb, B.; Auer, M; and Pospisil, P.; J. of Chr. Sc. 15, 53-63, February 1977.
2. Albert, D. K., Anal. Chem. 50, 1822-1829, November 1978.
3. Gallegos, E. J., Anal. Chem. 47, 1150-1154, June 1975.

:kab

Paper #MAMOA13

Application of GC/FIMS to Hydrocarbon Analysis

A.M. Hogg, Dept. of Chemistry, J.D. Payzant, I. Rubinstein and O.P. Strausz, Hydrocarbon Research Centre, University of Alberta, Edmonton, Alberta, Canada T6G 2E1

The analysis of complex mixtures of hydrocarbons has been pursued in this laboratory for some time using GC/EIMS/DS techniques. Single ion cross scans (mass fragmentograms) have provided the most useful output but the lack of abundant molecular ions under EI is a formidable limitation. Later an FI source in conjunction with a heated batch inlet was used to provide molecular weight profiles for the hydrocarbon mixtures.[1]

We have now coupled a GC to the field ionization mass spectrometer and are applying it to the analysis of hydrocarbon mixtures. The GC employed was a Varian 1200 fitted with a 2.15 m x 3 mm S.S. column packed with 3% OV-101. Helium flow was 45 ml min^{-1}, injection temperature 350° and the oven programmed from 60° to 350° at 2° min^{-1}. Approximately 4 mg of sample was employed for each run. The column exit was coupled to the modified[2] AEI MS-9 mass spectrometer by a heated capillary transfer line and a Watson-Bieman type ceramic separator. All internal surfaces were heated to 250° or over. The magnet cycle time was 11 sec and data was acquired with a DS-50S system.

The principle advantage of FI over EI is that for most types of hydrocarbons the molecular ion is the dominant (>90%) ion generated. This greatly simplifies the mass spectra. When two or more compounds co-elute from a GC column, the interpretation of the EI spectra is difficult. However by FI, if the materials have different molecular weights then they appear as separate mass peaks thus simplifying the interpretation.

There are various methods of displaying the GC/FIMS data. In figure 1 is shown the TIC (sum of ion intensities from m/z = 28 to 600 for the thiourea adduct saturated hydrocarbon fraction of Leduc Petroleum in central Alberta. This reproduces the GC that would be observed with a FID detector. Figure 2 shows a display of the molecular ions for the series of monocyclic alkanes present in this fraction. Material of formula C_nH_{2n} has molecular ions at m/z = 140, 154, 168, 182, 196 ... etc. for n = 10, 11, 12, 13, 14, 15 ... etc. Figure 2 is a sequential display of these molecular ion traces. As may be seen a number of homologous series are present.

The only type of hydrocarbon which fragments significantly under FI conditions is the acyclic alkanes (C_nH_{2n+2}). The fragment ions formed (m/z = 29, 43 and 57) correlate with terminal structures of the type ∿R, ⅄R and ⅄⅄R respectively. This is a sensitive measure of the molecular structure and when combined with the formula C_nH_{2n+2} gives valuable information on the structure of the material. No other fragment ions are formed in significant amounts under normal FI conditions. A full report of this work has been submitted for publication.[3]

1. J.D. Payzant, I. Rubinstein, A.M. Hogg and O.P. Strausz, Geochim and Cosmochim Acta (in press).

2. A.M. Hogg and J.D. Payzant, Int. J. Mass. Spec. and Ion Phys., 27, 291 (1978).

3. J.D. Payzant, I. Rubinstein, A.M. Hogg and O.P. Strausz, Anal. Chem. (submitted for publication).

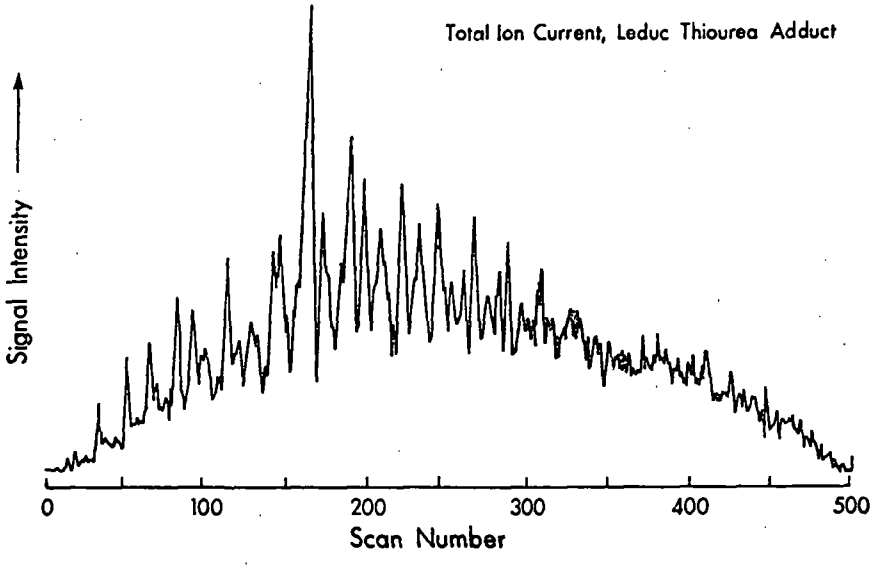


Figure 1.

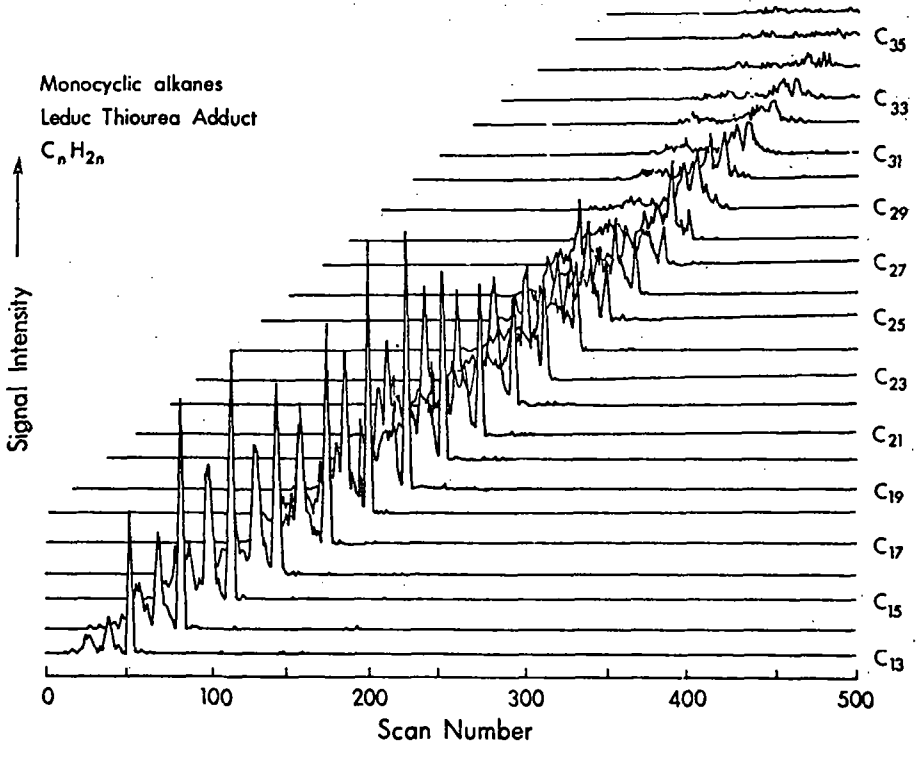


Figure 2.

THE HIGH TEMPERATURE PYROLYSIS OF AROMATIC HYDROCARBONS[a]

Richard D. Smith
Physical Sciences Department
Battelle, Pacific Northwest Laboratory
Richland, Washington 99352

The mechanisms and kinetics for formation of complex hydrocarbon compounds in the pyrolysis of simple fuels are of great interest in the study of combustion processes in addition to the environmental concern with a number of carcinogenic products. While the importance of the intermediates, reactions, and products of the high-temperature pyrolysis of fuels has been recognized, there have been relatively few studies of such high-temperature (>1200°C) pyrolyses. The reasons for this paucity of data are related to the technical problems in carrying out such pyrolyses at high temperature in a meaningful manner, and the requirement of universal detection for a variety of unstable and stable molecules. In the present work, we have used a newly constructed high-temperature Knudsen cell equipped with a gas inlet and modulated molecular beam mass spectrometric detection to analyze the products of toluene pyrolysis. This approach allows a direct examination of the chemistry occurring in the high-temperature region, if the increasing complex mass spectra can be interpreted.

The species effusing from Knudsen cells having 2 mm diameter orifices were examined for toluene pyrolysis at temperatures up to approximately 1900°C for the tungsten and 1400°C for the quartz cells. At low pressures, the residence time of species in this cell is approximately 3×10^{-3} (M/T) s, where M and T are the molecular weight and temperature. Estimates of Knudsen cell pressure suggest that usable results can be obtained for pressures ranging from approximately 10^{-5} torr at the lowest pressures to 10^{-1} torr at the highest pressures. A separate Knudsen cell with a 0.4 mm diameter orifice was used to obtain pressures approximately 20 times higher. Analysis of species flowing from the Knudsen cells utilized low energy electron impact, phase angle spectrometry, and appearance potential measurements. Concentrations of species present in the high-temperature zone have been measured at temperatures up to 1900°C and the effects of pressure have been studied over four orders of magnitude.

Figure 1 gives the concentration profiles for several of the minor species observed in the pyrolysis of toluene at 1280°C in a quartz cell, as a function of pressure (over a range of approximately 5×10^{-5} torr to 0.5 torr). The pyrolysis of toluene has been found to produce a number of higher molecular weight species (including radicals, polycyclic aromatic compounds up to $C_{20}H_{12}$, and polyacetylenes) efficiently at temperatures between 1200°C and 1500°C. At temperatures between 1200°C and 1400°C, C_3H_4, C_4H_2, C_4H_3, C_5H_3, C_5H_5, C_6H_4, C_6H_5, C_7H_5, C_7H_6, and C_7H_7 species were observed to have maxima in their concentrations as a function of pressure, suggesting a role in the formation of higher molecular weight compounds. At higher temperatures, the major products were C_2H_2, C_2H_3, C_2H_4, C_4H_2, C_6H_2, and C_6H_6; species containing even numbers of carbon atoms appear to dominate the reaction products. Figure 2 gives the concentrations (excluding H and H_2) of the major species observed in the pyrolysis of toluene as a function of temperature.

These results are described and discussed in detail in a paper accepted for publication in the Journal of Physical Chemistry, and the study is currently being extended to a series of aromatic hydrocarbons.

[a]This paper is based on work performed under United States Department of Energy Contract EY-76-C-06-1830.

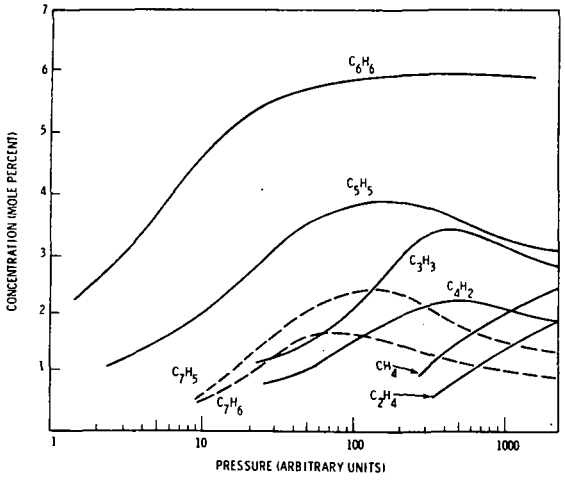


Fig. 1. Concentrations of C_7H_6, C_7H_5, C_6H_6, C_5H_5, C_4H_2, C_3H_3, C_2H_4, and CH_3 in a quartz Knudsen cell at 1280°C for pressures of approximately 5 x 10^{-5} to 5 x 10^{-2} torr.

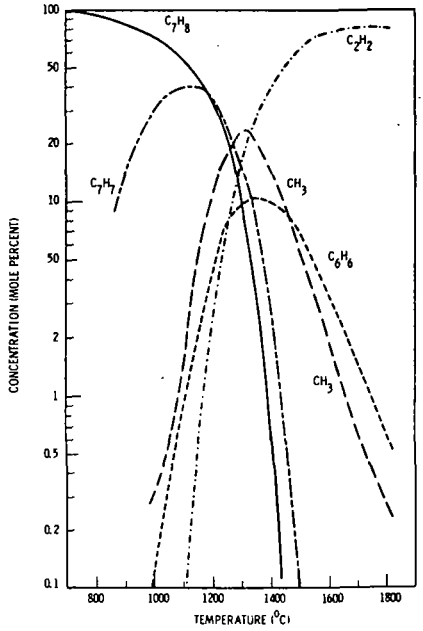


Fig. 2. Concentration of several of the major species (excluding H and H_2) in the pyrolysis of toluene in a tungsten Knudsen cell at approximately 10^{-2} torr.

THE APPLICATION OF MICROFABRICATION TECHNOLOGY TO THE CONSTRUCTION OF FIELD EMISSION IONIZERS

C.A. Spindt
SRI International, Menlo Park, California 94025

Field electron and ion emission have been known as research tools for many years. However, neither has received extensive use except by a few specialized groups employing highly developed technology. This limited usage can be attributed to the technological problems associated with the very high fields (10^7 - 10^8 V/cm) required and the high voltages generally used to achieve these high fields.

The application of microfabrication technology to the construction of field emission devices can reduce the voltage requirements for useful emission to levels that are low enough to prevent, or greatly reduce, the difficulties normally associated with collisions of high energy particles. For example, a 5000-tip array of the type shown in Figure 1 is capable of producing 100 mA of electron emission with less than 200 volts applied across the sandwich structure, and has been shown to be capable of over 10 mA at less than 100 volts at room temperature.

Figure 2 shows the effects of operating the cathode in hydrogen and air up to 1 X 10^{-5} torr. It is apparent that surface changes due to adsorption modify the emission characteristics of the cathode. However, no permanent change took place as a result of the high pressure operation, since the cathode returned to its original performance characteristic after each exposure. It has been determined that oxygen in the air causes the drop in emission during operation at 10^{-5} torr of air. Additional experiments showed that He, Ne, and Ar had no effect up to 10^{-6} torr, and CH_4, H_2S, and H_2O caused the emission to increase by as much as 10X. In all cases the emission returned to the original value when the sample gas was removed from the system, indicating that there was no damage to the emission tips by sputtering. This absence of sputtering damage is the direct result of the low voltage operation that is possible because of the very small distance between the tips and anode film ($\sim$ 0.5 μm). It also accounts for the very long lifetimes that have been obtained when operating in normal ultrahigh vacuum ($\sim 10^{-9}$ torr). Emission levels of 20 μA per tip have been maintained for over 35,000 hours with no change in performance.

The cathodes are fabricated by a combination of standard techniques developed by the semiconductor industry and electron beam lithography and thin film technology developed especially for this purpose. A metal/oxide/semiconductor sandwich structure can be formed by oxidizing a silicon chip and depositing a metal film over the oxide. Holes are then formed in the metal film by coating it with an electron sensitive resist and exposing the resist with a pattern of submicron-diameter spots in the desired configuration: Typically, this is an orthagonal array of spots with 12 to 6 microns between centers, covering an area up to 1 mm in diameter. (A parallel electron-beam exposure system was devised by Westerberg for this purpose[1].) The resist is developed leaving holes where the electrons have impinged on it; holes are etched in the metal film where it is exposed by the pattern of holes in the resist, and the silicon oxide is etched through the holes in the metal film producing a structure as shown in Figure 3a. A grazing angle deposition is then made while rotating the substrate about an axis normal to its surface as shown in Figure 3b. This deposited film is of a material that is selectively etchable with respect to all the other materials used in he structure, and thus can be used as a parting layer for subsequent depositions. When a suitable parting layer has been deposited, deposition is initiated from a metal source oriented to deposit a beam normal to the surface of the substrate as shown in Figure 3c. The depositions are continued until the hole has been completely closed as shown. A metal cone is formed in the hole by the decreasing aperture in the top film that results from the metal depositing on the sides of the hole. The parting layer is then dissolved, releasing the metal deposited on the top surface during the cone formation and revealing the structure shown in Figure 3d and Figure 1. This completes the cathode fabrication process.

Field ionization structures have been fabricated using similar techniques. The most recent of these has been the "volcano" field ionizer[2] structure, which was designed to minimize the voltage required for ionization, minimize the source size for high resolution application, and maximize the efficiency of ionization. The source consists of a tiny hollow cone through which the sample gas flows. Figure 4 is a scanning electron micrograph of the cone or volcano: This tip has a 20 μm OD and about a 15 μm ID through which the sample gas flows, although tips with ODs as small as 5 μm have been made. The volcano is mounted on the end of a tube and centered in an opening of a counterelectrode screen (250 lpi nickel) as shown in Figure 5. Spacing between the volcano rim and the screen is typically 25 μm. After activation, voltages of between 1 and 3 kV produce currents in the

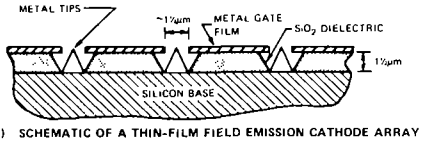
10^{-9}A range (10^{9} ions/sec) with pressures of about 500 microns of easily ionized organics such as toluene behind the volcano.

The fabrication of the device is straight-forward with the exception of the volcano itself[3]. Volcano fabrication begins with the formation of a hole having the desired shape in a suitable substrate. This hole is then used as a mold into which the volcano is cast in thin-film form by vapor deposition (Figure 6). If the thickness of the deposit is less than the radius of the hole, the cast structure will replicate the hole shape without closing it off. The deposited film is then parted from the mold, yielding the completed volcano structure. Applications of the volcano ionizer structure are discussed in other presentations at this conference.[4, 5, 6]

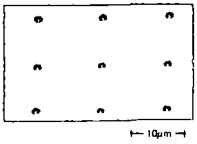
References

1. L.N. Heynick et al., IEEE Trans. Elec. Dev., 22, 400 (1975).
2. W. Aberth and C.A. Spindt, Int'l J. of Mass. Spec. and Ion Phys., 25, 183 (1977).
3. C.A. Spindt, U.S. Patent No. 4,141,405 (February 27, 1979).
4. S. Buttrill et al., 27th Ann. Conf. on Mass. Spec. and Allied Topics, MAMOB3 (1979).
5. W. Aberth et al. 27th Ann. Conf. on Mass. Spec. and Allied Topics, MPMP11 (1979).
6. S. Buttrill and G.A. St. John, 27th Ann. Conf. on Mass Spec. and Allied Topics, FAMP18 (1979).

*Supported in part by NASA-Lewis, Cleveland, O.; JPL, Pasadena, CA; NIH, Bethesda, MD.



(a) SCHEMATIC OF A THIN-FILM FIELD EMISSION CATHODE ARRAY



(b) SEM MICROGRAPH OF AN ARRAY OF FIELD EMISSION TIPS

FIGURE 1 THIN-FILM FIELD-EMITTER ARRAY CATHODE

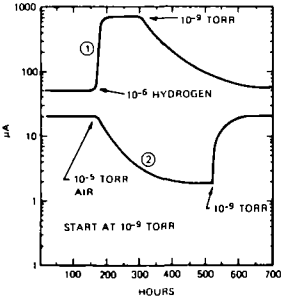


FIGURE 2 THE BEHAVIOR OF CATHODE EMISSION IN 10^{-6} TORR OF H_2 ①, AND 10^{-5} TORR OF AIR ②.

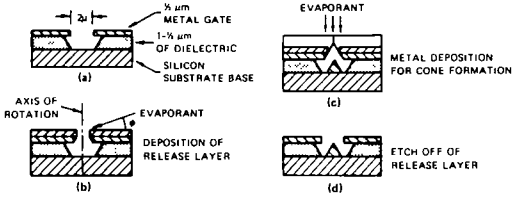


FIGURE 3 THIN-FILM FIELD EMISSION CATHODE FABRICATION

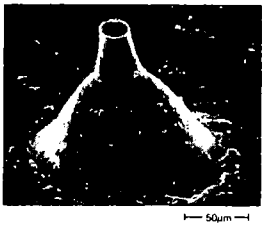


FIGURE 4 VOLCANO FIELD ION SOURCE

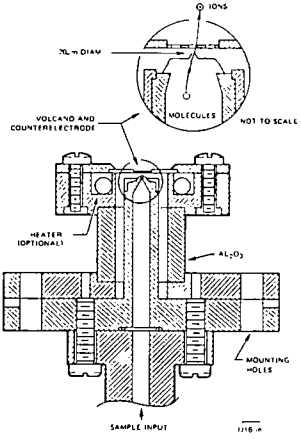


FIGURE 5 CROSS SECTION OF VOLCANO-TYPE FIELD-ION/ELECTRON EMITTER

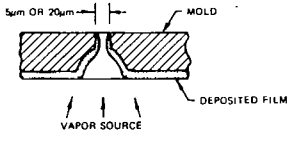


FIGURE 6 VOLCANO FABRICATION

IONIZATION BY PROTON ATTACHMENT, WOODFIN V. LIGON, JR., General Electric Company, Corporate Research and Development, Schenectady, NY 12301

We have observed the production of ion beams from the combination of simple gas phase organic molecules and a substrate bound mineral acid (polyphosphoric acid) under conditions of high field. For most molecules, the ion beams produced consist of protonated molecular ions and cluster ions of the form $(2M+H)^+$. For these molecules the sensitivity of the technique is related to the ease of protonation of the molecule not to its ionization potential. Fragments when observed can generally be attributed to proton induced chemical reactions. Odd electron processes are not observed.

Very weak spectra exhibiting $(M-1)^+$ ions and significant (even electron) fragmentation have recently been obtained for molecules which do not readily accept protons such as alkanes. The spectra observed are very similar to those obtained for the same molecules in methane chemical ionization mass spectrometry. This result suggests that under the influence of high field polyphosphoric acid has a much enhanced pKa and moreover suggests that the ions produced by this technique do not represent the equilibrium situation existing in the solution in the absence of the field. Figure 1 is the spectrum obtained from a mixture of acetone and isopropanol showing $(M+1)^+$ ions and mixed cluster formation. Figure 2 shows a portion of the mass spectrum of kerosene obtained by field ionization and by cation extraction. The alkane peaks at 156, 170, and 184 in the FI spectrum show both addition and elimination of protons in the cation extraction spectrum. Since n-alkanes such as dodecane (m/e 170) are known to show only $(M-1)^+$ ions, this observation suggests that the FI peak at 170 consists of at least two species which are resolved in the cation extraction spectrum.

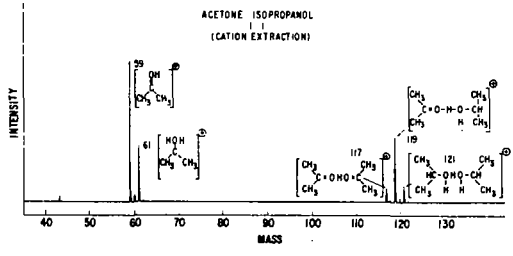


Figure 1

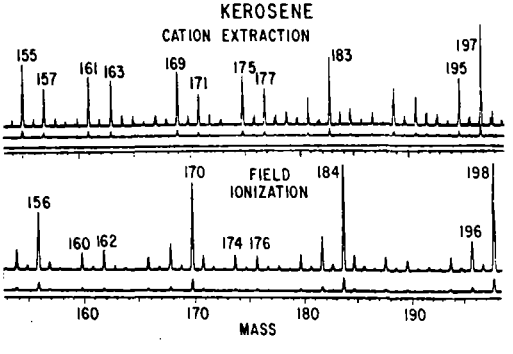


Figure 2

CHARACTERISTICS OF A VOLCANO-STYLE FIELD IONIZATION SOURCE AND MAGNETIC SECTOR MASS SPECTROMETER

S. E. Buttrill, Jr., G. A. St.John, and C. A. Spindt
SRI International, Menlo Park, CA 94025

The volcano-style field ionization source, developed by Spindt,[1] is the most efficient field ionizer known to us. The characteristics of this ion source combined with a quadrupole mass spectrometer have been reported previously.[2] Current versions of the source resemble inverted funnels with throat diameters of 15 to 30 μm. The high ionization efficiency is attributable to two characteristics: (1) the neutral sample molecules must pass through the field ionization region in order to exit the source, and (2) the active field ionization region is very small, which facilitates the focusing and collimation of the ion beam.

We have adapted the volcano source to operate in our 60° magnetic sector mass spectrometer at 5 kV accelerating potential. The ion optics are shown schematically in Figure 1. The use of dual electrostatic quadrupole lenses[3] allows both beam shaping and steering, and it increases sensitivity by a factor of five.

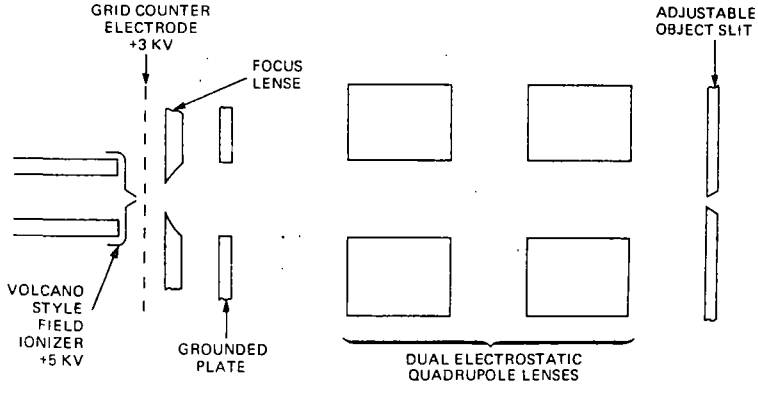
Figure 2 shows the ionization efficiency as a function of ionizer voltage for ammonia, hydrogen sulfide, and water. It is noteworthy that (1) the ionization efficiency is low, about 2 x 10^{-8} ions/molecule, and (2) the compounds with the higher ionization potentials have their curves shifted to higher ionizer voltages. For water, field desorption of ions from the layers of water molecules adsorbed on the emitter is far more probable than direct field ionization. In contrast, Figure 3 shows the ionization efficiency of xylene as a function of the potential between the ionizer and grid counterelectrode. Because of its much lower ionization potential, the ionization efficiency of xylene is about 2.4 x 10^{-6} ions/molecule in the plateau region of the curve.

An ionization efficiency of 2.4 x 10^{-6} ions/molecule means that on the average, 2.4 ions are counted at the detector for every 10^6 molecules entering the volcano source. In terms of the recommended[4] measure of mass spectrometer sensitivity, this is equivalent to 2.2 x 10^{-9} C/μg, comparable to the most sensitive of the commercially available EI or CI mass spectrometers and orders of magnitude better than other field ionization instruments.

Figure 4 compares the shapes of the ionization efficiency curves for some solid materials. For a new volcano source, the shape is similar for all compounds, but again is shifted to higher voltages for compounds with higher ionization potentials. The ionization efficiency curve for perylene obtained with the same source after it was damaged by an accidental discharge is not only shifted down by a factor of over 100, but is also very different in shape. This indicates that the lower efficiency field ionization produced by the damaged source involves not only different numbers, but also different types of active field ionization sites.

Figure 1

SCHEMATIC OF MAGNETIC SECTOR ION OPTICS. NOT TO SCALE



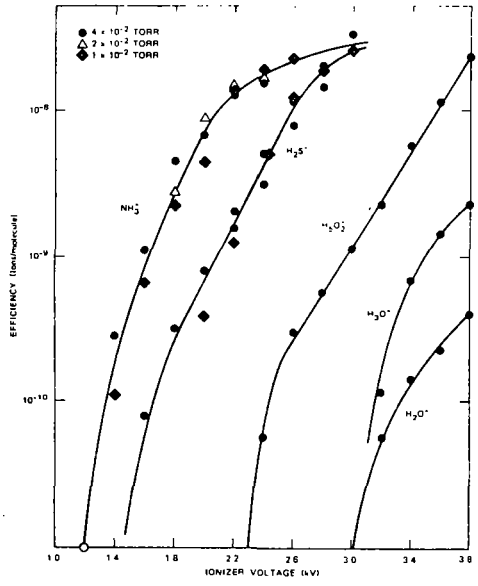


Figure 2

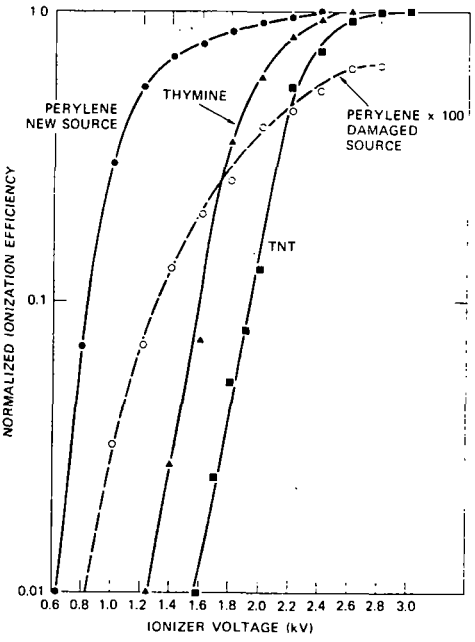


Figure 4

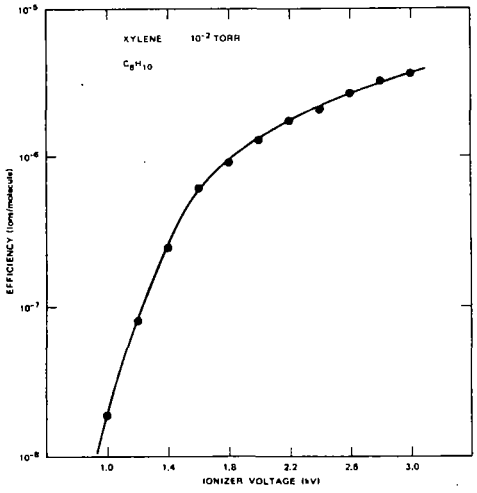


Figure 3

Because of the very low ionization potentials of polynuclear aromatic hydrocarbons, such as perylene, it is clear from Figure 4 that the volcano field ionization source may be operated as a highly selective detector for these compounds.

References

1. C. A. Spindt "Method of Fabricating a Funnel-Shaped Electrode for Use as a Field Ionization Source," U.S. Patent Application.
2. W. Aberth and C. A. Spindt, Int. J. Mass Spectrom. Ion Phys., 25, 183 (1977).
3. C. F. Giese, Rev. Sci. Instrum., 30, 260 (1959).
4. IUPAC Recommendations on Symbolism and Nomenclature for Mass Spectrometry, Org. Mass. Spectrom., 12, 115 (1977).

Characterization of Low Molecular Weight Polymers by Liquid Chromatography and Field Desorption Mass Spectroscopy

MAMOB4

by

Robert P. Lattimer*, Dale J. Harmon, and Kenneth R. Welch

The BFGoodrich Research & Development Center
9921 Brecksville Road
Brecksville, OH 44141

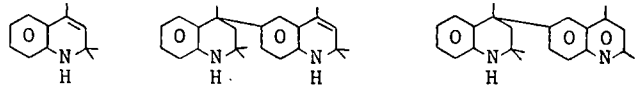
Considerable difficulties are encountered in the analysis of nonvolatile and thermally unstable materials by direct coupling of a liquid chromatograph with a mass spectrometer. It seems clear that for the present, at least, no suitable direct coupling technique has been devised that has proven to be satisfactory for the analysis of higher molecular weight oligomeric materials. Field desorption mass spectroscopy has been shown to be a very effective technique for determining molecular weights of labile and nonvolatile chemicals. This report describes the off-line coupling of LC with FDMS to characterize two low molecular weight polymer systems - polystyrene and poly-TMDQ (2,2,4-trimethyl-1,2-dihydroquinoline). LC-FDMS has proven to be a very effective combination for the characterization of these complex oligomeric mixtures.

The LC separations were performed on a Waters Associates ALC/GPC 202/R401 liquid chromatograph. A Waters Micro Bondapak C_{18} column, 30 cm x 3.9 mm ID, was used. The polystyrene sample was a commercial GPC standard (Pressure Chemical Co.) of reported M_n 750u. A linear solvent gradient (60 minute program) 100% methanol to 100% tetrahydrofuran was used. The chromatogram obtained is shown in Figure 1 (0.73 mg polystyrene on column). The poly-TMDQ sample was prepared by the acid-catalyzed polymerization of highly purified TMDQ. Gradient #7 (60 minute program) 50/50 tetrahydrofuran/water to 100% tetrahydrofuran was used with a five minute initial hold on injection. The chromatogram is shown in Figure 2 (0.55 mg poly-TMDQ on column.

The LC effluent peaks were trapped in glass vials, and the solvent was evaporated to dryness with gentle heating under a nitrogen stream. The residue from drying was taken up in a few microliters of tetrahydrofuran for syringe deposition on the field emitter. FD mass spectra were obtained on a Varian MAT 311A mass spectrometer.

Polystyrene oligomers containing up to eighteen monomer units (MW 1930) were identified via the LC-FDMS analysis (Figure 1). Molecular ions were the only prominent ions in the FD mass spectra from the LC cuts, even for the nonvolatile higher molecular weight components. The oligomers were separated by units of 104u (corresponding to styrene) and were "offset" by 58u, indicating that this was a butyl-terminated polymer. Very weak "satellite" peaks were observed for each oligomer at (M + 14) and (M + 16)u. The ion at (M + 14) apparently arises from an extra methylene group; the origin of (M + 16) is not clear.

Poly-TMDQ oligomers were observed (Figure 2) up to 1384u (octamer). The oligomers are separated by the TMDQ monomer unit (173u):



TMDQ MW 173 | TMDQ Dimer MW 346 | Demethylated Dimer MW 330

Reasonably intense impurity peaks were observed at masses both lower and higher than the principal components. The more abundant impurities appeared at (M - 16), (M + 16), and (M + 32) u. Accurate mass measurements showed that the (M - 16) components are "demethylated" oligomers (as MW 330 above), and that the higher mass impurities are all oxidation products, probably nitroxyl radicals and hydroxylamines.

The combination of liquid chromatography with field desorption mass spectroscopy has apparently received little attention in the past. The technique has considerable potential, however, and it is doubtful that this combination can be surpassed at present for the general characterization of complex mixtures of labile, nonvolatile organic compounds.

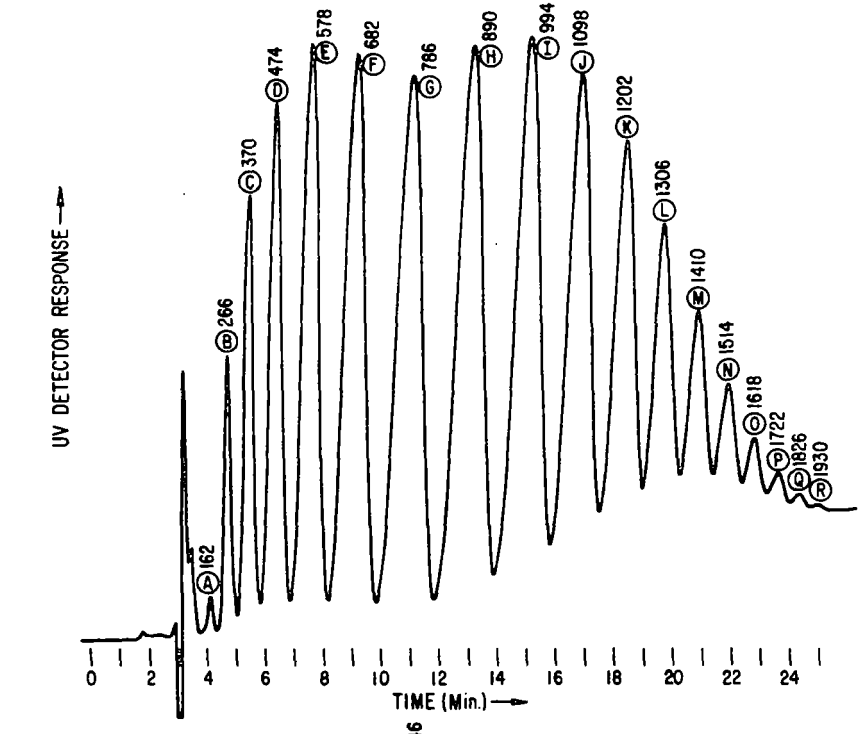


Figure 1. LIQUID CHROMATOGRAM of POLYSTYRENE

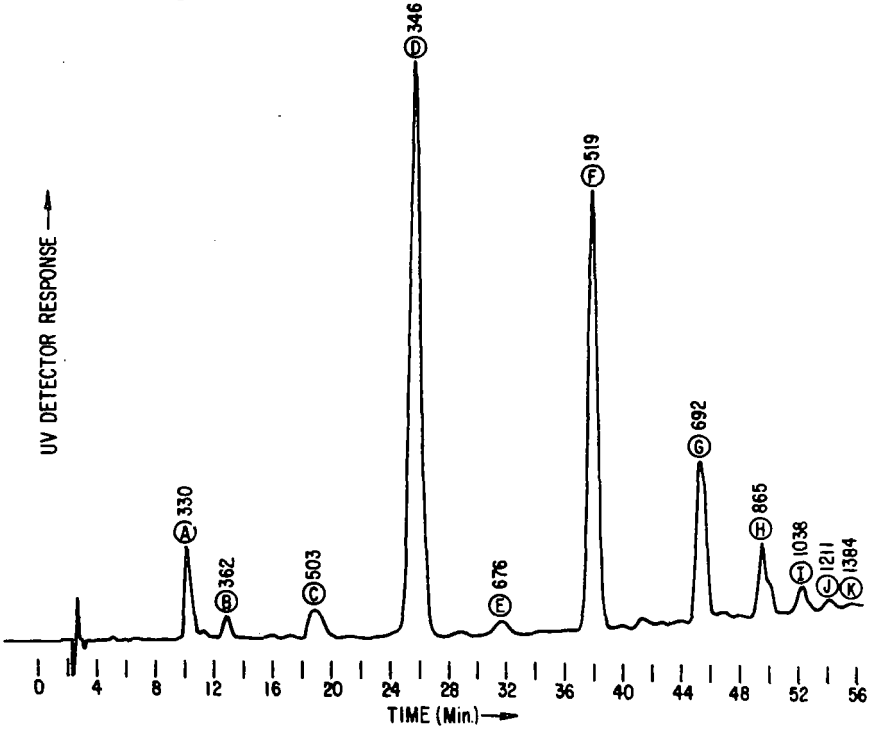


Figure 2. LIQUID CHROMATOGRAM of POLY-TMDQ

Electrohydrodynamic Ionization Mass Spectrometry Of Organic Salts MAMOB5

SHOOK -T. F. LAI and KELSEY D. COOK
School of Chemical Sciences, University of Illinois, Urbana, IL 61801

Electrohydrodynamic ionization mass spectrometry (EHMS)[1] depends on the action of a strong electric field (~6-8 keV) to withdraw naked and solvated ions directly from liquid solutions. Ionization occurs via salt dissociation and/or proton or ion attachment in the liquid phase prior to EH sampling. Adjustment of the polarity of the withdrawing field allows sampling of either positive or negative ions. In recent studies[2,3] data from positive and negative ion spectra of a variety of systems have proven complementary in illuminating some of the solution phase interactions which give rise to detected ions.

Spectra of sulfonates, quaternary ammonium salts, and sodium acetate in glycerol solution have been obtained. Glycerol is the solvent of choice because of its low vapor pressure at room temperature and its good solvation properties. Protonated glycerol clusters and (in the presence of alkali metal salts) simple cation-attached glycerol clusters usually appear in EHMS spectra of glycerol solutions. Except where these ions contain analyte moieties, they have been excluded from the data presented below. Ion abundances listed are relative to the most intense ion in each spectrum (100%).

In the positive ion spectrum of 2-naphthol-3,6-disulfonic acid, disodium salt (RNa_2), only $[Na]^+$ and its glycerol clusters were detected. The negative ion spectrum (Table 1)[2] consisted of three types of anionic species: $[G_n+R]^-$, $[G_n+R+H]^-$, and $[G_n+R+Na]^-$, where G represents a glycerol molecule and n is the number of glycerol molecules in a cluster. Similiar spectra were obtained for the disodium salts of 4,5-dihydroxy-2,7-naphthalenedisulfonic acid, indigo carmine and bromocresol green. These results indicate that (1) the sulfonates are highly dissociated in glycerol solutions and (2) there are proton transfers between the solvent molecules and the doubly charged anions.

Positive ion spectra of three quaternary ammonium compounds are summarized in Table 2. The solubilities of these three salts in glycerol are very low and concentrations ranged from 0.1 to 0.008 mole % (Mole % is *defined as moles of sample dissolved/ moles of glycerol* X 100%). In order to facilitate ionization, the conductivities of these solutions were increased by adding sodium iodide as a supporting electrolyte. Even at the low concentrations employed, organic cations and anions were observed (Tables 2 and 3). The absence of cation attached glycerol clusters $[G_n+NR_4]^+$ indicates that ammonium cations have low tendencies to interact with the solvent, consistent with the low solubilities of the salts.

EH mass spectra can provide information concerning the acid/base chemistry of salt solutions. Protonated glycerol clusters are present in the positive ion spectrum of a sodium iodide-glycerol solution[4], but disappear on addition of sodium acetate. The absence of $[G_n+H]^+$ reflects the buffer action of sodium acetate[5], which competes with glycerol for available protons. Instead of these solvent clusters, the positive ion spectrum of acetate solution contains rather unusual cationized ion pairs $[Na+NaOAc+G_n]^+$. (Table 4a). Solvated acetate anions are observed in the negative ion spectra (Table 4b).

Through these studies, we have begun to elucidate some of the interactions underlying observed EHMS spectra. Additional study should advance our understanding of these liquid phase phenomena.

ACKNOWLEDGEMENT

This work is supported by the NIH grant HEW-PHS-GM 19749.

REFERENCES

(1) B. P. Stimpson and C. A. Evans Jr., J. Electrostatics 5, 411 (1978).
(2) Shook-T. F. Lai and Charles A. Evans Jr., Org. Mass. Spectrom. 13, 733 (1978).
(3) S.-T. F. Lai, Electrohydrodynamic Ionization Mass Spectrometry, Ph.D. Thesis, University of Illinois, Urbana, IL, U.S.A., October 1978.

Table 1. Negative ion spectrum of 2-naphthol-3,6-disulfonic acid, disodium salt (RNa_2).

	Abundance (%)						
n	0	1	2	3	4	5	6
$[R+G_n]^{2-}$	0.47	0.16	0.24	0.39	0.11		0.06
$[R+G_n+H]^-$	0.17	0.12					
$[R+G_n+Na]^-$		0.41	1.63	2.41	1.03	0.09	0.08

Table 2. Positive ion spectra of tetrabutylammonium iodide, tetrabutylammonium borofluorate and benzyldimethylhexadecylammonium chloride.

	Abundance (%)		
	tetrabutylammonium iodide	tetrabutylammonium borofluorate	benzyldimethylhexadecylammonium chloride
$[cation]^+$	0.73	1.54	2.57

Table 3. Negative ion spectra of tetrabutlyammonium borofluorate.

	Abundance (%)		
n	0	1	2
$[G_n+BF_4]^-$	0.33	6.22	1.54

Table 4. (a) Positive ion spectrum of sodium acetate (NaOAc) and (b) Negative ion spectrum of sodium acetate (NaOAc).

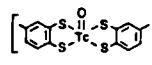
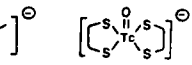
	Abundance (%)			
n	0	1	2	3
(a) $[G_n+NaOAc+Na]^+$	0.24	0.70	1.50	0.30
(b) $[G_n+OAc]^-$	0.37	5.51	35.48	1.44

FIELD DESORPTION MASS SPECTRA OF TRANSITION METAL CONTAINING ORGANIC COORDINATE COMPLEXES.

S.A. Carr, C.E. Costello, B.N. Wilson, C. Orvig, A. Davison, K. Biemann; Dept. of Chemistry, M.I.T., Cambridge, MA 02139

Although technetium (Tc^{99m}) complexes are widely used clinically as radioimaging agents, their structures are not well known. In an effort to aid structure determination FDMS of Tc-anion complexes was explored. Previous preliminary data had shown promise (1) and this work was extended to determine the most useful type of anion and cation. Oxo-bis-(3,4-toluene-dithiolato) technetate (TDT) and Oxo-bis-(ethane-dithiolato)technetate (EDT) were chosen as the anion in combination with a series of aliphatic and aromatic onium cations (see Table I) for this study.

TABLE I

	TDT	EDT
		
$(CH_3)_4N^+$		
$(C_2H_5)_4N^+$		$(C_2H_5)_4N^+$
$(C_3H_7)_4N^+$		$(C_3H_7)_4N^+$
$(C_4H_9)_4N^+$		$(C_4H_9)_4N^+$
$(C_5H_{11})_4N^+$		$(C_5H_{11})_4N^+$
$(C_6H_{13})_4N^+$		$(C_6H_{13})_4N^+$
$Ph_3\text{-}P{=}\overset{+}{N}{=}P\text{-}Ph_3$		$Ph_3\text{-}P{=}\overset{+}{N}{=}P\text{-}Ph_3$
Ph_4As^+		Ph_4As^+
Anion, Cation, M (M+Cation), $(Anion)_2$ $(Anion)_3$		Cation, (M+Cation) (NO Anions, M^+)

The FD mass spectrum of tetramethylammonium TDT is shown in Fig. 1. All spectra were taken on a Varian MAT 731 double focussing mass spectrometer equipped with an EI/FI/FD combination source. The base peak is $(anion)^+$ at m/e 423. Abundant ions ascribable to $(cation)^+$, $(M)^+$ and $(M+cation)^+$ are also observed. Of lower abundance is the anion dimer region at mass 346. The characteristic cluster of ions at mass 830 arises from the anion dimer by loss of oxygen and this loss has been confirmed by accurate mass measurement. The ion at m/e 692 has been assigned to a fragment of the anion dimer, as shown.

The spectra of the EDT salts are also straightforward. Fig.2 is the FD mass spectrum of tetrapentyl ammonium EDT. It consists almost entirely of $(cation)^+$, $(M+cation)^+$ and $(2M+cation)^+$. The mass of the anion can be obtained as the difference (M+cation)-(2 cations).

More complex spectra are obtained for both EDT and TDT anionic complexes, when the counter ion is aromatic. Fig.3 shows a spectrum of tetraphenyl arsonium TDT normalized to the base peak which is the cation at mass 383. Again, one observes ions corresponding to $(anion)^+$. There are also ions arising from phenyl ion attachment to the cation at mass 459 (confirmed by accurate mass measurement) and phenyl ion attachment to the anion, at mass 500. However, the abundance of these ions was so exceptionally high, that the signal to noise ratio for even relatively minor ions was quite good.

In Fig.4 the spectrum has been replotted and renormalized to bring out the rather rich spectral detail. All assignments are based on either accurate mass measurements or on homology to the other compounds in the series. The anion dimer region is quite abundant as are fragments and fragment plus ion clusters of the anion-for example, m/e 653 and 692. Doubly charged clusters were present at m/e 618.5, 625.5, 633.5 and 671.5 corresponding to the anion trimer region and anion trimer plus phenyl, all clearly shown in Fig.4. The peak at m/e 1189 corresponds to $(M+cation)^+$, m/e 1267 to anion trimer-2H and m/e 1344 to anion trimer plus phenyl.

In contrast, spectra of the EDT based anionic complexes do not show ions attributable to the EDT anion or cluster ions thereof. In addition none of the EDT complexes exhibited molecular ions. However, the spectra of the tetramethyl through tetrapentyl ammonium TDT salts included molecular ions with the trend again being that as the aliphatic cation size increased, the relative intensity of the respective molecular ions decreased.

The spectral differences between the TDT and EDT type complexes are summarized on the bottom of Table I and are attributed to the fact that in the former the positive charge generated by the loss of two e^- from the anion can be delocalized due to orbital overlap of the Tc with the aromatic rings which is not possible in the case of the non-aromatic EDT complexes. From these data it is evident that FDMS can play a major role in the characterization of Tc complexes and their synthetic intermediates.

Figure 1

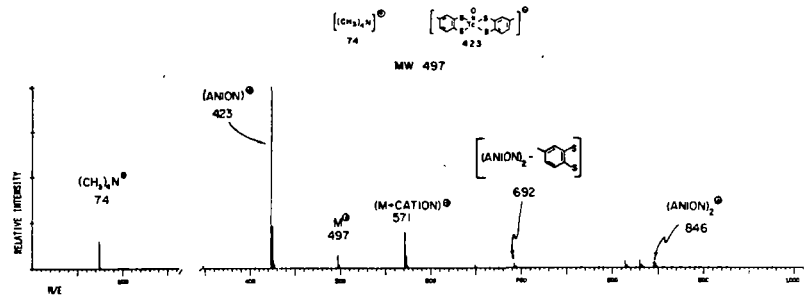


Figure 2

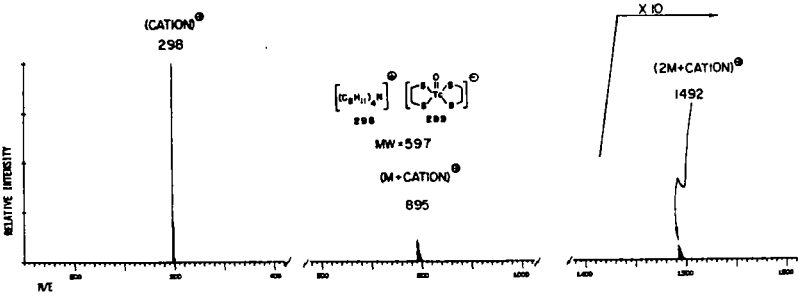
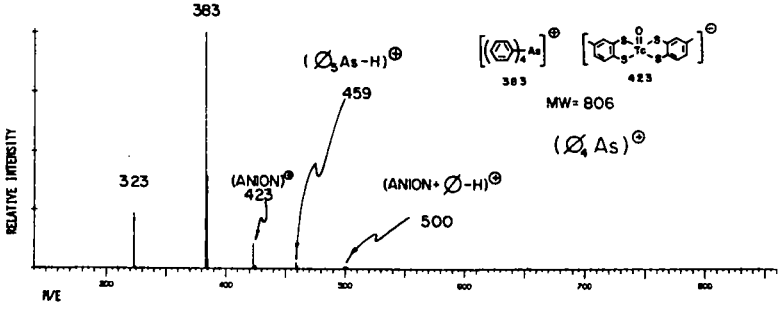


Figure 3



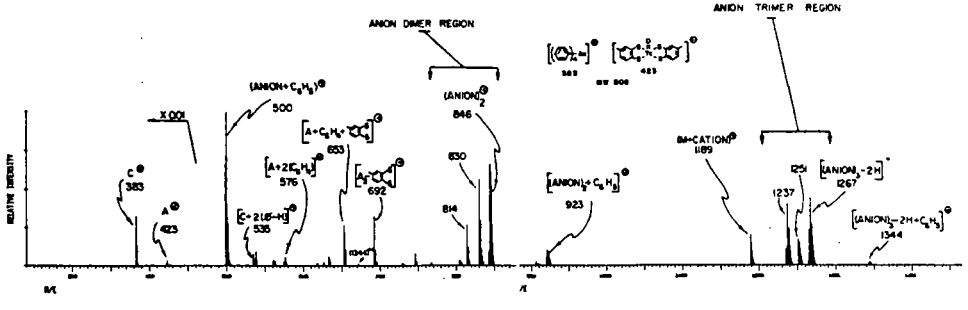


Figure 4

(1) B.W. Wilson, C.E. Costello, S.A. Carr, K. Biemann, C. Orvig, A. Davison, and A.G. Jones, Anal. Letters., 12(A3), 303-311 (1979).

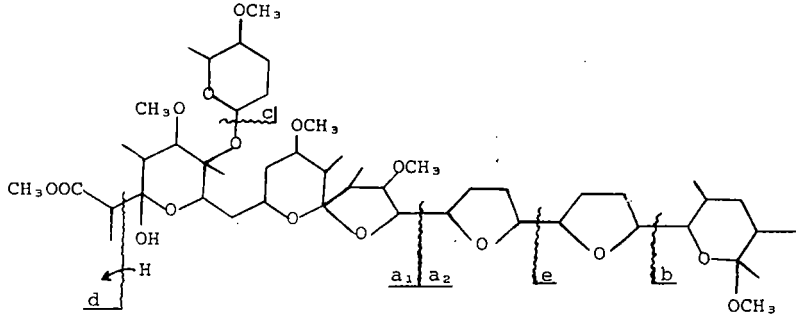
STRUCTURE INVESTIGATION OF HIGHER MOLECULAR WEIGHT POLYETHER ANTIBIOTICS USING FIELD DESORPTION MASS SPECTROMETRY, J. L. OCCOLOWITZ and R. L. HAMILL, Lilly Research Laboratories, Indianapolis, IN 46206

Previously, we have demonstrated the use of EI mass spectrometry in determining the structures of metabolites of monensin and the structure of narasin and related compounds. In our experience, the polyether antibiotic dianemycin (MW = 866) sets an upper limit to the MW of compounds which can be examined by EI alone. For higher MW polyether antibiotics, such as K41/A32887 (MW = 946) and A28695B (MW = 930), we have found it necessary to use a combination of FD and EI to obtain necessary structural information. This paper describes this combined approach in the structure determination of the latter two compounds and examines the FD spectra of other high MW polyether antibiotics of known structure.

Although the salts and free acids of the higher molecular weight polyethers give FD spectra which are characterized by intense molecular ions or cationized molecular ions, the spectra show very little fragmentation which can aid structural studies. When EI spectra of these compounds can be obtained by use of the "in-beam" technique, the spectra are difficult to interpret because most fragments do not arise from the molecular ions.

In order to obtain spectra which yield the most structural information, we have found it necessary to derivatize the higher molecular weight polyethers. This approach can be contrasted to mass spectral examination of lower molecular weight polyethers, such as monensin and narasin, where much structural information can be derived from examination of the EI spectra of their sodium salts.

For the compounds studied, structurally significant fragmentations occur in the FD spectra of the methyl ester methyl ethers. The fragmentation of A28695A (septamycin) methyl ester methyl ether shown here is typical of the spectra of corresponding derivatives of other similar polyethers.



The EI spectra of the derivatives are composed largely of ions corresponding to a_1 and its fragmentation products, including peaks resulting from the loss of molecules "d," "C-OH," and all or some of the methoxyl groups as molecules of methanol. The ions "a_2," "e," or "b" are not discernible in the EI spectra.

USE OF COMPLETE FIELD DESORPTION MASS SPECTRA FOR STRUCTURAL STUDIES IN BIOLOGICAL CHEMISTRY. C.E. Costello, S.A. Carr, N.R. Mancuso, and K. Biemann; Dept. of Chemistry, M.I.T., Cambridge, MA 02139

Although field desorption was initially welcomed as an ionization method which made possible the determination of the molecular weight of energy labile molecules, experience has shown that there are frequently present in the spectra fragment ions which provide some structural detail. Photoplate recording of the spectra facilitates the gathering of both types of information. Effective utilization of the technique has required the development of experimental protocols, the selection of suitable marker compounds and some modification of the photoplate reading programs routinely used for the measurement of electron impact spectra.

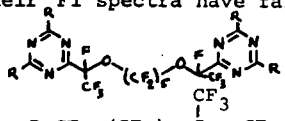
Exact mass determinations using photoplate recording of field desorption spectra are carried out at a resolution of M/ΔM 5000, after careful tuning of the ion source potentials using the FI signal of a reference compound and the combined beam monitor signals at the Z-plate and the β-slit. Because field desorption spectra have few lines which are multiplets, the use of relatively low resolution still permits accurate mass measurements (1). Microfilmed profiles of densitometer readings are useful to assess photoplate data for possible sample/marker doublets or to select the proper signal level for peak center calculation.

Theoretical and practical considerations for the selection of the marker ionization mode are summarized in TABLE I.

TABLE I
CHARACTERISTICS OF DIFFERENT SAMPLE/MARKER IONIZATION MODE COMBINATIONS

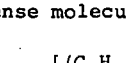
	FD/FD	FD/FI	FD/EI
Ion Formation	Simultaneous	May be simultaneous	Not simultaneous
Ionization Modes	Identical	Similar	Different
Repositioning of Ion Source Parts	None	None	Slight
Beam Monitor Integration or Feedback for Heating Control	Not usable	Usable if not Simultaneous	Usable
Number of Markers Needed	Many	Many	One
Ion Source Contamination	Serious	Serious	Minimal

Although FD/FD is of the greatest simplicity, the possibilities of emitter overloading and competitive desorption, together with the problems shown in Table I make it impractical. Since FD/FI also has low sensitivity and requires many marker compounds thus leading to ion source contamination, FD/EI emerges as the method of choice. A new series of fluorinated bis-triazines, such as the one of MW 2442 shown below, are promising as markers because they are quite volatile, their EI spectra exhibit a series of fragment ions providing calibration lines throughout the mass range, and their FI spectra have fairly intense molecular ions (permitting ion source tuning).



R=CF_3-$(CF_2)_2$-C(F)(-CF_3)-CF_2-O-C(F)(-CF_3)-

Bis-Triazine, MW 2441.8304

$[(C_6H_{13})_4N]^+[$  $]^-$

Cation	Anion
354.4100	298.8520

Hexyl EDT, MW 353.2620

Exact mass assignments of lines in the FD spectra of a number of compounds of biological significance have been made using this FD/EI technique. Excellent results for the $(M+cation)^+$ region of the spectrum of the Hexyl EDT complex (2,3)are shown in TABLE II. These data made possible the assignment of the group of lines near m/e 744 as the $(M+cation)^+$ region of the chloride complex, which may be either an impurity or an experimental artifact.

TABLE II

FD Hexyl EDT / EI 2,4,6-triperfluoroheptyl Triazine

M/E obs. (uncorr.)	M/E calc.	ΔMMU	
743.7941	743.7888	+5.3	$[(C_6H_{13})_4N^+]_2\,Cl^-$
744.7941	744.7921	+2.0	
745.7894	745.7859	+3.5	
746.7891	746.7892	-0.1	
1007.6759	1007.6719	+4.0	$[(C_6H_{13})_4N^+]_2EDT^-$
1008.6723	1008.6752	-2.9	
1009.6660	1009.6728	-6.8	

However, in another region of this spectrum, there is a very significant deviation (about 35 mmu.) between the assigned exact mass and its theoretical value (TABLE III).

TABLE III

FD Hexyl EDT / EI 2,4,6-triperfluoroheptyl Triazine

M/E obs. (uncorr.)	M/E calc.	ΔMMU	
352.3545	352.3944	-39.9	
353.3585	353.3977	-39.2	
354.3749	354.4100	-35.1	$(C_6H_{13})_4N^+$
355.3799	355.4133	-33.4	
356.9810	356.4166	-38.2	
357.3814	357.4199	-38.5	
382.4035	382.4413	-37.8	$(C_6H_{13})_3N^+(C_8H_{17})$
383.4062	383.4446	-38.4	

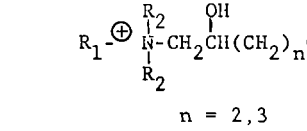
This discrepancy illustrates the caution with which one must approach these measurements. Although the FD/EI approach can be quite useful and can give accurate results, until one can explain and compensate for such phenomena, it is essential that a few known lines be present in the region of the FD spectrum in which assignments of unknown lines are to be made.

(1) B.W. Wilson, C.E. Costello, N.R. Mancuso, and K. Biemann, "Approaches to the Recording and Measurement of Field Desorption Mass Spectra Using Photoplates", 1978 ASMS Meeting, Paper No. TA-4.
(2) S.A. Carr, C.E. Costello, B.W. Wilson, C. Orvig, A. Davison, and K. Biemann, "Field Desorption Mass Spectra of Transition Metal Containing Organic Coordinate Complexes", 1979 ASMS Meeting, Paper No. MAMOB8.
(3) B.W. Wilson, C.E. Costello, S.A. Carr, K. Biemann, C. Orvig, A. Davison, and A.G. Jones, Anal. Letters, 12(A3), 303-311 (1979).

Field Desorption of Some Substituted Ammonio-Carboxylates, T. Keough and A. J. DeStefano, The Procter & Gamble Company, Miami Valley Laboratories, P.O. Box 39175, Cincinnati, Ohio 45247.

INTRODUCTION

Field desorption mass spectrometry has been used to characterize several hydroxy ammonio-pentanoates (n=2) and -hexanoates (n=3) whose structures are given below:



n = 2,3

$R_1 = CH_3$, $C_{14}H_{29}$, $C_{22}H_{45}$; $R_2 = CH_3$

$R_1 = R_2 = C_2H_5$

The molecular weights of these thermally unstable compounds can be determined directly from the FD spectra obtained at low emitter currents (<10mA). At higher emitter currents (~20mA) both intermolecular and intramolecular pyrolytic processes become important.

EXPERIMENTAL

All FD spectra were obtained on a Varian/Atlas SM-1B mass spectrometer modified to allow field desorption.[1] Samples were loaded from a concentrated solution onto high temperature activated benzonitrile emitters either by dipping or by direct syringe loading. Ion source focusing was accomplished mechanically with micromanipulators. The mass scale was calibrated with the aid of a Hall effect probe after obtaining FI or FD spectra of suitable reference standards. All spectra were output onto an oscillographic strip chart recorder but were replotted for convenience in presentation.

RESULTS AND DISCUSSION

The FD spectrum (6mA) of 4-hydroxy triethyl ammonio-pentanoate (Figure 1) is typical of the low-temperature spectra of the hydroxy ammonio-carboxylates that were studied. These spectra are dominated by two series of ions. The first consists of the protonated molecular ion and higher mass cluster ions, while the second consists of decarboxylation products.

Some irreproducibility problems led us to investigate the effect of emitter heating current on the FD spectra of this class of compounds. Results obtained from the analysis of 5-hydroxy triethyl ammonio-hexanoate are given in Figure 2. The upper spectrum (15 mA) exhibits a weak $(M+H)^+$ ion and is dominated by $(M+H-CO_2)^+$ as expected. The lower spectrum (20 mA) exhibits several interesting results: (1) The relative abundance of M^+ and $(M+H)^+$ increased as the emitter current was raised from 15 to 20 mA. This effect is just opposite of what might be expected given the thermal instability of this class of compounds. (2) The spectrum exhibits an intense ion 46 amu below the molecular ion. This is believed to result from thermal elimination of EtOH prior to ionization. (3) Surprisingly, no significant ion current resulting from intermolecular transfer of an ethyl group is evident at m/z 260. Intermolecular alkyl transfer of groups as large as $C_{10}H_{21}$ has been previously observed in the high temperature FD spectra of some non-hydroxylated ammonio-hexanoates.[1]

The FD spectrum (20 mA) of a hydroxy ammonio-hexanoate containing a $C_{22}H_{45}$ alkyl group attached to the quaternary nitrogen is given in Figure 3. Again, the relative abundance of M^+ and $(M+H)^+$ increased as the emitter current was raised from 15 to 20 mA. Alcohol elimination (loss of MeOH) is relatively less significant than previously observed for hydroxy ammonio-carboxylates containing only methyl or ethyl substituents attached to the quaternary nitrogen. In contrast to the spectra given in Figure 2, the ion formed by intermolecular methyl

transfer is the second most abundant ion in this spectrum.

We interpret the observed thermal effects according to the sequence given in Figure 4. The first pyrolytic process to occur involves intermolecular esterification with the transfer of one (MR^+) or two (rearranged form of M) alkyl groups. We believe that the product distribution is influenced by the nature of the substituents attached to the nitrogen. We have verified that M^+ is produced through a bimolecular process by analysis of a two component mixture of compounds containing different substituents attached to the quaternary nitrogen Once the hydroxy amino-ester form of the molecule is produced, it may undergo an additional pyrolytic process, i.e., intramolecular cyclization producing a 5- or 6-membered lactone depending on the structure of the starting material. Pyrolysis IR studies confirm these interpretations

CONCLUSIONS

FD is an excellent method for the qualitative analysis of hydroxy ammonio-carboxylates. However, the FD spectra are strongly dependent upon emitter heating current. At high currents (~20 mA) both intermolecular and intramolecular pyrolytic processes become important.

ACKNOWLEDGMENTS

We thank Bob Sanders for many useful suggestions during the course of this work and Dr. Bursey and the University of North Carolina for the loan of the FD source used in this study.

REFERENCE

1. R. A. Sanders, 26th Annual Conference American Society for Mass Spectrometry and Allied Topics, paper no. TA-5, St. Louis, Missouri, May 28-June 2, 1978.

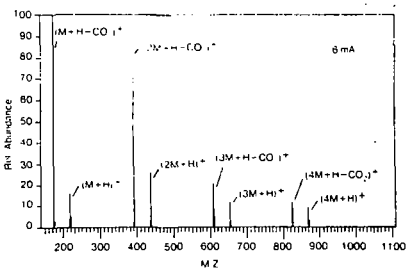


Figure 1: FD spectrum of 4-hydroxy triethyl ammonio-pentanoate.

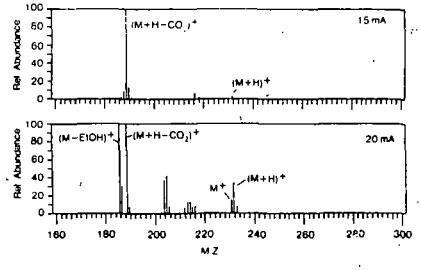


Figure 2: FD spectra of 5-hydroxy triethyl ammonio-hexanoate.

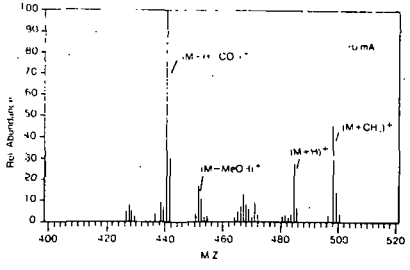


Figure 3: FD spectrum of 5-hydroxy dimethyl docosyl ammonio-hexanoate.

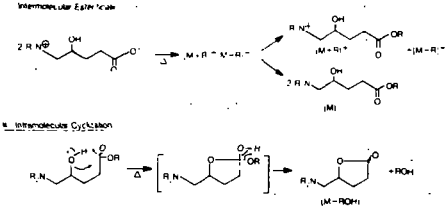


Figure 4: Mechanism of thermal decomposition of ammonio-carboxylates.

RAPID HEATING EVAPORATION OF $Pb(NO_3)_2$*

T. Radus, H. R. Udseth, and L. Friedman

Chemistry Department, Brookhaven National Laboratory, Upton, NY 11973

Lead nitrate was evaporated at a very rapid heating rate (up to ~5000°/s) by means of a pulsed heating technique into a mass spectrometer source under either chemical or electron impact ionization conditions. Evaporation under EI conditions revealed a two stage process. The first stage was a low temperature (250-500°C) evaporation of fragments from the decomposition of $Pb(NO_3)_2$. The second stage was a high temperature (700-900°C) evaporation of lead oxide species. Under CI conditions with NH_3 and H_2O as reagent gases, solvated ions of the molecular species $Pb(NO_3)_2$ as well as the fragment species $PbNO_3$ were seen. Using CH_4 and Ar as reagent gases, only various fragment ions were seen with no evidence of the molecular species or any solvated ions. Activation energies were measured for the evaporation process. Significant differences in activation energies for evaporation of species produced in chemical ionization sources as compared with ions produced in high vacuum by electron impact provide evidence for heterogeneous reactions between ions generated in the CI source and molecules on the surface of the sample probe.

*Research performed under the auspices of the U.S. Department of Energy.

Paper Number MIAM10812

An Electron Bombardment Heated Knudsen Cell Mass Spectrometer.

P.J. Turner, W.D. Unsworth.

VG-Isotopes Limited, Ion Path, Road Three, Winsford, Cheshire, CW7 3BX.

Introduction.

An electron bombardment heated Knudsen Cell has been developed for operation at temperatures up to 2500°C. The cell has currently been fitted to a Micromass 30 mass spectrometer fitted with a special electron impact ionisation source. This is a single focussing mass spectrometer using a 90° magnetic sector of mean radius 305 mm having an ultimate resolving power better than 6×10^3 (10% valley definition). The axis of the cell is vertical and two modes of temperature control are provided, thermocouple and total power. Temperature stability is better than $\pm$ 1°C over the temperature range room temperature up to 2500°C. Appearance potential measurements may be made in the range 3 to 100 eV with an accuracy of $\pm$ 0.1 volt, assuming proper source tuning.

Construction of Furnace.

The furnace is constructed off a water cooled base plate which is mounted on the bottom of a water cooled vacuum jacket. The vacuum vessel is pumped by means of a 700 l/s polyphenyl ether oil diffusion pump having an ultimate vacuum better than 5×10^{-9} torr. The cell itself is mounted on a support rod attached to a manipulator which may be used for centring the molecular beam axis. Two types of support rod are provided so that the cell may be run either at ground potential or at +2 kV. Two tungsten wire filaments are used to generate the electrons used for heating the cell, and the current through each of the filaments may be varied independently to minimise temperature gradients in the cell. With the cell at ground potential, the filaments may be floated to 1kV negative so that the heating power is divided between the cell and the inner shield. In this configuration, a heat input of 1 kilowatt is sufficient to raise the cell temperature to 2000°C. With the cell grounded, a thermocouple may be used to measure the cell temperature and also provide the control signal for the furnace electrical supplies. At low temperatures, the radiation from the filaments is sufficient to raise the temperature of the cell (up to approximately 700°C) and the controller is so designed that whether the heating is bombardment or radiation, temperature stability will be maintained.

In its alternative configuration with the K-cell biassed to 2kV positive, and the filaments at ground potential, all the electron bombardment energy is available for heating the cell, and an input of approximately 1.5 kilowatt is sufficient to raise the temperature to 2500°C. Control in this case is by means of total power. Emission current and cell voltage are measured, and the filament current is controlled so that constant power is provided to the cell.

Heat shields and support assemblies are in general made from tantalum, whilst the crucible support rod for work at 2500°C is made from tungsten.

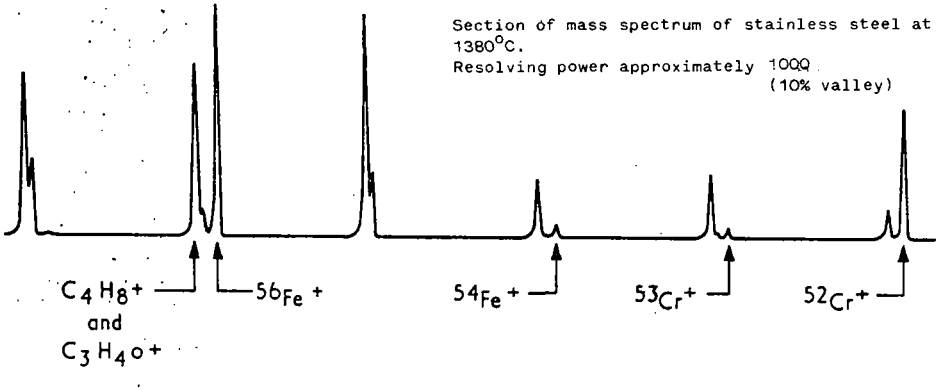
Control Unit.

A master control unit is used to drive the furnace through a filament slave unit and separate EHT supply. On this unit is a meter display of the current through each filament, with the facility to balance these currents. Total emission is also displayed, and also the EHT. Power of thermocouple control may be selected, and provision is made for either manual or externally programmable operation of the furnace. The thermocouple "set" voltage can be set using thumbwheel switches in the range 0 to 40mV with 10uV resolution. A meter is used to show the offset between the offset between the "set" temperature and the actual furnace temperature. The controller is essentially two term, the difference and integral terms being used, whilst the differential term is not.

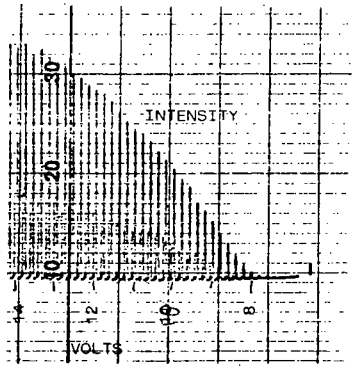
Electron Impact Source.

A special electron impact source has been developed in which the electron beam axis is at right angles to both the molecular beam axis and the length of the ion exit slit. Emission control may be either the conventional "trap" mode or "trap + source" mode. In this latter case a collimator plate between the filament and source block is used to define the beam entering the block and regulation is such that the current entering the ion block and trap is kept constant. The emission may be set in a 1,2,5 sequence between 10uA and 1mA. For analysis of gas samples, the maximum sensitivity is in excess of 10^{-3} amps/torr.

Examples of Results.



Section of mass spectrum of stainless steel at 1380°C.
Resolving power approximately 1000 (10% valley)



Appearance Potential Measurement for $^{107}Ag^+$
100 μA trap + source mode
0.2 volt steps
Repeller voltage + 1.8 volts.

MAM 10B12

PES OF HIGHER TEMPERATURE VAPORS

J. Berkowitz and C. H. Batson, Argonne National Laboratory

Argonne, IL 60439

The study of high temperature species by photoelectron spectroscopy is about 7 years old. We began this work in the early 1970's, using a newly-designed cylindrical mirror analyzer. Significant information was obtained on a number of inorganic systems, particularly metal halides and metal atoms. One significant difference that appeared was the characterization of bonding orbitals in the conventional (covalent) sense and bonding orbitals when ionic bonding is dominant. [Many high temperature species tend to be ionically bonded, whereas normally volatile materials tend to be covalently bonded.]

Our work (and those of other groups) seemed to reach a temperature barrier of ~1000°, for several reasons. In order to surmount this barrier, we designed a new apparatus. It consists of a hemispherical electron energy analyzer with a retarding-focussing entrance lens, and a radiatively heated oven, basically of the Nuclide Analysis Associates design. The oven has been modified from the Knudsen cell style by surmounting a large, thin tube. The base oven and the tube are independently heated by non-inductively wound heaters. The uncancelled magnetic fields of the two heaters are opposed, reducing the residual field further. Double-oven capability is thereby achieved, and temperatures in excess of 2000°C should be possible.

The electron energy analyzer is largely isolated from the oven and heating system. It can rotate (in θ and ϕ), enabling angular distribution studies to be performed. Scanning is achieved with the retarding lens, keeping the electron pass energy through the analyzer fixed.

We describe below one recently completed study, and make reference to others completed or underway.

The Alkali Halide Vapors

Early mass spectrometric work had revealed the presence of dimers, trimers, even tetramers in alkali halide vapors. This work showed that the complexity of the vapor increased from Cs → Rb → K → Na → Li halides. For cesium halides, dimers were ca. 1% of vapor, higher polymers insignificant. For lithium halides, dimers were ~50% of vapor, trimer around 10%. PES has heretofore been confined to Cs, Rb, K and Na halides, presumably for two reasons.

a) Temperatures required are somewhat higher for lithium halides.

b) Large dimer component would confuse the photoelectron spectrum.

The basic observations of this earlier work are:

a) In the VUV range, ionization occurs from the halogen end of an M^+-X^- diatomic molecule.

b) This p— like orbital splits in cylindrical symmetry into π and σ. The π splits further by spin-orbit interaction into $\pi_{3/2}$ and $\pi_{1/2}$.

c) One can therefore anticipate 3 peaks, but in most cases 2 of the peaks are not separated and one sees a doublet.

d) A dimer peak can be seen at somewhat higher energy, increasing in intensity as the percent of dimer increases.

The present work was performed on lithium halides, which have the largest dimer concentrations. Two types of spectra were obtained, one with essentially the saturated vapor, the other with superheated vapor. Some peaks were dramatically lower in the superheated vapor, and could immediately be assigned to dimer. Normalization and subtraction of the two spectra enabled us to obtain "pure" monomer and dimer spectra. The monomer spectra were about as expected from extrapolation and prediction of the other alkali halides. The dimer spectra were completely new. Six peaks are anticipated for these rhombic structures. In the case of Li_2I_2, we see 5 of these.

Conclusions

a) The first I.P. of dimer is higher than that of monomer in each lithium halide.

b) This can be obtained by ionic model calculations, and also by molecular orbital calculations. We have done such calculations using the Xα— DVM method. The calculations were performed by Dr. G. L. Goodman.

c) These calculations predict that trimer has lower IP than dimer, and tetramer has higher IP than trimer.

d) Electron impact measurements on LiF agree with this oscillatory trend, through trimer.

e) A crude ionic model calculation can also rationalize this behavior (assuming hexagonal trimer and distorted cube for tetramer).

A complete description of this work will appear shortly in the Journal of Chemical Physics. The partial cross sections of atomic iodine have also been studied, and will appear in the same journal.

This research was performed under the auspices of the Division of Basic Energy Sciences of the United States Department of Energy.

ANIONIC BEHAVIOR OF URANIUM(VI) IN A SULFATE-SULFURIC ACID SYSTEM*

R. Newbury, R. Carver, and J. Rego
Lawrence Livermore Laboratory
Livermore, CA 94550

We measured the effect of changing the relative proportions of both sulfate and sulfuric acid on the anionic behavior of uranium(VI). Previous investigators have described the anionic behavior of uranium in sulfuric acid solution. Others have observed similar anionic behavior in sulfate solutions.

In sulfate-sulfuric acid solution, uranium(VI) exists as a uranyl cation in equilibrium with UO_2SO_4, $UO_2(SO_4)_2^{2-}$, and $UO_2(SO_4)_3^{4-}$. The anionic complexes are quickly absorbed on the anionic exchange resin, and the equilibrium is shifted toward the formation of additional complexes. There is some indication that even the uncharged UO_2SO_4 may combine with SO_4^{2-} already absorbed on the resin.

We prepared five solutions containing a measured amount of $^{235}UO_2SO_4$ dissolved in standardized sulfuric acid. A weighed amount of Na_2SO_4 was added to each solution so that the total sulfate concentration increased in each succeeding sample while the acidity was held constant. We added a measured volume of each solution to a known weight of anion exchange resin (Dowex 1X8, sulfate form, 30-70 mm/min settling rate), and the mixtures were agitated daily for a week to ensure equilibration. The liquid was filtered away from the resin, and we determined the concentration of the unabsorbed uranium by isotope dilution mass spectroscopy.

This technique involved adding a known spike of ^{233}U to a measured portion of the ^{235}U solution and running the mixture through our standard anion exchange process to get rid of the voluminous Na_2SO_4 and, incidentally, any iron or other metals present.

The samples were analyzed on a 34-cm double-focusing mass spectrometer with magnetic sweep, utilizing two filaments (sample filament and surface ionizing filament) and operating in the pulse-counting mode. The information was taken from the multiplier, through the preamplifier and amplifier, and was dumped into an ND180 multisumming scaler in synchronization with the magnetic sweep. A PDP8 took the raw data, made coincidence and background corrections, and calculated the amount of ^{235}U in the sample. This technique allows continuous averaging so that, if the sample is large enough, any desired precision (to the limit of the equipment, ~0.2%) may be obtained. Typical sample sizes for medium-ionization-potential elements such as uranium are ~10-40 ng.

The experiment was repeated four times, varying the acid concentration from 0.03 to 7.3 N and varying the total sulfate concentrations from 0.15 to 8.1 N. Our measured K_D's ranged from 5 in high acid-high sulfate to 5550 in low acid-low sulfate solutions. The absorption onto anion exchange resin is much more sensitive to acidity than to the total sulfate concentration.

Nonsulfate anions compete for active sites on the resin; therefore, less absorption of uranium will occur in a system containing anions that do not complex with uranium(VI). To measure this effect, we prepared an additional set of samples. To that set we added a measured amount of $NaClO_4$ to make the total anion concentrations approximately equal. The $NaClO_4$ was dissolved in each solution before it was added to the anion exchange resin. The measured K_D's were smaller by as much as a factor of 100 from the matching set of samples without the $NaClO_4$.

*Work performed under the auspices of the U. S. Department of Energy, Contract No. W-7405-Eng-48.

NEGATIVE ION PRODUCTION USING RYDBERG ATOMS

R. W. Odom and R. M. Hill
Molecular Physics Laboratory, SRI International, Menlo Park, CA 94025

The production of negative ions from collisions of highly excited (Rydberg) atoms with electronegative molecules, written schematically as

$$A^{**}(n,\ell) + XY \xrightarrow{\sigma_t} A^+ + XY^- \text{ or } (X+Y) \quad , \tag{1}$$

has several characteristics which make it an ideal method for investigating low energy electron attachment processes. Since the energy of the excited electron in a Rydberg atom is very well defined and proportional to $1/n^2$ (where n is the electron's principal quantum number), the average kinetic energy of the Rydberg electron can be accurately varied over the range 0.136 eV (n=10) to 0.015 eV (n=30) simply by changing its n level. A second characteristic of this type of electron transfer process is that the electron transfer cross section, σ_t, can be very large ($\sim 10^{-11}$ cm^2). This large transfer cross section is the result of the large area swept out by the Rydberg electron which is proportional to n^4 and is, for example, equal to 3×10^{-11} cm^2 for n=20. A third characteristic of the Rydberg atom electron transfer process is the long time ($\sim 10^{-10}$ sec) the Rydberg electron interacts with the attaching molecule. This long interaction time increases the probability of electron transfer since the neutral attaching molecule has sufficient time to assume a favorable configuration for attaching the electron.

Our technique for investigating Rydberg atom electron transfer processes is to optically pump an effusive sodium beam to specific Rydberg levels inside a collision cell containing the attaching gas of interest. Two nitrogen pumped dye lasers are used to produce the Na Rydberg atoms by the two-step pumping process: 3s → 3p followed by 3p → n, ℓ. The n value of the Rydberg level can be easily varied between n=5 and n=30 using this pumping sequence. The negative ions formed in the collision cell are extracted, mass analyzed, and counted.

Figure 1 presents experimental results obtained in an investigation of negative ion formation resulting from collisions of Na Rydberg atoms with CCl_4 and SF_6. The major negative ions formed from these two molecules were Cl^- and SF_6^-, respectively, and the ratio of the electron transfer cross section, $\sigma_{Cl^-}/\sigma_{SF_6^-}$ is plotted in Figure 1 as a function of the Na Rydberg level. The most prominent feature of the data is that the cross section ratio increases with increasing principal quantum number of the Rydberg electron which indicates that the dependence of σ_t on electron velocity has a different functional form for Cl^- and SF_6^- formation.

The theoretical treatment of Rydberg atom electron transfer processes developed by Matsuzawa[1] predicts that the velocity dependence of σ_t is proportional to the cross section for free electron attachment, $\sigma_{e\ell}$, averaged over the velocity distribution of the Rydberg electron, i.e.,

$$\sigma_t(n) \propto \int_0^\infty \sigma_{e\ell}(v)\, v |\varphi_{n,\ell}(v)|^2 v^2 dv \tag{2}$$

where v is the electron velocity and $\varphi_{n,\ell}(v)$ is the wave function for a Rydberg electron in quantum states n and ℓ. If $\sigma_{e\ell}(v)$ for SF_6^- formation has a 1/v dependence, then $\sigma_t(n)$ for its formation is independent at n and the velocity dependence of free electron attachment to CCl_4 can be calculated from the $\sigma_{Cl^-}/\sigma_{SF_6^-}$ ratios using Eq. (2). The value of $\sigma_t(n)$ for SF_6^- formation for $25 \le n \le 40$ reported by Foltz et al.[2] as well as our own evaluation at n=10 show that this cross section is independent of n and equal to approximately 1.0×10^{-11}cm^2.

Using this value for the SF_6^- transfer cross section, the best fit for the velocity dependence of $\sigma_{e\ell}Cl^-$ formation calculated from Eq. (2) is shown in Figure 2 along with the velocity dependence of $\sigma_{e\ell}$ obtained from a swarm experiment.[3] The agreement between the two experimental methods is quite good especially at lower electron energies (higher n values) and the Rydberg data shows that it is possible to extend the cross section

measurements to electron energies not obtainable using thermal electron attachment techniques.

Since numerous classes[4] of molecules attach thermal energy electrons, the Rydberg atom technique can be used to determine the velocity dependence of the attachment process as well as bracket the electron affinity of the attaching species. In addition, since it is possible with cw pumping of alkali beams to produce Rydberg atom (low energy electron) densities which are 10^2 to 10^4 times greater than those possible with electron beam techniques, the Rydberg atom technique can be used as a very sensitive negative ion source.

References

1. M. M. Matsuzawa, J. Phys. B 8, 2114 (1975).

2. G. W. Foltz, C. J. Latimer, G. F. Hildebrandt, F. G. Kellert, K. A. Smith, W. P. West, F. B. Dunning, R. F. Stebbings, J. Chem. Phys. 67, 1352 (1977).

3. R. P. Blaunsteim, L. G. Christophorou, J. Chem. Phys. 49, 1526 (1968).

4. Atomic and Molecular Radiation Physics, L. G. Christophorou, Wiley Interscience, New York, 1971. p. 501.

Acknowledgements

This research was supported in part under grant PHY 76-24541 from the National Science Foundation.

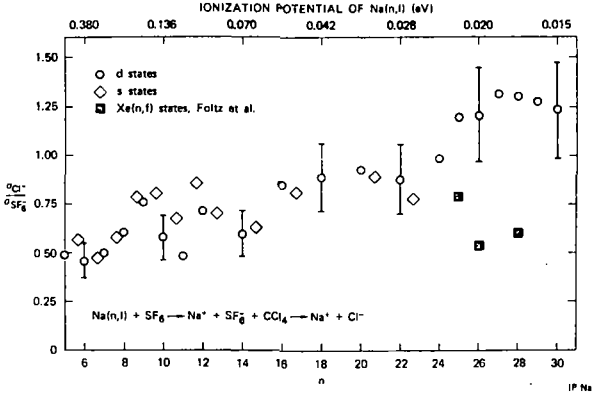


Figure 1. $\sigma_{Cl^-}/\sigma_{SF_6^-}$ ratio as a function of n.

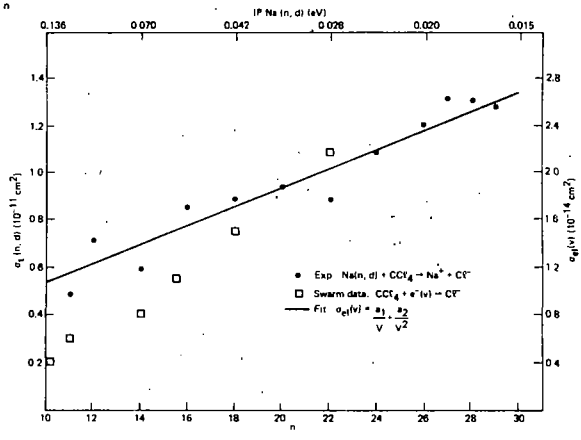


Figure 2. Comparison of Cl^- formation cross section using Rydberg atom and thermal electron attachment techniques.

MAMOC2 JOINT EXPERIMENTAL and THEORETICAL STUDY OF CO_2^- POTENTIAL SURFACES

R.L.C. WU and T.O.TIERNAN, Brehm Lab., Wright St. Univ., Dayton, OH 45435 and E.S. SACHS and D.G. HOPPER Theoretical Chem. Div., Science Applications, Inc., 4124 Linden Avenue, Dayton, OH 45432

The ground and excited state potential surfaces of CO_2^- and their relationship to the CO_2 ground state surface have been studied. Experimental (in-line tandem mass spectrometric) studies of the endothermic charge transfer processes $YO^-(CO_2,YO)CO_2^-$,$YO^-=O_2^-$, NO^-,O^-OH^-, yield several thresholds for CO_2^-. These thresholds correspond to electron affinity values of -0.30±0.1 eV (1st O_2^-,NO^- threshold), -0.97±0.1 eV (1st O^-,OH), and -4.19±0.1 eV (2nd O_2^-,O,OH^-). Theoretical (ab initio) MCSCF/CI and SCF electronic structure) studies yield the $CO_2^-(X^2A_1)$ geometry as R(C-O)=1.26A and θ(O-C-O)=134°. The vertical electronic spectrum of CO_2^- has been computed and will be used to interpret and assign the experimental results. The combined results have enabled the intersection locus of surfaces for the $X\Sigma_g^+(^1A')$ states of CO_2 and CO_2^-, respectively to be located.

LASER PHOTODETACHMENT OF CHLORINE MOLECULAR NEGATIVE IONS

R. O. Daubach and John R. Eyler

Department of Chemistry, University of Florida,
Gainesville, Florida 32611

The photodetachment of chlorine molecular negative ions ($h\nu + Cl_2^- \rightarrow Cl_2 + e^-$) has been studied from 460-630 nm using our pulsed ion cyclotron resonance (icr) mass spectrometer and a flash-lamp pumped dye laser system. The chlorine molecular negative ion was formed by charge transfer from NO_2^- according to the scheme

$$e^- + CH_3NO_2 \rightarrow CH_3 + NO_2^- \quad (1)$$

$$NO_2^- + Cl_2 \rightarrow Cl_2^- + NO_2. \quad (2)$$

The delay between the end of the grid pulse (formation of NO_2^-) and laser irradiation and subsequent detection of Cl_2^- was varied to determine the effects of collisions on the cross-section for photodetachment.

To establish that the photodestruction process observed was actually photodetachment a double resonance experiment was performed. In this experiment, the background Cl^- ions were brought into resonance and then ejected from the cell using a second oscillator (ω_2). Cl^- ions formed by photodestruction should, however, be observed. The results over the entire wavelength region (maximum Cl_2^- decrease ~10%) showed no photoproduction of Cl^-.

We believe that the Cl_2^- ions in our experiments possess very little internal energy because they are formed by a reaction which is only slightly exoergic and they undergo many ion-neutral collisions before laser excitation. This may help explain our observation of photodetachment rather than photodissociation for the Cl_2^-. In addition, we observe structure in certain regions of our photodestruction vs. wavelength curves. We are continuing our investigations of this molecule and other X_2^- and XY^- systems (X, Y = halogens).

NEGATIVE ION-MOLECULE REACTIONS IN SULFURYL HALIDES

Richard Robbiani* and J. L. Franklin
Department of Chemistry, Rice University, Houston, Texas

Reactions of negative ions in SO_2Cl_2, SO_2F_2 and SO_2ClF have been studied at ambient temperatures in a sector field mass spectrometer. A conventional ion source equipped to measure ion intensities as a function of either pressure or retention time was employed.

SO_2Cl_2 exhibited two resonance regions: one, having a maximum at about 2 eV electron energy, produced only Cl^- and Cl_2^- in the ratio 10:1 as primary ions; the second, having a maximum at about 5.5 eV electron energy, produced SO_2^-, Cl^- and Cl_2^- in the ratio 5:4:1 as primary ions. Any other primary ions were formed in amounts too small to be detected.

With increasing pressure and/or retention time Cl^- decreased in intensity forming both Cl_3^- and SO_2Cl^-. The latter reacts further to form Cl_3^-. Either Cl_3^- or SO_2Cl^- (or both) appear to form $SO_2Cl_3^-$. Unfortunately, the origin of $SO_2Cl_3^-$ could not be definitely established. Small amounts of $SO_2Cl_2^-$ also are formed, probably by charge exchange from Cl_2^-. In the higher energy resonance region SO_2^- also reacts rapidly, primarily to form Cl^-.

The rates of the principal reactions were measured by varying both pressure and retention times with results as follows:

	10^{10}, $cm^3\ sec^{-1}$	
$Cl^- + SO_2Cl_2 \rightarrow Cl_3^- + SO_2$	3.0	(1)
$Cl^- + SO_2Cl_2 \rightarrow SO_2Cl^- + Cl_2$	11.0	(2)
$SO_2Cl^- + SO_2Cl_2 \rightarrow Cl_3^- + 2SO_2$	7.5	(3)
$SO_2^- + SO_2Cl_2 \rightarrow Cl^- + SO_2 + SO_2Cl$	50.0	(4)

By adding SO_2 to SO_2Cl_2 in different proportions at elevated source pressures and varying the retention time, the equilibrium constant for reaction (1) was determined and from this $\Delta G(1)$ was found to be 0.86 kcal/mol. Assuming $\Delta S \approx 0$, we then compute $\Delta H_f(Cl_3^-)$ to be -71.8 kcal/mol. From the various reactions in which they are involved, we estimate $\Delta H_f(SO_2Cl^-)$ to be approximately -135 kcal/mol and $\Delta H_f(SO_2Cl_3^-)$ to be between -149 and -157 kcal/mol.

At an electron energy of 3.5 eV the primary ions formed in SO_2F_2 are F^-, F_2^- and SO_2F^- in the ratio 72:14:14. The SO_2F^- ion appears to be completely unreactive. The principal product is $SO_2F_3^-$ formed by the reactions

$$F_2^- + SO_2F_2 \rightarrow SO_2F_3^- + F \qquad (5)$$

$$F^- + SO_2F_2 \xrightarrow{M} SO_2F_3^- \qquad (6)$$

The rates of these reactions were found to be, respectively, 8.6×10^{-11} $cm^3\ mol^{-1}\ sec^{-1}$ and 1.3×10^{-27} $cm^6\ mol^{-2}\ sec^{-1}$. At pressures above about 0.02 Torr small amounts of $SO_2F_2^-$ were detected, probably by charge transfer from F_2^-.

The primary ions in SO_2ClF at an electron energy of 3.2 eV are F^-,

---

*Present address: Laboratorium für Org. Chemie, ETH-Zentium, CH-8092, Zurich, Switzerland.

Cl^-, SO_2Cl^- and FCl^- formed in the ratio 56:38:3:3. Both F^- and Cl^- react to form SO_2F^-. The F^- also forms Cl^- at a rather slow rate. FCl^- also disappears slowly by a reaction that could not be identified. The important reactions then are

$$F^- + SO_2ClF \rightarrow SO_2F^- + ClF \quad (7)$$

$$Cl^- + SO_2ClF \rightarrow SO_2F^- + Cl_2 \quad (8)$$

$$F^- + SO_2ClF \rightarrow Cl^- + SO_2F_2 \quad (9)$$

The rate of disappearance of F^- is given by the sum of the rate constants for reactions (7) and (9) and was found to be 2.1×10^{-9} $cm^3\ mol^{-1}\ sec^{-1}$. The data were not sufficiently reliable to permit the separate determination of these rate constants or of k_8.

Beauchamp[1] reported reaction (1) and Sullivan and Beauchamp[2] reported several reactions in SO_2F_2, SO_2FCl and SO_2Cl_2. Their results and especially the primary ions and their ratios differed considerably from ours. In their investigations they employed an ICR spectrometer with a 70 eV electron beam for primary ionization. Their negative ions were formed by attachment of thermalized secondary electrons to the molecule being studied. Our ions, on the other hand, were formed by more energetic electrons and thus were formed with more energy than were theirs. As a result, where Sullivan and Beauchamp[2] found SO_2Cl^- to be a major primary ion in SO_2Cl_2, we found none. Presumably, the larger amount of energy imparted by the electron in our studies was sufficient to cause the SO_2Cl^- to dissociate to form additional Cl^-. The differences in electron energy probably account for other differences in the primary ion spectra. Further, the primary ions in our system must have been formed with considerable kinetic and/or vibrational energy and this could account for the different ion-molecule reactions observed in the two laboratories.

We wish to express our gratitude to The Robert A. Welch Foundation for support of this research. One of us, R.R., is indebted to the ETH-Zurich for the award of a travel grant.

References

1. J. L. Beauchamp, "Interactions Between Ions and Moles", P. Ausloos, ed., Plenum Press, New York, N.Y., 1975, p. 442.

2. S. A. Sullivan and J. L. Beauchamp, Int. J. Mass Spectrom. Ion Phys., 28, 69 (1978).

THERMOCHEMISTRY AND STRUCTURE OF MOLECULAR NEGATIVE ION NO_3^-

Richard L. C. Wu and Thomas O. Tiernan
The Brehm Laboratory and Department of Chemistry
Wright State University
Dayton, Ohio 45435

The molecular negative ion NO_3^- plays a significant role in the negative ion chemistry of the D-region of the ionosphere.[1] The thermodynamic properties of this ion clearly affect its reactivity with various neutral species, and consequently, are important in determining the concentrations of gaseous ions in the earth's lower ionosphere. There is still considerable controversy and uncertainty with respect to the bond dissociation energy, heat of formation of this ion and the electron affinity of the neutral NO_3. Also, there is some indication that excited state of NO_3^- [1,2] exist, but the evidence for this is still not definite. The purpose of this paper is to present new experimental results bearing on the formation and energetics of the ground and excited states of NO_3^-. The experimental techniques employed here involve measurements of the thresholds for collision-induced dissociation (CID) of this ion upon impact with inert target gases. The CID method has previously been shown to be useful in detecting the presence of an excited state of O_3^-.[3] Also, several previous reports from our laboratory[4-6] have shown that reliable bond dissociation energies and ionic heats of formation can be obtained from such measurements.

An in-line tandem mass spectrometer, previously described[7] was used in the present study. The NO_3^- projectile ion was formed from two different gaseous mixtures. Electron impact on gaseous mixtures of O_3 and N_2O was employed in the first case, while a mixture of O_3 and NO was used in the second instance. Corrections of the measured translational energy thresholds were made to take account of the projectile ion energy spread and the Dopple motion of the neutral target. These correction procedures have been described previously.[5]

Excitation functions were obtained for various reaction channels for collision induced dissociation (CID) of NO_3^- on Ar. The cross sections and observed thresholds are found to be markedly dependent upon the method of formation of the NO_3^-. When NO_3^- was produced from electron impact on gaseous mixture of O_3 and N_2O, the translational energy thresholds for CID yield the bond dissociation energies of $D_0^\circ(O^- - NO_2) = 4.8 \pm 0.1$ eV, and $D_0^\circ(NO_2^- - O) = 3.8 \pm 0.1$ eV. These bond dissociation energies along with the heats of formation of O^-(1.12 eV)[8], O(2.582 eV)[8] NO_2(0.344 eV)[8], NO_3(0.76 eV)[9] yield the values of -3.3 ± 0.1 and -3.26 ± 0.1 eV respectively for the heat of formation of NO_3^- and yield the values of 4.16 ± 0.15 and 4.02 ± 0.15 eV respectively for the electron affinity of the NO_3 molecule. However, the NO_3^- ion formed by electron impact on gaseous mixture of O_3 and NO, exhibits much lower dissociation energies, $D_0^\circ(O^- - NO_2) = 1.8 \pm 0.15$ eV and $D_0^\circ(NO_2^- - O) = 1.0 \pm 0.1$ eV. This observation suggests that an excited state of NO_3^-* is formed in the latter case. The lifetime of this state must be on the order of several microseconds, since this is the transit time required for the ions to traverse the region from the ion source to the collision chamber. The heat of formation of this excited state of NO_3^- is calculated from the above two observed dissociation thresholds to be -0.34 ± 0.2 and -0.44 ± 0.15 eV respectively. The error limits are estimated on the basis of the ranges of calculated threshold functions which yielded a good fit to the experimental data. The typical excitation functions for the NO_3^-/Ar reactions for the ground and the excited states are shown in Figure 1.

A more detailed description of this study will be submitted for publication in the Journal of Chemical Physics.

Acknowledgment

This work was supported by the Air Force Office of Scientific Research under Contract F44620-76-C-007 with Wright State University.

References

1. E. E. Ferguson, D. B. Dunkin, and F. C. Fehsenfeld, J. Chem. Phys. 57, 1459 (1972).
2. J. T. Moseley, P. C. Cosby, J. R. Peterson and G. P. Smith, paper MA-7, 30th Annual Gaseous Electronics Conference, Palo Alto, CA (1977).
3. R. L. C. Wu, T. O. Tiernan, and C. Lifshitz, Chem. Phys. Lett. 51, 211 (1977).
4. T. O. Tiernan and R. L. C. Wu, Adv. Mass Spectrom. 7A, 136 (1978).
5. C. Lifshitz, R. L. C. Wu, T. O. Tiernan and D. T. Terwilliger, J. Chem. Phys. 68, 247 (1978).
6. D. G. Hopper, A. C. Wahl, R. L. C. Wu and T. O. Tiernan, J. Chem. Phys. 65, 5475 (1976).
7. T. O. Tiernan, B. M. Hughes and C. Lifshitz, J. Chem. Phys. 55, 5692 (1972).
8. J. L. Franklin, J. G. Dillard, H. M. Rosenstock, J. T. Herron, K. Drexel and F. H. Field, Ionization Potentials, Appearance Potentials and Heats of Formation of Gaseous Positive Ions, (U. S. Department of Commerce, NBS, Washington, D. C. (1969).
9. R. A. Graham and H. S. Johnston, J. Phys. Chem. 82, 254 (1978).

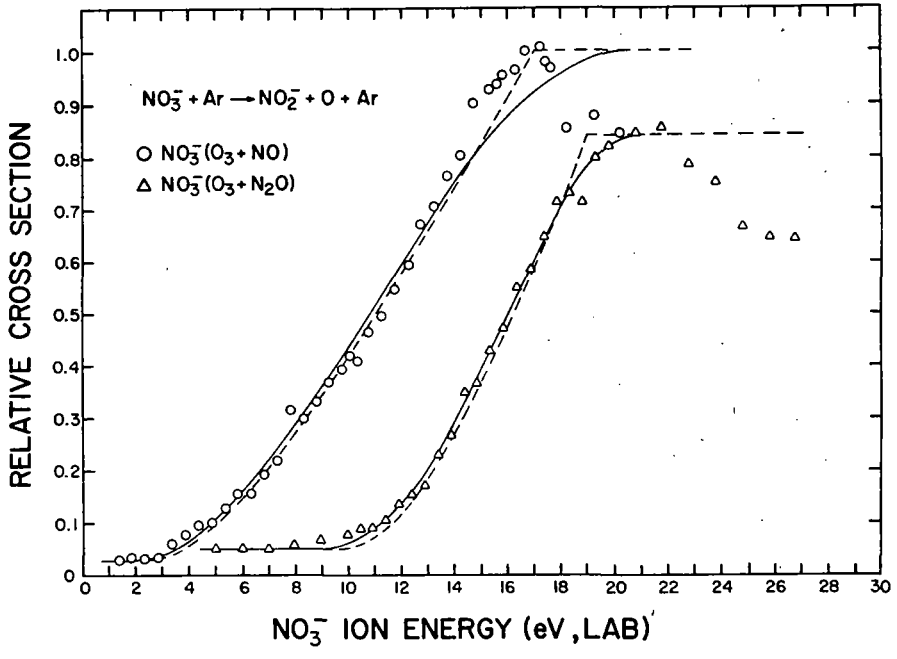


Figure 1. Relative cross section for the reaction NO_3^- + AR → NO_2^- + O + Ar as a function of translational energy. Δ-experimental data for NO_3^- from O_3 and N_2O; O-experimental data for NO_3^- from O_3 and NO. Solid lines are the calculated "best fit" excitation functions.

MAMOC7 ENHANCEMENT OF ELECTRON CAPTURE DETECTOR SENSITIVITY TO NON-ELECTRON ATTACHING COMPOUNDS USING N_2O CARRIER GAS DOPING, M. P. Phillips,[1] P. D. Goldan, R. Sievers,[1] and F. C. Fehsenfeld, Aeronomy Laboratory, NOAA/ERL, Boulder CO 80303

The response of the electron capture detector (ECD) to compounds such as N_2O depends not only on the initial attachment process but to the subsequent negative ion chemistry as well. This can be understood from the low pressure negative ion chemistry of N_2O.[2] Any compound that reacts with O^- or NO^- can increase the effective rate of attachment of electrons to N_2O. Because of this, the sensitivity of the ECD to N_2O can be increased by the presence of compounds such as H_2O and CO_2 in the ECD. By the same token, enhancement of ECD response has been observed for compounds that do not attach electrons such as CO_2, H_2, and CH_4 with N_2O in the ECD. The ion chemistry responsible for this will be described, the uncertainty that this chemistry places on atmospheric N_2O measurement using gas chromatography with ECD will be discussed, and the potentials and limitations of the technique for the detection of certain atmospheric trace gases will be outlined.

1. Chemistry Dept., Colo. Univ. Boulder CO
2. J. Chem. Phys. 58, 3267 (1973).

THE REACTION OF 2,3,7,8-TETRACHLORODIBENZO-P-DIOXIN IN AN OXYGEN RICH PLASMA AT ATMOSPHERIC PRESSURE

R. K. Mitchum and G. F. Moler
Department of Health, Education, and Welfare
Food and Drug Administration
National Center for Toxicological Research
Jefferson, AR 72079

Atmospheric Pressure Ionization Mass Spectrometry has been shown to be a very sensitive technique for the detection and quantitation of trace amounts of various organic residues[1]. The applicability of Negative Ion Atmospheric Pressure Ionization (NIAPI) Mass Spectrometry for the identification and quantitation of trace amounts of 2,3,7,8-tetrachlorodibenzo-p-dioxin (I) in fish has been explored.

The Atmospheric Pressure Ionization Mass Spectrometer vacuum housing was fabricated by Extranuclear Laboratories, Inc. and has been described[1a]. The system consists of an Atmospheric Pressure Ionizer utilizing a 1 mCi ^{63}Ni foil as the primary electron source. The source in flange mounted on a differentially pumped vacuum chamber housing the low pressure ion optics, quadrupole mass analyzer, and continuous dynode electron multiplier assembly. The ion source temperature was constant at 250°C with a carrier flow rate of 20 cc/min measured with an electronic flow cell (Matheson-LF-100).

GC/NIAPI analyses were performed with a Hewlett Packard 5700A gas chromatograph interfaced directly using 1/16 inch glass lined tubing connected to an auxillary port on the API ionizer. The nitrogen GC carrier was made up with 3% oxygen prior to ionization of the column effluent. A split of 2:1 based upon the ionizer throughout of 18 cc/min was maintained throughout the experiments to obtain a good GC resolution. The chromatographic column was packed with (glass 6 ft. X 1/4 inch) Dexil-300 on 80/100 mesh chromasorb-W.

The unique ion molecule reaction reported by Hunt[2] resulting in the formation of the 4,5 dichloro-1,2-benzoquinone anion was found to be the only detectable product anion formed in a 3% oxygen/nitrogen plasma. The predominant pathway under oxygen free conditions was found to be dissociative electron capture to I forming Cl^-. Two methods have been employed to introduce samples into the API ionizer. Direct insertion of the sample deposited on a platinum wire and via a gas chromatograph interface.

The detection sensitivity for I under oxygen rich conditions using direct insertion of the sample and monitoring only m/e 176 was found to be 5 pg with a signal to noise ratio of 4:1. The detection sensitivity for I using the GC interface was found to be 30 pg with a signal to noise ratio of 3:1.

The cleanup methodology used for the direct insertion analysis consisted of foam charcoal chromatography[3] of a neutral fish extract followed by silica gel HPLC, collecting the fraction corresponding to I and chromatographing on a C-18 reverse phase HPLC column, again collecting the fraction corresponding to I. Although this cleanup gave recoveries[4] of 70-80%, the cleanup was insufficient to allow direct probe analysis via NIAPI. The matrix components which co-chromatograph with I appear to have a higher electron affinity than either I or O_2. With rigorous cleanup using HPLC or conventional methodology[5] the GC/NIAPI/MS technique is the most useful. In the fish matrix no ions were found which interfere with the analysis monitoring m/e 176 (naturally occuring) or m/e 182 (carbon-13 labeled I).

1. a) M. W. Siegel and M. C. McKeown, J. Chrom., 122, 397 (1976); b) D. I. Carrol, I. Dzidic, R. N. Stillwell, M. G. Horning, and E. C. Horning, Anal. Chem., 46, 706 (1974) c) E. C. Horning, D. I. Carrol, I. Dzidic, S. N. Lin, R. N. Stillwell and J. P. Thenot, J. Chrom., 142, 481 (1977).

2. D. F. Hunt, M. T. Harvey and J. W. Russell, J. C. S. Chem. Comm., 151 (1975).

3. J. N. Huckins, D. L. Stalling and W. A. Smith, J. A. O. A. C., 61, 32 (1978).

4. Based upon fish spiked with Octachlorodibenzodioxin.

5. O'Keefe, J. A. O. A. C., 61, 621 (1978).

Advantages of Negative Ion-MS for Analysis of Pentafluorobenzyl-Phenyl Ethers

G.R. Dubay, D.L. Stalling, J.D. Petty, and L.M. Smith, Columbia National Fishery Research Laboratory, Columbia, MO 65201

Phenols are manufactured in large quantities for use in herbicides, fungicides, wood preservatives, and as intermediates for many industrial processes. The acute toxicity of phenols to fish and mammals is well documented. Though phenols are ubiquitous at varying levels within the environment, there are few general, yet sensitive methods for analysis of the wide range of phenols produced each year. An analytical method is needed which yields, first, good chromatographic separations; second, high and consistent sensitivity for routine analysis by GC; and third, high selectivity for molecular identification or confirmation by MS.

To provide these features we studied 9 of the 11 EPA consent decree phenols as part of an EPA/FWS interagency agreement. The phenols were separated with gel permeation chromatography from lipid interferences found in spiked fish extracts and isolated from neutral and basic contaminants using silica gel modified with CsOH. Derivatization with pentafluorobenzyl bromide made the pentafluorobenzyl (PFB)-phenyl ethers which enabled us to meet the first two criteria set out. PFB-phenyl ethers have a rather uniform yet highly sensitive response to electron capture/GC detection because of the pentafluorobenzyl moiety. Those ethers also chromatograph well using 6 ft glass columns packed with 1.5% SP 2250/1.95% SP 2401. Thus, when coupled with a specific and sensitive mode of MS analysis this method offers specific advantages.

Electron impact (EI) and positive chemical ionization (PCI) analysis have insufficient sensitivity for low level detection. Ions characteristic of the PFB-phenyl ethers or the phenolic groups are not present for a majority of the ethers below the 20 ng level using EI or PCI-MS. Sensitivity for the 10 different ethers (one is an internal standard) varies greatly in both EI and PCI-MS. The base peak in the EI spectra of all the PFB-phenyl ethers is the ion at 181 AMU representing the PFB functionality (Table 1). Thus, EI and PCI-MS are not good analytical tools for the identification or confirmation of PFB-phenyl ethers.

We have found that PFB-phenyl ethers form characteristic negative ions which can be detected at very low levels. Ionization of PFB-phenyl ethers in a methane plasma (recommended CI conditions) give negative ions, probably resulting from an electron capture process. The base peak for all PFB-phenyl ethers studied is the negative ion of the phenolic group (table 1). No other ion in the spectra has an intensity greater than 15% of the base peak. The consistency of this ionization process for negative ions provides a nearly uniform sensitivity.

Detection of negative ions of PFB-phenyl ethers is at least 1000 times more sensitive than either EI or PCI-MS analysis. Using the standard negative ion option for our Finnigan-4023 GC-MS, these samples were analyzed using full scan spectra from 50 to 650 AMU with a 6 ft 1.5% SP 2250/1.95% SP 2401 Supelcoport 100/120 mesh glass packed column. Under recommended CI source conditions the ion characteristic of the phenol group for all phenols was observed for 50 pg samples of each. Detection of 100 pg is possible for routine analysis when acquiring full scan spectra for a complex residue sample.

Our study, thus, demonstrated analysis of PFB-phenyl ethers by negative ion MS is more sensitive than analysis by EI or PCI-MS. When coupled with our separation of phenols using CsOH modified silica gel, the method advances the analysis of EPA consent decree phenols.

Table 1

Pentafluorobenzyl-Phenyl Ethers

Phenyl R Group	MW	Phenyl Mass	Base Peak EI	Base Peak PCI	Base Peak NI
H	274	93	181	275	93[c]
Dimethyl	302	121	181	303	121[c]
Chloro	308	127	181	181	127[c]
Nitro	319	138	181[a]	183	138[c]
Chloromethyl	322	141	181	323	141[c]
Dichloro	342	161	181	181[b]	161[c]
Trichloro	376	195	181	181[b]	195[c]
Iodo	400	219	181	181[b]	219[c]
Pentachloro	444	263	181	181[b]	265[c]

[a] No Molecular Ion at 30 ng level

[b] No Molecular or pseudomolecular ion at 120 ng sample

[c] No Molecular ion at 0.5 ng level

POSITIVE/NEGATIVE CHEMICAL IONIZATION MASS SPECTROMETRY OF MYCOTOXINS,
W.C. BRUMLEY, J.A.G. ROACH, P.A. DREIFUSS, D. ANDRZEJEWSKI, and J.A. SPHON,
Division of Chemistry & Physics, Food & Drug Administration, Washington,
DC 20204

Mycotoxins are a structurally diverse class of compounds of widely varying toxicity which are known to contaminate foods. Electron impact mass spectrometry (EIMS) has proved effective for the identification of many of these compounds. Positive and negative chemical ionization MS (CIMS) has now been applied successfully to the identification of mycotoxins. The aflatoxins give predominantly $(m+H)^+$ ions with CH_4 as the reagent gas by proton transfer and $M^{-\cdot}$, $(M-1)^-$, and $(M-15)^-$ ions by resonance electron capture (REC). Ochratoxins, versicolorins, and related compounds give abundant $M^{-\cdot}$ and $(M-1)^-$ ions by REC. Trichothecenes frequently produce a low abundance of molecular ions by EIMS and do not undergo significant ionization by REC. However, they may be ionized with little fragmentation using OH^- as the reagent ion. Additionally, the trichothecenes show a remarkable affinity for producing negative ion attachment spectra especially with chloride ion as the attachment reagent species.

A probe and a current control unit for field desorption activated emitters have been constructed to facilitate the introduction of samples into a chemical ionization source. Emitter orientation affects the ion output of the source. Sample introduction on an emitter permits low temperature ionization when a Townsend Discharge is used to generate reagent ions in the source. Activated emitters are superior to the conventional solids probe for the introduction of thermally labile mycotoxins.

SURVEY OF CHEMISTRY DEPARTMENT MASS SPECTROMETRY SERVICE FACILITIES IN THE UNITED STATES AND CANADA

Robert D. Minard and Fred W. Lampe

Department of Chemistry
Pennsylvania State University
University Park, PA 16802, U.S.A.

This survey was initiated in order to answer some questions about the operations of the mass spectrometry service facility at Penn State's chemistry department relative to similar operations at other universities in the U.S. and Canada. Forty-seven university chemistry departments were contacted and 30 supplied information. These were Alberta (A. M. Hogg), Brit. Columbia (G. Eigendorf), U. of Cal., Santa Barbara (M. Bowers), Caltech (J. Mitchell), Carnegie Mellon (R. M. Montgomery), Cornell (T. Wachs), Delaware (B. Munson), Harvard (B. P. Stimpson), Illinois (J. C. Cook), Indiana (L. Phillips), Iowa State (H. J. Svec), Johns Hopkins (W. S. Koski), Kansas (R. Drake), MIT (K. Biemann), Mich. State (J. G. Funkhouser), Minn. (R. A. Upham), Nebraska (P. Lyons), Ohio State (C. R. Weisenberger), Ottawa (J. Krause), Penn State, Pittsburgh (G. J. Meisner), Princeton (D. Nordlund), Purdue (R. G. Cooks), Rockfeller (F. H. Field), Toronto (A. G. Harrison), Utah (J. Futrell), Virginia (D. Hunt), Washington (M. Higgins), Wayne State (L. Kevan), Yale (D. O. Traficante).

Information on the following topics was elicited by letter and/or questionnaire. Not all respondents supplied information on all topics. In some cases additional information was included by other contacts.

I. MODELS AND AGES OF INSTRUMENTS AND DATA SYSTEMS (32 FACILITIES)

Format of information: Instrument manufacturer (# instruments; average age) [# data systems; average age] age is in years.

AEI-KRATOS (27; 11.1) [10; 6.8], VARIAN MAT (14; 4.7) [7; 3], FINNIGAN-INCOS* (9; 4.5) [5 and 3*; 4 and 2.5*], DUPONT (7; 6.5), HITACHI (6; 6), VG-MICROMASS (3; 2.6) [3; 2.3], LKB (2; 9), CEC (2; 14), OTHER (9; 12) [7; 3.5], OVERALL (79; 8.2) [35; 4.3].

II. TOTAL SAMPLE DISTRIBUTION (27 FACILITIES)

This is the total number of samples analyzed per year in each facilitiy including low resolution, high resolution, gc-ms, EI and CI FD, spark source and isotope ratio.

Data format: Range of total samples/year (number of facilities in this range; average no. of instruments/facility; average total samples/instrument for this group).

100-399 (4; 1.25; 218)	2200-2499 (0)
400-699 (3; 1.33; 374)	2500-2799 (2; 4; 673)
700-999 (2; 1.5; 494)	2800-3099 (1; 1; 3043)
1000-1299 (2; 1.0; 1043)	3100-3399 (1; 5; 662)
1300-1599 (5; 2.2; 660)	3400-3699 (0)
1600-1899 (13; 23; 746)	3700-3999 (0)
1900-2199 (3; 3.7; 541)	4000-4299 (1; 2; 2000)

III. SAMPLES/USER DISTRIBUTION

Using the A.C.S. "Directory of Graduate Research," the number of active research groups (organic, biochem., inorganic-organometallic,

analytical and at times, physical) that would probably use a mass spec. facility was determined for each chemistry department. This was 47.8% overall of the 786 active research faculty listed. The overall average was 108 samples per faculty user per year with the distribution as shown below.

1-25 samples/user/year: 2 facilities, 26-50: 3, 51-75: 3, 76-100: 4, 101-125: 6, 126-150: 3, 151-175: 2, 176-200: 1, 201-225: 0, 226-250: 1, 251-275: 0, 276-300: 1.

IV. GC-MS ANALYSIS

Of 27 facilities reporting, 19 offer gc-ms service. Because some facilities ran so few samples by gc-ms, we have selected 8 facilities based upon these criteria: 1) Separate gc-ms instruments; 2) Over 1300 total samples/year; 3) No known contract work. For this selected group the number of samples analyzed by gc-ms averaged 10.7% of all low resolution samples. The percentages for each facility were distributed as follows: 4.5%, 4.7%, 8.3%, 10.4%, 11%, 11%, 16.6%, 19%.

V. HIGH RESOLUTION ANALYSES

Twenty-two of the 27 facilities reporting this information offered high resolution analysis. Nine out of 27 used peak matching and these 9 analyzed 24% of all samples by this method. Thirteen of the twenty-seven reported that their high resolution analyses (19% of all samples) were done by computer. For 14 facilities running over 1300 total samples/year, the average percentage analyzed by high resolution was 17.4%.

VI. DOWNTIME

Facilities were asked how many days/year that they were unable to offer the full capabilities of their labs. There were 3 categories of downtime:

A. Maintenance: 12.8 days/year average (19 labs reporting, the range was 2-30 days)

B. Mechanical or Electronic Failure: 44.1 days/year (20 labs, range was 3-210). For 14 breakdowns described explicitly, 7 were due to mass spec. failure, 4 due to data system failure and 3 due to Acts of God.

C. Development Work-System Improvements: 12.7 days/year (18 labs, range 0-77)

There appeared to be little correlation with number of instruments or samples.

VII. SAMPLE TURN-AROUND TIME

Twenty-one facilities reported an average time of 2.1 days between the submission of sample for low resolution E.I. analysis and the completion of the request. This average turn-around time was 10 days for high resolution E.I. (13 labs reporting), 2.9 days for gc-ms (8 labs), 3.3 days for low res. C.I. (4 labs), and 5 days for FI/FD (2 labs).

VIII. STAFFING

Twenty-eight facilities had a total of 50 personnel directly involved with their operation. This averages .76 staff/instrument. For 36 facilities where degree information was given, 21 Ph.D.'s, 3 M.S.'s and 12 B.S.'s were involved; 13/28 had one or more full-time technicians in addition to a supervisor.

IX. ANALYSIS CHARGES

Sixteen out of twenty-eight facilities charge for mass spec. analysis. Using the assumption that a low res. analysis requires 0.5 hr.

and a high res. analysis requires 1.0 hr. in order to equate hourly and per sample charges, the following averages were calculated:

A. Low Resolution Analysis (14 labs): $13.87/sample - range = $2.50 to $40.00

B. High Resolution Analysis (13 labs): $22.37/sample - range = $2.50 to $75.00

C. GC-MS Analysis (10 labs): $27.13/sample - range = $5.00 to $50.00

Charges for samples from outside the department were often 2 to 4 times as much.

X. DISTRIBUTION OF THE SAMPLE MOLECULAR WEIGHTS

Facilities were asked what percentage of all samples had molecular weights above 800. The following distribution for 20 labs is found: 5 labs = 0%, 2 labs = <1%, 3 labs = ∿1%, 1 lab = 2%, 2 labs = ∿3%, 1 lab = 8.4%, 5 labs = ∿10%, 1 lab = ∿20%. Overall average = ∿4.6%.

XI. PLANS FOR THE FUTURE

Eighteen facilities had ordered or hoped to order new mass spectrometers. Twelve desired new or expanded data systems. Six planned to upgrade old electronics, 4 wanted to add CI to their capabilities, 3 wanted a high field or fast scanning magnet and 2 each planned introduction or development of FD, Laser, LC-MS, or pyrolysis. Other plans mentioned singly included glass capillary gc-ms, high res. gc-ms, increased charges, metastable scanning, more staff, positive-negative ion, turbopumps, and triple quad.

ACKNOWLEDGEMENTS. The authors extend their heartfelt gratitude to those who took time to reply to our questionnaire. We hope your plans for the future materialize. We would also like to thank Carla Hofland for her help in this project.

MAMP1 GC-MS Determination of Urinary Polyamines During Treatment of Acute Leukemia. M.D. DENTON, B. FINLEY, E.J. NORMAN, Univ. of Cincinnati College of Medicine, Cincinnati, OH 45267

The polyamines are intracellular amines which are found in all proliferating cells. Urinary polyamine levels reflect responses to chemotherapy for neoplastic disease. We are using GCMS with multiple ion monitoring of the heptafluorbutyryl derivatives to follow patients with acute leukemia during induction therapy. Patients with objective responses have shown marked changes in one or more of the urine polyamines studied (spermidine, spermine, acetylspermidine or the precursor diamine putrescine). Peak responses correspond to the peak action of an active drug. This may allow determination of the more effective drugs in a multidrug regimen and therefore allow adjustment of a chemotherapeutic program according to the susceptibility of an individual's leukemic cells. This would allow avoidance of unnecessary toxicity from drugs ineffective in a particular patient We believe the specificity and sensitivity of mass spectrometry are necessary for proper detection of the relevant changes during chemotherapy for acute leukemia.

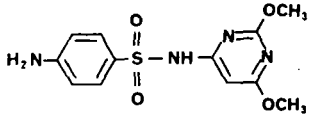
A gc-picims Stable Isotope Dilution Method for the Determination of Sulfadimethoxine in Cattle and Swine Livers and Kidneys at the 0.1 ppm Regulatory Limit

B. J. Hodshon, W. A. Garland
G. Chen*, G. Weiss*, and A. MacDonald*

Departments of Biochemistry and Drug Metabolism
and *Animal Health Research

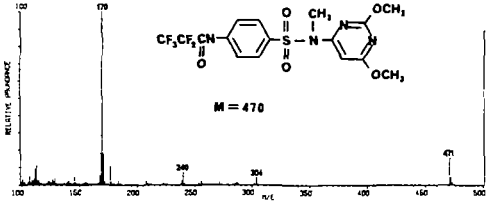
Hoffmann-La Roche Inc., Nutley, NJ 07110

Sulfadimethoxine (SDM) is a long acting sulfonamide used for the treatment of bacterial infections in various food producing animals. Federal regulations limit sulfonamide residues to a maximum of 0.1 ppm in edible meats.



SDM

Currently, a Bratton-Marshall colorimetric procedure is used to monitor SDM levels in tissues. Since a colorimetric procedure potentially lacks specificity, a gc-cims assay was developed to confirm the data from the Bratton-Marshall procedure. The developed assay features the addition of 0.2 ppm of a deuterated analog of SDM (SDM-d_6) to the tissue homogenate before processing by a previously published method[1]. The extract from the processed sample is treated consecutively with diazomethane and pentafluoropropionic anhydride and is then analyzed by gc-cims. Isobutane is used as gc carrier gas and as ci reagent gas (.3 Torr). The gc column, 5 ft x 2 mm id, is packed with 3% OV-17 *on Gas Chrom Q*. *The isobutane mass spectra of derivatized SDM and SDM-d_6* are characterized by relatively intense MH^+ ions. The base peak of both spectra is an ion which corresponds to the elements of protonated 4-methylamino-2,6-dimethoxy-pyrimidine.



For the assay, a Finnigan 3200 quadrupole mass spectrometer is set to monitor m/e 477, 471, 176 and 170 in the gc effluent.

SDM-d_6 is used in the assay to both verify the presence of SDM and to determine the drug's concentration. Three criteria must be satisfied for verification of the presence of SDM.

1. The retention time of SDM must be identical to the retention time of SDM-d_6.

2. The peak width at half height of the SDM m/e 471 ion must be the same as the peak width at half height of the m/e 477 ion from SDM-d_6.

3. The ratio of the m/e 170 to m/e 471 ions from SDM must be within 10% of the m/e 176 to m/e 477 ion ratio from SDM-d_6.

Quantitation of SDM is based on a comparison of the intensity of the m/e 471 to m/e 477 ions. The m/e 471 to m/e 477 ion ratios vs concentration data obtained from the analysis of samples spiked with 0.2 ppm of SDM-d_6 and either 0, 0.05, 0.1, 0.2, 0.4 or 0.8 ppm of SDM are subjected to a linear regression analysis. The slope (m) and its standard derivation (SD_m) and the intercept (b) and its deviation (SD_b) from the regression analysis are used to predict, employing the equation $R_L = (m-2SD_m)(0.1) + (b-2SD_b)$ an ion ratio limit (R_L), which if exceeded in an unknown sample spiked with 0.2 ppm of SDM-d_6, establishes that the sample is in violation of the legal 0.1 ppm residue limit. By using slope and intercept parameters which are two standard deviations below those determined by linear regression analysis, the R_L value can be determined statistically at the 95% confidence level.

The isobutane ci mass spectra of the commonly used sulfonamides listed below all have a substantial MH^+ ion and a fragment ion analogous to SDM's m/e 170. The mass spectra and relative retention times on the same 3% OV-17 column are presented in the following table:

Sulfonamide	MW of methyl PFP derivative	Mass spectrum m/e(relative intensity)	Retention time relative to SDM
1. SDM	470	471 (26) 170 (100)	1.00
2. sulfaisoxazole	427	428 (80) 127 (100)	0.49
3. sulfabenz	408	409 (100) 108 (93)	0.51
4. sulfapyridine	409	410 (90) 109 (100)	0.55
5. sulfathiazole	415	416 (73) 115 (100)	0.56
6. sulfadiazine	410	411 (87) 110 (100)	0.68
7. sulfachloropyrazine	445	446 (88) 145 (100)	0.71
8. sulfamethazine	438	439 (44) 138 (100)	0.72
9. sulfaethoxypyridazine	454	455 (37) 154 (100)	0.89
10. sulfadoxine	470	471 (52) 170 (100)	0.92
11. sulfachloropyridazine	444	445 (16) 144 (100)	0.94
12. sulfamethoxypyridazine	440	441 (32) 140 (100)	0.96
13. sulfamethylphenazole	488	489 (32) 188 (100)	1.38
14. sulfaquinoxaline	460	461 (23) 160 (100)	1.58

With the synthesis of the appropriate stable isotope analog, it should be possible to use a modified version of the procedure we have described to specifically measure other sulphonamides besides SDM. This analytical approach could become the method of choice for the sensitive and specific determination of this class of drugs in biological matrices.

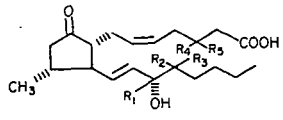
1. Fellig, J., Westheimer, J., J. Agr. Food Chem., 16, 738 (1968).

Determination of the Prostaglandin Analog TM-PGE_2 in Dog Plasma by Combined Capillary Column Gas Chromatography-Negative Ion Chemical Ionization Mass Spectrometry

B. H. Min, J. Pao, W. A. Garland, J. A. F. de Silva

Research Division
Hoffmann-La Roche Inc.
Nutley, New Jersey 07110

We report a quantitative method for the prostaglandin analog TM-PGE_2 (I) using capillary column gas chromatography-negative ion chemical ionization mass spectrometry with selected ion monitoring.

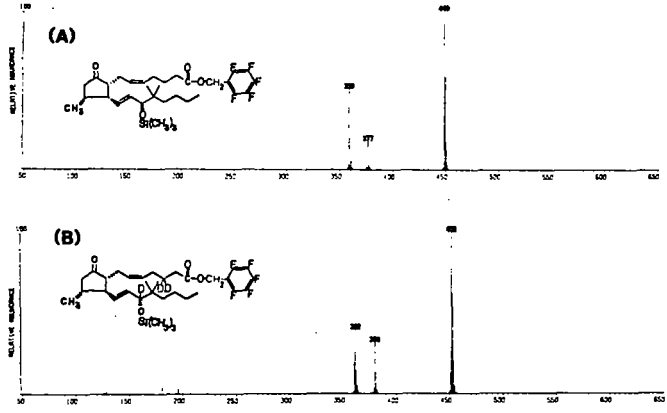


Compound	R_1	R_2	R_3	R_4	R_5
I	H	CH_3	CH_3	H	H
II	D	CH_3	CH_3	D	D
III	H	F	H	H	H

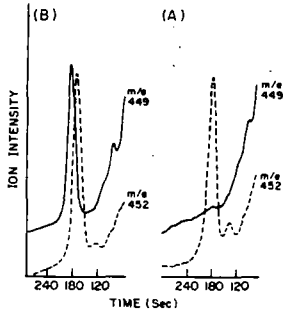
The compound to be determined, 2.5 ng of a trideuterated analog of TM-PGE_2(II) added as the internal standard, and 200 ng of a fluoro analog of TM-PGE_2 (III) added as a carrier were extracted from plasma buffered to pH 3 into a benzene-methylene chloride (9:1) solution. The residue from the extraction was derivatized with pentafluorobenzyl bromide and BSTFA and analyzed by capillary column gc-nicims.

The gc analysis was accomplished with a Finnigan model 9500 gc equipped with a 16 m x 0.5 mm id SE-30 SCOT column and a splitless injector. The effluent from the gc was coupled to a Finnigan 3200 quadrupole mass spectrometer which was modified to detect negative ions using the method of Stafford[2], i.e., the polarities of the ion source voltages were reversed and a conversion dynode was installed before the continuous dynode electron multiplier.

The methane nici mass spectra of derivatized I (A) and II (B) show no molecular anions. Intense fragment ions corresponding to the loss of pentafluorobenzyl radical can been seen at m/e 449 for I and m/e 452 for II. Smaller fragment ions corresponding to the loss of $(CH_3)_3$-SiOH and the loss of $CH_2 = Si(CH_3)_2$ from the base peak can be seen at m/e 359 and m/e 377 for I, and m/e 362 and m/e 380 for II. For the assay the m/e 449 and m/e 452 ions were monitored in the gc effluent.



Ion chromatograms from the assay of 1.0 ml of control plasma (A) and 1 ml of plasma from a dog who had received a 50 µg/kg i.v. dose of I (B) are shown below. The ion at m/e 452 represents 2.5 ng/ml of II. One µl out of available 100 µl was injected into gc-ms. The concentration of I in chromatogram B was determined to be 2.9 ng/ml.



To quantitate the level of TM-PGE_2, the peak height ratio m/e 449 to m/e 452 for each sample was calculated and converted to a concentration using previously established standard curves.

The standard curves were generated from a least squares analysis of the ion ratio vs amount added data from the assay of 1 ml control plasma samples each spiked with 2.5 ng of II and either 0, 0.1, 0.5, 1.0, 2.5, 5.0, 7.5 or 10 ng of I.

The overall procedure recovery was determined to be 55.7 ± 9% (SD) from the analysis of six replicate samples each spiked with 2.5 ng of compound I.

In summary:

1. Using only a simple extraction procedure, we have been able to analyze for a prostaglandin analog in dog plasma. The method was successfully applied to the determination of I in dog plasma following a single iv dose of 50 µg/kg of I and chronic oral doses of 500 µg/kg of I to dogs.

2. The derivative most commonly used in the determination of prostaglandins by ec-gc can also be used for the analysis of these compounds by nicims.

3. Compared to picims, nicims offers a significant enhancement in sensitivity. For the assay the lowest known sample analyzed contained 0.2 ng of TM-PGE_2. This represents 2 pg injected on the column. For authentic standards, gc-nicims is approximately 6 times more sensitive than ec-gc.

4. The general analytical approach should be useful in the measurement of other naturally occurring and xenobiotic prostaglandins.

References

1. A. J. F. Wickramasinghe and R. S. Shaw, Biochem. J., 141, 179 (1974).

2. G. Stafford, J. Reeker, R. Smith, M. Story in D. Price, J. F. J. Todd (ed.), Dynamic Mass Spectrometry Vol. 5, Heyden, London, 1978, p. 55.

APPLICATION OF CHROMATOGRAPHIC AND MASS SPECTROMETRIC TECHNIQUES TO DIFFERENTIATE LIDOCAINE FROM PHENCYCLIDINE AND PHENCYCLIDINE METABOLITES

S. D. Erk, M. R. Bogdan, R. O. Yelton and M. L. Taylor

The Brehm Laboratory and the Department of Pharmacology
Wright State University
Dayton, Ohio 45435

Phencyclidine [PCP; 1-(1-Phenylcyclohexyl) piperidine] is a frequently abused drug. Methodology commonly employed for detection and quantitation of PCP and metabolites thereof entails quantitation by gas chromatography. We report here an instance where a gas chromatographic (GC) procedure routinely applied in a coroner's laboratory to determine levels of PCP in blood and urine yielded results suggesting the presence of PCP; however, subsequent mass spectral (MS) analyses performed to corroborate GC data revealed that PCP was in fact not present. Surprisingly, the unknown drug was shown by MS to be lidocaine [lignocaine; xylocaine; 2-(Diethylamino)-N-(2,6-dimethylphenyl) acetamide] a well-known therapeutic agent not commonly abused. Details of the GC and MS techniques which were employed to differentiate lidocaine from PCP are given below.

Initial gas chromatographic analyses of an aqueous PCP standard (PCP, HCl, Applied Science Laboratories, Inc.) and urine from the deceased were performed using a Varian 3740 Gas Chromatograph with the following operating parameters.

Column:	20" x 1/8" OD stainless steel tubing packed with 5% OV 101 on 100/120 mesh Gas Chrom Q
Carrier Gas:	Nitrogen @ 30 cc/min
Temperatures:	Injection Port: 220° Detector: 250°
Column Temperature Program:	Initial T, 140° (1 min) increased to 200° at 60°/min rate, hold at 200° for 3 min

Injections of aliquots of the aqueous PCP standard and the urine of the deceased indicated the presence of a substance in the urine of the deceased which exhibited, within experimental error, a gas chromatographic retention time nearly identical to that obtained for PCP. The slight but consistent difference in retention times obtained for the unknown substance and the PCP standard suggested the need for more definitive analyses. Gas chromatographic retention times obtained for certain metabolites of PCP were found to be markedly different from either PCP or the unknown substance.

Solids probe mass spectral analysis of a chloroform extract of the urine of the deceased was accomplished using a Kratos AEI MS-25 Mass Spectrometer equipped with a DS50S Data System. No evidence for PCP was found. Subsequently chloroform extracts of an aqueous PCP standard and the urine of the deceased were prepared and the components were separated by thin layer chromatography (TLC). Each of the separated components were analyzed using a DuPont 21-491 mass spectrometer and data system described previously.[1,2] Comparison of the mass spectral data obtained for each of the compounds separated by TLC with data in the Cornell Library of Mass Spectra revealed the presence of lidocaine.

Lidocaine present in the urine of the deceased was then quantitated using a Varian 2740 Gas Chromatograph coupled with an Extranuclear Quadrupole Mass Spectrometer system.[3] The system was configured as follows:

Varian Gas Chromatograph Column:	2m x 3mm ID glass coil packed with 3% OV-7 on 100/120 Mesh Gas Chrom Q
Carrier Gas Temperatures:	Helium @ 65 cc/min Injector 240° Column 235° Transfer Line 285°
Extranuclear Quadrupole Mass Spectrometer:	Ionizing voltage 23.5 eV Source Envelope Pressure: 1.4×10^{-4} torr Analyzer Pressure: 6.0×10^{-6} torr Mass Monitored: m/e 86

Using SIM/GC/MS, lidocaine in the blood of the deceased was found to be present at a level of 21 µg/ml and lidocaine in the urine was present at a level of 80 µg/ml was found.

Subsequently, these analytical results were corroborated by clinical records which became available after the analyses were performed, which revealed lidocaine had been administered in sizeable quantities.

References:

1. D. T. Terwilliger, D. C. Walters, M. L. Taylor, and T. O. Tiernan, "A Mass Spectrometric Data System for Use With a Gas Chromatograph or Direct Insertion Probe, "Proceedings of the 25th Annual Conference on Mass Spectrometry and Allied Topics, Washington, D.C., 1977, Pages 652-654.
2. Michael N. Gardos, Thomas O. Tiernan, Michael L. Taylor, Dennis C. Walters, D. Thomas Terwilliger, and Larry L. Fehrenbacher, ASLE Transactions, in press.
3. Stanley D. Erk, Michael L. Taylor, and Thomas O. Tiernan, Chemosphere 8(1) 7-14 (1979).

ANALYSIS OF THE ENANTIOMERIC COMPOSITION OF WARFARIN IN HUMAN PLASMA BY CHEMICAL IONIZATION MASS SPECTROMETRY

WILLIAM N. HOWALD, ERNIE D. BUSH and WILLIAM F. TRAGER,
Dept. of Pharm. Sci., Univ. of Wash., Seattle, WA 98195
KATE MOTLEY and ROBERT O'REILLY,
Santa Clara Valley Medical Center, San Jose, CA 95128

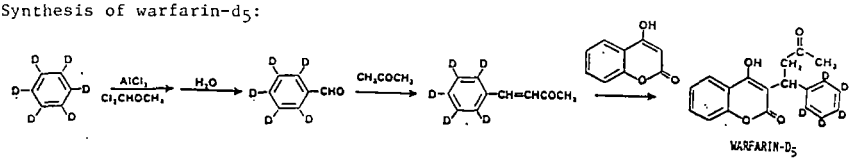
INTRODUCTION

The oral anticoagulant warfarin is classic in terms of a drug whose biological action is modulated by the presence of other drugs. Earlier studies indicated that at the molecular level these effects may, in part, be explained by induced changes in the stereoselective metabolism of the drug. To probe this pharmacological response a pseudoracemic mixture of warfarin was synthesized, in which the R and S enantiomers contained naturally occuring and specifically incorporated ^{13}C (90 atom %), respectively. The drug was administered as a single dose to volunteers in three separate studies: (1) by itself (control), (2) while under treatment with phenylbutazone and, (3) while under treatment with seconal. Analysis for enantiomeric composition and total warfarin of serial plasma samples taken during each study was accomplished by HPLC cleanup and direct probe CIMS multiple ion monitoring using a pentadeutero warfarin analog as an internal standard.

EXPERIMENTAL

Pseudoracemic warfarin in which the S-enantiomer contains 90% ^{13}C in the C-2 position was prepared as previously reported. [1] Burdick and Jackson glass distilled solvents were used for all HPLC and extraction procedures. HPLC chromatograms were run on a Micromeritics Model 7000 B liquid chromatograph. A Searle SRI Biospect Quadrupole CIMS with a Model 7551 Spectral Analysis Microprocessor DS was used in the mass spectral analysis.

Synthesis of warfarin-d_5:



Two sets of standards were prepared by mixing various amounts of (R)-warfarin with fixed amounts of warfarin-d_5 and (S) - warfarin-C2-^{13}C stock solutions made by dissolving 2.0 mg of each compound in 10 ml of acetonitrile. The first set was prepared by mixing 100, 200, 400, 1,000 or 2,000 µl of the (R)-warfarin stock solution with a solution containing 400 µl of (S)-C2-^{13}C-warfarin and 400 µl of warfarin-d_5 prepared from their respective stock solutions. The second set of standards was prepared by mixing 0, 200, 400 and 600 µl of (R)-warfarin stock solution with a solution containing 200 µl of (S)-C2-^{13}C-warfarin and 800 µl of warfarin-d_5. To generate a standard curve each of the nine standard solutions was applied to the probe tip, the solvent evaporated and the relative intensities of the ions at m/e 309, 310 and 314 determined as described below. For a given standard curve each point was measured from three to six times and the average taken. Plasma standards were prepared by the addition of 50 µl of each of the nine standard solutions to 2 ml of plasma.

Plasma extraction was accomplished using acid soaked glassware, rinsed in distilled water and oven dried prior to use. To 2 ml of plasma in a 60 ml flask was added 1 ml of internal standard solution containing 10 mcg/ml of warfarin-d_5. This was followed by the addition of 1.0 ml of 3N hydrochloric acid, 1.0 ml of distilled water and 20 ml of 1,2-dichloroethane. The mixture was shaken on a mechanical shaker at 120-150 oscillations/min for 10 min and then transferred and centrifuged at 10,000g at 4.0°C for 20 min. The aqueous phase was removed and discarded. The organic phase was transferred to a second 60 ml flask, 4.0 ml of 2.5N sodium hydroxide added and the mixture shaken as before. After centrifugation of the aqueous layer 3 ml of it were transferred to a third 60 ml flask and combined with 3 ml of 3N hydrochloric acid and 2 ml of 1,2-dichloroethane and shaken. The mixture was centrifuged and 1.5 ml of the organic phase was transferred to a liquid scintillation vial and evaporated to dryness under vacuum at room temperature.

The HPLC apparatus was equipped with a syringe loading loop injector fitted with a 1 ml loop, a 20 µm glass beak precolumn, a 250 x 4.6 mm stainless steel column packed with Dupont 5 µm Zorbax-CN. The mobil phase consisted of cyclohexane; isopropanol: glacial acetic acid in a ratio of 96:3.95:0.05, generated as used by programming the HPLC to mix cyclohexane with an isocratic solution of isopropanol containing 1% glacial acetic acid by volume. Both solvents were degassed under constant helium sparge prior to mixing. The flow rate of the mobile phase was 3.0 ml/min at 2650 psi. To each warfarin plasma isolate

was added 250 µl of mobile phase. The sample was vortexed and injected onto the HPLC. The warfarin peak had a retention time of 7 min and was detected using a 280 nm fixed wavelength detector. The warfarin fraction was collected in a concentration tube, the solvent evaporated and stored for mass spectral analysis.

The sample residues were taken up in 100 mcl of acetonitrile, vortexed and allowed to stand for 30 min. From 2 to 50 mcl were placed on a pyrophrylite probe tip, solvent evaporated, probe tip retracted, and the probe inserted into the mass spectrometer. Immediately following insertion, the electron multiplier and ion source supplies were turned on. Under computer controlled selective ion monitoring, 5 sec of background acquisition was allowed, followed by data acquisition with the probe tip fully extended. Twenty-five sec after initiation of data collection, this function was terminated, the electron multiplier and ion source supplies turned off, the probe removed, and background corrected data presented. Background corrected integrated total signal and signal ratios for each ion monitored were obtained using the software provided with the data system. The analysis of both standards and blanks were periodically repeated throughout the course of a given run to monitor the mass spectrometer's performance.

Calibration curves for total warfarin concentration were generated by a multiple regression program (MINITAB) based on the linear equation

1) $Y = mP + nQ + o$

where $Y = (R + S)/D$

R = concentration of (R)-warfarin

S = concentration of (S)-warfarin

D = concentration of warfarin-d_5 (I.S.)

P = 310/314 = the ratio of the ion intensities of the base peaks of (S)-warfarin-C2-^{13}C and warfarin-d_5 respectively

Q = 309/314 = the ratio of the ion intensities of the base peaks of (R)-warfarin and warfarin-d_5 respectively

m and n are slope coefficeints

o is an intercept coefficient

Since the ratio of 309/310 is not a linear function calibration curves were obtained using equation 2), shown below in the nonlinear least squares program (BMD x 85) on a CDC 6400 digital computer.

2) $$Z = \frac{R + cS + bD}{aR + (1-c)S + dD}$$

where Z = 309/310 = the ratio of the ion intensities of the base peaks of (R)-warfarin and (S)-warfarin-C2-^{13}C

a = fraction of warfarin due to ^{13}C natural isotopic abundance

b = fraction of warfarin-d_5 appearing as warfarin-d_0

c = fraction of (S)-warfarin-C2-^{13}C that contains ^{12}C at the C-2 position

d = fraction of warfarin-d_5 appearing as warfarin-d_1

R, S and D are defined above

Rearrangement of Equation 1) in terms of R and substitution of the expression for R into Equation 2) yields an equation, which upon further rearrangement yields an expression for S, equation 3).

3) $$S = \frac{DY\ (1-aZ) + D(b - dZ)}{Z(1-a-c) + 1-a}$$

This equation provides the concentration of (S)-warfarin present in each plasma sample and a basis for the propagation of error.

RESULTS and DISCUSSION

The standard curves for total warfarin concentration and the ratio of R/S was determined by least squares fit of 9 points for each curve. The curves defined a range of ratios for (R + S)/D and R/S of 0.25 to 3.5 and 0 to 5, respectively. Standard curves were redetermined each time a set of samples was run. Figure 1 is a typical Total Warfarin Ratio calibration curve with plasma standards superimposed. In this case the coefficients n,m and o are 0.8828 $\pm$ 0.0135, 0.6212 $\pm$ 0.0368 and -0.0317 $\pm$ 0.0245 respectively.

The linear equation shown in Figure 2 with a slope of 0.9992 and y-intercept of 0.000 illustrates the overall precision and accuracy of the individual enantiomer concentration determination. The R-warfarin values were obtained by subtracting calculated (S)-warfarin concentrations (Equation 3) from the calculated total warfarin concentrations. The coefficients a, b, c and d used in Equation 3 were 0.1383 $\pm$ 0.0028, 0.02219 $\pm$ 0.002643, 0.2200 $\pm$ 0.0020 and 0.01509 $\pm$ 0.002643, respectively. As expected the maximum standard deviation occurs in those coefficients which have the smallest absolute values.

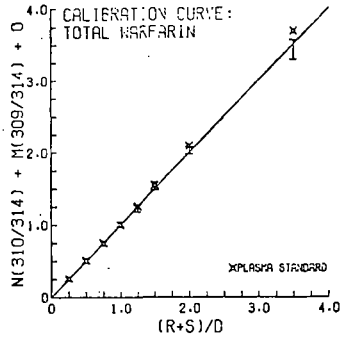


Figure 1

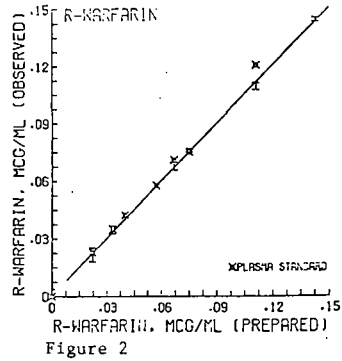


Figure 2

The assay described has been utilized to measure the enantiomeric composition of warfarin in over three hundred plasma samples within the last year. Figure 3 shows the results of a series of studies in a single individual in which the half lives of (R)- and (S)-warfarin were determined after the administration of warfarin alone, warfarin plus phenylbutazone and warfarin plus seconal. As may be seen the effect of phenylbutazone is to increase the half life of (S)-warfarin and decrease the half life of (R)-warfarin. Seconal decreases the half-life of both enantiomers but has a much greater effect on (S)-warfarin. These results are at least qualitatively consistent with the observed biological response elicited by these drug interactions. Whether or not these apparent metabolic effects account for the entire biological effect remains to be determined.

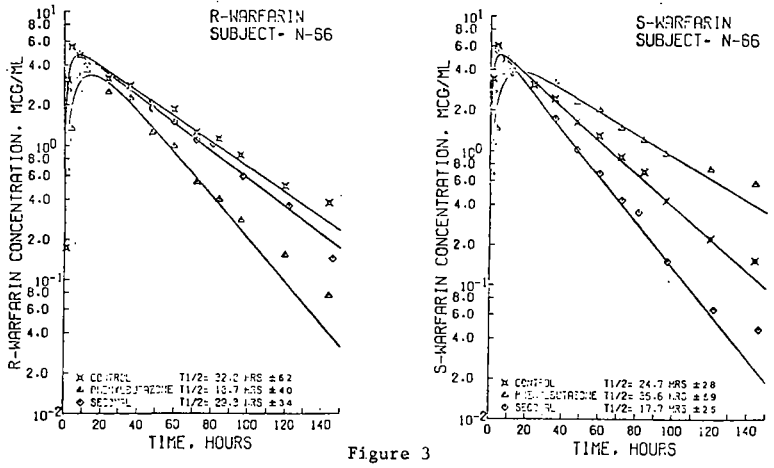


Figure 3

ACKNOWLEDGEMENTS

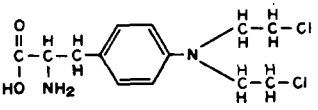
This investigation was supported in part by NIH Research Career Development Award (GM U-2111) and Research Grants (GM 25136 and GM 22860) from the Institute of General Medical Sciences (WFT).

1 Porter, W. R., Kunze, K., Valente, E. J., and Trager, W. F., J. Labeled Cmpds. Radiopharmaceuticals, in press.

A GCMS ASSAY FOR PHENYLALANINE MUSTARD, SHARON PALLANTE, MARK APPLER, R.BRUNDRETT, R.MENELL, O.M.COLVIN, AND CATHERINE FENSELAU, Dept. of Pharmacology and Experimental Therapeutics, Johns Hopkins University School of Medicine, 725 N. Wolfe St., Baltimore, MD 21205

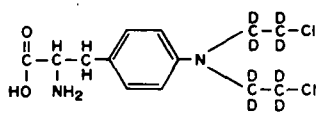
The compound phenylalanine mustard (L-PAM or Melphalan) has been used clinically since the late 1950's in the treatment of ovarian cancer, myeloma and breast cancer. The European method of IV administration is not favored in this country for several reasons: the IV preparation is more toxic to bone marrow, and the oral tablet is more stable as the drug is readily hydroxylated in aqueous solutions.

In examining the published analysis methods, we found that there was no data from patients on oral doses which looked specifically at unmetabolized drug levels below 50 ng/ml plasma. Published studies either involved IV administration of 0.6 mg/kg L-PAM with HPLC analysis at a minimum detectable level of 50 ng/ml (1) or both IV and PO administration with labelled L-PAM - a method which does not distinguish between the unmetabolized drug and its mono- and dihydroxylated metabolites (2). We, therefore, set out to develop a gas chromatographic mass spectrometric assay which exploited the sensitivity and specificity of chemical ionization and selected ion monitoring for evaluating blood levels in patients taking L-PAM orally in the 8 to 30 mg [0.25 mg/kg] range used in our clinic. The amount of unmetabolized drug available in the plasma was monitored over a 24 hour time course. The SIM and quantitation were made possible by the use of a chemically synthesized d_8-PAM internal standard coupled with a GCMS data system.



L-PHENYLALANINE MUSTARD dO

Figure 1



L-PHENYLALANINE MUSTARD d8

Figure 2

To each 2 ml of patient plasma is added 200 ng of the d_8-PAM (5 ng/µl in methanol). The samples are then flash frozen with dry ice-acetone until analysis. Each sample is then thawed and precipitated with 2 mls of 5% perchloric acid, centrifuged, and the supernatant stored on ice. The precipitate is washed with 1 ml of 5% PCA, centrifuged, and the combined supernatants applied to a Porapak Q column (Waters Associates). Pairs of samples are carried through the work-up to completion due to the instability of the drug. If all the samples were precipitated at one time, the rapid hydroxylation of the L-PAM in the aqueous PCA solution would lead to a loss of 40-45% of the total drug in the samples processed last (a lag time of 60 minutes).

The Porapak Q column (10 cm X 0.5 cm) is washed with 25 mls of cold distilled water and then eluted with 8 mls of MEOH. The MEOH eluant is dried immediately and derivatized. An N-trifluoroacetyl methyl ester is prepared by the addition of TFAA: Acetonitrile 1:1, drying with N_2, and then reacting with diazomethane, Figure 3. Several other derivatives were evaluated then rejected. The silylated derivatives provided a signal equally as intense with CI but the compound degraded over 24 hours. Preparation of the DMS-dialkyl acetyl derivative gave a response that was only 1/6 as intense as that of the TFA methyl ester.

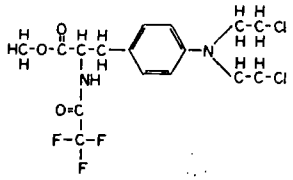
The use of the gas chromatographic resin Porapak Q as a liquid chromatography resin (3) was evaluated against XAD-2 using both labelled L-PAM and GCMS, Figure 4. Its use leads to much higher yields and cleaner GC runs. Even with the cleaner samples, the response from low levels of the drug was buried in the background of the total ion chromatogram regardless of whether EI or CI with isobutane was used, Figure 5.

By using selected ion monitoring on a DuPont Dimaspec 321 with Riber software calibrated to 0.1 amu the sensitivity was now increased to the point where quantitation is possible at levels down to 2 ng/ml plasma, Figures 6-9. A standard curve from plasma was produced, Figure 10, and five female patients undergoing treatment were evaluated, Figure 11. The unmetabolized L-PAM peaked in the plasma at 1-1/2 to 2-1/2 hours and the majority of the drug had cleared by 24 hours.

1) S. Y. Chang, et. al., J. Pharm. Sci. 67, 5, (1978).

2) M. H. N. Tattersall, et. al., Europ. J. Cancer, p. 507, May 1978.

3) J. E. Bakke, Bound and Conjugated Pesticide Residues, ACS Symposium Series 29, 65, (1976).



L-PHENYLALANINE MUSTARD
N-TRIFLUOROACETYL METHYL ESTER

FIGURE 3

COMPARISON OF PORAPAK Q AND XAD-2

USING RADIOACTIVE L-PHENYLALANINE MUSTARD

PROCEDURE	% RECOVERY OF LABELLED L-PAM	
	PORAPAK Q	XAD-2
COLUMN LOADING VOLUME	87%	n/a
25 ML H_2O WASH	33-35%	19-20%
8 ML METHANOL ELUANT	92-95%	73-78%
RECOVERY AS EVALUATED BY GCMS	90%	n/a

FIGURE 4

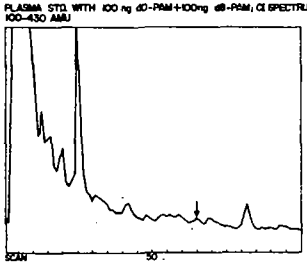


FIGURE 5

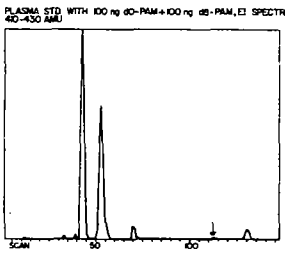


FIGURE 6

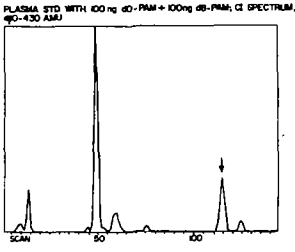


FIGURE 7

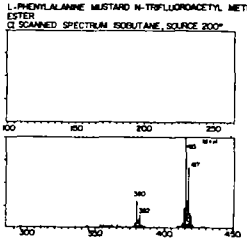


FIGURE 8

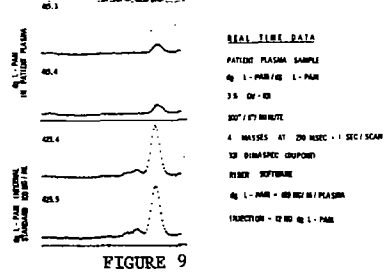


FIGURE 9

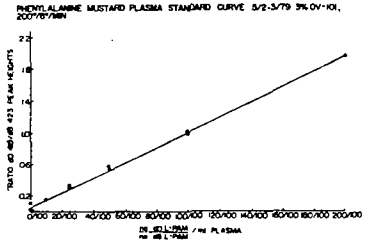


FIGURE 10

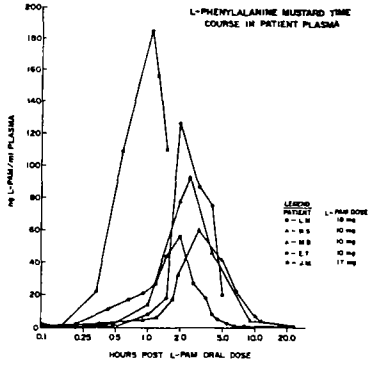


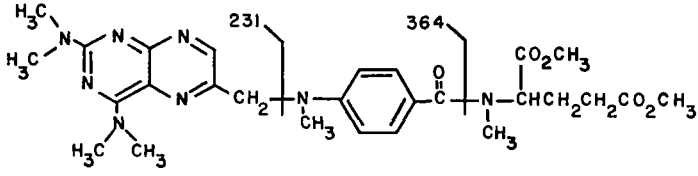
FIGURE 11

Mass Spectrometry of Folic Acid Analogues

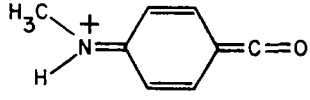
Ronald G. Smith, Yeu-Ming Wang, Joyce C. Pegues, David Farquhar, and Ti Li Loo.
Departments of Developmental Therapeutics and Pediatrics, The University of Texas System Cancer Center M.D. Anderson Hospital and Tumor Institute, Houston, TX 77030.

The dihydrofolate reductase inhibitor methotrexate (MTX) has been widely used in cancer chemotherapy, both alone and in combination with other agents. A method is presented for the identification of MTX and its metabolites isolated from patient samples.

The MTX metabolites were isolated from the urine collected from patients treated with high dose MTX (50-350 mg/kg) over a 6 hr infusion period followed by "rescue" therapy using citrovorum factor. Isolation involved column chromatography on DEAE cellulose using an ammonium bicarbonate buffer. The isolated components were derivatized by permethylation using sodium methylsulfinylmethide in DMSO followed by methyl iodide. The resulting product, shown below for MTX, was sufficiently volatile to obtain mass spectra with moderate heating (150-200°C) of the direct probe.



The resulting spectra typically exhibited molecular ions, strong ions corresponding to the fragmentations shown above for permethylated MTX, and a rearrangement ion derived from the p-methylaminobenzoyl moity, shown below.



m/e 134

The primary metabolite of MTX, 7-hydroxymethotrexate, was identified as its permethylated derivative and shown to be identical to that derived from synthetic 7-hydroxymethotrexate. Another metabolite, 4-amino-deoxy-N^{10}-methylpteroic acid was also identified as its permethylated derivative.

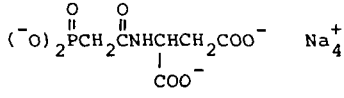
In addition to methotrexate and its metabolites, several other folic acid metabolites and analouges of interest in cancer chemotherapy have been examined.

(Supported by NCI Contract CM-87185, USPHS Grant CA-05831, and the Beebo Smith Memorial Fund for Bone Cancer Research.)

GC-MS-SIM Quantitation of the Antitumor Agent N-(Phosphonacetyl)-L-Aspartic Acid in Human Biological Fluids.

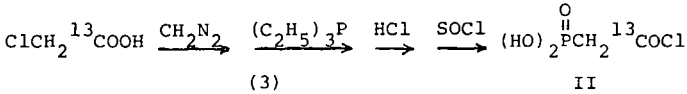
R.J. Bruni, Y. Merrill, A.R. Branfman, Arthur D. Little, Inc., Cambridge, MA 02140; J.M. Strong, Lab. of Chem. Pharmacology NIH, Bethesda, MD 20014; T.J. Ervin, Sidney Farber Cancer Institute, Boston, MA 02115.

The antitumor agent N-(phosphonacetyl)-L-aspartic acid (PALA, NSC 224131, I), a transition-state inhibitor of the enzyme aspartate

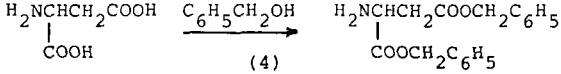


I

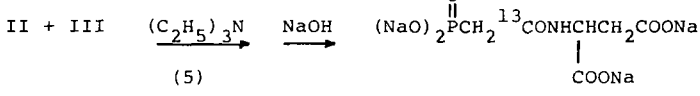
transcarbamylase (1,2), is currently under clinical study by the National Cancer Institute. To obtain clinical pharmacokinetic data we have developed a sensitive, specific method of analysis for PALA in plasma and urine by means of combined gas chromatography - mass spectrometry - selected ion monitoring (GC-MS-SIM). Our method utilizes the ^{13}C isotope-labeled internal standard N-(phosphon-^{13}C-acetyl)-L-aspartic acid (IV), which was synthesized according to the following scheme:



(3) II



(4) III



(5) IV

A previous report (6) described GC and GC-MS-SIM methods for the quantitation of PALA utilizing N-(phosphonacetyl)-L-glutamic acid as an internal standard. Both previous and present methods use methylation by diazomethane for derivatization of PALA and internal standards. The

methyl derivatives of PALA and ^{13}C PALA in the present method co-chromatograph as a single GC peak which allows simultaneous measurement of the monitored ions in the mass spectrometer. The mass spectral ions of interest were m/e 151 and 220 for PALA (7) and m/e 152 and 221 for ^{13}C PALA methyl derivatives. Although measurement of m/e 151, the base ion, would result in the highest sensitivity, m/e 220 (50% relative intensity) was measured to avoid interference from a substance in plasma which chromatographed close to PALA and possessed an ion at m/e 151. An outline of the procedure is as follows: Internal standard was added to samples of plasma or urine and the protein and drug were precipitated by acetone. The drug was extracted into tetrahydrofuran/methanol/HCl, dried and methylated with diazomethane. Drug recovery was 78%. Samples were chromatographed on a 3% OV-17 packed glass column and the eluted components were monitored for masses 220 and 221. Calibration curves which related ion intensity peak height ratios to PALA concentrations were linear over a range of 2 to 60 µg/ml of plasma or urine with a coefficient of variation of 1 to 12%. PALA concentrations in the plasma of cancer patients being treated with PALA at 1800 mg/m^2/day by continuous i.v. infusion for 5 days varied between 15 and 40 µg/ml during the infusion and decreased to the lower limits of sensitivity of the method by 24 hr after the end of the infusion. The pharmacokinetic data will be reported in a later paper.

Supported by Contract NO1-CM-87163 from DCT, NCI, NIH, DHEW.

REFERENCES:

1. R.K. Johnson, T. Inouye, A. Goldin and G.R. Stark, Cancer Res. 36, 2720(1976).
2. K.D. Collins and G.R. Stark, J. Biol. Chem. 246, 6599(1971).
3. R.M. Davidson and G.L. Kenyon, J. Org. Chem., 42, 1030(1977).
4. L. Zervas, M. Winitz, and J.P. Greenstein, J. Org. Chem., 22, 1515(1957).
5. Private communication from Starks Associates, Inc., via NCI.
6. J.M. Strong, Y.E. Kinney, A.R. Branfman, Y. Merrill and R.L. Cysyk, Cancer Treat. Rept. (in press).
7. A.R. Branfman, K.H. Valia, and R.J. Bruni, J. Chromatogr., 151, 71(1978).

MAMP10 CHARACTERIZATION OF THE GLUCURONIC ACID CONJUGATES FORMED DURING CLOFIBRATE METABOLISM, C. E. HIGNITE, C. TSCHANZ, S. LEMONS, D. H. HUFFMAN, AND T. L. AZARNOFF, V.A. Med. Center, Kansas City, MO 64128 and Univ. Kansas Med. Center, Kansas City, KS 66103

The commonly used hypolipidemic drug clofibrate is rapidly and essentially completely metabolized in man to liberate p-chlorophenoxyisobutyric acid (CPIB) which in turn is conjugated with glucuronic acid and excreted in the urine. Because of a report establishing the presence of two different glucuronic acids conjugates when only one, attachment of CPIB at C-1 of the β-pyranose form of glucuronic acid, would be expected, we studied the metabolism of clofibrate and have characterized four glucuronic acid conjugates of CPIB. The structures of these conjugates and their possible significance in metabolism studies will be discussed.

MAMP 11

Mass Spectra of Quaternary Ammonium Chlorides

Fred A. Elder, Lynn J. Bluett,
Kenneth M. Maloney, Raymond K. Crandall

Joseph C. Wilson Technology Center
Xerox Corporation
Webster, New York

Electron impact spectra of selected members of a homologous series of quaternary ammonium chlorides have been studied to establish gas phase species component types and their respective breakdown following ionization.

The major gas phase species were found to be chlorine, hydrogen chloride and the respective triamines.

A Study of the Decomposition of Arylazopyrolines

Fred A. Elder and Kenneth M. Maloney

Joseph C. Wilson Technology Center
Xerox Corporation
Webster, New York

The electron impact spectra of 4-phenylazo-3-methyl-1-phenylpyrazoline-5-one, 4-(p-methoxyphenylazo)-3-methyl-1-phenylpyrazoline-5-one, 4-(p-chlorophenylazo)-3-methyl-1-phenylpyrazoline-5-one, and 4-(p-nitophenylazo)-3-methyl-1-phenylpyrazoline-5-one have been recorded.

It was observed that the parent ions and their direct products account for 50% of the total ion current. The fragmentation was found to be sensitive to 4-phenylazo substitution. Four types of primary ions are observed: loss of the 1-phenyl group, loss of the 4-phenyl group and rupture of the azo bond. All fragmentation pathways are identified via metastable ions.

The azo rupture is particularly sensitive to the electronegativity of the 4-phenyl substitution. Electron donating groups enhance the fragmentation and electron withdrawing ones decrease it.

LIQUID IONIZATION AT ATMOSPHERIC PRESSURE: CLUSTER IONS FROM LIQUID PRODUCED BY CHARGE TRANSFER

M. Tsuchiya and T. Taira
Faculty of Engineering, University of Tokyo, Bunkyo-ku, Tokyo,Japan
K. Hiraoka
Faculty of Engineering, Yamanashi University, Kofu, Yamanashi

We have developed a new ionization method for the analysis of compounds either as liquids or in solution at atmospheric pressure. Cluster ions observed are shown to describe the information obtained by this method.

A conventional quadrupole mass spectrometer (ANELVA TE-600 GC-MS) was modified for our purpose and a schematic drawing of the instrument (a part) is shown in Fig.1. A carrier gas such as argon, helium or nitrogen is ionized by a corona discharge between a needle, electrode-1, and a gauze, electrode-2. The carrier gas ions and excited species flow beyond the gauze into an ionization chamber to ionize a sample. Liquid or solution enters the ionization chamber through a stainless steel tube such as is used in liquid chromatography into the carrier gas ions just in front of a pinhole (dia. 20 μm) through which ions are drawn into the mass spectrometer. A metal rod on which a liquid sample is deposited is another means of sample introduction. The sample appears to be ionized by interactions between ions in the carrier gas at or very near the surface of the liquid. The mass spectrometer is evacuated by an oil diffusion pump (3000 l/s) which maintains the pressure at $10^{-5} \sim 10^{-4}$ Torr when the pinhole is exposed to carrier gas at atmospheric pressure.

Figure 2a shows an example of the mass spectrum of water in the background of the instrument. Both $(H_2O)_n^+$ and $(H_2O)_nH^+$ are produced from water vapor which probably comes from water desorbed from the discharge tube or from outside air because the ion source is not airtight and no water is introduced deliberately. When the discharge chamber is heated by a stream of heated air (hair dryer), the abundance of all $(H_2O)_nH^+$ ions diminishes. The $(H_2O)_nH^+$ ions are known to be abundant when water vapor is ionized at high pressure whereas $(H_2O)_n^+$ has not been reported for water in the gas phase. When liquid water is introduced via the sample tube, the mass spectrum, consisting principally of $(H_2O)_n^+$ ions, shown in Fig.2b, is obtained. In the latter case, $(H_2O)_n^+$ ions are considered to be formed on the surface of the liquid water and are desorbed and carried into the mass spectrometer via the pinhole before any ion/molecule reactions resulting in protonation can take place. The number n varies mainly from 1 to 8 (values as high as 16 have been observed). The intensity distribution of the $(H_2O)_n^+$ ions depends upon experimental conditions such as temperature, the geometry and potentials of the electrodes of the ion source and contamination from the preceding samples. When the potential of the pinhole is increased, the intensity of $(H_2O)_n^+$ having smaller n, increases. The proof that the core ion is H_2O^+ will be described in elsewhere.

Cluster ions of acetonitrile with water are shown in Fig.3. Similar to the case for acetone, dimethyl sulfoxide and pyridine, the MH^+ and M_2H^+ ions are abundant but the M_3H^+ ions are few. This suggests that the structure of M_2H^+ ion is $CH_3CN\cdot\cdot H^+\cdot\cdot NCCH_3$ and the third molecule could not attach to the central proton of the cluster $M\cdot\cdot H^+\cdot\cdot M$ ion. It is interesting to note that the M_2HW^+ and M_3HW^+ (W means water molecule) ions are very abundant but no M_4HW^+ ion and no trimer ions, M_3^+ and M_3H^+, are observed. This big difference in stability between M_3HW^+ and M_4HW^+ suggests that the M_3HW^+ ion has the complete solvent shell as shown in Fig.3. The formation of such intermolecular cluster ions is considered to be another evidence for ionization at the liquid surface.

A set of reactions which might account for the production of M^+, MH^+ and cluster ions are:

A = carrier gas, H_2O

$$A^+ + M \longrightarrow M^+ + A \quad (1), \qquad A^+ + nM \longrightarrow M_m^+ + (n-m)M + A \quad (2)$$

$$M^+ + nM \longrightarrow M_mH^+ + (n-m)M\cdot(M-H) \quad (3) \qquad n \geq m = 1,2,\cdots n$$

At the liquid surface, charge transfer reactions such as (2) and hydrogen or proton transfer reactions such as (3) may occur to produce cluster ions.

This method provides informations not only about cluster ions but also about chemical nature of compounds in the liquid phase.

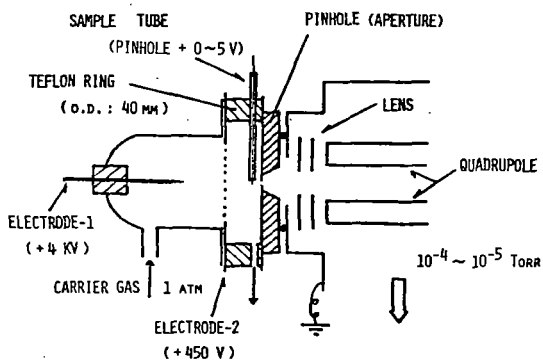


Fig.1 Schematic diagram of a new ion source

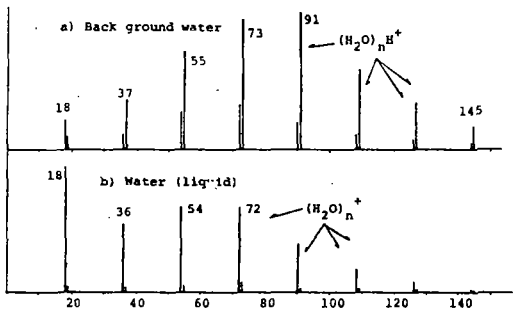


Fig.2 Mass spectra of water (cluster ions)

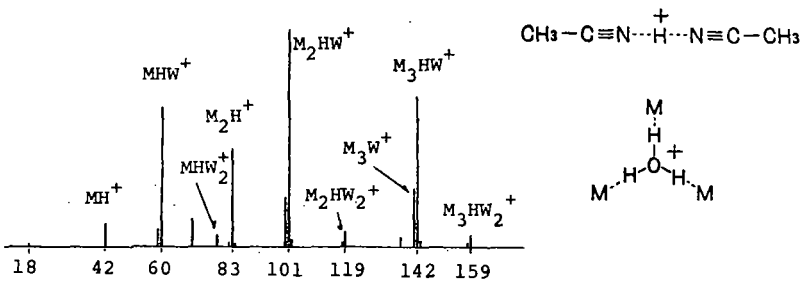


Fig.3 Mass spectra of acetonitrile with water

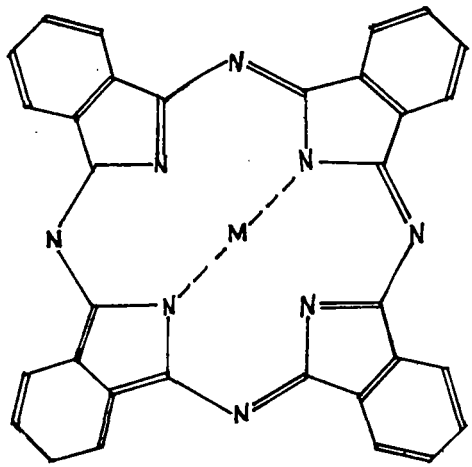
PHOTOELECTRON SPECTROSCOPY OF PHTHALOCYANINE VAPORS

J. Berkowitz, Physics Division, Argonne National Laboratory

Argonne, Illinois 60439

Statement of the problem:

Phthalocyanines have the structure



where M can be a metal atom or an H_2 unit. These highly symmetric structures are generically related to important biochemical molecules, such as hemoglobin and chlorophyll.

They have the unusual property (for such big organic molecules) of remaining intact (i.e. not decomposing) at temperatures as high as 500°C. In fact, such temperatures are required to vaporize these compounds.

We have obtained the He (I) photoelectron spectra of several metal phthalocyanines, and metal-free phthalocyanine vapor.

The objectives were to:

1. Determine the absolute ionization energies.
2. Deduce which peaks correspond to ionization from metal-like and ring-like orbitals.
3. Compare with existing molecular orbital calculations.

These molecules could then serve as good tests of molecular calculations aimed at determining the chemical behavior of large, biologically interesting molecules. The primary results from these data are:

1. A sharp peak at 4.99 eV is an artifact due to ionization of atomic helium by the He (II) radiation. This contradicts an earlier observation.
2. The first phthalocyanine peak in every case (metal-containing or

metal-free) occurs at ∿6.4 eV. Therefore, the uppermost occupied orbital must be ring-like, not metal-like.

3. The metal-like d orbitals lie at least 1— 2 eV deeper, except in the interesting case of Fe.

Höchst, et al [Phys. stat. sol. 76, 559 (1976)] have reported on the X-ray photoelectron spectra of solid phthalocyanines. Their energy scale refers to a Fermi edge, not to the vacuum level like ours. However, it is possible to match up the spectra.

We can then see the effect upon band intensities in going from VUV radiation to X-radiation. In the latter, the metal d-orbitals have higher ionization cross sections than the ring orbitals, and hence we can pick out the regions of metal-like ionization in each molecule. With these observations, we can list not only the absolute ionization energies, but the character of the orbitals (metal or ring-like) from which the corresponding electrons were ejected.

Conclusions:

1. We have successfully obtained the ionization energies of several phthalocyanine molecules.
2. The character of several of the orbitals from which ionization takes place has been deduced.
3. An Xα Multiple Scattering calculation by Case and Karplus on copper porphine [J.A.C.S. 99, 6182 (1977)] reproduces several of the features deduced here, including the nature of the first ionization, and the relative location of the Cu 3d-like bands. Other, more semi-empirical calculations (extended Hückel, Pariser-Parr-Pople) do not.
4. The Xα calculational technique, in a more refined form, looks promising as a tool for describing the chemical behavior of biological molecules.

An extensive article containing all of the photoelectron spectra, together with a more detailed analysis, has recently appeared in the Journal of Chemical Physics.

This research was performed under the auspices of the Division of Basic Energy Sciences of the United States Department of Energy.

ELECTRON IMPACT FRAGMENTATION OF THE METHYL AND ETHYL ESTERS OF FORMIC AND ACETIC ACIDS

by
Robert W. Kiser, P. A. Purdue and J. D. Tarrant
Department of Chemistry, University of Kentucky,
Lexington, Kentucky 40506

The simpler aliphatic esters of the monocarboxylic acids yield deceptively simple-appearing mass spectra that are produced by a series of rather complex fragmentation processes. A number of mass spectra of both high and low resolution have been reported for these compounds and are in general agreement. In order to gain information concerning threshold processes, several investigators have measured the appearance potentials for the more abundant ions in the mass spectra of these esters. King and Long conducted a reasonably comprehensive study of methyl and ethyl formate and methyl acetate. A more complete investigation of the mass spectra of these esters and ethyl acetate was initiated with the intention of providing unified, self-consistent fragmentation schemes and thereby to gain a more detailed understanding of their fragmentation processes and the energetics involved.

The mass spectrometer employed in this study is an Hitachi RMU-7 double-focusing instrument of Nier-Roberts geometry. Modifications made to this instrument for the electric sector voltage variation (ESVV) studies of metastable ions have been described previously; for the instrumentation used, r = 25.00 cm and d = 1.32 cm. Normal ESVV peaks (possessing no kinetic energy release) have full widths at half height of 1.1 (at 2400 V) and 1.6 V (at 3600 V). Kinetic energy releases measured have error values for reproducibility of ± 3 % of the kinetic energy determined. For metastable ions observed at apparent M/z values greater than 12 u, simple linear interpolation yielded M/z measurements usually to within ± 0.04 u when in the pseudo-linear increasing M/z scan mode. For a few m* values of less than 12 u, this approach was unsatisfactory. Consequently, the feedback circuit of the magnetic field scanner was interrupted and exponential decay scanning of the magnetic field was effected; using a simple computer program, the apparent M/z values were determined by extrapolation to within ± 0.05 u. Precise masses were determined using an AEI MSDS-II computer acquisition and data reduction program at a resolution of 7000 with ADR's SERF system as well as by the peak-matching method. Mass calibrations were accomplished using an admixture of low boiling perfluorokerosene with the compound being studied. Sample pressures employed were typically 2 x 10^{-4} Pa. The inlet system of the mass spectrometer was maintained at 450 °K. No thermal decomposition was noted in any of the compounds studied. Also, no indication was obtained that any of the metastable peaks observed were collision-induced.

Appearance potentials were determined by the method of extrapolated voltage differences. The electron emission current used during the appearance potential measurements was maintained less than 10 μA to minimize space charge effects. Further, the emission regulator was interrupted so as to minimize filament current and filament temperature variations. Repeller voltages were held at or close to 0 V. The energy scale was calibrated using admixtures of the sample being studied with krypton (I = 14.00 eV) and/or water vapor (I = 12.61 eV). The precise mass measurements were used together with literature values of the isotopic abundances of carbon and oxygen to reduce the recorded mass spectra to yield ion spectra, i.e., monoisotopic mass spectra. Identification of fragment ions was achieved by correlating the determination of metastable transitions and clastograms with information derived from appearance potentials, high resolution spectra and energetics. These results were projected into models to be used in the QET calculations for consistency confirmation. From the complete study of methyl formate emerges a complex picture of competing metastable decompositions.

The parent ion of methyl formate fragments into ten positive ions, given in order of metastable intensity: H_3COH^+, H_3CO^+, H_2CO^+H, HCO^+, HCO^+H, H_3CO^+C, CH_3^+, H_3CO^+CO, HO^+CO and HCO_2^+. These ions in turn fragment to form smaller ions whose multiple origins obscure the ion progenitor determinations and their relative importances. Hence, deuterated methyl formates (CD_3OOCH and CH_3OOCD) were also systematically analyzed in order to define the origin of the hydrogen atom(s) within the ionic species. Identification of ion fragments were confirmed with this additional information and it was deduced that there is little or no scrambling of formyl and methyl hydrogen atoms under electron impact. The structures indicated are inferred from these studies with the deuterated compounds. The appearance potential for CO^+ from methyl formate indicates that a significant amount of this ion is formed by direct ionization of the neutral molecule eliminated in other fragmentation steps. Also it was observed that the mass spectra of $HCOOCH_3$, $DCOOCH_3$ and $HCOOCD_3$ bear a striking similarity in the M/z = 26-36 u region to the mass spectra of CH_3OH, CH_3OD and CD_3OH.

The investigation of ethyl formate resulted in an even more complicated fragmentation analysis, to the extent that work on this compound and its deuterated analogs continues in our laboratory. Like methyl formate, many ions in the spectrum of ethyl formate have multiple origins. Ethyl formate bears little other similarity to methyl formate. Metastables that involve the parent ion are quite different from those of methyl formate with respect to neutrals lost, the positive ions formed, and the intensities of the metastable ions observed.

In addition to displaying some similarities to the mass spectrum of methyl formate, methyl acetate exhibits a base peak due to CH_3CO^+ that is also found in ethyl acetate. Unlike the methyl formates, the CH_3CO^+ ion arises from simple bond cleavage in methyl and ethyl acetate. The fragmentations observed in methyl acetate and the other esters indicate that primary ionization by electron impact in the esters involves the removal of an electron from the lone pair on the alkoxy as well as the carbonyl oxygen. The ionic species found in the spectrum of methyl acetate also provide evidence of the stability of the trivalent oxygen ion. Neither methyl acetate nor methyl formate parent ions show significant loss of the water molecule as is found with both the methyl and ethyl acetate parent ions.

The elimination of the vinyl radical to yield $C_2H_5O_2^+$ from $C_4H_8O_2^+$ in ethyl acetate strongly suggests that the $C_2H_5O_2^+$ ion is protonated acetic acid. The proton affinity of acetic acid has been measured by Yamdagni and Kebarle using proton transfer equilibria to be 784 kJ mol^{-1}; this value leads to $\Delta H_f(CH_3C(OH)_2^+)$ = 315 kJ mol^{-1}, in excellent agreement with the appearance potential data obtained in the present studies. Yamdagni and Kebarle also determined the proton affinity of methyl formate to be 786 kJ mol^{-1}; thus, $\Delta H_f(HC(OH)(OCH_3)^+)$ = 395 kJ mol^{-1}. These data add significantly to the conclusion that the M/z = 61 ion in the mass spectrum of ethyl acetate has the structure of protonated acetic acid, $CH_3C(OH)_2^+$.

Through the study of more than ten times the number of previously reported metastables, the fragmentation schemes of these esters have been found to be considerably more complex than reported earlier. Heats of formation calculated from the appearance potentials for ions formed in primary and some secondary reactions agree well with available literature data. Based on the data now available for these esters, it appears imperative that more extensive models be employed in QET calculations with these compounds.

The authors wish to thank Miss Mary Schwendemann and Mr. Glenn Nutter for their assistance in this work.

MAMP17 IONIC STRUCTURES OF DIENE IONS, ROBERT C. BENZ AND ROBERT C. DUNBAR, DEPT. OF CHEMISTRY, CASE WESTERN RESERVE UNIVERSITY, CLEVELAND, OHIO, 44106

Do double bonds migrate upon ionization? If so, how much? Can a rotation of a double bond take place? The structures of a number of diene ions have been determined by photodissociation spectroscopy and these questions have been answered. These studies have been done uning ion cyclotron resonance detection, taking advantage of the long trapping times to assume an equilibrium of ionic structure populations. The photodissociation spectral region examined includes the uv and visible regions. In this range peaks, corresponding to electronic excitations, are observed. In the uv region peaks appear as a result of $\pi \rightarrow \pi^*$ transitions, while the visible region shows $\pi \rightarrow \pi$ transitions in the case of congugated systems. Since the π spacings and the $\pi \rightarrow \pi^*$ spacings depend greatly on the structure of the ions and the double bond location, each structure has its own unique and predictable spectrum. The comparision of these spectra show which ions have rearranged and which ones have retained their original geometry.

MAMP18 PHOTODISSOCIATION OF PROTONATED ORGANIC CARBONYLS. JEFFREY P. HONOVICH and ROBERT C. DUNBAR, Dept. of Chem., Case Western Reserve Univ., Cleveland, Ohio, 44106

The low resolution UV photodissocation spectra of a series of protonated α,β-unsaturated carbonyls has been obtained. The intent is to examine the effect of alkyl substitution on the $\pi \rightarrow \pi^*$ transition associated with the protonated acrolein chromophore. Instrumentation consists of a pulsed mode ICR and a Hg/Xe arc photon source. Water or methane is used as a protonating agent to generate the ion from the corresponding nuetral. The proton is assumed not to change the nature of the chromophore and therefore comparison will be made between the spectrum of the neutral parent and that of the ion.

AUTOIONIZATION IN O_2.

A. Tabché-Fouhailé,[+] I. Nenner,[+] P.M. Guyon[++], P. Morin[+], L.F. Ferreira[++], K. Ito[++], K. Köllmann[+++], LURE, U.P.S., 91405 ORSAY CEDEX, France
+ DRA/SRIRMa, CEN/SACLAY, B.P. n° 2, 91190 GIF S/YVETTE
++ Lab. Collis. At. Mol., Bâtiment 351, UPS, 91405 ORSAY CEDEX.
+++ Institut für experimental physik, Univ. of Hamburg, 2 HAMBURG 36, RFA

Autoionization in O_2 was investigated by photon impact using ACO Orsay's storage ring - synchrotron radiation in the 12-26 eV spectral range. Firstly fluorescence measurements have been used in order to determine $b^4\Sigma_g^-$ and $A^2\Pi_u$ partial photoionization cross sections of O_2. Secondly, a double TOF spectrometer has been used for measuring total ionization cross section and electron time of flight distribution at various selected wavelengthsin order to measure branching ratios associated to autoionization.

EXPERIMENTAL.

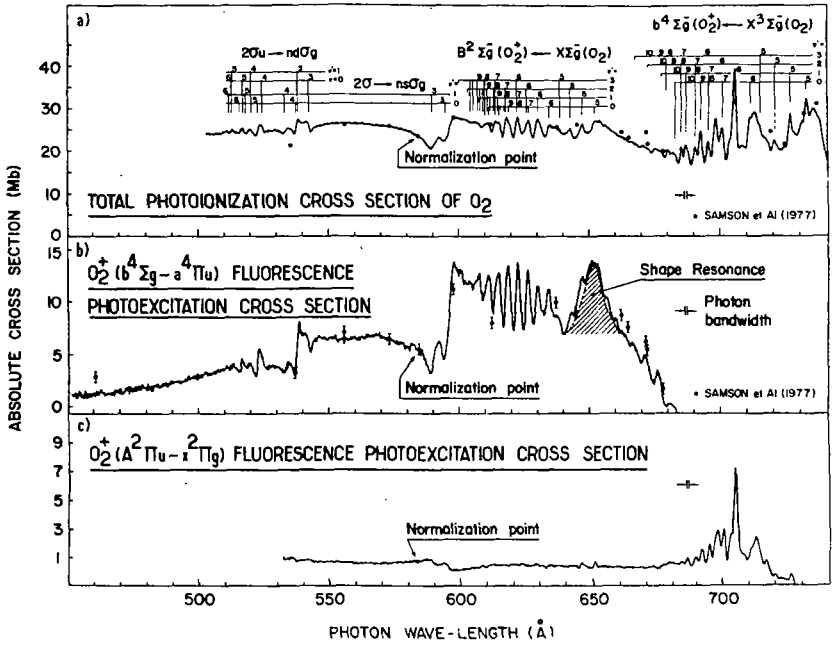
Visible fluorescence with appropriate filters has been measured as a function of exciting wavelength (0.3 Å,1Å bandwidth) out of a windowless cell filled with 5.10^{-3} Torr of oxygen. In this way the relative partial cross sections for the production of the $b^4\Sigma_g^-$ state monitored by the $b\ ^4\Sigma_g^- \rightarrow a\ ^4\Pi_u$ fluorescence (4900-8000 Å) and the $A\ ^2\Pi_u$ state monitored by the $A\ ^2\Pi_u \rightarrow X\ ^2\Pi_g$ fluorescence (2600-5000 Å) have been obtained separately.Single photon counting technique has been used. Secondly, the double time of flight spectrometer described elsewere (1) has been used on one hand for measuring the total photoionization cross section on another hand for measuring electron time of flight spectra : the electron signal detected perpendicularly to the light beam and a jet of gas within a small solid angle starts a time to amplitude converter which is stopped by the ACO signal given by a pick-up electrode mounted into the storage ring. The output is then fed into a pulse-height-analyser. The electron time of flight distribution is then converted to a photo-electron spectrum using as apparatus function, the electron TOF distribution obtained with helium at various wavelengths. Electron spectra TOF have been recorded at selected wavelengths in the whole spectral range.

RESULTS.

A) Partial photoionization cross sections.

Figure 1 shows a) the total photoionization cross section in O_2 from 740 to 500 Å (17 to 25 eV),

Figure 1



b) the partial photoionization cross section for the b $^4\Sigma_g^+$ state
and c) the partial photoionization cross section for the A $^2\Pi_u$ state

both obtained by the fluorescence technique. These three spectra have been recorded with a 1 Å resolution. The relative cross sections have been normalized to the results of Samson et Al. (2) (black dots) at 584 Å.

The spectrum b) has been also measured with a 0.3 Å resolution.

The three Rydberg series converging to the b $^4\Sigma_g^-$, B $^2\Sigma_g^-$ and c $^4\Sigma_u^-$ of O_2 are observed in the total photoionization cross section. The spectra b) and c) (spin-orbit coupling) show that the Rydberg states converging to B and c (electronic coupling) autoionize almost completely to b but not to A. The Rydberg states converging to b are of two kinds

1) the states located below b (v = 0) autoionize (~30 %) to A $^2\Pi_u$ (electronic coupling)
2) the states located above b (v = 0) decay to b by vibrational autoionization; this is more evident in the spectrum at higher resolution. The spectrum b) (σ(b)) shows a large structure centered at 650 Å (~19 eV) and of 0.44 eV FWHM which does not appear in the spectrum c) : σ(A). According to the calculations of Wallace et al. (3) in the frame of the "Multiple scattering model" theory, it is possible that this structure is a shape resonance expected in the σ_u channel (l = 3). The dipole selection rules allow the transition $3\sigma_g \rightarrow \sigma_u$ then a shape resonance is expected in b $^4\Sigma_g^-$ or B $^2\Sigma_g^-$ channels, but the transition $1\Pi_u \rightarrow \sigma_u$ is not allowed and no shape resonance is expected in the A $^2\Pi_u$ or a $^4\Pi_u$. Our results are in qualitative agreement with these predictions but there is still a discrepancy between theory and experiment for the energy and the width of this resonance.

B) Branching ratios for autoionization.

region above $\tilde{X}^2\Pi_g$ state of O_2^+

Photoelectron spectra have been obtained for a number of photon energies corresponding at various Rydberg series. Very different vibrational distributions of the $\tilde{X}$ state have been observed depending on the type of the Rydberg series.

region of the b $^4\Sigma_g^-$ state of O_2^+ (Figure 2)

Various photoelectron spectra obtained in the region of 7 eV above b (v = 0) have shown a shift of the b vibrational distribution from v = 0 for $E_{h\nu}$ 18.9 eV. It is probable that this behaviour is connected to the shape resonance in the b channel.

(1) T. Baer, P.M. Guyon, I. Nenner, A. Tabché-Fouhailé, R. Botter, L.F. Ferreira and T.R. Govers, J. Chem. Phys., 70(04), 1585 (1979)
(2) J.A.R. Samson, J.L. Gardner and G.N. Haddad, J. Electron. Spectrosc. Relat. Phenom., 12 (1977) 281
(3) S. Wallace, Ph. D. thesis, Boston University 1979;
S. Wallace, D. Dill and J.L. Dehmer (to be published)

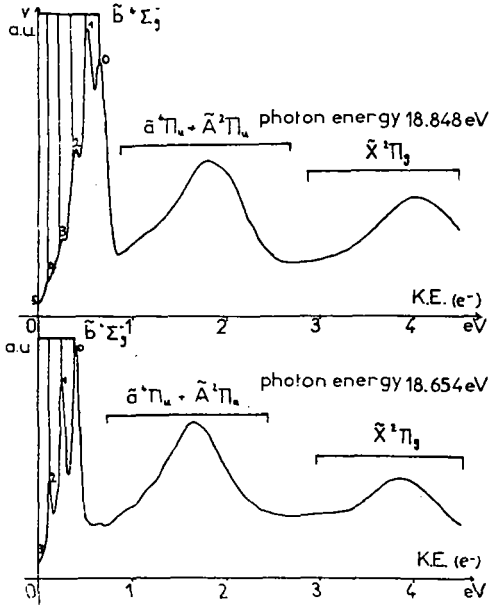


Fig. 2 : Photoelectron spectra of O_2 measured at 18.848 eV and 18.654 eV.

Observation of Highly Excited Vibrational States in Atmospheric Molecules

by

Roger Stockbauer

National Measurement Laboratory
National Bureau of Standards
Washington, D.C. 20234

ABSTRACT

The direct and autoionizing processes in a variety of atmospheric gases have been studied by threshold photoelectron spectroscopy. The technique uses variable wavelength photons so that all processes which emit an electron within the bandpass of the electron energy analyzer are detected. Through autoionizing processes, excited states of the ion not accessible directly from the ground state are observed. The results show that the ions of H_2, D_2, N_2, O_2, NO_2, NO, N_2O, CO, CO_2, H_2O, and D_2O are produced in highly excited vibrational states. In addition, the spectra for H_2O and D_2O show a break in their curves at the threshold for formation of OH^+ and OD^+. This is most probably caused by a change in the neutral vs ion processes competition at the fragmentation threshold. Results for H_2, D_2 and N_2 have been published in the Journal of Chemical Physics, 70 (1979) 2108.

State-Selected Fragmentation of Nitromethane Ions by Threshold Photoelectron Coincident Photoion Mass Spectrometry

Morris J. Weiss and G. G. Meisels
Department of Chemistry
University of Nebraska at Lincoln
Lincoln, Nebraska 68588

Abstract. Threshold Photoelectron-Coincident-Photoion Mass Spectrometry is used to prepare nitromethane ions in the second ionization band, which results from removal of an electron from the $(1a_2)$ (π), nonbonding orbital. The vibrational progression of this band reflects the excitation of the symmetric bending mode of the O-N-O group (ν_2). The first observable fragmentation is the formation of NO^+, at $\nu_2 = 2$ or 11.87 ev. This is 1.17 ev higher than the thermochemical threshold for the formation of this ion and CH_2OH and .76ev higher than threshold for formation of CH_3O. The kinetic energy release was found to be 0.054±0.005ev at onset. These observations are ascribed to a two-step process; the first is isomerization to methylnitrite ion with an activation energy of 0.80 eV., the second is rapid unimolecular dissociation to NO^+ and CH_3O.

Introduction. The study of the chemical fates of ions produced in selected internal energy states has only recently received appreciable attention (1,2). A particularly intriguing aspect is the possibility that excitation of different vibrational modes at nearly the same total energy may lead to different unimolecular reaction products, that is, that mode-specific chemistry might be observed (2). Unfortunately, only very few systems lend themselves to experiment because of the need for clearly assigned and well spaced vibrational progressions in the photoelectron spectra, in an energy range where thresholds for fragmentation exist.

One possible example is Nitromethane; it dissociates NO^+ in the region of the second photoelectron band (3), but at an energy considerably in excess of the thermodynamic threshold. The band within which this first dissociation process is observed belongs to a well-defined vibrational progression which has been assigned to the excitation of the O-N-O bending mode resulting from the removal of an electron from the non-bonding $1a_2$ π orbital, i.e., from the . . . $(1a_2)^1(5a_1)^2$, $^2A_2$ $(1a_2)^2(5a_1)^2$, $^1A_1$ transition. The unimolecular fragmentation can therefore be studied by varying solely the vibrational quantum number of the O-N-O bending mode.

Experimental. Photoions are prepared in a Threshold Photoelectron-Coincident-Photoion mass spectrometer (TPE-CPI MS) described earlier (2,4). The width at half height for Ar ionization was 0.023ev. The vibrational spacing in the second band is about 560 cm^{-1} or 0.069ev; at that electron energy, the transmission function is reduced to about 15%. Under favorable conditions individual states can therefore be prepared with an estimated purity of about 75 to 80%, the lower figure resulting from allowance for differences in transition probabilities and the remaining "tail" of the distribution (5). The Argon and Helium (Hopfield) continua were used as light sources as appropriate. The Extranuclear quadruple mass spectrometer was normally used as a flight tube only, with mass analysis by time-of-flight with a resolution of about 18m/m. Differentiation between NO_2 and CH_2NO^+ above 12.5 ev photon energy required its use as a mass filter in selected runs.

Nitromethane was purified by repeated bulb-to-bulb distillation on a high vacuum line, dried over anhydrous sodium sulfate, and stored in a sample bulb.

Results and Discussion. Three TPE-CPI spectra, using time of flight (TOF) mass analysis, at the lowest vibrational frequencies near onset of NO^+ formation are shown in Figure 1. The photon energies correspond to maxima in the (0,1,0) (a) and (0,2,0) (c) peaks, and to the valley between them (b). Observation of NO^+ in the valley could be the result of collision induced dissociation. We ascribe the appearance potential as coincident with the (0,2,0) level, or 11.87 ±0.05 ev.

The photoelectron spectrum (3) and the breakdown graph showing only NO^+ are compared in Figure 2. The onset and sharp rise in NO^+ formation appear to be accompanied by a slight but discernible broadening of the photoelectron band, which also begins with the (0,2,0) level. Since the onset is 0.76 or 1.17 ev in excess of the thermodynamic threshold for reactions leading to NO^+: (6)

$$CH_3NO_2 \xrightarrow{-e} \begin{cases} NO^+ + CH_3O & \Delta H = 11.11 \text{ ev} \\ NO^+ + CH_2OH & \Delta H = 10.70 \text{ ev} \end{cases}$$

it was of interest to see whether any part of the excess energy appears as kinetic energy of the fragment ions. Analysis of the peak shape at 11.87 ev (0,2,0) (fig. 1) indicates that fragments carry away 0.057 ± 0.01 ev.

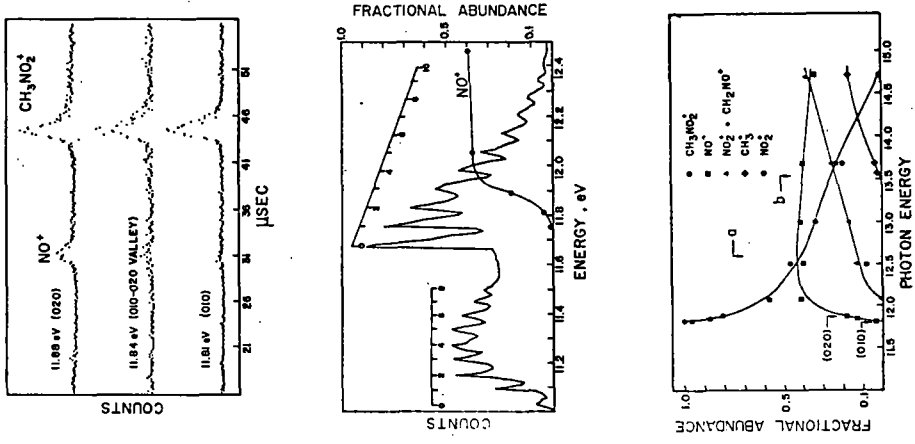
We propose that fragmentation of the molecular ion is preceded by rearrangement with an activation energy of 0.8 ev to the methylnitrite CH_3ONO^+ structure. The onset of NO^+ formation from CH_3ONO has been reported as 11.1 eV (7), corresponding closely to the thermodynamic onset. Since the methylnitrite ion should be about 0.43 ev more stable than nitromethane ion (6,7), the well depth should be 0.37 ev with respect to the methylnitrite ion. The fragmentation of the rearranged ion with 0.86 ev excess energy should occur readily within 10^{-9} seconds if it is statistical; energy randomization is supported by the measured kinetic energy release which is within experimental error of the 0.057 ev calculated for the measured excess energy and 15 degrees of freedom. The absence of a metastable peak in the electron impact mass spectrum (8) is not entirely explained on this basis. There should be an energy regime in which the isomerization process, the rate determining step, occurs with a rate constant which falls into the metastable range.

$CH_3NO_2^+$ vanishes only at the onset of the third band in the photoelectron spectrum at 13.85 ev. (fig. 4) It is probable that this is largely the result of an experimental complication resulting from a combination of the small but finite transmission of energetic electrons through the collimated hole structure and the window in the photoelectron spectrum between 12.3 and 13.9 eV which enhances the relative production of "hot" electrons.

ACKNOWLEDGEMENTS. We are grateful for the support of this investigation by the Department of Energy under Contract No. EY-76-S-02-2567, and thank Professor T. Baer for helpful discussions and suggestions.

1. Tomas Baer, "State Selection by Photoion-Photoelectron Coincident", in "Ion-Molecule Reactions" M. Bowers, Editor, Academic Press (1979).
2. Morris J. Weiss, Ta-Cheng Hsieh and G. G. Meisels, J. Chem. Phys., in Press.
3. J. W. Rabalais, J. Chem. Phys. 57, 960 (1972).
4. C. F. Batten, J. Ashley Taylor and G. G. Meisels, J. Chem. Phys. 65, 3316 (1976); ibid 69 2547 (1978).
5. Morris J. Weiss, Ta-Cheng Hsieh and G. G. Meisels, to be published.
6. H. H. Rosenstock, W. Drake, V. W. Steiner and J. T. Herron, J. Phys. Chem. Ref. Data 6, Suppl. 1 (1977)
7. M. A. Haney and J. L. Franklin, Trans. Faraday Soc. 65, 1794 (1969) "Theory of Unimolecular Reactions", Academic Press, New York (1973).
8. M. L. Gross, private communications.

Figure Legends:
Figure 1. Threshold photoelectron-coincident-photoion mass spectra of CH_3NO_2 the $^2A_2$ (π) state of the ion with one (curve a) and two (curve c) quanta in the O-N-O bending mode. Figure 2. He-I photoelectron spectrum (left scale; reference 3) and fraction of total ion current appearing as NO^+ (right scale) in the TPE-CPI MS. The energy scales are identical for both curves.
Figure 3. Breakdown graph of Nitromethane obtained by TPE-CPI.



Mass Spectrometric Measurement of Partial and Total Electron Impact Ionization Cross Section Functions of Rare Gas Atoms and Molecules

H. HELM, K. STEPHAN and T.D. MÄRK

Inst. f. Experimentalphysik, Abt. f. Kernphysik u. Gaselektronik,
Leopold Franzens Universität, A 6020 Innsbruck, Österreich (Austria)

The present paper deals with the upgrading of the quantitative knowledge of the electron impact ionization of the rare gases in the low energy regime (< 180 eV). The experimental setup consists of a Nier type electron impact ion source (Varian MAT Intensitron M), a high resolution double focussing mass spectrometer (Varian MAT CH5) and a gas handling system. Previous studies in our laboratory[1] with this instrument have shown, that measured partial ionization efficiency curves are strongly dependent on the extraction conditions of the ion source, and that the focussing potentials which guide the ion beam from the ion source to the mass spectrometer entrance slit also effect the shape and magnitude of measured efficiency curves. Meanwhile we have improved considerably the operating conditions of the ion source, i.e. achieving complete ion extraction by means of a penetrating field extraction and achieving complete measurement and analysis of the extracted ion current by means of a new sweeping mass spectrometer technique[2]. Thus it became possible to measure accurate relative partial ionization cross section functions and accurate partial cross section ratios.

Figures 1 to 4 give for He, Ne, Ar and Kr absolute partial ionization cross section functions, which have been obtained by normalizing our measured relative partial ionization cross sections with help of the measured ion current ratios to the well established absolute total cross section curves[3]. In the upper part of each figure the percentage deviation of our total cross section from those of Ref.3 is shown. It can be seen that the total cross sections agree in shape to within a few percent.

Using the same experimental technique relative cross sections for the electron-impact ionization of the rare gas Van der Waals dimers Ar_2, ArKr, Kr_2, KrXe and Xe_2 have been measured[4]. The following appearance potentials for the direct ionization from the corresponding neutral dimers have been found: Ar_2^+:(15,2 ± 0,2)eV, $ArKr^+$: (14,0 ± 0,2)eV, Kr_2^+: (13,45 ± 0,3)eV, $KrXe^+$:(12,2 ± 0,2)eV, and Xe_2^+:(11,75 ± 0,3)eV.

Work partially supported by the Österreichischer Fonds zur Förderung der Wissenschaftlichen Forschung under Project S-18/08

1. K. Stephan, H. Helm and T.D. Märk, Proc.IXth SPIG,Dubrovik (1978)7
2. H. Helm, K. Stephan and T.D. Märk, 31st GEC, Buffalo (1978) 98
3. D. Rapp and P. Englander-Golden, J.Chem.Phys., 43 (1965) 1464
4. H. Helm, K. Stephan and T.D. Märk, Phys.Rev.A, June 1979

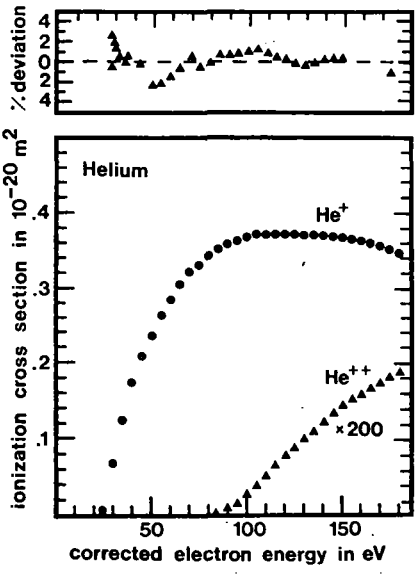


FIG. 1

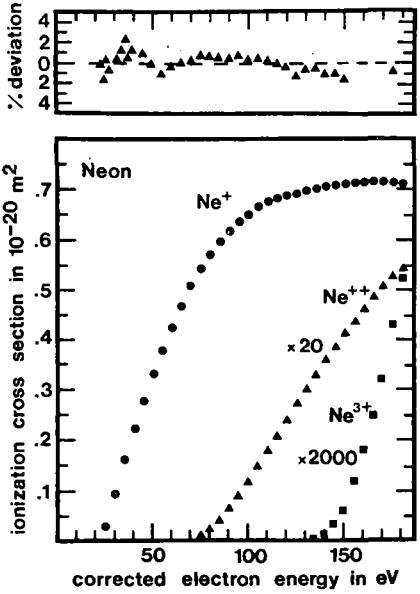


FIG. 2

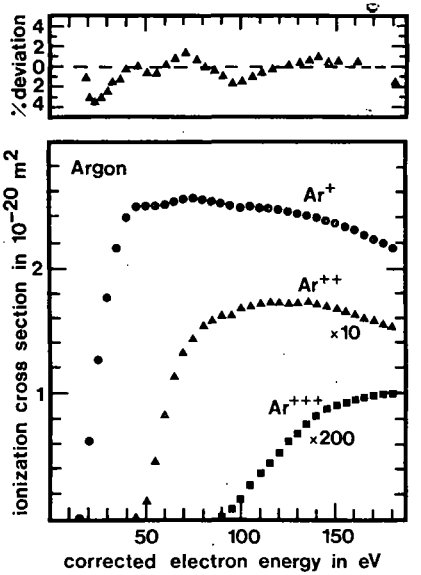


FIG. 3

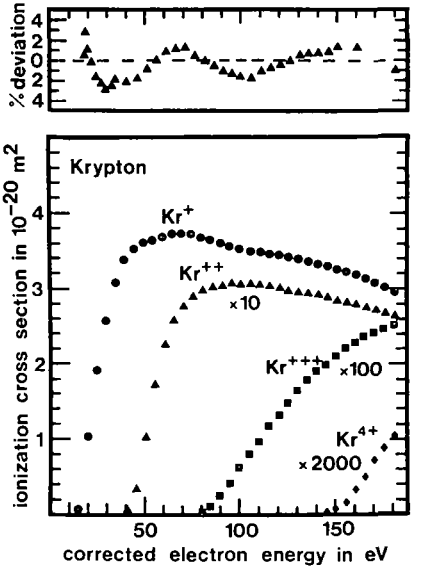


FIG. 4

ArF LASER MULTIPHOTON IONIZATION MASS SPECTROMETRY

Mark Seaver, J. W. Hudgens, J. J. DeCorpo, and J. R. Wyatt

Laser Chemistry Group
Code 6110
Chemistry Division
Naval Research Laboratory
Washington, DC 20375

Photoionization provides a monoenergetic means of producing ions. This energy resolution enabled mass spectrometrists to improve their understanding of molecular ionization and fragmentation pathways by observing changes in parent and fragment ion intensities as the photon energy was varied. Such photoionization experiments necessitate working with vacuum ultraviolet light sources.

We have begun to explore the feasibility of using multiphoton ionization to overcome the difficulties inherent in dealing with these short wavelength light sources. We obtain mass spectra from 27 organic molecules whose first ionization potentials lie between 8.8 and 12.6 eV following irradiation with the 193 nm (6.42 eV) output of an ArF eximer laser.

The data support a two-photon (12.84 eV) mechanism with the two possible pathways for these ionizations appearing in Fig. 1. On the left we depict a resonance enhanced (or resonant) transition, while the right portrays a nonresonant case. Experimentally, one distinguishes the two processes by an increase of up to several orders of magnitude in the overall transition rate for the resonant absorption. In addition to the enhanced ionization rate, we observe dramatic changes in the mass spectrum for the one strongly resonant transition, benzaldehyde, found in our data.

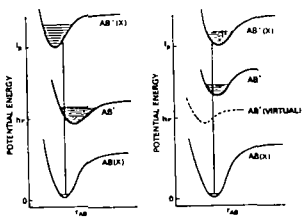


Figure 1

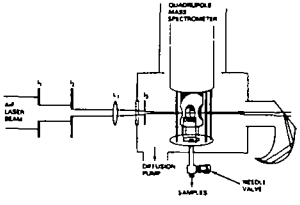


Figure 2

In these experiments great care must be taken to preclude surface effects in the ionizer due to stray photons. As shown in Fig. 2, our precautions include an iris behind the entrance window to block any reflections or refractions, enlargement of the crossed-beam ionizer ports and a Brewster's angle exit window which reflects any untransmitted laser light into a woods horn. Variations in ionization efficiency of over three orders of magnitude demonstrate the lack of surface ionizations in our experiments.

During initial experiments we estimated an absolute ionization efficiency of one ion (including fragments) reaching the detector for every 10^8 benzene molecules irradiated. In subsequent experiments we estimated the total ion count for each spectrum relative to NH_3 and converted these counts into an ionization efficiency relative to butane. The results span the range from 0.007 for chlorobenzene to 11 for benzaldehyde, with the majority of these relative efficiencies between 0.07 and 0.7.

Benzaldehyde stands out as the one case in which a strong one-photon absorption ($\varepsilon \sim 50{,}000$) occurs. In this case, the efficiency is ten times greater than any other molecule studied, and we see large amounts of C^+, C_2^+, C_3^+, etc. fragments with very little signal above 50 amu. We attribute these fragments to sequential decompositions and ionizations. Experiments with a tunable laser should enable us to determine if this strong resonance enhancement provides a means of selectively identifying the individual components in a gaseous mixture.

The remaining 26 molecules give multiphoton ionization mass spectra very similar to their electron impact ionization counterparts. In fact, we obtained electron impact mass spectra at 10, 15, 20, and 25 eV for most of the molecules studied. These electron impact spectra were taken in an attempt to pin down the amount of energy being deposited in the molecules. In general, the 10 eV spectra match most closely the multiphoton ionization results. This comparison provides the major impetus behind our conclusion that a two-photon process dominates the laser ionizations.

The molecules investigated include NH_3, OCS, CS_2, ethane, butane, neopentane, propene, 1-butene, methylacetylene, methanol, ethanol, isopropanol, acetone, acetaldehyde, ethylformate, diethylether, cyclopentanone, n-butylnitrile, benzene, toluene, chlorobenzene, benzaldehyde, and pyridine.

Details of the experiments and the observed mass spectra will be published in the International Journal of Mass Spectra and Ion Physics.

C.A. Cramers and P.A. Leclercq, Dept. of Chem.,
Eindhoven University of Technology, The Netherlands.

No doubt, maximum utility with the integrated GC-MS system is obtained when glass capillary columns are used. Discarding molecular separators as interfaces there are basically two coupling devices: closed and open-split connections.
The first type has the obvious advantage of 100% sample transmission, but depending on the restriction used the outlet of the column is at a more or less reduced pressure. Often it is claimed that a decreased outlet pressure has a deleterious effect on column efficiency. In this paper the effect of sub-atmospheric outlet pressure on the performance of open-tubular columns will be discussed. Band broadening in capillary columns is satisfactorily described by the Golay-equation extended to situations of appreciable pressure drop by Giddings [1,2,3]. Taking into account the decompression effect as described by above mentioned authors, the measured or apparent plate height equation, for an uniformly distributed liquid film, reads:

$$H = \left[2 \frac{D_{m,o}}{v_o} + \frac{11\,k^2 + 6\,k + 1}{24(1+k)^2} \frac{r^2 v_o}{D_{m,o}} \right] f_1 + \frac{k^3}{6(1+k)^2} \frac{r^2}{K^2 D_s} v_o f_2 \qquad (1)$$

This equation describes the effect of pressure gradient on the observed plate height ,H,.

$$f_1 = \frac{9}{8} \frac{(P^4 - 1)(P^2 - 1)}{(P^3 - 1)^2} \qquad (2)$$

By definition $P = \frac{P_i}{P_o}$ is the ratio of inlet to outlet pressure. $f_1 = 1$ for $P = 1$, for $P_{\to\infty}$ f_1 approaches $\frac{9}{8}$.

$$f_2 = \frac{3}{2} \frac{P^2 - 1}{P^3 - 1} \qquad (3)$$ Martin-James correction factor [4]

In equation (1) the following symbols are used:
- $D_{m,o}$ is the diffusion coefficient of a component in the mobile phase at column outlet pressure.
- v_o is the linear velocity at the column outlet (obtained from the retention time t_o of an unretained component, column length L and f_2), $\bar{v}$ being the average carrier gas velocity.

$$v_o = \frac{\bar{v}}{f_2} = \frac{L}{t_o f_2} \qquad (4)$$

- D_s is the diffusion coefficient of a component in the stationary liquid phase.
- r is the column radius.
- k is the capacity ratio of a solute = $K \frac{V_s}{V_m} = K.\beta$
- K is the partition coefficient of a solute.
- β is the volumetric phase ratio of stationary and mobile phase.

Eq. 1 can be written in a simplified form:

$$H = \left[\frac{B}{v_o} + C_{m,o}\, v_o \right] f_1 + C_s\, v_o\, f_2 \qquad (5)$$

By differentiating eq. 5 with respect to v_o, and setting the result equal to zero, the optimum value of v_o and the minimum value of H are found. It is shown in a separate paper [5] that for situations of large inlet to outlet pressure ratios (large values of P, as encountered when using sub-atmospheric outlet pressures) this differentiation yields the following equations describing the optimum gas chromatographic conditions:

$$v_{o,opt} = \sqrt{\frac{B_o f_1}{C_{m,o} f_1 + C_s (f_2 + y_2)}} \qquad (6)$$

$$H_{min} = \left\{ 2\, C_{m,o} f_1 + C_s (2\, f_2 + y_2 \right\} * \sqrt{\frac{B_o f_1}{C_{m,o} f_1 + C_s (f_2 + y_2)}} \qquad (7)$$

$$y_2 = v_o \frac{\partial f_2}{\partial v_o} \qquad (8)$$

Values of f_1, f_2 and y_2 in dependence of P are given in table 1.

Table 1
Variation of f_1, f_2 and $y_2 (v_o \frac{f_2}{v_o})$ with the ratio, P, of inlet to outlet pressure.

P_i	P_o	P	f_1	f_2	y_2
1	10^{-2}	10^2	1,1249	0,0150	-0,0075
1	10^{-1}	10	1,1157	0,1486	-0,0723
2.5	1	2.5	1,0510	0,538	-0,1864

The effect of operating at sub-atmospheric column outlet conditions is strongly dependent on the relative magnitude of the $C_{m,o}$ and C_s terms (describing the resistance to mass transfer of gas and liquid phase respectively).
In table 2 optimum gas chromatographic conditions are calculated for a 0.25 mm inside diameter capillary column. Three different values of the

C_s term, as met in practice, are used.
Depending on the film thickness of the stationary liquid phase and on the mode of liquid distribution the effect of C_s is larger. The largest value of C_s (7×10^{-3} s) is obtained from a stainless steel capillary column, apparently most liquid phase is accomodated in relatively deep pores in the column wall.

Table 2

Theoretical values of H_{min}, [cm], $v_{o,opt}$, [cm s^{-1}] and $\bar{v}_{opt}$, [cm s^{-1}] equations (6) and (7).
Conditions: 0.25 mm i.d. capillary column
$C_{m,o}$ at P_o = 1 atm: 0.0004 s

Pi	P_o	P	H_{min}	$v_{o,opt}$	$\bar{v}_{opt}$	
1.0	10^{-2}	10^2	0.099	596	8.9	
1.0	10^{-1}	10	0.098	59	8.8	$C_s = 7 \times 10^{-3}$ s
2.5	1	2.5	0.057	8.1	4.4	
1.0	10^{-2}	10^2	0.030	1643	24.6	
1.0	10^{-1}	10	0.029	164	24.4	$C_s = 4 \times 10^{-4}$ s
2.5	1	2.5	0.022	18.4	9.9	
1.0	10^{-2}	10^2	0.020	2087	31.3	
1.0	10^{-1}	10	0.019	209	31.1	$C_s = 2 \times 10^{-5}$ s
2.5	1	2.5	0.018	21	11.3	

Conclusions

Operating a capillary column at a reduced outlet pressure results in:

A. decreased column efficiency. The increase in plate height is strongly dependent on the relative magnitude of the C_s term. For uniformly distributed thin liquid films the deleterious effect is negligible.
B. The optimum carrier gas velocity shifts to appreciably higher values, this effect being larger for thin liquid films.

Combining these two statements it can be concluded:

1. When using longer capillary columns, operated at sub-atmospheric outlet pressure, the net effect will be more theoretical plates without an increase in analysis time.
2. For GC-MS combinations, it is advantageous to strive for thin, uniformly distributed, liquid films.

References

1. M. Golay, in "Gas Chromatography, 1958", Butterworth, London, 1959, (ed. D.H. Desty), p.36.
2. J.C. Giddings, S.L. Seager, L.R. Stucki and G.H. Stewart, Anal. Chem. 32, 867, 1960.
3. J.C. Giddings, Anal. Chem. 36, 741, 1964.

4. A.T. James and A.J.P. Martin, Biochem. J. 50, 679, 1952.
5. C.A. Cramers, F.A. Wijnheymer and J.A. Rijks, accepted for publication J. High Res. Chromatogr.

ON THE $(GC)^2$ IN $(GC)^2$-MS

by

M. Verzele,
Laboratory of Organic Chemistry, State University of Ghent,
Krijgslaan, 271 (S.4), B-9000 GENT (Belgium).

Is this talk on chromatography still necessary ? What if the separation can be achieved by Mass Spectrometry (MS) alone rather than by a combination with Gas Chromatography (GC) or even with Glass Capillary Gas Chromatography $(GC)^2$?
Recent successes of MS-MS (1) indeed point in this direction. My experience however that complex natural mixtures contain many compounds with the same molecular weight (terpenes !). We can therefore predict with confidende that coupling the two techniques is still important.

The first contribution to GC-MS of my laboratory goes back to 1968 (2) and therefore we have considerable experience in the field. For the moment the situation is as follows.
On coupling $(GC)^2$ to MS, the difficulties to be reckoned with are either in the $(GC)^2$ or MS part but not in the interface or actual coupling. In a recent contribution (3) comparing the performance of a glass capillary column with MS detection and with Flame Ionisation Detection (FID) our conclusion was : even with full sample transfer and without restriction between $(GC)^2$ and MS the efficiency loss is at most 25 %.

That coupling $(GC)^2$ to MS is easy, was further substantiated in the mentioned paper by 15 references coming more or less directly to the same conclusion. The above applies to quadrupole MS only; with other mass spectrometers the situation may be different; slightly more difficult, because the interface has to be more complicated.

Apparently many mass spectroscopists are attracted by $(GC)^2$-MS but a number of points create real difficulties and also, $(GC)^2$ has the reputation of being delicate and tricky.

What are these difficulties, how can they be solved or how do we get around them ?

1. The delicate character of glass capillary columns

Many $(GC)^2$ specialists have stated that the technological difficulties of glass capillary columns are not greater than those we had with glass columns maybe 10 years ago. This is indeed so. Practice will allow any technician to master the handling of glass capillary columns. This may take a few hours or days but is not more complicated than most laboratory techniques. Proof of this may be found in the fact that by now, hundreds of laboratories, mostly in Europe, have at least partly switched over from packed columns to glass capillary columns. In our laboratory nearly 60 chromatographs are all running on glass capillaries. Packed columns are only used for preparative scale separations or e.g. when molecular sieves are needed. Many of our chromatographs operate with 5 to 10 m columns and

indeed, I believe this is a very much overlooked possibility of capillary GC.

Handling the columns in $(GC)^2$ may become very easy in the future according to a recent development introduced at the latest Hindelang symposium (4). Very thin walled glass capillaries, coated on the outside with a suitable polymer are so tough that they can hardly be broken. A straight piece of such tubing can be tied into a knot and will only break when the knot circle is stretched to a diameter of less than 1 inch. In the mean time untill this development becomes generally available : learn to straighten glass capillary column ends in a micro flame, play around with shrinkable Teflon tubing and with glass inserts - you'll find it is fun, much less difficult than expected and well worth to do.

2. The short life time of glass capillary columns

Complaints often heard about glass capillaries are :

1) that their Maximum Allowable Operating Temperature (MAOT) is so much lower than for a corresponding packed column;
2) that quite rapidly the dreaded phenomenon of "droplet formation" destroys all of the column's initial efficiency.

These difficulties arise only because of a wrong choice of the stationary phase. This choice is indeed too often dictated by earlier experience or publications in GC. In $(GC)^2$ selectivity of the phase is of minor importance; efficiency is always large enough to solve all separation problems with a very restricted number of phases. In $(GC)^2$ only gum phases should be used. Gums lead to very stable films. They request only a minimum of column wall modification and give very high coating efficiencies (5). Most gums have very good thermal stability and are therefore ideally suited for $(GC)^2$-MS combination. Do not use or request a low viscosity liquid as stationary phase in $(GC)^2$ unless you know this is absolutely necessary ! This is the most important message in this paper. The number of gum phases is expanding; a list of some available ones with increasing polarity are given below.

What is it ?	Trade name	McR-R	MAOT in °C	Details in ref.
poly branched alkane	RSL-110	3110*	300°	5
polydimethylsilicone	SE-30, OV-1	3443	300-350°	-
poly branched alkene	RSL-210	4210*	275°	6
polyethylene glycol	Superox-4	5442	300°	7

Table 1 : List of some gum phases. Column McR-R stands for sum total of the McReynolds-Rohrschneider constants for as much that this could be measured. * stands for guessed value.
Sources : SE-30 - OV-1 : Ohio Valley - RSL-110, RSL-210 and Superox-4 : RSL, B-9830, Reinaertdreef, 19 or Alltech, Arlington Heights, Chicago.

We solve practically all our application problems with only two phases; n° 1 and 4 of table 1. An attractive feature of the Superox phases is their low bleeding even at high temperatures, allowing polar phase $(GC)^2$-MS without back ground trouble.

3. Splitter difficulties

Splitters have several characteristics which may be undesirable or even unacceptable : high operating temperature, large fraction of the injected sample is vented, discrimination, etc.The solution to this point is simply to leave the splitter out and to adopt on column or better in column injection. This is easy and fully documented in the literature (8). To avoid trouble, the beginner can opt for columns with an ID that is not too small - 0.3 to 0.5 mm rather than 0.2-0.25 mm.

4. High price or manufacturing difficulties

Commercial prices of glass capillary columns have a tendency to go down. Compare ! What about price per HETP or for comparable column length : capillary-packed ? Manufacturing difficulties are real. Although practically all know-how has been published, making a good glass capillary column is still not easy. The drawing of capillaries alone already requests much attention. If you need less than ∿50 columns per year it may be not worthwhile to start your own development. Making that many will keep a good technician practically full time busy. The starting up difficulties and the hard-ware investment should also be considered.

From a research view point, the difficulties of drawing glass capillary columns, roughening the inner wall and coating, have all been mastered. The remaining problems, attracting the attention of the moment, are high temperature activity-deactivation and quantitation with polar samples. Many deactivation techniques are described in the literature. A clear difference should be made between the MAOT for the phase and for the deactivation procedure.

Conclusions

Optimum results are easy to achieve in $(GC)^2$-MS provided that :

- no splitter is used
- the $(GC)^2$-MS combination is done as described in reference (3)
- a gum phase is used
- temperatures above 220° can be avoided. Higher t° can be used, but not with all samples and not with long column life.

REFERENCES

1. Cooks, R. : International Laboratory, 79 (1979).
2. Van Cauwenberghe, K., Vandewalle, M. and Verzele, M. : J. of Gas chromatography, 6 (1968) 72.
3. Vangaever, F., Sandra, P. and Verzele, M. : Chromatographia, vol. 12, n° 3 (1979).

4. Dandeneau, R. and Zerenner, E. : 3rd International symposium on glass capillary columns. Ed. R. Kaiser 1979 (81). To be published in the Journal of High Resolution Chromatography.
5. Bouche, J. and Verzele, M. : J. Gas chromatography, 6 (1968) 501.
6. Verzele, M. and Sandra, P. : 3rd International symposium on glass capillary columns. Ed. R. Kaiser, 1979 (375). To be published in the Journal of High Resolution Chromatography.
7. Verzele, M. and Sandra, P. : J. Chromatography, 158 (1978) 111.
8. Sandra, P., Verzele, M. and Vanluchene, E. : Chromatographia, 8 (1975) 499.

GAS LIQUID SOLID CHROMATOGRAPHY IN ENVIRONMENTAL AND TRACE ANALYSIS

FABRIZIO BRUNER
Laboratorio sull'Inquinamento Atmosferico del C.N.R.
Via Montorio Romano, 36
00131 - ROMA ITALY

By Gas Liquid-Solid Chromatography (GLSC) a particular Gas Chromatographic technique is meant, where the stationary phase consists of an adsorbent coated with a partition liquid. The adsorbent surface may be partially or totally coated depending on the needs of the analytical problem to be faced. The main feature of such technique is that it exploits the selectivity of adsorption and that of the functional groups of the liquid.

It should be remarked that the driving force of the chromatographic process is adsorption, that is "corrected" by the liquid phase. In this way, the active sites of the adsorbent are shielded by the liquid, yielding a linear isotherm even for highly polar compounds, such as free acid alcohols and aliphatic amine.

The possibility of exploiting such technique depends on the nature of the adsorbent, that must be of the "non specific" type, i.e. it should act only through the London non specific forces, being free of directional forces, such as hydrogen bonds. Of course, an adsorbent that fully meets these characteristics does not exists. However, graphitized carbon black is the most suitable material for the purpose of gas liquid solid chromatography.

Graphitized carbon black is the most non porous, non specific material available and this explains the success of it in many applications to trace analysis.

Due to the particular selectivity toward isomers and the total number of the external electrons in the molecules rather than toward functional groups, Graphitized Carbon Black as such has been successfully used for the separation of hydrocarbons (1), while modified with small amounts of non polar liquid phases was successfully used for the separation of isotopic mixtures.

When Graphitized Carbon Black is modified with polar liquid phases, it may be used for the elution of very polar compounds at extremely low levels of concentration, still maintaining the high selectivity due to the adsorption process. Thus, separation of all light sulfur gases (H_2S, SF_6, COS, SO_2, CH_3SH) was obtained at the ppb level (3).

The extraordinary selectivity of Graphitized Carbon Black is shown by the separation obtained of all the C_1-C_6 alcohols within 7 minutes with a standard 6' column (4). This was obtained by Di Corcia et al. by treating a Graphitized Carbon Black of about 9 m^2/g, commercially known as

Carbopack C with only 0.2% Carbowax 20M. The same author performed this separation in 2 min using a shorter column with finer particles. Also free carboxylic acids, aliphatic primary amines (5) and phenols (6) have been analyzed by this technique. The important fact is that such separations have been made in water solution and at the ppm level, making the direct analysis of several samples of interest, for example, in food chemistry.

One of the most important applications of GLSC is in the analysis of atmospheric samples obtained from working areas. In this type of problems, a relatively high number of samples should be analyzed, that contain usually the some compounds, most of them being organic and chloroorganic solvents. Repetitive analysis is required in such cases and both the selectivity and reproducibility of GLSC columns are extremely useful. This is also true for routine analysis of atmospheric samples, such as those needed for the understanding of photochemical smog (7). The same column has been used for the analysis of hundreds of samples during a summer monitoring campaign (8).

Another important application of GLSC is in the field of fluorochlorocarbon monitoring in air samples. Recentrly all C_1-C_2 fluorochlorocarbons (9) have been separated with a Carbopack B column, coated with 1% SP 1000. Carbopack B is a graphitized Carbon Black with a surface area of about 90 m^2/g.

It can be seen that the some adsorbent matrix, treated with different amounts of various liquid phases can yield the right column for every separation problem, the only limitation being the elution temperature, that is usually higher than in GLC.

For what GC-MS applications are concerned, the main feature of GLSC is that the column show a very low bleeding compared to the same phase used in GLC.

The last important application in this field is the definitive recognition of F21 ($CHCl_2F$) in atmospheric samples, by means of GC-mass fragmentrography (9).

REFERENCES

1) A. V. Kiselev and Y.I. Yashin, "Gas Adsorption Chromatography", Plenum Press, New York, N.Y., (1959).

2) F. Bruner, W. Bocola and G.P. Cartoni, "Nature", 209, 200, (1966).

3) F. Bruner, P. Ciccioli and G. Bertoni, "J. Chromatogr.", 120,200, (1976).

4) A. Di Corcia, A. Liberti, R. Samperi, "Anal. Chem.", 45, 1228, (1973).

5) F. Bruner, P. Ciccioli, E. Brancaleoni, A. Longo, "Chromatographia", 8, 503, (1975).

6) A. Di Corcia, "J. Chromatog.", 80, 69, (1973).

7) F. Bruner, P. Ciccioli, F. Di Nardo, "J. Chromatog.", 99, 661, (1974).

8) P. Ciccioli, G. Bertoni, E. Brancaleoni, R. Fratarcangeli, F. Bruner, "J. Chromatog.", 126, 757, (1976).

9) G. Crescentini, F. Bruner, "Nature", June 1979, in press.

MPMOA4 ENVIRONMENTAL AND BIOMEDICAL APPLICATIONS OF GLASS CAPILLARY GAS CHROMATOGRAPHY/MASS SPECTROMETRY, RODGER L. FOLTZ, DENIS C.K. LIN, SAM V. LUCAS, BRUCE A. PETERSEN, TINA M. ENGEL, GREGORY A. JUNGCLAUS, FRANK W. CROW, ALF BJORSETH, AND BRUCE J. HIDY, Battelle Columbus Laboratories, 505 King Ave., Columbus, OH 43201

Glass capillary columns can offer significant advantages over packed GC columns for both qualitative and quantitative GC/MS analysis of complex mixtures such as are often encountered in samples derived from environmental and biological sources. These advantages will be illustrated by examples of the use of glass capillary GC columns in combination with EI and CI mass spectrometry for the analysis of 1) pollutants in drinking water and sludge extracts, 2) polynuclear aromatic hydrocarbons in combustion emissions, and 3) drugs and drug metabolites in extracts of body fluids.

MPMOA5 ALTERNATIVES TO HIGH PERFORMANCE GLASS CAPILLARY GAS CHROMATOGRAPHY MASS SPECTROMETRY FOR THE ANALYSIS OF COMPLEX SAMPLES. T. Michael Harvey, Ford Motor Co., Dearborn, Michigan 48121

Combined high performance glass capillary gas chromatography/mass spectrometry (gc^2/ms) has been successfully applied to a number of analytical problems in our laboratory. Areas of application have included vehicle emissions with emphasis on catalyst performance and alternate fuels, stationary source emissions from manufacturing operations, ambient air and wastewater, materials characterization and workplace environments.

Set up and optimization time required for proper gc^2/ms analysis can become extensive. We have therefore explored a number of alternatives to gc^2/ms for solving our analytical problems. Some of these have included chromatographic separation using directly coupled packed columns, S.C.O.T. columns, or conventional packed columns combined with mass spectral detection by conventional or low voltage electron impact, positive or negative chemical ionization, or accurate mass measurements at low resolution. In addition, selective gc detectors (N, P, S, P, or EC) are often used as screening tools.

MPM0A6 CAPILLARY GC/CIMS ANALYSIS OF ISOMER/HOMOLOG MIXTURES IN STUDIES OF CI-INDUCED FRAGMENTATION. WILHELM J. RICHTER, WOLFGANG BLUM, JOACHIM LIEHR and ERICH SCHLUMPF, Central Function Research, Ciba-Geigy AG, CH-4002 Basel.

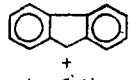
For the study of substituent effects governing CI fragmentation of certain classes of compounds, GC/CIMS analysis of artificial mixtures of properly substituted members can show major advantages over the customary direct sample by sample insertion. Thus, identical ionization conditions are easily secured for all components frequently prepared in batch, in a single chemical experiment. H_2O elimination from protonated 5 to 7-membered alicyclic ketones - strongly dependent on the degree of α-alkyl substitution - will be given as an example.

Attempts to implement recent advances in glass capillary GC (column preparation, injection techniques), essential for the high performance of the system needed for such analysis, will also be discussed.

MPM0B1 EI INDUCED CYCLIZATION OF ORTHO SUBSTITUTED DIPHENYLMETHANES. J.G.LIEHR, R.M. CAPRIOLI, Anal. Chem. Ctr., UTMSH, Houston, Tx. 77025, and A.G.Brenton, J.H.Beynon, Dept. of Chem., U. of Swansea, UK.

Mass spectra of 2-hydroxydiphenylmethane (I) and its ether derivatives in the upper mass region are characterized by an abundant ion m/z 165. Metastable ion measurements reveal that this ion is formed from the molecular ion of I by elimination of hydrogen and H_2O. A fluorenyl cation structure is proposed for this ion on the basis of the identity of CA MIKE spectra of ion m/z 165 generated from I and from fluorene by elimination of hydrogen. Four possible pathways of formation of a fluorenyl cation from the molecular ion of I will be discussed:

a) $M^{+\cdot} \rightarrow (M - H)^{+} \rightarrow$
b) $M^{+\cdot} \rightarrow (M - H_2O)^{+} \rightarrow$
c) $M^{+\cdot} \rightarrow (M - OH)^{+} \rightarrow$
d) $M^{+\cdot} \rightarrow (M - H_2)^{+} \rightarrow$



The contribution of each of these pathways (a-d) to the genesis of fragment m/z 165 was monitored in a reversed geometry instrument by measuring the first fragmentation in the first field-free region and the second fragmentation in the second field-free region.

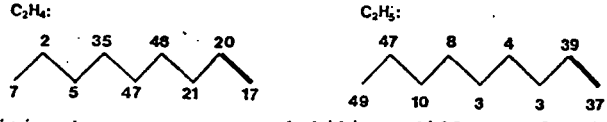
MULTIPLE LABELLING IN MASS SPECTROMETRY

T. Gäumann, D. Stahl & P. Tecon
Institute of Physical Chemistry
Federal School of Technology
CH-1015 Lausanne, Switzerland

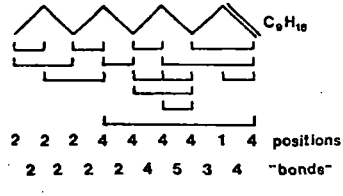
Labelling by ^{13}C and/or D is necessary to study the fragmentation pattern of hydrocarbons. We use 1-nonene to demonstrate for the loss of neutral fragments containing two carbon atoms how multiple labelling can be used to unrarel reaction schemes. In the following table we give the contribution of these fragments to the total ion current. They are rather minor products in the fast decay within the source, but their contributions in the mestastable region shows them to be important precursors for further decay :

m/z	loss of	% TIC -source-	% TIC metastable
98	C_2H_4	1.1	15
97	C_2H_5	2.1	31
96	C_2H_6	-	10

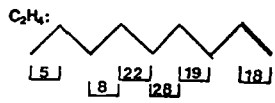
The probability of a given position to be lost to C_2H_4 or $C_2H_5^{\cdot}$ within the source is the following :

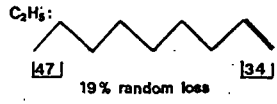


Every position has a nonzero probability, different for C_2H_4 and $C_2H_5^{\cdot}$. Multiple labelling allows two things : it gives information about losing two specified positionstogether, and it increases the number of equations available for a least square treatment of the results. In the former case a rather large number of doubly labelled products would be necessary in order to cover all possibilities. For evident reasons this can hardly be done and a compromise has to be found. Since a least square procedure will be used to evaluate the data, attention has to be paid to the fact that all positions to be lost and bonds to be broken have about equal probabilities. Otherwise a specific loss might be biased. The following ^{13}C doubly or triply labelled compounds were at our disposal :



The vertical bars connected by horizontal lines indicate the labelled positions. By a least square treatment we tried to find the most probable combinations of losing two carbon atoms together to the neutral fragment. The choice of the possible combinations is very limited : only a few possibilities give residual errors in the order of a few percent corresponding approximately to the error of measurement. We obtained the following best solutions :





For ethylene three major pathways have to be retained : a loss of either end and an internal expulsion of two consecutive positions. This general feature was also found for other n-olefines. Both terminal positions can be lost to the neutral fragment in the case of $C_2H_5^+$. Furthermore we have to assume one fifth of the ethyl to be split off by a "random loss", e.g. every position has an equal probability to be lost to the neutral fragment. This can be explained by consecutive reactions, where a C_2H_4 is lost from the $(M-1)^+$-ion. We have shown for n-alkanes that the contribution from this ion cannot be neglected [1] and that odd-electron ions have a tendency for a "random loss" because of rearrangement processes [2].

The probabilities to lose a given position for reaction within the source and metastable decay are compared in the following table :

pos.of label :		9-^{13}C		3,4-$^{13}C_2$		
nbr. of ^{13}C lost:		0	1	0	1	2
"source"	C_2H_4	93	7	54	27	19
	C_2H_5	51	49	93	7	0
meta-stable	C_2H_4	95	5	53	12	15
	C_2H_5	52	48	100	0	0
	C_2H_6	53	47	100	0	0

Two important conclusions can be drawn : firstly distribution for the "fast" and the "slow" reactions seems to be equal, contrary to field ionisation [3]. Secondly, the "random loss" does not contribute to the metastable decay. This is not astonishing because it is assumed to be a two-stage process. However it is in this case difficult to explain the important contribution of ethane that seems to stem from an additional H-loss from the $C_7H_{13}^+$-ion.

References

1. A. Lavanchy, R. Houriet, T. Gäumann, Org. Mass. Spectr. 14,79 (1979)

2. D. Stahl & T. Gäumann, Adv. in Mass Spectr. 7B, 1190 (1978), Inst. of Petroleum, London

3. P. Tecon, D. Stahl & T. Gäumann, Int. J. MS Ion Phys. 27,83 (1978), 29, 363 (1979).

EFFECTS OF SULFUR-FOR-OXYGEN SUBSTITUTION ON EI AND FI MASS SPECTRA OF ESTERS

Gordon W. Wood and Bernard T. Kiremire
Department of Chemistry, University of Windsor
Windsor, Ontario, CANADA N9B 3P4

Previous direct comparisons between mass spectral behavior of isomeric monothioesters have been limited largely to methyl and ethyl esters (1). In that work a number of features were identified in the mass spectra which apparently arose from the influence of the sulfur atom. Most notable among these results was the presence of abundant rearrangement ions from the thionesters, e.g.

$$PhC(=S)OR \longrightarrow PhCO^+ \quad ; \quad 6\% \text{ for } R = CH_3, \quad 92\% \text{ for } R = C_2H_5$$

This process, along with a number of others, appeared to require thiocarbonyl since the isomeric thiolester showed little evidence of the corresponding (reverse?) rearrangement:

$$PhC(=O)SR \not\longrightarrow PhCS^+ \quad ; \quad 0.2\% \text{ for } CH_3, \quad 0.5\% \text{ for } R = C_2H_5$$

Study of higher alkyl thiol- and thionesters related to acetic and benzoic acids has shown that the above rearrangement to produce (oxy) acyl ions is a general process which competes very effectively with other rearrangements and cleavages. Thus n-butyl thionacetate has m/z 43 (CH_3CO^+) as a major peak in EIMS (Fig 1) and a minor peak (1.5%)in FIMS.

Charged olefin (m/z 56) from McLafferty rearrangement is the base peak in EIMS of this compound, and the corresponding ionized styrene (m/z 104) becomes predominant in the ß-phenethyl analog (Fig 2).

Benzoates show even more dramatic amounts of rearrangement ions, as shown in Fig 3 where n-butyl thionbenzoate has m/z 105 as base peak. The major rearrangement ions from this compound are summarized (Fig 4) in terms of per cent of total ionization represented by each (%Σ).

1. A. Ohno, T. Koizumi, Y. Ohnishi and G. Tsuchihashi, Org. Mass Spectrom., 3, 261 (1970).

(a portion of this work has been submitted to Org. Mass Spectrom.)

Fig 1. EIMS of n-BUTYL THIOACETATES (M=132).

$CH_3\overset{O}{\overset{\|}{C}}SC_4H_9$	m/z	$CH_3\overset{S}{\overset{\|}{C}}OC_4H_9$
28	132	93
0.2	99	2
2	89	3
1	88	2
4	77	84
2	76	28
6	72	1
0.4	60	10
1	59	44
2	57	35
12	56	100
3	55	17
3	47	2
100	43	78

Fig 2. THIONACETATE REARRANGEMENTS

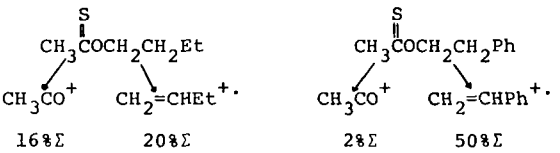
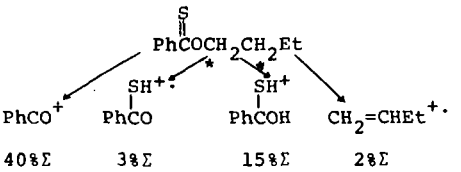


Fig 3. EIMS of n-BUTYL THIOBENZOATES (M=194)

$PhC\overset{O}{\overset{\|}{S}}C_4H_9$	m/z	$PhC\overset{S}{\overset{\|}{O}}C_4H_9$
9	194	31
0.5	161	8
4	139	37
1	138	8
3	134	0.2
2	122	10
0.5	121	35
100	105	100
23	77	22
0.5	56	6

Fig 4. n-BUTYL THIONBENZOATE REARRANGEMENTS



Chemical Ionization Mass Spectrometry of Aryl Substituted Cyclohexenes: Analogy to Solvolysis

G. Sudhakar Reddy, M. Vairamani and K. G. Das
National Chemical Laboratory, Poona-411008, India

H. Budzikiewicz
Institut für Organische Chemie der Universitat
Köln, West Germany

Mark M. Green
Clarkson College of Technology
Potsdam, New York 13676 USA

Abstract

In contrast to the usual expectation in chemical ionization (CI) mass spectrometry, the CI spectra of a series of aryl 4-nitro-Δ'-cyclohexenes show very low intensity protonated molecular ions while a major share of the ion current is carried by rearrangement ions. The intervention of a rearrangement long known in the solvolysis of cyclohexenyl carbenium ions can account for the observed CI behavior.

The analytical value of chemical ionization mass spectrometry[1] derives from the usual observation of simple spectra dominated by the intensity of the protonated molecular ion $(M+1)^+$. The isobutane CI spectrum of 3,5,6 triphenyl-4-nitrocyclohexene exhibits an $[M+1]^+$ ion carrying only 0.4% of the total ionization above m/z 90 ($\%\sum_{90}$) while the base peak in the spectrum which carries 30%$\sum_{90}$ is a rearrangement ion composed of two of the phenyl groups and a methine carbon $[(C_6H_5)_2CH]^+$.

Skeletal rearrangement processes which are common in electron ionization mass spectra[2] are of less frequent occurrence in chemical ionization nass spectra.[1,3]

In the case herein we shall see that the interesting extrusion of a single carbon bearing hydrogen and two aryl groups from the protonated triarylnitrocyclohexenes can be reasonably connected to the long known contraction of six to five membered ring carbenium ions.[4]

Moreover we have previously studied the EI behavior of this class of aryl nitrocyclohexenes[5] and the present study acts to complete this picture for the behavior of these materials in mass spectrometers subject to differential ionization mechanisms.

The materials under discussion are twenty different Δ'-4-nitrocyclohexenes bearing aryl and heterocyclic rings at positions 3,5,6.

A heuristic scheme, which must await further evidence for confirmation, would reasonably involve the initial protonation at the nitro group[9] so as to give loss of HNO_2. The loss of HNO_2 to lead to the carbenium ion might also be aided by the adjacent phenyl group[10] or by solvolytically precedented[11] participation of the homoallylic double bond. Thus the observation of a low intensity $[M+H]^+$ ion is reasonable and not of exceptional note. Protonation at various sites in multifunctional molecules can be expected[12] and leads to other ions in the spectrum. The key and striking observation in these molecules is the abundant extrusion of the charged fragments $[CHR_2R_3]^+$, $[CHR_1R_2]^+$ and $[CHR_1R_3]^+$. It is difficult to understand how the substituted cyclohexene structure could yield such ions. As outlined below, a reasonable solution to this apparent conundrum may be found in the literature of cyclohexyl carbenium ions.

Deno and Houser first reported on the basis of n.m.r. data the opening of bicyclic alcohols to cyclohexenyl cations which then undergo ring contraction to cyclopentenyl ions.[13] Further research in this area has led to details of the scrambling mechanisms available in these ions.[11,14-18]

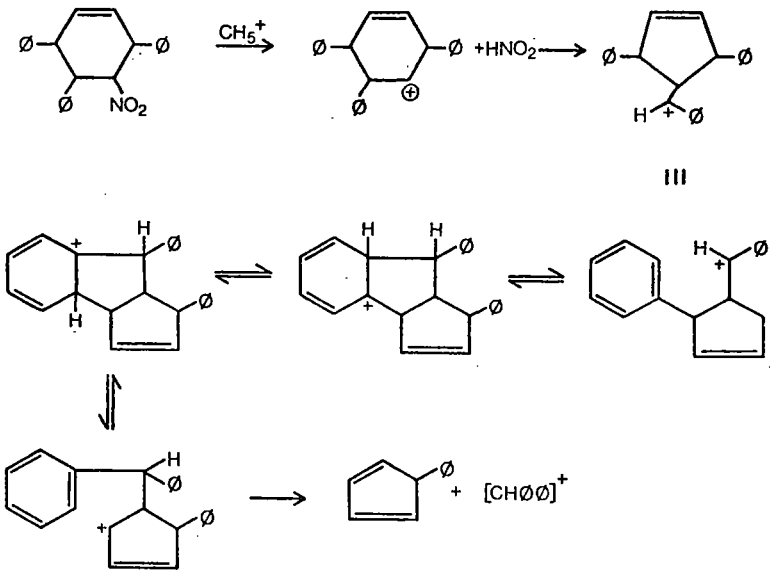
The research referenced above suggests the possibility of ring contraction in the $[M+H-HNO_2]^+$ ion produced in the CI of these triarylnitrocyclohexenes.

We are now offered an explanation for the expulsion rearrangement loss of $[CHRR]^+$. Ring contraction from the initially produced cyclohexenyl cation could cast one carbon out of, although for the moment still attached to, the cycle.

In the n.m.r. studies discussed above, it was found that the ring contracted ion rapidly transfers hydride so as to place the charge within the ring. A large body of evidence on intramolecular Friedal-Crafts alkylations and acylations[19] shows that carbocations located so as to close five membered rings are favorable. This is precisely the situation in the molecules discussed here and moreover such an intervention hypothesis could reasonably lead to the CI observed diarylmethinyl cation. This hypothesis leads to an overall mechanism which is outlined for one of the compounds in the Scheme below.

Scheme

Mechanistic Hypothesis



The proposal in the Scheme is supported by: analogy to known solution carbocation chemistry; the expulsion of diarylmethinyl cations predominantly containing aryl groups of widely varying structure; a strong stereochemical dependence. The latter two observations would be difficult to understand if more random and extensive rearrangements were occurring prior to fragmentation.

The present study indicates that the substituted cyclohexenyl cation undergoes the same type of rearrangements under solvolytic conditions and in the CI source.

References

1. A recent view is: A. L. Burlingame, C. H. L. Shackleton, I. Howe and O.S. Chizhov, Anal. Chem. 50, 346 (1978) and pages 355-356 in particular. See also: F. H. Field, Accounts Chem. Res. 1, 42 (1968) and subsequent papers in that series; F. H. Field, in MTP International Review of Science, Physical Chemistry Series One, Vol. 5, (A. Maccoll, Ed.), Ch. 5, Butterworths, London (1972). A beautiful recent example of this analytical value is: A. M. Sepulchre, P. Varenee, B. C. Das, S. D. Gero and H. E. Audier, Nouveau J. Chimie 2. 405 (1978).

2. P. Brown and C. Djerassi, Angew. Chem. Int. Ed. 6, 477 (1967). For general discussion, references and examples see: R. A. W. Johnstone, Mass Spectrometry for Organic Chemists, Cambridge Univ. Press, Cambridge, 1972; D. H. Williams and I. Howe, Principles of Organic Mass Spectrometry, McGraw-Hill, New York, 1972; F. W. McLafferty, Interpretation of Mass Spectra, 2nd Ed., Benjamin, Reading, Mass., 1973; K. G. Das, Organic Mass Spectrometry, India Book House, Bombay, 1977. Rearrangement reactions in EI and CI mass spectrometry are valuable probes of stereoisomerism. See: M. M. Green, in Mass Spectrometry of Natural Products, Pergamon Press, New York, 1978.

3. A few outstanding examples are: F. H. Field and M. S. B. Munson, J. Amer. Chem. Soc. 89, 4272 (1967); F. H. Field, ibid 90, 5649 (1968); ibid 89, 5328 (1967). J. G. Liehr and A. McCloskey, Org. Mass Spectrom. 9, 491 (1974); P. Longevialle, G. W. A. Milne and H. M. Fales, J. Amer. Chem. Soc. 95, 666 (1973). A recent excellent review is: W. Richter and H. Schwarz, Angew. Chem. Int. Ed. 17, 424 (1978).

4. N. C. Deno and J. J. Houser, J. Amer. Chem. Soc. 86, 1741 (1964).

5. K. G. Das and K. P. Madhusudanan, Org. Mass Spectrom. 11, 135 (1976).

6. J. S. Bindra, C. Jain and N. Anand, Ind. J. Chem. 9, 388 (1971).

7. K. P. Madhusudhanan, Ph.D. Thesis, Kerala University, Kerala, India (1974).

8. In addition, the EI spectra were recorded for all materials studied. The results support our earlier published observations.[5] We have in the course of this, recorded the normal metastable ions at 70 ev and determined the MIKE spectra for the $[M-NO]^+$ and $[M-HNO_2]^{\circ+}$ ions from compound (3) in our studies. These data and discussion may be found in: C. Sudhakar Reddy, Ph.D. Thesis, in preparation, National Chemical Laboratory, Poona, India, 1979. This work will form the basis of a future publication.

9. D. P. Martinsen, Org. Mass Spectrom. 11, 762 (1976).

10. R. H. Shapiro and T. F. Jenkins, Org. Mass Spectrom. 2, 771 (1969); W. J. Richter and W. Vetter, ibid 2, 781 (1969); G. W. A. Milne, T. Axenrod, H. M. Fales, J. Amer. Chem. Soc. 92, 5170 (1970).

11. G. A. Olah, G. Liang and Y. K. Mo., ibid 94, 3544 (1972).

12. See reference 3 and especially W. Richter and H. Schwarz therein.

13. N. C. Deno and J. J. Houser, J. Amer. Chem. Soc. 86, 1741 (1964). See also: N. C. Deno and R. R. Lastomirsky, ibid 90, 4085 (1968).

14. T. S. Sorenson and K. Rajeshwari, ibid 93, 4222 (1971); T. S. Sorenson and K. Ranganayakulu, ibid 92, 6539 (1970); T. S. Sorenson, ibid 89, 3794 (1967).

15. T. S. Sorenson and K. Rajeshwari, Can. J. Chem. 50, 2939 (1972); T. S. Sorenson, R. Cone, R. P. Haseltine and P. Kazmaier, ibid 52, 3320 (1974).

16. G. A. Olah and G. Liang, J. Amer. Chem. Soc. 94, 6434 (1972).

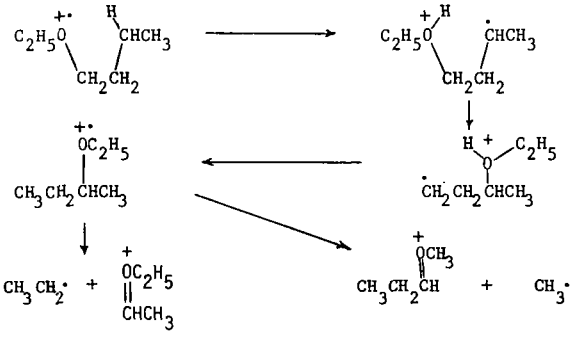
17. D. V. Nightingale and M. Maienthal, ibid 72, 4823 (1950); D. V. Nightingale, J. D. Kerr, J. A. Gallagher and M. Maienthal, J. Org. Chem. 17, 1017 (1952).

18. G. Seybold, P. Vogel, M. Saunders and K. B. Wiberg, J. Amer. Chem. Soc. 95, 2045 (1973); D. Forcaşiu, ibid 100, 1015 (1978).

19. L. Ross and C. Barclay in, Friedel-Crafts and Related Reactions, Vol. II, Ed. by G. A. Olah, Ch. XXII, Interscience, 1964; S. Sethna, ibid, Vol. III, Ch. XXXV.

LOSS OF ALKANE FROM IONIZED SECONDARY ETHERS. C.E. Hudson, R.D. Lerner, R. Aleman and D.J. McAdoo, Marine Biomedical Institute, Department of Human Biological Chemistry and Genetics, The University of Texas Medical Branch, Galveston, Texas 77550

We recently expanded the observation of Bernasek and Cooks[1] on the loss of ethyl from ionized n butyl ethyl ether.[2] The mechanism of decomposition in Scheme I is consistent with labelling results and with observed isotope effects.



Scheme I

However the metastable ion chemistries of n and sec butyl ethyl ethers differed considerably (Table I).

Table I
Metastable Decompositions of Ether Ions

	Species Lost			
Ether	C_2H_5	C_2H_6O	CH_3	C_2H_6
n Butyl Ethyl	100	13.4	2.4	0.8
sec Butyl Ethyl	< 47	0	0	100
sec Butyl Methyl	29	0	0	100

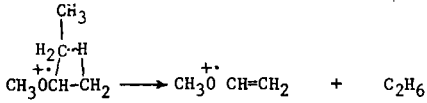
We suggested that C_2H_5 and C_2H_6 may be lost from separate electronic states. We have now studied ethers deuterated in the sec butyl group, (Table II)

Table II
Ethane Losses from Deuterated Ethers

Ether	C_2H_6	C_2H_5D	$C_2H_4D_2$	$C_2H_3D_3$
$CH_3CD_2CH(CH_3)OCH_3$[a]	0	15[b]	100	-
$CH_3CH_2CD(CD_3)OCH_3$[c]	100	0	-	-
$CH_3CH_2CH(CD_3)OCH_3$[d]	2.3	100	3.3	>18[e]

a. 98% d_2, 4% d_1 b. Probably largely $C_2H_3D_2$
c. 98% d_1, 2% d_o d. 96% d_3, 4% d_2, e. Not corrected for overlap with 90→58

and shown that the reaction is a 1,2 elimination to form an ionized vinyl ether.



This reaction is symmetry forbidden if it proceeds from the gound electronic state through the transition state of simplest geometry.

A comparison of the thermochemistry of this fragmentation with that of the loss of ethyl shows that the latter is less endothermic by about 3 kcal/mole.

$CH_3CH_2\overset{+}{O}=CHCH_3$	$C_2H_5\cdot$	$\Sigma\Delta H_f^{298}$
121.2 kcal/mole[3]	25.7[4]	146.9
$CH_3CH_2\overset{+\cdot}{O}CH=CH_2$	C_2H_6	
170.0[5,6]	-20.2[7]	149.8

It is surprising that a rearrangement reaction could dominate a direct cleavage which is more thermodynamically favorable. These observations support the suggestion that the differently derived sec-butyl ether ions decompose from different electronic states.

Other ionized ethers of secondary alcohols also lose alkane molecules. These losses are summarized in Table III. The loss of CH_4 is observed only in the isopropyl ether, which cannot elimate any other alkane by the same mechanism. The ethers which can form a secondary radical by five membered ring hydrogen transfer to oxygen also lose methanol.

Table III
Losses of Neutral Species from Metastable Ionized Ethers

Ether	CH_4	C_2H_6	CH_3OH	C_3H_8	C_4H_{10}
2-Methoxy Propane	100	0	0	0	0
2-Methoxy Pentane	0	0	100	19	0
3-Methoxy Pentane	0	100	0	0	0
2-Methoxy Hexane[a]	0	0	38	0	100
3-Methoxy Hexane	0	100	12	67	0

a. Loss of CH_3=52

Ionized ketones lose alkanes by a similar mechanism.[8] Ions derived from sec butyl benzene, N,N-dimetyl sec butyl amine, and di sec butyl sulfide lost ethyl but not ethane. No molecular ion or metastable peaks from it could be found for methyl tert pentyl ether.

Acknowledgment

Supported by the Robert A. Welch Foundation (Grant H-609). The adiabatic ionization potential of ethyl vinyl ether was measured by Henning Friege and Martin Klessinger of Orleansring University, Munster West Germany.

References

1. S.L. Bernasek and R.G. Cooks, Org. Mass Spectrom., 3, 126 (1970)
2a. C.E. Hudson and D.J. McAdoo, Org. Mass Spectrom., 14, 109 (1979)
b. C.E. Hudson and D.J. McAdoo, Proceedings of the 26th Annual Conference on Mass Spectrometry and Allied Topics 529 (1978)
3. R. Botter, J.M. Pechine, and H.M. Rosenstock, Int. J. Mass Spectrom. Ion Phys., 25, 7 (1977)
4. J.A. Kerr, Chem. Rev., 66, 464 (1966)
5. G. Pilcher, H.A. Skinner, A.S. Spell and A.E. Pope, Trans. Faraday Soc., 59, 316 (1963)
6. The adaibatic ionization potential of ethyl vinyl ether is 8.83 eV (H. Friege and M. Klessinger Private Communication)
7. E.J. Prosen and F.D. Rossini, J. Res. Nat. Bur. Stand., 34, 263 (1945)
8. R.G. Cooks, A.N.H. Yeo, and D.H. Williams, Org. Mass Spectrom., 2, 985 (1969)

MPM0B6

LOW ENERGY FRAGMENTATION OF THE MAJOR IONS OF CYCLOHEXANE BY TANDEM QUADRUPOLE MASS SPECTROMETRY

R.K. Latven, R.A. Yost and C.G. Enke
Department of Chemistry
Michigan State U., E. Lansing, MI

The triple quadrupole mass spectrometer developed in our laboratory was conceived primarily as an analytical tool for mixture determination and compound identification. It is now clear that it also has great value in the study of ion-molecule reactions and in the elucidation of compound structures and fragmentation pathways.

Figure 1 is a schematic diagram of the essential components of the instrument. Figure 2 shows how structure elucidation and mixture analysis is achieved by the triple quadrupole system. For a detailed description of the instrument and application see abstract # WAMP12 by R.A. Yost and C.G. Enke, this volume. Briefly, the sample, fragmented in the source, is accelerated into the first quadrupole, where an ion of interest can be selectively filtered into the second. These ions posess only about 10-20 eV of kinetic energy. A gas, maintained at between 10^{-2} and 10^{-6} torr, is bled into the RF-only quad collision chamber to provide a collision partner for the incoming ions. The resulting ionic products are scanned with the third quadrupole, and detected by an electron multiplier to produce a collision induced dissociation (CID) spectrum. CID spectra can be obtained for most cations generated in the source, including such low intensity ions as the M+1 isotope ion.

The 70 V electron impact spectrum of cyclohexane and selected CID spectra are seen in Figure 4. All spectra were recorded on our instrument. A comparison of the cyclohexane EI and 84^+ CID spectra shows that they are quite similar. Since the CID is a low energy process, many of the smaller peaks due to losses of various hydrogen seen in the EI are reduced or absent in the CID spectrum. Also, conspicuously diminished in the CID spectrum is the 39^+ peak, presumably the stable cyclopropenium cation. This implies that 39^+ is formed in the source by some process other than low energy fragmentation. However, since 39^+ appears in some other CID spectra of cyclohexane the 39^+ may be more readily produced by a secondary fragmentation. Also note the exclusion of C^{13} isotope peaks at 85, 70 and 57 in the CID spectrum.

Since normal mass spectrometry of hydrocarbons is that of odd electron ions, it is interesting to observe the mass spectra of even electron (EE) ions. We can compare the CID spectra of $C_6H_{10}^+$ (83^+), $C_5H_9^+$ (69^+), and $C_4H_7^+$ (55^+), each of which has one degree of unsaturation. Similarities are immediately apparent; for example, all three ions produce only EE ions. The similar fragmentation patterns may imply a common mechanism. These particular ions do not fragment to form single carbon fragment ions or single carbon neutral species. What is observed are only $C_nH_{2n+1}^+$ and $C_nH_{2n-1}^+$ fragment ions, where n ranges from 2 to M-C_2. The C_6 (83^+) parent ion thus produces 57^+, 43^+, and 29^+; and 55^+, 41^+, and 27^+. For the C_5 (69^+) parent ion, 43^+, 29^+, 41^+, and 27^+ are observed. Similarly, for 55^+ parent ions, only 29^+ and 27^+ are formed. The most favorable fragmentation seems to involve both the formation of ethyl cation, 29^+ as one major product and the loss of neutral ethylene to form another.

Four carbon fragments with varying degrees of unsaturation can also be compared. Figure 3 shows the CID spectra of $C_4H_7^+$ (55^+), $C_4H_5^+$ (53^+) and $C_4H_3^+$ (51^+), with one, two, and three degrees of unsaturation respectively. Except for cyclopropenium cation (39^+) the only major products are those with two carbons. The major peaks result from loss of neutral acetylene. The loss of ethylene also results in prominent $C_4H_7^+$ peak. The fragmentation of cyclopropenium cation, 39^+, the smallest of the aromatic ring system is also of interest. It is the most difficult ion of cyclohexane to fragment, as its molecular ion is some 16 times more intense than its most intense fragment ion, 38^+. Its fragmentation differs from other EE ions in that this most intense fragment is an odd electron species. It also readily loses H_2, which leaves the strange moiety C_3H^+ at about 50% relative abundance.

Future work on this instrument will involve elucidation of fragmentation mechanisms of cyclic hydrocarbons, using labeling techniques, and the study of ion-molecule reactions. We are pleased to acknowledge support for this project from the Office of Naval Research.

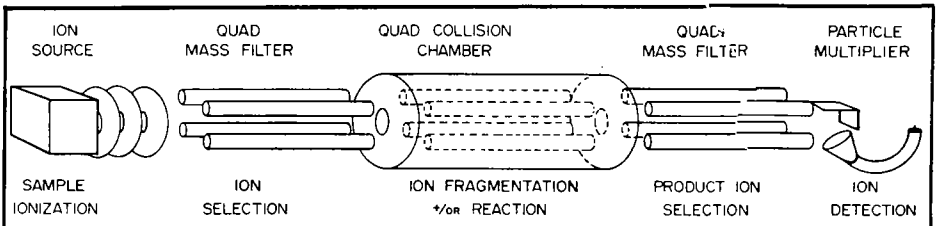


FIGURE 1

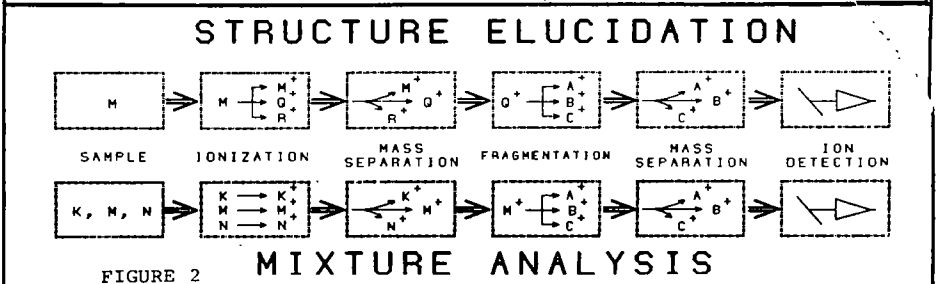
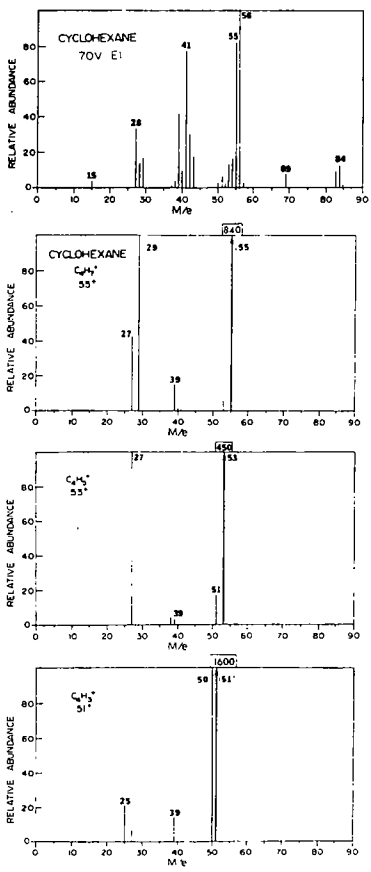


FIGURE 2

FIGURE 3



Applications of B/E Linked Metastable Scans to the Analysis of Natural Products

G A Warburton, R McDowell, D Hazelby, S Evans and K R Compson
Kratos Limited, Barton Dock Road, Urmston, Manchester M31 2LD

The B/E linked scan can be an extremely useful tool in the identification and structural analysis of compounds. The resolution obtainable within a B/E scan is good in comparison with other types of metastable scans and allows mass assignment of fragment ions to be easily performed. Artifact peaks can be produced but due to their low intensity and relatively great width (analogous to metastable peaks produced in normal mass spectra), they are easily distinguished.

A further advantage of B/E scanning is that source tuning conditions remain unaffected giving data which is more reproducible than that from other metastable scan modes (alteration of accelerating voltage for example normally changes source tuning conditions and effective source sensitivity).

Scanning over a wide mass range also becomes possible. For example, a B/E scan of m/e 1165 in Fomblin® oil shows peaks below m/e 169.

An important application of B/E scans is illustrated by the data in Figures 1 and 2. These are B/E scans of two stereoisomeric anhydrosugars, 1,5 anhydroxylofuranose and 1,5 anhydroribofuranose, shown in Figure 3. For all practical purposes the EI spectra of these compounds are identical. Any differences in ion intensity which might result from preferences in reaction pathways are lost in the overall spectra. B/E scans of the weak 115^+ ion (M-OH), however, show differences between the two, notably the relatively intense ion of m/e 72 formed by a loss of 43 amu (C_2H_3O) in 1,5 anhydroribofuranose.

Table 1 contains a summary of the intensity measurements taken from several B/E scans of one of the samples and illustrates the very acceptable reproducibility of the data. Hence, it is now possible to distinguish these isomers using data from a single B/E scan.

Another application of B/E scanning is its use in conjunction with soft ionisation techniques which on their own provide little structural information. For example, in the case of FD very few peaks are seen except M^+, $M+H^+$ or $M+Na^+$. Collision induced decomposition together with B/E scanning can help to provide extra information. Figure 4 shows part of a B/E scan from m/e 870 in the FD spectrum of the porphyrin, phaeophytin-a using helium as a collision gas to induce decomposition. The peaks observed can be explained in terms of successive losses from the phytyl side chain. It is interesting that m/e 660 and 606 are not seen in this scan but were present in the original FD spectrum. This suggests that these ions are due to impurities, for example, the related porphyrin, phaeophorbide-a (M.wt.606).

We wish to thank Dr Metzger of Oldenburg University for supply of the sugar samples and Professor A H Jackson and Dr D E Games of Cardiff University of supplying the porphyrin samples. We would also like to thank Dr J R Chapman for his help in this work.

Fomblin® is a registered trade mark of Montedison.

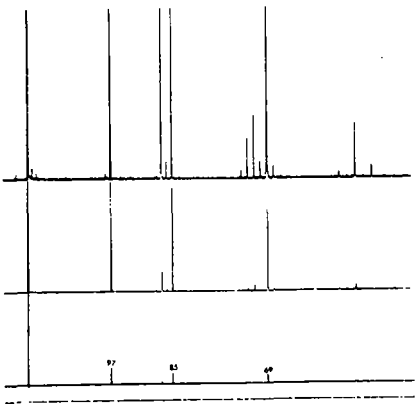


Figure (1)

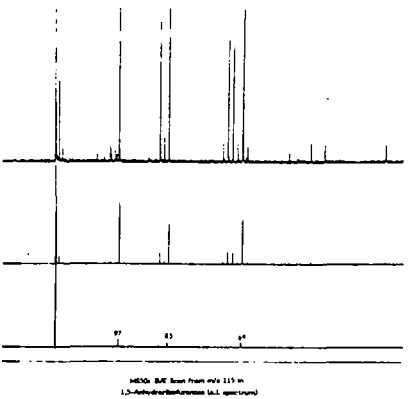
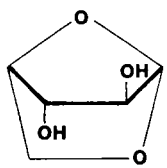
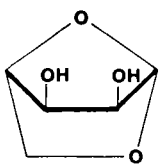


Figure (2)



1,5-Anhydroxylofuranose



1,5-Anhydroribofuranose

M/E VALUE	97	87	86	85	73	72	71	70	69	68	57	55
MEAN RELATIVE INTENSITY	100	17	3	40	4	13	17	3	51	3	3	3
COEFFICIENT OF VARIATION OF INTENSITY VALUES (%)	-	8	15	13	14	10	12	15	10	27	28	26

M55o REPRODUCIBILITY OF B/E SCANS FROM M/E 115 IN 1,5-ANHYDRORIBOFURANOSE

Table (1)

Isomeric anhydro sugars for metastable analysis

Figure (3)



M550 Part of B/E scan from parent ion in fd spectrum of phaeophytin a (M Wt 870)

Figure (4)

Diagnostic TMS-containing ions in the mass spectra of sterol derivatives

D.J. Harvey and Paul Vouros
Department of Pharmacology
Oxford University and
Institute of Chemical Analysis
Northeastern University
Boston, Massachusetts 02115

The mass spectra of the trimethylsilyl derivatives of selected hydroxy steroids have been studied with emphasis on the recognition of TMS-containing ions specific to the position of hydroxylation on the steroid system. Ions characteristic of 6-hydroxy substitution or hydroxylation on the 17β-side chain were examined. Specific ions whose formation is influenced by the presence of a 6-OTMS group were noted. The relative abundance of some of them was enhanced significantly by the presence of an additional 3-OTMS substituent.

Strong bifunctional group interactions characterized the mass spectra of derivatives possessing a 17α-hydroxy or TMSO group and one or more TMSO substituents on the 17β-side chain. Selective isotopic labeling revealed the "mixing" of TMS groups occurring in structurally diagnostic ions. Reciprocal exchange of a TMS group and a vicinal hydrogen was encountered in partially trimethylsilated sterols. The mechanisms of formation of major ions and the specificity of some of these interactions will be discussed.

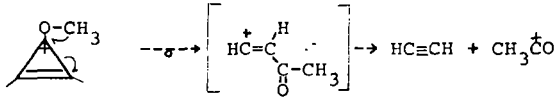
This work will be published in part in Biomedical Mass Spectrometry (1979)

STRUCTURE AND FORMATION OF GASEOUS $C_4H_5O^+$ IONS MPMOB9

JOHAN K. TERLOUW, UTRECHT UNIVERSITY, LABORATORY FOR ANALYTICAL CHEMISTRY, Cr esestraat 77a, 3522 AD UTRECHT, THE NETHERLANDS.

Characterization of $C_4H_5O^+$ ions in the gas phase using their metastable ion (MI) and collisional activation (CA) spectra shows that the following isomeric ions are stable for $\geq 10^{-5}$s. :
(i) the four isomeric $C_3H_5\overset{+}{C}=O$ ions ($CH_2=CH-CH_2-\overset{+}{C}=O$ (a), $CH_3CH=CH-\overset{+}{C}=O$ (b) $CH_2=C(CH_3)\overset{+}{C}=O$ (c) and cyclo-$C_3H_5\overset{+}{C}=O$ (d)) which were generated from a large number of precursor molecules. The structure identity of the cyclopropyl carbonyl cation follows immediately from the presence of a characteristic peak at m/z 55 (loss of CH_2) and also from the large kinetic energy release observed for the loss of CO in the MI spectrum.
(ii) the methoxy substituted propargyl cations $HC\equiv C-\overset{+}{C}H-OCH_3$ (e) and $CH_3O-C\equiv C-CH_2^+$ (f), $H-C\equiv C-CH_2-OCH_2^+$ and the cyclic ion $\underline{CH_2-\bar{C}H-\overset{+}{C}H-\bar{C}H-O}$ (g) which were generated from a series of acetylenic and allenylic ethers. Of these, the cyclic ion (g) is the most stable :its ion enthalpy ($\leq$ 165 kcal mol^{-1}) is close to that found for the acyclic $C_3H_5\overset{+}{C}=O$ isomers (a), (b) and (c). Based upon additional thermochemical evidence and analysis of deuterium and 13-C labelled precursor molecules it is concluded that loss of X$^\cdot$ from ethers of the type $X-C\equiv C-CH_2OCH_3$ involves isomerization into energy rich allenyl type ions $(X)HC=C=CHOCH_3^{4+}$. These ions undergo loss of X$^\cdot$ by simple bond cleavage, yielding (e) type product ions, when the C-X bond strength is relatively low (X= I,Br). When X=Cl and especially CH_3 or H, X$^\cdot$ is only lost after further rearrangement yielding the cyclic product ion (g). The mechanism for this cyclization reaction is related to that proposed in a previous study (Org. Mass Spectrom. 13, 470 (1978))for the ester → acid isomerization in the molecular ions of α,β-unsaturated carboxylic acids.
In contrast to the generation of $C_3H_3^+$ ions, where, irrespective of the structure of the (acyclic) precursor molecule studied, the cyclic cyclopropenium ion is always generated at the thermochemical threshold,it is found that the methoxy cyclopropenium ion (k) is not generated from acyclic precursor molecules. A possible reason is that the differences in heat of formation between the three methoxy substituted $C_3H_3^+$ ions ((e),(f) and (k)) are much smaller than that found for the two unsubstituted isomers (cyclo-$C_3H_3^+$ is more stable than $H-C\equiv C-CH_2^+$ by 26 kcal mol^{-1}). Calculations support this idea : an ab initio calculation related to STO 4-31 G with geometries taken from fully optimized MINDO/3 calculations even predicts that the methoxy cyclopropenium ion is less stable than the methoxy propargyl cation (e) (by 9 kcal mol^{-1}, species (f) is calculated to be 14 kcal mol^{-1} higher in energy than (e)). However, the methoxy cyclopropenium ion is a stable entity which can be generated by loss of $OCH_3^\cdot$ from ionized 2,2-dimethoxy-cyclopropene. Its MI and CA spectra are completely different from those of (e) and (f) type ions.(Ions (e) and (f) have loss of CO as base peak in the MI and

CA spectra whereas ion (k) exclusively loses C_2H_2 in the MI spectrum) We propose that the C_2H_2 loss involves a 1,2 methyl shift followed by ring opening:

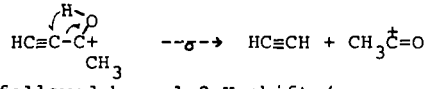


The Gaussian shaped metastable peak for this process (T0.5=45 meV) is similar to the narrow component of the composite metastable peak for loss of C_2H_2 from $HC{\equiv}C\text{-}\overset{+}{C}(OH)CH_3$ (i) type ions (vide infra).

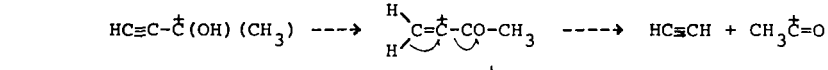
Acetylenic and allenylic alcohols were also investigated. **Linear alcohols** yield stable ions of the type $C_3H_3\overset{+}{C}HOH$ (l) and $HC{\equiv}C\text{-}\overset{+}{C}HCH_2OH$ (m) whereas loss of an alkyl group X· from acetylenic alcohols $HC{\equiv}C\text{-}C(X)(OH)(CH_3)$ and gas phase protonation of $HC{\equiv}C\text{-}CO\text{-}CH_3$ are shown both to yield stable $HC{\equiv}C\text{-}\overset{+}{C}(OH)(CH_3)$ ions. Ions of this structure are unique among all other $C_4H_5O^+$ isomers by having m/z 43 ($C_2H_3O^+$) as base peak in both the metastable ion and collisional activation spectra. It is concluded (thermochemical considerations and deuterium labelling) that the composite metastable peak for this process corresponds with two distinct reaction profiles which must lead to the same product ion, $CH_3\overset{+}{C}{=}O$, and neutral, $HC{\equiv}CH$.

We propose that the two pathways for loss of C_2H_2, whose energy requirements are very similar, respectively involve:

(1) a concerted four membered cyclic rearrangement (broad component metastable peak):



(2) a 1,4 hydroxyl-H shift followed by a 1,2 H shift (narrow component of the metastable peak):



It is further shown that the $C_4H_5O^+$ ions from related alcohols (like $HC{\equiv}C\text{-}CH(OH)(CH_3)$) which have an α-H atom available for isomerization into energy rich allenyl type molecular ions consist of a second stable structure $H_2C{=}C\text{-}\overset{+}{C}(OH){=}CH_2$. (j).

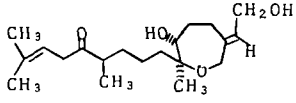
-o-o-o-o-o-o-o-o-

Mass Spectra of the Novel Oxepane Diterpenes from the Mexican Plant Zoapatle (Montanoa tomentosa): Zoapatanol and Montanol

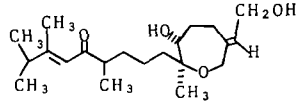
Charles J. Shaw, Robert Chen, Mary Lou Cotter, Ramesh M. Kanojia and Michael Wachter, Ortho Pharmaceutical Corporation, Division of Chemical Research, Raritan, New Jersey 08869

The isolation and identification of the biologically active components of the zoapatle plant, zoapatanol and montanol, has been recently reported[1].

These oils were separated by chromatography and identified by combined spectral data (IR, NMR, C^{13}-NMR, GC/MS), chemical transformations and x-ray crystallography of a derivative. The following structures were established for these novel oxepane diterpenes:



Zoapatanol 338



Montanol 352

The mass spectrum of zoapatanol had an apparent $[M]^{+\cdot}$ 320 followed by the elimination of water $[M-H_2O]^+$ 302 and cleavage of an isoprene unit $[M-C_5H_9]^+$ 251. The mass spectrum was further characterized by the m/z 69 base peak and low intensity fragments above mass 150. Montanol had an apparent $[M]^{+\cdot}$ 334 and a very intense m/z 111 base peak which accounted for a large portion of the total ion current. High resolution mass spectrometry indicated that the elemental composition of the apparent molecular ion of zoapatanol was $C_{20}H_{32}O_3$ and montanol was $C_{21}H_{34}O_3$. From other spectral techniques it appeared that the true $[M]^+$ was not being observed by EIMS.

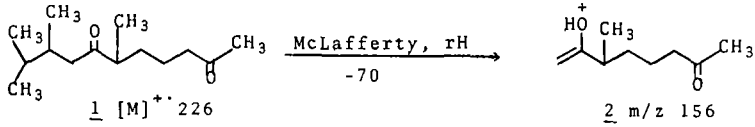
A variety of derivatives were prepared to establish the true mass of these diterpenoids. The thermally stable TMS derivative of zoapatanol had a $[M]^{+\cdot}$ 554 followed by the loss of trimethylsilanol $[M-90]^+$ 464 and a primary alcohol fragment $[464-103]^+$ 361. The elimination of three TMS groups [M-OTMS; HOTMS; CH_2OTMS]$^+$ 282 suggested that zoapatanol had three hydroxyl groups. However, the TMS derivative's $[M]^{+\cdot}$ 554 was inconsistent with the underivatized $[M]^{+\cdot}$ 320. It was postulated that one of the TMS groups resulted from reaction with an enol since a carbonyl absorption band was present in the infrared. A $[M]^{+\cdot}$ 511 obtained from the MOX:TMS derivative prepared according to Horning's procedure[2] confirmed this finding and indicated a 338 molecular weight for zoapatanol.

Montanol's TMS derivative mass spectrum had a $[M]^{+\cdot}$ 496 and a m/z 103 base peak indicating the presence of a primary alcohol. The TMS derivative suggested a starting molecular weight of 352. The $[M]^{+\cdot}$ 525 obtained from the combined MOX:TMS derivative established that montanol's mass was 352 and its structure contained two hydroxyls and a keto group.

Zoapatanol and montanol's molecular weight were confirmed from their CIMS. Methane CIMS of zoapatanol showed a protonated molecular ion $[M+H]^+$ 339 followed by two consecutive losses of water:m/z 321 and 303. The 339 cation became the base peak when isobutane was used. Montanol's CIMS had a $[M+H]^+$ 353.

The major differences between montanol and zoapatanol were that montanol's mass was 14 amu higher than zoapatanol's, zoapatanol contained a readily enolizable carbonyl and montanol had an intense m/z 111 fragment which accounted for a large portion of the total ion current. The m/z 111 fragment was found to result from cleavage of the terminal side chain ($C_7H_{11}O$) alpha to the carbonyl.

The fragment (2) obtained from McLafferty rearrangement of the montanol diketone degradation product (1), established the position of the additional methyl group in montanol's side chain as beta to the carbonyl.



1 $[M]^{+\cdot}$ 226

2 m/z 156

1. S. Levine, R. Adams, R. Chen, M. L. Cotter, R. Huettemann, A. Hirsch, V. Kane, R. Kanojia, P. Ostrowski, C. Shaw, M. Wachter, J. L. Mateos, L. Noriega, A. Guzman, A. Mijarez, L. Tovar. Zoapatanol and Montanol, Novel Oxepane Diterpenoids from the Mexican Plant Zoapatle (Montanoa tomentosa), ACS/CSJ Chemical Congress, Honolulu, April 1979, Medicinal Chemistry, Abstract #81.

2. W. L. Gardiner and E. C. Horning, Biochim. Biophys. Acta 115, 425 (1966).

Paper No.: MPMOB 11

The Stabilities of Unsaturated Carbocations

Donald H. Aue, W. R. Davidson, R. D. Betowski
E. Motell, and M. T. Bowers

Department of Chemistry, University of California, Santa Barbara
Santa Barbara, California 93106, U. S. A.

Proton affinities of unsaturated hydrocarbons have been measured by ion cyclatron resonance techniques. Proton transfer rates are slow ($0.1\text{-}5 \times 10^{-10}$ cc/molec./s) enough that equilibrium is not always completely achieved in such reactions. In these cases PA's are quoted to only $\pm$ 2 kcal/mole accuracy. From this proton affinity data, heats of formation can be calculated and compared with data from appearance potentials and radical ionization potentials. Hydride ions affinities, $HIA(R^+)$, can also be calculated from known heats of formation for the following hydride attachment reaction,

$$R^+ + H^- \rightleftarrows R - H$$

$$\Delta H^o = -HIA(R^+).$$

Table I. Thermodynamic Data for Carbocations at 25°C[a]

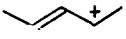
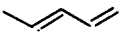
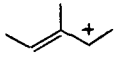
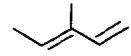
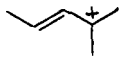
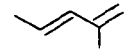
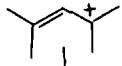
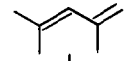
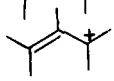
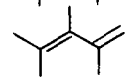
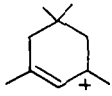
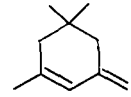
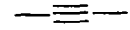
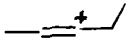
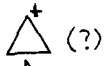
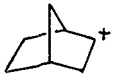
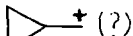
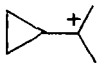
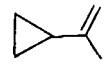
	$\Delta H_f^o(R^+)$	$HIA(R^+)$	PA(olefin)	olefin
CH_3^+	261[b]	312		
$CH_3CH_2^+$	219[b]	273	163.5	$CH_2{=}CH_2$
$CH_3CH^+CH_3$	192[b]	247		
	187.2	245.2	184.9[d]	$CH_2{=}CHCH_3$
$(CH_3)_3C^+$	164.0[c]	229.6		
	166.0	231.6	196.9	$CH_2{=}C(CH_3)_2$
$CH_3CH_2C^+(CH_3)_2$	159.8[b]	230.0	197.3	$CH_3CH{=}C(CH_3)_2$
	226[e]	256		
	204[e]	237		
	200	233	193	
	211[e]	248		
	184.9	224.7	200.4	
	183.5	224.6	201.8	
	175.9	224.3	202.1	

Table I (cont.)

	$\Delta H_f^o(R^+)$	HIA(R^+)	PA(olefin)	olefin
	173	221	205.7	
	170	219	207.9	
	158	212	213.1	
	154	211	210.6	
	200.7	225.7		
	199.1	224.1	200.0	
	149	207	216.1	
$HC{\equiv}C-CH_2^+$	281[e]	270		
	266[e]	287		
	230	258	182	
	215	251	187	
	204	244	198	
	201	242	196	
	235	256	198	
	190.3	235.9	201.6	
	214	241	191	
	179	218	209.3	

a) All values in kcal/mole. Based on $\Delta H_f^o(H^+)$ = 367.2, $\Delta H_f^o(H\text{-})$ = 33.2, and $\Delta H_f^o(t\text{-}Bu^+)$ = 166.0, PA(NH_3) = 205.0.

b) Lossing and Semeluk (1970) and Lossing and Maccoll (1976). Values may be too high because of nonadiabatic IP(R·).

c) Koeing, et al. (1975).

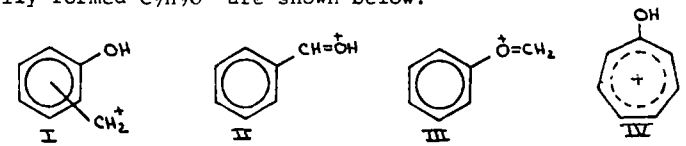
d) Yamdagni and Kebarle (1976).

e) Lossing (1971, 1972).

SOME ASPECTS OF THE UNIMOLECULAR DECARBONYLATION REACTION OF $C_7H_7O^+$ CATIONS*

D. H. Russell, D. C. Canada, and E. H. McBay
Analytical Chemistry Division
Oak Ridge National Laboratory
Oak Ridge, Tennessee 37830

The $C_7H_7O^+$ ion is an important secondary ion in the mass spectra of a variety of oxygen containing aromatic compounds, viz. alkyl phenols, substituted benzyl alcohols and substituted alkyl phenyl ethers. In addition, the $C_7H_7O^+$ ion is important with respect to the question of ring-expansion rearrangement reactions of aromatic ring systems, i.e., formation of the heteroatom tropylium ion. In this study we have investigated the unimolecular reaction chemistry of a number of $C_7H_7O^+$ ions generated from a variety of precursor molecules, e.g., the cresols, substituted benzyl alcohols, and substituted alkyl phenyl ethers. In addition, as a model for the heteroatom tropylium ion, we have generated the $C_7H_7O^+$ ion via hydrogen atom loss from the molecular ion of 3,5-cycloheptadienone. Possible structures for the initially formed $C_7H_7O^+$ are shown below.



The major unimolecular reaction channels ($k(E) \sim 10^6 s^{-1}$) for the $C_7H_7O^+$ ion is expulsion of CO and CH_2O, i.e., reaction (1) and (2), respectively. Typical branching ratios for reaction (1) and (2) are shown in Table 1.

$$C_7H_7O^+ \rightarrow C_6H_7^+ + CO \qquad (1)$$

$$C_7H_7O^+ \rightarrow C_6H_5^+ + CH_2O \qquad (2)$$

Although there are considerable differences for the branching ratios for the various $C_7H_7O^+$ ions, it is difficult to ascertain the reason(s) for these differences. That is, are the branching ratios different due to unique decomposing structures or differences in average-ion internal energies?

The results for metastable kinetic energy release measurements are consistent with different structures for the decomposing $C_7H_7O^+$ ions (see Table 1). For example, the phenol type $C_7H_7O^+$ ions (I) decompose via CO loss with the release of a large amount of kinetic energy, i.e., ca. 400 meV. The benzyl alcohol $C_7H_7O^+$ ions (II) which decompose via CO loss do so with the release of a moderate amount of kinetic energy, i.e., ca. 190 meV. Whereas, the $C_7H_7O^+$ ions generated from the phenoxy-alkyl compounds and substituted alkyl phenyl ethers (III) which decompose via CO loss give rise to a composite metastable peak shape, i.e., KE Rel ≅ 25 meV and 300 meV. The composite metastable for decomposing ions of structure III may arise from competing reaction mechanisms or two decomposing structural forms.

The $C_7H_7O^+$ ion generated from 3,5-cycloheptadienone, i.e., IV, which decompose via CO loss also gives rise to a composite metastable peak shape. In sharp contrast to III, the kinetic energy release for IV is composed of two large kinetic energy release processes, e.g., ∿400 meV and 900 meV.

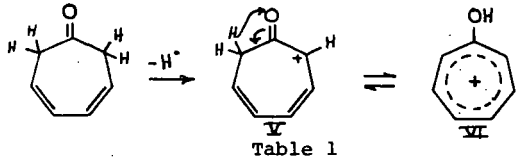
*Research sponsored by the U. S. Department of Energy under Contract #W-7405-eng-26 with the Union Carbide Corporation.

By acceptance of this article, the publisher or recipient acknowledges the U.S. Government's right to retain a nonexclusive, royalty-free license in and to any copyright covering the article.

The metastable kinetic energy release value for $C_7H_7O^+$ ions which decompose via reaction (2), i.e., CH_2O loss, are consistent with different structures for the $C_7H_7O^+$ ions, i.e., ca. 150 meV for phenol type ions (I) vs ca. 25 meV for methylene phenyl ether (III). The intensity of the metastable peak for ions of structure II decomposing via CH_2O expulsion was too low to measure reliably.

We interpret these experimental results, i.e., metastable branching ratios and metastable kinetic energy release, as unique structural forms for decomposing $C_7H_7O^+$ ions, viz. structures I-IV. However, these experimental results leave unanswered the question of why $C_7H_7O^+$ ions formed initially as III and IV give rise to composite metastable peak shapes. For $C_7H_7O^+$ ions of structure IV, the composite metastable peak may arise due to an equilibrating mixture of structures V and VI, i.e., keto-enol tautomerism.

Additional experiments are underway to explore further the mechanism for decomposition of $C_7H_7O^+$ ions.



V VI

Table 1

Experimental Data for Decomposing (k(E) $\sim 10^6 s^{-1}$) $C_7H_7O^+$ Ions

Compound	$C_7H_7O^+ \rightarrow C_6H_7^+ + CO$	$C_7H_7O^+ \rightarrow C_6H_5^+ + CH_2O$
m-chloroanisole	20/300[a] (95)[b]	30[a] (5)[b]
p-chloroanisole	25/300 (75)	25 (25)
2-phenoxyethanol	20/275 (95)	20 (5)
m-chlorobenzylalcohol	195 (99)	- (1)
p-chlorobenzylalcohol	195 (99)	- (1)
1,2-diphenylethanol	185 (99.8)	- (.2)
o-cresol	350 (90)	120 (10)
m-cresol	410 (65)	140 (35)
p-cresol	470 (60)	170 (40)
3,5-cycloheptadienone	390/930 (90)	140 (10)

[a]Metastable kinetic energy release expressed in milli-electron volts.

[b]Metastable branching ratios expressed as percent of total metastable ion current.

MPM0B13 STEREOSPECIFICITY AND HIDDEN HYDROGEN MIGRATION IN THE ELIMINATION OF METHANOL FROM CYCLIC DIESTERS UNDER ELECTRON IMPACT. ASHER MANDELBAUM, R. BAR-SHAI, J. SHARVIT AND I. MERSKSAMMER, Dept. of Chem., Technion, Israel Institute of Technology, Haifa

Deuterium isotope effect studies have recently shown that a hidden hydrogen transfer precedes the loss of a methyl group from methyl isobutyrate under electron impact.[1,2] The study of stereoselectivity and site specificity suggests that a hidden hydrogen transfer precedes the elimination of methanol from the molecular ion of trans-1,4-dicarbomethoxycyclohexane. The occurrence of hidden H-migrations in several other fragmentations will be discussed.

[1] A. WEISZ AND A. MANDELBAUM, J. CHEM. SOC., CHEM. COMM., 1978, 521.

[2] H. SCHWARZ AND C. WESDEMIOTIS, ANGEW. CHEM., 90, 724 (1978).

THEORY OF THE EFFECT OF THE ELECTRIC FIELD INHOMOGENEITY IN ION CYCLOTRON RESONANCE SPECTROMETRY

G. Baykut, K.-M. Chung, K.-P. Wanczek and H. Hartmann, Institute of Physical Chemistry, University, Frankfurt, FRG

The influence of the electric field inhomogeneity on the ICR spectrometrical data is studied theoretically applying quantum mechanical methods. The results obtained by the minimized wave packet approach are converted into classical quantities using the known energy relations. The inhomogeneity effects on the cyclotron frequency and the drift velocities of the ions is taken into account by a Schrödinger pertubation calculation. The coupled trapping and cyclotron motions can be decoupled because the motion is much slower than the second under the conditions utilized in the experiments. The potential is than:

$$V(y,z) = V_{\perp}(y,\langle z\rangle) + V_{\parallel}(\langle y\rangle, z)$$

where $V_{\perp}$ is the potential in y direction, perpendicular to the magnetic field and $V_{\parallel}$ is the potential in the direction of the magnetic field (z direction). $\langle y\rangle$ and $\langle z\rangle$ are parameters in the potential equations which are quantum mechanical averages using the wave packet approach. For the motion perpendicular to the magnetic field one can write:

$$V_{\perp}(y,\langle z\rangle) = V_{\perp,0}(y,\langle z\rangle) + V_{\perp,s}(y,\langle z\rangle)$$

where the unpertubed problem is:

$$V_{\perp,0}(y,\langle z\rangle) = V_T - \sum A_K(1 - B_K\langle z\rangle^2) + \sum C_K(1 - B_K\langle z\rangle^2)\, y$$

$$A_K = A_K(V_T, V_1, V_2, A, B) \quad ; \quad B_K = B_K(A) \quad ; \quad C_K = C_K(V_1, V_2, A, B)$$

For the motion parallel to the magnetic field a corresponding equation is obtained.

With the parametrized potentials the Hamiltonian can be decoupled

$$H = H_{\perp} + H_{\parallel}$$

$$H_{\perp} = \frac{1}{2M}\left(\vec{P} - \frac{q}{c}\vec{A}\right)^2 + q\,V_{\perp}(y,\langle z\rangle)$$

$$H_{\parallel} = \frac{p_z^2}{2M} + q\,V_{\parallel}(\langle y\rangle, z)$$

For the trapping motion the harmonic approximation is used. We obtain a *minimized and orthonormalized* wave packet:

$$\Psi_{\parallel}(\xi, t) = \sum_N p_N u_N(\xi)\ \exp\left\{-\left(\frac{i}{\hbar}(N_T + \frac{1}{2})\hbar\omega_T\right)t\right\}$$

$$p_N = \frac{1}{2^N (N!)^{1/2}} \exp\left\{-\frac{1}{8}\,\xi^2(t)\right\}\left\{\xi(t)\right\}^N$$

where the p_N's are the weight functions and the u_N's are the wave functions including the Hermite function. In the case of the cyclotron motion we obtain the minimized and orthonormalized wave packet:

$$\Psi_{\perp}(\vec{R}_{\perp}, t) = \sum p_N u_N(\vec{R}_{\perp}, \vec{R}_M) \exp\left\{-\frac{i}{\hbar}E_N t\right\}$$

$$P_N = \frac{1}{(N!\, e)^{1/2}} \exp\left\{ i N \left(\alpha + \frac{\pi}{2} \right) \right\} \; J_N \left\{ x (2/B)^{1/2} \right\}$$

$$= \frac{Q}{\hbar c} \left\{ \left(A_x + \frac{MC}{Q} v_D \right)^2 + \left(A_y \right)^2 \right\}^{1/2}$$

The wave function (screw function) has been given by Chung and Mrowka[1]. With the aid of this wave packet the behaviour of the ions in the plane perpendicular to the magnetic field can be described completely, for example the pertubation of the rotational energy and the changes of the translational energy due to the electric field inhomogeneity.

---

1. K.-M. Chung and B. Mrowka, Z. Physik 259, 157 (1973)

EXACT MASS DETERMINATION IN ION CYCLOTRON RESONANCE SPECTROMETRY

G. Baykut, K.-M. Chung, K.-P. Wanczek and H. Hartmann, Institute of Physical Chemistry, University, Frankfurt, FRG

We have given a minimized and orthonormalized wave packet which can be utilized to describe the ion in the direction perpendicular to the magnetic field. The pertubation energy of the ions is obtained as:

$$E^1_\perp = q \left\langle \psi_\perp \middle| V_{\perp,s}(\gamma, \langle z \rangle) \middle| \psi_\perp \right\rangle$$

$$= q \cdot \sum_{J=2}^{\infty} c_J \left\langle \psi_\perp \middle| \gamma^J \middle| \psi_\perp \right\rangle$$

With the quantum mechanical averages $\langle z \rangle$ of the coordinate of motion in the z direction and $\langle y \rangle$ of the coordinate in the plane perpendicular to the magnetic field one gets for the pertubation energy of the rotational mode:

$$E^1 = q (c_2 \gamma_M^2 + c_3 \gamma_M^3 + c_4 \gamma_M^4) + q \frac{S}{B} (c_2 + c_3 \gamma_M + c_4 \gamma_M^2) + \frac{3}{2} q c_4 \left(\frac{S}{B}\right)^2$$

$$S = \frac{M \omega_c^2 R^2}{2} - \frac{1}{2}$$

The effect of the inhomogeneous electric field on the translational energy is determined by calculation of the average values of the translational energy operator

$$H_D = \frac{1}{2M} \left(\vec{P} - \frac{q}{c} \vec{A} \right)_x^2$$

The change $\Delta \langle H_D \rangle$ due to the field inhomogeneity is approximately:

$$\Delta \langle H_D \rangle = \left\langle \psi_\perp \middle| H_D \middle| \psi_\perp \right\rangle - \left\langle \psi_\perp^0 \middle| H_D \middle| \psi_\perp^0 \right\rangle$$

$$= \left\langle \psi_\perp^1 \middle| H_D \middle| \psi_\perp^0 \right\rangle + \left\langle \psi_\perp^0 \middle| H_D \middle| \psi_\perp^1 \right\rangle$$

After some calculations one obtains the "quasi cyclotron frequency":

$$\omega = \omega_c \left[1 + \beta \frac{1}{B} + \gamma \frac{1}{B^2} \right]$$

where

$$\beta = \frac{2 E \gamma_M^2 c}{\omega_c W^2 J_0^2} \left(c_2 + \frac{3}{2} c_3 \gamma_M + 2 c_4 \gamma_M^2 \right),$$

$$\gamma = -\frac{4 E \gamma_M c^2}{\omega_c^2 W^2 J_0^2} \left\{ \left(\frac{V_1 - V_2}{B} \right) \left(c_2 + \frac{3}{2} c_3 \gamma_M + 2 c_4 \gamma_M^2 \right) + \frac{k_B T}{q} \left(\frac{3}{16} c_3 + \frac{2}{3} c 4 \gamma_M \right) \right\}$$

To compare the theoretical results with experiments the dependence of the factor f which can be obtained for uniform crossed magnetic and electric fields ($f = (m\omega_c)/B$) from the magnetic field strength is determined for several gas mixtures. For a mixture of H_2, D_2, H_2O, B_2H_6, N_2, O_2 and Ar the results are given in Fig. 1. (Δ p = $5.9 \cdot 10^{-5}$ Torr, $\odot$ p = $1.7 \cdot 10^{-5}$ Torr, ν_c = 288.02 kHz)

The theoretical results agree very well with the experimental data (theoretical results solid line).
The treatment has left out of account the effects of collisions and statistics and of the differences of ionization cross sections. Some of the fluctuations of the experimental points may be to these effects.

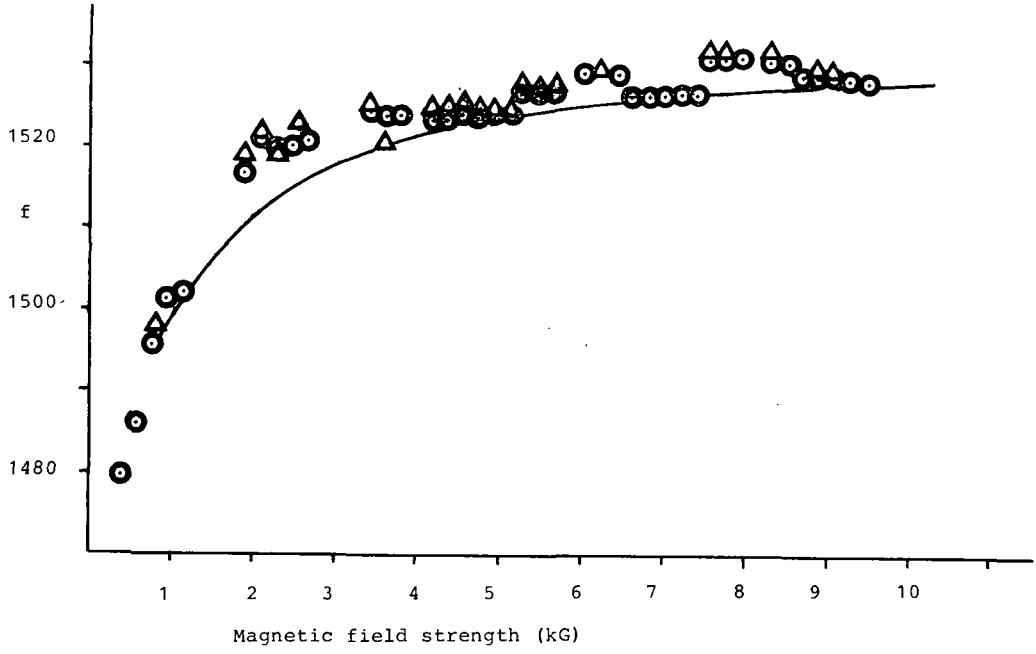


Fig. 1. Dependence of the factor f on the magnetic field strength.

ELECTRONIC EXCITATION IN ION-ATOM COLLISIONS*

E. Grant Jones

Department of Chemistry and The Brehm Laboratory
Wright State University
Dayton, Ohio 45435

Ion-atom reactions have been found to be an efficient method to produce selective electronic excitation.[1-3] Frequently the quantum states of the reactants are known and those of the products can be determined from studies of luminescence produced in single collisions. Thus, for some ion-atom reactions, it is possible to obtain precise knowledge of reaction cross sections and distribution of the available energy in the products. Such information is valuable in assessing and identifying laser pumping mechanisms. For symmetric rare gas systems, it provides insight into the potential curves for the dimer ions, Rg_2^+. Since absorption by Rg_2^+ may be an important loss mechanism, knowledge of the potential energy curves and transitions for Rg_2^+ is important in optimizing the rare gas halide lasers.[4,5]

Experiments were performed using a mass spectrometer to prepare a low energy mass selected ion-beam for impact on a target gas (1-2 m torr) located in a collision chamber. The ion-beam is chopped at 1 KHz and the luminescence emitted from short-lived ($<10^{-6}$s) products formed in single collisions is monitored by a McPherson 1 m vacuum UV monochromator using pulse counting techniques.

Previous studies in this laboratory[1-3] of He^+/Rg collisions, where Rg is Ar, Kr or Xe, have centered on charge-transfer reactions manifested by RgII luminescence. In symmetric collisions, three major reaction types can be considered.

$$Rg^+ + Rg \rightarrow Rg + Rg^+ \qquad \Delta H = 0 \qquad (1)$$

$$\rightarrow Rg^+ + Rg \qquad \Delta H = 0 \qquad (2)$$

$$\rightarrow Rg^+ + Rg^* \qquad \Delta H = >0 \qquad (3)$$

Resonant charge-transfer, (1), occurs with very large cross section for all of the heavy rare gases.[6] Reactions (2) and (3) involving elastic and inelastic collisions, can be studied in ion scattering experiments, but there is difficulty in directly classifying the excited products. Reaction (3) for krypton and xenon has been investigated over the collision energy range 10-100 eV (lab) by monitoring luminescence in the interval 115-620 nm. For the symmetric xenon system the spectrum is dominated by RgI resonance lines produced in the collisional excitation reaction (4).

$$Xe^+(^2P^\circ_{3/2,1/2}) + Xe(^1S_0) \rightarrow Xe^+(^2P^\circ_{3/2,1/2}) + Xe\ 6s[3/2]^\circ_1 \qquad (4)$$

Since no cascade contributions to the resonance lines are observed, the cross section for (4) is given by the emission cross section for the transition ($^1S_0$) $\rightarrow$ 6s[3/2]$^\circ_1$ observed at 147.0 nm. The cross section is found to depend strongly on the electronic state of the reacting xenon ions.[7] Because of the large splitting (1.31 eV) between the J-states of Xe^+, it is possible to operate the ion-source at ionization voltages in the vicinity of onset to study reaction (4) for J = 3/2. From experiments at higher ionization voltages, at which the precise beam composition of J = 1/2 and J = 3/2 states has been measured,[8] the cross section of reaction (4) for J = 1/2 can be obtained. The results are shown in Figure 1 and the data is summarized in Table I.

All observed reactions are endothermic and are driven by the conversion of translational into internal energy. The large cross sections attest to the efficiency of translational to internal energy transfer in the heavy ion systems. The proposed mechanism of reaction (4) involves a near-or-avoided-curve-crossing in the steeply repulsive regions. The cross section for reaction of the J = 1/2 state to excite the lowest xenon resonance level exceeds that for the J = 3/2 state at all energies above reaction onset. No apparent effect on J is observed in the collisional excitation of the second resonance level, 6s'[1/2]$^\circ_1$. The measured cross sections in the krypton symmetric system are smaller ($<10^{-16}$ cm^2) than those for xenon but qualitatively both systems are very similar.

Table I. ENERGY THRESHOLD AND REACTION CROSS SECTION SUMMARY

$$Xe^+(^2P^o_J) + Xe(^1S_o) \rightarrow Xe^+ + Xe6s[3/2]^o_1 \qquad (2)$$

$$Xe^+(^2P^o_J) + Xe(^1S_o) \rightarrow Xe^+ + Xe6s'[1/2]^o_1 \qquad (3)$$

State of Xe^+ Reacting Ion	Kinetic Energy Threshold eV (C.M.)		Cross Section for 100 eV(Lab) Collisions (10^{-16} cm^2)	
	(2)	(3)	(2)	(3)
$^2P^o_{3/2}$	12 ± 2	12 ± 2	1.1	0.3
$^2P^o_{1/2}$	11.5 ± 0.5	12 ± 2	11.	0.3

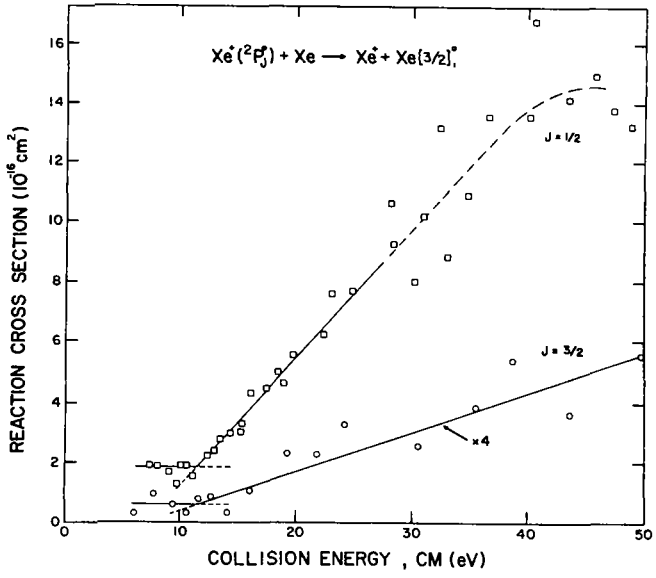


Figure 1.

* Sponsored by Air Force Aeropropulsion Laboratory, Air Force Systems Command, United States Air Force, Wright-Patterson AFB, under Contract No. F33615-77-C-3141.

References:

1. E. G. Jones, B. M. Hughes, D. C. Fee and T. O. Tiernan, Phys. Rev. A15, 1446 (1977).
2. E. G. Jones, B. M. Hughes, T. O. Tiernan, D. C. Fee and D. G. Hopper, Spectrochim. Act. 33B, 787 (1978).
3. E. G. Jones, D. C. Fee, T. O. Tiernan and B. M. Hughes, submitted to J. Chem. Phys.
4. J. E. Velazco and D. W. Setser, J. Chem. Phys. 62, 1990 (1975).
5. J. M. Hoffman, A. K. Hays, and G. C. Tisone, Appl. Phys. Lett. 28, 538 (1976).
6. See L. Squires and T. Baer, J. Chem. Phys. 65, 4001 (1976) and references therein.
7. The precise J state of the product xenon ions cannot be determined in the present experiments.
8. R. C. Amme and P. O. Haugsjaa, Phys. Rev. 165, 63 (1968).

LOW-ENERGY COLLISION PROCESSES IN TANDEM QUADRUPOLE MASS SPECTROMETRY MPM OC4

C.G. ENKE, J.A. CHAKEL, AND E.J. DARLAND
DEPARTMENT OF CHEMISTRY, MICHIGAN STATE UNIVERSITY, EAST LANSING, MI.48824

A tandem triple quadrupole mass spectrometer has been constructed in our laboratory. It consists of a combined CI/EI source, two quadrupole mass filters and a Channeltron ion detector. Between the two mass filters is a quadrupole collision chamber. Ions from the source are mass selected by the first quad and can undergo low-energy (2-100 eV) collision with neutral molecules in the quad collision chamber. The center quad is operated in RF-only mode to focus and transmit parent and product ions of all masses. The ionic collision products are mass analyzed by the third quad and detected. The resulting spectrum of the products is indicative of the processes that occur during or after the collision. For many molecules, the fragmentation of M^+ produced by collision-induced dissociation (CID) with Ar resembles the EI mass spectrum of the molecules. (See Figures in the Abstract of paper # MPM0B6 by Yost, Latven, and Enke.)

Previous CID mass spectrometry has been done in MIKES and CAMS instruments with ion energies of 3-10 KeV. The experiments described in this paper were designed to help characterize the clearly different low energy collision processes which occur in the triple quad instrument.

The effects of various sources of ion energy are considered first. The fragmentation of M^+ from cyclohexane was observed as the EI electron energy was varied. All fragments produced at high voltages were also produced below 30 eV, although at reduced intensity. Excess internal energy of the ions is thus not an essential factor in the fragmentation. Even less influenced by source energy are the CID spectra of fragment ions such as $(M-28)^+$. The loss of H from CH_4^+ through CID was observed for various axial energies from 0 - 110 eV. The formation of CH_3^+ is almost independent of axial energy, but loss of 2, 3, and 4 H's shows increasing axial energy dependence with a maximum C^+ production at 15 eV. The RF field in the collision chamber contributes only a few eV to the ion's kinetic energy. The fragmentation process occurs, therefore, by an efficient conversion of a portion of the ion's kinetic energy.

The fragmentation efficiency $F_i/(P + \Sigma F_i)$ (where F_i, ΣF_i, and P are the intensities of a specific fragment ion, all fragment ions, and the parent ion, respectively) was observed for the noble collision gases from He to Xe. The fragmentation efficiency for all fragments of CH_4^+ increases with increasing mass of the collision gas. The efficiency for N_2 falls between Ar and Kr.

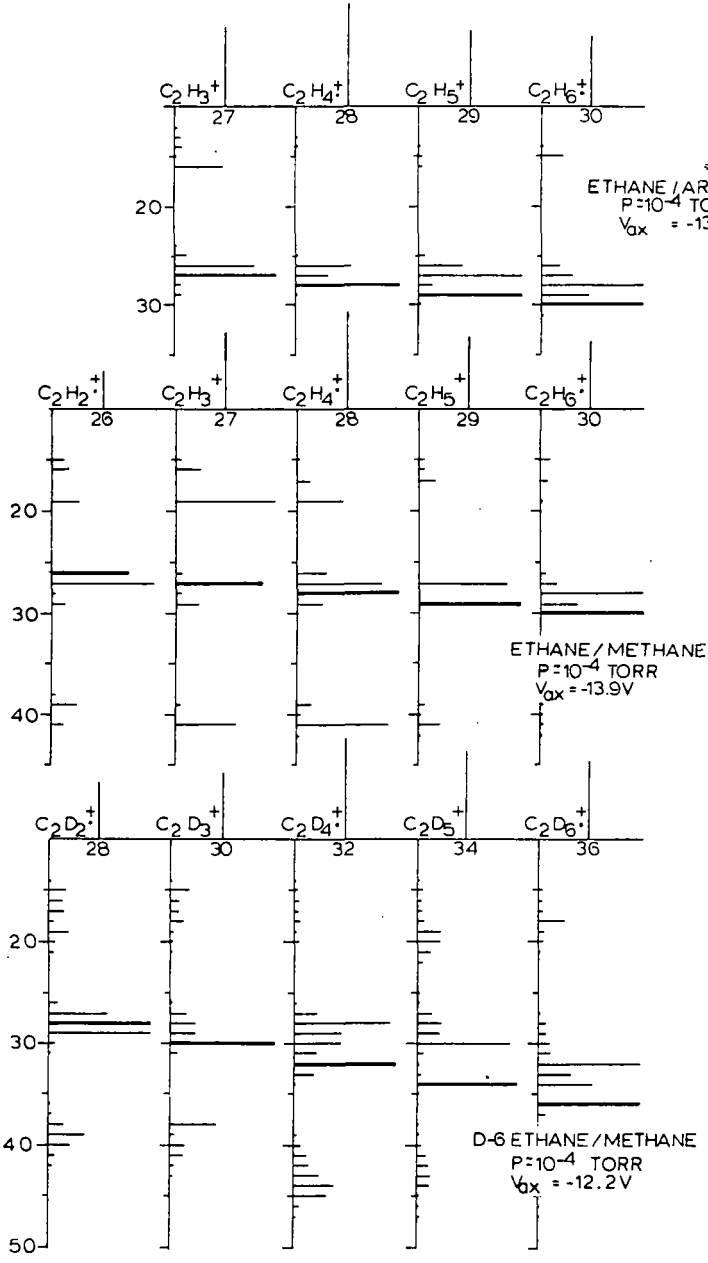
The effects of collision gas pressure on the fragmentation efficiency and scattering loss were also studied. The fragmentation efficiency for CH_4^+ increases with increasing pressure. Single-collision conditions exist below 10^{-5} torr and scattering losses are less than 50% up to 10^{-4} torr.

The possibility of a chemical reaction between the ion and collision gas was explored by colliding the ions of ethane with methane gas. The top two-thirds of Fig. 1 shows the CID spectra for the ethane ions $C_2H_3^+$ through $C_2H_6^+$ for both Ar and CH_4 gas. Ion-molecule addition reactions are clearly indicated for CH_4. The various products of the ethane ion/methane molecule reactions were observed as functions of the CH_4 pressure and the ion axial energy. All products increased with pressure up to about 10^{-4} torr, where those favored by further CH_4 collision (such as $C_3H_5^+$) increased further at the expense of those disfavored (such as $C_2H_3^+$). Hydrogen gain and loss are favored by increasing axial energy but $C_3H_5^+$ formation has a maximum at about 10 eV. A trade-off between increasing energy and decreasing interaction time probably exists for most reactions.

The reactions of the ions of d-6 ethane with CH_4 gas are also shown in Fig. 1 and clearly demonstrate H-D scrambling and a variety of other interesting products. Finally CCl^+ ion was obtained from CCl_4 and reacted with Ar, N_2, O_2, H_2O, and He collision gases. The collision products with Ar include C^+, Cl^+, Ar^+, CAr^+, and $ClAr^+$. Interesting

products were also observed for N_2, O_2, and H_2O, but He produced only C^+ and Cl^+ fragments.

From these experiments it appears that the low-energy ion-molecule interactions can involve significant momentum transfer and that the interaction can last long enough for a collision complex to form and a variety of reaction products to result. This work has been supported by the Office of Naval Research.



REACTIONS OF METHYL CATIONS WITH METHYL SILANES,

G. W. GOODLOE, E. R. AUSTIN, AND F. W. LAMPE, Dept. of Chem., The Penn. State Univ., Univ. Park, Pa. 16802

This paper describes a study of the gas-phase reactions of CH_3^+ with methyl silanes using a tandem mass-spectrometric apparatus.

Collisions of CH_3^+ ions with methyl silanes initiate a rather simple set of chemical processes as may be seen from Figure 1, which depicts the mass spectrum of the ionic products of the $CH_3^+ + (CH_3)_2SiH_2$ reaction.

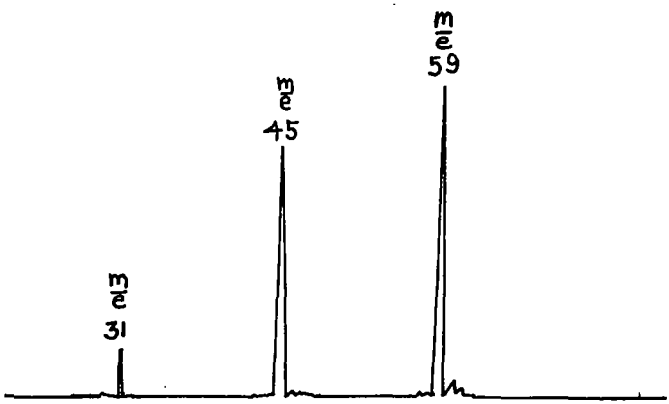


Fig. 1--Product-Ion Mass Spectrum in the Reaction of CH_3^+ Ions with $(CH_3)_2SiH_2$

As may be seen in this figure, there are three principal products: (1) $(CH_3)_2SiH^+$ (m=59 amu) which results from a hydride ion abstraction reaction; (2) $CH_3SiH_2^+$ (m=45 amu) which results from a reaction that is formally a CH_3^- abstraction process; and (3) SiH_3^+ (m=31 amu) which must arise from a more complicated process that may be a unimolecular decomposition occurring subsequent to hydride ion abstraction. These type processes appear to be common to all the methyl silanes in their reactions with CH_3^+ ions.

The major reactions observed in these collision systems along with the standard enthalpy changes and cross-sections at 1 eV (Laboratory) of CH_3^+ ions are shown in Table 1. It is to be seen from the table that hydride ion abstraction from target molecules containing Si-H bonds is a major process in all cases, a fact that is consistent with previous studies (1,2) of the reactions of CH_3^+ with SiH_4.

The unexpected phenomenon to be seen in Table 1 is the important role played by the methyl anion abstraction from the methyl silanes. Thus CH_3^- abstraction is of almost equal importance to hydride ion abstraction in $(CH_3)_2SiH_2$ and becomes significantly more important in $(CH_3)_3SiH$ and $(CH_3)_4Si$.

TABLE 1

Major Exothermic Reactions of CH_3^+ with Methyl Silanes Reaction[a]

Reaction	ΔH^o (kcal./mole)	$\sigma(\text{Å}^2)$
$CH_3^+ + CH_3SiH_3 \rightarrow SiH_3^+ + C_2H_6$	-37	15
$CH_3^+ + CH_3SiH_3 \rightarrow CH_3SiH_2^+ + CH_4$	-59	62
$CH_3^+ + (CH_3)_2SiH_2 \rightarrow SiH_3^+ + C_3H_8$	-28	8
$CH_3^+ + (CH_3)_2SiH_2 \rightarrow CH_3SiH_2^+ + C_2H_6$	-48	42
$CH_3^+ + (CH_3)_2SiH_2 \rightarrow (CH_3)_2SiH^+ + CH_4$	-74	59
$CH_3^+ + (CH_3)_3SiH \rightarrow CH_3SiH_2^+ + C_3H_8$	-39	19
$CH_3^+ + (CH_3)_3SiH \rightarrow (CH_3)_2SiH^+ + C_2H_6$	-64	66
$CH_3^+ + (CH_3)_3SiH \rightarrow (CH_3)_3Si^+ + CH_4$	-88	30
$CH_3^+ + (CH_3)_4Si \rightarrow (CH_3)_2SiH^+ + C_3H_8$	-55	19
$CH_3^+ + (CH_3)_4Si \rightarrow (CH_3)_3Si^+ + C_2H_6$	-78	73
$CH_3^+ + (CH_3)_4Si \rightarrow (CH_3)_4Si^+ + CH_3$	-7	32

[a]Ion-energy = 1 eV (LAB)

When CH_3^+ ions are replaced by CD_3^+ and $^{13}CH_3^+$ ions as reactants only negligibly small changes in the mass spectra of the hydride transfer and CH_3^- transfer products are observed. Hydride transfer for SiH_4 to a variety of reactant ions at 1 eV (Laboratory) has been shown (3,4) to be principally a direct process and it is likely that hydride transfer from the methyl silanes is also. This is in accord with the absence of any effect of labelling of the reactant ions on the products of hydride transfer. The absence of an effect of reactant ion labelling on the products of CH_3^- transfer suggest, but do not prove, that this process is also direct. At the very least, one may conclude that if intermediate complexes are involved the methyl groups in the complex are non-equivalent.

References

1. G. W. Stewart, J. M. S. Henis and P. P. Gaspar, J. Chem. Phys., 57, 1990 (1972).
2. T. M. H. Cheng, T. Y. Yu and F. W. Lampe, J. Phys. Chem., 77, 2587, (1973).
3. T. M. Mayer and F. W. Lampe, J. Phys. Chem., 78, 2195 (1974).
4. T. M. Mayer and F. W. Lampe, J. Phys. Chem., 78, 2429 (1974).

MPMOC6 A TANDEM-ION CYCLOTRON RESONANCE STUDY OF THE REACTION OF N_2^+ WITH SO_2, YUKIO NISHIMURA, ROBERT ORTH and JEAN H. FUTRELL, Department of Chemistry, University of Utah, Salt Lake City, Utah 84112.

The reaction of N_2^+ with SO_2 has been studied as a function of electron energy and ion source pressure in a tandem-ion cyclotron resonance mass spectrometer at less than 0.1 eV translational energy. As the pressure of N_2 in the ion source is increased, vibrationally excited N_2^+ ions are quenched, producing a corresponding increase in the branching ratio of the charge-transfer product SO_2^+ to the dissociative charge-transfer product SO^+. The total rate constant for charge-transfer was determined to be 6.5×10^{-10} $cm^3 molecule^{-1} sec^{-1}$ independent within experimental error of the vibrational excitation of the N_2^+ ion.

MPMOC7 ION-MOLECULE REACTION RATES USING A SELECTED ION FLOW TUBE,* A. V. VIGGIANO, F. Howorka, D. L. Albritton, and F. C. Fehsenfeld, Aeronomy Laboratory, NOAA/ERL, Boulder CO 80303

Ion-molecule reactions have been studied in a room temperature selected-ion flow tube. The results that will be discussed were obtained using electron-impact ion sources, as well as a hollow-cathode discharge source. The present results include reactions of CH^+, CH_2^+, CH_3^+, CH_5^+, C_2^+, C_2H^+, OH^+, and H_2O^+ with O, N, and NO. The reactions are of interest in connection with the ion chemistry of interstellar clouds. The reaction $NH^+ + O \rightleftarrows OH^+ + N_2$ was measured in both the forward and reverse direction allowing an estimation of the absolute proton affinity of N_2. Finally, the reaction of O^{++} with N_2 has been measured. This reaction is important in connection with the ion chemistry of the earth's upper atmosphere.

* Supported in part by Defense Nuclear Agency.

VIBRATIONAL ENERGY DEPENDENCE OF THE REACTION $C_2H_4^+ + C_2H_4 \rightarrow C_3H_5^+ + CH_3$

Timothy Su
Department of Chemistry, Southeastern Massachusetts University
North Dartmouth, Massachusetts 02747

and

Michael T. Bowers
Department of Chemistry, University of California
Santa Barbara, California 93106

The reaction of ethylene ion and ethylene has been a subject of considerable current interest both experimentally and theoretically. Verboom and Meisels[1] has reported the branching ratio of the formation of $C_4H_7^+$ and $C_3H_5^+$ via the reactions

$$C_2H_4^+ + C_2H_4 \xrightarrow{k_1} C_4H_7^+ + H \qquad (1)$$

$$C_2H_4^+ + C_2H_4 \xrightarrow{k_2} C_3H_5^+ + CH_3 \qquad (2)$$

and from photoionization of several C_4H_8 isomers. Their experimental results and theoretical calculations based on a modified RRKM theory showed that the ratio k_1/k_2 decreases as the total angular momentum of the system increases. Chesnavich and Bowers[2] has applied the phase space theory to calculate the relative reaction rate constant of reaction (2) as a function of the internal energy of $C_2H_4^+$, ε_v, [i.e. $k(\varepsilon_v)/k(\varepsilon_v=0)$ as a function of ε_v], and compared with experimental results performed in a high pressure mass spectrometer. Under the experimental conditions, the relative translational energies are much higher than thermal energies leading to a high total angular momentum. Consequently, reaction (2) dominates and it was assumed that reaction (2) is the only reaction channel. The experimental rate constant decreases much more rapidly with internal energy of $C_2H_4^+$ ion than is predicted by theory. Chesnavich and Bowers[2] pointed out that the phase space theory considers only the phase space available for each exit channel, which is good in predicting the product kinetic energy distribution. In calculating reaction rate constants, however, the characteristics of the potential surface in the region of $C_4H_8^+$ complex should also be considered. The following mechanism was proposed:[2]

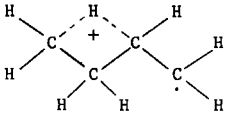
$$C_2H_4^+ + C_2H_4 \underset{k_1}{\overset{k_{cap}}{\rightleftharpoons}} \underset{(1)^{\ddagger}}{\underset{A^+}{CH_2CH_2CH_2\dot{C}H_2}} \underset{k_{-2}}{\overset{k_2}{\rightleftharpoons}} \underset{(2)^{\ddagger}}{CH_3CH_2\dot{C}HCH_2} \longrightarrow \underset{B^+}{C_3H_5^+} + \dot{C}H_3 \qquad (3)$$

We present here a theoretical study of the reaction rate constant as a function of the internal energy of $C_2H_4^+$ ion using a RRKM type calculation with conservation of angular momentum.

Assuming A^+ and B^+ in equation (3) are in steady state, the reaction rate constant is expressed in Eq. (4)

$$k_{rxn} = k_{cap} \frac{k_2 k_3}{k_1 k_3 + k_2 k_3 + K_1 k_{-2}} \qquad (4)$$

It is assumed that transition states $(1)^{\ddagger}$ and $(3)^{\ddagger}$ are orbiting transition states, and $(2)^{\ddagger}$ has a structure



The rate constant of each step is expressed by Eq. (5) or (6) depends on the type of transition state (k_{orb} for orbiting, and k_{sp} for saddle point transition states)[3]

$$k_{orb}(E, J) = G \frac{W_{ss}(E, J)}{h\rho(E_c, J)} \quad (5)$$

$$k_{sp}(E, J) = G \frac{W^{\ddagger}(E - B J^2)2J}{h\rho(E_c, J)} \quad (6)$$

In these equations, G is the reaction path degeneracy, J is the total angular momentum, $\rho(E_c, J)$ is the density of states of the energized reagent at energy E_c, $W_{ss}(E, J)$ and $W^{\ddagger}(E - B J)2J$, are the J conserved sum of states at the oribiting and saddle point transition states respectively. The relative reaction rate constant at a given ε_v is calculated by integrating over the angular momentum distribution and the relative translational energy distribution:

$$\frac{k(\varepsilon_v)}{k(\varepsilon_v=0)} = \int \frac{k(\varepsilon_v, \varepsilon_T, J)}{k(\varepsilon_v=0, \varepsilon_T, J)} P(J)\, P(\varepsilon_T)\, dJ d\varepsilon_T \quad (7)$$

In order to fit the experimental data, it is necessary to assume an extraordinary tight transition state $(1)^{\ddagger}$ in mechanism (3), that is, most vibrational frequencies are extraordinary high. This is very unlikely. Ceyer, et al.[4] has observed the existence of a loosely bound collision complex $C_2H_4^+ \cdot C_2H_4$ as a precursor to the $C_4H_8^+$ intermediate. The existence of the $(C_2H_4)_2^+$ dimer has little effect on the calculation of the overall rate constant.

A second possible mechanism involves two 1-2 shift of a H^- ion as follows:

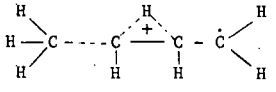
$$C_2H_4^+ + C_2H_4 \underset{(1)^{\ddagger}}{\rightleftharpoons} CH_2CH_2CH_2\dot{C}H_2 \underset{(2)^{\ddagger}}{\rightleftharpoons} CH_3\overset{+}{C}HCH_2\dot{C}H \underset{(3)^{\ddagger}}{\rightleftharpoons} CH_3CH_2\overset{+}{C}HCH_2 \xrightarrow{(4)^{\ddagger}} CH_3 + C_3H_5^+ \quad (8)$$

To fit the theoretical calculation with experimental data, again it is necessary to assume unreasonably tight transition states $(2)^{\ddagger}$ and $(3)^{\ddagger}$.

A third possible mechanism involves a 1-2 H^- shift followed by a simultaneous breaking of a C-C bond and a second 1-2 H^- shift as follows:

$$C_2H_4^+ + C_2H_4 \underset{(1)^{\ddagger}}{\rightleftharpoons} CH_2CH_2CH_2\dot{C}H_2 \underset{(2)^{\ddagger}}{\rightleftharpoons} CH_3\overset{+}{C}HCH_2CH_2 \xrightarrow{(3)^{\ddagger}} CH_3 + C_3H_5^+ \quad (9)$$

Transition state $(2)^{\ddagger}$ is assumed to have vibrational frequency distribution similar to those of 1-Butene. Transition state $(3)^{\ddagger}$ has the structure



In this mechanism, there are two adjustable parameters: the energies of $(2)^{\ddagger}$ and $(3)^{\ddagger}$. Setting energy of $(2)^{\ddagger}$ to be 17.3 kcal below the energy of the reactants and the energy of $(3)^{\ddagger}$ to be 9.2 kcal above that of the products, the theoretical calculated $k(\varepsilon_v)/k(\varepsilon_v = 0)$ agrees quite well with experimental data. Ceyer, et al.[4] has reported a barrier of 7.7 ± 1.5 kcal for $CH_3\cdot$ elimination. Thus the third mechanism presented above seems to be in consistent with experimental results.

References: 1. G.M.L. Verboom and G.G. Meisels, Proceedings of the 26th Annual Conf. on Mass Spect. and Allied Topics, 1978 p. 506; 2. W.J. Chesnavich and M.T. Bowers, J. Am. Chem. Soc., 98, 8301 (1976); 3. W.J. Chesnavich, T. Su and M.T. Bowers, J. Am. Chem. Soc., 100, 4362 (1978); 4. S.T. Ceyer, P.W. Tiedemann, C.Y. Ng, B.H. Mahan and Y.T. Lee, J. Chem. Phys., 70 2138 (1979).

MPM0C9 TRANSITION STATE ANALYSIS OF ION-DIPOLE CAPTURE DYNAMICS, W. J. Chesnovich, T. Su and M. T. Bowers, Dept. of Chemistry, Univ. of Calif., Santa Barbara, Ca. 93106

An analysis of the classical dynamics of ion-dipole capture collisions is presented. We show that by using methods based on transition state theory it is possible to impose various bounds on the capture rate due to energy, angular momentum, and flux restrictions. Examples of orbiting trajectories (i.e., accurate transition states) are presented. The ADO and Barker-Ridge capture theories are examined in light of the transition state theory analysis. Also, the question of energy transfer between translational and rotational motion is critically examined.

MPM0C10 INTERMOLECULAR FORCES AND COLLISION FREQUENCIES IN ION MOLECULE SYSTEMS, F. CELLI, G. WEDDLE, and D. P. RIDGE, Dept. of Chem., Univ. of Del., Newark, DE 19711

Various categories of forces between ions and molecules will be considered. In addition to the ion induced dipole force, the effect of ion induced quadrupole, London dispersion and repulsive forces will be considered. Polyatomic ions and molecules have many force centers rather than one. The consequences of this fact will be considered quantitatively. The importance of valence or exchange forces in ion molecule interactions will be considered. The effects of all of these forces on momentum transfer and capture collision frequencies will be discussed.

Ion Clustering Studies Using an Atmospheric Pressure Ionization Source

W. N. Allen, J. J. DeCorpo, F. E. Saalfeld, and J. R. Wyatt
Chemistry Division
Naval Research Laboratory
Washington, D. C. 20375

An atmospheric pressure ionization (API) source has been used to study ion clustering solvation reactions. The reactant is introduced into the source as a trace (~ppm range) constituent of the carrier gas (Ar or N_2) by flow dilution with a calibrated motor-driven syringe upstream of the source. Primary ionization is produced by β-rays from a ^{63}Ni foil.

Equilibrium constants for the system

$$NH_4^+(NH_3)_{n-1} + NH_3 \rightleftharpoons NH_4^+(NH_3)_n$$

up to n=4 were measured; the free energies (Table I) calculated from them are in good agreement with those reported by Payzant, et al.[1]

Table I

n-1,n	ΔG° This work	ΔG° Payzant, et al
0,1	16.5 ± 0.8	17.1 ± 0.5
1,2	8.0 ± 1.4	8.9 ± 0.3
2,3	6.2 ± 1.0	6.1 ± 0.2
3,4	4.7 ± 1.8	3.7 ± 0.5

Hydrazine, which is a stronger base than ammonia in the gas phase[2] but weaker in the liquid phase,[3] is also being investigated. Equilibrium constants for the reaction

$$N_2H_5^+(N_2H_4)_{n-1} + N_2H_4 \rightleftharpoons N_2H_5^+(N_2H_4)_n$$

for n=1 and 2 have been measured and the free energies for the reactions calculated (Table II).

Table II

n-1,n	K_{eq} (Std State = 1 atm)	ΔG° (Kcal/mole)
0,1	2.1×10^8	14.0
1,2	7.1×10^4	8.3

Further work on this system is in progress and will be submitted for publication in the near future.

1. Can. J. Chem. 51, 3242 (1973).
2. Proton Affinity, P. A. (N_2H_4) = 214 kcal/mole, J. J. DeCorpo, W. N. Allen, J. R. Wyatt, to be published.
3. Cotton and Wilkinson, Advanced Inorganic Chemistry, 2nd ed., Interscience (1963), p. 335.

MPMOC12 SOLVATION OF K^+ AND Cl^- BY DMSO, T. F. MAGNERA, J. SUNNER AND P. KEBARLE, Dept. of Chemistry, Univ. of Alberta, Edmonton, T6G 2G2, Canada.

The gas phase equilibria: $K^+(DMSO)_{n-1} + DMSO = K^+(DMSO)_n$ and $Cl^-(DMSO)_{n-1} + DMSO = Cl^-(DMSO)_n$ were studied with special high pressure ion source mass spectrometers, over a wide temperature and pressure range. van't Hoff plots of the equilibrium constants lead to $\Delta H^o_{n-1,n}$ and $\Delta S^o_{n-1,n}$. It was found that the K^+ binds DMSO, in the first shell, very much more strongly than the isoelectronic and of similar radius Cl^-. This is probably due to the location of a major part of the DMSO dipole on the S^+O^- group which can approach closely only the positive ion. A relatively large drop off in stability is observed between $K^+(DMSO)_2$ and $K^+(DMSO)_3$.

MPMOC13 Ion Cyclotron Resonance Studies of $TiCl_4$ and CH_3TiCl_3 Ion Chemistry with Some Organic Molecules, JACK S. UPPAL and RALPH H. STALEY, Dept. of Chem., Mass. Inst. of Tech., Cambridge, MA 02139

$TiCl_3^+$ and $TiCl_4^+$ in $TiCl_4$ react to give $Ti_2Cl_7^+$. In mixtures with CH_4, CH_3Cl, CH_2Cl_2, $CHCl_3$, CCl_4, C_2H_5Cl, and C_6H_5Cl, H^+, Cl^-, and $TiCl_3^+$ transfer reactions are observed yielding data on the relative proton affinity of $TiCl_4$ and the relative chloride affinity of $TiCl_3^+$. Transfer reactions of $TiCl_3^+$ promise to prove useful in determining relative $TiCl_3^+$ binding energies of π- and n-donor bases. In CH_3TiCl_3, $TiCl_3^+$ reacts to produce $CH_3TiCl_2^+$, indicating that substitution of CH_3- for Cl- in $TiCl_3^+$ decreases chloride affinity. Reaction of $CH_3TiCl_2^+$ with C_2H_4 gives C_3H_5-$TiCl_2^+$ with elimination of H_2, a possible mechanism for termination of Ziegler-Natta polymerization of ethylene. With C_2D_4, predominantly HD elimination occurs, suggesting formation of a $CH_3CD_2CD_2TiCl_2^+$ intermediate.

Ion-Molecule Reactions in Dimethylsulfoxide Studied by High Pressure Photoionization Mass Spectrometry

J.A. Stone and M.C. Lin, Department of Chemistry
Queen's University, Kingston, Ontario K7L 3N6, Canada

Ion-molecule reactions in DMSO at low pressure have received some attention but the kinetic data obtained are not in agreement. The rate constant for the disappearance of the molecular ion (M^+) is given as 1.9×10^{-9} (1) and 2.1×10^{-10} $cm^3 molecule^{-1} s^{-1}$ (2). In addition the rate of solvation of the proton by DMSO is noted to be low, an effect attributed to steric hindrance (2). We describe some experiments with a field free photoionization source (3) at pressures in the range 10^{-4} - 10^{-1} torr in which only the molecular ion is initially generated.

M^+ produced by krypton resonance radiation (10 eV) disappears in the following reactions:

$$CH_3SOCH_3^+ + CH_3SOCH_3 \longrightarrow H{\cdot}CH_3SOCH_3^+ + C_2H_5SO{\cdot} \quad (1)$$
$$\longrightarrow CH_3SO{\cdot}CH_3SOCH_3^+ + CH_3{\cdot} \quad (2)$$
$$\longrightarrow CH_3{\cdot}CH_3SOCH_3^+ + CH_3SO{\cdot} \quad (3)$$

$(k_1 + k_2 + k_3) = 2.0 \pm 0.2 \times 10^{-9}$ $cm^3 molecule^{-1} s^{-1}$ and this value is unchanged with increase in photon energy to 11.7 eV (argon resonance radiation). The ADO collision rate constant is 2.5×10^{-9} $cm^3 molecule^{-1} s^{-1}$. However $(k_2/k_1) = 1.5$ at 10 eV but the value increases to ~ 1 at 11.7 eV.

$H{\cdot}CH_3SOCH_3^+$ $\left((M+1)^+\right)$ and $CH_3SO{\cdot}CH_3SOCH_3^+$ $\left((2M-15)^+\right)$ disappear in apparently second order reactions to yield the proton bound dimer $(2M+1)^+$ which constitutes $\sim$ 80% of total ionization at 5 mtorr. At higher pressures the ion series $(nM+1)^+$ with $n \leq 5$ dominates the spectrum. Minor peaks are present in the two series $(nM+15)^+$ and $(nM-15)^+$ but the origin of these ions cannot be entirely due to solvation of the products of reactions 2 and 3, reactions of the $(nM+1)^+$ ions with DMSO must also contribute.

Neither H_2O nor CH_3OH ionize at 10 eV. In DMSO/CH_3OH mixtures a large yield of $(DMSO{\cdot}H{\cdot}CH_3OH)^+$ is observed for very low DMSO pressures (< 1 mtorr) and very high CH_3OH pressures ($\sim$ 60 mtorr). Only a very small $(DMSO{\cdot}H{\cdot}H_2O)^+$ peak is observed for H_2O/DMSO mixtures under the same conditions. With increased DMSO pressure the spectra are essentially the same as those for pure DMSO, no mixed solvation shell ions being present. However under these conditions much H/D exchange occurs in D_2O/DMSO mixtures and there is evidence for such exchange involving the DMSO methyl hydrogens. Such exchanges and reactions of these clustered ions may lead to complications in determining the thermodynamic parameters of proton solvation by DMSO.

1. A. Mackenzie Peers and J.C. Muller - Int. J. Mass Spectrom. Ion Phys. 16, 321 (1975).

2. W.B. Nixon, W.S. Woodward, M.M. Bursey and J.D. Henim - Int. J. Mass Spectrom. Ion Phys. 26, 115 (1978).
3. J.E. Kronberg and J.A. Stone - Int. J. Mass Spec. Ion Phys. 24, 373 (1977).

PHOTOELECTRON SPECTRA OF TRINUCLEAR METAL CLUSTER COMPLEXES

W. C. Trogler, Northwestern University and

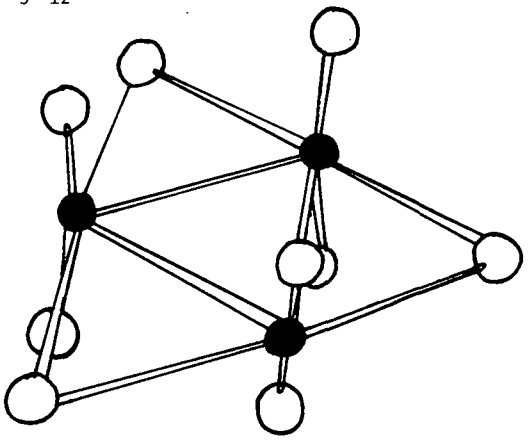
J. Berkowitz, Argonne National Laboratory

Metal cluster complexes can be generated and studied in the vapor phase, where detailed information about ionization energies and the atomic composition of the various valence orbitals can be deduced by photoelectron spectroscopy. One goal of such studies is to relate the molecular results to the nature of the bonding between various ligands and metal surfaces as in chemisorption. Another goal is to understand the nature of metal-metal bonding in metal clusters.

Knowledge about the nature of metal-ligand bonding in the cluster complexes could conceivably lead to a better understanding of their role in catalytic reactions.

Two general classes of metal cluster complexes are those containing either carbonyl or halide ligands. We have recorded the photoelectron spectra of Re_3Cl_9, $Ru_3(CO)_{12}$ and $Os_3(CO)_{12}$. For the latter two complexes both He I and HE II spectra have been recorded.

The assumed structure of Re_3Cl_9, based primarily on the known crystallographic structure of $Cs_3Re_3Cl_{12}$, is shown below. This structure was used in the Xα calculations.



Re_3Cl_9

The vapor phase photoelectron spectrum was obtained at 800°K. The spectrum shows a well-defined band at 9 eV splitting into components at 9.00 and 8.85 eV. Calculations of the SCC DV Xα type support a 23e" assignment for this band. This orbital possesses equal Re 5d and Cl 3p character due to covalent Re-Cl interactions. The

0.25 eV peak splitting is attributed to spin-orbit splitting of the $^2E''$ state into $E_{1/2}$ and $E_{3/2}$ components. The relatively narrow width is consistent with the delocalized nature of this orbital. Considerable structure is observed for the higher ionization energy region of the spectrum. Our calculations indicate that there are 21 additional valence orbitals which can contribute to this structure.

$Ru_3(CO)_{12}$ and $Os_3(CO)_{12}$

In the He I and He II photoelectron spectra of $Ru_3(CO)_{12}$ large CO peaks are evident at ∿14, 17 and 19.7 eV, due to partial decomposition of the sample upon heating. In comparing the He I and He II spectra, we note a lower ionization energy peak (at ∿6.5 eV) in the He II spectrum. This could be due to thermal decomposition yielding a molecular species $Ru_3(CO)_X$ ($X < 12$), or it may be attributable to ionization from the more energetic 256 Å line of He II.

The lowest ionization energy peaks are broad, indicating electron ejection from bonding orbitals. Their low energy implies large ruthenium atomic character. At this time, we cannot be certain whether the bonding is Ru—Ru, Ru—CO, or both. Calculations of the Xα DVM type are in progress, which we hope will help to clarify this point. The $Os_3(CO)_{12}$ spectra are similar to their ruthenium counterparts.

The spectrum of Re_3Cl_9 and its interpretation will appear shortly in the Journal of the American Chemical Society. The work on the ruthenium and osmium complexes is currently being prepared for publication.

This research was performed under the auspices of the Division of Basic Energy Sciences of the United States Department of Energy.

COMPARISON BETWEEN THE PHOTOELECTRON SPECTRA OF TRANSITION METAL BETA-DIKETONATE COMPLEXES AND THEIR IONIZATION EFFICIENCY CURVES IN THE THRESHOLD REGION

John B. Westmore and Charles Reichert
Department of Chemistry,
University of Manitoba,
Winnipeg, Manitoba, Canada R3T 2N2

The ionization energies of many beta-diketonate complexes of transition metals have been determined by electron impact methods. A review of these results is available (1). The methods used (semi-logarithmic plot, vanishing current, critical slope, extrapolated voltage difference, energy compensation) all involve certain assumptions about the threshold ionization behavior in an absolute and/or relative way as compared to reference species (such as Xe) used to calibrate the electron energy. Our own attempts to deconvolute the ionization efficiency curves using either the derivative methods (2) or the "energy distribution difference" (EDD) method (3) were not very successful. These methods are very sensitive to signal noise, but attempts at noise removal did not lead to sufficiently improved results. In fact, these methods should only be effective for a sequence of first order ionization processes with thresholds not too closely spaced, when using an electron beam with a "normal" energy spread. As will be described below, the title compounds obey second power threshold ionization laws and these would not be effectively revealed by the derivative or EDD methods.

The electron impact IPs reported in the literature did not show the variations anticipated on the basis of ligand field theory. The objective of the present study is to attempt to determine the importance of d electron participation near the ionization threshold of transition metal beta-diketonate complexes, by comparison of their ionization efficiency curves with those of the corresponding complexes of Al(III), and with photoelectron spectra (4).

Theoretical curves for the electron impact threshold ionization regions of the title compounds were compared with the experimental data points. The theoretical curves were obtained by convoluting the thermal energy spread (assumed Maxwellian) of the ionizing electrons with test threshold ionization laws. Standard methods lead to the following expressions:

First power threshold law: $p(E) \propto (E - IP)$

$$I_v = B(2kT - V - IP)\exp\left(\frac{V - IP}{kT}\right) \quad \text{for } V \leq IP$$

$$I_v = B(2kT + V - IP) \quad \text{for } V \geq IP$$

Second power threshold law: $p(E) \propto (E - IP)^2$

$$I_v = 2kTC(3kT - V + IP)\exp\left(\frac{V - IP}{kT}\right) \quad \text{for } V \leq IP$$

$$I_v = C\left[6(kT)^2 + 4kT(V - IP) + (V - IP)^2\right] \quad \text{for } V \geq IP$$

in which E = electron energy; V = electron acceleration voltage; B,C = proportionality constants.

When curve fitting procedures were adopted it was found that, unlike the ionization of many species, none of the metal complexes obeyed a first power threshold ionization law. Instead, excellent agreement with a second power threshold ionization law was obtained for complexes of Al(III), Mn(III), Fe(III) and Co(III) (d^0, d^4, d^5 and d^6 respectively). The quality of the agreement is illustrated for $Al(hfacac)_3$ in figure 1, in which the theoretical curve is fitted to experimental values of $\sqrt{(I_v/I_{50})\%}$ (least squares method) by varying the two parameters, IP and C (T was taken as 2500 K, for which kT = 0.215 eV). For complexes of Ti(III), V(III) and Cr(III) the experimental points lie above the "best fit" curves in an electron energy range correlating with band Y (assigned to electron removal from metal t_{2g} orbitals) in the photoelectron spectra, illustrated for V(III) complexes in figures 2 and 3. The data for the Mn(III) and Fe(III) complexes show no evidence for involvement of the metal e_g^* orbitals at lower energies.

References

1. J. B. Westmore, Chemical Reviews 76, 695 (1976)
2. J. D. Morrison, J. Chem. Phys., 19, 1305 (1951); 21,1767 (1953); 22, 1219,2090 (1954); 39, 200 (1963)
3. R. E. Winters, J. H. Collins and W. L. Courchene, ibid., 45 1931 (1963)
4. S. Evans, A. Hamnett, A. F. Orchard and D. R. Lloyd, Faraday Discuss. Chem. Soc., 54, 227 (1972)

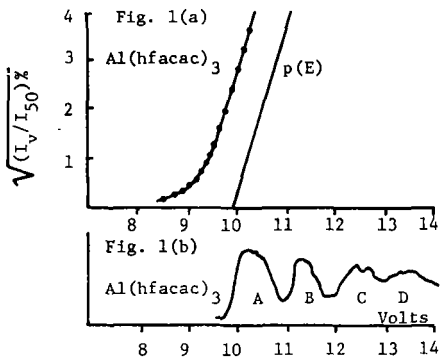
Figure captions

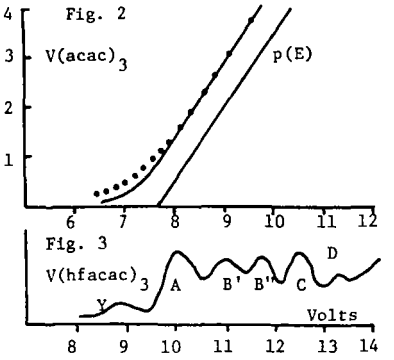
1(a). "Best fit" curve and p(E) function (with slope adjusted to parallel linear portion of "best fit" curve) for $Al(hfacac)_3$. Fits of similar high quality were obtained for $Al(acac)_3$, $Al(tfacac)_3$, $Mn(acac)_3$, $Fe(acac)_3$, $Fe(tfacac)_3$, $Fe(hfacac)_3$ and $Co(acac)_3$

1(b). PE spectrum of $Al(hfacac)_3$

2. "Best fit" curve and p(E) function for $V(acac)_3$. Similar, but larger, deviations were observed for $Ti(acac)_3$. The deviations for $Cr(acac)_3$, $Cr(tfacac)_3$ and $Cr(hfacac)_3$ were smaller but apparently real.

3. PE spectrum of $V(hfacac)_3$. Bands for $V(acac)_3$ for comparison with Figure 2 are expected to be shifted ~2 v to lower values.





IMPROVED SIMS ENERGY PREFILTER

J. R. Wyatt, R. J. Colton, J. D. Ganjei, J. J. DeCorpo, and J. S. Murday,
Chemistry Division, Naval Research Laboratory, Washington, D. C. 20375

The use of a quadrupole mass filter for SIMS requires reducing the energy spread of the sputtered ions. Our SIMS apparatus uses an Extranuclear quadrupole mass filter equipped with a "Bessel Box" type ion energy prefilter. The Bessel Box performance was improved dramatically by adding an extraction lens between it and the sample. This arrangement is shown in Figure 1. Screens were added to reduce the radial component of the field produced by the lens. Typical operating voltages referenced to the sample are: extraction lens, -18V; front and back of the Bessel Box, -15V; and center of the Bessel Box, OV.

To gain a better understanding of the prefilter, computer programs were developed to calculate the potential field and plot the ion trajectories within the prefilter. As the Bessel Box is a cylindrically symmetric system, the field, Φ, must satisfy the following differential equation.

$$\partial^2\Phi/\partial z^2 + \partial^2\Phi/\partial r^2 + \partial\Phi/r\partial r = 0$$

Using the boundary conditions imposed by the box this equation was solved by the Liebmann method.[1] Φ can then be scaled to the actual voltages of the system.

Ion trajectories were calculated by solving the following equation.

$$d^2r/dz^2 = (1 + (dr/dz)^2)(d\Phi/dr - d\Phi/dz * dr/dz)/2\Phi$$

This equation was numerically integrated twice to give the radial position, r, of an ion as a function of its axial position, z. The only approximation was to assume that Φ was constant over each increment of integration. A result of the calculations is shown in Figure 2. Here, the fraction of ions transmitted through the prefilter as a function of the ion's energy relative to the center-stop is shown for three different extraction lens potentials. In this case, the potential at the entrance and exit of the Bessel Box is 20V, and the initial energy of the ions is 9V. From Figure 2 the performance of the Bessel Box strongly depends upon the extraction lens potential. Without the extraction lens the field between the sample and Bessel Box entrance is determined by the entrance potential of the Bessel Box and cannot be adjusted for high energy resolution without degrading ion collection.

Verification of the calculated performance of the ion energy prefilter was obtained by connecting an external ramp voltage to the sample and measuring the intensity of mass-selected secondary ions as a function of the ramp voltage. Aluminum and vanadium samples were used for the experiment. Figures 3 and 4 show the intensity of the Al^+ peak as a function of the ramp voltage for various lens settings without and with the extractor attached to the prefilter. Without the extraction lens there is little change in the bandpass as a function of the entrance energy (Ll) of the ions to the Bessel Box. Ideally the bandpass should be proportional to the energy of the ions. With the extractor the bandpass is much sharper and correlates with the entrance energy as expected. The bandpass was calculated from the slope of the rising edge of the curves in Figures 3 and 4 and is given as half-width (HW) in volts. Additionally, the extractor increases the signal intensity by a factor of five when Ll = 20V.

[1] "Numerical Analysis," K. S. Kunz, McGraw Hill, 1957, p.296.

In summary we have shown both experimental and theoretical evidence that use of an extraction lens dramatically improves the performance of a Bessel Box type ion energy prefilter. The results include more intense SIMS spectra and improved energy resolution. Additionally, the performance of the quadrupole mass filter is improved since the ion beam entering it has narrower energy distribution and spacial divergence.

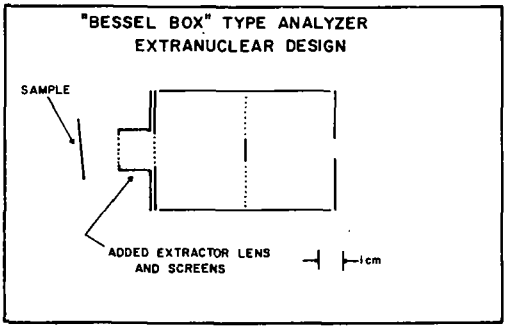


Figure 1

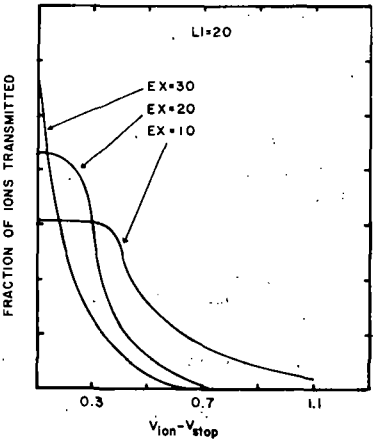


Figure 2

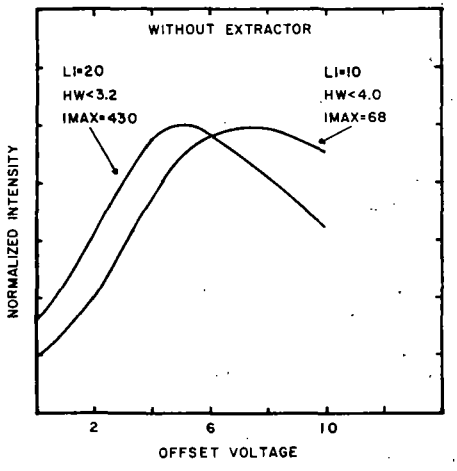


Figure 3

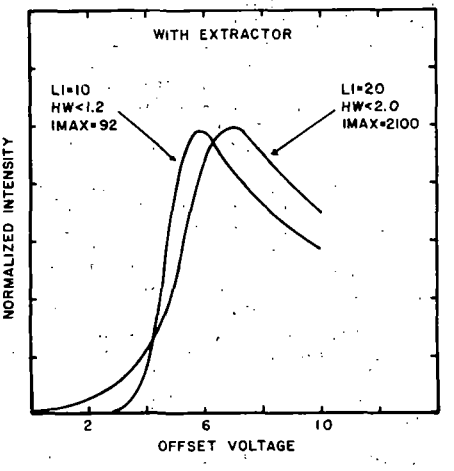


Figure 4

MPMP4 **The Automation of a SIMS System: Philosophy and Design,**

Margaret A. Frisch, IBM Research Center, Box 218, Yorktown Heights, N.Y. 10598

The SIMS instrument is under the control of an IBM System/7 computer. Using high precision digital/analog converters: 1) the quadrupole mass spectrometer can be scanned or stepped in many complex sequences, and 2) the focusing potential of the energy filter can be dynamically set, which is essential in determining charging effects and in optimizing ion collection. The ion signal is measured with 100 MHz pulse counting equipment. The gating of the scaler is controlled by a programmable timer, which also inhibits the scaler during the "non-window" portion of a raster.

Many programs are available for control and analysis. The measurement of the quadrupole dispersion is fully automatic. The experimenter can graphically observe in real time the profiling of a sample for as many ion species as desired. The user can also generate complex graphic displays, including overlays, normalizing to a reference species and subtracting an interference component. To aid in identification, a mass spectrum can be compared with a simulated spectrum, based on the isotopic distribution for a set of ionic species. The data can be displayed as a function of ion energy and integrated for relating total ion production to sputtering yield. Further, the data can be statistically analyzed, yielding averages and standard deviations.

MPMP 5

Rapid Measurement of Calcium Isotope Ratios Using a New Thermal Ionization Method.

A.L. Yergey, National Institute of Child Health and Human Development, NIH, Bethesda, Maryland 20205

Stable isotopes of calcium are required for tracer studies of inborn errors of calcium metabolism in children. The practice of determining metabolic kinetics by using two isotopes simultaneously makes mass spectrometry the preferred tool to measure changes in isotopic enrichments. Thermal ionization methodology was chosen for use in these studies because of its proven reliability and because calcium chelates were found to give unsatisfactory mass spectra for isotope tracer studies.

Clinical tracer studies require the ability to measure enrichments of from 20-150 atom % for the 42,43 or 48 isotope and enrichments of 50-1000 atom % for the 46 isotope all at accuracies and precisions of 1-2%. The volume of samples necessary for a typical clinical study demands an analysis time of 10-15 min. per sample. Existing thermal ionization methods for calcium require 3-4 hours per sample but yield accuracies and precisions of about 0.2%. It was felt that a simpler method than that presently used could be devised to permit the rapid analysis of samples and give results within the required error limits.

The new rapid method for measurement of calcium isotope ratios has as its basis a highly modified solids inlet probe. The tip of the probe is a receptacle for disposable filament assemblies that are made from nickel rods held at the desired separation by a glass bead. Rhenium ribbon filaments are spot welded across the rod tips. Samples are placed onto the degassed filaments and air dried under a heat lamp, placed into the probe tip, heated in air at 2A for 10-15 sec, cooled, and inserted into the solids probe inlet. Calcium samples consist of 15µl of 0.02 M $CaCO_3$ dissolved in 3% HNO_3 placed onto the probe tip from a Hamilton syringe.

A Finnegan 4021 Quadrupole Mass Spectrometer modified by replacing the standard diaphragm solids probe inlet valve with a 1/4 turn Con Vac off axis butterfly valve was used in this work. Isotope ratios were measured by scanning the appropriate mass windows with an Extra Nuclear 091-3 Mass Programmer and inputing data to the NIH Isotope Ratio Calculator, an 8080 µ-processor based device with an 8 bit A/D that has 8 pre-selectable gain ranges. Overall sensitivity is 10V-10MV with resolution of 40mV ± 10 to 40 µV ± 10.

Stable calcium ion signals of about 10^{-8}A for ^{40}Ca are obtained by heating the loaded filaments with currents of 3-3.6A using a +5V bias on the filament and multiplier voltages of about 2000V. A typical analysis requires about 6-10 min. of operating time on the mass spectrometer. Several replicate measurements from a single filament are generally possible. Filaments are not reused, but the holders can be used several times by cleaning them in an ultrasonic bath with 3% HNO_3,

Measurements of natural abundance (n.a.) isotope ratios (Table I) show that satisfactory accuracy and precision are obtained for 4 of the six isotopes. The 43 isotope cannot be measured at present due to a hydrocarbon background ion at m/e 43; the 46 isotope is at too low a level to be observed under the present conditions. Modifications to the 4021 are planned to correct both of these problems. An isotope dilution curve in the range of 5-1000 atom % enrichment of ^{44}Ca has been determined (Table II). These results are satisfactory to carry out the first series of clinical studies.

Table I

Natural Abundance Calcium

Isotope Ratios

	Ratio relative to m/e 42	
m/e	theoretical	observed
40	150	156 ± 8
42	---	---
43	0.207	N/A
44	3.22	3.21 ± .02
46	0.0026	N/A
48	0.288	0.287 ± .003

Table II

Isotope Dilution Curve for ^{44}Ca in n.a. Ca

% ^{44}Ca added	measured atom % enrichment ^{44}Ca
7.38	7.4 ± .1
16.2	14.9 ± .3
40.6	36 ± .9
81.1	82.3 ± 1.6

The regression line through these points is y = 1.01 x -1.5.

MPMP6 A NEW AUTOMATED UF_6 - MASS SPECTROMETER WITH MOLECULAR BEAM INLET AND MULTIPLE ION COLLECTOR. C. BRUNNEE, B. LASER, H. RACHE, and H. RAVENS, Varian MAT GmbH, Bremen, Germany

The analyzer uses stigmatic focusing (46 cm effective radius, 8 kV accelerating voltage) and is equipped with four collectors for simultaneous measurement of the isotopes 234, 235, 236, 238. An additional multiplier serves as a detector for trace impurities. Sample inlet is done via a collimated molecular beam of small aperture to avoid any contact of the UF_6 molecules with the ion source. Thus contamination of the source and memory effects are reduced to a minimum. All functions of the mass spectrometer including sample inlet are under control of an HP 9835 computer. Performance: precision $\pm$ 0.1 ‰, abundance sensitivity $< 1 \times 10^{-5}$, memory factor < 1.003, time for one analysis 5 minutes.

MPMP7

TWO PROGRAMMABLE CALCULATOR PROGRAMS FOR ISOTOPE DILUTION

E. H. Daughtrey, Jr., and J. K. Bostick, Jr.

Northrop Services, Inc.
P.O. Box 12313
Research Triangle Park, North Carolina 27709

The analytical method of isotope dilution offers sensitive, precise determination of specific elements. The method involves adding a known amount of separated isotope of the sought-for element to the sample. The altered isotopic ratio is then measured. Knowing weight and isotopic abundance of the sample and spike, the concentration can be calculated.

Having met the inherent stringent requirements on the altered ratio and with some prior knowledge of the sample, the I.C. spike program calculates the spike weight. Properly spiked, the depleted isotope will fall within the factor-of-three requirement of photoplate linearity. The bracketing method, using a logarithmic curve fit, can then be used and the concentration determined.

These programs simplify the cumbersome calculations necessary in isotope dilution and provide an intermediate step to the minicomputer.

This work was performed under Contract No. 68-02-2566 in support of the Environmental Monitoring and Support Laboratories, Environmental Research Center, Research Triangle Park, North Carolina.

References:

1. R. K. Webster, "Advances in Mass Spectrometry", I. D. Waldron, ed., Pergamon, London, 1959, p. 1.
2. H. Farrar, "Trace Analysis by Mass Spectrometry", A. J. Ahearn, ed., Academic Press, New York 1972, pp. 283-290.

Table 1

conc	=	the concentration in µg/g.
W	=	the weight of the isotopically enriched spike (in µg)
M	=	the weight of the sample (in g)
K	=	the ratio of the atomic weight of the naturally occurring element of interest to that of the enriched isotopic material.
Asp	=	the isotopic abundance of the enriched isotope A in the spike.
Bsp	=	the isotopic abundance of the depleted isotope B in the spike.
A	=	the natural isotopic abundance of isotope A.
B	=	the natural isotopic abundance of isotope B.
R	=	the measured altered ratio of isotope A to isotope B, from the mass spectrum.

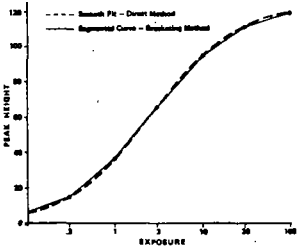
① MAGNETIC CARD STORAGE OF THE ELEMENTAL ISOTOPIC CONSTANTS

② KEYBOARD ENTRY
–DESIRED ALTERED ISOTOPIC RATIO
–SAMPLE WEIGHT
–EXPECTED CONC. OF SOUGHT FOR ELEMENT

③ $\frac{(CONC)\ (M)}{(K)} \left(\frac{RB - A}{Asp - R\ Bsp} \right)$ = SPIKE WEIGHT

④ UPPER AND LOWER LIMITS FOR ALTERED ISOTOPIC RATIO

⑤ A BRACKETING METHOD OF CALIBRATION IS USED, SEGMENTING THE CURVE INTO LINEAR PORTIONS



⑥ THE ISOTOPE'S PEAK HEIGHT, FALLING BETWEEN CALIBRATION POINTS, IS CONVERTED TO A RELATIVE EXPOSURE VIA THE CALIBRATION

⑦ $\frac{W \cdot K}{M} \left(\frac{Asp - R\ Bsp}{RB - A} \right)$ = conc

OPTIONAL: CALIBRATION COEFFICIENTS

B, M, R

Figure 1

```
I.D. SPIKE
①
          CU
②
          2.5          R
          0.05         WT
          128.         CONC
③
  9.343906848          SPK
```

```
ISOTOPE DILUTION
 * *  - *  * *  * *
①* *     CU * *   * *
            65.          MA
            63.          MB

         30.91          %A
         69.09          %B

         99.69          %ASP
          0.31          %BSP

         0.982          K
③
         9.345          SPK
         0.05           WTI
-------------------------
④
  321.5806452           UL
  .4473874656           LL
 * *   * *   * *   * *
⑤
 CAL.      EXP.    HT.
            1.          EXP
          2.9           HT
            3.          EXP
          5.4           HT
⑥
          5.4
            3.          A
          3.3
 1.192173326            B
 2.516412617            R
⑦
 128.9961085            PPM
-------------------------
```

Desorption Mechanisms and Their Relationship to the Apparent Locus of Ion Formation in Field Desorption Mass Spectrometry

J.F. Holland, B. Soltmann, R. Olinger and J. Dye

Departments of Chemistry and Biochemistry, Michigan State University, East Lansing, MI. 48824

Progress toward a clear understanding of the role of the high field in Field Desorption Mass Spectrometry has been impeded by the effect of the field on the measured intensities of the ions that are being collected and focused by the mass spectrometer.

The presence of sharp needle-like structures on the activated FD emitter will, when exposed to an electrical field, result in large field gradients in the vicinity of their tips. These gradients will affect both the processes of ion generation and ion collection.

The current collected from point sources is exponentially related to the applied voltage (1), and the observed increase in ion intensity with increasing voltage, as shown in Fig. 1, can mask the more subtle effects of the field on ion production due to the experimental variations of the intensity measurement.

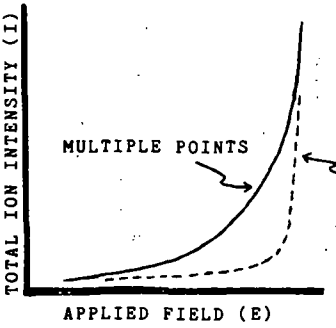


Figure 1

EFFICIENCY OF ION COLLECTION AS A FUNCTION OF APPLIED VOLTAGE

$\log i \propto 1/E$

The role of the field in ion generation may be considered as three generalized modes of action.

A. Field Induced Electron Tunnelling from the molecule to the conducting emitter surface as proposed by Muller (2) and Gomer (3) and expanded by Beckey (4). This is a resonant process that theoretically results in a molecular ion species of very low internal energy and, hence, very little fragmentation.

B. Field Assisted Electrophilic Attachment may occur between a molecule and an ion on or near the emitter surface. For example, reactions of the type;

$$M + \text{Cation}^+ \rightleftharpoons [M\text{-Cation}]^+$$

$$M + H^+ \rightleftharpoons [M\text{-H}]^+$$

Since there is no net charge difference involved in these processes the field may primarily affect them by imparting linear energy to the cations in the reaction zone. This increased energy and coincident mobility may serve to increase both the probability of collision and the rate of the ensuing attachment reaction with neutral species. In a more speculative vein, polarization of the neutral species in the high field may also influence their susceptibility to cation attachment.

C. Field Assisted Charge Transfer (FACT) reactions may occur in those situations where there is a charge difference between the reactants and the products. Consider the following processes occurring in the mobile phase on or near the emitter:

$$\text{molecules} \rightleftharpoons \text{molecular clusters} \rightleftharpoons \text{ion pairs} \rightleftharpoons \text{separated ions}$$

The equilibrium of the left hand reaction is primarily affected by the concentration of the material in the reaction zone and the temperature of the emitter. The other two equilibria will be affected by the high field, favoring the production and separation of ionic species. Calculations of the overall free energy change for the complete process predict that in situations where the field gradient is ~ 1 V/Å and the ion pair separation is greater than $\sim$ 4-5 Å, the production of ions by this mechanism is a favorable, spontaneous process (5). The conditions necessary for this ionization process often occur in the FDMS of organic molecules.

Table I lists the types of ions observed in FDMS.

Table I

Prior Ions
Tunnelled Species
F A C T Species
Reaction Products of the above with Neutral Species
Fragment Ions
Surface Ionization Products

If the point at which an ion responds exclusively to the external field (i.e. the point of ion generation and/or deshielding) varies for the different types of ions, they will receive varying amounts of kinetic energy from the applied field as they are accelerated and collected by the spectrometer. Table II shows the change in accelerating voltage of the Varian MAT CH5-DF mass spectrometer necessary to maximize the transmission of various molecular ions through the electric sector of the instrument. These reproducible differences in accelerating voltage indicate a difference in energy imparted to the various types of ions by the high field.

Table II

Variations in the Kinetic Energies of Selected Ions in FDMS

Compound	V
Acetone	0
Benzene	.1
Water	2.1
Nitrogen	3.9
Uridine	0
Cholesterol	0
Methanol	0
Butanol	0
Na^+ codesorption	-3.4
Na^+ surface	-5.4
K^+ codesorption	-3.4
K^+ surface	-5.3

These observations are consistent with the concept of a varying locus of ion formation and/or capture.

The data in Table II indicate that specific levels of ion energy exist for several types of compounds analyzed by FDMS under similar conditions. These differences in kinetic energy can be attributed to the various mechanisms of ion generation and can be associated with specific regions of ion formation and/or capture for each type of compound (Fig. 2).

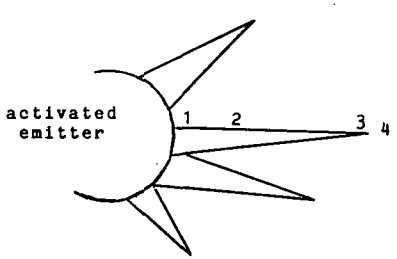


Figure 2

ZONES OF ION ENERGY

1 - Langmuir Ions - Temperature Induced Surface Ionization

2 - Prior Ions - Coevaporation

3 - Large Organic Molecules - Facts

4 - Small Molecules - Tunnelling

In conclusion, the observed differences in kinetic energy for the different types of ions support a model for FDMS consisting of more than one mechanism of ionization and indicate a locus of ion generation and/or capture that is dependent upon the specific type of ion and its mode of formation.

References

1. Eyring, C.F., MacKeown, S.S. and Milliken, R.A., Phys. Rev., 31, 900 (1928).
2. Muller, E.W., Phys. Rev., 1, 169 (1956).
3. Gomer, I., J. Chem. Phys., 31, 341 (1959).
4. Beckey, H.D., "Principles of Field Ionization and Field Desorption Mass Spectrometry," Permagon, London, England, 1977.
5. Holland, J.F., Soltmann, B. and Dye, J.L., 26th Ann. Conf. Mass Spec. and Allied Topics, p. 193 (1978).

THE APPLICATION OF FIELD DESORPTION MASS SPECTROMETRY (FDMS) TO ANALYSIS OF LIPID RADIOLYSIS PRODUCTS

C. Merritt, Jr. and S.G. Kayser, Food Sciences Laboratory, U.S. Army Natick R&D Command, Natick, MA 01760

W.W. Nawar, Department of Food Science & Nutrition University of Massachusetts, Amherst, MA 01002

M.R. Olinger and J.F. Holland, Department of Biochemistry, Michigan State University, E. Lansing, MI 48824

The application of high energy sterilizing radiation in the preservation of meats often produces changes in the meat that may affect its acceptability and wholesomeness. Fats comprise 10-20% of meat weight and are quite susceptible to chemical change. Prior studies[1,2] have shown the formation of several types of lipid fragments due to heating, oxidation and radiolysis. This study is concerned with the identification of the higher molecular weight species that are produced by the irradiation of triglycerides.

The analysis of recombination products induced by irradiation in triglycerides such as trilinolein (MW=878) is difficult due to their high molecular weight. Tributyrin (MW=302) was chosen as a model compound for preliminary investigation of the types of rearrangements that occur in samples of triglycerides under irradiation.

Ten grams of the triglyceride are exposed to beta and/or gamma radiation in doses of 50-100 megarads under controlled conditions. The products are separated from the resulting mixture by gel permeation chromatography on 60 Å Styragel followed by separation of the compounds by gas chromatography. The isolated fractions are analyzed by several mass spectrometric techniques.

The chromatograms are shown in Figures 1 and 2.

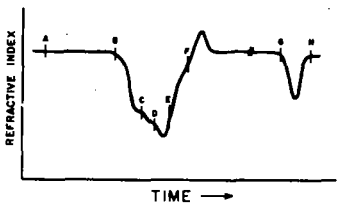


Fig. 1 Gel permeation chromatogram.

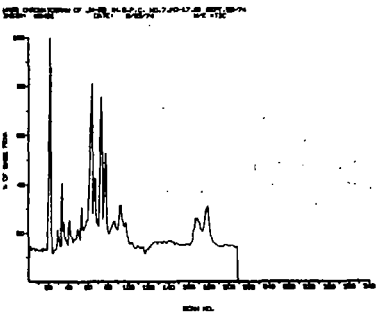


Fig. 2 Reconstructed total ionization gas chromatogram.

Ions in the mass spectra obtained by ordinary EI of the eluting components in GC/MS mode are found not to have sufficient abundance in the high mass range to allow identification of the compounds. In many cases parent ions are missing and many other ions in the spectra of lipid derived compounds are isometric. It is essential to be able to observe the parent ion and to assign the fragment ions in the high mass range to structurally related features of the spectrum. Field desorption (FD) and electron ionization desorption[3] (EI/D) are used to provide the information. The spectra are seen in Figures 3 and 4.

Field desorption has shown the presence of at least two major components in the GPC fraction having molecular weights of 516 and 602, respectively. The principle fragment ions are seen in the corresponding EI/D spectrum. In this example the compounds are seen to be identified as a dimer of tributyrin, M.W. 602 and a recombination product, M.W. 516, of tributyrin with a radiation induced free radical corresponding to propanedioldibutyrate. The structures and some of the key fragment ions are shown below.

CONCLUSIONS

The data show that irradiation produces high molecular weight recombination products and illustrates that EI/D and FD Mass Spectrometry are efficacious techniques for the elucidation of the structure of such lipid compounds.

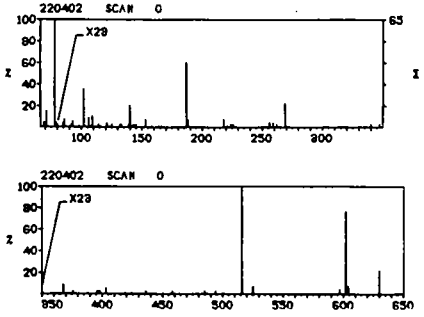


Fig. 3 FD Mass Spectrum

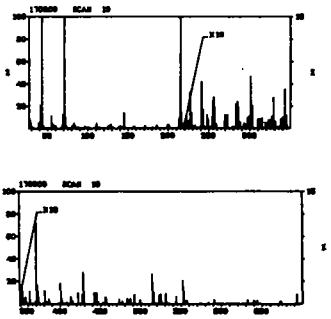
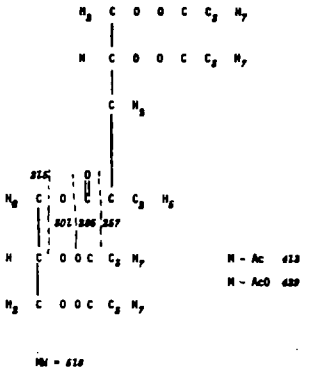
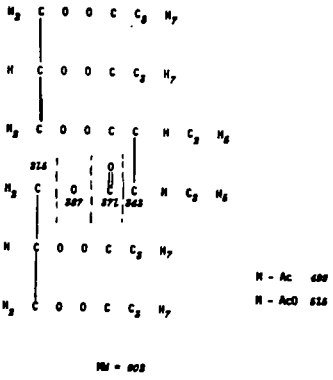


Fig. 4 EI/D Mass Spectrum





REFERENCES

1. Merritt, C., Jr., Angelini, P. and Nawar, W.W., Food Preservation by Irradiation Vol. II, Internation Atomic Energy Agency, Vienna, Austria (1978) pp. 97-112.
2. Meidani, J., Nawar, W.W., Yeomans, W.G. and Merritt, C., Jr., J. Am. Oil Chem. Soc., 54, 496 (1977).
3. Soltmann, B., Sweeley, C.C. and Holland, J.F., Anal. Chem., 49, 1164 (1977).

COMPARISON OF THREE METHODS OF OBTAINING METABOLIC PROFILES FROM URINE

B. Edwin Blaisdell, William Aberth, Alan Sheets, Constance Tsao, Joan C. Engels, Stuart MacGuire
Linus Pauling Institute of Science and Medicine, Menlo Park, California 94025

We have made a comparison of three methods of obtaining metabolic profiles of urine and of their effectiveness in distinguishing real world characteristics of the urine's sources. The methods are volcano field ionization mass spectrometry of urine (VFIMS) (1), capillary gas chromatography of volatiles of urine (GC) (2), and high pressure liquid chromatography of urine amines and amino acids (HPLC) (3). The urines were collected for successive 24-hour periods from 3 persons who were eating the same diet in the same proportions by weight at every meal according to the following schedule by days: (1) uncontrolled, (2, 3) basic diet plus tuna fish (canned, in water), (4, 5, 6, 7, 8) basic diet, (9, 10) basic diet plus 1 quart water per day, (11, 12, 13) uncontrolled. The basic diet: milk, shredded wheat, salted peanuts, apple, carrot, romaine lettuce, 2 grams vitamin C.

The analytic power for step changes in urine was accomplished by analysis of variance and covariance of the spectra for urine collection days 6, 7, 8, 9, 10 coding days 6, 7, 8 as diet (D), days 9, 10 as water (W), and persons as A, B, C with covariate the instrumental analysis sequence, which was assigned at random to the set of 30 measurements (15 sets of duplicates analyzed in close but not necessarily contiguous sequence). We used program P2V of the BMDP package (4). The covariate removes the influence of a small but significant linear instrumental drift observed in the recurrent analyses of a standard. Fifty-four out of the 55 selected peaks or peak combinations for HPLC (3) are effective at the 10% significance level in distinguishing at least one of the possible class differences and 20 of them are effective in distinguishing the interactions between diet and person, namely that it is possible to distinguish that persons respond in different ways to the change in diet of drinking much more water. Similarly 171 and 60 out of the 238 measured masses for VFIMS.

The analytic power for step changes in urine was also accomplished by discriminant analysis of the spectra for urine collection days 2, 3, 6, 7, 8 coding days 6, 7, 8 as diet (D), days 2, 3 as tuna (T), and persons as A, B, C. We used program P7M on the BMDP package (4). Good discrimination of the 6 subsets was achieved.

The analytic power for linear long-term changes in urine was accomplished by linear least squares of the spectra for days 4, 5, 6, 7, 8 as a linear function of collection date and of analysis sequence. Seventy-eight of 3 x 55 peaks for HPLC and 125 of 3 x 238 masses for VFIMS gave trends with collection date which were significant at the 10% level using program PIR of the BMPD package (4). Further details of the levels of significance obtained are shown in the histogram of Fig. 4; many are less than 1%.

References

1. W. Aberth, paper WAMP10, this conference.
2. A. B. Robinson, D. Partridge, M. Turner, R. Teranishi, L. Pauling, J. Chrom. 85, 19 (1973)
3. H. Dirren, A. B. Robinson, L. Pauling, Clin. Chem. 21, 1970 (1975).
4. BMDP, Health Sciences Computing Facility, UCLA, NIH Grant RR-3 (1975).

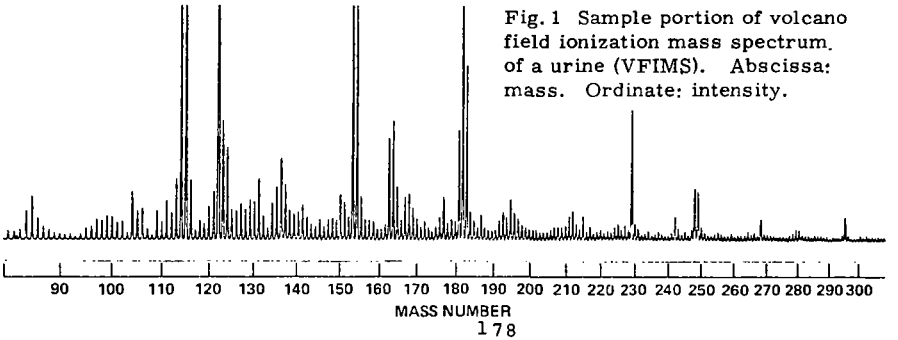


Fig. 1 Sample portion of volcano field ionization mass spectrum of a urine (VFIMS). Abscissa: mass. Ordinate: intensity.

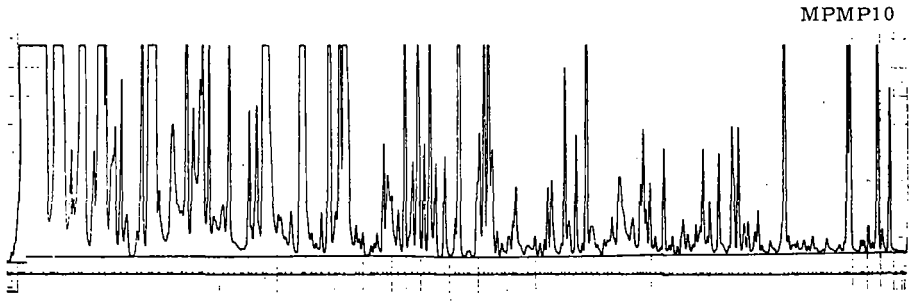


Fig. 2. Sample portion of chromatogram of urine volatiles (GC). Abscissa: number of selected combinations of one or more peaks. Ordinate: intensity.

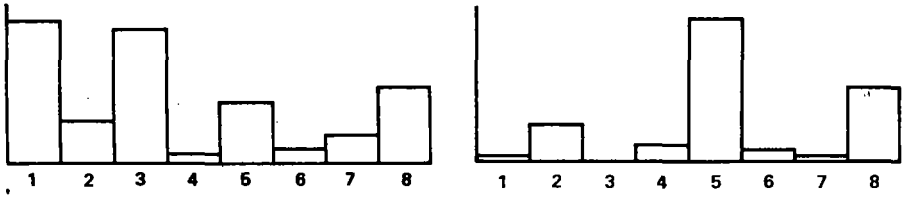


Fig. 3. Analytic power for step changes in urine. Left: VFIMS Right: HPLC. Abscissa: class of difference distinguished: (1) none, (2) only water, (3) only person, (4) only interaction between water and person, (5) both water and person, (6) both water and interaction, (7) both person and interaction, (8) all three of water, person, and interaction. Ordinate: count of number of masses (peaks) significant at 10% level out of 238 (55) possible.

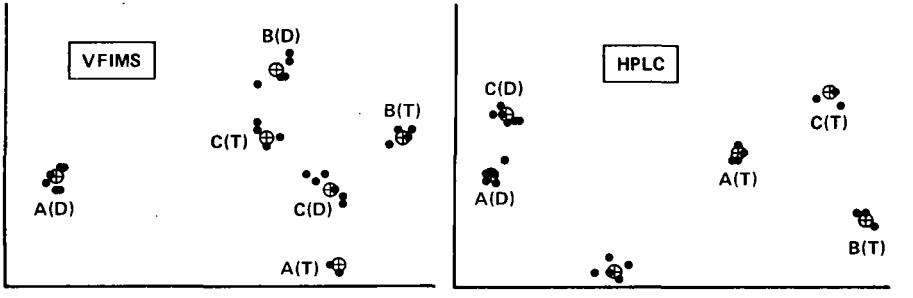


Fig. 4. Analytic power for step changes in urine. Left: VFIMS. Right: HPLC. Discrimination achieved with 2 best combinations of 10 (10) best discriminating masses (peaks) from 80 contiguous masses (peaks).

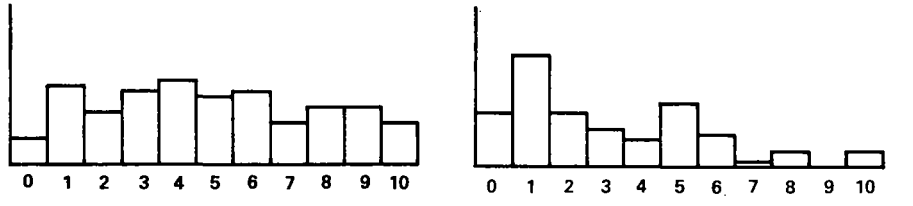


Fig. 5. Analytic power for linear long-term changes in urine. Left: VFIMS. Right: HPLC. Abscissa: Significance level ($\leq$10%) of linear trend over five days on constant diet. Ordinate: count of number of masses (peaks) out of 238 (55) possible.

A STUDY OF THE MECHANISM OF FIELD IONIZATION BY CONDITIONED GRAPHITE FILAMENTS

by

Derryl D. J. Allman, Paul L. Gutshall and Paul J. Bryant
University of Missouri-Kansas City
Department of Physics
Kansas City, Mo. 64110

Graphite filaments have been used by the authors as a field ionization and field desorption source in mass spectrometers for several years. The filaments consist of carbon layers rolled into a scroll-like filament 2 to 5 microns in diameter. Platelets on the surface of the filaments are the result of partial defoliation of the scroll-like structure. The platelets have edges whose radius is sufficiently small to produce field ionization at potentials as low as 2000 volts. The platelet density of the surface determines the sensitivity of the ion source. Exposure of the filaments to bromine gas enhances defoliation of the graphite.

Graphite filaments 3 millimeters long were mounted on a U-shaped support and placed in a vacuum system whereby the total field ion current could be measured. Ammonia was used as the ionizing medium for determining the ion current of the untreated filaments. After measuring the background current for a given filament, it was then exposed to bromine gas for 12 hrs. After exposure to bromine, the field desorption current for bromine and the field ionization current for ammonia were measured. The filaments where then placed in a vacuum furnace for 40 min. at 625°C to remove any residual bromine remaining in the filament. After the heat treatment, the field ionization current for ammonia was determined for the "clean filament."

The data shown in Table I are the average FI current obtained from 10 filaments.

Table I

FIELD IONIZATION OF AMMONIA BEFORE AND AFTER TREATING FILAMENTS WITH BROMINE

	Condition	Current (amp/torr-mm)
1.	Untreated	5.52×10^{-5}
2.	Treated with Bromine	1.24×10^{-5}
3.	Bromine removed by baking	9.61×10^{-5}

After exposure to Br, the ion current showed a decrease. This may be due to the decrease in the conductivity of the graphite—bromine system. Baking the filament removes the residual bromine which results in an improvement in the field ionization characteristics of the filament.

The field desorption current of bromine as a function of applied potential is shown in Fig. 1. The system pressure was less than 10^{-6} torr. The current initially decreased exponentially with time to 80% of its maximum value and then remained constant. The FD. measurements were made at 20°C.

The results indicate that the FI characteristics of the graphite filament can be altered by chemical treatment. Further improvement in the field ionization may be possible using different chemicals. The ability of the graphite filaments to field desorb at low temperatures and low potentials is also of interest in mass spectrometry.

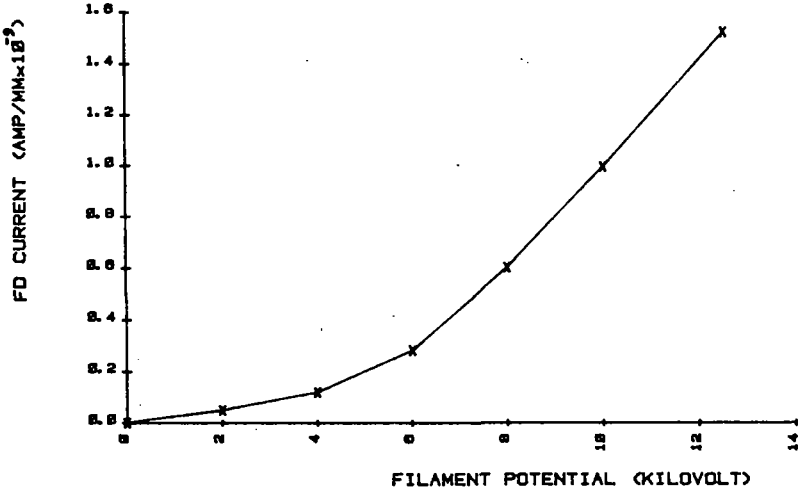


Figure 1. Average field desorption current of bromine from 10 filaments. Data taken at 20°C.

R. W. Odom and S. E. Buttrill, Jr., SRI International, Menlo Park, CA 94025

A new technique for producing field desorbed mass spectra has been developed. This technique consists of forming packets of ions by applying short (50-150 nsec), high voltage (-2 kV) pulses to the counter electrode (cathode) of an FD source and mass analyzing the desorbed ions by a time-of-flight (TOF) method. The mass resolution of the TOF analysis is significantly enhanced by incorporating the ion reflection technique originally developed by Mamyrin et al.[1] This method for generating FD mass spectra has the following advantages over conventional, continuous FD techniques:

(1) Simple design, consisting of FD source, flight tube, ion reflector and detector.

(2) No defining apertures or slits resulting in a high ion collection efficiency.

(3) Minimization of ion bombardment of the FD emitter during the short desorbing pulses.

(4) Ability to distinguish field desorption and field ionization processes occurring at the emitter.

Pulsed field desorbed mass spectra are generated using this technique in the following manner. Ions formed on the FD emitter during the high voltage counter electrode pulses are focused into the ion reflector located 1 M from the source. The uniform electric field in the ion reflector decelerates the ion beam and reverses its direction of motion over a distance of about 12 cm. The reflected ion beam is detected by a channel electron multiplier (CEM) located 1 M from the ion reflector and positioned directly above the source. A time-to-pulse-height converter (TPHC) and multichannel analyzer (MCA) generate a histogram of signal intensity versus the time between the application of the high voltage pulse and the arrival of an ion at the detector. This histogram is then converted to a mass spectrum.

Since the ion reflection technique results in second order time focusing of the ions with respect to ion energy, the time spread of an ion arriving at the detector is determined principally by the time width of its formation. The expression for the mass resolution under this condition becomes $M/\Delta M = t_f/(2\Delta t_p)$, where t_f is the flight time of an ion of mass M and Δt_p is the width of the ion formation pulse.

Field desorbed mass spectra of arginine and adenosine obtained using the technique are shown in Figures 1 and 2. These spectra were obtained using an activated tantalum foil (carbonaceous dendrites) at an emitter temperature of about 200°C. The emitter potential was +1.7 kV and the counter electrode pulses were -1.6 kV in amplitude, and 150 nsec in duration at a 8 kHz repetition rate.

The major peaks in the arginine spectrum due to the presence of arginine on the emitter are the M+1 ion at mass 175 and the M-16 ion at mass 158. These two ions comprise about 1.5% of the total ion counts for this spectrum. The relative intensities of the arginine related peaks obtained under pulsed and continuous[2] FD conditions are given below:

	Relative Intensity	
Mass	Pulsed FD	Continuous FD
175	100	27
158	49	100
117	-	30

Comparison of these relative intensities shows that significantly less fragmentation of the arginine molecule occurs under the pulsed field conditions. This lower extent of fragmentation may be the result of the low emitter temperature used in the pulsed spectrum

(200°C versus 220°C for the continuous spectrum) or the reduced extent of negative ion bombardment of the emitter in the pulsed method.

The adenosine spectrum obtained using the pulsed technique gives a base peak at mass 268 (M+1) and a molecular ion peak at mass 267 of 70% relative intensity. These two peaks comprise 4.4% of the total ion counts for this spectrum. Other major peaks in this spectrum include the protonated base peak at mass 135 (15% relative intensity), the sugar peak at mass 133 (27% relative intensity), and a peak due to loss of CH_2OH from the M+1 ion at mass 237 (24% relative intensity).

These two spectra illustrate that the pulsed field desorption technique can readily generate field desorbed mass spectra of nonvolatile compounds. The mass resolution (full width at half maximum) of the M+1 ion in both these spectra is about 230 and appears to be limited by the time spread resulting from ions striking different positions on the CEM.

Acknowledgments

This research was performed under contract DAAG29-78-C-0034 from the U.S. Army Research Office.

References

1. B. A. Mamyrin, V. I. Karataev, D. V. Shmikk, and V. A. Zagulin, Sov. Phys.-JETP 37, 45 (1973).
2. H. U. Winkler and H. D. Beckey, Org. Mass Spectrum. 6, 665 (1972).

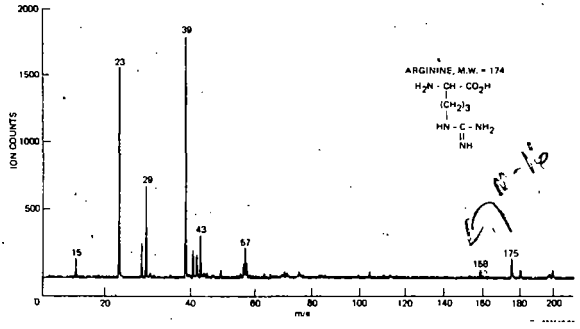


Figure 1. PFD spectrum of arginine.

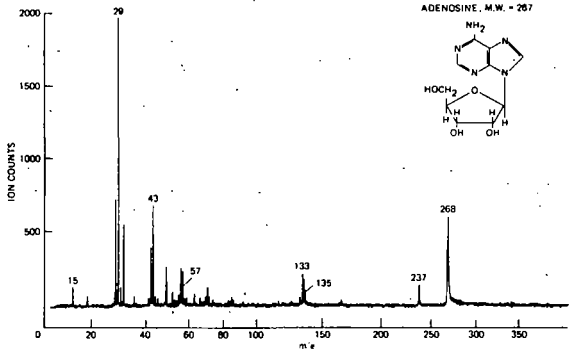


Figure 2. PFD spectrum of adenosine.

USE OF MODIFIED KRATOS/AEI MS-902 FOR FIELD DESORPTION/COLLISION-INDUCED DISSOCIATION (FC/CID) MASS SPECTROMETRY

MPMP13

H. Kambara, F.C. Walls, R. McPherron, K. Straub and A.L. Burlingame
Biomedical Mass Spectrometry Resource, Space Sciences Laboratory,
University of California, Berkeley, CA 94720

The analysis of highly polar, involatile samples has become a commonplace problem in mass spectrometry. While field desorption mass spectrometry (FDMS) has become the method of choice for dealing with such species, the lack of fragmentation data and poor reproducibility have hampered the routine use of FDMS as an analytical technique. Our laboratory has modified our existing Kratos/AEI MS-902 for FDMS, with provision for linked scanning of the magnetic and electric sectors of the instrument (B/E scan). This permits the use of three experimental modes of operation: (1) normal field desorption mass spectrometry; (2) field desorption B/E linked scan mass spectrometry -- this has the specific advantage of identifying which field desorbed species are related to each other, and in allowing the discrimination between gas phase reactions, surface reactions, and cationization or protonation reactions; and (3) field desorption/collision induced dissociation B/E linked scan mass spectrometry -- this technique permits the enhancement of fragmentation patterns from low internal energy field desorbed molecular ions. These three interrelated modes of operation have proven to be especially valuable when analyzing mixtures, as a FD/CID spectrum of each component can be generated without having to separate the components prior to analysis.

Modifications to the instrument include: (1) fabrication of a combined FD/EB ion source, based on the specifications of the Kratos/AEI MS-50 ion source. In FD mode, the EB volume of the source can be used as a gas collision cell by admitting helium to the volume *via* a capillary leak. The collision cell has a path length of *ca.* 1 cm; (2) addition of precision scan control circuitry (Space West Engineering, Model 100); (3) and addition of a linked scanning circuit, allowing the ESA voltage to be scanned as a function of the magnetic field (monitored *via* a Hall probe). These modifications have allowed us to make use of the high sensitivity, enhanced resolution capabilities of the MS-902 for field desorption and associated linked scanning techniques.

To support FD operations, our LOGOS-II computer system was modified to provide facilities for assigning masses to mass spectral peaks on the basis of electric sector voltage and magnetic field measurements. To accomplish this, the data acquisition hardware was first modified so that each data point in a peak profile would consist of detector, ESA, and Hall probe voltage samples instead of a detector voltage sample alone. The data acquisition software was then modified so that, when peak profiles were converted to centers of gravity, the successive ESA and Hall probe voltage measurements would be averaged so as to give the ESA and Hall probe voltages at the approximate midpoint of the peak profiles. Finally, the mass assignment software was modified so that masses were assigned according to the following equations:

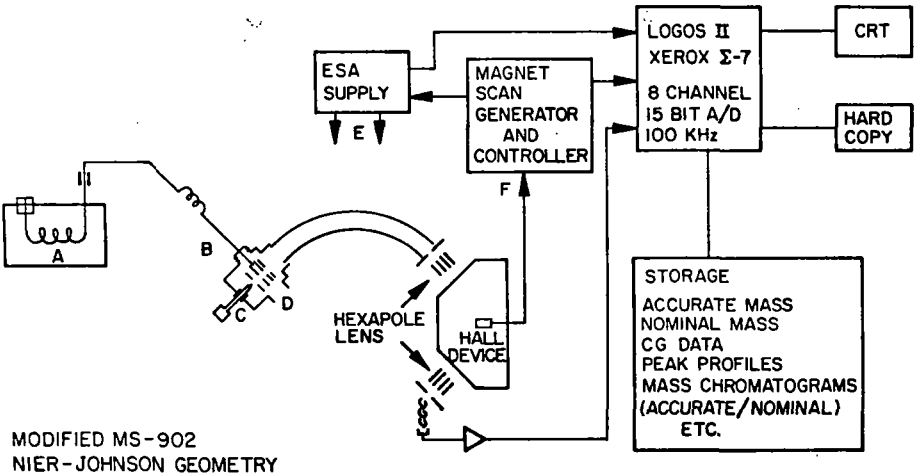
$$M = \left(\frac{V_{REF}}{V_{ESA}}\right) B^2 \quad \text{and} \quad B = aV_{HALL} + b$$

where V_{ESA} and V_{HALL} are the ESA and Hall voltages at the midpoint of the peak profile at mass M; V_{REF}, a, and b are calibration constants derived from the calibration of an EB mode PFK spectrum. Although not shown above, the a and b constants are, in fact, sets of constants that serve to linearize the Hall probe response curve in a piecewise fashion.

This time-sharing computer system, then, allows for data acquisition, real-time nominal mass assignment and real-time display of FD spectra, while permitting concurrent on-line operations by other instruments or data analysis by other users in the laboratory.

The results obtained were outstanding so long as instrument conditions remained unchanged relative to the time of calibration; mass assignments accurate to 0.1 AMU were routinely achieved over periods of hours without Hall probe temperature stabilization or compensation. Mass accuracy was degraded by factors ranging from 10 to 100, however, by changing the mass range scanned, or the scan rate, or by stopping the scan. In spite of these difficulties, FD mode real-time mass assignment and spectrum display proved to be an enormous improvement compared to strip chart and mass marker methods.

This work was supported by NIH Division of Research Resources Grant RR00719.



MODIFIED MS-902
NIER-JOHNSON GEOMETRY
DYNAMIC RESOLUTION 10,000
SCAN CYCLE TIME 9.5 SECONDS
MASS RANGE 70-800

(A) MODIFIED PERKIN-ELMER 900 GC
0.5 mm x 50 m $BaCO_3$ SE-52
WALL COATED OPEN TUBULAR

(B) CAPILLARY RESTRICTOR ADJUSTMENT
INTO ION SOURCE

(C) FD PROBE, SAME AS PROVIDED WITH
KRATOS MS-50

(D) SOURCE PUMPING SYSTEM MODIFIED
TO PROVIDE ~300 L/S PUMPING
AT ION SOURCE

(E) ESA SUPPLY - JOHN FLUKE
VOLTAGE CALIBRATOR

(F) SCAN GENERATOR/CONTROLLER
SPACE WEST MODEL 100

SOLUTION CHEMISTRY AS A GUIDE TO SELECTIVE SURFACE REACTIONS ON FIELD DESORPTION EMITTERS

MPMP14

Maurice M. Bursey, Tim L. Youngless, David F. Fraley, and Neil B. H. Henis

Department of Chemistry, The University of North Carolina at Chapel Hill, Chapel Hill, North Carolina 27514

Our experience with the reactivity of emitter surfaces led us to study whether controlled changes of the surfaces would give predictable changes in the field ionization and field desorption spectra of test compounds. We already had evidence that hydrogenation/dehydrogenation reactions of certain cyclic compounds occur very slowly on cobalt oxide surfaces, and that a silver nitrate surface increases the ionization efficiency of olefins and aromatics relative to their saturated analogs. Each of these reactions reflects well known solution chemistry.

We have found that at least one class of metal chelate, representative porphyrins, can exchange the central metal for a metal ion coated as a salt on an emitter surface. The least stable of the isolatable porphyrins, such as Cd, Mg, and Pb porphyrins, give substantial ions corresponding to the replacement of these metals by typical transition metals such as Co and Cu from the chloride salts. It comes as more of a surprise that the exchange peaks are also observed in Zn and Cu porphyrins coated on $CoCl_2$, but the results are in keeping with known orders of stability. Most surprising[2] is the observation that under Li cationization conditions the Cd may be replaced one or two Li ions. One cannot isolate Li porphyrins, and the reaction is unlike any exchange observed previously under EI conditions. This is the first example of metal exchange noted under cationization conditions; we do not know yet how general such reactions may be for chelate compounds.

Coating an emitter with boric acid produces reactions reminiscent of those found when one uses boric acid as a pre-column for the removal of alcohols from mixtures to be analyzed by gas chromatography. One sees ions corresponding to the alcohol, and also to the ester $B(OR)_3$. The alcohol may be admitted as a gas or coated on the emitter as a solid. In fact,[3] the alcohol may be deposited first and the boric acid coated over it. This suggests, and electron micrographs clearly show, that the emitters are not completely covered by either layer. The temperature dependence of the reaction suggests a process in competition with ionization of the alcohol; the reduced level of the process observed on emitters under EI conditions suggests that the process is partially field-induced. No intermediate stages of esterification are detected; the consideration of the crystal structure of boric acid suggests that esterification would occur most easily at the edges of the crystal plane, where only two or four hydrogen bonds hold H_3BO_3 molecules to their neighbor(s). In such cases, reaction could occur in a way so that[3] all intermediates would be held to the edge of the lattice by the same number of hydrogen bonds until the last step. The reaction does not occur for molecules not containing OH groups; a bit surprisingly, it does not occur for carboxylic acids; more surprisingly, it does not occur for phenols. Thus it may be useful for simple qualitative analysis in the mass spectrometer.

Covalent bonding to surfaces, both metal and carbon, has been explored by electrochemists. Their techniques may also be applied to emitter surfaces as well as electrode surfaces. ESCA results indicate a high concentration of -COOH groups on the surfaces of pyrocarbon emitters, analogously to pyrolytic carbon electrodes, and one expects that these will be located predominantly at the edges of graphite or graphite-like planes of organic material, which will also be at the tips of the emitters; the emitters should grow by extending these planes. Thus these polar groups may affect ionization. We tried several silanizing and alkylating reagents as capping reagents for the polar surface groups and found that ionization efficiencies in FI were altered, efficiency sometimes increasing by as much as a factor of 14. Metal emitters were modified by attaching silanes containing functional groups, and ESCA was used to show that the functional groups remain after subjecting the coated emitters to source conditions. An emitter with a $-CH_2CH_2CH_2NHCH_2CH_2NH_2$ group attached decreases the ionization efficiency of a carboxylic acid relative to a compound which does not react with an amine. An emitter with $-CH_2CH_2CH_2COOH$ attached increases the ionization efficiency of an amine relative to a non-reacting compound; also, the base peak shifts from M to M+1. Each of these results is easily interpreted by analogy to the formation in solution of ammonium carboxylates.

COAL TERPANE ANALYSIS BY METHANE CHEMICAL IONIZATION GC/MS

James G. Moncur, Finnigan Corporation, 2334 Walsh Avenue, Santa Clara, California 95050
R.M. Teeter, Chevron Research Co., 576 Standard Avenue, Richmond, California 94802

INTRODUCTION

The GC/MS quantitation and identification of minor terpane components found in saturate extract of pyrolyzed fossil fuel sources has been useful in establishing a taxonomy of geochemical relationships.[1] More specifically, the presence of an m/e 191 base peak[2] in electron impact/MID mode is now used to quantify triterpanes to an internal standard. Identification of structure is derived primarily using retention time and molecular ion mass/intensity data from capillary GC/MS runs.[3] A standard coal extract containing triterpanes was chosen to investigate any qualitative or quantitative benefits that methane chemical ionization GC/MS might present.

RESULTS AND CONCLUSIONS

The results of consecutively run full scan EI and methane CI experiments suggest that the m/e 191 base peak of EI also exists in CI, with CI giving a characteristic m/e 205 ion in the terpane fingerprint. (Figure 2.) The absolute intensities of quasimolecular $(M-1)^+$ ions in CI when compared to molecular $(M)^+$ ions of EI are similar. (Figure 3.) In conclusion, the CI experiment indicates potential usefullness in complementing EI data with additional quantitation and/or identification data.

REFERENCES

1. E.J. Gallegos, Advances in Chemistry No. 170, Analytical Chemistry of Liquids, Fuel Sources, Tar Sands, Oil Shale, Coal, and Petroleum, pages 13-36, 1978.
2. H. Budzikiewicz, J.M. Wilson, C. Djerassi, JASC, 85, 3688 (1963).
3. E.J. Gallegos, ibid, page 31.

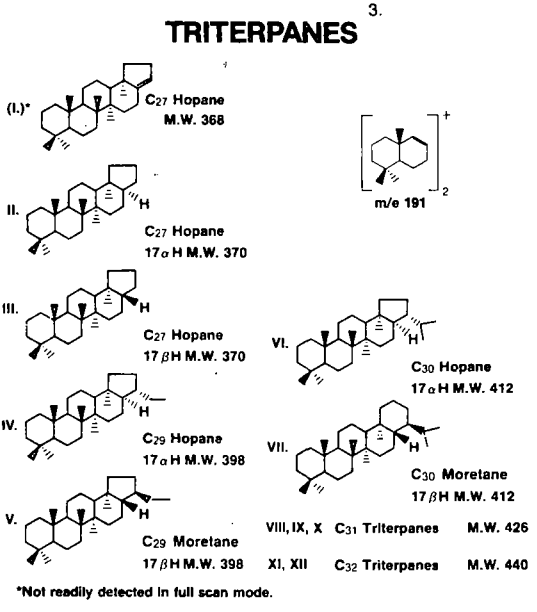


Figure 2

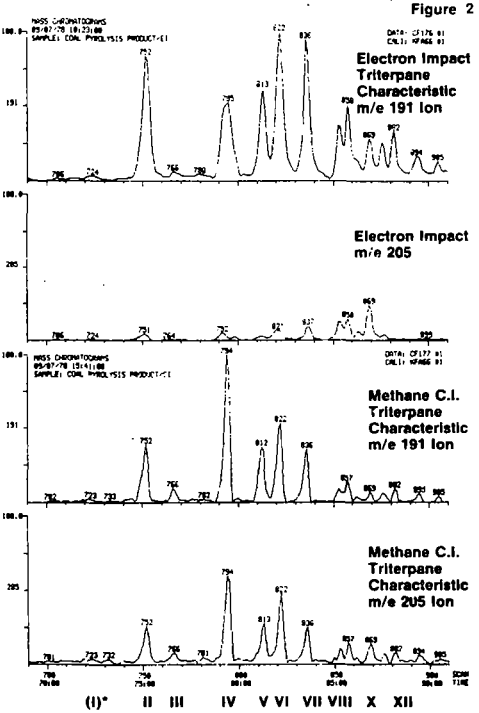
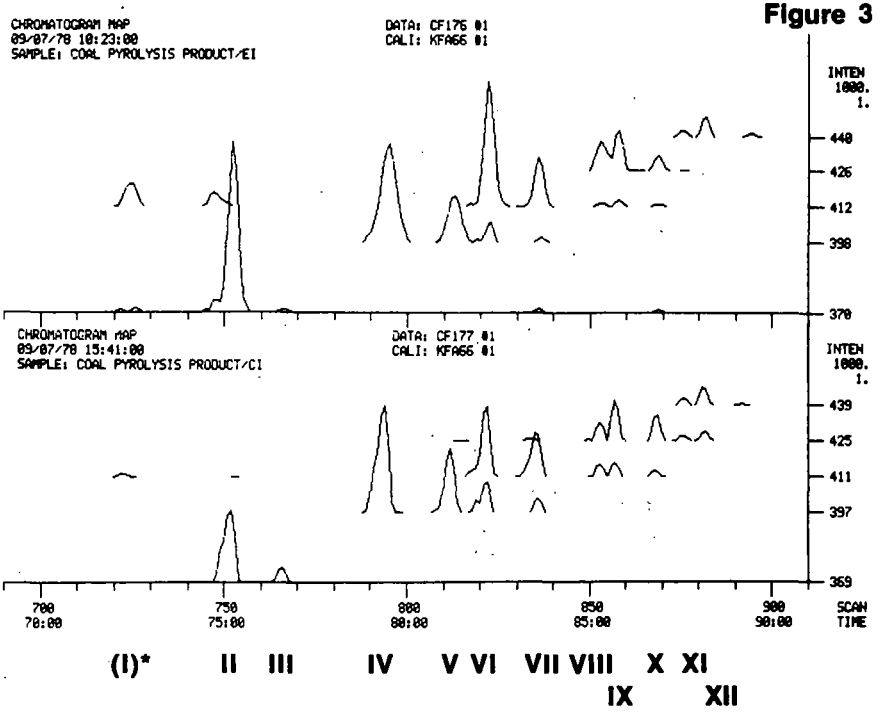


Figure 3



MPMP16

MASS SPECTROMETRY OF BITUMEN DISTILLATES AND RELATED STREAMS

I. P. Fisher and P. Fischer
Gulf Canada Limited, Research and Development Department
2489 N. Sheridan Way, Sheridan Park, Ontario, Canada, L5K 1A8

Introduction

Canada's goal of oil self reliance depends on bringing the Athabasca Tar Sands to the market place. The object of this study is to show in general terms how mass spectrometry may be used to:
1) characterize heavy oil distillates,
2) study the proposed upgrading routes, and
3) assess the impact of these streams on existing refineries.

Experimental

CEC 103C Low Resolution MS
AEI MS 902 High Resolution MS
In house analytical methods, 70 eV El, low eV EI and Field Ionization

Results and Discussion

Bitumen is highly viscous, dense oil with high S, N and a high C/H ratio. A marked feature is the lack of wax. This oil is recovered by surface mining followed by hot water extraction, then coking followed by catalytic hydrogenation. Deeper deposits are recovered by 'in situ' methods (steam, combustion, etc.).

Figure 1 shows a comparison between compositions of an untreated gas oil distilled from Athabasca bitumen and a conventional gas oil. The noteworthy differences are paraffin, aromatic and S contents. Table 2 shows typical middle distillate compositions.

Bitumen must be upgraded to produce a synthetic crude of acceptable yield structure and quality. Coking produces extensive hydrogen rearrangements resulting in distillates of lower quality than those in the original feed. These coker products must be hydrotreated. Table 3 shows an example of the coked gas oil and its hydrotreated product.

Other non-commercial processes have been studied e.g. thermal hydrocracking, catalytic hydrocracking. The products from the former appeared to need further hydrotreating before acceptable materials were obtained. The products from the latter had compositions somewhat similar to those from the coking-hydrotreating route providing residuum conversion was sufficiently high.

Conclusions

Considerable upgrading of raw bitumen is required before it may be used to replace conventional oil. The only way to achieve this is by increasing the hydrogen content of all fractions. Mass spectrometry is a particularly appropriate technique for studying the quality and processing of heavy oil in order to bring the yield/quality parameters up to those of conventional crude oil. Table 4 summarizes some of the applications of mass spectrometry to heavy oil programmes.

FIGURE 1 - IMPLICATIONS OF RAW BITUMEN COMPOSITION

AS AN EXAMPLE, COMPARE A CONVENTIONAL GAS OIL WITH A SIMILAR MATERIAL FROM BITUMEN (EX MINING)

	EX BITUMEN	CONVENTIONAL
PARAFFINS	1.7	22.1
CYCLOPARAFFINS	31.6	42.9
MONOAROMATICS	15.3	13.9
DIAROMATICS	12.1	9.0
TRIAROMATICS	8.9	3.4
TETRA+	15.7	6.4
AROMATIC SULPHUR	10.6	2.2

RAW BITUMEN CANNOT BE USED IN CONVENTIONAL REFINERIES AND MUST BE UPGRADED.

TABLE 2 - HOW DO 'IN SITU' RECOVERED MATERIALS COMPARE

AS AN EXAMPLE, COMPARE CONVENTIONAL DISTILLATE MATERIAL WITH THAT DISTILLED FROM 'IN SITU' RECOVERED HEAVY OIL.

	STEAM STIMULATED	FIRE FLOODED	CONVENTIONAL
PARAFFINS	3.6	9.6	35.5
MONO CYCLOPARAFFINS	10.0	8.4	17.3
COND. CYCLOPARAFFINS	40.5	18.0	21.7
MONO AROMATICS (- 6)	3.5	8.1	11.0
(- 8)	6.4	10.9	7.7
(-10)	11.0	6.2	2.8
DIAROMATICS	15.7	18.8	3.8
TRIAROMATICS+	6.3	3.1	0.2
AROMATIC SULPHUR	4.0	16.7	0.1
QUALITY	POOR	AWFUL	GOOD

'IN SITU' RECOVERED HEAVY OILS CANNOT BE USED IN CONVENTIONAL REFINERIES AND MUST BE UPGRADED.

TABLE 3 - CATALYTIC HYDROGENATION OF COKER GAS OIL

	COKED GAS OIL	$+H_2$ →	SYNTHETIC GAS OIL
PARAFFINS	2.3		4.4
CYCLOPARAFFINS	18.8		37.5
MONOAROMATICS	11.7		23.8
DIAROMATICS	14.8		17.9
TRIAROMATICS	10.7		7.1
TETRA+	23.4		6.9
AROMATIC SULPHUR	18.2		2.4
QUALITY	AWFUL		FAIR

TABLE 4 - APPLICATIONS OF MASS SPECTROMETRY TO BITUMEN - HEAVY OIL PROGRAMS

1. MAY DEFINE THE COMPOSITION OF DISTILLATES AND THUS DISTINGUISH BETWEEN DIFFERENT CLASSES OF HEAVY OILS.
2. MAY BE USED TO ASSESS PRODUCT QUALITY.
3. MAY BE USED TO OPTIMIZE UPGRADING SCHEMES BY BEING ABLE TO FOLLOW COMPOSITIONAL CHANGES ACCOMPANYING THE UPGRADING PROCESSES.
4. MAY BE USED TO MODEL UPGRADING PROCESSES BASED ON THE CHEMISTRY OF, E.G. HYDROGENATION MECHANISMS.

CALCULATION OF PHYSICAL AND CHEMICAL PROPERTIES OF PETROLEUM FRACTIONS FROM MASS SPECTROMETRIC COMPOSITIONAL DATA

M. P. Hahto
Gulf Canada Limited, Research and Development Department,
2489 N. Sheridan Way, Sheridan Park, Ontario, Canada, L5K 1A8

The concept of using MS compositional data for the calculation of physical and chemical properties of complex hydrocarbon (HC) streams has received only casual mention in the literature (1,2). Improved MS analytical methods, coupled with the ready availability of computational facilities in recent years, now makes it possible to derive useful correlations between composition and almost any physical or chemical property that can be defined or measured. This presentation will demonstrate the feasibility of the MS composition/property approach for calculating the following: density (d), average molecular weight (MW), vapour pressure (VP), %C, %H, % aromatic S (AS), mass spec distillation (MSD), heats of formation (H_f), vaporization (H_v) and combustion (H_c), aniline point (AP), kauri-butanol value (KBV), octane number (ON) and cetane number (CN).

The apparatus used in this work was a CEC 21-103C mass spectrometer. Data acquisition and processing was carried out on an IBM 1800 or Modcomp 11/221 computer. Two procedures were used to calculate physical-chemical properties.

Case I Additive properties (eg. d, VP): group contribution methods can be used.

Case II Non-additive properties (eg. ON, CN): a statistical-empirical approach utilizing regression analysis techniques is preferred. Briefly, the latter procedure involves the following: 1) measure property of a large number of samples, 2) analyze samples, 3) subject results from 1 + 2 to regression analysis, 4) test model on unknowns. The following equation is an example of a correlation model:

$$\text{Physical Property (eg. ON)} = A + X_1C_1 + X_2C_2 + \ldots\ldots X_8C_8$$

where A and X_1-X_8 are empirical constants and C_1-C_8 are MS-determined volume % concentrations of paraffins, monocycloparaffins, dicycloparaffins, tricycloparaffins, alkylbenzenes, other monoaromatics, naphthalenes, and remaining aromatics respectively.

For MS analysis hydrocarbon samples are normally categorized into 3 different boiling range fractions. These are covered separately below:

IBP-400°F Fraction (Gasolines, Naphthas, Reformates, Petroleum Solvents)
A modified ASTM D2789 method of analysis was used to obtain a HC group type analysis - Paraffins, Naphthenes, Alkylbenzenes, etc. - plus additional breakdowns such as HC type by carbon number, iso-/n- paraffin split, cyclopentanes/cyclohexanes split and light ends analysis. Properties which can be predicted from the compositional analysis include: d, MW, VP, %C, %H, MSD, AP, KBV, H_c and ON. Figure 1 compares a MSD to an ASTM D86 distillation and to a gas chromatographic distillation (GCD). Like a GCD, the MSD invariably produces lower initial boiling points and higher end points than the D86 method. This is due to the fact that D86 is a non-fractionating distillation giving a relatively poor separation as well as loss of light ends. The MSD may be considered to be a true boiling point (TBP) distillation - i.e., a distillation with fractionation. Figure 2 illustrates the predictive accuracy that can be expected for reformate octane numbers.

400-650°F Fraction (Middle distillates - Jet, Heating & Diesel Fuels)
Two MS methods of analysis were used - a modified ASTM Method D2425 and a procedure described by C.J. Robinson (3). Figure 3 shows the relationship between calculated CN and experimentally determined CN. Other properties which are readily calculated from middle distillate analytical data include d, MW, %C, %H, H_f, H_v and H_c.

650-1050°F Fraction (Heavy distillates - Lubricating and Gas Oils)

The MS method of analysis used was a modified combination ASTM D2786/D3239 procedure. Properties that can be calculated include: d, %C, %H, %AS, H_f, H_v and H_c. Table 1 compares the MS calculated %H with that determined in two commercial labs (using combustion techniques). The astonishing variability shown in replicate analyses by the commercial labs should be noted. It is believed that for HC samples boiling up to 1050°F, MS calculated %H (and %C) is superior to results obtained by combustion techniques.

The described procedures are not generally applicable to pure compounds nor to materials containing additives i.e., octane improvers. The calculation approach which uses regression techniques takes into account any systematic error generated by MS and to this extent the derived constants may not be universally applicable. It must be stressed, too, that inspection test data can in most instances undoubtedly still be measured more accurately than can be calculated from MS composition; nevertheless, such data can be satisfactorily estimated from MS compositional information.

Since only μL-size samples are required and since the MS analysis and subsequent multi-property calculation steps are very rapid, the described composition/property procedures are cost-effective and attractive for pilot plantprocess evaluation studies, process modelling, yield predictions and hydrogen consumption calculations. Future developments in this area of activity will undoubtedly include serious proposals for the monitoring of refinery process streams by mass spectrometry.

The assistance of G. deBoer, I. P. Fisher, R. M. Haynes, and J. Isojima is gratefully acknowledged.

References: 1) T. Aczel, H. E. Lumpkin, R. B. Williams, Annual Conf. on Mass Spectrometry and Allied Topics, Houston, 1975, Washington DC, 1977
2) S. Meyerson, ACS Meeting, Annaheim, Mar. 12-17, 1978
3) C. J. Robinson, Anal. Chem. 43 1425, 1971

Fig. 1 ASTM D86 DISTILLATION VS GC & MS DISTILLATION

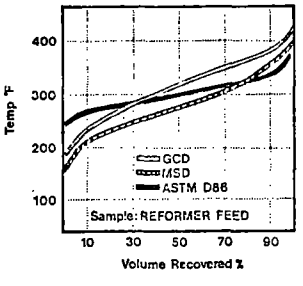


Fig. 2 OCTANE NUMBER

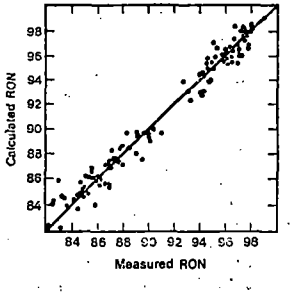


Fig. 3 CETANE NUMBER

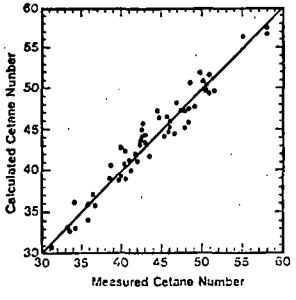


TABLE 1

HYDROGEN ANALYSIS – COMPARISON OF RESULTS

	SAMPLE DESCRIPTION			WT % HYDROGEN		
	Avg C#	%Sats	%Arom	Commercial Lab 1 (Range)	Commercial Lab 2	Mass Spec Calculated
1)	22	98.1	1.9	13.58 (13.41-13.74)*	13.90 (13.87-13.92)*	14.02
2)	26	64.4	35.6	12.00 (11.57-12.40)*	12.72 (12.53-12.86)●	12.52
3)	37	60.5	39.5	12.39 (12.3 -12.5)*	12.81 (12.41-13.02)●	13.05

* Duplicate Analyses
● Replicate Analyses (Six)

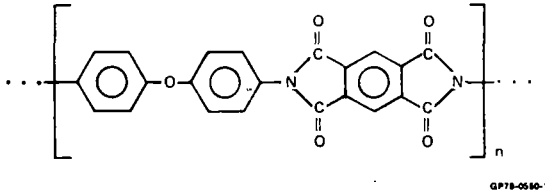
MPMP18 SELECTIVE CHEMICAL IONIZATION REAGENT GASES FOR CARCINOGENS IN SYNTHETIC FUELS, D. M. Schoengold, Battelle Pacific Northwest Laboratory, Richland, WA 99352

Determination of carcinogens in fuels normally requires extensive sample cleanup to avoid complicated chromatograms. This laboratory has previously shown that argon used as a chemical ionization reagent gas provides enough specificity for polynuclear aromatics (PNA's) to eliminate cleanup. We have extended this approach and studied the specificity of inert, hydrocarbon or inorganic gases used as chemical ionization reagent gases for determination of a series of carcinogens including PNA's, nitrogen substituted aromatics and polynuclear aromatics, and other compounds which might reasonably be expected to be found in fuels. For comparison, these same gases were used for non-carcinogenic compounds found in these samples such as hydrocarbons, phenols and nitrogen compounds.

Pyrolysis Mass Spectrometry of Poly (4, 4' Diphenylene Oxide Pyromellitimide)*

M.A. Grayson
McDonnell Douglas Research Laboratories
McDonnell Douglas Corp., St. Louis, MO 63166

Polyimides are a class of polymers that remain stable at high temperatures, typically $\leq$ 620 K. The thermal degradation of polyimides is of interest, but conventional pyrolysis/gas-chromatography/mass-spectrometry/data-system (PY/GC/MS/DS) studies provide information that is restricted to identifying those products with significant vapor pressures at 520 K. The identity of the less volatile products is required to determine thermal degradation mechanisms. The thermal degradation of poly (4, 4' oxydiphenylene oxide pyromellitimide) [structure shown in Fig. 1] was investigated from 700 to 870 K by pyrolysis mass spectrometry (PY/MS).



GP78-0510-1

Figure 1 Structure of poly (4, 4' diphenylene oxide pyromellitimide)

Experimental

The polymide film was pyrolyzed in the ion source of an MS-30 mass spectrometer with the aid of a specially constructed solids probe capable of attaining 870 K. Three separate types of PY/MS experiments were performed:

1) PY/MS at 70 eV ionization potential (IP) and M/ΔM = 1000 *(conventional).*

2) PY/MS at 9 eV IP and M/ΔM = 1000 *(low IP).*

3) PY/MS at 70 eV IP and M/ΔM = 3000 *(accurate mass).*

Mass spectral data were continuously acquired for the duration of the linear-temperature-programmed heating of the solids probe for both the *conventional* and *low IP* experiments. Peak matching techniques were used for accurate mass measurements during the *accurate mass* experiments using perfluorokerosene as a mass reference.

The onset of thermal degradation and the mass range of the pyrolysis products were determined from the *conventional* experiments. However, since a mixture of compounds is evolved upon pyrolysis, it is not possible to identify the products solely from the *conventional* experiments. Therefore, *low IP* experiments were performed to isolate molecular ions. Since pyrolysis products from the polyimide are predominantly aromatic, the *low IP* experiments were performed at approximately 9 eV. Selected ions were studied by *accurate mass* experiments, and elemental compositions were computed on the basis of exact mass data. Proposed structures of the pyrolysis products from poly (4, 4' diphenylene oxide pyromellitimide) are summarized in Table 1.

Results and Discussion

The onset of thermal degradation occurs at $\sim$ 740 K. A maximum in the evolution of degradation products occurs at $\sim$ 820 K. A number of major products are observed from 300 to 500 amu as the pyrolysis temperature increases from 740 K. Inspection of the product identifications (Table 1) indicates that major portions of the main chain are excised from the polymer to form high-molecular-weight products during pyrolysis.

The products indicate that thermal degradation proceeds by both scission of single bonds in the polymer main chain and cleavage of the polyimide ring. One of the most abundant products, phenol (m/z 94), is formed by scission of single bonds at ϕ-O and ϕ-N sites in the main chain. All product structures which have end groups of either phenol or benzene are also indicative of single-bond cleavage during pyrolysis.

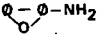
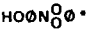
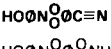
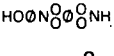
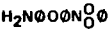
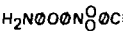
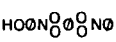
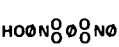
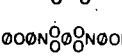
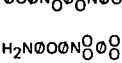
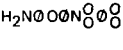
Another abundant product, aniline (m/z 93), provides evidence for destruction of the imide ring. The observation of both carbon monoxide and carbon dioxide as well as heavier products that terminate with nitrile or phthalimide groups provide further support for imide-ring cleavage during pyrolysis.

Examination of extracted ion-current profiles from the *low IP* experiments show that both m/z 93 and m/z 94 have similar profiles as the pyrolysis temperature increases. This behavior suggests that the formation of aniline and phenol occurs by the same process, i.e., the excision of phenol from the main chain is accompanied by the destruction of an imide ring to produce aniline.

The thermal degradation of a polyimide, poly (4,4' diphenylene oxide pyromellitimide), was performed, and the identity of the major products was obtained by the application of several PY/MS techniques. The products indicate that in addition to single-bond cleavage during pyrolysis, destruction of the imide ring also occurs.

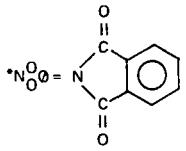
*This research was conducted under the McDonnell Douglas Independent Research and Development Program.

Table 1 Pyrolysis products from poly (4, 4′ diphenylene oxide pyromellitimide)

Molecular weight	Formula	Probable structure	Temperature of formation (°C)
17	NH_3		N.D.
28	CO		N.D.
44	**CO_2**		**N.D.**
78	C_6H_6	ØH	N.D.
93	**C_6H_7N**	**$ØNH_2$**	**480**
94	**C_6H_6O**	**ØOH**	**480**
109	**C_6H_7NO**	**$HOØNH_2$**	**480**
119	C_7H_5NO	Ø−N=C=O	540
128	$C_8H_4N_2$	N≡CØC≡N	560
168	$C_{12}H_8O$		540
183	**$C_{12}H_9NO$**		**500**
185	**$C_{12}H_{11}NO$**	**$ØOØNH_2$**	**490**
239	**$C_{14}H_9NO_3$**		**530**
264	**$C_{15}H_8N_2O_3$**		**530**
308	$C_{16}H_8N_2O_5$		515
330	**$C_{20}H_{14}N_2O_3$**		**510**
355	$C_{21}H_{13}N_3O_3$		525
384	$C_{22}H_{12}N_2O_5$		525
400	**$C_{22}H_{12}N_2O_6$**		**525**
476	$C_{28}H_{16}N_2O_6$		515
491	$C_{28}H_{17}N_3O_6$		525
567	$C_{34}H_{21}N_3O_6$		545
582	$C_{34}H_{22}N_4O_6$		545

N.D. = not determined

GP78-0159-246



CHARACTERIZATION OF MUSCLES FROM DUCHENNE MUSCULAR DYSTROPHY PATIENTS USING PYROLYSIS MASS SPECTROMETRY.

F. D. Hileman, H. L. C. Meuzelaar, L. H. Wojcik, J. H. Petajan
Flammability Research Center and Department of Neurology
University of Utah, Salt Lake City, Utah 84108

Pyrolysis mass spectrometry (Py-MS) has been shown to be an effective tool in the characterization and classification of biomaterials [1,2]. In this study this technique has been used to characterize muscle tissues taken from patients with Duchenne Muscular Dystrophy and from control (normal) patients.

Muscle biopsies were obtained from six patients, three control patients (patients A,B and C) and three dystrophic patients (patients D,E and F). The dystrophic patients were selected to show increasing degress of involvement with the disease (i.e. patient D was the least involved, while patient F was most severely involved). All biopsied samples were freeze-dried and subsequently ground to a powder, suspended in methanol and then applied to a ferromagnetic wire. These samples were then pyrolyzed by inductively heating the ferromagnetic wire and the low ionization voltage mass spectra of the pyrolysates were recorded using a rapid scanning quadrupole mass spectrometry [2]. The replicate analyses of the samples were then evaluated using multivariate statistical analysis procedures [3] to determine the characteristic differences between the normal and dystrophic tissues.

Figure 1 shows typical Py-MS spectra for a control tissue and the most severely involved dystrophic tissue. The arrows on the mass spectra for the dystrophic tissue indicate those peaks found by the multivariate statistical analysis program to be significant in differentiating the tissues. Upward indicating arrows show those pyrolysates which progressively increase in relative intensity with the onset of the disease while downward indicating arrows show the opposite trend.

These relationships are shown in a different manner in Figure 2 using a simple variable-variable plot of m/z 67 versus m/z 81. In this plot the control tissues are observed to cluster together while the dystrophic tissue move progressively away from these controls following the onset of the disease. The pyrolysates corresponding to m/z 67 and m/z 81 are believed to be pyrrole and methyl-pyrrole. These pyrroles are formed from the pyrolysis of proline and hydroxyproline containing proteins. This is illustrated in Figure 3 showing the difference spectrum obtained by subtracting the average spectra of the normal tissues from the average spectra of the dystrophic tissues. The positive component of the difference spectrum shows a characteristic pyrrole ion series at m/z 67, 81, 95 and 109. This is further confirmed by the actual Py-MS spectra of a proline containing tripeptide shown in Figure 4. The same ion series is again observed.

This interpretation of these results is very reasonable in view of what is known of the changes occurring in wasting of muscles due to the onset of Duchenne Muscular Dystrophy. The muscles have a buildup of connective tissue which is composed of collagen, a protein unusually rich in proline and hydroxyproline. Thus the relatively simple and rapid analysis procedure available in Py-MS has been shown to give results consistant with what is currently known about Duchenne Muscular Dystrophy and can be applied to study this disease in greater detail.

REFERENCES

1. Meuzelaar, H.L.C., and Kistemaker, P.G., *Anal. Chem., 45,* 587 (1973).
2. Meuzelaar, H.L.C., Kistemaker, P.G., Eshuis, W. and Boerboom, A.J.H., in N.R. Daly, ed., *Advances in Mass Spectrometry,* Vol. 7, Heyden and Son, London, 1978, p. 1452.
3. Eshuis, W., Kistemaker, P.G., and Meuzelaar, H.L.C., in C.E.R. Jones and C. A. Cramers, eds., *Analytical Pyrolysis,* Amsterdam, 1977, p. 151.

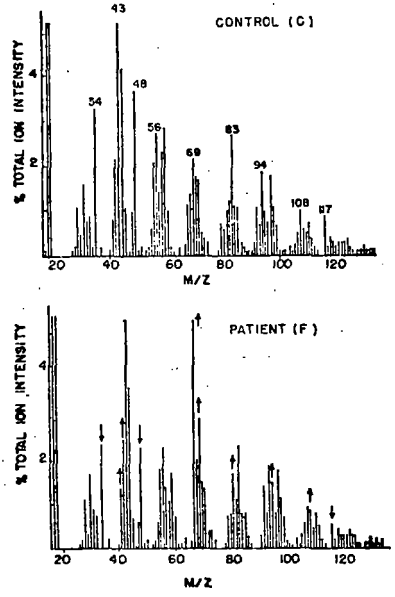


Figure 1. Pyrolysis mass spectra of muscle tissue from a control subject (C) and a dystrophic patient (F).

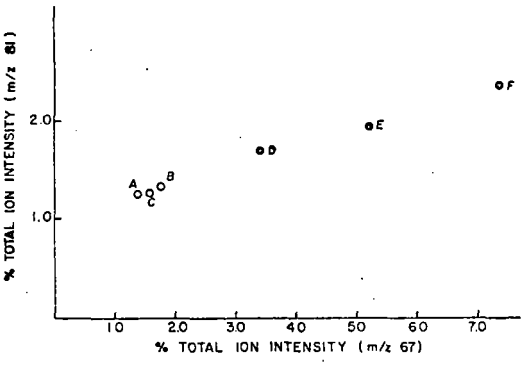


Figure 2. Scatter plot of the ion intensities at m/z 67 versus m/z 81 for the muscle biopsy samples, showing a strong increase in the dystrophic muscle (D,E,F) and a high degree of correlation (correlation coefficient = 0.91) between m/z 67 and 81.

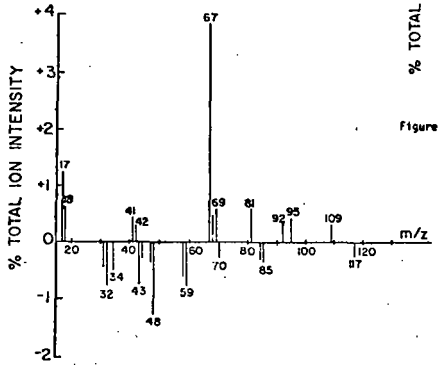


Figure 3. Difference spectrum obtained by subtracting the average pyrolysis mass spectrum of normal muscle samples from the average spectrum of dystrophic muscle samples.

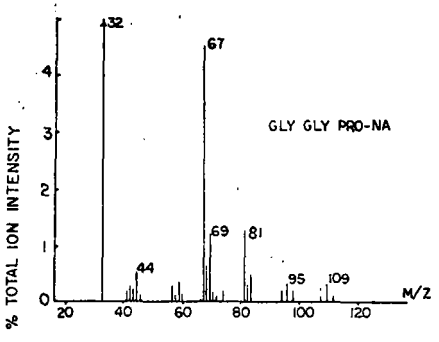


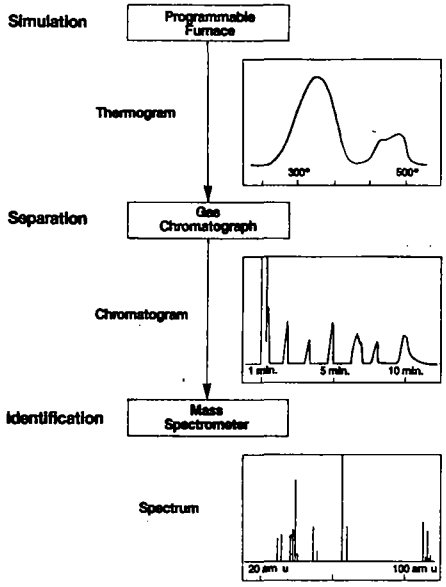
Figure 4. Pyrolysis mass spectrum of the sodium salt of the GlyGlyPro tripeptide. Note the strong resemblence between this spectrum and the difference spectrum shown in Figure 3.

A MULTI-PURPOSE THERMAL-MS SYSTEM AND TYPES OF APPLICATIONS IN INDUSTRIAL RESEARCH

Claudia Elkins
Stauffer Chemical Company
Dobbs Ferry, NY 10522

A system which facilitates the identification of the products of thermal processes has been constructed by coupling a modified commercial thermal analyzer directly to a mass spectrometer and to the spectrometer through a gas chromatograph. The technique can be illustrated:

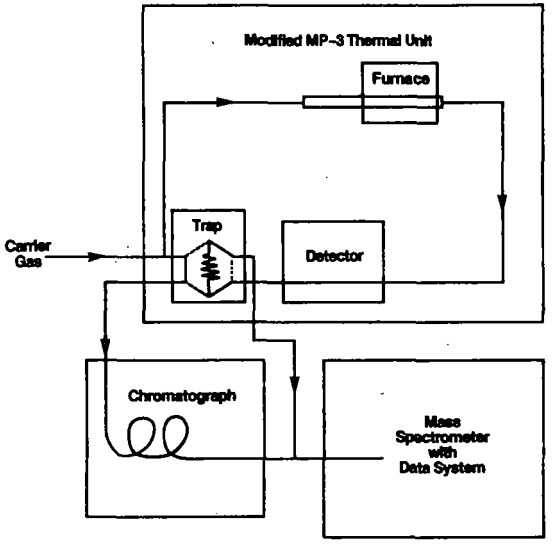
SCHEME FOR THERMAL-GC-MS TECHNIQUE



The thermal-MS system has proven useful for evaluating potential human exposure to chemical compounds during manufacturing processes and the end-use of products, identifying the causes of odors, clarifying thermal properties of substances, and elucidating chemical and physical properties of materials. The system consists of an MP-3 thermal analyzer (Chromalytics, Inc.), which has been modified for more automatic temperature programming; an MS-12 spectrometer (AEI Scientific), which has been modified for high-speed pumping (9-Systems, Inc.); a DS-50 data system (Kratos Inc.); and a Model 5750 gas chromatograph

(Hewlett Packard). The units are connected through the necessary heated lines and valves. A simplified schematic of the arrangement is shown below:

THERMAL-MS EQUIPMENT



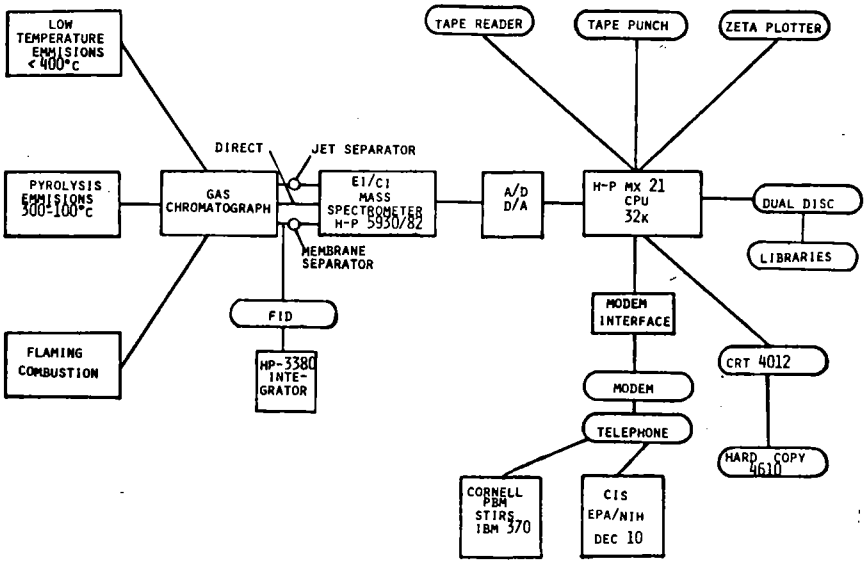
As a sample is heated in the thermal analyzer, the volatile compounds evolved can be carried into the spectrometer. Mass spectra are obtained in real time. Computer processing of the data allows the creation of "mass thermograms", plots of the intensity of specific ions as a function of temperature. These plots can be used to determine the temperatures at which different products are evolved. Alternatively the products from any range of the temperature program can be collected on an absorbent trap and thermally desorbed into the GC-MS configuration. The thermal-GC-MS mode allows the identification of low-concentration components in complex thermal products and also facilitates quantitation of individual compounds.

Analysis of Volatile Emissions From Polymers by GC/MS/COM,

JOSEPH P. HOPPESCH, CAROL J. PINSON, VIRGINIA H. SCHNEIDER, BORG-WARNER CHEMICALS INTERNATIONAL, ROY C. INGERSOLL RESEARCH CENTER, DES PLAINES, IL 60018

Gas chromatography-mass spectrometry has proven to be a viable means for determining the volatile emissions which are inherently released from polymers and polymer additives when these materials are heated, pyrolyzed or burned. Because many of these volatiles are present at very low levels, an acceptable methodology requires the separation, sensitivity, and identification capabilities afforded only by gas chromatography-mass spectrometry.

During compounding or molding operations, polymers may be subjected to temperatures ranging from 200-300° C. The small scale experiments described herein permit the rapid determination of the chemicals which are present and which may have the potential of becoming airborne during these operations. The possibility of accidental overheating of polymers during processing operations can result in pyrolysis of a polymer or additive. Potential degradation products can be determined using the described pyrolysis system coupled to the gas chromatograph-mass spectrometer. Recent concern for the identification of potentially toxic chemicals produced when materials are burned has prompted extensive studies by many investigators. One approach to determining these volatile chemicals which may develop during flaming combustion was also presented.



TAMOA1 CAPILLARY GC/MS OF TRIGLYCERIDES USING EI AND CI TECHNIQUES

by U. Rapp, G. Dielmann, M. Höhn, Varian MAT GmbH, Bremen, and E. Schulte, Institut für Lebensmittelchemie der Universität Münster, W. Germany

The separation and identification of the various components in naturally occuring triglyceride mixtures is very important in the many industrial applications of these compounds.

Until recently, it has been possible only to use packed columns in the GC/MS analysis of such mixtures. Although the greater efficiency of capillary columns was clearly recognized as very attractive for the separation of these mixtures, their use was obviated by the requirement for high temperature operation.

The authors have now used capillary columns with high temperature stability and excellent efficiency. Triglyceride mixtures have been analyzed using such columns, an "open-split" GC/MS interface and a combined EI/CI ion source. Excellent results have been obtained using ammonia as reagent gas for lard and beef-suet extracts. The techniques employed and the results obtained will be discussed.

TAMOA4 ELEMENTAL COMPOSITION DETERMINATIONS IN CAPILLARY GC RUNS USING MEDIUM RESOLUTION

by U. Rapp, H. Kaufmann and M. Höhn, Varian MAT GmbH, Bremen, W. Germany

The use of the mass spectrometer at medium resolving power in GC/MS work is well established. Special efforts have been made to cope with the very narrow GC peaks eluting from high performance glass capillary column.

A resolution of about 2-3000 allows the determination of accurate masses, when using scan speeds as fast as 2-3 s/d and a modern data system for acquisition and evaluation.

Examples of flavour extracts containing low molecular weight compounds and steroids covering the higher mass range will be presented and discussed. the high sensitivity and elemental composition determination will be illustrated.

RAPID INSTRUMENTAL TECHNIQUES FOR THE ANALYSIS OF VOLATILES IN CEREALS

J. B. STANLEY, M. G. LEGENDRE, H. P. DUPUY AND W. H. SCHULLER
SOUTHERN REGIONAL RESEARCH CENTER[1/]
NEW ORLEANS, LOUISIANA 70179

IN RECENT YEARS, CONSIDERABLE EFFORT HAS BEEN MADE TO EXAMINE THE VOLATILES AND TRACE COMPONENTS THAT CHARACTERIZE AND CONTRIBUTE TO FOOD FLAVORS. SOME EARLY ATTEMPTS TO MEASURE FOOD VOLATILE COMPONENTS BY GAS CHROMATOGRAPHIC METHODS CONSISTED OF ANALYZING HEADSPACE VAPORS TO DETECT VEGETABLE AND FRUIT AROMAS (1) AND VOLATILES OF VARIOUS FOOD PRODUCTS (2). THESE METHODS, HOWEVER, REQUIRE SPECIAL PREPARATION OF THE SAMPLE AND SUBSEQUENT TRANSFER OF A VAPOR ALIQUOT TO THE GAS CHROMATOGRAPH. EXTRACTION AND DISTILLATION TECHNIQUES HAVE BEEN PROPOSED TO PROVIDE QUANTITIES OF VOLATILES SUFFICIENT FOR INSTRUMENTAL DETECTION AND ANALYSIS (3,4,5,6). THESE METHODS ARE COMPLEX, TEDIOUS, TIME-CONSUMING OPERATIONS THAT CAN ALSO PRODUCE ARTIFACTS. MORE RECENTLY, A DIRECT GAS CHROMATOGRAPHIC PROCEDURE WAS REPORTED FOR THE EXAMINATION OF VOLATILES IN SALAD OILS AND PEANUT BUTTERS (7,8). THIS METHOD DOES NOT REQUIRE PRIOR ENRICHMENT OF VOLATILES AND IS RAPID AND EFFICIENT. ANALYSES OF FLAVOR-SCORED SOYBEAN OILS BY THIS DIRECT CHROMATOGRAPHIC METHOD, OR WITH A SUITABLE MODIFICATION (9,10,11), HAVE SHOWN THAT THEIR FLAVOR QUALITY CAN BE MEASURED BY INSTRUMENTAL MEANS.

OUR WORK PROVIDES ADDITIONAL EVIDENCE OF THE APPLICABILITY OF THIS RAPID, UNCONVENTIONAL GAS CHROMATOGRAPHIC TECHNIQUE FOR THE ANALYSIS OF VOLATILES IN CEREAL PRODUCTS BY DIRECT GAS CHROMATOGRAPHIC OR COMBINED GAS CHROMATOGRAPHY/MASS SPECTROMETRY (FIGURE 1). FOR GAS CHROMATOGRAPHIC ANALYSIS, THE SAMPLE IS SECURED IN THE GLASS LINER OF THE HEATED INJECTION PORT. THE COMBINED ACTION OF HEAT, MOISTURE, AND CARRIER GAS FLOW SWEEP THE VOLATILES FROM THE SAMPLE TO THE GAS CHROMATOGRAPHIC COLUMN. THE LINER WITH THE SPENT SAMPLE IS REMOVED, AND THE COLUMN OVEN IS TEMPERATURE PROGRAMMED TO RESOLVE THE VOLATILES. FOR THE MASS SPECTROMETRIC IDENTIFICATION OF THE VOLATILES, THE SAMPLE IS SECURED IN THE LINER AND PLACED IN AN EXTERNAL CLOSED INLET ASSEMBLY EQUIPPED WITH A SODIUM SULFATE

CONDENSER THAT REMOVES MOISTURE FROM THE VOLATILES (12). THIS PROCEDURE PERMITS EFFECTIVE IDENTIFICATION OF THE VOLATILE COMPONENTS. WITH THIS RAPID UNCONVENTIONAL APPROACH, THE ALDEHYDES, KETONES, ALCOHOLS, AND ESTERS OF FRESH AND AGED CEREALS WERE IDENTIFIED. CERTAIN ALDEHYDES AND KETONES INCREASE DURING STORAGE AND MAY BE INDICATIVE OF PRODUCT STABILITY.

1/ ONE OF THE FACILITIES OF THE SOUTHERN REGION, SCIENCE AND EDUCATION ADMINISTRATION, U. S. DEPARTMENT OF AGRICULTURE.

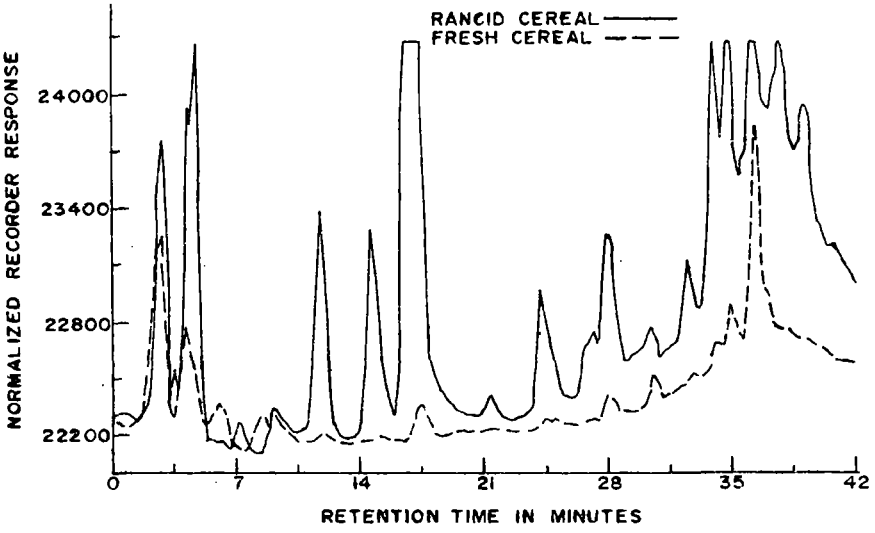


FIGURE 1

REFERENCES:

1. R. G. BUTTERY AND R. TERANISHI, ANAL. CHEM. 33, 1439 (1961).
2. R. TERANISHI, R. G. BUTTERY AND R. E. LUNDIN, ANAL. CHEM. 34, 1033 (1962).
3. D. E. SMITH AND J. R. COFFMAN, ANAL. CHEM. 32, 1733 (1960).
4. S. S. J. CHANG, J. AM. OIL CHEM. SOC. 38, 669 (1961).
5. C. H. LEE AND P. A. T. SWOBODA, J. SCI. FOOD AGRIC. 13, 148 (1962).
6. E. SELKE, H. A. MOSER AND W. K. ROHWEDDER, J. AM. OIL CHEM. SOC. 47, 393 (1970).
7. H. P. DUPUY, S. P. FORE AND L. A. GOLDBLATT, J. AM. OIL CHEM. SOC. 50, 340 (1970).
8. S. P. FORE, H. P. DUPUY, J. I. WADSWORTH AND L. A. GOLDBLATT, J. AM. PEANUT RES. EDUC. ASSOC. 5, 59 (1973).
9. H. P. DUPUY, E. T. RAYNER, J. I. WADSWORTH AND M. G. LEGENDRE, J. AM. OIL CHEM. SOC. 54, 445 (1977).
10. J. L. WILLIAMS AND T. H. APPLEWHITE, J. AM. OIL CHEM. SOC. 54, 461 (1977).
11. H. W. JACKSON AND D. J. GIACHERIO, J. AM. OIL CHEM. SOC. 54, 458 (1977).
12. M. G. LEGENDRE, G. S. FISHER, W. H. SCHULLER, H. P. DUPUY, AND E. T. RAYNER, J. AM. OIL CHEM. SOC. 56, 552-555 (1979).

CAPILLARY GC/MS ANALYSIS USING A COMPUTER CONTROLLED EI/CI MASS SPECTROMETER

E. M. CHAIT, T. A. BLAZER, E. I. du Pont de Nemours & Co., Inc.
Instrument Products, Wilmington, DE 19898

The technique of glass capillary gas chromatography $(GC)^2$ is regarded as the best way to obtain high performance chromatography using either a WCOT or SCOT column. It is realistic that it should be combined with a sensitive GC/MS instrument. Using the Du Pont DP-102 GC/MS system we have performed a variety of analyses over the last year indicating the value of what is now called $(GC)^2$/MS where the superior chromatographic resolution obtained from the use of glass capillaries provide advantages in mass spectrometry by producing spectra of single components leading to better library searches of the data. Using an instrument like the DP-102 which is a computer controlled mass spectrometer it is possible to reap other advantages from capillary chromatography. With the computer controlled instrument variables may be carefully controlled and remembered from experiment to experiment. Ionization mode may be selected from electron ionization or one of three chemical ionization gases with ease using a single keystroke on a computer terminal. Several examples are presented in this paper indicating the value of capillary gas chromatography combined with the mass spectrometer.

Earlier we introduced a method for interfacing open tubular columns to a GC/MS by conducting the column effluent into a conventional GC/MS jet separator with the addition of make-up gas to provide for the most efficient flow through the jet separator. It is now apparent that the technique offers several advantages. First among these is that column performance is not compromised as the end of the column is at atmospheric pressure. It is common to obtain similar numbers of theoretical plates as would be expected from normal capillary column operation. Ion source performance is not compromised by pressure fluctuations and furthermore any kind of open tubular column operating at a variety of flow rates, either WCOT or SCOT may be used. This interface can be used for a variety of applications in either split or splitless injections.

Based on the examples, glass capillary chromatography is an ideal choice for combination with mass spectrometry. Using either split or splitless injection, a variety of samples may be analyzed. Using the power of a computer controlled gas chromatograph and the ability to obtain both electron ionization and chemical ionization spectra from capillary GC separations increased versatility of analysis is allowed. Both operator interaction and automation of data processing to handle the large numbers of peaks obtained from a typical capillary analysis are possible.

METHODS OF UTILIZING A COMPUTER CONTROLLED GC/MS FOR IMPROVEMENT OF MASS SPECTRAL DATA

R. L. CONRAD, E. M. CHAIT, R. F. HOWARD, C. W. HULL, E. I. du Pont de Nemours & Co., Inc., Instrument Products Division, 1500 S. Shamrock Ave., Monrovia, CA 91016

When a GC/MS is run with computer control of the data, it is theoretically possible to take advantage of the computational power of the computer to enhance the mass spectral data. If applied uniformly, this technique can reduce day to day and instrument to instrument variations from mass spectra, and allow participating laboratories to report the same results on identical GC/MS samples. This is not the present situation in mass spectrometry, and this often leads to confusion in mass spectral interpretations, and unsuccessful library search results. The same computational techniques that lead to reproducible mass spectra from GC/MS data are also required to achieve reliable automatic data reduction.

The steps required to produce uniform spectra are:

- Maintain uniform ion source conditions.
- Meet minimum source tuning criteria on a suitable mass standard.
- Calibrate the instrument, including a record of the intensities of the standard masses.
- Scan the spectra, and correct the intensities based on deviations of the recorded standard mass intensities from an accepted standard pattern.
- Scan the instrument fast enough so that several complete spectra are recorded for each GC peak.
- Access the recorded spectra in a way that correctly interpolates each mass intensity for the selected retention time.
- Detect the GC peak, and enhance the mass spectrum by selecting those peaks that reach a maximum across the peak, discarding those that don't vary (background), and subtracting appropriately for those that are in the background on both sides of the peak.
- The resulting mass spectrum is substantially more free of instrument effects than an unprocessed GC/MS spectrum.

This scheme has been adopted for the Du Pont DP-1 GC/MS series. This instrument is well suited for this technique because it is a computer controlled GC/MS and because the ion source and ion optics have been especially designed for long periods of stable operation, even with normally contaminating samples. A special gold sputtering technique is also employed in the ion source to restore its performance when it finally does become contaminated. Also, the source temperature is controlled by the computer so that whenever a method is rerun, this critical parameter is reset correctly.

Source tuning is monitored by two routines. The TUNUP display is used to look at selected mass peak profiles, and is used for initial source tuning and mass scale alignment. This is similar to a conventional oscilloscope display. Final source tuning, however, is done with the aid of a display called PROMPTUNE. This is a real time display that shows the normalized pattern of the PFTBA standard compared to an idealized spectrum of this standard. The operator follows a simple source tuning procedure to make the real time spectra similar to the idealized standard. The tolerance of this procedure is not critical.

The calibration routine is run after source tuning is checked. For PFTBA, thirteen peaks are detected, their intensities ratioed to the idealized standard, and these ratios are stored in a table, along with the calibrated mass scale. As the GC/MS spectra are acquired, both mass position and mass intensity are then adjusted to conform to the calibration table. Thus, if the mass standard itself (PFTBA) is recorded, it will give an idealized spectrum.

TAMOA6

Quantitative Analysis with GC/MS

William L. Budde and James W. Eichelberger
U.S. Environmental Protection Agency
Environmental Monitoring and Support Laboratory
26 W. St. Clair St., Cincinnati, Ohio 45268

During the last ten years, the term quantitative analysis with GC/MS has become strongly identified with the selected ion monitoring method of data acquisition. The precision, accuracy, and sensitivity associated with this technique has been described by a number of authors. For many applications, e.g., broad spectrum analysis of environmental samples, the preferred data acquisition method is continuous, repetitive measurement of spectra as separated components emerge from the chromatograph. After the components are identified by examination of their mass spectra, it would be very cost-effective to quantify the components using the same raw data that is stored in a data system file. This report is concerned with an evaluation of the precision and accuracy of this process. With aqueous laboratory control standards having 5-10 components in the 0.1-10 µg/l concentration range, and using a single external concentration calibration standard, an average bias of -30% was obtained. This and other analogous data will be presented and analyzed. The full text of this paper will be submitted to Analytical Chemistry.

GC/MS IDENTIFICATION OF HIGH BOILING PRODUCTS FROM THE DIRECT PROCESS MANUFACTURE OF METHYLCHLOROSILANES

Gerald F. Dudding, William D. Kray and Alan Ritzer

Analytical Services Operation
GENERAL ELECTRIC COMPANY
Silicone Products Department
Mail Drop 12-07
Waterford, NY 12188

The direct process, formulated below for dimethyl dichlorosilane, is one method for manufacture of methylchlorosilanes.

$$Si + 2CH_3Cl \longrightarrow (CH_3)_2SiCl_2 + \text{other components}$$

A Finnigan 4000 GC/MS instrument, equipped with a glass capillary column, was used to characterize a laboratory purified product mixture from the direct process. Identification of many of the components was possible by interpretation of their mass spectra.

EXPERIMENTAL

Product from the direct process was purified in the laboratory by distillation through a glass Vigreaux column (15 cm x 1.5 cm). A fraction (bp 160°C/1 atm) was collected for analysis by GC/MS. Authentic samples of pentamethylchlorodisilane and trimethylsilyldimethylchlorosilylmethane were obtained from Silar Labs.

The GC/MS/Data System was a Finnigan model 9610 GC interfaced to a Finnigan model 4000 quadrapole MS with dual chemical/electron ionization (CI/EI) source. An Incos data system, equipped with a Data General Nova 3 computer, acquired and stored mass spectra from repetitive scans.

The gas chromatograph was equipped with a glass lined Finnigan injector/splitter and a Perkin Elmer glass capillary column (OV-101, 100M, 0.01 in. I.D., 0.03 in. O.D.). The injector/splitter was maintained at 225°C and was adjusted such that a 40 cc/min split flow was obtained using Helium carrier gas at 30 psi. The flow through the capillary was 1 cc/min. After 1 µl of sample was injected, the capillary was maintained at 70°C for 16 minutes, then temperature programmed to 225°C at 2°C per minute.

The Finnigan interface, which consisted of a platinum lined tube (0.005 in. I.D.) had 0.01 ml dead volume and was enclosed by a stainless steel sleeve (1/16 in. O.D.). It was heated at 200°C and passed into the ion chamber at a point just short of the electron beam to ensure no loss of GC resolution.

The MS operating conditions were: 70eV electron energy, 0.35 mA emission current, 1600 eV electron multiplier, 250°C source temperature, $2X10^{-6}$ torr high vacuum. A mass range of 35 - 300 amu was scanned in one (1) second.

RESULTS AND DISCUSSION

Four types of chlorosilanes were found: methylchlorodisilanes, dialkylchlorosilanes, bis-(alkylchlorosilyl) methanes and linear alkylchlorosiloxanes. Identification of each component in the reconstructed ion chromatogram (Figure 1) was based on interpretation of the respective mass spectrum. Characteristic fragmentation patterns in the mass spectra of chlorosilanes have been described by Smith[1]. The presence of chlorine atoms, with their natural isotopic distribution, is recognized from the "isotopic clusters" produced in the mass spectrum. Fragment ions at M/e 63, corresponding to SiCl; M/e 93, corresponding to $(CH_3)_2SiCl$; M/e 113, corresponding to CH_3SiCl_2 and those corresponding to the molecular ion (M^+) and $[M-CH_3]^+$ are common in the mass spectra from methylchlorosilanes.

Typical mass spectral fragmentation patterns for authentic analogs of methylchlorodisilanes were determined under similar EI conditions used to obtain Figure 1. For example, the mass spectra of authentic pentamethylchlorodisilane and trimethylsilyldimethylchlorosilylmethane were found to exhibit fragment ions characteristic of those from methylchlorosilanes.

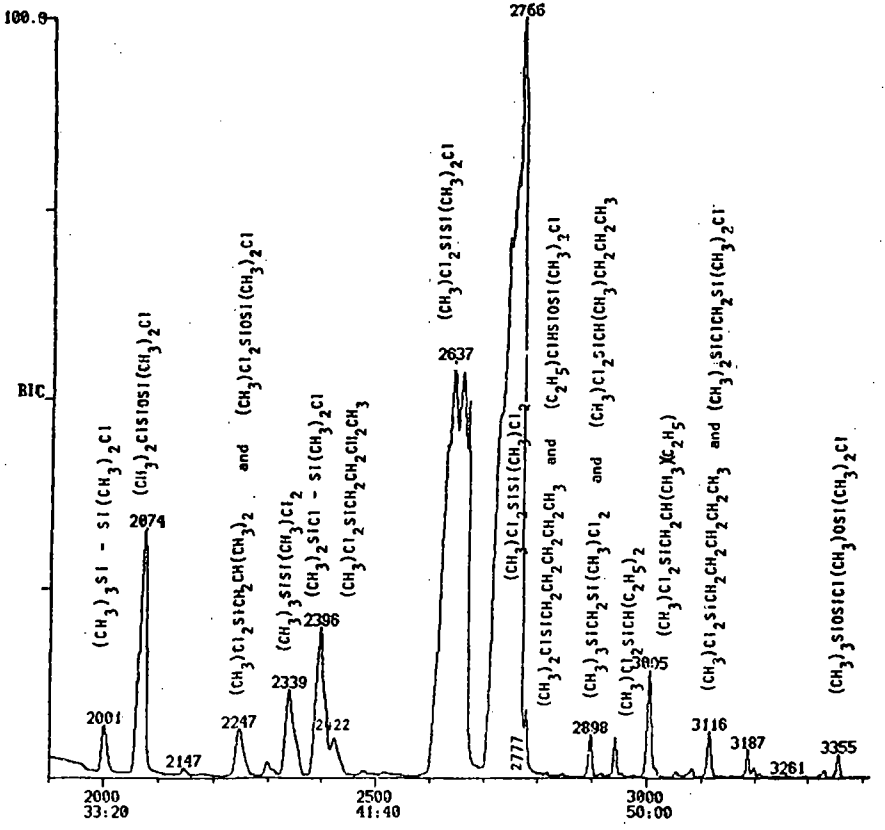
In conclusion, a discussion about the mass spectra obtained by GC/MS analysis of a mixture of methylchlorodisilanes will be presented.

REFERENCES

1. A. Lee Smith, ed., Analysis of Silicones, J. Wiley and Sons, New York, 1974, p. 331.

Figure 1

Reconstructed Ion Chromatogram



APPLICATIONS OF AUTOMATIC OPERATION OF A COMPUTER CONTROLLED GC/MS TO ENVIRONMENTAL AND BIOMEDICAL ANALYSIS

H. RODEN, E. M. CHAIT, T. A. BLAZER, E. I. du Pont de Nemours & Co., Inc. Instrument Products, Wilmington, DE 19898

GC/MS has now reached the stage of development where the techniques for operation of instruments and data processing are well established. Computer based data processing systems have always emphasized operator interaction and obtain much of their value from the ability of the operator to optimize experimental data. The large numbers of analysis now being performed in environmental and biomedical research require a large degree of automation of the GC/MS process. A computer controlled GC/MS is particularly suitable for this automatic operation.

The Du Pont DP-102 GC/MS system is a computer controlled GC/MS that operates in conjunction with an automatic analysis system. The automatic analysis system consists of a 60 position automatic sampler, a computer controlled solvent diverter valve and an automatic gas chromatograph oven door to allow for cooling of the column to begin temperature programmed runs. Under computer control the sampler can select any sample or a wash for the automatic syringe from any position on the 60 sample carousel. Accompanying the automatic analysis system making it more effective, is computer software for the complete automatic data processing of a sample and automatic quantitation of both mass resolved and selected ion monitoring GC/MS data. An additional advantage of computer control of the GC/MS and the use of the automatic sampler is the reproducibility of injections for quantitative analysis. The automatic sampler also allows injections during unattended processing of data because of the foreground/background ability of the central processing unit. In qualitative analysis reproducible retention time is assured by precise positioning of the injection point in the chromatogram.

An analysis using ratios was conducted for a typical environmental sample containing acenaphthene and fluoranthrene using D_{10} anthracene as an internal standard. The precision of automatic analysis for this sample was evaluated for nine injections using the automatic sampler. Acenaphthene was found with an average deviation in area counts of 2.1% and peak height 2.8% while the average deviation in area percent was 1.4%. Ratioing the peak areas of acenapthene and fluoranthrene at the 20 nanogram level to the mass chromatogram, m/e 188, representing D_{10} anthracene as an internal standard showed area ratio average deviations of 1.6% and 2.3% respectively for the acenapthene and fluoranthrene. Retention time average deviations were zero percent for acenapthene and 0.3% for fluoranthrene.

Identification of the Decomposition Products of $C_{10}H_{21}(OCH_2CH_2)_5OH$, A. J. DeStefano, D. W Leedy, and R. A. Sanders, The Procter & Gamble Company, Miami Valley Laboratories, P.O. Box 39175, Cincinnati, OH 45247

INTRODUCTION

Pentaoxyethyleneglycol monodecyl ether, $C_{10}H_{21}(OCH_2CH_2)_5OH$ (hereafter $C_{10}E_5$) is a common non-ionic surfactant which can be obtained in high purity for the study of its phase and physical properties. As with most compounds containing ether linkages, this compound can react slowly with the oxygen in air. Some of the observed degradation products were studied by GC and GC/MS techniques. The identifications made suggest that $C_{10}E_5$ is decomposing by an autoxidation free-radical pathway.

EXPERIMENTAL

The first drop from a distillation of a $C_{10}E_5$ sample which was several years old and known to be degrading with time was used for this analysis. A portion of the impurities mixture was derivatized using a silylating reagent and used for the GC and GC/MS analyses.

Stand-alone GC work was done on an HP5840 GC equipped with a 3% OV-17, 6' x 1/8" stainless steel column and a flame ionization detector. The oven temperature was programmed from 130°C to 250°C at 10°C/min. The He flow rate was 50 ml/min. GC/MS experiments were done on a KRATOS MS-30 dual-beam double-focusing mass spectrometer at a resolution of 3000 using a scan speed of 3 sec/decade of mass. The mass spectrometer was interfaced to a Perkin-Elmer Sigma II GC via a glass jet separator. The He flow rate was reduced to 30 ml/min to maximize the sample throughput of the GC/MS interface. Both electron impact and isobutane chemical ionization GC/MS analyses were done on the derivatized impurities mixture. All data from the mass spectrometer were processed using the KRATOS DS-50 and DS-50S data systems.

RESULTS AND DISCUSSION

The two most abundant sets of compounds are the lower $C_{10}E_x$ compounds (x=0-4) and the glycols ranging from diethylene glycol to pentaethylene glycol. Figure 1 shows the EI and isobutane CI spectra of $C_{10}H_{21}(OCH_2CH_2)_2OSi(CH_3)_3$. The EI spectrum contains alkyl chain fragment ions as well as a number of silicon-containing fragments. The $(M-15)^+$ ion is observed for the $C_{10}E_xOSi(CH_3)_3$ compounds from x=0-2 but no molecular weight information is available from the EI spectra of compounds with $x \geq 3$. However, the CI spectrum for each of the compounds observed in this study shows an intense $(M+1)^+$ ion and supplies the molecular weight data for each species identified.

The EI and CI spectra of the second set of compounds, the glycols, are typified by the spectrum of $(CH_3)_3Si(OCH_2CH_2)_3OSi(CH_3)_3$ shown in Figure 2. Several Si-containing species are observed in the EI spectrum. Two other sets of compounds identified include the oxidized glycol and oxidized $C_{10}E_x$ species $(CH_3)_3SiOC(=O)CH_2(OCH_2CH_2)_xOSi(CH_3)_3$, x=1-4, and $C_{10}H_{21}(OCH_2CH_2)_xOCH_2C(=O)OSi(CH_3)_3$, x=1-4, respectively. The final set had the form $C_9H_{19}C(=O)(OCH_2CH_2)_xOSi(CH_3)_3$, x=0-5, and was not predicted strictly from the autoxidation mechanism. The EI and CI spectra of the x=3 species are shown in Figure 3. The spectrum contains characteristic ions at m/e 155 and 199 as well as the expected Si-containing fragments.

A total of 25 species have been identified totalling about 90 area % of the FID chromatogram. The identifications made suggest that $C_{10}E_5$ degrades through a free-radical autoxidation mechanism. Possible products resulting from three sites of attack are shown in Figure 4. The $C_9H_{19}C(=O)(OCH_2CH_2)_xOH$ products are most probably condensation products of

the observed decanoic acid and the various glycols.

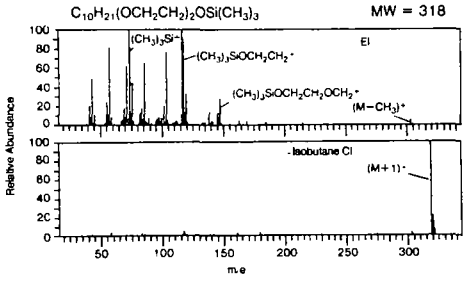


Figure 1

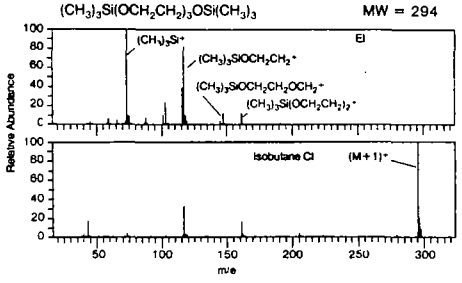


Figure 2

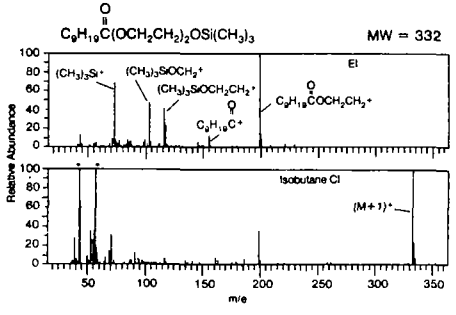


Figure 3

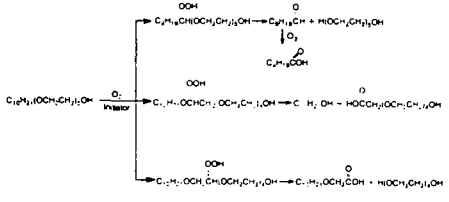


Figure 4

AUTOMATIC SEARCH, IDENTIFY, AND QUANTIFY MASS SPECTRAL DATAFILE COMPUTER PROGRAM FOR PRIORITY POLLUTANT ANALYSES

J.F. RYAN, R.A. NOVAK AND W.A. FARR

Gulf South Research Institute, New Orleans, LA

A computer program has been written which allows GC/MS datafiles to be processed such that a preselected list of compounds can be identified and quantified, based on three criteria. Those are (1) existence of appropriate extracted ion current profiles (EICP) within a given retention time window, (2) simultaneous maximization of the appropriate EICP's within that window, and (3) appropriate ratios of the peak areas of the three extracted ion current profiles. If a compound is determined to be present, the computer program will quantify the peak area and absolute amount injected.

This program was developed specifically to process priority pollutant data in a rapid, cost effective manner. However, it has shown its applicability to many other areas wherein selected compounds must be identified and quantified. The program system is divided into two parts (Figure 1), each operating independently but necessitating the existence of the other for its overall effectiveness. The library generation portion of this program is called CERFILE CREATE. In that portion of the program there are five options which the datafile user can execute. Option 1 allows the user to input a relative retention time (RRT) and relative response ratio (RRR), as well as up to five ions which may be searched through the datafile at a particular retention time window. Option 2, list, allows the user to list the CERFILE once it has been created. Option 3, list short form, allows the user to list only the relative response ratio, relative retention time, and first ion in a short tabular listing. Option 4 allows the user to enter any CERFILE and modify the library to change the ions which are searched, the relative retention time or the relative response ratio. Option 5 allows the user to take two separate CERFILES and merge them into one unified CERFILE. The last two options have great versatility in allowing changes to be made in the CERFILE without having to re-enter the entire data set. In addition, the user may set up small CERFILES based on particular classes of compounds and then tie them together as a major CERFILE once they have been collected.

The second part of the program is called ASIQM, which stands for automatic search, identify and quantify mass spectral data. This program is divided into two portions. The first allows the user to make a GC/MS run containing known quantities of standard compounds and then have the ASIQM program process that data to calculate the RRR and RRT values for that run. Using this capability, the analyst can update daily the values used for a particular data reduction and make adjustments in the CERFILE to account for changes in chromatographic performance or overall instrumental sensitivity.

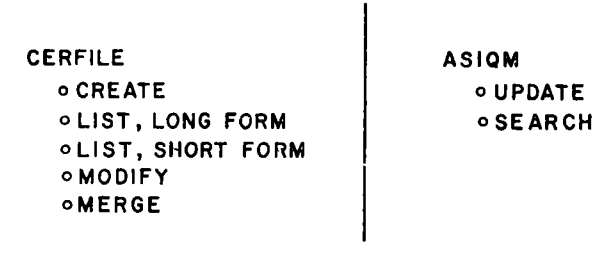


Figure 1. Options available for automatic search, identify and quantify search system.

The second portion of the ASIQM program involves the actual searching of the datafile for those compounds listed in the specified CERFILE. The output from this search routine can be presented either in tabular form or with appropriate graphical mass chromatograms as shown in Figure 2. The output automatically generates hardcopies of all data for archival storage.

This computer program is rapid, versatile, and powerful. It allows the user to build libraries slowly, while permitting modifications to the search parameters and fine tuning of the search design. This program operates on a complex datafile such that it will search 40 compounds in approximately 3 minutes, generate the data, including CRT hardcopies. The corresponding data reduction using manufacturer's commercially available software for priority pollutant analysis takes approximately 2 hours. The cost effectiveness of the program is significant.

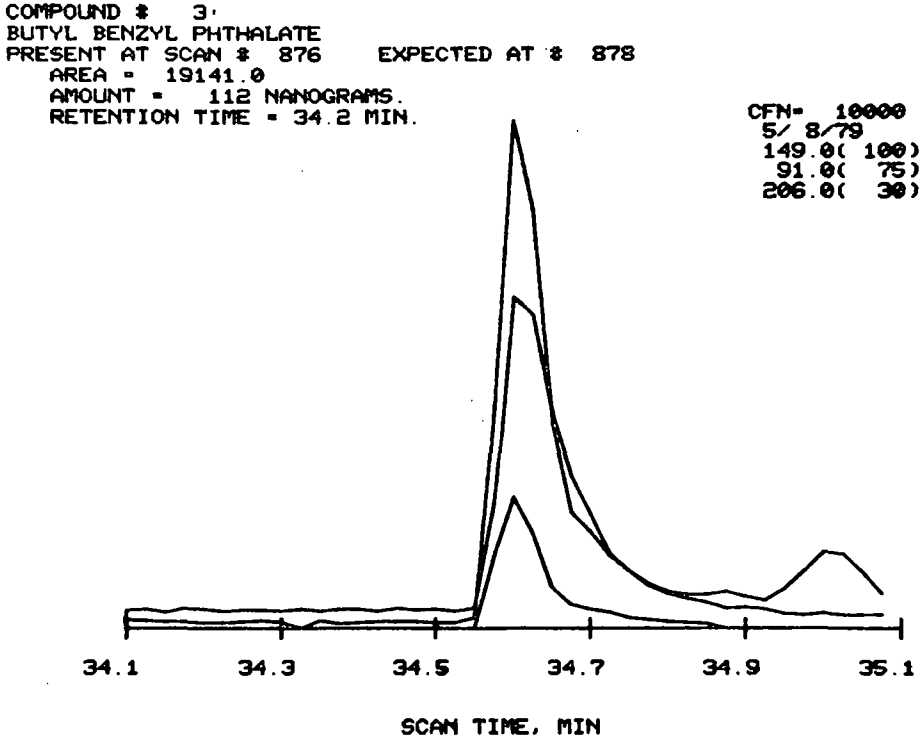


Figure 2. Mass chromatogram ASIQM output showing positive identification of butyl benzyl phthalate. Note features such as expected scan retention time vs. actual retention scan time, quantification, nanograms present and CERFILE ions used in search.

INVOLATILE SAMPLE ANALYSIS BY DENSE GAS CHROMATOGRAPHY/MASS SPECTROMETRY

A.L. Wahrhaftig and L.G. Randall
Department of Chemistry, University of Utah
Salt Lake City, Utah 84112

On the usual phase diagram for a one-component system, the line separating liquid and gas (HPLC and GC moving phases) ends abruptly at the critical point, P_c, T_c. The single phase remaining at $T > T_c$ and P close to or higher than P_c acts like a gas but has many liquid properties. It has unique properties as the moving phase in chromatography. There are several names applied to such a gas; I shall use the term dense gas and DGC. The most important property of a dense gas is shown in Figure 1, a plot of reduced density ($\rho_R = \rho/\rho_c$) vs. reduced pressure ($P_R = P/P_c$). By taking appropriate temperatures slightly above $T_R = 1$, the curves for the three dissimilar gases listed coincide. As P increases over the range $0.5\ P_c < P < 10\ P_c$, ρ increases rapidly and becomes comparable to the normal density of the liquid. Therefore, a dense gas has the solvent properties of a liquid. However, its viscosity (low) and diffusivity (high) are closer to those for gases (at STP) than for liquids, giving the GC advantages of rapid separations and sharp peaks. Also, pressure will have a major effect upon solubility in a dense gas, giving a new parameter, along with temperature and solvent composition, which can be varied to obtain separations.

Since the initial separations of several metal porphyrins using dense Freons by Klesper, Corwin and Turner in 1962, there have been quite a few additional studies of DGC and several reviews have been written.[1-3] The solvent power of dense gases also has been studied, in particular by Giddings,[4] and more recently by Stahl and Schilz[5] who find that involatile substances such as sugars, etc., dissolve in dense CO_2. In one determination, Jentoft and Gouw[2] clearly separated the polystyrene oligomers, C_4H_9-$[-CH_2-CH(C_6H_5)]_n$-H, n = 2-32 (molecular weights 266 to 3386) in one run using dense methanol (5%) - n-pentane at 215°C and pressure rising from 40 to 70 atm during the 80 min. run.

A major problem has been the lack of a highly sensitive, selective detector; the ones so far used, UV absorption, flame ionization, and thermal conductivity, have many disadvantages. The possibility of using a mass spectrometer as a detector in a DGC/MS system was first discussed by Giddings et al.[6] The method proposed was the direct expansion of the dense gas through a suitably sized pinhole (of the order of 10 μm diam.) followed by a skimmer and collimator so as to obtain a supersonic molecular beam which would then pass through the ionization chamber of the MS. They noted that formation of molecular aggregates, solute-solvent or of solute, would be complicating factors but that the process was so highly non-equilibrium that one could not hope to predict what would actually happen. Such a system should have great value, since it would combine the ability of HPLC to separate non-volatile and thermally labile molecules with the ability of MS to act as a highly sensitive detector giving detailed information about each compound eluted. In simplified form, without a column, it would be a useful inlet system for thermally labile molecules. There is no heating in such a DGC/MS instrument; the maximum temperature is determined by the critical temperature of the dense gas--usually the DGC temperature is 10 to 25°C above T_c.

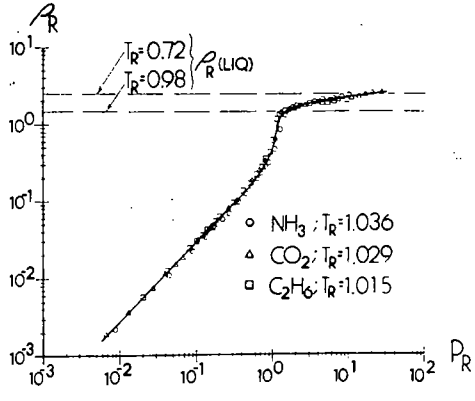


Figure 1

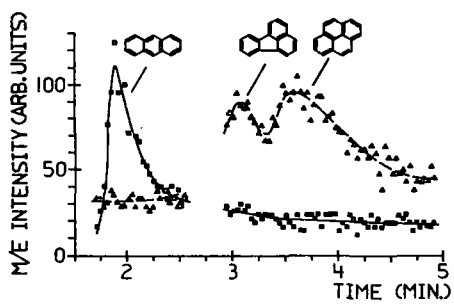
We have now constructed such a DGC/MS instrument by adding the necessary interface to an old PE-270 small, double-focusing mass spectrometer, used because it was

available. The details of this instrument are given in Poster Paper WAMP4, a brief description and some results have been published. Polymers have been observed out to $(N_2)_9^+$, $(C_2H_6)_{17}^+$, $(C_2H_4)_{20}^+$, and $(CO_2)_{13}^+$; also $(N_2O)_n^+$ with n about 15. However, these are very easily destroyed by glancing collisions at a pressure of 10^{-3} to 10^{-4} torr in the nozzle-skimmer region, a pressure which has no effect on solute molecules in the beam.

Studies of the variation with pressure and temperature of the capacity ratios for anthracene and pyrene on a Permaphase ODS column show the expected decrease (greater solubility in gas) with pressure increase, but an increase with temperature increase. The major effect of temperature increase is a decrease in gas density which lowers solubility. In the preliminary studies made to date, naphthalene, azobenzene, triphenylbenzene, phenanthrene, anthracene, fluoranthene, pyrene, and caffeine have been dissolved, eluted, and the parent peaks observed, using either dense CO_2 or N_2O, and both for some components. We have some, but not conclusive, evidence for transport of anthraquinone, ℓ-histidine, and inosine. The separation of a mixture of anthracene, fluoranthene, and pyrene is shown in Figure 2; the peak for caffeine is shown in Figure 3.

We believe we have demonstrated the feasibility of a DGC/MS instrument. However, we do not yet have a practical system. Many improvements are required: separate temperature control of sample chamber, column, and nozzle; a beam chopper and phase sensitive detection to eliminate background from non-beam molecules; a data handling system; a better sampling system; and a higher pressure dense gas system suitable for gas mixtures and for pressure programming. Finally, our present system is severely limited by the pumping speed available on the nozzle-skimmer region and by the poor sensitivity and resolving power of the mass spectrometer.

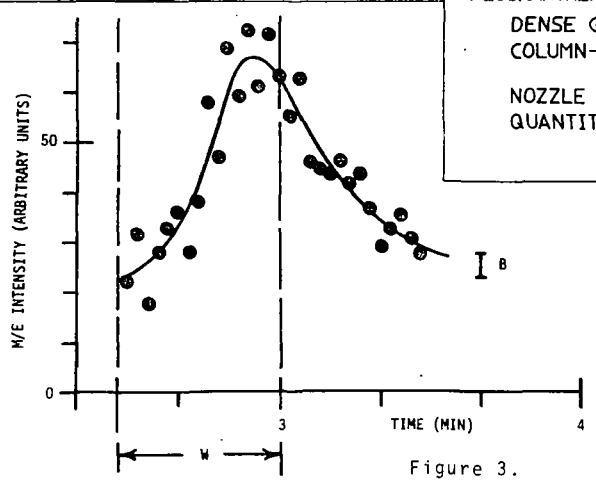
References: 1) N.M. Karayannis, Rev. Anal. Chem., 1, 43-83 (1971); 2) T.H. Gouw and R.E. Jentoft, Adv. Chromatogr. 13, 1-40 (1975); 3) M.S. Vigdergauz and V.I. Semkin, Russ. Chem. Rev., 40, 533-549 (1971); 4) J.C. Giddings, M.N. Myers and J.W. King, Jr. Chromatogr. Sci., 7, 276 (1969); 5) Egon Stahl and Winfried Schilz, Chem. Ing. Tech., 50, 535 (1978); 6) J.C. Giddings, M.N. Myers and A.L. Wahrhaftig, Int. J. Mass Spectrom. Ion Phys., 4, 9 (1970).



SEPARATION OF ANTHRACENE (M/E 178), FLUORANTHENE (M/E 202), PYRENE (M/E 202)

DENSE GAS - N_2O AT 102 ATM, 50 °C
COLUMN - PERMAPHASE ODS
50 CM x 1.5 MM I.D.
NOZZLE DIAMETER - 12.5 μM
QUANTITIES - 4 μG, 4 μG, 6 μG

Figure 2.



ELUTION OF CAFFEINE BY DENSE N_2O

SAMPLE SIZE- ~ 11 μG
CONDITIONS- 184 ATM, 39.0 °C
COLUMN- 6 M X 0.5 MM I.D. CAPILLARY
NOZZLE D- ENLARGED 5 μM (~ 8 μM)
W- TIME INTERVAL FOR ELUTION (TIME ABOVE BACKGROUND) OF A 2 μℓ $CHCl_3$ SLUG IN ANOTHER RUN UNDER SAME CONDITIONS
B- BACKGROUND INTENSITY OF M/E 194, PARENT MASS OF CAFFEINE

Figure 3.

PYROLYSIS GAS CHROMATOGRAPHY CHEMICAL IONIZATION MASS FRAGMENTOGRAPHY (PGC/CI/MF) TO ANALYZE CHOLINE AND ACETYLCHOLINE IN PICOMOLE QUANTITIES.

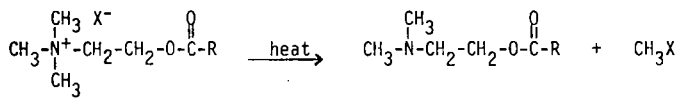
J.K. Khandelwal, P.J.A. Szilagyi, and J.P. Green, Mount Sinai School of Medicine, Department of Pharmacology New York, New York 10029.

Detailed studies of the central cholinergic system comprising measurement of steady state levels and turnover rates of acetylcholine and choline in discrete regions of rat brain require an accurate, sensitive and specific method that can simultaneously analyze isotopic variants. Bioassays[1], enzymatic[2,3], fluorometric[4] and chemical methods[5,6] have been employed but they lack specificity and are unable to monitor simultaneously isotopic variants of choline esters. A sensitive and specific gas chromatographic-electron ionization mass spectrometric method based on demethylation of choline esters with benzenethiolate has been reported[7,8]. The method, however, requires extremely anhydrous conditions and high purity of the demethylating reagent. Chemical ionization mass spectra of choline esters have also been reported[9]. Isobutane produced more intense protonated molecular ions and less fragmentation than did methane.

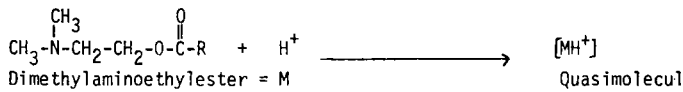
We have combined pyrolysis gas chromatography[10] and chemical ionization mass fragmentography in a specific, sensitive, simple and rapid method for simultaneous analysis of stable isotopic variants of acetylcholine and choline with a detection limit of approximately 10^{-12} mole. Acetylcholine and choline are extracted from brain tissue in acetonitrile in the presence of anhydrous magnesium sulfate and known amounts of deuterium labeled internal standards. Choline in the sample is derivatized with butyric anhydride to butrylcholine. The choline esters are taken into a small volume of potassium chloride solution and the excess butyric anhydride is removed by repeated ether wash. The choline esters are back extracted into acetonitrile and are pyrolyzed with butyltrimethylammonium chloride (BTMA), used as co-pyrolisant, for subsequent analysis by pyrolysis gas chromatography-chemical ionization mass fragmentography (PGC/CI/MF).

Principle of the Method:

Under controlled pyrolytic conditions, acetylcholine and other choline esters are quantitatively and reproducibly demethylated to the corresponding amino esters.



The demethylated products are volatile, possess good gas chromatographic properties and retain the full structural characteristic of the parent molecules bereft only of one methyl group. The demethylated derivatives form intense quasimolecular ions suitable for analysis with isobutane reagent gas in chemical ionization mass spectrometry.



Pyrolysis under controlled conditions causes mono-N-demethylation to form corresponding amino esters. In chemical ionization mass spectrometry these produce predominantly quasimolecular ions MH^+ with isobutane reagent gas. The relative ratios of the peak areas are linearly related to the amounts of choline esters and cover a large dynamic range. The recovery and reproducibility of the method are excellent and the method is well-suited to measure steady state levels and turnover rates of acetylcholine and choline in discrete regions of rat brain.

Pyrolysis Conditions:

Pyrolysis Temperature = 425°C
Duration of Pyrolysis = 5 sec
Ramp (rate of rise of temperature) = 5°/msec
Pyrolyzer Interface Temperature = 135°C
Size of Quartz Boat = 8mm
Capacity of Quartz Boat = about 12 µl

GC Conditions:

Column = 1.5ft, 2mm glass column packed with 1% Poly A-135 on Porapak P 100/120 mesh
Oven Temperature = 170°C
Carrier Gas Helium = approximately 25 ml/min
≡ 1 torr in ion source

MS Conditions:

Pressure of Isobutane = 0.35 torr
Internal Source Temperature = 175°C
Analyzer Temperature = 90°C
Electron Energy = 175eV
Electron Emission = 100µA

References:
1. Whittaker, V.P. (1963) Handbook of Experimental Pharmacology (edited by Koelle, G.B.) Vol. 15, p. 1. Springer, New York.
2. Saelens, J.K., Allen, M.P., and Simke, J.P. (1970) Arch. Int. Pharmacodyn. Ther. 186: 279-286.
3. Reid, W.D., Haubrich, D.R., and Krishna, G. (1971) Anal. Biochem. 42:390-397.
4. O'Neill, J.J., and Sakamoto, T. (1969) Fed. Proc., Fed. Am. Soc. Exp. Biol. 28:291.
5. Fellman, J.H. (1969) J. Neurochem. 16:135-143.
6. Eksborg, S., and Persson, B.A. (1971) Acta Pharm. Suec. 8:205-216.
7. Jenden, D.J., Hanin, I., and Lamb, S.I. (1968) Anal. Chem. 40:124-128.
8. Jenden, D.J., Roch, M., and Booth, R.A. (1973) Anal. Biochem. 55:438-448.
9. Hanin, I., and Skinner, R.F. (1975) Anal. Biochem. 66:568-583.
10. Szilagyi, P.I.A., Schmidt, D.E. and Green, J.P. (1968) Anal. Chem. 40:2009-2013.

METABOLISM OF TWO PCB ISOMERS BY RHESUS MONKEYS TAMOB2

H.T. CORY (1), G. DOYLE DAVES (1), R.G. SMITH (2) AND W.P. MCNULTY (3)
(1) OREGON GRADUATE CENTER, BEAVERTON, OR 97005
(2) M.D. ANDERSON HOSPITAL, HOUSTON, TX 77030
(3) OREGON REGIONAL PRIMATE CENTER, BEAVERTON, OR 97005

WE HAVE STUDIED THE METABOLISM OF TWO ISOMERS OF TETRACHLOROBIPHENYL (TCB) IN ADULT MALE RHESUS MONKEYS. THE TWO COMPOUNDS, 2,5,2',5'-TCB AND 3,4,3',4'-TCB DIFFER GREATLY IN THEIR TOXICITY: THE FORMER APPEARS TO BE NON-TOXIC, WHEREAS THE LATTER CAUSES SEVERE GASTRIC, SKIN AND THYMIC LESIONS, FOLLOWED BY DEATH, WHEN MIXED WITH THE DIET AT 1 TO 10 PPM.

THREE GROUPS OF 3 ANIMALS WERE FED WITH A DIET CONTAINING 3 PPM OF 3,4,3',4'-TCB, 2,5,2',5'-TCB AND NORMAL DIET (CONTROLS) RESPECTIVELY. ALIQUOTS OF URINE AND FECES WERE COLLECTED AT ZERO TIME AND AT MONTHLY INTERVALS OVER A 6 MONTH PERIOD. CRUDE CHLOROFORM EXTRACTS WERE PREPARED FROM THE SAMPLES BEFORE AND AFTER HCL HYDROLYSIS TO RELEASE ANY CONJUGATED METABOLITES. THE EXTRACTS WERE DRIED, CONCENTRATED AND TREATED WITH DIAZOMETHANE.

TWO MAJOR ANALYTICAL TECHNIQUES WERE USED, BOTH OF WHICH WERE SUITED TO THE DETERMINATION OF LOW LEVELS OF CHLORINE CONTAINING SUBSTANCES IN CRUDE, CONCENTRATED BIOLOGICAL EXTRACTS.

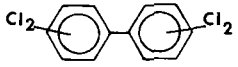
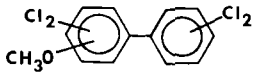
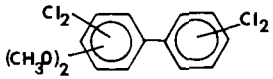
1. SELECTED ION MONITORING GAS CHROMATOGRAPHY MASS SPECTROMETRY

THE SAMPLES WERE EXAMINED FOR SPECIFIC COMPOUNDS OF KNOWN MOLECULAR WEIGHT CONTAINING FOUR CHLORINE ATOMS: THE FIRST TWO MASSES IN THE MOLECULAR ION CLUSTER WERE MONITORED. OPERATING CONDITIONS WERE:

GAS CHROMATOGRAPH: VARIAN AEROGRAPH 2700; G.C. COLUMN: 1 M X 2 MM GLASS COLUMN PACKED WITH 1 % SP 2250 ON 100/120 SUPELCOPORT; INJECTOR AND DETECTOR TEMP: 275°C; CARRIER GAS FLOW: 40 ML/MIN HELIUM; OVEN TEMP. 190° ISOTHERMAL OR TEMP. PROGRAM 150° TO 275° AT 10°/MIN.
MASS SPECTROMETER: DUPONT 21-491B MASS SPECTROMETER EQUIPPED WITH A 4-CHANNEL DUPONT SMID ACCESSORY AND GOULD BRUSH 6-CHANNEL RECORDER; IONIZING VOLTAGE: 70 EV; FILTER: 1 HZ; SAMPLING FREQUENCY 40 PKS. SEC^{-1}. LIMIT OF DETECTION: 10 PG OF 2,5,2',5'-TCB.

THE TABLE LISTS THE METABOLITES FOUND IN THE EXTRACTS OF HYDROLYSED URINE AND UNHYDROLYSED FECES SAMPLES. THE FINDING OF RING HYDROXYLATED METABOLITES IS IN AGREEMENT WITH A NUMBER OF REPORTS CONCERNING ANIMALS OTHER THAN RHESUS MONKEYS (CF 1). COMPARISON OF THE METABOLIC PATTERNS IN THE TWO EXPERIMENTAL GROUPS SHOWS THAT THE AMOUNT OF UNMETABOLISED TCB EXCRETED WAS THE SAME, AS WAS THE SUM OF THE LEVELS OF THE METABOLITES FOUND. NO TETRACHLORODIBENZOFURAN OR -DIBENZODIOXIN ISOMERS WERE DETECTED IN ANY OF THE EXTRACTS. THERE WAS ALSO NO EVIDENCE OF DECHLORINATION ACCOMPANYING HYDROXYLATION AS REPORTED ELSEWHERE (2). MOREOVER, A TETRACHLORINATED DIHYDRODIOL METABOLITE FOUND IN THE URINE

OF RABBITS (3) AND RHESUS MONKEYS (4) GIVEN 2,5,2',5'-TCB WAS NOT FOUND, BUT IT IS LIKELY THIS WOULD HAVE DECOMPOSED TO THE PHENOL UNDER THE ABOVE CONDITIONS. THERE WAS NO EVIDENCE FOR THE METABOLIC FORMATION OF O-METHYL ETHERS, AS REPORTED ELSEWHERE (CF 1).

COMPOUND	IONS MONITORED M/E	2,5,2',5'-TCB URINE	2,5,2',5'-TCB FECES	3,4,3',4'-TCB URINE	3,4,3',4'-TCB FECES
	290, 292	-	+	-	+
	320, 322	+	+	+	+
	350, 352	+	+	-	-

2. DUAL FLAME IONIZATION - ELECTRON CAPTURE GAS CHROMATOGRAPHY

THIS TECHNIQUE WAS USED AS A MEANS OF ESTIMATING THE TOTAL NUMBER OF CHLORINE CONTAINING METABOLITES IN THE EXTRACTS, SOME OF WHICH MAY NOT HAVE BEEN SUSPECTED AND COULD THEREFORE NOT BE MEASURED BY SELECTED ION MONITORING G.C.M.S. THE OPERATING CONDITIONS WERE AS FOLLOWS:

GAS CHROMATOGRAPH: VARIAN AEROGRAPH 2400; E.C. DETECTOR: ^{3}H ADSORBED ON Sc FOIL; GC COLUMN: 1 M SP 2250; OVEN TEMPERATURE 190° ISOTHERMAL OR TEMP. PROGRAM 190° TO 230° AT 3°/MIN; CARRIER GAS FLOW: 40 ML/MIN N_2; INJECTOR AND DETECTOR TEMP: 250°; EFFLUENT SPLIT RATIO 1:1.
THE LIMIT OF DETECTION WAS 1 NG 2,5,2',5'-TCB.

COMPARISON OF THE ELECTRON CAPTURE PROFILES OF THE URINE AND FECES SAMPLES OBTAINED BEFORE AND AFTER FEEDING OF THE TCBs INDICATED THAT UP TO TWO ADDITIONAL, UNKNOWN METABOLITES COULD BE PRESENT IN BOTH GROUPS OF EXTRACTS.

(1) SUNDSTRÖM G. & O. HUTZINGER (1976) CHEMOSPHERE 5, 267-298
(2) HUTZINGER O., W.D. JAMIESON, S SAFE, L. PAULMANN & R. AMMON (1974) NATURE 252, 698-9
(3) GARDNER A.M., J.T. CHEN, J.A.G. ROACH & E.P. RAGELIS (1973) BIOCHEM. BIOPHYS. RES. COMMUN. 55, 1377-1384
(4) HSU I.C., J.P. VAN MILLER & J.R. ALLEN (1975) BULL. ENVIRON. CONTAM. TOXICOL. 14, 233-240

A Comparison of the Analysis for Carbon-13 and Carbon-14 in the Serum of Dogs Following the Intravenous Infusion of Labeled Disodium Dichloromethanediphosphonate, Robert S. Ampulski, The Procter & Gamble Company, Miami Valley Laboratories, P.O. Box 39175, Cincinnati, Ohio 45247

INTRODUCTION

This report describes the results of a method developed to use carbon-13 as a tracer in disodium dichloromethanediphosphonate (Cl_2MDP) bioavailability studies in animals. Cl_2MDP (M.W. = 290) is a geminal diphosphonate with an affinity for calcium ions. Cl_2MDP has also been found to inhibit bone resorption in animal models of osteoporosis and arthritis. In order to determine the bioavailability of Cl_2MDP in humans an analytical method was needed that did not require dosing long-lived radionuclides, since Cl_2MDP is strongly adsorbed to bone and has a slow turnover. The method needed to be sensitive to low levels (<ppm) of drug in biological fluids. The bioavailability study further required that the method use small volumes of samples. A method was developed using carbon-13 tracer technology which met all these criteria.

EXPERIMENTAL

In this study serum samples from three dogs were analyzed for both carbon-13 and carbon-14 following an intravenous administration of 2.5 mg Cl_2MDP/kg enriched with 80 atom % excess carbon-13 plus 5μCi carbon-14. Five milliliter serum samples were taken at 0,5, 10, 15, 30, 45 minutes and 1, 2, 3, 4, 6, 12, 18, and 24 hours. The carbon-14 in the samples was quantitated by directly counting volume aliquots in scintillation gels on a Packard Tricarb Scintillation counter. In the carbon-13 method, the protein was precipitated from one-half milliliter serum. Fifty microliters of the supernatant liquid were oxidized in a static system using prepurified oxygen and a platinum ribbon catalyst (900-1100°C).[1] The molar volume of carbon dioxide produced (M) was determined manometrically.[2] The relative amount of $^{13}CO_2$ was measured by isotope ratio mass spectrometry (VG Micromass 903).[3] The corrected ^{13}C enrichment (δ_c) was determined for each sample relative to a standard. The absolute ratio of $^{13}C/^{12}C$ $R_{13}(t)$ was then calculated at various times (t) from

$$R_{13}(t) = \frac{\delta c R13(STD)}{1000} + R_{13}(STD).$$

It can be shown that the weight of drug (W) in a sample is

$$W = \frac{R_{13}(t) - R_{13}(0)}{R_{13}(0) + 1} \times M \times \frac{M.W.}{A}$$

Where $R_{13}(0) = R_{13}$ before dosing (t=0).

M.W. = Molecular weight of compound dosed

M = Moles of CO_2 per ml of serum

A = Percent ^{13}C in dose compound

RESULTS AND DISCUSSION

The precision of the 13-C method is shown in the table below. The precision of a single analysis on the mass spectrometer was $\pm$ 0.016 μg Cl_2MDP/ml. This is the precision of the mass spectrometer only. Using a single protein precipitate and combusting 10 aliquots there was a drop in precision to $\pm$ 0.16 μg Cl_2MDP/ml. When 7 aliquots of the same serum were precipitated, combusted and analyzed, the precision decreased further to $\pm$ 0.32 μg Cl_2MDP/ml serum. Another source of error in the reported weight of drug (W) is the 10% variation in the measured volume of CO_2. The major limitation seems to be in the ability to reproducibly pipet, combust, trap, and transfer the CO_2.

The standard curve for $^{13}Cl_2MDP$ in dog serum is shown in Figure 1. The method was linear over the range investigated (0.2 to 14 μg/ml). The limit of detection was 0.4 μg Cl_2MDP/ml.

Precision of Detecting ^{13}C in Dog Serum

Limiting Factor	# of Analysis	Vol of CO_2 m moles/ml	$R_{13} \pm$ S.D. ($\times 10^5$)	S.D. in µg Cl_2MDP/ml
Mass Spectrometer*	1	0.153	1103.03 ± .03	± .016
Combustion only	10	0.154 ± .023	1103.3 ∓ 0.3	∓ 0.16
Complete method	7	0.157 ∓ .013	1102.8 ∓ 0.6	∓ 0.32

*Difference of 10 ratios

A linear regression analysis comparing the ^{13}C method with the ^{14}C method is shown in Figure 2. The two methods are comparable. A typical drug clearance curve is shown in Figure 3.

CONCLUSIONS

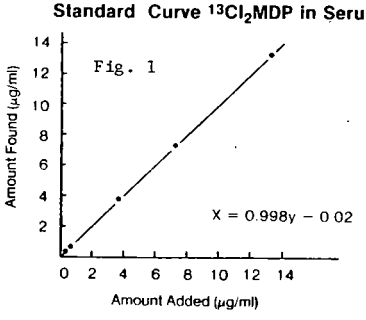
The carbon-13 tracer method described here was sufficient to quantitatively determine excess ^{13}C in concentrations greater than 1 x 10^{-9} moles/ml. The method uses small amounts of biological fluids (one-half milliliter or less). The carbon-13 results are comparable to those obtained by carbon-14 methods; though the carbon-14 method is twenty times more sensitive.

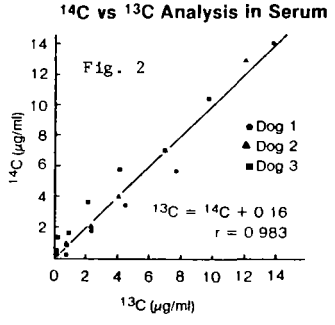
ACKNOWLEDGMENTS

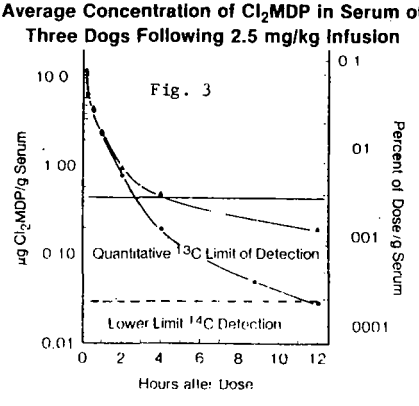
The valuable assistance of C. Slough is acknowledged for design and execution of the animal study. L. D. McCreary is acknowledged for the radioanalytical data. John Landgraf is acknowledged for his valuable contributions in developing the ^{13}C techniques and sample analysis.

REFERENCES

1. W. H. Lee, "Developments in the Preparation of Samples for Carbon Isotopic Analysis" Thesis, Indiana University, Bloomington, IN, 9/75.
2. R. T. Sanderson, "The Microvol," Industrial Engineering Chemistry, Analytical Edition, 15, 76 (1943)
3. R. S. Ampulski, "Automated Real Time Analysis of $^{13}CO_2$ in the Respired Breath of Rats Fed Sodium Acetate," Presented at the 26th Annual Conference on Mass Spectrometry and Allied Topics, May 28-June 2, 1978, St. Louis, MO Paper #RA 12







TAMOB4

GC/MS DETERMINATION OF THE METABOLIC PATTERN OF PROPRANOLOL

Van. T. Vu and Fred P. Abramson
Departments of Pharmacology and Pathology
George Washington University Medical Center
Washington, D.C. 20037

Our studies of the effects of drug interactions on the metabolism of propranolol have proceeded in four steps. We first had to develop an analytical method to quantify propranolol and its many metabolites from urine. At last year's ASMS meeting, that technique was discussed (1). To properly understand the chain of metabolic events in propranolol disposition, we felt it was necessary to perform in vitro metabolic studies with several propranolol metabolites in order to directly observed the sequence of reaction steps. The third aspect of this study was to quantify the pattern of propranolol metabolism under control conditions, that is, without administering any interacting drug. Finally, the effects of either chlorpromazine (CPZ) or phenobarbital (PB) pretreatment on the disposition of propranolol were measured. This abstract will deal primarily with the second of these sections with a summary of data obtained from the latter two aspects of our investigations.

One or two mg of propranolol or a metabolite were incubated for three hours at 37° with 10 ml of a 10,000 xG supernatant from dog liver, along with the necessary cofactors. The metabolites 4-hydroxypropranolol (4-OH-P), N-deisopropylpropranolol (N-DIP), alpha- naphthoxylactic acid (NLA) and propranolol glycol (GLY) were also used as substrates. In this incubation, propranolol was degraded 65%. Its products were: 4-OH-P, 30%; GLY, 6%; N-DIP, 20%; Naphthol, 9%. Incubations with N-DIP as the substrate showed a 21% loss of the starting product with 5% converted to GLY and 10% converted to naphthol. With GLY as the starting product, 18% was degraded and 11% was detected as a ring hydroxylated propranolol glycol. No products could be detected following the incubation of 4-OH-P and 88% was recovered. Incubations of NLA produced 48% naphthol with a 54% loss of substrate.

The metabolic pattern of propranolol published by Walle and Gaffney (2) was based only on observations of the in vivo and in vitro products of propranolol. Our incubations of metabolites suggest several revisions to their pathways. The incubation of NLA shows a facile conversion to naphthol. Despite the finding that NLA is the major urinary metabolite of propranolol following in vivo administration, we could not find NLA as a product in our in vitro studies. We conclude that NLA is very rapidly converted by liver enzymes to naphthol and that its role as an intermediate in the production of naphthol following incubations of either propranolol or N-DIP must be assumed. We conclude that propranolol does not undergo a dealkylation reaction to form naphthol directly. Naphthol's production involves first the formation of N-DIP followed by its rapid conversion to an aldehyde intermediate which then oxidized to NLA. Because this conversion utilizes monoamine oxidase and aldehyde oxidase, both ubiquitous enzymes, N-DIP will have only a short lifetime in the body.Our liver preparation would not reflect the total body capacity for these two reactions and thus does not correlate with the in vivo observation.

It has also been assumed that 1,4-naphthalenediol (DIOL) was produced from 4-OH-P. Our incubations fail to demonstrate that reaction. We assume that DIOL is produced from the hydroxylated metabolite of GLY although our incubation did not produce enough hydroxylated GLY to observe this secondary reaction product. Our in vivo studies seem to confirm this pathway because DIOL is only observed under dosing conditions where hydroxylated GLY is formed while DIOL production appears independent of 4-OH-P production.

With these pathways elucidated, we can study alterations in the disposition of propranolol in vivo. We have used 4 male beagle dogs as our experimental models. Propranolol has been shown to have markedly different metabolism following intravenous or oral administration (3). Because our single dose oral studies differed from other observations which used chronic dosing, we have compared three dosing schemes for propranolol: a single 6 mg intravenous dose; a single 40 mg oral dose; and continuous dosing at 160 mg/day. The results for the initial steps of propranolol disposition are shown in Table 1. The individual numbers of each process are the sums of all metabolites which are associated with that pathway, including conjugation. Thus, we see little difference in propranolol conjugation or side-chain degradation, but a large effect of route of administration on the formation of 4-OH-P. It is interesting that we see hydroxylation of propranolol following intravenous administration, since the one report which previously investigated this phenomenon (3) did not demonstrate any 4-OH-P at all.

Table 1. EFFECT OF ROUTE OF ADMINISTRATION ON PROPRANOLOL METABOLISM

PATHWAYS	MODE OF ADMINISTRATION Intravenous (6 mg)	Acute Oral (40 mg)	Chronic Oral (160 mg/day)
Conjugation	5.0 ± 2.4%	7.3 ± 1.1%	6.8 ± 0.2%
Side Chain Degradation	82.0 ± 5.2%	72.9 ± 1.6%	68.8 ± 2.1%
4-Hydroxylation	8.2 ± 4.4%	17.7 ± 1.2%	22.7 ± 1.9%
Unmetabolized	4.8 ± 0.4%	2.1 ± 0.3%	1.7 ± 0.2%

There are two major effects of drug interactions on the disposition of single oral doses of propranolol. Table 2 shows that CPZ pretreatment lowers the amount of 4-hydroxylation by nearly 50%, while PB increases that metabolic step by 62%. Because this pathway involves production of a metabolite with equal pharmacological potency to that of the parent drug, these interactions could have clinical importance. We also noted that, although CPZ increases the bioavailability of propranolol by 155%, the urinary excretion is lowered. Thus, CPZ inhibits the renal excretion of propranolol.

Table 2. THE METABOLIC DISPOSITION OF PROPRANOLOL FOLLOWING ACUTE ORAL ADMINISTRATION (40 mg)

PATHWAYS	CONTROL	CHLORPROMAZINE PRETREATMENT	PHENOBARBITAL CHRONIC TREATMENT
CONJUGATION	7.3 ± 1.1%	5.4 ± 1.0%	7.7 ± 1.1%
SIDE CHAIN DEGRADATION	72.9 ± 1.6%	84.6 ± 4.6%	60.4 ± 2.8%
4-HYDROXYLATION	17.7 ± 1.2%	9.0 ± 3.7%	28.7 ± 2.3%
UNMETABOLIZED	2.1 ± 0.3%	1.0 ± 0.1%	3.2 ± 0.8%

In summary, the availability of a sensitive and reproducible analytical method for the determination of propranolol and its metabolites even with concommitant administration of other drugs has led to an improved understanding of propranolol metabolism. The influence of the route of administration has been described in more detail than was previously known, and the particular sensitivity of the pathway which produces the active metabolite, 4-OH-P, to drug interactions was demonstrated.

Acknowledgements: This work was supported by The Washington Heart Association, The George Washington University Biomedical Research Support Grant No. 5 SO1-RR5359, and a Grant from the National Institutes of Health, No. HL 22718.

1. Vu, V.T., and Abramson, F.A., Quantitative analysis of propranolol and metabolites urine by a GC/MS/COM technique. Paper No. MC-9. Proc. 26th Annual ASMS Conference, 1978.
2. Walle, T.A., and Gaffney, T.E., Propranolol metabolism in man and dog: Mass spectrometric identification of six new metabolites. J. Pharmacol. Exp. Therap., 182: 83- 92, 1972.
3. Paterson, J.W., Conolly, M.E., Dollery, C.T., Hayes, A., and Cooper, R.G., The pharmacodynamics and metabolism of propranolol in man. Pharmacologica Clinica 2: 127-133, 1970.

TAMOB6 USE OF MS AND HPLC IN STUDIES OF THE IN VITRO METABOLISM OF GUTHION (AZINPHOSMETHYL) BY MICE AND RAT LIVER HOMOGENATES
SHEN-NAN LIN, CHUNG-YIING CHEN, RICHARD M. CAPRIOLI AND SHELDON D. MURPHY, Anal. Chem. Ctr. and division of Toxicology, The Univ. of Tx. Med School at Houston, Houston, Tx. 77025

Metabolic pathways of Guthion, a widely used insecticide, by mice and/or rat liver homogenates were confirmed by MS and HPLC techniques. The advantage of using HPLC over GC was that thermal decomposition of Guthion and its metabolites were prevented. Metabolic degradation of Guthion and its oxygen analogue, Gutoxon, to produce benzazimide have not been reported previously. The present study verified that Guthion was activated to Gutoxon and was also degraded to benzazimide. Gutoxon was degraded to benzazimide but at a slower rate than that of Guthion. Metabolism of Guthion by mice and by rat liver homogenates were compared.

Methodology described here is currently being applied to detect metabolic changes due to endogenous and exogenous variables.

TAMOB7 2,5-DI-tert.-AMYL-p-BENZOQUINONE: AN ANTIOXIDANT ENCOUNTERED DURING ANALYSES OF HUMAN TISSUES, BRIAN S. MIDDLEDITCH, HARRY B. HINES, Dept. of Biophys. Sci., Univ. of Houston, Houston, TX 77004, FRANK O. BASTIAN, and PATRICIA R. MIDDLEDITCH, Dept. of Pathol., St. Lukes Episcopal Hospital, Houston, TX 77030.

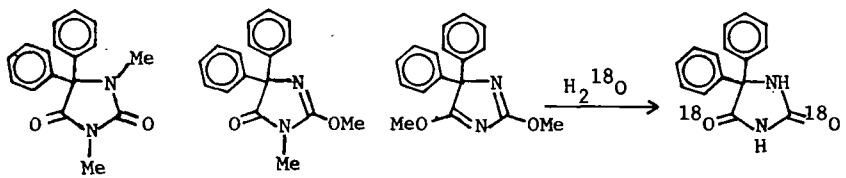
The title compound was encountered during analyses of human tissues (tumors, fetal organs, and adult control specimens) obtained during surgery and at autopsy. Possible sources of this and related compounds in the home, the hospital, and the laboratory are discussed.

FORMATION OF O- AND N-METHYLATED PRODUCTS IN THE DERIVATIZATION OF 5,5-DISUBSTITUTED HYDANTOINS WITH DIAZOMETHANE.

J.P. Thenot, A. Hung*, T.I. Ruo, and R. De Sagher*

Clinical Pharmacology Center, Anesthesiology Department, Northwestern University, Chicago and *Inst. Lipid Res., Houston, Texas

Diazomethane reacts with acidic functional groups such as carboxylic acids, phenols, and imines. Hence, with 5,5-disubstituted hydantoins, the main product is the 3-methyl derivative. After reaction of phenytoin (5,5-diphenylhydantoin) with diazomethane, three dimethyl derivatives that can be concentrated by extraction with hexane are also observed. The position of the methyl groups were identified by the products obtained by mild acidic hydrolysis (1N HCl at 60° C for 1 hr). In these conditions, the enol ethers are hydrolyzed while the N-methyl derivatives are stable. These dimethyl derivatives were thus identified as the 1,3-, 2,3-, and 2,4-derivatives. The electron impact ionization mass spectra confirm the structures. A characteristic fragmentation of O,O'-derivative is the elimination of the methyl group of the enol ether.



1,3-diMe 2,3-diMe 2,4-diMe

With 2-thio-5,5-diphenylhydantoin only the dimethyl derivatives were observed due to the higher reactivity of the sulfur. Again the 1,3-, 2,3-, and 2,4-derivatives are formed. Since the enol (or thio-enol) is easily hydrolysed to the parent hydantoin, the preparation of ^{18}O-labeled phenytoin can be achieved without any difficulty.

The formation of O-methyl derivatives reflects the partial SN_1 character of the reaction for the alkylation at the nitrogen is preferred in the classical SN_2 mechanism. This also explains why O-alkylation is preponderant with the silver salt(1,2).

1. H. von Pechman & O. Baltzer, Ber., 24, 3144 (1891).
2. N. Kornblum, R.A. Smiley, R.K. Blackwood, & D.C. Iffland, J. Amer. Chem. Soc., 77, 6269 (1955).

TAM 0B9

A GAS CHROMATOGRAPHIC-MASS SPECTROMETRIC ASSAY FOR LOW LEVELS OF RETINOIC ACID IN HUMAN BLOOD

Teh-Ching Chiang,
Central Analytical Laboratories
Johnson & Johnson Research Center
New Brunswick, New Jersey 08903

Introduction:

Recently, high performance liquid chromatography has become a popular method for separation and identification of natural retinoids (1,2,3,4). The limits of detection claimed by these authors varied from 1 nanogram (ng.)[1] to 6.7 ng.[2] of retinoic acid in standard solutions; however, no limit of detection was reported from actual experimental samples using nonradioactive retinoic acid.

A GCMS method was developed for detecting as low as 2 ng. of nonradioactive retinoic acid per ml. of human plasma. This method requires a simple clean-up and derivatization prior to GCMS analysis, thus it allows the analysis of a large number of clinical samples, with the limit of detection down to 1 ng. retinoic acid per ml. of blood.

Experimental:

Extraction

To each 10 ml. of plasma in a glass-stoppered centrifuge tube, 1 ml. of 2 N HCl, 10 ml. of ethanol, and 25 ml. of petroleum ether was added. After shaking on a mechanical shaker for 10 minutes, the tube was cooled and centrifuged at 3000 RPM for 5 minutes. The petroleum ether layer was evaporated to dryness in a 2 ml. amber vial with a stream of nitrogen gas, and the vial was immediately capped with a teflon-lined rubber seal.

GCMS Method:

Fifty microliters of dimethylformamide dimethylacetal was added to the vial to convert retinoic acid to its methyl retinoate.[5] The conversion of retinoic acid to the volatile methyl retinoate derivative enables separation on a glass GC column (6 ft. x 2 mm i.d.) packed with 3% SE-30 on 80/100 Chromosorb WHP (Supelco Inc.) at a column temperature of 230°C. Three microliters of the dimethylformamide dimethylacetal solution was used for each GCMS injection.

The molecular ion of methyl retinoate at m/Z = 314 was monitored by a Varian MAT 311A mass spectrometer.

Results and Discussion:

Spiked Samples

In order to determine efficiency of extracting retinoic acid from blood, blood samples were spiked with known amounts of retinoic acid, ranging from 2 ng./ml. plasma to 50 ng./ml. plasma, and extracted according to the procedure described under Experimental. Percent recovery of the spiked retinoic acid measured was found to be between 40 and 60%.

Clinical Samples

a) Subtotal Inunction

Ten female human subjects were applied with 0.025% Tretinoin Cream (a Johnson & Johnson product containing 0.025% retinoic acid) to the entire arms, legs and back two times a day for 28 consecutive days. Blood specimens were collected on days prior to application,

14 days and 28 days after application started. The specimens were analyzed according to the procedure described under Experimental using ^{14}C-labeled retinoic acid as internal standard. The results show that no retinoic acid at a 2 ng. retinoic acid per ml. plasma limit of detection, was found from any specimen.

b) Total Inunction

A male human volunteer was whole body treated with 1% retinoic acid cream, and a blood sample was collected for analysis. No retinoic acid was detected in the blood as a result of this rather drastic topical application of retinoic acid.

c) Intravenous Injection of Retinoic Acid Solution
A male human volunteer was intravenously injected with a total of 0.5 mg. of retinoic acid dissolved in methanol. Blood specimens were collected 5 minutes and 1 hour after the injection. The results show a level of 14.6 ng. and 5.4 ng. retinoic acid per ml. plasma, respectively.

Conclusion:

A relatively rapid, sensitive and very specific method for analysis of retinoic acid in human blood at a 2 ng./ml. of plasma limit of detection was developed. Results indicated that no detectable amount of retinoic acid was found in human blood after topical application of retinoic acid. Low levels of retinoic acid were detected in blood following 0.5 mg. intravenous injection.

References:

(1) A. M. McCormick, J. L. Napoli and H. F. DeLuca, Anal. Biochem. 86, 25 (1978)

(2) C. A. Frolik, T. E. Tavela dnd M. B. Sporn, J. Lipid Res. 19, 32 (1978)

(3) R. M. McKenzie, D. M. Hellwege, M. L. McGregor, N. L. Rockley, P. J. Piquetti and E. C. Nelson, J. Chromatogr. 155, 379 (1978)

(4) R. Hanni and F. Bigler, Hlev. Chim, Acta 60, 881 (1977)

(5) Pierce Previews, November 1972, published by Pierce Chem. Co., Rockford, Illinois

DETECTION OF METHADONE METABOLITES USING DEUTERIUM LABELLED ANALOGS

Frank S. Abbott, Gun Il Kang, and Roland W. Burton.
Faculty of Pharmaceutical Sciences, University of British Columbia, Vancouver, British Columbia, Canada, V6T 1W5.

Methadone continues to be widely used in the clinical maintenance of narcotic addiction and remains clinically useful as an analgesic for pain. The chronic use of this drug and the frequent combination with other drugs indicates a need to have a complete picture of methadone metabolism. While the reported metabolism of methadone in animals and man already describes many metabolites, there is evidence to suggest that not all of the minor metabolites are known.

To further explore the metabolism of methadone it was decided to use deuterium labelled analogs and GC-MS. Emphasis was placed on examining hydroxylated metabolites that are excreted as conjugates. Wistar rats (300-350 g) were bile duct cannulated to obtain the samples. The deuterium labelled analogs used were $^{2}H_{10}$ - methadone (label in the two aromatic rings) and $^{2}H_{3}$ - methadone (label in the methyl of the ketone side chain). Two labelled metabolites, $^{2}H_{10}$ - EDDP (2-ethylidene--1,5-dimethyl-3,3-diphenylpyrrolidine) and $^{2}H_{10}$ - EMDP (2-ethyl-5-methyl--3,3-diphenylpyrroline) were also prepared for study. The synthesis and mass fragmentation of these labelled derivatives is soon to be published.[1]

The compounds were administered to rats subcutaneously (15 mg/Kg) and bile collected for 24 hours. Bile was diluted with an equal volume of water and centrifuged to remove solids. The supernatant was adjusted to pH 7.0 and extracted with CH_2Cl_2 to remove the nonconjugated metabolites. The aqueous phase was then lyophilized and the residue treated with methanol and centrifuged to remove undesired solids. The methanol was evaporated and the residue was incubated with β-glucuronidase at pH 5.0 and 37° for 24 hours. The fraction of metabolites that were conjugated were then extracted with CH_2Cl_2. This extract was injected into the GC-MS, or was first derivatized with diazomethane. Analyses were performed on the Varian Mat 111 GC-MS (EI) using 3% OV-17 columns and temperature programming. An on-line computer has been adapted to this system. Since labelled and unlabelled analogs were injected into separate animals, metabolite identification was based primarily on a simple comparison of mass spectra or more frequently by comparing mass chromatograms generated by a judicious choice of selected ions.

The total ion chromatograms of these extracts contained many peaks resulting from endogenous bile components. Additional clean-up procedures during the extraction were not necessary, however, since mass chromatograms or selected ion monitoring was specific for the metabolites. For example, the derivatized sample extracts obtained from administering $^{2}H_{10}$ - EMDP to a rat gave coincident mass chromatogram peaks at m/e 276, 261 and 245 for the isolated dihydroxy - $^{2}H_{10}$ - EMDP and m/e 247, 232 and 216 for the monohydroxy - $^{2}H_{10}$ - EMDP. Corresponding ions for nondeuterated EMDP administration are m/e 238, 223 and 207 for the monohydroxy and m/e 268, 253 and 237 for the dihydroxy metabolite. These ions are all related to the diphenyl methyl cyclopropane fragment at m/e 208 that is common to methadone and most of the conjugated metabolites.

When rats were dosed with methadone the derivatized bile extract gave mass chromatogram peaks (m/e 237) for monohydroxy - EMDP, monohydroxy - EDDP, and dihydroxy - EDDP free of any other significant peaks. A new compound in this fraction was identified by producing a mass chromatogram of the ion at m/e 72. The retention time of this component exceeds that of dihydroxy EMDP and the peak did not shift following diazomethane treatment. The mass spectrum obtained for this component gave weak apparent molecular ion at m/e 309 with strong peaks at m/e 72 (base), 207, 253, 73, 208 and 129. A comparison of the results obtained following $^{2}H_{10}$ - methadone metabolism proved that this component was not ring hydroxylated. A clue to the identity of this apparently new metabolite was obtained from quite different circumstances. During oxidative degradation studies of the primary methadone metabolite EDDP, it was found that peracid oxidation of

EDDP under certain conditions gives a variety of breakdown products including EMDP plus a compound having an identical retention time and mass spectrum to that of the new component present in the bile extract. Sufficient quantities of this EDDP degradation product were isolated by preparative GC to obtain an accurate mass analysis (courtesy of Mr. G. Eigendorf, Chemistry Dept., U.B.C.). The structure that best fits the mass spectral evidence for the degradation product is the nitrone of N-demethylmethadone. A mechanism for the formation of this nitrone by peracid oxidation of EDDP has been proposed. A case can also be made for the formation of the nitrone of N-demethylmethadone during metabolism, arising from the breakdown of N-hydroxydemethylmethadone following or during enzymatic hydrolysis of conjugated metabolites. Confirmation of the structure of this new component from methadone metabolism requires the isolation of the material and additional chemical or spectroscopic evidence.

Reference

1. G. Kang, R. Burton, and F.S. Abbott, Synthesis and Mass Spectrometry of Deuterated Methadone and Methadone Metabolites. Biomed. Mass Spectrom. (IN PRESS).

POTENTIAL ROLE OF HYDROXY POLYENOIC FATTY ACIDS IN HUMORAL HYPERCALCEMIA OF MALIGNANT DISEASE

W. C. Hubbard, A. Hough, Jr., A. R. Brash, R. M. Johnson and J. A. Oates
Departments of Pharmacology, Pathology and Medicine
Vanderbilt University, Nashville, Tennessee 37232

Hypercalcemia is a frequent complication of malignant disease (1-6). Many examples of hypercalcemia associated with malignancy can be attributed to destruction of bone by metastatic tumor (4). Other examples of malignancy-associated hypercalcemia are those in which boney metastases are absent and remission of the hypercalcemia results from resection of the primary tumor thus leading to the assumption that the hypercalcemia in these instances is humoral in nature. The VX-2 carcinoma-bearing rabbit has been employed as an animal model of humorally-mediated hypercalcemia of malignant disease (7-11). Rabbits receiving implants of VX-2 carcinoma tissue intramuscularly (IM) develop significant hypercalcemia within 10-21 days. The evaluation in the serum calcium levels is preceeded by increased prostaglandin E_2 (PGE_2) production. Concomitant with the onset of hypercalcemia are osseous changes that are consistent with systemic bone resorption. Indomethacin, an inhibitor of PGE_2 biosynthesis, lowers or, in some instances, normalizes the serum calcium levels. Since PGE_2 is a potent osteoclastic stimulator in vitro (12,13) and is produced in relatively large quantities by rabbits bearing the VX-2 carcinoma IM, it has been postulated that the hypercalcemic syndrome in this tumor-bearing animal model is due to the secretion and release of PGE_2 which, in turn, leads to systemic bone resorption.

The effect of the presence of VX-2 carcinoma tissue in rabbits upon serum calcium levels varies in relation to the site of implantation of the tumor tissue. Rabbits receiving implants of tumor tissue intra-abdominally (IA) fail to develop hypercalcemia even in the presence of an extensive neoplastic burden (9). We have evaluated the differences in the serum calcium levels in normal and tumor-bearing rabbits in relation to PGE_2 production in vivo and to the metabolism of arachidonic acid, the fatty acid precursor of PGE_2, by VX-2 carcinoma tissue in vitro.

Comparisons of the serum calcium levels and levels of the 15-keto-13,14-dihydro-metabolite of PGE_2 ($15K\text{-}H_2\text{-}PGE_2$), an index of PGE production in vivo in normal and tumor-bearing rabbits are shown in Table 1.

Table 1

Serum Calcium Levels and Plasma Levels of $15K\text{-}H_2\text{-}PGE_2$ in Normal and Tumor-Bearing Rabbits

Site of Implant	Serum Ca^{++}, mg/dl	$15K\text{-}H_2\text{-}PGE_2$ Plasma, ng/ml
None (Control)	14.9±0.3	0.05±0.02
Intra-abdominally	13.9±0.5	11.1 ±6.0[a]
Intramuscularly	17.9±0.5[a]	15.2 ±3.8[a]

Samples for evaluation taken 4 weeks after tumor implantation

a = $p<0.001$

The data summarized in Table 1 illustrates that the differences in the serum calcium levels in rabbits bearing the VX-2 carcinoma are not related to PGE_2 production in vivo or to the level of $15K\text{-}H_2\text{-}PGE_2$ in the circulation.

In subsequent studies of the metabolic profile of arachidonic acid (AA), the fatty acid precursor of PGE_2, by homogenates of VX-2 carcinoma tissue, we observed no differences in the oxygenation of the fatty acid by tumor tissue harvested from IA and IA implant sites. One finding of the studies of the metabolism of AA by VX-2 carcinoma tissue in vitro, was that the fatty acid is a precursor to two monohydroxy-eicosatetraenoic acids (HETEs), 11-hydroxy-eicosatetraenoic acid (11-HETE) and 15-hydroxy-eicosatetraenoic acid (15-HETE). More significantly, we observed that linoleic acid is also oxygenated by VX-2 carcinoma tissue. The quantities of 9-hydroxy-octadecadienoic acid (9-HODD) and 13-hydroxy-octadecadienoic acid (13-HODD) produced by the tumor tissue from linoleic acid in vitro approximate that of PGE_2 biosynthesis. The conversion of AA and linoleic acid to HETEs and HODDs is inhibited by indomethacin.

Our data indicate that the differences in the serum calcium levels in rabbits bearing the VX-2 carcinoma IM and IA may be due to more complete pre-systemic inactivation of the humoral agent(s) released from IA implants by metabolism sequentially in the liver and the lung along than by the lung alone when the implants are IM. Since PGE_2 is rapidly converted to less active compounds by both the lung and the liver (14-17), the differences in the serum calcium levels in the two groups of animals may be related to different abilities of the lung and liver to remove the monohydroxy polyenoic fatty acids (HPFA) from the circulation or to inactivate the HPFA. The possibility that the differences in the serum calcium levels in rabbits bearing the VX-2 carcinoma IM and IA may be related to different abilities of the lung and liver to remove or inactivate HPFA warrants further investigation.

Acknowledgement: Supported by Grant GM 15431

References

1. Seyberth, H.W., Segre, G.V., Morgan, J.L., Sweetman, B.J., Potts, J.T., Jr., and Oates, J.A., N. Engl. J. Med. 293:1278-1283, 1975.
2. Powell, D., Singer, F.R., Murray, T.M., Munkin, C., and Potts, J.T., Jr., N. Engl. J. Med. 289:176-181, 1973.
3. Chopra, D. and Clerkin, E.P., Med. Clin. N. Am. 59:441-447, 1975.
4. Milch, R.A. and Changres, G.W., Cancer 9:340-351, 1956.
5. Bender, R.A. and Hansen, H., Ann. Intern. Med. 80:205-208, 1974.
6. Azzopardi, J.G. and Whittaker, R.S., J. Clin. Pathol. 22:718-724, 1969.
7. Voelkel, E.F., Tashjian, A.H., Jr., Franklin, R., Wasserman, E., and Levine, L., Metabolism 24:973-986, 1975.
8. Hough, A., Jr., Seyberth, H.W., Oates, J.A., and Hartman, W., Am. J. Pathol. 87:537-552, 1977.
9. Young, D.M., Fioravanti, J.L., Prieur, D.J. and Ward, J.M., Lab. Invest. 35:30-46, 1976.
10. Tashjian, A.H., Jr., Voelkel, E.F., and Levine, L., Prostaglandins 14:309-317, 1977.
11. Seyberth, H.W., Hubbard, W.C., Oelz, O., Sweetman, B.J., Watson, J.T., and Oates, J. A., Prostaglandins 14:319-331, 1977.
12. Klein, D.C. and Raisz, L.G., Endocrinology 86:1436-1440, 1970.
13. Dietrich, J.W., Goodson, J.M., and Raisz, L.G., Prostaglandins 10:231-240, 1975.
14. Samuelsson, B., Granstrom, E., Green, K., Hamberg, M., and Hammarstrom, S., Ann. Rev. Biochem. 44:669-695, 1975.
15. Samuelsson, B., Goldyne, M., Granstrom, E., Hamberg, M., Hammarstrom, S., and Malmster, C., Ann. Rev. Biochem. 47:997-1029, 197 .
16. Bakhle, Y.S. and Vane, J.R., Physiol. Rev. 54:1007-1045, 1974.
17. Hamberg, M. and Samuelsson, B., J. Biol. Chem. 246:1073-10 , 1971.

A MICROWAVE DISCHARGE ION SOURCE FOR CHEMICAL IONIZATION

M. W. SIEGEL
Extranuclear Laboratories, Inc.
Pittsburgh, PA 15238

The choice of primary ionization (reagent ion making) means in chemical ionization sources is relatively unimportant except in the context of the requirements of specific difficult applications. Thus the vast majority of chemical ionizers use a low cost, moderate energy electron gun, but other means such as Townsend discharge, corona discharge, and radioactive foils are in routine use. Faced with an application requiring analysis of trace concentrations of H_2 in He, where metal surfaces in the ion source are by experience inimical to trace H_2 analysis, we have developed a microwave discharge chemical ionization source. Since the microwave power is coupled into the active ionization region capacitively, inert non-metallic walls, e.g., quartz, are used, and neither hydrogen nor water are spontaneously evolved during operation. The method may be compared and contrasted to plasma emission (optical) spectroscopy: we find it advantageous to operate at low microwave power (~2 watts), where the ion mass spectrum is dominated by molecular ions, while plasma emission sources typically operate at high microwave power (~100 watts) to produce complete dissociation and as a result generate optical spectra of the constituent elements.

Our apparatus uses a coaxial cylindrical resonator terminated in a capacitive gap at a voltage maximum for the 2450 MHz excitation. The active discharge volume is the order of 1 cm^3, and the sampling aperture of the order of 0.5 mm diameter. The source operates reliably over a wide pressure range around 1 torr, the usable limits depending on matrix gas, microwave power level, and gross impurity level. Thermal ions are carried by the bulk gas flow into a differentially pumped vacuum system where they are collected, focused, and mass analyzed by apparatus similar to that previously described for our Atmospheric Pressure Ionizer/Mass Spectrometer and Simulscan CI-EI/Mass Spectrometer systems; the microwave discharge ionizer can, in fact, be installed on either of these systems.

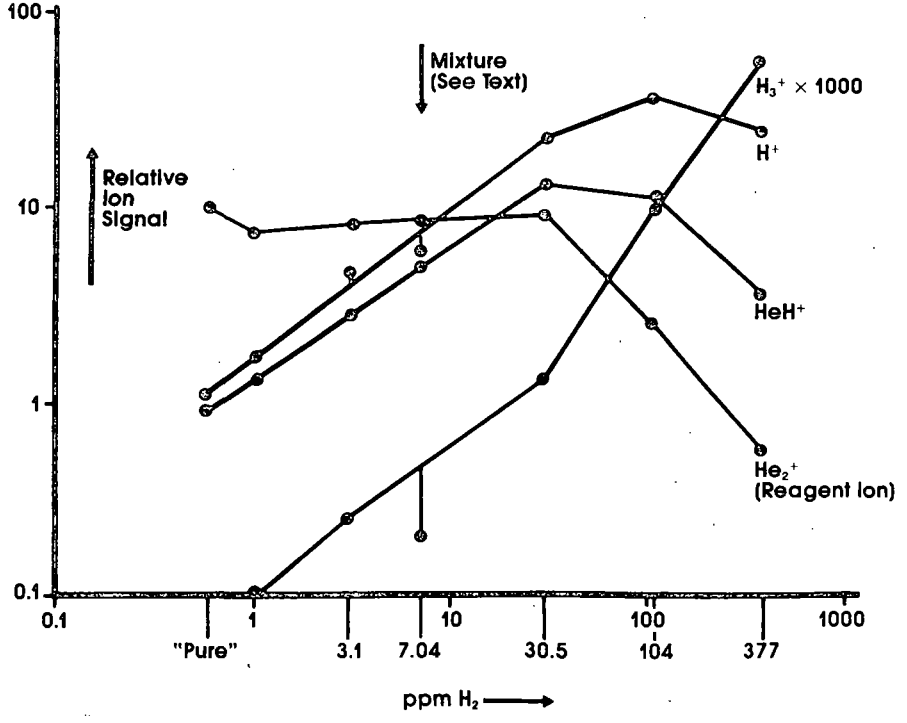


Figure 1

Figure 1 demonstrates the ability of the instrument to quantify the H_2 concentration in He in the 0-300 ppm range. By downward extrapolation of the 1-30 ppm data, the ion currents from nominally pure He are shown to correspond to a background level of apparently 0.6 ppm of H_2. The "pure" He is Research Grade Helium from Ideal Gas Products, Edison, New Jersey, and the 1 ppm H_2 mixture was prepared by the same manufacturer from the same helium stock. The 3.1, 7.04, 30.5, 104, and 377 ppm mixtures are standards of the Japan Atomic Energy Research Institute, at whose facility (Tokai) these data were collected. The 7.04 ppm mixture also contained ~10 ppm each of several other impurities, whose competition with H_2 for available reagent ions results in the somewhat too low hydrogen related ion signals for that sample. While the ion H^+ carries a little more of the total signal current that HeH^+, its intensity is more sensitive to discharge conditions and competing impurities, making HeH^+ the preferred ion for quantitation at low concentration. The relevant reactions are

$$He^+ + He \xrightarrow{He} He_2^+$$

and

$$He_2^+ + H_2 \longrightarrow HeH^+ + He + H$$

In contrast to the results of flowing afterglow experiments, in which He_2H^+ is reported as the main product of the $He_2^+ + H_2$ reaction, we have never observed an ion at mass 9.

At concentrations above 30 ppm the reagent ion density is severely depleted, with a resulting saturation and eventual decrease of H^+ and HeH^+ signals. The H_3^+ signal, apparently (from the shape of the curve in Figure 1) due to secondary reactions, one of which might be

$$HeH^+ + H_2 \longrightarrow H_3^+ + He,$$

provides a warning of this saturation, and perhaps a means for quantitating higher H_2 concentrations.

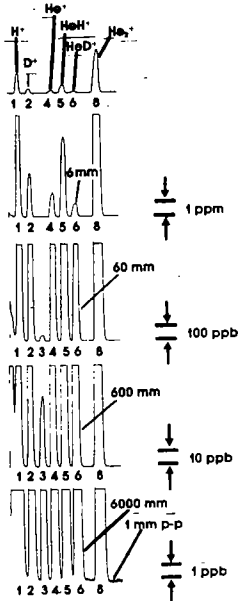


Figure 2

The residual HeH^+ and H^+ are confirmed, by LN_2 trapping, to be due to water vapor in the sample gas. Further confirmation is provided by adding a trace of D_2O vapor, which produces D^+ and HeD^+ as well as the expected heavier ions. To determine the ultimate sensitivity of the present configuration to hydrogen, the water interference was eliminated by examining a mixture of 1 ppm D_2 in Research Grade Helium. The result is shown in Figure 2, where a signal-to-noise ratio of approximately 6000:1 is observed for the HeD^+ ion. Thus, in the absence of interference, quantitation of H_2 in He at the ppb level should be easily attainable.

To illustrate the potential this system affords for analysis of other impurities, a 0-50 amu spectrum of Research Grade Helium is shown in Figure 3. Most of the ions seen are obviously associated with water vapor, air, and halocarbons. Further investigations along these lines, including considerations for GC-MS use of this ion source, are in progress.

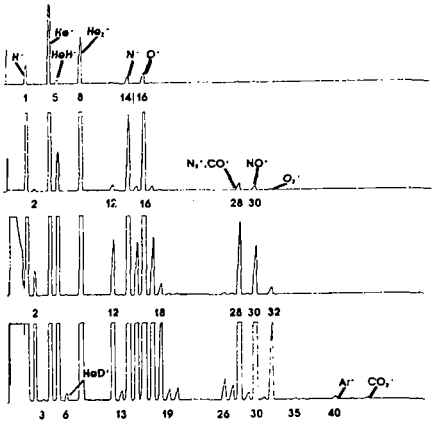


Figure 3

*N. G. Adams, D. K. Bohme, E. E. Ferguson, J. Chem. Phys. 52 5101-5105 (1970). F. C. Fehsenfeld confirms (private communication) the possibility that He_2H^+ is formed by clustering in the cold (200°K) flowing afterflow or in the sampling expansion.

LOW PRESSURE CI BY FT/MS*

Sahba Ghaderi, P.S. Kulkarni, R. B. Spencer,
E. Ledford, Jr., Charles L. Wilkins, and Michael L. Gross

Department of Chemistry
University of Nebraska-Lincoln
Lincoln, Nebraska 68588

It is well-known that conventional chemical ionization mass spectrometers require relatively high reagent gas pressures (0.1 to 1 torr) for ion molecule reactions to be observed. This requirement arises from the short ion residence times in these instruments. However, when ion trapping is employed, as in the QUISTOR[1] or in ion cyclotron resonance instruments[2], much lower pressures (ca. 10^{-6} torr) of reagent gas are sufficient to permit observation of chemical ionization mass spectra[3,4]. With the advent of Fourier Transform mass spectrometry (FT/MS)[5], it became possible to design a truly general-purpose analytical ICR mass spectrometer which would be capable of both EI and CI measurements using either positive or negative ion modes. As we have previously reported[6,7], such an instrument has been constructed in our laboratories and preliminary study of its analytical capabilities begun.

Here we report our most recent investigations of low pressure chemical ionization using the standard reagent gases methane, isobutane, water, and ammonia at pressures in the 10^{-6} torr range with a variety of analytes which were present at partial pressures about 100 times lower. Because the system was not equipped with a direct insertion probe at the outset of these studies, most of our evaluations to date have utilized fairly volatile analytes. Recently we have completed installation of a heated direct insertion probe and have begun to examine a variety of other samples which represent more realistic tests of the practical analytical capabilities of the system. With each of the reagent gases mentioned above, the first experiments were designed to determine appropriate conditions for obtaining routine and reproducible chemical ionization spectra. A key factor in choice of experimental conditions is the length of time allowed for reaction before applying the radiofrequency excitation

*This research was supported by Grant No. CHE-77-03964 and by a grant from the Gulf Research Foundation.

necessary to observe the mass spectrum. With methane, for example, the ratio of CH_5^+ (m/z=17) to $C_2H_5^+$(m/z =29) ions become constant after 100msec. Thus, when methane is the reagent gas, chemical ionization spectra are obtained by ionizing the methane at some convenient low voltage (e.g.50V), delaying 100-200 msec, rapidly (less than 1 msec) sweeping the rf excitation source through the range of frequencies where ions are expected to absorb, acquiring the data and Fourier transforming. Methane CI spectra obtained in this way are in good agreement with conventional CI spectra of representative compounds. Electron impact spectra are obtained by simply eliminating the delay time. Multiple ensemble-averaged spectra (for signal to noise enhancement) can be obtained in less than a minute.

The other reagent gases mentioned yield spectra that are good accord with published high-pressure CI data. As the delay times are accurately and precisely programmable under computer-control, it is possible to obtain time-resolved mass spectra of ion molecule reactions with time resolution in the millisecond range. Thus, the technique has considerable potential as a tool for fundamental kinetic studies of ion molecule reactions, in addition to its analytical potential. With the addition of the heated direct insertion probe, we have recently obtained positive ion CI spectra of benzaldehyde, as well as negative ion chloride CI spectra of p-nitrophenol, p-cyanophenol, and p-ethoxybenzoic acid with quantities of sample in the 50 nanogram range yielding full range spectra with usable S/N ratio. Additionally, we have demonstrated the utility of D_2O for the determination of active hydrogens in hydrocarbons.

References

1. R.F. Bonner, G. Lawson, and J.F.J. Todd, J. Chem. Soc. Commun., 1179 (1972).
2. R.T. McIver, Jr., Rev. Sci. Instrum., 41, 555 (1970).
3. R.T. McIver, E.B. Ledford, and J.S. Miller, Anal. Chem., 47,697 (1975).
4. R. L. Hunter and R.T. McIver, Jr., Anal. Chem. 51, 699 (1979).
5. M.B. Comisarow and A.G. Marshall, Chem. Phys. Lett., 25, 282 (1974).
6. E.B. Ledford, Jr., R.L. White, P.S. Kulkarni, R.B. Spencer, S. Ghaderi, C. L. Wilkins, and M.L. Gross, Abstr. No. 117, 1979, Pittsburgh Conference on Analytical Chemistry and Applied Spectroscopy.
7. S. Ghaderi, P.S. Kulkarni, M.L. Gross, C.L. Wilkins, R.B. Spencer, and E. B. Ledford, Jr., Abstr. No. 118, 1979, Pittsburgh Conference on Analytical Chemistry and Applied Spectroscopy.

TAMOC3

REAL TIME TRACE ANALYSIS BY ATMOSPHERIC PRESSURE CHEMICAL IONIZATION: SUPPLEMENTARY TECHNIQUES IN MOLECULAR ION IDENTIFICATION, N.M.REID, B.A. THOMSON, W.R. DAVIDSON, J.B. FRENCH AND J.A. BUCKLEY, SCIEX INC., 55 Glencameron Road, Thornhill, Ont., Canada.

This paper describes a series of supplementary techniques for molecular ion identification which have been developed for use with the TAGA™ 3000 (Trace Atmospheric Gas Analyser), a system which has been developed to realize the full potential of atmospheric pressure chemical ionization (APCI) coupled with mass spectrometric detection under complete micro-computer control. Instantaneous or real time analysis of trace components in a complex matrix is made possible by virtue of a combination of hypersensitivity, almost instantaneous response, the massive degree of pre-separation or preferential ionization, coupled to the production of molecular ion based spectra provided by APCI, together with the elimination of the ion clustering problems which complicated earlier APCI work .[1]

This capability of carrying out instantaneous trace analysis, under complete microcomputer control without requiring chromatographic separation, when embodied in a rugged, multipurpose design, has produced a versatile analytical system which has opened up a productive new area of the application of mass spectrometry to 'real world' problems. Results of an intensive application program with this new system have been reported in a series of publications[2,3]. These application studies have shown that this system is ideally suited for analytical situations which have been termed **"Targeted Compound-analysis in a complex matrix"**[4] as exemplified by such diverse applications as the rapid screening for pre-selected environmental contaminants in air, water or soil, the continuous monitoring of pre-selected compounds in occupational atmospheres, or the study of chemical species in dynamic systems such as industrial process development or in the medical field. However, during these studies it has been recognized that although simple, intense molecular-ion-dominated spectra can be produced by this technique from trace compounds in a complex media, as is illustrated in Figure 1, molecular weight information alone may not be sufficient to solve many of trace analysis situations encountered in the real world and that additional information is required to improve the certainty of identification of the final analysis. Several techniques for providing such supplementary information have been developed for use in conjunction with the TAGA™ over the last few years and these are described below.

1. CLASS SEPARATION BY SELECTIVE CHEMICAL IONIZATION - The general process of utilizing reactant ions produced by a primary ionization process in a carrier to ionize traces of interest in the carrier has been termed chemical ionization (CI). It has been shown that most of the reagents used in conventional 1 Torr CI can also be employed at atmospheric pressure. The first use of CI is to provide a massive degree of preferentional ionization of traces in the sample matrix, say nitrogen, air or other carrier gases so as to allow parts per billion to parts per trillion detectabilities which are typical using APCI. However this preferential or selective ionization capability can be extended to selective ionization of pre-chosen classes of traces, by judicious choice of the CI reagent. This instantaneous capability of **chemical class separation** which is provided by CI is taken advantage of in the TAGA™ system so as to substitute for **chromatographic separation** which is much slower and requires sample collection and laborious work up procedures in many cases. Examples of this are the use of $H^+(H_2O)_n$ and $O_2^-(H_2O)$ ions formed from an air carrier to carry out essentially acid or base extraction of traces instantaneously from a flowing air sample. Another example of class separation is illustrated in Figure 1 in which the $C_6H_6^+$ ion was used to preferentially ionize cyclic aromatic compounds in a complex matrix of hydrocarbon and other traces by virtue of the lowering in ionization potential produced by a conjugated ring system. **Chemical selectivity** can also be employed as in the example of the highly specific CI^- attachment to nitroglycerine[5] under the conditions existing in a TAGA™ APCI source. This produces a much lower detectability limit due to the combination of increased signal with a concomitant reduction in **chemical noise.**

2. CONTROLLED MOLECULAR ION FRAGMENTATION - This approach involves a patented programmable microcomputer controlled technique of controlling the internal energy of the declustered molecular based ions formed from selected trace compounds in the carrier, to produce a controllable molecular fragmentation. This technique provides a rich supplementary channel of information concerning the identity of the molecular ion and has been used and proven in a series of analytical situations during the last few years. This ability to control the degree of fragmentation is illustrated in Figure 2.

3. ISOTOPIC RATIO INFORMATION - if an intense molecular ion based spectrum can be produced then full advantage can be taken of the isotopic abundance information contained in the mass spectrum in any chemical compound. Figure 1 clearly illustrates the supplementary information contained in the Cl^{35}, Cl^{37} isotope ratio in chlorinated biphenyls as well as C^{12}, C^{13} ratio information. (See our companion paper). This supplementary channel has been used to great advantage in many of the application studies to date.

4. POSITIVE/NEGATIVE RESPONSE COMPARISONS - The TAGA™ System's ability to switch from positive to negative ion mode operation within seconds under programmable microcomputer control allows full advantage to be taken of improved compound assignment of a molecular mass by the comparison of the system's response in both polarity modes. Many compounds will only give a molecular ion in one polarity mode under controlled selective C.I. conditions. In other cases compounds will respond in both modes under similar C.I. conditions. This information channel can also be combined with a fast change in C.I. reagent to enhance the accuracy of the molecular ion identification process.

5. CONTEXT - In analytical situations termed "Targeted Compound Analysis" it is axiomatic that the **context** of the analytical task has played a critical role in the final choice of compounds to be monitored, screened or studied. However, in most of the application studies to date other molecular ions have been detected which were of interest to the analyst. Using various combinations of the previously described supplementary techniques together with a knowledge of the analytical context has enabled the identification of these peaks to be carried out with a high degree of confidence in many cases. This has been especially true for situations that have been described as **relatively closed**" or "**somewhat open**"[4] that is, for systems where there is some control of the entry of compounds into the system or that the entry of new compounds is possible but not likely or frequent.

In conclusion, the combination of all or any of the supplementary techniques as described above, with the instantaneous capability of producing intense molecular ion based spectra from traces in a complex media, with an analytical system under microcomputer control, has successfully opened up a new approach to trace mixture analysis. The TAGA™ system appears to offer an alternative approach to gas or liquid-chromatography mass spectrometry for certain important applications with attendant advantages of higher sensitivity and speed coupled to an enhanced ability to operate in the outside world as opposed to being limited to a laboratory setting.

1. J.B. French, N.M. Reid, C.C. Poon and J.A. Buckley, "A Solution to Ion Clustering Interference in API Mass Spectrometry", Proceedings of the 25th Annual Conference on Mass Spectrometry and Allied Topics, Washington, D.C., 122, (1977).
2. N.M. Reid, J.A. Buckely, D.A. Lane and A.M. Lovett, "TAGA™ 3000 - A New, Digitally Controlled APCI Mass Spectrometer Based System", Proceedings of the 26th Annual Conference on Mass Spectrometry and Allied Topics, St. Louis, 662, (1978).
3. TAGA™ Application Notes - SCIEX INC., 55 Glencameron Road, # 202, Thornhill, Ontario, Canada, L3T 1P2.
4. W.L. Budde, J.W. Eichelberger, "Organics in the Environment", Anal. Chem. 51(6), 567A, (1979).
5. B.A. Thomson, W.R. Davidson and A.M. Lovett, "Applications of a Versatile Technique for Trace Analysis - Atmospheric Pressure Negative Chemical Ionization", Environ. Health Perspectives, 1979. In Press.

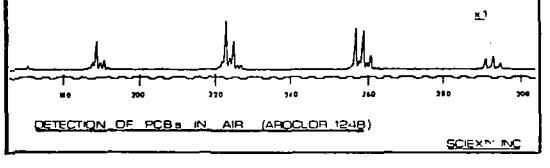


Figure 1.

Detection of PCB's in air using benzene as a CI reagent.

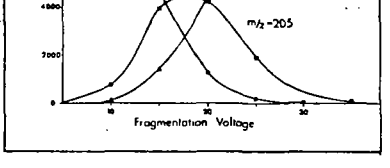


Figure 2.

Control of the degree of Molecular Ion Fragmentation in the TAGA™ System.

Electron Penetration: Characterization and Application of a Chemical Ionization Source with Coaxial Electron Entrance Aperature and Ion Exit Slit

Andreas J. Illies, Rafael Infante, Charles Polley and C. G. Meisels,
Department of Chemistry,
University of Nebraska,
Lincoln, NE 68588

A new pulsed high pressure ion source for the study of slow ion-molecule reactions and ion-molecule equilibria at near thermal energies is described. It was constructed from oxygen free copper, commercially gold plated, and installed in a modified commercial Varian MAT CH4-B mass spectrometer. (1,2)

The ion source is cylindrical and the electron entrance is coaxial with the ion exit slit. (Figure 1) The ion drift length is 2.29 cm. Two field shaping rings are included; these can be adjusted to produce parallel equipotential lines in the ion drift region over an area of about 25 $mm.^2$ (Figure 2) The source block contains a thermalizing chamber through which the sample gas passes before it enters the ionization region. The temperature is variable from 175 to 500 K and the source is operable at pressures up to 3 torr.

Sensitivity

Sensitivity studies were carried out on toluene and p-xylene using a chromatographic inlet. The studies involved selected ion monitoring of the $(M+H)^+$ ions using methane at 0.5 torr as the reagent gas. All ion intensities were monitored with the electron multiplier, whose gain had been determined by comparison with the response of a Faraday cup detector.

The limit of detection (signal/noise = 2) was 100 pg for toluene and 400 pg for p-xylene. By correlating the results of this source with an AEI MS50, which was about 10 times more sensitive, we calculate that the sensitivity of our source would be 8×10^{-11} coulomb/ g for methyl stearate.

Residence time Distributions and Mobility

Residence time distributions of Ar^+ in Ar in the limit of high pressure and low electron energy (see electron penetration below) are shown in Figure 3. The points are the experimental and the lines are the calculated distributions. (3,4) The reduced mobilities, K_o for the rare gases are presented in table I. The agreement is within 10% of the accepted literature values. (6,7)

Electron Penetration

Since the electron entrance aperature is coaxial with the ion exit slit, the residence time distributions depend on the distance which the ionizing electrons travel into the source; they are therefore sensitive to electron energy. Residence time distributions at three different electron energies demonstrate this dependence on Energy (Figure 3). Since the drift properties of the ion are known, residence times may be related to the point of ion formation or distance from the electron gun. Thereby one may obtain the range of the electrons. The Range is defined as the distance that the electron will penetrate a given substance before its kinetic energy is reduced to a value below which ionization can no longer take place; it has units of g/cm^2 (7,8) In this work range is defined as the distance from the electron entrance within which 97% of the ion formation occurs. Figure 4 shows the product of the pressure and the electron penetration in cm as a function of electron energy. This Figure demonstrates that the range is independent of pressure when expressed in units of density. Figure 4 also shows that the range is linear with electron energy in the region of 100-400 eV although this behavior is not expected to hold throughout a wide energy range. (8) Presented in table II are the ranges of electrons in the rare gases and methane. The last column gives the distance in cm that 200 eV electrons will penetrate at a pressure of 1 torr. Table II also includes an entry for the range of electrons in air determined by Cole. (8)

In the limit of low pressure and high electron energy (0.2 torr, 2000 eV) uniform ionization occurs throughout the drift region of the ion source. The experimental residence time distributions collected under these conditions can be numerically reproduced through a sum of calculated distributions as a function of the drift distance to yield an instrument function reflecting ion collection efficiencies as a function of the point of formation. Residence time distributions at lower electron energies (200 eV) can then be corrected for diffusive spread, and the instrument function to yield the initial ion concentration as a function of position of origin.

Acknowledgements

This research was supported by DOE under contract No. EY-76-S-02-2567.

Table I. Mobilities of Gaseous Ions

ION	Neutral	Ko, cm^2/v - sec This Work	Literature[5]
He^+	He	10.40±0.05	10.4±0.10
Ne^+	Ne	3.73±0.02	4.1-4.2
Ar^+	Ar	1.35±0.01	1.4 - 1.6
Kr^+	Kr	0.85±0.01	0.90
Xe^+	Xe	0.52±0.01	0.58
CH_5^+	CH_4	2.21±0.03	2.32±0.02[6]
$C_2H_5^+$	CH_4	2.06±0.03	2.29±0.02[6]

Table II. Electron Ranges

ION	Neutral	Millitorr cm/ev	cm at torr and 200 ev
He^+	He	5.68± 0.1	1.14
Ne^+	Ne	1.60±0.05	0.320
Ar^+	Ar	1.23±0.03	0.246
Kr^+	Kr	1.14±0.03	0.228
Xe^+	Xe	0.76±0.04	0.152
$C_2H_5^+$	CH_4	1.48±0.03	0.296
CH_5^+	CH_4	1.61	0.322
Air	Air	3.2	0.65

References

1. G. Sroka, C. Chang, and G. G. Meisels, J. Amer. Chem. Soc. 94, 1052 (1971)
2. G. G. Meisels, A. J. Illies, R. S. Stradling and K. R. Jennings J. Chem. Phys. 68, 866 (1978)
3. C. Chang, G. J. Sroka, and G. G. Meisels, Int. J. Mass. Spectrom. Ion Phys. 11, 367 (1973)
4. J. T. Moseley, I. R. Gatland, D. W. Martin and E. W. McDaniel, Phys. Rev. 178, 234 (1969)
5. E. W. McDaniel and E. A. Mason, The Mobility and Diffusion of Ions in Gases, Wiley, New York, 1973 Chap. 7
6. D. P. Ridge and J. L. Beauchamp, J. Chem. Phys., 64, 2735 (1976)
7. L. C. Northcliffe and R. F. Schillings, Nucl. Data, Sect. A., 7, 233 (1970)
8. A. Cole, Radiation Res. 38, 7 (1969)

Figure 1. Schematic diagram of the ion source. a is the extraction plate, b are the field shaping rings, c is the pressure sensing inlet, d is the electron gun and e is the gas inlet showing the thermalization chamber.
Figure 2. Equipotential lines and electric field lines inside the source
Figure 3. Experimental and calculated residence time distributions.
Figure 4. Residence time distribution at different electron energies
Figure 5. Linear range of electrons in Ar as a function of electron energy. The Ordinaete corresponds to electron penetration in cm at 1 torr.

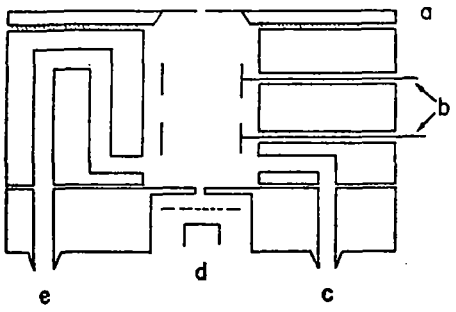


Figure 1

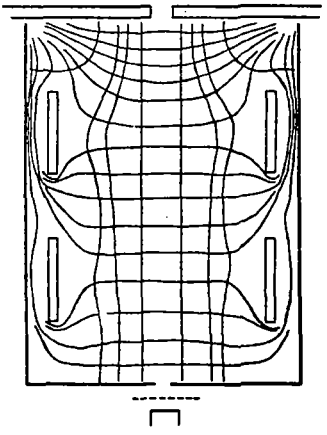


Figure 2

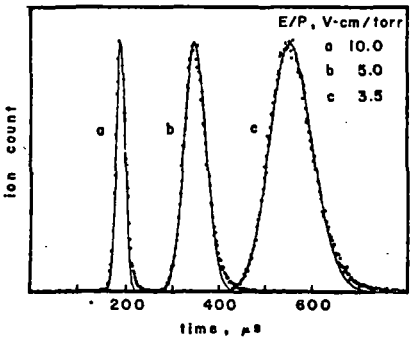


Figure 3

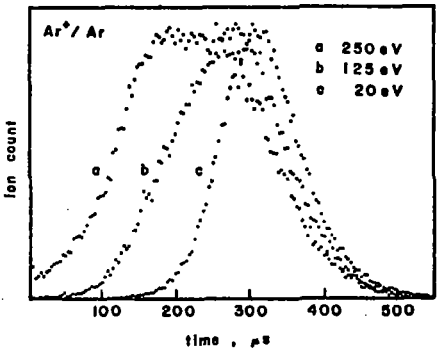


Figure 4

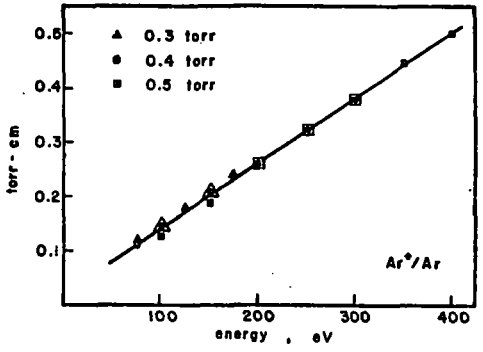


Figure 5

"FAST RADICAL REACTIONS OBSERVED BY CHEMICAL IONIZATION MASS SPECTROMETRY"

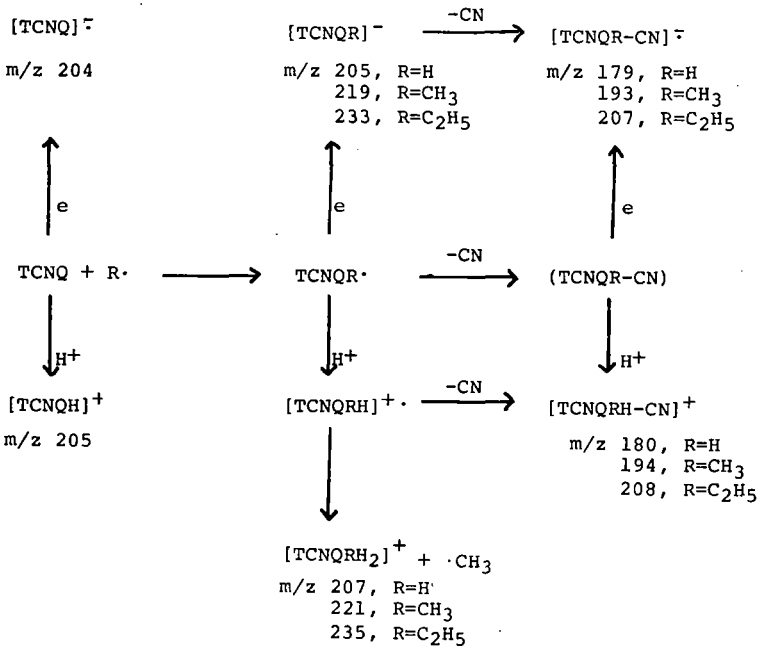
by C. N. McEwen and M. A. Rudat
Central Research and Development Department
E. I. DU PONT DE NEMOURS & CO.
Wilmington, Delaware 19898

Unusually facile alkyl radical addition to 7,7,8,8-tetracyanoquinodimethane(TCNQ) has been observed by positive and negative ion chemical ionization mass spectrometry. Products corresponding to addition of H, CH_3 and C_2H_5 to TCNQ and these additions with loss of cyanide dominate the high pressure methane negative ion TCNQ spectrum. These same additions with loss of cyanide and protonation are observed in the positive ion CI (methane) spectrum along with a series of ions corresponding to $[TCNQRH_2]^+$ where R=H, CH_3 or C_2H_5.

The proposed mechanism for formation of these ions involves initial radical addition to neutral TCNQ followed by ionization of the products as shown in Scheme I. Protonation of the radical addition products apparently produce a reactive radical cation which either loses a radical fragment or abstracts hydrogen from the reagent gas.

Pentacene, tetracyanoethylene and tetracyanopyrazine also react with alkyl radicals in the CI source. Reactive alkyl radicals are produced by hydrocarbon, ketone and various other reagent gases.

SCHEME I



STRUCTURAL ANALYSIS OF HYDROCARBON RADICALS PRODUCED IN A CI SOURCE USING COLLISIONAL ACTIVATION MASS SPECTROMETRY

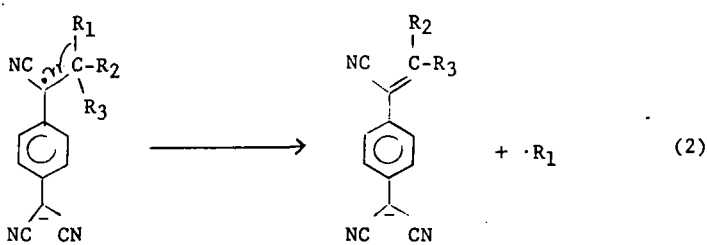
M. A. Rudat and C. N. McEwen
Central Research and Development Department
E. I. duPont deNemours & Co., Wilmington, Delaware 19898

As reported in the preceding paper, alkyl radicals from a variety of sources have been found to react with 7,7,8,8-tetracyanoquinodimethane (TCNQ) in a chemical ionization source. Collisional activation (CA)[1] mass spectrometry, in which a mass selected ion beam is subjected to collisions with a neutral gas in a field-free region to induce fragmentation of the ions, has been employed to study the structures of the radical-adduct ions and, in particular, the structures of the alkyl fragment adducts.

The ions chosen for study by CA are those represented by the reaction

$$TCNQ + R\cdot \xrightarrow{e} [TCNQR\text{-}CN]^{-} + \cdot CN \qquad (1)$$

The observed CA spectra can be envisioned as arising from an adduct ion having structure (1) decomposing by collision-induced cleavage:



(2)

1

The decomposition of the alkyl portion of the adduct ion completely dominates the CA spectra, very much simplifying interpretation. We have found that the structure of R· is maintained after formation, for C_3 and C_4 radicals. That is, n-propyl and iso-propyl radicals produce TCNQ adducts whose CA spectra show almost exclusive loss of $\cdot C_2H_5$ and $\cdot CH_3$, respectively. Primary, secondary and tertiary C_4 radicals likewise produce CA spectra of the adduct ions with predominant losses of $\cdot C_3H_7$, $\cdot C_2H_5$ and $\cdot CH_3$, and $\cdot CH_3$, respectively.

C_4H_9 radicals produced by the sequence

$$1\text{-Br-}C_4H_9 \xrightarrow{e} C_4H_9^+ \xrightarrow{e} \cdot C_4H_9$$

(ion-electron recombination) reveal through the CA spectra of the adduct ions that the $C_4H_9^+$ ion rearranged substantially from a primary ion to a mixture of primary, secondary, and tertiary ions prior to neutralization and radical formation.

Radicals of chain length $\geq C_5$ have been found to undergo intramolecular hydrogen transfer reactions by a back-biting mechanism. In spite of the resultant deterioration of the clarity of the CA spectra of the adduct ions, it has been found that different isomers give clearly different spectra that can be rationalized in terms of the back-biting mechanism.

This is the first convenient method of studying radical structures in the gas phase, and it is expected that this technique will be very useful not only in mass spectrometric studies of fragmentation mechanisms through radical cleavage, but also in the study of gas-phase intramolecular reactions of radicals, radical equilibria, radical-rich reactant systems, etc. It may also prove useful as a new analytical mass spectrometric tool.

1. P. F. Bente III and F. W. McLafferty in "Mass Spectrometry", Practical Spectroscopy Series, Vol. 3, Part B, C. Merritt and C. N. McEwen, eds., Marcel Dekker, N.Y., N.Y., 1979, Chapter 3.

5/21/79

mtk

NEGATIVE ION CHEMICAL IONIZATION MASS SPECTROMETRY OF EXPLOSIVES

Jehuda Yinon
Weizmann Institute of Science, Department of Isotope Research, Rehovot, Israel.

Chemical ionization (CI) mass spectrometry has become during the last years a commonly used method for the analysis of explosives (1-4). Various reagent gases have been used: hydrogen, water, methane, isobutane and ammonia.

Although direct CI-MS is being used for forensic identification of explosives, there are still several compounds which are characterized by considerable fragmentation. It has become common practice to use for the positive identification of an unknown explosive or explosives mixture, two different analytical techniques, for example CI and EI mass spectrometry (5).

In an effort to find an additional sensitive mass spectrometry method which can be complimentary to CI and can be applied to the same sample, we have investigated the use of negative ion chemical ionization (NCI) using isobutane as reagent, for the analysis of explosives. The use of isobutane as CI reagent facilitates the alternate recording of positive and negative CI mass spectra.

The application of NCI has been pioneered in several fields by various groups (6,7). The most likely reaction types to occur in the negative ion source with isobutane as reagent are electron resonance capture, producing low-energy electrons; dissociative electron capture, producing fragment ions; proton transfer reactions producing $(M-H)^-$ ions; and ion-molecule reactions, occuring mainly between the ions and molecules of the sample, producing ions of the type $(M+R)^+$.

Mass spectra were recorded on a Varian MAT CH7 single focusing mass spectrometer modified for CI and for negative-ion mode operation.

NCI mass spectra of TNT, nitroglycerin, PETN, RDX and HMX were recorded.

Figure 1 shows the NCI mass spectrum of TNT.

The ion at m/e 197 $(M-NO)^-$, m/e 210 $(M-OH)^-$, m/e 226 $(M-H)^-$ and the parent ion at m/e 227 are observed. It seems that the dominant reaction in TNT is proton transfer, producing the base peak $(M-H)^-$

Figure 2 shows the NCI mass spectrum of RDX.

Typical fragment ions are m/e 46 $(NO_2)^-$, m/e 93 $(NO_2HNO_2)^-$, m/e 129 $(M-NO_2HNO_2)^-$ and m/e 176 $(M-NO_2)^-$ which is the base peak. An $(M-H)^-$ peak and abundant $(M+H)^-$ peak are observed.

Adduct peaks due to ion molecule reactions are observed at m/e 252 $(M+NO)^-$ and at m/e 268 $(M+NO_2)^-$.

The sensitivity of the NCI mass spectra of the investigated explosives is in the order of magnitude as the positive ion CI mass spectra. This is because the electron multiplier is operated at a first dynode voltage of -2500 V. as for positive ions. (The accelerating voltage of the mass spectrometer is 3000 V.).

However, an increase in the kinetic energy of the impacting negative ions by applying a positive high voltage on the first dynode of the multiplier (and a higher positive voltage on the last dynode) should increase the detection sensitivity of the negative ions by one to two orders of magnitude

References

1. R.G. Gillis, M.J. Lacey and J.S. Shannon, Org. Mass Spectr. 9, 359 (1974).
2. J. Yinon, Biom. Mass Spectr. 1, 393 (1974).
3. S. Zitrin and J. Yinon, Advances in Mass Spectr. in Biochemistry and Medicine 1, 369 (1976).
4. P. Vouros, B.A. Peterson, L. Colwell, B.L. Karger and H. Harris, Anal. Chem. 49, 1039 (1977).
5. J. Yinon and S. Zitrin, J. of Forensic Sciences 22, 742 (1977).
6. R.C. Dougherty, J.D. Roberts and F.J. Biros, Anal. Chem. 47, 54 (1975).
7. D.F. Hunt and F.W. Crow, Anal. Chem. 50, 1781 (1978).

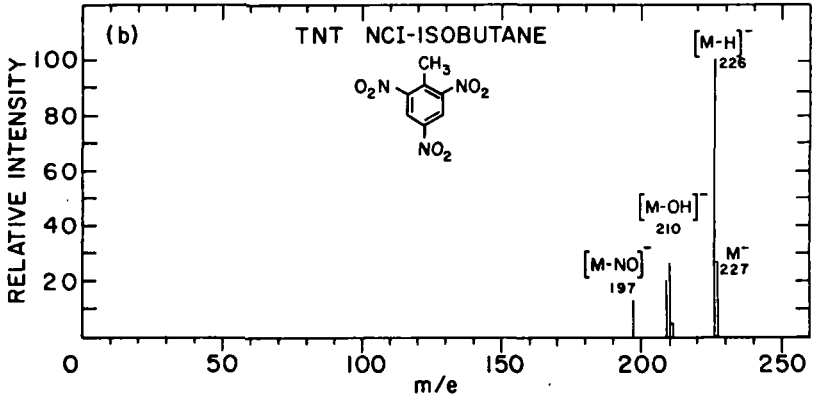


Figure 1.

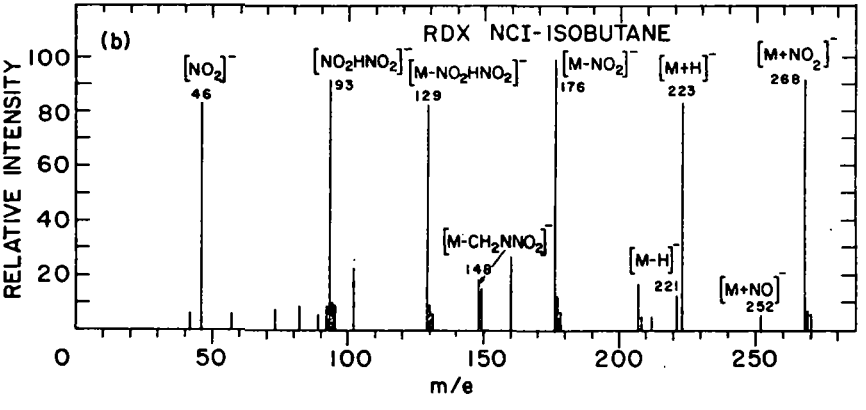


Figure 2.

ANALYSIS OF SILICONES BY CHEMICAL IONIZATION MASS SPECTROMETRY, H. GRADE and W. V. LICON, General Electric Company, Corporate Research and Development, Schenectady, NY 12309

Chemical ionization mass spectrometry (CI) has been used to great advantage in the analysis of organic materials. Its potential in the general field of organosilicones has, however, been largely ignored.[1] We report in particular the use of high resolution CI and GC-CI as being advantageous for the analysis of many classes of silicones, especially at relatively high mass (700-2000 amu), and for complex mixtures. The capability of chemical ionization is exemplified by Figure 1 in which the molecular ion region of a polymethylsilicone oligomer of molecular weight 1420 is displayed. Comparisons between CI and other ionization techniques help demonstrate the relative merits of CI for this class of materials.

[1]Coutant, J.E., Robinson, R.J., Futrell, J.H., and Elwood, T.A., 22nd Annual Conf. on Mass Spectrometry and Allied Topics, Philadelphia, May, 1974.

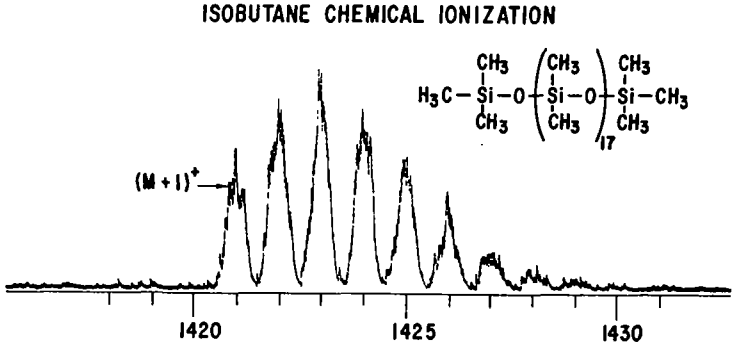


FIGURE 1

TAMOC9

AMMONIA CHEMICAL IONIZATION MASS SPECTROMETRY OF 16-MEMBERED RING MACROLIDE ANTIBIOTICS.

M. Suzuki, K. I. Harada, N. Takeda and A. Tatematsu
Faculty of Pharmacy, Meijo University, Nagoya 468 Japan

Chemical Ionization Mass Spectrometry (CIMS) is useful for structural characterization of macrolide antibiotics, which contain large lactone ring and sugar moieties. There are a few papers published in this area, however, Mitscher has reported CI mass spectra of well known macrolide antibiotics using iso-butane as a reagent gas [1].

Basic macrolide M-4365 G_2 and A_2 produced by *Micromonospora capillata* have been isolated and proposed their structures, recently by our group [2]. Concerning the CI (i-butane/NH_3) mass spectra of M-4365 G_2 and A_2 were previously reported [3], however, correct structures of amino sugar (desosamine)-derived ions and unusual behavior in hydrogen → deuterium exchange by ND_3 have been left as the unsolved problems. (cf. Fig.1 -M-4365 G_2-)

We have therefore investigated CI(NH_3/ND_3) mass spectra of the other type of macrolide antibiotics: Depoxycirramycin A_1 and Cirramycin A_1 (III,IV) and Desosaminyl-platenolides (V,VI [4]). Due to the same behaviors demonstrated in their mass spectra, CI(NH_3/ND_3) spectra of III and V were given in Figs.2 and 3, respectively.

Compared these mass spectra with that of M-4365 series, following results and discussions were obtained and developed:

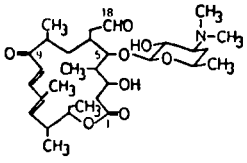
1. Protonated Molecular Ions (H → D exchange by ND_3)

M-4365 series(I,II) and Cirramycin series(III,IV) showed 5 and 6 mass-units shifting of protonated molecular ions, respectively, however, Desosaminyl platenolides (V,VI) indicated only 3 mass-units shifting in CI(ND_3) mass spectra.

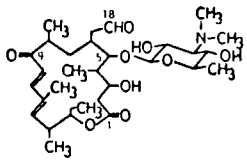
These observations suggest that excess 2 mass units in M-4365 and Cirramycin series, two hydrogen atoms at α-position of aldehyde function exchanged to deuterium by ND_3-reagent gas, through enolization mechanism.

2. Aglycone-derived Ions

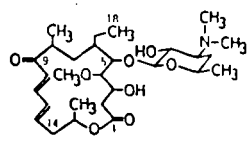
As shown in Figs.1,2 and 3, aglycone-derived ions of each series of macrolides exhibit similar two kinds of ions in CI(NH_3) mass spectra, and their structures were supported by individual shifting value in CI(ND_3) mass spectra. However, protonated aglycone-ion species observed even in CI(NH_3) mass spectra depending reagent-gas pressure. The cleavage producing aglycone-derived ions occures on both sides of glycosidic bond (A and B) in every cases. (cf., Fig.4.)



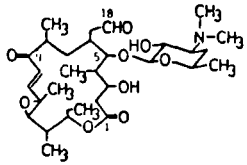
M-4365 G_2 (I)



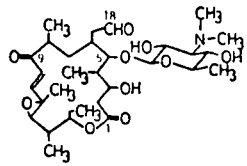
Depoxycirramycin A_1 (III)



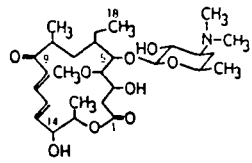
5-O-Desosaminyl-platenolide I (V)



M-4365 A_2 (II)



Cirramycin A_1 (IV)



5-O-Desosaminyl-14-hydroxy-platenolide I (VI)

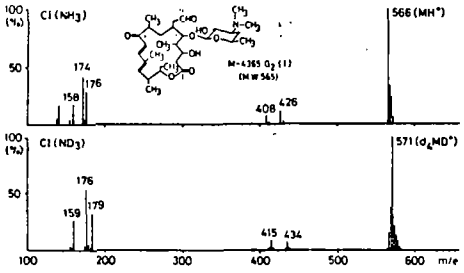


Fig.1.

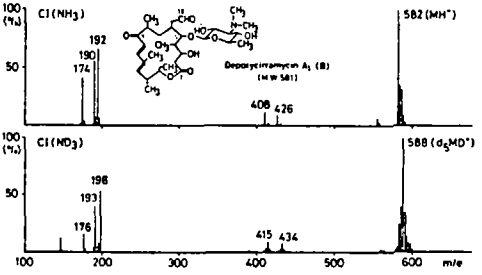


Fig.2.

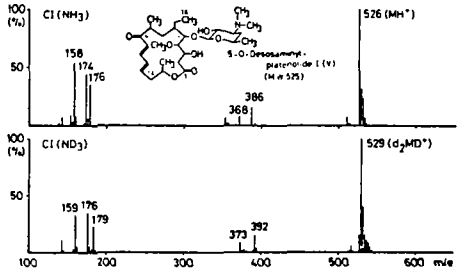
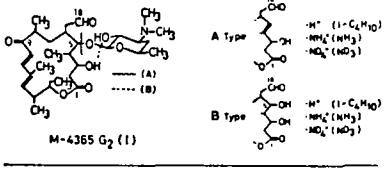


Fig.3.



	CI(-C_4H_{10})	CI(NH_3)	CI(ND_3)	Δu
(A)	m/e 391	m/e 408	m/e 415	7
(B)	409	426	434	8

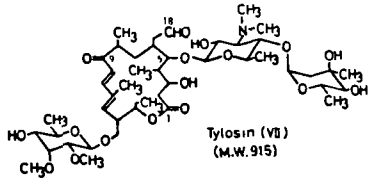
Fig.4.

Table I.

Amino Sugar-derived ions in CI Mass Spectra

Tylosin (mycaminose)			
CI (i-C_4H_{10})	m/e 192 (22.8)	m/e 190 (11.5)	m/e 174 (21.1)
CI (NH_3)	m/e 192 (47.7)	m/e 190 (10.7)	m/e 174 (11.4)
CI (ND_3)	m/e 196 (35.9)	m/e 193 (11.1)	m/e 176 (7.1)
Angolamycin (angolosamine)			
CI (i-C_4H_{10})	m/e 176 (14.9)	m/e 174 (11.1)	m/e 158 (30.7)
CI (NH_3)	m/e 176 (10.0)	m/e 174 (4.0)	m/e 158 (8.3)
CI (ND_3)	m/e 179 (13.0)	m/e 176 (7.1)	m/e 159 (3.8)

( )··· relative intensity.



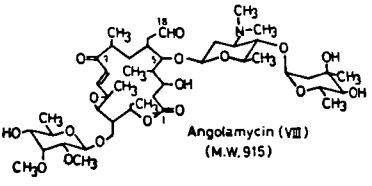
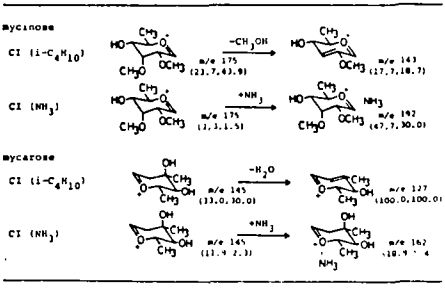


Table II.

Neutral Sugar-derived ions in CI Mass Spectra



( )··· relative intensity of Tylosin(VII) and Angolamycin(VIII), respectively

3. Sugar-derived Ions

3-1. Amino Sugar-derived Ions: From the behavior of CI(NH_3/ND_3) mass spectra of M-4365 series, we have proposed the structures of three kinds of desosamine-derived ions [3]. These proposals have now been supported by the same (Desosaminyl platenolide series) and rationally shifting (Δ 16 u; Cirramycin series) behaviors. Besides, high resolution mass spectral data [CI(i-butane)] have also supported completely the structures of such fragment ions (error, ± 3.5 mmu).

These results established the ion-structures, and simultaneously, they made clear that amino sugar-derived ions were produced by both-sides cleavage on the glycosidic bond in macrolide molecules. Furthermore, highest m/e ions (m/e 176-desosamine; m/e 192-mycaminose) are really charasteristic ions in CIMS.



R=H : m/e 176 (m/e 179)
R=OH : m/e 192 (m/e 196)

R=H m/e 158 (m/e 159)
R=OH . m/e 174 (m/e 176)

R=H : m/e 174 (m/e 176)
R=OH m/e 190 (m/e 193)

( ) ND_3 as reagent gas

3-2. Neutral Sugar-derived Ions: In order to determine the fragmentation pattern of neutral sugar moieties in macrolide molecule, we have measured CI(NH_3/ND_3) mass spectra of Tyrosin (VII) and Angolamycin (VIII). Both macrolides contain same neutral sugars, Mycinose and Mycarose, but different amino sugars, Mycaminose and Angolosamine with each other. The fragment ions and their shifting behaviors of producing amino sugar- and neutral sugar-derived ions are listed in Table I and II.

The results of producing amino-sugar ions were completely identical with above mentioned conclusions. On the other hand, concerning the neutral-sugar ions, they were clealy obtained from one-side cleavage of glycosidic bond in macrolide molecules.

Total results thus obtained from three series of macrolides: The behavior of glycosidic-bond cleavage in macrolide molecule is quite different depending upon the nature of containing sugar moieties, and the key step of fragmentation mechanism of amino-sugar moiety is "proton bridge formation" between glycosidic-oxygen and dimethyl amino-nitrogen atoms in each amino sugar.

These results are practically powerful for the characterization of macrolide molecule, and now, we are going to elucidate the structure of new family of 16-membered-basic macrolide antibiotics, applying CI(NH_3/ND_3) mass spectrometry and ^{13}C-NMR spectroscopy combination analysis.

References

1. L. A. Mitscher, H. D. H. Showalter, J. Chem. Soc. Chem. Comm., 1972, 796 and L. A. Mitscher, H. D. H. Showalter, R. L. Foltz, J. Antibiotics, 1973, 26, 55.
2. A. Kinumaki, K. I. Harada, T. Suzuki, M. Suzuki, T. Okuda, J. Antibiotics,1977, 30, 450.
3. M. Suzuki, K. I. Harada, N. Takeda, A. Tatematsu, Heterocycles, 1977, 8, 199.
4. I. Maezawa, A. Kinumaki, M. Suzuki, J. Antibiotics, 1978, 31, 309.

TAMOC10

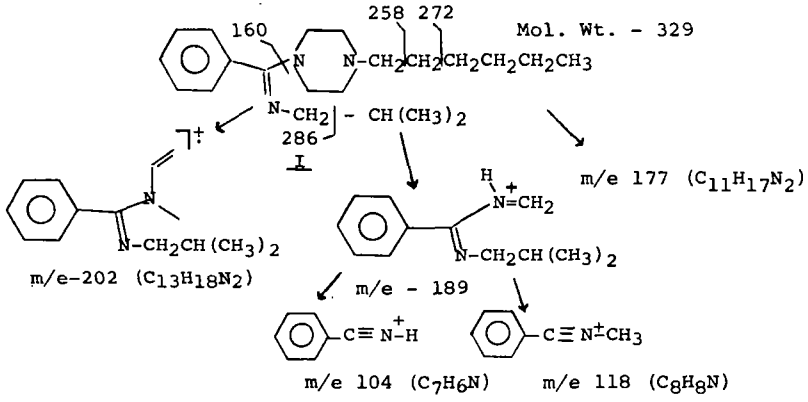
MASS SPECTRAL STUDIES ON THE MOLECULAR FRAGMENTATION AND URINARY METABOLISM OF A NEW ANTIARRHYTHMIC AGENT, N-HEXYL-N^4-(ISOBUTYLIMINOBENZYL)-PIPERAZINE, USV G-233.

M. O'Hare, R. Biniakewitz and J. Shroff,
USV Pharmaceutical Corp., Tuckahoe, NY 10707.

The experimental drug, USV G-233, has been investigated with respect to its molecular fragmentation under electron ionization and the detection of its urinary metabolites by chemical ionization mass spectroscopy.

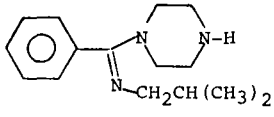
I. Molecular Fragments:

The molecular fragmentation of the title compound, I, was determined from precise mass measurements, deterium labelling and metastable defocusing studies. The fragment ions shown below represent unimolecular decompositions from the molecular species. Several of these processes involve cleavage of the piperazine ring accompanied by multiple hydrogen migration to basic nitrogen centers.



2. Detection of Urinary Metabolites:

A procedure was developed for the detection of *in vivo* urinary metabolites by stable isotope dilution and chemical ionization mass spectroscopy with a solid sampler. Accordingly, a (1:1) mixture of the unlabelled drug and its D_5-version were administered to two male beagle dogs. The urine was collected over a 6 hr. period, and extracted at pH 8. The organic residue was analyzed by direct chemical ionization (isobutane) mass spectrometry. Unequivocal detection of metabolites is demonstrated by the appearance in the mass spectrum of twin peaks of equal intensity separated by 5 amu. A metabolite of molecular weight 245 was detected and has been identified as a monosubstituted piperazine, II. This component is presumably formed by enzymatic oxidation of the N-hexyl substituent.



II Mol. Wt. 245

TAMOC11 DIRECT CI-MS ANALYSIS OF ESTROGEN IN PREGNANCY URINE, J. M. L. MEE, International Health Service, Ltd., Research Laboratories, Honolulu, Hi. 96816., and B. Halpern, University of Wollongong, Dept. of Chemistry, N.S.W., Australia.

A rapid procedure has been tested for analyzing and monitoring urinary estrogen by direct chemical ionization mass spectrometry(CI-MS). The identities of the estrogen molecules could be confirmed from their CI mass spectra which showed the presence of the protonated molecular ion $(MH)^+$ and the dehydrated ion species. Estriol in pregnancy urine were quantitatively determined using stable isotopically labelled analog as internal standard and the mass spectral results were compared with those obtained by a fluorescence method. The new analysis requires no chromatographic separation and permits rapid detection and measurement of estrogen level in 100 ul pregnancy urine. The analysis is reproducible (C.V. = 3.0%) and the instrument turnaround time is about 5 minutes.

SELECTED ION RECORDING DATA SYSTEM

L. K. Barden, R. L. Tate, A. R. Shultz, Computer Systems Laboratory, NIH
S. P. Markey and J. A. Oliver, Laboratory of Clinical Science, NIMH,
Bethesda, MD. 20205

Introduction

A data system specifically designed for selected ion recording in a biomedical research environment has been developed over the past three years. The purpose of embarking on this project was to tailor a system for repetitive quantitative analyses. The system was to be sufficiently versatile to permit programming changes as the tasks, equipment, and personnel change; transportable to other laboratories in other institutions because it has been developed in the public domain; and offer precision and accuracy exceeding commercial general purpose mass spectral data systems. SIRS is the result of this development effort. It is now routinely functioning for quantitative analyses on either quadrupole or magnetic sector mass spectrometers.

Hardware: The following components were selected for system reliability, wide dynamic range, and precision of control and recording.

Computer - DEC PDP-11/10 with 28K words of core memory, EAE, AR-11, serial and parallel digital digital interfaces.

Hard Disk - DEC RL-11 5.2 Mbyte cartridge disk.

Floppy Disks - DEC RX-11 dual floppy disks (256 Kbyte each).

X/Y Scope - Tektronix 607 variable persistence storage scope.

Printing Terminal - DEC LA-36 DECwriter II.

Graphics Terminal - Tektronix T4010.

Isolation - Optical isolation on all digital data and control lines, isolation transformers on computer and A/D converter a.c. power lines, isolated d.c. power supply for D/A converter

A/D Converter - Phoenix Data model 7215 autoranging 15 bit 20,000 conversions/sec, 1,000,000/1 dynamic range

D/A Converter - DATEL HR 16B

Accelerating Voltage (for magnetic sector instruments) - TREK model 608A programmable 200 - 5000 V high voltage power supply adapted by the manufacturer for mass spectrometer specifications (0-10 V control).

Software: All programs, except the time critical data acquisition routines, are written in FORTRAN. The entire system software is partitioned into program modules which operate under RT-11, a standard DEC mini-computer operating system. The operating system permits the user to modify or expand SIRS programs as well as utilize general purpose routines available from other sources.

While the SIRS software is written as stand-alone programs, the transition between modules is handled automatically and is essentially invisible to the user. Terse responses and default options accelerate user interaction in all modules.

Initialization: The initialization program supervises the selection and storage of basic operating parameters necessary for selected ion recording (spectrometer selection, mass values, retention time windows, etc). These parameters may be stored for recall and use in later runs.

Calibration: The calibration program permits the user to tune the spectrometer under computer control and observe peak shapes in real-time. Automatic mass scale calibration is performed on keyboard command after spectrometer tuning is complete.

Data Acquisition: This module signals the operator for injection start, records and displays up to five ions on a logarithmic scale during the selected time window, and then offers the options of repeating the previous injection, advancing to a new file automatically, incrementing the file number, or proceeding to data analysis.

End Run Analysis: Data previously acquired from individual sample injections can be processed via linear display of mass chromatograms, specification of time windows for integration, and specification of desired height and area ratios.

Automatic Multi-sample Analysis: After the operations for peak ratio measurement are specified in End Run Analysis, this program applies the same set of analytical operations to the other data files in that series without further user interaction.

Conclusion: The SIRS system is in routine use in our laboratory and has been tested by comparison with analog peak switching devices and commercial data systems. It offers significant improvements in operation, signal handling quality, dynamic range and speed. Operator's and system reference manuals are in preparation. Complete source copies of the software and hardware engineering drawings are available.

TAMP2

DATA COMMUNICATION FOR COMPUTER ASSISTED AMINO ACID SEQUENCE DETERMINATION

R. J. Madden, M. E. Jackson and R. A. Day, Department of Chemistry, University of Cincinnati, Cincinnati, Ohio 45221

Objective: To provide simple, inexpensive data communications from a VG 2025F2 (PDP-8/E) to an AMDAHL 470.V6 in order to transfer amino acid sequence containing information for higher order processing.

Introduction: Data systems for mass spectrometers enable large quantities of data to be handled in a convenient manner. However, higher order processing of these data by individual users generally requires an intimate knowledge of machine or assembly language programming. Also generally associated with such processing and archival storage is a sizable expenditure in under-utilized peripherals. This was the situation in our laboratory.

Upon the discovery of the various peptide derivatization reactions, it was realized that the need existed to be able to search large data files for specific ions and assimilate these data to decide on the amino acid sequence. It was then decided to design a system that would enable data to be transferred to a central computing facility via the most simple and least expensive way possible.

The specific reaction utilized for sequence determination is the sequential degradation of a peptide chain by 1,2-naphthoquinone.

The 1,2-naphthoquinone-peptide reaction: The 1,2-naphthoquinone reaction as reported in R. A. Day and Koka J., ACS National Meeting, September 1978, gives amino acid sequence information as a function of the relative position in the original peptide chain. This information comes in the form of reaction product type and relative yield of those products. The closer to the N-terminus, the greater the relative yield of the corresponding oxazinone and its characteristic ions. Additionally, the closer to the C-terminus, the greater the relative yield of the corresponding oxazole and the lower the relative yield of the oxazinone products this is seen in diagram I.

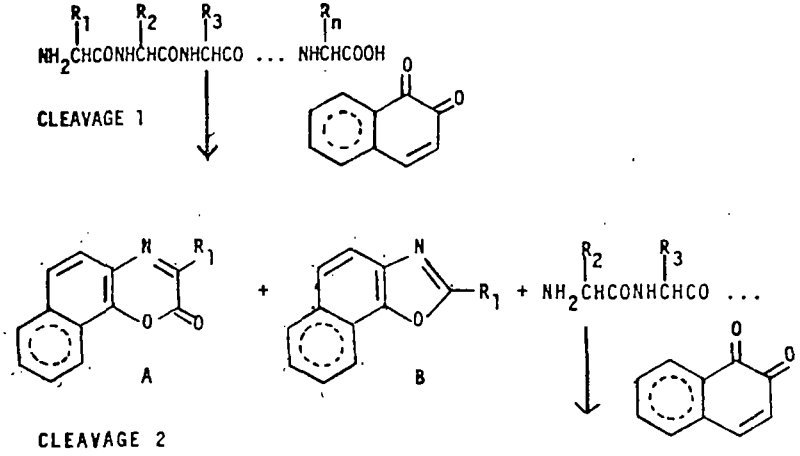


Diagram I Sequential Degradation of Peptides by 1,2-Naphthoquinone.

Data hardware description: The key piece of hardware is an additional asynchronous port, in this case a KL-8JA, added to our PDP-8/E (VG 2025F2). Additionally, a special cable is needed to connect the KL-8JA to an asynchronous originate-only modem (Anderson-Jacobson m/n 242 A). This enables an RS-232C port to accoustically couple with a standard telephone line.

This when coupled with the existing teleprocessing system at our central computing facility comprises the total of the system hardware.

Data link software description: In order to enable the hardware to function a small handler program had to be generated to support the second asynchronous port. This program proved to be simple and straightforward because of OS-8 user service routines (USR) provided by Digital Equipment Corporation (DEC) and through the ability to set the device code of the second port.

The final portion of the system was entrance into the central computing facility (AMDAHL) 470/V6). This was accomplished via use of the teleprocessing system WYLBER. Here, an "active" file was generated in the WYLER "collect" mode and thus the file being transferred could be held until data transfer was completed and disc storage effected.

Conclusion: The data transmission is completely effective. Once transferred, the full capabilities of the central computing facility are at the disposal of the individual user. Such peripherals as large discs, magnetic tape drives, high speed line printers and flat bed plotters become available for use. Also due to the nature of most central facilities, the amounts of memory available and software support make higher order processing well within the experience of most laboratories. Thus, the off-line sequence determination program, which in this case requires 256K bytes of memory runs in approximately 1.8 seconds.

Finally, the problem of data management is solved both in library storage and search/retrieval.

On the critical side, the transmission rate and overall time is dependent on baud rate and extent of character set available to the user.

A Microcomputer-based GC-MS Controller. T. Clem, W. Comstock, and H. M. Fales, Biomedical Engineering and Instrumentation Branch and Laboratory of Chemistry, NHLBI, NIH, Bethesda, MD 20205

Although there is no question that for maximum utility the data from a GC-MS system should be processed by a computer, not all laboratory situations can make equally effective use, nor justify the expense of such a system. Furthermore, in our opinion most modern GC-MS data handling systems leave much to be desired in terms of true, usable dynamic range, automatic detection and adjustment of base line (thresholding), detection of metastables and doubly charged ions, indication of noise level, and mass marking. For these reasons, we have preferred to maintain our LKB-9000 spectrometer in its original form but a method of operation was sought wherein, for routine samples, attendance at the console was unnecessary.

We have designed an Intel 8080-based microprocessor system using a PROM and limited amount of RAM which autmatically performs the following tasks formerly carried out by the operator:

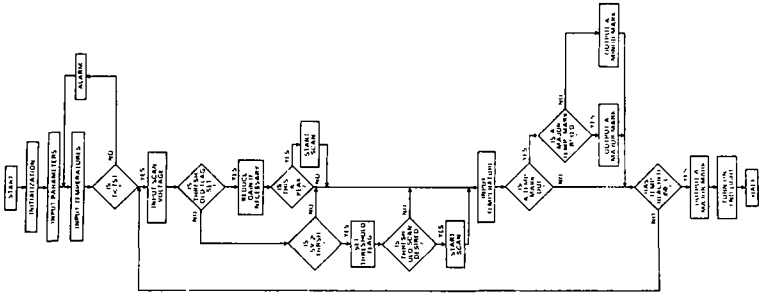
1. Marks the GC chart paper every 10°C with a different mark every 50°.

2. Scans the GC peak either when the signal exceeds and returns to a threshold value, or just after the peak maximum or both, as desired.

3. Attenuates the multiplier gain when the GC peak goes offscale, resetting automatically as it returns. This may be disabled for weak, high mass ions, metastables, etc.

4. Marks both GC and oscillograph chart simultaneously every fifth scan to aid in correlating GC peak and mass spectrum in complex chromatograms.

A simplified flow chart of the microprocessor program follows:



The system has been performing well in our laboratory for several months. During development, it was relatively easy to reprogram via the PROM chip as our requirements were updated. The PROM also enables others to modify the systems of operations to meet their own requirements.

The cost of parts is approximately $1500 and our programs are available in machine code either in paper tape or PROM form.

DATA TRANSFER BETWEEN AN INCOS DATA SYSTEM AND A VARIAN 620/L-100 MINICOMPUTER*

W. D. JAMIESON, E. W. DYER and F. G. MASON
Atlantic Regional Laboratory, National Research Council,
1411 Oxford Street, Halifax, N.S., Canada, B3H 3Z1

AND

M. WEISS
Finnigan Instruments, Sunnyvale, California, 94086

Three mass spectrometry instruments had been interfaced non-concurrently with a VARIAN 620/L-100 minicomputer (1, 2). An INCOS data system (dual acquisition, dual terminal) interfaced with two other mass spectrometers was installed. Cable distance between the two computer systems was about 60 metres. We investigated modifications to the VARIAN and INCOS systems which would make possible hardwired data transfers at 9600 baud (serial 8-bit binary) between the two systems. The data transfer rate was limited to this value by the existing I/O hardware although higher rates are probably feasible.

Minor modifications were made to the existing hardware. The software needed was developed in assembly language, partly on each system. The general scheme of the working system we have developed is shown in the Figure. Details of the hardware modifications and of the software developed are available on request to the authors.

Although the data transfer capability developed is widely useful, our applications have been to transfer VARIAN-acquired mass spectral data for processing by the INCOS system and to use VARIAN peripherals for archival data storage. The major use foreseen is transfer of VARIAN-acquired photoplate-derived high resolution mass spectral data for INCOS processing. A feature of the system developed is that INCOS-resident software accesses the VARIAN minicomputer in the same way that INCOS peripherals are accessed.

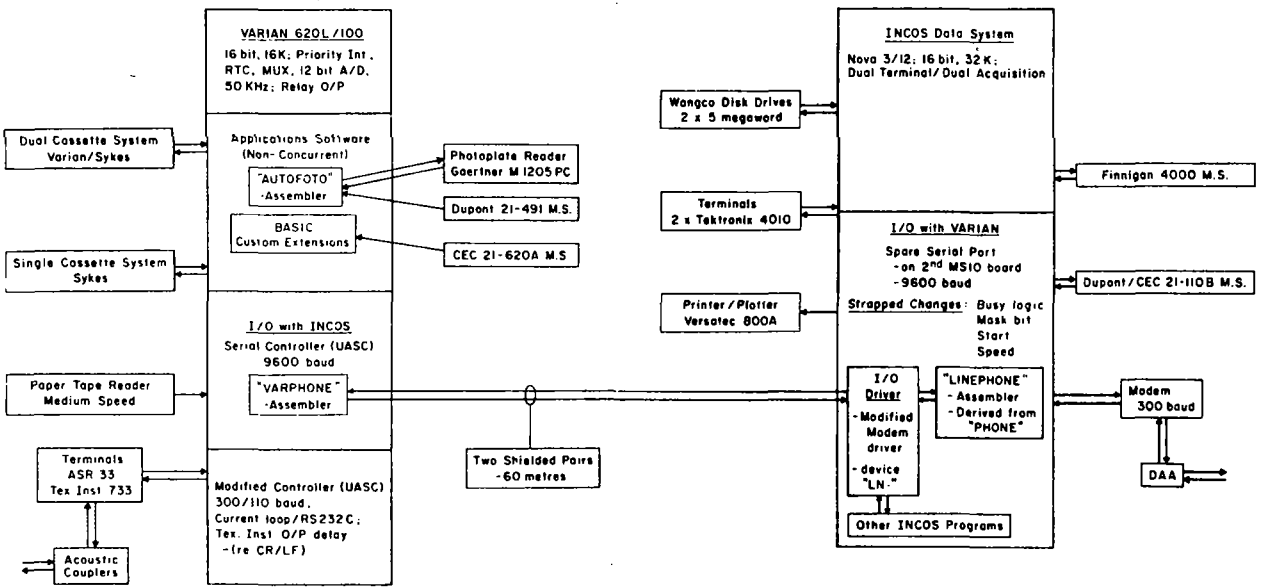
REFERENCES

1. W. D. Jamieson and F. G. Mason. Paper presented at the 23rd Annual Conference on Mass Spectrometry and Allied Topics, Houston, Tex., 1975. Proc., pp. 222-224.

2. W. D. Jamieson and F. G. Mason. Paper presented at the 25th Annual Conference on Mass Spectrometry and Allied Topics, Washington, D.C., 1977. Proc., pp. 668-670.

---

*NRCC No. 17525


VARIAN 620L/100
16 bit, 16K; Priority Int., RTC, MUX, 12 bit A/D, 50 KHz; Relay O/P
Applications Software (Non-Concurrent)
"AUTOFOTO" -Assembler
BASIC Custom Extensions
Photoplate Reader Gaertner M 1205 PC
Dupont 21-491 M.S.
CEC 21-620A M.S
Dual Cassette System Varian/Sykes
Single Cassette System Sykes
I/O with INCOS
Serial Controller (UASC) 9600 baud
"VARPHONE" -Assembler
Paper Tape Reader Medium Speed
Terminals ASR 33 Tex Inst 733
Acoustic Couplers
Modified Controller (UASC) 300/110 baud, Current loop/RS232C; Tex. Inst O/P delay -(re CR/LF)
Two Shielded Pairs -60 metres
INCOS Data System
Nova 3/12; 16 bit, 32K; Dual Terminal/Dual Acquisition
Wangco Disk Drives 2 x 5 megaword
Terminals 2 x Tektronix 4010
Printer/Plotter Versatec 800A
I/O with VARIAN
Spare Serial Port -on 2nd MSIO board -9600 baud
Strapped Changes: Busy logic Mask bit Start Speed
I/O Driver -Modified Modem driver -device "LN-"
"LINEPHONE" -Assembler -Derived from "PHONE"
Other INCOS Programs
Finnigan 4000 M.S.
Dupont/CEC 21-110B M.S.
Modem 300 baud
DAA

IMPROVEMENTS TO PBM AND STIRS FOR COMPUTER IDENTIFICATION OF UNKNOWN MASS SPECTRA

I. K. Mun, K. S. Haraki, B. L. Atwater(Fell), K. J. Bierre, K. Hosokawa, R. Venkataraghavan and F. W. McLafferty

Department of Chemistry, Baker Laboratory, Cornell University, Ithaca, New York 14853

Substantial improvements to the Probability Based Matching (PBM) system[1] have resulted from two major modifications. The "confidence value" ratings (such as K and ΔK, indicating the degree of match) and their modifiers (such as molecular ion presence, number of flags, and degree of skewing) are converted to their statistically determined probabilities before ranking the selected reference spectra. Secondly, to compensate for mass discrimination differences between reference and unknown spectra, the unknown peak abundances are automatically "skewed" as a function of mass and rerun through PBM to see if a better match is achievable.

Improvements to the program for molecular weight prediction using the Self-Training Interpretative and Retrieval System (STIRS) include abundance weightings based on the statistics of the condensed reference file (not the complete file), computer recognition of Cl/Br isotopes, and more accurate definitions of illogical neutral losses. Now molecular weight predictions are >90% accurate for the first choice and >95% for the first and second, as compared to the previous performance of 83% and 90%, respectively. A new list of 192 substructures selected from ∿10,000 candidates show an average recall of ∿70% with only 0.31% false positives, compared to 55% recall with 1.4% false positives for the previous list of 101 substructures. For the average unknown STIRS can identify correctly 8 nodes (non-H atoms), with one nearly correct and 0.5 incorrect.

[1]R. Venkataraghavan, H. E. Dayringer, G. M. Pesyna, B. L. Atwater, I. K. Mun, M. M. Cone and F. W. McLafferty in "Computer-Assisted Structure Elucidation", D. H. Smith, Ed., American Chemical Society, Washington, D.C. (1977), pp. 1-17.

PREDICTING MASS SPECTRA: APPLICATIONS TO STRUCTURE ELUCIDATION.

A. LAVANCHY, N.A.B. GRAY, D.H. SMITH, AND B.G. BUCHANAN,
Dept. of Chemistry, Stanford University, Stanford, CA 94305.

With GC-MS-systems now routinely available, computer aided structure identification from mass spectral data is now of great importance. We describe here a method for structure elucidation which makes use of mass spectral data by comparing predicted mass spectra for candidate structures for an unknown compound with the observed spectrum. Three steps can be distinguished:

1) SELECTION OF PROBABLE CANDIDATE STRUCTURES FOR THE UNKNOWN COMPOUND: This selection can be done ether intuitively by the chemist or more systematically by computer. For computer selection, we are currently using two interactive programs. The first (CONGEN) [1] generates all isomers (the candidate structures) of a given molecular formula within user-defined constraints. The second (REACT) [2] allows definition of reaction pathways which are used to generate biosynthetically plausible candidates from a given precursor.

2) PREDICTION OF FRAGMENTATION PATTERN. We have developed two methods for prediction of mass spectra, which differ by the theory used for the prediction. The first is based on the so-called "half-order theory". This theory, an extension of a theory allowing all bonds to cleave, specifies limitations on the kind and number of cleavages, the allowed transfers of neutral species such as hydrogen and the number of steps per process, and associates with each process a given plausibility. The predictions of this theory can be improved by including specific substructural cleavages, e.g., alpha-cleavage, McLafferty rearrangement. The second method takes as input a set of specific fragmentation rules which control the fragmentation processes. A rule contains information about the bonds to cleave, the substructural environment of the cleavage, the charge location, the accompanying neutral transfers, the probable intensity range of the derived ions and a factor expressing "confidence" in the occurrence of the process.

The half-order theory is very useful for general cases allowing quickly a significant reduction in the number of probable candidate structures. The rule-based prediction is slower and depend on the quality of the selected rules, but leads to high performance and discriminatory power for specific classes of compounds.

3) RANKING. The ranking of the candidates is based on the match between the predicted and observed spectra. Different scoring functions are used for each method of prediction. For the half-order theory the score for a predicted and observed ion is the product of the plausibility and the i) ion mass, ii) ion's observed intensity or iii) product of the ion mass and the ion's observed intensity. In the rule-based prediction method the score for a predicted ion is of the form $W^*(X \text{ or } -Y)$ or $W^*(Z \text{ or } 0 \text{ or } -Y)$, where X is the contribution when the peak is observed; Y the contribution when a peak is not observed (e.g., X=Y=1); Z the contribution when the observed peak is in the predicted intensity range; 0 the contribution when the observed peak is not in the predicted intensity range and W is a weighting factor (average peak mass or confidence factor or the product of both). The total score is the sum of the scores for all predicted ions.

APPLICATIONS: EXAMPLES AND RESULTS

EXAMPLE 1 : HALF-ORDER THEORY. This example illustrates the identification of the (constitutional) structure of an ester of molecular formula $C_{10}H_{11}O_2N$ based on the low resolution mass spectrum. The following substructural information was available and given as constraints for the generation of plausible candidate structures using the CONGEN program: the compound contains a benzyl group, a methyl ester group and an additional carbonyl function, but does not contain primary amine, cyanide or aldehyde functional groups. The program generated 39 structural candidates. In a second step the 39 candidate structures were ranked based on the correlation between the predicted and observed spectrum. Following score/frequency distribution was obtained: (29/3) (28/3) (27/1) (14/2).... Structures having a score less than or equal to 14 can be excluded in this example because such scores are clearly very poor compared to the highest score, leaving seven structures. A new ranking including two substructural cleavages (high plausibility of cleavage of X-C in X-C=O and X-C-NH) improved the separation of the top ranked structures leading to the following score/frequency distribution: (21/1) (20/2) (19/1) (18/1) (17/1) (16/1). In both rankings the correct structure had the best score.

EXAMPLE 2 : RULE-BASED PREDICTION. The problem consists of the identification of the (constitutional) structure of a natural occurring 4-demethyl marine sterol of molecular weight 426. Under the assumption that the nucleus is that of 5α-androstane-3β-ol (Δ^5, Δ^7 or $\Delta^{5,7}$) and the side chain is biosynthetically related to the desmosterol side chain, 214 candidates were generated by the REACT program [3]. The spectrum was analyzed in two steps: 1) identification of the sterol nucleus; and 2) identification of the side chain. In the first step, 16 rules, selected on the basis of a computer analysis of the high resolution mass spectra of 23 known marine sterols, were used to predict the fragmentation pattern of the different nuclei. The score based on comparison of predicted and observed spectra (scoring functions = Confidence * (1 or -3)) gave a score of 17.7 for the Δ^5, 10.6 for the Δ^7 and 7.7 for the $\Delta^{5,7}$nucleus, thus the nucleus of the unknown sterol is probably Δ^5-androstan-3β-ol. In the second step, the 99 candidates containing the Δ^5 nucleus, were analyzed using 10 empirically chosen fragmentation rules involving side chain cleavages and the scoring function used in step 1. The score / frequency distribution obtained was: (7.7/1) (6.8/10) (5.0/2) (4.6/9) (2.0/1)... The top-ranked (score 7.7) structure is Δ^{25}-24-isopropylcholesterol and was confirmed by NMR[4]. The second best-ranked structures (score 6.8) have all a 25-26 unsaturation in common.

REFERENCES:

1) C.J. Cheer, D.H. Smith, and C. Djerassi, **Tetrahedron**, 32, 1807 (1976).

2) T.H. Varkony, R.E. Carhart, D.H. Smith, and C. Djerassi, **J. Chem. Inf. Comp. Sci.**, 18, 168 (1978).

3) T.H. Varkony, D.H. Smith; and C. Djerassi, **Tetrahedron**, 34, 841 (1978).

4) W.C.M.C. Kokke, W.H. Fencial, C.S. Pak, and C. Djerassi, to be published.

ADVANCED SOFTWARE FOR A LOW-COST GC/MS

Jeff Justice
Hewlett-Packard Company, 1601 California Avenue
Palo Alto, CA 94304

A new set of software has been developed for the HP5992 GC/MS that uses the HP9825 computer and one to four HP9885 floppy disk drives. The features of the system are:

1. All spectra can be saved during GC runs. Each diskette can hold about 15 minutes of data. Storage can alternate between drives for unlimited storage space. Extracted ion chromatograms can be reproduced twenty per pass and integrated six per pass. Data acquisition mode can be changed during the GC run between saving all spectra and only saving the spectra that occur at GC peaks.

2. SIM data can be acquired 20 ions at a time. It may be integrated six ions per pass or reconstructed 20 ions per pass.

3. Both scan and SIM data are normalized to the DFTPP standard with the software.

4. Ten procedure files are available for storing the default conditions for data gathering and analysis.

5. A library of 375 drugs and 540 polutants is supplied with the software. Another library with up to 6464 entries can be filled by the user. Library search speed is greater than 100 spectra per second.

6. The quadrupole can be tuned for maximum sensitivity at one of eight masses.

7. A second data system can be added for less than $20,000 for off-line processing of the acquired data. This doubles the data processing power.

MODIFICATION OF THE DUPONT 094B DATA SYSTEM FOR REAL TIME CAPABILITY AND ENHANCED POST-RUN PROCESSING. JEROME J. SOLOMON AND LEE M. MORIN, LAB. ORG. CHEM. AND CARCINOGENESIS, INST. ENV. MED. AND DEPT. OF MICROBIOLOGY, NEW YORK UNIV. MED. CENTER, NEW YORK, N.Y. 10016

THE DUPONT 094B DATA SYSTEM HAS BEEN MODIFIED IN ORDER TO OBTAIN A PLOT OF THE TOTAL ION CURRENT DURING DATA ACQUISITION AND TO STOP AND RESUME DATA ACQUISITION WITH REDISPLAY OF RESULTS IN TERMS OF RETENTION TIME. NEW POST-RUN SOFTWARE, IN FORTRAN, PERMITS THE ADDITION OF LITERATURE SPECTRA TO THE LIBRARY AND ALLOWS EXAMINATION AND REMOVAL OF LIBRARY ENTRIES. OTHER NEW CAPABILITIES INCLUDE THE ABILITY TO EXAMINE MULTIPLE MASS CHROMATOGRAMS, THE SUM OF IONS IN A MASS REGION OF INTEREST AND THE SUM OF IONS THAT HAVE MAXIMIZED IN A PARTICULAR SCAN. THE PROS AND CONS OF DEVELOPING SOFTWARE WILL BE DISCUSSED.

OPTIMIZATION OF AUTOMATIC DATA REDUCTION FOR QUALITATIVE GC/MS STUDIES

by

B. N. Colby, M. E. Rose, A. E. Rosecrance

Systems, Science and Software
P.O. Box 1620
La Jolla, California 92038

The advent of commercial GC/MS data systems, capable of conditional branching based on the content of acquired data, makes possible the automation of what have become routine data system operations. For qualitative investigations, these routine operations include location of chromatographic peaks, production of background subtracted spectra, library searches, and GC peak area measurements for semiqualitative concentration estimates. The most serious difficulty in automating these procedures involves reducing the number of useless or uninterpretable spectra generated without sacrificing useful spectra in the process. This presentation will describe a combined set of decisions based on criteria which has been developed to maximize the production of useful spectra and minimize useless ones. Approximately 1,000 spectra have been examined and the results indicate that greater than 98 percent of useful spectra and less than seven percent of useless spectra are produced.

The NIH/EPA/MSDC Mass Spectral Data Base and Search System

D. P. Martinsen, Fein-Marquart Associates, Inc., Baltimore, MD 21212
R. S. Heller, Department of Computer Science, University of Maryland, College Park, MD 20742

The NIH/EPA/MSDC Mass Spectral Data Base is a comprehensive collection of low-resolution mass spectra data. The data base has been under development for a number of years; it currently contains the electron impact spectra of 31,800 compounds. These spectra have been selected from an archival file of nearly 60,000 spectra. All isotopically labelled compounds are removed; when more than one spectrum is present for a given compound, the best spectrum is chosen for the data base using a modification of an algorithm developed by McLafferty and co-workers (1). (The major change is that the source of the spectrum is not used in the calculation of the quality index.) Each compound in the data base has been assigned a Registry Number by the Chemical Abstracts Service, which provides a unique identification of the compound as well as a link to the chemical literature.

The data base is made available in a variety of formats. A magnetic tape copy of the 31,800 complete spectra may be leased from the National Bureau of Standards. This version contains information regarding the contributor, experimental conditions, compound name and synonyms, in addition to the spectral data. Printed volumes containing the plotted spectra have been published by the National Bureau of Standards and are available from the U.S. Government Printing Office (Stock # 003-003-01987-9). A listing of the compound names, molecular weight, formula, and CAS Registry Number may be obtained on microfiche.

The NIH/EPA/MSDC Mass Spectral Data Base is searchable on-line using the Mass Spectral Search System (MSSS), a component of the NIH/EPA Chemical Information System (CIS). CIS, which has been described elsewhere (2), allows the user to search a number of different data bases in addition to the Mass Spectral Data Base. The whole of CIS is now resident on a single computer network, so that a user may search all of the component data bases. In addition to mass spectral data, CIS contains CNMR data, X-ray powder diffraction data, crystallographic data, toxicity data, chemical structure, nomenclature, and formula, and a number of collections that group compounds of a particular type. These latter include active and inert ingredients in pesticides, environmentally controlled substances, toxicology collections, regulatory files, and others. All of these may be searched on the basis of structure, substructure, nomenclature, and molecular formula.

A number of developments have occurred within MSSS during the past year. The Ion Energetics Data Center of the National Bureau of Standards has compiled a summary of proton affinity and gas phase basicity values appearing in the literature through 1977. These values form the basis of two new searches: PA and GB. Compounds with specific proton affinity or gas phase basicity values may be retrieved and the citations to literature articles describing the associated measurements or calculations may be displayed. The files contain approximately 650 measurements.

A new MSSS subsystem, a search of chemical ionization mass spectra, has been developed. The search strategies are similar to those used in MSSS. The system is described more fully in paper FAMP1 in this volume.

MSSS has now become a fully integrated component of the CIS. This means that greater flexibility is allowed in retrieving and displaying information associated with other CIS components. Certain commands which are recognized throughout CIS may be used to display structural information, toxicity data, and manipulate files of results without the need to exit from MSSS. In addition, the new command MSHOW allows one to display mass spectral data without explicitly entering MSSS. Of course, MSSS still contains the molecular weight and formula searches, the peak and intensity searches, the complete spectrum searches (Biemann and PBM), and the Mass Spectrometry Bulletin searches.

References:

(1) D.D. Speck, R. Venkataraghavan, and F.W. McLafferty, Organic Mass Spectrometry, 13, 209 (1978).

(2) S.R. Heller, G.W.A. Milne, and R.J. Feldmann, Science, 195, 253 (1977).

TAMP13

COMPARISON OF FORWARD AND REVERSE SEARCH FOR THE AUTOMATIC PROCESSING OF GC/MS DTA

David Rosenthal and William F. Hargrove, Jr.
Research Triangle Institute
Research Triangle Park, North Carolina 27709

To further explore the potential of computer identification of components of organic mixtures by analysis of GC/MS data, a comparison of the reverse search and forward search procedures was carried out. An environmental sample obtained from ambient air was subjected to GC/MS analysis, and the components were processed by the RTI (forward) spectrum identification system, consisting of a cleanup and search procedure. The five best matches for each component were then subjected to reverse search against the GC/MS run.

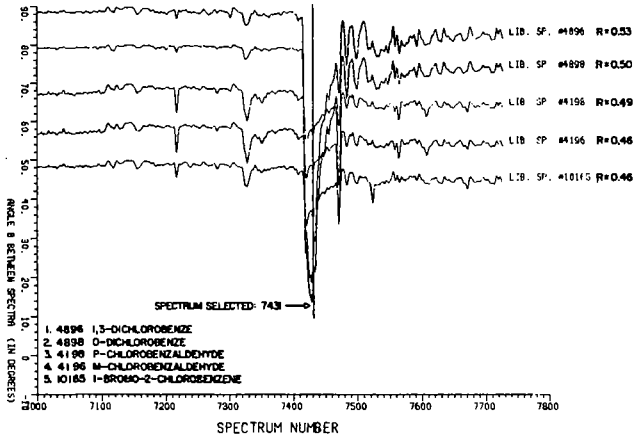
Reverse search is based on the principle that if two spectra are considered as vectors in a multidimensional space, the angle θ between the two spectra $\vec{M}$ and $\vec{M}'$ can be expressed by the vector relationship

$$\frac{\vec{M} \cdot \vec{M'}}{|M| \cdot |M'|} = \cos\theta$$

or

$$\theta = \cos^{-1}\left(\frac{m_1 \cdot m'_1 + m_2 \cdot m'_2 + \ldots m_n \cdot m'_n}{\sqrt{\Sigma(m_i)^2} \cdot \sqrt{\Sigma(m'_i)^2}}\right)$$

In this study, the output from each spectrum of the entire GC run was compared, spectrum by spectrum, with the five best matches from the forward search. The results were plotted as the angle between each library spectrum and each unknown spectrum in turn. A typical plot is shown below.



From this example, and several others obtained in the same run the following conclusions may be drawn.

1. Forward search in the method of choice, especially when the composition of the mixture is unknown.
2. Reverse search can be carried out efficiently with full spectra, whereas because of the size of the unknown library (>26,000 cpds.) forward search uses condensed spectra.
3. Reverse search can often exclude the presence of specific compounds, but taken alone, cannot definitely confirm the presence of a component.
4. Reverse search can detect low levels of components, even if their presence is obscured by unresolved eluants.
5. To be effective, reverse search must be combined with some other method or data, either a forward search or retention time information.
6. Reverse search can be used most effectively as an adjunct to, but not as a substitute for forward search.

COMPUTER FACILITATED COMPLEX MIXTURE ANALYSIS I. DETECTION AND IDENTIFICATION OF CO-ELUTING COMPOUNDS

M. N. Kan, J. Jugovich and J. Slayback

Finnigan Instruments
6110 Executive Blvd.
Rockville, Md. 20852

To separate and identify every compound in an unknown mixture by GC/MS can be a difficult and tedious task, especially in the analysis of complex mixtures wherein complete chromatographic resolution of each component cannot be achieved. To demonstrate how a combined GC/MS/Data System can facilitate an analysis of this type, an aromatic fraction of a coal liquefaction extract was run on a 60m capillary column. In this paper, we focus on various methods to detect and identify successfully minor components hidden under a dominant GC peak (10^3 concentration difference). The results of the programs used in this work, such as a sophisticated library search routine, an ion maximization peak-finding algorithm and a mass spectral background subtraction routine will be presented and discussed.

In the library search report, there are three values, namely PURITY, FIT, RFIT, which are indicative of the similarity between the unknown spectrum and the library spectrum. For the PURITY calculation, all masses and intensities of the unknown spectrum are taken into consideration whereas for the FIT calculation, only the masses in the unknown spectrum which occur in the library spectrum are considered. The RFIT calculation is the reverse of the FIT calculation. Therefore, a mixed spectrum will normally show a low PURITY value with a high FIT value. In this case, a library search of the spectrum, generated by subtracting the unknown from the library spectrum, usually reveals the identity of the second component.

An alternate method for purity determination and subsequent compound identification is use of the Biller-Biemann type peak-finding algorithm. This algorithm examines ion maximization within a given scan window. When a defined number of ions have simultaneously maximized within a given number of consecutive scans, it is defined as a unique "compound". Co-eluting components thus can be easily detected. Once compounds are located, automatic or manual background subtracted spectrum of each compound can be obtained, followed by library search routine to reveal the identity of each compound.

COMPUTER FACILITATED COMPLEX MIXTURE ANALYSIS II. RAPID AND SPECIFIC DETECTION OF ORGANIC COMPOUNDS BY REVERSE LIBRARY SPECTRAL-MATCHING

John Slayback, J. Jugovich and M. N. Kan

Finnigan Instruments
6110 Executive Blvd.
Rockville, Md. 20852

Analytical GC/MS/DS provides the chemist with one of the most powerful techniques for complex mixture analysis. Much of the power of the system can be provided by rapid and specific data reduction algorithms which allow the chemist to quickly detect compounds of interest. This paper describes the applicability of reverse library spectral searching. One salient feature of this search program allows the user to set a similarity index of matching. The results show that within a 14,000 scan coal extract capillary GC/MS run, the reverse search technique rapidly and specifically detected such compounds of interest as pyrene, phenanthrene, C-2 naphthalenes and dihydroacenaphthalene. Identification of these compounds was confirmed by elemental composition analysis, natural abundance isotope ratio measurements, library spectra comparisons and relative retention indices. The search program also detected compounds of interest in mixed, unresolved GC peaks.

The major advantage of this method vis a vis mass chromatography is specificity. For example, the mass chromatogram of m/z 154 (diagnostic ion for dihydroacenaphthalene) revealed over 30-40 GC peaks or compounds which contained that ion. Reverse library searching obviates the need for detailed knowledge of the spectra and user-selection of a unique mass for rapid identification.

COMPUTER-CONTROLLED MIKES ANALYSIS: A RAPID, CONVENIENT AND SENSITIVE METHOD OF DETECTING SPECIFIC COMPONENTS OF COMPLEX MIXTURES

Mark Weiss, Joel Karnofsky, Finnigan Corporation, 845 West Maude Avenue, Sunnyvale, California 94086; Ron Hass,Don Harvan, NIEHS, P. O. Box 12233, Res. Triangle Pk., North Carolina 27709

PURPOSE

We have developed computerized techniques for all aspects of obtaining MIKES and other metastable spectra, and for processing the acquired data. The data system is used to automate:

- locating and centering the main ion beam
- scanning for metastable ions, both full scan and MID
- acquiring metastable spectra
- smoothing, averaging, subtracting, and performing energy calculations -displaying data in various formats, including assigning correct mass, mass loss, energy, and energy loss
- creating automated procedures to link the above steps

INTRODUCTION

The use of MIKES (Mass-Analyzed Ion Kinetic Energy Spectroscopy) for detecting specific compounds in complex mixtures is potentially an important analytical tool. A MIKES analysis begins with the selection of a "main beam" mass peak by varying the magnetic field (B) and the accelerating voltage/electric sector (V/E); MIKES data is then acquired by decoupling V and E, then scanning E. Many other new developments in mass spectrometry have been due to the decoupling of V and E. V scans (holding E and B) give information on ion fragmentation, and linked scans (e.g. B/E, B^2/E, and E^2/V) give other parent-daughter ion correlations.

None of these metastable ion techniques has been easy to use, because data systems have not been developed to handle all the different problems associated with instrument set-up, scanning, and data processing. Several recent reports (1, 2) have presented the use of computers for controlling metastable scans, and for some data processing. We report here a computer system which assists or controls many aspects of metastable ion techniques.

SYSTEM DESCRIPTION

For this work, we used a ZAB-2F mass spectrometer (V. G. Micromass) with its scan selector control, coupled to an INCOS data system (Finnigan Corporation). The data system can hold one scan function constant while scanning a second.

Scan selector logic (not presently under computer control) chooses which parameter (E, V, or B) the data system holds, and which parameter (or pair for linked scans) to vary. The third parameter, if any, is preset.

Parameter linking is a hardware function.

AUTOMATIC MAIN BEAM FINDING

Since each MIKES (or metastable) experiment requires locating a different main beam mass, automating this process is of prime importance to making MIKES analyses rapid, reproducible, and convenient.

Automatic peak finding and centering starts with the user requesting that the data system FIND any mass. This is accomplished by:

1. At known E/V, moving the magnet to the approximately correct position
2. Holding B constant, the peak is located by scanning E/V and a new magnet position computed.
3. Reiterating these steps, the magnet is positioned at peak top, with an accuracy of 2^{-16} of the mass range.

Details of this process vary depending on the hysteresis characteristics of a given magnet. Using the ZAB, peaks are reliably located and centered in 20-45 seconds.

SCANNING FOR METASTABLES

Once the main beam is found and the scan selector logic change, the data system will perform any scan function desired.

- MIKES: linear down scans of E; single and multiple reaction monitoring or full-scale scan. E may be scanned both above and below main beam position.

- HIGH VOLTAGE SCANS: V is scanned linearly down while holding E; same scan flexibility as MIKES.
- B/E, B^2/E, and E^2/V: Inverse linear or linear scanning, with full scale or multiple reaction monitoring.

ACQUIRING AND STORING METASTABLE DATA

Three modes of data acquisition are allowed:

- PROFILE: metastable peak shape information is permanently recorded on the disc. Data can be recalled and processed repeatedly.
- TEMPORARY PROFILE: peak shape information is stored temporarily in memory. Data must be analyzed at once. However, hundreds of repeat scans can be averaged without using valuable disc space.
- CENTROID: only metastable peak size and energy (or mass) is stored on disc. This reduces storage needed, and is useful when quantitative information is required. No peak shapes are saved.

DATA PROCESSING AND DISPLAY

Metastable Profile data may be extensively processed and displayed in a large variety of formats.

Processing options include:

- software signal filtering, using a variable filter width;
- adding (averaging) collected scans;
- subtracting scans. Two registers provided for easier manipulation
- multiplying or normalizing scans before addition or subtractions
- automatically adjusting or aligning scans for best overlap before adding or subtracting
- calculating peak heights, areas, and centroids, and writing quantitation reports
- calculating peak area and energy spread
- processing by all other parts of the data system (including Library Search)

Display options include:

- automatic assignment of correct mass or energy values
- mass axis display or mass loss axis display
- energy axis display or energy loss axis display
- mass * 2 axis display (for doubly charged ions)
- reversing any axis
- adjustable normalization and vertical scaling; square root vertical scale
- dual graph display
- all displays can be hardcopied; comments may be added

AUTOMATION OF MIKES ANALYSIS

Peak-finding, data acquisition, and data processing can be combined in automatic sequences. The data system can have complete control of the entire operation with the exception of the scan selector/linked scan logic, which is currently under manual control.

A typical sequence might include making lists of main beam masses and reaction ion masses, and a data processing routine. Once sample is introduced, operator intervention is required only to change the scan selector switches. The data system would find main beams, scan over reation masses, and, perhaps quantitate the observed peaks.

REFERENCES

1. Development of a System for the Operation of an IKES Spectrometer under Computer Control. P. S. Bolton, G. W. Trott, R. P. Morgan, A. G. Brenton, and J. H. Benyon; Int. J. of M.S. and Ion Physics 29 (1979) 179-90
2. Computerized Mass Spectrometer Linked Scan System for Recording Metastable Ions. W. F. Haddon Anal. Chem. June 1979 (in press)

ELECTRON IMPACT FRAGMENTATION MECHANISMS OF 2,4,6-TRINITROTOLUENE (TNT) DERIVED FROM METASTABLE TRANSITIONS AND ISOTOPIC LABELING

SURYANARAYANA BULUSU
ENERGETIC MATERIALS DIVISION
LARGE CALIBER WEAPON SYSTEMS LABORATORY
US ARMY ARMAMENT RESEARCH AND DEVELOPMENT COMMAND
DOVER, NEW JERSEY 07801

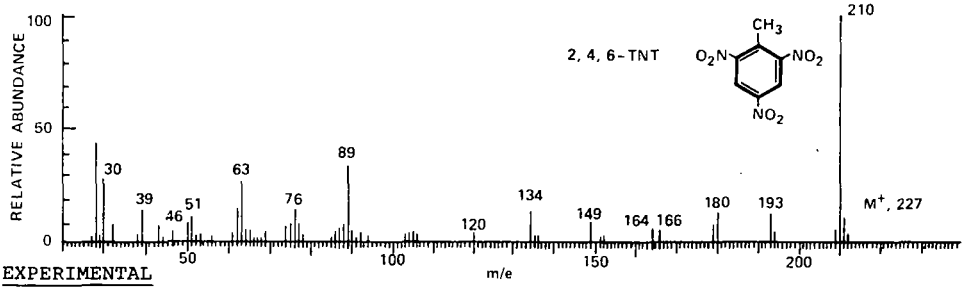
and

THEODORE AXENROD
DEPARTMENT OF CHEMISTRY
THE CITY COLLEGE OF THE CITY UNIVERSITY OF NEW YORK
NEW YORK, NEW YORK 10031

INTRODUCTION

In recent years the mass spectrometry of nitroaromatic compounds has been the subject of numerous investigations[1] which have emphasized either analytical applications or the modes of fragmentation induced by electron impact[2,3]. In view of the central role of 2,4,6-trinitrotoluene (TNT) as a high explosive and the importance of understanding the energy-releasing processes accompanying its decomposition, a comprehensive program was undertaken in these laboratories to study and compare electron-impact induced fragmentations with other modes of decomposition such as those induced by heat, light and ionizing radiation.

In the present study, metastable scanning techniques[4] and ^{15}N and ^{2}H isotopic shifts have been used to elucidate the competing and consecutive reactions which follow from the ionization of the parent 2,4,6-trinitrotoluene molecule. The spectrum of 2,4,6-TNT is shown in Figure I.



EXPERIMENTAL

A DuPont, Model 21-492 double-focusing mass spectrometer operating at an ionizing voltage of 70 eV was used. Samples were introduced via the direct insertion probe, and the source temperature during metastable scans was maintained at 110°. The scanning of the metastable ion transitions was accomplished by driving the 'metastable adjust' control with a slow speed motor. The variable accelerating voltage (monitored with a Dana Laboratories Model 5500 voltmeter) and the amplifier output (increased by 10^2 to 10^3 with a Keithly Model 427 current amplifier) were applied to the x- and y- coordinates, respectively, of an x-y recorder. Exact masses of selected ions were measured by the peak matching method.

RESULTS

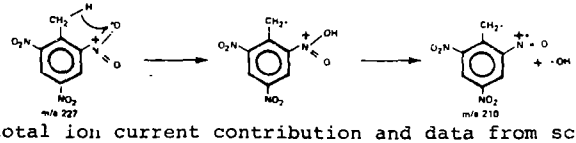
From about 25 ions in the TNT spectrum selected for detailed study, more than 100 transitions were observed and assigned. Some typical precursor-product relationships derived from the metastable scans are summarized in Table I.

Table 1. Some Precursor - product transitions determined by metastable ion scanning of selected TNT peaks

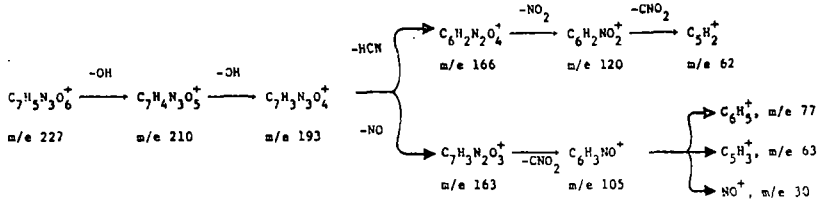
Product Ion scanned		Precursors found		Probable neutral loss
m/e	Formula	m/e	Formula	
210	$C_7H_4N_3O_5$	227	$C_7H_5N_3O_6$	OH
193	$C_7H_3N_3O_4$	210	$C_7H_4N_3O_5$	OH
		228	$^{13}CC_6H_5N_3O_6$	HNO_2
		211	$^{13}CC_6H_4N_3O_5$	NO
180	$C_7H_4N_2O_4$	210	$C_7H_4N_3O_5$	NO
		197	$C_7H_5N_2O_5$	OH
		227	$C_7H_5N_3O_6$	OH, HNO
166	$[C_6H_2N_2O_4]$	183	$C_6H_3N_2O_5$	OH
		181	$C_7H_5N_2O_4$	CH_3

The base peak in 2,4,6-trinitrotoluene appears at m/e 210. Exact mass measurements, and the presence of a metastable ion in the normal spectrum at m/e 194.2 confirm the formula of the m/e 210 ion to be $C_7H_4N_3O_5$, and indicate that this ion arises from the hydrogen rearrangement - hydroxyl elimination process shown in Scheme I.

SCHEME 1



In terms of total ion current contribution and data from scanning of the metastable transitions, the fragmentation of 2,4,6-TNT is dominated by several reaction sequences, which all emphasize the central role of the m/e 210 ion. One of these important fragmentation pathways is illustrated in the following reaction sequence:



CONCLUSIONS

Extensive metastable scanning data support the view that the electron impact fragmentation of TNT parallels the photochemical and thermal decomposition. The important fragmentation pathways involve the m/e 210 ion which arises from a hydrogen migration-hydroyl loss from the molecular ion.

REFERENCES

1. H. Budzikiewicz, C. Djerassi, and D.H. Williams, Mass Spectrometry of Organic Compounds, (Holden-Day, San Francisco, p. 512 (1967).
2. J.H. Beynon, R.A. Saunders, and A.E. Williams, The Mass Spectra of Organic Molecules, Elsevier, New York, P. 322-344 (1968).
3. S. Meyerson, R.W. Vanderhorn, and E.K. Fields, J. Org. Chem., 37, 4114 (1972).
4. R.G. Cooks, J.H. Beynon, R.M. Caprioli, and G.R. Lester, Metastable Ions, Elsevier, New York, (1973).

TAMP18 Applications of a New Interactive Colour Graphics Terminal in Organic GCMS.

T.S. Davis, J.C. Bill, M.J. Wallington and P. Powers.
VG Data Systems Limited, Tribune Avenue, ALTRINCHAM, England.

Conventional colour terminals do not offer the necessary combinations of speed and high definition that are required for use in Organic Mass Spectrometry.

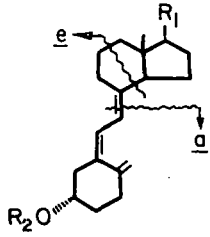
A new Interactive Colour Graphics Terminal has been developed especially for real time use in this field. Based on a high quality colour monitor and using dual microprocessor logic the terminal provides 19.2 kbaud operation with automatic axis generation on 4 graphs in any of 8 colours. Optional hardware fill under the trace, optional background colour, graphic and character cursors, inverse character video and highlight features combine to make the terminal a powerful addition to modern real time interpretive data systems.

The paper illustrates the use of this terminal in several typical GCMS situations and shows how the use of colour can greatly ease interpretive problems.

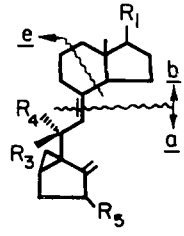
Mass Spectrometry of 3,5-Cyclo-Vitamins D_3.

Ze'ev V.I. Zaretskii, Department of Isotope Research, The Weizmann Institute of Science, Rehovot, Israel.

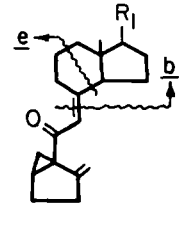
Proceeding with mass spectrometric investigation of vitamin D_3 and its analogues [1] we have studied the fragmentation pathways, on electron bombardment, of (6R)- and (6S)-stereoisomeric 3,5-cyclovitamins D_3, their methyl esters and the respective 7,8-epoxy derivatives, as well as of corresponding 6-keto-analogues, using high resolution mass spectrometry and metastable defocusing technique (Table 1-4). The mass spectra of 3,5-cyclovitamins D_3 differ sharply from the spectra of the corresponding vitamins D_3, which makes it possible, when studying vitamin D-3,5-cyclovitamin D inter-conversion, to differentiate between these isomers (Table 1,2). On the other hand, the difference in mass spectrometric behaviour of the (6R)- alcohols and ethers from that of their (6S)-epimers provides a basis for configurati nal assignments to the stereoisomers of 3,5-cyclovitamin D_3 series (Table 2,3).



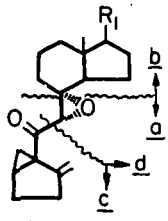
1 R_2=H
2 R_2=Me



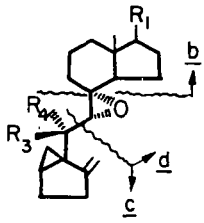
3 R_3=R_5=H, R_4=OH
3a R_4=OH, R_5=OAc, R_3=H
4 R_3=R_5=H, R_4=OMe
5 R_4=R_5=H, R_3=OMe



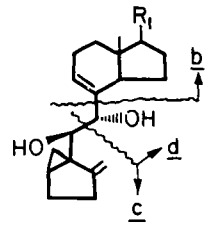
6



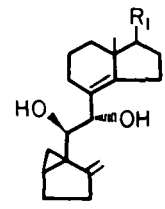
7



8 R_3=H, R_4=OH
9 R_4=H, R_3=OH



10
R_1 = C_8H_{17}



11

Acknowledgment

The author expresses his deep gratitude to Prof. Y. Mazur and Dr. M. Sheves (Dept. of Org. Chem., The Weizmann Inst. of Sci.) for the samples used in this study, and to Mrs. M. Ganz, A. Gorelov and E. Ne'eman for technical assistance.

References

1. (a) Z.V.I. Zaretskii, Biomed. Mass Spectrom., 5, 576 (1978);
(b) Z.V.I. Zaretskii, Nouveau J. de Chimie, 2, 531 (1978);
(c) Z.V.I. Zaretskii, Steroids, 33, in press (1979).

Table 1. Ion (m/e)

Compound	$M^{\cdot+}$ (384)	* (366)	** (351)	b (247)	*** (135)	e (176)	**** (158)	a (136)	***** (118)
(1)	51	7	41	2	18	15	45	100	100
(3)	19	47	22	69	100	-	61	67	75

* $(M-ROH)^{\cdot+}$; ** $(M-ROH-Me)^{+}$; *** (b-side chain+H)$^{+}$; **** $(e-ROH)^{\cdot+}$: ***** $(a-ROH)^{\cdot+}$

Table 2. Ion (m/e)

Compound	$M^{\cdot+}$ (398)	* (366)	** (351)	b (247)	**** (158)	a (150)	***** (118)
(4)	10	100	10	29	87	48	71
(5)	12	100	15	62	44	38	62
(2)	12	8	14	12	25	66	100

See footnotes of Table 1.

Table 3. Ion (m/e)

Compound	$M^{\cdot+}$ (400)	* (382)	d (277)	- (278)	b (247)	$(d-H_2O)^{+}$ (259)	*** (135)	c (123)	$(d-C_8H_{17}+H)^{+}$ (165)
(8)	13	8	70	26	96	34	97	100	50
(9)	13	7	50	43	57	33	98	100	41
(10)	2	6	38	70	31	4	15	69	100
(11)	20	16	89	89	92	82	43	100	72

See footnotes of Table 1.

Table 4.

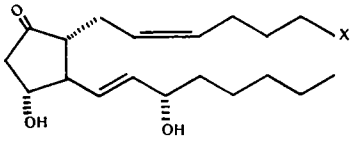
Compound	Transition	Parent-Neutral lost*
(3)	384 → 136 (a)	$M^{\cdot+} - C_{18}H_{32}$
(5)	398 → 366	$M^{\cdot+} - MeOH$
	398 → 357	$M^{\cdot+} - C_3H_5$
	398 → 325	$M^{\cdot+} - C_4H_9O$
	398 → 351	$M^{\cdot+} - C_2H_7O$
	366 → 351	$(M-MeOH)^{\cdot+} - Me$
	366 → 325	$(M-MeOH)^{\cdot+} - C_3H_5$
	357 → 325	$(M-C_3H_5)^{+} - MeOH$
	366 → 247 (b)	$(M-MeOH)^{\cdot+} - C_9H_{11}$
(7)	398 → 150 (a)	$M^{\cdot+} - C_{18}H_{32}$
	398 → 285	$M^{\cdot+} - C_8H_{17}$
	398 → 277 (d)	$M^{\cdot+} - C_8H_9O$
	398 → 247 (b)	$M^{\cdot+} - C_9H_{11}O_2$
	285 → 135	$(M-C_8H_{17}{}^{ii})^{+} - C_9H_{11}O_2$
	277 → 259	d - H_2O
	247 → 135	b - C_8H_{16}
	150 → 121 (c)	a - CHO
	121 → 93	c - CO

*Based on HR mass spectra; ^{11}C-17 Side chain; LR mass spectra were determined at 70 eV on a Varian MAT 731 double focusing Mass Spectrometer using a direct inlet system, and the standard sample probe (± 0.3° temp. stabilization). HR mass spectra were obtained at a resolution of 10,000 using Spectro-System SS-100. The metastable transitions were discovered in the first free field region of MAT-731 using "defocusing technique".

Rearrangement of N-Acyl Prostaglandin Carboxamides to Nitriles and Trimethylsilyl Esters, Fred C. Falkner, Drug Metabolism Department, Pfizer Inc., Groton, CT 06340

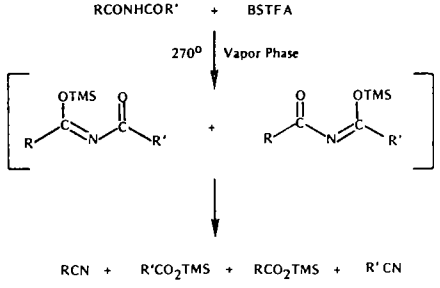
N-Acetyl-PGE_2 carboxamide (IIa) was treated under standard derivatizing conditions to prepare a MO-TMS derivative suitable for analysis by g.c. Analysis of the final reaction mixture by g.c. in the presence of excess BSTFA showed two doublets. The mass spectra of the second doublet showed these two peaks to be the syn and anti isomers of PGE_2-MO-TMS3 (1). The first doublet gave mass spectra consistent with the syn and anti isomers of the MO-TMS derivative of 9-keto-11,15-dihydroxy-prost-5,13-dienonitrile (III, PGE_2-nitrile).

That this unexpected formation of nitrile could also be observed for other prostaglandin analogs was confirmed by noting that N-acetyl-PGA_2 carboxamide gave PGA_2-nitrile-TMS and PGA_2-TMS2 under the same derivatizing and g.c. conditions. Varying the N-acyl moiety of the prostaglandin E_2 carboxamides from propanoyl to pivalyl (IIb-IIId) produced nitrile but decreasing amounts of ester. In the case of IIe no ester and only a small amount of nitrile were observed.



I X = CO_2H
IIa X = $CONHCOCH_3$
IIb X = $CONHCOCH_2CH_3$
IIc X = CONHCO-cyclopropyl
IId X = $CONHCOC(CH_3)_3$
IIe X = $CONHCOC_6H_5$
III X = CN

The residue obtained after removal of excess silylating reagent showed no silylation on the imide moiety. In addition, this residue dissolved in ethyl acetate was not stable to the g.c. conditions employed. However, if a volume of BSTFA equal to that of the ethyl acetate was added to the solution, the rearrangement products reappeared in good yield upon analysis by g.c. An attempt to reproduce the rearrangement in solution by heating IIa-MO in BSTFA at 150° for 1 hr was not successful.



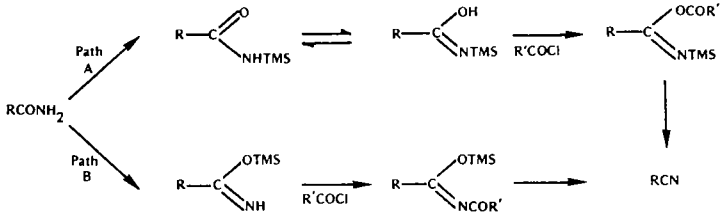
POSTULATED INTERMEDIATES IN THE CONVERSION OF TMS IMIDES TO NITRILES AND TMS ESTERS

SCHEME 1

This rearrangement of imides to nitriles in the presence of excess silylating reagent has not been previously reported and is proposed to occur as outlined in Scheme 1. No attempt was made to verify the presence of the presumed by-products of the reaction, namely, acetonitrile and trimethylsilyl acetic acid. The postulated scheme may have implications for mechanisms involving the conversion of TMS amides to nitriles. Previous studies (2) have shown that TMS amides, when treated with acyl chlorides, yield the corresponding nitrile in good yield. Path A postulating N-silylation (Scheme 2) was proposed to explain the conversion. However, in the light of present results, path B must also be considered as a viable pathway. O-Silylation followed by N-acylation would yield a TMS imide which would rearrange to the nitrile of the original amide, a situation in accord with experimental data (2).

1. B. S. Middleditch and D. M. Desiderio, J. Org. Chem. 38, 2204 (1973).

2. M. Hallenslebe, Tetrahedron Lett., 2057 (1972).



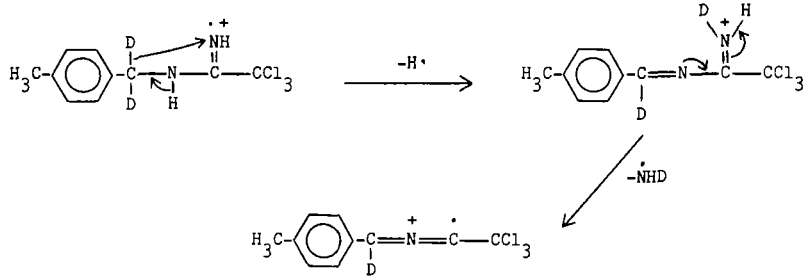
POSSIBLE PATHWAYS FOR THE REARRANGEMENT OF TMS AMIDES TO NITRILES IN THE PRESENCE OF AN ACYL CHLORIDE

SCHEME 2

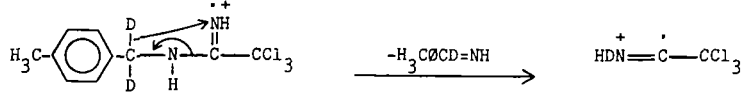
MASS SPECTROMETRIC ANALYSIS OF SOME BENZYL TRICHLOROMETHYLAMIDINES. R. E. Rhodes, A. G. Zacchei, J. R. Huff and W. S. Saari, Merck Sharp & Dohme Research Laboratories, West Point, Pa., 19486

A series of aromatic substituted amidines of the general structure type R-$\phi CH_2NHC(NH)CCl_3$ (R = H, CH_3, OCH_3) has been investigated using low and high resolution mass spectrometry and conventional metastable ion analysis.

In general, the 70eV spectra are characterized by weak molecular ions and base peaks due to the substituted benzyl nucleus. Intense peaks due to the substituted benzylamine moiety are also present. The molecular ion region is characterized by relatively intense M-H ions (when compared to the molecular ion). Also present are peaks due to the loss of the elements of NH_3 from the molecular ion. In order to elucidate these latter fragmentations, the deuterated analog N-(p-methyl-α,α-dideutero benzyl)-trichloroacetamidine was prepared. As can be seen from the spectra, there is no M-D peak. Furthermore, the loss of the elements of the NH_2D from the molecular ion is confirmed by high resolution measurements. We propose the following mechanisms to relationalize these fragmentations:



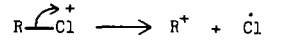
Transfer of the benzylic hydrogen is further evidenced by the formation of the peak at m/e 145. The elemental composition of this peak is $C_2H_2NCl_3$ by high resolution measurement. This peak is shifted to m/e 146 (C_2HDNCl_3) in the spectrum of the α,α-dideutero benzyl analog. The following mechanism seeks to rationalize this fragmentation:



Of further interest in the spectra of these compounds is the sequential loss of chlorine from the M and M-H ions. The following table tabulates these ions:

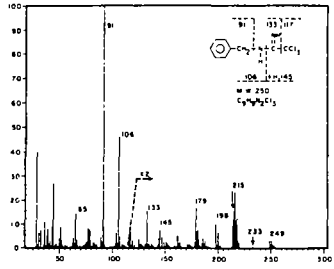
	ϕCH_2R	$H_3C\phi CH_2R$	$H_3C\phi CD_2R$	$H_3CO\phi CH_2R$
M	250	264	266	280
M-H	249	263	265	279
M-Cl	215	229	231	245
M-HCl	214	228	230	244
$M-Cl_2$	180	194	195	210
$M-HCl_2$	179	193	194	209
$M-Cl_3$	145	159	160	175
$M-HCl_3$	144	158	159	174

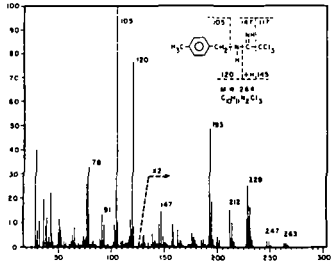
In many cases, metastable ions are discernable which confirm the chlorine losses. However HCl losses may also be involved. A single chlorine loss due to the mechanism

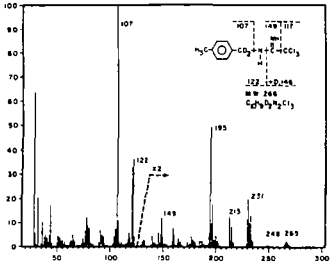


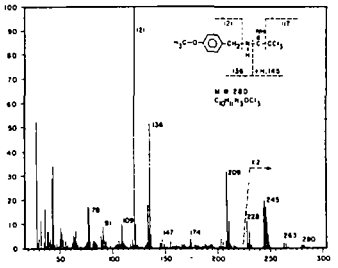
is consistent with previous work. However, what mechaism and the nature of the activated intermediate for the subsequent chlorine radical or ion losses is not yet understood.

A complete paper containing the high resolution and metastable ion data further exploring the nature of the fragmentation processes of the above compounds is currently in preparation.

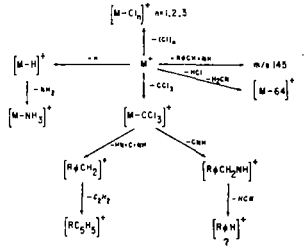








GENERALIZATION

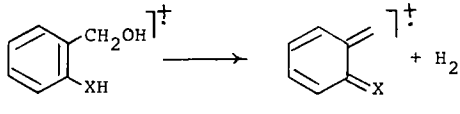


ENERGETIC ANALYSIS OF A 1,4 ELIMINATION

D.R. Hilker and M.L. Gross

Department of Chemistry
University of Nebraska
Lincoln, Nebraska 68588

Previously, we have reported an unusual trend for kinetic energy release in 1,4-eliminations of various ortho-substituted benzyl alcohols (see eq. 1) and benzoic acids.[1] Specifically, when X=CH_2, the kinetic energy release is about 30 times larger than when X = O. Furthermore,

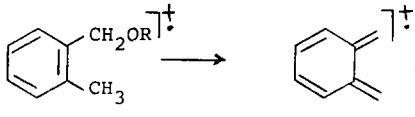


X = O, NH, CH_2

the loss of water from 1-tetralol is analogous to the o-methyl benzyl alcohol: both compounds show broadened metastable peak shapes for this process.

We find these differences to be difficult to explain within the present confines of current theory of kinetic energy release. That is, these eliminations appear to procede via a "loose" six-centered transition state. Accordingly, similar and narrow metastable ion peak shapes would be expected. However,a problem with the design of this study is the differing daughter ions produced from each member of the series.

In an attempt to generate further data to shed light on this phenomenon, we have studied a second series of compounds which all undergo 14,-eliminations of stable neutral molecules to give a common daughter ion. The system is represented in equation (2). The various molecular



R = H, CH_3, C_3H_7, CH_3CO

ions lose ROH by 1,4-process as demonstrated by deuterium labeling experiments. Linked metastable scans as well as previous ion-molecule reaction studies are in accord with a common daughter ion structure for all members of the series.

Knowing the heat-of-formation of the ortho-quinodimethane radical cation (estimated at 225 kcal/mole), the heats-of-formation of the various

neutral ROH's (from standard tables), and estimating the ΔH_f of the molecular ions, we can calculate the fraction of reverse activation energy which is released as translational energy provided the tranlational energy is measured, of course. We have made these measurements for metastable ions and find that when R=H, the fraction of energy released is approximately 100 times that when R = CH_3, C_3H_7 or CH_3CO. The same situation applies for the comparison of H_2O and CH_3COOH-eliminations from 1-tetralol and 1-acetoxytetralin[2] respectively.

Because the mechanisms appear to be the same by all criteria we have applied to date, we suggest that these results confirm our earlier hypothesis[1] that the results can be explained in terms of the relative locations of the transition state on the reaction coordinate.

References:

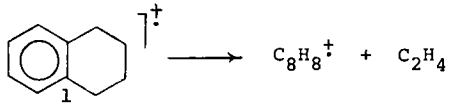
1. M.L.Gross, F.L. DeRoos, M.K. Hoffman, Org. Mass Spectrom.,12,258(1977).
2. S.F. Wojinski and M.L. Gross, ibid, 14, 135 (1979).

THE MECHANISM OF H/D RANDOMIZATION OF THE MOLECULAR ION OF TETRALIN

S.M. Arghestani, E.K.Chess, and M.L. Gross

Department of Chemistry
University of Nebraska
Lincoln, Nebraska 68588

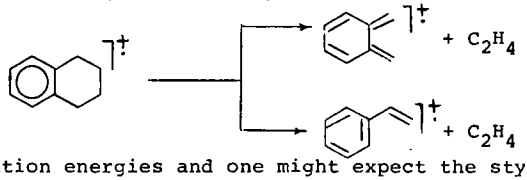
The mechanism for elimination of ethylene from the molecular ion of tetralin (1) has been one of classic questions in organic mass spectrometry.



(1)

Among the possibilities in the literature are (1) a retro Diels Alder reaction, (2) elimination of carbons 1 and 2 to form a styrene-type radical cation, (3) rearrangement of the tetralin nucleus to give a phenyl cyclobutane radical cation or a tetrahydroazulene radical cation and (4) benzylic bond cleavage followed by ring expansion to give a substituted tropylium ion.

Based on a study of tetralols completed in our lab in 1976,[1] we suggested that the experimental data could be understood in terms of two competitive processed (eq. 2). These processes would obviously have



(2)

different activation energies and one might expect the styrene ion formation to dominate at lower energies (based on stability considerations).

This has been recently verified by field ionization kinetics studies done in Germany.[2] Specifically, at 10^{-11} sec, the retro Diels-Alder reaction comprises 70% of the total pathways for C_2H_4 elimination, whereas at 10^{-5} sec, the percentage has dropped to about 10%. The normal mass spectra of C-13 labeled tetralins show that the ratio of C_1-C_2: C_2-C_3: C_3:C_4 losses is 1:1:1[3], which is now understood as a fortuitous integration of the two mechanisms shown in equation (2).

The results for various deuterium labeled tetralins are in accord with the C-13 results cited above with the exception that a small amount of H/D scrambling has begun (see table 1). These measurements were made on a

Kratos MS-50 mass spectrometer at a resolution of 75,000

Table 1. Comparison of Losses of Deuterated Ethylenes (at R=75,000) with Results of C-13 Labeling.

		$-C_2H_4$	$-C_2H_3D$	$-C_2H_2D_2$
1,1-$\underline{d}_2$-tetralin:	Predict*:	67	—	33
	Observe:	61	15	24
2,2-$\underline{d}_2$-tetralin:	Predict:	33	—	67
	Observe:	32	5	63

* Prediction based on C-13 labeling results which indicate 1:1:1 loss of C_1-C_2: C_2-C_3: C_3-C_4.

To complete our understanding of this simple organic system, we have investigated the mechanism of H/D scrambling for slow decompositions (metastable ions). The dissociations exhibit extensive H/D randomization as determined by both linked $V^{\frac{1}{2}}/E$ (MS-50) and MIKES (Hitachi RMU-6D). Nevertheless, the mechanism for the scrambling can be determined from the data. Our proposed model involves complete (by 10^{-5}sec) equilibration of the four benzylic and the four aromatic hydrogen atoms. Furthermore, the results are complicated by a small amount (20%) of total scrambling (i.e., all 12 hydrogens mix). The comparison of the observed values with those calculated based on this model is given in Table 2.

Table 2. Comparison of Experimental Data for Metastable Losses of Deuterated Ethylenes with Calculated Results Based on H/D Scrambling Model*

Compound		$-C_2H_4$	$-C_2H_3D$	$-C_2H_2D_2$	$-C_2HD_3$
1,1-$\underline{d}_2$-Tetralin	Predict:	52	42	6	-
	Observe:	51	35	12	-
2,2-$\underline{d}_2$-Tetralin	Predict:	48	10	42	-
	Observe:	43	13	44	-
5,6,7,8-$\underline{d}_4$-Tetralin	Predict:	23	47	29	1
	Observe:	30	41	21	5

*See text for description of Model.

In conclusion, the ethylene is eliminated from tetralin via two competitive processes (eq. 2). Prior to this loss, hydrogen atom scrambling takes place primarily involving the four aromatic and the four benzylic hydrogens.

References: 1. M.L.Gross and F.L.DeRoos, J. Am.Chem.Soc., 98,7128 (1976).
2. R. Stolze, H.Budzikiewicz,K. Levsen, and F. Borchers, Org. Mass Spectrom., 13, 510 (1978).
3. R. von Gretler, E. Askitoglu, H. Kühne, and M. Hesse, Helv. Chim. Acta, 61, 5 (1978).

RATES AND MECHANISMS OF THERMAL ION-MOLECULE REACTIONS

John I. Brauman

Department of Chemistry
Stanford University
Stanford, California 94305

Although many ion-molecule reactions occur on essentially every collision, it is now well established that a substantial number of reactions have rate constants which are considerably slower than this. Obviously the magnitude of such rate constants are related to some of the details of the ion-molecule interaction. In certain cases the behavior of the system may correspond to that expected from a statistical model and consequently reflect some of the details of the potential surface. We believe that many thermal ion-molecule reactions, especially those of large organic systems, may be described by such a model, and we are exploring some of its consequences.

The fairly large number of reactions which occur with efficiencies between 1 and 0.001 suggests that there should be a model which has the generality to describe all of these reactions. The model which we have proposed involves a surface with two minima separated by a barrier which is lower in energy than the entrance (or exit) channel centrifugal barrier.

$$A^+ + B \underset{k_{-1}}{\overset{k_1}{\rightleftharpoons}} AB^+ \underset{k_{-2}}{\overset{k_2}{\rightleftharpoons}} CD^+ \rightleftharpoons C + D^+$$

In general, the reaction efficiency is determined by the relative rates of k_2 and k_{-1}. Although k_{-1} (dissociation to separated ion and molecule) is energetically less favorable than k_2 ("chemical" transformation), it still competes favorably because of entropy considerations--free rotations, etc.

This model, which can be described quantitatively, suggests a number of effects in which the reaction rate can be affected. These include chemical stability as reflected in energy-rate correlations, steric effects, and effects involving rotational energy loss. We have found evidence for these effects in displacement reactions and proton transfer reactions. The model appears to be quite reasonable in describing rates and isotope effects.

PROTONIC ACID-BASE EQUILIBRIA: GAS PHASE AND SOLUTION

Robert W. Taft
Department of Chemistry
University of California, Irvine
Irvine, California 92717

Advances in the methods of determination of gas phase protonic acidities and basicities, and of stabilities of ion-molecule complexes, coupled with advances in theoretical ab initio calculations, provide a very effective means for the attainment of new understanding of both intrinsic effects of molecular structure and solvation effects on acid-base behavior. This paper is limited to considerations of the acid-base behavior of neutral organic bases, although there are equally important new results available for acidities of organic acids.

Structural effects on inherent basicities are usefully considered by methods of linear free energy relationships, i.e., in terms of the effect of a substituent replacing hydrogen at a given base site or functional group. The general applicability of polarizability effects, inductive-field effects, and pi electron delocalization (resonance) effects is demonstrated by a combination of both linear and non-linear relationships between corresponding effects of substituents on the proton affinities of amines, alcohols, ethers, mercaptans, thioethers, nitriles, and carbonyl compounds.[1] The predictive utility of generalized linear structure-energy relationships is stressed.

The alternative approach to prediction of substituent effects on proton affinities via theoretical molecular orbital calculations at the STO-3G level of approximation is also examined. The comparison of observed and calculated substituent effects on isodesmic proton transfer reaction is shown by a variety of applications to be generally good.

Qualitative interpretations of the relationship of gas phase basicities to aqueous solution basicities are illustrated in terms of non-specifically solvated acid-base pairs and highly specifically solvated acid-base pairs.[1] The results of both theoretical and experimental studies comparing the effects of formation of discrete ion-solvent molecule complexes in the gas phase with corresponding observed aqueous medium effects are presented.

Close equivalence has been obtained (Taagepera, Hehre, and Taft, unpublished results) between large aqueous medium effects on proton transfer reactions between a series of primary amines and simplified "model" hydration effects calculated by the use of the Gaussian-70 program. It is assumed in obtaining the calculated results for these reactions that the only role of water is the selective stabilizing effects of single water molecule attachments to all three protonic sites of RNH_3^+ and the single lone pair site of RNH_2. While the good agreement obtained cannot necessarily be taken as "proof" of the assumptions made, it does support the idea that complex

formation involving a relatively small number of water molecules is the predominant contribution to the observed aqueous medium effects on these proton transfer equilibria.

Table 1 gives the results of experimental studies by the ICR equilibrium constant method of the effects of formation of single molecule-ion complexes on proton transfer equilibria between oxonium ions. Both the single (S) molecule attachments and aqueous medium effects are shown to favor the formation of the oxonium ion having the greater charge localization at the protonic site. The order of increasing stabilization by S of gaseous ion-molecule complexes is shown not to parallel the proton affinity but instead the hydrogen-bond acceptor parameter, β, of Taft and Kamlet.

Reference

(1) for a recent summary cf. R. W. Taft, in "Kinetics of Ion-Molecule Reactions," P. Ausloos, Ed., Plenum Publishing Corporation, 1979, pp 271-293.

Table 1

DIFFERENTIAL SOLVATION EFFECTS FOR CHARGE DELOCALIZED vs CHARGE LOCALIZED MONOPROTONIC OXONIUM IONS

$$B_1H^+_{(g)} + :B_{2(g)} \rightleftharpoons B_2H^+_{(g)} + :B_{1(g)};\ \Delta G^0_{(1)}$$

$$B_1H^+\cdots S_{(g)} + :B_{2(g)} \rightleftharpoons B_2H^+\cdots S_{(g)} + :B_{1(g)};\ \Delta G^0_{(2)}$$

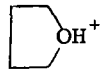
$$B_1H^+_{(aq)} + :B_{2(aq)} \rightleftharpoons B_2H^+_{(aq)} + :B_{1(aq)};\ \Delta G^0_{(aq)}$$

all in kcal/mole at 298 °K

Charge-Delocalized

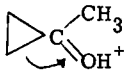
$B_1H^+ = C_6H_5C(H)=OH^+$

Charge-Localized

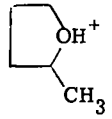
$B_2H^+ =$ 

$-\Delta G^0_{(1)}$	S	$-\Delta G^{0\,a}_{(2)}$	$\Delta G^0_{(1)} - \Delta G^0_{(2)}$	$\Delta G^{0\,b}_{(aq)}$	$\Delta G^0_{(1)} - \Delta G^0_{(aq)}$
- 1.5	$(CH_3)_2O$	- 0.1	+ 1.4	+ 3.1	+ 4.6
	CH_3CN	+ 0.5	+ 2.0		
	$(CH_3)_2CO$	+ 0.9	+ 2.4		

Charge-Delocalized

$B_1H^+ =$ 

Charge-Localized

$B_2H^+ =$ 

$-\Delta G^0_{(1)}$	S	$-\Delta G^{0\,a}_{(2)}$	$\Delta G^0_{(1)} - \Delta G^0_{(2)}$	$\Delta G^{0\,b}_{(aq)}$	$\Delta G^0_{(1)} - \Delta G^0_{(aq)}$
- 2.0	CH_3CN	- 0.5	+ 1.5	+ 0.9	+ 2.9
	$(CH_3)_2CO$	0.0	+ 2.0		
	$HCONH_2$	+ 0.7	+ 2.7		

a) from J. Bromilow and R. W. Taft, unpublished results.

b) from G. Scorrano and R. W. Taft, unpublished results.

TPMOA3

STRUCTURE AND CHEMISTRY OF GASEOUS ORGANIC IONS STUDIED BY COLLISIONAL ACTIVATION MASS SPECTROMETRY

F. W. McLafferty, D. C. McGilvery and P. J. Todd

Department of Chemistry, Baker Laboratory,
Cornell University, Ithaca, New York 14853

The collisional activation (CA) mass spectrum is characteristic of an ion's structure and independent of its internal energy. This complements information from metastable ion (MI) mass spectra, which represent higher energy precursor ions; however, MI spectra can be dependent on precursor ion internal energies.

Helium is the preferred collision gas, giving the highest sensitivities for high energy decompositions. At the collision gas pressure giving maximum CA ion intensities (precursor ion intensity reduced to ~25% of its original value) ions undergo multiple collisions; although this can cause some isomerization of the precursor ion, lowering the specificity of the CA spectrum, the remaining differences between isomeric CA spectra are still reliable characteristics of the precursor ion structure. CA ion decompositions resemble those of normal electron-ionization mass spectra, so that structural information can be obtained by CA spectral interpretation. For example, the $C_7H_5D_2^+$ ions obtained at 13 eV from $C_6H_5CD_2I$ show mainly CD_2 (not CHD) losses, supporting the benzyl ion structure.

The utility of CA spectra in ion chemistry studies is illustrated by two cases in which competitive isomerizations are possible in both the precursor and product ions of a decomposition reaction. The more stable isomer can be favored by M^+ isomerization at lowest energies, and by product ion isomerization at highest energies, with a maximum of less stable isomers formed at intermediate energies. Thus variation of the ionizing electron energy gives a maximum at intermediate energies for [benzyl$^+$]/[tropylium$^+$] from toluene and for $[H_3CS^+]/[H_2C{=}SH^+]$ from CH_3SSCH_3.

A new CA instrument employs high resolution analysis of the primary ion beam followed by acceleration at 30 KV and collision with a molecular beam of helium and secondary mass analysis. CA spectra of the $C_4H_9^+$ (m/z 57.070) and $C_3H_5O^+$ (m/z 57.034) show <2% contamination of the latter spectrum by the former. The higher collision energies make possible the resolution of ions formed with substantial energy release, such as C_5^+-$C_5H_6^+$ from $C_7H_8^+$. Computer automation of both mass analyzers further improves its applicability to such ion chemistry problems and its utility in MS/MS.

"Solvation Energies - The Link Between Ionizations in the Gas Phase and Solution"

Edward M. Arnett and Norbert J. Pienta
Department of Chemistry
University of Pittsburgh
Pittsburgh, PA 15260

The activation of neutral molecules by conversion to less stable charged intermediates is one of the simplest and most widely useful of chemical processes. Such ionization processes have provided some of the most basic information about the relationships between molecular structure and reactivity which lie at the heart of organic- and bio-chemistry. However, until the last decade, there has been no clear means for separating unequivocally, stability factors such as resonance, polarity or steric contributions (which are inherent to the molecules themselves, and their related ions) from solvation contributions. Three mass spectral methods - ion cyclotron resonance, high pressure mass spectrometry, and "flowing afterglow" - have provided, at last, a means for accomplishing gas phase ionization reactions with sufficient ion-molecule collisions so that a Boltzmann distribution of energies is approached in the gas phase which is comparable to that in solution at the same temperature. During the past decade several hundred acid-base reactions have been examined in the gas phase by these methods with generally good agreement (1-3). At the same time, the means for studying a very wide range of acids and bases in solution have been developed so that comparison of many types of ionization processes can be made in the presence and absence of solvents.

A surprisingly large number of gas phase ionization processes respond to variation in molecular structure in a manner which is closely parallel to that for the same processes in solution. The formation of resonance stabilized carbanions, resonance stabilized carbonium ions, pyridinium ions, enolate, phenolate and carboxylate ions are such cases. On the other hand, the formation of charge-localized ammonium ions or alkoxide ions show drastically different behavior in the two kinds of media.

As can be seen from the following cycle, the entire difference between the effects of structure in the gas phase and solution is attributed to the variation in solvation energies of the neutrals (N) and their related ions $I^{\pm}$

$$\begin{array}{lcl} I_o^{\pm} + N_1 \rightleftharpoons I_1^{\pm} + N_o \text{ (gas)} & & \Delta P_i^{\circ} \\ \Delta P_s \downarrow \quad \downarrow \Delta P_s & & \downarrow \Delta P_s \quad \downarrow \Delta P_s \\ I_o^{\pm} + N_1 \rightleftharpoons I_1^{\pm} + N_o \text{ (solution)} & & \Delta P_i^{\circ} \end{array}$$

For such an isodesmic exchange reaction the ionization of a given neutral acid or base, N_1 is compared with that of a standard acid or base, N_o, as they go to their respective cations, I_o^+, or I_1^+, or their anions, I_o^-, or I_1^-. The solvation properties ΔP_s may be the solvation enthalpies ΔH_s°, the standard free energies of solvation ΔG_s° or the corresponding entropies ΔS_s°. If the relative free energies of solvation of the neutrals, $\delta\Delta G_s^{\circ}$, are available from Henry's Law constants, the relative free energies of the ions can be calculated by combining the relative standard free energies of ionization, $\delta\Delta G_i^{\circ}$, in the gas phase and in solution with $\delta\Delta G_s^{\circ}$ for the neutrals. In the same manner, the relative enthalpy of solvation of the ion $\delta\Delta H_s$ (I_1) can be gotten from the heats of solution of N_1 and N_o from the gas phase to the solvent and the heats

of ionization. Heats of solvation from the gas phase to infinite dilution can be derived from heats of vaporization of the pure liquid or solid acids or bases and from their heats of solution in the solvent. We have reported a number of such analyses for aliphatic ammonium ions (4,5,6), pyridinum ions (7,8), alkoxide ions, phenolate and enolate anions (9,10).

Of particular interest to mass spectrometry and petroleum chemistry is the behavior of carbonium ions. Recently we described a low temperature calorimeter (11) which could be employed for measuring the heats of ionization of many alkyl chlorides and fluorides to simple alkyl carbonium ions by reaction with SbF_5 at low temperatures in solvents of very low nucleophilicity such as SO_2ClF. The conditions for forming such ions have been reported extensively by Olah and his colleagues (12).

Although such ionization processes are of inherent interest they can only be used to evaluate the heats of formation of the carbonium ions themselves if the heats of formation of the alkyl chlorides are known with an accuracy which is at least as good as that for the ionization processes. Until now only a few such reliable data were available for alkyl chlorides. However, many excellent data are available for the heats of formation and vaporization of alkenes. During the past winter we have found that rapid, clean addition of HCl to branched olefins to yield tertiary alkyl chlorides may be accomplished in a calorimeter at -55° in dilute CH_2Cl_2 solution. The resulting heat of hydrochlorination may be combined with the heat of formation of the olefin and HCl with appropriate heats of solution of the olefin and alkyl chloride to provide finally the heat of formation of the carbonium ion in solution. Figure 1 presents a plot of such derived values for carbonium ions (probably as ion-pairs) produced from RCl + SbF_5 in SO_2ClF at -55°. Comparison with corresponding estimates of heats of formation of the carbonium ions in the gas phase leads to clear evidence that the relative solvation energies of these ions is minimal (although of course the electrostatic solvation energies are very large indeed).

Several important points emerge at once. First, that charge-localized carbonium ions behave very differently in their solvation energies in SO_2ClF than do ammonium or oxonium ions in water (13,14). The absence of hydrogen bonding interactions between ion and solvent in the former case seems to be a likely reason for the difference. Secondly, the close correspondance of solution phase behavior with that in the gas phase may provide a useful check on gas phase processes where the structure of the ion is debatable. It also provides useful primary data for comparison with energies calculated by various quantum mechanical methods. Thirdly, we note that the method is not limited to the determination of the heats of formation of tertiary chlorides. Many primary or secondary chlorides rearrange instantly to tertiary carbonium ions. If the same ion is produced quantitatively from several isomeric chlorides, any difference in their heats of ionization can be directly referred to the differences in heat of formation of the original chlorides. Accordingly, if the heat of formation of only one of the isomeric chlorides can be determined from the olefin, the heats of formation of the others can be calculated from their heats of conversion to a common ion.

Finally, it is important to emphasize that knowledge of the heats of formation of neutral precursors is essential for resolving problems where contributions from ion stability are implied. Many arguments regarding rates, free energies or enthalpies of ionization have been treated solely in terms of the relative stabilities of the ions or transition states involved. We have shown recently (11) that large errors can be produced through such reasoning. The method of determining heats of formation of alkyl halides and subsequently of the resulting carbonium ion provides a useful method for resolving this problem.

Acknowledgements: This work has been supported generously by the Petroleum Research Fund of the American Chemical Society and by the National Science Foundation.

References

1. J. F. Wolf, R. H. Staley, I. Koppel, M. Taagepera, R. T. McIver, Jr., J. L. Beauchamp and R. W. Taft, J. Amer. Chem. Soc. 99, 5417 (1977).

2. D. H. Aue and M. T. Bowers in "Gas Phase Ion Chemistry", M. T. Bowers, Ed., Academic Press, N.Y., 1979.

3. P. Kebarle, Ann. Rev. Phys. Chem., 28, 445 (1977).

4. E. M. Arnett, F. M. Jones, III, M. Taagepera, W. G. Henderson, J. L. Beauchamp, B. Holtz and R. W. Taft, J. Amer. Chem. Soc., 94, 4724 (1972).

5. D. H. Aue, H. M. Webb and M. T. Bowers, J. Amer. Chem. Soc., 94, 4726 (1972); 98, 311, 318 (1976).

6. F. M. Jones, III and E. M. Arnett, Prog. Phys. Org. Chem., 11, 263 (1974).

7. E. M. Arnett, B. Chawla, L. Bell, M. Taagepera, W. J. Hehre and R. W. Taft, J. Amer. Chem. Soc., 99, 5729 (1977).

8. E. M. Arnett and B. Chawla, ibid., 100, 214, 217 (1978).

9. E. M. Arnett, L. E. Small, D. Oancea, and D. Johnston, J. Amer. Chem. Soc., 98, 2346 (1976).

10. E. M. Arnett, L. E. Small, D. Oancea, and D. Johnston, Faraday Symposium Chem. Soc. # 10, 206 (1975).

11. E. M. Arnett and C. Petro, J. Amer. Chem. Soc., 100, 5402, 5408 (1978).

12. G. A. Olah, Science, 168, 1298 (1970) and many subsequent articles. See especially "Carbonium Ions", ed. by G. A. Olah and P. von R. Schleyer, Vols. 1-5, J. Wiley, New York.

13. E. M. Arnett and G. Scorrano, Adv. Phys. Org. Chem., 13, 83 (1976).

14. R. W. Taft, J. F. Wolf, J. L. Beauchamp, G. Scorrano and E. M. Arnett, J. Amer. Chem. Soc., 100, 1240 (1978).

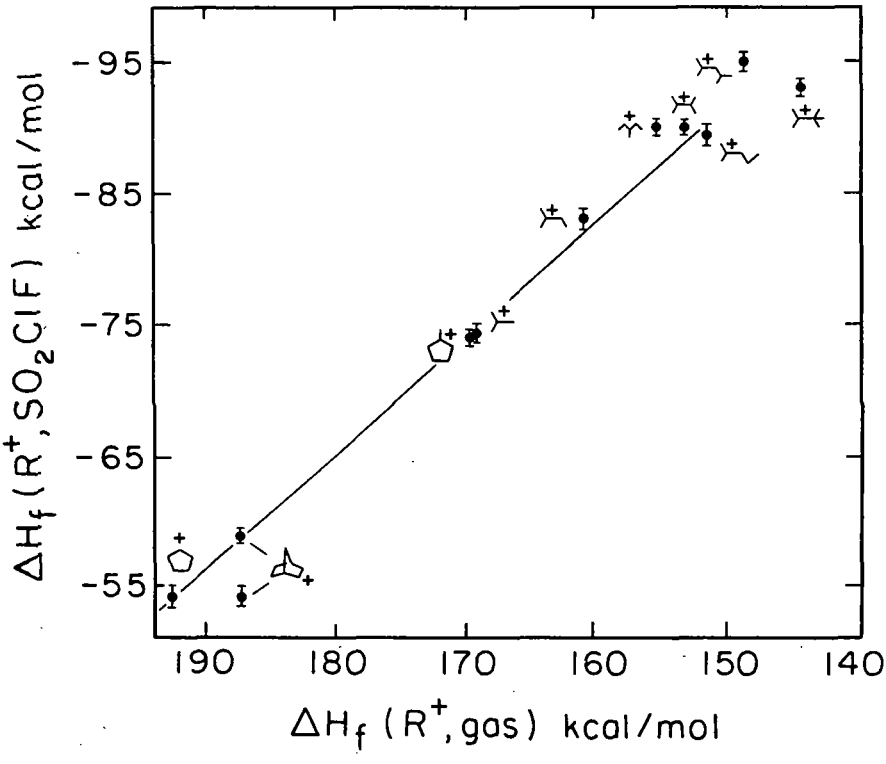


Figure 1. Correlation of Heats of Formation of Carbonium Ions in Solution and in the Gas Phase (see P. Kebarle, ref. 3). Slope of line is 1.09 and coefficient of correlation is 0.966.

TPM0A5 ION-SOLVENT MOLECULE CLUSTERS IN GAS PHASE AND ION SOLVATION IN LIQUID SOLVENTS, P. Kebarle, Edmonton T6G 2G2, Canada.

Measurement of the gas phase ion-solvent molecule equilibria $I^{\pm}(Sl)_{n-1} + Sl = I^{\pm}(Sl)_n$ leads to $\Delta G^{o}_{n-1,n}$, $\Delta H^{o}_{n-1,n}$ and $\Delta S^{o}_{n-1,n}$. Correlation of these data with behavior in liquid solvent is best obtained by comparing solvation of two different ions in the same solvent. Three different types of behavior are observed: (1) solvation difference in gas phase approaches that in solution after only one solvent molecule (Example carbonium ions and CH_2Cl_2 solvent). (2) Solvation in gas phase approaches that in liquid solution for n ≈ 5-10 (positive and negative ions in aprotic solvents). (3) Solvation gas phase does not come close to that in liquid solution (substituted pyridines in H_2O). Explanation of these results can be given and is of fundamental interest.

A COMPARISON OF SURFACE ANALYTICAL TECHNIQUES

Charles A. Evans, Jr.
Charles Evans & Associates
1670 S. Amphlett Blvd., Suite 120
San Mateo, CA 94402

The demands of modern science and technology have fostered the development of a variety of surface analytical techniques. Most of the techniques employ a spectroscopy in which the analytical signal has a shallow escape depth (3-20 Å) combined with energetic ion sputtering to advance this shallow analytical volume through the depth of interest. These techniques are:

1. Auger electron spectroscopy (AES) - A focused electron beam impinges on the sample surface and causes inner shell electrons to be ejected. An outer shell electron falls into this vacancy and another outer shell electron is ejected to provide an energy balance to the atom. The kinetic energy of the ejected electron is characteristic of the emitting atom and can traverse only 3-20 Å before losing some of its characteristic energy. Thus, electron spectroscopy of the ejected electrons contains discreet peaks from the atoms in the outermost atomic layers superimposed on a high background due to inelastically scattered electrons from the deeper layers. Ion sputtering generally employs 500-3000 eV Ar^+ to accomplish in-depth analysis. Lateral analyses can be accomplished by focussing the primary electron beam and localizing the analytical excitation. The commercially available instruments have differing capabilities with spot sizes of 300 Å, 2000 Å, 3 μm and 50 μm diameters available in the different instrumental configurations.

2. Electron Spectroscopy for Chemical Analysis (ESCA) - This is the second of the surface electron spectroscopies and employs x-ray bombardment of the sample to eject an inner shell electron. This ejection is via an elastic energy transfer process thereby transferring the total photon energy to the electron. In leaving the atom, this photoelectron must give up its binding energy, thereby having an energy of

$$E_{kinetic} = E_{photon} - E_{binding}$$

when it leaves the sample surface (there is a small but constant correction for the instrument's work function). Thus, electron energy spectrometry of the ejected electrons give not only an elemental identification but also a measure of the actual electron binding energy. Since this energy is influenced by the other atoms surrounding or bonded to the emitting atom, the chemistry of the sample surface can be probed. Due to the difficulties of focussing x-rays, the ESCA technique provides little lateral analysis capability. This surface spectrometry can be combined with ion sputtering for in-depth analysis but one must be aware of the possibility of chemical alteration of the surface by the sputtering process.

3. Ion Scattering Spectrometry (ISS) - During the energetic ion bombardment of a surface, a certain fraction of the impinging ions are scattered from the outermost surface atoms rather than being immediately incorporated in the sample surface. These scattered ions lose energy during the scattering process depending on their mass (m) and that of the impacted or recoiled atom (M).

$$E_{final} = E_o \left(\frac{M-m}{M+m}\right) \quad \text{for } 90^o \text{ scattering}$$

Thus, the determination of the scattered ion energy (using an electrostatic sector or cylindrical mirror analyzer) provides a mass identification of the atoms present in the outermost atomic layer. This capability is unique among the surface analytical techniques. The ion scattering process is accompanied by sputtering of the surface thereby permitting in-depth distributional analysis. It should be noted that the atomic mixing which accompanies the sputtering process will mix adjacent layers to the extent that the intrinsic depth resolution advantage of the ISS technique will not be fully realizable. In most cases the attainable resolution will be the same as any of the other surface techniques employing the same energy sputtering ions. Lateral resolution in the ISS technique is controlled by the probing ion beam diameter and commercial instrumentation is available with approximately 100 μm resolution.

4. Secondary Ion Mass Spectrometry (SIMS). A fraction (10^{-1} - 10^{-5}) of the atoms ejected from a surface by the sputtering process leave the surface as positive and negative ions. This ion flux is representative of the outermost atomic layers and can be extracted in a mass spectrometer for mass-to-charge analysis and detection. Due to the relatively high ionization efficiency, the high transmissions of magnetic mass spectrometers (10^{-2} - 10^{-1}) and low background noise attainable for ion detection (<1 cps), the SIMS technique is by far the most sensitive of the surface analytical techniques. Routinely, detection limits of better than 1 ppm can be attained per data point in a depth profile when sampling a volume 150 μm in diameter and 10-20 Å in depth. Lateral resolutions of 0.3 μm to 2 μm can be attained by localizing the ion emission in the ion microscope or the ion microprobe instrument.

It should be noted that the main contributor to (or detractor from) depth resolution in an in-depth profile is generally the quality of the sputtering process, not the escape depth of the particular analytical signal. Thus, in a well-behaved matrix, such a single-crystal or amorphous layer, the depth resolution of a profile can approach 50 Å or 1% of the depth, whichever is greater. This performance is degraded by the use of high ion impact energies (>2-5 keV), inert gas ion sputtering, poor ion beam or sputtered crater shape or study of polycrystalline matrices. There are numerous operating "tricks" used to overcome the artifacts of the sputtering process and the reader is referred to the literature to learn these.

There is one surface and thin film analytical technique which does not use ion sputtering to obtain an in-depth analysis: MeV He^+ backscattering spectrometry. When an MeV He ion impinges on a surface, a small fraction (10^{-6} - 10^{-7}) of the ions backscatter from the surface atoms with an energy loss during the recoil process. For those ions backscattered 180^0, the final energy, E_f, can be related to the initial energy, E_0, by the relationship

$$E_f = E_0 \left(\frac{M-m}{M+m}\right)^2$$

where m is the mass of the probing ion and M is the mass of the recoiled ion. The backscattered ion can be detected with a surface barrier detector and its energy characterized by the detector pulse height distribution. As those highly penetrating ions, which were not backscattered, traverse successive atomic layers, kinetic energy is lost to coulombic interactions with the electrons in the target by a well characterized process and quantitatively related to the amount of material traversed. Should a probe ion recoil from a subsurface atom, it will lose energy according to the above Rutherford relationship but with E_0 (the energy as reduced by the coulombic interactions). Moreover, the backscattered ion will lose energy after the scattering event as it goes back toward the surface. Thus, the detected energy will be characteristic of not only the mass of the target atom but also the depth at which the interaction took place. Since the probing ion beam simultaneously samples all depths to about a micrometer, backscattering spectrometry provides a rapid survey analysis of the material. The depth resolution is controlled by the detector resolution and statistical nature of the energy loss process and is generally taken to be 150-300 Å. As generally practiced, the lateral resolution is 1-2 mm but some laboratories have constructed units with 10-20 μm diameter probes.

For a more detailed discussion of the capabilities, limitations, comparative features and applications of these techniques, the reader is referred to the following references:

1. "Comparison of Backscattering Spectrometry and SIMS Analysis of Ta_2O_5 Layers," W.K. Chu, M-A. Nicolet, J.W. Mayer, and C.A. Evans, Jr., Analytical Chemistry 46, 2136 (1974).

2. "Thin Film Compositional Analysis - A Comparison of Techniques," C.A. Evans, Jr., Journal of Vacuum Science and Technology 2, 144 (1975). (Invited article.)

3. "Surface and Thin Film Analysis," C.A. Evans, Jr., Analytical Chemistry 47, 855A (1975). (Invited article.)

4. "Surface and Thin Film Compositional Analysis: Description and Comparison of Techniques," C.A. Evans, Jr., Analytical Chemistry 47, 818A (1975), (invited article). These two invited articles are also being reprinted.

5. "A Comparison of the Techniques for Silicon Surface Analysis," C.A. Evans, Jr., NBS Workshop Report on the ARPA/NBS Workshop on Surface Analysis for Silicon Devices (NBS, Washington, D.C., 1975), NBS Special Publication SP-400-23.

6. "Workshop on Surface Analysis and Secondary Ion Mass Analysis," C.A. Evans, Jr., B.N. Colby, G.L. Kearns, W. Singer, Analytical Chemistry 45, 398A (1973).

7. "Modern Experimental Methods for Surface and Thin Film Chemical Analysis," C.A. Evans, Jr., and R.J. Blattner, Surface and Thin Film Chemical Analysis, Annual Review of Materials Science, R.A. Huggins, Ed., Vol. 8 (1978).

8. "Modern Ion Beam and Related Techniques for Materials Characterization," R.J. Blattner and C.A. Evans, Jr., Fifth International Conference on Crystal Growth, Boston, July 17-22, 1977, Proceedings.

AN ISS-SIMS STUDY OF SAPPHIRE SURFACES AND THE SILICON/SAPPHIRE INTERFACE

William L. Harrington and Charles W. Magee
RCA Laboratories, Princeton, N. J. 08540

It is widely accepted that the semiconducting properties of heteroepitaxial silicon on sapphire are strongly influenced by the incorporation of reaction products during initial stages of Si growth.[1,2] In previous SIMS investigations in collaboration with Cullen, Corboy, and Smith of RCA,[3,4] we have observed, for example, that over a distance of about 500 Å from the Si/substrate interface the Aℓ concentration in the Si film increases as one profiles from the surface to the substrate; this distance is in good agreement with the minimum thickness required for complete coverage of the substrate during growth.

In addition to contamination of the Si by substrate material, it is also recognized that foreign contamination from numerous sources can exist on a sapphire substrate at the time of Si deposition. Thus polishing and cleaning of these wafers is a critical step in controlling properties.

It is the purpose of this study to combine the capabilities of several techniques to (1) determine the elemental surface composition of sapphire from various sources and processed by several polishing and cleaning procedures--this phase uses low energy ISS where very low sputter rates and high surface sensitivity even on insulating materials are considerable assets; (2) grow thin layers of Si (<1000 Å) on these same 3" diameter substrates and examine the resulting interfaces with SIMS; and (3) finally correlate these findings with electrical properties of the layers such as carrier mobility and comparative lifetime.

Results to date can only be considered a preliminary progress report rather than a completed study. The preliminary indications are promising, however, and the work reported here demonstrates the usefulness of the techniques for investigation of this system.

The surface sensitivity of ISS and its usefulness in shallow depth profiles of interfaces have been described in numerous publications[5,6] and will not be repeated here. The instrument utilizes the 3M Model 515 cylindrical mirror analyzer with a simple tray holder allowing an entire 3" diameter sapphire wafer to be mounted for analysis. Micrometer adjustment allows successive analyses for uniformity studies over about 2" of the wafer. Figure 1 shows a series of spectra obtained for an "as-received" wafer. Vendors will not be identified at this time. Each spectrum represents a static spot analysis with $^4He^+$ at 2000 eV with a beam diameter of about 150 μm. During each scan the instrument sweep is under computer control (HP1000) and pulse-counted signals from the channel multiplier are digitally stored for later processing and plotting. A program-addressible voltmeter samples the output at a rate of 1000 Hz and averages 500 readings for each point of the spectrum. Three hundred points were taken for each scan so that data for each analysis spot were accumulated in 150 seconds. The spectra are offset vertically by a constant amount to show the relative uniformity across the wafer. It is obvious that the process used to polish and clean this wafer leaves a uniformly contaminated surface. After polishing, there must have been an HF-containing cleaning step that leaves a large amount of F on the surface. Fe is also uniformly present, and Cℓ is variable across the surface.

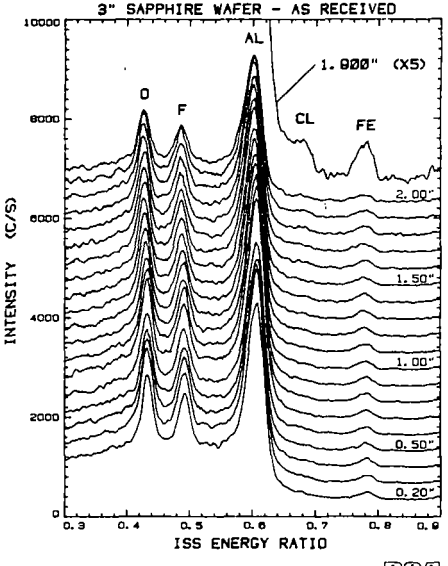


FIGURE 1

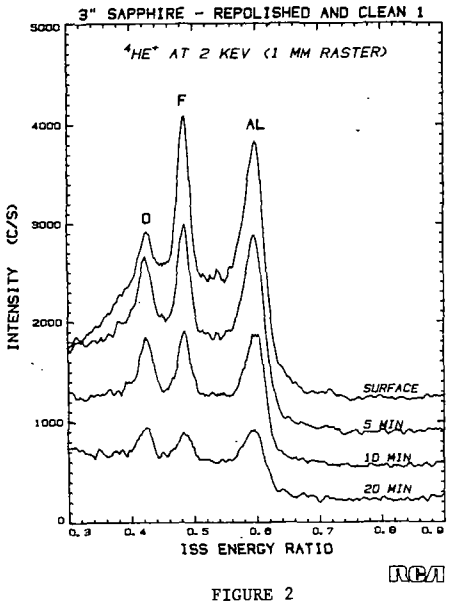


FIGURE 2

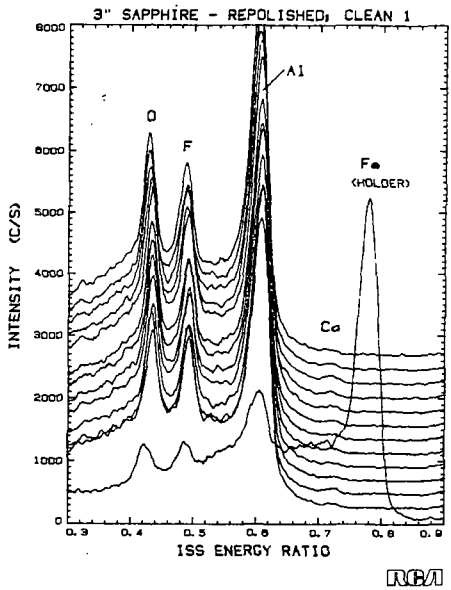


FIGURE 3

A second wafer from the same source was repolished and cleaned in solutions incorporating oxidizing agents. This procedure is labeled Clean #1 in Figures 2 and 3. Figure 2 shows spectra taken with a rastered beam in one sample location, i.e., a very shallow depth profile covering only about 2-10 Å for the entire 20-minute series. This series shows still the presence of F concentrated at the surface, and at expanded scales there is no indication of Fe or Cℓ as in the as-received sample, but a slight indication of Ca. The presence of a large, non-conducting sample plane slightly defocusses the beam near the center of the sample. This results in overall decreased intensities as the surface contamination is sputtered away.

Figure 3 shows the results of static beam analysis across the wafer for direct comparison with Figure 1. The bottom scan was taken on the edge of the wafer with part of the beam striking the stainless steel holder. Note that no Fe is detected at the second location, thus showing that Fe on the as-received wafer (Figure 1) is not contamination from the surroundings. Cℓ, which would occur at $E_1/E_0 = 0.68$ is not present, but Ca is now present uniformily across the surface. The presence of F, even after cleaning, shows this element to be tightly bound as a non-volatile species rather than simply adsorbed on the surface.

Wafers from other sources and having experienced other processing have been and are being analyzed in a similar manner. These surfaces range in appearance from no detectable F to highly contaminated with Na, Ca, and other heavy metals.

Although the second phase of this effort is only slightly underway, we have established conditions for high sensitivity SIMS depth profiling with the quadrupole-SIMS system previously described by C. Magee[7]. By first sputtering through a Si layer to the sapphire substrate, optimum charge neutralization conditions for the electron beam[8] can be determined. This neutralization minimizes artifacts at the insulating interface.

Figure 4 illustrates the SIMS profiling capability of this system on a 6000 Å Si film on sapphire which had been implanted with H atoms. For this very preliminary evaluation, the Aℓ secondary ion response was not calibrated under these conditions, and is plotted with an arbitrary scale factor. This shows that once the sapphire is reached, no charging occurs and a steady, artifact-free signal can be obtained. Although not optimized in this example, very large raster/gate ratios will be used with thinner films as a guard against unevenly sputtered craters.

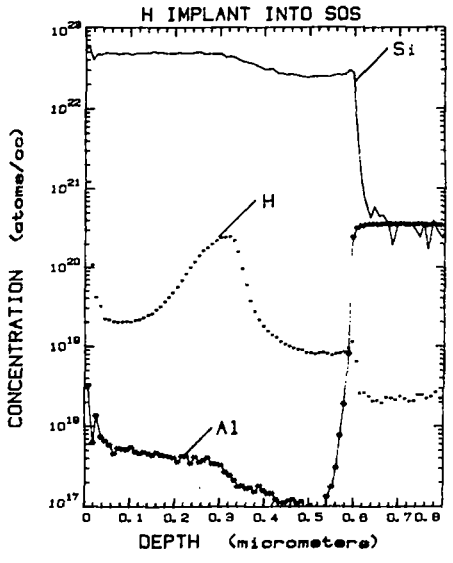


FIGURE 4

In conclusion, we have demonstrated that variable surface contamination is present on sapphire wafers as a result of polishing and cleaning. In addition, we have established conditions for careful SIMS depth profiling of Si films deposited on such surfaces with the hope of understanding the resulting interface and relating these properties to electrical behavior.

REFERENCES

1. G. W. Cullen, J. Crystal Growth 9, 107(1971).

2. H. M. Manasevit, J. Crystal Growth 22, 125(1974).

3. W. L. Harrington, C. W. Magee, G. W. Cullen, and J. F. Corboy, 24th Ann. Conf. on Mass Spec. and Allied Topics, San Diego, CA, Paper No. M-4, 1976.

4. G. W. Cullen, J. F. Corboy, and R. T. Smith, J. Crystal Growth 31, 274-283(1975).

5. W. L. Harrington, NBS Special Publication 400-23, ARPA/NBS Workshop IV, Surface Analysis for Silicon Devices, issued March, 1976.

6. W. L. Harrington, R. E. Honig, A. M. Goodman, and R. Williams, Applied Phys. Lett. 27, No. 12, 644-645(1975).

7. C. W. Magee, W. L. Harrington, and R. E. Honig, Rev. Sci. Instrum. 49, 477(1978).

8. C. W. Magee and W. L. Harrington, Applied Phys. Lett. 33, No. 2, 193-196(1978).

A QUANTITATIVE SIMS ANALYSIS OF DECALIBRATED CHROMEL VERSUS ALUMEL THERMOCOUPLES USING INDEXED SENSITIVITY FACTORS*

W. H. Christie, R. E. Eby and T. G. Kollie
Oak Ridge National Laboratory
Oak Ridge, Tennessee 37830

In this study we have used secondary ion mass spectrometry (SIMS) to determine the failure mode responsible for the large decalibrations observed in sheathed, MgO-insulated Chromel versus Alumel, compacted thermocouple assemblies, exposed to temperatures above 1100°C. Thermocouples sheathed in Inconel-600 and type 304 stainless steel were studied in this work. Quantified SIMS data showed that the observed decalibrations were due to significant alterations that took place in the Chromel and Alumel thermoelements. The amount of alteration was different for each thermocouple and was influenced by the particular sheath material used in the thermocouple construction. Relative sensitivity factors, indexed by a matrix ion species ratio, were used to quantify SIMS data for three nickel-based alloys, Chromel, Alumel, and Inconel-600, and an iron-based alloy, type 304 stainless steel.

After exposure to high temperature in air in a calibrated temperature gradient tube furnace, a number of transverse cross sections were cut from the thermocouples for analysis. The specimens and the required standards were imbedded in epoxy and polished until a smooth metallographic finish was obtained prior to SIMS analysis. Table 1 lists the compositions of the various materials analyzed in this work.

Table 1. Nominal Compositions (Atom %) of Standard Materials Investigated in This Study

	Chromel	Alumel	304 S.S.	Inconel 600	NBS NX -980	NBS NX -1285
Al	0.02	4.19	0.0014	0.40	0.55	0.38
Si	0.92	3.53	1.95	0.41	0.22	0.49
Cr	10.37	0.0008	19.96	17.42	16.73	17.85
Mn	0.01	3.01	1.99	0.21	0.40	0.32
Fe	0.35	0.031	66.42	7.39	8.93	6.92
Ni	88.33	88.76	9.32	74.28	72.31	73.16
Co	0.04	0.48	0.014	-	-	-

In the nickel-based alloys, Alumel, Chromel, Inconel-600 and two NBS standards, we found that the ratio NiO^+/Ni_3^+ was very sensitive to oxygen surface coverage. Sensitivity factors for Cr and Fe, determined from Chromel and the two NBS standards were plotted as a function of the NiO^+/Ni_3^+ indexing ratio and are shown in Fig. 1. Although these three standard materials are different in composition (See Table 1), the S.F.'s for Cr when indexed by the NiO^+/Ni_3^+ ratios fall on the same line. The S.F. plots that we used in analyzing the Chromel and Alumel wires from the decalibrated thermocouples are presented in Figs. 1 and 2. Aluminum, Mn, Co, and Si values were determined from the Alumel standard as these elements were present at higher abundances than in the Chromel standard. The S.F.'s for Cr and Fe were determined from Chromel for similar reasons.

The shape of these S.F. curves verifies the observation that higher accuracy and more reproducible results are obtained with O_2 flooding in the sample region when oxidizable metallic samples are being analyzed. In this system of Ni-based alloys, we found that oxygen pressures of $4\text{-}8 \times 10^{-6}$ torr and current densities of .2 mA cm^{-2} tended to keep the NiO^+/Ni_3 ratio above 20 and thereby allowed S.F.'s from the flat region of the S.F. response curve to be used.

*Research sponsored by the U. S. Department of Energy under Contract #W-7405-eng-26 with the Union Carbide Corporation.

By acceptance of this article, the publisher or recipient acknowledges the U.S. Government's right to retain a non - exclusive, royalty - free license in and to any copyright covering the article.

The stainless steel sheath of thermocouple I, being an iron alloy, was analyzed using a different set of S.F.'s based on Fe as the reference element. The indexing ratio used was FeO^+/Fe^+. The S.F.'s derived from this alloy are shown in Fig. 3. A different type response was observed in this system. As O_2 surface coverage increased, the observed S.F. range, with the exception of silicon, decreased and at high coverage tended to converge on the reference element value (Fe ≡ 1).

Chromel and Alumel thermocouples, sheathed in reactive metals (Inconel-600 and type 304 stainless steel) decalibrate significantly when exposed to temperatures above 1100°C. The decalibration is caused by the alteration in composition of the Chromel and Alumel thermoelements. Significant migrations of Al, Si, Cr, Mn, and Fe were seen to occur in the Chromel and Alumel thermoelements and in the sheath materials. For example, Cr which was present in virgin Alumel at the 0.0008 atomic % level was observed to increase a factor of 1500 in regions of the thermocouple exposed to temperatures above 1100°C. The source of this Cr was the Chromel thermoelement and the sheath. The specific nature of the compositional alteration was influenced by the chemical environment present in the hot thermocouples.

The use of single, unindexed S.F.'s for calculating these data was found unacceptable. Oxygen pressure >2 x 10^{-6} torr in the sputtering region gave a more reproducible set of sensitivity factors and indexing with a matrix ion species ratio allowed the correct set of S.F.'s to be chosen for any given set of analytical conditions (oxygen pressure, current density, sample composition, etc.). A detailed account of this work has been accepted for publication in *Applications of Surface Science*.

FIG. 1. Cr AND Fe SENSITIVITY FACTORS DETERMINED FROM CHROMEL, NBS STANDARDS NX-1285 AND NX-980

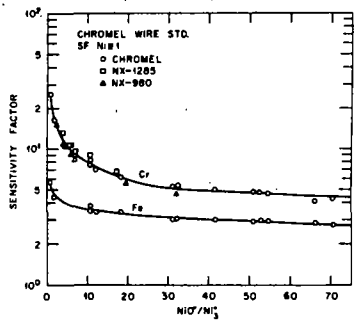


FIG. 2. Al, Mn, Co AND Si SENSITIVITY FACTORS DETERMINED FROM ALUMEL

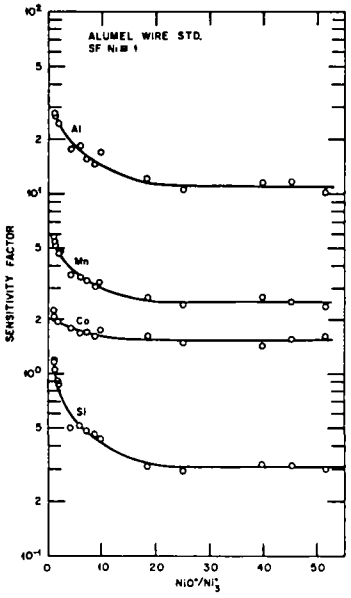
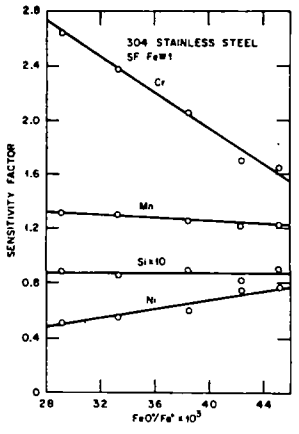


FIG. 3. Cr, Mn, Si, AND Ni SENSITIVITY FACTORS DETERMINED FROM TYPE 304 STAINLESS STEEL



INITIAL ENERGY DISTRIBUTIONS OF SECONDARY (+) IONS FROM THE SPUTTERING OF METALS WITH 10 KeV Ar^+*

Frank G. Satkiewicz
The Johns Hopkins University, Applied Physics Laboratory
Laurel, Maryland 20810

In order to test theories of ion production and to provide a basis for quantitative SIMS analyses, secondary ion energy distribution (SIED) curves from the sputtering of metals must be obtained. Previous results on species sputtered from various glasses[1] showed that for some elements, sizeable errors in relative ion yields arise if differences in distribution are not taken into account. In the current phase of characterizing solids by ion sputtering at APL, a number of pure metals were studied using the GCA IMS 101-B prototype[2]. For obtaining the ion distributions, the α and β apertures were reduced to give approximately a 5 eV energy window. The extraction conditions for the secondary ions were studied to provide a basis for reproducible results. A primary beam of 10 KeV Ar^+ was used to sputter high purity targets at current densities of 15 ma/cm^2 (focused) and 500 μA/cm^2 (defocused). The condition of the target surface was evaluated from a succession of spectra. Results were obtained in the ultimate vacuum (~10^{-7} Torr) and with varying O_2 partial pressures up to 10^{-5} Torr. To compare the SIED curves, the first moment $\bar{E}$, the square root of the second moment, $\sqrt{m_2}$, the coefficient of skewness, a_3, and the coefficient of kurtosis, a_4, were calculated. As an example, the moments for Fe^+ are shown in Table I; note the significant effect of oxygen. Oxygen also lowers $\bar{E}$ for Al, Co, Si, Mo, Mn, and Mg; raises it for W and Ta; and does not affect Ni, Cu, and Ag greatly. A comparison of $\bar{E}$'s obtained in this work was made with values reported by Hennequin[3], Jurela[4], DÜsterhöft[5], and Snowdon and MacDonald[6]. An attempt was made to compare data obtained with similar primary and background conditions. The results are shown in Table II for the energy range 0-150 eV. The data of Jurela, and Snowdon and MacDonald, were adjusted to lower values since they used 40 KeV Ar^+ vs. 10 KeV in this work. Considering the variety of experimental methods and differences in surface and extraction conditions, the agreement is good although values reported by Jurela for Cu and Au appear to be on the low side. Table III shows the comparison with Hennequin's data which were obtained in the range 0-400 to 500 eV. Table IV shows that $\bar{E}$ in the range 0-150 eV falls far short of $\bar{E}$ in the broader range indicating that distribution data in a more narrow range can be in error when used in testing theories of ion production.

---

(1) Satkiewicz, F. G., Proc. 25th Annual Conf. on Mass Spectrometry, 1977, pp. 312-314.

(2) Herzog, R. F. K., Poschenrieder, W. P., Satkiewicz, F. G., "Mass Spectrometer Analysis of Solid Materials with the Ion-Microprobe Sputter Source," Final Report NASA Contract No. NA55-9254, NASA CR-683, 1967.

(3) Hennequin, J., Le Journal de Physique, 29, 655 (1968).

(4) Jurela, Z., Int. J. of Mass Spectrom. Ion Phys., 18, 10, (1975).

(5) DÜsterhöft, H., Ihlenfeld, A., Phys. Stat. Sol. (a) 39, K147 (1977).

(6) Snowdon, K. J., MacDonald, R., Int. J. Spectrom. Ion Phys., 28, 233 (1978).

*Supported by APL IR&D funds. (Naval Sea Systems Command N00024-78-C-5384).

Table I

Effect of oxygen on the secondary ion energy distribution of Fe^+ (10 keV Ar^+on Fe).

OXYGEN PRESSURE, $p \times 10^8$ Torr	$\bar{E}$, eV	$\sqrt{m_2}$, eV	a_3	a_4
960*	52.5	83.2	2.61	10.6
10	74.7	108.7	1.96	6.33
7	84.5	117.4	1.78	5.42
3	98.6	127.9	1.48	4.24

*ADDED O_2

Table II

$\bar{E}$ from sputtering metals with Ar^+ (0 – 150 eV).

X^+	SATK.	DUST.	JUR	S&M
Mg	35.6	23	13.9	
Aℓ	29.0	8.5	13.3	36.9
Si	36.6	60	44.1	
Fe	38.3			40.1
Co	32.4	37	38.0	
Ni	34.3	32	69.3	45.4
Cu	56.7	30	11.7	43.7
Mo	36.3	39	28.4	
Ta	53.1	63	47.4	
W	27.9	79	48.6	37.4
Au	51.0		3.3	38.6

Table III

$\bar{E}$ from sputtering metals with Ar^+.

(0 – 400 to 500 eV)

X^+	SATK.	HENN	X^+	SATK.	HENN
Mg	135	120	Ge	(60)*	
Aℓ	64	50	Mo	87	
Si	80	70	Ag	128	220
Mn	127		Ta	77	70
Fe	86	140	W	45	
Ni	96	160	Pt	(34)	
Co	73	170	Au	120	
Cu	132	160			

*VALUES IN ( ) OBTAINED USING 50 eV BAND WIDTH CORRECTED TO 5 eV.

Table IV

Comparison of $\bar{E}$ in two energy ranges.

X^+	MEAN ENERGY, $\bar{E}$, eV	
	(0–150eV)	(0–500eV)
Mg	36	135
Aℓ	29	64
Si	37	80
Fe	38	86
Co	32	73
Ni	34	96
Cu	57	132
Mo	36	87
Ta	53	77
W	28	45
Au	51	120

Etching of SiO_2 and Si By A Helium-Fluorine RF Discharge

by

Michael J. Vasile
Bell Laboratories
Murray Hill, New Jersey 07974

The ionic and neutral gas phase products from an RF discharge in a helium-20% fluorine mixture were investigated. Positive ions directly sampled through the RF electrode or through a grounded electrode that were representative of the gas mixture were He^+, F^+ and F_2^+. Impurity ions resulting from chemical attack on the discharge vessel or from the gas mixture itself were O_2^+, OF^+, COF^+ and CF_3^+. Notably absent were the ions HF^+ and SiF_3^+. Atomic fluorine could not be detected effusing from the discharge, with a detection limit of ca. 2%. Introduction of a specimen of 10^4 Å SiO_2 on single crystal silicon showed that direct ion sampling can be used to monitor the plasma etching of such substrates, when placed either on the RF electrode or on a grounded electrode. Etch rates for SiO_2 ranged between 90-100 Å/min. when the specimen was mounted on the ground electrode, and between 350 to 450 Å/min. when mounted on the RF electrode. The RF electrode was subjected to a higher flux of F^+ than the ground electrode, and the maximum kinetic energies of both F^+ and F_2^+ were of the order of 25 to 30 Volts on the RF electrode and 13 to 15 Volts on the ground electrode. These results suggest that energetic ion bombardment significantly enhances etch rates in this system.

TPM0B6 DETAILED EXAMINATION OF THE OUTER SURFACE BY COMBINED TECHNIQUES:SIMS COMBINED WITH ISS AND SEM, GENE R. SPARROW, 3M Company, Analytical Systems, St. Paul, Minnesota 55133

A new push-button SIMS control designed for rapid versatile surface analysis will be described. SIMS coupled with high depth resolution by ISS can be used routinely to chemically characterize the outer few Å of a material in great detail. Physical characterization of a specimen is readily accomplished at very high spatial resolution using a Scanning Electron Microscope. Combining SIMS with either ISS, SEM or other techniques results in highly complementary systems. Practical applications of these techniques will be reviewed.

A COMPUTERIZED DATA ACQUISITION SYSTEM FOR QUADRUPOLE SECONDARY ION MASS SPECTROSCOPY

Bradway F. Phillips and Nancy E. Lares
Perkin-Elmer Corporation, Physical Electronics Division
6509 Flying Cloud Drive, Eden Prairie, Minnesota 55344

One of the factors which has slowed the acceptance of Quadrupole Secondary Ion Mass Spectroscopy (QSIMS) as a surface analytical technique has been the lack of a reliable method for recording the data. This is a particularly serious problem when one attempts to obtain a depth profile because the signal levels of the various elements of interest can vary over a range of 10^6-1. In order to overcome this limitation, an adaptation of our Multiple-Technique Analytical Computer System (MACS) has been designed to integrate the operation of the QSIMS unit with our Scanning Auger Microprobe (SAM) and Electron Spectroscopy for Chemical Analysis (ESCA) instruments. In line with these other two techniques, we can record the following types of data files: Survey, Profile and Multiplex.

In the Survey mode one may select a portion of the mass spectrum of any width, set the step size in multiples of .05 AMU, the time spent at each step and the number of scans through the selected portion of the mass spectrum. Also available are bookkeeping statements for ion beam voltage (BI), ion beam current (II), condenser lens setting (CND), X-raster (XR), Y-raster (YR), signal gating percentage (GP), pass energy (PE) and retard energy (RE). These are demonstrated in the stainless steel spectrum of Figure 1. Another option is a logarithmic signal display shown in Figure 2 of the same data as Figure 1. In Figure 2 the data was smoothed using a 3 point smoothing routine, and the amount of smoothing is indicated by the S3 in the left margin. Also included is a counts routine which displays both the total counts in any one selected channel and the counts per second at that point.

The second option is the Profile mode in which the integral of single atomic mass peaks is calculated from -1/2 AMU to +1/2 AMU and displayed as a function of sputtering time for up to 20 selected peaks. Also included is the option to set the mass spectrometer on the top of the mass peak and count for a preset time. This option is particularly useful in collecting data from very small peaks that approach the residual noise level of 1 pulse every 2 to 5 seconds. Figure 3 shows the results obtained by profiling through a thin Cr film into a Si substrate. Again the bookkeeping functions are recorded as a part of the profile so that the ion gun and QSIMS spectrometer data needed to set up equivalent profiles in the future is available.

In the third mode, Multiplex, a number of single AMU or short range mass scans can be taken automatically for a number of cycles to average the signals obtained over a specific depth in the specimen being analyzed. This mode is most useful for doing bulk analysis of materials with unchanging composition versus depth characteristics. It is also used to allow a very small peak to build up to a readable level by signal averaging for an extended time.

The technique of QSIMS is greatly enhanced by the ability to record signals in a reproducible manner. We feel that this system of data collection answers most of the questions raised by the formerly inexact methods used to record QSIMS data because not only can all of the primary ion beam and mass spectrometer conditions be recorded, but also the original data file is stored and can be redisplayed without the effects of previous data manipulation distorting the data.

STAINLESS STEEL SURVEY SPECTRUM
LINEAR SCALE

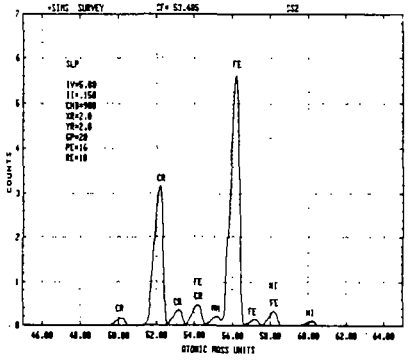


Figure 1

STAINLESS STEEL SURVEY SPECTRUM
LOG SCALE

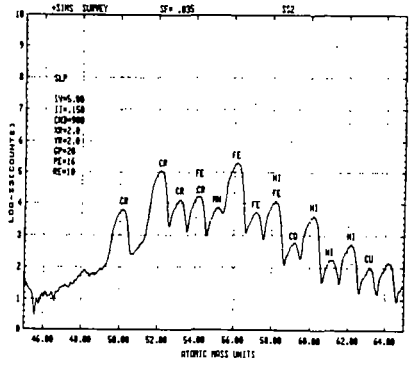


Figure 2

Cr ON Si DEPTH PROFILE
LOG SCALE

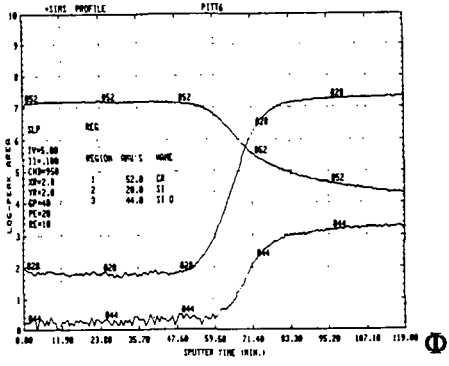


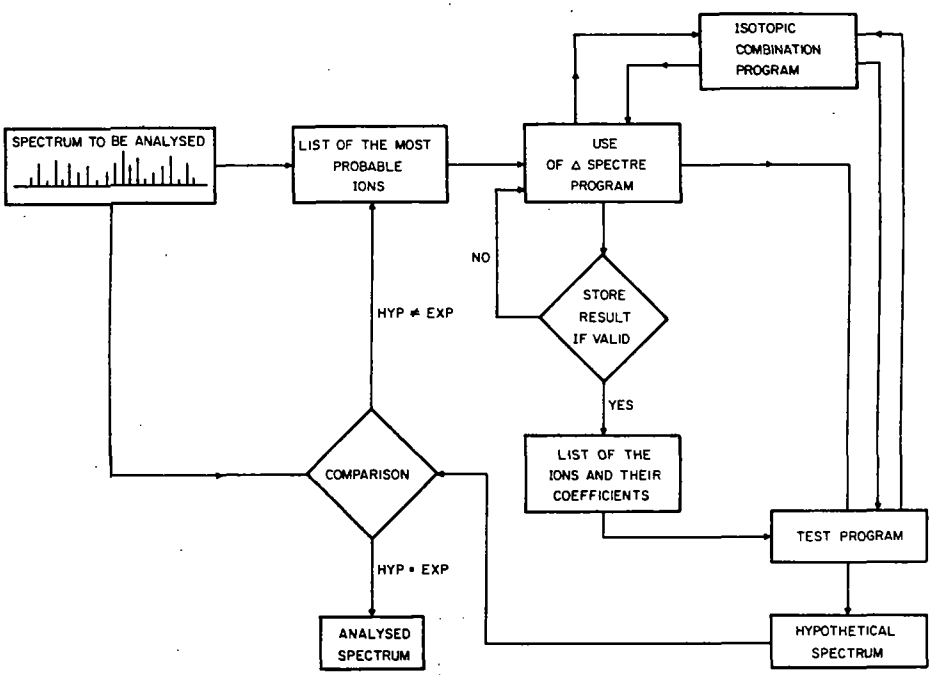
Figure 3

SIMS SPECTRA OF STEEL AND THEIR ANALYSIS BY COMPUTER

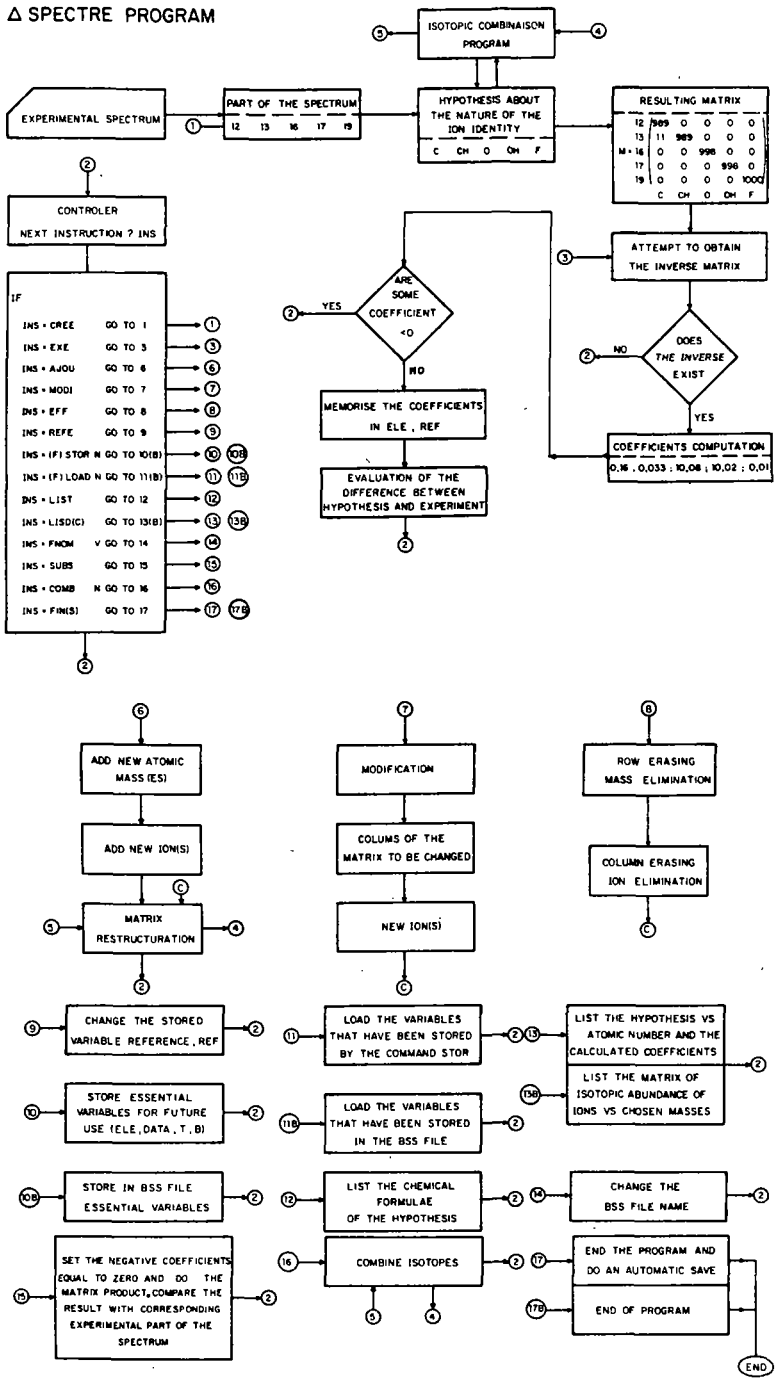
Marcel Baril

Département de physique, Université Laval
Sainte-Foy, Québec, Canada G1K 7P4

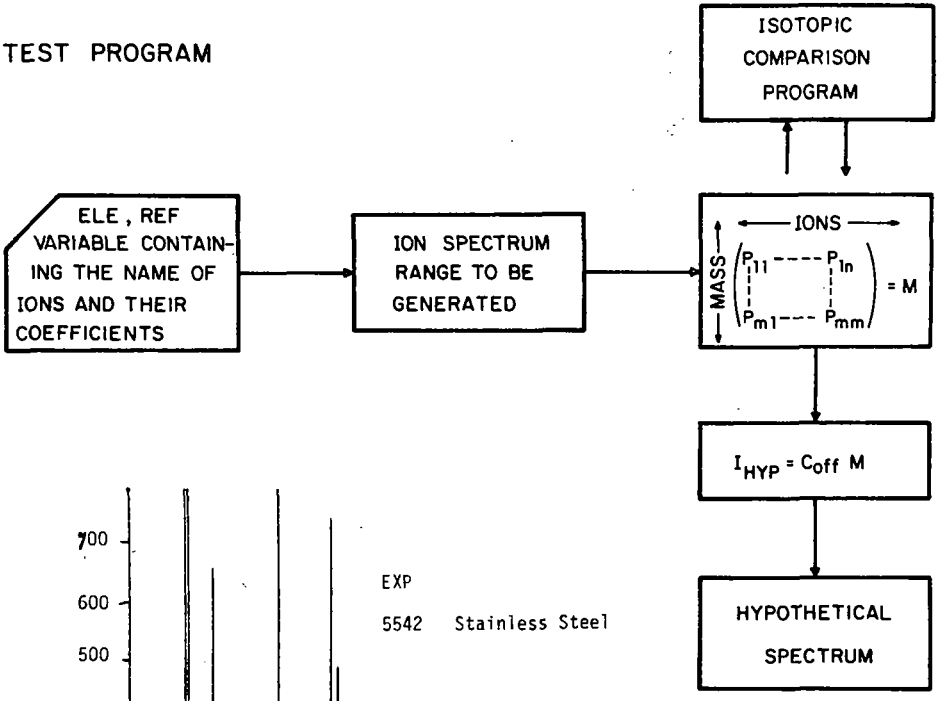
The analysis and interpretation of spectra produced by Secondary Ion Mass Spectrometry with Cs^+ as primary beam is very different from computer file search for organic spectra. Many facts must be taken into account. The presence of such a reactive constituant as Cs result in an enhancement of some peaks. Not only are atomic ions produced but also molecular ones such as oxydes, hydroxydes, hydrides, dimers, trimers, etc. Cluster ions are formed containing one, two or three atomic species. The search is done in a library containing catalogs of the preceeding information. But the 92 elements and their hundreds of isotopes will generate so much possibilities that it will be a waste of time. By selecting probable atomic constituants and working interactively to fit successive portions of the spectrum, it is possible to minimize the number of uninterpreted or multi-interpretated peaks. The following figures present the flow chart of the programs written in APL language. An example of the data and result is also given.

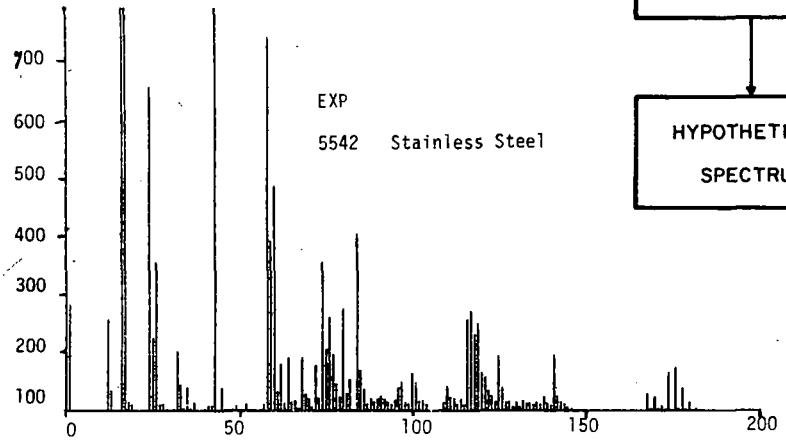


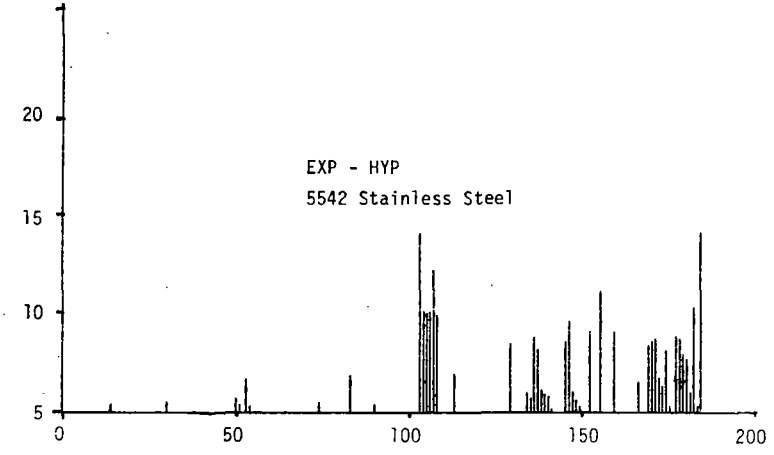
Δ SPECTRE PROGRAM



TEST PROGRAM







TPM0B9 SAMPLE MOUNTING TECHNIQUE--A SIGNIFICANT SOURCE OF BIAS IN THERMAL IONIZATION MASS SPECTROMETRY, E. L. GARNER and K. A. BRLETIC, National Bureau of Standards, Washington, DC 20234

Sample mounting is that part of the thermal ionization mass spectrometry procedure in which a solution of the analyte element is dried on the filament. The sample is then treated in a manner which will yield either a salt or a metal. The form used for analysis is usually not well known but is selected empirically on the basis of the precision of the isotope ratio. Sample mounting is one of the most vulnerable and neglected parts of the procedure because it is generally believed that nothing can occur which will bias the ratio measurement. However, if the evaporation process in the ion source is mass dependent, then the element(s) or salt forms on the filament, and the elemental or molecular species evaporated from the filament are critical.

Isotopic ratio data for sample mounting studies of uranium will be utilized as the primary example of biases which are traceable to sample mounting technique. Corroborative data will also be provided for other elements including Ag, Pu, and Cs.

Experiences with a Fully Automatic Thermal Ionisation Mass Spectrometer.

R.C. Haines, T.O. Merren, P.J. Turner, S. Sayyid.
VG-Isotopes Limited, Road Three, Winsford, Cheshire, CW7 3BX.

Summary.

This paper gives analytical results obtained for a suite of uranium standards run automatically on an Isomass 54 mass spectrometer. Results are also given of data obtained on a strontium standard, on different mass spectrometers, using both single and double collector techniques.

On uranium, for samples of one microgram the accuracy (95% confidence) for the 235/238 ratio for the suite is 0.09%, for the minor peaks 0.1 to 1% the accuracy (95% confidence) is 0.5%. For lower levels in the 20 to 50 ppm range the accuracy is 3%.

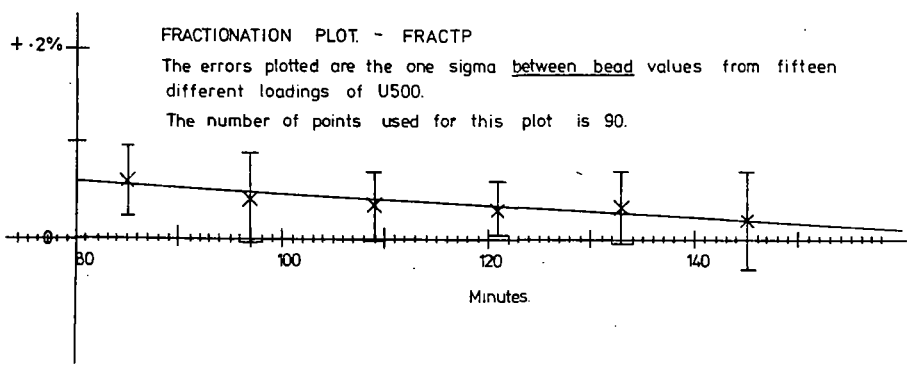
On strontium, the between bead precision obtained was 0.005% (95% confidence) with a value which agreed using both single and double collection techniques.

Measurements on Uranium.

The object of the experiments carried out was to demonstrate the accuracy that can be obtained on an automatic thermal ionisation machine, and therefore a large sample (one microgram total) was loaded on each triple rhenium bead. The information required of results varies from laboratory to laboratory. Representative data was taken as measurements of 234, 235, 236 and 238. This sequence is in no way limited by the hardware or software ; any number of channels could have been selected by the software, even different elements could have been introduced in the same barrel loading. The time required to make a measurement was taken as being of secondary importance. Initially the measurement accepted occured at approximately one hundred minutes, although current results are taken at 60 minutes (ten values over ten minutes).

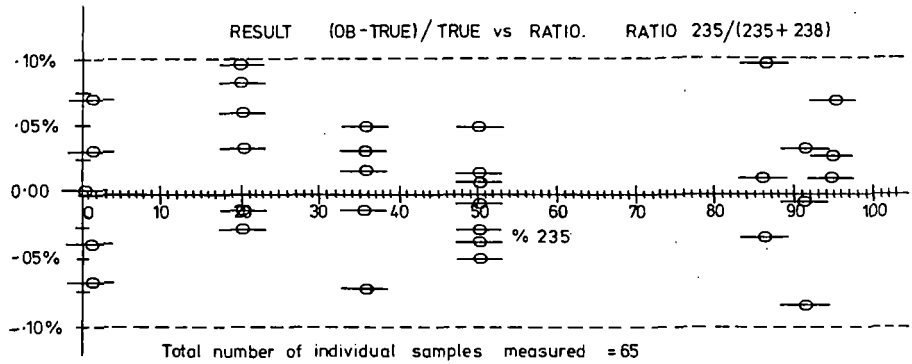
Fractionation Effects.

Fractionation of the sample was found to give the major errors to the values obtained. Care was taken to load the samples similarly, and to take results only after one hour, by which time the irregular effects of fractionation had disappeared. Fifteen different loadings of U500 were used to obtain the fractionation curve. The limits plotted on each point indicates the one sigma between bead precision of the results, that is the 95% confidence on any single measurement of U500, each of the fifteen loadings being measured six times over a period of approximately one hour. The value of bias to be applied to other results was determined from the mean value at 90 minutes. One single value was determined which was applied to all other reference samples.



Suite of Uranium Samples.

Sixty five reference samples were run with 235 content being between 0.5% and 93%. The percentage difference between the observed and the quoted reference value is plotted against percentage of 235. For clarity overlapping results have been omitted. The diameter of the circle plotted is typical of the internal precision. The deviation of all the values of observed/true is unity with a 95% confidence of .09%.



Minor peaks in the ppm range could be better measured on the Daly multiplier using the 235 as reference. A comparison of the results on the Faraday and Daly was made on six samples.

Measurements on Strontium.

Strontium is run using the 86/88 as an internal spike, therefore fractionation is not a contributing error. Approximately 200 values were made on each bead.

One microgram samples of strontium were loaded on single filament beads, and results obtained in overnight runs. Two different machines were used to obtain results for both single and double collector measurement techniques. The results are tabulated below. The results illustrate that a better internal precision is obtained using the double collector method, but the external precision is similar for both cases. The main improvement in accuracy in the use of the double collector is seen when for example rock samples produce a beam which is not stable.

	SINGLE COLLECTOR ISOMASS 54			DOUBLE COLLECTOR MM30	
NO.	RATIO 87/86	ERROR PER MIL 2 SIGMA (INT)	NO.	RATIO 87/86	ERROR PER MIL 2 SIGMA (INT)
1	0.710252	.03	1	0.710243	.015
2	0.710293	.06	2	0.710287	.014
3	0.710265	.08	3	0.710277	.016
4	0.710270	.02	4	0.710298	.014
5	0.710282	.02	5	0.710268	.014
6	0.710278	.02	6	0.710295	.018
7	0.710295	.02	7	0.710253	.016
8	0.710239	.02	8	0.710258	.014
			9	0.710247	.016
			10	0.710269	.014
MEAN	0.710272	0.05 per mil (95% confidence)	MEAN	0.710270	0.05 per mil (95% confidence)

ANALYSIS OF U AND PU RESIN BEAD SAMPLES WITH A SINGLE STAGE MASS SPECTROMETER*

David H. Smith, R. L. Walker, L. K. Bertram, and J. A. Carter

Analytical Chemistry Division
Oak Ridge National Laboratory
Oak Ridge, Tennessee 37830

Restrictions in sample size caused by recently imposed limits on the amounts of fissionable isotopes that can be shipped has created a keen interest in minimizing the amount of sample required for analysis for Safeguards purposes. Use of the resin bead sampling technique[1] allows shipment of nanogram quantities of U and Pu for mass spectrometric analysis for isotopic composition and, through the use of isotope dilution, quantity.

Application of this technique to Safeguards has been investigated with a single-stage mass spectrometer.[2] The instrument has a 90-degree sector magnet with a 30 cm central radius of curvature. The instrument was designed and built at ORNL, but does not differ in any significant way from several widely used commercially available mass spectrometers. The small samples require a pulse-counting detection system to supply the necessary sensitivity.

To evaluate the single stage-resin bead combination, several samples were analyzed. Standards (Table 1) gave results in good agreement with NBS certified values. Other samples, previously run on multi-stage instruments, were analyzed and gave good agreement with the earlier results (Table 2).

Precision of our results is not as good as that obtainable under the optimum conditions of very large samples and a Faraday cup collector; however, our results are comparable in quality to those obtainable from current integrating detectors. External precisions of ±0.5% are obtained on isotopic ratios of about 0.01; precisions on quantitative measurements are ±1.0%.

Table 1. Results from Standards

	NBS-010		NBS-500	
	234/235	235/238	234/235	235/238
NBS	0.00538	0.01014	0.01043	0.9998
ORNL	0.00549 ±0.00032	0.01013 ±0.00004	0.01041 ±0.00010	1.0006 ±0.0036
	8 analyses		13 analyses	

	NBS-947			
	238/239	240/239	241/239	242/239
NBS*	0.00370	0.24147	0.04309	0.01559
ORNL	0.00377 ±0.00013	0.24119 ±0.00069	0.04327 ±0.00031	0.01557 ±0.00021
	22 analyses			

*Corrected to August 13, 1978.

*Research sponsored by the U. S. Department of Energy under Contract #W-7405-eng-26 with the Union Carbide Corporation.

By acceptance of this article, the publisher or recipient acknowledges the U.S. Government's right to retain a non-exclusive, royalty-free license in and to any copyright covering the article.

Table 2. Results from Comparison Samples

SAU-14

U	No. of Analyses	234/235	235/238		
2-stage		0.01030	0.01216		
1-stage	4	0.01015 ±0.00025	0.01220 ±0.00008		
Pu		238/239	240/239	241/239	242/239
2-stage		0.0093	0.3116	0.1020	0.03149
1-stage	4	0.0097 ±0.0006	0.3121 ±0.0008	0.0992 ±0.0008	0.03153 ±0.00011

K-1

U	No. of Analyses	234/235	235/238	238/233	
2-stage (unspiked)	2		0.00198 ±0.00001		
1-stage (unspiked)	4		0.00202 ±0.00003		
2-stage (spiked)	2	2.42 ±0.03	0.00236 ±0.00004	2.113 ±0.010	
1-stage (spiked)	4	2.34 ±0.04	0.00244 ±0.00004	2.096 ±0.013	
Pu		238/239	240/239	241/239	242/239
2-stage (unspiked)	2	0.00057 ±0.00028	0.05858 ±0.00022	0.00219 ±0.00001	0.00019 ±0.00001
1-stage (unspiked)	4	0.00022 ±0.00006	0.05862 ±0.00014	0.00224 ±0.00001	0.00037 ±0.00001
2-stage (spiked)	2	0.00033 ±0.00007	0.05863 ±0.00006	0.00223 ±0.00001	0.3415 ±0.0002
1-stage (spiked)	4	0.00023 ±0.00003	0.05864 ±0.00024	0.00231 ±0.00001	0.3397 ±0.0017

References

1. R. L. Walker, R. E. Eby, C. A. Pritchard, and J. A. Carter, Anal. Lett., 7, 563 (1974).

2. D. H. Smith, ed., USDOE Report ORNL/TM-6485, Oak Ridge, TN, November, 1978.

PAPER #59

The Diffusion of Trace Metals in Metals and Alloys and its Applicability to Environmental Assays by M.E. Koslin* and F.A. White, Dept. of Nuclear Engineering, Rensselaer Polytechnic Institute, Troy, N.Y. 12181

Many techniques can be used for determining diffusion parameters in metals and alloys. The most common are: serial sectioning, the residual activity method, surface decrease method, and autoradiography. These methods give good results at temperatures below 800°C. However, at higher temperatures the diffusing system tends to react with its environment. Additionally, rapid heating and cooling of the solute-solvent system often adversely affect the diffusion measurements. Thus, in 1960, McCracken and Love[1] developed a system utilizing thermal ionization mass spectrometry to determine diffusion parameters.

The advantages to a mass spectrometric approach are many. They are: (1) since the mass spectrometer analyzes for only one mass at a time, no ambiguity is caused by interfering masses; (2) the sensitivity of the mass spectrometer allows the solue level to be less than one ppb - thus no doping of a sample is required; (3) utilizing a thermal ionization source constructed out of the material of interest, diffusion coefficient measurements at various temperatures can be made without changing samples; (4) as the filament is small, the time involved in heating and cooling is small; (5) and because the source mounting is in the high vacua of the mass spectrometer there is negligible interaction between the diffusing system and the surrounding environment at the experimental operating temperatures.

In this work, a thin ribbon filament of solvent material was used with its own solute (impurity) concentrations. As the mass spectrometer source chamber pressure is well below the vapor pressure of the solute material in the desired temperature range, the solute atoms diffuse to the filament surface and evaporate immediately. This results in a zero solute concentration at the filament surface after the filament temperature is raised to the desired level. Further, as the ribbon thickness is much less than its length or width, the diffusion may be considered to be one dimensional. Thus Fick's second law for diffusion in a thin plate can be utilized. When this is combined with the Langmuir-Saha equation for the ratio of emitted positive ions to emitted neutrals, the following relationship of solute ion current out of the filament as a function of time is obtained.

$$J_{ion} = \exp\left(-\pi^2 Dt/x^2\right)$$

Where D is the diffusion coefficient for a given temperature, x is the filament thickness, and t is time. Thus, the slope of the plot of the natural logarithm of solute ion current versus time will yield the diffusion coefficient for the experimental temperature.

After D has been determined for various temperatures, other important diffusion parameters such as the frequency factor, D_o, and the activation energy, Q, can be determined by the following equation.

$$D = D_o \exp (-Q/RT)$$

Where R is the Rydberg constant and T is in degrees Kelvin. Thus Q may be found from the slope of the plot of ln D versus 1/T, and D_o is the y-intercept of this plot.

This work looked at the diffusion properties of the alkali metals in tantalum, zircaloy-2, and 304 stainless steel. These metals represent a transition from a pure metal to a highly alloyed material. The purpose was to illustrate the universal capability of this technique for real material analysis. Some of the results are listed in the following table.

Diffusion Coefficients at 1200°K (10^{-8} cm/sec)

Solvent	Li-7	Na-23	K-39	Rb-85	Cs-133
Ta	1.20	1.66	0.42	0.51	0.38
Zr-II	--	0.81	1.71	0.28	5.83
304 SS	0.21	0.17	0.26	0.93	2.10

This method for determining diffusion parameters can be applied to the determination of trace metal environmental analysis utilyzing thermal ionization mass spectrometry. In this situation a sample is deposited on a rhenium filament and is then coated with a thin film of rhenium by RF sputtering.

This encapsulation of the sample within a matrix of high work function refractory metal minimizes the direct relationship between evaporation and ionization efficiency. In this matrix, the sample atoms must thermally diffuse to the surface where they can be either evaporated as ions or neutral atoms. However, since thermal diffusion is generally a slower process than direct evaporation, the filament can be operated at higher temperatures. Thus, higher ionization efficiencies are obtained without the rapid loss of the sample. This encapsulation enables the analysis of extremely small samples (approximately 10^8 atoms has been achieved).

An example of the utilization of this technique is the determination of actinide elements in samples of air and water from a nuclear power plant and the emissions from a coal fired power plant.

Sample	Uranium Content
Reactor Coolant	2.38×10^{-6} gm/cc of water
Air Sample	1.97×10^{-14} gm/cc of air (background)
Coal Fired Plant Stack Emissions	5.61×10^{-9} gm/V (unknown volume of air)

Thus, the mass spectrometer becomes a valuable tool in characterizing diffusion properties of materials; while the diffusion process enables one to analyze extremely small environmental contaminants via mass spectrometry.

References

1. McCracken, J.M. and H.M. Love, Phys, Rev. Letters., 5,201,1960.

* Present Address: The Perkin-Elmer Corp., Aerospace Division
Pomona, California 91767

PHOTOIONIZATION AND THRESHOLD PHOTOELECTRON-PHOTOION COINCIDENCE STUDY OF CYCLOPROPENE FROM ONSET TO 20 eV

by

Albert C. Parr* and Andrew J. Jason

Department of Physics and Astronomy
The University of Alabama
University, AL 35486

and

Roger Stockbauer

National Measurement Laboratory
National Bureau of Standards
Washington, D.C. 20234

ABSTRACT

The photoionization efficiency curves have been obtained for cyclopropene and its fragments $C_3H_3^+$, $C_3H_2^+$, and C_3H^+ from threshold to 20 eV. The threshold photoelectron spectra and breakdown curves are given over the same energy range. The breakdown curve is almost identical to those obtained previously for allene and propyne when put on a common energy scale. This suggests that all three ions isomerize to a common ion structure before fragmentation. The results have been submitted to The International Journal of Mass Spectrometry and Ion Physics for publication.

* National Bureau of Standards, Intergovernmental Personnel Act, Appointee 1978-79

MASS SPECTRA OF ORGANIC COMPOUNDS IN LIQUID PHASE AT ATMOSPHERIC PRESSURE : LIQUID SURFACE IONIZATION

M. Tsuchiya and T. Taira
Faculty of Engineering, University of Tokyo
Hongo, Bunkyo-ku, Tokyo, Japan 113

Most mass spectrometric techniques require the sample molecules to be in the gaseous state prior to ionization. While field desorption[1] and in beam techniques[2,3] could be used for liquid and solid samples, they are ordinarily not suitable for continuous analysis of liquids and solutions. We have developed a new atmospheric pressure ionization method[4] for the analysis of organic compounds either as liquids or in solution. The method and the instrument are described in the abstract (MAMP 13) for this Conference.

The mass spectra of aniline measured by this method (LI) at the potentials of a pinhole of 20 V and 100 V are shown in Figs. 1a and 1b, respectively. The pinhole potential means the voltage applied to the pinhole mount respect to the earth (refer Fig.1 in MAMP13). At 20 V, the molecular ions, M^+ and MH^+, are most abundant accompanied by the dimer ions, M_2^+ and M_2H^+, and the trimer ions, M_3^+ and M_3H^+, but no fragment ions are observed. In contrast, at 100 V the higher mass peaks diminish, while fragment ions such as $C_6H_5^+$ and $C_4H_3^+$ appear, corresponding well to the structure of the compound. The fragmentation mechanism is somewhat different from that of EI ionization. That is:

$$C_6H_5NH_3^+ \xrightarrow{-NH_3} C_6H_5^+ \xrightarrow{-C_2H_2} C_4H_3^+$$

$$C_6H_5NH_2^+ \xrightarrow{-NH_2} C_6H_5^+$$

The latter process was confirmed using Penning ionization. As shown in the EI spectrum (Fig.1c), the main fragmentation reactions under electron impact involves HCN elimination. Thus the mass spectrum obtained by the new method is easier to understand when compared with the EI spectrum.

The mass spectra of 1,4-butanediol-2,2,3,3-d_4 at pinhole potentials of 20 V and 100 V are shown in Figs. 2a and 2b, respectively. These are compared with the EI and CI (CH_4) spectra (Figs. 2c and 2d). In Fig.2a the peak at m/z 95, MH^+, is the base peak accompanied by M_2H^+ and a small peak at m/z 77 which disappears at 15 V. At 100 V, the M_2H^+ peak diminishes, while the fragment peaks at m/z 77, 31 et cetera increase, indicative of the structure of the compound. The peaks at m/z 77 $(MH - H_2O)^+$ and at m/z 59 $(MH - 2H_2O)^+$ are formed by decomposition of the MH^+ ions due to the excess internal energies of the MH^+ ions, because the spectral pattern is similar to the CI spectrum. The spectral pattern in the middle mass region is somewhat different from that of EI spectrum. The peak at m/z 47 in the new spectrum may be due to the $CD_2CH_2OH^+$ ion, while the peak at m/z 46 in the EI spectrum is due to the $CD_2CD_2CH_2^+$ ions. Therefore the fragmentation mechanism in LI must be different from that of other ionization methods. The electric field near the pinhole is considered to cause the decomposition of the molecular ions.

When a solution of an organic compound is introduced into the ionization chamber, the mass spectrum obtained is mainly that of the solute. For example if the solution is ~1% dibutylphthalate (MW=278) in acetone, the mass spectrum shown in Fig. 3d is obtained with a slight heating at the pinhole potential of about 100V. At 20 V, only the molecular ions, M^+ and MH^+, are obtained without any fragment ions. Thus both information about the molecular weight and the structure of the solute molecule is available. Heat seems to have a significant effect on molecules with high boiling points. Heat gives ions the translational energies which help the ions to desorb from the liquid surface. Similar results were obtained for compounds whose boiling points are around 300°C.

This method provides not only the molecular weight of a compound but also information about its structure and its properties in the liquid phase. The method should be applicable to many separation techniques, including liquid chromatography.

REFERENCES
1. H.D.Beckey, Int. J. Mass Spectrom. Ion Phys., 2, 500 (1969)
2. M.A.Baldwin and F.W.McLafferty, Org. Mass Spectrom., 7, 1353 (1973)
3. D.F.Hunt, J.Shabanowitz, F.K.Botz and D.A.Brent, Anal. Chem., 49,1160 (1977)
4. M.Tsuchiya and T.Taira, Mass Spectroscopy (Japan), 26, 333 (1978)

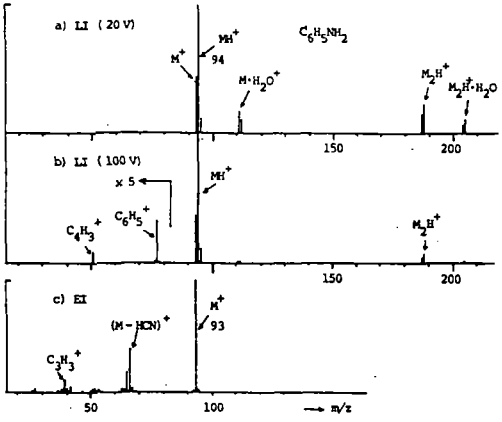


Fig.1 Mass spectra of aniline

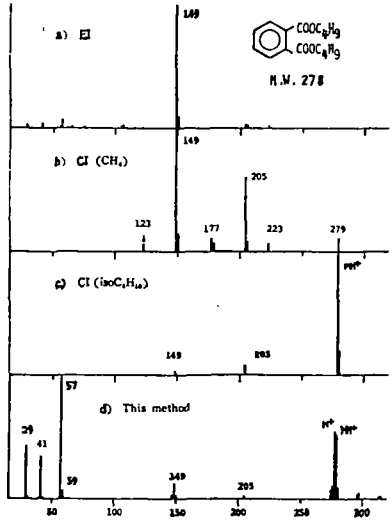


Fig.3 Mass spectra of n-butylphthalate

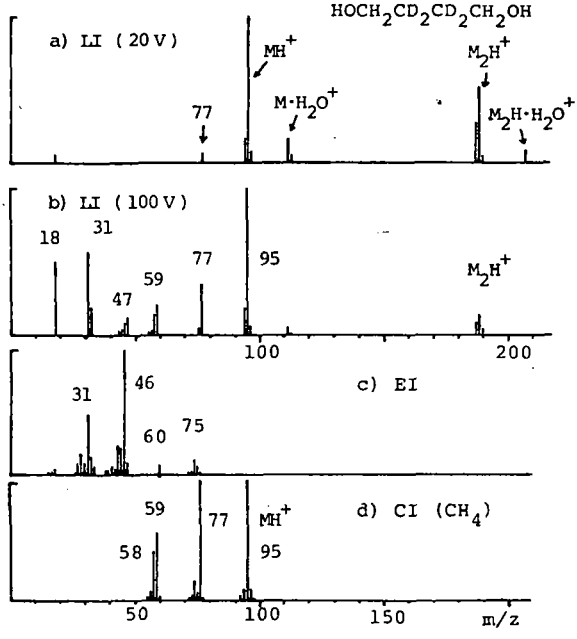


Fig.2 Mass spectra of 1,4-butanediol-d_4

ANGULAR DISTRIBUTIONS IN MOLECULAR ION DISSOCIATIONS OBSERVED BY PHOTOELECTRON-PHOTOION COINCIDENCE SPECTROSCOPY

J. H. D. Eland, Physics Division, Argonne National Laboratory
Argonne, Illinois 60439

If a molecule could be held fixed in space before ionization the angular distributions of both the ejected electrons and of the fragment ions would be richly structured. In contrast to the familiar $a + b\cos^2\Theta$ distributions, their description would require sums $\sum_n a_n\sin^n\Theta + b_n\cos^n\Theta$ with both odd and even terms to high order. Such rich angular structure is not observable in mass spectrometry nor in photoelectron spectroscopy using randomly oriented target molecules. When electrons and ions are detected in coincidence, on the other hand, the full angular distributions characteristic of fixed molecules can in principle be observed. This is easily visualized in extreme cases: if electrons can be emitted only along a single direction in the molecular frame, the fragment ion distribution in coincidence with electrons at a single laboratory angle will be the fixed-molecule fragment ion distribution. Conversely, if fragment ions leave the molecular frame in a single direction, the electron angular distribution in coincidence with ions of defined laboratory angle will be the fixed-molecule electron angular distribution. In practice we can observe at most a fold of the two fixed-molecule angular distributions. Any rotation of the molecular ion after electron ejection but before fragmentation also reduces the sharpness of the distribution. The effects of molecular rotation on the expected distributions are characterized by the parameter $\Gamma\omega$, the angle of rotation during one mean lifetime. (Γ is the mean lifetime, ω the angular rotation rate.) When $\Gamma\omega$ is zero the full distribution is observed: when it is large ($\Gamma\omega \gtrsim 2$) odd terms in the distribution vanish, and the coefficients of even terms are reduced by factors proportional to $1/2^n$. Even after infinite time an initial anisotropy does not vanish completely in the absence of collision processes, though it may in practice become undetectable.

In fixed wavelength photoelectron-photoion coincidence work electrons are detected at a single laboratory angle (or in a small range of angles). For a fragment ejected with a velocity v_o in center of mass the time-of-flight deviation (under time-focusing conditions) is: $t - t_o = v_o\cos\Theta/a$ where a is the acceleration in the source field, and Θ is the laboratory angle of the fragment from the mass spectrometer axis. The lateral position of the ion at the detector (away from the axis) is $x - x_o = tv_o\sin\Theta$. Thus if v_o is known (single velocity release) a measurement of the tof distribution alone determines the angular distribution. If v_o if unknown, measurements of the time-of-flight and the position of impact of each ion at the detector are needed to determine both the velocity and angular parts. Conversely, if the velocity distribution is unknown, it can never be derived from tof measurements alone without knowledge or an assumption of the angular distribution.

In diatomic ion fragmentation v_o is known (or limited to very few values) because only atomic assymptotes are possible, and the initial ion energy is selected by the photoelectron energy. Linear momentum conservation requires axial recoil of the fragments in the CM frame, so anisotropic electron distribution can be expected in all cases where dissociation is sufficiently rapid. Although the observations refer directly to fragment ion angular distribution they are equivalent to those of electrons from fixed

molecules if effects of the unpolarized light propagation direction are negligible.

Coincidence measurements have been made on a number of diatomic and small polyatomic ion fragmentations;[1] the angular distributions observed are summarized in Table I. The essentially isotropic distributions of O^+ from the B and c states of O_2^+ and of S^+ from $D_2S^+(\tilde{A})$ are consistent with long lifetimes of these ionic excited states. The anisotropic distributions found for $N^+/NO^+(c)$ and for I^+ from diatomic interhalogens demonstrate that the decay lifetimes are there shorter than the rotation periods. It is expected, on the basis of these results, that the majority of fast molecular ion dissociation will show angular anisotropies when examined by the coincidence method.

This research was performed under the auspices of the Division of Basic Energy Sciences of the United States Department of Energy.

1. J. H. D. Eland, J. Chem. Phys. 70, 2926 (1979).

Table I. Angular distributions in molecular ion decays

Fragment Ion	Precursor Ion (state)	Ionizing Light	Angular Distribution
I^+	I_2^+ (B)	584Å	Sharp minimum at 90°
I^+	IBr^+ (B)	584Å	Broad minimum around 90°. Slight forward-backward asymmetry.
I^+	ICl^+ (B)	584Å	Dip at 90°, broad peaks at 50°, 135°.
O^+	O_2^+ (B)	584, 304Å	Isotropic
O^+	O_2^+ (c)	304Å	Isotropic
O^+	$O_2^+ (^2\Pi_u)$	304Å	Peaked near 90° (see ref. 1)
N^+	NO^+ (B)	304Å	Isotropic
N^+	NO^+ (c)	304Å	Peaked at 180° (electron emitted from O end)
S^+	D_2S^+ ($\tilde{A}$)	584Å	Isotropic

Photoionization of Formic Acid: Fragmentation Mechanisms and the Proton Affinity of Carbon Dioxide

K. E. McCulloh
National Bureau of Standards
Washington, D. C. 20234

The photoionization of HCOOH has been investigated from the ionization threshold at 11.33 eV to a maximum photon energy of 13.40 eV. The $HCOOH^+$ yield exhibits a staircase structure extending through the accessible vibrational levels of the lowest electronic state of the ion, but it shows no prominent features assignable to the second electronic state or the Rydberg manifold converging to the vibrational levels of this state.

The second electronic state of the ion is unstable with respect to predissociation. The CO_2H^+ onset consists of a step at 12.38 eV, followed by a second step at 12.51 eV. These steps coincide in energy with the first two peaks in the second photoelectron band.[1] The photoionization yield of CO_2D^+ from HCOOD exhibits steps at 12.38 and 12.50 eV. The CO_2H^+ onset from HCOOD consists of a weak step at 12.50 eV. From the observed CO_2H^+ onsets from these two isotopic species and the isotopic shift in molecular zero point energy it is inferred that ΔH_{f0}° (CO_2H^+) lies within the bounds 143.1 $\pm$ 0.2 and 145.0 $\pm$ 0.2 kcal/mol.

The yield of CO_2H^+ in the photoionization of acetic acid shows a temperature shift which is consistent with the hypothesis that the internal energy of the molecule is available for fragmentation. On this basis a threshold of 12.17 $\pm$ 0.01 eV at 0 K is inferred, leading to an upper bound of 145.0 $\pm$ 0.2 kcal/mol for ΔH_{f0}° (CO_2H^+), in excellent agreement with the results from formic acid. Hence, there is strong support for a value near 145.0 kcal/mol. These results lead to a proton affinity

$$PA(CO_2) = 126.2_{-0.2}^{+2.1} \text{ kcal/mol}$$

at 0 K.

From this value and a proton affinity difference derived from equilibrium data[2] it is calculated that for methane

$$PA(CH_4) = 127.4_{-0.2}^{+2.1} \text{ kcal/mol}$$

at 0 K. Since both bounds lie well within the wider limits reported on the basis of a direct study of the reaction of CH_4^+ with CH_4,[3] the present results for $PA(CO_2)$ are proposed as absolute bounds for the proton affinity network.

References

1. C. R. Brundle, D. W. Turner, M. B. Robin, and H. Basch, Chem. Phys. Lett. 3, 292 (1969).
2. R. S. Hemsworth, H. W. Rundle, D. K. Bohme, H. I. Schiff, D. B. Dunkin, and F. C. Fehsenfeld, J. Chem. Phys. 59, 61 (1973).
3. W. A. Chupka and J. Berkowitz, J. Chem. Phys. 54, 4256 (1971).

Laser-Induced Fluorescence as a Probe of Ground State Ions Formed by Electron Impact,[1] John Allison, Keith Jackson, and Richard N. Zare, Department of Chemistry, Stanford University, Stanford, CA 94305

To date, the spectroscopy of several dozen molecular ions has been investigated[2] with N_2^+ the most widely studied ion in emission work. While emission is a sensitive probe of the internal energy of excited states of ions formed by electron impact, the ground state ions thus formed are more difficult to probe. Recently it has been shown that the technique of laser-induced fluorescence (LIF) can be used to determine ground state ion product distributions. Work typified by that of Miller and Bondybey[3] has shown that LIF can be used to probe ions formed under "high pressure" conditions. We present here a simple technique for studying ground state ions formed by controlled electron impact on low pressure gases, under conditions where nascent energy distributions can be obtained.

Figure 1 shows the experimental setup. The experiment is pulsed, since electron impact on a gas results in emission, and an LIF signal cannot be detected in its presence. Therefore, we turn off the electrons, wait for excited species to radiate, then fire the laser. The laser-induced emission is detected and monitored as a function of excitation energy as the laser wavelength is scanned. Figure 2 shows an LIF spectrum of N_2^+ formed from 100 eV electrons on N_2 at 3×10^{-4} torr.

A plot of log[Intensity/(N'+N"+1)] vs N"(N"+1) for the rotational lines of this (0,0) band gives a straight line, indicating a Boltzmann rotational distribution. The slope reveals a rotational temperature (T_R) of 323±5 K. 60 eV electrons form ground state N_2^+ ions with T_R = 342±10 K. Below 50 eV, the signal-to-noise of the experiment prohibited good determination of the rotational temperature. These experiments do indicate slight rotational heating with decreasing ionizing energy, which may parallel trends seen in $N_2^+(B^2\Sigma_u - X^2\Sigma_g^+)$ emission studies.[4,5]

We have also studied the polarization of ions formed by electron impact, by monitoring the $N_2^+(B^2\Sigma_u - X^2\Sigma_g^+)$ emission from electron impact on N_2. Polarization (P) is defined in terms of the emission polarized with its electric vector parallel to the electron beam ($I_{||}$), and that polarized perpendicular to the beam ($I_\perp$) by

$$\%P = \left(\frac{I_{||} - I_\perp}{I_{||} + I_\perp}\right)100$$

We find that %P is positive for this N_2^+ emission and is a function of electron energy, reaching a value of ∿10% at 35 eV. Based on the symmetries of the electron impact ionization process and the N_2^+ B-X emission process, we expect %P to be positive. The energy dependence of %P is presently under study.

In determining the heats of formation of ionic and neutral fragments from electron-impact appearance potentials, the information usually missing is the internal energy of the molecular fragments. In this context we have used LIF to probe fragments such as CN from electron impact on ICN (NB: I^+ is a major ion in the mass spectrum of ICN). We find that $CN(X^2\Sigma^+)$ is formed with T_R of several thousand degrees, but vibrationally cool. This contrasts with CN from electron impact on CH_3CN, where both vibrational and rotational excitation is observed.

In conclusion, we have shown that LIF is a useful tool for probing the internal energy of ionic and neutral species formed by electron impact. Such studies will lead to a better understanding of this method of excitation.

Support by the Air Force Office of Scientific Research is gratefully acknowledged.

1. Parts of this work have been accepted for publication in Chem. Phys. Lett.
2. G. Herzberg, Chem. Soc. Quarterly Reviews 25, 201 (1971).
3. T. A. Miller and V. E. Bondybey, Chem. Phys. Lett. 50, 275 (1977).
4. G. Culp and A. T. Stair, J. Chim. Phys. 1, 57 (1967).
5. J. H. Moore and J. P. Doering, J. Chem. Phys. 50, 1487 (1969).
6. G. H. Dunn, Phys. Rev. Lett. 8, 62 (1962).

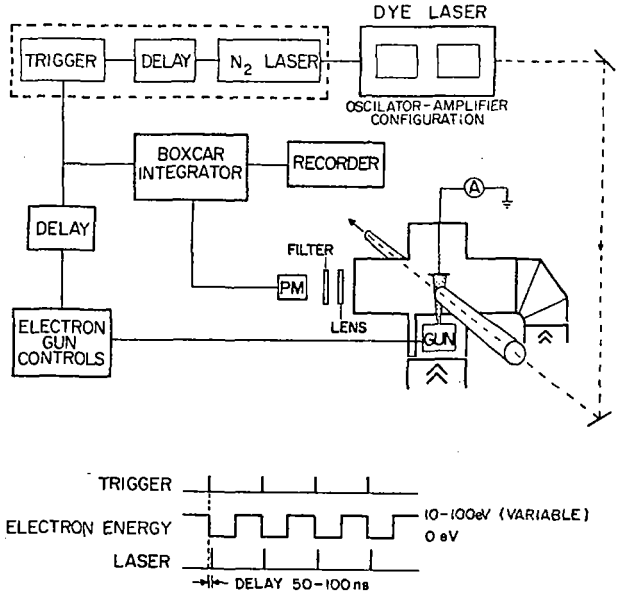


Fig. 1 Schematic diagram of the Experiment

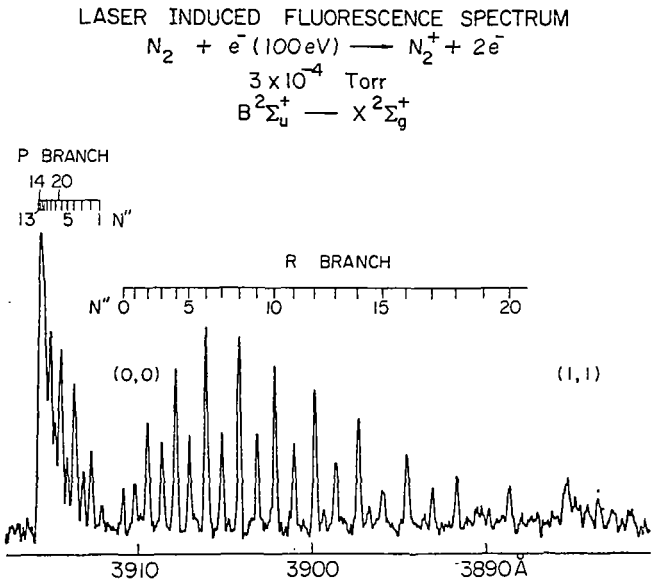


Fig. 2 Excitation spectrum of N_2^+X state produced by 100 eV electrons on N_2 (4×10^{-4} torr)

LASER PHOTODISSOCIATION OF POSITIVE AND NEGATIVE IONS

J. Hiller, J. Robeson, and M. L. Vestal
University of Houston, Department of Chemistry, Houston, TX 77004

The tandem quadrupole mass spectrometer described previously[1] has been combined with a tunable dye laser pumped by a pulsed N_2 laser for photodissociation measurements on ions. A set of parallel mirrors has been added to the ion-photon interaction region to allow operating either in a single pass mode to obtain reliable absolute cross sections or in a multiple pass mode with enhanced sensitivity. With this instrument high resolution photodissociation measurements are possible over the entire fundamental tuning range of the laser (360-750 nm). Recently, this instrument has been applied to measurement of photodissociation cross sections for Ar_2^+, Ne_2^+, N_4^+, $(CO_2)_2^+$, and high resolution studies of several positive and negative ions of atmospheric importance. Our most recent results on CO_3^- may be of particular interest.

In earlier work, Moseley, Cosby, and Peterson[2] measured laser photodestruction cross sections for CO_3. They observed detailed structure in the range between 1.8 and 2.35 eV which was interpreted as reflecting the vibrational spacings of a predissociating excited electronic state. These data gave an upper limit for $D(CO_2\text{-}O^-)$ of 1.85 eV. Recent flowing afterglow experiments[3] indicate that $D(CO_2\text{-}O^-)\text{-}D(O_2\text{-}O^-) \geq 0.58$ eV and from laser photodetachment measurements[4] the electron affinity of O_3 has been determined to be 2.1028±0.0025. Since $D(O_2\text{-}O^-)=EA(O_3)+D(O_2\text{-}O)-EA(O)$ and $D(O_2\text{-}O)$ and $EA(O)$ are known to be 1.05±0.02 and 1.462±0.003, respectively, these values give a lower limit for $D(CO_2\text{-}O^-)$ of 2.27 eV. The discrepancy of 0.42 eV between these two determinations is at least an order of magnitude larger than the estimated experimental errors and clearly at least one is incorrect.

In our earlier work[1] we observed structure in the photodissociation cross section for CO_3^- which was similar to that obtained by Moseley, et al.[2]; however, our absolute cross sections were smaller by nearly an order of magnitude. Furthermore, we observed that the amplitude of the structure decreased with increasing ion source pressure, perhaps indicating that at least a portion of observed transitions occurred from vibrationally or electronically excited CO_3^-. In the present work we have measured the CO_3^- photodissociation cross section at intervals of 1 nm or less throughout the range from 1.95 to 3.1 eV (400-630 nm). A portion of these results is shown in Figure 1. In the region of overlap our results reproduce our earlier work; however, at shorter wavelengths the cross section increases and shows a series of steps rather than the peaks observed at longer wavelengths. This structure is the type expected for a direct dissociation process in which the upward breaks in the curve correspond to opening of new product channels; in this case, these channels correspond to producing CO_2 in higher vibrational states. With this interpretation in mind, the known vibrational spacings of CO_2[5] were compared to the observed structure and the best fit was obtained as indicated approximately in Figure 1 and more precisely in Table I. Attempts to shift the O-O transition to either higher or lower upward breaks significantly reduce the quality of the fit. As shown in Table I all eight breaks observed between 2.2 and 2.65 eV are satisfactorily accounted for by the vibrational levels of CO_2 and only two vibrational levels are not clearly discernible. In both cases these levels lie slightly higher in energy than levels which are observed and they are apparently either not present or not resolved. The best fit of the CO_2 vibrational spacings with the observed upward breaks in the CO_3^- photodissociation cross section data gives $D(CO_2\text{-}O^-)=2.222\pm0.004$ eV. This value is about 0.05 eV lower than the "lower limit" value discussed above but may be within the experimental uncertainty of that value. This result implies that the electron affinity of CO_3 is $EA(CO_3)=D(CO_2\text{-}O^-)\text{-}D(CO_2\text{-}O)+EA(O)=3.22\pm0.17$ where the only significant uncertainty is in the value of the neutral dissociation energy $D(CO_2\text{-}O)=0.46\pm0.17$ eV.

We gratefully acknowledge financial support of this research from the Robert A. Welch Foundation.

References
1. M. L. Vestal and G. H. Mauclaire, J. Chem. Phys. 67, 3758 (1977).
2. J. T. Moseley, P. C. Cosby, and J. R. Peterson, J. Chem. Phys. 65, 2512 (1976).
3. L. Dotan, J. A. Davidson, G. E. Streit, D. L. Albritton, and F. C. Fehsenfeld, J. Chem. Phys. 67, 2874 (1977).
4. S. E. Novick, P. C. Engelking, P. L. Jones, J. H. Futrell, and W. C. Lineberger, J. Chem. Phys. 70, 2652 (1979).
5. D. M. Dennison, Revs. Mod. Phys. 12, 175 (1940).

TABLE I. Analysis of Structure Found in CO_3^- Photodissociation Cross Sections between 2.2 and 2.7 eV.

Break No.	$h\nu$(eV)	CO_2 Vib.	E_V(eV)[5]	$D(CO_2\text{-}O^-)$ (eV)
1	2.220	000	0	2.220
2	2.305	010	0.083	2.222
3	2.388	020	0.160	2.228
4	2.445	030	0.240	2.205
5	2.495	110	0.258	2.237
6	2.513	001	0.292	2.221
7	2.566	200	0.348	2.218
8	2.616	050	0.389	2.227

Mean=2.222±0.004

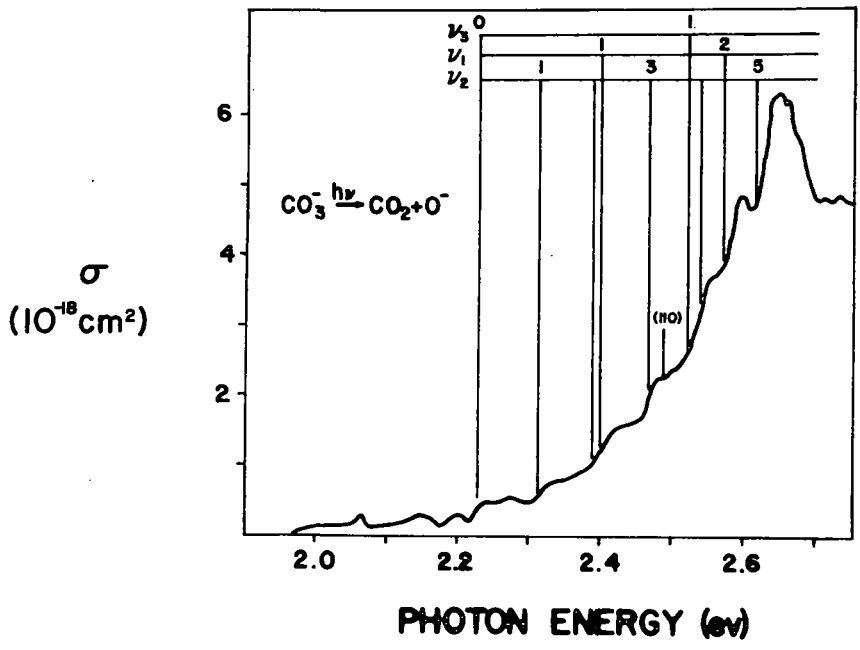


Figure 1: Cross section for photodissociation of CO_3^- as a function of photon energy. The vertical lines correspond to the indicated vibrational state of the CO_2 product if the O-O transition for the reaction were at 2.23 eV.

LASER PHOTODISSOCIATION OF MOLECULAR IONS

Lee N. Morgenthaler and John R. Eyler

Department of Chemistry, University of Florida
Gainesville, Florida 32611

The pulsed icr pulsed laser technique has been used to probe a number of physical processes in excited molecular ions in the gas phase. A detailed spectrum, related to the absorption spectrum, of the ion can be obtained at a time when it has undergone anywhere from zero to several hundred collisions with the background gas. The spectra of collisionally unstable ions may be studied before they decompose or react and collision-induced changes in apparently stable ions can be followed spectroscopically.

Chloroethane molecular ion is an example of a collisionally unstable species that has been investigated successfully by this technique[1]. The photodissociation spectrum indicates that the first excited electronic state of this ion is weakly bound or flat and that the second excited state is purely repulsive with respect to scission of the carbon-chlorine bond. In addition, there is a strongly energy-dependent competition between two reaction channels. This effect is <u>not</u> predicted by quasi-equilibrium theory, which indicates that the dynamics of the decay processes are dictated by the potential surfaces of the excited electronic states of the ion.

We have carried out several experiments which attempt to probe the dynamics of rearrangement processes that have been investigated using continuous icr techniques. In the first case, benzyl chloride, the results obtained in our work are not the same as those obtained in the continuous icr experiment, with up to 60% dissociation of the $C_7H_7Cl^+$ ion observed, as compared to only 30% in the previous study. A kinetic scheme which reconciles the two results has been developed. Based on our results one cannot be sure that rearrangement has occurred at all. In the second example, cis-trans isomerization in the 1,3,5 hexatriene cation, emission spectroscopy indicated that the structure of the ions formed from the two isomers of the parent compound were different on the time scale of 10^{-8} s. However, continuous icr photodissociation spectroscopy indicated that the two structures were identical on the time scale of several seconds. Our results indicate that the ions of the two isomers are the same within 10 ms of ionization. No information about the kinetics of the rearrangement process can be obtained in

this case.

The collisional relaxation of vibrationally excited 1,3,5 hexatriene molecular ions has also been studied. The rate of quenching by the parent molecule was observed to depend on the ionization energy. Ions formed at higher ionization energy (11 eV) were quenched on every nonreactive collision with the parent molecule. This result is consistent with other studies of similar processes in molecular ions. Ions formed at lower ionization energy (9 eV) were quenched less efficiently by a factor of four--an unexpected result. Quenching by argon atoms was also investigated and found to be extremely rapid--about two orders of magnitude faster than the corresponding process in neutrals.

1. L. N. Morgenthaler and J. R. Eyler, J. Chem. Phys., in press.

LASER-ENHANCED IONIZATION OF INVOLATILE SAMPLES IN SOLUTION

E. R. Lory and F. W. McLafferty

Department of Chemistry, Baker Laboratory,
Cornell University, Ithaca, New York 14853

Direct solution introduction into a chemical ionization source, such as used in one LC/MS interface,[1] can produce solution droplets of ~5 μm diameter. Milne[2] and Giddings, Myers, and Wahrhaftig[3] proposed the gas phase isolation of molecules from a high pressure jet; recent work[4] is promising, but a practical system still has not been demonstrated for non-volatile molecules. The apparatus proposed[5] combines these techniques utilizing a laser to vaporize droplets of a $\sim 10^{-4}$ M solution so rapidly (100 nsec) that the involatile solute molecule should not agglomerate extensively; diffusion times for such intermolecular distances should be 10^{-8} - 10^{-6} sec. Vaporization of ~10 μm droplets could be achieved with 100 nsec pulses from a CO_2 Lumonics model 103 laser, energy >1 Joule. Approximate threshold measurements indicated energy requirements of 1.5-4.5 μJ per drop. However, the repetition rate of 0.1 Hz gave vaporization of only 1 in $\sim 10^5$ droplets. Thus it is not surprising that no solute ions were detected in chemical ionization experiments with this technique.[5]

Vaporization of all droplets conceivably could be accomplished with a 200 watt CW laser focused to a 50 μm spot with a 2 MHz rate of 100 nsec pulses. However the complicated optical system and severe positioning requirements of this have led us to examine alternative methods of rapid droplet vaporization.

[1] F. W. McLafferty, R. Knutti, R. Venkataraghavan, P. J. Arpino and B. G. Dawkins, Anal. Chem., 47, 1503-5 (1975).

[2] T. A. Milne, Int. J. Mass Spectrom. Ion Phys. 3, 153 (1969).

[3] J. C. Giddings, M. N. Myers, and A. L. Wahrhaftig, ibid, 4, 9 (1970).

[4] L. G. Randall and A. L. Wahrhaftig, Anal. Chem., 50, 1703 (1978).

[5] E. R. Lory, B. G. Dawkins, P. J. Arpino, P. A. Hoffman, and F. W. McLafferty, ASMS Meeting, St. Louis, May 1978.

TPM0C9 PHOTODISSOCIATION SPECTROSCOPY OF CYCLOOCTADIENE RADICAL CATIONS. JOHN D. HAYS and ROBERT C. DUNBAR, Dept. of Chemistry, Case Western Reserve University, Cleveland,OH 44106.

Photodissociation spectra have been obtained for several $C_8H_{12}^{+\cdot}$ radical cations using a pulsed ICR technique employing microprocessor controlled data acquisition. The spectrum of the 1,3 cyclooctadiene radical cation is compared with the spectra of the nonconjugated cyclooctadiene isomers and analyzed for structural information. The correlation of peak positions and cross sections indicates a thermal conversion of 1,4 cyclooctadiene to 1,3 cyclooctadiene, with 1,5 cyclooctadiene undergoing only a partial rearrangement to the conjugated isomer. The latter process has been further studied by time resolved photodissociation of the 1,5 cyclooctadiene radical cation. Spectra and electronic transitions will be compared, along with those observed by other methods.

Ion Focusing Properties of a "Thick" Retardation Lens

G. L. Merrill, C. A. Calkins, and C. L. Peterson

General Electirc Company, Pleasanton, CA 94566

Several authors have documented that a retardation lens (RL) added after the final stage of a magnetic sector mass spectrometer provides a substantial improvement in abundance sensitivity for thermal ionization applications. We constructed a lens that duplicated the geometry of one described by Kaiser ans Stevens[1] except that the entrance and exit focal points were initially reversed to accommodate the existing vacuum housing and Daly detector. Optimization of RL performance on our tandem magnet system was a very sensitive function of the ion beam angle of entry, offset from the axis of symmetry, and the voltage difference, ΔV, between the source voltage and the RL setting. Maximum transmission occurred about 18 volts below the ion source accelerating potential but it is decreased again as the potential barrier was further reduced. Only at the lowest settings available did the transmission tend to increase. For simple conditions of a narrow, parallel, and on-axis beam, one would expect the transmission to remain high as the RL voltage was lowered (i.e., high pass plateau and cutoff).

A review of the properties of einzel lenses suggested that by varying the potential on such a lens, different operating ranges hence different focal lengths would result for off axis rays. For other studies we had developed numerical techniques for both potential field determination and trajectory calculations, all of which could be run on an in-house minicomputer (DEC PDP15). Solving Laplace's equation numerically saved considerable time and effort from traditional resistance paper or tank methods. To determine the potential field in the lens, a 121x51 mesh grid was formulated and the Laplace difference equation solved by the method of successive over-relaxation. To determine the trajectories, a fourth order Runge-Kutta integration was applied with a variable time step since the ion velocity changed greatly through the lens. Results for parallel rays in our original geometry are shown in Fig. 1. Angle effects are even more severe. We have not vigorously analyzed the accuracy of the computed results. Due to the fairly coarse mesh used and boundary effects, we surmise there may be some uncertainty in the trajectories. However, our analysis enabled us to build a new RL housing on a rotatable and translatable carriage which, in fact, allowed us to attain a broad, high transmission, precise isotope ratio capability, and a high abundance sensitivy ($>10^8$ for ^{236}U). In conclusion, use of a "thick" RL specifically as an energy filter for wide beams ($\sim$0.5mm) requires consideration of the focusing properties of the lens and of the acceptance of the ion detector to properly interpret experimental results.

[1] K.A. Kaiser and C.M. Stevens, ANL-7393, Nov. '67.

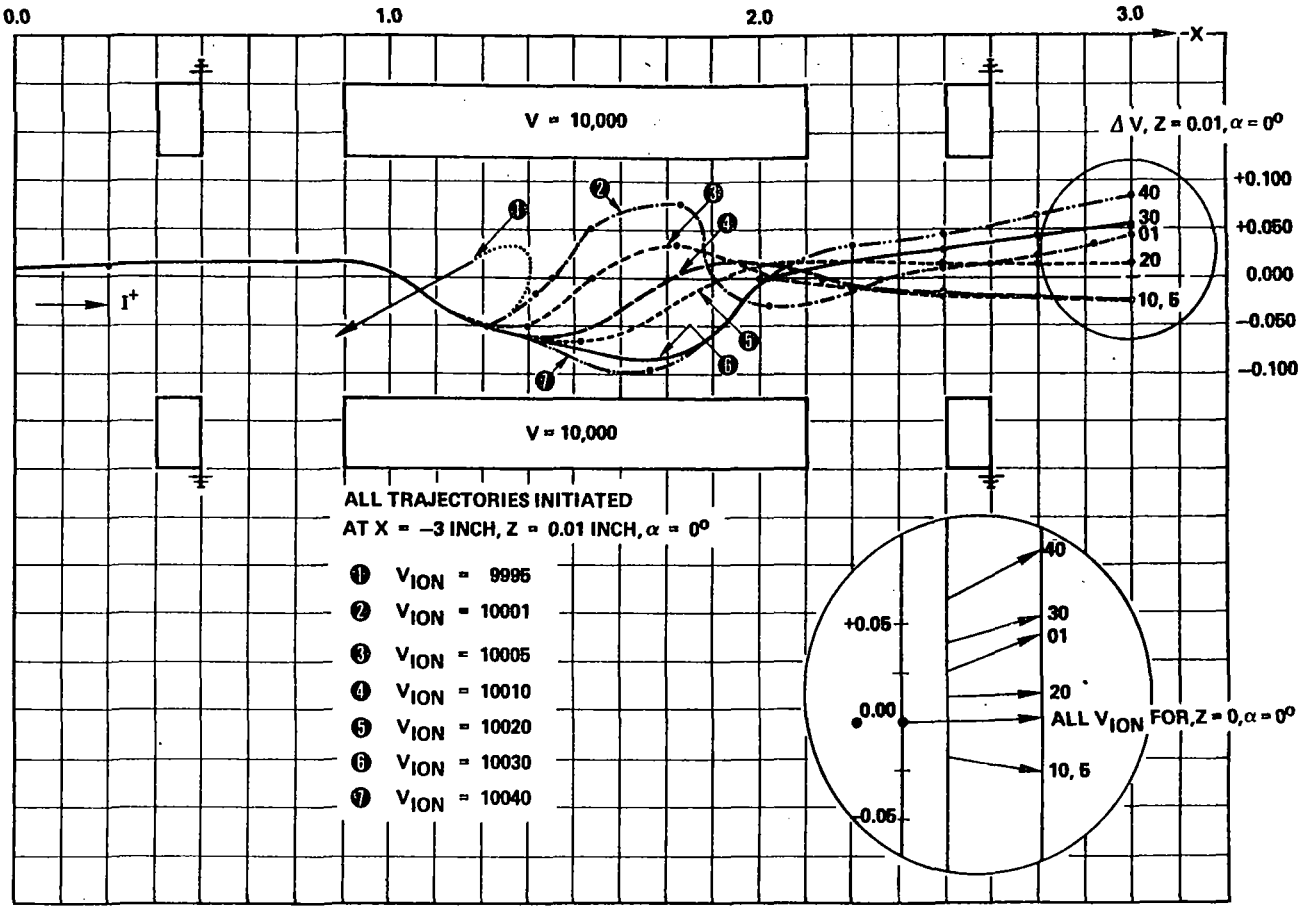

0.0
1.0
2.0
3.0
-X
V = 10,000
V = 10,000
I+
ALL TRAJECTORIES INITIATED
AT X = −3 INCH, Z = 0.01 INCH, α = 0°
❶ V_ION = 9995
❷ V_ION = 10001
❸ V_ION = 10005
❹ V_ION = 10010
❺ V_ION = 10020
❻ V_ION = 10030
❼ V_ION = 10040
Δ V, Z = 0.01, α = 0°
+0.100
+0.050
0.000
−0.050
−0.100
40
30
01
20
10, 5
+0.05
0.00
−0.05
ALL V_ION FOR Z = 0, α = 0°

Figure 1

THE INTERFACE OF DESORPTION CHEMICAL IONIZATION (DCI) IN MASS SPECTRAL IONIZATION METHODS

D.E. Games, J.L. Gower and E. Lewis;Department of Chemistry, University College. P.O.Box 78, Cardiff, CF1 1XL, Wales. U.Rapp and G. Dielmann, Varian MAT GmbH, Postfach 144062, 2800 Bremen 10, W. Germany.

In recent years the development of techniques for obtaining mass spectral data from salts, highly polar and thermally labile organic molecules have received considerable attention. Recently[1] activated field desorption emitters have been used for obtaining methane and ammonia CI spectra of a wide range of salts and thermally labile organic compounds. Rapid heating from a teflon surface[2] or tungsten wire[3] with NH_4^+ as a proton transfer agent has proved useful in studies of underivatized peptides. Last year[4] we reported on CI spectra obtained from rapidly heated non-activated tungsten wires. The technique has been called Desorption Chemical Ionization (DCI). We present here a comparison of results obtained with DCI, CI and FD. DCI spectra were obtained using Varian MAT44 and 311A mass spectrometers, FD spectra were obtained with a Varian CH5D mass spectrometer and CI spectra were obtained using the LC/MS interface of a Finnigan 4000 mass spectrometer.

Underivatized sugars provide little useful EI information. FD has proved useful in their characterization,[5] however it is difficult to obtain reproducible spectra and often samples from biological sources fail to provide any useful spectral information. Since Ammonia CI has proved useful in characterization of underivatized mono and di-saccharides[6] we felt that studies in this area would be useful. Isobutane CI of the disaccharide trehalose failed to provide MW information, the highest mass ion appearing at m/z 325. With ammonia an $(M+NH_4)^+$ ion was present at m/z 360 (20%) together with ions at m/z 198 (48) 180 (100) and 162 (18) due to cleavage of the two sugar units. DCI with isobutane gave an M+1 ion at m/z 343 (5) together with m/z 325 (97) and m/z 163 (100). In contrast the base peak in the ammonia DCI spectrum was at m/z 360, ions were also present at m/z 342 (2), 198 (18), 180 (55) and 162 (20). The trisaccharide raffinose failed to provide MW information with ammonia CI, the highest mass ion being observed at m/z 342. In contrast ammonia DCI gave a $(M+NH_4)^+$ ion at m/z 522 (1%) together with ions at m/z 504 (15), 360 (4), 342 (9), 198 (24), 180 (100) and 162 (18). Encouraged by these results we examined a series of glycosides. The flavanoid glycoside naringin (1) on FD from acetone solution shows a $(M+1)^+$ ion at m/z 581, at higher wire currents fragment ions appear at m/z 434, 272 and 147. When spectra were obtained from a methanol solution the $(M+1)^+$ was of low intensity and the base peak in the spectrum appeared at m/z 603 $(M+Na)^+$. Ammonia CI failed to show ions above m/z 435 whereas both ammonia and isobutane DCI enabled molecular weight assignments to be made. Ammonia DCI gave ions at m/z 598 (47), 581 (8), 435 (5), 418 (23), 326 (100), 273 (76), 180 (12), 164 (26), 146 (17). Isobutane DCI from methanol and acetone solutions gave similar spectra to ammonia without the presence of NH_4^+ attachment ions at m/z 598, 435, 326, 164, 180. An interesting aspect of these DCI spectra is the strong abundance of the ion m/z 325 which is not observed in FD and is weak on ammonia CI. It is formed from the diglycoside portion of the molecule. Riboflavin (MW 376) on DCI with ammonia gave a protonated molecular ion together with ions at m/z 243, 257, 260 due to the aglycone portion of the molecule. The base peak in the spectrum was at m/z 137 due to a 4C sugar fragment with ammonia attachment. The ammonia CI spectrum shows similar ions but with only a weak ion (10% rel. int.) at m/z 137. Similarly FD although showing fragment ions characteristic of the aglycone showed no fragment ions which can be assigned to the sugar. The diglycoside cascaroside (2) confirms this behaviour having an ion at m/z 180 as the base peak in its spectrum which we assign to cleavage of the glucose portion of the molecule with ammonia attachment. A strong ion is also present at m/z 436 with a weak ion at m/z 596 which is two mass units lower than would be expected for $(M+NH_4)^+$. Whilst DCI gives no direct information about the aglycone portion of the molecule, FD shows ions at m/z 256 and 280 together with m/z 418 and m/z 603 (M+Na), similarly ammonia CI shows ions at m/z 180, 257, 287 and 436, but fails to provide MW information. The utility of DCI in this area is confirmed by the obtaining of an $(M+NH_4)^+$ ion at m/z 886 for the cardiac glycoside dioscin which contains a trisaccharide unit.

A series of salts have also been studied and again some contrasts in behaviour have been observed. FD provides information about the size of the cation and sometimes the nature of the anion for Wittig salts, but usually little additional structural information is available. Isobutane DCI of the Wittig salt (3) showed ions at m/z 383 (9), C^+; 263 (100), 187 (17), 121 (89) enabling the nature of the substituents on the phosphorous to be ascertained. Ammonia CI gave similar information but the ion at m/z 383 was of less than 1% relative intensity. The drug propantheline (4) illustrates the area where FD is superior to the other techniques for molecular weight determination. Both conventional CI and DCI (ammonia) failed to give an ion at m/z 368 for the cationic portion of the

molecule, the highest mass ion is m/z 354 in both cases, and is due to loss of the methyl group from the salt. FD in contrast gives an ion at m/z 368 as base peak in the spectrum.

From our studies to date it appears that the ionization mechanism in DCI is more closely related to conventional CI than FD. Some interesting contrasts in behaviour in DCI and CI have emerged, particularly in the case of the glycosides and we feel that DCI provides a useful addition to the range of mass spectral techniques available for structural studies and should be particularly useful, where FD facilities are not readily accessible.

References

1. D.F. Hunt, J. Shabanowitz, F.R. Botz and D.A. Brent, Anal. Chem., 1977, 49, 1160; D.F. Hunt and S.K. Sethi, in "High Performance Mass Spectrometry: Chemical Applications", edit. M.L. Gross, American Chemical Society, Washington, 1978, p.150.

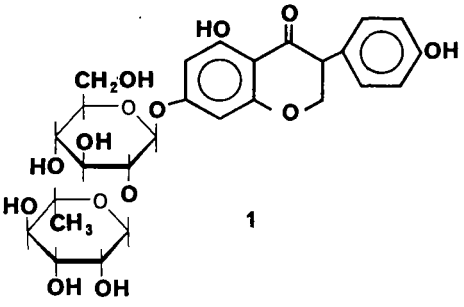
2. R.J. Beuhler, E. Flanigan, L.J. Greene and L. Friedman, J. Amer. Chem. Soc., 1974, 96, 3990; Biochemistry, 1974, 13, 5060.

3. W.R. Anderson Jr., W. Frick, D.G. Daves Jr., D.F. Barofsky, I. Yamaguchi, D. Chang, K. Folkers and S. Rosell, Biochem. Biophys. Res. Commun., 1977, 78, 372.

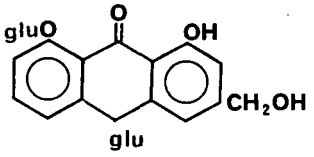
4. B. Jelus, U. Rapp and W.A. Wolstenholme, 26th Annual Conference on Mass Spectrometry and Allied Topics, St. Louis, Mo, May 1978, 187.

5. J. Moor and E.S. Waight, Org. Mass Spectrometry, 1974, 9, 903.

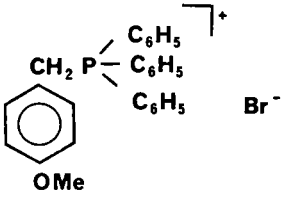
6. A.M. Hogg and T.L. Nagabushan, Tetrahedron Letters, 1977, 4827.



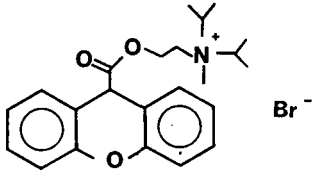
1



2



3



4

TPMOC12 ION CYCLOTRON RESONANCE STUDY OF REACTIONS OF IONS WITH ATOMIC HYDROGEN, V. G. ANICICH, Z. KARPAS, and W. T. HUNTRESS, JR., Jet Propulsion Laboratory, Pasadena, CA 91103.

The JPL ion cyclotron resonance mass spectrometer has been coupled to a microwave discharge radical source. The rate constants for the reactions of atomic hydrogen with H_2^+, HeH^+, CO_2^+, CO^+, N_2^+, and HCN^+ were measured. These reactions are important in the atmospheres of the outer planets and in comets. At the top of the planetary atmospheres of Jupiter, Saturn, Uranus, and Neptune, the principle neutral species are He, H_2, and H. The H_2^+ ion transfers charge to H atoms to form H^+. The H^+ ion does not react with H_2 and He. H atoms serve as a sink for positive charge in the ionospheres of the outer planets and is the major ion present in their upper atmospheres. CO_2^+, CO^+, and N_2^+ ions have been detected in the atmospheres around comets. Hydrogen atoms are also the principle constituent of the extended cometary coma, so that the reactions of CO_2^+, CO^+ and N_2^+ with H may be an important loss process for these ions in comets.

TPMOC13 CHARGE AND PROTON TRANSFER REACTIONS OF NH_3^+ (v) ON NH_3: THE EFFECT OF INCIDENT ION VIBRATIONAL AND TRANSLATIONAL ENERGY ON THE REACTION CROSS SECTION, P. TERRENCE MURRAY AND TOMAS BAER, Dept. of Chem., Univ. of North Carolina, Chapel Hill, NC 27514

We have measured the absolute cross sections for both charge and proton transfer reactions of NH_3^+ ($^2A_1$, v) on NH_3 with the incident ion in selected vibrational (v = 0-10) and translational (1 eV - 3000 eV) energies. The photoion-photoelectron coincidence (PIPECO) technique coupled with TOF ion analysis in both single and double chamber experiments was used. The results indicate that the proton transfer reaction dominates at low vibrational and kinetic energies. The increase in the charge transfer reaction from v = 0 to v = 10 is less than a factor of 3 at low translational energies. At high translational energies, the effect is even less. These results raise serious question about the use of Franck-Condon factors in calculating charge transfer reactions.

This work was supported by the National Science Foundation and the Army Research Office.

A CONVENIENT METHOD FOR ANALYSIS OF THE ^{18}O CONTENT OF WATER AND PHOSPHATE

Thomas R. Sharp and Robert D. Minard

Department of Chemistry
Pennsylvania State University
University Park, PA 16802, U.S.A.

Introduction

One of the most convenient forms of ^{18}O for use in isotopic labeling experiments is $H_2{}^{18}O$. Paradoxically, this is one of the most difficult chemicals in which to measure O^{18}, because of interfering desorption of $H_2{}^{16}O$ in the mass spectrometer. Most current methods involve transfer of the oxygen to CO_2 which is then analyzed. This involves sealed tubes and extensive gas handling equipment. In the course of our work on the analysis of ^{18}O incorporated into phosphate, we devised a much simpler and more convenient method for determining the ^{18}O content in $H_2{}^{18}O$.

Conversion of H_2O to H_3PO_4

Under a relatively dry atmosphere, a few grains of vacuum sublimed reagent grade PCl_5 are placed in a conical-bottom reaction vial. The H_2O sample to be analyzed (10-20 microliter) is added and allowed to react.

$$H_2O^* + PCl_5 \rightarrow H_3PO_4^* + HCl$$

Capped samples are quite stable at this stage and can be stored for an extensive period before methylation.

Conversion of H_3PO_4 to Trimethyl Phosphate

The H_3PO_4 is esterified by adding a drop or two of methanol followed by an ethereal solution of diazomethane.

$$H_3PO_4 + \text{excess } CH_2N_2 \rightarrow (CH_3O)_3P{=}O$$

The solutions can be concentrated under a stream of dry N_2.

Isotope Analysis by GC-MS-SIM

Instrumentation: Finnigan 3200 with 6000 data system.

Chromatographic Conditions:
- Column - 1.5 x 2 mm id glass column packed with 10% silar 10C on 100-120 GCQ
- Temperature - 140° isothermal
- Carrier gas - ~20 cc/min He
- $(CH_3O)_3P{=}O$ retention time - ~6 mins.

Selected ion monitoring:
Electron impact ionization
Ions monitored:

M^+	m/q 140	$(CH_3)_3P^{16}O_4$
$(M+2)^+$	m/q 142	$(CH_3)_3P^{16}O_3{}^{18}O_1$
$(M+4)^+$	m/q 144	$(CH_3)_3P^{16}O_2{}^{18}O_2$
$(M+6)^+$	m/q 146	$(CH_3)_3P^{16}O_1{}^{18}O_3$
$(M+8)^+$	m/q 148	$(CH_3)_3P^{18}O_4$

Data Collection

Since only 4 ions can be monitored at once, each sample was injected 5 times and the following mass abundances were determined by SIM.

1st injection	m/q	140	142	144	146
2nd injection	m/q	140	142	144	148
3rd injection	m/q	140	142	146	148
4th injection	m/q	140	144	146	148
5th injection	m/q	142	144	146	148

The missing intensity in each set of numbers is estimated by a simple ratios method.

Results

The peak areas are input to a relatively simple FORTRAN computer program which calculates the intensity for the missing ion in each cluster. Percents of total for each of the isotopically labeled species calculated by taking the intensity of each m/q as a percentage of the sum of all 5 species, routinely shows a standard deviation of $\pm$.5 or less. The final calculated atom % ^{18}O takes into account the contributions of each of the 5 species to the total oxygen content of the $(CH_3O)_3PO$. Anyone wishing to have a copy of this program can contact T. R. Sharp.

Eighteen samples were prepared by sequential dilution of 99 atom % $H_2{}^{18}O$ so that a fairly representative set of samples with ^{18}O content ranging from natural abundance to 99 atom % could be analyzed and the accuracy of the method roughly determined. A comparison between expected and experimentally determined atom % ^{18}O in these water samples is shown in Table I.

Table I

Experiment	Expected	Observed $\pm$ S.D. Mean
1	99%	94.05% $\pm$ 0.74%
2	49.5	49.63% $\pm$ 0.09%
3	24.75	22.38% $\pm$ 0.2%
4	12.38	12.86% $\pm$ 0.22%
5	6.19	5.88% $\pm$ 0.04%
6	3.09	3.03% $\pm$ 0.31%
7	1.54	1.77% $\pm$ 0.06%
8	0.77	1.15% $\pm$ 0.04%
9	0.39	0.81% $\pm$ 0.07%
10	9.90	9.54% $\pm$ 0.47%
11	64.0	64.36% $\pm$ 0.42%
12	56.88	56.56% $\pm$ 0.16%
13	0.2	0.3% $\pm$?
14	0.2	0.3% $\pm$?
15	1.0	0.9% $\pm$?
16	1.5	1.6% $\pm$?
17	4.0	3.7% $\pm$?
18	8.0	6.8% $\pm$?
19	?	28.54% $\pm$ 0.05%
20	?	28.53% $\pm$ 0.04%

*Replicate analysis on same water sample.

The error due to incorrect integration is fairly small for samples with 25 to 75 atom % ^{18}O. For example, when the peak areas for a particular ion (140, 142, 144, 146, or 148) were increased or decreased by 10% for all 5 injections, the results for the 49.5 atom % ^{18}O sample were still all in range 48.99 to 50.27 atom % (actual result 49.63 atom %).

Acknowledgement: The authors would like to thank S. Benkovic for his support for this project and Carla Hofland for her help with the presentation of this paper. T.R.S. is a Postdoctoral Research Fellow of the American Cancer Society, Grant PF-1615.

A METHOD FOR THE ISOTOPIC ANALYSIS OF BIOSYNTHETIC ^{13}C-CARBON MONOXIDE BY GC/MS

ADRIAN SWANSON AND M. W. ANDERS
DEPARTMENT OF PHARMACOLOGY
UNIVERSITY OF MINNESOTA
MINNEAPOLIS, MINNESOTA 55455

THE QUANTITATIVE AND/OR ISOTOPIC ANALYSIS OF CARBON MONOXIDE BY GC/MS IS OFTEN HAMPERED BY LARGE AND NOISY BACKGROUNDS AT MASSES 28 AND 29. WHEN THE CO OF INTEREST IN A SAMPLE CAN BE CONVERTED QUANTITATIVELY INTO CARBON DIOXIDE THE SIGNAL TO NOISE RATIO OF THE MEASUREMENTS WILL IMPROVE TO THE EXTENT THAT THE BACKGROUNDS AT MASSES 44 AND 45 ARE SMALLER AND MORE STABLE.

WE REPORT HERE THE USE OF ACTIVE HOPCALITE ® (PART NUMBER 41566, MINE SAFETY APPLIANCES COMPANY, PITTSBURGH, PA 15208) AS A VERY USEFUL AND EFFICIENT MEDIUM TO EFFECT SUCH A CONVERSION AS THE CO IS ELUTED FROM THE COLUMN PRIOR TO MASS ANALYSIS. ACTIVE HOPCALITE IS A PROPRIETARY MIXTURE OF OXIDIZERS AND CATALYSTS WHICH WE HAVE FOUND TO BE ABLE TO SUSTAIN THE TOTAL CONVERSION OF CO TO CO_2 IN THE ANAEROBIC CONDITIONS PREVAILING THE CARRIER GAS STREAM OF THE GC. NO ADDITIONAL SOURCE OF OXYGEN IS REQUIRED.

ANY CONVENTIONAL GC/MS EQUIPPED WITH A JET-ORIFICE SEPARATOR IS EASILY ADAPTED TO USE THIS TECHNIQUE. A GAS SAMPLING VALVE WITH A 1 ML CAPACITY IS RECOMMENDED AND SHOULD BE INSTALLED WITH THE GC FLOW CONTROLLER BYPASSED (TO MINIMIZE BASELINE UPSET). THE COLUMN IS PACKED WITH MOLECULAR SIEVE 5A, 100/120 MESH, WITH AN I.D. OF CA. 2MM AND A MINIMUM LENGTH OF 3 METERS. APPROXIMATELY 0.1 GM OF ACTIVE HOPCALITE (AS RECEIVED) CAN EITHER BE PLACED DIRECTLY INTO THE EXIT ARM OF THE COLUMN OR ASSEMBLED INTO A SEPARATE REACTOR CONNECTED BETWEEN THE COLUMN AND THE SEPARATOR INLET.

USING SUCH A REACTOR WE HAVE FOUND THAT A LINEAR DOSE-RESPONSE RELATIONSHIP PREVAILS OVER THE RANGE OF CO CONCENTRATIONS EXAMINED (50 PPM TO 10% CO IN NITROGEN) AND THAT THE SPECIFIC RESPONSE OF THE $CO \rightarrow CO_2$ SYSTEM IS 20-30% GREATER THAN THAT OF THE NON-CONVERSION CASE. WHILE THE REDUC-

TION OF BACKGROUND NOISE LEVELS IS IDIOSYNCRATIC BETWEEN SPECTROMETER SYSTEMS WE HAVE EXPERIENCED ON THE AVERAGE A FACTOR OF 100 AS THE MEASUREMENTS ARE SHIFTED FROM MASSES 28 AND 29 TO 44 AND 45. FOR THE SIMPLE DETECTION OF CO WE ESTIMATE THE NOISE LIMIT OF THIS METHOD TO BE 10 PPM CO (IN AIR); HOWEVER, CONSIDERABLE PEAK BROADENING IS EVIDENT. 200 TO 500 PPM CO SUFFICE FOR A $^{13}C/^{12}C$ DETERMINATION.

ALTHOUGH THE EFFICACY OF THE REACTANT MEDIUM CAN BE DESTROYED BY ITS DELIBERATE EXPOSURE TO SEVERAL 1 ML SAMPLES OF NEAT CO, WE HAVE ASSAYED UNLIMITED ($N < 100$) SAMPLES IN THE CONCENTRATION RANGE OF 100 TO 800 PPM CO IN AIR WITH NO EVIDENT CHANGE IN CONVERSION EFFICIENCY.

AN IMPORTANT BENEFIT OF THE USE OF A MOLECULAR SIEVE 5A COLUMN IN THIS TECHNIQUE IS THAT IT EFFECTIVELY SCRUBS THE CARRIER GAS AND THE GAS SAMPLE ITSELF OF ANY POTENTIALLY INTERFERING CO_2.

IN OUR LABORATORY THIS TECHNIQUE IS PRIMARILY DIRECTED TO THE ISOTOPIC ASSAY OF BIOSYNTHETICALLY GENERATED CO. A TYPICAL APPLICATION MIGHT INVOLVE 200 NANOMOLES OF CO GENERATED IN A CLOSED REACTION FLASK HAVING A 10 ML HEADSPACE OF ROOM AIR. A 5.0 ATOM-PERCENT EXCESS OF ^{13}C-CO CAN BE DETERMINED TO A PRECISION OF 0.5 A-% USING A 1 ML GAS SAMPLE. OUR EXPERIENCE SUGGESTS THAT THERE ARE NO SIGNIFICANT MEMORY EFFECTS ASSOCIATED WITH THE USE OF ACTIVE HOPCALITE.

THIS RESEARCH SUPPORTED BY U.S.P.H.S. GRANT NO. ES01082 AND IS IN PREPARATION FOR PUBLICATION.

EVALUATION OF LONG-TERM STABILITY IN CHROMATOGRAPHIC RELATIVE RETENTION TIME AND MASS SPECTROMETRIC RELATIVE RESPONSE RATIOS IN GC/MS DATAFILES

J.F. Ryan, R.A. Novak, B.J. Dowty, and R.M. Segesta

Gulf South Research Institute, New Orleans, Louisiana

As part of a survey study, Gulf South Research Institute (GSRI) has collected a number of GC/MS datafiles containing capillary column GC/MS data on 38 compounds. These compounds were injected in known quantities over the period from October 1, 1978 to February 28, 1979. Resulting data were evaluated to determine how much relative retention time (RRT) and relative response ratio (RRR), both measured against an internal standard, could be expected to vary as a function of time. This study of changing RRR and RRT was facilitated by the use of a priority pollutant data reduction program written at GSRI, which allows standard runs to be updated, thereby determining RRR and RRT values daily. This program has been described in a previous presentation at this meeting.

Relative retention times were found to be least variable with higher retention times, and most variable with compounds such as TMS-phenol which elute early. The coefficient of variation ranges from 0.1% to 3.9%, with a median value of 0.5%. Thus, relative retention time is apparently not a significant variable with respect to identification of those compounds of interest over the examination period. Experimentally, this is borne out by the fact that in the priority polltuant data reduction program developed at GSRI, the retention time window has been set at 30 scans on either side of the expected scan number. In all cases the compounds have been found within those 60 scans, which corresponds to approximately a minute and a half retention time window. Quite often, the compounds are found within two scans of their expected position.

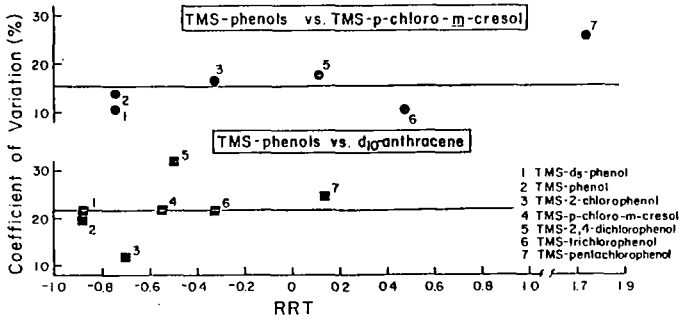
A second objective of the study was to determine how much the relative response ratio would change over a six-week period. Response ratios were calculated relative to d_{10}-anthracene. For the 18 compounds selected the relative response ratios were found to have a coefficient of variation of 11% to 46%, with a median value of 25.3%. This variability seemed to be independent of retention time (Table 1).

This last observation indicated that it would be worthwhile to study the coefficient of variation of RRR as a function of retention time within a given chemical class. Therefore, relative response ratios for selected classes of phthalates, polynuclear aromatics, and TMS-phenols were calculated with respect to d_{10}-anthracene and to internal standard of similar chemical functionality. In all three cases, the coefficient of variation of the relative response ratio was less for those response ratios calculated with a chemically similar internal standard than for those calculated with respect to a dissimilar internal standard. As can be seen, the precision of the quantification would be better with a chemically similar internal standard. When these data are examined mathematically, the points are seen to cluster closer to the median with respect to a chemically similar internal standard. Also, it is apparent that there is very little slope to the linear regression line, which indicates that there is little relationship between precision of the RRR measurement and relative retention time. Therefore, we conclude that the best internal standard would be one which is close in fuctionality to the chemical of significance. One may speculate that this relationship is caused by similarity in fragmentation mechanism. This effort will be explored in subsequent work.

TABLE 1

Compound	Mean RRR	CV* (%)
TMS-d_5-phenol	1.3248	21.4
naphthalene	1.6941	12.3
d_8-naphthalene	1.5277	13.5
TMS-2-chlorophenol	0.8099	11.4
acenaphthene	0.9904	13.1
diethyl phthalate	0.8375	19.5
d_{10}-anthracene	1.0000	--
TMS-trichloroguaiacol	0.8189	17.6
TMS-pentachlorophenol	0.6647	25.4
di-n-butyl phthalate	2.7792	18.0
diamyl phthalate	1.8258	23.3
TMS-oleic acid	0.1880	23.7
TMS-linoleic acid	0.2198	41.3
TMS-linolenic acid	0.0698	26.2
TMS-d_{35}-stearic acid	0.3772	33.0
chrysene	1.2373	17.0
di-n-octyl phthalate	1.3757	30.5
TMS dichlorodehydroabietic acid	0.2427	46.4

*CV = coefficient of variation; $CV = \frac{\text{standard deviation}}{\text{mean}} \times 100$



INTERNAL STANDARD	COMPOUND CLASS	MEDIAN CV (%)
d_{10}-anthracene	PNA	13.3
TMS-p-chloro cresol	PNA	28.1
d_{10}-anthracene	phthalates	22.9
diamyl phthalate	phthalates	12.6
d_{10}-anthracene	TMS phenols	21.7
TMS-p-chloro-m-cresol	TMS phenols	15.2

TPMP4

GAS CHROMATOGRAPHY AND MASS SPECTROMETRY OF NUCLEIC ACID HYDROLYSATES

David L. Smith and James. A. McCloskey, University of Utah, Salt Lake City, Utah 84112.

Methylated bases in DNA play a key role in recognition of cleavage sites by restriction endonucleases; study of other possible roles has in general been hampered by low levels of occurrence. This work is directed toward development of methods of base analysis with greater sensitivity and selectivity than current methods, which in conjunction with the appropriate biological experiments will, in principle, expose more fully the role of modified bases in DNA.

Samples of DNA have been analyzed after hydrolysis to bases (88% HCO_2H, 150°, two hours); the hydrolysate may be analyzed without further treatment, by direct probe high-resolution mass spectrometry (Varian MAT 731), for detection of modified bases. Spectra are photographically recorded, and exact mass data reduced (Varian SS-100 data system) to give a list of elemental compositions for each ion, which is manually searched for presence of ions corresponding to plausible modifications of the usual bases.

5-Methylcytosine (m^5cyt) is a major methylated base in DNA. If present, its level can range from several percent vs cytosine (cyt) in calf thymus, to one residue per bacteriophage ϕX174 genome (5386 residues) or even to currently undetectable levels. Figure 1 illustrates the detection of m^5cyt in a small amount of DNA, even when present at the 0.01% level. The peak at 125.0591 represents 0.7 ng m^5cyt; peaks at 125.008 and 125.0347 represent PFK and M - H of thymine, respectively.

Direct analysis of bases obviates problems associated with GC/MS methods, such as incomplete derivatization or column reactivity. Since the entire hydrolysate is analyzed simultaneously, a potential disadvantage of this method is interference of ions from extraneous components with ions of modified base components. For example, salmon sperm DNA hydrolysates give about nine ions at nominal mass 125. This problem can be eased by use of resolving power greater than 20,000.

Information complementary to that described above may be obtained by analysis of the TMS derivative of the hydrolysate by selected ion monitoring or high resolution photoplate mass spectrometry, with sample introduction via gas chromatography. DNA base analysis by capillary column GC has not previously been reported. We have found this method to be particularly advantageous because: (1) increased resolution permits separation of modified bases from interfering substances usually present, (2) GC/MS system sensitivity is enhanced(10-100 fold) because capillary columns may be directly coupled to the mass spectrometer, (3) the glass columns used in this work are particularly inert.

Glass capillary columns are prepared as follows: 1.2 m lengths of 8 mm OD glass are cleaned (2M KOH saturated with $KMnO_4$) and thoroughly rinsed with distilled H_2O, conc. HCl, then distilled H_2O. The glass is then drawn into a capillary (0.25-0.50 mm ID) which is then deactivated and coated with stationary phase.

Although TMS derivatives of DNA bases are quite volatile, they are highly reactive; for this reason the capillary columns must be thoroughly deactivated before use. We have deactivated columns by several methods: (1) conventional silanization, (2) dynamic coating with surfactants (bistriphenyl phosphonium chloride or sodium tetraphenyl boron) either directly or added to stationary phase prior to coating, or (3) dynamic coating of the glass with 0.5% carbowax 20 M; the column is dried, then baked five hours at 280° under He flow. The latter treatment may be repeated for more complete deactivation. Although all treatments yield good columns, we have had most consistent results using the carbowax 20 M treatment.

Deactivated columns were coated with SE-30 (methyl silicone) or SP-2300 (36% cyanopropylsilicone) to a film thickness of 0.7 and 0.2 μm, respectively. One to three percent carbowax 20 M added to SE-30 reduces tailing of the peaks.

Chromatographic separation of cytosine from 5-methylcytosine is illustrated in Figure 2. SE-30 was used because it was found to yield a larger number of theoretical plates for a column of this length (~25,000). However where m^5cyt is present in orders of magnitude lower levels than cyt, its peak may appear only as a small bump on the tail of the cyt peak.

In gas chromatography of cyt/m^5cyt on the more polar SP-2300 phase, 5-methylcytosine elutes first and is more apparent when present in low levels. SP-2300 does not coat the glass evenly, however, and generally results in fewer effective theoretical plates per unit length. We hope to improve performance of SP-2300 columns by optimizing phase coating parameters.

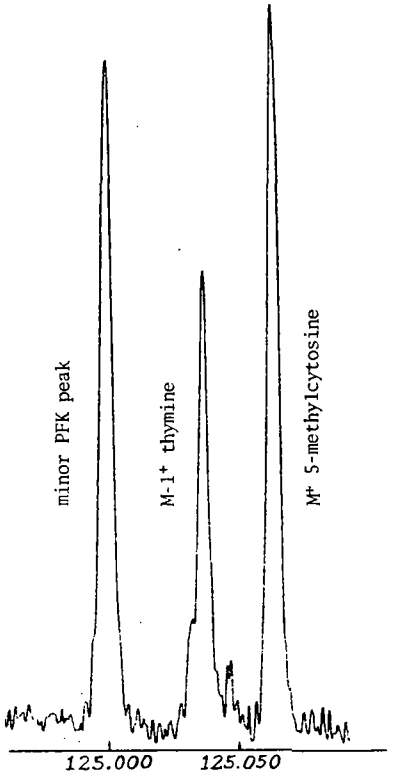


Figure 1: Microdensitometer recording of m/z 125 region (5-methylcytosine molecular ion) from 10 µg ΦX174 DNA, resolution (FWHM) 30,000. *See also:* J.Deutsch, A. Razin and J. Sedat, Anal. Biochem. 72, 586 (1976).

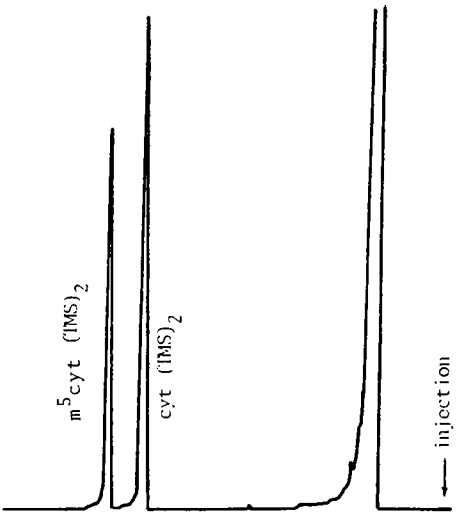


Figure 2: Separation of the TMS derivatives of the cytosine/5-methylcytosine pair. Column length 22 m, SE-30, 160°.

APPLICATIONS OF GCMS IN PLASTICS RESEARCH AND DEVELOPMENT

Max A. Haney
Gulf Oil Chemicals Company
P. O. Box 79070
Houston, TX 77079

GCMS has proven to be a valuable tool in the plastics laboratory. Monomers and low molecular weight intermediates can be investigated directly by GCMS. Most plastics additives are amenable to analysis in the solid probe inlet of the Mass Spectrometer. Liquid chromatographic separation of the additives is usually required. The structure of the polymers themselves may be probed by pyrolysis on line with the GCMS.

Major applications in our laboratory have been in the following areas:

1. Intermediates in polymer synthesis.
2. Pyrolysis of polymers.
3. Technical problem troubleshooting.
4. Analysis of competitor products.

Examples of data are shown from each of these areas.

TPMP6 Direct Analysis of Mixtures by MIKES. R. G. Cooks, A. E. Schoen, M. L. Sigsby, S. E. Unger, D. Zakett, V. M. Shaddock and T. L. Kruger, Department of Chemistry, Purdue University, W. Lafayette, Indiana 47907

This paper introduces several new analytical methods and areas of application of MIKES. Improvements in methodology include use of negative chemical ionization, charge inversion, charge stripping and multiple reaction monitoring. Emphasis is on determinations which are not possible using gc/ms or lc/ms. The ability to examine small samples for specific compounds allows tissue to be mapped on a microscale for particular molecules (molecular mapping). Chemotaxonomy is facilitated using intact plant material or simple extracts and following the distribution of particular compounds (tetrahydroisoquinolines) in related plant species. The MIKES results extend and in some cases lead to revisions of classical phylogenetic relationships. Applications to constituents in blood and in coal liquids and to stereochemical analysis will also be given.

THE MECHANICS OF CAPILLARY COLUMN GC/MS AND ON-COLUMN INJECTION.

Curtis B. Norwood and James L. Lake
Environmental Protection Agency
Environmental Research Lab
Narragansett, R.I. 02882
401-789-1071

The tremendous resolving power of a WCOT capillary column can be quite easily interfaced with the fast scan potential of a quadrapole Mass Spectrometer. One very simple and very low dead volume connection between the capillary column and 1/16" Glass Lines stainless steel Tubing (GLT), which can be used as a transfer line to the MS, can easily be fabricated from a few readily available components. In addition, if a glass rod is heated to the softening point and drawn quickly to a very thin filament, a short section of it (of just the right diameter to fit very snugly inside of the GLT) can be broken off and inserted in the column end of the GLT to act as a restrictor.

At the head of the column, a number of different injection modes have been used successfully in the past to introduce the components of interest onto the capillary column. Quite recently, one of these, that of On-Column injection, has been shown to offer certain advantages over traditional split or splitless injection. On-column injection consists of inserting the needle directly inside of the capillary column so that the sample components are deposited directly on the column head, as opposed to into a heated injection port. The On-column injection system presented here consists of a septum, needle guides, and a simple connection to the head of the capillary column. The long, 33 gauge syringe needle is externally supported by a telescoping needle guide and is guided through the septum and injector by the use of small bore GLT guides. The injector remains completely outside of the heated oven area, and includes a cooling system to ensure that the end of the needle, which penetrates well into the oven area, remains cool during injection.

In general, On-column injection has the advantages of eliminating thermal degradation due to a hot injection port, eliminating ghosting of septum bleed peaks during temperature programmed runs, and generating results of greater reproducibility, especially for less volatile material. In addition, this specific design also allows the use of flow controlled carrier gas, does not require column end straightening, and has all the advantages inherent to syringe injection, e.g. ease of use and easily variable injection size and speed.

However, care must be exercized during injection to avoid damaging the column, or causing flash expansion of the sample back into the cold areas of the injector, or having too little solvent effect because of improper injection speed, size or temperature. For example, 1 ul of sample should be injected within 3 to 5 seconds at 15°C above the boiling point of the solvent.

Nearly all of the components used to fabricate the injector are available from Scientific Glass Engineering. (Mention of a specific manufacturer does not constitute endorsement of the product by the EPA.)

STUDIES OF HERBICIDES AND DRUGS BY COMBINED LC/MS

D.E. Games, Margaret E. Knight, E. Lewis, and N.C. Weerasinghe; Department of Chemistry, University College, P.O. Box 78, Cardiff, CF1 1XL, Wales.

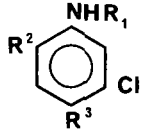
Pesticides of the carbamate type are widely used. GC and GC/MS techniques are not ideal for studies of molecules of this type since they are thermally labile. Hence TLC and LC are important in studies in this area. The utility of LC/MS has already been shown.[1] We have utilized this technique in studies of the metabolism of the herbicide CIPC (1a) in rats and paddy plants. Crude plant and urine extracts are first subjected to FD to provide MW profiles which serve as a check for absorption and/or decomposition during LC/MS. LC/MS with both EI and CI is then performed. The results obtained allow structural formulations to be made, which are confirmed by comparison with synthetic material. To date the known[2] metabolites (1b) and (1c) have been identified in paddy plants and the known[3] metabolites 1(d-g) have been found in hydrolyzed urine. Both in paddy and rat a number of additional metabolites have been located and are currently undergoing structural study.

Our quantitative LC/MS studies[4] of the drug disopyramide have continued. Using $[^2H_{14}]$ labelled drug as an internal standard, calibration in the CI mode using spiked plasma samples has been attempted. To date our studies have shown reasonable reproducibility of repetitively injected samples but we have been unable to maintain instrumental performance in the CI mode for sufficient periods of time to obtain calibration data at levels of drug below 500 ng/ml of plasma.

The conjugates of drugs and their metabolites is a potentially interesting area for LC/MS studies. By spotting solutions of glucuronide metabolites onto our moving belt LC/MS interface we have obtained good ammonia CI spectra in a number of cases. The spectra having ions characteristic of the molecular weight of the conjugate and its aglycone. As a prelude to on-line LC/MS studies in this area we have investigated the LC/MS of a number of bile acids and their conjugates. Using an ODSI column and eluting with a solvent system of water made pH_2 with phosphoric acid:methanol at 0.5 ml/min we were able to obtain an excellent separation and TIC trace for a mixture of lithocholic, cholic, chenodeoxycholic, taurocholic and glycocholic acids. The ammonia CI spectra of the free acids showed $(M+NH_4)^+$ ions together with $M^{+\cdot}$ ions and other ions resulting from loss of water from the molecule. Glycocholic acid showed $(M+1)^+$ and $(M+NH_4)^+$ ions together with abundant ions assigned to successive losses of water from the molecule. Taurocholic acid failed to yield molecular weight information, the highest mass ion appearing at m/z 462 which we assign to the loss of three molecules of water from the $(M+1)^+$ ion. Currently studies are in progress to see if the technique can be used to identify bile acids and conjugates in biological samples.

References

1. L.H. Wright and E.O. Oswald, 26th Annual Conference on Mass Spectrometry and Allied Topics, St. Louis, Mo., 1978, 47.
2. J.L. Wiedmann, G.C. Ecke and G.G. Still, J. Agric. Food Chem., 1976, 24, 588 and references therein.
3. S.C. Fang, E. Fallin, M.L. Montgomery and V.H. Freed, Pesticide Biochemistry and Physiology, 1974, 4, 1, and references therein.
4. D.E. Games, M.L. Games, E Lewis, M. Rossiter and N.C. Weerasinghe, 26th Annual Conference on Mass Spectrometry and Allied Topics, St. Louis, Mo, 1978, 656.



1a R_1 = $COOCH(CH_3)_2$, R^2 = R^3 = H
b R_1 = $COOCH(CH_3)_2$, R^2 = OH, R^3 = H
c R_1 = $COOCH(CH_3)CH_2OH$, R^2 = R^3 = H
d R_1 = $COOCH(CH_3)_2$, R^2 = H, R^3 = OH
e R_1 = $COOCH(CH_3)CH_2OH$, R^2 = H, R^3 = OH
f R_1 = R^2 = H, R^3 = OH
g R_1 = $COCH_3$, R^2 = H, R^3 = OH

ANALYSIS OF INSULATION INTEGRITY OF LARGE ELECTRICAL GENERATORS USING GC/MS/COM

J. W. Auld and D. B. Kehoe

Engineering Research Department
THE DETROIT EDISON COMPANY
Detroit, MI 48226

The integrity of electrical insulation in 300 MW and larger electric power generators is very critical with respect to performance, reliability, and productivity of these generators. Failures of the polymeric insulating materials which result in unscheduled outages can be very costly, possibly running into tens of millions of dollars in lost revenue.

The primary means for detection of insulation overheating in electrical generators is an ion chamber device. Installed on stream in a loop of the hydrogen cooling gas, this device detects smoke particles in the .1 to .001 micron size range. More specific information, however, is usually required for operational and maintenance decisions. A GC/MS analysis of the compounds present in the hydrogen cooling gas of these machines has been found to be the most viable method for providing more specific information which may confirm the present of overheating insulation.

In order to investigate this problem, Detroit Edison has established a long-term project which embodies the use of GC and GC/MS/COM. GC analysis is used as a routine screening method and GC/MS/COM is used where warranted to obtain more detailed information on the nature of the substances present.

Sampling of impurities in generator cooling gas is accomplished using Tenax-GC packed tubes for vapors and either glass mat filters or sintered stainless steel filters for particulate. Ten generators are sampled at least once per month and at the time of each ion chamber alarm. The analysis of these monthly samples provides us with a typical set of background compounds for each generator. Surveillance of these compounds allows for the detection of trends and the ability to predict future problems.

The samples to be analyzed by GC/MS/COM are introduced into the GC by heating the Tenax trap in a split tube oven in series with the carrier gas line just prior to the column inlet. The desorped vapors are reconstituted on the head of the column using a liquid nitrogen trap. The components are released by removing the liquid nitrogen. Thus, the compounds enter the column in a mode similar to a syringe injection.

A typical chromatogram is shown in Figure 1 as a total ion current plot and gives the experimental parameters for the analysis. The Riber Data System controls the scanning of the DuPont 21-491 double focusing mass spectrometer. Data from two (2) seconds/decade scans are stored by the computer for subsequent analysis. Bargraphs illustrating spectra from two specific compounds are illustrated in Figure 2. The bargraphs are used to determine designate ions which are most discriminating in the confirmation of the compound in the mixture[1]. In addition to the designate ions, other ions are selected to increase the statistical reliability of a confirmation. These ion sets are employed in a program under development that will use them in concert with retention indices[2]. Retention indices will be determined by comparision with toluene which is normally present in the samples. Quantification will be carries out by comparison with a gas injected by a sampling valve during the run.

Investigations to date have revealed that semi-quantitative sets of pyrolysis products can be used to determine what major insulation types may be overheating. Table I lists two of the compound sets that have been found from pyrolyzing major insulating polymers.

References: 1. Gates, S. C., Young, N. D., Holland, J. F., and Sweeley, C. C. "Advances in Mass Spectrometry in Biochemistry and Medicine," Spectrum, N.Y., 1976, Ch. 44, p. 483.

2. Nau, H., Biemann, Analytical Chemistry, 46, 426, (1974).

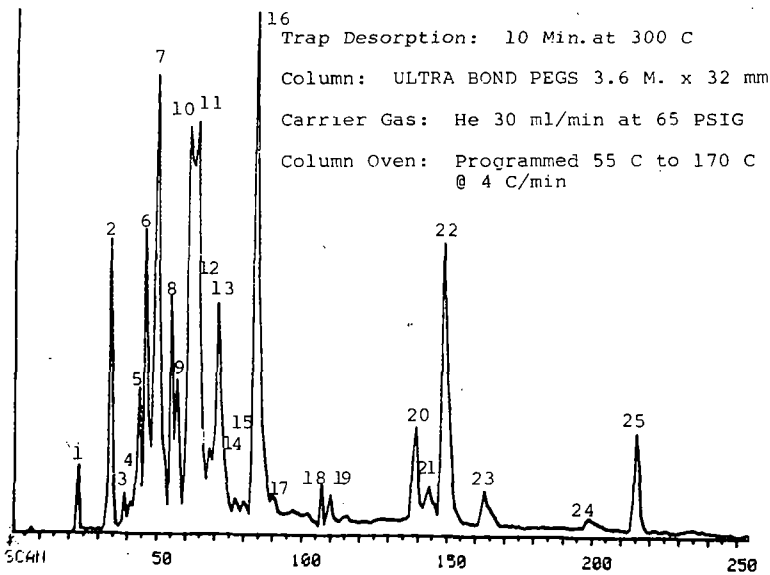


FIGURE 1

TOTAL ION CHROMATOGRAM

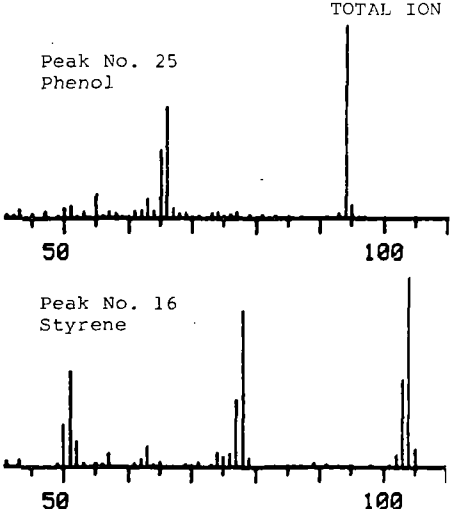


FIGURE 2
TYPICAL SPECTRA

TABLE NO. I

POLYESTER	
Phenol	4%
Styrene	3%
Acetophenone	22%
Benzaldehyde	58%
Dibutylphthlate	7%
EPOXY	
Phenol	33%
Meta-isopropylphenol	5%
Butanol	3%
Toluene	4%
Isopropylbenzene	26%

A GAS CHROMATOGRAPH/FIELD IONIZATION MASS SPECTROMETER (GC/FIMS) SYSTEM

S. E. Young, S. E. Buttrill, Jr.,* and G. A. St. John
SRI International, Menlo Park, CA 94025

Nonfragmenting field ionization is an obvious and desirable alternative to electron impact ionization and offers the potential of a large decrease in susceptibility to interferences without any loss in sensitivity. Field ionization produces only molecular ions from the vast majority of chemical compounds. Electron impact ionization usually produces many different ions in varying amounts from most compounds, and often does not produce a strong molecular ion peak. The electron impact mass spectrum of a mixture is complex and its decomposition into the spectra of the individual substances is often impossible. In contrast, the field ionization mass spectrum of a mixture is very simple, with each component substance producing a single ion, corresponding to its molecular weight. The fact that all of the ionization is concentrated in the molecular ion results in a uniformly high sensitivity for a wide variety of compounds.

The above considerations led us to couple a gas chromatograph with a field ionization mass spectrometer equipped with the SRI volcano-style source. The performance of the ion source and mass spectrometer were described in an earlier paper at the meeting. The interface between the gas chromatograph and the ion source is shown schematically in Figure 1. The innermost tube is 0.5-mm Pyrex and carries the GC effluent directly to the 0.16 cm^2 dimethyl silicone membrane. Helium carrier gas and excess sample flow back through the annular space to be vented to the laboratory. The quartz interface is heated by a nichrome wire coil as illustrated. Separate heaters for the volcano-source mount and grid support are not shown.

The gas chromatograph was a Hewlett-Packard Model 5700 equipped for on-column injection. A variable splitter was used to partition the GC column effluent between a heated line connected to the mass spectrometer and a flame ionization detector (FID). In the "open" position, two-thirds of the effluent went to the mass spectrometer and one-third to the FID. In the splitters "closed" position, the entire flow went to the FID.

The GC column was 2.2-m or 3-mm OD glass tubing packed with 3% OV-17 on 80/100 mesh Supelcoport and cured at 250°C. Samples were run isothermally with 30 cm^3/min helium carrier gas flow. Anthracene and dimethyl naphthalene were analyzed with oven temperatures of 200° and 150°C, respectively. Other temperatures were as follows: FID 250°; vent 200°; transfer line 180°; membrane separator 158°; volcano source 180°.

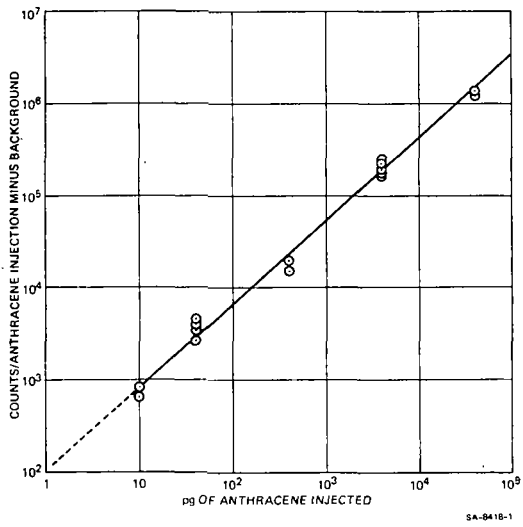


FIGURE 2 DEMONSTRATION OF THE DYNAMIC RANGE FOR THE DETECTION OF ANTHRACENE BY GC/FIMS

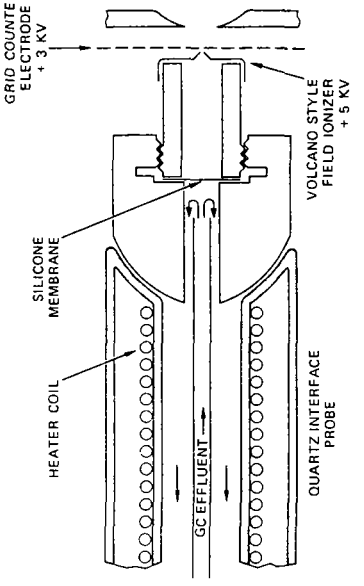


FIGURE 1 GC-MS INTERFACE SYSTEM FOR VOLCANO STYLE FIELD IONIZATION MASS SPECTROMETER SOURCE

The dynamic range of GC/FIMS is illustrated by the calibration curve for anthracene shown in Figure 2. The total counts at m/z 178 due to the anthracene peak were obtained by correcting the counts recorded during a 20-sec period, including the anthracene peak for the background recorded during a similar period following the peak. Figure 2 is a plot of the net ion counts due to anthracene versus picograms of anthracene injected onto the GC column. The linearity of the plot over four orders of magnitude clearly shows that GC/FIMS is well suited to the quantitation of samples containing as little as 10 pg of anthracene.

For 10-pg injections, the peak-to-peak S/N was greater than 3, as shown in Figure 3. The reproducibility of replicate injections was excellent; the three 10-pg injections produced the same peak height and total counts within ± 10%. The solvent peak produces a small disturbance in the baseline, which is only visible on the most sensitive ranges of the rate meter. Comparison of the negative going 1-mg cyclopentane solvent "peak" with 10-pg anthracene peak shows that the selectivity for detection of the PNA anthracene relative to the saturated hydrocarbon cyclopropane is greater than 10^8.

In order to assess the affects of the FIMS interface on the GC resolution, a sample of impure dimethyl naphthalenes (DN) was examined. The dimethyl naphthalene molecular ion at m/z 156 was monitored. Figure 4 compares the single ion chromatogram of a 10-ng sample of DN with the FID chromatogram of a 400-ng sample. Note that at this sensitivity, there is no detectable peak due to the one mg of cyclopropane solvent in the m/z 156 ion chromatogram. Clearly, the mass spectrometer interface does not affect the chromatographic resolution. Several small peaks in the FID chromatogram are seen by comparison with the FIMS data to be due to impurities in the DN sample.

The sensitivity of the volcano-style field ionization source used in these experiments was 2×10^{-6} ions/molecule. By direct comparison with the responses measured from injections of known amounts of anthracene on the GC column, the yield of the interface is found to be slightly less than 1%. Increasing the membrane area to 16 cm^2 should increase the yield to the FIMS to at least 50%. It should also be possible to reduce the background in the mass spectrometer to less than 5 counts per second. The combination of these two improvements will lower the detection limit to about 10^{-14} g in the single ion monitoring mode and allow detection of as little as 10 pg while repetitively scanning several hundred mass units.

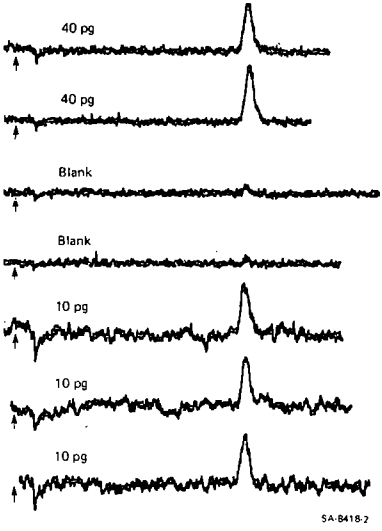


FIGURE 3 GC/FIMS SIM AT M/Z 178 OF 40 PG OF ANTHRACENE INJECTED WITH BLANKS (upper) AND 10 PG OF ANTHRACENE INJECTED (lower)

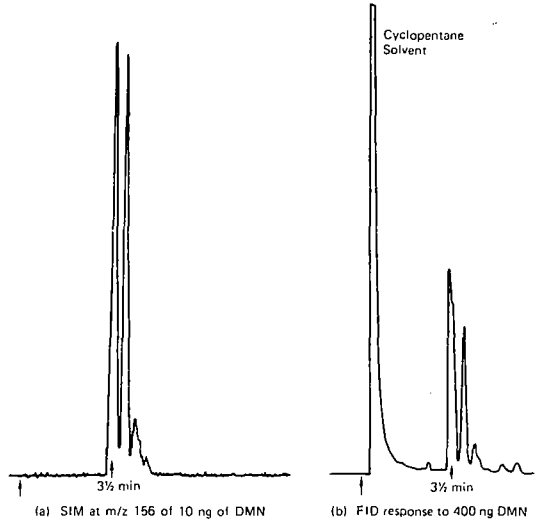


FIGURE 4 RESOLUTION OF GC/FIMS VS FID FOR DETECTION OF DMN

TPMP11 AN ION CYCLOTRON RESONANCE SPECTROMETER AS A DETECTOR FOR A GAS CHROMATOGRAPH, MINH THUY NGUYEN, J. WRONKA and D. P. RIDGE, Dept. of Chem., Univ. of Del., Newark, DE 19711

If some of the effluent of a gas chromatograph is admitted to an ion cyclotron resonance spectrometer, the full range of icr techniques becomes available to characterize sample materials. Reactant ion monitoring and product ion monitoring are both enhanced in utility by the long ion residence time characteristic of icr and the ability to do double resonance. The long residence time of ions makes it possible to observe reactions between sample ions and sample molecules. Such reactions effect the shape of the gc peak from which ion molecule reaction rates may be deduced. Double resonance makes it possible to monitor a reactant ion-product ion pair. Very reactive species such as metal ions can be used as chemical ionization reagents. Monitoring the intensity of non-reactive ions provides information on sample polarity. Resolution problems can be minimized by using a low molecular weight carrier gas.

DESIGN AND TESTING OF A TWO DIMENSIONAL GAS CHROMATOGRAPHY SYSTEM FOR MASS SPECTROMETRY, RALPH J. MAY and WOODFIN V. LIGON, JR., General Electric Company, Corporate Research and Development, Schenectady, New York 12301

We report a design and test results for a fully proportional two dimensional gas chromatography system for mass spectrometry. The device was conceived to facilitate analysis of thermal desorption samples of unknown composition and to facilitate analysis of trace components in organics of moderate volatility such as Di-2-ethylhexylphthalate. The device in its primary separation phase is shown in Figure 1. The secondary separation phase is shown in Figure 2. The device functions by first splitting a small fraction of the effluent of the primary column to a flame ionization detector. The remainder of the sample passes to a region in which it is diverted by vacuum to a cold trap or allowed to vent. The vacuum induced flow into the cold trap is modulated by the output of the flame ionization detector. In the second stage the vacuum and vent valves are closed and the cold trap heated. A fraction of the flow from the primary packed column is used to provide carrier gas for the secondary capillary column.

As a peak elutes from the primary column it is sampled continuously into the cold trap at a rate inversely proportional to its intensity and corrected for detector non-linearity. Only at very large signal levels is the peak not sampled at all.

This combination allows the injection or thermal desorption of samples of completely unknown composition into a system which ultimately provides full capillary resolution without concern for overloading of either the capillary or the mass spectrometer.

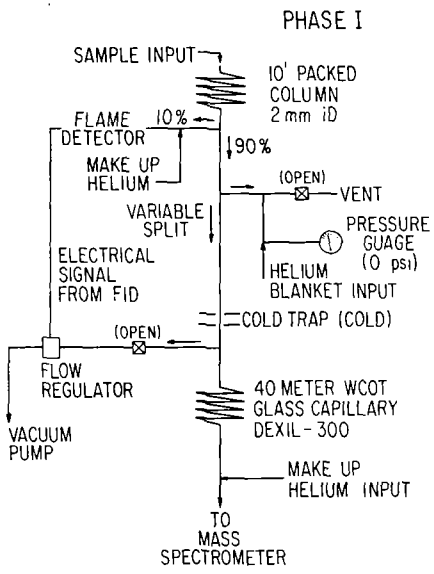


Figure 1

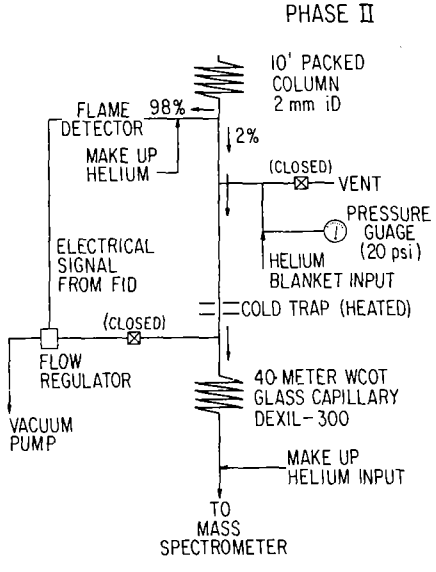


Figure 2

A COMPARATIVE EVALUATION OF QUANTITATIVE TECHNIQUES FOR SCANNING GC/MS ANALYSIS

by

A. E. Rosecrance, M. E. Rose, B. N. Colby

Systems, Science and Software
P.O. Box 1620
La Jolla, California 92038

Quantitative techniques for GC/MS require the use of reference standards for calibration. There are a variety of approaches to this standardization process. Typically, these include some form of external standard or internal standard, either labeled or non-labeled. Calibration can be accomplished by several methods. The most simplistic method utilizes a single data point plus the origin to establish the calibration; more complex procedures involve regression analysis. This presentation will provide a comparative evaluation of all the commonly used techniques for quantifying GC/MS data acquired in the scanning mode.

TPMP14 COMPARISON OF PACKED AND CAPILLARY CHROMATOGRAPHY FOR QUANTIFICATION OF DRUGS FROM BIOLOGICAL SAMPLES BY GC/CIMS.

F. W. CROW and R. L. FOLTZ, Battelle, 505 King Avenue, Columbus, Ohio 43201.

Glass capillary column gas chromatography is compared with packed column gas chromatography with respect to the quantitative analysis of drugs in biological fluids. Capillary columns are employed in order to increase resolution to separate the peak of interest from interfering background. Typically capillary columns produce narrower peak widths than packed columns which increases the signal-to-noise ratio. Comparisons using diazepam, N-desmethyldiazepam, Δ9-tetrahydrocannibinol and it's metabolites as model compounds will be shown. Chromatographic considerations to be discussed will include capillary column length, stationary phase, split vs. splitless injection, and interfacing to the mass spectrometer.

AN HPLC-MS STUDY OF SOME POLYCYCLIC AROMATIC HYDROCARBONS, CARBAMATES AND HYDRAZINES

Fred L. DeRoos and Rodger L. Foltz
Battelle Columbus Labs
Columbus, Ohio

Introduction

With the advent of a workable LC-MS interface it has become possible to analyze many environmental samples previously unamenable to separation and mass spectral analysis. In this study a selection of polycyclic aromatic hydrocarbons, carbamate pesticides, and dinitrophenylhydrazine derivatives were examined. Parameters such as mobile phase, mobile phase flow rate, split ratio, drive chamber temperatures and sample vaporizer temperatures were studied to determine their effect on sensitivity and quality of the spectra.

Experimental

The LC-MS analyses were carried out using a Finnigan Model 4000 mass spectrometer interfaced to a Finnigan/INCOS Model 2300 data system. The HPLC system was comprised of an Altex Model 420 system controller and two Model 110A pumps. The HPLC was interfaced to the mass spectrometer using a Finnigan direct coupled LC-MS interface. The ultraviolet detector was a Laboratory Data Control Model UV-III. Optimum HPLC conditions were worked out before commencement of the LC-MS analyses. The polycyclic aromatic hydrocarbons were separated on a Lichrosorb RP-18 column using a mobile phase of 70% acetonitrile in water to 100% acetonitrile over a period of ten minutes. A Lichrosorb RP-8 column was used for the carbamate study. The mobile phase was 40% methanol in Ph 2.5 phosphate buffer which was liquid-liquid extracted into an organic phase prior to deposition onto the interface belt. A Spherisorb-ODS column with a mobile phase of 10% methanol in methylene chloride was used for the dinitrophenylhydrazine study.

Results

The data indicate that HPLC-MS is applicable to the analyses of these types of compounds. Although the sensitivity is somewhat less than obtained by GC-MS, it is adequate for many studies. Further refinements in the chromatography and interface parameters will undoubtedly result in increased sensitivity.

Good quality data were obtained for the PAH's by both electron impact ionization and isobutane chemical ionization. In all cases the base peaks were the molecular ions or MH^+ ions. Additional ions corresponding to the loss of O, NO, and NO_2 were also observed.

The carbamates were studied using isobutane chemical ionization. The data shown resulted from the injection of 100 ng on column of each of the compounds. For each compound the base peak was the MH^+ ion with the only other peaks of any significance resulting from the loss of $CH_3N{=}C{=}O$ or $CH_2{=}CHCH_3$.

The dinitrophenylhydrazine derivatives were also studied under isobutane chemical ionization conditions. As expected the base peaks are due to the MH^+ ions with loss of O, NO, and NO_2 accounting for the remaining high mass ions.

Conclusions

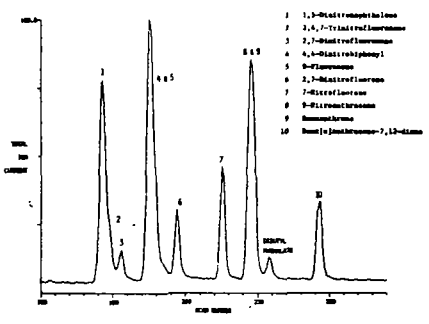
Sensitivity is limited by the background noise level and the transfer efficiency of the interface. The sensitivity is approximately 10 - 100 times less than obtained by GC-MS.

Transfer efficiency is a function of the sample volatility. It ranges from approximately 10% to 50%.

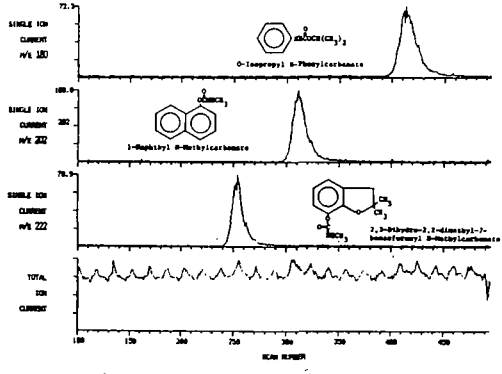
Background noise level results mainly from solvent impurities and pressure fluctuations in the source. Source pressure fluctuations can be minimized by careful control of the mobile phase flow rate and the drive chamber heater temperature.

Peak broadening is minimal and does not cause any observable problems.

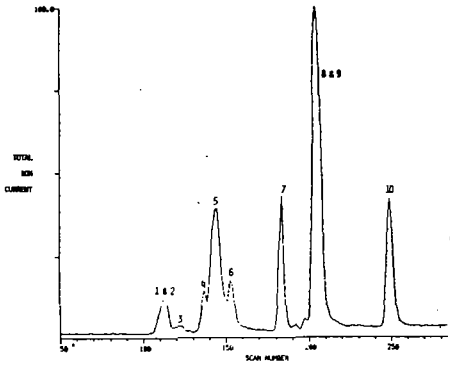
Mobile phase flow rate is dependent upon the volatility. The interface can accommodate approximately 1.0 ml/min of hexane or methylene chloride, but only 0.3 ml/min of acetonitrile or organic/water phases.



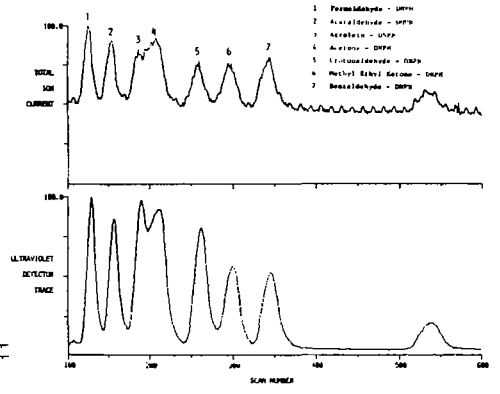
RECONSTRUCTED ION CURRENT TRACE FOR POLAR PAH MIX - ISOBUTANE CHEMICAL IONIZATION



RECONSTRUCTED ION CURRENT TRACE FOR CARBAMATE MIX - ISOBUTANE CI



RECONSTRUCTED ION CURRENT TRACE FOR POLAR PAH MIX - ELECTRON IMPACT



RECONSTRUCTED ION CURRENT TRACE FOR DINITROPHENYLHYDRAZINE DERIVATIVES - ISOBUTANE CHEMICAL IONIZATION

QUANTITATION OF Δ^9-THC, 11-HYDYOXY-Δ^9-THC, AND 11-NOR-Δ^9-THC-9-CARBOXYLIC ACID FROM PLASMA USING CHEMICAL IONIZATION GAS CHROMATOGRAPHY / MASS SPECTROMETRY

B. J. HIDY, R. L. FOLTZ, AND D. L. PERRY

BATTELLE COLUMBUS LABORATORIES COLUMBUS, OHIO

OBJECTIVE. The purpose of this research is to develop a method for the quantitation of Δ^9-THC and two of its major metabolites in physiological fluids. The method should be capable of accurate quantitation for sample concentrations as low as 50pg/ml and permit the routine analysis of a large number of samples (50-100/wk.)

METHOD. The method developed consists of a solvent extraction of the physiological fluid followed by concentration and derivatization. Quantitation of the derivatized extract is obtained by gas chromatography/ chemical ionization mass spectrometry(Figure 1 shows a Flow Diagram for this method).

EXTRACTION. The extraction procedure consists of the addition of deuterated internal standards tothe sample(approx. 50ng/ea),buffering to pH 2.0,and extract twice with hexane + ethly acetate 7:1. the combined extracts are washed once with aqueous 0.2N H_2SO_4, then evaporate to dryness under reduced pressure using a Buchler Vortex-Evaporator.

DERIVATIZATON. The evaporated solvent extract is derivatized with BSTFA+1% TMCS. The derivatized sample shows good stability when stored at -20 C until analyzed.

QUANTITATON BY CI-MS USING SELECTED ION MONITORING. For cannabinoids as for many drugs we find that the best sensitivity and selectivity is obtained by using a mixture of methane and ammonia (10:1) as CI reagent gas. The methane-ammonia CI mass spectra of each of these cannabinoids gives a single major ion which corresponds to the protonated molecule ion (MH^+). By using a computer program to control the mass spectrometer during selected ion monitoring we can automatically monitor different sets of ions for specific intervals during the GC-MS analysis.

PACKED COLUMN VERSUS CAPILLARY COLUMN GAS CHROMATOGRAPHY. For previous cannabinoid analyses a 3% OV-17 (2m X 2mm)glass packed column provided good resolution and peak shape. However, an endogenous component of the physiological fluid gave a peak in the M/z 387 ion current profile which was unresolvable from the peak due to Δ^9-THC-TMS. The same extract when analyzed on a SE-52 glass capillary column (15m X.25mm) gives a well

resolved peak with no interference for Δ^9-THC-TMS. In addition, the increased resolution of the capillary column produces a much sharper, narrower peak (6sec. vs 24sec.) which improves the over-all sensitivity of the analysis.

CONCLUSIONS. A method for the simultaneous extraction of Δ^9-THC and two of its major metabolites has been developed which has the required sensitivity and selectivity when used in conjunction with glass capillary GC / methane-ammonia CI-MS using selected ion monitoring. With this method we can routinely analyze 50-100 samples per week.

ACKNOWLEDGMENT. This work is supported by the National Institute on Drug Abuse, Contract HSM-42-72-183.

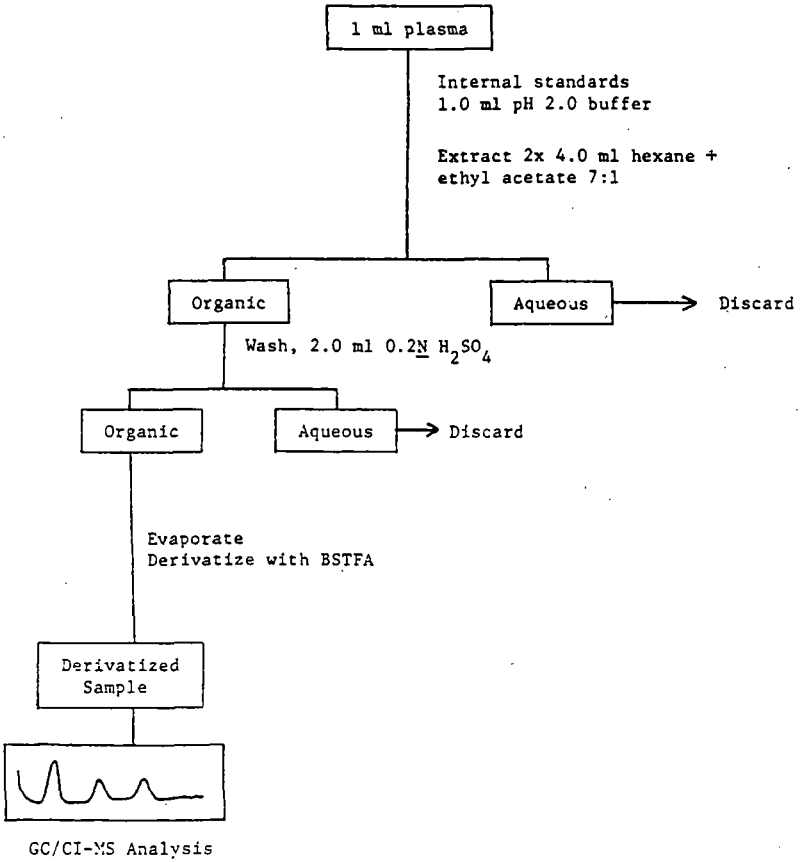


FIGURE 1

FLOW DIAGRAM FOR ANALYSIS OF Δ^9-THC AND ITS TWO MAJOR METABOLITES IN PHYSIOLOGICAL FLUIDS

DEVELOPMENT OF PROGRAMS TO IMPROVE ON-LINE DATA COMPUTATION CAPABILITY OF HEWLETT-PACKARD (H.P.) 5933A DATA SYSTEM INTERFACED WITH H.P. 5930A GC-MS.

J.K. Khandelwal and H. Weinstein, Mount Sinai School of Medicine, Department of Pharmacology, New York, NY 10029.

Our behavioral studies require simultaneous measurements of steady state levels and turnover rates of acetylcholine, choline and their isotopic variants in discrete regions of rat brain by pyrolysis gas chormography-chemical ionization mass fragmentography. Such analysis results in the generation of a large body of experimental data that needs to be processed efficiently and expediciously from the information stored automatically. Current Hewlett-Packard Computer programs do not fulfill our specific needs. We have, therefore, developed three new computer programs to improve on-line data computation capability of the system and to facilitate the processing of a large body of data in an integrated manner suitable for our research needs.

Program 'COMBINE' pools the desired number of SIM (Selected Ion Monitoring) data files into a temporary file numbered 9999. This combined temporary file is utilized in the other two programs. The SIM data file can not save more than 20 entries in a single file. Our 'COMBINE' program has overcome this limitation and has enabled pooling of large body of entries in a single file.

Program 'STANDARD' plots calibration curves on a linear scale between the amount of choline esters and the area ratio and calculates both the slope and intercept values for use in calculations of choline ester concentrations in tissue samples.

Program 'UNKNOWN' calculates the amount of choline esters in individual tissue samples and the concentration of esters per gram tissue weight for use in turn over studies.

Conclusions:

The three new programs have enhanced the on-line data computation capability of our data system and have facilitated efficient and expeditious calculations of a large body of experimental data in a manner suitable for our turn over studies in behavioral pharmacology. The programs can be used in other studies as well.

Documentation of the programs is available upon request.

Supported by NIMH Grant MH24949 and NIDA Grant DA01875.

THE CARRIER EFFECT IN GC/MS

T. A. BLAZER, E. I. du Pont de Nemours & Co., Inc., Instrument Products, Wilmington, DE 19898

The addition of co-elutants to gas chromatographic mixtures prior to an injection in order to increase the sensitivity of certain components has been a long recognized technique. This principle has been extended into the field of GC/MS. This presentation describes the carrier effects in GC/MS. The carrier effect in GC/MS is demonstrated by the addition of compounds which are analogs to the desired components by the addition of compounds which are of a similar nature but have a different functionality and by the addition of compounds which are dissimilar. The conclusion to this study of the carrier effect is that the carrier effect compensates for active sites in the gas chromatographic column or the GC/MS interface by tying up these sites and thus permitting the desired components to pass through the system in greater yield.

CHEMICAL AND ANALYTICAL APPLICATIONS OF AN LC/MS INTERFACE

Attilio Melera
Scientific Instruments Division, Hewlett Packard Co.
1601 California Avenue
Palo Alto, CA 94304

One year ago at this meeting[1] preliminary data obtained from a modified version of McLafferty's[2] direct liquid inlet LC/MS interface were presented. Results from a more thorough characterization of the interface are given here. In this version the sample is introduced into the MS source area by means of a removable probe through which the eluate of the LC column is transported (Fig. 1).

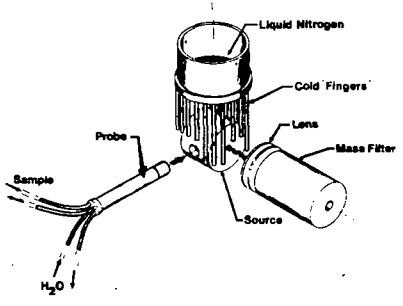


Fig. 1

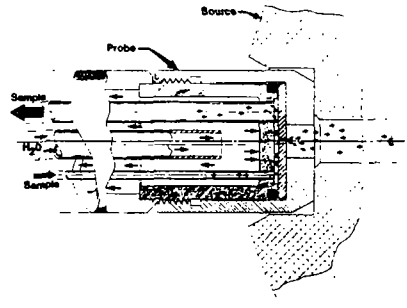


Fig. 2

At the tip of the probe a small portion of the eluate (1-4%) is split from the main stream through a small bore hole (5-10μ DIA) located in the center of a stainless steel diaphragm (Fig. 2). The jet of small droplets emerging from the tip[3] enters a desolvation chamber where the solvent is evaporated and a gaseous solvent/sample mixture is formed which is then ionized in the MS source operating in the CI mode of operation.

A cryogenic pump, a set of copper fingers located in the area surrounding the source and cooled by means of LN_2 (Fig. 1), increases the pumping speed for the most common solvents used in HPLC by a factor of ten over comparable operation with the standard diffusion pump thus allowing to introduce more sample into the ion source (approx. 20 mg/min) while keeping optimum pressure conditions for maximum CI sensitivity. Further improvements in sensitivity have been achieved by means of shorter LC-columns operated at lower flowrates than the standard 25cmx4.6 mm columns.

Typical sensitivities with a 5cmx4.6 mm column packed with 5μ RP-8 material are 50-500 ng on column for a spectrum and 2-20 ng for a SIM detection, depending on the CI properties of the samples. Buffered ammonium acetate solutions in acetonitrile/water have been successfully

used for the separation of alkaloids such as strychnine and brucine and for the biologically important bases cytosine, adenine and adenosine. Fig. 3 shows the chromatogram of adenosine at the 1µg level together with the spectrum obtained on top of the LC peak.

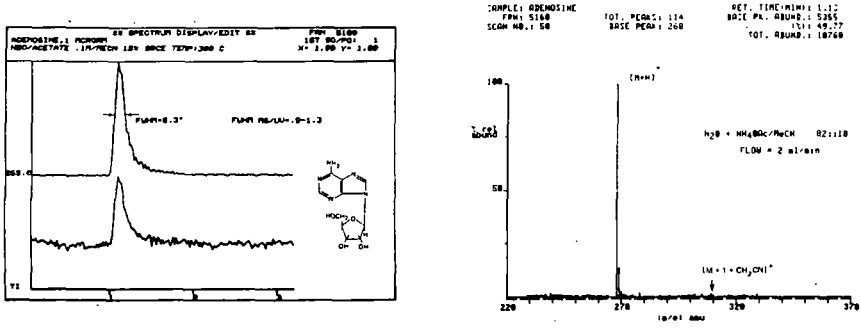


Fig. 3

Stability, reproducibility and linear dynamic range of the interface were also investigated. Results are presented for a mixture of benzanilide/ indomethacine (750 ng each) and for a mixture of cortisone, dexamethasone corticosterone (500 ng each on column) in the scanning mode, with precision in the range of 3-10% obtained for hand injected 1 microliter quantities (Fig. 4)

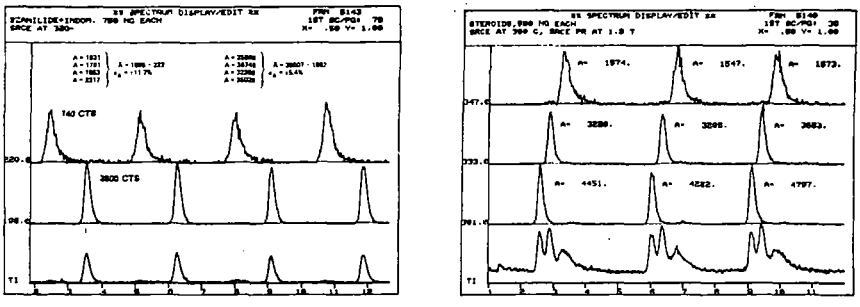


Fig. 4

Linear dynamic range for the $[M+1-60]^+$ ion of Cortisol in SIM mode is illustrated in Fig. 5a. Different detector gains were needed to accommodate the 5 order of magnitude investigated.

Stability of the signal obtained from a 5 PPM solution of cortisol and 1 PPM of benzanilide in water/acetonitrile 1:1 continuously sprayed into the source and monitored in the scanning mode at 100 amu/sec show an excellent stability during a period of 15 minutes with a standard deviation better than 10% (Fig. 5b)

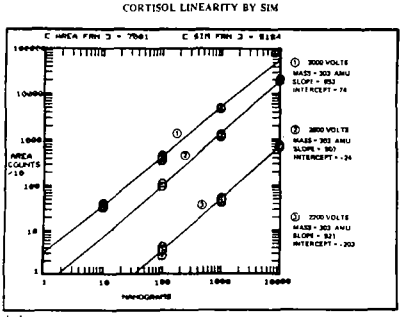


Fig. 5a

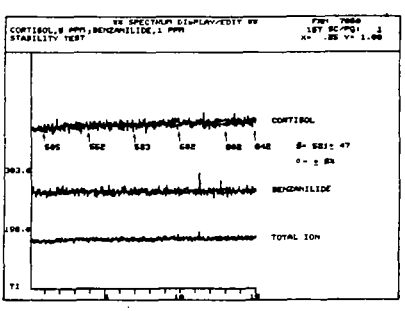


Fig. 5b

Summary:

- Performance parameters of the direct liquid introduction LC/MS interface have been characterized.
- Alkaloids, purine and pyrimidine bases, eluted with appropriate buffer solutions of temperature sensitive organic buffers have been successfully analyzed.
- Protic and non-protic solvents as well as gradient elutions have been used with greater emphasis given to the popular reverse phase systems operating at high water percentages
- Good stability, precision, sensitivity and linear dynamic range for thermally unstable and non volatile compounds has been demonstrated.

1) Serum, J. W. and Melera, A., Paper No. RP-8, 26th ASMS Meeting, St. Louis, May 28 - June 2, 1978.

2) Arpino, P., Dawkins, B. G., and McLafferty, F. J. Chromatogr. Sci., 12, 574 (1974).

3) Linblad, N. R. and Schneider, J. Sci. Instr. 42, 635 (1965)

TPMP20

PROGRESS IN LC/MS INTERFACING BASED ON THE DLI CONCEPT.

Patrick J. ARPINO and Georges GUIOCHON, Ecole Polytechnique, Laboratoire de Chimie Analytique Physique, F-91128 Palaiseau.

Gerard DEVANT and Paul Krien, Nermag Inc.F-92502-Rueil-Malmaison.

In the course of developing improved methods for on-line LCMS analysis, the different factors influencing the transport of a liquid solution through an interface for Direct Liquid Introduction (DLI) have been investigated.

It is easy to increase the pumping speed of the vacuum equipment of a conventional quadrupole MS by adding a large active surface cryopump chilled by liquid nitrogen. For a surface of 300 - 500 cm^2, about 30 - 70 µL /min of liquid solution from the LC column output can be directly sampled into the CI ion source block. The cryopump shows self regulating action against over pressures in the source housing. It saturates after 5-8 hours of continuous LCMS operations. The best method for regenerating the cryopump is to break the vacuum in the source housing, to remove it completely, and to evaporate the solvent under a hood using a heat gun. The complete cycle of regeneration between two consecutive LCMS runs can take as short as 10 - 15 min in our apparatus.

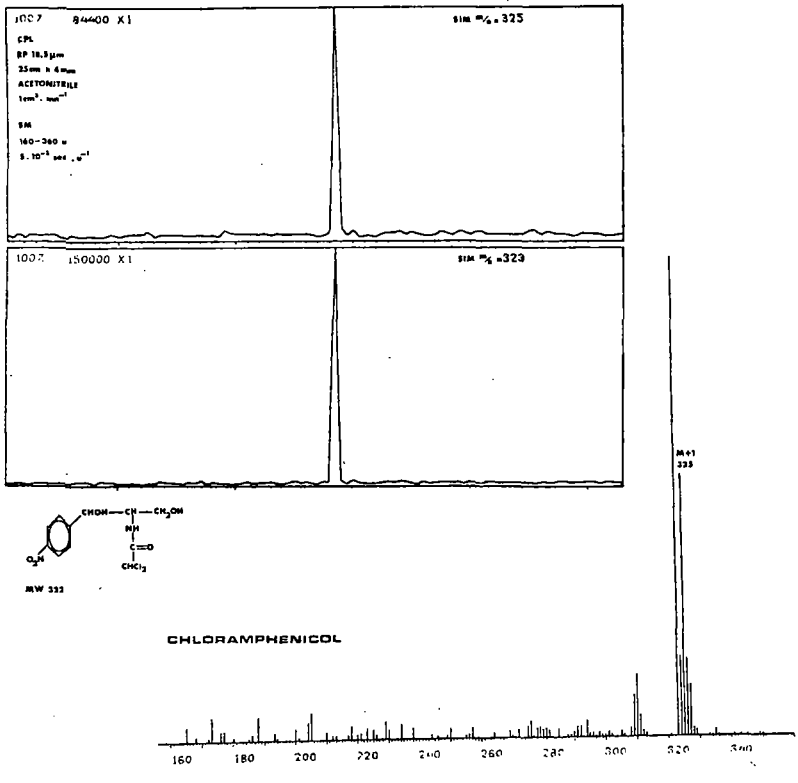
For constant flow rate introduction of a solvent with molecular weight M, the pumping speeds of the cryopump and of the diffusion pump reduce roughly as $1/\sqrt{M}$, whereas the amount of solvent vapor being produced by vaporization of the liquid reduces as 1/M. Thus the tolerable input flow rate of liquid increases with $\sqrt{M}$ for constant ion source pressure. The higher limit in mass range for the value of M is set by the difficulty of evaporating high MW solvents, the possible overlay of solute mass spectra , and loss of MS resolution and transmission because of ion-molecule interactions in the ion optics.

The volume of the interface between the HPLC column outlet and the ion source block must be smaller than $(1+k')V_o/5\sqrt{N}$ to avoid degradation of the chromatographic peak (V_o is the retention volume of an inert solute, k' is the capacity ratio, N is the number of theoretical plates). This causes severe contraints on the size of the interface. For a 4 mm i.d. column, 50 cm long, 50 000 plates and k'=3, the acceptable dead volume is 30 µL.

Our first model of DLI interface was based on a long (30cm) and narrow (0.1 mm id) capillary glass tube. The purposes of the tube were to meter a small flow of liquid inside the CI source block, and to reduce all critical post-column dead volumes. Although long

and trouble free LCMS runs could be sometimes achieved, it was demonstrated that solutes with boiling point under atmospheric pressure of about 500°C could not be correctly eluted due to the vaporization of the solvent inside the capillary tube, consequentely, other designs of DLI interface were investigated.

We have verified that performances are significantly improved when droplets of liquid solution are sprayed inside the ion source. The optimum situation is probably reached when the droplets fly and evaporate shortly before intersecting the ionizing electron beam. A small diaphragm (10 µ) kept at ambiant temperature was used for producing droplets of liquid solution, and a 2 cm long glass tubing was inserted between the diaphragm and the ion source block to increase the flight length of the droplets. Under those conditions, CIMS spectra of non volatile drugs such as ampicilline and chloramphenicol could be obtained. It appears then, that it is probably important to control the number, the size, and the life time of the droplets.



A COMBINED DATA-BLOCKING, CROSS CORRELATION PEAK DETECTION METHOD FOR COMPUTERIZED GC-MASS SPECTROMETRY

Wm. Bryant, M. Trivedi, B. Hinchman, and S. Sofranko
Departments of Analytical Chemistry and Computer & Statistical Operations, Pennwalt Pharmaceutical, Rochester, N.Y. 14623

P. Mitachek, Jr., Department of Chemistry
St. John Fisher College
Rochester, N.Y. 14618

During the development of a data system to support on-line GC-MS, we found it advantageous to modify a cross-correlation peak detection procedure previously reported by Bell (1) and to combine it with a data-blocking detection method based on the use of a digital clock and a threshold comparitor. Both methods are linked through program LOCPK so that, data within a scan, is automatically processed using either the data-blocking(CTIME) or cross-correlation (CROSS) subroutine as required by the complexity of the digital record.

In operation, LOCPK first calls CTIME to examine the clock values transmitted with each conversion taken by the interface, then uses these values to find regions of continuous data transmission. A break or discontinuity in data transmission occurs when the ion response falls below the 5-10 mv threshold set by the user. These breaks are located by comparing values of the clock for adjacent conversions. If the number of conversions between breaks does not exceed 1 a.m.u., CTIME applies a threshold test to eliminate noise spikes, then determines intensity and mass position before processing continues for the rest of the scan. When the data range between breaks exceeds 1 a.m.u., then CROSS is required to locate individual peaks within the data block.

A significant feature of CROSS is that it locates mass peaks through simple sign checking. CROSS takes advantage of a property of D_t (Eq.1) which causes it to become negative just before and just after mass peaks. This property allows peak detection by CROSS to be both simple and rapid.

$$D_t = -I_{(n-3)} + I_{(n-1)} + 2I_{(n)} + I_{(n+1)} - I_{(n+2)} \qquad \text{(Eq.1)}$$

Tests conducted in this laboratory over the past year show that, at least half of the peaks in a typical integer resolution mass spectrum can be located by CTIME alone. For example, a typical mass spectrum of p-methylanisole (I) acquired with the use of the threshold comparitor set to transmit data for which the intensity exceeds 10 mv, consisted of a digital record of 382 conversions (1528 words). This scan contained 29 ions of which 17 were found by CTIME and 12 required further processing by CROSS. The performance of program LOCPK can be readily checked by turning the comparitor off. This causes all data to be processed by CROSS. For I, the complete digital under these conditions contained 3008 conversions (12, 032 words). Spectra of I, processed by LOCPK (A) and by CROSS only (b), were submitted for identification via the Cornell University Probability Based Matching system (2). The largest confidence factor, K, for I-A was 90 (Δ K = 8); that for I-B was 92 (Δ K = 6). The excellent agreement between the K factors indicates that the results of the combined, data-blocking cross-correlation method compares favorably with that from cross-correlation analysis alone. The magnitude of the K factors, along with the low values of Δ K, demonstrates good agreement with the literature spectrum for this compound.

(1) Bell, N.W., Twenty-First Annual Conference on Mass Spectrometry, San Francisco, Ca., 1973.

(2) Atuater (Fell), B.L., Mun, I.K., Harak, K.S., VenKataraghovan, R., and McLafferty, F.W. Twenty-Sixth Annual Conference on Mass Spectrometry and Allied Topics, St. Louis, Mo., 1978, p.574.

TPMP22 LC-MS Analysis of Drugs

J.D. BATY, Dept. of Biochemical Medicine, Ninewells Hospital, Dundee.
D.A. YORKE and B.N. GREEN, V.G. Organic Ltd., Altrincham, England.

Applications of a new liquid chromatography-mass spectrometry interface to the analysis of drugs and related compounds will be presented. The interface is connected to a Vacuum Generator MM-16F instrument and a VG2040 Data System. Urine extracts from subjects receiving analgesic drugs can be analysed by HPLC on a reverse phase column and the drug and metabolites directly identified by LC-MS. Benzodiazepine drugs can be analysed following HPLC on silicic acid columns.

TPMP 23

A Newsletter for Practical Mass Spectrometry Communication

Walt Hyde
Veterinary Diagnostic Lab, ISU, Ames, Iowa 50011

With the increased interest in GC/MS as an analytical tool, has come a wealth of practical information for utilizing the technique efficiently and economically. Unfortunately, few mediums exist for the transfer of this type of information.

The goal of the Mass Spec Notes newsletter is to collect information from readers and redistribute it to all users. The Notes depends entirely upon user/reader contribution for its content. Issues are published approximately bimonthly or whenever enough information is collected to make up an issue. Past subjects have been:

vacuum problems and solutions,
service tips for maintaining instrumentation,
electro polishing source parts,
cheaper sources of replacement parts,
MS manufacturer schools - a review,
user-generated software,
and instrument modification

to mention a few.

Any subject of interest to mass spec users is possible. The Notes is meant for the practicing mass spec users.

The Notes is striving to present information from users of all mass spec equipment available. Techniques of problem solving are generally universal and applicable to most instrumentation.

Also, the Notes will try to share concerns of users about instrument support for older systems, service reliability of manufacturers, and other such matters

Please help the Notes succeed. Contact us with any information you think would help someone else utilize his MS equipment more fully.

CHARACTERIZATION OF THIOETHER CONJUGATES OF ACETAMINOPHEN BY FIELD DESORPTION MASS SPECTROMETRY

WAM0A1

T.A. Baillie*, H. Kambara*, S.D. Nelson+ and Y. Vaishnav§
*Biomedical Mass Spectrometry Resource, Space Sciences Laboratory, University of California, Berkeley, Ca. 94720; +Department of Pharmaceutical Sciences, University of Washington, Seattle, Wa 98195; §Baylor College of Medicine, Houston, Tx 77030

Studies on the metabolic fate of the analgesic acetaminophen (paracetamol) have indicated that the tissue damage observed at high doses of the drug is associated with the formation of a reactive electrophilic intermediate. This metabolite, produced via a cytochrome P450 mediated oxidation of the parent drug and believed to possess an imidoquinone structure, reacts with cellular nucleophiles, e.g., glutathione, to form covalent adducts. The acetaminophen-glutathione thioether conjugate formed by this pathway is further metabolized to the corresponding cysteine adduct and, subsequently, to the mercapturic acid derivative prior to excretion in the urine (1).

Of the above thioether conjugates of acetaminophen, only the mercapturic acid is amenable to study by EI mass spectrometry because of the highly polar nature and thermal instability of this class of compounds. CI techniques, in which the sample is inserted directly into the reagent gas plasma, have been employed (with limited success) in the characterization of the cysteine adduct, while attempts to study the glutathione conjugate by mass spectrometry have hitherto been unsuccessful. In connection with our interest in the identification of polar drug conjugates by FD mass spectrometry, we decided to investigate the utility of FD techniques for the analysis of two thioether conjugates of acetaminophen, viz. the cysteine and glutathione adducts.

The required conjugates were produced in vitro, using a preparation of mouse liver microsomes fortified with NADPH and to which had been added the appropriate thiol to serve as a "trapping agent". Aliquots of the incubation products were analyzed directly by HPLC (2) and metabolites believed to be the glutathione and cysteine conjugates of acetaminophen were collected from the HPLC column and subjected to analysis by FD mass spectrometry. A modified AEI MS-902 instrument was used, equipped with a combined EI/FD source and provision for collision-induced dissociation (CID) studies (3). Samples, dissolved in methanol ($\sim$1 $\mu g\ \mu l^{-1}$), were applied to the emitter using the syringe technique; approximately 200 ng was required for FD studies while 1-2 μg of sample was employed for FD/CID work. FD/CID spectra were recorded using the EI source chamber as a collision cell and the B/E linked scan technique (4).

Results from the analysis of the acetaminophen cysteine conjugate are shown in Fig. 1. In the FD spectrum, prominent M^+ and $[M+Na]^+$ species are present, together with an intense ion at m/z 183, corresponding to cleavage of the CH_2-S bond with charge retention on the thiophenol moiety. This ion also dominates the corresponding FD/CID spectrum which, in addition, contains ions derived from fragmentation of the amino acid and acetamido functional groups, thus providing further evidence for the proposed structure.

The FD spectrum of the acetaminophen glutathione conjugate (Fig. 2) again exhibits a prominent parent ion (MH^+, m/z 457) and its cationized equivalent at m/z 479. Cleavage of the γ-glutamyl peptide bond gives the doublet at m/z 129/130, while the fragment at m/z 307 corresponds to the glutathione moiety and the ions at m/z 229, 240 and 251 to doubly charged species. The intense m/z 151/152 pair corresponds to $[acetaminophen]^+$ and its protonated counterpart, respectively; the possibility that these ions may result from thermal degradation of the conjugate on the emitter surface is suggested by their absence from the FD/CID spectrum, in which only those species which result from direct fragmentation of the MH^+ species are recorded. CID of the γ-glutamyl side-chain appears to be an important process, as evidenced by the prominent ions at m/z 327 and 382.

As demonstrated in this study, FD techniques are extremely useful in the characterization of labile thioether conjugates of acetaminophen by mass spectrometry. The use of normal FD and FD/CID analyses gives valuable complementary information on molecular structure and fragmentation pathways.

Acknowledgments: This work was supported in part by NIH Division of Research Resources Grant RR00719-04 to Dr. A.L. Burlingame and in part by NIH Grant GM25418.

References

1. D.J. Jollow, S.S. Thorgeirsson, W.Z. Potter, M. Hashimoto and J.R. Mitchell; Pharmacol. 12, 251 (1974).
2. A.R. Buckpitt, D.E. Rollins, S.D. Nelson, R.B. Franklin and J.R. Mitchell; Anal. Biochem. 83, 168 (1977).
3. A.L. Burlingame, H. Kambara and F.C. Walls; 26th Annual Conference on Mass Spectrometry and Allied Topics, St. Louis, Mo., May 1978, p. 184.
4. R.K. Boyd and J.H. Beynon; Org. Mass Spectrom. 12, 163 (1977).

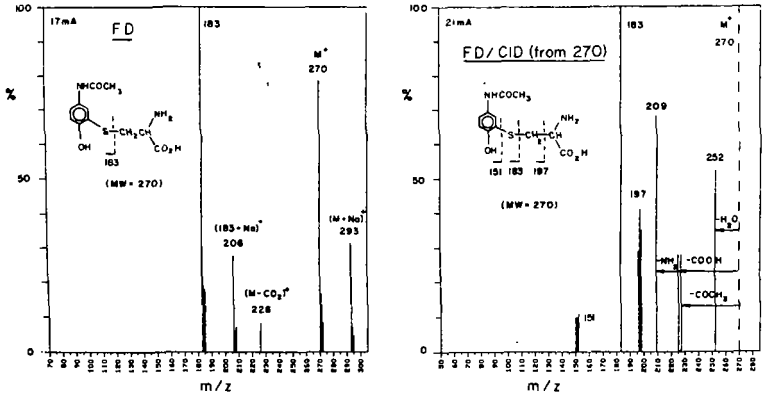


Figure 1. FD (left) and FD/CID (right) mass spectra of the acetaminophen cysteine conjugate.

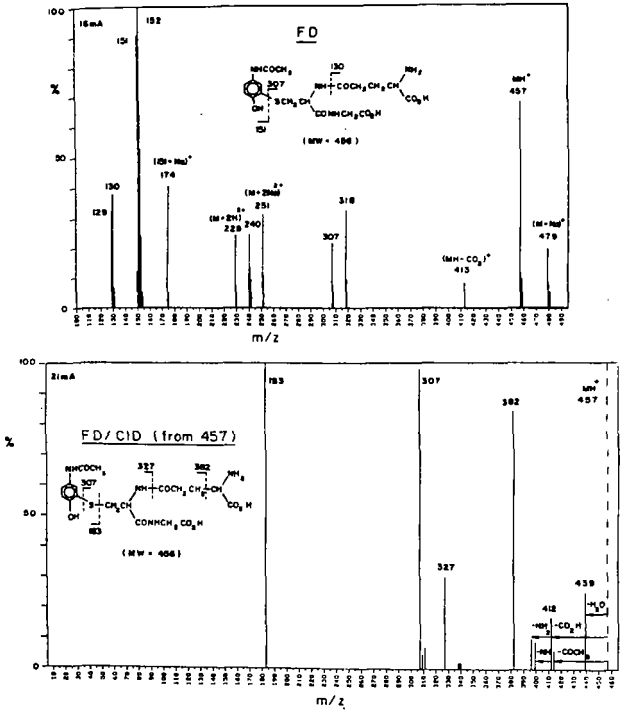


Figure 2. FD (upper) and FD/CID (lower) mass spectra of the acetaminophen glutathione conjugate.

Preparation and GCMS Studies of N-Ethyl Derivatives Of Desmethyl Metabolites of Antidepressant and Antipsychotic Drugs

WAMOA2

N. Narasimhachari and R. O. Friedel
Department of Psychiatry
Medical College of Virginia
Richmond, Virginia 23298

Determination of plasma levels of tricyclic antidepressant drugs is considered necessary to evaluate the clinical response to the drug. The secondary amino tricyclics, desimipramine (I), nortriptyline (II) and protriptyline are in clinical use as antidepressants and I, II and desmethyldoxepin are also the active metabolites formed when imipramine, amitriptyline and doxepin are administered as antidepressant medication. We have recently reported a procedure for N-ethylation of these secondary amines using dimethylformamide-diethyl-acetal.[1] These N-ethyl derivatives are stable and have excellent GC and GC-MS characteristics, thus making them suitable for quantitation by GC-MS-SIM technique. We have now used this procedure for the simultaneous quantitation of the tertiary amino tricyclic antidepressants, imipramine, amitriptyline and doxepin and their desmethyl metabolites in a single injection using both EI and CI mass spectrometry. For this quantitation we used d_4-desipramine and d_4-imipramine as common internal standards. The ions monitored for the drugs and the internal standards in EI and CI mode are shown below:

	EI m/e	- int.std.	CI m/e	- int.std.
Imipramine	234	238	281	285
N-Et-Desipramine	208	212	295	299
Amitriptyline	-	-	278	285
N-Et-Nortriptyline	232	212	292	299
Doxepin	-	-	280	285
N-Et-Desmethyldoxepin	234	212	294	299
N-Et-Protriptyline	190	212	292	299

We have now extended this reaction to several desmethyl metabolites of antipsychotic drugs of different classes, such as alkylamino phenothiazines, e.g. norpromazine, norchloropromazine and piperazino-phenothiazines, e.g. norperazine, norchloroperazine. All desmethyl compounds yield quantitatively the corresponding N-ethyl compounds. Direct inlet solid probe mass spectra taken at various temperatures do not show any unchanged product or by-products. Gas chromatography shows only single reaction products and mass spectra of N-ethyl derivatives agree fully with the structures postulated for the derivatives. As *illustrative examples the gas chromatogram and mass spectra of N-ethyl derivatives of* norpromazine and norchloropromazine are shown in Fig. 1. We have obtained the mass spectra for N-ethyl derivatives of desmethyl thiothixene, norvalium and norcocaine. Full details will be published shortly.

References

1. N. Narasimhachari and R. O. Friedel, Anal. Lett., 12(B1), 77-88 (1979).

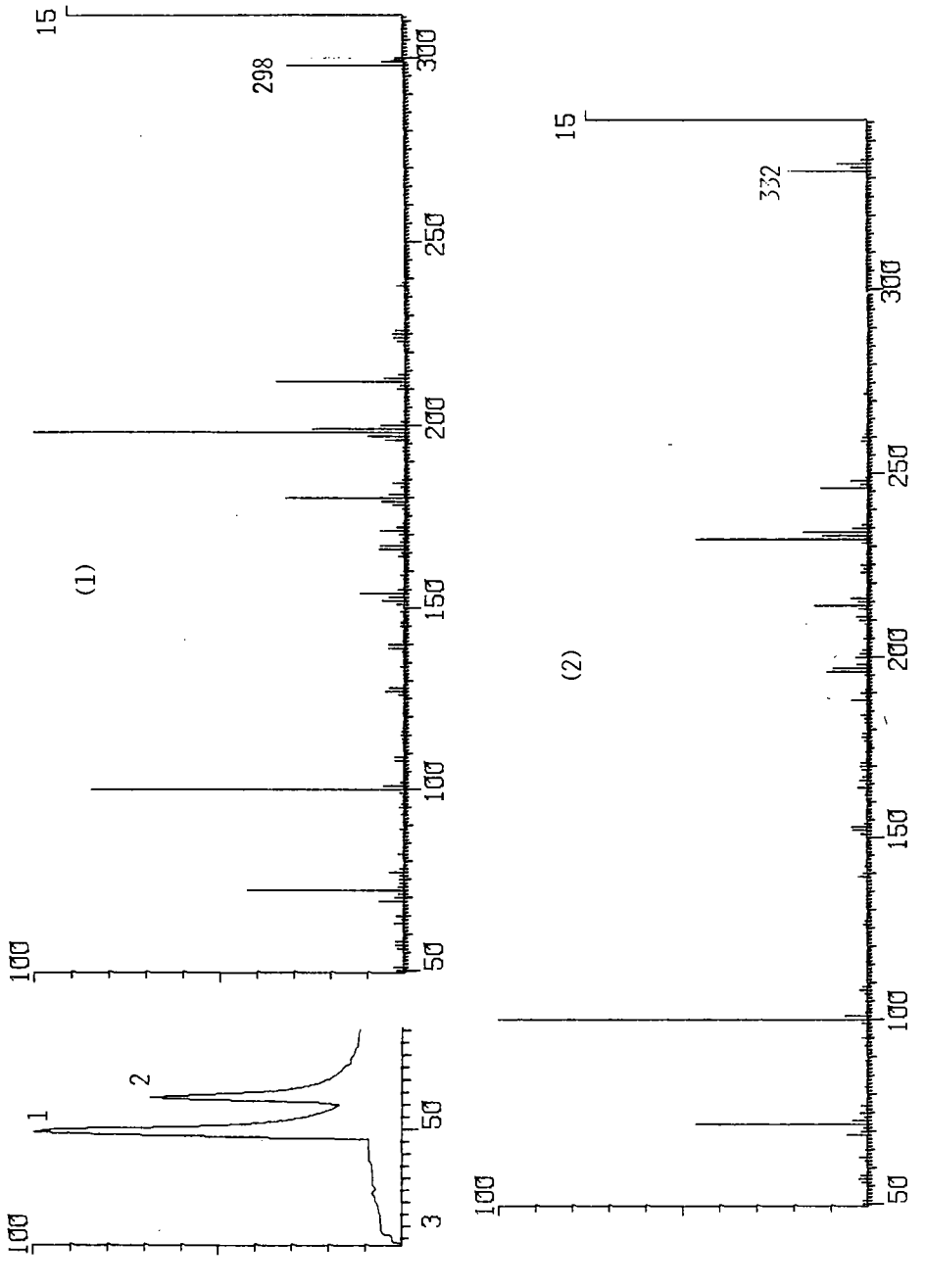


Fig. 1

Norpromazine (1) + Norchlorpromazine (2) N-Ethyl Derivatives

MASS SPECTROMETRIC TECHNIQUE FOR DETERMINING N-PHOSPHONOACETYL-L-ASPARTIC ACID (PALA) IN SERUM.

John Roboz, Robert Suzuki, Esther Rose, and Takao Ohnuma

Department of Neoplastic Diseases
The Mount Sinai School of Medicine
City University of New York
New York, N.Y. 10029

PALA is a potent inhibitor of aspartic acid transcarbamylase in vitro. Impressive efficacy has been shown against certain murine tumors in vivo. PALA is now undergoing Phase I clinical trials. Initial experiments revealed that PALA is not metabolized to phosphonoacetic acid (PAA) in humans. Thus, PALA may be quantified in serum after in vitro conversion to PAA.

Deproteinized serum (perchloric acid) is hydrolyzed with 8N HCl at 100°C for 3 hr. PALA is thereby converted to PAA and aspartic acid. PAA is quantified by monitoring the $(M+1)^+$ ions of the protonated TMSi derivatives of PAA and phosphonopropionic acid (int. std.) obtained by chemical ionization with methane as previously described[1]. Limit of detection is 0.5 μM (150 ng/ml) PALA using 1 ml serum.

PALA was given to 37 patients with advanced cancer. Courses were either 24hr infusion with dose escalation from 0.5 to 10.5 g/m^2/24hr or 5day infusion with dose escalation from 4.0 to 8.7 g/m^2/5days. Comparative blood level data gave maximum levels at the end of infusion in the 100-500 μM range. The biphasic decay gave $T_{\frac{1}{2}\alpha} \simeq$ 100min and $T_{\frac{1}{2}\beta} \simeq$ 8hr. Increase in $T_{\frac{1}{2}\alpha}$ correlated with increased clinical toxicity.

[1]Roboz, J., Suzuki, R., Bekesi, G., and Hunt, R. Biomed. Mass Spectrometry, 4, 291 (1977).

This work was partially supported by Grant # 5P01-CA 15936-05 from the National Cancer Institute, National Institutes of Health.

QUANTITATIVE MEASUREMENTS OF INDICINE-N-OXIDE IN THE URINE AND PLASMA OF CANCER PATIENTS

WAMOA4

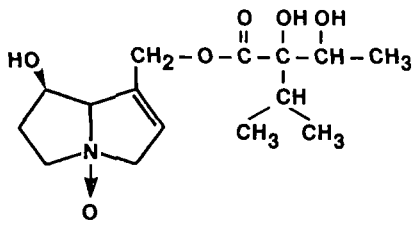
James V. Evans, Sylvia K. Daley and Carl Johann Nielsen
Biological Markers Program, NCI Frederick Cancer Research Center,
Frederick, Maryland 21701

Indicine-N-oxide (INO) (see below), a plant-extracted, pyrrolizidine alkaloid, has demonstrated significant antitumor activity in the National Cancer Institute Tumor Screen. INO can be analyzed by GC/MS after trimethylsilylation to either of two different products. The details of these reactions have been described elsewhere (1). One set of reaction conditions gives the trisubstituted pyrrolizidine derivative (INOPYZ) while a slightly different set of conditions gives the trisubstituted pyrrole derivative (INOPYL). An extension of this work has been the development of a quantitative procedure that applies this derivatization scheme to samples from cancer patients in clinical trials.

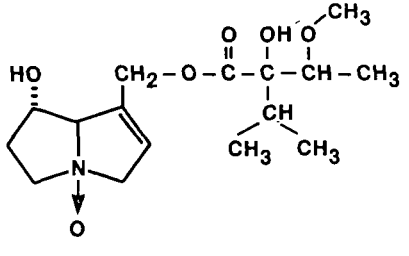
To reliably quantitate drug levels in such samples by gas chromatography, our first concern was to obtain a suitable internal standard. For this, we employed heliotrine-N-oxide (HNO) which is structurally very similar, differing only by a methyl group on the side-arm and by the orientation of the ring hydroxyl group (see below). In addition, the internal standard behaves chemically very similarly to INO. HNO produces analogous pyrrolizidine and pyrrole forms (HNOPYZ and HNOPYL, respectively) under the same derivatization conditions as INO does. In addition to displaying good gas chromatographic qualities, the HNO derivatives possess comparable mass spectral characteristics. As in the spectra of INOPYZ and INOPYL, the pseudomolecular ions differ by two mass units (m/e 457 for HNOPYZ and m/e 455 for HNOPYL). Moreover, HNOPYZ and HNOPYL fragment very similarly to their INO analogs. For example, the base peaks are 210 and 208 for HNOPYZ and HNOPYL, respectively, which are due to the cleavage of the ester bond. Furthermore, a number of other side-arm and ring fragments are directly analogous to those seen in the spectra of the INO derivatives.

The derivatization reactions are essentially complete after 2-3 hours of heating at 65°C. In both cases, prolonged heating was not desirable due to the lability of the ester bond in these compounds. Since the pyrrolizidine derivatives were somewhat unstable, we concentrated our quantitation efforts for biological samples on the pyrrole derivatization procedure, although we were able to generate good standard curves with the pyrrolizidine derivatives.

Once the derivatization conditions were established for the two reactions, we prepared standard curves utilizing HNO as the internal standard. Data employing the pyrrolizidine reaction and the pyrrole reaction were each plotted as peak area ratios of drug to internal standard as a function of drug concentration. The correlation coefficients for both least squares lines were greater than 0.99 for three experimental determinations



INDICINE-N-OXIDE



HELIOTRINE-N-OXIDE

over a range of 10 µg to 1 mg/ml of sample. This range serves as the working range for analyzing the levels of drug in the urine and plasma of cancer patients. In addition, we determined the lower limit of detection to be 40 nanograms of derivatized drug injected on column. Using the gas chromatographic column packing material 3% OV-101 on 100/120 mesh Chromsorb WHP employing temperature programming allowed the internal standard to be well resolved from the drug. In addition, all four derivatives are resolvable from each other using these chromatographic conditions.

Early quantitative studies of the drug in biological samples indicated that a clean-up procedure was necessary in order to obtain as high a sensitivity as possible. Without such a step, the derivatization was hindered severely. The sample containing the drug was spiked first with the internal standard. Methanol was then added to precipitate most of the protein which, of course, was more substantial in plasma than in urine samples. After centrifugation, the methanol supernate was reduced to about 1 ml, and then applied to a strong cation exchange column of SP Sephadex. The drug and internal standard were retained by the resin during a thorough water wash. Both compounds were then quantitatively eluted from the resin with 1% aqueous pyridine. The eluent was lyophilized and derivatized for GC analysis. The yields of this clean-up procedure were determined by comparing a weighed sample derivatized directly to a weighed sample in urine and plasma derivatized after the clean-up procedure. The yields fall in the 95 to 99% range based on three determinations for each, and very few interfering substances survived the clean-up. Because of this, we found it possible to detect INO down to 100 nanograms/ml of urine and 100 nanograms/ml of plasma.

This methodology can be used to study the pharmacokinetics of INO by analyzing samples collected from cancer patients taking part in the Phase I clinical trials. In collaboration with the Southwest Oncology Group at the University of Kansas Medical Center, we obtained frozen urine and plasma samples from several cancer patients receiving the drug. Aliquots of patient urine or plasma were carried through the clean-up procedure and derivatized using the pyrrole reaction conditions. The cumulative percent recovery of the drug in the urine of one patient showed that as much as 98% of the drug was eliminated in the first 48 hours after administration. The half-life of the drug is around 3-4 hours. Plasma levels of the drug from another patient confirmed its relatively short stay in the body. A semi-logarithmic plot of mg of drug/ml of plasma as a function of time after administration was biphasic in nature showing a sharp decrease in the first phase ending after about 4 hours.

In summary, many times the development of a drug is hindered by the lack of an analytical method capable of determining quantities of the drug in biological samples with accuracy, sensitivity and selectivity. This partial purification allows one to prepare biological samples for the direct analysis of INO by GC or GC/MS after trimethylsilylation. HNO has properties very similar to INO and, therefore, can be incorporated as an internal standard to reduce the variabilities that arise with such quantitative measurements. We have demonstrated with patient samples that this approach can be applied to the analysis of samples of clinical importance. Finally, these methods should be directly applicable to further pharmacological investigations into the mechanism of action of the drug.

Acknowledgment

Research supported by the National Cancer Institute under Contract No. NO1-CO-75380 with Litton Bionetics, Inc.

Reference

1. J.V. Evans, A. Peng and C.J. Nielsen, Biomedical Mass Spectrometry, 6(1), 38 (1979).

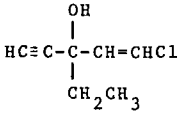
IDENTIFICATION OF RAT AND HUMAN URINARY METABOLITES OF PLACIDYL® (ETHCHLORVYNOL).

M. D. Scamuffa, S. Mueller, J. Wang, and J. Machinist.
Abbott Laboratories, North Chicago, Illinois 60064.

The rat and human urinary metabolites of Placidyl (1) were investigated by utilizing drug labeled with carbon-14 in the acetylene moiety. The label permitted GLC identification of drug-related species, and facilitated the TLC separation of the various ^{14}C-metabolites from one another and from the rest of the rat and human urine constituents.

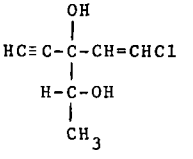
The structures of the different metabolites were determined by performing EI and CI GC/MS analyses on the metabolites, as well as; their trimethylsilyl derivatives.

The major urinary metabolite (Metabolite I) of both the rat and the human was identified as a mixture of diastereomeric alcohols (2a and 2b). Metabolite II, also found in the urine of both species, is a minor metabolite identified as the primary alcohol (3). Metabolite III is a minor metabolite found in human urine only, and is the secondary alcohol with an altered acetylene group (4).

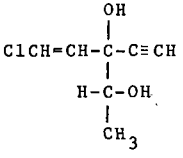


(1)

Placidyl



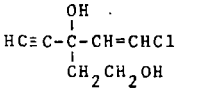
(2a)



(2b)

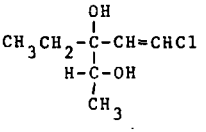
Metabolite I

Major Urinary Metabolite for Rat and Human
Diastereomeric Secondary Alcohols



Metabolite II

Minor Urinary Metabolite for Rat and Human
Primary Alcohol



(4)

Metabolite III

Minor Urinary Metabolite for Human

CHARACTERIZATION OF URINARY METABOLITES OF PGD_2 IN THE MONKEY USING GC/MS

B. J. Sweetman, C. K. Ellis and J. A. Oates
Departments of Pharmacology and Medicine
Vanderbilt University, Nashville, Tennessee 37232

There has been great interest shown in recent years in the series of highly-biologically active compounds derived from arachidonic acid. These are represented by the so-called primary prostaglandins, thromboxane, prostaglandin I_2 formerly called prostacyclin, and several hydroperoxy unsaturated fatty acids. These compounds occur in almost all tissues generally in trace amounts. They are rapidly biosynthesized and metabolized, which often makes their measurement an unreliable indicator of their biosynthesis. Hence, a great deal of effort has gone into characterizing stable metabolites so that they might be measured as an index of prostaglandin biosynthesis. Prostaglandin D_2 (PGD_2) (Figure 1) was one of the compounds whose metabolism had not been explored and has a number of interesting and unique biological properties.

2 mg of biosynthesized [$^3H_7$]-PGD_2 was infused (6.5 hr.) into the left femoral vein of a male Cynomolgus monkey. Urine collected (0°, 24 hr.), was chromatographed in sequence on XAD-2 (pH 3.2), silicic acid, RPPC (2 steps) and HPLC (μ-Porasil). Fractions were converted to the methyl ester, methoxime (MO), trimethylsilyl ether derivatives and chromatographed on a GC-radioactivity monitor system to determine which GC peaks were PGD_2-related. Low resolution E.I. mass spectra at 70 ev were obtained for all the PGD_2-related peaks using the LKB-9000 instrument--PDP-12A computer and a 1 m. 2 m.m. I.D. column of Dexsil 300. Various other derivatives such as deuterated MO and TMS derivatives, ethyl esters and ethoximes were prepared as appropriate in order to aid in the interpretation of fragmentation patterns and in the determination of the structures of individual metabolites. This lead to the identification of some 20 urinary metabolites of PGD_2. The metabolic processes postulated involved various combinations of 15-dehydrogenation, reduction of the 13:14 double bond, ω-hydroxylation ω-oxidation and one or more stages of β-oxidation on both chains. The interesting finding was that about half of the metabolites retained the PGD ring, but the other half contained a PGF ring (dihydroxy-cyclopentane), which implies the action of a keto-reductase enzyme as a major mechanism of metabolism. It is not clear yet whether the parent PGD_2 or some of the early metabolites or both serve as substrates for the keto-reductase, or whether this is a different enzyme (9-keto reductase) to the one known to convert PGE_2 to $PGF_{2\alpha}$ in some circumstances. The ratios of actual amounts of PGF-ring metabolites found are very different to the ratios found in studies of the metabolism of $PGF_{2\alpha}$. For example, the major urinary metabolite of PGD_2 is 2,3-dinor-$PGF_{2\alpha}$ representing about 9% of the radioactivity in the urine. Dinor-$PGF_{2\alpha}$ has not been described as a metabolite of $PGF_{2\alpha}$. Conversely, the major urinary metabolite of $PGF_{2\alpha}$ is a minor metabolite of PGD_2 (<2%). These metabolic differences may be related to differences in substrate specificity and enzyme location. It is apparent that previous investigations assessing biosynthesis of $PGF_{2\alpha}$ using quantitation of PGF-ring metabolites should be re-evaluated, as should studies of biological responses to PGD_2 as $PGF_{2\alpha}$ itself is a metabolite of PGD_2.

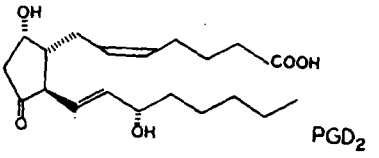
During the course of this investigation, several interesting fragmentation mechanisms were defined. It was observed that all the metabolites having the 11,15 di-MO groups showed an ion at M-63 corresponding to combined expected loss of MeOH and $^{\cdot}$OMe. However, there was also an ion at M-61 in all of these spectra. Examination of the spectra of the corresponding di-d_3-MO and ethoxime derivatives showed that the formation of the M-61 ion involved loss of $^{\cdot}OMe+CH_2O$ as shown in Figure 2. The sequence in Figure 2 was supported for several metabolites by observation of the appropriate "metastable peak." A similar fragmentation mechanism occurs in some PGI_2 metabolite derivatives containing the 6:15 di-MO groups, but not to any significant extent in metabolite derivatives of PGE_2 containing the 9:15 di-MO groups. This mechanism obviously requires the spatial proximity of the two MO groups and so the mass spectra of a number of model di-MO's were examined. The only di-MO that we found which lost the elements of formaldehyde (M-30) as a major mode of fragmentation was the dimethoxime of cis-bicyclo [3.3.0] octane-3:7-dione. This mechanism seems possible for di-MO's but a similar mechanism might apply for one MO and a second close hydrogen-accepting group.

Another ion which was of diagnostic value, occurring in every metabolite retaining the PGD_2 ring and having a reduced 13:14 double bond was at m/z 200. A suggested mechanism for its formation is shown in Figure 3.

A detailed report of this work will appear in the Journal of Biological Chemistry.

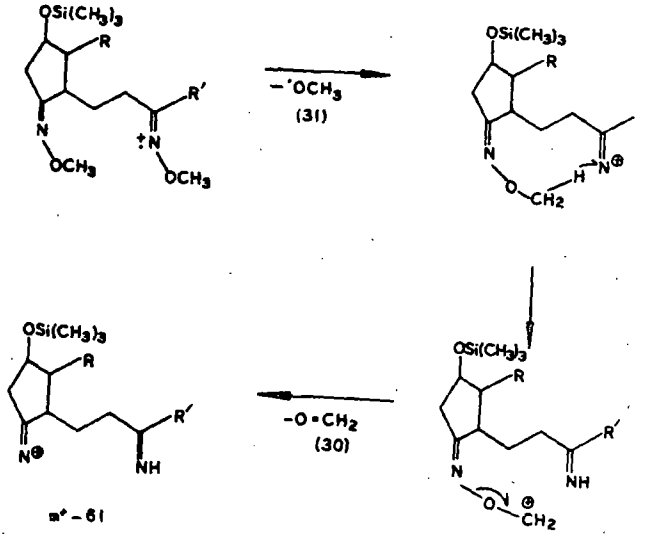
The valuable suggestions of Drs. A. R. Brash, D. F. Taber and J. T. Watson are gratefully acknowledged. This work was supported by NIH GM 15431 and NIH Training Grant GM 00058. J. A. Oates is the Joe and Morris Werthan Professor of Investigative Medicine.

1

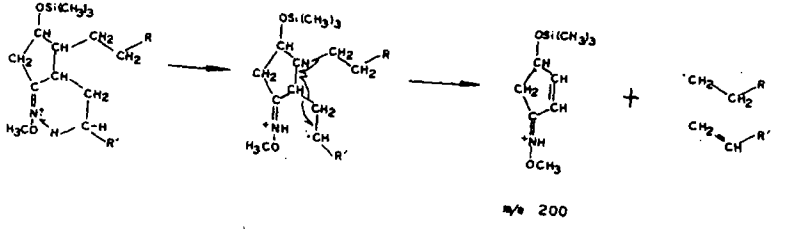


PGD_2

2



3



m/e 200

5-Methoxytryptamine in Rat Hypothalamus and Human CSF A Fact or Artifact?

N. Narasimhachari
Department of Psychiatry, Medical College of Virginia
Richmond, Virginia 23298

The identification and quantitation of 5-methoxytryptamine (5-MT) in the hypothalamus of the rat was reported by Green et al. [1], and a possible role for this compound as a neurotransmitter has been suggested by Koslow [2].

Banerjee and Synder postulated the formation of 5-MT from serotonin (5-HT) by an enzyme capable of O-methylating serotonin with methyltetrahydrofolate (MTHF) as the methyl donor [3]. Subsequently we reported the absence of O-methylation with MTHF-dependent N-methyltransferase [4]. This finding was later confirmed by other investigators. The only proven O-methylation of indoleamines is that by acetylserotonin methyltransferase (E.C. 2.1.1.4), which methylates N-acetylserotonin to melatonin. In view of the significant biological role for this new neurotransmitter, we have reinvestigated the identification of 5-MT in the rat hypothalamus using thin-layer chromatography (TLC), microspectrofluorometry, gas chromatographic-mass spectrometry and field ionization mass spectrometry.

Experimental

Twenty adult male Sprague-Dawley rats were divided into two groups of 10. The animals in one group were injected intraperitoneally with 1 mg of tranylcypromine (parnate) daily for 3 days and the control group was injected with saline. One hour after the third injection the rats were killed by decapitation; the brain was quickly removed and the hypothalamus separated from the brain and immediately prepared for analysis.

The hypothalami from three brains (0.325 g) were homogenized with 2 ml of 1 N ethanolic HCl and centrifuged. The supernatant was drawn off and the residue was washed with 0.5 ml of the same reagent. The combined washings and supernatant were evaporated to dryness under reduced pressure. Four drops of ammonium hydroxide were added to bring the pH to 10 and the residue was reconstituted in 5 ml of ethyl acetate which was removed by evaporation. The extract thus obtained was used for TLC and GC/MS identification of 5-MeO-tryptamine.

TLC and Spectrofluorometry: Two dimensional thin layer chromatography and o-phthalaldehyde spray and modified o-phthalaldehyde method were used for the qualitative identification and quantitative determination of 5-methoxytryptamine.

GC/MS: The isothiocyanate (NCS) derivative and N_1-TMS derivative were used for quantitation by GC-MS-SIM, monitoring m/e 160 and 232 respectively.

Field Ionization Mass Spectrometry: The fluorescamine derivative was prepared from the extract and the $(M-18)^+$ ion at m/e 450 monitored by field ionization mass spectrometry.

Results

In all experiments in the several batches of rats treated with saline or tranylcypromine no 5-MT could be detected. At the same time 10 ng of 5-MT added to the homogenate could be identified by all the methods.

In view of the discrepancy between our results and those of Green et al., we repeated their procedure using pentafluoropropionyl (PFP) derivatives and for this purpose prepared the PFP and trifluoroacetyl (TFA) derivatives of reference standards of melatonin, 5-methoxytryptamine, serotonin and N-acetyl serotonin. In our experiments on acylation of melatonin using pentafluoropropionic anhydride we found multiple products by GC/MS (Fig. 1). Of the three major peaks the first one was identical with 5-methoxytryptamine-PFP derivative (mass spectrum shown in Fig. 2). The characteristic fragment ions m/e 306 and 319 are of the same relative intensity as standard 5-MT-PFP. Similar results were obtained with the TFA derivative. Selected ion recording of ions m/e 256, 269 and 310 of the TFA derivative of melatonin is shown in Fig. 3. Identical results were obtained in acylation of N-acetyl serotonin and N-acetyl-N-methyl tryptamine using trifluoroacetic or pentafluoropropionic anhydrides. The corresponding fluoroacyl derivative of the parent amine, serotonin, and N-methyl tryptamine were formed as major by-products. The identity of these by-products was confirmed by comparison of GC retention times and mass spectra of reference standards. Thus transacylation of N-acetyl tryptamines by fluoroacylation seems to be a general reaction. Such a transacylation was also reported by Blau et al. with butyloxy 5-methoxytryptamine [5]. These results suggest that under the conditions of derivatization procedure used by Green et al., 5-methoxytryptamine could be formed as

an artifact from melatonin, which was shown to be present in rat hypothalamus. The methods we used do not cause any artifact from melatonin and therefore our negative results would emphasize the need for a more unambiguous method of confirming the presence of this postulated new neurotransmitter.

References

[1] Green, A.R., Koslow, S.H. and Costa, E., Brain Res., 51, 371 (1973). [2] Koslow, S.H. In E. Costa, G.L. Gess and M. Sandler (eds.), Advances in Biochemical Psychopharmacology, vol. 11, Raven Press: New York, 1974, pp. 95-100. [3] Banerjee, S.P. and Snyder, S.H., Science, 182, 74 (1973). [4] Lin, R.-L. and Narasimhachari, N., Res. Commun. Chem. Pathol. Pharmacol., 8, 535 (1974). [5] Blau, K., King, G.S. and Sandler, M., Biomed. Mass Spec. 4, 232 (1977).

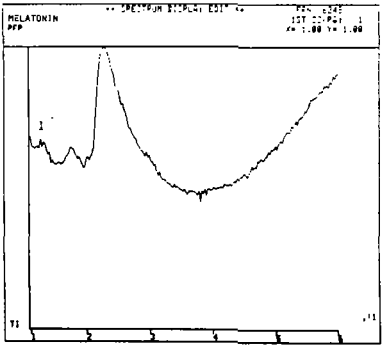


Fig. 1

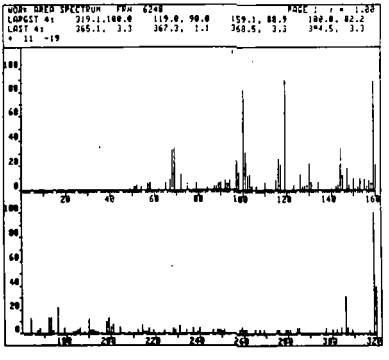


Fig. 2

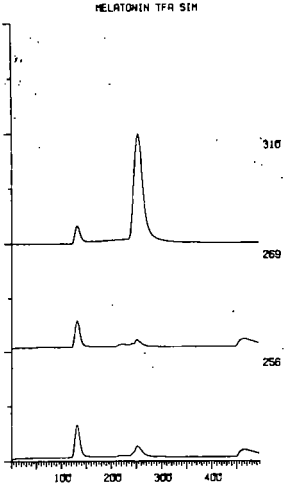


Fig. 3

Mass Spectrometric Analysis of Deuterium Triple-Labeled Blood Lipids[1]

William K. Rohwedder and Edward A. Emken
Northern Regional Research Center, Agricultural Research, Science and Education Administration, U.S. Department of Agriculture,[2] Peoria, Illinois 61604

Introduction

Hydrogenated soybean oil constitutes about 44% of the total visible fat eaten in the United States. During hydrogenation cis-trans and double bond positional isomerization occurs, scattering the unsaturation up and down the fatty acid carbon chain. The work reported here is the analysis part of an experiment to determine the distribution of these fatty acids in human blood lipids (1-3). In the metabolism experiment, mixtures of fatty acids labeled with 2, 4, and 6 deuterium atoms were fed as triglycerides to human subjects. Blood was drawn at 10 intervals, separated into about 30 different blood lipid fractions, converted to methyl esters, and analyzed by selected ion monitoring GC-MS.

This experimental approach is different from most in that the internal standard, deuterated oleic acid, is fed to the subject along with the labeled experimental material. The purpose of this paper was to determine the relative precision of dual and triple label measurements using different combinations of mass peaks.

Experimental

The materials used in this experiment were methyl oleate, methyl oleate-d_2 (methyl cis-9-octadecenoate-9,10-d_2), methyl elaidate-d_4 (methyl trans-9-octadecenoate-13,13,14,14-d_4), and methyl oleate-d_6 (methyl cis-9-octadecenoate-8,8,13,13,14,14-d_6). The dual-label test material was prepared by mixing equal weights of methyl oleate-d_2 and methyl elaidate-d_4, and the triple-label material used equal weights of methyl oleate-d_2, methyl oleate-d_4, and methyl oleate-d_6. These samples were diluted with unlabeled methyl oleate to form test samples containing 50%, 10%, and 2% label where the term label refers to the sum of deuterium labeled compounds in the samples. These samples were diluted with isooctane so that 10 µl injected put 5 µg of the total methyl esters into the GS-MS.

The mass spectrometer used was a Nuclide 12-90-DF operated in a low resolution mode connected to a Modcomp II computer through a PDP-8 computer. The GC was a Packard model 7400 equipped with 4 ft x 4 mm glass columns packed with Apiezon M on 80/100 Chromasorb W at 210°C. The mass spectrometer computer system was set up to do SIM on four different sets of peaks, 264-269; 264-271; 296-301; and 296, 298, and 300. The three samples and four different SIM combinations were given numbers 1 to 12 and run in the order of a table of random permutations of 12.

Results and Discussion

The results are given in Table I. The means of the percent value ($\bar{X}$) deviate from the weighed values 52.7 vs. 50%, 26.2 vs. 25%, and 21.1 vs. 25% because the methyl elaidate has slightly less of its total ionization in the mass regions measured than methyl oleate. The data appear to be self consistent in that the means all fall within three standard deviations of their expected values. The first three rows tested the fragment ion region masses 264 to 269 used in the early metabolism work (1,4). This region consists of the rearrangement ion M-CH_3OH and the cleavage ion M-CH_3O, which together constitute 5% of the total ionization. Normally isotope work is done in the molecular ion region if possible, which is masses 296 to 301 in this case. The data in rows 4, 5, and 6 represent only 1% of the total ionization and, as can be seen from the standard deviations, the results are poorer than the dual-label 6 fragment region. The dual-label samples consist of three compounds and it should be possible to determine three components by measuring only three peaks. As stated in our dual-label papers (4), we have chosen to use twice the minimum numbers of peaks so that our least squares computer program can provide an error

---

[1] Presented at American Society for Mass Spectrometry, Seattle, Washington, June 3-8, 1979.

[2] The mention of firm names or trade products does not imply that they are endorsed or recommended by the U.S. Department of Agriculture over other firms or similar products not mentioned.

sum which is an independent evaluation of the quality of the data. With the dual label in the fragment ion region, there was relatively little loss of sensitivity because the second peak ($M-CH_3O$) was 64% of the most intense peak. In the molecular ion region, the carbon 13 peak is only 21% of the most intense peak and when measuring 6 peaks, the data acquisition system will spend half of its time measuring these relatively small peaks. Data based on the three molecular ion peaks 296, 298, and 300 can be compared with the six molecular ion peaks, and it can be seen that the standard deviations are considerably smaller for the 3 peaks as compared to the 6 peaks. The triple-label 8 fragment ion set was run to see if the increased number of compounds and mass peaks observed would cause a noticeable reduction in precision. It can be seen from Table I that the standard deviations for the dual label-6 fragment measurements are approximately the same as the triple label-8 fragment measurements.

The technique has been used in a triple-labeled study to follow the incorporation of cis-9-octadecenoic-d_6 acid, cis-12-octadecenoic-d_2 acid, and trans-12-octadecenoic-d_4 acid into human blood lipids with excellent results.

Acknowledgments

The authors wish to acknowledge the contributions of Wayne L. Everhart, Darhal J. Wolf, and Mike Wilhelm.

References

1. E. A. Emken, W. K. Rohwedder, H. J. Dutton, R. Dougherty, J. M. Iacono, and J. Mackin, Lipids 11, 135-142 (1976).

2. E. A. Emken, W. K. Rohwedder, H. J. Dutton, W. J. DeJarlais, R. O. Adlof, J. F. Mackin, R. M. Dougherty, and J. M. Iacono, Metabolism 28, 575 (1979).

3. E. A. Emken, W. K. Rohwedder, H. J. Dutton, W. J. DeJarlais, R. O. Adlof, J. F. Mackin, R. M. Dougherty, and J. M. Iacono, Lipids 14, in press (1979).

4. W. K. Rohwedder, W. F. Kwolek, D. J. Wolf, and W. L. Everhart, Biomed. Mass Spectrom. 6, 67-71 (1979).

Table I

COMPARISON OF METHODS
(5 µg of each sample injected 6 times)

	Label		MeOl		MeOl d_2		MeEl d_4		MeOl d_6	
	(%)	Method	$\bar{X}$	S	$\bar{X}$	S	$\bar{X}$	S	$\bar{X}$	S
1. Dual	50	6	52.7	0.19	26.2	0.12	21.1	0.13		
2. 5% Tol.	10	Frag.	89.6	0.33	5.8	0.28	4.6	0.11		
3. Ioniz.	2	Ions	97.6	0.25	1.4	0.20	1.1	0.08		
4. Dual	50	6	50.8	1.83	24.8	1.57	24.4	0.98		
5. 1% Tol.	10	Mol.	88.9	1.14	4.8	0.95	6.2	0.29		
6. Ioniz.	2	Ions	97.8	0.96	0.48	0.61	1.85	0.50		
7. Dual	50	3	53.4	1.16	21.8	0.48	24.9	0.68		
8. 1% Tol.	10	Mol.	90.2	0.56	4.5	0.42	5.3	0.24		
9. Ioniz.	2	Ions	98.2	0.65	0.64	0.41	1.2	0.27		
10. Triple	50	8	52.2	0.27	16.7	0.15	14.9	0.07	16.2	0.13
11. 5% Tol.	10	Frag.	90.4	0.45	3.6	0.24	2.9	0.06	3.1	0.11
12. Ioniz.	2	Ions	97.5	0.43	1.1	0.26	0.58	0.08	0.7	0.16

Dual label = 50% MeOl d_2 + 50% MeEl d_4.
Triple label = 33.3% MeOl d_2 + 33.3% MeEl d_4 + 33.3 MeOl d_6.

Effects of Sample Storage Time on Precision and Accuracy in Measuring Picomole Quantities of Monoamine Metabolites in Plasma by Selected Ion Monitoring

Susan E. Hattox, D. Harold Landis and James W. Maas

Departments of Psychiatry and Pharmacology
Yale University School of Medicine
New Haven, Connecticut 06510

Increased attention has recently been focused on the precision and accuracy of measurement of trace quantities by selected ion monitoring. Little is known, however, about the effects of sample storage on these parameters. Biological samples are particularly prone to present problems after storage due to degradation of the various components in the highly complex mixtures; yet clinical samples often must be stored since their collection is dependent upon patient population availability. For these reasons, we have undertaken a study designed to determine: (1) the length of time samples may be stored at -70°C before significant changes in precision occur; and (2) whether it is necessary to add internal standards to the samples before storage to maintain accuracy of measurement.

The study was carried out using previously developed methods for the simultaneous measurement of three neurotransmitter metabolites, 3,4-dihydroxyphenylacetic acid (DOPAC), 3-methoxy-4-hydroxyphenylacetic acid (HVA) and 5-hydroxyindoleacetic acid (5HIAA), in plasma (1). A pool of plasma was acidified (pH 2.0) with 0.5N HCl and sodium metabisulfite was added to stabilize the easily oxidized compounds. The plasma was divided into two pools, one to be stored with deuterated internal standards added and one without. The latter pool was carefully divided into 6 aliquots, each of which, after storage at -70°C for a given period of time, would be thawed, have the deuterated internal standards added, and be split into five samples for analysis. Deuterated standards were added to the other pool of plasma and individual samples, five for each time point, were stored at -70°C. A series of calibration curves, evaporated to dryness, were also stored and used to calculate the results for these latter samples. HVA, DOPAC and 5HIAA were measured as their pentapropionyl derivatives by selected ion monitoring as previously described (1). Each sample was injected 3-4 times in random order to allow determination of the instrumental variance and sample variance.

It was found that for samples analyzed without freezing there was no significant difference between instrumental and sample variance. Since degradation leading to late-eluting interfering peaks will result in increased instrumental variance, the variance for the total procedure, including both instrumental and sample components, was used as a measure of precision for samples which had been stored. The results for samples stored up to 28 days can be seen in Table 1A. Within one week a significant increase in variance occurred in the measurement of DOPAC in those samples to which deuterated standards had been added. No significant reduction in precision was seen for the other compounds in plasma stored up to 28 days. Loss of accuracy in plasma stored without internal standard was calculated by comparing ng/ml found in samples stored without internal standard as a percentage of ng/ml in samples stored with internal standard. Table 1B shows the decreasing accuracy of measurement when samples are stored without deuterated standards. It can be seen here that DOPAC was being rapidly lost. It is not known whether the increased variance in DOPAC measurement in samples stored with deuterated standards is due to degradation of DOPAC-d_5 of one of the other two standards. It may, therefore, be possible to store samples for DOPAC analysis if deuterated DOPAC is the only internal standard added or if another compound is used as internal standard. However, unless that is proven, the evidence suggests that plasma DOPAC samples are stable less than one week while HVA and 5HIAA are stable for at least one month. Although data are presented here for samples stored only up to 28 days at -70°C, the study will be continued for a total of six months.

In summary, the stabilities during storage of plasma metabolites such as HVA, DOPAC and 5HIAA were found to differ radically from one another, both in rate of loss of precision and rate of loss of accuracy. Such findings suggest that an experimental design as described above allows careful examination of any changes in precision and accuracy in selected ion monitoring, giving essential information concerning biological sample treatment prior to analysis.

TABLE 1

A. Variance

Storage time (days)	HVA t_o	HVA t_a	DOPAC t_o	DOPAC t_a	5HIAA t_o	5HIAA t_a
0	.04462		.19362		.125897	
7	.02697	.01695	.59552*	.30067	.02352	.03314
14	.02682	.03642	.36029	.02367	.11945	.06618
28	.02971	.03429	.54400*	.15638	.10924	.06552

*denotes significant difference from time 0, $p < .05$.
$t_o \equiv$ deuterated standard added before storage.
$t_a \equiv$ deuterated standard added after storage.

B. Percentage of metabolite remaining

0	100	100	100
7	96	61	106
14	95	42	100
28	94	47	90

Reference

(1) Hattox, S. E., Downey, A. L., Roth, R. H., and Maas, J. W., presented at the Twenty-sixth Annual Conference on Mass Spectrometry and Allied Topics, St. Louis, May, 1978.

This work was supported by NIMH Grant #25642.

CANDIDATE DEFINITIVE METHODS FOR THE DETERMINATION OF URIC ACID AND GLUCOSE IN HUMAN SERUM BY ISOTOPE DILUTION MASS SPECTROMETRY

A. Cohen, H. Hertz, R. Schaffer, L. Sniegoski, M. Welch, and E. White V

National Bureau of Standards
Washington, D. C. 20234

Introduction

Accurate determinations of serum glucose and uric acid levels are subjects of much concern in clinical chemistry. Two independent isotope dilution mass spectrometric methods for serum glucose, which warrant consideration as definitive methods, have been used in our laboratory. In addition, an IDMS method for serum uric acid, utilizing separate analyses of two tetraethyluric acid isomers, shows promise as a definitive method.

Methods

Calibration Standards. For each glucose method, a series of calibration standards was prepared by mixing weighed amounts of uniformly ^{13}C labeled glucose and NBS Standard Reference Material (SRM) glucose such that the measured ratios between labeled and unlabeled species were in the range of 0.85 to 1.37. For uric acid, 1,3-$^{15}N_2$-uric acid was added to NBS SRM uric acid in ratios ranging from 7.3:1 to 9.3:1. The high proportion of labeled material was used to facilitate the isolation steps. The standard mixtures were derivatized in the same manner as the serum samples.

Sample Preparation. Glucose DAG - Our first method (1) for glucose involves preparation of 1,2:5,6 di-O-isopropylidene-D-glucofuranose (DAG). After addition of the labeled D-glucose and equilibration, the serum is freeze-dried. To the dried residue is added acetone containing a small amount of sulfuric acid and excess dehydrating agents. The solution is shaken for 48 hours, followed by neutralization with anhydrous sodium carbonate. Sublimation and three thin-layer chromatography steps separate the DAG from the matrix, including other monosaccharide derivatives.

Glucose BBA - The second glucose method involves preparation of D-glucofuranose cyclic 1,2:3,5-bis(butylboronate) 6-acetate (glucose BBA) (2). After addition of the labeled D-glucose and equilibration, the sample is treated with ethanol to precipitate protein. The supernatant is passed over an ion-exchange resin and freeze-dried. A solution of butylboronic acid in pyridine is added, and the mixture is heated at 95° for 30 minutes, followed by addition of acetic anhydride to complete the derivatization.

Uric Acid - After addition of the labeled uric acid and equilibration, the serum is freeze-dried. Tetraethyluric acids are prepared by ethylation with triethylanilinium carbonate. The products are sublimed and the two most abundant tetraethyluric acid isomers (designated A and C) are isolated by thin-layer chromatography.

Sample Measurement. Introduction of samples into the mass spectrometer was via a Varian Aerograph model 2700 gas chromatograph. For DAG and tetraethyluric acid, a 1.8 m x 3 mm (OD) ss column with 3% OV-17 on 100-120 mesh Gas Chrom Q was employed. The column was operated isothermally at 170° for DAG, 192° for the tetraethyluric acid A isomer, and 205°C for the C isomer. Retention times were 5 min for DAG and 6.5 min for each of the tetraethyluric acid isomers. A 100 m glass SE-30 SCOT column was employed for the BBA samples. A capillary column is required to obtain baseline separation of glucose BBA from other monosaccharide BBA derivatives, which are not separated in the sample preparation procedure. At 197°, glucose BBA has a retention time of 45 min.

The gas chromatograph was interfaced to the mass spectrometer via a Biemann-Watson single-stage separator. For capillary work, make-up gas was added at the end of the GC column.

The mass spectrometer was a Varian MAT CH7A, operated in the EI mode at 70 eV with magnetic switching between the ions of interest. Other measurement procedures followed have been previously reported (3). For DAG, $(M-15)^+$ ions at m/z 245 (unlabeled) and at m/z 250 (labeled) were monitored. For glucose BBA, the $(M-57)^+$ ions, which are highly specific for glucose BBA relative to other monosaccharide BBA derivatives (4), were monitored at m/z 297 (unlabeled) and m/z 302 (labeled). For both isomers of tetraethyluric acid, the M^+ ions at m/z 280 (unlabeled) and m/z 282 (labeled) were monitored.

To improve precision, samples and calibration standards are run under identical conditions. Immediately preceding and following analysis of each

sample, standards which closely bracket the sample in ratio are run. The quantity of analyte in the serum sample is then calculated by linear interpolation. The analysis is repeated on a second day, with the order of the bracketing standards reversed. The mean of the two days' results is taken as the reported value.

Results and Discussion

Glucose. Table I shows the results of a comparative study of the two glucose methods on identical samples processed in parallel. Three sets of samples were prepared at one week intervals, with a set consisting of two samples each from the three serum pools for each method. The precision of each method was excellent for all three pools, but there is a systematic difference between the two methods, with the largest relative difference occuring for the pool with the lowest glucose concentration. Possible sources for these differences are under investigation at this time.

Table I
Glucose-Comparative Study

mg Glucose/g Serum

	DAG Results		BBA Results		DAG-BBA
Pool	Mean	R.S.D. (%)	Mean	R.S.D. (%)	Difference (%)
A	0.68427	0.29	0.67793	0.19	+0.93
B	1.80257	0.15	1.79028	0.17	+0.68
C	2.91919	0.24	2.90116	0.18	+0.62

Uric Acid. Table II shows the results of analyses of six serum pools for uric acid. Pools 1-5 were run as a group with five separate samples analyzed from each pool. The results of seven separate samples prepared at one time from the remaining pool (W), are also shown. For every serum pool, the A-C difference was less than 1%, with the agreement for pool W markedly better than the rest. Overall, the precision was satisfactory, but not as good as with glucose. This poorer precision is not due to imprecision in the mass spectrometric measurements, since agreement between day 1 and day 2 values were generally as good as was found for glucose by either method. Much of the imprecision and isomer bias effects observed may relate to subtle differences in sample preparation from one set to another, and are being investigated.

Table II
Uric Acid-Composite Results

mg Uric Acid/g Serum

	A Isomer		C Isomer		A-C
Pool	Mean	R.S.D. (%)	Mean	R.S.D. (%)	Difference (%)
1	.041388	1.44	.041229	1.04	+0.22
2	.099320	0.92	.098672	0.42	+0.65
3	.023409	1.24	.023215	0.94	+0.83
4	.035453	1.04	.035185	0.44	+0.76
5	.055210	0.52	.054985	0.40	+0.41
W	.044873	0.42	.044911	0.45	-0.08

References

(1) R. Schaffer, Pure and Appl. Chem., 45, 75 (1976).
(2) D. Bier, W. Sherman, W. Holland, and D. Kipnis, Proc. Int. Conf. Stable Isot. Chem., Biol., Med., 1st, 397 (1973).
(3) A. Cohen, H. Hertz, R. Schaffer, L. Sniegoski, T. Sun, and E. White V, presented at the 26th Ann. Conf. on Mass Spectrometry and Allied Topics, St. Louis, Mo., May 28-June 2, 1978.
(4) J. Wiecko and W. Sherman, J. Am. Chem. Soc., 98, 7831 (1976).

Identification of any commercial product does not imply recommendation or endorsement by the National Bureau of Standards, nor does it imply that the material or equipment identified is necessarily the best available for the purpose.

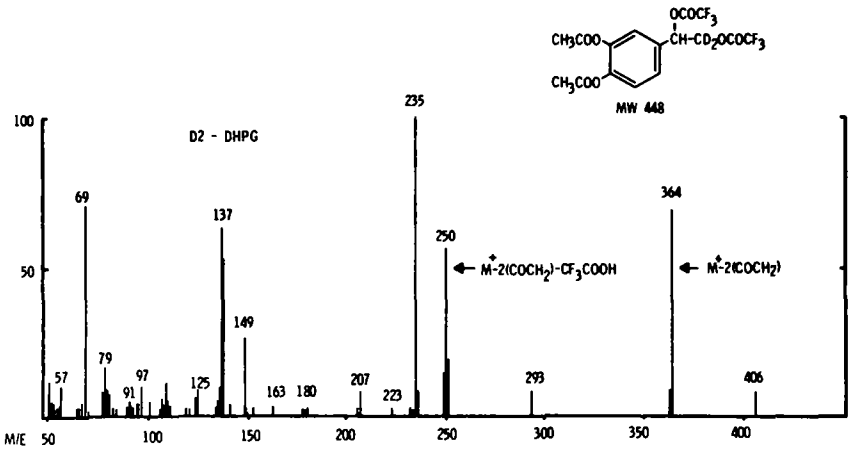
SIMULTANEOUS GC-MS ASSAY OF RAT BRAIN 3,4-DIHYDROXYPHENYLETHYLENE GLYCOL (DHPG) AND 3-METHOXY-4-HYDROXYPHENYLETHYLENE GLYCOL (MHPG). Damodar D. Godse and Jerry J. Warsh, Clarke Institute of Psychiatry, Section on Biochemical Psychiatry, 250 College Street, Toronto M5T 1R8, Ontario, Canada.

In the central nervous system of the rat, the catecholamine neurotransmitter norepinephrine is preferentially metabolized to the glycol end products 3,4-dihydroxyphenylethylene glycol (DHPG) and 3-methoxy-4-hydroxyphenylethylene glycol (MHPG). Several GC-MS methods have been described for the quantitation of MHPG in rat brain. However, DHPG has not been previously determined using specific GC-MS techniques. We describe here a sensitive and specific GC-MS assay that permits simultaneous quantitation of these two glycols in whole rat brain and individual brain regions.

Methods

Formic acid homogenates of whole rat brain or brain areas were subjected to enzymatic hydrolysis with aryl sulfatase (16 h., 37°C, pH 5.9). Under basic conditions (pH 10-10.5), DHPG and MHPG were simultaneously acetylated and extracted into ethyl acetate containing acetic anhydride (0.5%). The acetylated glycol products were acylated with trifluoroacetic anhydride and quantitated by multiple ion mass fragmentography on a Finnigan 3200 GC-MS system. Separation of the acetyl-di-trifluoroacyl derivatives of DHPG and MHPG was carried out on 1.5 m x 2 mm i.d. glass columns packed with 3.8% SE-30 on diatoport S, 80-100 mesh size, at 170° isothermal. Instrumental parameters were: injector temperature 230°, separator temperature 230°, ion source temperature 70°, electron energy 65 eV, emission current 1mA and ionizing mode electron impact. At 170° the retention times for the acylated derivatives of MHPG and DHPG were 100 and 140 second, respectively.

For internal standards D_2-DHPG was synthesized by reduction of 3,4-dihydroxymandelic acid with D_3-borane methyl sulfide, while D_3-MHPG was synthesized by the method of Karoum et al. (J. of Neurochem. 25, 653, 1975). D_2-DHPG yields of 8-15% and isotopic enrichments greater than 99 mol % were obtained. The mass spectrum of D_2-DHPG shows the base peak at m/e 235 and major ions at m/e 250 and 364. The M^+ was not detectable.



Mass fragmentography was performed using the positive ions at m/e 248 and 362 for DHPG, and m/e 250 and 364 for D_2-DHPG. As previously described (Takahashi et al., Clin Chim Acta 81, 183, 1977) the positive ions at m/e 249 and 376 were monitored for MHPG while for D_3-MHPG the positive ions at m/e 252 and 379 were monitored.

Results

As shown in the table below the fragmentation ratios for DHPG and MHPG in tissues were essentially identical to those obtained from reference standards. Linear calibration curves were obtained from 1.0 to 100 ng for both DHPG and MHPG and the procedure permits quantitation of at least 1 ng of each glycol in a sample. Recoveries of standards added to tissues were 100 ± 1.35% ($\bar{X}$ ± S.E.M., n=6) for MHPG and 102 ± 1.67% (n=6) for DHPG. The within assay coefficient of variation (2 C.V.) was 4.4% for MHPG and 2.4% for DHPG at a concentration of 20 ng/sample.

Fragment ion ratio		Standards (n=5)	Brain areas	t-test
DHPG	m/e 362 / m/e 248	0.97 ± 0.02*	1.03 ± 0.03	N.S.
DHPG-d_2	m/e 364 / m/e 250	1.08 ± 0.01	1.06 ± 0.03	N.S.
MHPG	m/e 376 / m/e 249	0.462 ± 0.006	0.476 ± 0.009	N.S.
MHPG-d_3	m/e 379 / m/e 252	0.506 ± 0.002	0.516 ± 0.003	p = 0.04

* Data are expressed as the mean ± S.E.M. for 5 or 7 determinations. N.S. indicates no statistically significant difference between the fragment ratio of standards and samples.

Whole rat brain DHPG (115 ± 2.6 ng/g) was of the same order of magnitude as brain MHPG (87.0 ± 1.8 ng/g). Unconjugated DHPG and MHPG accounted for 12% and 11%, respectively, of total brain DHPG and MHPG concentrations. Regional brain total DHPG concentrations varied from 963 ± 37 ng/g (n=6) in hypothalamus and 450 ± 70 ng/g (n=6) in septum to 76 ± 10 ng/g (n=6) in the caudate. Total DHPG was significantly higher than MHPG in hypothalamus and septum (molar ratio of DHPG/MHPG = 6.9 ± 0.44 and 3.91 ± 0.31, respectively.

In conclusion, the present GC-MS procedure represents a simple, sensitive and specific technique for simultaneous assay of DHPG and MHPG in rat brain and brain regions.

USE OF [1-^{13}C]LEUCINE TO MEASURE HUMAN WHOLE BODY LEUCINE AND PROTEIN TURNOVER

D.E. Matthews, K.J. Motil, D.K. Rohrbaugh, J.F. Burke, V.R. Young, and D.M. Bier

Department of Medicine, Washington Univ. Sch. Med., 660 S. Euclid, St. Louis, MO 63110 and Department of Nutrition, M.I.T., Cambridge, MA 02139

Using chemical ionization SIM-GCMS and conventional isotope ratio mass spectrometry, we have redesigned and improved previous continuous [1-^{14}C]leucine infusion techniques for measuring whole body amino acid and protein metabolism. Whole body leucine turnover, oxidation, incorporation into proteins, and protein breakdown rates can be calculated from plasma leucine ^{13}C enrichment and expired breath $^{13}CO_2$ enrichment obtained during a primed, continuous 4h infusion of L-[1-^{13}C]leucine. The entire study requires less than a 10 ml blood loss. We have applied this technique to quantify various aspects of leucine metabolic adaption to dietary protein alteration in 8 adult volunteers each studied at 3 levels of protein intake: 1.5 (excess), 0.6 (sufficient), and 0.1 (deficient) g-protein $kg^{-1}d^{-1}$.

Use of Volatile Metal Chelates for Isotope Ratio Analysis of Biomedical Samples

D. L. Hachey, J. C. Blais, and P. D. Klein
Bioanalytical Center
Division of Biological and Medical Research
Argonne National Laboratory
Argonne, IL 60439

Trace elements play an important role in maintaining good nutrition in man. There are, however, areas of clinical nutrition that remain largely unexplored, due either to ethical constraints that prohibit radioisotope studies in certain patient groups, or to inadequacies of existing technology. The object of the present work is to explore the use of volatile metal chelates for isotopic tracer studies of biologically important elements using conventional GC/MS instrumentation (1). Several questions must be resolved before one proceeds to use metal stable isotopes in clinical studies. What are the best ionization and sample introduction techniques? What are the limits for accuracy and precision of the isotope ratio measurement? What are the minimum detection limits for isotope dilution studies?

Volatile metal chelates used in this study were prepared by established techniques (1). Specific compounds used included magnesium and calcium bis-(1,1,1,2,2-pentafluoro-6,6-dimethylheptane-3,5-dionate); iron, chromium, and cadmium trifluoroacetylacetonate (TFA); and copper and nickel N,N'-ethylene-bis (trifluoroacetylacetoneimine) ($en(TFA)_2$). EI/MS studies were done on a Perkin-Elmer 270 spectrometer and CI/MS studies were done on a Chemetron Medical Products BIOSPECT spectrometer. Isotope ratios were obtained using a dedicated microprocessor based data system. Samples were introduced through the GC inlet (Cr, Cu, and Ni chelates) or through the solids probe inlet (Mg, Ca, Fe, Cd chelates).

Alkaline earth chelates containing fluorinated side chains and bulky t-butyl groups were sufficiently volatile for MS studies. They are best analyzed by EI/MS, because under CI conditions ions related to the free ligand predominate in the spectra. Transition metal chelates can be analyzed by either technique, although better sensitivity is obtained for CI/MS analysis of Ni and $Cu(en(TFA)_2)$. Table 1 summarizes isotope ratio data obtained for analysis of several natural abundance isotopic standards. Precision of the isotope ratio measurements show standard deviations ranging between $\pm$ 0.03% and $\pm$ 0.72%. The higher isotope ratio values generally exhibit a higher absolute standard deviation, but the relative standard deviation is a more constant measure which is generally 0.5-1.0%. Abundances of the individual isotopes can be obtained from the raw isotope ratio data by solving a set of simultaneous linear equations containing terms for the isotopic contributions of ^{13}C, ^{2}H, ^{15}N, ^{17}O, and ^{18}O that are due to the ligand (2). As shown in Table 1, excellent agreement was obtained between the observed isotopic abundances and the established natural abundance. The absolute difference between the two values ranged between 0.04 and 0.79%. The errors are random and indicate that hydride abstraction is not significant in these studies. For the homologous series of cadmium isotopes, the random error in the natural abundance measurement and the good agreement with established values indicate that isotope fractionation within the ion source is not significant over a 10 amu mass range. Figure 1 shows a set of isotope dilution curves for chromium, nickel, and copper chelates analyzed by GC/CI/MS. These curves are linear over the range 0.1% to 20 atom % excess and exhibit a correlation better than 0.999. The data indicate that isotope dilutions as great as one part per thousand can be measured accurately.

Work supported by the U. S. Department of Energy under contract No. W-31-109-ENG-38.

References

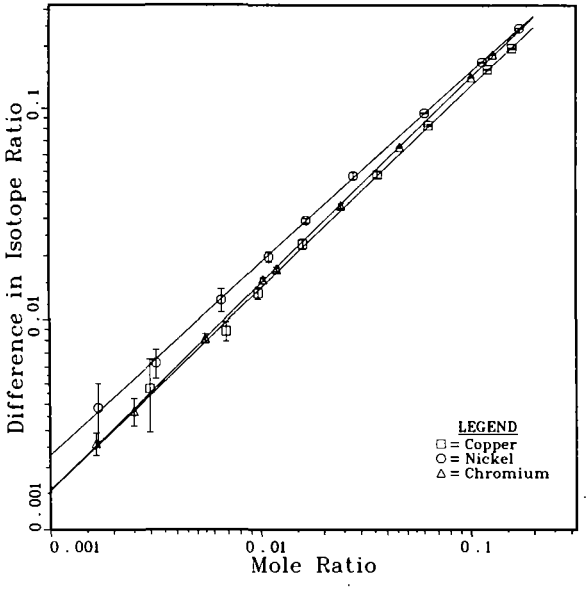
1. D. L. Hachey, J. Johnston, and P. D. Klein. Stable Isotopes: Proceedings of the Third International Conference. Editors, E. R. Klein and P. D. Klein. Academic Press, New York, 1979:157-163.
2. J. I. Brauman. Anal. Chem. 38:607, 1966.

The submitted manuscript has been authored by a contractor of the U.S. Government under contract No. W-31-109-ENG-38. Accordingly, the U.S. Government retains a nonexclusive, royalty free license to publish or reproduce the published form of this contribution, or allow others to do so, for U.S. Government purposes.

Table 1. Isotopic ratios and natural abundances measured for a series of isotopic standards.

ISOTOPE	ISOTOPE RATIO (mean ± SD)	% ABUNDANCE FOUND by MS[a]	% DIFFERENCE[b]
^{24}Mg	100.00	78.44 ± 0.10	-0.26
^{25}Mg	29.38 ± 0.12	10.92 ± 0.09	0.79
^{26}Mg	17.63 ± 0.06	10.64 ± 0.05	-0.53
^{40}Ca	100.00	96.87 ± 0.07	-0.10
^{42}Ca	3.67 ± 0.07	0.96 ± 0.10	0.32
^{44}Ca	2.40 ± 0.05	2.18 ± 0.07	0.12
^{54}Fe	6.59 ± 0.04	6.03 ± 0.04	0.21
^{56}Fe	100.00	91.43 ± 0.07	-0.23
^{57}Fe	18.98 ± 0.08	2.15 ± 0.07	-0.04
^{58}Fe	3.31 ± 0.03	0.39 ± 0.03	0.06
^{106}Cd	4.17 ± 0.13	1.27 ± 0.04	0.05
^{108}Cd	3.18 ± 0.12	0.95 ± 0.04	0.07
^{110}Cd	39.52 ± 0.21	12.02 ± 0.06	-0.37
^{111}Cd	45.71 ± 0.22	12.58 ± 0.07	-0.17
^{112}Cs	84.24 ± 0.72	24.09 ± 0.23	0.02
^{113}Cd	51.14 ± 0.57	12.65 ± 0.18	0.39
^{114}Cd	100.00	28.67 ± 0.09	-0.19
^{116}Cd	26.83 ± 0.36	7.76 ± 0.11	0.18

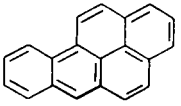
[a] Isotopic abundances were corrected for the natural abundance of ^{13}C, ^{2}H, ^{18}O present in the ligand.
[b] The difference was obtained by subtracting the established isotopic abundance from the experimentally determined value.



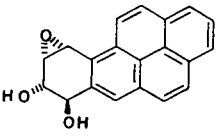
APPLICATIONS OF FD/CID MASS SPECTROMETRY TO MODIFIED NUCLEIC ACIDS

K. M. Straub and A. L. Burlingame
Biomedical Mass Spectrometry Resource, Space Sciences Laboratory,
University of California, Berkeley, CA 94720

The covalent modification of DNA by exogenous alkylating agents is believed to be a key initial event responsible for cell transformation by chemical carcinogens. Many types of chemical carcinogens require metabolic activation to a reactive electrophilic species which can then undergo covalent binding to cellular macromolecules such as DNA. Benzo(a)pyrene (I), for example, undergoes metabolism *in vivo* to the reactive species (+)-r-7,t-8-dihydroxy-t-9,10-epoxy-7,8,9,10-tetrahydrobenzo(a)pyrene (*anti*-diol epoxide, II).[1]



I



II

The modified sites on DNA are usually present at extremely low levels, typically one site per 10^4 or 10^5 base pairs. In addition to this, the modified nucleosides are characterized by high molecular weight (>500 d.), extreme polarity, and thermal lability. While derivatization has proven to be of value in the electron-impact mass spectral analysis of these structures, material losses encountered during derivatization of submicrogram quantities of a compound limit the minimum sample size with which one can reliably work, and molecular weight considerations limit practical work to modified monomers only. The latter point is important, since enzymatic hydrolysis of modified biopolymers to the monomer level is not always possible.

We have been investigating the use of field desorption mass spectrometry (FDMS) in conjunction with collision-induced dissociation (CID) techniques to provide both molecular weight and structural information on carcinogen modified nucleotides. In addition, the use of a linked scan of the electric and magnetic sector fields of the mass spectrometer (a modified Kratos/AEI MS-902) allows for the observation of collisionally-induced metastable ions. This "B/E" scan enables one to identify daughter ions M_2^+ formed from M_1^+ in the first field-free region of the mass spectrometer, as well as allowing for the direct analysis of single components within a mixture without prior chromatographic separation.[2] Our current studies are directed toward evaluating the usefulness and limitations of these techniques, when applied to the analysis of carcinogen-modified oligonucleotides.

We had previously reported on the results of an investigation by FDMS of the major products obtained in the reaction of (±) *anti*-diol epoxide with calf-thymus DNA.[3] A complete FDMS analysis of the monomeric adducts obtained in the reaction of *anti*-diol epoxide with DNA under "high" (*ca.* 200 times physiological) alkylating agent concentrations is summarized in Table 1. These results are important because they identify the nucleoside moiety present in minor products on which it had previously not been possible to obtain information by conventional electron-impact mass spectrometry. These results have enabled us to assign all of the structures present in the mixture of adducts, making possible the observation of stereoselective binding of a carcinogen to double-stranded DNA.[4]

Recent findings indicate that short range specificity for binding to DNA probably occurs, so that not all dinucleotide sequences will react with equal probability. Analysis by FD/CID mass spectrometry of oligonucleotides obtained from carcinogen-modified DNA will allow us to establish whether or not specific polynucleotide binding sites exist for a given alkylating agent, and will help to define those parameters that influence specific alkylation reactions. With these goals in mind, we have begun analyzing a series of modified dinucleotides by FDMS. Fig. 1 shows the results obtained on a dinucleotide-*anti*-diol epoxide adduct [d(ApT)-diol epoxide, as the N^6-exocyclic amino adduct of adenine] over the region m/z 500-900. Peaks marked with an asterisk (*) indicate that these fragment ions were detected as metastables in the linked scanning mode, confirming that they are derived from mass 857 rather than from thermal or surface reactions. Preliminary results on *anti*-diol epoxide-modified dinucleotides obtained by enzymatic hydrolysis of modified high molecular weight DNA

indicate a preference for pyrimidine-purine or purine-pyrimidine sequences. Such specificity has been observed for other compounds (ethidium bromide, actinomycin D) in spectroscopic investigations of their interactions with synthetic oligonucleotides.[5] We are presently evaluating the use of CID to determine whether or not structurally meaningful fragmentations can be generated from selected field desorbed ions of this type. These results will allow a study of the potential of FD/CID mass spectrometry for sequencing these modified oligonucleotides, thus identifying both the modified residue and its nearest neighbor.

This work was supported by NIH Division of Research Resources Grant RR00719.

Table 1. FD/MS on monomeric diol epoxide-DNA adducts.

Peak #	FD/MS (m/z)	Identity
1	529 + >600	deoxycytidine adduct plus modified oligonucleotide
		tetrahydroxy-tetrahydro-benzo(a)pyrene
3	529, 552	deoxycytidine adduct
4	569, 592	deoxyguanosine adduct
5	529, 552, 320	deoxycytidine adduct plus tetrahydroxy-tetrahydro-benzo(a)pyrene
6	569, 592	deoxyguanosine adduct
7	569, 592	deoxyguanosine adduct
8	553, 576	deoxyadenosine adduct
9	553, 576	deoxyadenosine adduct
10	553, 576	deoxyadenosine adduct

References

1. E. Huberman, L. Sachs, S.K. Yang, and H.V. Gelboin, Proc. Natl. Acad. Sci. USA, 73, 607 (1976).
2. A.P. Bruins, K.R. Jennings, and S. Evans, Int. J. Mass Spectrom. Ion Phys. 26, 395 (1978).
3. K. Straub, T. Meehan, H. Kambara, A.L. Burlingame, and S. Evans, presented at 26th Annual Conf. on Mass Spectrometry & Allied Topics, St. Louis, Mo., 1978, p. 499.
4. T. Meehan and K. Straub, Nature 277, 410 (1979).
5. C.G. Reinhardt and T.R. Krugh, Biochemistry 17, 4845 (1978).

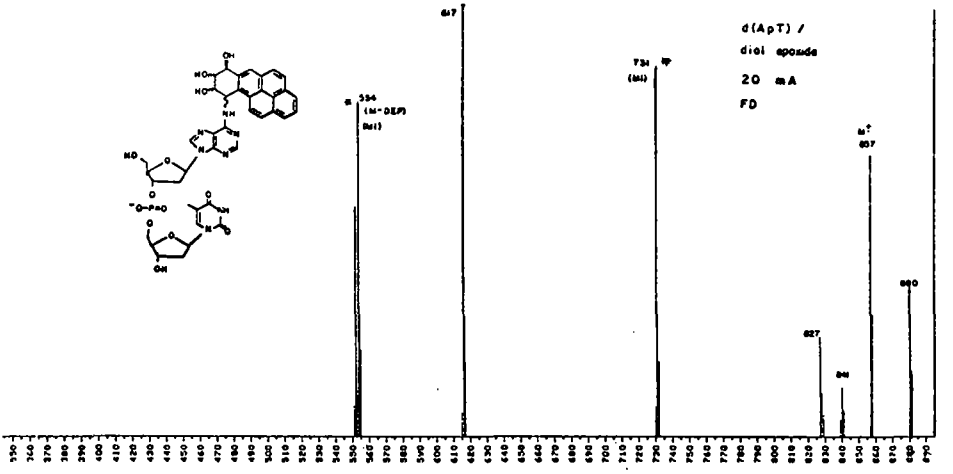


FIGURE 1

Analysis and Identification of Microparticles in the Ion Microprobe

John Gavrilovic - Walter C. McCrone Associates, Inc.

INTRODUCTION

Chemical analysis of microscopical samples has advanced tremendously in the past 20 years. Ultra micro samples, one nanogram or less, corresponding to small particles of <10 μm have been chemically characterized for a long time by various microchemical tests. However these tests are usually slow and often ambiguous and depend on the skill of the microscopist and his familiarity with a specific type of sample. The need for more efficient and reliable techniques for very small samples and microparticles was emphasized by the developments of microelectronics, miniature servo systems, and delicate inertial guidance devices in the early 1950's. On older devices such as printed circuits and larger servo systems, the presence of common airborne particles, less than 10 μm in size, had very little effect. The arrival of integrated circuits with conductive leads several microns wide and a fraction of a micron thick, and gyroscopes with tolerances of <1 μm, has dramatically changed this situation and increased our awareness of microparticles and airborne artifacts[1]. A single particle of sodium or calcium chloride which is a common artifact in cold weather may cause a breakdown of an electronic system. Similarly the uncontrolled introduction of several micron size microparticles in the fluid of a gyro can cause seizure of the rotor and eliminate a major part of the navigational system of an aircraft.

Increased levels of air pollution in certain areas also demanded full characterization and identification of airborne microparticles in order to determine and hopefully eliminate their source.

By far the most common tools for chemical characterization of microparticles are the Scanning Electron Microscope (SEM) and electron microprobe with energy dispersive x-ray systems (EDS)[2], and to a much lesser degree the Scanning Auger Microprobe (SAM). The first two instruments equipped with EDS will provide chemical analysis of a microparticle down to submicrometer size in a matter of minutes for most elements above 0.3 to 1% . Chemical analysis of microparticles for elements below 0.3 to 1% requires, however, an enormous increase in effort and counting time. The Scanning Auger Microprobe is primarily a surface analysis tool and is rarely used for chemical analysis of microparticles.

The ion microprobe analyzer offers in such cases several significant advantages. It will detect all elements, including hydrogen, with the detection limits range being from 0.1 to 0.001% (in a reasonable analysis time). It will also measure isotope ratios and detect thin films on the particles[3]. Trace element capability becomes a very significant factor in determination of the exact nature and origin of certain microparticles and pollutants.

SAMPLE PREPARATION AND MOUNTING

Perhaps the most important step in identification of microparticles in an ion microprobe is their preparation for analysis and mounting on a substrate.

Small particles are invariably examined in the light microscope prior to mounting and analysis. Optical and morphological properties are noted since identification of microparticles is a complex process that relies on a number of optical properties besides elemental composition.

Microparticles may be analyzed "in situ" but in virtually all cases it is advantageous to physically remove them and place first on a glass slide for microscopical examination and then on special substrates for analysis. A substrate for ion microprobe analysis of microparticles has to satisfy the following conditions:

- should be flat with a mirror-like surface
- has to be chemically pure and not very reactive
- free of inclusions
- electrically conductive
- should have relatively low secondary ion yield
- should have simple mass spectrum, i.e., few isotopes

Two substrates which satisfy most of these conditions and are in use at McCrone Associates are high purity gold and vitrified graphite. Gold is preferred because of its very high reflectance which facilitates microscopical inspection of the smallest microparticles. Gold beads of 99.9999% purity are placed between specially cleaned glass or quartz slides in the mounting press. Under gradually increasing pressure, gold planchettes of 5-10 μm diameter are produced with mirror-like clean surfaces. For small particle mounting and analysis, a small rectangular grid is inscribed on the gold using fine pointed tungsten needles.

Micropraticles >3 μm are then lifted off the samples using tungsten needles with tips electrochemically etched to >1 μm point. The particle is then transferred on the gold substrate as described on Figure 1 and fixed with a drop of very diluted collodion. More elaborate removal and mounting procedures necessary for microparticles smaller than 3 μm are described in detail in the Atlas of Small Particles by McCrone and Delly [1] and other articles [2]. Electrically conductive particles in most cases do not require collodion for mounting. They will remain on the gold plate provided they are carefully handled. After first contact with the high energy ion beam sputtered and possibly resputtered ions from the particle and the substrate efficiently bond them together as shown on Figure 2.

ANALYSIS

Microparticles, mounted on a substrate with low secondary ion yield such as high purity gold, are analyzed by subjecting them to a partially focused beam of high energy oxygen, nitrogen, argon or cesium ions. The choice of primary ion beam is not very critical and in general oxygen is good for stable secondary emission. Argon and nitrogen are suitable for analysis of oxides, while cesium is excellent for noble metals and other elements that have low secondary ion yield with an oxygen beam.

It has been established that microparticles can be analyzed using a positive primary ion beam. The main reasons seem to be low density of the ion beam, small size of the particles, and possible resputtering of the metal substrate on the particle. Both positive and negative secondary spectra are produced readily with a positive primary ion beam.

Small particles can be analyzed with a scanning or stationary ion beam that is at least twice, and sometimes five times, larger than the projected area of the particle. Assuming a Gaussian distribution of ion intensity across the beam one can calculate the volume under the curve from the equation:

$$2\pi\int_0^r te^{-x^2}dx = \pi\left(1-e^{-r^2}\right)$$

where r = radius of microparticle
x = distance from the center of beam (variable of integration)

A plot of percent of beam size vs percent of total ions intercepted by a microparticle is given in the graph on Figure 3, and numerical values are given in the following table:

Table 1: Relationship of particle/ion beam size vs. proportion of ions striking a microparticle. Ion beam diameter is assumed to be three standard deviations or an area containing 99% of the total ion beam intensity.

Particle/beam diameter (D)%	5	10	20	30	40	50	70	90	100
Percent of incident ions striking a microparticle of size D	2.2	8.6	30.3	55.4	76.4	89.4	98.7	99.9	100

A 2 μm particle under a 10 μm beam will receive, if properly centered, approximately one-third of the total intensity of the ion beam. The full scan for mass range 1-260 will take approximately five minutes and will display most elements present in a microparticle of 0.1% or higher. For lower concentrations ranging from 1000 down, to 100 ppm, scanning times become prohibitively long. Particle erosion is then so severe that by the end of the scan most of the signal is derived from the area surrounding remnants of the particle.

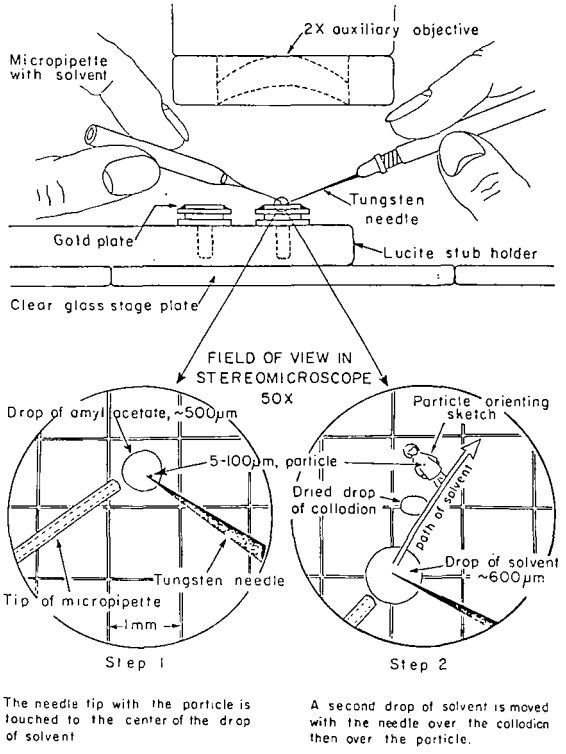


Fig. 1 - Securing a single microparticle >3 µm under a stereomicroscope, to a gold plate attached to an aluminum stub.



Fig. 2 - A spherical microparticle of fly ash on a gold substrate that has been bombarded by an off center argon beam. Note the resputtered gold on the lower side of the particle which effectively bonds it to the substrate.

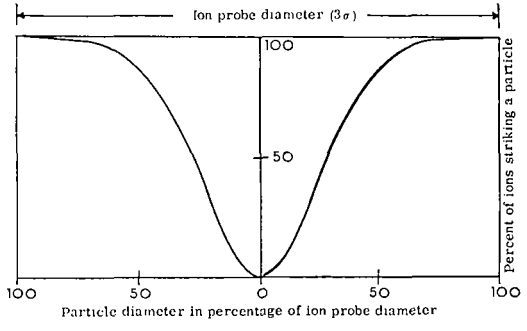


Fig. 3 - A diagram showing the relationship between particle size and proportion of incident ions striking it.

The most efficient approach to detection and analysis of trace elements in microparticles appears to be first to examine the particle for the presence of such elements by scanning a small fraction of the mass spectrum where such peaks are expected. After that, if time and/or particle erosion permit, a full mass scan from 0-300 m.u. may be performed in order to detect major and minor elements.

RESULTS AND INTERPRETATION

In the first 10 to 20 seconds only about 20-50 nm of particle surface is removed. In most cases this layer is surface contamination, such as organic thin films and submicron size dust particles. After preliminary etching, the microparticle will be cleaned and subsequent analysis will produce a full mass spectrum such as shown on Figure 4. Various stages of etching are shown on Figures 5,6 and 7. The spectrum was recorded in an ARL ion microprobe that was under the control of a

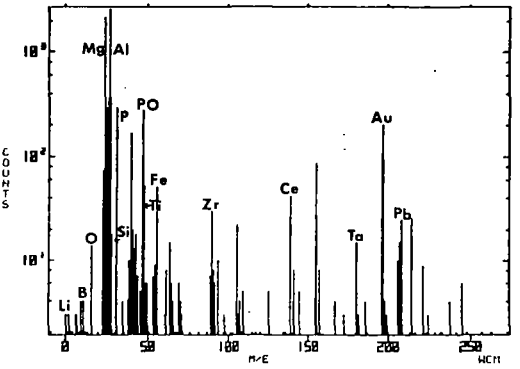


Fig. 4 - Mass spectrum of a 3 µm glass microparticle mounted on a high purity gold substrate. Glass is NBS K-497 with the following chemical composition in percent by weight: Li-0.0005, B-0.05, O-52.6, Mg-5.2, Al-5.8, Si-0.1, P-33.2, Ti-0.2, Fe-0.2, Zr-0.4, Ce-0.6, Ta-0.8, Pb-0.9. Primary beam argon, 2nA, 20 kV.

Data General 32K computer. Program for analysis was developed at GEC Vallecitos Nuclear Center and is particularly suitable for small particles. For trace analysis, a small fraction of the mass spectrum should be collected that display all isotopes and possibly oxides of the trace element. Measuring the intensity of only one isotope is seldom adequate because of the frequent mass peak overlaps that are common in a heterogeneous material such as atmospheric dust and various contaminants. A 50-200 sec. scan is sufficient to identify even a heavy trace element such as lead in microparticles. Low temperature ashing of organic aggregates and microparticles will frequently raise trace element content by an order of magnitude. For example, traces of vanadium in carbonaceous agglomerates, usually point to oil fired power station ash while higher sulfur and iron will indicate a coal power plant. Elements such as Ti, Br, Sb or Ba as trace elements help in differentiating various types of plastic even if the organic component is severely degraded and cannot be identified by other methods.

Computer programs can quantify the elements present in a microparticle using appropriate sensitivity factors. Even when results are semiquantitative the information on major, minor and trace elements will enable an experienced particle analyst to identify and even trace the origin of a small particle.

References

1. W.C. McCrone, J. Delly, "The Particle Atlas Two", Ann Arbor Science Publishers, Ann Arbor, MI

2. M. Bayard, "Application of the Electron Microprobe to the Analysis of Free Particulates" - C. A. Andersen Ed., Wiley, NY, 1973

3. C.A. Andersen, "Analytical Methods and Applications of the Ion Microprobe Mass Analyzer" - C.A. Andersen, Ed., Wiley, NY, 1973 Chapter 17

4. A. Teetsov, J. Brown, "Some Techniques for Handling Particles in SEM Studies", Proc. Scanning Electron Microscopy, 1976 (Part III), IIT Research Insititute, Chicago, IL

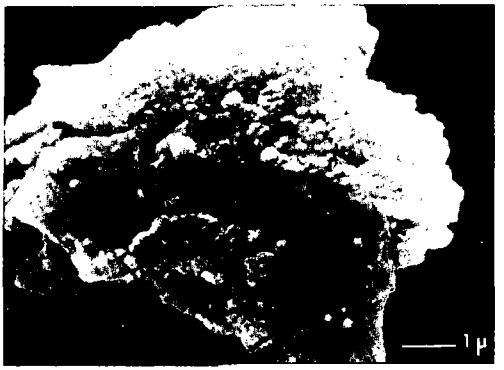


Fig. 5 - Microparticle with surface contamination mounted on a gold substrate.



Fig. 6 - Microparticle shown on Fig. 5 after 30 sec. of ion etching-cleaning.



Fig. 7 - Remnants of microparticle after prolonged IMA analysis (20 min). Note shadowing effect and etching of the substrate that shows the shape of inverse Gaussian curve.

ION MICROPROBE CHARACTERIZATION OF PARTICULATE MATTER

C.A. Evans, Jr. and V.R. Deline
Charles Evans & Associates
1670 S. Amphlett Blvd., Suite 120
San Mateo, CA 94402

Our initial studies of environmental particles used bulk analytical techniques, particularly spark source mass spectrometry, and particle sizing to determine the particle size distribution of the trace elements in fly ash from coal-fired power plants. This study found that the bulk concentration of trace elements, especially those considered to be toxic, exhibited a 1/r dependence. That is to say that the smaller the particle, the greater was the concentration of the toxic element. The implications of these findings were quite far-reaching since it is the smallest particles which escape conventional containment devices, can reside and travel in the atmosphere the longest and can penetrate the pulmonary system the deepest. We proposed that this 1/r relationship resulted from volatilization of the elements of interest in the high temperature fire bed and condensation on the fly ash surface in the cooler regions of the flue. Since the surface area per gram of particles changes as 1/r, the bulk concentration would also change with 1/r.

In order to confirm the proposed enhanced surface concentration of the toxic elements, several of the common surface analytical techniques were used to study the fly ash for in-depth distributions. In the general case only, the ion microprobe mass spectrometer was sufficiently sensitive to detect the elements of interest, although Auger electron spectrometry was of limited utility in confirming the ion probe results. Ion microprobe depth profiles confirmed that the elements exhibiting a 1/r concentration dependence were more concentrated in the outer 50-200 Å of the particles by as much as a factor of ten in some cases.

The last stage of the study used solvent leaching (H_2O and DMSO) to show that these concentrated outer layers were easily removed by biological like fluids. Ion microprobe depth profiles and bulk solution analyses showed that the surface layers were removed from the particles and quantitatively transferred to the solution phase.

More recent studies of particles have shown that the SIMS technique is readily capable of accurate isotopic analysis of individual particles. Using oxygen ion bombardment of individual 25 μm lunar particles, the $^{25}Mg/^{26}Mg$ ratio can be measured with .2% relative standard deviations with measurements made over a one day period.

Bibliography

1. "Toxic Trace Elements: Preferential Concentration in Respirable Particles," D.F.S. Natusch, J.R. Wallace, and C.A. Evans, Jr., Science 183, 202-204 (1974).

2. "Trace Metals in Airborne Particles," D. Natusch, R. Davison, R.E. Lamb, J.R. Wallace, and C.A. Evans, Jr., Proceedings of the Third Clean Air Congress, Dusseldorf, C12-14 (1973).

3. "Trace Metals in Fly Ash: Dependence of Concentration on Particle Size," Richard L. Davison, David F.S. Natusch, John R. Wallace, and C.A. Evans, Jr., Environmental Science and Technology 8, 1107 (1974).

4. "Surface Associations of Toxic Elements in Airborne Particulates," R.W. Linton, D.F.S. Natusch, P. Williams, C.A. Evans, Jr., Science 191, 852 (1976).

5. "Concentration of Toxic Species in Submicrometer Size Airborne Particles -- The Lung as a Preferential Absorption Site," D.F.S. Natusch, J.R. Wallace, and C.A. Evans, Jr., American Institute of Chemical Engineering Symposium Series - Polution Control and Clean Energy 71, 25 (No. 147).

6. "Determination of the Surface Predominance of Toxic Elements in Airborne Particles by Ion Microprobe Mass Spectrometry and Auger Electron Spectrometry," R.W. Linton, Peter Williams, C.A. Evans, Jr., D.F.S. Natusch, Analytical Chemistry 49, 1514 (1977).

7. "Characterization of Trace Elements in Fly Ash," D.F.S. Natusch, C.F. Bauer, H. Matusiewicz, C.A. Evans, Jr., J. Baker, A. Lon, R.W. Linton, and P.K. Hopke, International Conference on Heavy Metals in the Environment, Toronto, pp. 553-576 (1975).

8. "Surface Characterization of Environmental Particles," R.W. Linton, D.F.S. Natusch and C.A. Evans, Jr., Environmental Science and Technology (in press) (Invited).

WAM0B4 ENVIRONMENTAL AND ISOTOPE DILUTION REFERENCE STANDARDS, PAUL J. PAULSEN, Center for Analytical Chemistry, National Bureau of Standards, Washington, DC 20234

The Office of Standard Reference Materials at the National Bureau of Standards has a variety of SRM's useful for the analysis of environmental samples. These include gases in air, coal and coal fly ash, urban particulates, plant and animal tissue, water, and spikes for isotope dilution analysis. An overview will be presented of the presently available SRM's for environmental analysis, SRM's now in the process of being certified, and SRM's slated for production in the near future.

ISOTOPE DILUTION MASS SPECTROMETRY OF COAL AND FLY ASH*

D. L. Donohue, J. A. Carter, R. L. Walker
and J. C. Franklin

Oak Ridge National Laboratory
Oak Ridge, Tennessee 37830

The isotope dilution method is described for use with two types of mass spectrometers. Spark source mass spectrometry is used to survey a large number of elements simultaneously. Multi-element analyses are possible using isotope dilution techniques, provided certain criteria are met. A discussion is presented on the sources of error in such an analysis. In general, the detector limits ultimate precision due to its dynamic range characteristics and the amount of time spent measuring each isotope. For a photographic plate, it can be shown that a measured isotope 'spike' ratio of 1:1 is not always the most desirable. Incomplete dissolution and equilibration of the sample with the 'spike' can be a major cause of poor accuracy in this or, indeed, any isotope dilution analysis.

The second method described utilizes a thermal ionization mass spectrometer to make very precise isotope ratio measurements for one or two elements at a time. The use of pulse counting detection extends the dynamic range of the spectrometer and changes the contribution from various sources of error compared to SSMS. The use of resin bead technology allows smaller samples to be used, with relatively few interferences. Data are shown for both methods which demonstrate the precision, accuracy and sensitivity which can be achieved.

*Research sponsored by the U. S. Department of Energy under Contract #W-7405-eng-26 with the Union Carbide Corporation.

By acceptance of this article, the publisher or recipient acknowledges the U.S. Government's right to retain a non-exclusive, royalty-free license in and to any copyright covering the article.

Sample Preparation of Particulates for Multi-Element Examination by Spark Source Mass Spectrography

M. L. Jacobs and S. L. Sweeney
Commercial Testing & Engineering
490 Orchard Street
Golden, CO 80401

Preparation of particulate samples for multi-element examination requires a careful assessment of sample preparation to avoid inadvertant element contamination. A great part of our spark source mass spectrographic laboratory work has been evaluation of particulates for the Level I Source Assessment Sampling System or SASS train. Particulates from a combustion stream are collected in one of two ways; either by the use of a cyclone or caught on a fiberglass filter. The cyclones size the particulates into 1, 3 and 10 μ fractions. These particulates are generally not a problem in sample preparation as they can easily be mixed with compactable graphite used in normal spark source sample preparation. The mixture is then reduced to compacted pins for presentation to the spark source.

Problems arise in preparation of the particulate fractions caught on fiberglass filters in the SASS train which are used as prefilters to remove > 1 μ particulates in the gas stream prior to contact with the XAD-2 resin bed and liquid impingers.

In the normal sequence of events the analyst will try to remove at least 100 mg from the surface of the fiberglass at the same time minimizing the removal of any glass fibers. In our laboratory, this is called the "shake and take" technique. This technique does not remove any fine particulates caught in the interior of the fiberglass filter and thus makes the assumption that particulate sample removed from the surface is the same as that trapped in the interior of the fiberglass filter.

If normal sample preparation methods of "shake and take" don't work the real problems begin, then we must fall back on our next preparation technique. The next best method for the fiberglass filters is to cut a portion of the filter and place it in a glass centrifuge tube. We then cover the filter with alcohol. The centrifuge tube and alcohol is subjected to an ultrasonic shaking, hopefully, to remove particulates from the surface and interior of the filter. The main portion of the cleaned filter is then removed and rinsed with alcohol and the tube centrifuged for a few minutes. Some glass fibers from the filter generally are shaken loose with the particulate from the main filter but are found on the surface of the centrifuged particle matter and can be carefully removed prior to preparation of the subsequently dried particulates in the normal manner for spark source examination.

If, as in some cases, no particulate is removable from the fiberglass filter in the above manner, we then have several choices to make in a last ditch effort to obtain a multi-element examination by spark source of the particulates.

None of the choices are appetizing. A high pressure oxygen Parr bomb equipped with a quartz liner using platinum electrodes and platinum ignition wire can be used to ignite a mixture of fiberglass and particulates with benzoic acid as an accelerator over a HNO_3 solution. The mixture is combusted in a quartz cup at 30 atmospheres of oxygen pressure. If all is successful, the mixture combusts without fracturing the quartz liner or cup. The fiberglass, owing to the high combustion temperatures, melts into glass balls usually carrying some of the particulates into the glass spheres in an unretrievable fashion. The mixture must be filtered to remove the particulates that did not go into solution, as well as removing the glass spheres. The next problem using this method is to put the undissolved material into solution without excessive contamination of the sample. This objective has been accomplished by

HF/HCL/HNO_3 digestion or a fusion technique. Neither works with much success since contamination risks are very high and large dissolved silica levels create electrode preparation problems.

Another preparation method is to remove the particulate by solublizing them selectively leaving the fiberglass filter unchanged. This is tried using a hot aqua-regia digestion extraction. Unfortunately high trace element blank levels and poor or totally unknown trace elements recovery makes this method a poor choice.

Another digestion method would involve total digestion of the fiberglass filter and particulates using a mixture of HF/HNO_3/HCL. This creates problems because of the high trace element blank levels found in the fiberglass filters and the difficulty of fixing the trace element and silicon fluorides formed for evaporation onto the graphite for electrode preparation. The "fixing" of the volatile fluoride is usually accomplished by adding massive amounts of boric acid causing high trace element contamination levels.

The last and poorest choice is to attempt to grind the fiberglass filter and particulates, then mix and compact with graphite to make electrodes. The fiberglass does not grind well, and if accomplished, the resulting compaction with graphic results in an electrode with fiberglass whiskers. The fiberglass whiskers tend to cause disintegration of the electrodes when Rf sparking voltages of approximately 30 thousand volts are applied to the electrodes. Even if the examination of the electrodes sample pins is successful, high trace element concentrations in the blank fiberglass cause difficulty in attributing the resulting trace element analysis to the particulates originally under investigation. A brief table of selected trace element blank levels found by some of the preparation techniques described follows.

To sum up, the easiest technique with the highest probability of success that we have found is the "shake and take" routine, even with the technique's assumption of sample homogeneity. The ultrasonic and centrifuge preparation of the particulates offers the next most viable preparation alternative. The remaining preparation techniques have been used with only limited success because of the problems discussed and unfortunately offer limited hope of a successful multi-element sample preparation technique.

SELECTED TRACE ELEMENTS IN BLANK FIBERGLASS FILTERS BY DIGESTION

ELEMENT	*PPM OF GLASS FILTER*	
	HCL/HNO_3	*HF/HCL/HNO_3*
Lead	65	2
Barium	190	210
Silver	75	0.4
Molybdenum	100	2
Zirconium	58	50
Strontium	31	56
Arsenic	830	1
Gallium	13	3
Zinc	64	260
Copper	44	900
Nickel	3	160
Iron	470	> 1000
Chromium	22	230
calcium	>1000	> 1000
Sulfur	600	> 1000
Fluorine	≈ 250	> 1000
Beryllium	> 0.8	0.2

Elemental Characterization of Fuels and Effluents from Waste-to-Energy Systems by Spark Source Mass Spectrometry

G. M. Trischan
Midwest Research Institute, 425 Volker Boulevard, Kansas City, Missouri 64110

The use of urban refuse as an alternate energy source has been the focus of recent interest. Considering the production of approximately 3 to 5 lb of refuse per person per day which consists of approximately 80% combustible materials, the importance of refuse as an energy source can be realized.

Several different approaches to energy production through refuse utilization have been taken which invoke either direct refuse combustion or production of an intermediate fuel gas or oil from refuse precursors. In direct refuse combustion processes, refuse may serve as the single fuel source or, after removal of metallic and glass components, the combustible refuse fraction may be co-fired with conventional fuels such as coal or oil. The less direct alternative approach is the production of intermediate fuels from refuse through anaerobic digestion or pyrolysis. With the increasing interest in and construction of such refuse utilization systems as energy sources, detailed information concerning potentially hazardous emissions and process chemistry is receiving increasing attention. As a result, a unique series of analytical problems and considerations have been encountered.

Problem areas may be divided with respect to sampling and analysis. A thorough assessment of a combustion system must necessarily include all unique input and outlet streams. As a result, representative sampling of solid, liquid, and gaseous streams is often required. The often non-homogeneous state of the process streams and cyclic nature of many processes further complicate representative sampling procedures. Collection of gaseous samples for either organic or inorganic analytes is frequently a problem due to the lack of thoroughly validated collection techniques for many potentially gaseous materials. Finally, collection of sufficient materials to assure successful analysis is often a problem, especially for relatively clean gas outlet streams.

Analytical considerations involve three basic interdependent concerns: (1) the nature of the information desired, such as the analyte(s) of interest and corresponding sensitivity, accuracy, and precision; (2) the selection of suitable analytical techniques to obtain the desired information; and (3) the choice of appropriate sample preparation methods to insure compatibility with the selected analytical methods and to maintain sample integrity. Since it is frequently necessary to identify materials of concern in previously untested systems, survey information to identify the specific materials of interest and their approximate concentrations in process streams is often valuable. Subsequent sampling and quantitative analysis to accurately determine analyte concentrations then may be performed.

Evaluation of systems, such as waste-to-energy processes, requires understanding of the process being tested as well as knowledge of sampling and analysis limitations. Considerations of cyclic regional and/or seasonal process variations must be made to assure valid data interpretation. Finally, the extremely large mass flow rate of materials ($> 10^6$ g/min) compared to the relatively small ($\leq$ 1 g) of material actually analyzed should be realized.

The purpose of this work has been to survey a variety of waste-to-energy systems to generate preliminary data to identify potential process-specific emission problems. The results of spark source mass spectral survey analyses from three different waste-to-energy systems have been considered which are indicative of several trends in trace elemental emissions from refuse-fueled processes. The data are the result of at least three sampling and analysis runs of each material at each site. Supplementary analyses of selected elements by atomic absorption spectrophotometery and ion selective electrode techniques were performed to provide additional high integrity analytical data to validate SSMS observations and to identify possible problem areas.

The systems tested include a conventional 125 MW utility boiler fueled with a mixture of refuse derived fuel (RDF) and coal; a municipal refuse incinerator; and a refuse pyrolysis unit.

Refuse for the RDF-coal co-firing boiler was shredded and the more dense non-combustible materials were removed by an air classifier prior to being fed into the boiler. A baseline study during coal-only operation was also conducted. In addition to chemical changes, physical changes in the density, color, and electrical conductivity were noted in the bottom and fly ash samples.

The municipal incinerator was operated using raw refuse without preliminary processing. Combustible and non-combustible materials were fed directly into the boiler combustion zone on a travelling grate. A key sampling problem in this test was the coarseness of the refuse feed and the presence of non-combustible materials. Glass and metallic materials were segregated from the fuel samples and the remaining material was ground to a fine consistency for continued chemical characterization.

In the refuse pyrolysis unit, urban refuse was shredded, magnetically susceptible components were removed, and the remaining material fed into a pyrolysis reactor. A fuel gas was produced which was subsequently passed through a scrubber and an electrostatic precipitator. Solids and oils accumulated by the collecton devices were to be recycled to the pyrolysis reactor. For testing purposes a package boiler was connected to the fuel gas stream. Baseline characterizations of the boiler emissions were made using natural gas as the fuel.

The results of SSMS analyses of fuel, bottom ash, and fly ash streams from the utility boiler during operation using coal-only and coal-RDF supplemented fuel and the incinerator using municipal refuse as received, are presented in Table 1 for selected elements. Values for the unprocessed refuse feed stream of the incinerator are deceptively low due to the analysis of the feed material after removal of metallic or glass components, although glass and metallic materials were actually fed into the incenerator system. Three major groups of elements have been identified. Concentrations of the first group of elements are found to increase in both bottom ash and fly ash with increasing proportions of refuse burned. The most dramatic cases are observed for concentrations of relatively volatile elements, e.g., Pb or Cd in fly ash. It must be noted that the observed elemental quantities in the incinerator ashes most likely include contributions from the noncombustible fraction of the refuse feed. Cases of significant contributions to elemental concentration in ashes from noncombustible refuse components are classified in the second major group of elements. Although selected elemental concentrations in ashes vary slightly as coal is supplemented with RDF, dramatic concentration increases for the same elements are observed in the incinerator ashes. Such behavior suggests relatively small contributions from the combustible fraction of refuse while large proportions of these metallic and nonmetallic elements originate in the noncombustible fraction of refuse. Ash concentrations of the third group of elements are found to decrease or remain constant as larger proportions of refuse including non-combustible components are burned.

Data for the refuse, slag, and fuel gas scrubber inlet and outlet waters for the pyrolysis system are summarized in Table 2. Direct analysis of boiler outlet gas particulates was not possible due to extremely low particulate loadings. Additionally, mass balance was not possible since solid and liquid materials scrubbed from the pyrolysis gas were not recycled to the pyrolysis unit as intended and were not available for analysis. While the relatively volatile elements such as Sb, Pb, and Cd were found in slag at concentrations less than or equal to the original refuse concentration, less volatile elements were found at increased concentrations in slag. Vaporization of the more volatile elements into the pyrolysis gas is likely. This appears to be the case for at least six elements as evidenced by significant concentration increases in the scrubber outlet water. Additional elements of intermediate volatility are most likely condensed in the material which are removed from the pyrolysis gas. Had recycling devices been in operation it is expected that selected elemental concentrations would significantly increase in both the slag and scrubber outlet water.

TABLE 1

SELECTED TRACE ELEMENT CONCENTRATIONS IN COMBUSTION SYSTEM STREAMS[a/]

	Element	Fuel				Bottom Ash			Fly Ash		
		Coal	Fuel Supplement[b/] Coal	Fuel Supplement[b/] RDF[d/]	Refuse[c/]	Coal	Fuel Supplement	Refuse	Coal	Fuel Supplement	Refuse
Group 1	Sb	0.07	1.4	86	0.42	1.5	8.5	30	10	22	270
	Cd	0.12	0.13	28	< 0.31	0.68	1.5	2.2	2.6	4.5	37
	Cu	20	12	2,900	14	150	560	~ 900	240	240	720
	Pb	2.3	18	2,200	12	30	340	440	290	670	> 5,000
	Sn	0.28	0.43	130	1.1	9.9	19	96	14	42	1,200
Group 2	Ba	68	57	2,000	20	1,500	900	> 3,400	5,200	570	900
	Bi	0.04	0.21	9.3	< 0.15	0.47	0.47	8.3	7.4	4.4	58
	Cr	33	64	2,000	6.1	130	790	150	210	130	560
	Mn	9.8	11	770	15	360	360	250	630	210	1,600
	Ag	~ 0.04	< 0.1	7.1	< 0.14	0.40	0.71	4.6	3.9	1.2	21
	Zn	31	90	~ 4,800	42	300	~ 800	~ 1,000	~ 6,900	~ 1,200	> 5,000
Group 3	Br	1.3	41	58	20	3.4	13	10	14	8	280
	Cl	580	800	~ 2,200	16	130	~ 460	120	260	70	> 9,000
	F	69	85	470	18	110	220	57	1,100	110	1,700
	I	0.23	2.5	0.53	< 0.1	1.2	0.39	< 0.87	2.3	1.8	5.5
	P	26	170	> 5,000	330	~ 4,400	~ 2,800	1,700	~ 3,000	~ 3,100	> 10,000
	S	~ 2,000	730	> 10,000	540	~ 4,800	~ 2,600	2,300	~ 5,800	~ 4,800	> 7,500
	As	1.8	14	22	< 0.39	13	15	12	180	140	15
	Ga	1.3	2.0	12	< 0.20	13	6.5	3.4	40	16	5.7
	Ge	1.5	5.3	3.3	< 0.1	1.4	2.8	< 0.48	49	20	2.4
	Ni	9.8	32	~ 830	3.4	100	290	40	300	220	200
	Se	1.1	2.1	3.8	< 0.17	0.94	0.94	0.41	9.3	8.6	6.0
	Ti	640	1,300	> 8,300	~ 1,000	> 5,000	~ 4,600	> 4,000	> 8,300	> 5,000	> 5,000
	V	19	63	35	31	100	100	90	~ 1,100	120	100

a/ All concentrations in micrograms per gram.

b/ Coal and refuse co-fired at ratios of approximately 3:1 by weight.

c/ Coarse urban refuse used as received without additional processing.

d/ Refuse derived fuel produced by shredding and separation of non-combustibles from urban refuse.

Analysis of the boiler stack gases for vaporous species revealed elevated concentrations of mercury and chlorine during pyrolysis gas combustion as compared to natural gas combustion.

In all systems investigated, other elements, e.g., the rare earth series of metals, were not generally found at significant concentrations (> 10 ppm). Common elements such as Na, K, Ca, Mg, Al, and Si were found in major proportions (> 1%) in refuse and ash or slag wastes.

Survey information from three different refuse-consuming systems have demonstrated the mobility of relatively volatile elements or their compounds in combustion systems. The mass burning of unprocessed refuse (incineration) for an alternate energy source appears to present the greatest potential emissions problems. The potential impact of conventional fuel supplimentation using RDF appears to present emission problems comparable to those encountered in a conventional coal-fired boiler. Although a relatively clean-burning fuel gas can be produced by refuse pyrolysis, other waste streams from the pyrolysis reactor may present significant emission and disposal problems.

TABLE 2

SELECTED TRACE ELEMENT CONCENTRATIONS IN A REFUSE PYROLYSIS SYSTEM

Element	Refuse[a]	Slag[a]	Scrubber Inlet Water[b]	Scrubber Outlet Water[b]
Sb	30	13	< 0.001	0.002
Cd	2.5	3.9	< 0.001	< 0.004
Cu	180	∿ 2,200	0.013	0.017
Pb	1,600	50	0.009	0.32
P	≥ 0.31%	3,600	0.029	1.4
Sn	22	46	< 0.001	0.002
Ba	490	890	0.097	2.1
Br	28	5.0	0.51	0.80
Cl	570	150	21	360
Cr	140	710	< 0.001	0.016
F	150	∿ 140	0.1	0.84
Mn	220	2,000	0.029	0.70
S	1,400	1,700	10	35
Zn	630	460	0.095	3.8
Ga	3.4	4.2	< 0.001	< 0.001
Ge	1.2	0.53	< 0.001	< 0.001
Ni	24	49	0.014	0.005
V	14	33	< 0.001	0.003
As	3.8	4.9	0.002	0.028
Bi	7.5	≤ 4.2	< 0.001	< 0.003
I	0.83	≤ 0.51	0.005	0.013
Se	0.24	0.41	< 0.001	< 0.002
Ag	0.62	1.9	0.001	0.001
Ti	≥ 3,400	> 0.5%	0.003	0.020

a/ Concentrations in micrograms per gram.
b/ Concentrations in micrograms per milliliter.

WAMOB7 Comparison of Spark Source Mass Spectrometry with Other Methods in the Analysis of Ambient Air Particulate Samples, E. Hunter Daughtrey, Jr. and J. Kent Bostick, Jr., Northrop Services, Inc., P.O. Box 12313, Research Triangle Park, North Carolina 27709

Spark source mass spectrometry (SSMS) has found utility as a complimentary means of analysis to other methods used for analysis of ambient air particulates. The two chief routine methods used by EPA for elemental analysis are neutron activation analysis and ICP optical emission spectrometry. Where there are extraction recovery problems or poor detection limits by these methods, SSMS can be of service in many cases. A comparison is offered for the three techniques. Demonstration of the capability of SSMS is illustrated by the analysis of NBS SRM 1648 Urban Particulate Matter. Improved precision and accuracy can be obtained by the use of enriched isotope addition, as illustrated by the results for copper.

This work was performed under contract 68-02-2566 in support of the Environmental Monitoring and Support Laboratory, Environmental Research Center, Research Triangle Park, North Carolina.

COMPARISON OF ANALYTICAL METHODS

	METHOD		
	OES (ICP)	SSMS	NAA
Sample Preparation	extraction with mixed acid and ultrasonicate	mix with graphite and from electrodes	nil
Normal Precision (%RSD)	10%	25%	25%
Number of Elements Routinely Sought	48 (20)	~70	30 (20)
Time required for analysis of one sample	1 day	1 day	12 elements < 1 day 12 elements < 1 wk. rest < 6 wks.
Number of samples per day	50	3-4	20
Data system	minicomputer	programmable calculator	minicomputer
Special requirements			Nuclear Reactor

RESULTS OF ANALYSIS OF NBS SRM 1648 URBAN PARTICULATE MATTER

(μg/g)

A. NBS "CERTIFIED" ELEMENTS

Element	NBS	SSMS
Cr	403	422
Fe	39,100	26,700
Ni	82	<300
Cu	609	746
Zn	4,760	3,660
As	115	108
Cd	75	42
Pb	6,550	6,720
U	5.5	8.1

B. NBS "INFORMATION ONLY"

Element	NBS	SSMS
Na	4,000	3,160
Mg	8,000	7,870
Al	33,000	21,900
Si	125,000	111,000
K	10,000	8,700
Sc	7	10
Ti	4,000	3,310
V	130	131
Mn	860	677
Co	18	<90
Se	24	34.8
Br	500	450
Ag	6	9.8
Sb	45	49.3
Cs	3	3.7
Ba	737	1,000
La	42	23
Ce	55	56
Sm	4.4	3.6
Eu	0.8	1.1
Th	7.4	7.9

COMPARISON OF GENERAL SURVEY AND ENRICHED ISOTOPE ADDITION SSMS DETERMINATION OF COPPER

Results (μg/g) are given as the mean $\pm$ s.d. of 4-6 determinations

	NBS SRM 1632 Coal	NBS SRM 1633 Fly Ash
General survey	26.6 $\pm$ 7.7	136 $\pm$ 36
Enriched Isotope Addition	17.8 $\pm$ 1.2	128 $\pm$ 12.6
NBS value	18 $\pm$ 2	128 $\pm$ 5

LEVEL 1 ENVIRONMENTAL ASSESSMENT WITH THE SOURCE ASSESSMENT SAMPLING TRAIN,

FRANK BRIDEN and JAMES DORSEY, Industrial Environmental Research Laboratory, U.S. Environmental Protection Agency, Research Triangle Park, NC 27711

The use of mass spectrometric techniques in conducting an environmental source assessment survey of the streams associated with industrial and energy processes is described. The basic components of an "environmental source assessment" program include (1) a systematic evaluation of the physical, chemical, and biological characteristics of the streams associated with a given process; (2) predictions of the probable effects of the streams on the environment; (3) the prioritization of the streams; and (4) identification of any necessary control technology.

The sampling and analytical program is a systematic survey of the characteristics of the primary discharge from a given process or group of processes. The overall strategy incorporates three "levels" (phases) of information development. The Level 1 screening program emphasizes completeness of detection of elements and classes of organic materials in process streams. Level 2 seeks to identify specific substances existing in any classes identified in Level 1 as potential environmental problems. Level 3 is a quantitative study of the effect of process variables on the emission rates of specific substances identified in Level 2.

The Level 1 methods of sampling and analysis were chosen on the basis of information outputs, cost effectiveness, availability, reliability, and ease of application. The goal is to identify the pollution potential of a source with a target accuracy factor of 3, i.e., the final result obtained should be between 1/3 and 3 times the "true" value.

The objective of Level 1 organic analysis is to identify the major classes of organic compounds present in a process or effluent stream and to estimate their concentrations. The majority of the samples require extraction with an organic solvent prior to analysis. The scheme then proceeds to initial analyses of volatile (TCO) and nonvolatile (GRAV) organic material and a preliminary infrared (IR) spectral analysis. The sample extract is separated by silica gel liquid chromatography (LC) using a 7-fraction solvent series of varying polarity. A low resolution mass spectrum (LRMS) is obtained on each LC fraction that has sufficient quantity (TCO plus GRAV), when referenced to the source, to exceed decision criteria concentrations. The mass spectrometer used in this determination should have a resolution ($\overline{M}/\Delta M$) of 800 to 1,000, batch and direct probe inlet, variable ionizing voltage source, and electron multiplier detection. Spectra are normally obtained at 70 eV ionizing voltage, but low voltage (10 eV) spectra may provide much simpler data and thus aid in interpretation in some cases.

Table 1 is the final summary of organic data showing the information obtained on particulates greater than 3 microns, less than 3 microns, rinses, resin, and condensate from a ferromanganese plant stack sample. The Level 1 organic analysis scheme accurately determined the presence of polynuclear aromatics and other classes as later verified with gas chromatography/mass spectrometry.

Level 1 inorganic analysis uses spark source mass spectroscopy (SSMS) to achieve a semiquantitative analysis of 73 elements. All samples are analyzed on an "as received" basis except those high in organics (>50%) which are Parr bombed. A single element internal standard is added to the sample which is then run at exposures separated by a factor of 3. Detection is by photoplate and is quantified by the visual "just disappearing line" technique.

Table 2 gives a comparison of the means and relative standard deviations for "just disappearing line" (JDL) and densitometry data for 12 elements, each with 7 replicates, in a doped NBS flyash. Antimony and arsenic are two elements which in the past were analyzed by atomic absorption spectroscopy (AAS) for Level 1 but these data show very good results. The data also implies that for analyses under these conditions the densitometry information does not offer any real advantage over the more economical JDL technique.

For Level 1 environmental assessments the quantities used have been derived on the assumption that an overall accuracy factor of ±3 could be achieved. This factor was a subjective judgement based on experience in the field. Since the SSMS data provided 13 replications for many of the elements, it has been possible to test the factor of 3 validity to a 95% confidence level. The error factors were determined using logs of the data for the 19 elements for which the NBS certified and information only values and the doped values were known (mercury is not determinable by SSMS and titanium was a major component). The use of a mean error value is not meaningful and error factors for individual elements must be considered. Of 19 elements, there were 3 having an error factor greater than the prescribed 3. It is suspected that the problems with these particular elements arose from sample preparation procedures and modifications are under consideration to prevent these elemental losses. For the balance of the elements, an error factor of less than ±3, with a confidence level of 95%, is achievable and significant.

The attributes of SSMS for elemental analysis and LRMS for organic compound identification have been examined. Both of these techniques have proven to be invaluable tools in the Level 1 environmental assessment scheme although there remain several areas which need investigation and improvement. Our basic conclusion, however, is that these mass spectroscopic techniques afford the most cost-effective approach for screening a wide range of samples from industrial and energy processes.

TABLE 1. SASS Organics Summary Report

Compound Categories	Particulates			Sorbent Module		Total
	>3μ	<3μ	Rinses	Resin	Condens.	
Aliphatic Hydrocarbons		0.1	1.9	3.9		5.9
Aromatic Hydrocarbons		0.1	0.1	3.5		3.7
Fused Aromatics <216		0.2	14	370		380
Fused Aromatics >216	4.5	33	22	390	0.3	450
Heterocyclic S				37		37
Heterocyclic N	1.1	7.9	0.8	70	0.07	80
Ketones	0.8	6.4	7.8	53	0.05	67
Alcohols			0.2			~ 0.1
Esters		0.06	0.08	0.8		0.9
Carboxylic Acids		0.06		4.2		4.3

All results mg/m^3

TABLE 2. SSMS Accuracy and Precision for Selected Elements

Element	True Conc	JDL Mean	DENS Mean	JDL Relative Std Dev	DENS Relative Std Dev
U	6.0	12.4	11.4	27.4	50.2
Pt	92.0	15.7	16.3	26.9	23.7
Gd	3.7	2.4	3.7	32.4	40.3
Nd	17.8	18.3	17.9	44.4	24.7
I	1.4	0.6	0.5	43.8	48.2
Te	2.4	0.3	0.5	52.9	56.3
Sb	3.4	4.0	3.1	45.6	28.6
Cd	27.0	6.9	4.6	54.8	21.3
Se	15.5	18.3	18.6	12.9	11.1
As	34.2	36.6	32.9	33.3	25.3
Ni	207.0	210.0	185.7	35.7	27.1
Be	6.0	3.8	6.5	127.7	125.0

TABLE 3. Reliability of SSMS Data

Element	Error Factor for 95% Confidence Level	Element	Error Factor for 95% Confidence Level
U	2.1	As	1.3
Th	1.3	Zn	1.3
Pb	1.8	Cu	1.3
Tl	1.4	Ni	1.3
Hg	-	Co	1.4
Pt	6.1	Mn	1.4
Sb	1.4	Cr	1.7
Cd	4.9	V	1.2
Sr	1.8	Ti	-
Rb	1.3	Be	4.2
Se	1.2		
		Mean	2.02

A CLOSER LOOK AT THE ALCHEMY OF FIRE

L. L. Lamparski, T. J. Nestrick, S. S. Cutie'
Analytical Laboratories
The Dow Chemical Company
Midland, Michigan 48640

During the summer of 1978, the Michigan Division of The Dow Chemical Company conducted a study to investigate various sources of chlorinated dibenzo-p-dioxins to the environment. Up until this time, it was assumed that the major, if not only, sources of chlorinated dioxins to the environment were chlorinated phenolic pesticides (such as 2,4,5-T, Silvex, 2,4,5-trichlorophenol or pentachlorophenol). In short, what we observed during this study was that chlorinated dioxins and a variety of other compounds were produced in many common combustion processes.

This study was intended to identify areas in which we felt that further work should be done. Since much of the sampling was not statistical in nature, we want to stress that this is a preliminary report. It was not intended to elucidate all of the chemical reactions occurring at the part-per-billion and part-per-trillion levels during combustion. Indeed, the combustion process appears to create a sea of reactive intermediates which can form a tremendous variety of products. Conditions such as temperature, excess oxygen, trace elements which act as catalysts may affect the formation rates of some of these trace products. Indeed, as the title suggests, at this time we know very little of what really occurs at trace levels during combustion.

A total of 75 isomers of chlorinated dibenzo-p-dioxins are possible. Although all of the isomers have not been synthesized or subjected to biological testing, the most biologically active of the dioxins observed to date is the 2,3,7,8-tetrachloro isomer. As chlorine substitution increases, the toxicity generally appears to decrease; the mono-, di-, and trichloro isomers are considered to be relatively non-toxic. It's not all that simple though, because wide variations in biological activity (factors of 10,000) have been observed within a single degree of chlorine substitution such as tetrachloro isomers. For this reason it is necessary to be able to identify, as much as possible, the isomeric structure of any dioxins observed.

The analytical methodology consists of three basic parts: 1) separation of the dioxin fraction from the sample matrix, 2) liquid chromatographic separation of dioxins from common chemical residues (PCB's, DDE), 3) measurement of dioxin content by packed column GC-MS.

The dioxins are removed from the particulate matter by a 16 hour Soxhlet extraction with benzene. This extract is then purified through a column system consisting of two 1 x 10 cm columns placed in series and packed with various reactant-modified adsorbents. The top column contains one gram of activated silica over 5.0 g of 44% H_2SO_4 on silica. This column removes polar and oxidizable species while allowing dioxins and related compounds to pass through.

The second column contains 1.5 g of caustic silica which is a 33% mixture of 1N sodium hydroxide or activated silica followed by 1 g of activated silica. This system is useful in removing acidic species while again allowing the dioxins to pass directly through. The solvent is evaporated to dryness before proceeding to the next separation step. At this point, the residue can usually be dissolved in 5 ml hexane.

The second column system is designed to chemically and chromatographically remove a variety of compounds from the sample extract. The top column is a 1 x 3 cm bed of 1.5 g 10% $AgNO_3$ on silica. This reagent chemically removes chlorinated aliphatics, such as DDE, and sulfides. The effluent from the first column is run directly onto the second column of the system which is a 6 x 210 mm bed containing 5.0 g of activated basic alumina. This is the first chromatographic separation of residues. The hexane fraction contains chlorobenzenes and other low polarity compounds. A 50% CCl_4/hexane fraction removes most PCB's, about half of the chlorinated terphenyls, chlorinated diphenyloxides, and chlorinated naphthalenes. The dioxin fraction is eluted with 50% CH_2Cl_2/hexane and also can contain some PCB's, chlorinated terphenyls. This fraction is now subjected to a final HPLC cleanup to separate these various compounds.

The chromatographic conditions for the reverse-phase high performance LC separation are shown below:

Instrument:	Perkin-Elmer LC-65T
Column:	6.2 x 500 mm ZORBAX-ODS
Mobile Phase:	methanol at 2.5 ml/minute
Column Temperature:	50°C
UV Detector:	0.02 AUFS at 235 nm

Appropriate fractions containing dioxins of interest are collected and extracted prior to GC-MS analysis under the conditions shown.

Instrument:	Hewlett-Packard Model 5992A GC-MS
GC OPERATIONAL PARAMETERS	
Column:	2 mm ID x 210 cm - glass, silylated.
Packing:	0.60% OV-17 + 0.40 Poly S-179 over an 80/100-mesh specially deactivated support
Column Temperature:	230° → 280°C at 10°C/minute (TCDDs)
	230° → 300°C at 10°C/minute (Cl_6-Cl_8 DDs)
Injector:	280°C, on-column
Carrier:	Helium at 13 cc/minute
MS OPERATIONAL PARAMETERS	
Separator:	Single-stage glass jet
Electron energy:	70 eV
Resolution:	Unit
Ions monitored:	TCDD - 320, 322, 324
	HxCDD - 388, 390
	HpCDD - 424, 426
	OCDD - 458, 460

Method validation analyses to determine the useful concentration range, precision, accuracy, and overall-recovery of the procedure yielded the data shown below:

Component	Number of Analyses	Range (ppt)	Average Recovery	Relative Standard Deviation
2,3,7,8-tetrachloro dibenzo-p-dioxin	15	10-5000	106%	5.2% @ 50 ppt
hexachlorodibenzo-p-dioxin	15	$50-10^6$	73%	6.0% @ 250 ppt
heptachlorodibenzo-p-dioxin	15	$50-5 \times 10^6$	78%	10.8% @ 250 ppt
octachlorodibenzo-p-dioxin	15	$200-10^7$	80%	9.2% @ 1000 ppt

The advantages of using a sophisticated sample preparation procedure prior to GC-MS analysis are obvious. Additional specificity can be built into the analysis using chemical and/or liquid chromatographic separations. Production of a "clean" sample extract allows greater concentration factors and thus, improved sensitivity can be achieved. Finally, analysis of such samples prolongs the useful life-time of GC-columns and mass spectrometer source cleanliness by minimizing the amount of unwanted residues introduced into the system.

WAM0810 THE ANALYSIS OF ORGANIC SOLIDS BY METAL ION ATTACHMENT IN SIMS. R. G. Cooks, R. J. Day, and S. E. Unger, Department of Chemistry, Purdue University, W. Lafayette, IN 47907

Argon ion bombardment of organic solids admixed with metal salts gives secondary ion mass spectra which include cationized molecules as well as characteristic fragment ions, both metal containing and not. Transition metals (e.g. Cu, Fe, Co) attach to a variety of compounds giving molecular weight and molecular structural data. In some cases, such as with phenanthroline, chelation occurs and the properties of the gas phase chelate can be compared with those of its solution analog. The methodology finds application in studies on natural products such as alkaloids. Studies on hydrodesulfurization catalysts using molecular SIMS will also be described. Organic salts can be ionized directly by SIMS and this provides insight into the ionization mechanism. The mechanistic relationship of SIMS to field desorption, plasma desorption and laser desorption will be considered.

HAZARDOUS PRODUCTS FROM THE COMBUSTION OF ORGANOCHLORINE COMPOUNDS

Yves Tondeur*, Ralph C. Dougherty*, Christopher Rappe† and Hans-Rudolf Buser††

*Department of Chemistry, Florida State University, Tallahassee, FL 32304
†Organic Chemistry Department, University of Umea, S-901 87 Umea, Sweden
††Swiss Federal Research Station, CH-8820 Wädenswil, Switzerland

The hazards associated with products of cellulosic and fossil fuel combustion are well known. The formation of polynuclear aromatic hydrocarbons in oxygen-deficient flames has been the subject of considerable investigation. Indeed, the occurance of scrotal cancer in chimney sweeps in Great Britain was the first recognized occupational cancer, apparently caused by the presence of polynuclear aromatic hydrocarbons in chimney residues.

The formation of polychlorinated polynuclear aromatic hydrocarbons (PCPAHs) through the combustion or pyrolysis of organochlorine compounds is a less widely recognized environmental hazard.

We have used negative chemical ionization (NCI) mass spectrometry[1] using an AEI MS-902 mass spectrometer equipped with an SRIC chemical ionization source for examination of polychlorinated molecules that result from combustion and/or pyrolysis of organochlorine compounds and appropriate reference standards. We have also used GC mass spectral analysis, using a 25m OV-17 glass capillary column coupled to a Finnigan 4000 quadrapole mass spectrometer for analysis of those combustion products of polychlorinated organics, and fly-ash from a municipal incinerator and an industrial heating facility[2]. The cleanup procedure used for examination of smoke condensates by NCI mass spectrometry involved steam distillation of the condensates which had been diluted with 10% sulfuric acid, using a modified[3] version of the steam distillation head that was introduced by Veith[4]. In the case of GC mass spectrometry, samples were cleaned-up by extraction with methylene chloride, followed by chromatography on a micro-column of silica, followed by chromatography on a micro-column of basic alumina. In this case, the polychlorodibenzodioxin (PCDD) fraction was concentrated and directly used for GC-MS analysis.

In order to investigate the possibility that inorganic chlorides contribute to the presence of organochlorine residues in smoke condensates and fly-ash from cellulosic or fossil fuel fires, we constructed a quartz combustion chamber with a smoke trap and then undertook the combustion of pressure-treated lumber that had been treated with copper-napthanate-arsenate-chromate and filter paper that had been saturated with sodium chloride. There was no indication of the presence of organochlorine residues in the smoke condensates or ash from either of the fires. The detection sensitivity in the NCI experiments is between 1 and 100ng. The amounts of material burned in each case was 5g, thus the yield of polychloropolynuclear aromatics must have been at or below parts-per-billion in these experiments.

The combustion of wood that has been pressure-treated with pentachlorophenol or polyvinylchloride products produced abundant quantities of PCPAHs. We have previously shown that pyrolysis or combustion of polychlorophenols leads to the formation of polychlorodibenzodioxins[2] and combustion of polychlorobiphenyls leads to the formation of polychlorodibenzofurans[5].

Negative chemical ionization spectra utilizing isobutane-oxygen as the reagent gas on the smoke condensate obtained from combustion of polyvinylchloride initiated with a hydrocarbon flame contained a series of ions which corresponded to the oxygen exchange ions, (M-19)$^-$, for the series of polychlorodibenzodioxins, polychlorobiphenyls and polychlorodiphenylethers. Confirmation of the presence of polychlorodioxins by selective adsorption on activated carbon[6] followed by NCI analysis is the subject of current investigation.

The possibility that polychlorodibenzodioxins may arise in the course of ordinary cellulosic combustion or combustion of fossil fuels has been the subject of recent public discussion. We have examined fish tissue obtained from a series of rivers and lakes in the midwestern and northeastern United States, for the presence of polychlorodibenzodioxins, polychlorodibenzofurans and other planar polychlorinated aromatic hydrocarbons[3].

Cleanup was accomplished by Soxhlet extraction, gel permeation chromatography to separate the bulk of the lipids from the polychloro aromatics, and adsorption chromatography on activated carbon to very selectively isolate the planar aromatic hydrocarbons from the rest of the sample. The planar hydrocarbons were then desorped from the activated carbon with a reverse flow of toluene[6]. By use of negative chemical ionization screening, we were able to detect the presence of polychlorodibenzofurans in fish collected in the Ohio River in 1970 and 1971, Lake Michigan at Saginaw in 1974, the Connecticut River in 1970, and the Hudson River in 1974. Of the thirteen fish samples examined, only two gave any indication of the presence of polychlorodibenzodioxins. These two samples were taken from the Tittabawassee River in Michigan. The Tittabawassee River is adjacent to Dow's manufacturing facility in Midland. If ordinary combustion were responsible for the presence of polychlorodibenzodioxins in the environment, it would seem likely that we would have uncovered evidence for dioxins in fish taken at sites remote from the Dow plant.

In spite of the fact that we were unable to find polychlorodibenzodioxin in any samples that were not adjacent to a manufacturing facility for polychlorophenols and related products, the formation of polychlorodibenzodioxins and dibenzofurans through combustion of organochlorine compounds may present a significant addition to the cancer burden in the United States and other industrialized countries. The detection limits in our fish screening experiments were at or above 1ppb. In view of evidence that suggests that TCDD is carcinogenic at 5ppt in the diet, low levels of this molecule from combustion sources may be significant.

The production of chlorine gas in the United States is approximately 100 lbs. per person annually. Eighty percent of the chlorine that is produced is converted to organochlorine compounds. If, over time, 30% of the organochlorine compounds that are produced are subjected to combustion, this would represent the combustion of more than one-billion pounds of carbon-bound chlorine every year in the United States alone. If the yield of polychloro polynuclear aromatics from the combustion of highly chlorinated organics was only 1ppm the combustion of organochlorine compounds in the United States would result in the release of more than 2 tons of PCPAHs into the environment annually. If only 0.01% of the PCPAHs produced in this way entered the food chain, this would represent a burden of roughly 10ppt per person annually, if there were no biomagnification.

Our investevation has shown that high temperature oxidation of polychlorobiphenyls produced between 1% and 25% yields of polychlorodibenzofurans. Pyrolysis and/or combustion of polychlorophenols produced greater than 0.1% yields of polychlorodibenzodioxins. Polychlorodibenzodioxins and dibenzofurans were produced in greater than 0.1% yields by thermal reactions of polychlorodiphenylethers. The concentration of polychlorodibenzodioxins in municipal incinerator fly-ash ranged between 0.1 and 1ppm[2]. This data suggest that our estimate of the amount of PCPAHs produced by combustion of organochlorine compounds in the U.S. may be low by as much as two to three orders of magnitude.

The analysis above suggests that it would be prudent to seriously examine the waste processing technology in the United States and to take remedial action to control the combustion of highly chlorinated organic compounds in municipal incinerators or industrial furnaces. Addition of organohalogen compounds to gasoline should also be reexamined

Acknowledgments: This work has been supported by grants from the National Institutes of Health and the U.S. Environmental Protection Agency.

References:

1. (a) R.C. Dougherty, J. Dalton and F.S. Biros, Org. Mass Spectrom., 6, 1171 (1972); (b) R.C. Dougherty and K. Piotrowska, Proc. Nat. Acad. Sci. U.S., 73, 1777 (1976).
2. H-R. Buser, H-P. Bosshardt and C. Rappe, Chemosphere, #2, 165 (1978).
3. R.C. Dougherty, L. Smith, D. Stalling and D.W. Kuehl, Envir. Health Pers., in press (1979).
4. G.D. Veith and L.M. Kiwus, Bull. Envir. Contam. Tox., 17, 631 (1977).
5. H-R. Buser, H-P. Bosshardt, C. Rappe and R. Lindahl, Chemosphere, #5, 419 (1978).
6. J.N. Huckins, D.W. Stalling, W.A. Smith, J.A.O.A.C., 61, 32 (1978).

THE DISSOCIATION DYNAMICS OF FURAN STUDIED BY PHOTOION-PHOTOELECTRON COINCIDENCE, WAMOC1

Gary D. Willett, Tomas Baer and James J. Butler. Department of Chemistry, University of North Carolina at Chapel Hill, North Carolina 27514.

The threshold photoelectron spectrum (TPES), the photoionization efficiency (PIE), curves and photoion and photoelectron coincidence (PIPECO), time-of-flight (TOF), distributions for ionic furan are used to elucidate it's decay mechanism near the threshold for dissociation.

The metastable reactions studied are:

1. $C_4H_4O^{+\cdot} \rightarrow C_3H_4^{+\cdot} + CO$ (Thermodynamic Dissociation Energy = 10.9 eV)
2. $C_4H_4O^{+\cdot} \rightarrow C_2H_2O^{+\cdot} + C_2H_2$ (Thermodynamic Dissociation Energy = 11.7 eV)
3. $C_4H_4O^{+\cdot} \rightarrow C_3H_3^{+} + HCO$ (Thermodynamic Dissociation Energy = 11.9 eV)

The TPES and PIE curves were recorded on a spectrometer which has been described previously (1). The basic components of the spectrometer are a H_2 many-line resonance photon source, a steradiancy electron energy analyser and a quadrupole mass filter.

For the PIPECO experiment, threshold photoelectrons are recorded in delayed coincidence with their concomitant photoions. The electron and ion signals are used as start and stop inputs for a time-to-pulse-height converter after which fragment ion TOF distributions, such as those shown in Fig. 1, are recorded on a multichannel analyser.

Asymmetric TOF distributions are observed for ions with microsecond lifetimes because of initial acceleration of the photoion as a parent and final acceleration as a daughter. By convoluting either a Lorentzian or parent TOF distribution with an exponential decay function, calculated TOF distributions such as those shown as solid lines in Fig. 1, yield the total unimolecular dissociation rates. Subsequent modelling of these fragmentation rates using statistical theory yields important clues concerning the threshold energy dissociation mechanisms (1).

Fig. 2 illustrates the TPES and PIE curves for furan. From the TPES, we can determine both the energies of the first three molecular ion states and the presence of resonant autoionization. This last phenomenon has beer discussed in a previous paper (2). The PIE curves for furan illustrate two important points. First, mass 40 (presumably allene$^{+\cdot}$) does not onset until ~ 0.8 eV above its thermodynamic onset. Secondly, mass 39^+ shows a different variation in its PIE curve to those of masses 40^+ and 42^+.

Relevant heats of formation required for an RRKM statistical calculation are shown in Fig. 3. There are at least two other isomers of furan which have similar heats-of-formation to that of furan (3). For simiplicity, only one of these, vinyl-ketene (VK), is shown in this figure since its structure most closely resembles the structures of allene$^{+\cdot}$ and ketene$^{+\cdot}$. The activation energies shown in Fig. 3 together with suitably chosen structures for the furan molecular ion ($F^{+\cdot}$) and transition state ($F^{\ddagger}$) serve as inputs for the RRKM calculations. The calculated rates shown in Fig. 4 (solid lines) compare well with the experimental dissociation rates (points). These experimental rates were determined using the total measured rates k_T (see Fig. 2), assuming that $k_T = k_{39} + k_{40} + k_{42}$, together with the PIPECO branching ratios R_1 and R_2 where $R_1 = \frac{I_{42}}{I_{40}} = \frac{k_{42}}{k_{40}}$ and $R_2 = \frac{I_{39}}{I_{40}} = \frac{k_{39}}{k_{40}}$ by solving for k_{39}, k_{40} and k_{42}.

Since the height of the reverse activation barrier for mass 40^+ is not known experimentally, it was estimated by fitting the RRKM rates to the experimental rates. When allowance is made for a small kinetic shift, the calculated height of 0.67 eV compares well with the measured onset at about 0.8 eV above its thermodynamic onset.

Only the calculated curve for $C_3H_4^+$, VK^+, $VK^{\ddagger}$ is shown in Fig. 4 as the calculated rates for masses 39^+ and 42^+ using the VK system are similar to those obtained using the furan system. Contrary to previous PIPECO studies on molecular ion isomerization (1), this last result indicates that isomerization of furan to VK must be rate determining. This is because if $k_5 \gg k_6$, k_7 (see Fig. 3) we would be able to detect only mass 40^+ and Fig. 2 shows that this is not the case.

Fig. 4 illustrates that the rate of production of mass 39^+ is not expected to be greater than the rates for masses 40^+ and 42^+. One possible explanation for the "unusual" behaviour of the mass 39^+ PIE is that near threshold furan dissociates via a tight transition state. As the internal energy is raised, competition from isomerization

(to say cyclopropenal*) leads to a rate determining step that involves a loose transition state. Above ~ 13 eV, competition from the $CH_2 - C \equiv CH^+$ (Thermodynamic Dissociation Energy 13.0 eV) channel will complicate the mechanism even further.

REFERENCES

1. T. Baer, G. D. Willett, D. Smith and J. S. Phillips, J. Chem. Phys. 70, 4076 (1979) and references cited therein.

2. P. T. Murray and T. Baer, Int. J. Mass Spectrom. and Ion Phys., June 1979.

3. Professor John Holmes has kindly supplied us with the heats of formation of 11 $C_4H_4O^+$ isomers.

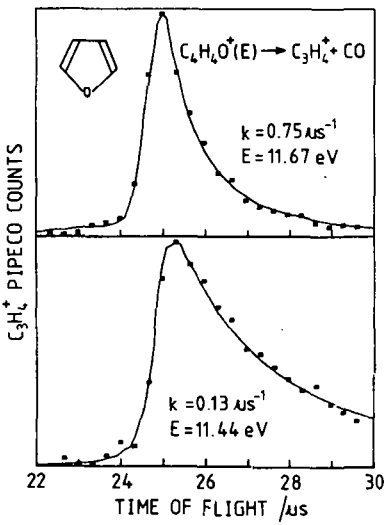


Fig. 1

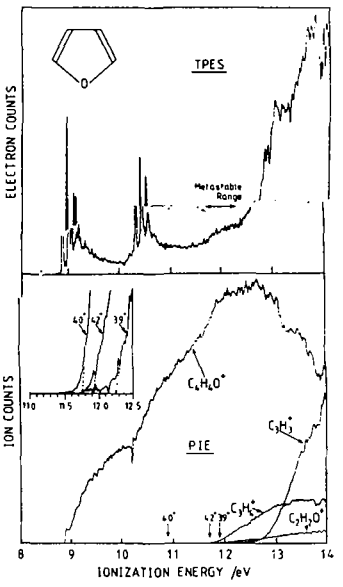


Fig. 2

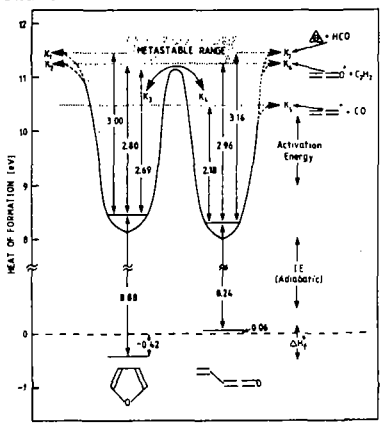


Fig. 3. All energies have been corrected for the thermal contribution of vibrations and rotations.

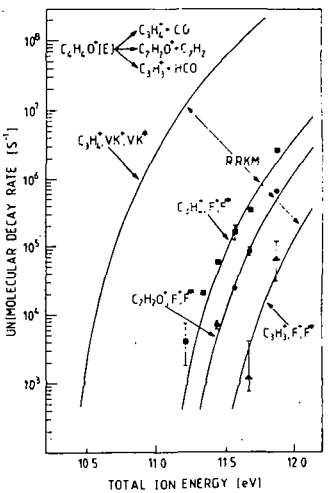


Fig. 4

ENERGY DEPENDENT FRAGMENTATION OF $C_6H_{12}^{+\cdot}$ MOLECULAR IONS

A. G. Harrison, Y.-H. Li, and N. E. Middlemiss
Department of Chemistry, University of Toronto, Toronto, Canada

Although the C_3 to C_5 olefins show very similar behaviour on electron impact indicating extensive isomerization of the molecular ions prior to fragmentation, the $C_6H_{12}^{+\cdot}$ molecular ions show substantial differences in both their collision activation mass spectra[1] and in their relative metastable ion abundances[2] indicating that the isomeric molecular ions do not completely interconvert prior to fragmentation. The 2-methyl-1-pentene and 2-methyl-2-pentene systems have been discussed in detail by Bowen and Williams[2] who estimate that the intermediate for the double bond shift has a ΔH_f similar to that of the fragmentation products and conclude that fragmentation should be competitive with isomerization.

To provide more detail on the energy dependence of the fragmentation reactions we have determined the CS_2^+ (10.2 eV), Xe^+ (12.6 eV weighted), CO^+ (14.0 eV) and N_2^+ (15.3 eV) charge exchange mass spectra of a variety of C_6H_{12} olefins. The CS_2 reagent ion was produced by electron impact ionization of a 20% CS_2 - 80% N_2 mixture. With the range of recombination energies (given in brackets above) we have constructed approximate breakdown graphs for the various olefins.

Comparison of the breakdown graphs for 2-methyl-1-pentene and 2-methyl-2-pentene (Fig. 1) shows that the terminal olefin has a dominant low energy route to formation of $C_4H_8^{+\cdot} + C_2H_4$, the process which provides the dominant metastable ion. For the 2-methyl-2-pentene fragmentation begins at higher energies and leads predominantly to $C_5H_9^+ + CH_3$ (again the fragmentation giving the dominant metastable peak) with the $C_5H_9^+$ fragmenting further at higher internal energies to $C_3H_5^+ + C_2H_4$.

For both the 3-methyl-1-pentene and 3-methyl-2-pentene isomers (Fig. 2) the dominant low energy fragmentation of the molecular ion involves loss of $CH_3^{\cdot}$ although for the former isomer, which has an allylic ethyl group, loss of C_2H_5 becomes an important fragmentation route at higher energies.

4-Methyl-1-pentene is similar to 2-methyl-1-pentene in showing a dominant low energy fragmentation to $C_4H_8^{+\cdot} + C_2H_4$, even though this is not the product expected by the normal McLafferty rearrangement. This favourable low energy rearrangement reaction is replaced by an apparent simple bond cleavage to form $C_3H_7^+$ at higher internal energies (Fig. 3). The 4-methyl-2-pentene shows the dominant fragmentation to be loss of methyl to form $C_5H_9^+$ with further fragmentation to $C_3H_5^+$ at higher internal energies.

The large differences observed in the breakdown graphs for 2-methyl-1-pentene and 2-methyl-2-pentene indicate that the barrier for interconversion of the two molecular ions may be considerably higher than the activation energy for fragmentation of either isomer. This conclusion is supported by the observation (Fig. 4) that while the metastable peak for C_2H_4 loss from 2-methyl-1-pentene shows a low kinetic energy release with a distribution characteristic of a single fragmentation process, the similar fragmentation process for 2-methyl-2-pentene shows a composite metastable peak, the major contributor showing a considerably higher kinetic energy release.

Although the results for these compounds can be rationalized by simple rearrangements or bond cleavage reactions, the possibility of more complex mechanisms cannot be ruled out in the absence of isotopic labelling.

Full details of this work will be published elsewhere.

1. T. Nishishita and F. W. McLafferty, Org. Mass Spectrom., 12, 75 (1977)

2. R. D. Bowen and D. H. Williams, Org. Mass Spectrom., 12, 453 (1977)

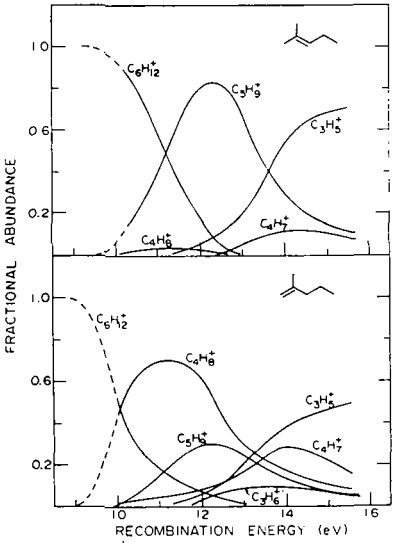


Figure 1

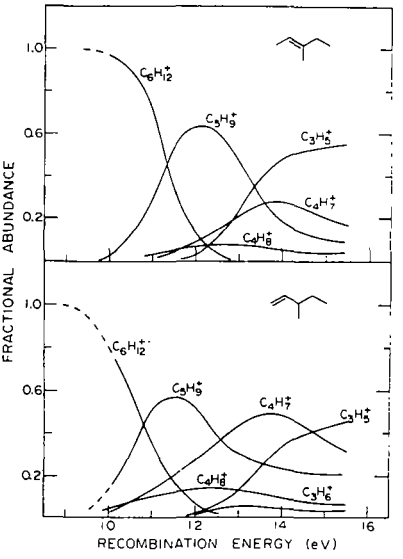


Figure 2

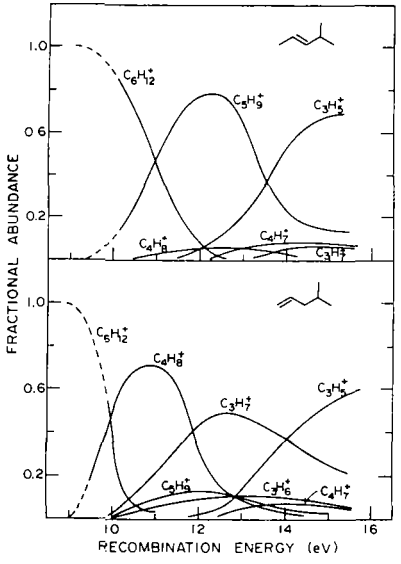


Figure 3

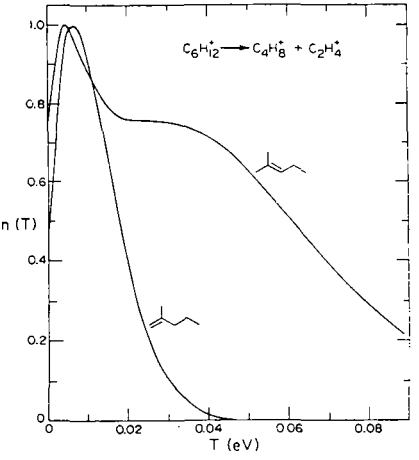


Figure 4

ISOMERISATIONS OF HYDROCARBON MOLECULAR IONS

P. WOLKOFF and J.L. HOLMES. (Chemistry Dept., University of Ottawa, Ottawa, Ontario K1N 9B4 Canada)

The possible isomerisation of the molecular ion of butane to that of methylpropane prior to decompositions on the μs time-scale and the structures of daughter ions resulting from the loss of $H^{\cdot}$, $CH_3^{\cdot}$ and CH_4 from the two hydrocarbons have recently been discussed in detail[1].

In order unequivocally to identify for $[butane]^{+\cdot}$ the participation of non-terminal C atoms in methyl and methane eliminations therefrom, the ^{13}C labelled butane $^{13}CH_3CH_2CH_2{}^{13}CH_3$ was prepared and the metastable peaks for losses of $CH_3^{\cdot}$, CH_4 and $^{13}CH_3^{\cdot}$, $^{13}CH_4$ were measured; the results are shown in the Table. From these values, assuming that no isotope effect is operating, the proportions of internal and terminal C atom participation were calculated (see Table). It is evident that no appreciable positional loss of identity of C atoms takes place before fragmentation. These results must now be compared with those reported previously[1] for deuterium labelled butanes and which are also shown below.

Metastable peak areas; methyl and methane losses from labelled butanes.

	Fragment lost			
	$CH_3^{\cdot}$	CH_4	$^{13}CH_3^{\cdot}$	$^{13}CH_4$
$CH_3CH_2CH_2CH_3$ (1)	54.8	45.2	--	--
$^{13}CH_3CH_2CH_2{}^{13}CH_3$ (2)	4.3	[5.7] ← 56.3 → [50.6]		39.4

	$CH_3^{\cdot}$	$CH_4(CH_2D^{\cdot})$	$CH_3D(CHD_2^{\cdot})$	$CD_3^{\cdot}(CH_2D_2)$	CD_3H	CD_4
$CH_3CD_2CD_2CH_3$ (3)	51.2	24.3	14.6	3.9	5.7	< 0.2
$CD_3CH_2CH_2CD_3$ (4)	5.9	< 0.5	6.1	48.8	21.6	17.0

Terminal methyl loss. Examination of the Table shows that terminal methyl loss involves no significant isotope effect. Similarly, terminal methane loss involves no significant isotope effect when the overall process is considered; compound (2) 39.4%; (3) 38.9% and (4) 38.6%. However, the reaction can formally be separated into 1,2 + 1,3 and 1,4 eliminations. For (3) the 1,2 + 1,3-elimination contributes 14.6% and the 1,4 process,

24.3%. In contrast, for (4) the 1,2 + 1,3 contribution is 21.6%, the 1,4 reaction, 17%. These results are compatible with normal deuterium isotope effects favouring (CH_3-H) over (CH_3-D) and (CD_3-H) over (CD_3-D) for (3) and (4), respectively.

Internal methyl loss. The absence of $CH_2D^{\cdot}$ loss from (4) and, by inference from the small changes in methyl: methane ratios among the compounds examined, that loss of $CHD_2^{\cdot}$ does not contribute to the overall reaction $(3)^{+\cdot} \rightarrow m/z$ 45 + 17, indicates the participation of only (secondary) methylene H atoms rather than (primary) terminal H atoms in the internal methyl loss. Some small isotope effect is apparent from the relative losses of $CH_3^{\cdot}$(4.3%), $CD_3^{\cdot}$(3.9%) and $CH_3^{\cdot}$(5.9%) from (2), (3) and (4), respectively.

Internal methane loss appears related to internal methyl loss because the relative abundance for loss of $^{12}CH_4$ from (2) is similar to those of CD_3H from (3), and CH_3D from (4).

Many of the above results could be explained by invoking partial isomerisation of $[butane]^{+\cdot}$ to $[methylpropane]^{+\cdot}$ prior to fragmentation. For example, as shown below:

$$CH_3CD_2CD_2CH_3^{+\cdot} \rightarrow \underset{\underset{5}{}}{CH_3\text{-}\underset{CD_3}{\underset{|}{CD}}\text{-}CH_3^{+\cdot}} \begin{cases} \rightarrow CD_3\overset{+}{C}DCH_3 + CH_3^{\cdot} \\ \rightarrow C_3H_5D^{+\cdot} + CD_3H \end{cases}$$

$$CD_3CH_2CH_2CD_3^{+\cdot} \rightarrow \underset{\underset{6}{}}{CD_3\text{-}\underset{CH_3}{\underset{|}{CH}}\text{-}CD_3^{+\cdot}} \begin{cases} \rightarrow \overset{+}{C}DCHCD_3 + CH_3^{\cdot} \\ \rightarrow C_3D_5H^{+\cdot} + CH_3D \end{cases}$$

The non-involvement of the tertiary H(D) in the methane elimination has been well established[2]. Although the above rationale seems plausible it must be deemed unlikely because metastable ions of (5) were found to lose CH_4, CH_3D and CD_3H in ratios 78 : 18 : < 1, i.e., CD_3H loss was a very minor process[1] (with no isotope effect CH_4:CD_3H would be 1:2). Indeed, the participation of methylpropane molecular ions is further rendered unlikely from observations of (6). Here loss of CH_3D predominates (91%) with CH_2D_2 (4%), CD_3H (4%), and CD_4 ($\sim$ 1% as minor processes (compare (4)).

It is concluded from the above observations that the processes leading to loss of methyl and methane from butane molecular ions (and possibly from alkane ions in general) are best described as concerted and not step-wise reactions, i.e., although the reacting configurations for loss of C2 (or C3) as methyl or methane from $[butane]^{+\cdot}$ may resemble those for the corresponding reactions of $[methylpropane]^{+\cdot}$ ions, the latter are not involved as discrete reaction intermediates.

References

1. P. Wolkoff and J.L. Holmes, J. Amer. Chem. Soc., 1978, 100, 7346.
2. P.J. Derrick, A.M. Falick and A.L. Burlingame, J. Chem. Soc., Perkin 2, 1975, 98; idem, J. Chem. Soc. Faraday Trans. I, 1975, 1503.

ELECTROCYCLIC RING OPENING OF THE CYCLOBUTENE RADICAL CATION

Michael L. Gross and David H. Russell

Department of Chemistry
University of Nebraska
Lincoln, Nebraska 68588

The electrocyclic ring opening of cyclobutene to give 1,3-butadiene is a well-understood chemical isomerization. The process occurs with a lower than anticipated activation energy presumably because it is an "allowed" reaction. In order to ascertain whether the electrocyclic ring opening occurs for the gas-phase cyclobutene radical cation, we have undertaken a comparative study of the chemical properties of ionized cyclobutene and 1,3-butadiene. Both ions exhibit nearly identical chemical reactivities with a variety of neutral molecules including methyl vinyl ether, furan, ethene, propene, isomeric butenes, and isomeric pentenes. The explanation proposed to account for these results is that the cyclobutene ion rapidly undergoes (within less than 2 ms) an electrocyclic isomerization to give the 1,3-butadiene ion. The maximum activation energy for this process is estimated to be less than 7 kcal/mol. The chemical properties of the molecular ions of 1,2-butadiene, 1-butyne, and 2-butyne were determined using the same reactant neutral molecules, and they differ considerably from the 1,3-butadiene and cyclobutene ions. The results are interpreted to exclude other isomeric [$C_4H_6^{+}\cdot$] species in the electrocyclic reaction.

1. Michael L. Gross, and David H. Russell, J. Amer. Chem. Soc., 101, 2082 (1979).

DECOMPOSITION OF THE 1,3-BUTADIENE RADICAL CATION ON THE MICROSECOND TO PICOSECOND TIME SCALE

D.H. Russell, M.L. Gross, J. van der Greef, and N.M.M. Nibbering

Department of Chemistry
University of Nebraska
Lincoln, Nebraska 68588

Department of Chemistry
University of Amsterdam
Amsterdam, The Netherlands

The decomposition of ionized 1,3-butadiene to give $C_3H_3^+$ and $\cdot CH_3$ has been studied over the time interval of approximately 10^{-11}-10^{-5}s using the complementary techniques of field ionization kinetics (FIK) and mass-analyzed ion kinetic energy spectroscopy (MIKES). By employing both carbon-13 and deuterium labeled 1,3-butadiene, it has been established that (1) hydrogen atom randomization takes place very rapidly and is complete by approximately 10^{-11}s, (2) carbon atom randomization occurs at a slower rate which is competitive with the decomposition reaction. The hydrogen atom randomization is postulated to take place by isomerization to other acyclic C_4H_6 ions without change in the carbon skeleton. The near lack of carbon atom interchange at short times (10^{-9}-10^{-11}s) is explained by invoking a high-energy formation of a methylcyclopropene which occurs as a rate-determining step. For more slowly decomposing (metastable) C_4H_6 ions, the ring-opening reaction of this intermediate to re-form the 1,3-butadiene cation becomes more competitive with dissociation, and this explains the nearly complete carbon atom randomization at longer times.

1. D.H.Russell, M.L.Gross, J. van der Greef, and N.M.M. Nibbering, J. Amer. Chem. Soc., 101, 2086 (1979).

PROTON-TRANSFER REACTIONS INVOLVING SPECIFICALLY SOLVATED IONS

D. Smith, N. G. Adams and M. J. Henchman,* Dept. of Space Research, University of Birmingham, Birmingham B15 2TT, England

Using a new SIFT apparatus (selected ion flow tube) with a flowing afterglow source,[1] the hydrated hydronium ions $H_3O^+(H_2O)_{0,1,2}$ have been prepared and, after mass selection, have been selectively injected into the helium flow tube at ~ 300 K. Addition of a neutral reactant downstream allows the chemistry of these ions to be explored as a function of their hydration number under uniquely controlled conditions. First, no contaminant is present -- just the pure ion, the pure neutral and the buffer gas: second, the system is truly thermal, thereby fulfilling a necessary requirement for comparison with the chemistry of this species in aqueous solution. This preliminary study has focussed on two fundamental reactions -- the symmetric proton-transfer reaction to water itself, this being thermoneutral, and the asymmetric transfer to ammonia, which is exothermic. Rate constants and product-ion distributions have been measured, with particular emphasis on deuterium labelling for insight into mechanism.

Reaction with water

The six isotopic-exchange reactions involving $H_3O^+(H_2O)_{0,1,2}$ with D_2O and $D_3O^+(D_2O)_{0,1,2}$ with H_2O have been shown to proceed at or near to the gas kinetic limit, ~ 2(-9) cm^3 $molecule^{-1}$ s^{-1}. A typical example of the branching ratios which were measured is given by:

$$D_3O^+ + H_2O \longrightarrow \begin{cases} D_2HO^+ + DHO & (65\%) \\ DH_2O^+ + D_2O & (35\%) \end{cases}$$

and should be compared with the predictions of 67% to 33% from a statistical model involving complete mixing of the hydrogens within a bound intermediate. The complementary experiment of H_3O^+ on D_2O gave essentially the identical result of 70% to 30%, thereby establishing the absence of significant kinetic isotope effects. All the evidence, both on these six reactions and the subsequent further reactions of the product ions with water, supports the statistical model. Thus the notion that the reaction of D_3O^+ with H_2O involves the simple discrete transfer of a D^+ from D_2O to H_2O is not upheld: rather an intermediate is formed, with a lifetime longer than the time required for hydrogen scrambling, and it decomposes, losing a water molecule statistically. Such scrambling is plausible since the intermediate is highly excited (with an excitation energy equal to its binding energy of 20-30 kcal mol^{-1}) and its lifetime is in excess of 10^{-9} s, as estimated from the magnitude of third-body rate constants for stabilizing the intermediate as a cluster. For example, facile transfer of H^+ (or D^+) between water molecules, coupled with rotation of the H_3O^+ moiety, is one simple mechanism for randomizing the hydrogens.

Further corroboration of the scrambling comes from the preparation in the ion source of partly deuterated $H_3O^+(H_2O)$ and $H_3O^+(H_2O)_2$ type ions and their selective injection at high energy into the flow tube. Water loss by collisional dissociation yielded fragment ions whose isotopic distribution revealed that the deuterium labels had again been randomized throughout the clusters.

Reaction with ammonia

In the reaction of the hydrated hydronium ions with ammonia, the difference in proton affinity[2] can present a choice between competing channels.

$$H_3O^+ + NH_3 \longrightarrow NH_4^+ + H_2O \quad + 32 \text{ kcal} \quad (1)$$

$$H_3O^+(H_2O) + NH_3 \longrightarrow \begin{cases} NH_4^+ + 2H_2O & + 0 \text{ kcal} \quad (2) \\ NH_4^+(H_2O) + H_2O & + 17 \text{ kcal} \quad (3) \end{cases}$$

$$H_3O^+(H_2O)_2 + NH_3 \longrightarrow \begin{cases} NH_4^+ + 3H_2O & - 20 \text{ kcal} \quad (4) \\ NH_4^+(H_2O) + 2H_2O & - 3 \text{ kcal} \quad (5) \\ NH_4^+(H_2O)_2 + H_2O & + 12 \text{ kcal} \quad (6) \end{cases}$$

Reactions (1), (2) and (5) were observed exclusively, again at the gas kinetic limit ($\sim 2(-9)$ cm^3 molecule s^{-1}) and the latter two reactions become exothermic if the two product water molecules remain bound (binding energy 4.6 kcal[3]). Experiments using the corresponding deuterated ions revealed the discrete transfer of D^+, D_3O^+ and D_3O^+ respectively without scrambling. Thus the NH_3 abstracts the proton together with the minimum number of waters for the process to be allowed energetically. One can rationalize the prevention of proton exchange within the intermediate in terms of the greater proton affinity of ammonia, and, in the case of (1), a shorter lifetime for the intermediate.

Further insight comes from a study of nonreactive collisions between NH_4^+ and D_2O [(1) in reverse], where the rate constant for hydrogen exchange was measured to be $3(-12)$ cm^3 molecule^{-1} s^{-1}. Here the intermediate lifetime will be long, the excitation energy 20 kcal but the disparity in proton affinity restricts the proton exchange to one collision out of every thousand.

* Permanent address: Chemistry Department, Brandeis University, Waltham, MA 02254

(1) D. Smith and N. G. Adams, "Gas Phase Ion Chemistry", Vol. I (ed. M. T. Bowers) Academic Press, New York (in press) 1979.
(2) Thermochemical data from P. Kebarle, Ann. Rev. Phys. Chem. 28, 445 (1977).
(3) H. Kistenmacher, G. C. Lie, H. Popkie and E. Clementi, J. Chem. Phys. 61, 546 (1974).

REACTIONS OF ORGANIC ANIONS IN THE GAS PHASE

Charles H. DePuy, Veronica M. Bierbaum, Robert J. Schmitt,
Joseph J. Grabowski and Gary K. King
Department of Chemistry, University of Colorado, Boulder, Colorado 80309

The formation of gas phase organic anions by proton abstraction can often lead to mixtures of isomers, either because of the presence of more than one acidic site in the parent neutral or because of rearrangement in the act of abstraction. Using a flowing afterglow system[1,2] we have developed a method to specifically generate a carbanion from a trimethylsilyl (TMS) derivative using fluoride ion as a displacing agent.

$$(CH_3)_3SiCH_2\text{-}CH{=}CH_2 \xrightarrow{F^-} (CH_3)_3SiF + {}^-CH_2\text{-}CH{=}CH_2$$

$$CH_3C{\equiv}C\text{-}TMS \xrightarrow{F^-} CH_3C{\equiv}C^-$$

$$TMSCH_2C{\equiv}CH \xrightarrow{F^-} {}^-CH_2\text{-}C{\equiv}CH$$

$$C_6H_5CH_2TMS \xrightarrow{F^-} C_6H_5CH_2^-$$

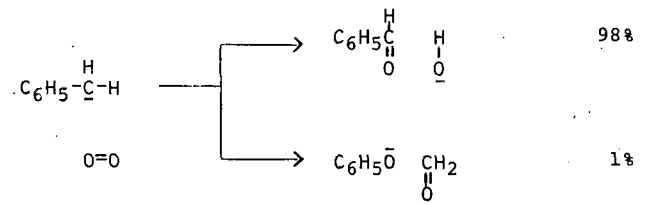
While the method allows generation of many anions, it has so far been unsuccessful for the production of anions more basic than allyl; tetramethyl silane, for example, adds fluoride ion rather than displacing to give CH_3^-.

$$(CH_3)_4Si \xrightarrow{F^-} (CH_3)_4SiF^-$$

Using this and other methods for carbanion formation, we have investigated several different types of reactions. We have found, for example, that delocalized anions react with molecular oxygen giving rise to cleavage products at the carbons bearing the negative charge.

$$\begin{array}{ccc} CH_2{=}CH\text{-}CH{=}CH\text{-}\bar{C}H_2 & & CH_2{=}CH\text{-}CH{=}CH\text{-}O^- \\ \updownarrow & \xrightarrow{O_2} & \\ CH_2{=}CH\text{-}\bar{C}H\text{-}CH{=}CH_2 & & CH_2{=}CH\text{-}O^- \end{array}$$

The benzyl anion reacts with oxygen by cleavage of a methylene proton to give hydroxide ion and benzaldehyde as the major products.



Bohme and Young[3] observed that alkynyl anions can be cleaved by molecular oxygen. For example, the propynyl anion gives the ketene anion and formaldehyde as the major products.

We have found that some carbanions, such as the acetonitrile anion, will not react with ground state molecular oxygen. These species will, however, react with singlet oxygen, $O_2(^1\Delta g)$. Singlet oxygen is produced by passing oxygen through a microwave discharge before introduction into the flowing afterglow. The anions of acetaldehyde and methanol, which also do not react with ground state oxygen, as well as the anion of acetonitrile are cleaved by singlet oxygen.

$$N\equiv C-\bar{C}H_2 + O_2(^1\Delta) \longrightarrow NCO^- + H_2C=O$$

$$H-\overset{O}{\overset{\|}{C}}-\bar{C}H_2 + O_2(^1\Delta) \longrightarrow H-\overset{O}{\overset{\|}{C}}O^- + H_2C=O$$

$$CH_3O^- + O_2(^1\Delta) \longrightarrow HO_2^- + H_2C=O$$

We have also found that carbanions react readily with nitrite esters to form nitroso anions.

$$CH_2=CH-\bar{C}H_2 \quad \overset{O}{\overset{\|}{N}}-OCH_3 \longrightarrow \left[CH_2=CH-CH_2-\overset{O}{\overset{|}{N}}-OCH_3\right]^-$$

$$\downarrow$$

$$\left[CH_2=CH-CH_2-N=O \quad {}^-OCH_3\right] \longrightarrow CH_2=CH-\bar{C}H-N=O \quad HOCH_3$$

Amide reacts with ethyl nitrite to give primarily NO_2^- by an E2 or an S_N2 reaction. Using neopentyl nitrite, in which these two pathways are suppressed, leads to the production of large amounts of HN_2O^-.[4]

The acetone anion reacts with neopentyl nitrite to give two products.

$$CH_3\overset{O}{\overset{\|}{C}}\bar{C}H_2 \xrightarrow{RONO} CH_3\overset{O}{\overset{\|}{C}}\bar{C}HNO + \bar{C}H_2N=O$$

35% 65%

The first is the expected product based on the mechanism given above. The second presumably arises by attack of the alkoxide ion on the carbonyl carbon in the intermediate complex.

In summary, we have developed new methods of specific carbanion generation using fluoride ion displacements of a trimethylsilyl derivative, and have demonstrated cleavage reactions of carbanions using ground state and singlet oxygen and reactions with nitrite esters.

References

1. V. M. Bierbaum, C. H. DePuy, R. H. Shapiro, and J. H. Stewart, J. Am. Chem. Soc., 98, 4229 (1976).

2. J. H. Stewart, R. H. Shapiro, C. H. DePuy and V. M. Bierbaum, J. Am. Chem. Soc., 99, 7650 (1977).

3. D. K. Bohme and L. B. Young, J. Am. Chem. Soc., 92, 3301 (1970).

4. C. H. DePuy, V. M. Bierbaum, R. J. Schmitt and R. H. Shapiro, J. Am. Chem. Soc., 100, 2920 (1978).

WAMOC8 ORGANOMETALLIC ION CHEMISTRY: PARALLELS BETWEEN GAS PHASE AND CONDENSED PHASE, R. FREAS, K. KALMBACH, J. WRONKA, and D. P. RIDGE, Dept. of Chem., Univ. of Del., Newark, DE 19711

The ion chemistry observed in gaseous mixtures of transition metal compounds and organic compounds will be compared with condensed phase transition metal chemistry. The role of oxidative addition in both of these chemistries will be emphasized. Insights into the mechanisms of catalytic and synthetic reactions available from studies of the gas phase ion chemistry will be discussed. Specific examples considered will include the cleavage of alkanes and the metal assisted synthesis of cyclic ketones. Evidence from the ion molecule reactions relating to the thermochemistry of covalent bonds to metals, particularly metal-carbon and metal-hydrogen bonds, will be summarized and evaluated.

WAMOC10 Spectroscopic Properties of Ions in the Gas Phase and in Solution. W. D. Reents, Jr. and B. S. Freiser, Purdue University, Department of Chemistry, W. Lafayette, Indiana 47907.

Spectroscopic studies of carbonium ions in solution primarily by NMR have yielded much structural information pertaining to these chemically important species. In the gas phase, new mass spectrometric techniques are currently being developed which provide further insight into the structure and chemical properties of these ions in the absence of complicating solvation effects. In particular, ion cyclotron resonance (ICR) spectroscopy has emerged in the forefront of this area due to its unique ability to trap ions for long periods of time approaching minutes, permitting the study of bimolecular encounters between ions and neutrals, as well as the study of unimolecular processes following electron or photon impact. To illustrate the types of information obtainable by these techniques, results from a comparative study of isomeric $C_6H_6NO^+$ ions in the gas and solution phases will be presented and discussed.

GAS PHASE BASICITIES OF SOME MAIN GROUP FLUORIDES AND OXOFLUORIDES

C. E. Doiron and T. B. McMahon
Department of Chemistry
University of New Brunswick
Fredericton, N.B. Canada E3B 5A3

The gas phase proton affinities of a number of fluorine and trifluoromethyl substituted carbonyl compounds have been investigated using trapped ion cyclotron resonance techniques to examine bimolecular proton transfer equilibria. Equilibrium constants for a number of reactions outlined in Fig. 1 were determined and these subsequently converted to enthalpy changes for proton transfer using $\Delta G = -RT\ln K_{eq}$ and assuming ΔS for proton transfer to be accurately estimated by changes in rotational symmetry numbers. As a reference point for these gas phase basicity determinations a value of 157 kcal/mole was assumed for the proton affinity of SO_2, as suggested by Munson [1].

In addition to the fluorocarbonyl compounds basicities of the group V trifluorides were investigated relative to SO_2 and SO_2F_2. The basicities of PF_3 and NF_3 found agreed with previous more approximate estimates [2,3]. However AsF_3 had not been previously investigated and the trifluoroarsonium ion, $HAsF_3^+$, was found to undergo nucleophilic displacement reactions with a number of bases. For example, with AsF_3 itself, reaction (1) occurs via HF displacement.

$$HAsF_3^+ + AsF_3 \rightarrow As_2F_5^+ + HF \qquad (1)$$

This reaction appears to be general with a variety of bases, B, whose proton affinities are greater than that of HF but less than that of AsF_3, eqn. (2). Subsequent reaction of $BAsF_2^+$ with AsF_3 leads to

$$HAsF_3^+ + B \rightarrow BAsF_2^+ + HF \qquad (2)$$

B = N_2, CO_2, N_2O, CO, CH_3F, NF_3, CF_2O.

displacement of B by the stronger base, AsF_3.

References

1. D. E. Smith and B. Munson, J. Am. Chem. Soc., 100, 497 (1978).

2. R. R. Corderman and J. L. Beauchamp, Inorg. Chem., 17, 1585 (1978).

3. D. Holtz, J. L. Beauchamp, W. G. Henderson and R. W. Taft, Inorg. Chem., 10, 201 (1971).

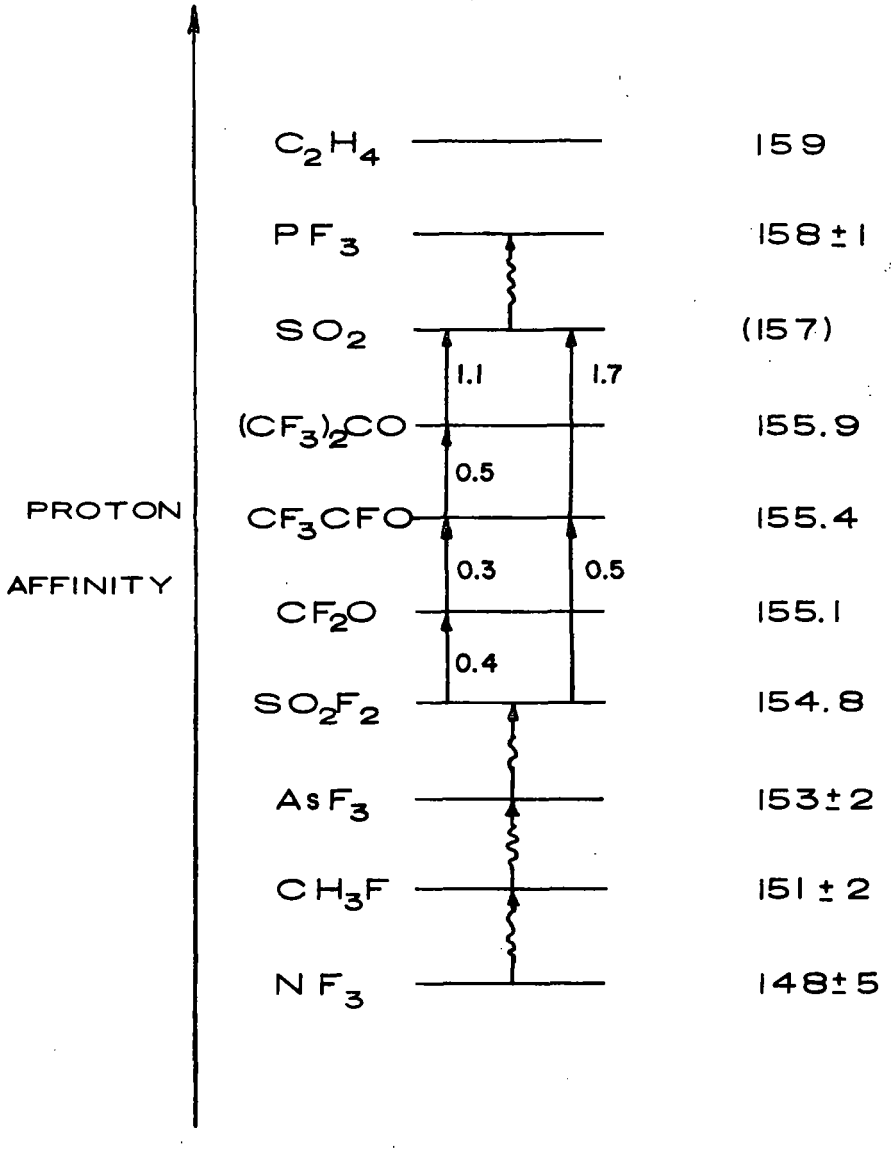


Fig. 1. Enthalpy changes for proton transfer equilibria studied and absolute proton affinities based on an assigned value of 157 kcal/mole for the proton affinity of SO_2. Straight arrows indicate equilibrium results. Curved arrows indicate equilibrium measurements were not possible but the exothermic direction of proton transfer was determined by ICR double resonance.

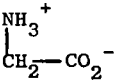
THE CHEMISTRY OF GLYCINE IN THE GAS PHASE: ACIDITY, BASICITY, STRUCTURE

by

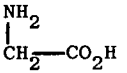
M.J.LOCKE, R.L.HUNTER, and R.T.McIVER, JR.
Dept. of Chem., Univ. of Cal., Irvine, CA 92717

Using pulsed equilibrium ion cyclotron resonance (ICR) mass spectrometry in a one-region trapped cell, we were able to determine the relative gas-phase acidities and basicities of glycine and three methyl substituted isomers of glycine.[1-3] These measurements allowed us to determine the sites of protonation and deprotonation of glycine, as well as the structure of the gas-phase neutral of glycine. In addition, by comparing the energetics of these gas-phase reactions with similar reactions in aqueous solution, the heats of solvation for the glycine ions have been determined.

It is well known that in the crystalline state and in aqueous solution glycine exists as a dipolar, or zwitterion. The nonionic structure of



zwitterion



nonionic

glycine in the gas phase has been discussed previously by several workers, although definitive data was heretofore unavailable.[4-7] Our preliminary work[3] on the acidity and basicity of glycine also indicated the nonionic structure. Our present work based on methyl substituent effects provides further proof of the existence of glycine in the gas-phase as the nonionic structure.

The nonionic form of glycine contains three types of hydrogen atoms. If one alkyl group (methyl in our studies) is substituted for one of these hydrogens, an increase in the gas-phase basicity is observed. The magnitude of the increase is proportional to the closeness of the substituted methyl group to the site of protonation of glycine. Thus, if glycine protonates on nitrogen, the largest increase is basicity is expected for sarcosine, with smaller increases expected for alanine and glycine methyl ester. Our results are shown in Figure 1, and support the proposition of the nonionic form protonating on nitrogen. Figure 2 shows the results of methyl substitution on the gas-phase acidity of glycine. The acidity data shows slight increases in the acidity for sarcosine and alanine, and a large decrease in acidity for glycine methyl ester. These results are consistent with the nonionic structure deprotonating at the carboxylate group. A more detailed discussion of alkyl substituent effects has recently been made by Taft, et al.[1]

The energetics of the gas-phase acidity and basicity of glycine can be compared to similar reactions in aqueous silution, as shown in Figure 3. Enthalpies for the various processes shown in Figure 3 have been determined as follows. The absolute proton affinity (basicity) of glycine as

determined by our ICR measurements is 214.9 kcal/mole. In aqueous solution the value for this reaction is 1.0 kcal/mole.[8] The enthalpy of solvation for neutral glycine (-19.4 kcal/mole) is obtained by combining the sublimation enthalpy[9] and the solution enthalpy of the neutral.[10] The solvation enthalpy for the proton (-270.1 kcal/mole)[11] can be combined with the above data to yield the single ion enthalpy of transfer (gaseous-phase→aqueous-phase) for the glycine cation (-75.6 kcal/mole).

The heterolytic bond dissociation enthalpy (acidity) of glycine in the gas-phase (343.0 kcal/mole) as determined by our ICR measurements[3] can be compared to the similar reaction in aqueous solution (10.6 kcal/mole).[8] This comparison combined with the solvation enthalpies noted above for neutral glycine (-19.4 kcal/mole) and the proton (-270.1 kcal/mole) yields the single ion enthalpy of transfer (gaseous-phase→aqueous-phase) for the glycine anion (-81.7 kcal/mole).

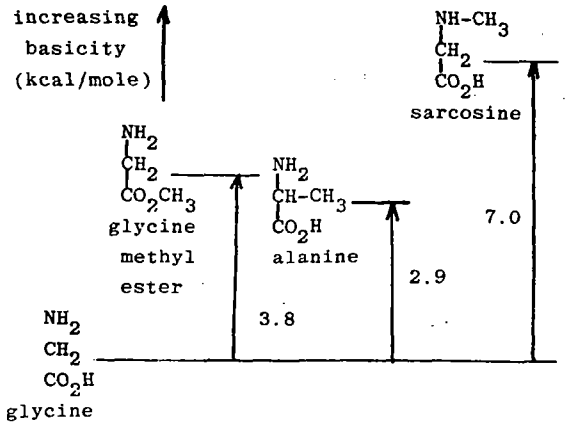


Figure 1. Effects of methyl substitution on the relative gas-phase basicity of glycine.

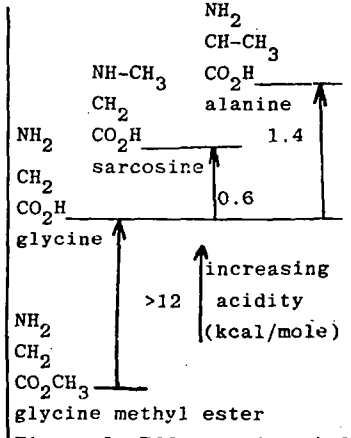


Figure 2. Effects of methyl substitution of the relative gas-phase acidity of glycine

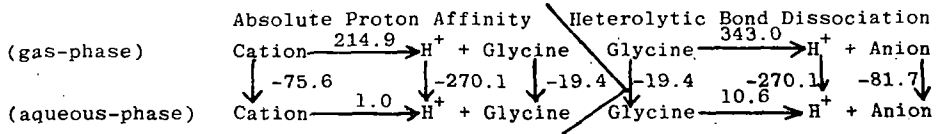


Figure 3. Thermodynamic values for gas-phase and aqueous-phase glycine.

References:

1) Taft,et al, JACS, 99, 5417 (1977).
2) McIver, Rev.Sci.Instr.,49, 111 (1978).
3) Locke, et al, JACS, 101, 272 (1979).
4) Svec, et al, JACS, 85, 839 (1963).
5) Grenie, et al, J.Chem.Phys., 53, 2980 (1970).
6) Brown, et al, J.S.S.Chem.Comm., 547 (1978).
7) Newton, et al, JACS, 100, 4329 (1978).
8) Greenstein, et al, Chem. of Amino Acids, Wiley,N.Y. 1961.
9) Friedman, et al, JACS 99, 4293 (1977).
10) CRC Handbook of biochem,CRC,Cleveland, OH.
11) DeLigny, Elecanal.Chem. Interfacial Electochem.57,265(1974)

WAMOC12 PROTON BOUND DIMERS: THERMOCHEMISTRY AND APPLICATIONS TO STEREOCHEMICAL ANALYSIS, T. L. KRUGER, G. M. McCLUSKY, D. CAMERON and R. G. COOKS, Dept. of Chemistry, Purdue University, W. Lafayette, IN 47907

Conjunction of low energy ion-molecule reactions for ion synthesis with high energy ion-molecule reactions for analysis provides new access to gas phase thermochemistry and structure. The species $A_1^- \cdots H^+ \cdots A_2^-$ and $B_1 \cdots H^+ \cdots B_2$ are generated by CI, mass-selected by MIKES and dissociated in high energy collisions. The resulting MIKE spectra provide a sensitive means of ordering acidities and basicities in the gas phase. Comparison of these results with those of strictly thermochemical methods for both gas phase and solution will be made. Experiments with these dimeric ions can also be used to distinguish stereoisomers, the species A_2 (or B_2) serving as a three dimensional probe of the structure of A_1 (or B_1). Examples are given where epimers can readily and sensitivitely be distinguished even in mixtures.

WAMOC13. BONDING ENERGIES AND RESONANCE STABILIZATION IN DIMER IONS OF POLYCYCLIC AROMATICS. M. MEOT-NER (MAUTNER), E.P. HUNTER, and F.H. FIELD, The Rockefeller University, New York, N.Y. 10021

Abstract

Dissociation energies ($\Delta H°_D$, kcal mol^{-1}) were measured for radical dimer ions $B^+ \cdot B$ and protonated dimer ions $BH^+ \cdot B$ of C_{10} (naphthalene) to C_{24} (coronene) polycyclic aromatic hydrocarbons. Bonding in the radical dimer ion is always stronger than in the corresponding protonated dimer. Interactions in the latter are assumed to be purely electrostatic; this is confirmed by measurements on asymetric dimers $B^+ \cdot A$. The stronger bonding in the symmetric radical dimer is than assigned to the resonance $B^+ \cdot B \longrightarrow B \cdot B^+$, and its magnitude is measured by $\Delta H°_{res} = \Delta H°_D (B^+ \cdot B) - \Delta H°_D (BH^+ \cdot B)$. $\Delta H°_{res}$ decreases with increasing molecular size, as intramolecular charge delocalization in B^+ makes intermolecular delocalization less significant. The measurements were made by ion-molecule equilibrium methods. Some experimental results: (B, $\Delta H°_D(B^+ \cdot B)$, $\Delta H°_D(BH^+ \cdot B)$, $\Delta H°_{res}$): benzene, 17.0, 11.0, 6.0; naphthalene, 17.8, 14.1, 3.7; biphenylene, 16.0, 13.6, 2.4; phenanthrene, 17.8, 15.7, 2.1; anthracene, 16.4, 16.0, 0.3; pyrene, 19.1, 16.5, 2.6; perylene 19.7, 19.1, 0.6; chrysene, 18.2, 17.8, 0.4; 1,12-benzoperylene, 21.6, 21.4, 0.2. (all kcal mol^{-1})

Paper No.: WAMOC 14

The Stabilities of Proton-Bound Dimers in the Gas Phase

L. D. Betowski, D. H. Aue, H. M. Webb and M. T. Bowers

Department of Chemistry, University of California, Santa Barbara
Santa Barbara, California 93106, U. S. A.

Ammonium ions and oxonium ions undergo efficient condensation reactions with neutral amines or oxides to form proton-bound dimer ions. The mechanism of these reactions has been investigated in detail to reveal that the proton-bound dimers are initially formed with excess vibrational energy which can be dissipated at high pressures to form stable dimer ions (Neilson, et al., 1978). Kebarle's group (1972, 1977) has directly measured equilibrium constants for reactions such as reaction (1) using high pressure mass

$$BH^+ + B \rightleftarrows BHB^+ \qquad (1)$$

spectrometry. Knowledge of the stabilities of these proton-bound dimer ions and of more highly condensed ions is basic to an understanding of the solvation.

Drift-cell ion cyclotron resonance experiments are carried out in a convenient pressure range for the stabilization and study of proton-bound dimers. In such experiments on mixtures of amines A and B, the proton-bound dimers in equation (2) appear to be in equilibrium, since their ratios remain constant with increasing pressure (Bowers, et al., 1971). From these experiments and those of Yamdagni and Kebarle (1973), a scale

$$AHA^+ \underset{A}{\overset{B}{\rightleftharpoons}} AHB^+ \underset{A}{\overset{B}{\rightleftharpoons}} BHB^+ \qquad (2)$$

of molecule-pair gas-phase basicities (MPGB's, Table I) can be constructed, where the MPGB of a pair of molecules A and B is defined as the negative of ΔG^o for reaction (3).

$$A + B + H^+ \rightleftarrows AHB^+ \qquad (3)$$

$$-\Delta G^o = \text{MPGB}; \quad -\Delta H^o = \text{MPPA}$$

Yamdagni and Kebarle's (1973) absolute MPGB's for dimethylamine and trimethylamine approximately agree with the relative values obtained in a series of equilibrium experiments for reaction type (2). This agreement and the self-consistency for overlapping thermodynamic cycles in the determination of relative MPGB's suggests that reaction (2) has indeed achieved equilibrium under drift cell ICR conditions (Aue, Betowski, Webb and Bowers, 1978, to be published; see also Taft, 1975).

The MPGB's in Table I have values that generally parallel the GB's of the amines involved. In some cases, however, steric effects play a significant role in determining MPGB's. For example, the MPGB of diisopropylamine is ca. 2 kcal/mol lower than that of piperidine, even though its GB is 3.5 kcal/mol higher.

TABLE I

Gas-Phase Basicities, Proton Affinities, Molecule-Pair Gas Phase Basicities and Molecule-Pair Proton Affinities of Amines at 25° C[a]

Compound	GB	PA	MPGB	MPPA[b]
NH_3	196.4	205.0	213.5[c]	229.8[c]
$MeNH_2$	205.7	214.1	220.4[c]	235.8[c]
Me_2NH	212.3	220.5	225.4[c]	241.3[c]
Me_3N	216.5	224.3	229.5[c]	246.8[c]
$MeNH_2$	205.7	214.1	219.8	235.7
Allyl NH_2	208.1	216.5	221.5	237.4
$EtNH_2$	208.7	217.1	222.1	238.0
n-$PrNH_2$	210.1	218.5	223.4	239.3
i-PrNH2	211.0	219.4	223.7	239.6
n-$BuNH_2$	210.6	219.0	224.2	240.1
i-$BuNH_2$	211.1	219.5	224.2	240.1
s-$BuNH_2$	212.1	220.5	224.9	240.8
Me_2NH	212.3	220.5	225.4	241.3
Pyridine	212.6	220.4	226.5	242.0
c-hexyl NH_2	212.9	221.3	226.6	242.5
Azetidine	214.5	222.7	228.7	244.6
MeNHEt	214.8	222.6	227.2	243.1
Pyrrolldine	216.1	224.3	229.9	245.8
Me_3N	216.5	224.3	228.3	244.6
Et_2NH	216.9	225.1	22818	244.7
Piperidine	2.7.2	225.4	230.2	246.1
Me_2NEt	218.8	226.6	229.7	245.6
i-Pr_2NH	220.7	228.9	228.4	244.3
N-Me-Piperidine	221.0	228.8	231.1	247.0

[a]All values in kilocalories per mole taken from Aue et al. (1978d). See also Taft (1975). Relative values based on MPGB of Me_2NH from Yamdagni and Kebarle (1973).

[b]Calculated from MPGB using an entropy term based on that fro Me_2NH($-T\Delta S^\circ$ = 15.9 kcal/mole) from Yamdagni and Kebarle (1973) and corrected for symmetry entropy differences

[c]Yamdagni and Kebarle (1973).

The Hydrogen Deuterium Kinetic Isotope Effect Bridge Between Mass Spectrometry and Electrochemistry

M. M. Green, G. Mayotte and L. Meites
Department of Chemistry, Clarkson College, Potsdam, New York 13676

Photochemical excitation, anodic oxidation and electron impact ionization all lead 2-hexanone to a reactive state in which a hydrogen atom is transferred from C-4 to the carbonyl oxygen.[1a,b,c] In the photochemical and mass spectrometric experiments this event leads to fragmentation of the rearranged molecule to produce propene and respectively, the enol of acetone and the cation radical of the enol of acetone.[2] This famous example of parallelism between mass spectrometry and photochemistry is sullied by the comparison of the hydrogen deuterium kinetic isotope effects which is nearly six[3] for the photochemically reactive triplet state and nearly one for the cation radical produced in the mass spectrometer.[4]

Because isotope effects may be reduced in magnitude by increasing the internal energy of the reacting molecules, as by raising the temperature,[5] the reduced isotope effect in the cation radical produced by electron impact could be assigned to a high internal energy residue left by the ionization process. Such a conclusion would be in conflict with the quasi-equilibrium theory of mass spectrometry[6] which predicts that a reaction with a slow pre-exponential factor and a low energy of activation should only occur from molecular cation radicals of low internal energy.[7] The McLafferty rearrangement under discussion here is a process which is characterized by these kinetic parameters.[1c]

An alternative explanation would relate the low isotope effect to the earlier transition state demands of the cation radical compared to the triplet as in the long known difference in isotope effect between chlorine atom and bromine atom abstraction of hydrogen or deuterium on the methyl group of toluene: the isotope effects are nearly one for chlorine atom and nearly five for bromine atom.[8] In further support of this notion the isotope effect for the γ-hydrogen abstraction of the primary amine cation radical intermediate of the Hofmann-Loeffler-Freitag reaction is 1.2 while the same reaction for the stabilized N-alkyl substituted amino group cation radical is 3.2.[9]

Because the anodic oxidation takes place in solution at known temperatures and therefore with known internal energy for the reactive 2-hexanone cation radical we have therefore reproduced Miller's electrochemical oxidation of 2-hexanone[1b] with deuterated material to measure k_H/k_D. In addition to isolation of the previously described γ-acetamedo-2-hexanone (1) we have also obtained a second new material 2,5 dimethyl-3-acetyl-Δ pyrroline (2)[10] substituted at the γ-position which is apparently the result of internal capture of the intermediate precursor to (1). Both (1) and (2) should show the same k_H/k_D. The intramolecular hydrogen transfer is expected to be, and is supported by Miller's evidence,[1b] as the rate determining step.

Table I presents the results of these electrochemical experiments. We have moreover subjected γ-deutero-2-hexanone to electron impact mass spectrometry at varied ionizing voltage and temperature and measured the deuterium to hydrogen ratio of the $[C_3H_6O]^{\cdot+}$ product of the McLafferty rearrangement. These data are presented in Table II.

Table I [a,b]

Isotope Effect (k_H/k_D)

	1	2
0°C	1.27±.14	1.24±.10
20°C	1.47±.10	---
40°C	1.38±.19	1.28±.12

a. The deviations are the precision of a few runs taken over some months;
b. The oxidations were conducted in an H-cell at +2.3V following Miller[1b] except that $LiBF_4$ was the supporting electrolyte. The products were separated and collected by extraction followed by GC on SE-30.[10]

Table II [a]

Isotope Effect (k_H/k_D)

temp/ev	50°C	75°C	125°C
10 ev	1.4±.15	1.4±.15	1.5±.15
70 ev	1.6±.1	---	1.6±.1

a. Ratios of m/e 58 to m/e 59 as shown corrected for ^{13}C contribution; Electron voltages are uncalibrated (ev); temperatures are of the ion source, the inlet was at room temperature. Measured on a DuPont 21-490 mass spectrometer.

Inspection of the isotope effects in Table I and II show the numbers in almost all cases to be within experimental error and in the remainder to be nearly so. These observations are consistent with the thesis that the low isotope effect in the mass spectrometer does not derive from high internal energy of the cation radicals produced via electron impact.[11] The correspondence is remarkable and draws one to the difficult conclusion that 2-hexanone cation radical demands the same transition state for γ-hydrogen abstraction in vacuum as in the complex solvent medium of an electrochemical cell. The molecular cation radicals undergoing the McLafferty rearrangement in the mass spectrometer cannot be distinguished from thermal molecules in their discrimination for hydrogen over deuterium.[12]

References

1. (a) P. J. Wagner, Acc. Chem. Res. 4, 168 (1971) discusses the nature of this process and gives leading references to the earlier literature; (b) Y. J. Becker, L. R. Byrd, L. L. Miller and Y-H. So, J. Amer. Chem. Soc. 97, 853 (1975); (c) D. G. I. Kingston, J. T. Bursey and M. M. Bursey, Chem. Revs. 74, 215 (1974) is a review of these observations.

2. See 1(a) above and S. Meyerson and J. D. McCollum, in "Advances in Analytical Chemistry and Instrumentation," Vol. 2, Wiley, New York, 1963, p. 184 ff. and the references in 1(c) above.

3. D. R. Coulson and N. C. Yang, J. Amer. Chem. Soc. 88, 4511 (1966); A. Padwa and W. Bergmark, Tetrahedron Lett., 5795 (1968); F. D. Lewis, J. Amer. Chem. Soc. 92, 5602 (1970).

4. See 1(c) above and J. K. MacLeod and C. Djerassi, ibid 89, 5182 (1967).

5. For a general treatment of these effects see: K. B. Wiberg, Chem. Revs. 55, 713 (1955); L. Melander, "Isotope Effects on Reaction Rates," Ronald Press, N.Y. 1960; F. H. Westheimer, Chem. Rev. 61, 265 (1961); R. P. Bell, Chem. Soc. Revs. 3(4), 513 (1974); C. J. Collins and N. S. Bowman, "Isotope Effects in Chemical Reactions," ACS monograph 167, Van Nostrand, 1970.

6. H. M. Rosenstock, M. B. Wallenstein, A. L. Wahrhaftig and H. Erying, Proc. Natl. Acad. Sci. USA 38, 667 (1952).

7. D. H. Williams and I. Howe, "Principles of Organic Mass Spectrometry," McGraw-Hill, 1974, Ch. 4.

8. See K. B. Wiberg, in reference 5 herein.

9. M. M. Green, J. M. Moldowan, M. W. Armstrong, T. L. Thompson, K. J. Sprague, A. J. Hass and J. J. Artus, J. Amer. Chem. Soc. 98, 849 (1976) and references therein.

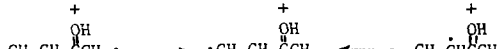
10. Details of this work are available in the M.Sc. Thesis of G. Mayotte, Clarkson College, 1979.

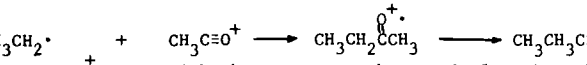
11. M. M. Green, T. J. Mangner, S. P. Turner and F. J. Brown, J. Amer. Chem. Soc. 98, 7082 (1976); M. M. Green, R. J. Giguere and J. R. P. Nicholson, ibid 100, 8020 (1978).

12. The independence of temperature for k_H/k_D in both systems (Table I and II) is consistent with recent results and predictions for bent transition states. See: H. Kwart, D. A. Benko and M. E. Bromberg, J. Amer. Chem. Soc. 100, 7093 (1978) and references therein.

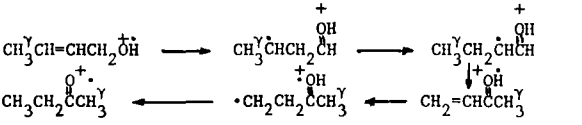
DECOMPOSITIONS OF METASTABLE $C_4H_8O^{+\cdot}$ IONS. D.J. McAdoo, C.E. Hudson, and D.N. Witiak, University of Texas Medical Branch, Galveston, Texas.

The observation of strong metastable losses of methyl and ethyl from ionized n-butanal prompted us to investigate the metastable decompositions of other $C_4H_8O^{+\cdot}$ ions (Table I). Previous work[1,2] has demonstrated that the enolic 2-butanone ions decompose as follows:



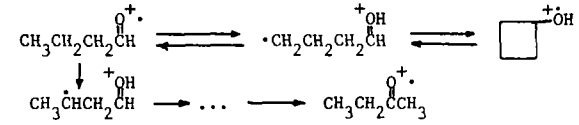


Most $C_4H_8O^{+\cdot}$ ions with the oxygen on the terminal carbon showed strong losses of methyl, ethyl and water and a weak loss of C_2H_4 (Table 1). The energies released in the metastable decompositions of the first fifteen ions in Table 1 are in the range 0.02-0.03 eV. The energy releases and metastable decomposition patterns are similar enough to be consistent with the rearrangement of the ions with the oxygen on the terminal carbon (except $(CH_3)_2\dot{C}C(=\overset{+}{O}H)H$ and  $CH_2\overset{+}{O}H$) to a common intermediate prior to their decompositions. Deuterated forms of the ions with the oxygen on the first carbon showed complementary labeling patterns in their losses of methyl and ethyl (Table 2), demonstrating that the losses of methyl and ethyl take place via the 2-butanone ion. Deuterated forms of $CH_3\dot{C}HCH_2C(=\overset{+}{O}H)H$ and $CH_3CH=CHCH_2\overset{+}{O}H$ lost the terminal methyl and its complementary ethyl in about half of their losses of methyl and ethyl, and methyl containing three of the hydrogens on carbons 1,2 and 3 and the complementary ethyls in the other half. Hydroxyl deuteriums were lost only in the ethyl. $CH_3CH=CH^{13}CH_2\overset{+}{O}H$ lost only $^{12}CH_3$ and $^{12}C_2H_5$, indicating that the initial carbon-oxygen bond is not broken, contrary to earlier conclusions.[3] The apparent scrambling between carbons 1,2 and 3, nonscrambling at C-4 and loss of the terminal methyl and its complementary ethyl are rationalized as follows:



We have not devised a satisfactory mechanism for the remaining losses of methyl and ethyl.

$CD_3CH_2CH_2\overset{+\cdot}{O}CH$ undergoes intense scrambling of its methyl, and loses $CH_3\cdot$, $CH_2D\cdot$, $C_2H_5\cdot$ and $C_2H_4D\cdot$ at similar rates. We rationalize these observations by the following rearrangements:



The 5-membered ring hydrogen rearrangement is proposed based on an analogous process in butanoic acid ions.[4]

Acknowledgments: The Robert A. Welch Foundation (Grant H609) provided financial support and Professor Michael Gross and the NSF Mass Spectrometry Center at the University of Nebraska assisted with energy release measurements.

Table 1. The Decompositions of Metastable $C_4H_8O^{+\cdot}$ Ions

Ion	Source	$-CH_3$	$-C_2H_5$	$-H_2O$	$-C_2H_4$
$CH_3C(=\overset{+}{O}\cdot)CH_2CH_3$	2-butanone	83	100		
$\cdot CH_2CH_2C(=\overset{+}{O}H)CH_3$	1-methylcyclopentanol	92	100	3	1
$CH_3CH_2C(=\overset{+}{O}H)CH_2\cdot$	3-heptanone	73	100	1	<1
$CH_3\dot{C}HC(=\overset{+}{O}H)CH_3$	3-methyl-2-heptanone	100	88	<0.5	<0.3
$CH_3CH(\overset{+}{O}H\cdot)CH=CH_2$	3-buten-2-ol	100	74	3	<1
$^{+}CH_2CH_2CH(OH)CH_2\cdot$	1-hepten-3-ol	73	100	4	1
$CH_3CH_2\dot{C}HC(=\overset{+}{O}H)H$	2-ethylbutanal	100	40	16	4
$CH_3\dot{C}HCH_2C(=\overset{+}{O}H)H$	3,4-dimethylcyclopentanol	100	55	18	5
$CH_3CH=CHCH_2\overset{+}{O}H$	2-buten-1-ol	100	55	20	3
$CH_3CH_2CH_2C(=\overset{+}{O}\cdot)H$	n-butanal	100	52	23	4
$\overbrace{CH_2CH_2CH_2}CH\overset{+}{O}H$	cyclobutanol	100	58	19	4
$CH_2=CHCH_2CH_2\overset{+}{O}H$	3-buten-1-ol	100	45	17	2
$CH_3CH(CH_3)CH\overset{+}{O}\cdot$	2-methylpropanal	100	69	32	4
$CH_2=C(CH_3)CH_2\overset{+}{O}H$	2-methyl-2-propen-1-ol	100	50	18	3
$(CH_3)_2CCH=\overset{+}{O}H$	2,2-dimethylbutanal	63	<40	7	100
$\overbrace{CH_2CH_2}CHCH_2\overset{+}{O}H$	cyclopropylmethanol	98	17	<10	100

Table 2. The Decompositions of Metastable $C_2(H,D)_8O^{+\cdot}$ Ions

Ion	$-CH_3$	$-CH_2D$	$-CHD_2$	$-CD_3$	$-C_2H_5$	$-C_2H_4D$	$-C_2H_3D_2$	$-C_2H_2D_3$
$CH_3CH(\overset{+}{O}D\cdot)CH=CH_2$	100	<1			3	90		
$CH_3CD(\overset{+}{O}H\cdot)CH=CH_2$	100	8			3	90		
$CH_3\dot{C}HCH_2C(=\overset{+}{O}D)H$	100	<0.4			5[a]	52		
$CH_3\dot{C}HCH_2C(=\overset{+}{O}H)D$	100	48			25[a]	62		
$CH_3\dot{C}HCD_2C(=\overset{+}{O}H)H$	100	42	41		24[a]	24[a]	53	
$CH_3\dot{C}HCD_2C(=\overset{+}{O}H)D$	100	27	66		17[a]	35[a]	13[a]	64
$CH_3CH=CHCH_2\overset{+}{O}D$	100	1			0.6[a]	36		
$CH_3CH=CHCD_2\overset{+}{O}H$	100	55	26		24[a]	31[a]	66	
$CD_3CH=CHCH_2\overset{+}{O}H$	65	7	19	100	88[a]	12[a]	5[a]	27
$CH_3CH_2CD_2CH\overset{+}{O}\cdot$	100	88	28		24[a]	51[a]	51[a]	
$CD_3CH_2CH_2CH\overset{+}{O}\cdot$	35	100	77	17	a	33[a]	39	11
$\overbrace{CH_2CH_2CH_2}CH\overset{+}{O}D$	100	67				40[a]	53	
$\overbrace{CH_2CH_2CH_2}CD\overset{+}{O}H$	100	38				26[a]	77	
$CH_2=CHCH_2CH_2\overset{+}{O}D$	100	72				45[a]	58	
$CH_2=C(CH_3)CH_2\overset{+}{O}D$	100	0.7				3[a]	39	

a. Contains small contributions from loss of $C_2(H,D)_4$

1. D.J. McAdoo, F.W. McLafferty and T.E. Parks, J. Am. Chem. Soc., 94, 1601 (1972).
2. B. Grant and C. Djerassi, J. Am. Chem. Soc., 96, 3477 (1974).
3. D.J. McAdoo, C.E. Hudson and D.N. Witiak, Org. Mass Spectrom., 1979 (in press).
4. D.J. McAdoo, D.N. Witiak, F.W. McLafferty and J.D. Dill, J. Am. Chem. Soc., 100, 6639 (1978).

A FINNIGAN 4000 MS INTEGRATED THERMAL DESORBER FOR AIR-SAMPLING CARTRIDGES, R. Narang and PAUL P. DYMERSKI, Division of Laboratories and Research, New York State Department of Health, Albany, NY 12201. J. KNIGHT, Finnigan Corp., Sunnyvale, CA 94086

The capillary injector port of a Finnigan 9610/4000 GC/MS was modified to permit insertion of thermal-desorption air-sampling cartridges for "trapped volatiles" analysis (Fig. 1). The GC microprocessor-controlled "Grob" valving automates sample desorption (Fig. 2), giving reproducible desorption efficiencies and retention times.

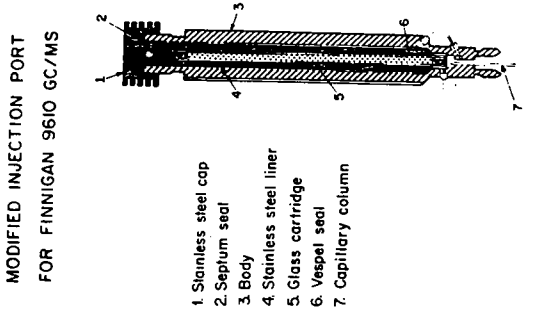
Two cartridge packing materials were tested. Tenax is well accepted but has low breakthrough volumes for very volatile compounds (Table 1). Porapak N, on the other hand, retains very volatile compounds two to four times better than Tenax. These values were determined by sampling a known volumn of a generated standard atmosphere, eluting the cartridge with methanol, and quantitating by GC/ECD.

Thermal desorption of Porapak N just below its decomposition temperature (170°C) is incomplete for compounds with boiling points above 80°C. Relative to a direct standard injection, Tenax shows no boiling point effect; its best desorption temperature is 220. The minimum detection levels at the breakthrough volume, assuming a 10ng quantitation level, are listed in Table 1. For Porapak N these values are corrected for the desorption efficiency. For thermal desorption of compounds more volatile than benzene Porapak N is clearly the preferred packing. For methanol-elution analysis Porapak N is equal to or better than Tenax with volatile and semivolatile compounds, including naptha-lene.

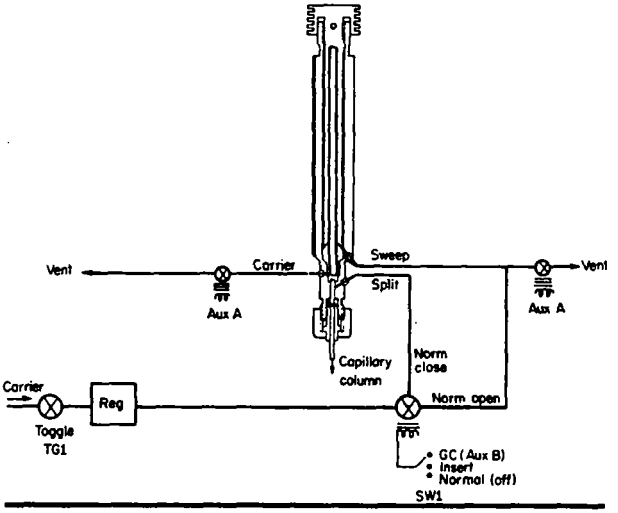
This system was applied to several hundred samples and standards using a SF96 WCOT glass-capillary column (oven temperature during desorption was -30°C), a SP 2250 DA packed column for semivolatiles, and more recently a Carbopak C/0.1% SP1000 packed column. In each case retention times were reproducible, and quantitation results were linear to 500 ng of cartridge loading for each compound.

Design and Operation: The capillary injection port of the gas chromato-graph was modified, courtesy of Finnigan Corp., to accept 1/4" OD X 4" glass tubes. This was accomplished by replacing the standard septum cap, glass, spring, and metal inserts of the injection port with a one-piece cap and liner (Fig. 1). The liner and the injection-port housing were beveled at the bottom edges to accomodate a double-ended Vespel ferrule. The insert was designed to make a gas-tight seal simultaneously at the lower end of the glass tube and at the cap. Conversion between normal injection and cartridge takes less than a minute.

A three-way automatic valve under microprocessor control was added to the carrier gas stream to reroute the carrier gas through the SWEEP line during desorption. With the Vespel seal in place carrier gas is forced through the glass trap and onto the column head. At the end of the desorption cycle the carrier gas is routed through the SPLIT inlet at the base of the port, sweeping the port clean to reduce tailing while maintaining a column flow of 25 ml/min for packed column.



CARTRIDGE DESORPTION
FINNIGAN 9610 GC



FLOW ROUTE

	Insert	Desorb	Separate
Carrier	Off	Off	Off
Sweep	Off	Carrier	Vent
Split	Off	Off	Carrier

Table I. Volatile Organics

Compound	Breakthrough Volume[a] Porapak N	Tenax	Minimum Detectable level (ng/m^3)[b] Porapak N	Tenax
Benzene	54	27	300	370
Toluene	>67	120	<3000	83
Chlorobenzene	>67	230	∞	44
Dichlorobenzene	>67	450	∞	22
Dichloromethane	27	4	370	2500
1, 2 Dichloroethane		15		667
Tetrachloromethane	40	10	250	1000
1, 1, 1, Trichloroethane	40	7	250	1428
Trichloroethene	47	25	213	400
Tetrachloroethene	60	100		100
Trichloromethane	33	12	300	934
Chloroethene	>67		∞	
Bromodichloromethane	40	300	500	33
Ethylbenzene	>67	650	<450	15

[a] Liters/0.5-g cartridge at 27°C; elution with methanol.

[b] Corrected for thermal desorption efficiency and assuming 10-ng quantitation limit.

A TANDEM DOUBLE-FOCUSING MASS SPECTROMETER FOR CA/MS AND MS/MS STUDIES

P. J. Todd, D. C. McGilvery, M. A. Baldwin, G. J. Wendel
M. R. Wixom and F. W. McLafferty

Department of Chemistry, Baker Laboratory,
Cornell University, Ithaca, New York 14853

This instrument consists of an Hitachi RMH-2 double-focusing mass spectrometer (MS), a special ion acceleration and collision region, and a second double-focusing MS, controlled by a DEC PDP 11/45 computer.[1] It is now operational except for the second magnetic sector. The high-resolution (∿50,000) primary ion beam is accelerated to 30 KV with a triple-element ion lens and focused on a collision region consisting of an orthogonal molecular beam (<40 μm thick ribbon) of helium. This collisional activation (CA) produces secondary ions which are focused on the entrance slit to the second ESA with a similar lens.

The narrow collision region and higher energies have resulted in greatly improved sensitivity and resolution for CA mass spectra. CA of 7.2 KV CH_4^+ ions give a total yield of 8% for the fragment ions C^+ - CH_3^+. Higher accelerating potentials increase CA ion yields especially for ions formed by high energy processes. Complete resolution of the C_5^+ - $C_5H_6^+$ region of the CA spectrum of $C_7H_8^+$ ions from toluene can be achieved at 18.8 KV accelerating potential, despite the severe energy-release broadening.

The high resolution and mass range of the primary ion beam have greatly extended the applicability of the instrument to important ion structure problems and to complex mixture analysis by MS/MS. For example, the 70 eV EI mass spectrum of 5-methyl-3-hexanone produces significant $C_4H_9^+$ ($\underline{m}/\underline{z}$ 57.070) and $C_3H_5O^+$ (57.034) ions; the CA spectrum of the $C_3H_5O^+$ on this instrument showed <2% contribution of $C_4H_9^+$.

[1] F. W. McLafferty in "Analytical Pyrolysis", C.E.R. Jones and C. A. Cramers, Eds., Elsevier Amsterdam, 1977, pp. 39-48.

QUADRUPOLE ION STORE
CHARACTERIZATION AND APPLICATION

M.A. Armitage, J.E. Fulford, R.J. Hughes and R.E. March.
Department of Chemistry
Trent University
Peterborough, Ontario, Canada, K9J-7B8.

The quadrupole mass filter [1], the related monopole mass spectrometer [2] and the quadrupole ion storage trap (QUISTOR) [3] are analyzers which employ the criterion of ion path stability in radiofrequency electric fields. The geometry of the QUISTOR, which was first described [4] in 1953, is, in effect, that of a hyperboloid of one sheet combined with a hyperboloid of two sheets forming the ring and end-cap electrodes, respectively. In order to conform to the Laplace condition that the field gradient is uniform throughout the interior of the device ($\nabla^2\phi=0$) the inscribed circle of the quadrupole (radius r_0) becomes an ellipsoid with half axes r_0, z_0 such that $r_0^2=2z_0^2$.

The principle of operation of the QUISTOR is analagous to that of the two dimensional quadrupole. The two endcaps are electrically connected together and DC/RF potentials are applied between them and the ring electrode. Due to the asymmetry of the device the restoring force on an ion with respect to motion in the z-direction is twice that in the r-direction. The equations of motion for ions in the QUISTOR take the general form of the Mathieu equation

$$\frac{d^2u}{d\xi^2} + (a_u - 2q_u \cos 2\xi)u = 0 \qquad (1)$$

where u=r or z; $q_z = -2q_r = \frac{-4eV}{mr_0^2\Omega^2}$; $a_z = -2a_r = \frac{-8eU}{mr_0^2\Omega^2}$ and $\xi = \frac{\Omega t}{2}$; U is the DC voltage, V is the o-p RF voltage, m/e is the mass-to-charge ratio and Ω is the radial frequency of the RF voltage. The limits of stability may thus be defined in terms of a and q, and expressed as a stability diagram. Ions are created by electron bombardment of sample molecules within the device. The normal working pressure range is 0.1 to 10^{-4} Pa. Ion detection may be effected either by resonance absorption of auxiliary RF power applied to the endcaps or by ejection of the ions on to an electron multiplier.

QUISTOR Characterisation.

Experimental stability diagrams have been obtained for assemblies of ions under a variety of storage conditions. The diagrams are shifted in a,q space with respect to the theoretical diagram. The magnitude of this shift is related to the space charge of the stored ions. The motion of stored ions may be characterized by secular frequencies, ω_r and ω_z, in the r- and z-directions, respectively, where $\omega = \beta\Omega/2$ and β is approximately equal to $(a + q^2/2)^{\frac{1}{2}}$. The magnitude of the space charge of an assembly of ions, and hence the number of ions stored can be determined from the differences between observed and theoretical secular frequencies.

Monte Carlo calculations have been applied to the study of ionic motion

in the QUISTOR, with charge exchange and momentum exchange collisions permitted. The results suggest that ions migrate collisionally towards the centre of the device with a corresponding increase in extraction efficiency and a decrease in ion kinetic energy. In the two ion simulation model, charge exchange between Ne^+ and carbon dioxide competes with ion migration and can mask the migration of Ne^+.

QUISTOR Applications.

(i) Under total ion storage (a=o), the QUISTOR is a reactor for the study of negative and positive ion/molecule reactions. For the determination of rate constants, reactions mechanisms and equilibria the QUISTOR is mounted in place of the ion source of a conventional quadrupole mass filter.

(ii) The QUISTOR may be operated in a mass selective ion storage mode [5]. Applied potentials are chosen to yield pairs of a,q values close to either the upper or lower apex of the stability envelope, i.e. only ions of one particular mass are stable at any one time. A mass spectrum is generated by varying U and V at a constant ratio of U/V such that for each mass the a,q co-ordinates move along a locus described as a scan line.

(iii) In a mixed mode, spatial separation of the RF and DC voltages combined with a pulsed DC potential permits operation of the QUISTOR in a mass selective mode with relaxation to a total ion storage mode. In this mode the QUISTOR may act as a specific ion reactor. [6]

(iv) Stored ions may be selectively excited and ultimately ejected from the QUISTOR by irradiation at the secular frequency ω. As the resonant excitation is mass dependent, the technique of QUISTOR resonant ejection (QRE) is similar to ion cyclotron double resonance (ICDR). Resonant perturbation of precursor ions can be used to identify precursor-to-product ion dependencies for the elucidation of reaction mechanisms. QRE may be employed to isolate a single reactant ion species, e.g. Ar^{2+}, for study of partial charge transfer reactions.[7]

(v) Cylindrical ion storage traps have been investigated. The potential within the cylindrical ion store has been derived. Potential distributions have been calculated numerically and compared with those of the QUISTOR. In a collaborative programme with J.F.J. Todd et al of the Univ.of Kent, Canterbury, U.K., stability diagrams have been determined for 3 different cylindrical ion stores and operation of cylinders in the mass spectrometric mode has been demonstrated. Resonant ion ejection has been used for the elucidation of reaction mechanism e.g. in the formic acid-water system.[8]

REFERENCES:

1. W.E. Austin, A.E. Holme and J.H. Leck in P.H. Dawson (Ed.), Quadrupole Mass Spectrometry and Its Applications, Elsevier, Amsterdam, 1976, Ch. VI.
2. R.F. Herzog in P.H. Dawson (Ed.)s Quadrupole Mass Spectrometry and Its Applications, Elsevier, Amsterdam, 1976, Ch. VII.
3. J.F.J. Todd, G. Lawson and R.F. Bonner, in P.H. Dawson (Ed.), Quadrupole Mass Spectrometry and Its Applications, Elsevier, Amsterdam, 1976, Ch. VIII.
4. W. Paul and H. Steinwedel, Z. naturf., 1953, 8a, 448; U.S. Patent 2939 952, 7 June 1960
5. R.E. Mather, R.M. Waldren and J.F.J. Todd, in Dynamic Mass Spectrometry Vol. 5 (Ed. D. Price and J.F.J. Todd), Heyden, London, 1978.
6. J.E. Fulford and R.E. March, Int. J. Mass Spectrom. Ion Phys. 26 (1978) 155.
7. M.A. Armitage, J.E. Fulford, D.N. Hoa, R.J. Hughes and R.E. March. Can. J. Chem.
8. R.F. Bonner, J.E. Fulford, R.E. March and G.F. Hamilton, Int. J. Mass Spectrom. Ion Phys., 24 (1977) 255.

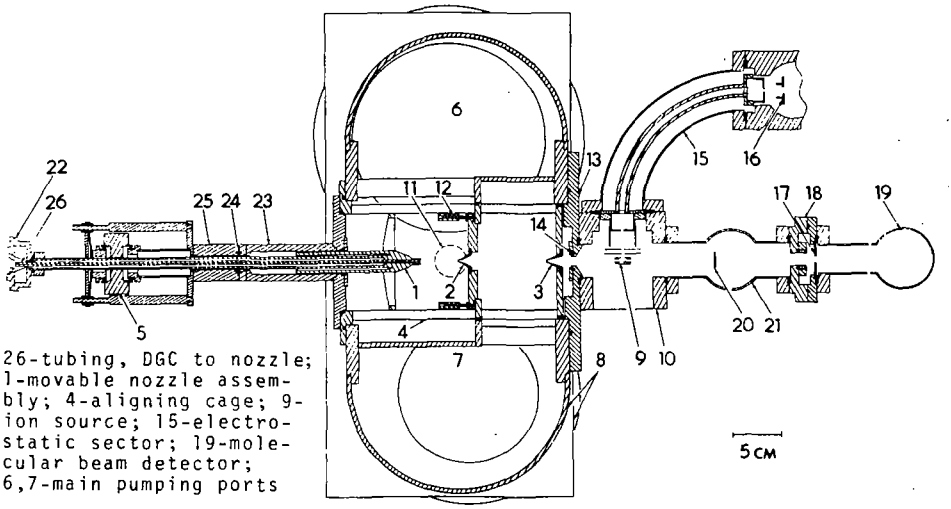
DESIGN OF A DENSE GAS CHROMATOGRAPH/MASS SPECTROMETER INSTRUMENT FOR INVOLATILE SAMPLE ANALYSIS

L.G. Randall and A.L. Wahrhaftig
Department of Chemistry, University of Utah
Salt Lake City, Utah 84112

A new instrument has been developed for involatile sample analysis by MS: a dense gas chromatograph/mass spectrometer (DGC/MS). The preliminary results along with pertinent aspects of dense gas chromatography (DGC) are outlined in paper TAMOA 11 of this conference.

A supersonic molecular beam was deemed the most promising interface for a DGC/MS instrument because of its characteristics of fast expansion, collisionless transport, high to low pressure capability, low temperatures, and centerline concentration of heavy components in light/heavy mixtures. Because solute solubility is such a sensitive function of solvent gas pressure, the system requires that essentially all the pressure drop occur at the nozzle orifice. With further design assumptions of small DGC volume for safety and construction ease, implementation of 0.5 mm I.D. capillary tubing, and no sample splitter, the result is that the nozzle diameter must give a gas flow rate appropriate for a DGC column without overloading the molecular beam expansion chamber pumping system.

Figure 1 is a schematic of the molecular beam interface and the MS. A modified, double focusing PE-270 is used. The molecular beam is also detected by an ion gauge placed on the beam axis. The interface housing has several functions: precise alignment and coupling of the molecular beam system with the MS, vacuum isolation of the various chambers, support for the diffusion pumps and associated equipment, and compact placement of those pumps with short, high-conductance leads. There are two vacuum locks; one provides differential pumping across the sliding o-ring seal of the nozzle assembly, and both plus a shared slide valve allow nozzle subassembly removal without system pressurization.



26-tubing, DGC to nozzle; 1-movable nozzle assembly; 4-aligning cage; 9-ion source; 15-electrostatic sector; 19-molecular beam detector; 6,7-main pumping ports

Figure 1: Cross Section of Interface

Solvent gas is supplied to the DGC from a thermostatted dense gas supply which compresses and stores cylinder gas and which has a maximum pressure of 270 atm. Nozzle assembly movement (below) requires chromatograph movement so all DGC components are mounted on an open frame suspended in a stationary, thermostatted water bath. Figure 2 shows the components.

DGC effluent is expanded through a nozzle into vacuum forming a supersonic jet. A skimmer removes the central core of the jet to form a beam of unidirectional molecules which travels with further definition by the collimator to the MS source. The three beam generating components are mounted in and aligned by an open cage-like structure which allows unimpeded pumping of the nozzle exit region and provides vacuum isolation of the various regions from each other (including the MS). Presently the pumping speed on the nozzle-skimmer expansion chamber is 2400 ℓ/sec and on the skimmer-collimator chamber, 1200 ℓ/sec. This speed limits the dense gas pressure to 120 atm with a 12.5 μm nozzle diameter.

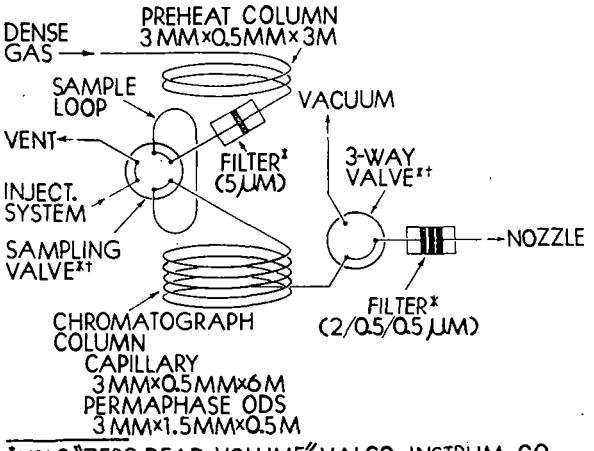


Figure 2: Dense Gas Chromatograph

The heart of the molecular beam interface is a commercial laser-drilled pinhole mounted as a converging nozzle. Several diameters have been used: 100, 25, 12.5 and 5 μm. The nozzle design permits a wide choice and easy replacement of orifices. The nozzle assembly (Figure 3) provides leak-tight clamping of the pinhole foil; alignment with the skimmer, collimator, and ion source; an adjustable, measured nozzle-skimmer separation up to 70 mm; and water circulation from the DGC bath to within 5 cm of the orifice. There are several considerations in skimmer design: small external angle, large internal angle, sufficient height, a sharp-edged orifice, and easy removal. Less care is needed in collimator design because of the low pressure in the skimmer-collimator region ($\leq 10^{-4}$ torr); recent experiments used an orifice in a flat plate.

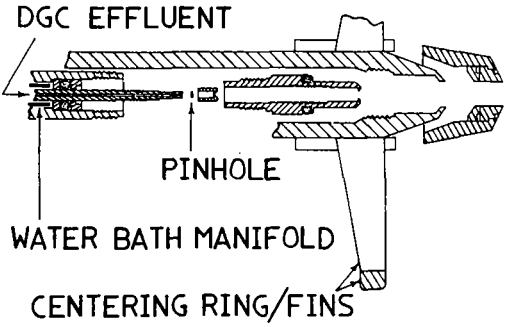


Figure 3: Nozzle Assembly

The results presented in paper TAM0A 11 prove the feasibility of DGC/MS which promises to be a compromise between HPLC/MS and GC/MS with unique properties. Besides analytical chromatography applications, it will be useful for species identification and monitoring in high pressure reactions and extractions which are becoming important in the fuel (coal gasification, extraction; ore extraction), pharmaceutical and food industries. This instrument has advantages for areas other than DGC/MS: 1. provides a molecular beam source with easily varied stagnation conditions, a wide variety of cheap nozzle orifices, and easily seeded species; 2. allows determination of mass spectra of involatile and/or thermally labile compounds; 3. provides cold, isolated molecules for MS without special ion source designs; and 4. extends the range of molecular beam sampling to much higher pressures both for MS and other purposes than heretofore commonly used.

Multiple Ion Detection at 10,000 Resolution

With a Modified AEI MS 902S

D. A. Durden,
Psychiatric Research Division,
University Hospital,
Saskatoon, Saskatchewan,
Canada S7N 0X0

We have recently modified an AEI MS 902S double focussing mass spectrometer so that its accelerating and electrostatic analyser potentials can be controlled by an externally generated 10 volt signal for use with a multiple ion detector controller.

In the original circuit, the electrostatic analyser reference is a floating power supply or battery (fig. 1). For external control, a centre grounded power supply is required and this necessitated redesigning the way in which the decade box controls the ESA and accelerating voltages during peak matching. The decade resistance is placed on the input of a high impedance inverting amplifier so that the output voltage is inversely proportional to the decade reading. Thus the original peak matching equation M (high) = M (low) (1 + decade) can be used, for conventional mass measurements, or to verify the reference ion to be used for MID. The ESA voltages in the new system are derived from a VG organic 70-70 ESA supply modified so that a 10 V input gives ± 250 V out, and the accelerating voltage is obtained from a Spellman RHSR 10 PN 60 power supply which gives 8000 V output for 10 V input. The 10 V reference signal may be generated in three ways: from a 10 V reference in the ESA supply, from an Analog Devices AD 2700 precision reference, or from the 0 to 10 V output of a VG digital MID controller which is attached to the VG 2000 Data System.

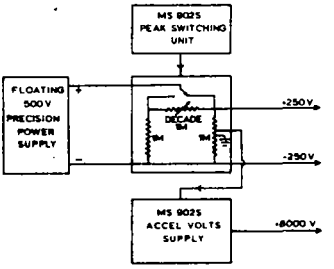
The stability of the system is better than 5 ppm/sec and the drift less than 20 ppm/h. These figures enable resolutions up to at least 10,000 to be used during multiple ion detection or peak matching. The ability to focus on ions over a wide mass range is limited only by the slew rate of the Spellman power supply. Using 0.5 sec voltage steps, a 10% mass change causes a 10 ppm error in the observed mass. At 30% this is 30 ppm and at 50% is 60 ppm. Under low resolution conditions (1000 resolution) shorter step times (0.1 sec) may be used as the peaks are flat topped.

Fig. 4 illustrates the use of high resolution MID for the analysis of meta and para-hydroxyphenyl acetic acids as their methyl-heptafluorobutyrate derivatives using deuterated internal standards. The detection of the following ionic species is shown: $C_{13}H_9O_4F_7$, m/e 362.0389 due to the molecular ion of the proton acids, $C_{13}H_5O_4F_7D_4$, m/e 366.0640, due to the meta standard, $C_{13}H_4O_4F_7D_5$ due to the para standard and $C_8F_{14}9$, m/e 375.9807 from the mass reference PFTBA. Two methods of observing the ions are possible. In fig. 4a, a narrow scan is superimposed on the steps so that the ion profiles are visible and the masses may be verified by observation of their superpositions on an oscilloscope. Alternately, only the peak tops may be detected (fig. 4b). The derivatives were separated on an SGE OV17 40 m x 0.50 mm SCOT column, which is capable of separating the protonated and deuterated species as well as the meta and para isomers.

Acknowledgements

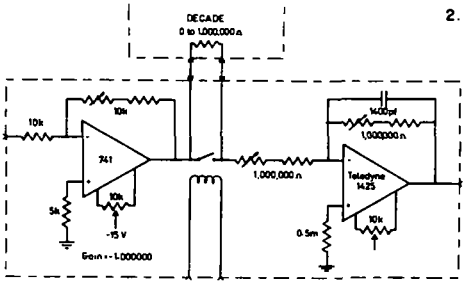
I wish to acknowledge the assistance of P. Hoiland and E. Johnson for technical assistance, and Saskatchewan Health, Province of Saskatchewan and the Medical Research Council of Canada for financial support.

1.



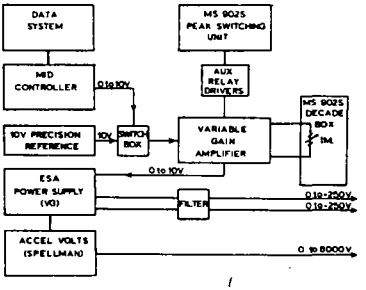
ORIGINAL ESA and ACCELERATING VOLTAGE CONTROL

2.



VARIABLE GAIN AMPLIFIER

3.



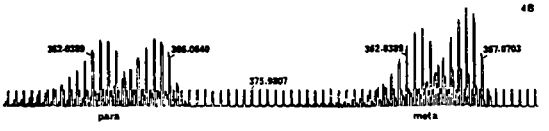
NEW ESA and ACCELERATING VOLTAGE CONTROL

4A



MID with 100 ppm scan; Resolution 120 ppm

4B



MID without scan; Resolution 120 ppm

A RF-ONLY QUADRUPOLE MASS FILTER

P.H. Dawson, M. Meunier and Wing-Cheung Tam

Division of Physics, National Research Council
Ottawa, Ontario, Canada K1A 0R6

A quadrupole mass spectrometer with only a radio-frequency voltage applied between the rods usually acts only as a high-pass filter. This work describes a simple device which eliminates high mass ions according to their final distributions of position and transverse velocity, providing a very narrow band pass.

The experimental set up is shown in Fig. 1, with $2r_o = \frac{1}{4}$". Mass filtering is effected by the coaxial circular ion stop, on which an accelerating voltage of up to a few hundred volts is applied. The set of octopole rods (1/8" dia.) helps to make the ion beam cylindrically symmetric[1]; its presence is not essential. A mass spectrum is obtained by scanning the magnitude of the RF voltage (V).

Figure 2 shows the mass spectra for the isotopes of xenon at two different pressures. The FWHM stays at 0.108 amu and a step-like structure at the low-mass side of each ion peak is evident. This is attributed mainly to scattering in the analyser, since the ratio of step to peak height decreases with decreasing pressure and becomes almost unnoticeable in the 1.0 μtorr spectrum.

The mass spectrum for perfluorokerosene is shown in Fig. 3. The peak shapes are different for different masses and the characteristic shapes persist even when the pressure is lowered ten times. This suggests an intrinsic tailing at the low-mass side of the fragment ion peak, probably due to the in-flight decomposition of the parent ions. The limiting resolution ($m/\Delta m$) is proportional to the product of the mass and the RF frequency squared ($R_{lim} \propto m\omega^2$). At ion energies (E) above $\sim$5 eV, $R \propto E^{-2} \propto n^4$, where n is the number of cycles the ions spent in the RF field. The origin of this dependence is not fully understood at the present time.

Phase space dynamics have been employed to calculate, as a function of $q(= 2\,eV/m\omega^2 r_o^2)$, the area in phase space for ion transmission at <u>all</u> initial phases. This is represented by the dotted curve in Fig. 4. Also shown is the area of a domain of combinations of initial position and initial velocity for which ion transmission is blocked off by an ion stop of radius r_o. This is represented by the full curve marked "shadow of ion stop", calculated for a hypothetical case of 40 cycles of RF field and 2 cycles of fringing field. The oscillations are due to the special imaging conditions of the quadrupole field[2]. The linearity of the Mathieu equations allows scaling of the curves for different radii of the ion stop (r_s). The curve for $r_s = 0.71\ r_o$ is shown in Fig. 5.

The effect of limiting the source radius is represented by horizontal lines in Fig. 5. The acceptance area above each of these lines cannot be utilised by a source aperture of that particular radius. The difference between the limiting curves and the shadow area will give the intensity of the transmitted ions a function of q. Some peak-shapes are shown in Fig. 6. When $r_a < \sim 0.3\, r_o$, the low-q edge of the remaining single peak can be trimmed off to increase the mass resolution at the expense of intensity. In practice, peaks are smoothed out, but these calculations suggest that a high-brightness but well-collimated source is desirable.

The experimentally attainable resolution seems to be limited by field imperfections but, for a given geometry, exceeds that in the normal mass filter mode of operation by a factor of at least 3. This device also offers some intrinsic advantages at high masses because of the absence of the detrimental effects of the DC fringing field on slow

ions[2], and because the resolution and peak shape improve with mass. The peak shape problems with daughter ions may, however, limit applications to sources with high parent ion intensities.

References

1. K. Birkinshaw, D.M. Hirst and M.F. Jarrold, J. Phys. E. 1037 (1978).

2. P.H. Dawson, editor "Quadrupole Mass Spectrometry and its Applications", Elsevier, Amsterdam 1976.

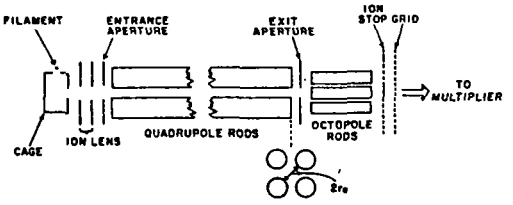


Fig. 1

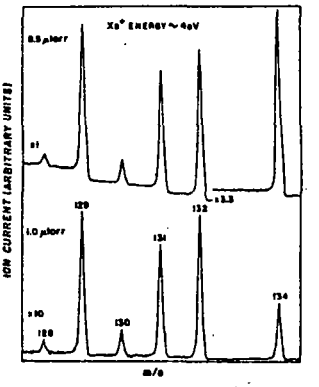


Fig. 2

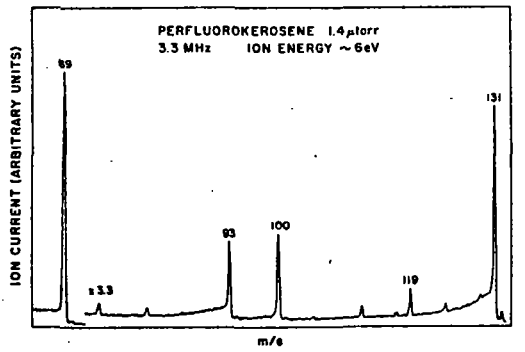


Fig. 3

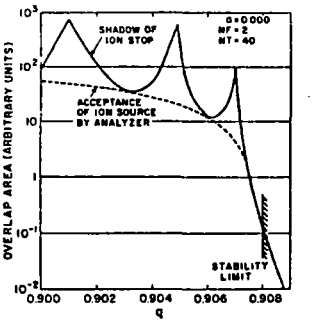


Fig. 4

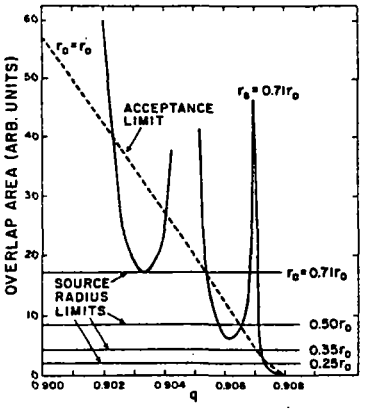


Fig. 5

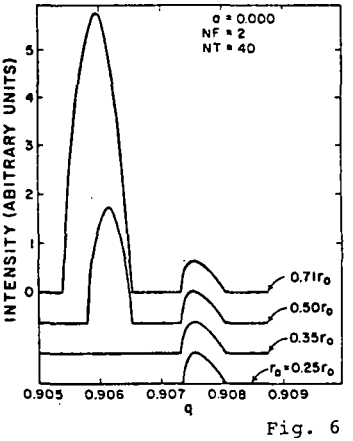


Fig. 6

WAMP7 A NEW APPROACH TO FAST SCANNING PYROLYSIS/MASS SPECTROMETRY, GREGORY WELLS, KENT J. VOORHEES and JEAN H. FUTRELL, Departments of Materials Science and Engineering and Chemistry, University of Utah, Salt Lake City, Utah 84112.

A fast scanning pyrolysis/mass spectrometer capable of scan rates in excess of 20,000 amu/sec has been fabricated around the electronics and mass filter of a Finnigan 3200 quadrupole system. An open ion source housed in 9" x 9" x 9" pumping station was connected to the mass filter by a series of extraction lenses and two einsel lenses. A 6" Edwards Diffstak was used to pump the source area. The pyrolysis apparatus used was a capacitor discharge ribbon probe. This probe is positioned below the ion source by an adjustable inlet valve. Two liquid nitrogen cooled plates are present above and below the source area. The bottom plate serves as spray plate to prevent contamination of the lens system. A small aperture in the bottom plate allows a portion of the pyrolysis products to enter the ion source as a molecular beam. The top plate traps the unionized pyrolysis beam to minimize background. The mass spectrometer is interfaced to a PDP 11/45 computer through a Tracor Northern 1710 multichannel analyzer.

WAMP8 WIDE BAND FAST FOURIER TRANSFORM ION CYCLOTRON RESONANCE, VINCENT G. ANICICH and WESLEY T. HUNTRESS, JR., Jet Propulsion Laboratory, Pasadena, CA 91103.

FFT ion detection instrumentation has been added to the authors' ion cyclotron resonance mass spectrometer. The use of the FFT ICR in a wide band (2MHz) mode as a broad range (3 - 100 amu), low resolution ($^{m}/\Delta m$=100) detector will be presented. Power requirements for the excitation pulse in the CW and chirp mode will be shown. Explicit instrumentation requirements will be shown, as well as presently understood limitations of the technique.

CHARACTERISTICS & DESIGN OF A FINGERPRINT FIELD IONIZATION MASS SPECTROMETER

William Aberth
Linus Pauling Institute of Science and Medicine
Menlo Park, California 94025

A mass spectrometer, utilizing a volcano type (1, 2) field ionization source and a Wien filter (3) mass separator, has been specifically designed to obtain routine mass profiles from multi-component samples (see Fig. 1). The instrument is single stage and operates in the magnetic scanning mode. A PDP 11/20 computer controls the mass scanning by means of a 16 bit D/A converter coupled to the 60 ampere voltage programmable Wien filter magnet supply. Signal is obtained by ion pulse counting. The mass spectrum is divided into discrete segments of equal time duration. The count obtained during each segment is added to the sum of counts registered from all the previous scans during the same mass segment. At the conclusion of the analysis, a single spectrum that represents the sum of all the mass scans is recorded on magnetic tape for further processing.

An important feature of the mass spectrometer is its capability of operating routinely at high accelerating voltage which is presently 30KV. The use of higher accelerating voltages increases the transmission efficiency as is demonstrated in Fig. 2. This is especially important for field ionization type sources that have relatively low ion signals and relatively high divergence of ions at the source. In addition, the high beam energy reduces the mass spread caused by source energy spread and makes it possible to obtain a higher resolution for a single stage instrument. Fig. 3 shows a recorder plot of a toluene mass scan and demonstrates the instrument resolution of 3500 FWHM. This resolution is presently limited by the size of the volcano field ion source which is 20 um in diameter. Smaller size sources of 5 μm dimensions are being developed and should produce a corresponding improvement in resolution.

The sensitivity of the mass spectrometer was measured using 75 ng of eicosane ($CH_3(C_{18}H_{36})CH_3$, molecular weight 282) in a solid sample probe, positioning the detector at mass 282 at a resolution of about 1,000 and counting signal ions for forty minutes while the probe heated to 185°C. A plot of the signal counting rate vs. time is shown in Fig. 4. The net efficiency obtained for eicosane was about 5×10^{-7} or 3×10^{17} counts/mole. In the scanning mode of operation the efficiency will decrease by about 3,000 for a full spectrum scan (masses 1-400), thus yielding a scanning efficiency of 10^{14} counts/mole.

An important feature of the mass spectrometer is its ability to perform routinely for long periods of time. This is due primarily to the long lifetime of the volcano field ionization source. The principal application of the mass spectrometer is for mass analysis of urine specimens. Each analysis utilizes 1 μl of untreated urine sample which is placed in a solid sample probe. Most of the water in the sample is pumped away in the source chamber vacuum before the probe is connected to the volcano source structure and temperature cycled. No discernable physical or operational changes have occurred in the volcano source for up to 130 hours of operation on urine specimens. The true lifetime of the volcano source is probably many times greater than this value under proper operating conditions. The high source efficiency which makes it feasible to use very small amounts of sample, thereby reducing the probability of gaseous voltage breakdown and contamination, undoubtedly contributes greatly to the stable source operation. In addition, protective circuitry has been installed on the source to reduce the destructive effects of voltage breakdown on the volcano.

References

1. W. Aberth, J. Wilder, A. L. Burlingame, & C. A. Spindt, Advances in Mass Spectrometry 7B, 999 (1977).

2. W. Aberth & C. A. Spindt, Int. J. Mass Spectrom. Ion Phys. 25, 183 (1977).

3. Model 300-6 Wien Filter, Colutron Research Corp., P. O. Box 1288, Boulder, CO 80302

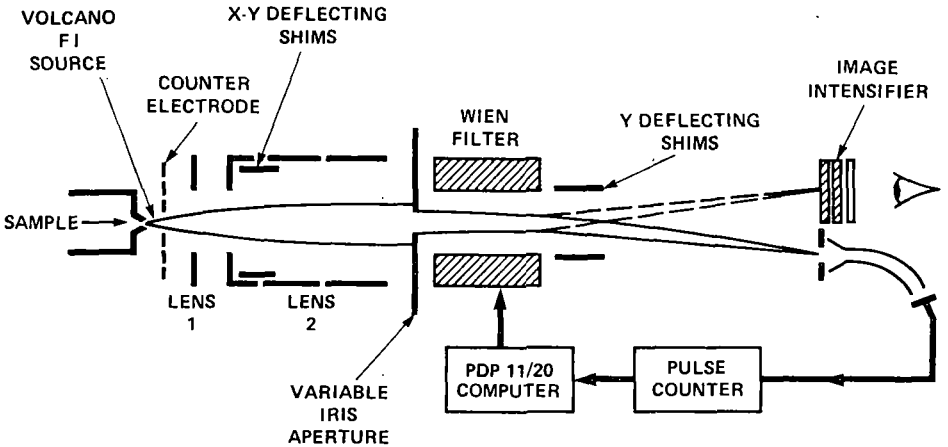


Figure 1. Schematic of the mass spectrometer

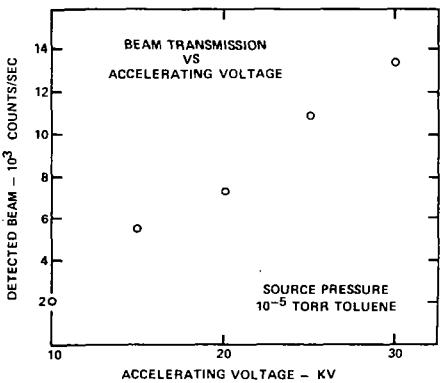


Figure 2. Signal counting rate vs time for 75 ng sample of eicosane $CH_3(C_{18}H_{36})CH_3$, m.w. 282, demonstrating a sensitivity of 5×10^{-7} or 3×10^{17} ion/mole at a resolution of 1000.

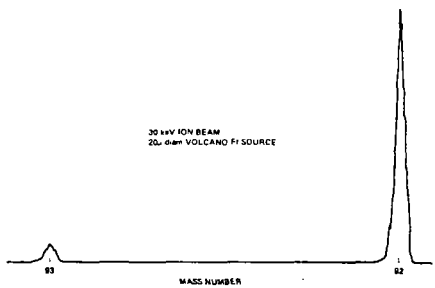


Figure 3. Mass scan of toluene demonstrating a resolution of the instrument of 3500 at 1/2 FWHM.

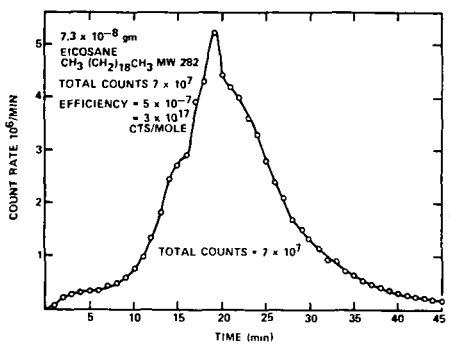


Figure 4. Transmission of the mass spectrometer vs accelerating voltage.

WAMP11 AUTOMATED MASS SPECTROMETER ADJUSTMENT FOR QUADRUPOLE MASS SPECTROMETERS, MICHAEL S. STORY, EDWIN L. MARKEL, Finnigan Instruments, 845 W. Maude Ave., Sunnyvale, Ca. 94086

With the advent of complete data system control of the mass spectrometer has come the challenge of automated ion source and quadrupole adjustment. In order for this to be accomplished the subjective weighing of transmission, peak shape, sensitivity and resolution has had to be quantitatively weighted and prioritized.

Such an algorithm has been developed with reproducible quantitative results as its goal. The results of complete ion source, analyzer and detector control will be shown.

A TRIPLE QUADRUPOLE MASS SPECTROMETER FOR DIRECT MIXTURE ANALYSIS AND STRUCTURE ELUCIDATION

WAMP12

R.A. Yost and C.G. Enke
Dept. of Chem., Mich. State U., E. Lansing, MI 48824

We recently introduced the concept of performing selected ion fragmentation (MS/MS) with a triple quadrupole mass spectrometer. In this system, the selected ion fragmentation process can provide enhanced selectivity and discrimination over normal mass spectrometry without loss of sensitivity. In structure elucidation applications, any fragment ion in a compound's normal mass spectrum is selected with the first mass analyzer; this ion is fragmented, and the mass spectrum of the resulting daughter ions is determined by scanning the second mass analyzer. The elucidation of organic structures and the analysis of mixtures benefit greatly from having the fragmentation spectrum of each source ion.

For mixture analysis, the molecular ions for each component can be separated by the first mass analyzer, and the individual fragmentation mass spectra obtained by scanning the second. The elimination of chemical noise that results often improves the detection limit.

The triple quadrupole mass spectrometer is a particularly simple and efficient approach to MS/MS. The selected ions are fragmented by collision-induced dissociation (CID) in an RF-only quad which provides ion focusing and is highly efficient. The instrument consists of, in series, a dual CI/EI ionization source, a quad mass filter, an RF-only quad that can be pressurized for CID, a second quad mass filter, and an electron multiplier. Possible modes of operation for the instrument are: 1) Normal mass spectrum. The first quad is scanned with the second and third quads in RF only (total ion) mode. 2) Spectrum of all the daughter ions from a selected parent ion. The third quad is scanned while the first quad selects the parent. With no collision gas, the "metastable" ions will be measured. 3) The spectrum of all parent ions that fragment to produce a given daughter ion. The first quad is scanned with the third quad fixed on the daughter ion mass. 4) The observation of a specific neutral mass loss. Both mass filters are scanned with a fixed difference in mass. 5) Single or multiple reaction monitoring. Both mass filters are set for a particular parent/daughter pair.

A scale drawing of the triple quad spectrometer appears in Figure 1. Detailed specifications are given in the table.

Samples may be introduced through a heated glass inlet system or a heated direct-insertion probe. The components of the mass spectrometer are enclosed in three differentially pumped stainless steel chambers, each pumped by an oil diffusion pump with water-cooled baffle (see figure 1). The vacuum system is interlocked to provide fail-safe operation. The entire system has been designed for computer control.

The use of quads as mass filters and as the CID chamber has provided excellent selectivity and sensitivity. The quads provide resolution up to 1 part in 1500 for masses up to 1000. The high sensitivity (detection limit of 10^{-15} mole) results from the very efficient low-energy CID process and the high transmission of each component along the ion path.

The overall sensitivity of the instrument is estimated from the efficiencies of the individual processes as one ion detected per 2×10^7 molecules (neglecting the CID process). The current due to one ion per second or 5×10^{-13}A can be detected. The electrical noise is typically 3×10^{-13}A. Chemical noise can be below the 10^{-13}A level. Based on these data, a detection limit of 20 femtograms for methane is estimated at a S/N ratio of 2. A sample of 10 ppm CH_4 in N_2 at a sample flux of 20 femtograms per sec of CH_4 was analyzed by monitoring the $CH_4^+ \rightarrow CH_3^+$ reaction and gave a 16 femtogram detection limit for CH_4. The chemical noise introduced by background $^{14}N^+$, $^{15}N^+$ and O^+ peaks was eliminated by this procedure.

The transition $NO_2C_6H_5^+ \rightarrow C_6H_5^+$ was monitored at unit mass resolution in both mass filters, with the parent ion produced by EI with a sample of 10 ppm nitrobenzene in N_2. A detection limit of 120 femtograms (S/N=2) was obtained with a sample flux of 200 femtograms/sec.

A mixture of five components at equal concentration was analyzed with the triple quad MS: the isomers 3-heptanone and n-heptaldehyde (114); n-octane (also 114); cyclohexane (84), and 2-pentanone (86). The CID spectrum of the 114^+ ion from the mixture shows unique fragmentations; 99+ (M-15) for 3-heptanone, 96^+ (M-18) for n-heptaldehyde and 70+ (C_5H_{10}) for

n-octane. The two isomers in the mixture are also identified by the match between the CID spectra of 99^+ and 81^+ with the CID spectra of 99^+ from pure 3-heptanone and 81^+ from n-heptaldehyde, respectively. The other two components are easily identified by matching the CID spectra of pure cyclohexane (84^+) and 2-pentanone (86+) with the CID spectra of these ions from the mixture.

The EI spectrum showed peaks at 120^+ and 105^+ which could not be attributed to any of the five known components. The CID spectra of these ions suggested acetophenone as an unexpected impurity, as confirmed with reference CID spectra.

Further experiments indicated an acetophenone concentration of approximately 5 parts per thousand in the n-heptaldehyde.

CI/EI SOURCE (FINNIGAN)	(TYPICAL)	(RANGE)
Conductance	0.5 ls^{-1}	
Sensitivity	1 ion/$2x10^5$ molecules	
QUADRUPOLE MASS FILTERS (EXTRANUCLEAR, 20 cm x 0.95 cm d.)		
Axial ion energy	-10 ev	(-100→+100 ev)
Transmission, 1/200 resol.	10%	(5→15%)
Transmission (RF-only)	60%	(50→75%)
QUADRUPOLE COLLISION CHAMBER (HOME BUILT, 21.6 cm x 0.95 cm d.)		
Axial ion energy	-10 ev	(-100→+100 ev)
RF-only mode voltage	35 V pRF	(0→150 V pRF)
Transmission	100%	
Collision Gas Pressure	$1x10^{-4}$torr	($2x10^{-6}$→$1x10^{-2}$torr)

CHAMBER PRESSURES, torr

Source Chamber, $6x10^{-7}$. Center Chamber, $2x10^{-6}$. EM Chamber $2x10^{-6}$.

SCALE DRAWING - TOP VIEW

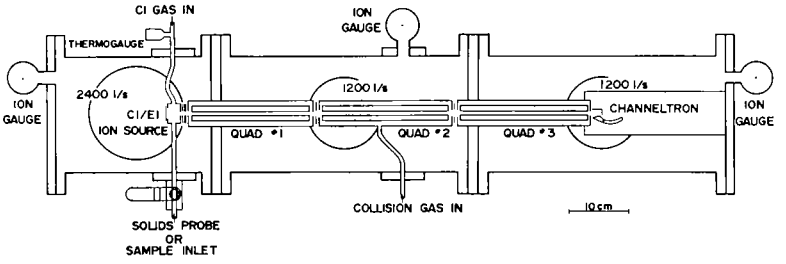


Figure 1.

CONSTRUCTION OF A FOURIER TRANSFORM MASS SPECTROMETER

S. Ghaderi, E.B. Ledford, Jr., R.B. Spencer, C.L. Wilkins and M.L. Gross

Department of Chemistry
University of Nebraska
Lincoln, Nebraska 68588

A Fourier Transform Mass Spectrometer has been built in our laboratory using the vacuum system and magnet of a Varian ICR-9, and by the addition of a trapped ion cell, a computer, a frequency synthesizer and the necessary electronic controls and computer interface.

The cell which serves as ion source and analyzer is based on the one section cell design of McIver (1). It is a cubic box with six gold plated faces, one square inch each, which are electrically isolated from each other. The trapping plates are biased at a positive or negative potential on the order of ca. + 1 or -1 volt to trap positive or negative ions respectively. All the other plates are at ground potential.

Electrons emitted from a filament (20 to 100 nA of emission current) pass through the cell via 1/16" diameter holes on the trapping plates and are collected on a target outside of the cell. The ions formed by electron impact at low pressure can be trapped for as long as 60 seconds due to the magnetic and electric fields present in the cell. A routine trapping time for the cell is 5 sec at 10^{-7} torr. Each trapped ion undergoes a cyclotron motion with a frequency which depends on the m/q of the ion, and the magnetic field. In addition, there is a small correction of the frequency which involves the trapping voltage, V_T, and the distance between the trapping plates, ℓ. The relation is known as the Beauchamp-Armstrong equation (2).

$$\omega = \{[qB/m]^2 - [4qV_T/m\ell^2]\}^{1/2}$$

In order to excite the cyclotron motions of the ions, a fast sweep of radio frequency in the range of ions of interest is applied to the two plates perpendicular to the magnetic field lines (transmitter plates) with a typical duration of less than one millisecond and an amplitude of 5 to 15 volts (peak-to-peak). The coherent motion of all the excited ions induces image currents in the other two plates (receiver plates) perpendicular to the magnetic field lines.

The frequencies of the induced image currents are detected using a wide band, low noise, high common mode rejection ratio differential amplifier for pre amplification. In our system, a Tektronix 5A22N differential scope amplifier is employed. The output of this amplifier is fed into a set of high pass, low pass filters to cut the undesired noise and a limiter amplifier to clip the high amplitude rf feed-through and other spikes to a safe level. The output of this circuit has an amplitude of about one volt for a typical transient and has the same characteristics of the initial transient signal. This signal is often input directly to a fast ADC (5MHz) for digitization. A full spectrum from mass 10 to infinite mass is obtained corresponding to an rf sweep at 0 to 1.843 MHz at 12 K Gauss magnetic field strength.

The digitized data is transmitted to memory of the Nicolet 1180 computer through a 32 K buffer memory and then submitted to Fourier transformation. The computer has a solid state memory of 40K. The output can be directed to a variety of devices including a dual density disk (Diablo Model 40), a magnetic tape (Kennedy Model 9700), a terminal (Tektronix Model 4010), a digital plotter (Tektronix Model 4662) and a fast printer (Texas Instrument Model 800).

When it's desirable to scan over a narrower band width, a mixer is used before the digitizer to mix the signal with a frequency equal to the maximum rf sweep frequency (local frequency). This mode of operation gives rise to a heterodyne frequency from addition and subtraction of each individual frequency in the composite transient decay and the local oscillator frequency. A low pass filter (Krohn-Hite model 3200) which can be set to pass any frequency up to the local oscillator frequency without discrimination is used to filter out the additional frequencies. The local frequency is provided by the fixed output of the Rockland frequency synthesizer through an electronic gate and amplifier on the mixer circuits.

Double resonance experiments are performed using a single frequency of variable amplitude output from the Rockland to eject the ions from the cell prior to detection. The frequency and amplitude of both the excitation and double resonance rf can be selected by means of computer commands with very high resolution, accuracy and reproducibility.

In order to maintain accurate timing for all the pulses and events (which is essential for signal averaging), a Nicolet 293A programmable pulser has been modified and improved in our laboratory. The pulsing characteristics are computer controlled and have variable duration using appropriate keyboard commands. The following pulses are employed:

1. Quench Pulse: This activates the quench and trapping control system to provide a $\pm$ 15 volts for 1 msec on the trap plates. This ejects all the trapped ions to the walls before the formation of new ions.
2. Beam Pulse: This activates the filamentand emission control and supply system to bias the filament from + 5 volts at OFF state to 0 to -100 volts electron energy at ON state. The beam is on typically for 1-5 msec.
3. Excitation or Transmition Pulse: An electronic gate is opened and the Rockland is activated to provide a sweep of frequency which is amplified using a wide band rf power amplifier to a desired amplitude for ion excitation. The typical amplitude ia about 15 volts peak-to-peak.
4. Receiver Pulse: The ADC is now triggered for data acquisition. In addition, the gate for the local oscillator frequency and the mixer circuit is opened if the mixer mode is chosen.

There are options for introducing to the cell a double resonance ion ejection frequency before the excitation frequency and also for variable delay times between ion formation and excitation. The latter option is used for chemical ionization and for time resolved studies of ion-molecule reactions. CI experiments can be conducted also by allowing a steady state of ions to exist in the cell by foregoing the quench pulse.

We intent to publish the details of the apparatus in Review of Scientific Instruments.

Acknowledgement: We wish to thank the Nicolet Company for consultation and many helpful discussions. The research has been supported by grants from the NSF (#CHE77-03964) and Gulf Oil.

References:

(1) R.T. McIver, Jr., Rev. Sci. Inst., 41, No. 4, 555 (1970).

(2) J.L. Beauchamp and J.T. Armstrong, Rev. Sci. Inst., 40, 123 (1969).

MICROCOMPUTER-BASED FOURIER TRANSFORM ION CYCLOTRON RESONANCE MASS SPECTROMETER

R. J. Doyle, Jr., T. J. Buckley, and John R. Eyler

Department of Chemistry, University of Florida
Gainesville, Florida 32611

We have expanded our microcomputer-based Fourier transform ion cyclotron resonance (fticr) mass spectrometer system so that all aspects of the fticr experiment (ion irradiation, storage of transient response, and discrete Fourier transformation) are now controlled or performed by a combination of two microcomputers (KIM-1 and Apple II). Figure 1 shows an overall block diagram of the system. The KIM-1 microcomputer provides timing pulses used to gate on and off both the excitation oscillator and the reference oscillator, as well as to control switches S_1 - S_4 which alternately route r.f. excitation to the upper and lower cell plates and permit the ion-induced current to flow to the detection circuitry. The microcomputer also acts as a signal averaging device, acquiring digitized transient responses from the ions in the icr and adding them to previously obtained data.

Signal averaged data from the KIM-1 microcomputer can be transferred directly (via serial output port-modem-telephone line) to our campus computer for Fast Fourier Transformation (FFT) and plotting. Alternatively, data can be transferred to the Apple II microcomputer for FFT analysis, with the results displayed on a video monitor.

Fast Fourier Transforms are currently being carried out by the Apple II computer using a BASIC program. This requires ca. 2½ min. for a 256 point transform, and 5 min. for a 512 point transform. We are developing a double precision (16 bit) 6502 machine language FFT subroutine which will drastically shorten (ca. 5 s for a 256 point transform) program execution time and allow 1K or 2K transforms to be carried out in a reasonable length of time. We also plan to add a hard copy output device to the Apple II computer so data does not have to be transferred to the campus computer for plotting.

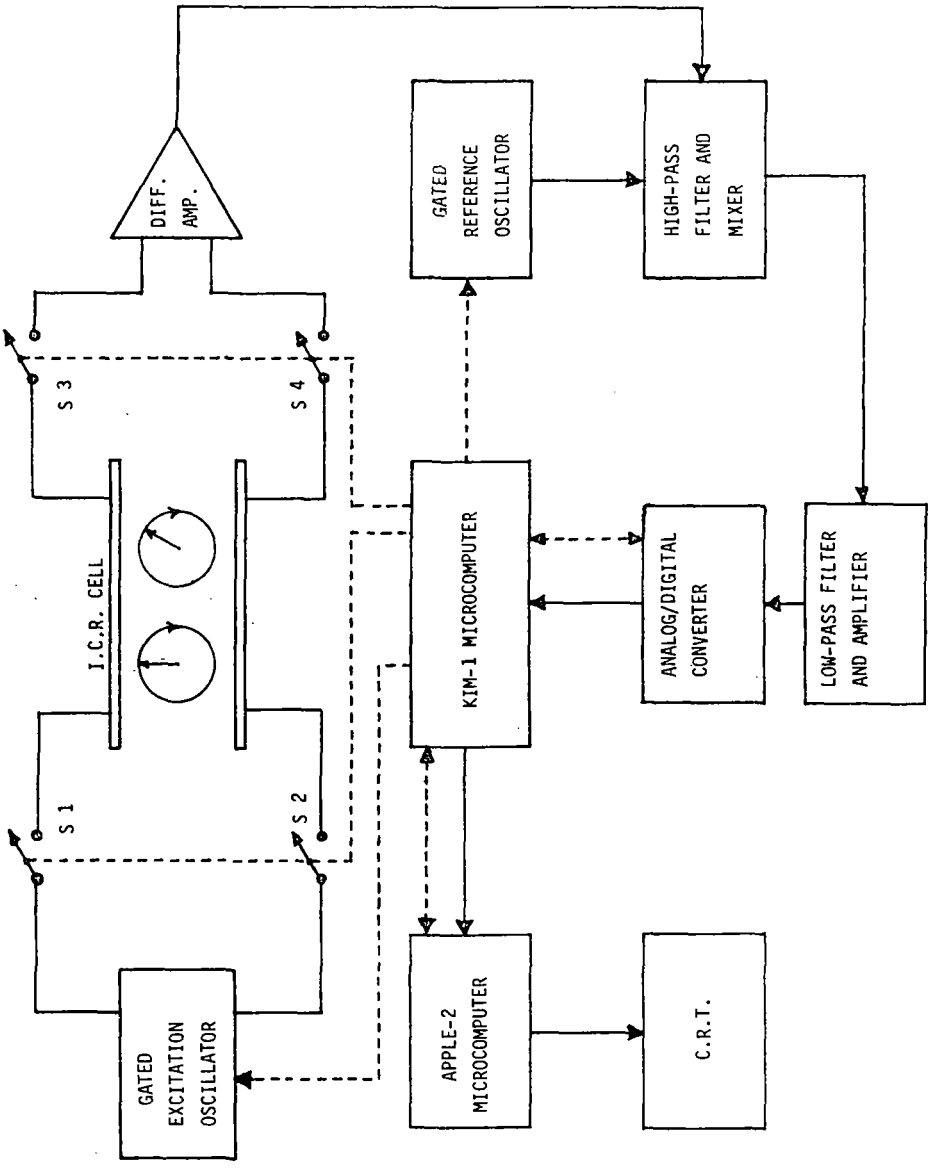


Figure 1. Overall Block Diagram of Microcomputer-Based Fourier Transform Ion Cyclotron Resonance Detection System

GAS CHROMATOGRAPH COLUMN EFFLUENT VENTING SYSTEM FOR THE DUPONT 490 GC/MS

David L. Winmill and Robert L. Williams, Hercules Incorporated
Development Department, Research Center, Wilmington, DE 19899

The impetus for this project arose during the analysis of synthetic lubricant samples that had been hydrolyzed and derivatized to trimethylsilyl (TMS) ethers and esters. One microliter aliquots of the sample solutions, that consisted mainly of the necessary excess reagents were injected into the gas chromatograph-mass spectrometer under normal operating conditions. After about thirteen such runs, the sensitivity of the dual source had fallen by a factor of three. At this point, the sensitivity was not high enough to obtain a calibration from perfluorinated kerosene in the batch inlet system. Therefore, the instrument had to be vented and the dual source removed, cleaned, and reassembled to continue operations.

The various solutions to this problem that were considered were as follows:

(1) Remove TMS reagents from the samples before GC/MS analysis.
(2) Turn off the source heater and ionizing filament during the TMS reagent elution period.
(3) Construct a venting system so that TMS reagents do not enter the mass spectrometer.

The removal of the bulk of the TMS reagents from a sample by evaporation can cause losses of more volatile components as well as hydrolysis, particularly of the TMS esters. Turning off the source heater and ionizing filament was not tried as a technique, but has the disadvantage of disturbing the source equilibrium as well as only preventing the effects due to decomposition by the heater and filament.

The design and construction of a venting system was undertaken as it would be most convenient in operation and most generally applicable. For example, such a system would be useful for venting the following:

(1) TMS and other corrosive reagents.
(2) Solvent peaks and air peaks.
(3) Large sample peaks in mid-chromatogram.
(4) Column bleed and high Mol. Wt. materials in samples where only the low Mol. Wt. components are of interest.

The major considerations for the design of the venting system were as follows:

(1) Maintain the integrity of the all glass construction from the GC column to the mass spectrometer.
(2) The system must be capable of withstanding the maximum operating temperatures of the GC column oven and the detector oven (350°C).
(3) Must not broaden or diffuse the GC peaks flowing to the flame ionization detector or mass spectrometer.
(4) Must not alter the normal operation of the GC/MS system.
(5) Should preferably give the same GC peak retention times with venting as without use of the venting system.

Some experiments were made to investigate the column exit as the point for venting unwanted GC eluents. By removing the column from the GC column oven exit fitting and replacing it with a pressure gauge, it was found that a pressure of 13 psig is maintained at this point when the make-up valve is open (See Figure).. This is due to the back pressure exerted by the splitter restrictors to the flame ionization detector (FID) and jet separator. Replacement of the pressure gauge with a soap film flowmeter showed that a flow rate of 20 ml/min was obtained when the exit was at atmospheric pressure. This is due to a pressure of 50 psig upstream of the restrictor that is between the make-up valve and the FID and jet separator restrictors. Therefore, if a tee junction is introduced at the end of the column and the column oven exit, the column effluent plus a flow of make-up helium will flow through the tee to atmosphere. When the tee is closed off and the make-up valve closed, the system will be returned to normal operation.

The tee junction was made by silver soldering 1/16" O.D. S.S. tubing into a 1/16" radial hole through the feed-thru assembly at a point coinciding with the end of the glass GC column. The internal diameter of this tubing was 0.05" to provide maximum flow with minimum back pressure. The common port of the valve (Port No. 2) was connected to an existing vent to

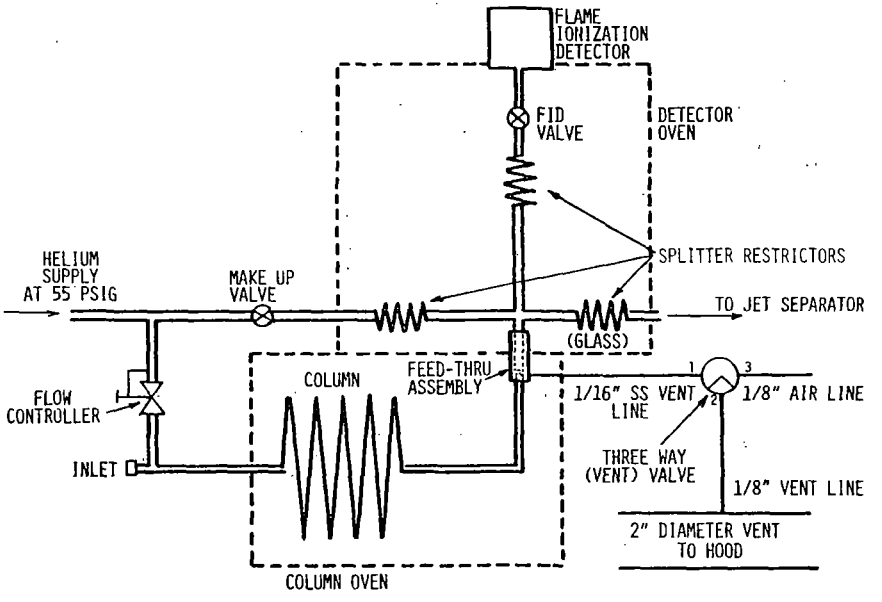
a fume hood and the third port was connected to an air line controlled with a needle valve to deliver 60-80 ml/min. No other modifications were required except that the Swagelok® metal to glass fitting after the make-up gas restrictor had to be scrupulously tight to prevent a venturi effect admitting small quantities of air into the system when the make-up valve was on.

In normal operation, the three-way valve is kept closed (no port connected to any other) and the make-up valve is also closed. Under these conditions, the column effluent (20 ml/min He) is split in about a 50/50 ratio between the mass spectrometer and the FID. When unwanted peaks are to be vented, the make-up valve is opened and the three-way valve turned to connect ports 1 and 2. The column effluent now flows through the vent line and three-way valve together with the helium make-up flow. After the peaks are vented, the three-way valve is turned to the closed position and the make-up valve is closed. If the compounds vented are toxic or corrosive, the three-way valve can be turned to connect ports 2 and 3 so that an air flow purges the lines to the fume hood.

CONCLUSIONS

Appropriate use of this venting system greatly decreases the build-up of contamination in the source and therefore decreases the frequency of source cleaning. As the chromatographic performance is not affected by use of the system, it can be used whenever required: for solvents and corrosive reagents, for large peaks in mid-chromatogram or for high molecular weight materials and column bleed in temperature programmed runs.

SCHEMATIC OF GC/MS COLUMN AND SPLITTER ARRANGEMENT WITH VENTING SYSTEM



Fomblin: A High Molecular Weight Reference Compound

G A Warburton, R McDowell and K R Compson
Kratos Limited, Barton Dock Road, Urmston, Manchester M31 2LD

Advances in magnet design and soft ionisation techniques have led to an increase in the useful mass range of mass spectrometers so that spectra of compounds of over 2,000 molecular weight are routinely accessible. As a consequence the need has arisen for a reference material for data system calibration and accurate mass measurement by peak matching at these high masses.

Presented here are details of Fomblin® oil, a perfluorinated polyether. This material has desirable sample handling characteristics and provides a good mass spectrum with a relatively intense regular series of peaks to masses in excess of 3,000. Figure 1 shows a spectrum of Fomblin oil recorded at full accelerating voltage using an MS50 fitted with a high field magnet and a DS50S data system.

The spectrum shows consistent differences of 16, 16 and 18 amu. Metastable ion studies on Fomblin have shown that most ions belong to series formed by losses of 66, 116 and 166 amu. Peak matching studies using the MS50 confirms these losses as CF_2O, C_2F_4O and C_3F_6O. This is in agreement with the following general structure for Fomblin:

$$\left[\left(O-\underset{\displaystyle CF_3}{\underset{|}{CF}}-CF_2-O-\underset{\displaystyle CF_3}{\underset{|}{CF}}-CF_2\right)_x O-\left(CF_2\right)_y\right]_z$$

The base peaks of three major series are m/e 335, 285 and 235 from which higher masses can be formed by addition of 66, 116 or 166 mass units. Figure 2 shows these major ion series present in Fomblin as determined by the use of B/E linked scans and V scans. Figure 3 illustrates an example of a B/E linked metastable scan of m/e 501 in Fomblin. Predominant fragment peaks occur at m/e 335 (loss of C_3F_6O) and 169 (loss of $(C_3F_6O)_2$).

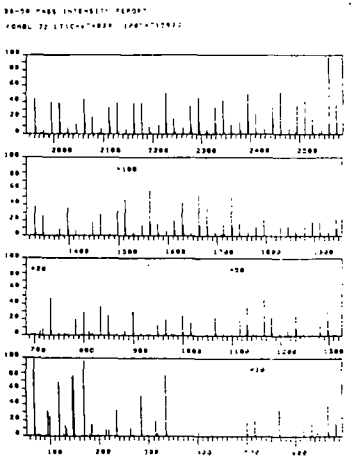
Confirmatory peak matches were performed up to mass 1,000 using PFK and tris (perfluoroheptyl) s-triazine as reference compounds. Additional checks were then made to m/e 1861 by peak matching Fomblin against itself. Because of the regularity of the spectrum and the predictability of their atomic composition, higher accurate masses were calculated and not confirmed by peak matching.

At the low mass end of the spectrum a few major peaks appear not to belong to the major series. These ions are formed by losses not common to the major series. For example m/e 313 has an intensity of 16% of the most intense peak. It also appears as a relatively weak fragment peak in the B/E scans of m/e 501, 451 and 401 formed by losses of C_3F_8, C_2F_6 and CF_4 respectively. Because of their deviations from the major series, the formulae of peaks such as m/e 313 were confirmed by accurate mass measurement.

A full listing of the accurate masses together with relative intensities of major peaks in Fomblin is available on request from the authors.

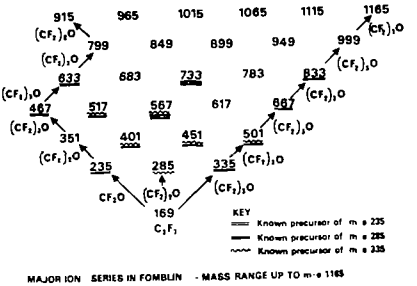
We would like to thank Dr J R Chapman for useful discusssions and help with this paper.

Fomblin® is a registered trade mark of Montedison.



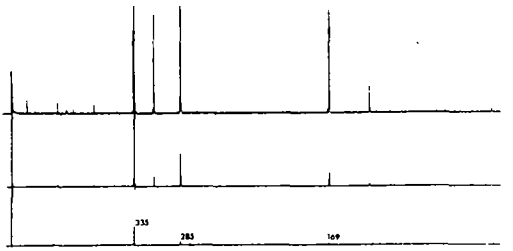
MS50: Spectrum of Fomblin® in Mass 2575

Figure (1)



MAJOR ION SERIES IN FOMBLIN - MASS RANGE UP TO m·e 1165

Figure (2)



MS50: B/E Scan of m/e 501 from Fomblin® Oil

Figure (3)

WAMP17 APPLICATIONS OF A NEW MASS SPECTROMETER TO QUANTITATIVE HYDROCARBON ANALYSIS., G.A. ERROCK, D.J. HOY, K.T. TAYLOR, K.R. COMPSON, KRATOS LTD, BARTON DOCK ROAD, URMSTON, MANCHESTER, M31 2LD, ENGLAND.

A small double focussing mass spectrometer (MS25Q) for quantitative analysis of mixtures has been described at a previous meeting [1].

We now present the results of measurements of the reproducibility of peak intensities as required by the ASTM test procedures numbers D2425 (middle distillate hydrocarbons), D2789 (gasoline hydrocarbons) and D3239 (Aromatic hydrocarbons in gas oil).

A statistical assessment of the results has been carried out. This shows that the sensitivity, stability and reproducibility of analyses with MS25Q exceed comfortably the requirements of these standard methods.

Ref Paper RP8 ASMS No. 26 1978

A REVIEW OF RECENT DEVELOPMENTS IN DATA ACQUISITION FOR TIME-OF-FLIGHT MASS SPECTROMETERS

Kenneth A. Lincoln

Ames Research Center, NASA, Moffett Field, California 94035

Various fast recording techniques for time-of-flight mass spectrometry were reviewed by Meyer[1] in 1969. The intent of this paper is to outline some of the more recent techniques employing commercially available instruments to capture and record in digital memory the time-of-flight mass spectra that is generated from transient phenomena. This discussion is limited to instrumentation for acquiring and temporarily storing the spectra and, for the most part, excludes equipment for the subsequent steps of data handling and analysis.

In the examples described here a CVC (Bendix) Model MA-2 time-of-flight mass spectrometer (TOFMS) was used and all the output signals were taken from the scope anode via an amplifier with a gain factor of 10. Five independent techniques for recording either a limited number of spectra or limited parts of sequential spectra are presented:

1. Programmable Waveform Digitizer (Tektronix, Model 7912AD). This is a complete system which uses two microprocessors to control the instrument, pre-process data, and direct storage of measurement in local memory. The waveform (in this case the TOFMS spectrum) is recorded on a diode array in analog form, then the diode array is subsequently scanned and digitized and placed in memory. Spectra are automatically normalized for CRT display and hardcopy output and, overall, it is convenient to use. Time windows as short as 5 ns can be digitized, making this the fastest available instrument for spectrum recording. However, resolution in the array is limited to the equivalent of about 500 time increments; this is adequate for recording only segments of a TOFMS spectrum, i.e., only a limited mass range for reasonable spectral resolution. This is its chief weakness. Also, the instrument is limited to recording about one TOFMS spectrum per 15ms, due to the scan-digitize time.

2. External Gating of Preselected Mass Peaks. All gating operations are performed external to the TOFMS multiplier and many simultaneous outputs of the spectra are provided. A more detailed description of this instrumentation has been reported at an earlier occasion,[2] but is briefly included here because it provides a convenient interface for all of the data acquisition equipment as well as meeting the specific objective of gating out from the spectra a limited number of mass peaks, integrating each one and stretching it to a 3 μs output pulse whose amplitude is proportional to the integrated value (total charge). The salient features of the technique are as follows:

- o No interference between any of the signal displays
- o Number of mass peaks monitored is not limited by the multiplier
- o Permits use of a less complicated electron multiplier
- o Improves speed and sensitivety of measurements for fast events
- o Output pulse height is proportional to the integral of that mass peak
- o The stretched mass peaks facilitate further data handling

This is the preferred instrumentation for time resolving and quantitatively measuring individual mass peaks during short-term events.

3. Single Spectrum Recording by a Transient Recorder. One of the best instruments for this is the Biomation, Model 8100 Transient Recorder, because it has a 2000 point memory and can digitize analog signals at the rate of 10 ns per point. Thus, it can record a time window of 20 μs which is equivalent to a mass range of 1 to 200. In this case a spectrum stored in the memory of the transient recorder can be displayed on a CRT and/or a strip-chart, and it can be fed digitally into a signal averager or computer. Although fidelity to the approximately 10 ns rise and fall times of the mass peaks is limited by the slewing rate of the input amplifier and the sampling rate of 10 ns per point, it is evidently adequate for defining low resolution spectra; in fact, we have found it useful in performing limited quantitative analyses. However, there are several other drawbacks that should be noted: a) despite the ability of the TOFMS to produce a spectrum every 25 μs, only one spectrum can be recorded during a fast event (on the order of milliseconds) because about 3 ms is required to dump the memory out of the transient recorder. b) a single spectrum permits no averaging of the ubiquitous statistical variations that occur in the intensities of the mass peaks from cycle to cycle in the TOFMS.

4. Multiple Spectra Recording by a Transient Recorder. This provides a limited number of time-resolved spectra for fast events by recording portions of successive spectra in the 2000 address memory of the transient recorder. The main purpose for trying to get more than one spectrum into memory is to overcome the drawbacks cited under section 3 above. In many applications, the multiple spectra can be averaged to overcome the statistical variations in peak intensity.

The technique for recording successive spectra within a reduced mass range is depicted in the block diagram of Figure 1. The primary addition to the previously described instrumentation is the 100 MHz pulse generator which drives the external time base of the transient recorder at the required sampling rate (the Biomation 8100 is specified to only 50 MHz external drive, but we have succeeded in driving it at nearly 100 MHz). This pulse generator must be amenable to being gated off and on by another pulse generator that establishes which portion of the mass spectrum will be sequentially stored in the memory. The delay generator is synchronized with the mass spectrometer and triggers the gating generator at a preselected starting mass in the spectra. The optional peak sense and hold unit can provide improved peak height measurement by the transient recorder but at the expense of degraded spectral resolution.

5. Signal Averager Coupled to Transient Recorder. The Nicolet Model 1170 Signal Averager can be coupled directly to the transient recorder to provide signal averaging for continuous spectra or to record time-resolved spectra from moderately fast events or various combinations of both. The rate-determining step is the approximately 3 ms required to dump the 2000 word memory of the transient recorder into the averager. Thus, with the 12K memory option in the Model 1170, six individual 2K word spectra can be stored or twelve individual 1K word spectra can be stored at a minimum of 3 millisec increments. When the event under study is of the order of a second or so, then a specific number of spectra can be averaged during storage in each of the memory units. For example, 33 spectra can be averaged per 0.1 sec time increment; the resulting averaged spectra will have considerably improved precision in mass peak intensities.

CONCLUSIONS

This discussion has been an attempt to describe some progress made in obtaining the mass spectra of transient events by using presently available equipment. The commercial instruments referenced here are not necessarily the only ones which will do the jobs prescribed, but are those with which we have had personal experience. Moreover, at the present rate of advancement in microelectronics, the ultimate goal of capturing and storing every mass peak from every cycle of a TOFMS at a reasonable cost may be within grasp in the near future. However, for the present we are left with a more pragmatic modus operandi: All of the mass peaks can be captured some of the time, some of the peaks can be captured all of the time, but all of the peaks cannot be captured all of the time.

REFERENCES

1. R.T. Meyer in D. Price and J.R. Williams (Ed.), The Time-of-Flight Mass Spectrometer, Pergamon Press, Oxford, 1969. pp. 61-68.
2. K.A. Lincoln, paper presented at the 23rd Annl. Conf. on Mass Spectrometry and Allied Topics, May 25-30, 1975. Houston, Texas.

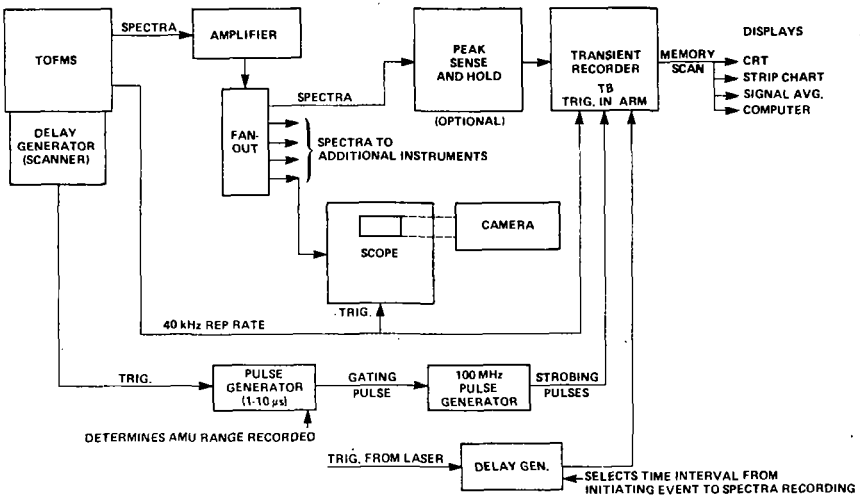


Fig. 1. Instrumentation for storing multiple spectra in a transient recorder

Positive ion composition measurements in the stratosphere - Experimental aspects and results.

E. Arijs, J. Ingels and D. Nevejans

Belgian Institute for Space Aeronomy, Ringlaan 3, B-1180 Brussels, Belgium.

Recently it has been discovered that upper atmospheric ion composition is mainly controlled by minority gases, and that ion composition data may be relevant in determining trace gases. The scientific objective of the balloon-borne ion mass spectrometer ION constructed at the Belgian Institute for Space Aeronomy, is to determine the positive ion composition of the stratosphere at altitudes between 30 and 40 km.

Experimental aspects

The present ion mass spectrometer is a 2nd generation payload evolving from a simpler one, after a series of preliminary balloon flights during 1974 and 1975. Basically, the actual payload consists of a quadrupole mass filter combined with a high speed liquid helium cryopump (1), and the appropriate electronics. Ambient positive ions are sampled through a small hole with a diameter between 0.01 and 0.03 cm. Before launching, this aperture is covered by a polyimide plunger, removable by a spring loaded aluminium arm and a pyrotechnical cable cutter. The opening device is activated by telecommand after the gondola has reached the chosen floating altitude (1). Then, positive ions and neutral gas can enter the mass spectrometer. Neutral gas is pumped by the high speed liquid helium cryopump, resulting in a vacuum of approximately 10^{-5} Torr, in the mass spectrometer region. The flange with ion sampling hole is electrically insulated from the gondola. Therefore a negative "draw-in" potential on this flange will attract positive ions and will overcome possible charging up of the payload. Positive ions focussed by an electrostatic lens into the quadrupole mass filter, are filtered there according to mass-to-charge ratio. After passing the mass filter, they reach a spiraltron electron multiplier, giving rise to charge pulses counted by an appropriate electronic unit. Pulse counting techniques are absolutely necessary in view of low stratospheric ion densities encountered (10^2 to 10^4 cm^{-3}). Ion counter contents are transmitted by telemetry as pulse code modulated signals. The electronic units of the actual payload consist of a set of batteries, a power regulator of the booster type, a quadrupole power supply, high voltage units for electron multiplier and vacuum gauge, a pulse counter, a mass controller and auxiliary instruments measuring pressure and temperature in the gondola and the liquid helium level in the cryopump. All electronic units are housed in a hermetically sealed container, pressurised with dry air at

1 ATM, AVOIDING SPARKING IN HIGH VOLTAGE COMPONENTS. THE MASS RANGE OF THE QUADRUPOLE IS FROM 0 TO 109 AMU, ITS RESOLUTION IS VARIABLE AND CAN BE CHANGED BY TELECOMMAND. TELECOMMAND POSSIBILITIES ARE EXTENDED BY A PROGRAMMABLE CONTROL UNIT (2), ALLOWING THE CHOICE OF 16 MEASURING TASKS WITH 16 TELECOMMAND CHANNELS ONLY. SWITCHING THE EXPERIMENT ON AND OFF IS PERFORMED BY TELECOMMAND ALSO. DATA ARE PROCESSED ON LINE BY A MINI-COMPUTER, THEREBY FACILITATING SELECTION OF RESOLUTION AND MASS DOMAIN SCANNED BY THE QUADRUPOLE, ACCORDING TO SIGNAL STRENGTH.

DISCUSSION AND IMPLICATIONS ON THE POSITIVE ION-MOLECULE CHEMISTRY OF OF THE STRATOSPHERE

THE SCIENTIFIC RESULTS OBTAINED DURING THE SEPTEMBER 1977 CAMPAIGN OF THE CENTRE NATIONAL D'ETUDES SPATIALES IN AIRE-SUR-L'ADOUR (FRANCE), WERE PUBLISHED IN NATURE (271, 642, 1977) (3). THE REACTION SCHEME GIVING RISE TO PROTON HYDRATES (PH) WAS KNOWN ALREADY (4). THE EXPECTED PROTON HYDRATES HAVE BEEN OBSERVED, HOWEVER NON-PROTON HYDRATES (NPH) WERE ALSO OBSERVED. ALL OBSERVED NPH MASSES FIT THE FORMULA $H^+X_M(H_2O)_N$ (SEE TABLE), SUGGESTING THAT A NEW STEP HAS TO BE ADDED TO THE REACTION SCHEME, NAMELY :

$$H^+(H_2O)_N + M\ X \longrightarrow H^+X_M(H_2O)_{N-M} + M\ H_2O$$

X SHOULD BE A MOLECULE WITH A PROTON AFFINITY (P.A.) LARGER THAN THAT OF H_2O AND SHOULD HAVE A MASS OF 41 ± 2 AMU. IN VIEW OF THIS, SEVERAL POSSIBLE X MOLECULES HAVE BEEN SUGGESTED, HOWEVER NaOH SEEMS TO BE THE MOST LIKELY ONE SO FAR (5). ALL PROPOSED MOLECULES REMAIN SPECULATIVE AS LONG AS HIGHER RESOLUTION ION MASS SPECTRA COMBINED WITH NEUTRAL COMPOSITION MEASUREMENTS ARE NOT AVAILABLE.

THESE INVESTIGATIONS ARE NOW PREPARED AT THE BELGIAN INSTITUTE FOR SPACE AERONOMY.

REFERENCE

1. J. INGELS, E. ARIJS, D. NEVEJANS, H.J. FORTH AND G. SCHÄFER, LIQUID HELIUM CRYOPUMP AND RELIABLE OPENING DEVICE FOR A BALLOON-BORNE MASS SPECTROMETER, REV. SCI. INSTRUM., 49, 782-784, 1978.
2. E. ARIJS AND D. NEVEJANS, PROGRAMMABLE CONTROL UNIT FOR A BALLOON-BORNE QUADRUPOLE MASS SPECTROMETER, REV. SCI. INSTRUM., 46, 1010-1015, 1975.
3. E. ARIJS, J. INGELS AND D. NEVEJANS, MASS SPECTROMETRIC MEASUREMENTS OF THE POSITIVE ION COMPOSITION OF THE STRATOSPHERE, NATURE, 271, 642-644, 1978.
4. E.E. FERGUSON, IN THE NATURAL STRATOSPHERE OF 1974, CIAP MONOGRAPH 1, 5.42-5.54, 1974.
5. E.E. FERGUSON, SODIUM HYDROXIDE IONS IN THE STRATOSPHERE, GEOPHYS. RES. LETTERS, 5, 1035-1038, 1978.

WAMP20 A NEW MASS SPECTROMETER FOR HYDROCARBON MIXTURE ANALYSIS.

C. BRUNNEE, H. RACHE, H. RAVENS, and B. WINDEL, Varian MAT GmbH, Bremen, Germany

The instrument has been designed for high stability of cracking pattern and sensitivity. It is based on the MAT 250 gas mass spectrometer (46 cm effective radius, 8 kV acceleration voltage). Two inlet systems are provided: one for gases (metal) and one for liquids and solids (glass, 350 °C). The source has three independent inlet parts and is thermostated to within 0.1 °C. Integral part of the system is a PDP 11/03 computer for instrument control and data evaluation. Performance data with respect to stability and accuracy will be presented.

THE EFFECTS OF HIGH INPUT CURRENT PULSES UPON CHANNEL ELECTRON MULTIPLIERS

E. A. Kurz
Galileo Electro-Optics Corp.
Sturbridge, MA 01518

Experiments have been conducted recently in order to study the effects of extremely high pulsed input currents upon the short term gain stability of Channeltron® Electron Multipliers (CEMs) operated at high gains[1]. All data was taken on 4800 Series CEMs at a pressure of approximately 10^{-7} torr. The channels were operated continuously, producing a steady state output of 0.5 μA, enabling gain to be monitored continuously throughout the experiment. A large electron input current pulse, from a gated filament, was imposed on top of the steady signal in order to observe its effects upon short term gain stability. The results of these tests are shown in Figures 1, 2, and 3.

All of this was obtained on CEMs which had been properly preconditioned (operated at approximately 4×10^7 gain, producing 0.1 μA output current for at least 24 hours) prior to testing. This preconditioning, by mechanisms which are not clear at this time, enables the CEM to withstand exposure to high input currents without permanent gain degradation. This point cannot be overstressed. CEMs operated identically to those previously discussed but without the preconditioning exhibited permanent gain degradation which was typically as large as a factor of ten. With conditioning, these CEMs exhibited characteristics consistent with those reported above , although at higher voltages necessitated by the permanent gain degradation incurred due to the premature exposure to the high input current pulses.

It is hypothesized this temporary loss of gain is due to the electron bombardment induced desorption of an adsorbed layer of residual gas molecules . As this layer is desorbed its contribution to the secondary emission coefficient is reduced, resulting in a net decrease in gain. When the large input is removed readsorption occurs with a concurrent increase in gain. The gain stabilizes when equilibrium is re-established.

This simple model alone does not account for two of the observed phenomena. First, the model does not account for the differences observed, in terms of gain recovery, between preconditioned CEMs and those without preconditioning. Secondly, it does not account for the occasionally observed occurrence of delayed depresssion of gain (for example, the 14 and 80 millisecond exposures of Figure 1).

This work was partially funded under NASA Contract NAS 5-24411.

1. E. A. Kurz "The Effects of High Current Input Pulses Upon Channeltrons®" submitted to the Review of Scientific Instruments.

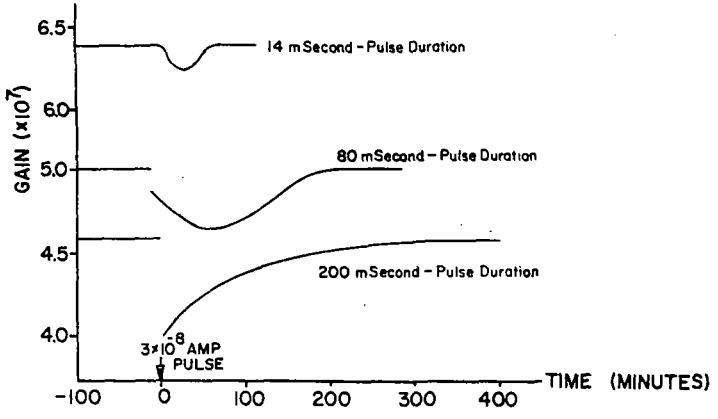


FIG. 1 GAIN VERSUS TIME AFTER PULSE

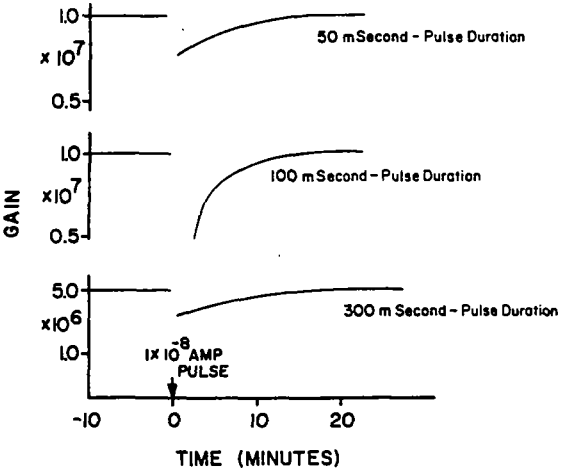


FIG. 2 GAIN VERSUS TIME AFTER PULSE

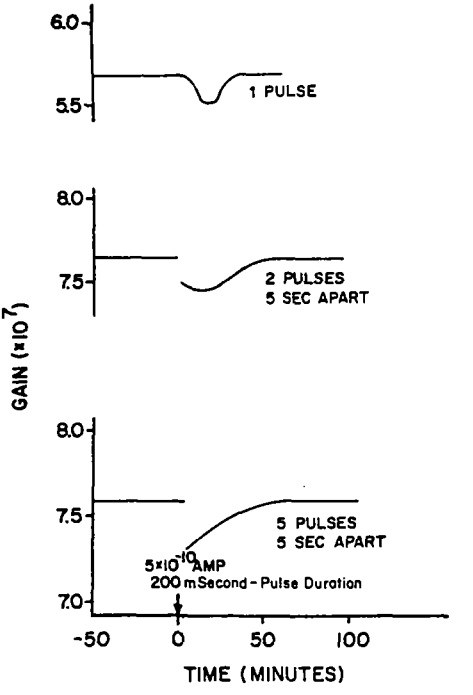


FIG.3 GAIN VERSUS TIME AFTER A SERIES OF PULSES

A DUAL OUTPUT CHANNELTRON®

E. A. Kurz and R. L. Roy
Galileo Electro-Optics Corp.
Sturbridge, MA 01518

A new detector is under development which will increase the dynamic range over existing Channeltron Electron Multipliers (CEMs) by a factor of between 10^2 and 10^3. The dynamic range of a standard CEM is typically 10^7. Figure One shows the typical dynamic range for a CEM operating at 10^7 gain. By varying gain, count rate capability can be adjusted.

The new detector differs significantly from the standard CEM in that it has one input and two outputs. An operational schematic of this detector is shown in Figure Two. Channel 1 operates at a low gain, resulting in a proportional analog output signal for high input levels. This output is sensed by Grid 1. Part of Channel 1's output also passes through grids 1, 2, and 3 and enters Channel 2, where further gain occurs. The overall gain of Channels 1 and 2 can be very large (a few times 10^8). The output of Channel 2 exhibits a peaked pulse height distribution and is quite suitable for use with standard pulse counting techniques. When the input is very large, as sensed by either or both the analog grid and the pulse counting anode, a voltage is applied to Grid 3, preventing any signal from entering Channel 2. Grid 2 isolates the anode from the effects of varying voltages on Grid 3.

Figure 3 graphically illustrates the increase in dynamic range obtained from this dual output CEM system.

Figure 4 shows the final design configuration of an actual detector of this design. Important features such as the Faraday cup/deflector, Channel 1, Channel 2, and the grid assembly are indicated.

This work was funded under NASA 5-24411.

FIGURE 1

OUTPUT CURRENT vs COUNT RATE
SINGLE OUTPUT CHANNELTRON®

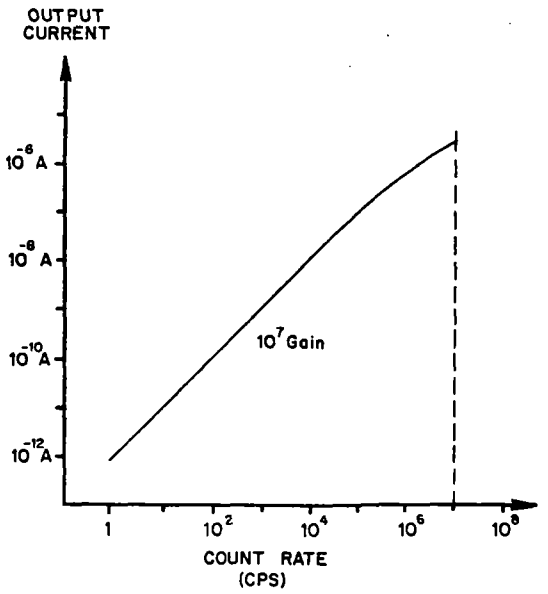
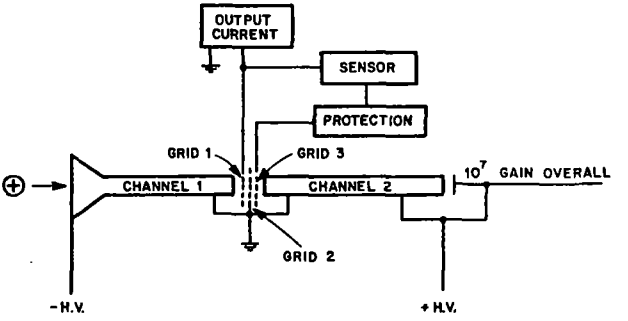


FIGURE 2



DUAL OUTPUT CHANNELTRON®

FIGURE 3

OUTPUT CURRENT vs COUNT RATE
DUAL OUTPUT CHANNELTRON®

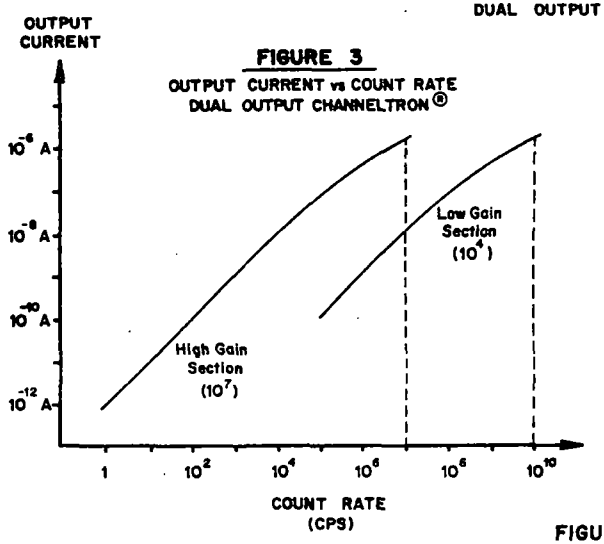
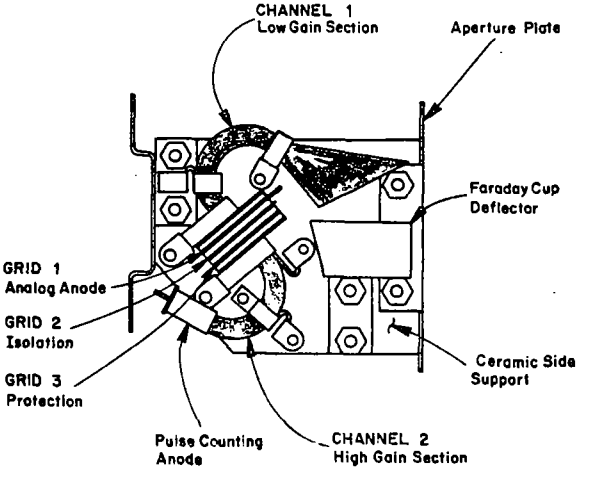


FIGURE 4



MULTICHANNEL SCALING FOR ULTRASENSITIVE DATA ACQUISITION ON THE VARIAN-MAT 731, WOODFIN V. LIGON, JR., General Electric Company, Corporate Research and Development, Schenectady, New York 12301

We have implemented a Tracor-Northern Model 1700 (8K) multichannel scaler in combination with a Johnson Laboratories Model PAD2 preamplifier-amplifier-discriminator to provide signal averaging on a Varian-Mat 731. Using the full memory (8K), ions are counted at rates up to 10MHz with dwell times per channel of about 0.5ms. Spectra are accumulated using repetitive electric scans. A mass range of up to 600AMU at mass 3000 (200AMU mass 1000) can be acquired with a single magnet setting. Using the full 8K memory and unit resolution there are 13 channels per nominal mass in a 600AMU scan at mass 3000.

This technique has allowed high resolution data acquisition in field desorption mode and data acquisition at very high mass (>3900AMU). In addition we have been able to observe a very weak (0.1 ion/channel/scan) tetracharged field desorbed ion. This data is shown in Figure 1. The ion count at the peak maximum is 10 ions/channel. Figure 2 shows the results of a 300AMU scan centered at mass 3721. The ion count at peak maximum is ~100 ions/channel. The off signal ion count is zero. The sample is a high boiling fraction of Fomblin L. The upper trace is an expanded region around mass 3671. In the expanded display all channels are shown. In the full scan only every 16th channel is displayed.

This data acquisition technique is applicable to all mass spectrometers with stable highly reproducible scan functions.

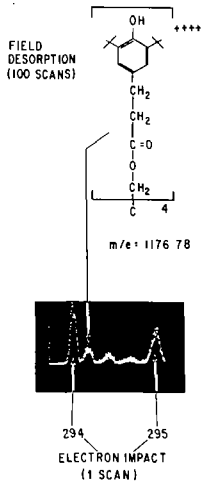


Figure 1

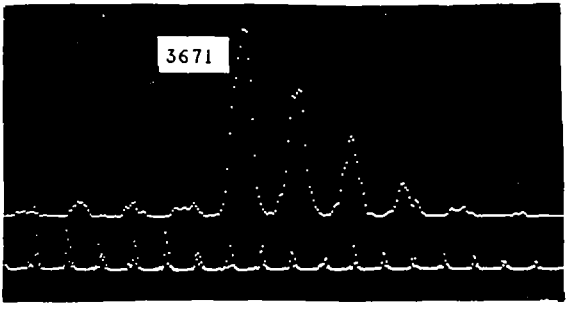


Figure 2

Biomedical Applications of Steroid Metabolic Profiling by GC/MS. P. G. Marsh and P. V. Fennessey, Dept. of Pediatrics, Univ. of Colo. Health Sciences Center, Denver, CO.

The investigation of inborn errors in human metabolism was greatly facilitated by the introduction in 1971 of metabolic profiling by gas chromatography and mass spectrometry (gc/ms) (1). For over half a decade our laboratory has been actively engaged with the gc/ms analysis of the organic acids present in the urine and plasma of children afflicted with various enzyme deficiencies (2). In the last year we have extended our capabilities to include the comprehensive analysis of the steroid metabolites found in the urine of normal populations, and in the urine of a few selected pediatric patients with either known or suspected endocrine problems. This presentation a) briefly describes the particular procedure involved, b) shows some of our data on the normal variation of particular steroid levels with age, sex and stress, c) emphasizes the potential value of being able to directly examine the relative concentrations of certain key metabolites in a urine sample, and d) illustrates, with four case histories, the emerging significance of metabolite profiling in the diagnosis of congenital lesions in steroid biochemistry.

Our method, a blend of the better procedures described in the literature (3), begins with a XAD-2 chromatography of 10-50 ml of urine in order to remove interfering salts, sugars, macromolecules, and blood cells (etc.) if present. Sulfate and glucuronide steroid conjugates are washed from the column, along with the free steroid metabolites, with methanol. After evaporation of the solvent and addition of pH 4.0 acetate buffer to the residue, these conjugates are cleaved enzymatically. All of the steroidal species are then extracted into methylene chloride, the internal standard, cholesterol n-butyrate (CB) is added, and the solvent is removed under a stream of nitrogen. The resulting residue is thoroughly dried and the steroids therein are derivatized to form the more stable and volatile "MOX-TMS" derivatives in standard use. These derivatives are separated on a 25 m glass capillary column housed in a temperature programmable gas chromatograph. Concentration values for each desired species are calculated directly by an integrating computer coupled to the chromatograph. Identifications are made using a highly reproducible methylene unit (MU) retention index and a gc/ms/computer system. With this system, we have compiled an extensive library of authentic steroid "MOX-TMS" spectra, and with the additional aid of several sophisticated data "clean-up" and interactive search routines we are able to quickly identify all major steroid metabolites.

The steroid profile of a normal adult male is shown in Figure 1; steroid metabolites of particular interest are identified and the normal variance within our control group of eight adult and teenage males is reported. The data is handled in terms of absolute concentration (µg/ml and mg/day) of each species, and also in terms of the measured amount relative to the amount of tetrahydrocortisone (THE) present in the sample. Since THE is

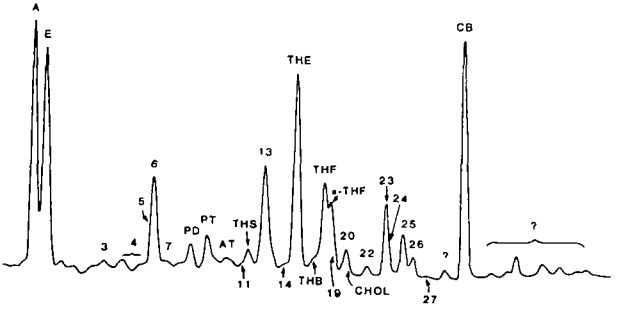


FIGURE 1
Gas chromatographic profile of normal urinary steroids from an adult male (retention time and oven temperature increase to the right).

	STEROID	µg/ml ± σ	% of THE ± σ
A	androsterone, 5α-pregnan-3α-ol-17-one	3.5 ± 1.2	96.0 ± 32.1
E	etiocholanolone, 5β-pregnan-3α-ol-17-one	2.5 ± 1.3	67.3 ± 27.8
PD	5β-pregnan-3α,20α-diol	.68 ± .34	20.8 ± 9.2
PT	5β-pregnan-3α,17α,20α-triol	.88 ± .31	26.3 ± 14.0
THS	5β-pregnan-3α,17α,21-triol-20-one	.49 ± .13	15.0 ± 4.2
13	4-pregnen-17α-ol-3,20-dione	1.0 ± .9	26.0 ± 14.8
THE	5β-pregnan-3α,17α,21-triol-11,20-dione	3.6 ± 1.5	100.0
THF	5β-pregnan-3α,11β,17α,21-tetrol-20-one	2.4 ± 1.3	64.1 ± 19.3
a-THF	5α-pregnan-3α,11β,17α,21-tetrol-20-one	2.2 ± 1.4	60.4 ± 25.0

the major metabolite of the important glucocorticoid, cortisone, and since its "MOX-TMS" derivative elutes as a sharply resolved peak in the middle of the gas chromatogram, "% of THE" values provide a way to assess interrelationships among the various metabolites in normal and abnormal steroid profiles. It is this capability to examine all of the steroid levels simultaneously that makes this method vastly superior to a series of independent radioimmunoassays for specific major metabolites.

The most obvious clinical application of steroid metabolic profiling is in the diagnosis of congenital adrenal hyperplasia (CAH). This condition results from the lack of one or more of the enzymes necessary for normal steroid metabolism. The exact position of the block determines the clinical course of the syndrome, and is also readily deduced from the metabolic profile. For example, the lack of the enzyme 17α-hydroxylase precludes the formation of 17α-hydroxypregnenolone and thus blocks the production of any androgen or estrogen hormones. The enzyme defect also blocks the biogenesis of cortisol, leading to high levels of circulating ACTH and progesterone, and to the excretion of large amounts of pregnanediol in the urine. In lieu of metabolites of 17α-hydroxyprogesterone, urinary steroids with 1β- and 16α-hydroxy groups become detectable, and the 11β- and 21-hydroxy steroids predominate along with the 11-keto homologues. Males with no 17α-hydroxylase activity have often been raised as girls because of their female habitus. Since their fetal adrenal glands could not synthesize the essential precursor for testicular transformation to the androgen hormones, the development of male genitalia was never triggered. We have derived a steroid profile from such a male pseudohermaphrodite, who, at 18, had his undeveloped and hidden testes removed and an artificial vagina implanted. The profile is compatible with a complete lack of 17α-hydroxylase and is essentially identical with a profile recently published (4). We are currently studying the urine collected for this patient after stimulation tests with hCG and ACTH in order to see the effect of these hormones on steroid equilibria in this restricted biochemical system.

Surprisingly, a second case of this extremely rare metabolic disorder in our locale was detected by our method in a 5-year-old girl with a large clitoris. Her profile was very similar to that of the prior case, except that small quantities of 11-ketoetiocholanolone, 11β-hydroxyetiocholanolone, THE and cortolone were also detected. This indicates that this 17α-hydroxylase deficiency is not complete and this individual can synthesize some androgens and cortisone. Other laboratories are planning to determine the karyotype of this child and to conduct hCG and ACTH stimulation studies. The metabolic profiles obtained during these studies will be compared to those obtained for the first patient under similar conditions. Depending upon the actual gender of the pediatric patient, the early diagnosis may enable treatment and a normal life.

A more subtle form of CAH is demonstrated by an 18-hydroxylase deficiency. Since the 18th position is only hydroxylated in the transformation of corticosterone to the potent mineralocorticoid, aldosterone, the lack of this enzyme may be deduced from a metabolic profile which is fairly normal except for a greatly increased amount of tetrahydrocorticosterone THB). We have derived the baseline metabolic profile for a boy diagnosed as having primary hypoaldosteronism who is now being treated successfully for that salt-wasting CAH syndrome. As expected, THB was his major urinary steroid metabolite, with the concentrations of the normal metabolites elevated by a factor of ten above their usual values, reflecting an indirect ACTH feedback stimulation of general steroid biogenesis.

Some of the tantalizing intricacies of steroid metabolism have been impressed upon us in our investigation of a 4-year-old boy who had grown pubic hair at 1 year of age, and who currently has a large penis (10 x 3 cm) and is the height and weight of a boy of six. His metabolic profile is fairly normal in appearance, except for the fact that THB is the major steroid metabolite present. The observation of pregnan-3α,20α,21-triol-11-one and pregnan-3α,11β,20α,21-tetrol in relatively large amounts is also of interest; the latter substance is a further reduced metabolite of THB, while the former substance implies the presence in the circulation of an oxidized form of corticosterone. We are currently analyzing the urine from the boy's grandfather who also had a precocious puberty. We hope to find a clue when comparing the two metabolic profiles that will enable us to know how to slow the rate of growth and sexual maturation so that this boy will have a chance for a normal childhood.

References:

1. a) E.C. Horning & M.G. Horning, J. Chromatographic Sci., 9, 129 (1971).
   b) M. Novotny & A. Zlatkis, Chromatography Reviews, 14, 1 (1971).
2. J.A. Thompson, B.S. Miles & P.V. Fennessey, Clin. Chem., 23, 1734 (1977).
3. a) K.D.R. Setchell, B. Alme, M. Axelson & J. Sjövall, J. Steroid Biochem., 7, 615 (1976)
   b) G. Phillipov, R.F. Seamark, & L.W. Cox, Aust. & N. Zealand J. Med., 8, 63 (1978)
4. J.W. Honour, J. Tourniaire, E.G. Biglieri, & C.H.L. Shackleton, J. Steroid Biochem. 9, 495 (1978).

Analyses of Organic Acids and Amino Acids in Amniotic Fluid by GC/MS/COM System

Toshihiro Shinka, Izumi Maruyama, Tomiko Kuhara, Isamu Matsumoto, *Katsuichi Kabashima, *Hiroshi Abe and *Toshi Kato

Research Institute of Medical Mass Spectrometry and *Department of Obstetics and Gynecology, Kurume University School of Medicine, Kurume, Fukuoka, Japan.

In order to establish an early diagnosis for the inborn errors of metabolism during pregnancy, we have been stydying the profile of the organic and amino acids in human amniotic fluid using GC/MS/COM system. Amniotic fluid is a dynamic system, and there are considerable changes in concentrations of its chemical components as gestation proceeds. Constituents may be contributed from the metabolic processes of the fetus and of the mother. On this viewpoint, studies on the profile of amniotic fluid have been reported from several laboratories (1-3), but detailed quantitative changes of amniotic fluid components during pregnancy have not been reported except catecholamine. In this report, we will detail the profiles of organic acids and amino acids in amniotic fluid and the quantitative changes of some organic acid components at four stages of gestation.

Twenty-four specimens of amniotic fluids from 20- to 40-weeks gestation were obtained. After deproteinization by cold ethanol, the organic acids were extracted using first diethyl ether and then ethyl acetate at acidic condition. The organic extracts were combined and evaporated to dryness under nitrogen stream, and the residue was trimethylsilylated with N,O-bis-trimethylsilyl-trifluoroacetamide (BSTFA). The amino acid fraction was separated with cation exchange resin (AG 50W x 12) after deproteinization, and trimethylsilylated with BSTFA and acetonitrile. These TMS derivatives were directly applied to GC/MS analysis. For the GC/MS analysis, JEOL JMS-D100 was used combined with JMA 2000 mass data analysis system. A 2m glass column packed with 3% OV-17 was used for the separation of both organic acids and amino acids. Column temperature was programmed from 80 to 290°C at 6°C/min.

We have detected and confirmed the amino acids in amniotic fluid. They were valine, glycine, proline, threonine, glutamate, phenylalanine, ornithine, lysine and tyrosine. The quality and quantity of these compounds are comparable to the previous paper of Schulman et al. (4). We have also detected more than 46 peaks in organic acid fraction of amniotic fluid and confirmed 25 compounds (Fig. 1). Several previously unidentified components of amniotic fluid were found in our organic acid profile. They were 3-hydroxypropionate, oxalate, fumarate, 2-deoxytetronate, α-glycerophosphate and β-glycerophosphate. We have also identified lactate dimer. But it is still obscure whether the latter compound is an endogeneous one or an artificial one.

The quantitative variations of several components show that there are three groups of compounds (Fig. 2). In the first group, the concentration reached maximum at 28- to 34-weeks gestation, then decreased rapidly. They were 3-hydroxybutyrate, citrate, succinate and oxalate. In the second group, the compounds decreased steeply as pregnancy advanced. They were lactate and glycolate. In the last group, the compounds maintained the concentration constant while the gestation proceed. They were 2-hydroxybutyrate, palmitate and stearate. During the third trimester, fetal bone formation, lung formation and so on were known to be enhanced in order to establish the fetal maturation. The increase of keton body and TCA cycle-related compounds at this period may reflect these situations.

References

1. Hagenfeldet, L. and Hagenfeldet, K., Clin. Chim. Acta, 42, 219 (1972).
2. Zambotte, F., Blau, G., King, G. S., Campbell, S. and Sandler, M., Clin. Chim. Acta, 61, 247 (1975).
3. Nicholls, T. M., Hagnel, R. and Wilkinson, S. P., Clin. Chim. Acta, 84, 11 (1978).
4. Schulman, J. D., Queenan, J. T. and Doores, L., Amer. J. Obstet. Gynec., 144, 243 (1972).

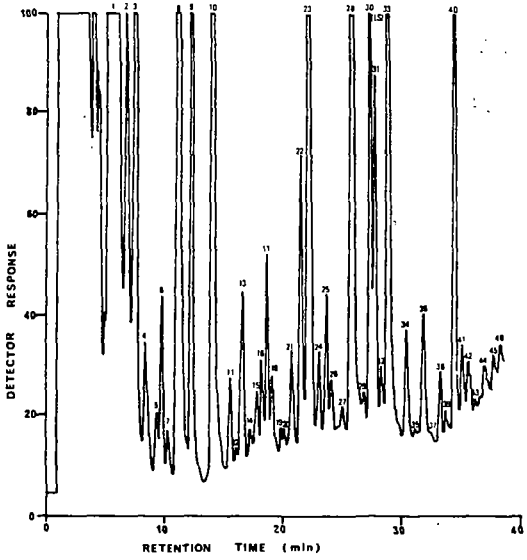
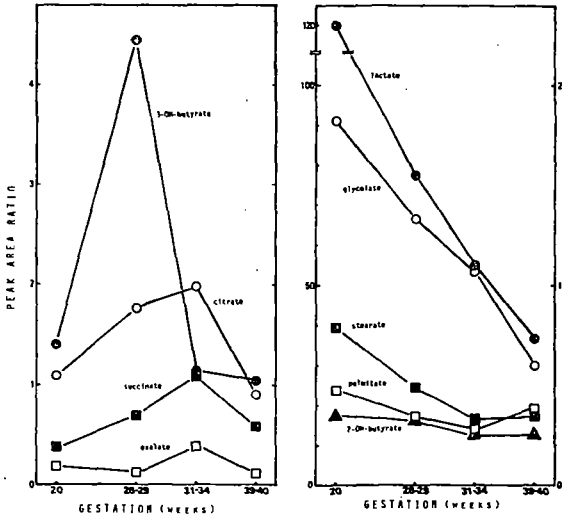


Fig. 1 Metabolic profile of organic acids in amniotic fluid.

1:lactate, glycolate, 2:2-OH-butyrate, 3:3-OH-butyrate, 3-OH-propionate, 4:oxalate, 8:urea, phosphate, glycerate, 9:succinate, fumarate, 10: 2-deoxytetronate , lactate dimer, 11:malate, 18: laurate, 21: β-glycerophosphate, 22:α-glycerophosphate, 23:citrate, myristate, 24:vanillate, 25:glucronolacton, 28:plmitate, hippurate mono-TMS, 30:heptadecanoate (I.S.), 33:stearate.



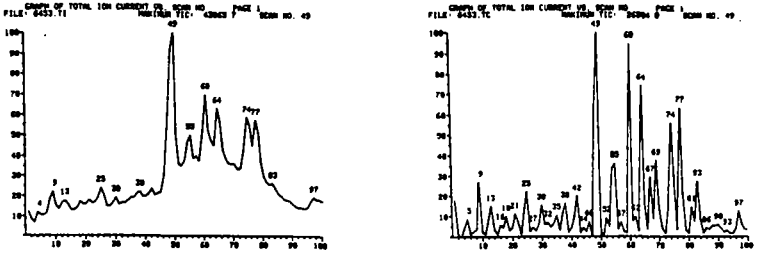
Fiig. 2 Quantitative variations of organic acids in amniotic fluid at different gestational stages. The value plotted in the vartical axis indicates the relative peak area ratio against internal standard which was added depend on creatinine concentration.

The Detection of Biochemical Markers in Disease. The Use of Quantitative GC/MS in the Discovery of New Disorders of Metabolism.
P.V. Fennessey, C. Butler, S. Kibler, P.G. Marsh and S. Tjoa. University of Colorado Health Sciences Center, Denver, Colorado 80262.

Our laboratory is involved with both the identification of unknown peaks detected during the course of the analysis of samples received from our national screening program for inborn errors of metabolism and from samples we obtain because of our location in a tertiary care hospital for the Rocky Mountain Region. These two sources result in the running of an average of 20 complete gc/ms runs per week on our single instrument. Because of this sample load and the complexity of the data generated from each of these runs we have added a second computer which is programmed to carry out the additional data processing.

The computer system we have added is a NOVA 3/12 with 32K of memory, hardware multiply/divide, two floppy disks and a 2.5 M byte removable disk unit. The first major program we added to our system has turned out to be a combination of "Cleanup" as described by the Stanford group (1) and the simpler program described by Biller and Biemann (2). Dr. D. Smith of Stanford sent us a complete copy of their program but we had to make substantial changes because of the differences in our equipment (both computer and mass spectrometer). We have found that it is important to be able to control the number of scans searched for a maxima and the conditions for saving a peak (or a part of the peak) because of the wide variety of sample types we have to deal with ranging from volatile, short-chained acids to steroids.

The wide range in the chemical properties of the compounds mentioned above leads to a wide difference in the separation obtained on our gc/ms system. An example of a raw and cleaned spectrum is given below.



Having clean data has become a great help in the automatic identification of known compounds and their subsequent quantification.

In an attempt to reduce our workload and make the data more easily understood we have developed a program to report the following data for each of the compounds found in the analysis of a particular compound class.

Scan #	M.U. (calc.)	Area/Area of i.s.	Normal area (mean min-max)	Score	Name
59	14.49	43.8%	74.0% 14.0-370.0%	-0.43	Succinic Acid

This type of data presentation allows one to scan the information and quickly pick out those peaks that are well outside accepted ranges, by a comparison of both the area/area of i.s. as compared to the mean and the score which is related to the number of standard deviations the compound's area is away from the mean compound. We have used this system for the following studies:

Case 1:

A six-year-old child with a history of poor growth, frequent episodes of drowsiness to the extent of being completely comatose in more critical situations, poor learning in school and a concern of possible mental retardation. Except for the frequent "spells" a physical exam was unremarkable. His history revealed a small bowel resection at two weeks of age with apparent full recovery. The gc/ms analysis of his urine, looking at both acids and neutrals, revealed a moderate peak for glutaric acid which is not seen in normal aged matched controls. Other cases where glutaric acid was reported in the urine and with measured enzyme deficiencies, had completely different clinical presentations. Subsequent enzyme work up on this child showed normal values. During one of the episodes requiring hospitalization the patient was treated with antibiotics because of a respiratory tract infection. A subsequent urinary gc/ms analysis showed a normal pattern. Additional studies confirmed the disappearance of glutaric acid in the urine every time antibiotics were given. We concluded that the glutaric acid was the result of its absorption as gut bacteria metabolites and its reexcretion in the urine. This and possibly other metabolites were the cause of the toxic side effects and the patient has been maintained for 1 year on an Rx of oral antibiotics twice a week. He has had some very mild reoccurrences of dizzy spells but has not been hospitalized once in that time.

Case 2:

A child that was apparently normal at birth developed a neurological problem at 6 months of age and has continued to be slow in reaching developmental milestones. Muscle biopsy showed unusually large vacuoles but other tissue suggested a less severe storage.

The child's mother has an exercise-induced cramping and excessive fatigue. She also reported several amnesic episodes lasting 12 hours following ingestion of 1 bottle of beer.

GC/MS analysis of the urinary acids and neutrals demonstrated elevated levels of α-glycerol phosphate and glycerol. A defect was suspected in the mitochondrial α-glycerol phosphate-dehydroxyacetone phosphate hydrogen ion shuttle.

This defect is closely related to the new inborn error of metabolism detected in our laboratory two years ago, namely, glycerol kinase deficiency (3). Those children also had an unusual muscle appearance and easy fatigue.

Case 3:

A family with an unusual disease that required institutionalization around puberty and was progressively debilitating over the next few years was studied. Analysis of their urine showed low levels of all metabolites except for a large unknown peak at m.u.=24.00. All affected members showed this peak which had the appearance in the low resolution spectrum of a glutaconic acid derivative. We were unable to obtain a lead as to the structure of this compound until we obtained high resolution data. The results of this study will be reported in a separate paper at this conference (4).

Acknowledgement

The authors wish to thank Gil Giron for his excellent technical help and the following agencies for financial support: NIH NICHD Grant HD 08315-05, Maternal and Child Health Project 252 and BRSC Grant RR-0537.

References

(1) D.H. Smith, M. Achenbach, W.J. Yeager, P.J. Anderson, W.L. Fitch and R.C. Rindfleisch, Anal. Chem. 49, 1623 (1977).
(2) J.E. Biller and K. Biemann, Analytical Letters 7, 518 (1974)
(3) E.R.B. McCabe, P.V. Fennessey, M.A. Guggenheim, B.S. Miles, W.F. Bullen, D.J. Sceats and S.I. Goodman, Biochem. and Biophys. Res. Comm. 78, 1327 (1977)
(4) See paper RAMOA6 in this conference

Profile of Organic Acids in Mouse Brain Homogenates

Shigeto Yamada, Tomiko Kuhara, Isamu Matsumoto and *Kazutoyo Inanaga

Research Institute of Medical Mass Spectrometry and *Department of Psychiatry, Kurume University School of Medicine, Kurume, Fukuoka, Japan.

In order to obtain much information about brain metabolism, we have studied on the profiles of organic acids in mouse brain homogenates by the use of gas chromatography-mass spectrometry (GC/MS). To make the profiles of organic acid fraction in tissues, it is the first thing to settle a suitable method for sample preparation. In this paper, we report the identification of the compounds in the organic acid fraction of mouse brain homogenates and the comparison of several procedures for sample preparation.

Materials and Methods

The mice were decapitated and the heads were immediately frozen in a liquid nitrogen. The brain was removed from the head in a cold room. The tissue (0.4g) was homogenated with 800 ul of 0.1 N-HCl in 99% methanol by Potter's homogenizer. Each 100 ug of heptadecanoate and sebacate was added as an internal standard. For deproteinization, either 4 ml of 0.3 N-perchloric acid (PCA) or 12 ml of 80% ethanol was added to the homogenates. The homogenates were mixed well and stood for 1 hr in the cold and centrifuged at 12,000 rpm/min for 15 min at 0°C. The supernatant from PCA-treated homogenate was neutralized with 1.5 N-KOH according to the method of Folbergrova (1). The supernatant from ethanol-treated homogenate was concentrated to 1 ml in order to remove ethanol completely. The organic acid fraction was obtained either by DEAE-Sephadex separation according to the method of Gates et al. (2) or by extraction with diethyl ether, and was then evaporated to dryness and derivatized with BSTFA. The derivatized samples were analyzed with a Shimadzu GC-6A gas liquid chromatograph and with a JEOL D-100 gas chromatography-mass spectrometer. The analyses were performed with a 2 m x 2 mm glass column packed with 3% OV-17 on 80-100 meshed Gas Chrom Q. The oven temperature was programmed from 80 to 280°C at 6°C/min.

Results and Discussions

The profile of organic acids in sample preparation obtained by ethanol deproteinization and diethyl ether extraction is shown in Fig. 1. Fourteen compounds in this profile were identified by the comparison of their mass spectra and retention times with those of authentic samples, such as, lactate, glycolate, 2-hydroxybutyrate, 3-hydroxybutyrate, glycerol, glycerate, succinate, fumarate, 2-deoxytetronate, malate, N-acetyl-aspartate, citrate, palmitate and stearate. Other compounds which were numbered in Fig. 1, 2 and 3 were tentatively estimated by the comparison of their mass spectra with those which have been reported (3). Major compounds in Fig. 1 were polyhydroxy-monocarboxylic acids, such as 2-deoxy-tetronate, dideoxypentonate, 2-C-hydroxymethyl-3-deoxytetronate and 3-deoxypentonate. Succinate was only compound of polycarboxylic acid which could be detected in this profile. Long chain fatty acids could be clearly detected in this profile as compared with those in the other sample preparation method. N-Acetylaspartate which was known to exist at high concentration in the brain was detected at peak No. 49. In comparison of ethanol deproteinization with PCA depropeinization (Fig. 2), long chain fatty acids and the compounds with relatively higher moleculer weight could be detected clearly in sample preparation of ethanol deproteinization, while the sample preparation of PCA deproteinization gave undesirable results. However, phosphate peak was always present in sample preparation of ethanol deproteinization and this peak concealed the peaks of glycerate, 2-methyl-glycerate and succinate. On the other hand, these three compounds were detected clearly due to disappearance of phosphate peak in sample preparation of PCA deproteinization. In comparison of DEAE-Sephadex separation with diethyl ether extraction, polycarboxylic acid, such as malate, succinate, N-acetylaspartate and citrate were detected distinctly in DEAE-Sephadex-treated sample preparation (Fig. 3).

In conclusion, it is necessary to choose adequate sample preparation method according to the nature of the compouds to be analyzed.

References
1. Folbergrova, J., MacMillan, V. and Siesjo, B. K., J. Neurochem., 19, 2497 (1972).
2. Gates, S. C., Dendramis, N. and Sweeley, C. C., Clin. Chem., 24, 1674 (1978).
3. Petersson, G., Tetrahedron, 26, 3413 (1970).

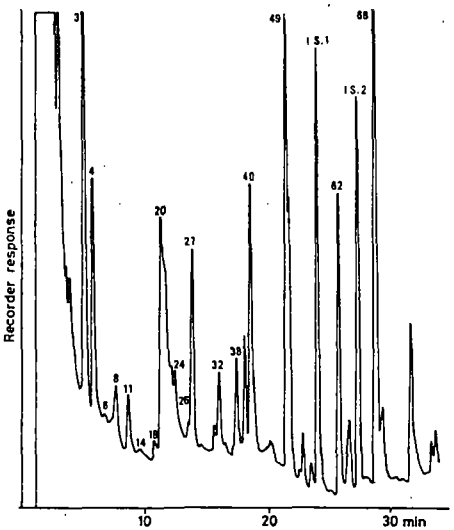


Fig. 1 Gas chromatogram of organic acids in mouse brain homogenate (By ethanol deproteinization and by ether extraction).

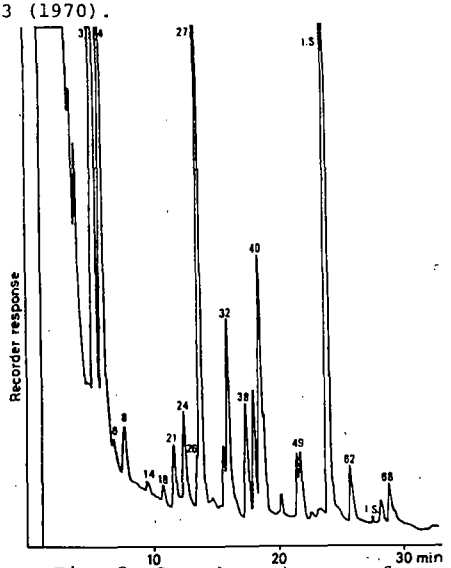


Fig. 2 Gas chromatogram of acids in mouse brain homogenate (By perchloric acid deproteinization and by ether extraction).

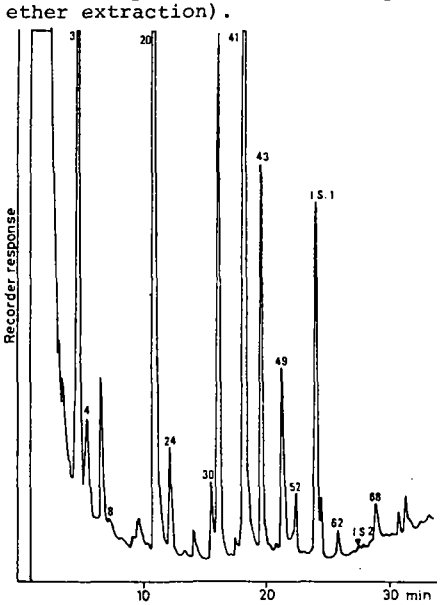


Fig. 3 Gas chromatogram of organic acids in mouse brain homogenate (By ethanol deproteinization and by DEAE-Sephadex chromatographic separation).

Peak
No. 3 lactic acid
4 glycolic acid
6 2-hydroxybutyric acid
8 3-hydroxybutyric acid
3-hydroxypropionic acid
11 cresol
14 glycerol
18 2-methylglyceric acid
20 phosphate
21 glyceric acid
24 succinic acid, fumaric acid
26 3-deoxytetronic acid
27 2-deoxytetronic acid
30 malic acid
32 dideoxypentonic acid
38 2-C-hydroxymethyl-3-deoxy-tetronic acid
40 3-deoxypentonic acid
41 glutamic acid
43 N-acetylaspartic acid-tri TMS
49 N-acetylaspartic acid-di TMS
52 citric acid
I.S. 1 sebacic acid
62 palmitic acid
I.S. 2 heptadecanoic acid
68 stearic acid

RAMOA5 RADIOGAS CHROMATOGRAPHY/MASS SPECTROMETRY IN DRUG MODE OF ACTION STUDIES

BY

I.M. Campbell, D.L. Doerfler, J.M. Malloy
I.R. McManus, J.D. Naworal and E.R. Rosenblum

Department of Biological Sciences
University of Pittsburgh
Pittsburgh, PA 15261 U.S.A.

If the flow of carbon through intermediary metabolism in cells in culture could be monitored comprehensively under various conditions of growth, a superior method of studying drug mode of action would be at hand. The pattern of flow in drug-treated and control cells could be compared. Any differences between the carbon flow patterns could be attributed to drug action, particularly if the extent of the difference correlated positively with administered drug levels. Moreover, since altered flow in any section of intermediary metabolism would necessarily indicate an alteration in the catalytic activity of specific enzymes in that section, this approach to the problem would pin-point which particular enzyme (s) was (were) antagonized by the drug.

Radiogas chromatography/mass spectrometry (RGC/MS) used in conjunction with ^{14}C-labelled substrate incorporation experiments can be used to monitor carbon flow in cultured cells. This is particularly true if the mass spectrometer (MS) is driven in the selected ion monitoring (SIM) mode. To illustrate the use of RGC/MS in this type of drug mode of action study, reference is made to the effect of 20,25-diazacholesterol (DAC) on sterol metabolism in cultured chick muscle cells.

The anti-cholesterolemic properties of DAC were discovered in 1963 (1). Since animals and humans treated with the drug accumulate desmosterol (Δ^{24}-cholesterol) in their serum it has been held for sometime that DAC acts by antagonizing a steroid Δ^{24}-reductase that is positioned at the last stage in the cholesterol biosynthetic pathway (2). In terms of an RGC/MS experiment, this means that normal cells should transfer radioactivity from a steroid biosynthetic precursor such as ^{14}C-acetate through a small metabolic pool of desmosterol to accumulate in cholesterol. DAC treated cells, on the other hand, should accumulate both mass and radioactivity in desmosterol with very little radioactivity passing to cholesterol. The cholesterol pool will still be significant as a result of biosynthetic activity prior to exposure to DAC.

Cultured chick embryo pectoral muscle cells were used in this work. They were prepared according to Konigsberg (3) and were plated at an initial density of 5×10^6 cells/15cm collagen-coated Petri dish in the medium of Coleman and Coleman (4). On the 7th day cells were depleted of serum for 4 1/2 hours and were treated with 1-^{14}C-acetate (10μCi) and DAC (1μg/ml culture fluid). Control cells were prepared similarly but the DAC was omitted. After 12 hours exposure to drug and tracer a chloroform/methanol extract was made. These extracts were analysed directly or after methanolysis.

Figure 1 shows the total current/radiocounter profile of control (I) and treated (II) cell extracts following methanolysis. Both samples had been spiked with a mixture of cholesterol (A), desmosterol (B), and lanosterol (E). Unexpectedly, radioactivity is lost from both the cholesterol and the desmosterol elution zone. Instead radioactivity is accumulated in elution zone D. Figure 2 shows the selected ion current profile at m/e 271 of treated (I) and control (II) extracts prior to methanolysis. The m/e 271 is the base peak of the desmosterol mass spectrum but is of low intensity in cholesterol. Elution zones X and Y correspond to cholesterol and desmosterol respectively. It can be calculated that relative to cholesterol the pool size of desmosterol drops by about half on DAC treatment. The pool size of a third compound (Z) doubles on DAC treatment.

These data are not consistant with the hypothesis that DAC's only action is to antagonize a Δ^{24}-reductase that operates late in the steroid biosynthetic pathway in muscle cells. Rather they indicate that a more pleiotrophic action is involved.

REFERENCES.

1. Counsell, R.E., Klimstra, P.D., and Ranney, R.E., (1962) J. Med. Pharm. Chem., 5, 1224-1233.

2. Laskowski, M.B., and Dettbarn, W.D., (1977) Ann. Rev. Toxicol., 17, 387-409.

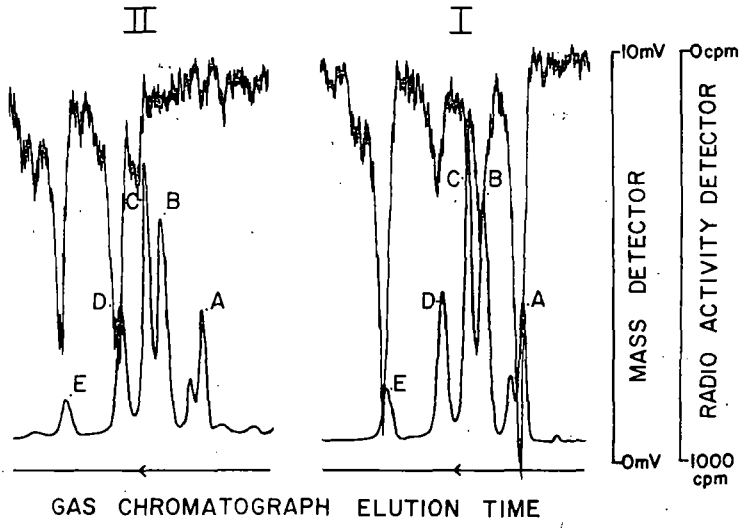


FIGURE 1

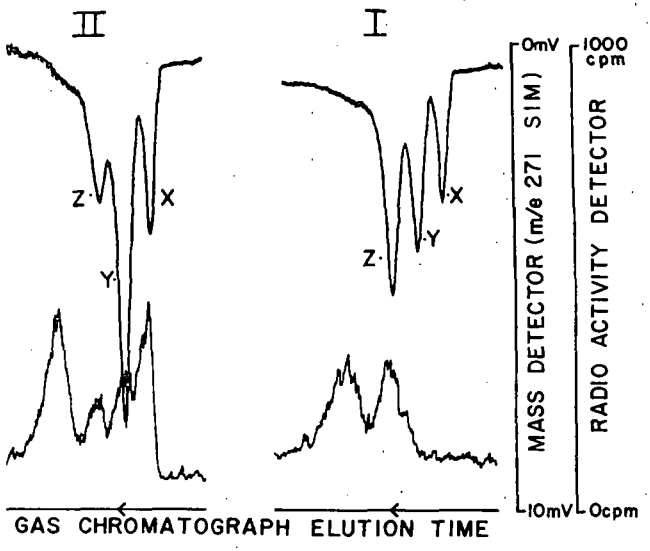


FIGURE 2

REFERENCES (continued)

3. Konigsberg, J.R., McElvain, N., Toothe, M. and Herrmann, H., (1960), J. Biophys. Biochem. Cyto., 8, 333-343.

4. Coleman, J.R., and Coleman, A.W., (1968) J. Cell Physiol., 72, Suppl. 1, 19-33.

APPLICATIONS OF GLASS CAPILLARY GAS CHROMATOGRAPHY/HIGH RESOLUTION MASS SPECTROMETRY TO PROBLEM AREAS OF URINARY ORGANIC ACID ANALYSIS

RAMA06

Sydell Lewis and A. L. Burlingame
Biomedical Mass Spectrometry Resource, Space Sciences Laboratory,
University of California, Berkeley, Ca. 94720
P. V. Fennessey
Dept. of Pediatrics, University of Colorado Medical Center, Denver, Col. 80262

A specialized technique which couples the efficiency of glass capillary chromatography (HRGC) with elemental composition determinations from accurate mass measurements (1,2) has been applied to identifying two unknown organic acids, each associated with an undiagnosed disease state. Mass spectra obtained from initial analyses of these components by routine gas chromatography/mass spectrometry were not readily interpretable.

Samples of organic acid extracts were prepared by a modified Thompson and Markey method (3) and were derivatized with BSTFA. Routine GC/MS (3) was performed using OV-22 packed columns (2).

Results and Discussion: Sample "K" was obtained from an infant having the symptoms of acidosis and failure to thrive. The compound elutes at RI ~ 1600 on an OV-22 packed column and the mass spectrum (Fig. 1) was located in the HRGC/HRMS total ion current chromatogram at RI 1363 using nominal mass chromatography (2). A reasonable set of elemental compositions was obtained (Fig. 1) from the accurate mass data which establishes the molecular ion at m/z 231.0742 ($C_6H_8O_2NSTMSi$). The ion at m/z 71.0616 results from a loss of CO_2 from the M-15 ion (m/z 216.0511) indicating that oxygen is not silylated. CO_2 expulsion plus the acidic nature of the mixture points to a lactone structure. The compositions of the ions at m/z 82.0699 (C_5H_8N) and m/z 91.0040 (HSTMSi) clearly indicate a silylated sulfur and the presence of a sulfhydryl group. The nitrogen must therefore be imino or fully substituted in order to have survived extraction and escaped silylation. In addition, several minor fragments that are free of sulfur contain silylated oxygen or nitrogen (Table 1), suggesting TMS migration. With all these structural constraints in mind, we developed a model (Fig. 2a) from the following biochemical reactions. Homocysteine is transaminated to a ketomercaptobutyric acid which condenses with ethanolamine to form a Schiff base which in turn lactonizes to form the proposed molecule in Fig. 2a. Although structures for all the major ions could be rationalized from this model, they would be more likely to result from the molecule in Fig. 2b. TMS migration can occur in both. Synthesis will be required for structural confirmation.

The unknown compound from sample "L-F" appeared in the urine of two siblings with an undiagnosed neurological disorder in which deterioration became manifest at the onset of puberty. The compound elutes at RI ~ 2400 on both OV-22 packed columns and GE SE-52 capillary columns. Elemental composition data confirmed the presence of a uronic acid moiety and indicated the presence of three chlorines in the molecule (Fig. 3). This led to the structure of urochloralic acid (Fig. 4), a conjugate of glucuronic acid (4) with a metabolite of chloral hydrate (the hydrate of trichloracetaldehyde, a sedative). It is formed by catalytic reduction of alcohol dehydrogenase of the aldehyde to 2,2,2-trichloroethanol and then conjugation to the glucuronide by the transfer of glucuronic acid from uridine diphosphate (UDP) glucuronic acid by UDP-glucuronyltransferase. No evidence of chloral hydrate administration appears on the patients' records. However, analysis of urine from another patient who had been given chloral hydrate revealed the same GC/MS peak and an identical spectrum. Urochloralic acid is being synthesized for confirmation.

Conclusion: The identification of an unexpected chlorinated drug metabolite (urochloralic acid) and the unequivocal determination of the elemental composition of a compound containing both sulfur and nitrogen, while both were constituents of complex biological mixtures, could have only been accomplished by HRGC/HRMS.

Acknowledgments: We wish to thank T.A. Baillie for helpful suggestions which led to determination of the proposed structures shown in Fig. 2. This work was supported by National Institutes of Health Division of Research Resources Grant RR00719.

References:

1. J. Meili, F.C. Walls, R. McPherron and A.L. Burlingame, J. Chromatogr. Sci. 17, 26 (1979).
2. Sydell Lewis, C.N. Kenyon, Juerg Meili and A.L. Burlingame, Anal. Chem., in press (July 1979).
3. T.H. Bindel, P.V. Fennessey, B.S. Miles and S.I. Goodman, Clin. Chim. Acta 66, 209 (1976).
4. "The Merck Index", Ninth Ed., Merck and Co., Inc., Rahway, N.J., 1976.

FIG. 1 Unknown Urinary Organic Acid - TMS
HRGC/HRMS Analysis (Fennessey Sample "K")

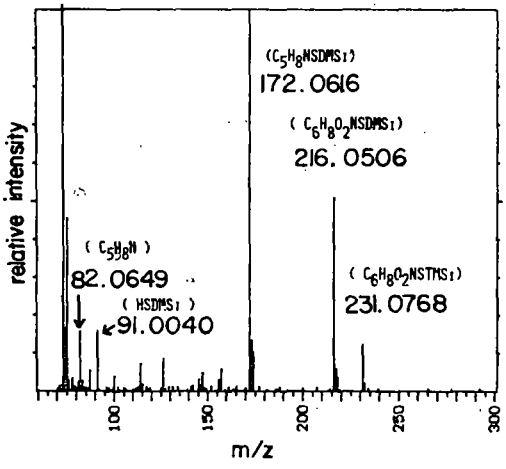


FIG. 3 UNKNOWN URINARY ORGANIC ACID - TMS DERIVATIVE
HRGC/HRMS ANALYSIS (FENNESSEY SAMPLE)

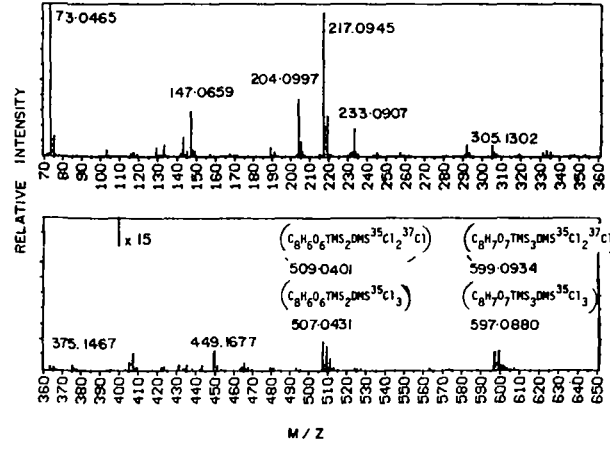


TABLE 1

ACCURATE MASS	ELEMENTAL COMPOSITION
114.0390	$C_2H_2ONDMSi$
126.0744	C_3H_3NTMSi
117.0384	COOTMSi

FIG. 2a

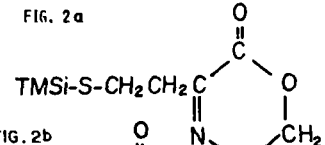


FIG. 2b

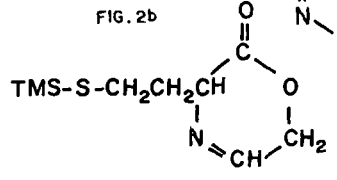
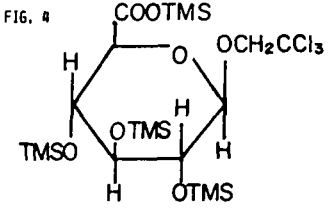


FIG. 4



Urochloralic Acid tetra TMS
(β,β,β-trichloroethyl-D-glucuronide)

RAMOA7 Analysis of Trace Levels of Organic Compounds using the New Electro-Optical Ion Detector Mass Spectrometer (EOID/MS) at JPL. Heinz G. Boettger, C. E. Giffin, and R. A. Britten, California Institute of Technology, Jet Propulsion Laboratory, Pasadena, California 91103.

The objective of this paper is to describe applications of the new EOID/MS at JPL in the field of trace analysis of biochemical compounds in physiological samples. The identification and estimation of many physiologically active compounds in plasma, urine or tissue requires high sensitivity and selectivity in detection. EOID/MS singly and in combination with GC and HPLC is under investigation as a means for the analysis of trace levels of organic compounds in biomedical samples. Procedures for the identification and quantitation of animo acid and steroids at the subpicogram level are described, demonstrating the unique advantages of an instrument system capable of recording complete spectra of trace components at sensitivity levels equal to those achieved by single ion monitoring. The detector system permits integration times from a few milli-seconds for rapidly changing concentration profiles to many minutes for slowly evolving substances.

Cf-252 Plasma Desorption Mass Spectrometry of Synthetic Gene Fragments*

C.J. McNeal and R.D. Macfarlane
Department of Chemistry, Texas A&M University, College Station, Texas 77843

Using the method of Cf-252 PDMS, the base sequence and molecular weight of a chemically protected oligonucleotide can be obtained (1). The positive ion mass spectrum is dominated by the presence of the oligonucleotide molecular ion and the negative ion spectrum is characterized by a nested set of fragment ions extending from the 3'-or 5'-terminal nucleotide to the opposite terminal nucleotide thereby identifying the sequence. The utility of this method has been demonstrated by the sequence determination of protected tetra-, penta-, hexa-, and decanucleotides synthesized by the improved phosphotriester method (2).

Very little fragmentation is observed in the positive ion mass spectrum above mass 500. The principle ion detected beyond this mass occurred 23 mass units higher than the average molecular weight of the parent molecule corresponding to ions of the type $(M+Na)^+$. The intense singular presence of this ion in the higher mass range unambiguously identified the average mass of each intact protected nucleotide and, in addition, verified the purity of the compound. The presence of the protecting group had the effect of increasing the positive molecular ion intensities relative to that of the naturally occurring oligonucleotides of comparable length. For example, the positive molecular ion intensity of dbzA$\bar{T}$ibuG$\bar{T}$bzA$\bar{T}$T(OBz) is of similar magnitude to that observed for corresponding molecular ions of GMP and (G-A).

In contrast to the positive ion spectra, the negative ion spectra were distinguished by an intense fragmentation pattern from which the base sequence could be determined. Bond cleavages occurred primarily at either the C5'-O5' or C3'-O3' internucleotidic links, liberating a nested set of fragment ions each bearing a negatively charged external phosphodiester group on the 3' or 5' end respectively. If the protected oligonucleotide had a hydroxyl group at the 5' terminus and an acyl function on the 3' terminus, there was a preference for cleavage to occur primarily along the C5'-O5' bond, rather than the C3'-O3' bond so that the set of negative ions terminated by a negatively charged external 3'-phosphodiester group was more intense than the set terminated by the corresponding 5'-phosphodiester group. However, the pattern was reversed for ions of the terminal nucleotide unit, in this case, the 5'-mononucleotide was barely detectable whereas, the 3'-mononucleotide was the most intense fragment ion.

It was possible to measure mass differences with sufficient precision to identify the base sequence of a protected oligonucleotide. Further, the simplicity of the positive ion spectrum can be used to detect the presence of impurity oligonucleotides down to the 10% level. These results show that Cf-252 PDMS can be used to sequence fully protected, synthetic oligonucleotides.

References

1. McNeal, C. J., Narang, S. A., Macfarlane, R. D., Hsiung, and H. M., Brousseau, R., (to be published).
2. Hsiung, H. M., Brousseau, R., Michniewiez, J., and Narang, S. A.(1979) Nucleic Acid Res. 6, 1371.

Research supported by the National Institute of General Medical Sciences (GM22950) and the Robert A. Welch Foundation (A258).

STEROID ANALYSIS USING CHEMICALLY LABELED IMMUNOASSAY

Frank M. Bockhoff and Heinz G. Boettger
California Institute of Technology
Jet Propulsion Laboratory
Pasadena, California 91103

The purpose of this work is to develop a simplified and sensitive procedure for the analysis of steroids in complex mixtures such as biological fluids. Our approach was to use the basic techniques of radioimmunoassay (RIA) analysis[1] but to substitute a chemically labeled standard in place of a radiolabeled tracer and to use mass spectrometry to separate and analyze the components.

Immunoassay is based on the principal that antibodies can specifically and competitively bind both an antigen (steroid) and a chemically similar standard or tracer. The disadvantages of RIA include problems associated with radioactive materials and the frequent inability to distinguish the antigen from immunochemically related molecules.

17B-Estradiol was chosen as a representative steroid for analysis. 6-methoxime-17B-estradiol, synthesized from 6-Keto-estradiol by reaction with methoxyamine hydrochloride in pyridine,[2] was selected as a chemically labeled standard. After incubation of the steroids with an estradiol specific antibody, the bound steroid phase is separated from the free phase by precipitation with a 4-fold excess of acetone. The solutions are centrifuged, the supernatant removed, and the bound precipitate dried under nitrogen. The bound complex is inserted into the mass spectrometer (AEI MS-901) via the direct probe (source temp. 140-150°C), the steroids are thermally liberated from the antibodies, and concentrations are measured by monitoring of the molecular ions. A standard curve may then be prepared from the ratio of estradiol to methoxime.

The major problem encountered with this technique is the background introduced by slow pyrolysis of the antibodies on the probe. While peak areas from estradiol and 6-methoxime antibody complexes qualitatively follow steroid concentrations in the low nanogram range, pyrolysis background currently limits the detection of estradiol to ~100 pg. Improvements in the sensitivity are hoped for by going to chemical ionization, using a specially designed pyrolysis probe, and measuring spectra with an electro-optical ion detection system.[3]

REFERENCES

1. D. S. Skelley, L. P. Brown and P. K. Besch, Clinical Chem., 19, 146 (1973).

2. J. H. Fried and A. N. Nutile, J. Org. Chem., 27, 914 (1962).

3. H. G. Boettger, C. E. Giffen and R. A. Britten, 27th Annual Conference on Mass Spectrometry and Allied Topics, Seattle, WA., June 1979, Paper RAMOA7.

Studies of Chlorophyll a Solvation by ^{252}Cf-PDMS

J.E. Hunt and R.D. Macfarlane

Department of Chemistry, Texas A&M University

College Station, Texas 77843

Introduction

The conversion of solar energy to chemical energy in the primary events of photosynthesis is accomplished by chlorophyll molecules. The majority of the chlorophyll molecules serve to funnel radiant energy, which they absorb, to a "reaction center" where photochemistry can occur via charge separation of these few special chlorophyll molecules. The nature of antenna and photoreaction center chlorophyll are central questions in photosynthesis research.

Chlorophyll a (Chla) is a reduced porphyrin, with two additional hydrogens on ring IV. This lower oxidation state becomes important for the π-system and thus for the electronic transition spectra. Chlorophyll normally represented is coordinatively unsatured as the axial positions on the magnesium atom are unfilled. From infrared and NMR studies, it has been shown that in polar solvents the chlorophyll occurs as the chlorophyll a monomer with one or both axial positions filled by solvent molecules [1]. Chlorophyll itself also posses such nucleophiles in the oxygen functions on the molecule. So, in non-polar solvents the chlorophyll can exist as dimers and oligomers.

Due to the nature of these coordination interactions in vitro models can be made which show the activity of in vivo chlorophyll.

Results and Discussion

These states of aggregation were investigated by Plasma Desorption Mass Spectrometry (PDMS), which has shown itself to be mild technique and sensitive to solid state ordering. Electron impact (EI) mass spectra show only pyrolysis products and no molecular ions of chlorophyll.

Monomer chl a samples which absorb at 660 nm show an extensive fragmentation pattern from mass 400 to 650 in both the negative and positive ion spectra. This fragmentation is not observed in field desorption (FD). One of the prominent fragment peaks, due to the loss of the phytyl tail from the chlorophyll macrocycle, occurs in both positive and negative ion spectra. The molecular ion is present in both positive and negative ion spectra, however, the negative ion spectra show additional peaks due to the attachment of extraneous nucleophiles to the chlorophyll molecule. This extra stability found in the anion bears significance on the model system for the primary act in photosynthesis.

The PD spectrum of the oligomer (680 nm) clearly shows that the chlorophyll-chlorophyll interactions and chain length are much greater than those of the monomer (660 nm). The intensity ratio of the monomer (mass=893) to dimer (mass=1787) is 40:1 in benzene versus 9:1 for the oligomer solution. It is known that in concentrated chl a solutions the oligomeric chain length can be as high as 10-20 units [2]. Although FD shows the presence of pheophytin a (the exchange of two protons for the central magnesium). PD does not show this reaction in this case. Furthermore the oligomer

shows the same fragmentation pattern as the monomer with only a portion, some 1% to appear as $M^{+\cdot}$, $2M^{+\cdot}$ and trimer. Absorption of energy to the unbound states in the manifold cause the molecule to dissociate creating the fragmentation pattern, while some of the oligomer chains in the ground or low lying energy states are ionized as a result of the shock wave produced by the rapidly moving fission fragment.

The PD of chlorophyll a hydrates is most unique in that the anion dihydrate of chlorophyll a is quite intense in addition to the molecular ion (M=893) in both negative and positive spectra. Also found in the spectra, in this case, is the pheophytin ion formed from pheophytin already present in the sample. This dihydrate anion indicates that the bond energy of water attached to the chlorophyll molecule anion is much larger than the corresponding bond energy for the cation. This result bears strongly on the photoreactions of photosynthesis as related to model systems for the photoreaction center.

Conclusions

We have shown that PDMS is a delicate probe into the chemical physics of chlorophyll states and by a similar mechanism to light absorption mimics the charge separation proposed for the primary event in photosynthesis. We intend to extend this study with the added support of molecular orbital calculations of chlorophylls and reduced porphyrins in interpreting the PD spectra of chlorophyll dimers and higher aggregates as related to the structure of chlorphyll in vivo.

We wish to thank J.J. Katz (Argonne National Lab) for generous donation of chlorophyll samples and R. C. Dougherty for assistance in interpretation of data.

The financial support of the National Science Foundation (CHE75-21554), National Institutes of Health (GM-26096) and the Robert A. Welch Foundation is greatfully acknowledged.

References

1. Katz, J. J., et al., J. Amer. Chem. Soc., 90, 734 (1968).
2. Shipman, L. L., Cotton, T. M., Norris, J. M., and Katz, J. J., J. Amer. Chem. Soc., 93, 8222 (1976).

In Vivo Study of Metabolism of Chirally Labeled Valine in Rats. I. J. AMSTER, D. J. ABERHART,* and K. TANAKA. Yale University School of Medicine, New Haven, CT 06510; *The Worcester Foundation of Experimental Biology, Shrewsbury, MA 01545

Steps in valine metabolism have extensively been studied in the past two decades but there are still several steps which remain to be elucidated. To study the mechanisms of the following unknown metabolic reactions, we synthesized valine and isobutyrate chirally labeled at the pro-S methyl group with ^{13}C or ^{2}H and studied their metabolism in rats in vivo.

Stereospecific mechanism of isobutyryl CoA dehydrogenation

We have previously shown that with the administration of isobutyrate in amounts of 40 to 100 mg per 100 g body weight, rats excreted a large amount of 3-hydroxyisobutyrate. This hydroxy acid was produced by α,β-dehydrogenation and subsequent hydration of methacrylate since α-deuterium of [2-^{2}H]isobutyrate was lost in the resulting 3-hydroxyisobutyrate (1). Therefore, when rats are loaded with isobutyrate labeled with 3 ^{2}H at the 2-pro-S methyl group, if one proton each were extracted from 2 pro-S methyl and α-methine, then the resulting 3-hydroxyisobutyrate and 2-methylmalonate would have two and no deuterium atoms, respectively. In contrast, if protons were extracted from 2-pro R methyl and α-methine, the resulting 3-hydroxyisobutyrate and methylmalonate would have 3 ^{2}H remaining at the 2-methyl group (Fig. 1).

We loaded two normal rats with 2S-[3,3,3-$^{2}H_3$]isobutyrate, and analyzed urinary 3-hydroxyisobutyrate as the methyl ester and isopropyl ester. The mass spectra of the isopropyl ester clearly indicated that 95% of 3-hydroxyisobutyrate from the rat's urine is labeled with 2 ^{2}H at the hydroxymethyl group and 5% is labeled with 3 ^{2}H at the methyl group. Thus, dehydrogenation of isobutyrate takes place almost exclusively from 2 pro-S methyl group and α-methine (2) (Fig. 2).

Stereospecific mechanism of methacrylyl CoA hydration

We isolated 3-hydroxyisobutyrate from the urine of rats loaded with natural isobutyric acid by a combination of distillation and thin layer chromatography. Optical rotation of the methyl ester of this acid was +25.8° indicating S-configuration (3). This data indicate that methacrylate is hydrated with the addition of a proton at carbon 2 from the same side as the hydrogen was removed in isobutyryl CoA dehydrogenation (Fig. 2).

Physiological significance of keto-enol tautomerization of 2-ketoisovaleric acid in vivo

At the 2-keto acid stage which precedes isobutyrate, 3proS-keto acid can be racemized to 3proR-keto acid by keto-enol tautomerization. This was clearly shown by the identification of L-allo-isoleucine in patients with maple syrup urine disease in whom oxidative decarboxylation of branched 2-keto acids is blocked (4). However, the significance of this reaction was not known in normal man nor in an other animals who do not have the metabolic block.

To study the magnitude of keto-enol tautomerization in valine metabolism in animals in which oxidative decarboxylation of branched 2-keto acids is not blocked, we injected 2RS,3S-[4-^{13}C]valine in amounts of 45-85 mg/100 g to vitamin B_{12} deficient rats and analyzed urinary methylmalonic acid by monitoring ions at m/e 146 and 147 as well as those at m/e 59 and 60. The ions at m/e 146 and 147 are the molecular ions of the unenriched and enriched compounds, respectively. The ions at m/e 59 and 60 are due to unenriched and enriched methoxycarbonyl groups, respectively. The isotope peak due to the natural

abundance of ^{13}C was subtracted from the intensity of the m/e 147 and 60 peaks.

We found that 23.4% of the methylmalonic acid is labeled with one ^{13}C atom and 19% of it is labeled at one of the carboxyl groups. Therefore, 4.4% of the urinary methylmalonic acid is enriched at the 2-methyl group. This result indicates that about 19% of the labeled methylmalonic acid is tagged at the methyl and that the remaining 81% is tagged at one of the carboxyls. Since we have shown that about 5% of isobutyrate was dehydrogenated at the 3proR methyl, we conclude that about 14% of valine administered was racemized by keto-enol tautomerization under these conditions.

Acknowledgement

We thank Ms. Ellen Jenkins, Department of Medicinal Chemistry, University of Utah for performing selective ion monitoring and Ms. Marilyn Feldman for preparing this manuscript. This study was supported by an NIH grant (AM 17453) and by a grant (1-378) from the National Foundation-March of Dimes.

1. Baretz, B.H., and Tanaka, K. J. Biol. Chem. 253, 4203 (1978)
2. Amster, I.J., and Tanaka, K. Submitted to J. Biol. Chem.
3. Amster, I.J., and Tanaka, K. Biochim. Biophys. Acta (in press)
4. Norton, P.M., Roitman, E., Snyderman, S.E., and Holt, L.E. Lancet 1, 26 (1962)

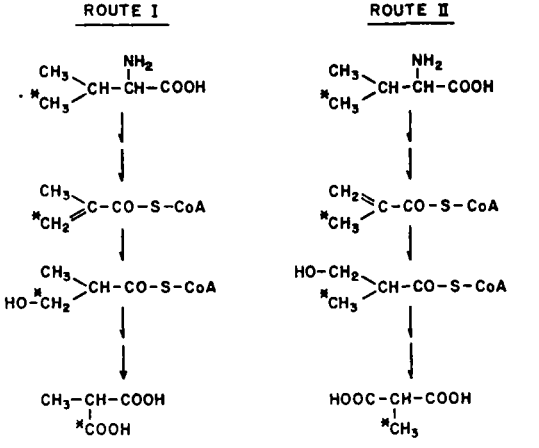


Fig. 1. Two possible stereospecific pathways of valine metabolism

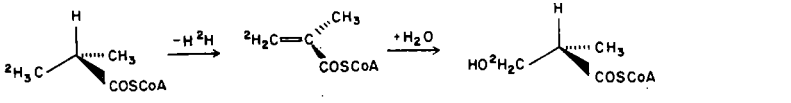


Fig. 2. Stereospecific mechanisms of isobutyryl CoA dehydrogenation and methacrylyl CoA hydration

RATE OF FORMATION OF Ar_3^+

D. C. Conway
Dept. of Chemistry
Texas A&M University
College Station, TX 77843

Werner et al.,[1] in their analysis of the cause of the deterioration of laser power at high pressures in the Ar excimer laser, postulate that the rate constant k_1 for the reaction

$$2Ar + Ar_2^+ \underset{k_{-1}}{\overset{k_1}{\rightleftharpoons}} Ar_3^+ + Ar \qquad (1)$$

is 4.2×10^{-33} cm^6/sec at room temperature. Liu and Conway[2] determined k_1 to be 3.2×10^{-30} cm^6/sec at 77°K in a drift tube mass spectrometer. The two values of k_1 appear to be in disagreement because k_1 is not expected to have such a strong temperature dependence.

The RRKM method[3] in the semiclassical approximation was used to compute k_{-1}. The rate constant k_1 was computed from Kk_{-1}.

The equilibrium constant K was measured from 144 to 217°K and the derived thermodynamic data were used to extrapolate K to the temperatures of interest.[4] Ar_3^+ was assumed to be linear. The Ar_2^+-Ar bond energy of 5.05 kcal/mole as well as the Ar_3^+ vibrational frequencies computed from the vibrational entropy for various vibrational models[4] were used in the computation of k_{-1}. The theoretical k_1 values are $3\text{-}5 \times 10^{-31}$ cm^6/sec at 77.3°K and about 7×10^{-32} cm^6/sec at 298°K. These values are not in agreement with either of the experimental results. However, the temperature dependence of k_1 was found to be small, so one (or both) experimental k_1 values is (are) in error by more than an order of magnitude.

Acknowledgment: This research was supported by the Robert A. Welch Foundation.

[1] C. W. Werner, E. Zamir, and E. V. George, Appl. Phys. Lett. 29, 236 (1976).

[2] Wei-cheng F. Liu and D. C. Conway, J. Chem. Phys. 62, 3070 (1975).

[3] G. M. Wieder and R. A. Marcus, J. Chem. Phys. 37, 1835 (1962); R. A. Marcus, J. Chem. Phys. 43, 2658 (1965).

[4] D. L. Turner and D. C. Conway, submitted to the J. of Chem. Phys.

Fragmentation of SO_2^+ Prepared in State-selected Vibrational Levels

Morris J. Weiss, Ta-Cheng Hsieh and G. G. Meisels, Department of Chemistry, University of Nebraska-Lincoln, Lincoln, NE 68588

INTRODUCTION

A simple and direct approach to the study of specific state chemistry deals with unimolecular processes originating from intermediates prepared in selected vibrational and rotational states (1,2). The recent development of Threshold Photoelectron - Coincident Photoion (TPE-CPI) mass spectrometry provides a valuable tool for the study of such reactions. It permits the detection of molecular ions and of fragmentation products resulting from primary ionization processes in which internal energies of the initial ion are defined within 0.018eV. For simple molecules, this permits one to select individual vibrational states. We describe here a study of SO_2 where high resolution photoelectron spectroscopy (4,5) has clearly delineated electronic states and vibrational progressions.

The thermodynamic onset of fragmentation of SO_2^+ falls within the third band of the photoelectron spectrum of SO_2; it consists of three electronic states arising from the removal of electrons successively from the $4b_2$, $2a_1$ and $2b_1$ orbitals (5,6). An earlier photoelectronphotoion coincidence study with a resolution of about .180eV (7) reported that the band is fully predissociated to $SO^+ + O$ in their ground states and that processes leading to S^+ formation are too weak to be measured meaningfully.

We have used the location of the vibrational band energies reported by Lloyd and Roberts (5) to prepare SO_2^+ ions in specific vibronic states and have followed their fate.

EXPERIMENTAL

The Threshold Photoelectron-Coincident Photoion Mass Spectrometer (TPE-CPI-MS) has been described elsewhere (3). The apparatus has been modified by incorporation of a quadrupole mass spectrometer. SO_2 was Matheson research grade and used after bulb-to-bulb distillation.

RESULTS

The results of the TPE and TPE-CPI fragmentation studies on SO_2 may be summarized as follows:

(a) The shape of the TPE spectrum closely parallels that of the HeI photoelectron band obtained by Lloyd and Roberts (5). Autoionizing structure is absent; the location of the peaks in the photoelectron spectrum can be correlated well with our observed photoelectron efficiency curve. It appears that the heretofore unobserved (410) levels and perhaps even the (510) level of SO_2^+ $^2B_2$ are excited. These levels appear as shoulders on the low energy side of the (100) and (200) levels of the $^2A_1$ state. The (310), (410) and (510) levels were not resolved in the VUV photoelectron study of Lloyd and Roberts (5).

(b) The third photoelectron band is partly predissociated to SO^+ and S^+. Parent molecule-ions formed with an internal energy in excess of the fragmentation threshold to SO^+ and O are still present (~5%) near the maximum of the third band.

(c) S^+ ions begin to be produced at a photon energy of 16.334eV, above the thermochemical threshold of 16.225eV (8), from SO_2^+ ($^2B_2$) ions, but only within an extremely narrow range of internal energies (Figure 2). The dissociation onset is coincident with the (310) level of SO_2^+ $^2B_2$.

(d) SO^+ ions are formed below the onset of the $^2B_2$ (000) state. The onset of SO^+ formation is at a nominal photon energy of 15.930 ± 0.005eV. This compares favorably with a calculated value of 15.95 ± 0.05eV obtained by combining the photoelectron spectroscopic ionization potential of the SO molecule with D (O-SO) of 5.60eV (8). Comparison of the SO_2^+ peak shape, for example at 16.180 e.v., with those of the other ions shows clearly that SO^+ is produced with excess kinetic energy as reported earlier (7).

The difference of our results from those reported earlier (7) can probably be ascribed to the higher sensitivity and energy resolution of the present study.

DISCUSSION

Our results suggest that the complex third photoelectron band of SO_2 includes a state or states which are not fully predissociated to $SO^+ + O$ but are stabilized by emission. We note, for examples that SO_2^+ is not observed at 16.674 eV, coincident with the levels $(200)^2B_1$ and $(300)^2A_1$. This may indicate that the $^2A_1$ state is stabilized long enough to radiate to the SO^+ ^{2} ground state but that the $^2B_1$ state predissociates to $SO^+ + O$. This suggests a rather long dissociative lifetime of the B^2A_1 and perhaps other states, on the order of 10^{-9} to 10^{-10} sec.

This is probably a result of the symmetry disallowed energy flow from ν_1 (symmetric stretch) to ν_3 (asymmetric stretch) required for asymmetric fragmentation to SO^+ and O. This intermodal energy flow does not occur unimolecularly in neutral SO_2 within the microsecond range. (10)

The energy at which SO^+ fragment ions can barely be detected is 15.930eV. We estimate the onset of SO^+ formation at 0^oK to be 15.965eV on the assumption that two degrees of rotational freedom contribute to the dissociation of SO_2^+ (11) and .009eV arise from the photon bandwidth of 0.8A. (12)

The formation of S^+ occurs only over a very narrow energy range, apparently entirely from the $^2B_2$ state. It is irrelevant whether this results from direct ionization or from autoionization to the states involved. The separation of the states within the $^2B_2$ band is at least 0.045 ev, so that about 85% of the ions detected result from the precursor states selected by the incident photon energy, except for the unresolvable overlap between the $^2A_1(000)$ and $^2B_2(310)$ as well as the only weakly resolved (0.019 ev) $^2A_1(100)$ and $^2A_1(100)$ and $^2B_2(410)$ states. Both S^+ and SO^+ appear to be formed from the (n00) and (n10) series of the $^2B_2$ state, suggesting that energy is more important in determining the outcome of the competition than the mode in which it resides at the time of formation.

We believe that this is the result of two factors. First, it is not possible to produce initially SO_2^+ in the $^2B_2$ state with more than one quantum of vibrational excitation in the ν_2 (bending) mode. However, one expects that this mode must be excited, either directly or by intermodal energy transfer, for the thermodynamic onset, yet the 0-0 bond distance in SO_2 and SO_2^+ is much in excess of that in O_2. The second factor is the energy dependence of the rate of intermodal energy flow. As the number of quanta in a given mode increases, the effects of anharmonicity become more important and one would expect that these should favor excitation of the assymetric mode since the difference in quantum size between ν_1 and ν_3 is probably smaller than that between ν_1 and ν_2 (Table I). This is consistent with the observation, in neutral SO_2, that collision induced intermode transfer to the bending mode is considerably less efficient than that to the asymmetric stretch mode (10).

The picture we propose is competition between intermodal energy flow from the ν_1 into the ν_2 and ν_3 modes with the latter being favored with increasing excitation of the ν_1 mode, with initial excitation of the ν_2 mode assisting in the fragmentation to give S^+. This is consistent with the earlier observations that the fragmentation is not statistical (7), and differs only slightly from that proposed by Brehm, et. al. (7).

ACKNOWLEDGEMENTS. We are grateful for the support of this investigation by the Department of Energy under contract EY-76-S-02-2567 and by the University of Nebraska Research Council. A full paper will appear in the Journal of Chemical Physics.

REFERENCES

1. R. B. Bernstein, Chapter 1 in "State-to-State Chemistry", ACS Symposium Series, No. 56, Philip R. Brooks and Edward F. Hayes, Editors, Amsterdam, 1977, pg. 3.
2. (a) W. A. Chupka and M. E. Russell, J. Chem. Phys. 49, 5426 (1978).
   (b) P. M. Dehmer and W. A. Chupka, J. Chem. Phys. 62, 4525 (1975).
3. C. F. Batten, J. A. Taylor and G. G. Meisels, J. Chem. Phys. 65, 3316 (1976); ibid. 69, 2547 (1978).
4. J. H. D. Eland and C. J. Danby, Int. J. Mass Spectrom Ion Phys., 1, 111 (1968).
5. D. R. Lloyd and P. J. Roberts, Molec. Phys. 26, 225 (1973).
6. I. H. Hillier and V. R. Saunders, Molec. Phys. 22, 193 (1971).
7. B. Brehm, J. H. D. Eland, R. Frey and A. Kustler, Int'l. J. Mass Spectrom. Ion Phys. 12, 197 (1973).
8. V. H. Dibeler and S. K. Liston, J. Chem. Phys. 49, 482 (1968).
9. K. T. Wu and A. J. Yencha, Can. J. Phys. 55, 767 (1977).
10. G. W. Flynn, Ch. 18 in "State-to-State Chemistry", ACS Symposium Series, No. 56, Philip R. Brooks and Edward F. Hayes, Editors, Amsterdam, 1977, pg. 145 and references cited therein.
11. W. A. Chupka, J. Chem. Phys. 48, 2337 (1968).
12. P. M. Guyon and J. Berkowitz, J. Chem. Phys. 54, 1814 (1971).

DISSOCIATIVE PHOTOIONIZATION

Toshio Masuoka and James A. R. Samson

Dept of Phys., Univ. of Nebraska, Lincoln, NE 68588

Until recently, few reliable data were available for the probability of dissociative photoionization of molecules. The main reason for this is that most previous measurements have been affected by ion discriminatory effects caused by the initial kinetic energies of the dissociated fragments, leading to underestimation of the fragmentation ratios. The kinetic energies of ion fragments formed in H_2, CO, N_2, and O_2 have been reported by Gardner and Samson[1], extending up to about 5eV for N_2, O_2, and CO and up to 12eV for H_2 ions at 304A. The initial energy of the dissociated fragments causes spatial spread of an ion beam and hence discrimination in the collection efficiency of standard mass spectrometers. The second problem is the variation in secondary electron emission produced at the first dynode of a charged particle multiplier such as an open-ended electron multiplier due to ions of different masses and energies. This effect is well known and is commonly encountered in the use of electron multipliers operated in a dc mode. However, the problem is less severe in the counting mode, especially, if the ions have several kV of energy.

We have successfully constructed a time-of-flight mass spectrometer (Fig. 1) completely free from such discriminatory effects and have measured the fragmentation ratios for hydrogen, nitrogen, oxygen, and some other simple molecules, at 584 and 304A helium resonance lines.

In the present experiment, electron pulses serve to start a time-to-amplitude converter (TAC) and ion pulses to stop it. Discriminatory effects have been reduced to a bare minimum by providing an appropriate high field (~1500V/cm) in the ionization region and by using a large diameter chevron CEMA (40mm in diameter).

The fragmentation ratios to the parent ions obtained at 584 and 304A are given in Table 1 for H_2, N_2, and O_2 and are compared with previously published data.[2-4] It is clear from this table that the fragmentation ratios reported by other authors are affected by ion discriminatory effects.

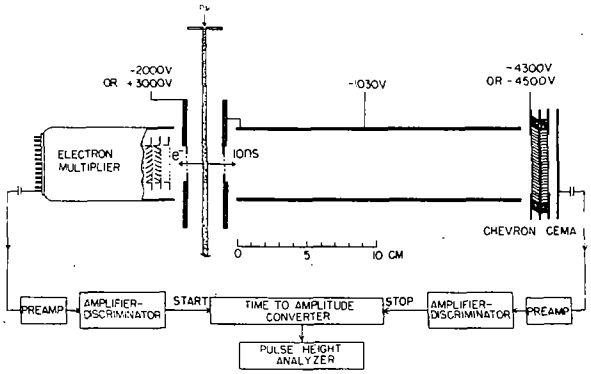


Fig. 1 Experimental setup of the coincidence time-of-flight mass spectrometer

TABLE 1 Fragmentation Ratios for Hydrogen, Oxygen, and Nitrogen.

Gas	λ (Å)	Present Work	Ref. 2	Ref. 3	Ref. 4
H_2	584	$H^+/H_2^+=0.222 \pm 0.001$	0.0206		
	304	$H^+/H_2^+=0.116 \pm 0.003$	0.108		
O_2	584	$O^+/O_2^+=0.238 \pm 0.004$	0.204	0.180	0.068
	304	$O^+/O_2^+=0.641 \pm 0.016$	0.42	0.518	0.182
N_2	304	$N^+/N_2^+=0.307 \pm 0.003$	0.25	0.250	0.082

References

(1) J.L. Gardner and J.A.R. Samson, Phys. Rev. A, 12 (1975) 1404.

J.L. Gardner and J.A.R. Samson, J. Chem. Phys., 62 (1975) 1447.

J.L. Gardner and J.A.R. Samson, J. Chem. Phys., 62 (1975) 4460.

(2) J. Fryar and R. Browning, Planet. Space Sci., 21 (1973) 709.

(3) C.E. Brion, K.H. Tan, M.J. Van der Wiel, to be published.

G.R. Wight, M.J. Van der Wiel, and C.E. Brion, J. Phys. B, 9 (1976) 675.

C. Backx, G.R. Wight, and M.J. Van der Wiel, J. Phys. B, 9 (1976) 315.

(4) P.L. Kronebusch and J. Berkowitz, Int. J. Mass Spectrom. Ion Phys., 22 (1976) 283.

STOICHIOMETRY OF THE REACTION OF ELECTRONS WITH $CBrCl_3$ IN AN ELECTRON CAPTURE DETECTOR

E. P. Grimsrud and S. H. Kim

Department of Chemistry
Montana State University
Bozeman, MT 59717

The electron capture detector (ECD) responds sufficiently sensitively to certain halogenated molecules as to cause nearly 100% ionization of these while they pass through this gas chromatographic detector. This observation has prompted investigations of the use of the ECD as a gas phase coulometer (1) in which the number of electrons lost by the electron capture reaction with sample is measured from the GC-ECD peak area and is related by calculation to the amount of sample.

If the ECD is to function successfully as a gas phase coulometer, several individual criteria of the overall method must be met. One of these is that the stoichiometry of the reaction of thermal electrons with the sample molecule in one atmosphere pressure of carrier gas must be 1:1 (or some other known ratio). We would like to report here an investigation of this criterion for the case of $CBrCl_3$. This compound is one which we expect to react extremely rapidly with thermal electrons. Furthermore, with $CBrCl_3$ we hoped that the measurement of its likely electron capture products, Cl^- and Br^-, might provide insight into the mechanism of its reaction with electrons.

Experiments were performed using an atmospheric pressure ionization mass spectrometer, the ion source of which is modified so that it is also an ECD (2). With this instrument ECD responses and negative ion measurements were made for various concentrations of $CBrCl_3$ diluted into nitrogen carrier gas. Also, the source temperature and carrier gas flow rate were varied.

In every experiment (at all $CBrCl_3$ concentrations, at all temperatures, and for all flow rates), the measured ratio of Br^- to Cl^- concentrations was 3.8 ± 0.4. The independence of this ratio from changes in all experimental variables is consistent with the mechanism written below:

$$e^- + CBrCl_3 \rightleftharpoons \begin{matrix} Br^- + CCl_3 \\ Cl^- + CCl_2Br \end{matrix}$$

Upon electron attachment by the parent molecule, the parent negative ion falls apart prior to its collisional stabilization to form Br^- and Cl^-. Br^- formation is favored by about 14 kcal over Cl^- formation, but the route taken by the $CBrCl_3^-$ species is only somewhat sensitive to this energy difference while it possess about 47 kcal of excess energy prior to its stabilization by collisions. Thus, for all experimental conditions a constant ratio of Br^- to Cl^- is observed. The neutral products, CCl_3 and $CBrCl_2$, do not appear to undergo further electron attachment. If further reactions of the neutral products where important, the observed ratios of Br^- and Cl^- would have varied with sample size and with flow rate.

These results support the chemical criterion of gas phase coulometry - that the stoichiometry of the reaction of electrons with this sample is 1:1. These and other related experiments have been described in more detail elsewhere (3).

(1) J. E. Lovelock, R. J. Maggs, and E. R. Adlard, Anal. Chem., 43 , 1962 (1971).
(2) E. P. Grimsrud, S. H. Kim, and P. L. Gobby, Anal. Chem., 51, 223 (1979).
(3) E. P. Grimsrud and S. H. Kim, Anal. Chem., 51, 537 (1979).

Kinetic Shift in Chlorobenzene Ion Fragmentation and the Heat of Formation of the Phenyl Ion

Henry M. Rosenstock, Roger Stockbauer and Albert C. Parr*

National Measurement Laboratory
National Bureau of Standards
Washington, D.C. 20234

ABSTRACT

The fragmentation of chlorobenzene ion has been studied by photoelectron-photoion coincidence techniques[1]. By varying the residence time it is possible to obtain breakdown curves on a function of residence time. The parent-daughter transition region shifts to lower energies as the residence time is increased (kinetic shift). The shift is of the order of 0.4 eV in going from 0.7 μsec to 8.9 μsec. A systematic analysis of the breakdown curves and residence time effects has been carried out using quasiequilibrium theory. The experimental results and analysis lead to

$$\Delta H_{f_0}^{\circ}\ (\text{Phenyl Ion}) = 275 \pm 1\ \text{kcal/mol}\ (1151 \pm 4\ \text{kJ/mol})$$

The systematic analysis shows that this experiment leads to a quite accurate rate-energy curve in the range of 10^4 - 10^6 sec^{-1}. The sensitivity of the QET model has been studied, and the limitations to the determination of activated complex parameter is critically discussed.

The results obtained here differ from the results of a previous experimental study by Baer et al[2].

Full details of this study have been submitted to the Journal of Chemical Physics.

*Intergovernmental Personnel Act appointee, permanent address, Department of Physics, University of Alabama, University, Alabama 35486.

[1]R. Stockbauer and H. M. Rosenstock, Int. J. Mass Spectrom. Ion Phys. 27 (1978) 185.

[2]T. Baer, B. P. Tsai, D. Smith and P. T. Murray, J. Chem. Phys. 64 (1976) 2460.

RAMOB6 Ionization Energies, Proton and Hydrogen Affinities of Polycyclic Aromatics. M. MEOT-NER (MAUTNER), E.P. HUNTER and F.H. FIELD, The Rockefeller University, New York, N.Y. 10021

Abstract

Proton Affinities (PA) and ionization energies ($\Delta H°_f$) of polycyclic aromatic hydrocarbons (PAH) were determined by gas phase ion equilibrium measurements with an accuracy of ±1 kcal mol^{-1}. Hydrogen atom affinities (HA) of the radical ions are calculated from $HA=PA+\Delta H°_f-\Delta H°_f(H)$. Some results: (PAH, $\Delta H°_f$, PA, HA, all in kcal mol^{-1}) naphthalene, 187.7, 196.3, 70; phenanthrene, 183.3, 201.1, 71; fluorene, 183.0, 202.4, 72; chrysene, 175.8, 203,3, 66; pyrene, 173.0, 208.5, 68; picene, 172.6, 205.8, 65; anthracene, 171.9, 209.4, 68; coronene, 170.8, 207.0, 64; 1,12-benzoperylene, 167.4, 210.6, 64; perylene, 165.2, 213.0, 64; azulene, 171.1, 222.0, 79. Decreasing HAs with increasing molecular size reflect increasing stabilities of the radical ions (B^+) vs protonated ions (BH^+). The HA's of naphthalene, anthracene and phenanthrene are lower by 9.5 and 3 kcal mol^{-1}, respectively, then HA's of partially hydrogenated analogues, reflecting resonance stabilization of the radical ions in the fully aromatic species. However, factors other than π resonance are also significant in determining ion stabilities. Correlation between PAs and IPs, in conjunction with results from ion-neutral interactions in dimers, are used to estimate PA of graphite as 278 kcal mol^{-1} and HA of ionized graphite as 64 kcal mol^{-1}.

CHEMICAL ACCELERATOR STUDIES OF ION-MOLECULE REACTIONS: $X^+ + CH_4$

Peter M. Hierl

Department of Chemistry
University of Kansas
Lawrence, Kansas 66045

Using chemical accelerator techniques, we have measured integral reaction cross sections (σ) and product velocity vector distributions as a function of the reactant's relative translational energy (T) for several exoergic ion-molecule reactions of the general type

$$X^+ + CH_4 \rightarrow XH^+ + CH_3.$$

Results have been published for the cases where X = Ar,[1,2] Kr,[3,4] and N_2.[5] We report here the results of an extension of these studies to the case X = Xe.

In the reactions studied previously[1-5] H-atom abstraction from methane was found to be dominated by a direct mechanism (i.e., to proceed on a time scale shorter than a typical rotational period) over the entire energy range studied, 0.4 to 35 eV in the center-of-mass (CM) system. Two unusual features were observed in all three reactions: (1) product translational energy distributions consistently peaked at values about 0.1 eV less than those predicted by the spectator stripping model (SSM), and (2) integral reaction cross sections decreased sharply at relative collision energies below about 5 eV (CM), giving the appearance of a translational energy threshold of about 0.1 eV for these exoergic reactions.

These features led us to suggest that the potential energy hypersurface for each of these reactions contains a basin which, at the lowest collision energy, could result in the formation of a XCH_4^+ complex which preferentially decomposes via various exoergic charge transfer channels rather than by XH^+ production. Since Xe^+ in its $^2P_{3/2}$ ground state is energetically incapable of undergoing charge exchange with methane, it was hoped that the present study might provide additional information on complex formation and the subsequent competition between charge transfer and chemical reaction (i.e., atomic rearrangement) in these systems at low collision energies.

The instrument used in this study is a single beam - collision chamber type of chemical accelerator with which product velocity and angular analyses are possible.[6] The reactant ions are produced by impact of 33 eV electrons, so that nearly all (>98 percent) of the Xe^+ ions are in the ^2P state, presumably distributed statistically in a 2:1 ratio between the $^2P_{3/2}$ and $^2P_{1/2}$ states.

The integral reaction cross sections for production of XeH^+ increase monotonically from approximately 0.1 Å^2 at T = 8 eV to about 1.0 Å^2 at T = 1.5 eV. At the higher collision energies, the cross sections are thus similar in magnitude to those measured for the formation of ArH^+, KrH^+, and N_2H^+ from CH_4. This similarity indicates that the small cross sections observed for these reactions are not simply a consequence of competition from fast charge transfer channels, as such processes are energetically forbidden in the Xe^+ case. At low collision energies, however, the monotonically increasing cross section for XeH^+ formation with decreasing collision energy contrasts with the rapidly decreasing cross sections observed in the other three reactions at collision energies below 5 eV. It is entirely possible, therefore, that competition from charge transfer may become an important factor at the lower collision energies, thus causing the observed decrease in XH^+ production in those systems (X = Ar, Kr, and N_2) for which charge transfer to CH_4 is exoergic.

At high collision energies (T > 2 eV) the XeH^+ velocity vector distributions are also quite similar to those observed previously for ArH^+, KrH^+, and N_2H^+ at comparable collision energies: the ionic product is sharply peaked in the forward direction, indicating that reaction proceeds by a direct mechanism and principally in glancing (i.e., large impact parameter) collisions at these energies. The most probable

product velocity is similar to - but somewhat less than - that predicted by the SSM.

When the collision energy is lowered to 1.58 eV, however, there is increased broadening of the XeH^+ angular distribution and the formation of a low-velocity tail entending back toward the CM. Again, similar behavior (although somewhat less marked) has been observed at collision energies below 1 eV for the analogous reactions of Ar^+, Kr^+, and N_2^+ with CH_4. This has been interpreted as indicating increased interaction between the incident ion and the CH_3 fragment at the lower collision energies, with a possible transition from a direct mechanism at higher energies to a long-lived complex mechanism at the very lowest energies.[1,4,5]

At T = 1.08 eV, the low-velocity tail of the XeH^+ distribution has extended behind the CM into the backward hemisphere, although the peak in the velocity vector distribution still remains considerably forward of the CM. At T = 0.43 eV, however, the amounts of forward and backward scattering are nearly equal, and the peak of the XeH^+ distribution itself has shifted much closer to the CM. This behavior contrasts markedly with the earlier studies which showed no backward scattering of the XH^+ (X = Ar, Kr, N_2), even at the lowest collision energies studied.

The observation that XeH^+ is scattered in a nearly symmetric manner about the CM at T = 0.43 eV suggests that the reaction of Xe^+ with CH_4 proceeds in large part via the formation of an $XeCH_4^+$ collision intermediate whose lifetime at this energy exceeds a rotational period. The direct observation of the $XeCH_4^+$ ion in high-pressure[7] and tandem mass spectrometric[8] studies indicates the stability of this species under certain conditions.

The results of the present study, therefore, are consistent with the interpretation we proposed for the earlier experiments and thus lead to the following picture for this series of $X^+ + CH_4$ reactions: at collision energies above 2-3 eV, reaction proceeds in a direct manner, with XH^+ formation being relatively inefficient ($\sigma < 0.5$ Å^2) but essentially the same in all four cases. The SSM, while providing a reasonable approximation to the reaction dynamics, consistently overestimates the product translational energy by 0.1-0.5 eV. At collision energies below 1 eV, however, a transition occurs to a reaction mechanism involving the formation of a lonf-lived XCH_4^+ collision complex. In three of the reactions (X = Ar, Kr, N_2) the production of XH^+ is drastically reduced because the XCH_4^+ intermediate preferentially decomposes via the available charge transfer channels because of their greater exoergicity, as one might expect from simple statistical considerations.[8] Such charge transfer channels are unavailable in the Xe^+ reaction, however, with the result that only in this reaction does the cross section for XH^+ production continue to increase as the collision energy is lowered.

REFERENCES

1. J. R. Wyatt, L. W. Strattan, S. C. Snyder, and P. M. Hierl, J. Chem. Phys. 62, 2555 (1975).
2. J. R. Wyatt, L. W. Strattan, S. Chivalak, and P. M. Hierl, J. Chem. Phys. 63, 4582 (1975).
3. J.R. Wyatt, L.W. Strattan, and P.M. Hierl, J. Chem. Phys. 63, 5044 (1975).
4. J.R. Wyatt, L.W. Strattan, and P.M. Hierl, J. Phys. Chem. 80, 2911 (1976).
5. J.R. Wyatt, L.W. Strattan, S.C. Snyder, and P.M. Hierl, J. Chem. Phys. 64, 3757 (1976).
6. J.L. Franklin and F. H. Field, J. Am. Chem. Soc. 83, 4509 (1961).
7. T.O. Tiernan and P.S. Gill, J. Chem. Phys. 50, 5042 (1969).
8. See, for example, R. B. Bernstein and R. D. Levine, Molecular Reaction Dynamics, Oxford University Press, New York (1974), pp. 221-224.

KINETIC AND INTERNAL ENERGY OF H_2S^+ IONS PRODUCED IN THERMAL-ENERGY CHARGE TRANSFER FROM Xe^+ TO H_2S

G.MAUCLAIRE, R.DERAI, S.FENISTEIN and R.MARX

Laboratoire de Résonance Electronique et Ionique
Université de Paris-Sud, 91405 Orsay, France

These last years, our work on charge transfer reactions at thermal energy has been focussed on the release of kinetic energy in the products [1]. The observation of translationally excited parent molecular ions is specially interesting since it implies momentum transfer during the collision.

Now, it has long been assumed that direct conversion of appreciable amounts of electronic energy into kinetic energy is inefficient and negligible for these thermal reactions. In fact,using an ICR spectrometer specially designed with ion kinetic energy measurement capability we have recently shown that with Ar^+, Kr^+ or Xe^+ primary ions, thermal energy charge transfer on small molecules very often goes through non-resonant mechanisms, sometimes with quite high rate constant [1,2]. However our results also confirm that when an energy resonance between the recombination energy (RE) of the primary ion and a state of M^+ occurs, simultaneously with reasonable Franck-Condon factors for the transition from M to this M^+state, the charge transfer usually goes through a resonant long distance electron jump, with no kinetic energy release.

To investigate which parameters govern such reactions , the Xe^+ on H_2S system is quite interesting, due to the existence of the $^2P_{3/2}$ and $^2P_{1/2}$ states of Xe^+, having respective recombination energies of 12.13 and 13.44 eV: As shown by the photoelectron spectrum (fig.1) the $^2P_{1/2}$ state is resonant with the v=6 level in the υ_2 mode of H_2S^+ $\tilde{A}$ state ($\tilde{A}$ state appearance potential:12.76 eV) whereas the $^2P_{3/2}$ state may only populate the $\tilde{X}$ state (appearance potential 10.47 eV).

Though the appearance potential for S^+ ions from H_2S is 13.36 eV, we could not detect any: if formed, this ion represents less than 1% of the ionic products. The reaction rate constant has been measured as being $(6\pm0.6)\times10^{-10}cm^3s^{-1}$, using 20 eV ionizing electrons (at this energy, the relative abondances of the two Xe^+ states are probably close to their statistical weights). We are not aware of previous determination for this rate constant at thermal energy. This rate constant value is to be compared with a locked dipole model calculated value of $2.66\times10^{-9}cm^3s^{-1}$.Kinetic energy measurements [1] have been performed for the only product ion, H_2S^+. A plot of the fraction of H_2S^+ ions effectively trapped in the ICR cell as a function of the square root of the trapping voltage V_T exhibits two distinct breaks. As shown on fig.2, this plot can be deconvoluted into curves B and C, indicating that $\sim$ 48% of the H_2S^+ ions have $\sim$ 0.8 eV of mean kinetic energy and that the remaining 52% H_2S^+ ions have $\sim$0.25 eV. Moreover, it has to be noted that $f(H_2S^+)$ extrapolates linearly to zero for V_T= 0: consequently, resonant processes are negligible in this system, since very few, if any, of the H_2S^+ ions have zero kinetic energy*. Furthermore, when supressing the production of the $^2P_{1/2}$ Xe^+ ions by lowering the ionizing electron energy to 12.5-13.0 eV, the same results concerning kinetic energy values and relative abundances of the two kinds of H_2S^+ions are obtained: This indicates that, in spite of a possible energy resonance with the $\tilde{A}$ state of H_2S^+, Xe^+ ($^2P_{1/2}$) does not react with H_2S, or react with a much lower rate than Xe^+ ($^2P_{3/2}$)does. This lower Xe^+ state charge transfers rather efficiently via a non resonant process, populating near equally two different vibrational modes of ground state H_2S^+, characterized by rovibronic energies of 0.65 and 1.34 eV. The sharpness of the observed corresponding breaks suggests a narrow vibrational distribution around these values. Results are summarized in table 1.

A systematic study of the repartition of the reaction excess energy into kinetic and vibrational energy in similar non resonant charge transfer reactions is in progress. Concerning the non reactivity of the $^2P_{1/2}$ state of Xe^+ with H_2S, it is worth noting that this state does not react either with CH_4 (in spite of the existence of a near-resonant energy state), nor with O_2 [3]and N_2O. However we found Xe^+ ($^2P_{1/2}$) ions to react slowly with H_2O [2] .

---

* T.R.GOVERS and M.GERARD-AIN (this same laboratory) in a thermal energy investigation of the Xe^+/H_2S system by emission spectroscopy, could not detect H_2S^+ ($\tilde{A} \rightarrow \tilde{X}$) emission, in agreement with this conclusion.

1 G.MAUCLAIRE, R.DERAI, S.FENISTEIN and R.MARX, J.Chem.Phys., 70 , 4023 (1979)

2 G.MAUCLAIRE, R.DERAI, S.FENISTEIN and R.MARX, to be published

3 J.M.AJELLO and J.B.LAUDENSLAGER, Chem.Phys.Lett., 44, 344 (1976)

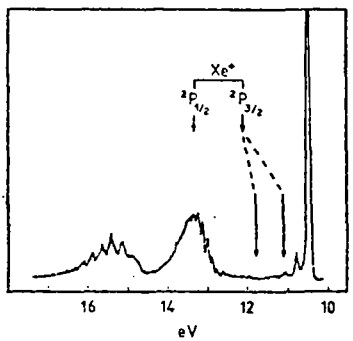


Fig.1: Photoelectron spectrum of H_2S. The lower arrows indicate the energies reached by charge transfer with Xe^+.

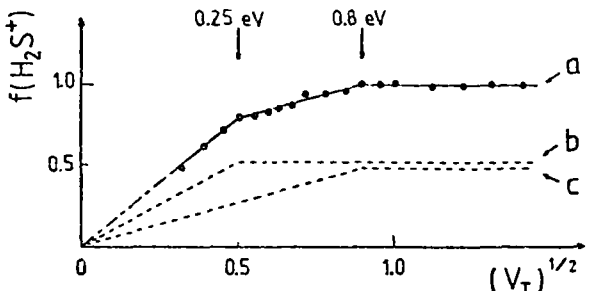


Fig.2: Fraction of H_2S^+ ions trapped in the cell vs square root of trapping voltage. Curve a: experimental plot; curve b and c: deconvolution of curve a

P^+	R.E.	$k \times 10^{10}$	S^+	K.E. H_2S^+	tot. K.E. H_2S^+, X_e	$E_{int.}$	$E_{vib.}$
$Xe^+ {}^2P_{3/2}$	12.13	~9	$H_2S^+ \tilde{X}$	0.25 0.80	0.32 1.01	11.81 11.12	1.34 0.65
$Xe^+ {}^2P_{1/2}$	13.44	< 0.6	—	—	—	—	—

Table 1: (all energies are in eV, k is in $cm^3 s^{-1}$)

RAMOB10 ION-MOLECULE HALF-REACTIONS,*
CORNELIUS E. KLOTS, Health and Safety Research Division, Oak Ridge National Laboratory, Oak Ridge, Tenn. 37830

Ionization of, or electron attachment to, van der Waals molecules can be used to simulate ion-molecule reactions which would be difficult or impossible to study directly. Even when the ion-molecule reaction is feasible, study of the "half-reactions" of molecular clusters affords greater control of experimental parameters such as energy and angular momentum. This will be discussed and results from studies of silane and oxygen dimers, simulating the reactions of the unknown SiH_4^+ and the short-lived O_2^- ions, will be presented.

*Operated by the Union Carbide Corporation with the U.S. Department of Energy.

RAMOB11 FT-ICR STUDY OF THE ION MOLECULE CHEMISTRY OF $CpCr(CO)_2NS$ AND RELATED COMPOUNDS. M. COMISAROW and G. Parisod, Chemistry Department, University of British Columbia, Vancouver, B.C., Canada V6T 1W5

Using the technique of Fourier transform ion cyclotron resonance (FT-ICR) spectroscopy, we have investigated the positive ion and negative ion gas phase ion-molecule chemistry of η^5-$CpCr(CO)_2(NS)$. Rate constants and product distributions from self-condensation reactions have been investigated. The condensation chemistry is very rich with higher order products observed at masses up to 700. Contrasts and comparisons with the ion molecule chemistry of $CpMn(CO)_3$ and $CpCr(CO)_2NO$ will be made.

A GC/MS STUDY OF THE TOTAL FLUORESCENCE METHOD FOR THE ANALYSIS OF POLYNUCLEAR AROMATIC COMPOUNDS IN SEA WATER*

W. D. JAMIESON, J. B. ADDISON and M. D. MACKINNON,
Atlantic Regional Laboratory, National Research Council,
1411 Oxford Street, Halifax, N.S., Canada, B3H 3Z1;
W. J. CRETNEY, Institute of Ocean Sciences, Fisheries and Oceans
Canada, Sidney, B.C., Canada, V8L 4B2; D. R. GREEN, Seakem
Oceanography Limited, Sidney, B.C., Canada, V8L 3S1

The total fluorescence of a sample and of fractions eluting from a high performance liquid chromatograph (HPLC) are parameters used for quantitative analysis of polynuclear aromatic compounds present in sea water (1). Hexane extracts are usually examined. We have used GC/MS and further HPLC to determine compounds present in fluorescing fractions of hexane extracts of sea water.

Sea water samples (4 ℓ) from stations in the Vancouver harbour area (Figure) were extracted with hexane (400 mℓ). The extract was concentrated to 500 µℓ, of which 240 µℓ were used for quantitative analysis by normal phase HPLC (hexane; 5 µm Lichrosorb Si60; fluorescence detection, 308/383 nm). Polar and non-polar fractions (2 mℓ) were collected, then concentrated to 100 µℓ for examination by reverse phase HPLC (10 µℓ injected; acetonitrile/water, 1.5 ml/min, gradient; 10 µm RP18, 40°; detection (UV, 254 nm; fluorescence, 240/370 and 280/370 nm)) and by GC/MS (50 µℓ concentrated to 5 µℓ, 5 µℓ injected; 3% OV1, 100/120 Gas Chrom Q, 3 mm X 2 m, glass; 25 ml/min; 110-250°, 6°/min; Finnigan/INCOS 4023; 2 sequenced 3 sec multiple ion detection descriptors (15 ions, 12 ions); m/z interval widths, 0.5 u; centred on formula m/z ± 0.005 u; baseline biased, 5 mv). Further details are shown in the Figure.

Quantitative analytical data for total extracts from filter (300-400/400 nm) and grating (308/383 nm) fluorometry and for fractions (non-polar, total) from fluorometric normal phase HPLC were compared using chrysene for reference (correlation coeffs: grating/filter, 0.84; grating/HPLC non-polar, 0.92). Compounds tentatively identified by reverse phase HPLC and GC/MS included naphthalene, alkylated naphthalenes, anthracene, alkylated anthracenes, phenanthrene, alkylated phenanthrenes, fluoranthene, pyrene, methyl pyrene, chrysene, perylene and benzo(a)pyrene.

The results show a 2 ℓ sample of estuarine or coastal sea water would provide enough material for total fluorescence analysis and normal phase HPLC analysis. Polar and non-polar fluorescent fractions from normal phase HPLC are suitable for further analysis by reverse phase HPLC and GC/MS. Compounds present can be characterized by HPLC retention volumes, fluorescence excitation specificity, GC retention times and GC/MS with multiple ion detection. Quantitative determination of compounds in such natural samples (concentrations <1 ppb) requires the sensitivities available reliably from fluorescence detection in HPLC and multiple (or "specific") ion detection in mass spectrometry. Under the above conditions, the mass spectrometric sensitivity was <10 pg phenanthrene (178 u, 10/1 S/N). The revised INCOS MID software used will be supplied on request.

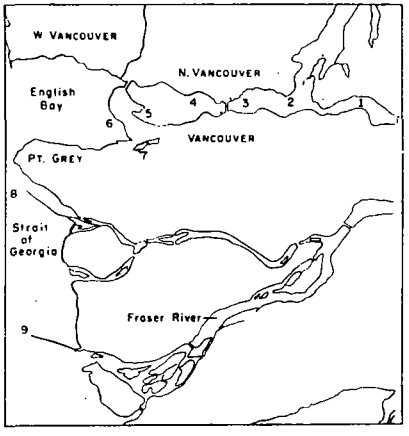
REFERENCES

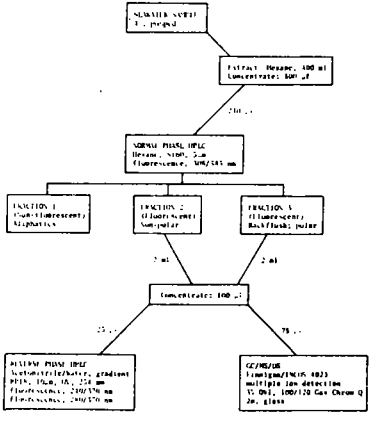
(1) W. J. Cretney and C. S. Wong. Marine Pollution Monitoring (Petroleum), pp. 175-7, NBS Spec. Publ. 409 (1974).

---

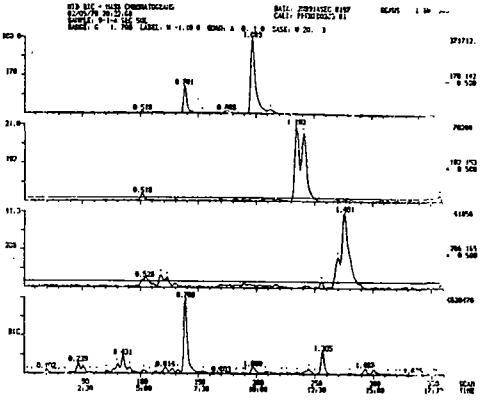
*NRCC No. 17365

SAMPLE LOCATIONS





COMPOUND	GC/MS (SE OV1)	HPLC (RP18)
NAPHTHALENE	0.136	0.67
2-METHYLNAPHTHALENE	0.273	0.88
1-METHYLNAPHTHALENE	0.288	0.80
1,1'-BIPHENYL	0.389	0.79
2,6-DIMETHYLNAPHTHALENE	0.419	1.07
1,3-DIMETHYLNAPHTHALENE	0.449	1.08
ACENAPHTHYLENE	0.547	0.92
FLUORENE	0.677	0.94
PHENANTHRENE	1.00	1.00
ANTHRACENE	1.02	1.06
2-METHYLANTHRACENE	1.18	1.29
2-METHYLPHENANTHRENE	1.19	1.24
1-METHYLPHENANTHRENE	1.23	1.38
9-METHYLANTHRACENE	1.27	1.38
3,6-DIMETHYLPHENANTHRENE	1.36	2.40
PYRENE	1.41	1.26
FLUORANTHENE	1.48	1.19
1,2-BENZO-FLUORENE	1.61	1.31
2,3-BENZO-FLUORENE	1.64	1.33
1-METHYLPYRENE	1.69	1.47
9,10-DIMETHYLPHENANTHRENE	1.82	2.40
1,2-BENZANTHRACENE	1.92	1.42
CHRYSENE	1.96	1.39
BENZO(a)PYRENE	2.36	2.01
PERYLENE	2.47	1.82
1,2,3,4-DIBENZANTHRACENE	2.47	2.06
9,10-DIPHENYLANTHRACENE	2.66	2.44
1,2,5,6-DIBENZANTHRACENE	2.73	2.19
BENZO(ghi)PERYLENE	-	2.39
CORONENE		3.03



```
MID 26/05/79  DESC: PL (CALIBRATED)
INST: MID     CAL1: FFKMID
                (ON: 01/05/79)
MASS DEFECT AT 100 AMU    30 MMU
FOSTER RATE          16384
TOTAL ACQU TIME      2.707 SECS
MIN  SCAN TIME       2.907 SECS
TOTAL SCAN TIME      3.000 SECS
CENT SAMP INT        0.200 MS
MASS RANGE      1 TO 1024 AMU
CAL1:  25 PEAKS FROM  51 TO  393 AMU
```

15. INT #	ONE MASS	62.773 BEGIN MASS	228.375 END MASS	1.000 TIME REQUEST	3.036 (SECS) ACTUAL	I MPW	93 MFW	0 MR	1 TH	0 BL	2 CS1/INT	MS/AMU
1.	63	62.773	63.274	0.020	0.826	1	120	0	1	2	131	52
2.	77	76.789	77.289	0.020	0.826	1	120	0	1	2	131	52
3.	128	127.812	128.313	0.200	0.216	1	120	0	1	2	1046	419
4.	142	141.828	142.328	0.200	0.210	1	120	0	1	2	1046	419
5.	149	148.774	149.274	0.882	0.882	1	120	0	1	2	0	3
6.	154	153.828	154.328	0.188	0.185	1	120	0	1	2	523	210
7.	156	155.844	156.344	0.188	0.185	1	120	0	1	2	523	210
8.	166	165.828	166.328	0.200	0.218	1	120	0	1	2	1045	419
9.	170	169.859	170.359	0.200	0.210	1	120	0	1	2	1045	419
10.	178	177.820	178.320	0.498	0.419	1	120	0	1	2	2092	839
11.	192	191.844	192.344	0.200	0.210	1	120	0	1	2	1045	419
12.	202	201.828	202.328	0.498	0.419	1	120	0	1	2	2092	839
13.	205	205.859	206.359	0.200	0.216	1	120	0	1	2	1079	432
14.	216	215.844	216.344	0.200	0.210	1	120	0	1	2	1045	419
15.	220	219.875	220.375	0.200	0.210	1	120	0	1	2	1045	419

```
AT/ 10:48: 4 MMS /
```

CAPILLARY ON-COLUMN INJECTION AND GC/MS ANALYSIS OF ORGANIC POLLUTANTS IN MARINE SAMPLES

Curtis B. Norwood and James L. Lake

Environmental Protection Agency
Environmental Research Lab
Narragnasett, RI 02882
401-789-1071

On-column injection (as described elsewhere in these proceedings - Norwood and Lake) can be used to considerable advantage when performing capillary (WCOT)column GC/MS analyses of organic pollutants in environmental samples. Not only does all of the sample material get deposited on the head of the column, but also the thermally labile material does not suffer degradation due to a hot injection port. In addition, On-colum injection has been shown to produce more quantitative recovery of material than either conventional split or splitless injection. On-column injection is now used for all of the GC/MS research at this EPA laboratory.

Quantitation reproducibility was demonstrated with seven injections of standard Polynuclear Aromatic Hydrocarbons (PAH's) analyzed by temperature programmed GC/MS over a period of two days. Full mass range data were collected and quantitation was based on the molecular ions. Amounts of individual components injected ranged from 8 to 55 nanograms. The relative standard deviations for the individual components were found to range from 6 to 11 percent and averaged 7.5%. To obtain a better measure of the true reproducibility of the injection system, as opposed to the possible longer term fluctuations in MS sensitivity and column performance, repeated isothermal injections of n-Decane were analyzed using a very limited scan range (50-60amu) so that the quantitation could be based on the m/e 57 ions. This resulted in a relative standard deviation of 1.7% for four injections.

Much of this lab's past research has investigated the PAH assemblages in marine waters, sediments and organisms. As an example of this, the Total Ion Current Profile (TICP) of an extract of mussels which had been suspended in the water column in the relatively heavily polluted upper Narragansett Bay was displayed. In spite of the large mound of unresolved complex material, Extracted Ion Curren Profiles corresponding to the molecular ions of 2, 3, 4 and 5 ring PAH's were obtained and showed the characteristics typical of these pollutants.

Another example was that of an F2 cut (eg. alkenes and aromatics)of an XAD resin extract of material from the upper Narragansett Bay waters. In addition to the biogenic methyl esters shown in the m/e 74 EICP, there were an abundance of organic pollutants, including 2, 3, 4 and 5 ring PAH's, chlorinated and oxygenated aromatics, and diphenyl amine.

In conclusion, the simplicity of the On-column injection system coupled with its ability to chromatograph more of the sample components, not just those that make it out of the injection port, make this an exciting tool for future environmental studies.

INSTRUMENTAL APPROACHES TO A MASTER SCHEME FOR ANALYSIS OF ORGANICS IN WATER

J. Bursey, K. Tomer, L. Sheldon, E. Pellizzari, and C. Sparacino
Research Triangle Institute
Research Triangle Park, North Carolina 27709

Because of recent and proposed legislation for regulation of organic compounds in the aqueous environment, there is increasing demand for improved analytical methodology. EPA anticipates analysis of thousands of samples within the next few years to assess distribution and impact of hundreds of organic chemicals in water: accurate, cost-effective, wide range analyses. The Master Scheme research program aims to develop and/or validate methodologies for qualitative and quantitative analysis of volatile organic chemicals in water using GC/MS/COMP as the major analytical tool in three phases: 1) a state-of-the-art literature review; 2) experiments to develop the scheme; and 3) application/improvement of the scheme. Phase 1 is complete (except for updating); the second is in progress. Phase 2 is limited to chromatographable organics (or those which can be made chromatographable, for example, by derivatization). Areas being investigated include collection/preservation/shipment of samples, storage/physical stability, particulates, volatile organics, extractable organics, intractable organics (those which cannot be purged or extracted), chemical derivatization, and GC and GC/MS analysis.

Experiments are currently in progress to define as strict a procedure as possible for attaining reproducible tune and "standard" spectra, stable over time. Since a wide range of variation is obviously possible, it will be essential to analyze a suitably defined standard mixture at least once daily (possibly more frequently) to be able to guarantee quality and reproducibility of results.

A question to be addressed in the Master Scheme is choice of standards for quantitative information by relative molar response factors. Two factors were assumed crucial in selection of standards: 1) a close chemical correspondence to the compound of interest; and 2) elution from the chromatograph in relatively close proximity to the compound of interest. To assess a selection of types of compounds for use as standards, a multicomponent mixture was analyzed in replicate and responses relative to different components of the mixture calculated. Selected ion peak heights were used as a measure of system response. In our laboratories, peak heights and peak areas have been found to be closely equivalent for selected ion profiles. The deviation seen in the response factors is shown in Table 1. Standards chosen in this group of compounds were d_{10}-anthracene, 2-chloronaphthalene, and *p*-chlorotoluene (a 25 m SE-30 WCOT column). The standards cover the elution range of the compound mixture with no one standard "best" over the entire range. Each standard seems to minimize deviation in response factors for those compounds which elute in its vicinity. The same effect is seen: 1) on a 100 m SCOT SE-30 column where deviations in response factors over the entire range are good (never more than $\pm$15%) but demonstrably better in close proximity to the position of elution of the standard; 2) on a packed column (OV-101) where deviations in response factors are significantly lower in the vicinity of the standard (the standard used for polybrominated biphenyl isomers is decachlorobiphenyl, which is chemically extremely similar). Standard deviation and coefficient of variation calculated for the multicomponent mixture are shown in Table 2. d_5-Phenol and d_7-quinoline (some more polar standards) did not prove to be significantly better standards, even for their undeuterated analogs, than the standards originally present in the mixture. When elution of the polar constituents from a Carbowax 20M WCOT (wide-bore, 0.5 mm) (Table 3) column is presented, a similar effect is observed. Use of a polar compound as a standard does not necessarily give better precision for response factors than use of a chemically dissimilar standard which elutes in closer proximity. Several factors will have to be considered in the selection of standards and of a number of standards for a given determination. The time, effort, and expense of selecting and using multiple standards for a given chromatographic analysis must be weighed against additional precision which can be gained by using multiple *vs.* single standards.

This work was supported under EPA Contract No. 68-03-2704.

Table 1

AVERAGE OF THE ± DEVIATION (PERCENT) AS A FUNCTION OF INTERNAL STANDARD AND "BEST" STANDARD ON CARBOWAX

Compound	Relative Retention[a]	Std. 126[b]	162[c]	99[d]	136[e]	188[f]	"Best"
Methylthiophene	.18	12	6	11	13	8	162
Ethylbenzene	.60	12	17	14	16	20	126
Ethylthiophene	.62	11	29	7	23	14	126,99
Pyridine	.64	11	34	37	27	31	126
p-Chlorotoluene	1	-	24	35	19	14	162
Methylpyridine	1.02	5	18	10	14	17	126
1,2,4-Trimethyl-benzene	1.07	12	17	14	16	20	126
Indan	1.11	10	21	13	12	20	126
2,3-Benzofuran	1.27	12	18	13	13	19	126
Indene	1.32	8	17	10	10	9	126
Naphthalene	1.64	19	12	8	9	7	99,188
d_5-Phenol	1.74	6	20	-	4	9	136,(99)
Phenol	1.74	6	20	3	10	13	99
o-Cresol	1.79	6	14	7	9	12	99,126
Methyl indole	1.88	27	5	27	8	12	162
p-Cresol	1.88	18	36	19	23	25	126,99
d_7-Quinoline	1.88	14	10	4	-	9	99(130)
Quinoline	1.88	17	4	7	7	8	162,136,99
3,5-Dimethyl-phenol	2.02	14	11	10	3	8	136
2-Chloronaph-thalene	2.03	28	-	15	16	7	162(188)
3,4-Dimethyl-phenol	2.08	11	11	11	8	7	136,188,99, 162,126
Methylquinoline	2.15	14	10	11	8	5	136,188
Indole	2.29	9	13	4	7	9	99,136
Dibenzofuran	2.29	24	4	12	4	6	136
Phenanthrene, Anthracene	2.78	18	6	17	11	8	136
d_{10}-Anthracene	2.80	14	11.5	10	10	-	99,136

[a] relative to p-Chlorotoluene
[b] 126 = p-Chlorotoluene
[c] 162 = 2-Chloronaphthalene
[d] 99 = d_8-Phenol
[e] 136 = d_7-Quinoline
[f] 188 = d_{10}-Anthracene

Table 2

VARIANCE IN RESPONSE FACTORS (SE-30 Column)

	"Best" Standard	Standard Deviation	Coefficient of Variation
Toluene	DA	0.23(.62,.50)	9 (20,11)
Methylthiophene	PCT(DA)	0.24	12
Pyridine	All(PCT)	0.05	29
Ethylbenzene	PCT	0.47	7
Methylpyridine	All(DA,CN)	0.04,0.04,0.05	44
Phenol	CN(PCT)	0.09	9
p-Chlorotoluene	PCT(CN)	0.08	12
2,3-Benzofuran	PCT	0.02	5
1,2,4-Trimethylbenzene	PCT	0.15	3
Indan	PCT	0.16	5
Indene	CN	0.09	4
o-Cresol	PCT	0.02	2
p-Cresol	CN	0.04	6
Naphthalene	CN	0.04	7
3,5-Dimethylphenol	CN	0.05	6
3,4-Dimethylphenol	CN	0.03	3
Quinoline	CN	0.02	3
Methylindole	CN(DA)	0.17	5
Indole	DA(CN)	0.08	12
2-Chloronaphthalene	CN(DA)	0.09	17
Biphenyl	DA	0.28	14
4-Methylquinoline	DA	0.01	6
Dibenzofuran	DA	0.007	4
Phenanthrene	DA	0.09	7
d_{10}-Anthracene	DA(CN)	0.12	6
Anthracene	DA	0.10	9

Table 3

VARIANCE IN RESPONSE FACTORS (Carbowax Column)

	$\sqrt{\frac{2(x-\bar{x})^2}{n-1}}$				Coefficient of Variation = $100\frac{s}{\bar{x}}$				Best Standard Deviation		Best Coefficient of Variation	
	126	162	99	136	126	162	99	136				
Pyridine	.08	.14	.04	.07	8	26	21	22	.04	D5	8	PCT
Methylpyridine	.05	.15	.03	.06	4	17	9	11	.03	D5	4	PCT
Phenol	.23	.62	.03	.19	5	16	2	8	03	D5	2	D5
o-Cresol	.15	.30	.05	.10	6	14	7	8	05	D5	6	PCT
Methylindole	1.08	.21	.30	.40	20	5	20	16	21	CN	5	CN
p Cresol	.52	.81	.16	.34	14	28	18	20	18	D5	14	PCT
Quinoline	.39	.08	.05	.07	13	4	6	5	05	D5	4	CN
3,5-Dimethylphenol	.28	.20	.06	.02	10	10	8	2	.02	Q7	2	Q7
3,4-Dimethylphenol	21	.15	.05	.07	9	8	8	6	.05	D5	6	Q7
Methylquinoline	.43	.26	.01	.12	10	8	1	6	01	D5	1	D5
Indole	.40	.59	.05	.13	7	13	3	5	.05	D5	3	D5

PEAK LOCATOR PROCEDURE

LYDELL B. HANSEN
Food and Drug Administration
3032 Bryan Street
Dallas, Texas 75204

GC/MS systems are valuable tools for the analysis of a variety of environmental contaminants. Typically, residues are analyzed chromatographically using one or more columns with specific and sensitive detectors, eg., electron capture. A relatively simple chromatogram is usually obtained by this procedure. If a contaminant is detected, the residue is then concentrated and subjected to GC/MS analysis for confirmation, or identification of unknown components. Three factors complicate the analysis at this point: (1) The resulting non-specific "total ion" chromatogram is usually different from the original "specific" chromatogram. In many cases the peaks of interest, representing nanogram to picogram quantities, are among coextracted natural components in microgram quantities. (2) A major complication is the need to temperature program the GC/MS column in order to maintain narrow peak widths and sensitivity for the trace components. (3) Usually the column and the chromatographic conditions cannot be fully duplicated in the GC/MS laboratory. Therefore, it may be difficult to locate a trace peak from a simple isothermal "specific" chromatogram in the complex temperature programmed "total ion" chromatogram. Figure 1 demonstrates the problem with the pesticide residue. Peaks I, II and III of chromatogram A (specific, FPD) can be relatively easily located in chromatogram B (total ion, MS). Peak IV is not easy to locate in the total ion chromatogram.

An aid for locating retention times in complex chromatograms is to use an index mixture which can be used to standardize both systems to each other. A simple Kovats type mixture of saturated hydrocarbons may not be adequate <1>. The McReynolds polarity of the contaminants may require the use of the same type components for a retention index <2>. The retention mixture standardizes columns of the same type to each other. Variations in column length, loading, flow rate or temperature are indexed to each other. Any differences in either system are self compensating. The technique allows temperature programmed columns to be standardized to isothermal columns. Capillary columns can be standardized to packed columns. Different liquid phases can be standardized to each other as long as the polarities are the same for the same sample type.

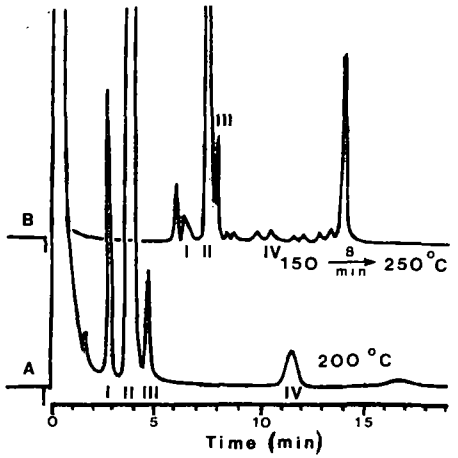


Figure 1. Pesticide Residue Chromatograms.

For pesticide residue analysis a mixture containing lindane, aldrin, endrin, pp'-DDT and guthion produces a retention mixture suitable for electron capture system indexing. (Approx. 1-5 mg/ml for the GC/MS and 1/1000 dilution for the EC system.) A full temperature range phosphate index can contain malaoxon, parathion, oxadiazon, trithion, guthion, coumaphos oxygen analog, and coumaphos. This mixture should be stored cold in opaque containers. The two coumaphos components may be excluded if the system is not temperature programmed above 230°C. The relative retention times of these components are not integer values, but they are well spaced on non-polar and moderately-polar columns.

Figure 2 shows chromatograms of the phosphate mixture obtained with a non-polar (OV-101) column. Chromatogram A is an isothermal (220°C) analysis with an FPD. Chromatogram B is a concentrated mixture, temperature programmed from 150 to 250°C at 4°/min with an FID.

A graphical analysis of the two column system is shown in the log-linear plot of Figure 3 <1,3>. The observed retention times of the isothermal column are plotted on the log axis vs. the observed temperature programmed times on the linear axis. The resulting straight line plot may be used to locate any intermediate retention times on the alternate column. For example, peak IV of Figure 1, chromatogram A (at 11.5 min) can be

located in the programmed chromatogram at 7.0 min. Conversely, cursory analysis of the mass spectrum of the total ion peak at 6.7 min indicated an aromatic symmetrical phosphate. However, the absence of an FPD peak at 11.0 min suggested that closer study of the mass spectrum was necessary. The peak was identified as a fatty acid gamma lactone coextracted with the residue.

A mathematical analysis of the retention times can be obtained with a computer or a programmable calculator. A curve fit program will yield the constants of the equation

$$Y = A + B \ln X \quad (1)$$

where X is the isothermal retention time and Y is the programmed retention time of the mixture.

$$(\text{Prog Time}) = A + B \ln (\text{Iso Time}) \quad (2)$$

Solving equation (2) for X allows programmed retention times to be located on the isothermal chromatogram.

$$(\text{Iso Time}) = e^{\left(\frac{\text{Prog Time} - A}{B}\right)} \quad (3)$$

The constants for the two columns of Figure 2 in minutes are: A = 1.439, B = 5.373 and degree of fit r^2=0.996. These constants and the equations transpose retention data to either column.

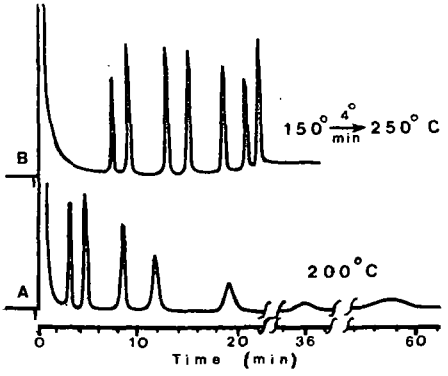


Figure 2. Phosphate Mixture Chromatograms.

A long initial hold or a multiple rate temperature programmed column could be indexed to an isothermal column. The curved plot in Figure 3 shows the graphical analysis of the phosphate mixture temperature programmed from 180 to 230°C at 4°/min after an initial 10 min hold at 180°C. The plot is non-linear because several peaks elute before the temperature starts to increase. But the plot allows the location of retention times on the alternate column. Mathematical analysis may not be practical in this case, even though extrapolation between near neighbors may give satisfactory results.

The units of measurement used allow a great deal of flexibility in analyzing a system. The usual units would be time in minutes or in centimeters. Any required units may be used in either the graphical or mathematical analysis. Also, the units can be transformed as required: to Kovats index values, simulated distillation temperatures, fatty acid ECL values, etc. Figure 4 shows a series of transformed axes for a temperature programmed standard mixture. The peak of interest can be found at the specified location, regardless of the units used.

(1). E. Kovats, Helv Chim Acta, 41, 1915 (1958).
(2). W. O. McReynolds, Characterization of Some Liquid Phases, J of Chrom Sci, 8, 685, (1970).
(3). W. E. Harris and H. W. Habgood, Programmed Temperature Gas Chromatography, Wiley, New York, N. Y.

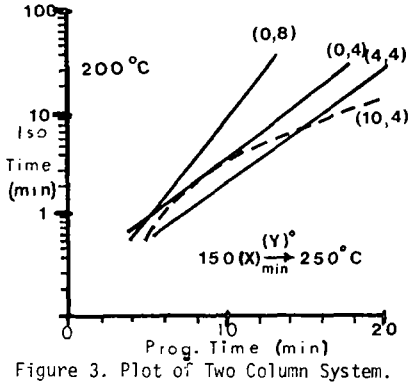


Figure 3. Plot of Two Column System.

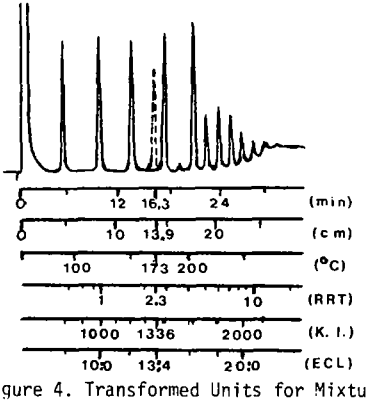


Figure 4. Transformed Units for Mixture.

PRACTICAL CONSIDERATIONS IN THE ANALYSIS OF INDUSTRIAL WASTE STREAMS

J. Bouldin, R. Stowe, K. Shewbart, and M. J. McAdams
Dow Chemical, Freeport, Texas

During 1976 the EPA was required to begin a program to establish industrial wastewater effluent limitations for a group of priority pollutants. The first step in determining what the limitations should be was to identify and quantitate these priority pollutants in various wastewaters from a number of industries. The Texas Division of the Dow Chemical Company would be one of these industries. The Texas Division ranks among the chemical industries largest complexes in both physical extent and volume of production. It has two plant sites covering 3,000 acres in Freeport, Texas. There are more than 100 different production units operating around the clock for a daily output of 40 million pounds of basic, intermediate, and fine chemicals and chemical products.

There are many real problems facing the industrial chemist concerning the consent decree.

One problem is the definition of a waste stream. A waste stream is water which has been used in a chemical process which will eventually end up back in the environment. Depending on the use of the water it may or may not contain contaminants. Condensate water is often cleaner when it is returned to the environment. Process water is water which is either recycled through a plant or is to be used by another chemical plant for some specific purpose. This water may also be returned to the environment from time to time. A waste stream may be turned into process water at any time depending on availability and water requirements.

Sampling procedures may also cause problems. Analytical results obtained in the laboratory can never be more reliable than the sample upon which the tests are performed. More results are in error because of poor sampling procedures than because of faulty laboratory techniques. Some grab and composite sampling techniques are discussed. Sample procedures include flushing lines and checking with each plant control room to be sure no recent production upset has occurred.

From a large industrial complex the wastewater samples are somewhat open in that entry of new components is possible but not frequent or likely, and the components are somewhat defined. GC/MS is the analysis method of choice, for samples which are most frequently involved in rule making. These include (1) the supply water, (2) influent to treatment and effluent from treatment. In plants which the inputs and reations are well defined, the waste streams can be analyzed by chromatography with GC/MS analysis required only when process changes occur. Mass spectrometry is an excellent qualitative tool and can also be used as a compound specific detector to quantitate organics. Criteria is discussed for defining a GC peak and for quantitation by mass spectrometry.

While procedures exist for extraction of organics from wastewater, recovery efficiencies from individual complex waste streams are not available. Often these streams vary in composition on an hourly basis. There are still no standard methods for analyzing complex waste streams. An isotope dilution method for the analysis of several complex waste streams is mentioned. This procedure includes spiking and cooling samples in the field and analysis by GC/MS.

GLASS CAPILLARY GC/MS ANALYSIS OF DRINKING AND ADVANCED WASTE TREATMENT WATER CONCENTRATES. DENIS C.K. LIN, R. FOLTZ, S. LUCAS, B. PETERSEN, AND L. SLIVON, Battelle Columbus Laboratories, 505 King Avenue, Columbus, Ohio 43201.

To examine the health effects of water, the organics in drinking and advanced waste treatment water from various origins have been concentrated by the reverse osmosis process (1). The water concentrates have been tested for mutagenesis and other types of biological activities. The concentrates that show biological significance are analyzed in this project. The objectives of this project are:

- to identify organic compounds that can be gas chromatographed
- to confirm the compound identifications
- to quantitate compounds confirmed.

An analytical scheme has been developed to achieve the above objectives. The scheme uses an extensive sample preparation step to separate the complex water concentrates into acidic, basic and four neutral fractions. The details of this fractionation step has been described (2). After sample preparation, the main analytical tool is capillary GC/MS using two types of columns (SP2100 and SP1000). The results show that the sample fractionation is a very essential step to identify the components by their low resolution electron impact mass spectra. The massive volume of data is interpreted with the aid of a computer. The computer also performs a semi-automatic routine to search for specific compounds in the data. The routine is based on selected ion summation (3) and GC retention time window. The compound identifications are considered to be tentative until the mass spectra and the relative retention times are shown to match those of authentic reference compounds. Deuterated compounds are added in the analysis for the purpose of calculation of appropriate relative retention times. Furthermore, they are used to monitor the fractionation and as internal standards for quantitation.

ACKNOWLEDGEMENT

We acknowledge EPA for its financial support under contract No. 68-03-2548.

REFERENCES

(1) Kopfler, F. C., Coleman, W. E., Melton, R. G., Tardiff, R. G., Lynch, S. C., and Smith, J. K. Ann. NY Acad. Sci. Vol. 298, 20 (1977).

(2) Lin, D.C.K., Foltz, R. L., Lucas, S. V., Petersen, B. A., Slivon, L. E., and Melton, R. G. ASTM Symposium Volume on 'Organic Pollutants in Water and Wastewater, June, 1978' ASTM, Philadelphia, PA (in press).

(3) Kuehl, D. W. Anal. Chem. Vol 49(3), 521 (1977).

A COMPARATIVE STUDY OF VOLATILE HALOGENATED HYDROCARBONS IN MAN AND THE ENVIRONMENTAL MEDIA BY GC/MS/COMP

E. D. Pellizzari, R. A. Zweidinger, R. N. Williams, M. D. Erickson, B. Harris, III, D. S. Smith, K. B. Tomer and M. Ray
Research Triangle Institute
Research Triangle Park, N. C. 27709

Currently this laboratory is involved in a research program to make a comparative analysis of selected halogenated compounds in man and the environmental media. One objective of this program is to demonstrate the body burden of volatile halogenated hydrocarbons in selected individuals by examining urine, blood and breath and to determine the occurrence of halogenated hydrocarbons in the environment to which these individuals are exposed.

A pilot study for this program was initiated in the Old Love Canal area of Niagara Falls, New York. This area was used as a toxic chemicals dump for a 25-30 year period up to 1953. In the late 1950's a housing development was built on adjacent land. Heavier than normal rains over the past several years have raised the ground water level above the dump site, causing the buried chemicals to begin seeping laterally into adjacent basements. In early 1978 we analyzed the chemical compounds accumulating in basements in this area. In this earlier study, elevated concentrations of halogenated hydrocarbons were found in the ambient basement air of the homes.

Since the potential exposure of this small population was quite high, there was a good opportunity to demonstrate the applicability of our analytical methodology to such a multimedia study. The core of this methodology is the application of the techniques of capillary GC/MS/COMP to the analysis of environmental and biological samples. The mass spectral data are utilized to provide both qualitative and quantitative information concerning pollutants in environmental samples.

It was also hoped that this pilot study would show a qualitative correlation between the halogenated compounds found in the environment and those found as a human body burden.

The results presented in this paper deal with one individual's body burden and environment. Table 1 summarizes our quantitative results for the environment of this individual while Table 2 presents our quantitative body burden results for this individual. A surprising result is that the levels of the volatile compounds examined were generally higher outside the home than inside. The outside air composition is in fact comparable to the previously determined basement air levels.

The levels of halogenated compounds found in the air inside the home of the participant are remarkable in that the heavier halogenated hydrocarbons were rarely detected. This is in contrast to the data obtained in the basements in February, 1978 during our earlier study.

These data also show that these volatile halogenated hydrocarbons found in the environment also occur as human body burden as demonstrated by their occurrence in the biological media-urine, blood and breath.

In the absence of a wider data base, it is not possible to say whether or not the levels of halogenated compounds found as body burdens are elevated or not.

In addition, the chronic health effects, if any, of chemicals at these levels are unknown and thus one cannot state with certainty whether or not these levels are health hazards.

The quantitative results of the at-large air samples are shown in Table 3. Quite high levels of some of the compounds, especially chlorobenzotrifluoride and chlorotoluene, are noted. It is interesting to note that Yurawecz in J. Assoc. Offic. Anal. Chem., 62, 36(1979) has reported the presence of chlorinated trifluorotoluene residues in Niagara River fish.

These results are indicative of the qualitative and quantitative information that can be obtained by bringing the technique of GC/MS/COMP to bear on environmental problems and are illustrative of the power of this technique. The experience obtained from this study is being used in larger multimedia studies on halogenated compounds in man and his environment which are now in progress.

Acknowledgement

We would like to acknowledge Mr. K. Krost, Organics Methodology Branch, EPA, RTP and Mr. B. Librizzi of the Office of Toxic Substances, EPA Region II, Edison, N. J., who initiated our involvement in the Old Love Canal Study.

We would like to acknowledge the United States Environmental Protection Agency for contract numbers 68-02-2764, 68-01-4731 and 68-01-3849, Task I and V. J. DeCarlo and J. Breen of the Office of Toxic Substances, EPA, Washington. We also wish to acknowledge the cooperation of the Niagara City Health Department, Dr. Francis J. Clifford and the N. Y. State Department of Health and Dr. M. Vienna. We especially wish to acknowledge our appreciation for the cooperation given us by the people of Niagara Falls, N. Y.

Table 1

ESTIMATED LEVELS OF VOLATILE HALOGENATED COMPOUNDS IN THE ENVIRONMENT OF THE PARTICIPANT

Compound	Outside air (ng/m^3)	Inside air (ng/m^3)	Tap water (ng/l)
Chloroform	51,692	2,392	9,542
1,2-Dichloroethane	–	–	–
1,1,1-Trichloroethane	1,444	1,216	417
Carbon tetrachloride	1,000	T	192
Trichloroethylene	–	T	65
Tetrachloroethylene	400	1,334	2,875
Chlorobenzene	T	588	42
Dichlorobenzene isomer(s)	T	3,980	825
Trichlorobenzene isomer(s)	T	–	542
Tetrachlorobenzene isomer(s)	T	–	658
1,2-Dichloropropane	T	–	–
Dichlorotoluene isomer(s)	T	–	–
Trichlorotoluene isomer(s)	T	–	–
Tetrachlorotoluene isomer	T	–	–
Dichlorobenzaldehyde isomer	T	–	–
1,2-Dibromoethane	T	–	–
Bromochlorotoluene	T	–	–
1,3-Hexachlorobutadiene	T	–	–
Bromodichloromethane	–	–	10,375
Dibromochloromethane	–	–	3,108

Table 2

BODY BURDEN OF VOLATILE HALOGENATED HYDROCARBONS FROM ONE PARTICIPANT

Halogenated Compounds	Breath (ng/m^3)	Blood (ng/ml)	Urine (ng/l)
1,1-Dichloroethane	–	–	–
Chloroform	37,447	1.54	1,250
1,2-Dichloroethane	243	–	–
1,1,1-Trichloroethane	329	.85	183
Carbon tetrachloride	689	.04	150
Trichloroethylene	–	–	67
Tetrachloroethylene	1,152	.49	692
Chlorobenzene	–	.055	117
Dichlorobenzene isomer(s)	5,294	2.77	1,433

Table 3

ESTIMATED LEVELS OF SITE-SPECIFIC HALOGENATED COMPOUNDS (ng/m^3) IN AMBIENT AIR IN NIAGARA FALLS/BUFFALO, N.Y.

Compound	Site 2	Site 4	Site 5
Chlorobenzotrifluoride isomer(s)	ND	523	19,586
Chlorotoluene isomer(s)	427	527	12,274
Dichlorobenzotrifluoride isomer(s)	ND	ND	193
Dichlorotoluene isomer(s)	43	ND	446
Trichlorobenzene isomer(s)	39	43	324
Hexachlorobutadiene	54	ND	389
Trichlorotoluene isomer(s)	ND	ND	568
Tetrachlorobenzene isomer(s)	ND	ND	451
Pentachlorobenzene	ND	ND	17

A QUALITY CONTROLLED OPERATING PROCEDURE FOR GENERAL TYPE GC/MS ANALYSES

Virgil L. Warren[1]

A procedure is described for analyzing a simple or complex environmental or pollution sample both qualitatively and quantitatively on one run of the sample. Why such a procedure is necessary is discussed for quadrupoles and results obtained on synthetic mixtures and spiked real samples are given, using both packed and glass capillary columns and electron impact ionization. Accuracies of from 5 to 20 percent of the amount present per analysis are obtained on low nanogram quantities.

The procedure consists of two parts: (1) a tune-up and calibration procedure and (2) a quantitative or semi-quantitative method of analysis using extracted ion current profiles (EICP's) - not selected ion monitoring as is normally used for quantitation by GC/MS. The main object of the entire procedure is to be able to analyze a simple or complex sample, with the appropriate standards run but not necessarily all on the same day or at the time that the sample was run.

The prime requirement, is that the spectra of the compounds remain essentially the same from day to day or week to week or longer, that retention times remain constant and that sensitivities or relative response factors remain fairly constant and be known. Also, spectra of both high and low molecular weight compounds must be "authentic" or not distorted and be of such quality that they will be found by manual or computer library search schemes.

Quadrupoles are widely used for the type of work considered here and they are well suited for it - if they are properly cared for and used. However a quadrupole can be tuned to give a spectrum which looks widely different from time to time. They can look widely different from that of magnetic instruments or they can be made to look essentially identical to them or to anything in between. Relative abundances which differ by a factor of ten or more from the "normal" are not uncommon, and the spectra can be enhanced at the low m/e end or the high m/e end or the middle or any combination. This is not difficult to understand if one obtains the profiles of the various source plates and deflection devices (that is, the voltage or its equivalent VS the response of various ions such as m/e 69, 219, and 502 for perflurotributylamine. These curves (some ten or more for such things as the repeller, drawing out plate, ion focus, entrance lens, X-ray deflection, electron multiplier high voltage, filament emission, electron energy, beam width controls, etc.) have irregular and sometimes unpredictable shapes generally different for ions in the low, medium or high mass range. Abundance ratios are dependent on the voltages producing these curves. A "high m/e tune", "low m/e tune" or "normal" tune can be obtained and used as needed. For this particular procedure a "normal" tune is selected. This is one which gives a decafluortriphenylphosphine (DFTPP) spectrum which agrees with that proposed by Budde and Eichelberger[2] of the EPA. The limits and target values for PFTBA and DFTPP used to obtain this tune are shown in Table 1. The exact way to tune up is subject to debate but I always use a set procedure (as much as possible) to arrive at the fixed target values as shown in Table 1, and operate in the stable positions on the profile curves, together with having symmetrical peaks of equal width, no precursors, and essentially baseline resolution at the 502, 503 region.

After the instrument is given the "normal" tune on PFTBA, a four component mix is run to check out the tune on DFTPP, the retention times, resolution, mass calibration and the sensitivities of several different types of compounds, in terms of extracted ion current profile areas. This four component mix (DFTPP, heptachlorepoxide, methyl stearate and dieldrin) also checks out the entire GC/MS/DS to see that all components are in good working order and that no significant changes have ocurred since the last time it was run under these same conditions. It also permits records to be kept for preventive maintenance and later use of sensitivities for semi-quantitation.

If this quality control sample is run satisfactorily, one can be assured that the instrument is ready and any results obtained within the next 10 hours or so are "authentic". One also knows the sensitivity and the retention times for a variety of compounds. This completes the tune up and calibration procedure. It takes about 20-30 minutes. If problems occur, especially if the instrument hasn't been operated in several days or the source and/or rods are dirty it might take several hours.

The instrument is now ready to be used in the general quantitative method of analysis in which it may be desired to identify and quantitate from one to twenty or more compounds in a given sample, running it only once if need be or several times if more accurate or precise results are desired. This particular method is almost as sensitive as SIM and almost as precise as GC methods, if used under the controlled conditions.

Basically the method uses what has commonly been called limited mass search peaks, mass chromatograms, or probably more correctly, extracted ion current profiles (EICP's). These are computer generated plots of the ion currents of designated m/e's as a function of the scan number. The data used for these plots are stored in the various register channels and are available for each scan number in the form of total intensity counts (normalized with respect to the integration time used to acquire them). The areas or peak heights are used for quantitation by relating the area counts for standard and sample run under the same conditions. Fragment ions and/or molecular ions can be used, and the areas are usually linear from 5 to 300 ng or more. Internal standards can be used for quantitation and relative retention times if desired.

This method was first used on a round robin laboratory test of known pesticide mixes and spiked extracts using packed columns. True accuracies of +5% can be obtained with care. The more usual case is to obtain accuracies of from 10 to 30 percent. For capillary columns it has been as good or better, both with regard to area measurements and retention times, although no round robin test of such has been made. Accuracies of ± 2% to 5% have been obtained with great care; and ± 10 to 20% of the amount present per analysis can generally be obtained on 20 to 300 ng. The key requirement for capillary work is that enough scans per peak be made, at least 6 and preferably 15 or so. This requires fast scanning, good resolution and high sensitivity. Sometimes this requires what is called "interval scanning" or limited repetitive scanning where only the important sections of mass ranges are used. For example 230-250, 265-280, 530-560 instead of 45-650, resulting in an increase of sensitivity of about 10.

TABLE 1
PERFORMANCE CRITERIA FOR TUNE-UP AND CALIBRATION COMPOUNDS

PFTA
(perfluorotributylamine $C_{12}F_{27}N$, M.W. = 671)

M/e Ratio	Range	Target
219/69	0.3 to 0.5	0.35
219/502	20 to 30	25
513/414	0 to 0.05	0
501/502	0 to 0.05	0
503/502	0 to 0.15	0.10
131/219	1 to 3	1.5
100/131	0.2 to 1	0.3
502/69	1% to 2%	1.3

DFTPP
(Decafluorotriphenylphosphine $C_{18}H_5F_{10}P$, M.W. = 442)

M/e Ratio	Range	Target
		Can be greater if all criteria are met.
442/198	0.4 to 0.8	
443/442	0.17 to 0.23	0.20
441/443	less than 1	0.6
365/198	0.01	0.01
197/198	0 to 0.01	0
199/198	0.05 to 0.1	0.06
68/69	0 to 0.02	0
70/69	0 to 0.02	0
51/198	0.4 to 0.7	0.5
127/198	0.4 to 0.7	0.5

[1]Present address Univ. of New Orleans, New Orleans, La. Formerly with the Food & Drug Administration in Washington, D.C.

[2]Eichelberger, James W., Harris, Lawrence E. and Budde, William L., Analytical Chemistry 47, 995-1000. June 1975.

RAMOC9 GC/MS Verification of Identity of Chlorinated Pesticides and Biphenyls in Municipal Sewage Treatment Plant Sludge. Charles F. Rodriguez, Carter P. Nulton, and William A. McMahon, Department of Environmental Sciences, Southwest Research Institute, San Antonio, Texas 78284.

The overall objective of the study of which this work was a part was to provide a method for the analytical determination of the priority pollutant chlorinated pesticides and biphenyls (PCB's) in activated sludges from sewage treatment plants. It was required that the method be available within six months of initiation of the work, hence, it was to be adapted from existing EPA analytical protocols for monitoring the priority pollutants in wastewaters of various origins. In these methods, the pesticides and PCB's are normally determined by gas chromatography/electron capture detection (GC/ECD) as part of the base-neutral extract group of compounds. The requirements for this method included that it stand alone, that quantification be at a minimum detectability level of 15μg/L, and that verification of identity be included in the procedure. The first two specifications were met by the following analytical procedure.

1. Liquid-liquid extraction with centrifugation to break any resultant emulsion,
2. Liquid column chromatography on Florisil adsorbant to minimize organic interferences,
3. Contact of the extract with metallic mercury to remove elemental sulfur, and
4. Separation and determination of the individual compounds by GC/ECD.

The method proved applicable to 14 single-compound pesticides, two multi-component pesticides, and the multi-component polychlorinated biphenyls. Attempts were made to verify the identities of compounds in the extracts by GC/MS but the mass spectra could not be used for identification because the amount of extract that saturated the mass spectrometer did not contain enough analyte for recognition. Consequently, another approach was pursued to cleanup the extracts prior to GC/MS determination.

Gel permeation chromatography (GPC) was found to remove up to 80% of the background interference material in contrast to Florisil which removed only about 10% and resulted in merely distributing the remainder into two fractions. Sephadex S-X2 with dichloromethane as the eluant produced an extract clean enough for GC/ECD but still too complex for useful GC/MS at the detectability limits sought. Sephadex S-X3 with cyclohexane as the eluant provided a broader elution band of the chloroorganics from which narrower fractions were caught. The relative amounts of chlorinated and interfering compounds were changed enough that the response of the pesticides and PCB's could be recognized in these fractions.

Authentic standards of the subject chloroorganic compounds were spiked in known concentrations into several different sludges. The sludges were acquired from municipal sewage treatment plants receiving varying ratios of domestic and industrial influents. The spiked sludges were equilibrated at 4°C with occasional shaking for a minimum 18 hours. The sludge was then extracted, cleaned up by GPC, and analyzed by GC/MS. It was found there was no need to remove elemental sulfur prior to GC/MS determination.

A spectrum, relatively free of background, was generated for each standard and reconstructed single ion mass chromatograms made for the characteristic ions. Comparison with the characteristic ions recommended by the EPA wastewater screening protocol showed good agreement of prospective useful ions. Three ions and their relative abundances for each compound, in combination with chromatographic retention characteristics, were found to provide strong evidence of a compound's identity.

The method was tested for applicability to sludges from three municipal sewage treatment plants from areas ranging from mainly domestic influent to one of high industrial influent. Only indication of Chlordane in concentrations below 150μg/μL was found in the sludges, confirming the results of GC/ECD.

The GC/MS procedure for confirmation of identity has been recommended for inclusion in the EPA interim method for screening activated sludges for chlorinated pesticides and biphenyls. The results provide a limited data base for expansion of the method and development of procedural refinements and statistical evaluation for qualification as a quantitative verification method.

APPLICATIONS OF RECENT MASS SPECTROMETRIC TECHNIQUES TO THE ANALYSIS OF ENVIRONMENTAL MATERIALS

D.J. Harvan, J.R. Hass, and K.L. Busch

Environmental Chemistry Branch
National Institute of Environmental Health Sciences
P.O. Box 12233
Research Triangle Park, North Carolina 27709

The analysis of biological samples for the presence of 2,3,7,8-tetrachlorodibenzo-p-dioxin at the part-per-trillion level is a particularly difficult analytical problem. Three inherent obstacles are:

1) There is a large amount of interfering chlorinated materials in any biological sample (i.e. polychlorinated biphenyls and their associated contaminants or chlorinated pesticides, such as DDT or DDE).

2) There is a degree of uncertainty introduced into any analysis that is operating at its lower limits of detection (i.e. electronic noise is larger at high gain levels, as are relative sample losses due to adsorption and sample manipulation).

3) There are 22 positional isomers of TCDD, therefore, introducing uncertainty even with exact mass measurements.

Removal of chemical interferences has been attempted by:

1) Extensive sample clean-up (Ref. 1).

2) Specific mass spectrometric detection systems (e.g. high resolution selected ion monitoring).

3) Use of gas chromatography for sample introduction.

We have attempted several new techniques in order to effect a more sensitive and specific detection of TCDD. Our first approach was the use of negative ion mass spectrometry. This method has been shown to be very sensitive for highly chlorinated molecules (Ref. 2). Unfortunately, TCDD was not as easily detected, having a minimum detectability of ca. 15 pg, as effluent from a GC column. We also found that milk samples had a co-eluting material which interfered with analyses even at 10-100 ppt levels, and thus, the method was unsuitable. The use of a capillary column may enable lower detection limits.

Another specific detection method is the use of field-free region reactions. Linked scanning of the magnet and electric sectors to monitor the reaction

$$M^{+\cdot} \rightarrow (M\text{-}COCl)^{+}$$

was found to be limited in sensitivity. The minimum detectable quantity was ca. 200 pg. It should be noted that this value was observed for the unimolecular reaction, because no collision cell was available at the time. This may be improved by monitoring the collision induced reaction.

We have also investigated mass-analyzed ion kinetic spectrometry (MIKES) as a method of monitoring the above reaction. This technique has recently been used for analysis of different samples without prior cleanup (Ref. 3). A S/N of greater than 5:1 was observed for 2 pg of TCDD by direct probe sample introduction. Good linearity and reproducibility were also demonstrated.

The direct probe method suffered some limitations from matrix effects. The signal from 100 pg TCDD was reduced to 67% of its former value by addition of 1 µg of methyl stearate to the probe cup. Also, 1 µg methyl stearate alone gave a signal equivalent to ca. 5 pg TCDD. Another problem is positive interferences arising from xenobiotic materials in the sample. It was observed that 53 ng of Aroclor 1260 gave a signal corresponding to 15 pg TCDD. Interferences were also observed for individual hexa-, hepta- and octa-chlorobiphenyl isomers, although pentachlorobiphenyl gave no response from 1 µg material.

Similar positive interferences were observed for the higher chlorinated dioxins, especially penta- and hexachloro isomers. Due to these matrix effects, direct probe MIKES analyses appear limited to higher levels (0.01%) of analysis.

The use of GC-MIKES enables removal of most of the matrix problems. However, we have experienced co-eluting contaminants that made ppt-level analyses impossible in several milk samples. The use of capillary column GC-MIKES will be investigated in future work.

At the present time, the three obstacles to ppt analyses are best met by means of capillary column, high resolution (10,000) GC-MS. However, the use of field-free region reactions and negative ion techniques offer promise as confirmatory as well as replacement methods.

References

1. Baughman, R. and Meselson, M.: Environmental Health Perspectives, 5, 27-35, 1973.

2. Hass, J.R., Friesen, M.D., Harvan, D.J., and Parker, C.E.: Anal. Chem., 50, 1474, 1978.

3. Kondrat, R.W., McClusky, G.A., and Cooks, R.G.: Anal. Chem., 50, 2017, 1978.

GC/MS ANALYSES OF VOLATILE PURGEABLE HALOGENATED ORGANIC COMPOUNDS IN HUMAN SERUM RAMOC11 AND ADIPOSE TISSUE. CARL D. PFAFFENBERGER, Department of Epidemiology and Public Health, The University of Miami School of Medicine, 15655 S.W. 127th Avenue, Miami, FL 33177.

Organohalogens have been detected in virtually all chlorinated drinking waters. During a nationwide study, concentration levels in the finished drinking water of 79 cities of the United States were established for six volatile purgeable halogenated hydrocarbons (VPHHs): chloroform ($CHCl_3$), bromodichloromethane (BDCM), dibromochloromethane (DBCM), bromoform ($CHBr_3$), carbon tetrachloride (CCl_4) and 1,2-dichloroethane (DCE). The health implications of these findings stimulated the development of a project to determine if any of these six substances or trichloroethylene (TCE) could be detected in relatively small samples of human adipose tissue (250 mg) or blood serum (0.5 ml) obtained from residents of Dade County, Florida, an area in which chloroform levels in excess of 300 µg/l (ppb) have been reported. Accordingly, the purge/trap/desorb method of Bellar and Lichtenberg was modified to accomplish these objectives. The procedure reported here is relatively rapid in that it requires no extraction or clean-up step.

Quantitative analyses were performed using a Tekmar Model LSC-1 liquid sample concentrator interfaced to a Tracor Model 222 gas chromatograph (GC) equipped with a Hall electrolytic conductivity detector which was operated in the halide specific mode. The chromatographic column was a 6-ft x 0.25-in. I.D. glass U-tube containing n-octane on 100-120 mesh Porasil C packing. The GC operating conditions included: a nitrogen carrier gas flow-rate of 30 ml/min, an inlet temperature of 140°, and a transfer line temperature of 210°. The Hall detector furnace was maintained at 900° with a hydrogen flow-rate of 40 ml/min and a solvent (1:1 n-propanol:distilled water) flow of 0.4 ml/min. A Finnigan Model 4000 gas chromatograph/ mass spectrometer (GC/MS) analytical system interfaced to a Tekmar liquid sample concentrator was used to confirm the identities of the compounds quantified by the gas chromatographic procedure. Both the GC and the GC/MS systems utilized a hot plate stirrer and a glycerol bath to heat the sample in the Tekmar purging device.

For adipose tissue: Between 200 and 500 mg of frozen adipose tissue is cut into thin strips and pushed to the bottom of a pre-purged, 5-ml Tekmar purging device. The purge flow-rate is adjusted to 10 ml/min, and the lower portion of the device is immersed in a 115° stirred glycerol bath for 20 min. After the volatile components have been purged from the liquefied fat, the adsorbed compounds are desorbed and transferred to the analytical column (60°) by heating the trap at 150° for 6 min. The GC column is then temperature programmed 7°/min to 140°. Hexane is added to the purging device containing the purged adipose tissue, and the residue is quantitatively extracted to separate the fat component from residual connective tissue. Values are reported in ng VPHH/ g hexane extractable fat. Ten fat samples, taken from near the anterior abdominal wall at autopsy, were analyzed. Chloroform concentrations ranged from 20 to 460 ng per gram of hexane extractable fat as indicated in Table 1.

For blood serum: One ml of 1% aqueous Dow Corning antifoam emulsion B is added to a 5-ml purging device and the sample concentrator is operated in the Trap Bake Mode for 20 min while the trap temperature is 200°. (This procedure purges the system of all potentially interfering compounds; however, a blank run may be made at this time to ascertain that the system is uncontaminated.) The trap is then cooled to the ambient temperature. By means of a gas tight syringe, 0.5 ml of serum is introduced into the purging device and a purge flow-rate of 10 ml/min is started. The lower portion of the purging device is immersed in a 115° stirred glycerol bath for 30 min. (Both serum and fat appear to possess an inherent binding capacity for halogenated organic compounds which can be overcome by purging the sample at elevated temperatures.) To prevent steam contamination of the Tenax/silica gel trap, a small glass vapor trap or interceptor is placed between the purging device and the adsorbent trap. After the purge/trap period is complete, the adsorbed compounds are desorbed and transferred to the analytical column (60°) by heating the trap at 150° for 6 min. The GC column is then temperature programmed 7°/min to 140°. Chloroform concentrations ranged from 2 to 189 ppb as indicated in Tables 2 and 3. Table 2 indicates serum levels of chloroform found in 100 white/hispanic females between the ages of 25 and 65 who ingest most of the time municipal drinking water reported (National Organics Reconnaissance Survey) to have a chloroform level of around 300 ppb. Table 3 indicates levels found in 80 other white/hispanic females between the ages of 25 and 65 who drink mostly non-chlorinated water from privately owned wells located in southern Dade County, Florida. Finally, Table 4 indicates serum levels of tetrachloroethylene (PCE; perchloroethylene) and chloroform, a metabolite of PCE, in four workers of a dry cleaning establishment.

Chloroform was the major VPHH identified during analysis of human adipose tissue and blood serum by the above procedures. The identities of PCE and chloroform were confirmed by LSC/GC/MS methods. When coupled with the appropriate GC retention data, the cluster

having m/e = 83, 85 and 87 corresponding to the respective positively charged fragments $CHCl_2^{35}$, $CHCl^{35}Cl^{37}$ and $CHCl_2^{37}$ was particularly useful to confirm the presence of chloroform in the biological samples.

The exact source of the chloroform detected in human fat and serum by this procedure is presently unknown. Possible sources include municipal drinking water and chronic exposure to trichloroethylene (TCE) and/or tetrachloroethylene (perchloroethylene; PCE). Municipal drinking water contains both residual chlorine and chloroform generated during the chlorination process from reactions between humic substances in raw water and either dissolved chlorine or hypochlorous acid. It has also been proposed that "intermediate bonding states" between halogen and various organic molecules can exist. If this latter situation occurs to any great extent, ingestion of municipal drinking water could conceivably lead to in vivo generation of chloroform from the precursors. Moreover, the residual chlorine in finished drinking water could also form chloroform precursors after the water has been consumed. A clear explanation of the origin of chloroform in human tissue is thus not currently possible.

A satisfactory explanation is even more difficult if exposure to TCE and/or PCE is considered. During an earlier study and from periodic water analysis reports, neither of thesecompounds has been detected in amounts comparable to the chloroform levels usually found in Miami drinking water. However, both TCE and PCE are metabolic precursors of chloroform, and Fishbein has reviewed two additional routes of exposure, air and food. McConnell and co-workers reported tissue ranges of TCE and PCE for humans between less than 0.5 µg/kg and 29 µg/kg wet tissue. These values are far less than the chloroform levels reported here for adipose tissue. Although it is impossible to rule out the possibility that some of our experimental subjects had been exposed to these two organochlorides, it is reasonable to assume that they were not. None of the subjects (except those in Table 4) were involved in either degreasing or dry cleaning occupations nor did any of them work or live near these types of establishments. If a portion of the serum chloroform reported in this investigation is traceable to metabolized TCE or PCE, the intact chlorinated ethylene(s) will be present in corresponding samples of adipose from the individuals. Such a study is in progress.

Table 1
Human Adipose Tissue
Chloroform Levels

Sample	ng/g*	Sample	ng/g*
F-1	80	F-6	20
F-2	230	F-7	28
F-3	460	F-8	140
F-4	65	F-9	95
F-5	240	F-10	240

*hexane extractable fat.

Table 2
Serum Levels of Individuals Who
Drink Highly Chlorinated Water

% of Samples	ppb Chloroform Range	Average	Median
25	26-189	59	41
50	10-25	15	13
25	6-9	8	7

Table 4
Blood Serum Levels in Dry Cleaners
Who Use Perchloroethylene (PCE)

	$CHCl_3$ (ppb)	PCE (ppb)
In the PCE dip room	6000	2300
In & out of the dip room	3000	800
Occasionally in dip room	350	100
Spot cleaner	300	150

Table 3
Serum Levels of Individuals Who
Drink Non-chlorinated Water

% of Samples	ppb Chloroform Range	Average	Median
25	13-25	18	18
50	5-12	8	7
25	2-5	4	4

The technical assistance of Mrs. A.J. Peoples, Mr. J.J. Freal, III and Mr. J. Guerra is gratefully acknowledged as is the financial support of EPA Research Grant No. R-804611.

References:

Peoples, Pfaffenberger, Shafik and Enos, Bull. Environ. Contam. Tox., September, 1979.

Pfaffenberger, Peoples and Enos, J. Chromatogr., September, 1979.

THE KINETIC ISOTOPIC FRACTIONATION EFFECT FOR CARBON AND OXYGEN IN THE REACTION CO + OH*

C. M. Stevens, L. Kaplan, R. Gorse, S. Cohen, S. Durkee, and K. Bielling

Chemistry Division, Argonne National Laboratory
Argonne, Illinois 60439, USA

The reaction CO + OH is the principal scavenging process for atmospheric CO [1] and hence its kinetic isotope fractionation effect (K.I.E.) is useful in isotopic studies aimed at determining the origin and production rate of the natural sources of atmospheric CO [2-4]. The K.I.E. for both carbon and oxygen in this reaction were measured using the photolysis of H_2O_2 as a source of OH radicals under static conditions with various gases at pressures between 0.2 and 1.1 atm. The K.I.E. for carbon ($^{12}k/^{13}k$) with air as the third body gas varied from 0.997 at 0.2 atm of air to 1.007 at 1.1 atm. With oxygen over the same pressure range the carbon K.I.E. varied from 0.994 to 1.002, and for argon, from 0.990 to 1.000. The oxygen K.I.E. ($^{16}k/^{18}k$) was the same for air, oxygen, or argon and varied from 0.989 to 0.991 over the pressure range 0.2 to 1.0 atm.

These results support the model for the reaction CO + OH in which the radical HOCO is produced by deactivation from an excited complex HOCO* and the subsequent formation of CO_2 from this state competes with the direct dissociation of the excited complex to CO_2 + H [5-7]. The variation of the carbon K.I.E. is interpreted as due to different amounts of the two reaction modes with the low value or inverse K.I.E. at low pressures corresponding to the direct decomposition and the high value, or normal K.I.E. corresponding to the deactivation of the excited complex.

[1] H. Levy II, Science 173, 141-143 (1971).
[2] B. Weinstock and Tai Yup Chang, Tellus XXVI, 108-115 (1974).
[3] D. H. Ehhalt and A. Volz, "Coupling of the CH_4 with the H_2 and CO cycle: Isotopic Evidence," in Microbial Production and Utilization of Gases (H. G. Schlegel, G. Gotteschalk, N. Pfennig, eds.), E. Goltze:KG, Göttingen, 1976, pp. 23-33
[4] C. M. Stevens, L. Krout, D. Walling, A. Venters, A. Engelkemeir, and L. E. Ross, Earth Planet. Sci. Lett. 16, 147-165 (1972).
[5] A. Y. M. Ung and R. A. Back, Can. J. Chem. 42, 753-763 (1964).
[6] I. W. M. Smith and R. Zellner, Chem. Soc. Faraday II: 69, 1617-1627 (1973).
[7] I. W. M. Smith, Chem. Phys. Lett. 49, 112-115 (1977).

*Work performed under the auspices of the Office of Basic Energy Sciences of the U. S. Department of Energy.

Quantitation of Individual Organic Compounds in Shale Oil, L. R. Hilpert, H. S. Hertz, W. E. May, S. N. Chesler, S. A. Wise, F. R. Guenther, J. M. Brown, and R. M. Parris, Organic Analytical Research Division, National Bureau of Standards, Washington, D. C. 20234

Introduction

In order to enhance the accuracy of environmental measurements associated with the development of alternate fuels, the analytical expertise necessary to certify the concentrations of several phenols, N-heterocycles, and polynuclear aromatic hydrocarbons (PAH) in shale oil is being developed and NBS will issue the shale oil as a Standard Reference Material (SRM). Acid-base solvent extraction and high performance liquid chromatography have been investigated as independent methods of shale oil fractionation prior to quantitative determinations of individual compounds by various gas chromatographic, gas chromatographic-mass spectrometric, and high performance liquid chromatographic methods.

Experimental

Shale Oil Sample - The shale oil analyzed in this work is from a 150-ton retort for in situ simulated combustion operated by the Laramie Energy Research Center, Laramie, Wyoming. The shale is from the Mahogany zone of the Colorado Green River formation. An 8 L sample of this shale oil was obtained by NBS from Oak Ridge National Laboratory, Oak Ridge, Tennessee. The shale oil underwent centrifugation at Oak Ridge to separate water (∿40%) and sludge from the oil. A sub-sample of 1 L was removed from the 8 L bulk sample, and aliquots of ∿5 mL each were sealed in amber glass ampoules for subsequent analyses.

Acid-Base Extraction - The shale oil sample was separated into three fractions (acids, bases, and neutrals) using an extraction procedure adapted from Schmeltz (1). For the determination of the PAH, an additional liquid-liquid partition step using dimethylformamide (DMF)/water and hexane was utilized to remove the aliphatic hydrocarbons from the PAH neutrals. This procedure for the isolation of PAH in complex mixtures has been previously reported by Bjørseth (2).

HPLC Extraction - The shale oil sample was diluted (∿0.1 g/mL) prior to fractionation on a preparative scale aminosilane column (30 cm x 7 mm i.d.). A sample containing from 10-15 mg of shale oil was injected onto the column using a loop injector. A mobile phase flow rate of ∿5 mL/min was employed. Standards of the compounds to be determined and the compounds utilized as internal standards were injected to determine the appropriate elution volumes for fraction collection. After collection of the fractions in 15- or 40-mL centrifuge tubes, the fractions were reduced to 50-500 µL by passing N_2 over the sample.

Quantitation

Liquid Chromatographic (LC) - LC analyses were performed using a standard liquid chromatograph. A 254 nm filter photometric detector was used for detection of the N-heterocycles, a multiwavelength UV detector was used for measurement of phenol and o-cresol at 270 nm, and a spectrofluorometer was used for fluorescence detection of the PAH. Quantitative results were based on measurement of chromatographic peak heights. An external standard method was used for the PAH and N-heterocycles, and an internal standard method for the phenols.

Gas Chromatographic (GC) - GC analyses were performed on a standard gas chromatograph which was modified for use of wall coated open tubular (WCOT) columns. Quantitative results were based on measurement of peak areas using a digital integrator. An internal standard method was used for all determinations.

Gas Chromatographic-Mass Spectrometric (GC-MS) - GC-MS analyses were performed on a quadrupole mass spectrometer. A standard addition technique was used for individual species quantitation for all compounds except the benzopyrenes, which were determined using an internal standard method. Four standard additions were made covering a range of 0 to 3X the approximate concentration of the species being determined (based on a preliminary quantitation of the compound in the shale oil using an external standard method). The "spiked" shale oil samples were subjected to either the acid/base solvent extraction, or the HPLC fractionation described above to generate fractions for GC-MS analysis. A second compound known to be present in the shale oil, and in the same compound class as the compound

being determined, was also monitored as a volume correction standard to compensate for variable injection volumes onto the GC column.

Selected ion monitoring was used for the analyses to enhance sensitivity and selectivity. The molecular ions for the compound of interest and the internal standard (volume correction standard) were monitored in 0.1 amu increments to insure that the voltage was sampled at the top of the mass peak. Dwell times of 50 or 100 ms were employed to insure at least 20 data points across the chromatographic peak. Single ion record peak areas were integrated after each run, and ratios of peak areas for the compounds of interest to the peak areas of the internal standard were computed. These ratios were plotted vs the concentration of the compound added to the shale oil. A linear least squares regression analysis was used to determine the concentration of the compound in the shale oil.

Results and Discussion

Quantitative determinations of individual components in a complex matrix such as shale oil require that the sample be cleaned up prior to analysis to remove non-analyte interferences. This sample clean-up step has traditionally involved a solvent extraction such as that reported by Schmeltz (1). This extraction step is a laborious procedure which requires 1-2 man days to generate the acidic, basic, and neutral oil fractions. Furthermore, once the extraction step has been completed, the sample must be subjected to a high resolution chromatographic separation to allow individual components to be quantified free from interferences. Quantitative determinations for the compounds in the solvent extracted fractions were performed by gas chromatography or, were additional specificity was required, by gas chromatography/mass spectrometry with selected ion monitoring. The results of these determinations are presented in Table 1, under the heading "Acid/Base Extraction".

Table 1. SHALE OIL ANALYSIS
(ppm, 95% confidence level)

	HPLC Extraction			Acid/Base Extraction	
	Quantitation by			Quantitation by	
Compound	LC	GC	GC/MS	GC	GC/MS
pyrene	108±16	101± 4	102± 9	94±10	--
fluoranthene	53±6	55± 6	62± 5	75± 5	--
benzo(a)pyrene	21.0±2.8	--	21± 5[a]	--	24± 2
benzo(e)pyrene	--	--	20± 6[a]	--	22± 5
phenol	383±50	387±26	416±28	--	334±63
o-cresol	330±34	334±86	350±16	--	322±45
2,4,6-trimethyl pyridine	--	912±26	1214±64	988±56	--
acridine	6.0±2.4	--	4.4±0.3	--	--

[a]Internal standard of perylene used instead of standard addition.

A novel, rapid method of preparing shale oil fractions of subsequent quantitative determinations has been developed which involves a high performance liquid chromatographic separation of the shale oil on a preparative scale aminosilane (μBondapak NH_2) column (3). By modifying the mobile phase composition from 100 percent hexane to 100 percent CH_2Cl_2, it is possible to selectively elute a wide range of compounds from non-polar PAH to the more polar phenols and N-heterocycles. The HPLC shale oil fractions obtained were analyzed for the individual compounds by various high performance liquid chromatographic, gas chromatographic, and gas chromatographic/mass spectrometric techniques. The results of these determinations are also shown in Table 1. As can be seen, the agreement among values obtained by independent quantitative techniques is excellent at the 95 percent confidence level. Results from determinations on fractions obtained by an acid/base extraction vs those obtained from the HPLC generated fractions are also in excellent agreement. Although the "true"

or "actual" concentrations cannot be verified with current state-of-the-art methodology, the intralaboratory precision obtained using independent techniques of shale oil fractionation and quantitation give us confidence in the results obtained.

Aliquots of the shale oil sample were sent to several laboratories currently involved in characterizing alternate fuels. The laboratories were requested to determined the concentrations of the phenols, N-heterocycles, and PAH listed. Preliminary results of this limited interlaboratory exercise are presented in Table 2. The scatter of the results indicate the variability of state-of-the-art quantitative analyses for individual compounds in a complex matrix. It also stresses the need for an SRM, such as the shale oil, which laboratories responsible for quantitative measurements can use to gauge the accuracy of their analytical methods.

Table 2. INTERLABORATORY COMPARISON OF RESULTS OF SHALE OIL ANALYSES

		Laboratory					
Compound	NBS[a]	2	3	4	5	6	7
pyrene	107	155	360	150	168	212	141
fluoranthene	61	102	220	80	108	104	112
phenol	395	392	180	--	--	--	399
o-cresol	338	350	150	--	--	--	381
2,4,6-trimethyl pyridine	1060	468	460	--	950	--	1092

[a]Results reported by NBS represent the mean of values obtained by GC, GC/MS, and HPLC.

References

(1) Schmeltz, I., Phytochem. 6:33 (1967).
(2) Bjørseth, A., Anal. Chim. Acta 94:21 (1977).
(3) In order to specify procedures adequately, it has been necessary to identify some commercial materials in this report. In no case does such identification imply recommendation or endorsement by the National Bureau of Standards, nor does it imply that the material identified is necessarily the best available for the purpose.

Acknowledgements

Partial financial support from the Division of Biomedical and Environmental Research of the Department of Energy is gratefully acknowledged. The following laboratories participated in the interlaboratory comparison reported herein: Ames Laboratory, Iowa State University, Ames, IA 50010; Chemical Engineering Dept., MIT, Cambridge, MA 02139; Argonne National Labs, Argonne, IL 60439; Pittsburgh Energy Research Center, Pittsburgh, PA 15213; Los Alamos Scientific Lab, Los Alamos, NM 87545; and Analytical Chemistry Division, Oak Ridge National Laboratory, Oak Ridge, TN 37830.

The Determination of Polycyclic Aromatic Hydrocarbons at the ng/L Level in Drinking Water

F.M. Benoit, G.L. LeBel and D.T. Williams, Environmental Health Directorate, Health and Welfare Canada, Ottawa, Canada, K1A 0L2

In June and October 1978 the drinking water at six water treatment plants (A-F) in Eastern Ontario were monitored for twelve selected low molecular weight (128-228) polycyclic aromatic hydrocarbons (PAH) and four oxygenated derivatives (O-PAH) using Amberlite XAD-2 macroreticular resin for analysis at the ng/L level according to the method of LeBel et al.[1] At two plants (E and F) the raw waters were also analysed in the October sampling. The compounds monitored were selected on the basis of their prominence in area waters in previous studies[2].

The waters sampled are located in neighbouring but demographically distinct water basins. Basin 1 drains a heavily populated urban area with a high industrial activity, basin 2 drains a lightly populated rural area with little industrial activity and basin 3 drains a moderately populated urban area with moderate industrial activity. As a measure of the relative quality of the waters analysed, aggregate levels were computed by summing the concentrations of the individual PAH and O-PAH, respectively for each water treatment plant. The average aggregate PAH and O-PAH levels for each water basin were computed from the aggregate levels for the plants in each basin.

The individual PAH concentrations ranged from 0.1 to 6.4 ng/L in treated waters and from 0.1 to 34.4 ng/L in raw waters. The aggregate PAH concentrations ranged from 3.3 to 30.3 ng/L in treated waters and from 13.1 to 74.3 ng/L in raw waters. Aggregate PAH concentrations showed no discernible seasonal trend. The raw waters analysed contained higher (plant E, 74.4 ng/L raw vs 30.3 ng/L treated) or equal (plant F, 13.1 ng/L raw vs 12.3 ng/L treated) aggregate levels of PAH; a similar trend was observed for O-PAH levels (plant E 28.5 ng/L raw vs 4.7 ng/L treated and plant F 3.3 ng/L raw vs 3.4 ng/L treated).

The individual O-PAH concentrations ranged from 0.1 to 2.1 ng/L in treated waters and from 0.3 to 10.6 ng/L in raw waters. At five plants (A,B,C,D,E) the aggregate O-PAH levels were higher in the October sampling than in the June sampling. The O-PAH levels at plant F was the same for both test periods.

For both test periods the average aggregate PAH and O-PAH levels were lower in basin 2 which has the lowest anthropogenic activity. The difference between aggregate O-PAH levels for basins 1 and 2 however was small (~ 10%). This suggests that PAH and O-PAH contaminants are deposited mainly in the aquatic system of the basin in which they

are produced.

Conclusions

PAH and O-PAH are present at the low ng/L level in all the waters sampled and the level of contamination is related to the anthropogenic activity within the water basin. The level of contamination of a raw water supply may vary considerably over a relatively short period of time and water treatment techniques are unable to remove completely PAH and O-PAH from the final product. The level of O-PAH contamination is generally higher in the autumn probably because of the accumulation of oxidation products of PAH during the summer when surface waters are exposed to higher levels of sunlight and atmospheric oxidants.

1. G.L. LeBel, D.T. Williams, G. Griffith and F.M. Benoit, J. Assoc. Off. Anal. Chem. 62, 241 (1979).

2. F.M. Benoit, G.L. LeBel and D.T. Williams, Intern. J. Environ. Anal. Chem., in press.

THE ANALYSIS OF TETRACHLORODIBENZODIOXIN (TCDD) AT THE PARTS-PER-TRILLION LEVEL

P.A. Lyon, J.O.Lay, D.L.Miller, and M.L. Gross

Department of Chemistry
University of Nebraska
Lincoln, Nebraska 68588

During the past two years, we have established a facility for the trace analysis of TCDD in environmental and biological samples. The research has involved both the sample preparation and the actual analysis by gas chromatography/high resolution mass spectrometry.

Traditionally the focus of attention has been on the presence of dioxins as by-products in the production of 2,4,5-T based herbicides. A growing concern over the effects and fate of dioxins in the environment led this spring to an EPA ban on the sale and use of trichlorophenoxy herbicides. However, recent reports suggest that chemical waste landfills and certain combustion processes (1) are also contributing to the levels of dioxins.

Monitoring studies are becoming more complex, due to the nature of the matrices, and more exacting with respect to sensitivity. Analyses today are demanding of both instrumentation and the chemical workups. To accomodate these demands, we have installed a Perkin-Elmer Sigma 2 gas chromatograph to operate with the MS-50 mass spectrometer via an interface of our own design, and a Nicolet Model 1170 Signal Processor for data acquisition and reduction. A three fold increase in GLC resolution over standard commercial columns (OV-1, OV-3, SE-30) was attained by using 0.60% OV-17 and 0.40% Poly S-179 coated on 100% methyl silicone bonded to 80/100 mesh chromosorb W-AW, a recently developed column packing at Dow Chemical. (We thank Dow Chemical for allowing us to evaluate this column packing.)

The improved chromatography and signal averaging have permitted us to improve detection limits to the 0.2 to 1.0 parts-per-trillion level for the analysis of a 10 g sample of human milk or adipose.

The confidence in data produced in this demanding analysis can be increased by validation studies in which standard solutions and biological extracts are submitted as blind samples to various analytical laboratories. The U.S. Environmental Protection Agency conducted a study of this nature in late 1977, and the results were reported in the popular scientific press (2). Briefly, the measured values correlate very well with the true values over a range of concentration of 9-81 parts-per-trillion for both standard solutions and beef fat extracts. The 95% confidence limits for a single analyses were established to be $\pm$ 6-7 parts-per-trillion over the entire range. This means that an unknown containing 50 parts-per-trillion can be extracted (using the "acid-base" procedure) and analyzed to yield a value within the range of 43 to 56 parts-per-trillion. No "false positives" or "false negatives" were found in this work although samples containing 4 parts-per-trillion (5 g sample) or less were not found.

Very low detection limits are required to monitor dioxin levels in samples such as plant materials, mother's milk, fish, fly ash and water. An example of this work was a cooperative study with the New York State Health Department (3) to assess bioaccumulation of TCDD in fish. The New York scientists prepared the fish samples for analysis in our laboratory. Initial findings showed the presence of dioxins at 4 ppt (detected with a S/N of about 10:1) in fish taken from lake Ontario. Levels were quantitated using internal ^{37}Cl spike and verified by checking the ratio of m/e 320:322 for the native dioxin (observed ratio agrees with theory to within 10%).

Another application of the analytical methodology is the assessment of the fate of TCDD in primates. W.P. McNulty at the Oregon Regional Primate Research Center, in cooperation with our laboratory, has completed a study of abortions in rhesus macaques caused by exposure to TCDD (4). Among samples analyzed for the study, aborted placentas were worked up and found to contain 45 and 90 ppt dioxin. These were the first reported TCDD

measurements for such samples, and the work demonstrates that TCDD can be monitored in tissue taken from animals in feeding studies.

Improved chemical workups have been required to analyze soils from chemical waste landfills. These soils contain high levels of contaminants, requiring a more rigorous clean-up procedure. We have shown in the case of a soil extract, when conventional LC clean-up methods are inadequate, HPLC (3) can be used successfully. The use of HPLC has been applied to the analysis of dioxins in drum contents from a landfill site. These drums often contain exclusive chemical wastes--potentially the worst matix in which to analyze for TCDD. We are developing methods that will permit the analysis of dioxins in these more complex matrices.

References:

1. "Trace Chemistry of Fires--A Source of and Routes for the Entry of Chlorinated Dioxins into the Environment" Chlorinated Dioxin Task Force, Midland Division of Dow Chemical, U.S.A.

2. Nature, 278, 109-110, March 8, 1979.

3. New York State Health Lab, P. Dymerski, D. Hilker in mass spectrometry; P. O'Keefe, B. Bush and R. Smith in chemical methods.

4. W.P. McNulty, "2,3,7,8-Tetrachlorodibenzo-p-dioxin: Abortions in Rhesus Macaques" Science (in press).

HEAT DEGRADATION STUDIES ON SOLAR HEAT TRANSFER FLUIDS

T. R. Henderson, C. R. Clark, T. C. Marshall, R. L. Hanson and C. H. Hobbs

Lovelace Inhalation Toxicology Research Institute
P. O. Box 5890
Albuquerque, New Mexico 87115

Expanded use of solar heating and cooling of buildings and homes is anticipated in the near future. This will result in introduction of large quantities of new materials into structures which are not utilized in present types of construction. Relevant chemical characterization and toxicity data is needed about these materials and possible products which may be formed from them in normal use, in fires or other types of malfunctioning.

The typical active solar collector involves circulation of a heat transfer fluid through copper collectors exposed to solar irradiation. A pump circulates the fluid through the collector and back to a central reservoir of several thousand gallons or more. As long as the pump is operating, the temperatures of the fluids are maintained in the range of 75 to 300°C. If the pump fails, or is turned off when the reservoir is fully charged, the temperature of the collectors during stagnation may approach 200°C in flat plate collectors and up to 300°C in evacuated tube collectors. The residual fluids in collectors thus may be exposed to hot metal surfaces and the possibility for thermal degradation products to form and accumulate is increased. Air admitted during draindown cycles may also contribute to the formation of oxidation degradation processes. Little information is available as to what types of heat degradation products may accumulate in heat transfer fluids used in solar collectors(1), or what potential toxicity problems may occur.

GC/MS procedures, in combination with data systems, provide a useful approach for characterizing complex mixtures and identification of biologically active compounds. We report on one approach to fractionating heat transfer fluids for concentration of components into fractions which are more amenable to GC/MS analysis, and which provide adequate amounts of material for in vitro mutagenesis screening systems, such as the Ames test(2).

METHODS

Samples of commercial solar heat transfer fluids were investigated under simulated stagnation conditions, by distillation in the presence of air over a temperature range of 200 to 400°C. Copper wire fragments were added to simulate the effects of metal surfaces.

GC/MS analyses were carried out by injection of 0.1 to 1 µl samples into a Finnigan 4023 GC/MS equipped with an INCOS data system. The GC conditions were 20 m SP-2100 glass capillary column, operated either splitless or with 1:100 split, with direct passage of the column effluent into the MS through the standard glass-lined capillary. The GC carrier gas was He, 2 ml/min. The temperature program was 60°C hold for 5 min; 60 to 150°C at 6°/min; 150 to 250°C at 2°/min; and 250°C hold for 10 min.

The Salmonella, mammalian microsome, mutagenicity bioassay (Ames) was carried out as described previously(2). Samples were dissolved in DMSO and 0.1 ml of the DMSO extract or dilutions thereof were used in each assay.

Fractionation of aromatic petroleum based heat transfer fluids was carried out by a modification of existing procedures. Ten ml of fluid was diluted with 90 ml of hexane in a separatory funnel. This organic layer was extracted 3X with 5% HCl. The HCl layer was extracted 3X with diethyl ether and neutralized to pH 12. The ether extract was evaporated in a rotary evaporator (Fraction I Basic). The hexane/heat transfer fluid layer was extracted similarly with 5% NaOH to yield Fraction II Acidic, then 3X with DMSO to yield a DMSO extract: Fraction III. Dilution of the DMSO extract with 2 volumes of water, followed by extraction into hexane and evaporation produced a Fraction IV Aromatic and Fraction V DMSO/water residue. The organic layer remaining after DMSO extraction was evaporated to yield Fraction VI Aliphatic. These samples were dissolved in DMSO for Ames bioassay or into methylene chloride for injection into the GC/MS.

RESULTS AND DISCUSSION

Destructive distillation of typical solar heat transfer fluids results in a variety of detectible products being formed. The early distillation fractions contained undegraded, low boiling components such as water, ethylene glycol, propylene glycol or low

boiling hydrocarbons. As the distillation proceeded, a point was reached where only slightly volatile materials remained, and thermal degradation ensued.

The glycol/water heat transfer fluids exhibited degradation products may result from dehydration of the parent glycol. No effects related to catalytic effects of Cu were noted. Ethylene glycol based fluids exhibited traces of 1,4-dioxane and ethylene oxide in the pyrolysis products. Propylene glycol fluids exhibited traces of proplyene oxide. Glycerol-based fluids exhibited traces of 2-propene-1-ol and 1,2-epoxy-4-propanol and appreciable residues of non-volatile residues which exhibited higher molecular weights than glycerol on CI/solid probe analysis.

The other types of fluids investigated included a diethylamine salt of butoxy,ethyl phosphate and a high aromatic petroleum base fluid. The former yielded 1,4-dioxane, 1,1'-oxybispropane,2-methyl and 1-(2-butoxyethoxy)-ethanol. The high aromatic fluid exhibited fractions which were high in aza-arenes in the first fraction and high in methyl-substituted naphthalenes, phenanthrenes and pyrene when analyzed by glass capillary GC/MS. The aza-arenes detected included methylquinolines, dimethyl-indolizines and dimethyl and trimethyl quinolines. Since the aza-arenes have been reported to be mutagenic in Ames bioassay, efforts were made to fractionate the high aromatic heat transfer fluid to investigate this possibility. It was found that the aza-arenes could be removed by extraction and the residue fractionated to enable Ames testing of all fractions as well as GC/MS analysis.

Mutagenic responses were detected with both Salmonella strains TA-100 and TA-98 with the basic fraction extracted from the high aromatic heat transfer fluids. A dose-response relationship was observed from dilutions of 1:1.5 to 1:5 (relative to original fluid), the number of revertants observed increased from 113 background for TA-100 to 353 for 1:5; 525 for 1:2.5; and 662 for 1:1.5. TA-98 exhibited increases from 59 background to 703 for 1:5; 1290 for 1:2.5; and 1788 for 1:1.5. All of these reversion rates were observed only in the presence of S-9, so the extracts required metabolic activation for expression of mutagenic activity. Other fractions of the high aromatic fluid were toxic to the Ames tester strains and required 1:100 to 1:500 dilution to obtain bioassays with minimum toxicity. However, the other fractions, with the exception of the basic fraction, did not yield positive mutagenic responses.

Analysis of the basic fraction of the high aromatic fluid yielded glass capillary gas chromatograms which matched with known aza-arenes by the INCOS/NBS data system of a Finnigan 4023 GC/MS. The peaks identified were (a) quinoline/isoquinoline; (b) methylquinolines; (c) dimethylquinoline/ethylquinolines; (d) trimethylquinolines; (e) benzoquinolines, in this order of elution. Specific ion chromatograms for aza-arenes peaks, 129; 143; 157; 171; 179; 193; and 203 showed that all of the peaks reported to occur in air particulates occurred in the high aromatic heat transfer fluid also(3).

Benzoquinolines and higher aza-arenes were detectible in extracts from unheated fluids, but they were undetectible in fractions from heat degraded fluids. Reverse search INCOS programs as well as specific ion chromatograms showed no benzoquinolines were detectible in heated fractions, suggesting that certain of the aza-arenes (but not the methylated derivatives) were heat labile.

The origin of aza-arenes in solar heat transfer fluids is uncertain. The presence in gasifier tars as well as air particulates suggest that they may be formed as a by-product of combustion. The presence in aromatic heat transfer fluids derived from petroleum suggest that they may be present in petroleum and be distilled over during the refining process.

REFERENCES

1. Arnold, C., and R. E. Trujillo, "Composition Stability and Degradation Products of Selected Materials for Solar Heating and Cooling," Technical Report Sand 78-0681, Sandia Laboratories, Albuquerque, NM, 1979.

2. Ames, B. N., J. McCann and E. Yamasaki, Mutat. Res. 31: 347-363, 1975.

3. Dong, M. W. and D. C. Locke, Environ. Sci. and Technol. 11: 612-618, 1978.

ACKNOWLEDGEMENTS

This research was performed under U. S. Department of Energy Contract No. EY-76-C-04-1013. We are indebted to Dr. D. R. Royer, Dr. R. F. Henderson, Mr. Ambrose Sanchez and Dr. J. Benson for criticism and comments.

ABSTRACT #322

Ubiquitousness of Long Chain Hydrocarbons and Derivatives in Industrial Waste Waters As Identified by G.C.M.S.D.S., Robert G. Teece, Satu M. Somani, and David Schaeffer, Southern Illinois University, and Illinois Environmental Protection Agency, Springfield, IL 62708

Long chain hydrocarbons (LCH) (C_{10}-C_{35}) and their derivatives have been found in both potable and industrial waste water effluents. These compounds have not attracted as much environmental attention as the EPA "Priority Pollutants". Effluents from 12 industries of various types, one sewage treatment plant and deionized-distilled (d-d) water samples were extracted and analyzed. "Grab" samples (3.8 L) were adjusted to pH 11 for isolating base-neutral extractable compounds and pH 2 for isolating acid extractable compounds. The samples were then serially extracted with methylene chloride (400, 200, 200 ml). The serial extractions were combined and K-D evaporated to 5-10 ml. The samples were then eluted through a Supelcosil column (3.0 g) with 36 ml of methylene chloride and re-evaporated to 5.0-0.5 ml. Fifty ul aliquot of the acid extractable fraction was N_2 evaporated to dryness and then brought up with 50-100 ul of methylating agent. XAD-2 amberlite resin and activated carbon columns were also used for sampling and they were eluted with 2 bed volumes of acetone (30 ml) followed by 8 bed volumes of chloroform. The samples were concentrated in the same manner as were the liquid-liquid extracted samples. The organic compounds were separated by gas chromatography and their electron impact spectra were taken and processed by the mass spectrometer data system against spectra from the Aldermasten library. The 14 samples analyzed by g.c.m.s.d.s. generated a total of 508 computer matched organic compounds of which 212 represented different compounds. Fifty seven of the 212 compounds were matched as LCH or derivatives. Alkanes were 49%, methyl esters of long chain organic acids were 21%, long chain alcohols were 16%, and alkenes were 14%. The number of LCH or their derivatives ranged from 1-17 per sample. Eleven of these compounds were found in sewage treatment plant effluent and 13 in d-d water from our laboratory. The ubiquitousness of these compounds in samples from industrial waste water effluents, to raw drinking water, to deionized distilled water should be of environmental concern and warrants further study.

RAMP8

Measurements of Organic Compounds in Sediment, Soil, and Material from Chemical Waste Dumps

James W. Eichelberger and William L. Budde
U.S. Environmental Protection Agency
Environmental Monitoring and Support Laboratory
26 W. St. Clair St., Cincinnati, Ohio 45268

Sediment is defined as wet solids taken from the bottom of a stream, river or lake. Sediment analysis for organics is important because many water pollutants are in an equilibrium between the aqueous phase and the sediment adsorbed phase. Similar analytical problems are encountered in the analysis of contaminated soils and materials from chemical waste dumps. The Environmental Monitoring and Support Laboratory of EPA in Cincinnati has recommended a sediment extraction procedure and this basic method was evaluated. For a broad spectrum organics analysis or a search for specific organic compounds, GC/MS is the method of choice. Six solvents were used to extract organics with an ultrasonic homogenizer. The identification and measurement of the organics in a sediment from a highly polluted area was accomplished by GC/MS using internal and external concentration calibration standardization. The results from the methods are compared and discussed. The full text of this paper will be submitted to Analytical Chemistry.

A UNIQUE SCAN CIRCUIT FOR USE IN MULTIPLE ION, GC-HIGH RESOLUTION MS DETERMINATIONS OF PICOGRAM QUANTITIES OF CHLORODIOXINS

J. G. Solch, C. D. Miller, R. O. Yelton, M. L. Taylor, and T. O. Tiernan

The Brehm Laboratory, Wright State University, Dayton, Ohio 45435

The continual refinement of analytical methods for determining trace levels of 2,3,7,8-tetrachlorodibenzo-p-dioxin (TCDD) in environmental samples has been necessary to more clearly define the extent of TCDD contamination in the environment. Continued literature reports of TCDD contamination in biological tissues,[1] soil and water samples,[2] and incinerator fly ash[3] have focussed attention on methods of achieving more accurate low picogram level determinations of TCDD in complex matrices. In our laboratory we have developed a multi-ion gas chromatographic-mass spectrometric method that has been demonstrated capable of identifying low picogram levels of TCDD contamination in various environmental samples. Details of this method are given below.

Instrumentation: Varian 3700 Gas Chromatograph coupled through an AEI Silicone Membrane Separator to an AEI Scientific Apparatus MS-30 Double Beam Mass Spectrometer

Chromatographic Conditions: 2 m x 2 mm I.D. coiled glass column packed with 3% Dexsil 300 on Chromosorb W H/P. 30 cc/min helium carrier gas. Column and injector temperatures held at 240°C.

Separator Temperature: 215°C

Mass Spectrometer Source Temperature: 250°C

Mass Spectrometer Resolving Power: 1:13,000 (Static, 10% Valley)

Data Acquisition: Nicolet 1072 Signal Averager

Multiple ion GC-high resolution MS determinations of picogram quantities of TCDD have been accomplished by coupling a new rapid scan circuit designed and built in this laboratory to an AEI MS-30 mass spectrometer. Schematic representation of this scan circuit, which can simultaneously monitor up to four mass spectrometric peaks, is illustrated in Figure 1. The circuit sequentially steps the ESA voltage up to three times during each rapid scan. In this way narrow portions of the mass scale (typically 0.07 AMU) which bracket four separate peaks of interest can be simultaneously monitored. During actual analysis, scanning is begun as TCDD elutes from the gas chromatographic column into the mass spectrometer source and ends when the peak has totally eluted. Compounds which are not adequately resolved from TCDD solely on the basis of chromatographic resolution can be distinguished from TCDD by the mass spectrometric information. Although a 1:13,000 resolution cannot discriminate all interferences during single ion monitoring of the base peak for TCDD (m/e 321.8936), simultaneous scanning of the m/e 320, m/e 322, m/e 326, and m/e 328 windows provides state-of-the-art mass spectrometric information for picogram determinations of TCDD. The m/e 320 to m/e 322 ratio exhibited by an authentic native TCDD standard (0.78) provides a decision criteria for TCDD identification that is based on two m/e ratios. In addition, monitoring of m/e 328 permits the use of ^{37}Cl fortified TCDD as an internal standard. Evidence of PCB and PBB contamination of the sample extract, which can generate interfering ions at m/e 320, m/e 322, and m/e 328, is indicated by monitoring m/e 326. Further confirmation of TCDD levels can be obtained by recalibrating the multi-ion scan circuit to monitor four other m/e ratios that are indicative of TCDD.

Figure 2 illustrates a typical high resolution mass scan of four masses obtained for an injection of 40% of an extract prepared from human mothers' milk doped with 10 parts per trillion (ppt) of 2,3,7,8-TCDD and 2500 ppt of ^{37}Cl TCDD. Table 1, which summarizes the results obtained during an in-house quality control study, indicates that extraordinary accuracy can be obtained for samples which contain as little as 5 ppt of TCDD. A similar blind study conducted on EPA doped samples produced absolute errors of 2 ppt or less for 8 samples containing between 3 and 11 ppt of 2,3,7,8-TCDD.

In conclusion, the gas chromatographic-high resolution multi-ion mass spectrometric method described above has been implemented in assaying approximately 150 extracts of varying environmental types, and has been found to yield accurate results for samples containing 5 ppt levels of TCDD.

References:

1. A. diDomenico, F. Meril, et al, Anal. Chem. 51, Page 735-740 (1979).
2. A. L. Young, J. A. Calcagni, C. E. Thalken and J. W. Tremblay, USAF OEHL-78-92 (1978).
3. H. R. Buser, H. Bosshardt, and C. Rappe, Chemosphere 2, Page 165-172 (1978).

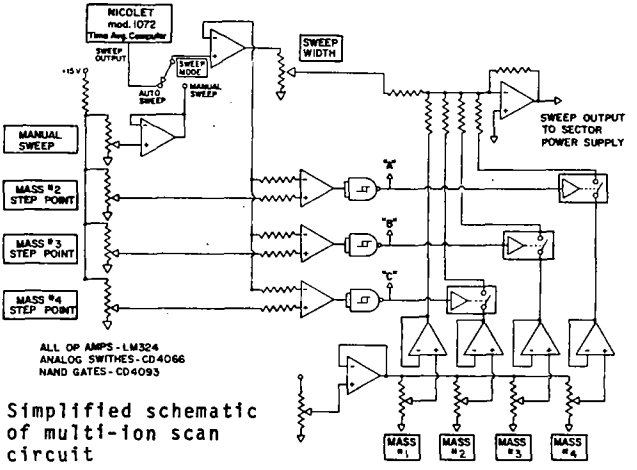


Figure 1. Simplified schematic of multi-ion scan circuit

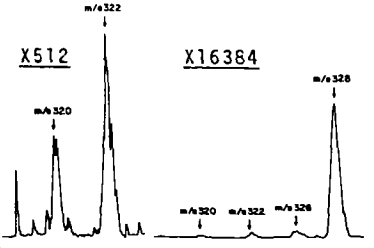


Figure 2. High Resolution Mass Scan of Four Masses For an Injection of 40% MMVS-9 (Doped). Injection Contained 40 Picograms 2,3,7,8-TCDD and 1000 Picograms of ^{37}Cl Fortified TCDD

Table 1. RESULTS OF BLIND DOPING STUDY USING EPA MOTHERS' MILK EXTRACTS SPIKED BY THE BREHM LABORATORY

Sample Number	Native TCDD Dope Level (ppt)	320/322	Native TCDD Found (ppt) 320	322	Ave
MMVS-5	25	0.84	25	23	24
MMVS-6	5	0.42	3	5	4
MMVS-8	20	0.79	21	21	21
MMVS-9	10	0.50	7	11	9
MMVS-13	5	0.83	5	5	5
MMVS-14	50	0.89	59	52	56
MMVS-15	20	1.05	24	17	21
MMVS-18	10	1.02	11	9	10
MMVS-19	35	0.50	27	42	35
MMVS-21	15	0.48	14	23	19

DETERMINATION OF THERMAL DECOMPOSITION PROPERTIES OF TOXIC ORGANIC WASTES

Judith A. Mescher and Wayne A. Rubey

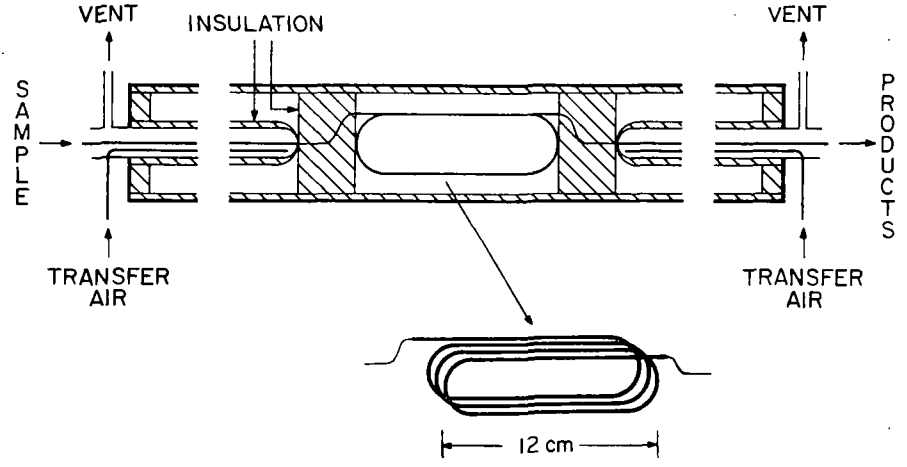
University of Dayton Research Institute

Dayton, Ohio 45469

Information regarding the conditions for the destruction of organic wastes has been obtained using an integrated thermal decomposition - GCMS-COMP system. This System features an in-line thermal destruction unit and adsorbent trap as inlet to a GCMS. The continuity of sample flow from entrance into the thermal reactor through transport into the GCMS makes this instrumentation not only unique, but also contributes to the safe handling of toxic materials in a research laboratory.

The performance of the high temperature reactor is the key to the determination of thermal decomposition properties of toxic organics. As indicated in the following schematic, the reactor is made entirely of narrow-bore quartz tubing which allows rapid transport of gas into and out of the reaction zone. The reactor is enclosed in a high temperature

NARROW - BORE QUARTZ REACTOR



Lindberg furnace (R.T. to 1150°C), and destruction temperatures can be measured precisely with an accuracy of ±2°C throughout the temperature range. Residence time, reactor internal pressure and gaseous environment (oxidative/inert) are all precisely controlled.

The analytical system features high resolution glass capillary columns to provide optimum separation of decomposition products and an LKB2091 GCMS-COMP system for product identity. To date, thermal decomposition profiles have been obtained for selected chlorinated pesticides, PCB isomers, and various industrial process wastes.

This work was supported by U.S. EPA Grant #R805117.

ENVIRONMENTAL APPLICATIONS OF CROSSED-BEAM LC/MS

M. J. McAdams,* C. R. Blakley and M. L. Vestal
The University of Houston

Polar and involatile compounds are often not measured or identified in environmental samples because they are not amenable to the gas chromatographic techniques commonly employed for these analyses. Recent advances in instrumentation and column technology have made high performance liquid chromatography (HPLC) a promising alternative for these difficult analyses; however, the lack of a truly universal detector with sufficient sensitivity is a serious limitation. The mass spectrometer is an obvious potential solution to the HPLC detector problem, and the challenging task of mating liquid chromatography with mass spectrometry is being actively pursued in several laboratories.[1-6]

In our laboratory we have recently developed a new approach to the problem of interfacing a liquid chromatograph with a mass spectrometer. This approach employs laser heating to rapidly vaporize both the solvent and the sample as it emerges from a capillary nozzle and crossed-beam techniques to efficiently transport and ionize the sample while minimizing contact of the sample with solid surfaces. This concept is based partly on the work of Friedman and coworkers[7] which showed that rather involatile samples can be vaporized intact by rapid heating of material deposited on relatively inert surfaces. The crossed-beam LC-MS which we have developed provides either electron impact or chemical ionization mass spectra and may be operated in either positive ion or negative ion modes.

In the original conception of the crossed-beam LC-MS, the laser beam intersected the liquid jet issuing from the capillary nozzle and the liquid evaporated in the very short time required for the liquid jet to cross the laser beam. Original feasibility calculations suggested that this should be possible using the focused output of a 50 watt CO_2 laser at flow rates up to one ml/min of water. However, in our initial experimental tests we experienced difficulty in maintaining stable vaporization with the laser beam intersecting the liquid jet in free space, but if the laser beam were shifted so that the liquid jet nozzle was heated by the laser beam then stable vaporization could be achieved. Furthermore, even though the tip of the nozzle was often operated at red heat, there was little indication that pyrolysis of the sample was occurring during the vaporization process. By operating in this "indirect" heating mode, successful operation of the crossed-beam LC-MS was achieved under both ion-exchange and reversed phase LC conditions for a variety of relatively involatile samples. A description of the apparatus and some of the earlier results are published elsewhere.[8]

An example of the data obtained for a series of polycyclic aromatic hydrocarbons is given in Figure 1. Even though there are several gas chromatographic methods available for the analysis of polycyclic aromatic hydrocarbons, effort is being spent on the development of LC methods for their analysis in water samples.[9] A UV chromatogram and mass chromatograms for the LC/MS analysis of PAH's are given in the figure. Separation of components was obtained using a 25 cm x 4.6 mm Partisil 10-ODS/2 column with 10% water in methanol isocratic at 0.5 ml/min mobile phase.

The present paper is primarily concerned with recent applications of the crossed-beam LC-MS using "indirect" laser heating to analyze samples of environmental interest. The emphasis in this work is placed on analyses of classes of compounds which are difficult to handle quantitatively as trace components in water samples by conventional GC or GC/MS techniques. Classes of compounds studied include phenols, amines, polynuclear aromatics, organic acids, and several herbicides. Present detection limits for these compounds typically correspond to about one nanogram injected into the LC with the mass spectrometer operating under CI conditions scanning at ca. 100 amu/sec. We have obtained EI and positive and negative CI mass spectral data on several representatives of each class of compounds in conjunction with LC separation, generally under reversed phase conditions using methanol-water mixtures as solvents. The EI spectra obtained are in good agreement with library spectra and the CI spectra generally show intense quasi-molecular ions, indicating that pyrolysis is not a serious problem under present operating conditions.

*Present address the Dow Chemical Company, Freeport, TX 77541
This work supported by the National Institute of Health (NIH)

References

1. V. E. Skurat, Russ. J. Phys. Chem. 46 (1972) 570.
2. F. W. McLafferty, R. Knutti, R. Venkataraghavan, P. J. Aprino and B. G. Dawkins, Anal. Chem., 47 (1975) 1503.
3. E. C. Horning, D. I. Carroll, I. Dzidic, S. N. Lin, R. N. Stillwell and J. P. Thenot, J. Chromatgr. 142 (1977) 481-495.
4. P. R. Jones and S. K. Yang, Anal. Chem. 47 (1975) 1000.
5. R. P. W. Scott, C. G. Scott, M. Munroe, and J. Hess, Jr., J. Chromatogr., 99, 395 (1974).
6. W. A. Darl, W. H. McFadden, D. L. Bradford, J. Chrom. Sci. 15, 454 (1977).
7. R. J. Buehler, E. Flanigan, L. J. Green and L. Friedman, J. Amer. Chem. Soc., 96, 3990 (1974).
8. C. R. Blakley, M. J. McAdams, M. L. Vestal, J. Chromatogr., 158 (1978) 261-276.
9. K. Ogan, "Analysis of Consent Decree PAH's in Water", Pittsburgh Conference, March, 1979, 52.

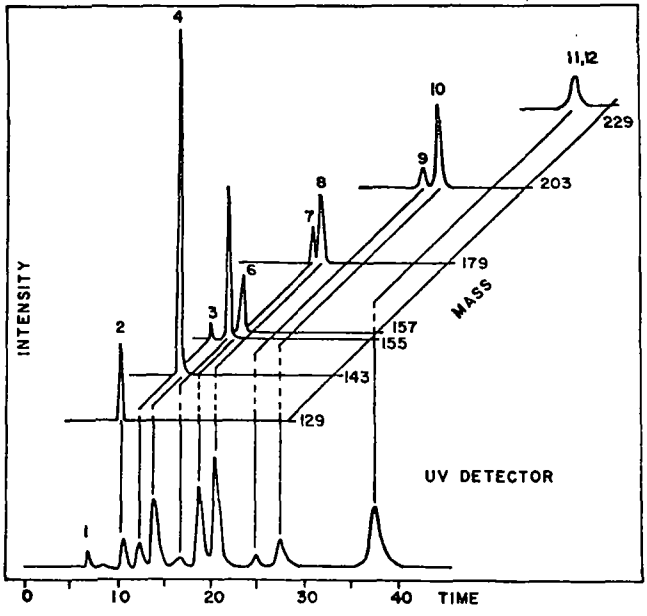


Figure 1 - UV and mass chromatograms are given for a polycyclic aromatic hydrocarbon (PAH) mixture. The LC peaks listed in order are (1) unknown, (2) 0.9 ug naphthalene, (3) an unknown phthalate ester, (4) 4.4 ug 1-methyl and 1.6 ug 2-methylnaphthalene, (5) 1.5 ug acenaphthalene, (6) 2.2 ug dimethylnaphthalene, (7) 0.6 ug phenanthrene, (8) 0.8 ug anthracene, (9) fluoranthene, (10) 0.6 ug pyrine, (11) 0.9 ug chrysene, and (12) 0.9 ug 1,2-benzanthracene.

APPLICATION OF MASS SPECTROMETRY TO ENVIRONMENTAL PROBLEMS. THE STRUCTURE OF AQUATIC HUMIC ACID.

M.-J. Bobenrieth*,+J.R. Hass*, W.-T. Liao+
R.F. Christman+ and F.K. Pfaender+

*Environmental Chemistry Branch
National Institute of Environmental Health Sciences
P.O. Box 12233
Research Triangle Park, North Carolina 27709

+Department of Environmental Science & Engineering
University of North Carolina
Chapel Hill, North Carolina 27514

Introduction

The formation of chlorinated products from aqueous organics during water treatment processes has recently been recognized as a major source of such chemicals in municipal water supplies (1). Naturally occurring materials like humic acid generally account for approximately 80% of the organic carbon dissolved in municipal drinking water supplies. These humics have been found to give low molecular weight chlorination products under typical water treatment plant conditions. Thus, a knowledge of humic acid structure is fundamental to our understanding of halocarbon production in water supplies.

Humic acid is a complex organic molecule which must be degraded before mass spectrometric techniques can be applied. In this paper we report observations resulting from the application of gas chromatography/mass spectrometry (GC/MS) using electron impact (EI) or isobutane positive ion chemical ionization (BPCI) at low and high spectrometer resolution and mass-analyzed ion kinetic energy (MIKE) spectrometry using collision-induced-dissociations (CID) of ions produced by BPCI and direct probe sample introduction.

Gas Chromatography/Mass Spectrometry

Combined GC/MS continues to play a prominent role in trace organic analysis and proved to be useful for this problem. As illustrated by the total ion current (TIC) plot the oxidative degradation products comprise a complex mixture. Preliminary identification of the degradation products was made by a computer assisted comparison of each low resolution EI spectrum with a 25,000 spectrum library. Each spectrum was then interpreted to give a tentative structure. Molecular weight assignments were then confirmed by BPCI. Further support for the structural assignments was then obtained by performing GC/MS at medium resolution using EI. This had two beneficial effects: doublets occurring at low m/z were resolved so that more representative spectra were available for interpretation from complex GC peaks and exact mass measurements were possible by use of an internal reference compound. The resulting elemental compositions increased the reliability of the identifications. When possible, structures are being confirmed by comparative chromatography.

Mass Analyzed Ion Kinetic Energy Spectrometry

The application of CID-MIKE spectrometry in conjunction with direct probe introduction and chemical ionization has been found useful for the analysis of crude mixtures (2,3). Reference spectra from the MH^+ or $(MH\text{-}CH_3OH)^+$ ions from benzene polycarboxylic acid methyl esters were obtained. The major collision-induced reactions can be rationalized in terms of CH_3, CO, CH_3O, CH_3OH and CH_3OCO loss or combinations thereof. The CID-MIKE spectra of the $(MH\text{-}CH_3OH)^+$ ions give a more characteristic fingerprint of the compound than does the EI, CI or CID-MIKE spectrum of the MH^+. As expected, the BPCI spectrum of the humic acid degradation products was to complex to permit deductions about structure. However, the CID-MIKE spectra of appropriate ions are simpler and exhibit losses typical of benzene polycarboxylic acid methyl esters. The m/z 221 spectrum also contains significant ions unexpected on the basis of the reference spectra, indicating the presence of a compound (or compounds) not detected by GC/MS.

The rate of sample analysis for CID-MIKE spectrometry is limited by sample loading and the pump-out time of the direct probe to ca. 2-3 minutes per sample. For a given m/z main beam, actual data acquisition is ca. 15-30 S. This is a considerable time savings compared to the 1-2 hrs required for GC/MS analysis. On the other hand, GC/MS gives information about isomer distribution not readily available by the direct probe CID-MIKE spectrometry technique.

Conclusions

Insomuch as humic acid degradation products constitutes a typical complex sample for trace organic analysis, a few general conclusions may be drawn. GC/EIMS is the most useful single experiment for compound identification. Medium resolution measurements are considerably more powerful than low resolution ones, especially if the reliability of the identification is a major concern. Molecular weight confirmation by BPCI was helpful and justified the second GC/MS analysis. The CID-MIKE spectrometry technique gives a more detailed fingerprint of the compounds studied and is also much faster. This method should be useful for comparing the degradation products of humic substances from different sources, for the presence of particular compounds; also, structural information not available by GC/MS techniques seems to be accessible.

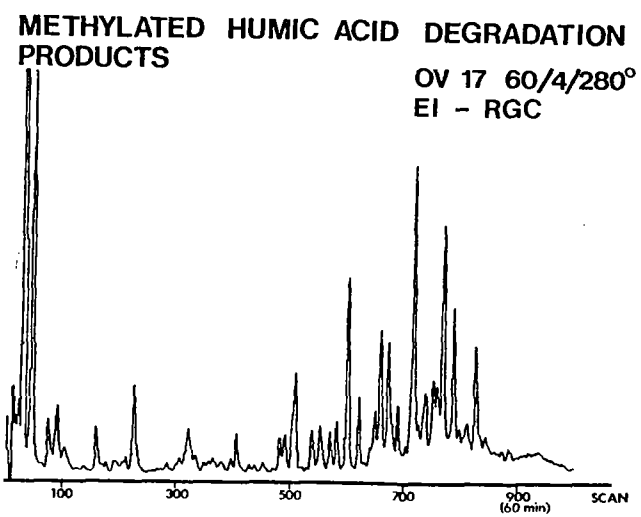
References

1. For a recent review, see R.L. Jolley, H. Gorchev and D.H. Hamilton, eds., "Water Chlorination: Environmental Impact and Health Effects", Vol. 2, Ann Arbor Science Publ., Ann Arbor, Michigan, 1978.

2. R.W. Kondrat, G.A. McClusky and R.G. Cooks, Anal. Chem., 50, 2017 (1978).

3. G.A. McClusky, R.W. Kondrat and R.G. Cooks, J. Am. Chem. Soc., 100, 6045 (1978).

4. R.F. Christman, J.D. Johnson, J.R. Hass, F.K. Pfaender, W.T. Liao, D.L. Norwood and H.J. Alexander, in "Water Chlorination: Environmental Impact and Health Effects"; Vol. 2, R.L. Jolley, H. Gorchev and D.H. Hamilton, eds., Ann Arbor Science Publ., Ann Arbor, Michigan, 1978, p. 15.



RAMP 14

HIGH PRESSURE NEGATIVE ION MASS SPECTRA OF ORGANOMETALLIC COMPOUNDS

K.L. Busch*[+], N.B.H. Henis[+], J.R. Hass* and M.M. Bursey[+]

*Environmental Chemistry Branch
National Institute of Environmental Health Sciences
P.O. Box 12233
Research Triangle Park, North Carolina 27709

[+]Department of Chemistry
University of North Carolina
Chapel Hill, North Carolina 27514

Negative ion mass spectra have been obtained for a variety of organometallic compounds using methane as a moderator gas at a pressure of 1 torr in the source of a chemical ionization mass spectrometer. Porphyrins, dialkyldithiophosphates, and triphenyltin compounds were among those investigated.

Spectra were obtained with a Finnigan 3300 quadrupole mass spectrometer with the appropriate source potentials reversed and a conversion dynode electron multiplier. Sample introduction was by means of the direct probe. Source temperature was held constant at 140°C.

The negative ion mass spectra of porphyrin derivatives contain both $M^{-\cdot}$ and $(M+1)^-$ ions, as shown in Figure 1 for the zinc compound. No other fragments are observed. The spectrum of the porphin derivatives investigated contain an $(M+1)^-$ ion, but no $M^{-\cdot}$. The cadmium derivative spectrum contained an $(LH)^-$ ion, but no others did. The lead derivative spectrum alone contained a metal exchange peak. These spectra are shown in Figures 2 and 3, respectively.

Several nickel dialkyldithiophosphates were investigated. The negative ion mass spectrum of the ethyl derivative, shown in Figure 4, contains only the negative molecular ion and the diethyl dithiophosphate ion. The other compounds of this class behave similarly. The cyclohexyl derivative is prone to decomposition upon heating of the probe.

Nickel and platinum dithioethylene compounds were also studied. Negative molecular ions are observed in the spectra of all compounds. When the ligand is substituted with phenyl or chlorophenyl, a peak for the ligand is observed as well, but such an ion is not produced if the substituent is hydrogen or a methyl group. Figure 5 is the negative ion mass spectrum of the platinum dimethyl compound.

Interest in triphenyltin compounds was initiated by the discovery of triphenyltin hydroxide in samples of polychlorinated biphenyls dumped on North Carolina highways in 1978. This compound is formed from tetraphenyltin, an anti-oxidant added by some manufacturers to transformer fluids manufactured in the 1950's. The spectra of triphenyltin hydroxide and chloride were obtained. Neither contains a peak for the negative molecular ion. In the spectrum of the chloride derivative, shown in Figure 6, ligand exchange produces the base peak corresponding to the diphenylchlorotin ion and further exchange produces the dichlorophenyltin ion. Chloride attachment to form the $(M+35)^-$ ion is also observed.

Within the scope of a limited study involving the nickel and platinum dithioethylene compounds, variation of substituent on the ligand did not affect the response in negative ion analysis. The responses of nickel or platinum compounds are similar.

The sensitivity of these compounds is such that detection of 1 ng of compound can easily be accomplished by selected ion monitoring, and 50-100 ng of compound should be sufficient for a scanning mass spectrum. Detection of 1.4 ng of a dimethyl dithioethylene nickel compound is shown in Figure 7.

In conclusion, negative ion mass spectra of a wide variety of organometallic compounds are characterized by $M^{-\cdot}$, $(M+1)^-$ or ligand ions, although ligand exchange or other ion/molecule reactions can occur. Fragmentation is minimal, and selected ion monitoring of the abundant ions provides a detection limit in the low ng range.

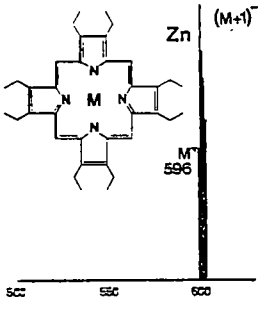


Figure 1

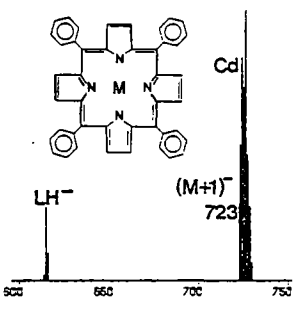


Figure 2

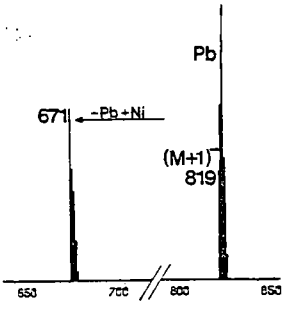


Figure 3

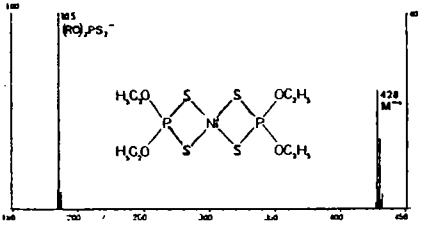


Figure 4

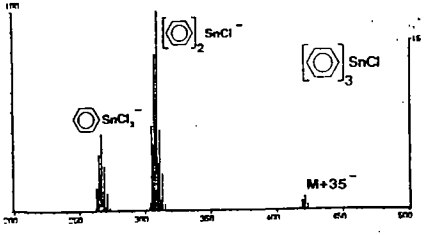


Figure 6

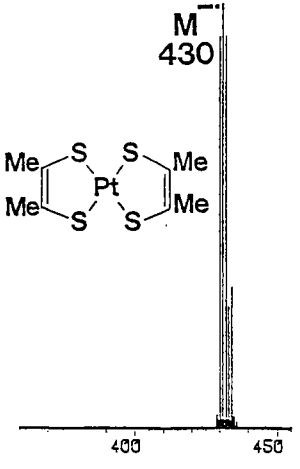


Figure 5

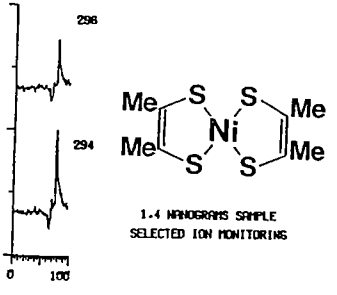


Figure 7

METHANE ENHANCED NEGATIVE ION SPECTRA OF ORGANIC NITRILES

C.E. Parker*, K.L. Busch*[+], D.J. Harvan*, J.R. Hass*, and M.M. Bursey[+]

*Environmental Chemistry Branch
National Institute of Environmental Health Sciences
P.O. Box 12233
Research Triangle Park, North Carolina 27709

[+]Department of Chemistry
University of North Carolina
Chapel Hill, North Carolina 27514

Experimental

Methane enhanced negative ion mass spectra were obtained on a Finnigan 3300 quadrupole mass spectrometer interfaced directly to a Finnigan 9500 gas chromatograph. A 1.6 m glass column packed with 3% OV-17 on 100/200 Gas-Chrom Q was used to elute the sample through a heated inlet line into the source of the mass spectrometer. Methane (Linde, ultra high purity grade) was used as the carrier gas, and its flow through the column was adjusted to give a source pressure of 1 to 2 torr. Modifications to the standard configuration of this mass spectrometer necessary for operation in the negative ion mode have been previously described (1). Data acquisition and reduction were under the control of a Finnigan 6100 data system. All spectra were obtained with the source conditions reproduced as nearly as possible. The source temperature was held constant at 180°C except when intentionally varied.

Results and Discussion

The spectra of twenty-five aliphatic nitriles, benzonitriles, acetonitriles, and aryl-acetonitriles were examined by methane enhanced negative ion mass spectrometry. In general, the spectra of organic nitriles contain intense peaks due to $(M-1)^-$ ions, characteristic ion/molecule reaction products, and few fragmentation products. Ion source temperature has a significant effect on the spectra produced and must be carefully controlled to ensure reproducibility.

For unsubstituted nitriles, the sensitivity of this method is comparable to that of positive ion electron impact methods. Greater sensitivity is possible for those compounds with additional electrophores.

The fragmentation of the negative molecular ion from dichloroacetonitrile was examined by MINDO/3 (2). The program had been modified to accommodate molecules containing both chlorine and nitrogen. Good agreement was found between predicted bond strengths and the observed fragmentation. Calculations indicated that the weakest bonds were the C-Cl and the C-H bonds. The base peak in the methane enhanced negative ion mass spectrum corresponded to the Cl^- ion with a large $(M-1)^-$ ion also present. No CN^- was observed in the spectrum.

Further theoretical and experimental studies were carried out on the $(M-1)^-$ ion from 4-fluorobenzonitrile. Energy levels predicted by MINDO/3 indicate that the ion resulting from the loss of the ortho-H is 2.96 kcal more stable than that resulting from the loss of the meta-H. The 2,6-d_2 derivative of 4-fluorobenzonitrile was synthesized and its spectrum examined. This compound showed the loss of hydrogen and not deuterium, implying loss of the meta-H. Correcting the calculated energy levels for the difference in zero point energies for C-D versus C-H bonds reduces the energy difference to 1.76 kcal, but ortho loss is still predicted over meta loss by MINDO/3.

In order to explain the discrepancy between the predicted and experimental results, an alternative mechanism was postulated. This involved $(OH)^-$ attack on the neutral species followed by H_2O loss, giving the $(M-1)^-$ ion. Presumably the hydroxyl group would attack at the ring carbon with the highest positive charge density. Unfortunately, MINDO/3 calculations still predict $(OH)^-$ attack at the ortho position.

Conclusions

Negative ion mass spectra of organic nitriles contain useful molecular weight information. These compounds also readily form dimers and adduct ions. The spectra show a strong temperature dependence, and this parameter must be carefully controlled to ensure reproducibility.

Two members of this class of compounds were selected to examine the applicability of the MINDO/3 molecular orbital approach to the prediction of the structure and fragmentation reactions of negative ions. For one compound, good agreement was obtained with experimental results, but for the other compound the predictions were shown to be incorrect. This indicates that it would be unwise to use the results of such calculations without experimental confirmation.

References

1. M.D. Friesen, Ph.D. Dissertation, Kansas State University, 1977.

2. R.C. Bingham, M.J.S. Dewar, and D.H. Lo, J. Am. Chem. Soc., 97, 1285 (1975).

PROPOSED APPLICATIONS OF FOURIER TRANSFORM* MASS SPECTROMETRY

M.L. Gross, S. Ghaderi, E. Ledford,
P.S. Kulkarni and C.L. Wilkins

Department of Chemistry
University of Nebraska
Lincoln, Nebraska 68588

Much like Fourier Transform NMR, FT/MS is well suited for investigations of fundamental and applied problems in chemistry. It's chief advantages are the high resolving power, the ability to rapidly acquire time resolved mass spectra, and the capacity to employ chemical ionization techniques at low pressure. In this poster presentation, we discussed results from representative studies of exact mass measurements, sensitivity, and low pressure chemical ionization. The types of reactions in CI which can be employed in FT/MS include conventional systems (CH_5^+, H_3O^+, $C_4H_9^+$, NH_4^+), negative ion abstraction, nucleophilic displacements, and H/D exchange for counting active hydrogens. The spectra are comparable to those obtained by conventional methods. Exact mass measurements have been performed at a resolution of about 1000 with a precision of $\pm$ 3 parts-per-million over a mass range of 18 amu. Samples sizes of 10 ng of cyclohexene are sufficient to obtain full mass scans in a CI mode.

To illustrate the capability of FT/MS for ion chemistry studies, the ion-molecule reactions which occur in a mixture of anisole and 2-propyliodide have been identified using time-resolved measurements and pulsed double resonance.

*This research was supported by Grant No. CHE-77-03964 and by a grant from the Gulf Research Foundation.

TEMPERATURE DEPENDENCE OF MOMENTUM TRANSFER RATE CONSTANTS

Denise C. Parent and Michael T. Bowers
Department of Chemistry, University of Santa Barbara
Santa Barbara, California 93106

We have recently looked at the temperature dependence of the momentum transfer rate constants of several systems, comprising polar and nonpolar neutrals with positive and negative ions. From this temperature dependence we hope to gain some information about the form of the interaction potential.

The momentum transfer rate constants were determined from collisional line-broadening in the drift cell of an ion cyclotron resonance spectrometer.(1) Experimental pressures were in the 10^{-4} to 10^{-2} torr range and the temperature was varied from 170 to 400°C.(2) The reduced mobility Ko is calculated from the momentum transfer rate constant ξ/n using

$$Ko = \frac{273}{760T}\frac{q}{m\xi/n} \qquad (1)$$

where q and m are the ion charge and mass, respectively.

The reduced mobility at a given temperature can be calculated theoretically if the interaction potential is known.(3) Since this is not usually the case, a parametrized form of the potential is assumed and the theory fit to the data by varying the parameters. For these experiments we used an n-6-4 potential given by

$$\epsilon/2[(1 + y)(\frac{r_m}{r})^n - 4y(\frac{r_m}{r})^6 - 3(1 - y)(\frac{r_m}{r})^4] \qquad (2)$$

where ϵ is the well depth, r_m is the potential minimum, n is the degree of steepness of the repulsion and y (which ranges from 0 to 1) is a measure of the relative strengths of the r^{-6} and r^{-4} terms.

A graph of the experimental quantities $\mu^1/_2$Ko versus temperature, where μ is the reduced mass, is compared to a graph of the theoretical quantities $1/T^{*1}/_2\,\Omega^{(1,1)}$ versus T^*. T^* is given by kT/ϵ and $\Omega^{(1,1)}$ is a collision integral dependent on the interaction potential. The comparison gives the four potential parameters ϵ, r_m, y and n when the polarization limit condition is applied, given as

$$3\epsilon r_m^4(1 - y) = q^2\alpha \qquad (3)$$

where α is the neutral polarizability.

The systems investigated are the following: Ar^+, N_2^+, CO^+, CH_2F^+, CF_3^+, CH_5^+ with He and Ne, also CF_3^+ with CF_4, $C_4H_9^+$ with n-C_5H_{12} and Cl^- with He, Ar, N_2, CH_4, CH_3F, CHF_3, CF_4 and NH_3. Most of these systems could be fit only with n equal to 8 (but not equal to 12) and a small value for gamma. The well depths are about 0.5-2 kcal/mole, or weak van der Waals bonding.

The exceptions are CO^+ with He, Cl^- with CH_4 and CF_4, and as expected, Cl^- with CH_3F, CHF_3 and NH_3. For these three polar systems the dipole contribution to the r^{-8} and r^{-4} terms increases the temperature dependence beyond that possible to explain with a nonpolar 8-6-4 potential.

This technique is subject to the following limitations. The theoretical curves vary slowly, which leads to a range of values for the potential parameters ϵ, r_m and y which will fit the data. We were able to cover only a relatively small temperature range (170-400°C). Also there is a relatively large uncertainty associated with the data. Due to these limitations precise determination of the potential parameters is not possible in most cases. Rather, we can find the general features of the potential and determine a range of values for the well depth and potential minimum, and see how these parameters vary as the neutral collision partner is changed.

Ref.

(1) D. P. Ridge and J. L. Beauchamp, J. Chem. Phys. 64, (1976), 2735.

(2) M. T. Bowers, P. V. Neilson, P. R. Kemper and A. G. Wren, Int'l. J. Mass Spectrom Ion Phys. 25, (1977), 103.

(3) E. A. Mason and H. W. Schamp, Jr., Ann. Phys. (New York) 4, (1975), 233.

RAMP18 PROTONATION OF ALKENES; HEATS OF FORMATION OF ALKYL IONS, P. AUSLOOS and S. G. LIAS, National Bureau of Standards, Wash., D. C. 20234

Information about the relative heats of formation of t-$C_4H_9^+$, sec-$C_4H_9^+$, sec-$C_3H_7^+$, c-$C_5H_9^+$, and c-$C_6H_{11}^+$ is derived from measurements of the rate constants of proton transfer from the alkyl ions (AH^+) to selected proton acceptors of known relative proton affinity ($AH^+ + M \rightarrow MH^+ + A$), and from the MH^+ species to the conjugate alkene base (A). It is shown that in cases for which equilibrium constants can not be determined directly because of the occurrence of isomerization or other competing processes, internally consistent estimates of relative PA(A) are obtained in this way. The relative values of $\Delta H(AH^+)$ derived from the results are compared with recent values obtained in threshold experiments. Protonation of 2-butene leads to the formation of t-$C_4H_9^+$ and 2-$C_4H_9^+$. The degree of skeletal rearrangement increases with the lifetime of the collision complex, which in turn depends on the enthalpy change of the proton transfer reaction.

Mobilities of CH_5^+, $C_2H_5^+$, $C_3H_5^+$, and $C_3H_7^+$ Ions in Methane Gas, M. SAPOROSCHENKO, Dept. of Physics and Astronomy, Southern Illinois University, Carbondale, IL 62901

Mobility measurements as a function of E/N (E is the electric field intensity, N is the gas number density) have been obtained for positive ions CH_5^+, $C_2H_5^+$, $C_3H_5^+$, and $C_3H_7^+$ in methane gas using the "four-gauze" electrical shutter method with an electron impact ion source. Measurements were made at 22-31° C gas temperature over a range of E/N from 20 to 280 Td (1 Td=10^{-17} V · cm^2) and in a pressure range for 0.7 to 1.3 torr. The ions have been identified mass spectrometrically simultaneously with the measurements of their mobility. Extrapolation of the low-field measurements to zero yields the values of the mobilities 2.74, 2.65, 2.54, and 2.51 cm^2/ V · sec for CH_5^+, $C_2H_5^+$, $C_3H_5^+$, and $C_3H_7^+$, respectively. It has been observed that the larger ion $C_2H_5^+$ moves faster than the CH_5^+ ion in the range $62 \leq E/N \leq 158$.

RELATIVE PROTON AFFINITIES OF SOME HALOBENZENES AND HALOTOLUENES

By

D. K. Bohme, J. A. Stone, R. S. Stradling, R. S. Mason and K. R. Jennings

Department of Chemistry and Molecular Sciences,
University of Warwick, Coventry, CV4 7AL, U.K.

A pulsed ion source has been designed and constructed for use with an MS50 mass spectrometer in studies of chemical ionization at high pressures (> 1 torr), specifically for measurements of equilibrium and rate constants of ion-molecule reactions at different temperatures. The ionization region, which is housed in a gold-plated copper block, is maintained field-free to allow thermal ion energy distributions to be established at the pressures employed.

The principle of operation of the pulsed source is similar to that of other high pressure sources (1). Reactant and product ion intensities are measured at reaction times up to 5.6 msec. CH_4 is used as the buffer gas and either CCl_4 or SF_6 is added to quench electrons and so decrease the rate of diffusion. Gases and volatile liquids are premixed to contain *ca.* 0.2% of the electron quencher and *ca.* 0.1% of the sample compounds under investigation. Ionization is initiated by 400 eV electrons.

The first measurements with this source were restricted to proton transfer equilibria involving halogenated benzenes and toluenes. Equilibrium constants for the halotoluenes were measured at a single temperature (370 K) at pressures in the range 1 to 4 torr and for concentration ratios varying by as much as a factor of $\sim$ 80. The resulting standard free energy changes are given in Table 1 in the form of a ladder of proton affinities. ΔG° may be assumed to be approximately equal to ΔH° for the reactions

$$CH_3C_6H_4XH^+ + CH_3C_6H_4Y \rightleftarrows CH_3C_6H_4YH^+ + CH_3C_6H_4X$$

where X and Y may be F, Cl, or Br. The changes in proton affinity caused by substitution at the various ring positions are in keeping with classical arguments concerning the influence of the halogen substituent on the charge distribution on the benzene ring (2). The gaps between the meta and ortho, and ortho and para isomers for a specific halogenated toluene decrease considerably when the substituent changes from F to Cl to Br. This may be due to an increased degree of protonation at the halogen position rather than protonation of the ring.

The equilibrium constant was measured as a function of temperature in the range from *ca.* 300 to 600 K for the reactions

$$C_6H_7^+ + C_6H_5F \rightleftarrows C_6H_5FH^+ + C_6H_6$$

and

$$C_6H_5ClH^+ + C_6H_5F \rightleftarrows C_6H_5FH^+ + C_6H_5Cl \ .$$

The results are consistent with the previous high pressure source measurements of Kebarle (3) but disagree with the ICR measurements reported recently by Hartman and Lias (2). The discord with the ICR results had introduced questions regarding the viability of the 'intermolecular entropy' change which has been invoked by Lias and co-workers (2,4) in the estimation of entropy changes for gas-phase ion-molecule equilibria. The measurements will be extended to other systems to provide further insight.

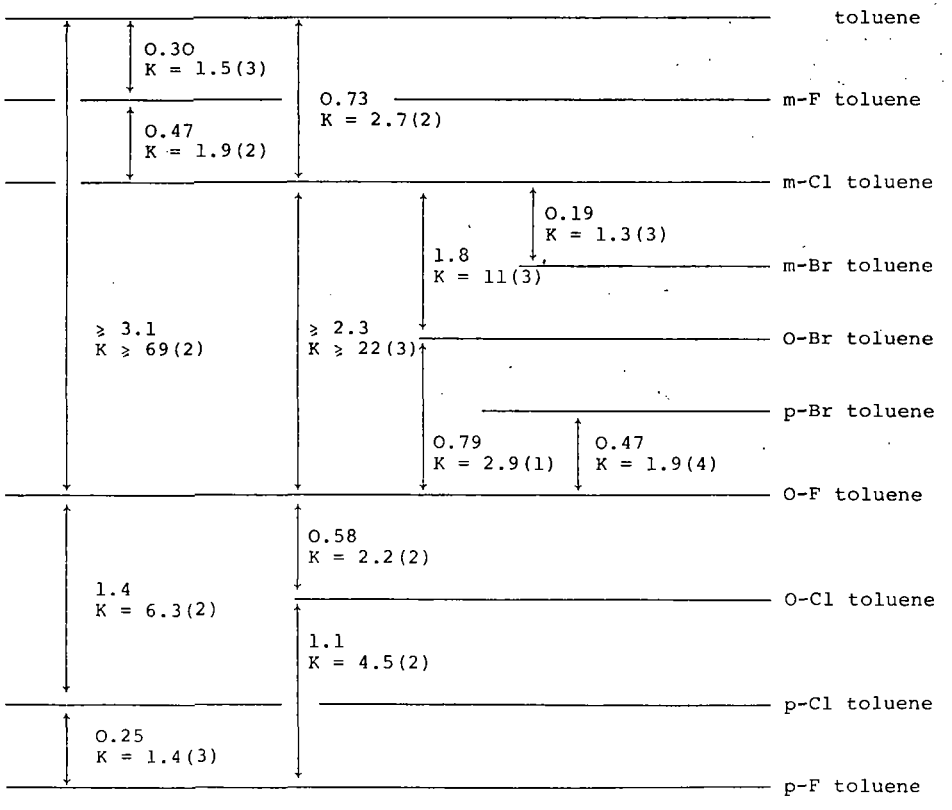
(1) P. Kebarle, in 'Interactions between Ions and Molecules', P. Ausloos (Ed.) Plenum Press, New York, 1975

(2) K. G. Hartman and S. G. Lias, *Int. J. Mass Spectrom. Ion Phys.*, 28, 213 (1978)

(3) Y. K. Lau and P. Kebarle, *J. Am. Chem. Soc.*, 98, 7452 (1976)

(4) S. G. Lias and P. Ausloos, *J. Am. Chem. Soc.*, 99, 4831 (1977)

TABLE 1: Proton affinity ladder showing values of ΔG°_{370} (in kcal mole^{-1}) for the halotoluenes along with the measured equilibrium constants. The number of measurements at different concentration ratios is given in parentheses.



DETERMINATION OF PROTON AFFINITIES BY REACTANT ION MONITORING RAMP21

Vinh Thi Tran and Burnaby Munson, Department of Chemistry, University of Delaware, Newark, DE 19711.

The proton affinities of a series of organometallic compounds were determined by Reactant Ion Monitoring in GC/CIMS.

The sample, M, was introduced into the source of the mass spectrometer with a direct insertion probe, vaporized, and protonated by the reactant ion in isobutane, $t\text{-}C_4H_9^+$, or by the reactant ions in CH_4, CH_5^+ and $C_2H_5^+$:

$$M + t\text{-}C_4H_9^+ \longrightarrow MH^+ + i\text{-}C_4H_8 \qquad (1)$$

A mixture of amines of known proton affinities was separated on a gas chromatographic column and allowed to flow into the source of the mass spectrometer. The ion current of the $(M+H)^+$ ion was monitored during the GC separation.

If the proton affinity of the eluting amine, B, is greater than that of the sample, the decrease of the intensity of the $(M+H)^+$ ion is observed due to the fast proton transfer process.

$$MH^+ + B \longrightarrow BH^+ + M \qquad (2)$$

However, if the proton affinity of B, the amine that is eluting from the chromatographic column, is less than the proton affinity of the sample, M, no significant change is observed in the ion current of MH^+.

In the experiment of Fig. 1, diethylamine, n-butylamine, di-iso-propylamine, and triethylamine are separated by the GC and mixed in the source of the MS with CH_4 containing a small amount of trimethylamine. Rapid proton transfer occurs from the remaining $C_2H_5^+$ to all of these amines as indicated by the trace of ion current for $(CH_3)_3NH^+$, however, shows rapid proton transfer from $(CH_3)_3NH^+$ to di-isopropylamine and to triethylamine, slow proton transfer to diethylamine and no reaction with n-butylamine. Consequently, we say that $216 < PA[(CH_3)_3N] < 223$ kcal/mole; the accepted literature value is 222.1 kcal. Similar observations can be made about $PA(C_2H_5NH_2)$ from the data of Fig. 2 and related experiments.

The proton affinities of triphenyl compounds of group Va were determined:

$PA(2\text{-}ClC_5H_4N) < PA(\emptyset_3N) < PA(n\text{-}PrNH_2)$; $PA(\emptyset_3N) \cong 214 \pm 2$ kcal/mole

$PA[(iPr)_2NH] < PA(\emptyset_3P) < PA(Et_3N)$; $PA(\emptyset_3P) \cong 228 \pm 1$ kcal/mole

$PA(2\text{-}ClC_5H_4N) < PA(\emptyset_3As) < PA(nPr\ NH_2)$; $PA(\emptyset_3As) \cong 214 \pm 2$ kcal/mole

$PA(i\text{-}C_4H_8) < PA(\emptyset_3Sb) < PA(4F\emptyset NH_2)$; $PA(\emptyset_3Sb) \cong 200 \pm 6$ kcal/mole.

The proton affinities of a series of phenylphosphine oxides, $R_1R_2\emptyset PO$ (R_1 = Me, i-Pr, t-Bu, $\emptyset$; R_2 = Me, $\emptyset$) were determined to be the same within our experimental precision:

$PA(4ClC_5H_4N) < PA(R_1R_2\emptyset PO) < PA(nPr\ NH_2)$; $PA(R_1R_2\emptyset PO) = 214 \pm 2$ kcal/mole.

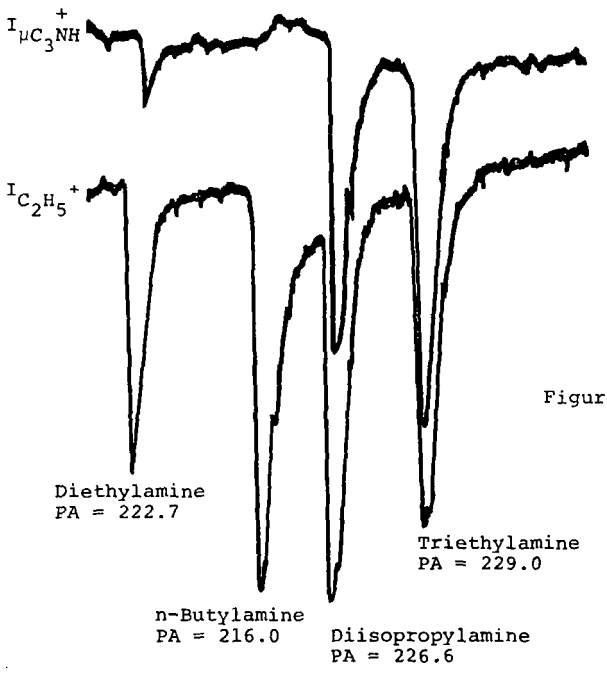


Figure 1

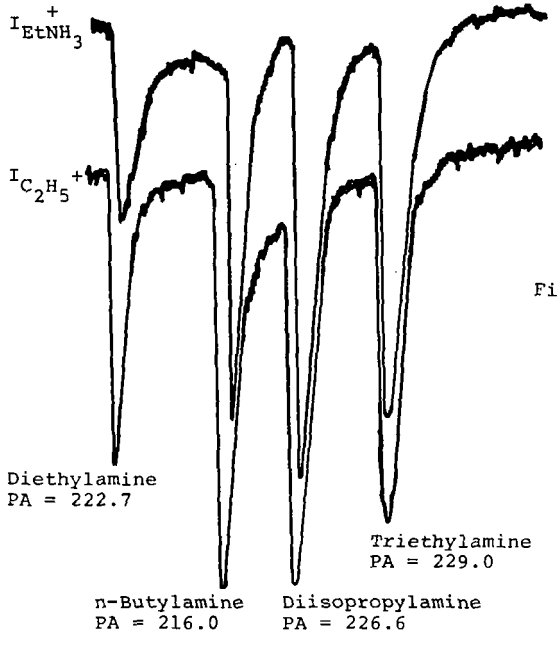


Figure 2

NEGATIVE ION CHEMISTRY OF THE VINYL GROUP

J.E.Bartmess and R.L.Hays
Department of Chemistry
Indiana University
Bloomington, IN 47405

Addition reactions of the type $A^- + B \rightarrow AB^-$ are not usually observed at low pressures in the gas phase since there is no solvent to carry away any excess energy deposited in the product. We have thus investigated several common solution addition reactions by ion cyclotron resonance spectrometry, to determine their alternate reactivities in the gas phase. Methoxide from methyl nitrite does not add to acrylonitrile in the pulsed ICR at 10^{-6} Torr, but deprotonates it to give a stable M-1 anion. Acrylonitrile, measured relative to known acids[1], is 2 kcal/mole more acidic than its saturated analog, propionitrile, consistent with sp carbon in the rehybridized anion being more electronegative than sp^2. Acrolein also gives an M-1 with methoxide, but the major peak is M+1 from hydride transfer. Nitroethylene gives a small M-1 and mostly radical anion.

Reaction of these vinyl compounds with monosolvated methoxide obtain via the Riveros reaction[2] (1) now provides a pathway for stabilization of the exoergonic addition product and M+31 ions are seen:

$$MeO^- + HCOOMe \longrightarrow MeO^- \cdots HOMe + CO^* \qquad (1)$$

$$MeO^- \cdots HOMe + CH_2{=}CHCN \longrightarrow MeOCH_2CHCN^- + MeOH \qquad (2)$$

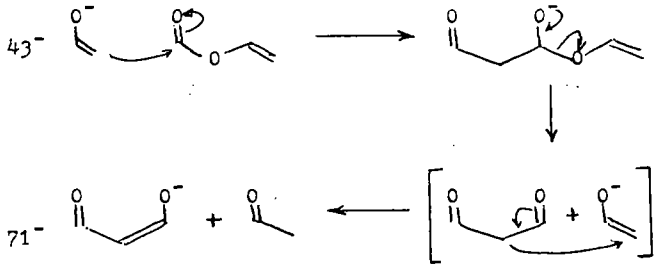
It is the first molecule of solvent which changes the mechanism from a "gas phase" to a "solution" one; futher solvation may change the size and rates but the qualitative effects are all in the first solvent molecule.

A true Michael addition requires a carbanionic nucleophile. We added acetaldehyde to the mixture and saw exchange with the solvated methoxide to form solvated enolate in reaction (3) but only a trace

$$MeO^- \cdots HOMe + CH_3CHO \longrightarrow MeOH \cdots {}^-OCH{=}CH_2 + MeOH \qquad (3)$$

of the additionproduct with acrylonitrile was seen. This M+43 anion is a quaternary ion; the time window in the ICR is not long enough for appreciable amounts of it to form. An attempt to produce it via a direct Riveros reaction of methoxide with vinyl formate gave only the unclustered enolate 43^-. We believe for thermochemical reasons[3] that the solvated enonalte forms but breaks up due to excess energy being present. At long times the enolate reacts with vinyl formate to give 71^-. This is the M-1 of vinyl formate but based on known substituent effects on anion stability we do not believe that this is a deprotonation product of the formate.

This 71^- is rather explicable in terms of a gas phase Claisen condensation:



Studies with other esters to confirm this structure indicate that the condensation goes for enolate attack on CH_3COY only if YH is more acidic than neopentyl alcohol (step 2 exoergonic) and less acidic than the β-diketo structure formed(step 3 exoergonic). We emphasize that free energies, not enthalpies, must be used in the thermochemical analysis of addition reactions such as these since entropy effects are not negigible.

References

(1) J.E.Bartmess andR.T.McIver,Jr., "The Gas Phase Acidity Scale" in "Gas Phase Ion Chemistry", V.2, M.T.Bowers, Ed., Academic Press, 1979

(2) L.K.Blair, P.Isolani, and J.M.Riveros, J.Am.Chem.Soc.,95, 1057 (1973)

(3) J.E.Bartmess and R.L.Hays, in preparation

ION-MOLECULE REACTIONS OF ALKYNES

C. Lifshitz, S. Gefen, Y. Gleitman and U. Shainok
Department of Physical Chemistry,
The Hebrew University of Jerusalem,
Israel

Relatively little work has been done on ion-molecule reactions of alkynes other than acetylene itself[1]. We have recently studied ion-molecule reactions in a series of alkynes and some of their isomers, including propyne, allene, 1-butyne and hexadiyne. These were induced by photon or electron impact. A medium-pressure (10^{-3} to 10^{-1} torr) photoionization mass spectrometer was employed to study mass spectra as a function of pressure. Trapped ion mass spectrometry (TIMS) was employed to study mass spectra as a function of time. Typical results for propyne and butyne are shown in Figs. 1 and 2, respectively. The results of Fig. 1 were obtained at a low ionizing electron energy of about 13 eV. The data of Fig. 2 were obtained with the Kr resonance lines at 10.03 and 10.63 eV. The major reactions in each system are proton transfer from the parent ion and condensation followed by dissociation. Results may be compared with previous medium pressure electron impact[2], and ICR[3] data. A suggested formation route for the tertiary ion $C_7H_7^+$ (tropylium?) in propyne is

$$C_6H_7^+ + C_3H_4 \rightarrow C_7H_7^+ + C_2H_4 \qquad \Delta H \leq -25.2 \text{ kcal/mole}$$

Rate coefficients were determined for the disappearance of reactant ions and agreement with previous data, where available, is very good.

REFERENCES

1. C. Lifshitz and A. Mandelbaum, "Mass Spectrometry of Acetylenes", Chapter 6 in 'The Chemistry of the Carbon-Carbon Triple Bond', Saul Patai editor, John Wiley & Sons, 1978.

2. J.J. Myher and A.G. Harrison, J. Phys. Chem. 72, 1905 (1968).

3. M.T. Bowers, D.D. Elleman, R.M. O'Malley and K.R. Jennings, J. Phys. Chem. 74, 2583 (1970).

Reaction schemes

Propyne

$C_3H_4^+ + C_3H_4 \rightarrow C_3H_5^+ + C_3H_3$ proton transfer

$\rightarrow [C_6H_8^+]$ condensation

↓ major dissociation channel

$C_6H_7^+ + H$

1-Butyne

$C_4H_6^+ + C_4H_6 \rightarrow C_4H_7^+ + C_4H_5$ proton transfer

$\rightarrow [C_8H_{12}^+]$ condensation

↓ major dissociation channel

$C_7H_9^+ + CH_3$

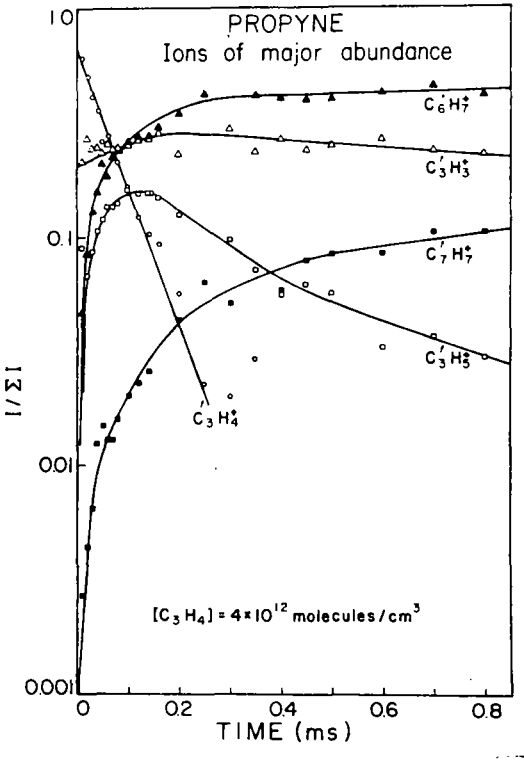


Fig. 1 Trapped-Ion Mass Spectrometry; Ion-intensities vs. time, propyne.

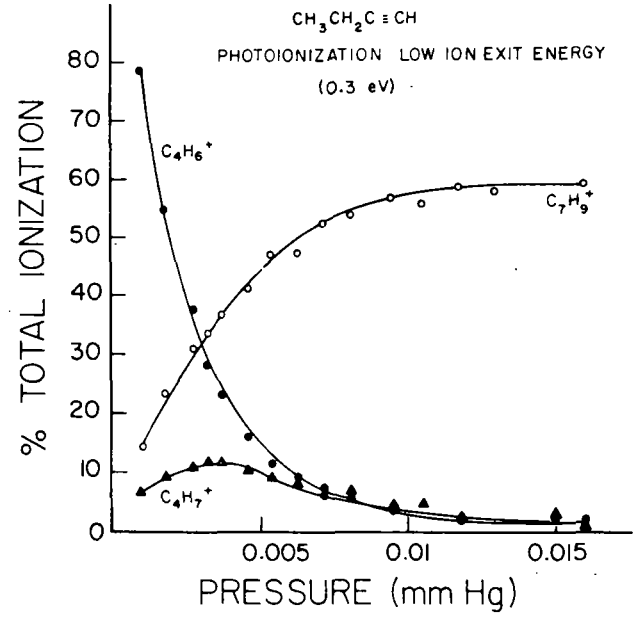


Fig. 2 Photoionization Mass Spectrometry; Ion-intensities vs. pressure, 1-butyne.

ON THE BEHAVIOR OF VIBRATIONALLY-EXCITED MOLECULES

R. A. Marcus
Arthur Amos Noyes Laboratory of Chemical Physics
California Institute of Technology,* Pasadena, California 91125

In the present lecture several topics on the behavior of vibrationally-excited molecules are considered. The first is the translational energy distribution of products of molecular beam reactions proceeding via molecular complexes. The second is the behavior of vibrationally-excited molecules inferred from recent quantum, classical and semiclassical theoretical studies--a largely statistical behavior at high vibrational energies and a nonstatistical one at low energies.

The translational energy distribution of products of bimolecular reactions involving intermediate complexes, such as

$$F + CCl_2 = CH_2 \xrightarrow{\alpha} FCCl_2 - \dot{C}H_2 \xrightarrow{\beta} Cl + FCCl = CH_2 \qquad (1)$$

$$F + C(CH_3)_2 = CH_2 \xrightarrow{\alpha} FC(CH_3)_2 - \dot{C}H_2 \xrightarrow{\beta} CH_3 + FCCH_3 = CH_2 \quad , \qquad (2)$$

depends on (a) the energy distribution in the transition state of step β in these reactions, and on (b) subsequent coupling, in any, of the internal modes of motion to the translational motion of the separating products in step β. When that coupling is negligible, the energy distribution of the products can readily be related to that of the transition state.[1] Since RRKM theory attempts to describe the energy distribution in the transition state, it can then be tested by measurements of the energy distribution of reaction products. Some information on the coupling in (b) is obtained from the steric factor of the reaction for the reverse of step β. A steric factor of unity implies a loose transition state and so no such coupling. Probably the steric factors of (1) and of (2) are of the order of unity and 10^{-3}, respectively. Data on (1) agreed well with the theoretical (e.g., RRKM) predictions[2] while (2) required a fuller analysis of the coupling effects in (b).[3] One treatment, which assumes the reverse of (2) to be translationally rather than vibrationally "driven", was given in Ref. 3.

Some examples of classical mechanical trajectory calculations for a system of anharmonically coupled oscillators are described next. For the Hamiltonian

$$H = \tfrac{1}{2}(p_x^2 + p_y^2 + \omega_x^2 x^2 + \omega_y^2 y^2) + \lambda x(y^2 + \eta x^2) \quad , \qquad (3)$$

the classical mechanical equations of motion for coordinates x and y and for momenta p_x and p_y have been integrated numerically on a computer to yield these variables as a function of time. A typical trajectory is given in Fig. 1 for the case of incommensurable ω_x and ω_y.[4]

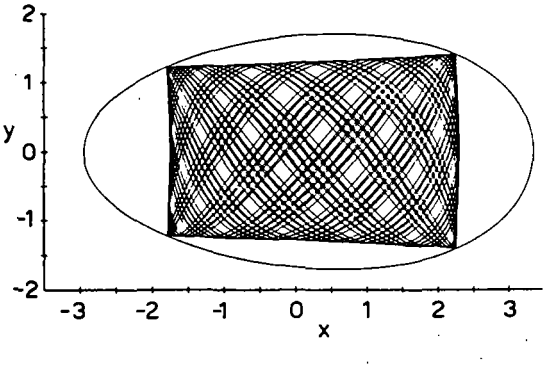


Fig. 1. A trajectory for Hamiltonian (1) with ω_x and ω_y incommensurable. The oval is the place where the potential energy equals the total energy E.

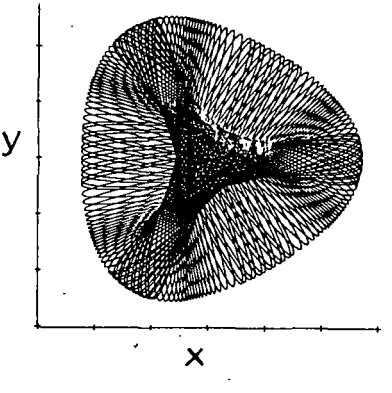


Fig. 2. As in Fig. 1 but $\omega_x = \omega_y$.

One sees from Fig. 1 that not all of the energetically accessible configuration space is occupied by the trajectory. In the four-dimensional phase space (x, y, p_x, p_y) at a given energy E, the instantaneous value of p_y is determined, apart from sign, by the instantaneous value of x, y, and p_x of the trajectory, by energy conservation. Thus, the system moves on a three-dimensional surface in this phase space. However, for quasi-periodic trajectories, such as that in Fig. 1, it moves in a more restricted way--on a two-dimensional surface! It winds around a torus (doughnut), ultimately covering it uniformly when $\omega_x \neq \omega_y$.[5] A projection of the torus onto the (x, y) plane yields Fig. 1. One can plot p_x versus x each time the trajectory in Fig. 1 crosses the plane $y = 0$, with $p_y > 0$, as in Fig. 4 of Ref. 4. By calculating the area $\oint p_x\, dx$ and setting it equal to

$$\oint p_x\, dx = (n_x + \tfrac{1}{2})h \quad , \tag{4}$$

where n_x is an integer, and doing the same for a p_y vs. y plot, composed of points noted each time the trajectory crosses the $x = 0$ axis, with, say, $p_x > 0$,

$$\oint p_y\, dy = (n_y + \tfrac{1}{2})h \quad , \tag{5}$$

one can "quantize" the trajectory, thereby making use of a semiclassical theory bridging classical and quantum mechanics.[4] The initial conditions of the trajectory, including the total energy E, are adjusted until the n_x and n_y determined by (4) and (5) are integers. The energy eigenvalues calculated in this way agree well with the quantum mechanical eigenvalues.[4]

Related remarks apply to the cases where ω_x and ω_y are commensurable, for example 1:1 or 2:1.[6,7] An example of the 1:1 case is given in Fig. 2.[6] One now has extensive energy exchange between the x and y coordinates, but the motion is still quasi-periodic rather than statistical: One again has simple patterns in the momentum versus coordinate plots, and eigenvalues can again be calculated reasonably accurately using curvilinear analogs of Eqs. (4) and (5).[6] Indeed, at low energies for these and other systems, one typically has this nonstatistical behavior of the vibrational motion of the molecules ("KAM" theorem).[5]

According to the semiclassical theory the vibrational wavefunction should be large (but oscillatory) in the region occupied by the trajectories, e.g., in Figs. 1 and 2. This expectation was verified by a large basis set variational calculation of the wavefunction.[7]

The spectral lines were also calculated from trajectories in this "quasi-periodic" regime (defined in the standard way as a Fourier transform of the autocorrelation function of a coordinate) and suitable semiclassical analysis.[8] They yielded a spectrum composed of a few lines, and these agreed well with the quantum mechanically calculated lines.[8]

At high energies the vibrationally-excited molecule behaves very differently. The trajectory now tends to occupy all of the energetically-accessible region as in Fig. 3.

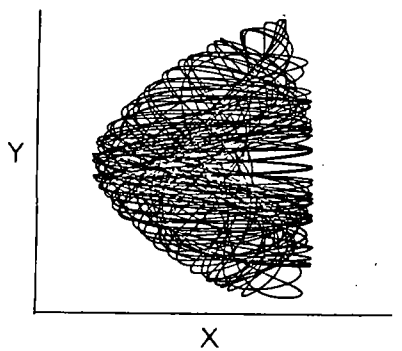


Fig. 3. As in Fig. 1 but for a high energy trajectory (statistical regime).

The p_x vs. x plot at $y = 0$ and the p_y vs. y plot at $x = 0$ now resemble a shotgun pattern,[5,7] and so no area can be calculated for Eq. (4) or (5). Similarly, the quantum mechanical wavefunction tends to occupy the energetically accessible space;[7] the classical

mechanical spectrum now contains many lines, and the quantum mechanical spectrum also contains various lines, fewer than those in the classical spectrum but in the same region as the classical lines.[9]

In the high energy ("statistical") regime each quantum state thus behaves as though it tries to occupy all of the relevant phase space and so a theory such as RRKM would be valid under such conditions. At low enough conditions the reverse is true and a different, more dynamical approach is required. The energy region where the statistical behavior sets in is given by Chirikov's theory of overlapping internal resonances:[10] The system can oscillate between two "modes" in a resonance, and continue to behave in a nonstatistical fashion, but when there are many overlapping resonances, it moves from one mode to many other modes and ultimately, for a sufficient number of overlapping resonances, occupies all of the energetically accessible phase space.

An internal resonance results in a slow energy exchange superimposed on the natural fast oscillations, and so contributes additional lines, displaced from the main frequencies by an amount equal to the frequency of this transfer. When there are many resonances, one would expect, on this basis, to have numerous lines, as observed. Thus, this observed result of Refs. 8 and 11 offers support for Chirikov's theory. Averaging over many trajectories converts the line classical spectrum in this statistical case to a continuous curve.

The semiclassical wavefunction for the quasi-periodic bound state systems can be written as[12]

$$\psi \doteq \sum_{b} A \exp iS/\hbar \tag{6}$$

where A is determined from S by normalization (the Van Vleck determinant), S is $\int(p_x\,dx + p_y\,dy)$ and the sum b is over all four branches of S corresponding to the four possible combinations of signs of p_x and p_y, and is such that the classical variables of the trajectory producing S correspond to the specified integer values of n_x and n_y in Eqs. (4) and (5). (A fuller discussion is given in Refs. 12, 6, and 7.)

In the statistical regime the semiclassical wavefunction is not yet known, since the $\oint p\,dq$ integrals no longer rigorously exist under these conditions. One possibility, a rather approximate one, is that ψ now includes contributions from all zeroth order sets of integers n consistent with the given energy E (say, N sets):

$$\psi_E \cong \sum_n a_n \psi_n \ , \qquad |a_n| \cong 1/\sqrt{N} \tag{7}$$

where each ψ_n is of the form in (6) and the sum is over all sets of integers n for that E, within some uncertainty δE related to the rate of modal energy exchange between the ψ_n's. Because of the large number of n's contributing, one expects destructive interference of cross-terms in computing averages with this ψ_E. (This interference would occur, for example, when there is a random distribution of signs of the a_n's subject to the constraint imposed by orthogonality of the N ψ_E's in the $(E, E + \delta E)$ range.) The average of any function f in such a state is then

$$\int \psi_E^* f \psi_E \, dq \cong \frac{1}{N} \sum_n \int \psi_n^* f \psi_n \, dq \tag{8}$$

where dq denotes the volume element in coordinate space. One can show, when the semiclassical expression for ψ_n in Eq. (6) is introduced, that this average effectively equals the microcanonical average:

$$\int \psi_E^* f \psi_E \, dq \cong \int f \, dq dp \, \delta(E - H(q, p)) / \int dq dp \, \delta(E - H) \ . \tag{9}$$

Here, E is the energy eigenvalue of the exact wavefunction ψ_E. Eq. (9) can be, but has not yet been, tested by numerical comparison of both sides of the equation for various f's. δ is the Dirac delta function, ensuring a microanonical average.

Related remarks may apply to the computation of off-diagonal matrix elements such as those involved in the calculation of spectra, e.g., for a spectral line of frequency $\nu = (E' - E)/h$, one calculates $\left|\int \psi_{E'}^* x \psi_E \, dq\right|^2$, which would become $\Sigma \left|\int \psi_m(E') \, x \, \psi_n(E) \, dq\right|^2 / N(E)N(E')$, with Σ over m and n, when cross-terms are neglected. There are fewer lines in the quantum spectrum in the statistical case than in the classical spectrum,[9] perhaps because of the restriction in the former case on the allowed n's (integers) and not on the latter. Thereby, there are fewer resonances between the different modes in the quantum case and so a smaller number of lines.

In summary, we believe that a quantum state in the statistical regime already has statistical properties, with the excitation distributed among many zeroth-order modes of vibration, and RRKM behavior is then anticipated. Further calculations will test this possibility, e. g., via testing Eq. (9). At low enough energies ("quasi-periodic" regime) a quite different, highly nonstatistical behavior prevails.

References:

* Supported in part by the National Science Foundation.

1. S. A. Safron, N. D. Weinstein, D. R. Herschbach, and J. C. Tully, Chem. Phys. Lett., 12, 564 (1972).
2. Y. T. Lee, et al., cited in Ref. 3 of J. Chem. Phys., 62, 1372 (1975).
3. R. A. Marcus, J. Chem. Phys., 62, 1372 (1975); G. Worry and R. A. Marcus, ibid., 67, 1636 (1977).
4. D. W. Noid and R. A. Marcus, J. Chem. Phys., 62, 2119 (1975).
5. E. g., J. Ford, in "Fundamental Problems in Statistical Mechanics", E. D. G. Cohen, ed. (North Holland, Amsterdam, 1975), Vol. I.
6. D. W. Noid and R. A. Marcus, J. Chem. Phys., 67, 559 (1977).
7. D. W. Noid, M. L. Koszykowski, and R. A. Marcus, J. Chem. Phys. (in press).
8. D. W. Noid, M. L. Koszykowski, and R. A. Marcus, J. Chem. Phys., 67, 404 (1977).
9. M. L. Koszykowski, Ph. D. Thesis, University of Illinois, April 1978, p. 71.
10. E. g., G. M. Zaslavskii and B. V. Chirikov, Sov. Phys. Usp. Engl. Transl., 14, 549 (1972).
11. R. A. Marcus, D. W. Noid, and M. L. Koszykowski, in "Stochastic Behavior in Classical and Quantum Hamiltonian Systems, Volta Memorial Conference, Como, 1977" G. Casati and J. Ford, eds., Lecture Notes in Physics, Vol. 93 (Springer Verlag, New York, 1978/79), p. 283.
12. J. B. Keller, Ann. Phys. (N. Y.), 4, 180 (1958); R. A. Marcus, Faraday Disc. Chem. Soc., 55, 9 (1973). Note presence of $\pi/2$'s in exponents in these papers.

CLASSICAL TRAJECTORY STUDIES OF UNIMOLECULAR DYNAMICS

William L. Hase, Department of Chemistry
Wayne State University, Detroit, MI 48202

There are many important questions which exist concerning the dynamics of unimolecular reactions. The purpose of this paper is to outline these questions and to survey the role classical trajectory calculations have played in answering them. This survey will be restricted to polyatomic unimolecular systems; i.e., those that contain four or more atoms. A discussion of the methodology of unimolecular classical trajectory calculations will be given. Finally, recent trajectory results for chloroacetylene and ethyl radical dissociation will be presented.

A convenient means of discussing a unimolecular reaction is to divide the molecular phase space into three parts: (1) the region which encloses the internal states of the excited molecule XY*; (2) the dividing surface or region which separates the XY* region of the molecular phase from the remaining regions; and (3) the region of exit-channel coupling which occurs as the system passes the dividing surface and separates to products X and Y.

Molecules are classified as intrinsically RRKM if the rate of vibrational energy redistribution within XY* is more rapid than the unimolecular dissociation rate.[1] There is much interest in determining which molecules are intrinsically non-RRKM. One would also like to know the rates of intramolecular vibrational energy redistribution and to know for which vibrational degrees of freedom is intramolecular vibrational energy redistribution the slowest.

An assumption of the RRKM and activated complex theories is that there is a dividing surface which separates the reactant and product regions of phase space and that a trajectory crosses this dividing surface only once. It is also assumed that there is a statistical distribution of energy at the dividing surface. The validity of these assumptions is currently not known. Nor is the relationship between an energy distribution at a dividing surface and a unimolecular lifetime clearly understood. Finally, little is known about exit-channel coupling effects. This coupling may significantly alter product energy distributions from their forms at the dividing surface.

Classical trajectory calculations yield the type of information required to answer these questions. A trajectory study can be divided into four major parts: (1) Monte Carlo selection of initial states; (2) derivation of the potential energy surface; (3) integration of the classical equations of motion and (4) collection and analysis of the trajectory results. The trajectory study may be viewed as either a model or a realistic type, depending upon the potential energy surface used in the calculations. The Monte Carlo technique used for selection of initial states is determined by the type of experimental condition that is being simulated. To date there have been five different unimolecular decomposition trajectory studies of molecules consisting of four or more atoms. These five molecules are CH_3NC,[1] (NaBrKCl) complex,[2] H-C≡C-Cl,[3] $CD_3Cl(H)$,[4] and C_2H_6.[5]

Between 200 and 135 kcal/mole we have found H-C≡C-Cl decomposition to be an intrinsically RRKM process.[3] A summary of the overall intramolecular vibrational energy relaxation rates deduced from the trajectory calculations is given in Table I. An analysis of energy transfer from excited internal coordinates shows that the C-H stretching coordinate is the most poorly coupled mode. The H-C≡C-Cl trajectory calculations have recently been extended to study the relationship between unimolecular lifetime and relative translational energy distributions. The results are shown in Fig. 1. The total energy is 175 kcal/mole with the "HCC modes" initially excited. As expected, the lifetime distribution for H-C bond rupture differs significantly from the RRKM prediction. However, the relative H+C≡C-Cl translational energy distributions for trajectories that dissociate in the 0-1.5 x 10^{-13} sec. range and in the 1.5-4.5 x 10^{-13} sec. range are both in agreement with the RRKM theory prediction. From this

result, one may deduce that RRKM translational energy distributions do not necessarily imply RRKM lifetimes.

To answer questions raised about the dynamics of alkyl radical decompositions,[6] we have undertaken a trajectory study of the reaction $C_2H_5 \rightarrow H+C_2H_4$. An analytic form for the potential energy surface was derived from ab initio, thermodynamic and spectroscopic information.[7] Here, results are presented for the decomposition of randomly excited C_2H_5 at total energies of 150 and 100 kcal/mole. As shown in Fig. 2 at 100 kcal/mole C_2H_5 dissociation to $H+C_2H_4$ is predicted to be intrinsically non-RRKM. Relative $H-C_2H_4$ translational energy distributions are shown in Fig. 3. The relative translational energy distributions at the exit-channel barrier are in excellent agreement with the RRKM predictions. However, exit-channel coupling effects broaden the translational energy distributions and shifts the final distributions to higher values. The $\Delta E_{rel} = E_{rel}(\text{barrier}) - E_{rel}(\text{final})$ distributions illustrate the complexity of the exit-channel coupling. The E_{rel}(final) distributions are similar to those observed in the $F+C_2H_4 \rightarrow C_2H_4F \rightarrow H+C_2H_3F$ molecular beam study.[6]

TABLE I. OVERALL INTRAMOLECULAR RELAXATION RATES WITHIN VIBRATIONALLY EXCITED H-C≡C-Cl

Energy (kcal/mole)	Relaxation Rates (sec^{-1})
200	4-11 x 10^{12}
175	3-8 x 10^{12}
150	1-4 x 10^{12}
135	< 1 x 10^{12}

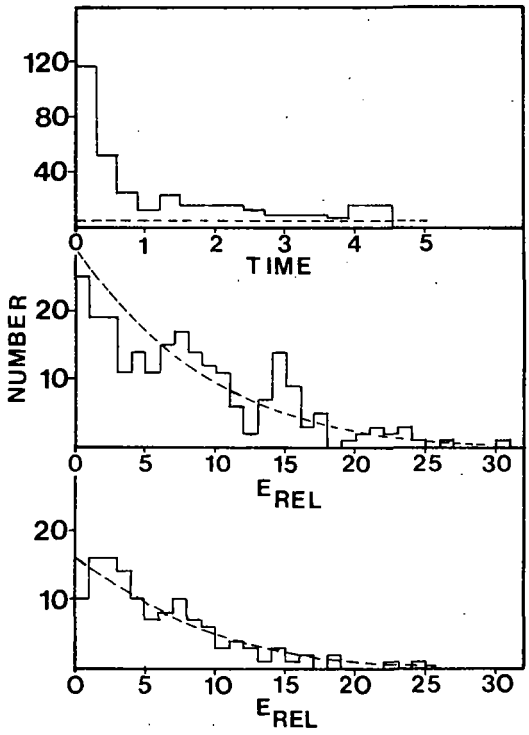


Fig. 1: Trajectory results for H-C≡C-Cl dissociation at 175 kcal/mole, with the HCC modes initially excited. (a) lifetime distribution for HC bond rupture; (b) H+C-C-Cl relative energy distribution for trajectories that dissociate between Time=0 to 1.5; (c) same as for (b) but for Time=1.5 to 4.5. Dashed lines are RRKM predictions. Energy is in kcal/mole and Time is in 10^{-13} sec.

To unravel the various C_2H_5 potential energy coupling terms we have reduced the dimensionality of the system and studied H-C-C → H+C=C dissociation on different model potenenergy surface. The results of these trajectories show intrinsic non-RRKM behavior for alkyl type radical dissociations, and suggest that the broadening and shift in the E_{rel} distributions is not due to couplings between the HC stretch and HCC bend coordinates. Also, a large number of long-lived periodic trajectories were found in these studies.

In summary, there are many questions which remain unanswered about the dynamics of unimolecular reactions. Classsical trajectory calculations are beginning to provide some understanding of different experimental observations. However, it is not yet possible to make broad generalizations. The trajectories do seem to promise a richness and complexity of dynamical details, and the possibility of discovering new principles.

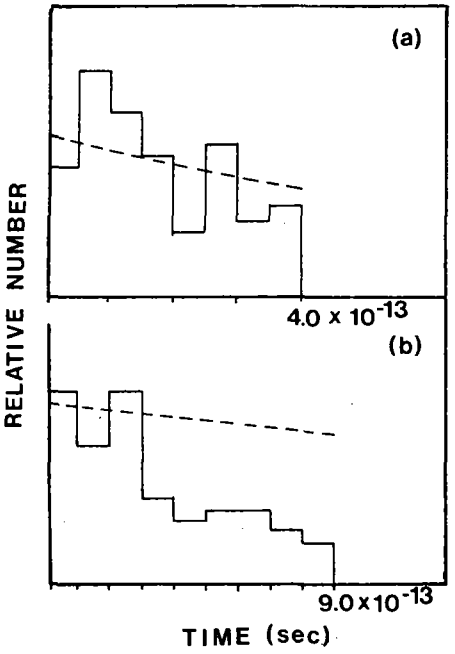


Fig. 2. Lifetime distributions for randomly excited C_2H_5 dissociating to $H+C_2H_4$. Dashed lines are the RRKM predictions (a) 150 kcal/mole (b) 100 kcal/mole.

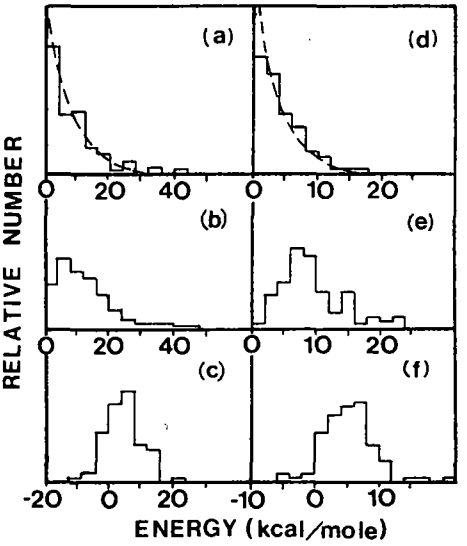


Fig. 3. Relative $H-C_2H_4$ translational energy (E_{rel}) distributions. (a), (b) and (c) are for C_2H_5 randomly excited at 150 kcal/mole. (d), (e) and (f) are for C_2H_5 randomly excited at 100 kcal/mole. (a) and (d) E_{rel} at exit-channel barrier; (b) and (e) final E_{rel} distribution; (c) and (f) $\Delta E_{rel} = E_{rel}$ (final) - E_{rel}(barrier) distributions.

Acknowledgements:

This research was supported by the National Science Foundation. I wish to thank Mr. R. J. Wolf for his help in preparing this manuscript.

References

1. D. L. Bunker and W. L. Hase, J. Chem. Phys., 59, 4621 (1973).

2. P. Brumer and M. Karplus, Faraday Discuss. Chem. Soc., 55, 80 (1973).

3. W. L. Hase and D. F. Feng, J. Chem. Phys., 61, 4690 (1974); ibid, 64, 651 (1976); and C. S. Sloane and W. L. Hase, J. Chem. Phys., 66, 1523 (1977).

4. J. D. McDonald and R. A. Marcus, J. Chem. Phys., 65, 2180 (1976).

5. E. R. Grant and D. L. Bunker, J. Chem. Phys., 68, (1978); and J. Santamaria, D. L. Bunker and E. R. Grant, Chem. Phys. Letters, 56, 170 (1978).

6. J. M. Farrar and Y. T. Lee, J. Chem. Phys., 65, 1414 (1976).

7. C. S. Sloane and W. L. Hase, Faraday Discuss. Chem. Soc., 62, 210 (1977); and W. L. Hase, G. Mrowka, R. J. Brudzynski and C. S. Sloane, J. Chem. Phys., 69, 3348 (1978).

RPM0A3 THE ROLE OF ELECTRONICALLY EXCITED STATES IN THE FRAGMENTATION OF LARGE IONS, H. M. ROSENSTOCK, National Bureau of Standards, Washington, DC 20234

The initial ionization process produces ions in Franck-Condon accessible portions of the ion ground state and some excited states. In discussing the subsequent fragmentation process it is generally assumed that the fragmentation process is preceded by internal conversion of electronic excitation energy to vibrational energy of the ion ground state. The validity of this assumption for benzene ion fragmentation has been examined by a number of workers in recent years, using a variety of experimental techniques and modes of interpretation. The present status of this problem is reviewed in detail. Tests of this assumption for other large ions is briefly summarized.

THE STATISTICAL THEORY AND THE DECAY OF STATE SELECTED IONS

Tomas Baer
Department of Chemistry
University of North Carolina
Chapel Hill, North Carolina

During the past 5 years, we have measured a number of unimolecular decay rates using photoion-photoelectron coincidence (PIPECO). The apparatus has been described previously.[1] Briefly vacuum U.V. light from a continuum lamp is dispersed by a 1 meter normal incidence monochromator. Ionization takes place in a 5.5 cm long acceleration region in which electrons and ions are accelerated in opposite directions. Threshold electrons are collected in coincidence with ions which pass through a 10 cm long drift region prior to detection. Ions which dissociate between .1 and 50 μs give rise to assymmetric daughter ion time-of-flight distributions from which we can determine their rate of decay.

In our studies, we have measured the decay rates of ions from various neutral precursors. If the ground state energies of the ionic isomers differ, as is usually the case, their rates of decay should also vary because the decay rates are strong functions of the activation energy. In fact in all but one set of isomers studied, the measured decay rates are identical when compared at the same total energy (photon energy + neutral ion heat of formation). This is convincing evidence that these ions isomerize to a common precursor from which the fragmentation reaction proceeds.

On the basis of these studies,[1-4] the following molecular ions are known to isomerize prior to fragmentation.

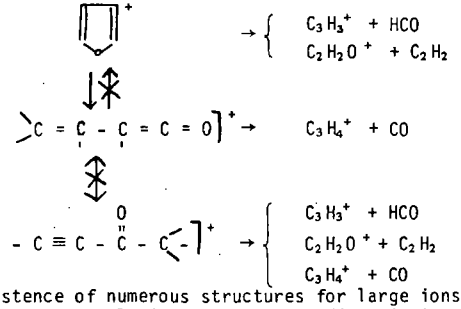
1,3 butadiene; 1,2 butadiene
cyclobutene; methylene-cyclopropene
2 butyne; 1 butyne
$\rightarrow$ 1,3 butadiene $\rightarrow C_3H_3^+ + CH_3$

1-butene; methyl-cyclopropane
cis-butene; isobutene
trans-butene
$\rightarrow$ trans-butene $\rightarrow C_3H_5^+ + CH_3$

2,4 hexadiyne
1,5 hexadiyne
benzene
$\rightarrow$ benzene $\rightarrow$ $C_6H_5^+ + H$; $C_4H_4^+ + C_2H_2$; $C_3H_3^+ + C_3H_3$

cyclooctatetraene
styrene
$\rightarrow$ styrene $\rightarrow C_6H_6^+ + C_2H_2$

We have now found an ion which does not isomerize completely prior to dissociation. This is Furan and two of it's isomers.



The existence of numerous structures for large ions (benzene has over 200 isomers) raises problems for analyzing the rates of dissociations because sequential and multiple reaction paths can create a bewildering set of intermediates and transition states.

Consider the simple scheme:

$$h\nu + A \rightarrow A^+ \qquad \text{ionization} \qquad (1)$$

$$A^+ \xrightarrow{k_1} P_1^+ + N_1 \qquad \text{product 1 formation} \qquad (2)$$

$$A^+ \underset{k_3}{\overset{k_2}{\rightleftarrows}} B^+ \qquad \text{isomerization} \qquad (3)$$

$$B^+ \xrightarrow{k_4} P_2^+ + N_2 \qquad \text{product 2 formation} \qquad (4)$$

This mechanism is quite general in that P_1^+ and P_2^+ could be the same. The rate of production of P_1^+ and P_2^+ is:

$$\frac{dP_1^+}{dt} = k_1 A^+ \qquad \frac{dP_2^+}{dt} = k_4 B^+ \qquad (5)$$

In order to determine the rate, we need to know the time dependences of A^+ and B^+. These are given by the coupled, linear, homogeneous differential equations (6). (The plus sign indicating ions will not be included for the remainder of this paper.)

$$\left.\begin{aligned} \frac{dA}{dt} &= (-k_1 - k_2)\, A + k_3 B = a_1 A + b_1 B \\ \frac{dB}{dt} &= k_2 B + (-k_3 - k_4)\, B = a_2 A + b_2 B \end{aligned}\right\} \qquad (6)$$

Solutions are of the form:

$$A = \alpha e^{-\lambda t} \qquad B = \beta e^{-\lambda t} \qquad (7)$$

substituting into (6) yields

$$\begin{pmatrix} a_1 + \lambda & b_1 \\ a_2 & b_2 + \lambda \end{pmatrix} \begin{pmatrix} \alpha \\ \beta \end{pmatrix} = 0 \qquad (8)$$

and $$\lambda_\pm = \frac{-(a_1 + b_2)}{2} \pm \frac{1}{2}\sqrt{(a_1 + b_2)^2 + 4a_2 b_1 - 4a_1 b_2} \qquad (9)$$

the general solutions are

$$\left.\begin{aligned} A &= c_1 \alpha_+ e^{-\lambda_+ t} + c_2 \alpha_- e^{-\lambda_- t} \\ B &= c_1 \beta_+ e^{-\lambda_+ t} + c_2 \beta_- e^{-\lambda_- t} \end{aligned}\right\} \qquad (10)$$

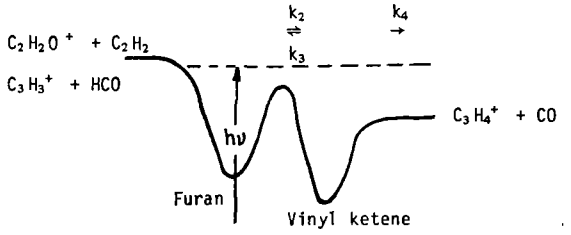
From Eqs. (8) and (9), the α's can be determined in terms of the β's which can be set equal to 1. Furthermore, according to (1) B(t=0) = 0. Therefore A and B are given by:

$$\left.\begin{aligned} A &= \alpha_- e^{-\lambda_- t} - \alpha_+ e^{-\lambda_+ t} \\ B &= e^{-\lambda_- t} - e^{-\lambda_+ t} \end{aligned}\right\} \qquad (11)$$

The rate of product formation is then given by Eqs. (5) and (11). It is evident that these rates are not simple exponentials. In fact, they are given by the <u>differences</u> between two exponentials.

Because λ_+ and λ_- are rather complicated, it is helpful to approximate them for various limiting cases.

Consider the case of Furan shown in Fig. 1. The justification for this potential diagram will be presented in future publications.[5,6] The point here is that for dissociation to $C_3H_4^+$, $k_1 = 0$. If we assume that once isomerized the dissociation is rapid i.e.



$k_4 > k_2 \approx k_3$ Eq. (9) yields λ_+ and λ_- such that the rate is given by Eq. (12)

$$\text{Rate} = \exp\left[-\left(k_2 - \frac{k_2 k_3}{k_4 + k_3 - k_2}\right)t\right] - \exp\left[-\left(k_4 + k_3\right)t\right] \approx \exp(-k_2 t) - \exp(-k_4 t) \quad (12)$$

Because $k_4 \gg k_2$, the effect of the second term is negligible in this case. In other words, the rate limiting step is isomerization which is consistent with the experimentally observed evidence for a simple exponential decay. However, there must be numerous cases in which exponential decay takes place. One example[6] is Cl loss from propargyl chloride. Here it seems that both P_1 and P_2 (Eqs. 2 and 4) give the same product namely $C_3H_3^+$. The data are consistent with $k_1 \approx k_2 > k_4 > k_3$. Because P_1 and P_2 are the same, the rate of $C_3H_3^+$ production is given by the sum $k_1 A + k_4 B$. When the boundary conditions are applied with $k_3 = 0$, the rather complicated expression results:

$$\text{rate} = \frac{k_1(k_1 + k_2 - k_4) - k_2 k_4}{k_1 + k_2 - k_4} e^{-(k_1 + k_2)t} + \frac{k_2 k_4}{k_1 + k_2 - k_4} e^{-k_4 t}$$

1. A. S. Werner and T. Baer, J. Chem. Phys. 62, 2900 (1975).
2. T. Baer, D. Smith, B. P. Tsai and A. S. Werner, Adv. Mass Spectrom. 7A, 56 (1978).
3. T. Baer, G. D. Willett, D. Smith and S. Phillips, J. Chem. Phys. 70, 4076 (1979).
4. D. Smith, T. Baer, G. D. Willett and R. C. Ormerod, Int. J. Mass Spectrom. Ion Phys., in press, 1979.
5. a) J. L. Holmes and J. K. Terlouw, private communication.
   b) G. D. Willett and T. Baer, to be published.
6. T. Baer, B. P. Tsai and A. S. Werner, J. Chem. Phys. 62, 2497 (1975).

ION PHOTOFRAGMENT SPECTROSCOPY

J. T. Moseley and P. C. Cosby
Molecular Physics Laboratory, SRI International
Menlo Park, California 94025

Introduction

The technique of ion photofragment spectroscopy consists basically of interacting a fast beam of molecular ions with photons, usually from a laser, and detecting the ionized photofragments produced. The intensity and the energy and angular distributions of the photofragments can be measured as functions of wavelength. If the ion beam and the laser are made coaxial, advantage can be taken of the compression of the velocity distribution of the ions when they are accelerated to permit sub-Doppler resolution of transition energies, and the beam velocity can be varied to fine-tune the absorption wavelength. From these basic measurements it has been possible to measure vibrational level spacings,[1-3] determine transition symmetries,[3-5] construct diatomic ion potential curves,[4,5] resolve rotational structure of predissociated states,[6] determine bond dissociation energies,[4-8] measure transition energies with sub-Doppler resolution,[6,9,10] and study the lifetimes of predissociated levels.[6,10,11] Examples of each of these types of measurements will be discussed, using the very detailed studies of the quartet states of O_2^+ as an example.

Normal Photofragment Spectroscopy

The technique of photofragment spectroscopy as originally conceived and used at Orsay[1] and FOM[2] consists of crossing a laser beam with an ion beam and measuring the energy distribution of the photofragment ions. Figure 1 shows a photofragment kinetic energy spectrum for the transition

$$O_2^+(\underline{a}\,^4\Pi_u) + h\nu \rightarrow O_2^+(\underline{f}\,^4\Pi_g) \rightarrow O^+ + O \qquad (1)$$

studied extensively at Orsay,[3] where the $\underline{f}\,^4\Pi_g$ state was observed for the first time, and its general shape and location determined. This work also resulted in the discovery[12] of a very interesting predissociation which will be discussed later.

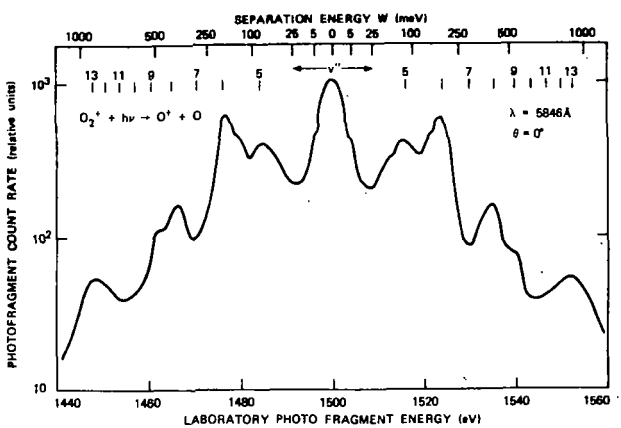


Figure 1. Photofragment kinetic energy spectrum for transition (I).

This spectrum can be understood by reference to the O_2^+ potential curves shown in Figure 2, where the transition under consideration here is labeled I. The peaks on the right and left side of separation energy W=0 correspond to the forward and backward ejected ion photofragments originating from various vibrational levels of the ground state. The spacing of these levels, determined from spectra obtained at a number of wavelengths, identifies the ground state of this photodissociation as the metastable $\underline{a}\,^4\Pi_u$. The fact that the angular distribution peaks for the laser polarization along the ion beam direction identifies the transition as parallel,[13] and thus the dissociative state as the previously unobserved $^4\Pi_g$. The fact that the dissociation occurs for W=0 shows that the $^4\Pi_g$ state is bound. Thus this state has the general shape and location shown in Figure 2, in agreement with recent calculations.[14]

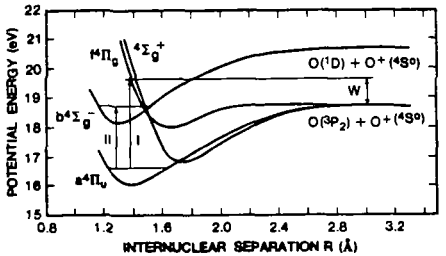


Figure 2. O_2^+ quartet state potential curves.

Predissociation Photofragment Spectroscopy

In addition to the transition in the O_2^+ quartet system described by Equation (2) and by Transition I of Figure 2, a second transition, II,

$$O_2^+(\underline{a}\,^4\Pi_u) + h\nu \rightarrow O_2^+(\underline{b}\,^4\Sigma_g^-) \rightarrow O^+ + O \quad , \quad (2)$$

can be observed for vibrational levels of the b state of $v'=4$ or greater, since these levels are predissociated. These transitions were first observed by the Orsay group,[12] with the correct identification made by the Southampton group.[8]

A detailed study of transitions to the $v' = 4$ and 5 levels of the b state has been made at 0.2 Å resolution by Tadjeddine, Abouaf, Cosby, Huber and Moseley.[9] Two CW jet-stream tunable dye lasers were used, one crossed and one coaxial with the ion beam, pumped by argon and krypton ion lasers. The primary experimental data were scans of the laser wavelength from 5750 to 5870 Å, covering all of the expected (4,4) and (5,5) transitions while observing the photofragment current for fragment ions corresponding to total separation energies W centered at 0, 12, 25, 50 and 100 meV.

Figure 3 shows a predissociation spectrum obtained for W=0 with crossed beams. The resolution of the peaks in this spectrum is seen to be about 0.2 Å, and the uncertainty in the absolute wavelength scale is also about 0.2 Å. From the width and spacing of the peaks it is clear that rotational structure is resolved.

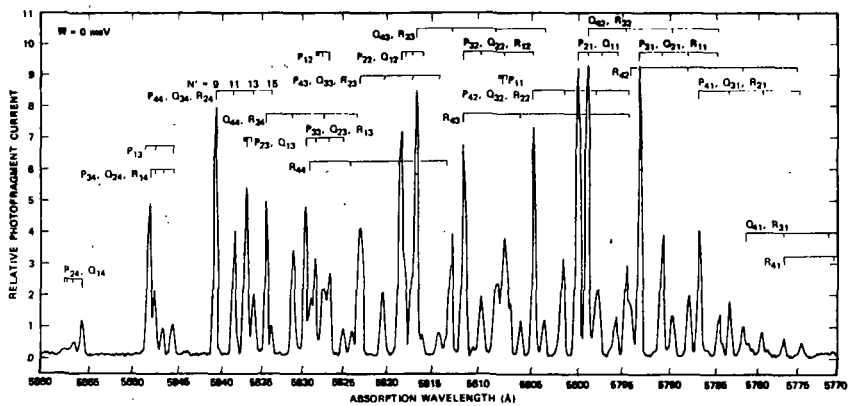


Figure 3. Predissociation spectrum for $O_2^+(\underline{a}) + h\nu \rightarrow O_2^+(\underline{b}) \rightarrow O^+ + O$ and W=0.

The identifications of the transitions were made using molecular constants[15] based on lower vibrational levels which are not predissociated. Because of its high multiplicity, the structure of this band is quite complex. In principle, 48 transitions can be observed which obey the selection rule $\Delta J = 0, \pm 1$, and terminate in a given N' level of the b state. However, with the present resolution of 0.2 Å, only 24 branches can be resolved, 16 of these consisting of blends of two or three transitions. Even in the highest-resolution optical spectroscopy only 40 branches can be resolved.

Velocity-Tuned Coaxial Beams Spectroscopy

The use of a single mode laser coaxial with the ion beam provides both the ability to obtain sub-Doppler resolution and a convenient way of tuning the absorption wavelength, namely variation of the ion beam velocity.[8] It also allows the resolution of transitions that are blended in the data of Figure 3, and in normal emission spectroscopy.

The experimental data to be discussed here were obtained in the following way. A beam of O_2^+ ions was established at an energy of 3600 eV. The single mode laser was tuned by tilting its etalons until its Doppler-shifted frequency was in the vicinity of one of the absorptions already studied in detail[6] at lower resolution (0.2 Å). The velocity of the beam was then scanned by varying the potential on the electrostatic cage. As the absorption wavelength was Doppler-tuned into resonance with a transition, photofrag-

ment ions appeared at the energy analyzer. If the energy analyzer was set to pass ions of the energy of these photofragments, counts could be observed at the detector.

A typical scan is shown in Figure 4. Such a scan, which covers about 0.5 cm^{-1}, required a variation in the ion beam energy of approximately 500 eV. The kinetic energy (and hence absorption wavelength) scan is controlled by a multichannel scaler, and thus each channel of the scaler corresponds to a specific absorption wavelength. The wavenumber listed at the center of Figure 4 is that of the single mode laser beam. The abscissa of the figure gives the Doppler shift from that value due to the ion velocity. The absolute value of the wavelength was determined[9] using a digital wavemeter inteferometer, relative to the iodine absorptions near 5145 Å, to an accuracy of 0.003 cm^{-1}. The designation of the peaks is as previously described,[6] with the value of N' included here in brackets.

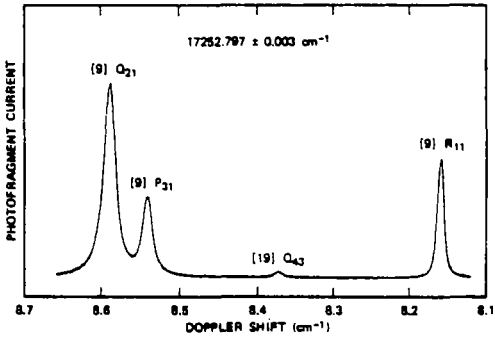


Figure 4. Predissociation spectrum for O_2^+ obtained using a single mode laser.

Data such as those shown in Figure 4 were obtained for over 1000 transitions in the (3,3), (4,4), (4,5), and (5,5) bands of normal[9] and isotopic O_2^+. A statistical analysis of the data[10] shows that the precision of the measurements for transitions terminating in $v'=4$ is 0.003 cm^{-1}. This is an order of magnitude better than the best previous optical spectroscopy on these transitions, which was limited by the normal Doppler width. The peaks labeled $[9]Q_{21}$ and $[9]P_{31}$ in Figure 4 would blend in normal optical spectroscopy; here they are easily resolved.

The present data, which include higher vibrational levels than previously existing data on the $\underline{b} \leftarrow \underline{a}$ transitions,[15] and are of higher precision, have allowed an improvement in the Hamiltonian description[10] of the $\underline{a}$ and $\underline{b}$ states.

Lifetimes of Quasi-Bound Levels

The fact that the peaks in Figure 4 have different widths indicates that the linewidths are not dominated by the apparatus-induced Doppler width, but contain information about the natural lifetime of the levels. The Doppler contribution to the linewidths can be accounted for in a relatively straightforward manner,[11] and the lifetime of each predissociated level obtained. The extensive nature of the present data allowed a study[11] of the variation of lifetime with quantum numbers v', N', and F_i', and with isotopic composition, in which it was concluded that the dissociation occurs by interaction of both the $^4\Sigma_g^+$ and $^4\Pi_g$ states with the $^4\Sigma_g^-$ (see Figure 2).

Angular Distributions and Bond Energies

Bond energies for diatomic ions can be determined[4,5] directly from the kinetic energy spectra with an accuracy of about 20 meV, while angular distributions are normally studied by rotating the laser polarization in a crossed beams configuration. However, for the predissociated levels of the $O_2^+\underline{b}$ state it was possible to determine both[8] β from kinetic energy distributions obtained using coaxial beams, with a single-mode laser. Figure 5 shows an experimental kinetic energy spectrum for the $[18]Q_{11}$ line of $^{16,18}O_2^+$ ($a \rightarrow b$). Experimental values of the anisotropy parameter β, which describes the angular distribution of the photofragments, were obtained by fitting the experimental energy distributions obtained from a Monte-Carlo computer simulation of ion trajectories in the apparatus. From this same fit, W values could be obtained with an uncertainty of less than ± 0.2 meV.

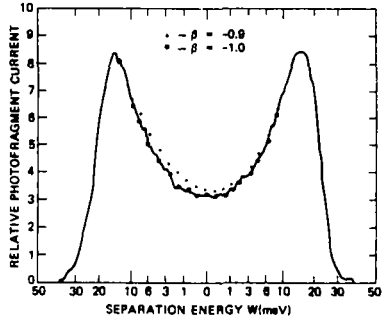


Figure 5. Photofragment kinetic energy spectrum for O_2^+ obtained using a single mode laser.

One unique result from this study was the demonstration that when all relevant quantum numbers are specified the angular distribution depends not on the symmetry of the electronic transition but on ΔJ. Another unique result was the determination of the bond energy of the O_2 ground state, using the measured values of W, to a higher precision than had been possible using purely optical spectroscopic data.

Acknowledgments

The authors are pleased to acknowledge the participation of others at SRI and Orsay in parts of the work presented here; in particular, Jean Durup, Jean-Bernard Ozenne, Mireille Tadjeddine, Bernd Huber, Roberta Saxon, Alberto Beswick, Abdallah Tabché-Fouhaillé, Robert Abouaf, Christiane Pernot, Tom Miller, and James Peterson. The assistance of and helpful discussions with D. L. Albritton and R. N. Zare are appreciated. The work at SRI was supported by AFOSR, NSF, and ARO.

References

1. J.-B. Ozenne, J. Durup, R. W. Odom, C. Pernot, A. Tabché-Fouhaillé, and M. Tadjeddine, Chem. Phys. 16, 17 (1976) and references therein.
2. N.P.F.B. van Asselt, J. G. Maas, and J. Los, Chem. Phys. 11, 253 (1975) and references therein.
3. A. Tabché-Fouhaillé, J. Durup, J. T. Moseley, J.-B. Ozenne, C. Pernot, and M. Tadjeddine, Chem. Phys. 17, 81 (1976).
4. J. T. Moseley, R. P. Saxon, B. A. Huber, P. C. Cosby, R. Abouaf, and M. Tadjeddine, J. Chem. Phys. 67, 1659 (1977).
5. R. Abouaf, B. A. Huber, P. C. Cosby, R. P. Saxon, and J. T. Moseley, J. Chem. Phys. 68, 2406 (1978).
6. M. Tadjeddine, R. Abouaf, P. C. Cosby, B. A. Huber, and J. T. Moseley, J. Chem. Phys. 69, 710 (1978).
7. D. L. Albritton, J. T. Moseley, P. C. Cosby, and M. Tadjeddine, J. Mol. Spec. 70, 326 (1978).
8. C. Pernot, J. Durup, J.-B. Ozenne, J. A. Beswick, P. C. Cosby, and J. T. Moseley, J. Chem. Phys. (in press).
9. A. Carrington, P. G. Roberts, and P. J. Sarre, Mol. Phys. 34, 291 (1977); Mol. Phys. 35, 5123 (1978).
10. P. C. Cosby, J.-B. Ozenne, J. T. Moseley, and D. L. Albritton, J. Mol. Spec. (in press).
11. J. T. Moseley, P. C. Cosby, J.-B. Ozenne, and J. Durup, J. Chem. Phys. 70, 1474 (1979).
12. J. T. Moseley, M. Tadjeddine, J. Durup, J.-B. Ozenne, C. Pernot, and A. Tabché-Fouhaillé, Phys. Rev. Lett. 37, 891 (1976).
13. R. N. Zare and D. R. Herschback, Proc. IEEE 51, 173 (1963); R. N. Zare, Ph.D. Thesis, Harvard University (1964); Molec. Photochem. 4, 1 (1972).
14. N.H.F. Beebe, E. W. Thulstrup, and A. Anderson, J. Chem. Phys. 64, 2080 (1976).
15. D. L. Albritton, A. L. Schmeltekopf, W. J. Harrop, R. N. Zare, and J. Czarny, J. Mol. Spec. 67, 157 (1977).

ENERGETICS AND DYNAMICS OF MOLECULE-IONS BY PHOTOIONIZATION OF VAN DER WAALS MOLECULES

S. Ceyer, P. Tiedemann, T. Hirooka, S. Anderson
B. H. Mahan and Y. T. Lee

Materials and Molecular Research Division
Lawrence Berkeley Laboratory and
Department of Chemistry
University of California, Berkeley, California 94720

The method of molecular beam photoionization of van der Waals molecules provides exciting new possibilities of deriving information on the energetics and dynamics of molecular ions. In this method a dispersed vacuum UV photon beam is crossed with a beam of van der Waals molecules formed in an adiabatic expansion. The resulting molecule-ions are extracted and then mass analyzed as a function of wavelength of the incident beam.

It is the energy threshold for the ionization of the van der Waals dimer, A_2, that allows the stability of the resulting molecule-ion, $(A^+)A$, to be calculated. For example, the formation of Kr_2^+ and $(HCl)_2^+$ is considered as excitation of one of the partners in the neutral dimer to an excited electronic state, $(Kr^*)Kr$, followed by almost immediate autoionization, which is in fact very close to a zero kinetic energy associative ionization to form the dimer ion, Kr_2^+. Figure 1 shows the good correlation between the Rydberg levels of the Kr atom and the structure in the photoionization efficiency curve of Kr_2^+. Thus the thresholds as measured in this method are not determined by the small Franck-Condon factors for direct ionization to the dimer ion state nor are limited by the uncertainty of a finite kinetic energy between the neutral species and the ion. Figure 2 shows the photoionization efficiency curves for the $(HCl)_2$ system and Figure 3 shows the calculation of the $(HCl^+)HCl$ binding energy from the experimental threshold of $(HCl)_2^+$, the dissociative ionization energy of HCl and the binding energy of the neutral HCl dimer. All the dimer ion binding energies measured by this method are shown in Table I.

As the photon energy is increased beyond the threshold the maximum level of vibrational excitation of the dimer ion also increases since most of the excess energy is retained as vibrational excitation during the associative ionization step. With increased vibrational excitation some

of the dimer ions eventually decompose unimolecularly. Hydrogen containing dimer ions may fragment via a proton transfer reaction yielding a protonated molecule. Combined with other thermodynamic data this threshold yields the proton affinity of the molecules in the neutral van der Waals dimer. The photoionization efficiency curve of H_2Cl^+ and the calculation of the proton affinity of HCl are also shown in Figures 2 and 3. Similarly, the proton affinities of H_2O (165.8 ± 1.8 kcal/mole), HBr (140 ± 1 kcal/mole) and NH_3 (202.1 ± 1.3 kcal/mole) have been measured. Photoionization and subsequent fragmentation of the larger van der Waals clusters like $(NH_3)_{x>2}$ yield the solvation energies of a proton by two or more NH_3 molecules. The energetics for the NH_3 system are illustrated in Figure 4.

Fragmentation other than proton transfer may also occur as the vibrational energy is increased. Upon photoionization of $(C_2H_4)_2$, methyl radical and hydrogen atom elimination occur resulting in the $C_3H_5^+$ and $C_4H_7^+$ ions being produced. The appearance potential of $C_4H_7^+$ occurs at an energy which corresponds to the heats of formation of $C_4H_7^+$ and H whereas the appearance potential of $C_3H_5^+$ occurs at a value 8 kcal/mole larger than the one predicted from the heats of formation. This indicates an activation energy barrier in the exit channel of 8 kcal/mole for methyl radical elimination from $(C_4H_8^+)^{\ddagger}$. In a conventional ion-molecule experiment, the large total energy of the system would prevent the determination of both the stability of the $(C_2H_4)^+ \cdot C_2H_4$ collision complex and the potential barrier along the reaction coordinate. The reaction coordinate is shown in Figure 5.

Competing with the associative ionization process of the electronically excited (A*)A dimer is predissociation of the dimer. This competition has been studied by comparing the H_3^+ photoionization curve produced by photoionization and fragmentation of $(H_2)_2$ to that of H_2^+ since in the absence of vibrational predissociation of $H_2^* \cdot H_2$, the H_3^+ curve should be very similar to that of H_2^+. It appears that states of $H_2^* \cdot H_2$ which have to autoionize by $\Delta v \geq 2$ process have a lower ion intensity due to a rapid rate for vibrational predissociation than states which autoionize by a $\Delta v = 1$ transition. Thus, from the reported autoionization rates for the

vibronic states of H_2, the vibrational predissociation rates are estimated to be $\geq 10^9$ sec^{-1} for states which have to autoionize via $\Delta v > 2$ transitions and $< 10^{11}$ sec^{-1} for $\Delta v = 1$ transitions.

Thus, the mechanism of ionization and stabilities of the resulting molecule-ion complex can be successfully probed by photoionization of van der Waals molecules. In addition, thermodynamic information such as proton affinities and potential barriers can be reliably obtained with this method.

This work was supported by the Division of Chemical Sciences, Office of Basic Energy Sciences, U. S. Department of Energy under contract No. W-7405-Eng-48.

Table I.

	kcal/mole		kcal/mole
$(NO^+)NO$	13.6 ± .5	$(Ar^+)Ar$	28.4 ± .5
$(C_2H_4{}^+)C_2H_4$	18.2 ± .5	$(Kr^+)Kr$	26.5 ± .4
$(NH_3{}^+)NH_3$	18.2 ± 1.1	$(Xe^+)Xe$	23.8 ± .2
$(H_2O^+)H_2O$	36 ± 3	$(KrAr)^+$	13.6 ± .5
$(HBr^+)HBr$	23 ± 2	$(XeAr)^+$	3.2 ± .5
$(HCl^+)HCl$	20 ± 2	$(XeKr)^+$	8.5 ± .5

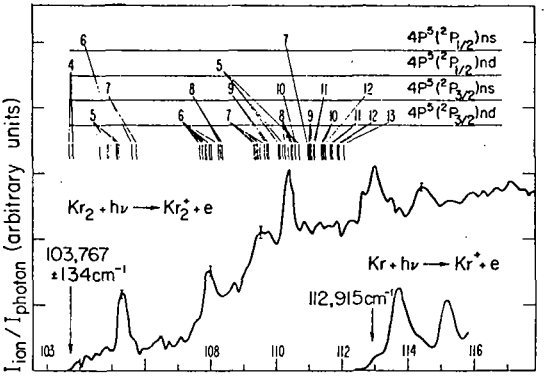


Figure 1

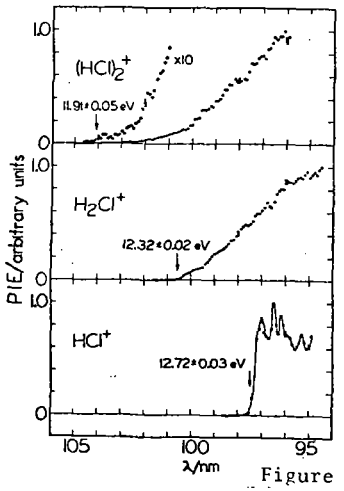


Figure 2

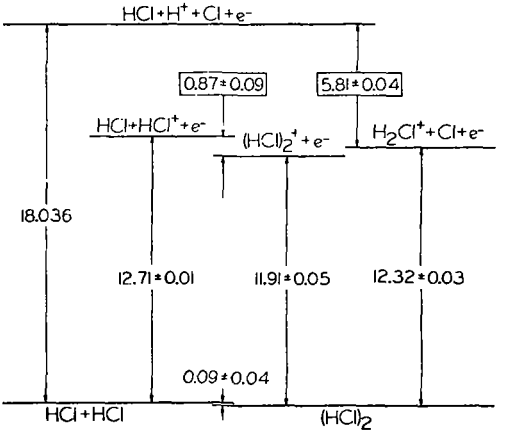


Figure 3

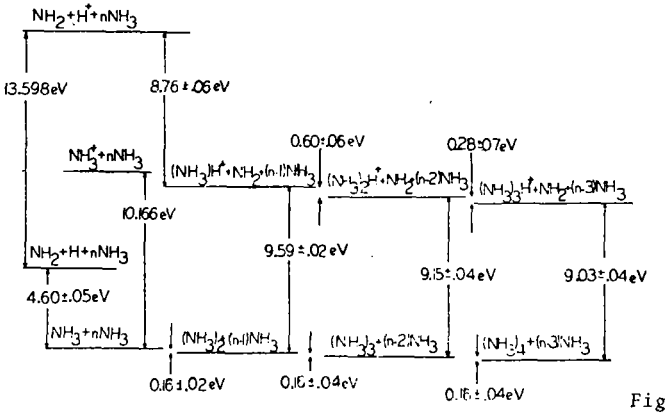


Figure 4

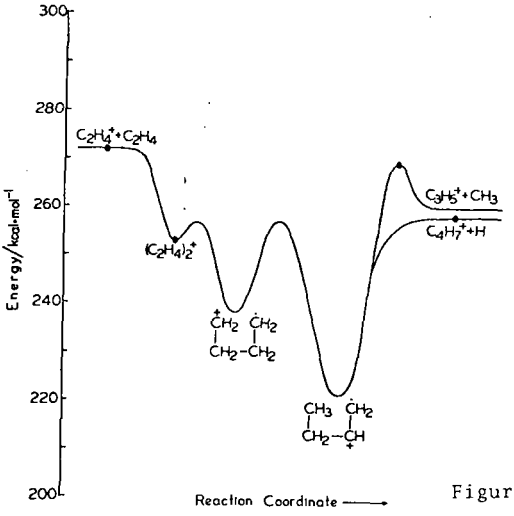


Figure 5

Computer Controlled Mass Spectral Data Acquisition with a Fast New High Dynamic Range Interface

J. C. Bill, W. E. Morden, P. Powers and M. J. Wallington, VG Data Systems Limited, Tribune Avenue, ALTRINCHAM, England.

The past few years have seen many significant advances in GCMS analysis, but of all these perhaps one of the more far reaching has been the improvement of instrumental signal-to-noise ratio.

A number of approaches have been made towards accommodating such increased dynamic range as far as the data system is concerned, but few of these have really set out to meet the chemist's requirements. It is important to identify two different aspects of these requirements:-

1. Dynamic range within each acquired spectrum, and
2. Overall Dynamic range from one scan to another

Dynamic range can be expressed in either of two ways. The first is to use a peak height (or signal-to-noise) basis and the second a peak area basis. Each has their own specific advantage, but comparison of different approaches must be made on similar bases.

The table below indicates the level of dynamic range that is needed from both the mass spectrometer and data system if the chemist's basic requirement is to be able to measure peak intensity down to 0.1% base to a 10% accuracy anywhere over a gas chromatogram which itself involves a wide intensity variation.

Dynamic Range Requirements

	Dynamic Range	
1. Within a Scan	Height	Area
Monitor peaks of 0.1% base	1,000	100,000
Measure peaks of 0.1% base to ± 10 to 20%	x10	x10
Accommodate base peaks which are 20% TIC	x 5	x 5
Required Range within a Scan	50,000	5×10^6
2. Within a Run		
Monitor 0.1% GC Peaks	x 1000	x1000
Required Total Dynamic Range	5×10^7	5×10^9

A new type of interface has been developed which recognises these two quite different aspects of dynamic range and which more than meets the requirements set out above.

High Dynamic range within a scan is provided by fast simultaneous dual sensitivity acquisition with a decision on which signal is in range being taken separately for each acquired mass spectral peak in true real time. High GC dynamic range is provided by automatic amplifier gain changing between scans over a range of 1000 to 1. The combination of these two approaches yields the performance in the table below which is fully able to utilise the capability of modern mass spectrometers.

Dynamic Range Performance

	Dynamic Range	
	Height	Area
Within a Scan	65,520	8×10^6
Within a Run	6.5×10^7	8×10^9

Perhaps one of the simplest tests of dynamic range within a scan is the analysis of a compound such as carbon tetrachloride whose isotopic pattern involves a quite significant intensity range. Figure 1 shows such a test with this compound using the mass range 117-124 and using peak height measurements. The right-hand column shows results obtained with $\frac{1}{5}$ of the sample size used to obtain the data in the left-hand column.

An overall intensity range of 60,000:1 is recorded with a peak height ratio of 10,000:1 and with the smallest peak being measurable to $\pm$ 1 in 6 or 17%.

Computer control of amplifier gain between scans to accommodate a high GC peak intensity variation is of particular importance since many modern applications of GCMS relate to the ability to identify small components hidden under very complicated GC traces. A typical example is that of an oil spill sample where the analyst is concerned to discover whether or not undesirable components can find their way into the food chain.

Figure 2 shows a portion of a chromatogram from the Amoco Cadiz oil spill which has undergone, and is still undergoing, extensive tests in France.

Figure 3 shows the 500 scan section of this run which encompasses some well-known components, but the areas of real interest are those around scans 2876 and 3242 where phenanthrene and the isomers of methyl phenanthrene can be expected to be present in the background.

Automatic control of amplifier gain over a wide range has always been difficult to implement in these circumstances since the high level of background frequently confuses the gain change decision process.

This problem was overcome in this development by using the data system's ability to produce mass measured data in true real time exactly in step with the data as it is acquired. The decision to adjust amplifier gain between scans is then made on mass measured data in either of two ways according to whether peak intensity is being measured by height or area.

Peak Height Mode :	Use intensity of base peak above a specified mass
Peak Area Mode :	Use value of TIC formed from all ions above a specified mass

One example of the success of this approach in the oil spill sample is seen in Figure 4 which shows the location of the isomers of methyl phenanthrene by tracing m/z 192 over the 500 scan section mentioned above.

Figure 5 emphasises this by showing the high quality of spectrum produced from such hidden components by high dynamic range acquisition and the corresponding high level of library match when compared against the NBS library.

A mass spectrometer-data system combination with high dynamic range capability can bring a new ease of analysis to problems which hitherto have presented a challenge to the analyst.

ACKNOWLEDGEMENT

The authors would like to acknowledge the valuable assistance of Mr. K. Hall in the analysis of the samples for this paper.

CTH4 2 05-JAN-71 AUTO-GAIN= 1 1. 1

MM305 RP=500+20 SEC/DEC. SAMPLE OF CCL4

MASS	RMT. MOD.	ABS HT.	MASS	RMT. MOD.	ABS HT.
117	100.000	62654	117	100.000	20192
118	1.068	669	118	1.055	213
119	96.782	60640	119	96.910	19568
120	1.036	649	120	1.075	217
121	30.899	19360	121	30.903	6240
122	0.335	210	122	0.337	68
123	3.366	2109	123	3.264	659
124	0.043	27	124	0.030	6

DYNAMIC RANGE TEST USING CARBON TETRACHLORIDE

Fig. 1

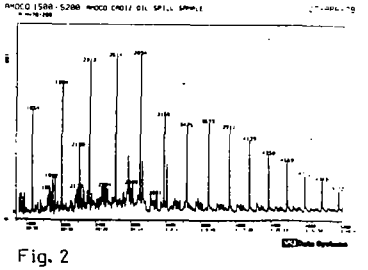


Fig. 2

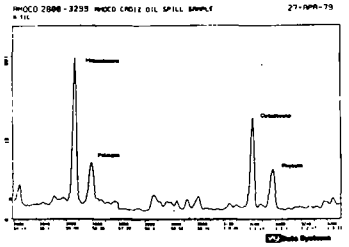


Fig. 3

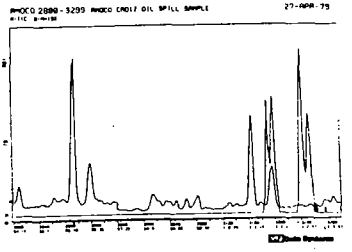


Fig. 4

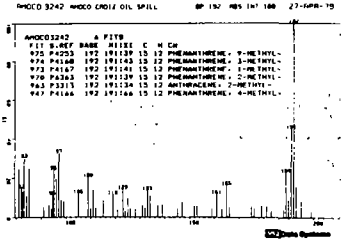


Fig. 5

MICROPROCESSOR CONTROLLED SAMPLE HEATING CURRENT PROGRAMMER FOR DIRECT EXPOSURE PROBES

Robert J. Cotter, Dept. of Pharmacology, Johns Hopkins Sch. of Medicine, Baltimore, MD 21205

Several investigators have reported the importance of sample temperature or heating rate on the production of molecular ions for non-volatile and/or thermally labile compounds using direct exposure probes. These studies have used activated FD emitters (1-3), fast-heated tungsten wires (4), and indirectly heated "inert" probes (5-8) in both EI and CI sources. Cotter and Fenselau (8) have demonstrated the role played by the heating rate in the production of molecular ion in competition with thermal decomposition.

In our laboratory, a microcomputer controlled current source has been constructed for programmed direct heating of tungsten wires used as solids probes in a Dupont 491 mass spectrometer. The system (FIGURE 1.) consists of an RCA COSMAC Evaluation Kit, a magnet scan interface, and a programmable current interface. The microcomputer contains a CDP1802 processor, 256 bytes of RAM, a ROM monitor, a Microterminal for programming in hexadecimal op code, and on-board input and output ports.

The current interface is connected directly to the output port of the COSMAC and consists of two parts. The optical isolation circuit (FIGURE 2.) electrically isolates the digital outputs from ground, since the 491 source block is operated at 1800 volts. The current source (FIGURE 3.) performs 4-bit digital-to-current conversion. A VMOS power FET provides a greater degree of linearity than bipolar transistors. In addition, the interface is operated in a "mixed" D/A and pulse-width-modulation mode to provide currents from 0 to 4 amperes with 12-bit (1 mA) accuracy. The magnet scan interface (FIGURE 4.) is "autoranging", and is used to synchronize changes in heating current with mass scan and acquisition, controlled by a Finnegan/INCOS data system.

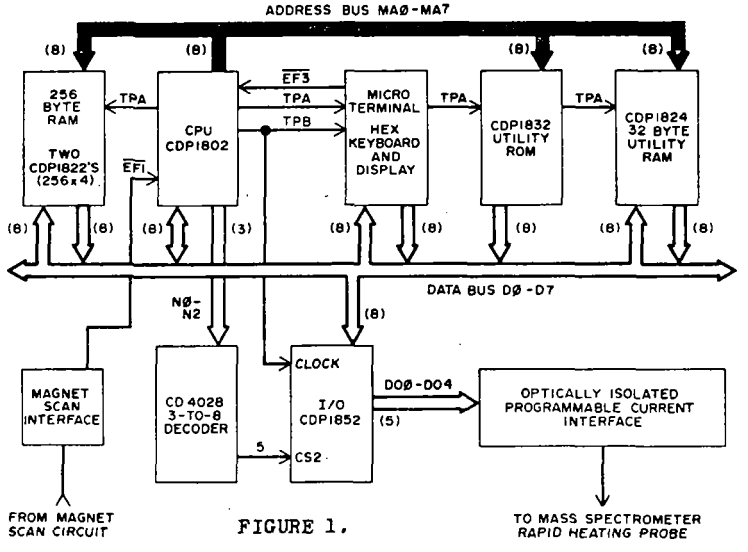


FIGURE 1.

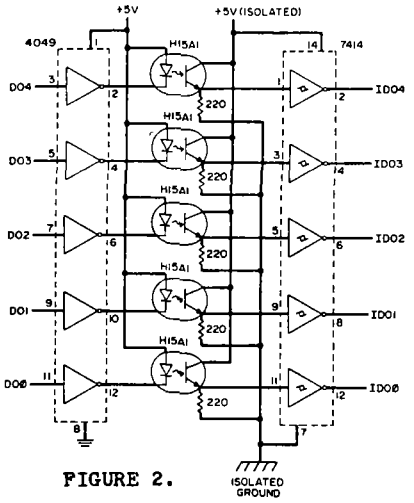


FIGURE 2.

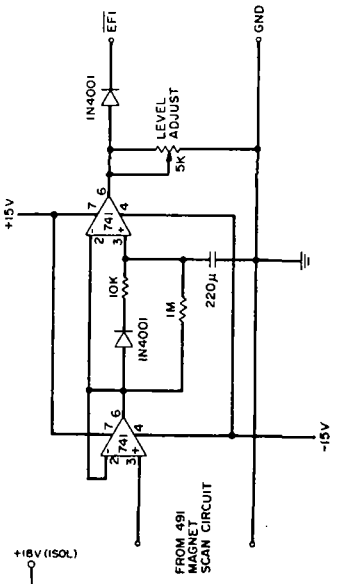


FIGURE 4.

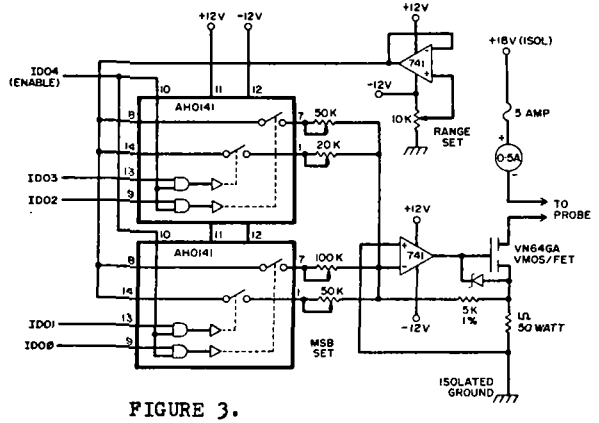


FIGURE 3.

1 J.F. Holland, B. Soltmann, and C.C. Sweeley, Biomed. Mass Spectrom., 3, 340 (1976)

2 B. Soltmann, C.C. Sweeley, and J.F. Holland, Anal.Chem., 49, 1164 (1977)

3 D.F. Hunt, J. Shabanowitz, F.K. Botz and D.A. Brent, Anal. Chem., 49, 1160 (1977)

4 W.R. Anderson, Jr., W. Frick, and G.D. Daves, Jr., J. Am. Chem. Soc., 100, 1974 (1978)

5 R.J. Beuhler, E. Flanigan, L.J. Greene, and L. Friedman. J. Am. Chem. Soc., 96, 3990 (1970)

6 G. Hansen and B. Munson, Anal. Chem., 50, 1130 (1978)

7 R.J. Cotter, Anal. Chem., 51, 317 (1979)

8 R.J. Cotter and C. Fenselau, Biomed. Mass Spectrom., (in presss)

AUTOMATED QUALITATIVE AND QUANTITATIVE ANALYSIS OF GC/MS DATA FROM COMPLEX ORGANIC MIXTURES

Glenn I. Ouchi, Finnigan Corporation, 845 W. Maude Avenue, Sunnyvale, Califonria 94086

An automated minicomputer-based method has been developed for the qualitative and quantitative analysis of GC/MS data acquired from complex organic mixtures. The method has two major parts. In the first, called confirmational analysis, specific target compounds are sought in the sample. If the target compound is found, it is quantified by either internal or external standard methods using selected mass chromatograms (extracted ion current profiles, EICP). In the second part, called survey analysis, forward library search is used to identify all other components detected by a Biller-Biemann max-mass algorithm[1] which were not identified via confirmational analysis. Thus, both specific target compounds sought and other unknown components in the sample are identified. This method can also be used for quantitative mixture profiling.

Confirmational analysis answers the question: is this specific target compound present in the sample? This type of GC/MS analysis[2] has found broad applications in the forensic and clinical chemistry and the analytical screening protocol for the concent decree priority pollutants. This method is potentially useful for the huge analytical task of reporting impurities in manufacturing use products, formulated use products and monitoring chemicals regulated by the Toxic Substances Control Act.[3]

Compound identification is based on relative retention time of the compound with respect to internal standard(s) and mass spectral pattern matching. This is accomplished by performing a reverse search[4] in a one-minute window centered on the expected relative retention time for the compound. If a spectrum in the window has a match value greater than a specified threshold, the compound is considered detected and identified. The compound is then quantified by performing the appropriate calculations on the peak areas of a selected mass chromatogram (EICP) for both the compound and an internal standard. By using selected mass chromatograms, background and coeluting compound interferences are minimized.[5]

Compound spectra for reverse search are generated from standard compound mixtures or for quantitative mixture profiling a selected control sample. This data is also used to calculate relative response factors and relative retention times. Periodically the standard mixture should be reanalyzed so the various parameters can be updated. This updating procedure is an important part of the method and these parameter are saved for system documentation.

Survey analysis performs a forward library search on all detected compound spectra not identified by the confirmational analysis. The name of the best matching library spectra above a specific match value threshold is reported along with the number of other library spectra having match values above the threshold. If no library spectra have match values above the threshold NOT IDENTIFIED is reported. The peak containing the scan is then quantified using the sum of the ion intensities of those masses present in the best matching library entry. This raw quantitative data gives the area of the resulting peak and the relative amount of the compound in the sample.

Operationally, the method requires the following steps:

1) Prepare and acquire GC/MS data on a standard mixture of the compounds to be sought and quantified. For quantitative profile analysis, this would be a selected control sample.

2) Enter reverse library search parameters (mass spectra, retention times, mass chromatogram to use for quantification) into a library.

3) Run an initialization program that finds the internal standards, and calculates relative response factors and retention times for all compounds.

4) Data process acquired unknown sample GC/MS data.

5) Periodically, the standard mixture is reanalyzed and reverse search parameters are updated. A history of all previous parameters are kept for system documentation.

Programs for steps 3, 4, and 5 are automatic, and require no operator interaction during the processing. These programs run in a low priority background mode while new acquisitions are made in foreground. Clear cut identifications and quantifications are made by the data system. If any criteria for compound identification or quantification are incomplete, the reports generated by the programs focus the chemists attention to those compounds for direct human interpretation. In this way final data interpretation is a team effort with both the data system and the chemist participating.

1. J. E. Biller and K. Biemann, Anal. Lett., 7, 515(1974).

2. W.L. Budde and J.W. Eichelberger, Anal. Chem., 51, 467A (1979).

3. W. T. Donaldson and A. W. Garrison, Anal. Chem., 51, 458A (1979).

4. F. P. Abramson, Anal. Chem., 47, 45 (1975)

5. S. C. Gates, M. J. Smisko, C. L. Ashendel, N. D. Young, J. F. Holland, and C. C. Sweeley, Anal. Chem., 50, 433 (1978)

RPM0B4

SIMULATION OF THE QUADRUPOLE MASS FILTER, J. E. CAMPANA[1] AND P. C. JURS, Department of Chemistry, Pennsylvania State University, University Park, PA 16802.

The quadrupole mass filter is currently the most popular type of mass spectrometer, but its characteristics are not fully understood. A simple iterative method of numerical computation has been used to simulate ion trajectories in an ideal quadrupole field. The method is based on elementary equations of classical physics rather than numerical integration of the Mathieu equation.

In the elementary approach (herein called "QUAD"), the acceleration at t=0 for an ion is calculated. The velocity and position of the ion are then evaluated at a time Δt later using simple kinematic equations. A new acceleration can be calculated at $t + \Delta t$ and this computation cycle is repeated iteratively for the length of the quadrupole field.

Simulation studies using numerical integration of the Mathieu equation have been based on the Runge-Kutta Method of Integration. This study used the fourth-order Runge-Kutta integration as one method of numerical integration of the Mathieu equation. The Runge-Kutta method suffers from deficiencies as an integration technique[2]. It should only be used when past information is not available and three or four accurate points on the solution curve are needed for a predictor-corrector method of integration. A predictor-corrector method (Hamming's) of integration was also investigated because the elementary approach was to be evaluated and contrasted to an accurate method of numerical integration.

The three methods of ion trajectory computation gave visually identical trajectories. Hamming's method was the slowest method while the QUAD method was more than an order of magnitude computationally faster than the Runge-Kutta method. The Runge-Kutta and QUAD methods were relatively poor with respect to stability, which was demonstrated by the observation that the actual exit coordinate values of a given trajectory would not converge by decreasing the step size, Δt. It was realized from several contrasting studies that the imprecision of the QUAD method would not significantly affect ion transmission and exit location distribution studies.

Ensembles of m/z 57, 59, 150, and 305 ions were studied and at a mass resolution identical to the m/z of the ion. The transmission of the ions were found to decrease with increasing resolution and mass. The percent transmission of ion through the mass filter was found to be 61.2, 60.5, 46.2, and 37.7 for masses and resolutions of 57, 59, 150, and 305 respectively for the particular set of entrance conditions. The graphical relationship between ion transmission and the RF phase angle at the time the ion enters the field and also between the ion transmission and (a, q) values can be obtained.

Figure 1 demonstrates a square array representing the ion exit distribution of an ensemble of ions. This distribution has been simulated from the exit distribution of ions that entered the field in the positive (+, +) quadrant and represents ions entering all four quadrants. A visually useful way of displaying such an exit distribution is by a three-dimensional histogram and is shown in Figure 2.

It appears that ions are focused about the center of the exit aperture.

The QUAD method offers the advantage of speed when other methods may not be practically applicable to a simulation problem. Future research will be directed at building a large data base of simulation data. If the analysis of a large data base reveals interesting facts, these will be investigated instrumentally.

1 - Present address: The Department of Pharmacology and Experimental Therapeutics, the Johns Hopkins University School of Medicine, 725 N. Wolfe St., Baltimore, MD 21205

2 - Forman S. Acton, "Numerical Methods That Work", Harper & Row Publishers, New York (1970).

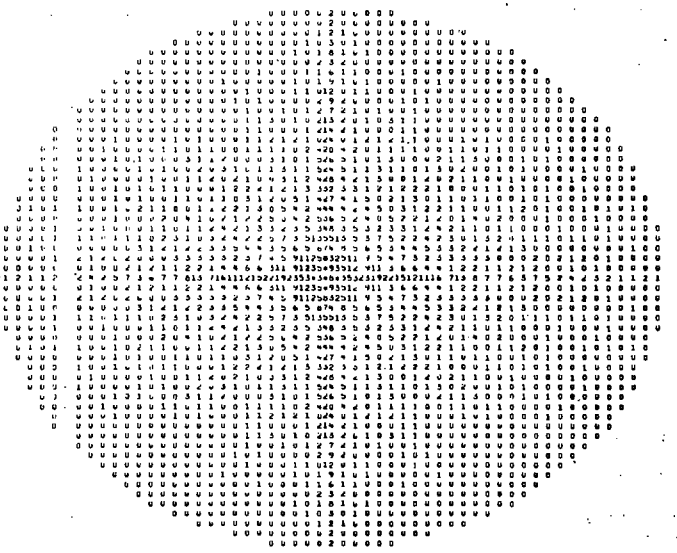


Figure 1

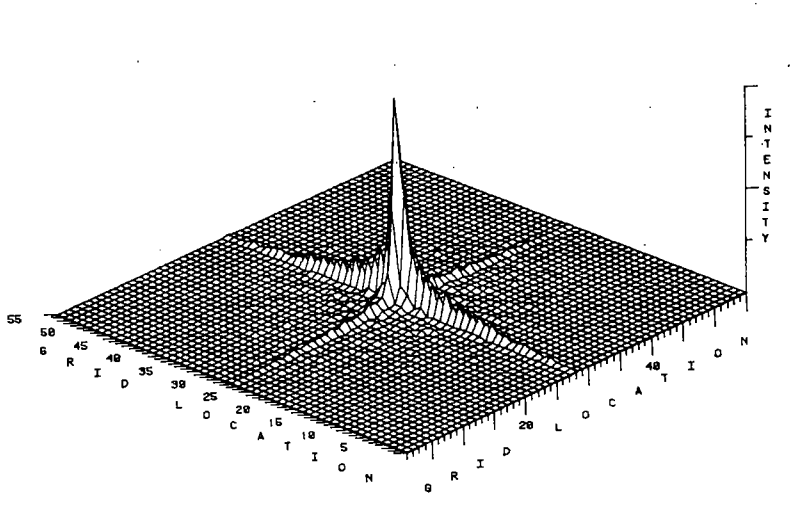


Figure 2

ELEMENTS OF A COST EFFECTIVE MASS SPECTROSCOPY DATA SYSTEM

David E.Smith, Philip L. Warren, Finnigan Corporation, 845 West Maude Avenue, Sunnyvale, California 94086

The elements of a mass spectroscopy data system to be discussed in this presentation are CPU, disc and tape drive, and software. The CPU, or central processing unit, is the heart of the entire data system. All data is acquired, processed, and recalled via the CPU. The disc drive is used to store data in real time, and for on-line storage of acquired data, mass spectral libraries and software. Typically, 1-3 days of acquisition can be stored on a single disc before its capacity is exceeded. A 9-track magnetic tape system is used for off-line archival storage of data. A single tape can store the contents of 1-4 discs, depending on the disc and tape size, at 20% of the cost of a disc system. The third element, software, may be the most important feature of the mass spectroscopy data system when considering cost effectiveness. It is with the software that data acquisition parameters are selected, and all data processing is performed.

In an examination of cost effectiveness of a mass spectroscopy data system, the capital cost of each component must be considered. Improved technology and manufacturing techniques have enabled hardware costs to decrease; however, software is constantly increasing in complexity, and labor costs do not decrease. The net result is that software accounts for a higher proportion of the total data system costs than hardware.

For fast data acquisition and processing, the CPU must have a large buffer area and a CRT input/output. The size of the buffer area is one factor that determines how fast the data can be acquired and processed. If the buffered area is too small, high data acquisition rates will cause the buffer to overflow and data will be lost.

A CRT terminal is necessary for inputing commands to the data system for interactive data display. Any other input/output device, e.g., a teletype with an impact line printer, is too slow to be interactive and cost effective. Viewing spectra or reduced data with a CRT display is nearly an instantaneous process; however, any device that relies on a printer for data display requires from a few seconds to minutes for data output. Depending on the size of the data file, processing data through a CRT terminal rather than a teletype may result in a savings of several hours.

The disc drive functions as an on-line storage device. Typically, MS data systems employ a dual disc system with software and mass spectral libraries residing on a fixed disc and acquired data on a removable disc. For a disc drive to be cost effective, it must be large enough to hold at least eight hours of acquired data. Any less space will result in lost time copying data files to tape, disc, or deleting files. For most applications, a 5 Megabite removable disc is the minimum size required to store at least one day's acquisition.

A disc can be used for data storage; however, the cost of disc storage may be up to 80% higher per unit than a nine-track tape. Storage of disc packs requires 2-3 times the space of a single tape that can store the data from four discs. Considering these factors, storing large volumes of MS data for extended periods is most effectively done on tape.

There are three components to a cost effective software package: foreground/background (F/B) capability, automated data reduction, and system diagnostics. The most common versions commercially available will be discussed below.

Foreground/background capability means that the data system can acquire data and perform one other job, e.g., data processing, simultaneously. Foreground/background can be of the 50/50 time share, or priority interrupt type. In time share F/B the data system spends 50% of the time on acquisition and 50% on the second job. Priority interrupt gives priority to data acquisition and allows available CPU time for the second job. Typically, acquisition will require 20-25% of the CPU time, leaving 75-80% for the second job.

The 50/50 F/B has many disadvantages. When used, the maximum scan speed is reduced by 50%. This may affect the ability to perform analyses by capillary columns as high scan rates (500u/s) are often required. At high data rates, the CPU may not have enough time available for acquisition and data may be lost.

Prior to the availability of automated data processing routines,

analysis of wastewater samples by MS generally required one hour for data acquisition, and ten hours for processing. At this time the ratio of acquisition to data reduction is 1:1, if the most cost effective automated routines are used.

There are three types of data reduction most often performed on MS data: confirmational analysis; survey analyses; and, a combination of the two. In confirmational analysis an unknown sample is examined using a preselected list of compounds, and if a compound is detected, quantitative analysis is performed. In a survey analysis, an attempt to identify from one to all compounds in a sample is made with relative concentrations estimated. A cost effective software package must include both types of analysis options in an automated form.

Autoprocessing may be performed in two modes: batch or using foreground/background. In batch processing, a group of data files are processed sequentially without interruption or operator interaction. At the time of processing, no data acquisition can take place. In the F/B mode, data processing occurs simultaneous with data acquisition. To maximize throughput and minimize analysis costs, the F/B mode is pre-ferred. Using batch processing instead of F/B will require a larger disc, throughput is limited and analysis costs are higher. A discussion of these points follows.

The usual situation for a laboratory using batch processing would be to acquire data for a period of time, e.g., eight hours, then process that data overnight without an operator in attendance. The processed data would be examined interactively with the data system during the following day simultaneous with acquisition of additional samples. The net result is that two sets of data must reside on the data system at one time: one set for manual confirmation, and one newly acquired. This doubles the required disc size.

Sample throughput is limited by batch processing. Assuming an acquisition every hour and 40 minutes for autoprocessing, the maximum practical throughput is limited to 14 samples/day. To process the 14 samples would require 9.3 hours and complete a 24-hour day. However, using F/B, data reduction is continuous, and for every sample acquired, a sample can be processed both automatically and interactively by the operator. Thus, in 24 hours, 24 samples could be acquired, and 23 samples would be completely processed.

Higher throughput is a factor that reduces analysis costs; however, the operational elements of data reduction must also be considered. The delay in reporting results when using batch processing may affect sample throughput. For example, when performing confirmational analysis using internal standards, it is a common practice to analyze a standard mixture at least every fifth sample. If there is an error in the standard analysis, it will remain undetected for up to 16 hours. When the error is finally discovered, five samples must be reanalyzed with a new standard. Even if the standard mix is always within the quality control limits, an internal standard may not be. In this case, the sample will have to be reanalyzed one day later with a new standard mixture.

When using F/B processing, any error is discovered immediately, and corrective action can be taken. This saves analysis time and eliminates the possibility of continuing to acquire data that is out of quality control limits.

To maintain sample throughput the MS and data system must be operational. Excessive down time either for the problem diagnosis, or waiting for repairs, can be a very frustrating and costly experience. To minimize problem diagnosis time, the data system should have a set of diagnostic software that is able to pinpoint hardware faults either in the MS or a data system component.

Diagnostic software should also examine acquired and processed data to determine if it is reliable. Saturated peaks must be identified in spectra and quantitation reports. A well defined match criteria for mass spectral library matching is necessary and a numerical output indicating the quality of the identification should be present in all qualitative reports.

All three general topics discussed, CPU, disc and tape drives, and software, are interrelated and the performance of the MS data system is dependant of all three factors being optimized for sample acquisition, data processing, and data reliability. With F/B and automated data analysis, a GC/MS system can produce organics analyses at a cost comparable to any technique available today.

RPMOB6

SIMULATION OF HYDROCARBON MASS SPECTRA

H. A. Clark and P. C. Jurs
Department of Chemistry
The Pennsylvania State University
University Park, PA 16802

The low resolution, electron-impact mass spectra of hydrocarbons can be simulated with equations derived by multiple linear regression analysis of experimental data. Spectra of 274 hydrocarbons from different sources, including acyclic alkanes and alkenes, and cyclic alkanes and alkenes were simulated. A randomly selected sample of ten spectra was removed from the set of spectra used to find the simulation equations. Calculated molecular parameters were regressed against log-transformed intensities for selected m/e. The parameters considered include molecular weight, substructure presence, substructure environment, and molecular connectivity index. The linear correlation coefficient between the simulated and observed intensities was calculated for each spectrum. The range of values for those spectra used in the model was 0.65 to 0.99 and the median 0.95. For the spectra not included, the range was 0.84 to 0.97 and the median 0.93. Matching the simulated against the experimental spectra rarely identify unambiguously the correct structure, but consistently place the simulated spectrum among a group of similar structures.

MICROCOMPUTER CONTROL OF A MASS SPECTROMETER FOR TRACE NOBLE GAS DETERMINATION*

John C. Newton, Ray G. Bedford, Hal R. Brand,
Richard W. Crawford, and John R. Elliott

General Chemistry Division
Lawrence Livermore Laboratory
Livermore, CA 94550

In the underground testing of nuclear devices in Nevada, gases, consisting principally of air, are pumped from the cavity to the surface and are sampled. For the last few years we have routinely analyzed these cavity gases to determine the noble gas concentrations (He, Kr, and Xe) at the ppm level. The results are used to assess device performance.

The analysis of a cavity gas sample consists of: a) the determination of the percent noble gases in the original sample by pumping a small aliquot with a titanium sublimation pump, b) concentrating the noble gases from about 800 cc (STP) of cavity gas by gettering active gases with molten calcium and c) analyzing the concentrated sample by mass spectrometry. Pure gases and air samples processed like the cavity gas samples are used to calibrate the mass spectrometer.

Recently, new requirements arose for the analyses of these samples. The results of analyzing the first five samples were needed within 48 hours. Starting with a 1 liter (STP) sample of gas, the noble gas components were to be analyzed at the 0.1 to 1000 ppm level with a combined accuracy and precision of ±1%. In addition to the absolute concentrations of each gas, the isotope ratios of the He, Kr and Xe were to be determined with similar accuracy and precision. In order to facilitate meeting these requirements, the mass spectrometer was placed under the control of a microcomputer.

The microcomputer selected to control and acquire data from the CEC 21-103C mass spectrometer is a DEC LSI-11. The mass spectrum is acquired by scanning with the high voltage being controlled by a 16-bit digital-to-analog converter. The ion signal is detected with a Keithly Model 640 electrometer using a 10^{12} Ω resistor. A 5 MHz voltage-to-frequency converter and a 20-bit counter are used to digitize the peak heights. Data and computer codes are stored on a dual floppy disk.

The computer programs which control the mass spectrometer are written in BASIC which has been modified with assembly language calls. These calls set the DAC voltage, the integration periods for the V/F converter, the delay times between readings and the variables which record the number of counts observed. Codes to calculate absolute concentrations and isotope ratios are also written in BASIC. In addition, statistical calculations are made on the ion signals observed on the baseline and peak tops.

*Work performed under the auspices of the U.S. Department of Energy by the Lawrence Livermore Laboratory under contract number W-7405-ENG-48.

These modifications have improved the technique in several ways. Computer control has eliminated numerous operations previously performed by the analyst. Strict timing of the scanning procedures is achieved. Monitoring the baseline has particularly improved the quantitative values and isotope ratios for xenon. The BASIC codes are easily modified for methods development and analyses of non-routine samples. Most important, these modifications have improved both the accuracy and precision for the determination of trace noble gases. The standard deviation is typically less than ±1% for duplicate analyses.

RPM0B8 ACCURATE MASS MEASUREMENT USING A COMPUTERIZED ION CYCLOTRON RESONANCE MASS SPECTROMETER, RICHARD L. HUNTER and ROBERT T. McIVER, JR., Dept. of Chem., Univ. of Calif., Irvine, CA 92717

In principle, the m/e of an ion in an ion cyclotron resonance (ICR) mass spectrometer can be determined by knowing the magnetic field strength and applied excitation frequency using the simple expression:

$$\omega = qB/m$$

However, this has been shown to be accurate to within only about 1 part per hundred due to higher order terms related to applied electric fields and the number of ions. A scheme for correcting for these effects has been developed for use with a pulsed ICR mass spectrometer. The system uses a programmable frequency synthesizer and a minicomputer data system to obtain accurate mass measurements.

RPM0B9 Applications of A Multi-User, Multi-Instrument Data System. P.R.J. Matejcek and W. A. Wolstenholme, Varian MAT Mass Spectrometry, Florham Park, N.J.

The use of Mass Spectrometry, in particular GC/MS, in modern analytical laboratories is continuing to increase. Many laboratories are now equipped with more than one mass spectrometer and a variety of well-known analytical reports may be generated from a single set of data. GC/MS data is characterized in particular by it's large volume and it's wide range of intensities. The efficiency of data handling is enhanced when it is possible to generate several reports simultaneously with data acquisition from one or more mass spectrometers. A wide dynamic range of intensity measurement in a single scan is also highly desirable.
The Varian MAT SS200 is a PDP 11/34 - based Mass Spectrometry Data System designed for Multi-User, Multi-Instrument use with a wide dynamic range (10 high 4 to 1) in a single spectrum. The system has been used in a variety of applications including the analysis of a complex flavor mixture. The flexibility and wide dynamic range of the system will be illustrated.

A GC-MS-DS TO SUPPORT PHARMACEUTICAL RESEARCH: PRACTICAL DESIGN CONSIDERATIONS IN VIEW OF THE PENDING GOOD LABORATORY PRACTICES REGULATIONS

Wm. Bryant, M. Trivedi, B. Hinchman, and S. Sofranko
Departments of Analytical Chemistry and Computer & Statistical Operations, Pennwalt Pharmaceutical, Rochester, N.Y. 14623

P. Matachek, Jr., Department of Chemistry
St. John Fisher College
Rochester, N.Y. 14618

In the Spring of 1976, the Departments of Analytical Chemistry and Computer and Statistical Operations began a project to construct a data system (DS) to provide on-line support to the Mass Spectrometry Laboratory. At the time the project began, it was apparent that certain regulations then being formulated by the Food and Drug Administration (FDA) would have a direct bearing on some experimental operations of this laboratory. The pressing need to automate operations within this laboratory dictated that we could not wait until the nature of the forthcoming regulations became entirely clear. The DS project thus began under the general guidelines that the system developed must facilitate the conduct of good experimental practices and should provide explicit routines for on-line data collection, processing, data storage and retrieval as well as instrument calibration.

Two local factors had an immediate and profound effect on the project. The first was the decision that maximum use would be made of existing facilities; the second was that there should be minimum interference with an important series of clinical studies with which we were then involved. The first factor meant that the DS would have to operate on a computer already supporting two large information systems. The second led us to develop the DS in two phases. In the first phase, initial efforts were concentrated on software and hardware developments for quantative applications. Once these became operational, the system was expanded in a second phase such that the DS would support repetitive mass scanning capabilities for the acquisition of mass spectra.

The mass spectrometer included in this work consists of a quadrupole mass filter and control equipment manufactured by Extranuclear Laboratories, Inc. It is linked to a Digital Scientific 4/1800 computer through an interface designed and built in our laboratory. Data taken by the interface is transferred to the computer as a block of four words consisting of intensity, mass voltage, clock and clock. The double precision digital clock forms an integral part of the peak detection algorithm covered in poster secession TPM21.

Programs for on-line data acquisition and mass peak identification are written in assembly language. Those for instrument calibration, data processing, storage and retrieval, as well as those provided by Tektronix® for operation of the video terminal, are in Fortran. All programs have been divided into modules and efficiently linked so that the largest area of core required is 9.6K words. The terminal is operated at 9600 baud to maintain maximum operating efficiency.

When the user initiates system operation, four options become available: (1) Mass Calibration (MCL), (2) Selected Ion Monitoring Calibration (SMCAL), (3) Record-MS, and (4) Record-SIM. Standard procedures for MCL involve the use of a reference standard such as decafluorotriphenylphosphine or FC-43. The spectrum of the reference standard is tabulated and the user enters any corrections. Thereafter, the user may select from among the three remaining options depending on the type of experiment scheduled.

For option (2) the known molar ratios of unlabeled and labeled internal standard are entered for a series of prepared mixtures. The response ratios are measured and the calibration constants determined through least-squares linear regression. The data for all standards

and the calibration constants are stored as an integral part of the study record.

When data for mass spectra is to be analyzed, scans to be displayed are selected by examination of the total ion current chromatogram. Spectra may be entered into a Holding File while the rest of the chromatogram is assessed. Unknown mass spectra may be identified by invoking a Probability Based Matching routine which causes spectra from an in-house library to be compared to specific entries in the Holding File. For permanent retention, mass spectra are transferred to the Library File.

For specific experiment, the computer file is identified by a unique, 5-character alpha/numeric code which is based on a laboratory-wide experiment protocol numbering system. Files for quantative experiments are divided into two distinct areas. The first area contains data for all calibration curves recorded during the experiment. Each calibration is identified by a unique, sequential number which is automatically assigned when the SMCAL option is invoked. The second area contains data for samples. Each sample is identified by a 4-section code which comes directly from the experiment protocol. This code contains the subject or animal number, the specified period within which the samples were collected (such as day 14, etc.), a dosage or formulation code, and the time when the samples were collected. Any or all sections of the sample identifier may be specified in retrieval options. Thus, it is any easy matter to organize data for statistical evaluation or report generation.

During long-term experiments it is advantageous to be able to check instrument calibration. With this system, standards used in calibration may be reinjected to verify system stability and consistency. Data for these standards are stored in order of acquisition with the data for samples. Thus, an exacting record is maintained for each experiment.

Retrieval options for mass spectra are also based on a sample identifier. Prior to running a sample, the user fills in an identifier block which has been drawn on the screen of the video terminal. The name of the compound, experiment number, compound number, sample/run number, and 60-characters of descriptive information can be entered. Any or all of these fields may be specified when searching the Holding or Library Files.

COMPUTERIZATION OF THE HITACHI-PERKIN ELMER RMH-2 MASS SPECTROMETER, D. Thomas Terwilliger, Department of Chemistry, University of Pennsylvania Philadelphia, PA 19104.

The RMH-2 is a high resolution, double focussing, Nier Johnson mass spectrometer designed prior to wide-spread use of data systems and therefore, not compatible with them. The most serious problem was that only a linear current scan was available for the magnet, whereas most data systems require an exponential scan. In addition, most of its power supplies were not stable enough to provide the needed accuracy.

The list of modifications that were made to the RMH-2 to remedy these defects are given in table 1. The data system was in considerably better

TABLE 1 NECESSARY RMH-2 MODIFICATIONS

1. Rewired the scan circuit from linear to exponential.
2. Rewired the relay control circuits for the computer.
3. Added a total-ion current monitor.
4. Replaced the accelerating voltage and E.S.A. power supplies.
5. Added a continuous voltage control for the ion multiplier.
6. Rebuilt the entrance and exit slits.

TABLE 2 DS-50 MODIFICATIONS MADE

1. Added a second disk for under $1200.
2. Wrote a program to measure dynamic resolution.
3. Modified the peak-average program to screen out noise.
4. Wrote a program to analyze overlapping isotopes.

condition, but a number of modifications, listed in table 2, were necessary. The most important of these consisted of the dynamic resolution program. This is an absolute necessity, as the position of the magnet necessary for optimum resolution in the static mode is considerably different from that necessary for even a slow scan rate of 30 seconds per decade.

The results of the above modifications are given in table 3. The

TABLE 3 RESULTS OF THE MODIFICATIONS

1. The RMH-2 has been successfully computerized.
2. Both low and high resolution spectra can be run routinely.
3. Calibration can be routinely achieved to m/e 855 at the full 8kV accelerating voltage.
4. Mass accuracies of better than 3 ppm can usually be obtained for the major fragments.

RMH-2 is the primary instrument in the University of Pennsylvania mass spectrometry service laboratory. Spectra are provided to members of the chemistry department and a growing number of users from outside the university. Since the primary users are synthetic chemists, the center must be capable of handling the wide variety of samples submitted. In particular, many samples contain multiple hetero-atoms such as selenium and tellurium which have many isotopes. This can produce a number of problems when running high resolution spectra, as there will be numerous unresolved multiplets at the same integer mass.

It is a well known fact that data systems can produce mass accuracies which far exceed the instrumental resolution. In our case, spectra run at a resolution of 1 in 7000 usually give mass accuracies of 1 in 300000 or better. When analyzing spectra containing multiple hetero-atoms, the formula matching program in the data system will not operate correctly, as it attempts to match an averaged experimental mass with individual isotopic formulas. The program "isotope" calculates the expected isotopic distribution for any formula. Weighted exact masses are calculated for peaks that lie within the instrumental resolution, which can then be matched manually to the experimental data. Eventually I plan to integrate this directly into the formula matching program to produce automatic analyses.

An example of the utility of this approach can be demonstrated in the spectrum of $C_2H_4Se_3$, which is typical of the samples of this type that are submitted for high resolution. For each formula, the program isotope was

run and the results were compared to the experimental data. In some cases intensity agreement could be obtained only by adding in contributions from formulas differing by several hydrogens. The utility of the program in determining the existence of these additional fragments is apparent, as none of them could be observed directly. The results are given in table 4.

TABLE 4 ISOTOPE ANALYSES

FORMULA(S)	RMS DEVIATIONS AVERAGED OVER THE ISOTOPIC ENVELOPE: MEASURED - MOST ABUNDANT ISOTOPE	MEASURED - ISOTOPIC AVERAGE	AVERAGE - MOST ABUNDANT ISOTOPE
$C_2H_4Se_3$	1.62 mmu	1.47 mmu	0.66 mmu
Se_3	1.20	1.07	0.67
$C_2H_4Se_2$	1.04	1.12	0.55
Se_2 and HSe_2	0.99	0.40	0.75
C_2H_4Se, C_2H_3Se, and C_2H_2Se	2.98	1.36	2.96

Column 2 gives the results from the formula matching program. RMS deviations of the errors of the most abundant isotope from each peak are given. Peaks consisting of primarily one isotopic formula have been excluded. Column 3 gives the results of matching the experimental masses with those calculated by the program isotope. The errors are lower, although not by as much as expected. This is due to the relatively large experimental error, which often cancels the error from ignoring the overlapping isotopes. Column 4 gives the RMS difference between the calculated mass of the most abundant isotope and the average isotopic mass. This is the best that could be obtained with any instrumentation if no allowance is made for the overlapping isotopes. The resolution necessary to resolve these multiplets ranges from 9000 for formulas with different numbers of hydrogens, to 600000 for different isotopes of the same formula, well beyond the capability of most instrumentation.

Another specialized experiment we have run involves determining the isotopic enrichment of water samples. Since there is no multiple peak monitoring capability available, I used a slow scan from m/e 20 to 17.5 at a rate of 130 seconds per decade, the upper limit of the data system. The resolution was reduced to 600 to improve ion statistics. Various data system modifications produced on-line mass conversions and accurate intensity ratios. Distilled water was employed as a standard to correct for H_3O^+ formation. The results of preliminary work used to evaluate this technique are given in table 5. Column 2 gives the calculated atom precent deuterium

TABLE 5 DEUTERIUM ANALYSES OF WATER

	SAMPLE	ATOM PERCENT D	ERROR
1.	Distilled water	0.0150 ± 0.0069	------
2.	1/10000 enriched water	0.0246 ± 0.0057	0.0004
3.	1/1000 enriched water	0.1035 ± 0.0073	0.0115
4.	Repeat of 3	0.1191 ± 0.0058	0.0041
5.	Second repeat of 3	0.1206 ± 0.0058	0.0056
6.	Average of 3 - 5	0.1144	0.0006

and the standard deviation of 20 to 30 scans. Column 3 gives the absolute error determined from the known sample enrichment. These numbers may be fortuitously low; the standard deviations of roughly 1 in 20000 are probably a better indication of our sensitivity and accuracy.

In conclusion, I have successfully computerized an instrument that was never designed to be. Both high and low resolution spectra are run on a routine basis. Unresolved isotopic multiplets, which occur quite frequently in our samples, can be analyzed successfully. The utility of the instrument in determining isotope ratios has been demonstrated with a sensitivity comparable to that obtained by multiple peak monitoring.

AUTOMATIC NORMALIZATION OF MASS ABUNDANCES IN SCANNED MASS SPECTRA

Jeff Justice
Hewlett-Packard Company, 1601 California Ave.
Palo Alto, CA 94304

This paper explains how software is used to normalize the mass abundance ratios of the HP-5992 and the advantages of doing this.

Some of the factors that influence mass abundance ratios in a mass spectrometer are:

1. the entrance conditions to the quadrupole
2. the exit conditions from the quadrupole
3. the electron multiplier response factor
4. the voltages on the optics elements of the source
5. the cleanliness of the source
6. the procedure used by the operator to tune the source

Eichelberger, Harris, and Budde have developed a standard for mass abundance ratios based on a study of four magnetic sector instruments and eleven quadrupole instruments. The standard (published in Analytical Chemistry, Vol. 47 in 1975) is based on the compound decafluorotriphenylphosphine (DFTPP) which gas chromatographs well and has large fragments in the most-used mass ranges. The standard includes tests for whether the mass-spectrometer has adequate resolution and sensitivity. The parts of the standard that refer to mass abundance ratios are shown in this table:

Standard Mass Abundance Ratios for DFTPP

Mass	Relative Abundance
51	30% to 60%
127	40% to 60%
198	100%
275	10% to 30%
442	40% to 100%

Previously, instruments have conformed to this standard by varying voltages in the analyzer. Unfortunately, this tends to lower sensitivity and put an additional constraint on the design of the mass spectrometer. Normalizing spectra with software eliminates these problems.

The method for software normalization of abundances is as follows:

1. The voltages in the instrument are set for maximum sensitivity in the desired mass range. This is done automatically on the compound PFTBA.
2. The heights of six peaks in the PFTBA spectrum are measured. The height of these peaks is then ratioed to a secondary standard for PFTBA:
   MASS ABUNDANCES RATIOS FOR PFTBA (SECONDARY STANDARD)

MASS ABUNDANCES RATIOS FOR PFTBA (SECONDARY STANDARD)

Mass	Abundance
50	1.2%
69	100.0%
131	55.0%
219	55.0%
414	2.5%
502	2.5%

PFTBA is used as a secondary standard because it is volatile, and can be introduced into the chamber continuously. The ratio of the standard height to the measured height forms the normalization factor for the above six masses. The normalization factor for other masses is formed by a linear interpolation between the standard masses. The normalization factor for masses below 50 is the same as for mass 50 and the factor for masses above 502 is the same as for mass 502.

3. All spectra taken by the GC/MS acquisition program are multiplied by the normalization factors. To check the secondary standard, a spectrum of DFTPP may be recorded. If it does not meet specifications, then another program can be run to recalculate the normalization factors based on the primary standard.

THE DEVELOPMENT OF AUTOMATIC SAMPLER AND LIBRARY SEARCH SYSTEMS FOR COMPUTER CONTROLLED GC/MS OPERATION

H. Roden, R. L. Conrad, E. I. du Pont de Nemours & Co., Inc.
Instrument Products Division, 1500 S. Shamrock Ave., Monrovia, CA 91016

Over the past several years our laboratory has been developing GC/MS systems that are inherently more reliable and easier to maintain than were classical systems. These new systems also run under computer control, making automatic analysis not only possible, but practical. A project to implement this capability was conducted for the Du Pont DP-1 GC/MS.

Beyond a reliable computer controlled GC/MS, an automatic sampling device and a complete set of automatic analysis software is required to successfully do automatic analysis. The typical mission of automated GC/MS is to run a set of samples and produce a prescribed report in which the GC peaks are detected, identified, and quantitated. However, the variety of possible samples and reports for a typical laboratory is very large, so that system flexibility, along with ease of system programming, is very important. Also, once the system is automated, the capability to do single sample analysis and to interact with the data processing must also be maintained. An added feature that we have found useful is to allow the system to have random access to the loaded samples. With this capability, the operator can alter the analytical sequence, recall samples for further analysis, or use the system as a single sample injector. In this sense, the sampler is treated like a computer peripheral device.

The auto sampler is programmed by selecting the initial GC temperature, the type of syringe wash, the location of the wash position by rack and vial numbers, and sample size and sample position by rack and vial numbers. When this program is run, the GC door automatically opens and cools the oven to the initial temperature, the sample brings the wash into position and cleans the syringe, and then brings the specified sample into position and loads the syringe. Injection is controlled by the data acquisition programs.

The system has several levels of possible control. After the syringe is loaded it is possible to call up and run a data acquisition operation, and after that operation has run, to initiate a data processing and display operation. It is also possible to string these same operations together, and they will run in sequence. In addition, after a particular operation has been programmed by selecting the running parameter, it is possible to declare that operation as a method, and to then recall and run that method or a string of methods. Thus the system operator has the flexibility to program the instrument for his types of analyses.

IDENTIFICATION OF CHEMICAL RESIDUES FOUND IN PEANUT BUTTER

David L. Heikes
U.S. Food and Drug Administration
Kansas City, Missouri 64106

The Food and Drug Administration (FDA) conducts a program for the surveillance of pesticides and industrial chemicals in processed foods. This survey, known as the Total Diet Program, is headquartered in the Kansas City District Laboratory. Each sample or market basket represents the food consumed by a 16-19 year old male - our nation's largest consumer - in a two-week period. The various items of each market basket are divided into twelve composites, and analyzed by procedures found in the Pesticide Analytical Manual of the FDA. Residues of pentachloronitrobenzene (PCNB) and related compounds have been found consistently in the composite containing fats and oils. Peanut butter has been found to be the main source of PCNB in this composite.

PCNB is an effective soil fungicide[1] and has been used extensively for a number of years. Its use in the control of some fungi found on peanuts has also been established.[2] Metabolism of PCNB to pentachloroaniline (PCA) is common to various organisms, and metabolism to pentachlorothioanisole (PCTA) is specific for several fungi.[3] Residues of these metabolites as well as PCNB impurities of hexachlorobenzene (HCB) and pentachlorobenzene (PCBZ) have been reported in soil and vegetables.[4,5]

Initial GC/MS analyses of peanut butter showed residues of PCNB, PCA, PCTA, PCBZ and HCB. Pentachloroanisole (PCAS) which tends to co-elute with HCB on most packed GC columns, has also been identified. The levels of PCAS found appear to correlate with the levels of PCNB and related compounds, indicating that PCAS may be a previously unreported residue of PCNB. Since it has been demonstrated that pentachlorophenol (PCP) can be methylated microbiologically to PCAS[6], the samples were also analyzed for PCP. The levels of PCP found seem to correlate with those of PCNB and related compounds. Residues of tetrachloronitrobenzene (TCNB) were found in all peanut butter samples. Analysis of Terraclor®, a commercial preparation of PCNB, indicates that TCNB as well as HCB and PCBZ are impurities.

In this study, peanut butter from several market basket samples was analyzed for PCNB and related compounds. The oil extracted from the peanut butter was first passed through a gel permeation column (GPC) of OR PVA 2000 beads with 30% methylene chloride in acetone. The eluate containing the residues of PCNB and related compounds is 99% fat free.[7] One-half of this eluate was methylated with diazomethane and both halves were then individually passed through a florisil column with 6% ethyl ether in petroleum ether. The eluates were quantitated using glass capillary gas chromatography (GC^2) with electron capture (Ni^{63}) detection. The quantity of PCP in each sample was represented by the difference of PCAS in the methylated and unmethylated eluates.

All eight compounds were found in each peanut butter sample. The results of analysis of seven peanut butter samples are listed in Table 1.

Table 1 Residue levels of PCNB and related compounds in seven peanut butter samples. Results are given in ppb.

Compound	Ave.	Range
PCNB	4.4	0.8 - 9.4
PCBZ	19	1.8 - 62
HCB	9.7	0.97 - 38
TCNB	1.2	0.31 - 4.3
PCA	45	3.4 - 140
PCTA	22	2.4 - 61
PCP	18	1.8 - 62
PCAS	12	1.5 - 33

1. B. Strecker; Z. Pflanzenkrakenheiten u. Pflanzenschutz, 64 9-35 (1959).

2. C. R. Jackson; Plant Disease Reptr. 49(11) 928-31 (1965).

3. T. Nakanishi and O. Hachiro; Hippon Shoknbutsu Byori Gakkaiho, 35 (5) 339-46 (1969).

4. J. H. Smelt, M. Leistra; Agric. Environ. 1 (1) 65-71 (1974).

5. N. Iwata, T. Suda, K. Yamada; Gumma-Ken Nogyo Shikenjo Hokoku, 18 65-74 (1978).

6. A. J. Cserjesi, E. L. Johnson; Can. J. Microbiol., 18 (1) 45-9 (1972).

7. M. Hopper; to be published.

GC/MS DETECTION OF MAMMALIAN URINE

Gabriel D. Castillo and Reno B. Bradicich

Food and Drug Administration, Dallas, Texas 75204

Food and drug products may become contaminated with animal filth by the use of unclean raw materials or the preparation of these products under insanitary conditions. Therefore, the law requires that food and drug production and storage be kept free from infestation by animals such as insects or rodents. Accordingly, the Food and Drug Administration has the responsibility of detecting and demonstrating such problems in plants under its jurisdiction so that corrective action may be taken.

In demonstrating rodent infestation a case can be established by the evidence collected at the site during inspection and by laboratory findings. These may include positive identification of rodent hairs or excreta pellets or confirmation of the presence of rodent urine on stained packaging material collected by the inspector. Earlier confirmatory tests were based on the microchemical identification of urea in the stained material and there were several tests that were satisfactory for this purpose.

Since these tests did not provide information concerning the source of the urea, a need remained for a more specific confirmation of rodent urine, especially in those cases where there is no additional supportive evidence. In 1973, Thrasher reported such a specific test based on the TLC detection of urea, allantoin and urinary indican (1). This method is highly accurate and has been used successfully in our laboratory in testing various materials. However, this method is long and requires considerable effort, so we recently decided to investigate the possibility of analyzing for the three compounds by GC/MS. This report describes our initial approach to provide a useful procedure.

Urea and urinary indican (potassium indoxyl sulfate) give suitable chromatographic response directly, although the latter may decompose to indoxyl (3-hydroxyindole). However, allantoin (5-ureidohydantoin) was retained on the columns tried, so we decided to use the trimethylsilyl derivatives for the analysis. Because of the possible very low urine levels in some samples, selected ion monitoring was chosen for the determination.

All three compounds have more than one reactive sites and it was found that the urea and indican give the di-TMS derivatives in high proportion. In the latter, the sulfate ester is hydrolyzed and the resulting indoxyl forms the derivative. Allantoin gives approximately equal amounts of the tri- and tetra-TMS derivates, but the mass spectrum of the latter has the non-specific mass 73 as the predominant ion, therefore, the tri-TMS derivative was selected for analysis.

Three ions were selected for its detection from the mass spectrum of urea di-TMS: two high intensity ions, 147 and 189, and the molecular ion 204. The mass spectrum of indican di-TMS exhibits two major ions, 73 and 277, the molecular ion. The latter and three low intensity ions, 163, 202 and 262, were used to detect this compound. The four ions of the mass spectrum of allantoin tri-TMS that were monitored are 189, 259, 359, and the molecular ion 374.

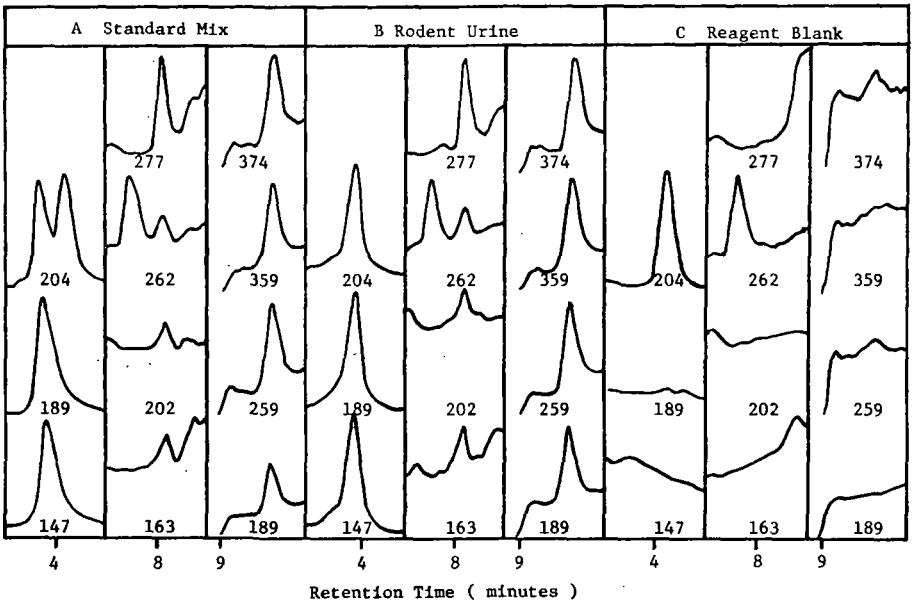
The analytical procedure is described briefly as follows. A standard mix solution was prepared containing urea 4 mg/ml, indican 0.1 mg/ml and allantoin 4 mg/ml. Normally the urea concentration in urine is five times as much but this was adequate for our purposes. As in the original TLC procedure, the suspected material was extracted four times with 5-10 ml of boiling acetone and the extracts were combined in a screw-capped vial. The solvent was evaporated under a stream of nitrogen with gentle heating on a steambath and the residue was dissolved in approximately 50 µl of dry dimethylformamide. The TMS derivatives were prepared by adding 100 µl each of bis-trimethylsilyl-fluoroacetamide and dry pyridine. The vial was capped and placed in a water bath at 50°C for 1 hour. A reagent blank and 1 ul of the standard mix were similarly treated. The cooled solutions were analyzed by GC/MS. A column of 3% OV-101 on Chromosorb W-HP was used and the temperature was held at 105°C for 2 minutes and then programmed at 16 degrees/minute. Preliminary chromatography of the individual components gave the following retention times of the derivatives (in minutes): urea - 3.9, indican - 8.1, and allantoin - 9.5.

Figure 1 A, B and C are composites of the relevant areas of the SIM

chromatograms of the standard mix, a rodent urine sample, and the reagent blank respectively. A and B each exhibit the three ions monitored for urea di-TMS at 3.9 minutes. The four indican di-TMS ions are present at 8.1 minutes in A and B. And at 9.5 minutes on these same two chromatograms, we see the four allantoin tri-TMS ions. There is also an intense mass 204 peak at 4.1 minutes in Figure 1 A. This is present in the reagent blank chromatogram and is reduced to a shoulder of the urea peak in the urine sample due to the high urea level. Figure 1 C shows that the monitored ions are absent in the reagent blank at the retention times of interest.

Although the lower limits of detection were not determined, the amount of the standards analyzed, i.e., 4 µg urea, 0.1 µg indican, and 4 µg allantoin, were readily detected, making this procedure at least as sensitive as the TLC procedure.

Figure 1 SIM Chromatograms of TMS Derivatives



References

1. Thrasher, J. J., JAOAC 56, 637 (1973).

RPM0C3 ANALYSIS OF THE URINARY METABOlites of the carcinogen acrylonitrile, Yong Y. Lin and Ahmed E. Ahmed, Univ. of Texas Medical Branch, Galveston, Texas 77550

Acrylonitrile (VCN) a widely used monomer in polymer industry is demonstrated carcinogen in animals and humans. To study the biological fate of VCN, urine of rats receiving an oral 0.5 LD50 dose of VCN was collected. The metabolites were separated and purified. From these metabolites n-propyl ester and acetate derivatives were synthesized. Methane chemical ionization GC/MS analysis of the derivatized samples indicated the presence of three compounds: 1) N-acetyl-S-acetoxyethyl-cysteine propyl ester [m/e: 292(M+H), 232(M-$OCOCH_3$ and M-H_2NCOCH_3), 204(M-$CH_2CH_2OCOCH_3$), 172(M-$SCH_2CH_2OCOCH_3$)], 2) N-acetyl-S-chloroethyl-cysteine propyl ester [m/e: 268(M+H), 232(M-Cl), 208(M-H_2NCOCH_3), 204(M-CH_2CH_2Cl), 172 (M-SCH_2CH_2Cl), and 3) N-acetyl-S-propoxy-carbonylethyl-cysteine propyl ester [m/e: 320(M+H), 260(M-H_2NCOCH_3), 232(M-$COOC_3H_7$), 204(M-$CH_2CH_2COOC_3H_7$), 172(M-$SCH_2CH_2COOC_3H_7$)]. This study shows the great utility of GC-MS for monitoring both occupational and environmental exposure to VCN.

IDENTIFICATION OF METABOLITES OF HEXAZINONE BY MASS SPECTROMETRY

Robert W. Reiser, Irvin J. Belasco, Robert C. Rhodes
Biochemicals Department, Research Division
E. I. du Pont de Nemours & Co., Inc.
Wilmington, Delaware 19898

Figure 1 shows the structure and mass spectrum of hexazinone [3-cyclohexyl-6-(dimethylamino)-1-methyl-1,3,5-triazine-2,4(1H,3H)dione], which is the active ingredient in Du Pont's Velpar® Weed Killer. Velpar® is registered in the United States and many foreign countries for non-crop weed control, such as: industrial plant sites, and railroad right-of-ways.

Radiolabeled hexazinone, employing ^{14}C, was used for metabolism and environmental fate studies. Early metabolism studies were done with rat liver microsomes and stem-injected plants. The major metabolites obtained in these studies were identified by mass spectrometry, and were synthesized for use in further metabolism and residue studies. In general, the same routes of metabolism were obtained in subsequent studies with plants, animals, and soil, but more extensive degradation occurred due to the longer exposure times.

The base peak in the mass spectrum of hexazinone at m/e 171 is due to loss of the cyclohexyl group with a double hydrogen rearrangement, and the fragment at m/e 128 is due to loss of HOCN from the m/e 171 via the retro Diels-Alder Reaction. Figure 2 shows a proposed mechanism for the double hydrogen rearrangement, which is likely obtained by transfer of two hydrogen atoms from the cyclohexyl group to the carbonyl oxygens through 6-membered cyclic transition states. The driving force for this rearrangement is due to the resonance stabilization of both the ion and radical products formed. This fragmentation is responsible for the base peak in the spectrum of hexazinone and all of its major metabolites.

Figure 3 shows the metabolic pathways of hexazinone. All of these metabolites were identified by mass spectrometry. The metabolites were separated by thin-layer chromatography, and mass spectra were obtained by direct probe or GC/MS. In some cases, it was necessary to prepare the TMS or TFA derivatives for GC/MS analyses. The major metabolic reactions were hydroxylation and demethylation. Deamination was a minor reaction in most biological systems.

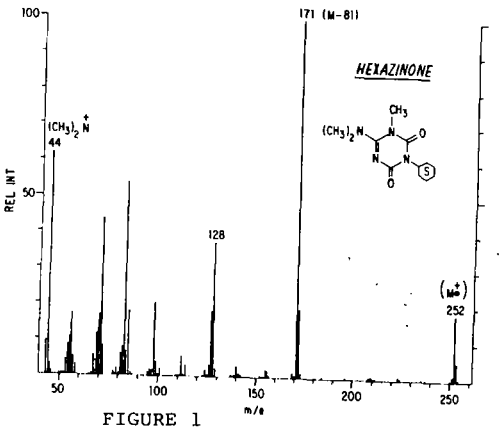


FIGURE 1

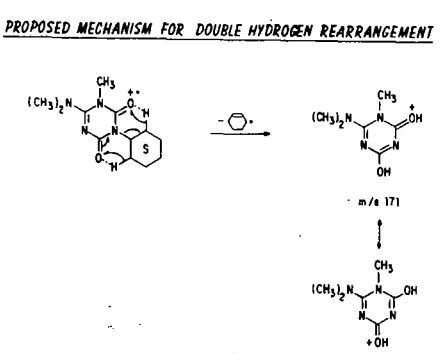


FIGURE 2

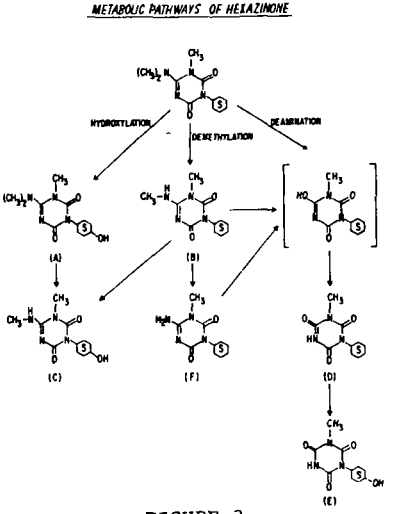


FIGURE 3

An On-Line Segmented Flow LC/MS Combination

B.L. Karger, D.P. Kirby and Paul Vouros
Institute of Chemical Analysis
Northeastern University
Boston, Massachusetts 02115

and

B. Hidy and R.L. Foltz
Battelle Columbus Laboratories
505 King Avenue
Columbus, Ohio 43201

The addition of a modified segmented-flow extractor between a liquid chromatograph (LC) and a mass spectrometer (MS) permits the direct combination of an LC operated in reverse phase to an MS without compromising the operational characteristics of either. This combination is accomplished by the extraction of solutes into a volatile organic solvent which is then transported into the MS via a moving belt interface. The system has been tested with a mobile phase consisting of 40/60 MeOH/H_2O, 0.1 M NaH_2PO_4, pH 2.5 at a flow rate of 0.5 ml/min, and was operated for a significant period of time with no deterioration of the performance of the MS. The applicability of the interface to the analysis of carbamate pesticides has been examined. The effects of the interface on peak broadening and sample recovery will also be presented.

This device provides a means of performing reverse phase liquid chromatography, even with non-volatile buffers, in an on-line combination with an MS.

THE USE OF MEMBRANE INLET SYSTEM FOR THE DETERMINATION OF TRACE ORGANICS IN AIR

Ashby W. Spratley, Jr. and Dale Talbert
Union Carbide
Chemicals and Plastics
Taft, Louisiana 70057

The typical analytical mass spectrometer is not ordinarly considered a sensitive instrument. Equipped with the usual inlet system for the routine analysis of liquid and gas sample, this is certainly true. However, considering the minute quantity of the material used by the source to produce a spectrum, the mass spectrometer actually has sensitivity comparable to that of the flame ionization detector. The difference is, with the flame ionization detector, the compound being sought can be diluted by a large amount of any gas not detected by the system. The mass spectrometer, however, is affected by the total amount of material present. Large amounts of a diluting gas severely reduce the sensitivity of the mass spectrometer even if its spectrum does not interfer with that of the compound sought. Therefore to utilize the high sensitivity of the mass spectrometer, the compound of interest must somehow be introduced onto the source without introducing the gas containing it.

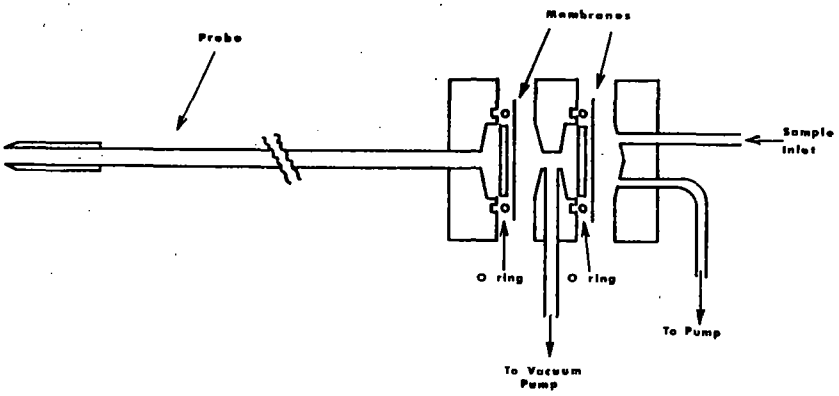
Mr. Meier[1] described the use of a membrane inlet system, probably based on the Llewellyn membrane separator, that seemed to do just this job with the portable mass spectrometer developed for the army. Therefore we built a membrane inlet to study. Figure One is a simplified cross section diagram of how the devise is constructed. Briefly, it consist of three disc. The membrane is supported on the low pressure side of a sintered glass plate (filter disc) that fits flush into stainless steel disc. The outside edges of the membranes are sealed with "O" rings fitted into a groves machined into the disc when the assembly is pulled together. Sample is drawn through an 1/8 inch tube into the small space over the first membrane and out a second 1/8 inch tube by a small diaphram pump. The space between the membranes is pumped with a small mechanical vacuum pump. Material that passes through the second membrane goes to the source of the mass spectrometer through the tube attached to the third plate. This is inserted into the mass spectrometer in place of the solids probe. In use, the membranes are heated with two cartridges heaters that fit in wells toward the outside of the separator. For simplicity, they are not shown.

Using this devise in very straight forward. The device is inserted and pumped down simular to introducing the solids probe. As soon as the probe end is pumped down, the vacuum pump connected to the space between the membranes is started. The heat is turned on and the separator gradually heated to operating temperature. The system is usually allowed to pump for one to two hours to remove background and allow temperature to stabalize. The output signal of the Mass Spectrometer is recorded with a multirange strip-chart recorder. Synthetic samples over the range of interest are prepared in ten liter plastic bags using standard industrial hygiene techniques. The mass spectrometer is adjusted to bring a selected large, and if possible unique, fragment into register. It is often helpful to feed a high concentration sample through the inlet to aid this adjustment. To run a sample or standard, the sample bag is attached to the inlet line of the membrane inlet system with the diaphram pump running. The recorder pin will rise to some value and stabalize. The sample is removed and the recorder pen returns to base line. The mass spectrometer should be occasionally checked to be sure the desired fragment is still in register. Comparison of the signal from samples to that of known synthetics allows calculation of the amount present.

One actual analytical problem solved with the membrane inlet system involved the determination of ethylene dichloride in the air over some sumps in our waste treatment area. Conventional analysis for ethylene dichloride with gas chromatograph equipped with a flame ionization detector had given values in excess of 70 ppm. However the chromatographs obtained were very complex due to the mixed hdyrocarbons present and the peak attributed to ethylene dichloride was suspected to be actually due to a hydrocarbon. Ethylene dichloride synthetics were prepared and found to work

very well with the membrane inlet. As little as 0.1 ppm could be detected Ten liter samples were collected at each location and analyzed by this technique using the m/e 62 fragment. They were first run with the instrument adjusted to the 10-100 ppm range. Then rerun with the instrument adjusted to 10 ppm full scale. One sample showed 3.7 ppm and the other two 0.2 ppm proving the high values by VPC were due to interference. A mass spectrum, run on the sample containing the 3.7 ppm, contained all of the large fragments common to ethylene dichloride and hence its presence could not be ruled out. These results are considered maximum values as the mixture spectrum was too complicated to prove ethylene dichloride present.

The membrane inlet is a very useful inlet system. It is very easy to construct and use. A problem with our present device is somewhat slow response which may well be the cause of it not working well below 0.1 to 1 ppm. We expect to see if heating the tube carrying the sample from the second membrane to the source would not improve its operation. Actually, this is the first one we have built and thought it works well, it is very likely not an optimum design. Using this inlet in place of the trap in "purge and trap" type analysis has been suggested along with many other ideas we hope to try.



MEMBRANE INLET SYSTEM

Figure One

[1]A Field Portable Mass Spectrometer for Monitoring Organic Vapor, by Robert W. Meier, American Industrial Hygiene Association Journal, Vol. 39, No.3, pg. 233 (1978)

RPM0C8 ANALYSIS OF POLYNUCLEAR AROMATIC HYDROCARBONS (PAH) IN DIESEL EXHAUST PARTICULATE BY GC/MS, BRUCE A. PETERSEN, CHENG C. CHUANG, AND RALPH M. RIGGIN, BATTELLE COLUMBUS LABORATORIES, 505 KING AVENUE, COLUMBUS, OH 43201

A method is being developed to determine the quantity of pyrene, benz(a)anthracene, chrysene, benz(a)pyrene, and perylene in diesel exhaust particulate by capillary column gas chromatography-low voltage electron impact mass spectrometry. In this study, perdeutero analogs of each of the above PAH are used as internal standards. A novel method of introducing the internal standards into the diesel exhaust is used so that the deuterated PAH associates with the diesel exhaust in the same manner as the native PAH. Quantification of the native PAH is conducted by Selected Ion Monitoring (SIM) techniques. This method is also being used to study whether artifacts are generated in the exhaust or in the sample collection process. Our experimental method and progress in this study will be described in this presentation. This research is supported by the Coordinating Research Council, Contract CAPE-24-72.

LC/MS USING CONTINUOUS SAMPLE PRE-CONCENTRATION

R. G. Christensen, H. S. Hertz, S. Meiselman, and E. White V

Center for Analytical Chemistry
National Bureau of Standards
Washington, D. C. 20234

A variety of methods for combining HPLC with mass spectrometry have been reported, and the strengths and weaknesses of various methods have been noted [1,2]. We have designed and constructed an LC/MS system which allows the use of conventional LC flow rates, a wide range of solvents, and a differentially pumped quadrupole mass spectrometer of conventional design.

The effluent from a liquid chromatograph is concentrated by allowing it to flow down an electrically heated wire (figure 1). The wire consists of three segments, since it is desirable that the resistance and the diameter of the wire be large at the top where the flow is greatest and small at the bottom where the flow is least. Maximum usable flow rates for various solvents are shown in the table.

The lowest segment of the concentrator wire crosses a gap in a nickel tube through which the remaining liquid stream is drawn into the ion source of the mass spectrometer. The size of the liquid drop in the gap is sensed with a photocell, feedback from which controls the heating current to the wire. The ion source-end of the inlet tube is cold-formed so that the orifice is about 25 μm in diameter. The flow rate of liquid into the mass spectrometer is controlled by means of a tungsten wire with a pointed end, which serves as a tiny needle valve as it seats in orifice.

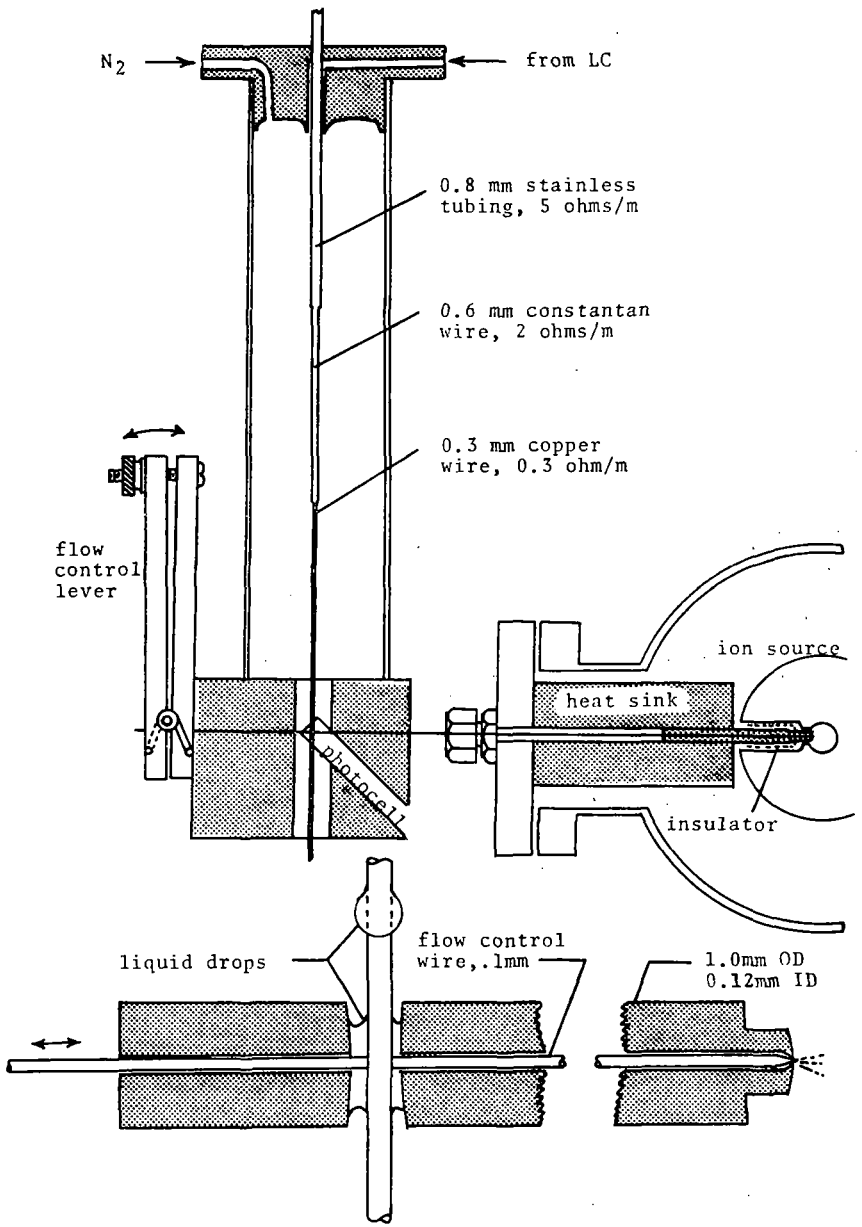
Chromatographic peaks which are about 30 s wide at a UV detector inserted in series between the column and the concentrator wire, are broadened by about 15-20 s and delayed about 1 min at the mass spectrometer. The first trials indicate detection limits for polynuclear aromatic hydrocarbons of about 2 ng of material injected on the column, and a signal enhancement of about 20-fold by the use of the concentrator wire. It is expected that further development will increase the overall sensitivity considerably.

Solution flow rates into the ion source can be adjusted within the range of 2-20 μL/min, allowing spectra of either purely CI or mixed EI/CI character to be obtained with the source and pumping configuration used. Spectra have been recorded for phenanthrene, fluoranthene, chrysene, benzo(a)pyrene, and other polynuclear aromatic hydrocarbons, as well as for phenazine, azafluorene, and adenine.

[1] Games, D. E., Gower, J. L., Lee, M. G., Lewis, I. A. S., Pugh, M. E., and Rossiter, M. in "Methodological Surveys in Biochemistry", vol. 7, "Blood Drugs and Other Analytical Challenges", Reid, E., ed., John Wiley and Sons, New York, pp. 185-194 (1978).

[2] Dawkins, B. S. and McLafferty, F. W. in "GLC, HPLC Determination Ther. Agents, Part I", Tsuji, K. and Morozowich, W., eds., Marcel Dekker, New York, chapter 7 (1978).

Solvent	Max. Flow Rate	ΔH_V
n-pentane	3.0 ml/min	90 cal/g
i-octane	2.8 ml/min	90 cal/g
methanol	1.7 ml/min	260 cal/g
50% MeOH/H_2O	0.7 ml/min	410 cal/g


N_2
from LC
0.8 mm stainless tubing, 5 ohms/m
0.6 mm constantan wire, 2 ohms/m
0.3 mm copper wire, 0.3 ohm/m
flow control lever
ion source
heat sink
photocell
insulator
liquid drops
flow control wire,.1mm
1.0mm OD
0.12mm ID

LC/MS INTERFACE USING MOLECULAR BEAM TECHNIQUES

C. R. Blakley, M. J. McAdams, and M. L. Vestal
Department of Chemistry, University of Houston, Houston, TX 77004

Initial testing has been performed on a new method of interfacing a liquid chromatograph (LC) with a quadrupole mass spectrometer (MS). The entire effluent from the LC is injected into a 0.05 cm ID x 1 cm long copper tube that is heated to about 1000°C by four oxy-hydrogen torches. Vaporization is effected by contact of liquid with the walls and by heat conduction through the vapor. Helium is added to increase the heat transfer efficiency. The resulting vapor expands into an evacuated chamber and is sampled by a skimmer before entering a chemical ionization source where the solvent vapor serves as the reagent gas. Overall sample transfer efficiency is on the order of a few percent.

Basically, this method is similar to that described previously[1] except that the oxy-hydrogen torches have replaced the laser and the large diffusion pump has been eliminated. These changes permit a considerable reduction in cost and size of the interface while retaining the advantage of minimal contact with surfaces. More importantly, the increased heating power and efficiency available with the torches substantially eases the difficult problem of vaporizing water. Thus far, the interface has been used at flow rates of 0.5 cc/min for water and 1.5 cc/min for methanol.

Applications have been oriented toward the components of nucleic acids: bases, nucleosides, and nucleotides. Representative data are shown in Figure 1 which is a chromatogram of a mixture of uracil, 5-hydroxy-methyl-cytosine, 5-methyl-cytosine-hydrochloride, N^6-methyl-adenine, and 7-methyl-guanine. A Partisil PXS 10/25 ODS-2 column was used at 0.4 cc/min with a 10 minute gradient from water, acidified with formic acid, to methanol. Sample sizes varied from 2 to 5 micrograms. At the top is the UV trace from the LC while just below it is the reconstructed liquid chromatogram (RLC) generated by the mass spectrometer data system from 5 second (40 amu/sec) scans. The mass fragmentograms show that, except for uracil and 5-methyl-cytosine-hydrochloride, good separation was obtained. Although not shown, the mass spectra (above m/e 100) at the elution peaks consist almost entirely of the protonated parent except in the case of 5-methyl-cytosine-hydrochloride which appeared solely as protonated 5-methyl-cytosine.

Mass spectra for arginine and guanosine are shown in Figures 2 and 3 which were obtained by injecting about 5 micrograms each into a 0.75 cc/min flow of 50:50 water:methanol without a column installed on the LC. These thermally labile molecules are difficult to analyze by the more usual techniques. Thus the intense protonated molecular ions and the apparent lack of severe pyrolysis demonstrate the utility of the oxy-hydrogen torch as a menas of vaporizing the LC effluent.

The authors gratefully acknowledge the support of the National Institutes of Health under grant GM24031.

---

[1]C. R. Blakley, M. J. McAdams, and M. L. Vestal, J. Chromatogr., 158, 261 (1978)

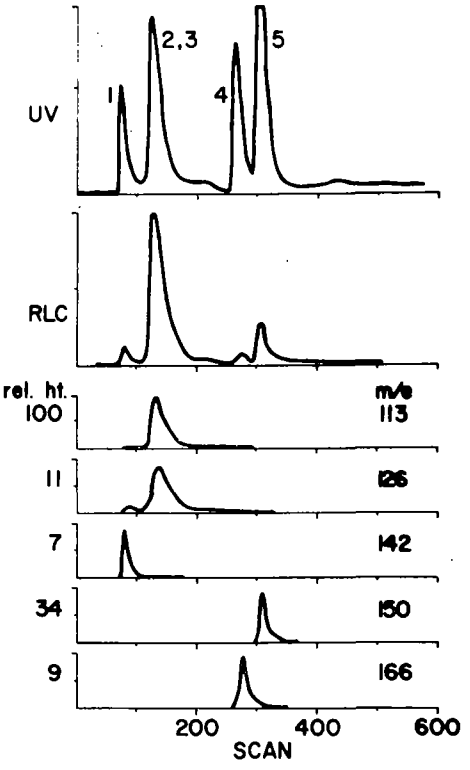


Figure 1: LC/MS chromatogram of a mixture of (1) 5-hydroxy-methyl-cytosine; (2) 5-methyl-cytosine-hydrochloride; (3) uracil; (4) 7-methyl-guanine; and (5) N^6-methyl-adenine. At the top is the UV trace followed by the reconstructed liquid chromatogram (RLC) and the mass fragmentograms.

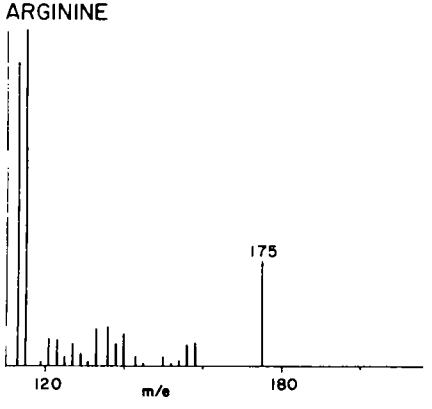


Figure 2: CI mass spectrum of arginine with methanol as the reagent.

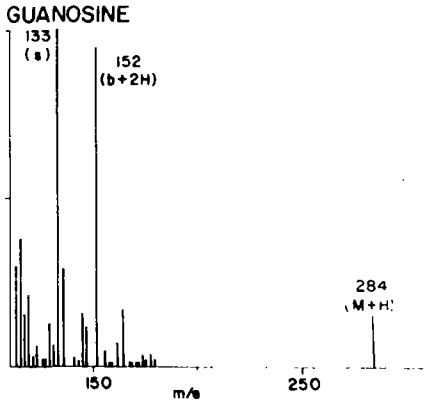


Figure 3: CI mass spectrum of guanosine with methanol as the reagent.

RPMOC11 A NEW HPLC/MS INTERFACE,
D.A.YORKE, P.BURNS and D.S.MILLINGTON,
VG-Organic Ltd., Altrincham, England.

The most versatile method for coupling high performance liquid chromatography (HPLC) with mass spectrometry is a moving belt interface[1] to which the entire column eluate is applied. A new moving belt system has been developed, which has several major differences from those described earlier. In particular, the belt enters the ion source chamber, where the sample is evaporated, while maintaining a seal to allow operation in either EI or CI mode. In addition, the probe on which the belt is supported is insulated from the source chamber so the LC interface is suitable for both magnetic sector and quadrupole spectrometers. The system can be conveniently inserted or removed from the MS as required without interfering with the other inlet systems.

1. W.H.McFadden, H.L.Schwartz and S.Evans, J. Chromatog. 1976, 122, 389-396.

HIGH EFFICIENCY RADIALLY COMPRESSED LIQUID CHROMATOGRAPHY/MASS SPECTROMETRY (RCLC/MS) - IS IT THE ANSWER?, DAVID HILKER and Paul P. DYMERSKI, Toxicology Center, Division of Laboratories and Research, New York State Dept. of Health, Albany, NY 12201, P. CHAMPLIN, Waters Assoc., Milford, MA 01757

Liquid chromatographic electron impact mass spectrometry (LCMS), using a Finnigan moving belt interface, has been applied in our laboratory to several areas of toxicology and environmental research. These areas include complex mixtures of fish and animal extracts, not amenable to gas chromatography, but requiring the specificity of mass spectrometry. LCMS data produced under the same conditions as those used by the chromatographer (column type, flow rate, solvent system, etc.) permitting direct correlation of retention times is essential for complex mixture analysis of this type.

Application of normal phase LCMS has proved valuable. Solvent flows above 1 ml/min of hexane are possible without splitting. Since reversed phase liquid chromatography using acetonitrile/water or methanol/water is most often preferred, however, an effort was made to make LCMS more compatible with these solvent systems by increasing the solvent volume evaporated by the interface and by searching for LC conditions compatible with current LC techniques but less demanding on the interface. (The standard interface will accommodate less than 0.4 ml/min of 80% acetonitrile/water necessitating excessive sample/solvent splitting, thus reducing sensitivity.

The LCMS interface was modified by the addition of a 40 watt "stick" heater to each of the differentially pumped chambers (Fig. 1). Solvent evaporation in each chamber cools the interface making evaporation more difficult. By adding heat in the vicinity of the transfer belt, vaporization is assisted, and flow rates up to 1.0 ml/min of acetonitrile/water or methanol/water can be tolerated. The limiting heater temperature is, of course, vaporization of the sample along with the solvent. At a flow of 1 ml/min, 25% is the practical limit of water as solvent in acetonitrile or methanol due to pressure bursts from water droplets entering the vacuum system. The effectiveness of these auxillary heaters can be demonstrated under the adverse conditions of 50% water/acetonitrile.

Column selection for LCMS is determined by the efficiency of separation at the limiting flow rate of the interface. This in turn is determined by the solvent system necessary for the desired separation. With these parameters in mind, four columns were tested on a mixture of ten polynuclear aromatics (PNA). This group was chosen for its wide range of molecular weights and difficulty of separation by liquid chromatography. Each column was tested with several solvent systems compatible with the interface and the best choice for each is reported in Table 1. The novel Radially Compressed Solvent System (Water Assoc.) was reported to have superior separation capabilities under a wide range of solvent systems. This is listed in Table 1 with the suggested conditions (to fast a flow for the LCMS interface), and the best acceptable conditions. The μC_{18} column (Waters Assoc.) is the most widely used column while the Brownlee RP8 low resolution column, using a similar coating, promised lower flow rates albeit lower resolution. Finally, the Zorbex ODS (DuPont) column is more "active" than most and was found to give better separation with shorter retention times (lower k' values) with several solvent systems (Table 1).

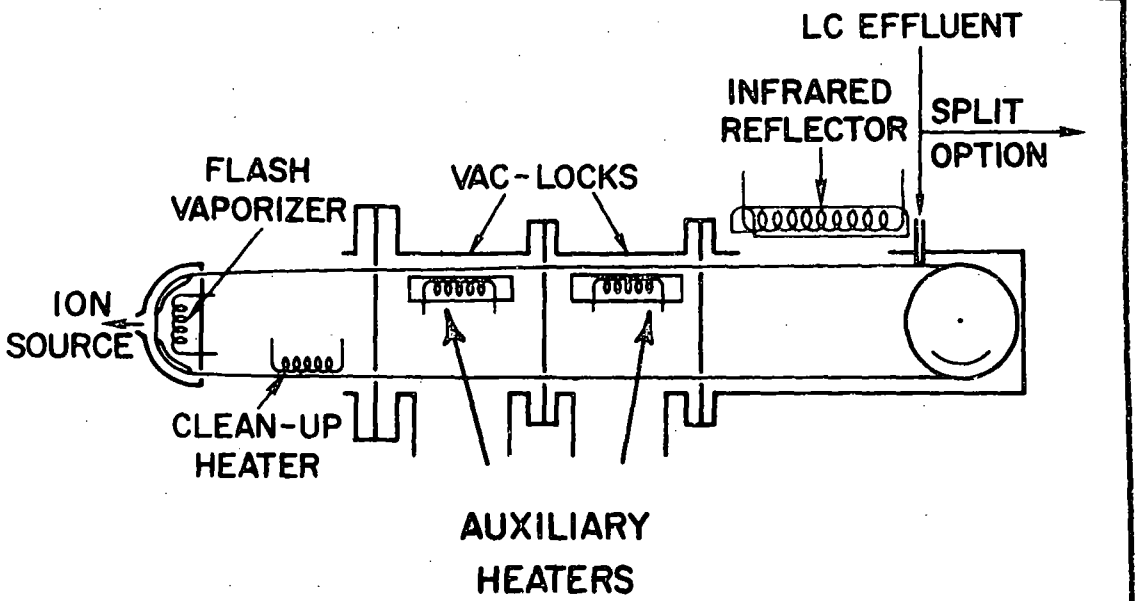
Comparison of the conditions in Table 1 shows that no one column separates all 10 of the compounds by LC/UV (254nm) detection, while the LCMS system monitoring the ion characteristic of each compound can detect all 10 in only 2 cases. Note that for the Zorbex column (chloroform/acetonitrile) unacceptable overlap occurred for LC/UV detection but resolution was maintained when monitored by LCMS specific ion detection.

LCMS ANALYSIS OF 10 PNA STANDARDS

Column	Conditions	Total Retention Time (Min.)	Peaks Separated UV (254nm)	MS	k'(a)
Waters RCSS	60-100% acetonitrile/ water @ 3 ml/min	13.0	8	-	2.6
Waters RCSS	80-100% acetonitrile/ water @ 1 ml/min	18.0	8	10	2.5
Waters μC_{18} 25 cm	80% acetonitrile/ water @ 1 ml/min	20.9	8	9	1.25
DuPont ODS 25 cm	100% Methanol @ 0.7 ml/min	20.3	7	10	1.1
Brownlee RP8 10 cm	75-100% acetonitrile/ water @ 0.8 ml/min	14.5	8	9	4.26
DuPont ODS 25 cm	20% Chloroform/acetonitrile @ 0.9 ml/min	6.3	7	9	.597

(a) Benz(a)pyrene

MODIFIED INTERFACE



Adapted from W. H. McFadden, Finnigan Corporation, Sunnyvale, California.

Combined LC/MS in Studies of Natural Products

D.E. Games, Christine Eckers, P. Hirter, E. Lewis and K.R.N. Rao; Department of Chemistry, P.O. Box 78, Cardiff, CF1 1XL, Wales.

In chemo-taxanomic studies and in the search for new natural products, the availability of rapid methods for the screening of crude or partially purified extracts of natural material are important. Combined GC/MS of derivatized or underivatized material is ideal for many studies; however,often the compounds being investigated may be thermally labile, or insufficiently volatile for GC study.[1] Chemical derivatization cannot always overcome these problems. Combined LC/MS offers a complementary or preferable alternative for studies of this type, since there is considerably less danger of decomposition of the sample and volatility presents no problems.

Our studies[2] in this area have used a commercial LC/MS system of the moving belt type.[3] Samples for investigation are first studied by field desorption mass spectrometry to provide molecular weight profiles. This provides a check for decomposition and/or absorption during LC/MS study. Once suitable LC conditions have been established, LC/MS studies in the EI and/or CI mode are carried out. If known compounds are present their identity is confirmed by comparison of LC retention and mass spectral data. When compounds of unknown structure are located preparative LC is carried out to isolate the compound, which is subsequently subjected to standard chemical and spectroscopic methods for structural study.

In order to illustrate the viability and utility of the technique, some examples from our current studies are presented. Fig. 1 shows the total ion current trace (TIC) obtained during EI LC/MS of a mixture of natural coumarins (1-7) of the type found in the Umbelliferae family. A similar trace was obtained under CI conditions and excellent EI and CI spectra were obtained. In our studies of plant extracts containing coumarins of this type we have found CI data particularly useful since many of the compounds show low intensity $M^{+\cdot}$ ions in their EI spectra. Recently we have commenced a research programme aimed at identifying new minor components in Ergot. Fig. 2 shows the TIC trace obtained from an extract of Claviceps purparea. The main components (1) and (3) are the known alkaloids agroclavine and elymoclavine, (4) proved to be the recently reported alkaloid 6,7-secoagroclavine[4] and (2) remains to be identified. Further extracts are currently undergoing investigation.

Combined LC/MS should be invaluable in peptide sequence studies[5] and Fig. 3 shows an example of our preliminary results in this area. Our recent studies of the cephalosporin antibiotic cephalexin (Fig. 4) suggest that small underivatized peptides should be amenable to study with our system since with ammonia CI cephalexin gave an M+1 ion at m/z 348 (10%) and the base peak in the spectrum was m/z 304. The fact that excellent CI spectra can be obtained from underivatized tetrapeptides spotted directly onto the belt interface reinforces this view.

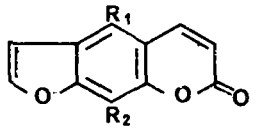
To date we have found LC/MS a valuable additional technique in our studies of natural products.

References

1. D.E. Games, J.L. Gower, N.J. Haskins, M. Rossiter and P. Scourides, in "Advances in Mass Spectrometry" Vol. 7, ed. N. Daly, Heyden, London, 1978, p. 1561.
2. D.E. Games, J.L. Gower, M.G. Lee, I.A.S. Lewis, M.E. Pugh and M. Rossiter, in "Blood Drugs and Other Analytical Challenges", ed. E. Reid, E. Horwood, Chichester, 1978, p. 185.
3. W.H. McFadden, H.L. Schwartz and S. Evans, J. Chromatog., 1976, 12, 389.
4. D.C. Horwell and J.P. Verge, Phytochemistry, 1979, 18, 519.
5. B.G. Dawkins, P.J. Arpino and F.W. McLafferty, Biomed. Mass Spectrometry, 1978, 5, 1.

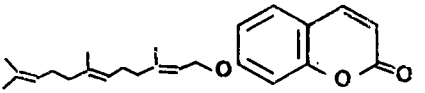
Key to Figures

Fig. 1: TIC trace obtained by EI LC/MS of a mixture of natural coumarins, Partisil 5, 1,2-dichloroethane:cyclohexane:acetonitrile (60:23:17) 1ml/min. Fig. 2: TIC trace obtained by EI LC/MS of an extract of Ergot, ODS 5 μ Spheresorb, methanol, water, ammonia (85:15:0.2) 1ml/min. Fig. 3: TIC trace obtained by EI LC/MS of Ac.Thr(OBz). Ala.Leu.OMe (1), Ac.Cys (SBz). Ala-Leu-OMe (2), AcPhe.Ala-Leu.OMe (3), Ac.His.Ala.Leu.OMe (4), Ac.Tyr. Ala.Leu.OMe (5); Partisil 5 with 6% methanol in chloroform, 0.8 ml/min. Fig. 4: TIC trace obtained by NH_3 CI LC/MS of cephalexin. ODS 5 μ Spheresorb, 0.3 ml/min of water (0.2g ammonium acetate per 100 ml of water buffered to pH5 with acetic acid), acetonitrile, 40:60.



2 R_1 = $OCH_2CH=C(CH_3)_2$ R_2 = H
3 R_1 = H R_2 = $OCH_2CH=C(CH_3)_2$
4 R_1 = $OCH_2CH(O)C(CH_3)_2$ R_2 = H
5 R_1 = H R_2 = $CH_2CH(O)C(CH_3)_2$
6 R_1 = OCH_2CH(Oangeloyl)$C(CH_3)_2OH$ R_2 = H
7 R_1 = $OCH_2CH(OCOCH_3)C(CH_3)_2OH$
R_2 = H

Fig 1



1

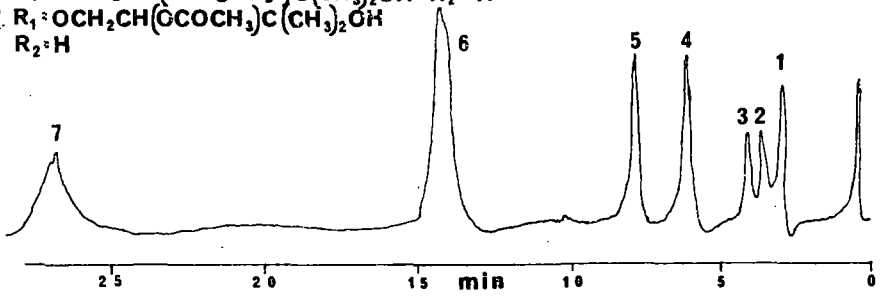


Fig 2

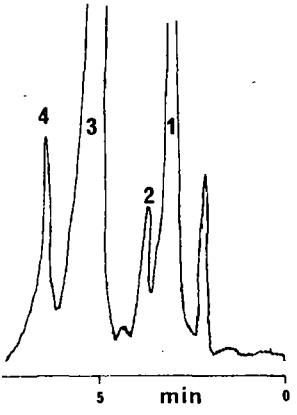


Fig 3

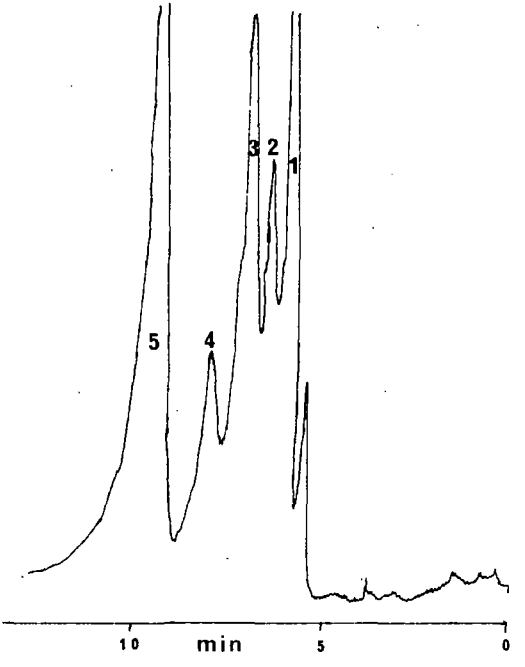
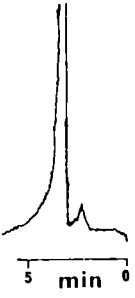


Fig 4



RPMP1 THE APPLICATION OF MASS SPECTROMETRIC TECHNIQUES TO THE RECOGNITION OF ORGANOPHOSPHATE PESTICIDE TRANSFORMATION PRODUCTS, IN A CASE OF HUMAN POISONING BY AN UNKNOWN TOXIC AGENT, R. L. HARLESS, G. W. SOVOCOOL, D. E. Bradway, L. H. Wright, E. M. Lores and I. E. Feige, Health Effects Research Laboratory, US EPA, MD-69, Research Triangle Park, NC 27711

An individual exhibiting symptoms of acute organophosphate poisoning, including low blood cholinesterase activity, was admitted to a hospital. However, examination of the poisoning solution by gas chromatography using phosphorus specific flame photometric detectors failed to identify intact pesticide. Mass spectrometric techniques of field ionization/field desorption and chemical ionization were used to define molecular ions of: 152, 168, 180, 196, 198, 302, 334 m/z. Exact mass measurements at high resolution, yielded several possible compositions. Recognition of key fragments as being of the same composition as ring fragments in the mass spectrum of the pesticide, Diazinon, led to the structural assignments of several transformation products of this pesticide.

Screening of The Inherited Metabolic Diseases by GC/MS/COM

Isamu Matsumoto, Toshihiro Shinka, Tomiko Kuhara, Shin-Ichi Haraguchi, Naotoyo Hisanaga, *Tokuo Mizuno and *Yasuhiro Itagaki

Research Institute of Medical Mass Spectrometry, Kurume University School of Medicine, Kurume, Fukuoka and *Japan Electron Optics Co. Ltd., Tokyo, Japan.

In the last few years, a great number of papers describing gas chromatography-mass spectrometric analyses of inherited diseases have been published and most of these works were aided by data processing with a computer. The approach of Sweeley and his coworkers appears to be the most extensively develped, providing reliable automated identification of the separated compounds, based on g.l.c. retention times as well as mass spectra. However, to make the works easier, it is necessary to develope a more sophisticated computer program for a fully automated system. We have recently developed a new computer program providing quite reliable diagnosis of the diseases.

The data analysis involves construction of the comparison table and the table of diseases using patient's or synthetic urine, measurement of unknown samples, comparison with standard chromatogram, detection of abnormal level, reference to the table of disease, library search and output of the name of disease. For construction of the comparison table and the table of disease, retention times of each separated peak were corrected to 4 internal standards of succinic acid, 4-hydroxyphenylacetic acid, heptadecanoic acid and hexacosane by quadratic equation, so that retention time of each peak relative to an internal standard was quite accurate and thus it made the identification of the corresponding peak in unknown samples easy. The program was evaluated in its applicability to the patient's urine of tyrosinosis, phenylketonuria, methylmalonic aciduria and some other diseases.

After urinary organic acids were isolated by diethyl-ether extraction, dehydrated with anhydrous sodium sulfate and evaporated to dryness under reduced pressure, the residue was converted to trimethylsilyl(TMS) derivatives with BSTFA by heating at 60°C for 1 hour. The mixture of TMS derivatives was separated on a 2 mm x 2 m glass column packed with 3% OV-17 on Gas Chrom Q, with temperature programmed from 80 to 290°C at 6°C/min. The magnet of a mass spectrometer (JEOL JMS D-100) was scanned repetitively over field strength corresponding to m/z 40 to 600 at every 5 second and mass spectra were stored on a disk memory of a JMA 2000 mass data analysis system (JEOL Co. Ltd.) for subsequent analysis by a new program called "Diagnostic Program".

About 80 peaks were detected on TIM chromatogram and 63 compounds were identified. The deficiency of 4-hydroxyphenylpyruvic acid oxidase in a patient with neonatal tyrosinemia caused the excretion of a large amount of 4-hydroxyphenylpyruvic acid and 4-hydroxyphenyllactic acid, as expected. In addition to these two abnormal metabolites, elevated levels of phenylpyruvic acid and phenyllactic acid were observed in urine of a patient of one-month-old boy. This indicates that the patient impaired the metabolism of phenylalanine hydroxylase like phenylketonuria, probably due secondarily to a primary defect of 4-hydroxyphenylpyruvic acid oxidase. The more complicated feature was obtained in a patient with hereditary tyrosinemia, that is, elevated level of adipic acid and suberic acid, which were characteristic for ketotic acidosis, was detected in addition to 4-hydroxyphenylpyruvic acid and 4-hydroxyphenyllactic acid. Thus, it is obvious from the above 3 cases of tyrosinosis that gas chromatogram of the patient with tyrosinosis greatly differs in the cases. The complicated feature of the disease makes this diagnosis difficult. Since, a new program we developed selected two abnormal metabolites, 4-hydroxyphenylpyruvic acid and 4-hydroxyphenyllactic acid, for the disease and the above 3 cases were diagnosed as tyrosinosis properly. The complicated chromatograms were also obtained from urine of the patients with phenylketonuria and methylmalonic aciduria as shown in Fig. 2. The new computer program, however, selected phenylpyruvic acid and phenyllactic acid for phenylketonuria, and methyl-

malonic acid for methylmalonic aciduria, so that the difficulty was overcomed.

In conclusion, a newly developed computer program for diagnosis of inborn errors of metabolism by GC/MS/COM system was tested to its applicability for the patients' urine of tyrosinosis, phenylketonuria and methylmalonic aciduria with fairly complicated feature of gas chromatogram and the system showed that the program was quite reliable and useful. The results also suggested that all of the diseases were not simple and gave rather complicated clinical features.

Gates, S. C., et al., Anal. Chem., 50, 433 (1978).

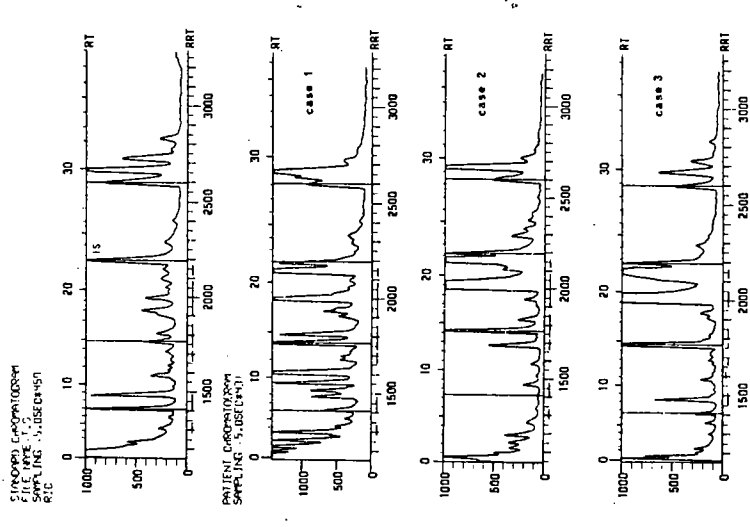


Fig. 1 RIC chromatograms of tyrosinosis.

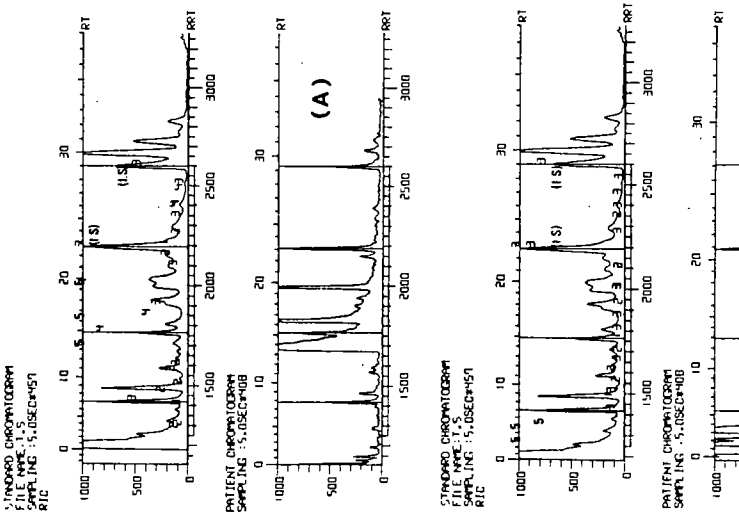


Fig. 2 RIC chromatograms of phenylketonuria (A) and methylmalonic aciduria (B).

ANALYSIS OF ORGANIC ACIDS IN CSF OF VARIOUS NEUROLOGICAL DISORDERS BY GC/MS

Masafumi Yoshida*, Tomiko Kuhara, Toshihiro Shinka, Isamu Matsumoto and Shinken Kuramoto*
Department of Neurosurgery* and Research Institute of Medical Mass Spectrometry, Kurume University School of Medicine, Kurume, Fukuoka, Japan

In order to obtain information concerning the metabolism in the central nervous system from biochmical view point we have recently been working to establish the metabolic profile of the cerebrospinal fluid(CSF) in normal subjects by GC/MS system. It also is our interest to find out an alteration of this metabolic profile in the various neurological disorders. In the central nervous system(CNS) with various neurological disorders many biochemical changes are very likely to be involved other than the one which is related to neurotransmitters. This study is of interest and may have clinical application because the alteration of the metabolic profile of the CSF can reflect some of the characteristics of basic pathology of neurological disorders. In this report organic acid profile of CSF both in normal and in various neurological disorders are presented.

MATERIAL. The lumbar and ventricular CSF was obtained from the patients with various neurological disorders(Table 1.). The control CSF was obtained from lumbar subarachinoid space from patients without apparent neurological disorders and in majority of cases during spinal anesthesia for orthopedic procedures. The CSF was stored at -20°C until analysis.

EXTRACTION. One ml of cerebrospinal fluids, after addition of 20 μg of heptadecanoic acids as internal standard, was deproteinized by adding 4 ml of cold ethanol. After ethanol in supernatant was evaporated under reduced pressure, the remaining aqueous layer was adjusted to pH 1.0 with 2N-HCl and extracted twice with diethyl ether and ethyl acetate respectively. The organic solvent was combined and concentrated to dryness under reduced pressure. The residue was trimethylsilylated with 100 μl of N,O-bis-trimethylsilyltrifluoroacetamide and 2 μl of the reaction mixture was injected into gas chromatograph and GC/MS.

GAS CHROMATOGRAPHY-MASS SPECTROMETRY. A JEOL JMS D-100 GC-MS on lined to JMA 2000 data analysis system was used throughout the experiments. For gas chromatographic analysis, the temperature of injection port was set at 290°C and separator and ion source were kept at 290°C and 200°C respectively. Column temperature was programmed at 6°C/min. from 80° to 290°C. An ionization voltage and an ion current were 75 eV and 300 μA respectively and the scanning was performed every 5 seconds.

RESULTS AND DISCUSSION. The organic acids profile of the normal cerebrospinal fluids and currently identified materials are presented in Fig. 1. The presence of various organic acids in various quantities in CSF, as currently studied, gives us fairly good insight into the metabolism in the CNS in normal human beings. Thus relatively high activity of the TCA cycle is extrapolated from the relative abundance of its metabolic intermediates, i.e., succinate, malate and citrate. The presence of highly

active urea cycle in the CNS is very likely because of presence of urea together with the data of amino acid analysis as previously reported.[1] The presence of large amount of 3,4-dihydroxybutyrate is of interest because of its possible link to the GABA metabolism in the CNS.[2] This compound seems to be more prevalent in ventricular CSF than in lumbar CSF. In parkinsonism 2-hydroxybutyrate seems to be higher in lumbar CSF than in ventricular CSF, whereas in brain tumor and in hydrocephalus this compound is relatively high intraventricularly. In brain tumor and in hydrocephalus the amount of some compounds, e.g., lactate, fluctuates largely. This may represents different state of metabolism in these conditions, but other factors such as hydrodynamics of CSF, turn over rate of compounds in CSF and state of blood-brain barrier should be taken into consideration in pathological conditions.

REFERENCES. 1. Matsumoto,I., Hisanaga, N., Shinka, T., Kuhara, T., Yoshida, M,. Kusano, N. and Kuramoto, S. Metabolic profile of ventricular cerebrospinal fluids. In Advances in Mass Spectrometry in Biochemistry and Medicine, Spectrum Publication, Inc., New York (In press).

2. Lee, C.R. and Pollitt, R.J. (1974). Gas chromatography-mass spectrometry applied to the study of urinary acids in a patient with periodic catatonia. In Mass Spectrometry in Biochemistry and Medicine, Ed. Frigerio, A. and Castagnoli, N., Raven Press, New York, pp. 365-371.

Lumbar CSF		Ventricular CSF	
Group	Number	Group	Number
Control	15	Parkinsonism	6
Parkinsonism	5	Neck Tremor	1x2*
Huntington's Chorea	1	Central Pain	2
Neck Tremor	1	DMD	1
Brain Tumor	2	Brain Tumor	4
Cerebrovascular Diseases	2	Hydrocephalus	2

* CSF obtained from the same patient, but on different occasions.

Table 1. Clinical material

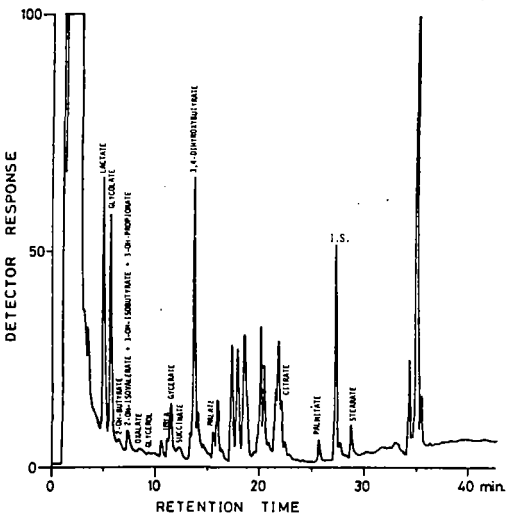


Fig. 1. Gas chromatogram of organic acids in cerebrospinal fluid

E.I./C.I./F.I. MASS SPECTRA OF SELECTED PROSTAGLANDIN DERIVATIVES AND ANALOGS

by L. Baczynskyj

Physical and Analytical Chemistry Research Laboratories

The Upjohn Company

Kalamazoo, Michigan 49001

Electron impact ionization (E.I.) mass spectra of naturally occurring prostaglandins and of some synthetic analogs has been studied in the past. These spectra usually do not exhibit molecular ions. Thermal and chemical stability can be increased by preparing appropriate derivatives, especially trimethylsilyl (TMS) derivatives. Usually such derivatives exhibit molecular ions. However, for certain synthetic prostaglandin analogs, the E.I. mass spectra of the TMS derivatives do not show molecular ions. Also, in the case of salts, the preparation of TMS derivatives is not straightforward. For these reasons, one has to use other ionization techniques such as chemical ionization (C.I.) or field ionization (F.I.) to obtain molecular ions.

The electron impact ionization mass spectra of 16,16-dimethyl prostaglandin $F_{2\alpha}$ was compared with the chemical ionization and field ionization mass spectra of the same molecule. The chemical ionization mass spectra were recorded using isobutane and ammonia as reagent gases. The E.I. mass spectrum does not show a molecular ion. The C.I. (isobut.) and C.I. (NH_3) spectra did show intense protonated molecular ion and $(M+NH_4)^+$ respectively. The F.I. mass spectrum shows a $(M^{+\cdot}-2H_2O)$ (18% R.A.) with the most intense ion occurring at m/z 99.

The E.I. mass spectrum of the TMS derivative of 16,16-dimethyl $PGF_{2\alpha}$ also shows no $M^{+\cdot}$ and the F.I. mass spectrum shows an $(M-99)^+$ ion (50% R.A.) and the most intense ion occurs at m/z 99. In the C.I. (isobut.) mass spectrum, the molecular ion is 5% of the most intense ion occurring at m/z 581 $(M-99)^{+\cdot}$. In the C.I. (NH_3) mass spectrum, the $(M+NH_4)^+$ is the most intense ion.

When the E.I., F.I., and C.I. mass spectra of the tromethamine (THAM) salt of prostaglandin $F_{2\alpha}$ were recorded, the following observations were made: The E.I. mass spectrum shows no $M^{+\cdot}$ for the free acid or the prostaglandin salt. The F.I. mass spectrum shows an $(M+1)^+$ at m/z 122 corresponding to the protonated tromethamine and the most intense ion occurring at m/z 90, which corresponds to the $(M-\cdot CH_2OH)^+$ ion of tromethamine. However, the C.I. (isobut.) mass spectrum showed a weak $(M+1)^+$ ion at m/z 476 of the $PGF_{2\alpha}\cdot$THAM salt while the base peak occurs at m/z 122 corresponding to the $(M+1)^+$ ion of tromethamine. As the probe temperature was increased, the ions at m/z 476 and 122 decreased, while the $M^{+\cdot}$ and $(M+1)^+$ of $PGF_{2\alpha}$ free acid increased and the most intense ion at m/z 337 corresponds to $[(M+H) - H_2O]^+$. A similar behaviour was observed for the C.I. mass spectrum using ammonia as reagent gas. However, at higher temperatures, the $(M+NH_4)^+$ ion at m/z 372 corresponding to the ammonium adduct of $PGF_{2\alpha}$ free acid became the most intense ion.

A similar comparison of E.I./F.I./C.I. mass spectra was performed for 16,16-dimethyl-9-deoxo-9-methylene $PGE_2\cdot$adamantylamine salt. The E.I. mass spectrum showed a very weak (0.01% R.A.) molecular ion of the prostaglandin free acid. The F.I. mass spectrum showed a weak $(M-18)^+$ ion with a base peak at m/z 151 corresponding to the molecular ion of adamantylamine. As in the previous case, the C.I. (isobut.) mass spectrum showed, at lower probe temperature, a weak (1.4% R.A.) ion at m/z 530 corresponding to the protonated prostaglandin salt, whereas at

higher temperatures, the $(M+1-H_2O)$ and $(M+1-2H_2O)$ became dominant. Similarly, the C.I. mass spectra using ammonia as reagent gas showed at lower temperatures a weak $(M+1)^+$ ion of the protonated prostaglandin salt and at higher temperatures a $(M+NH_4)^+$ of the prostaglandin free acid as the most abundant ion.

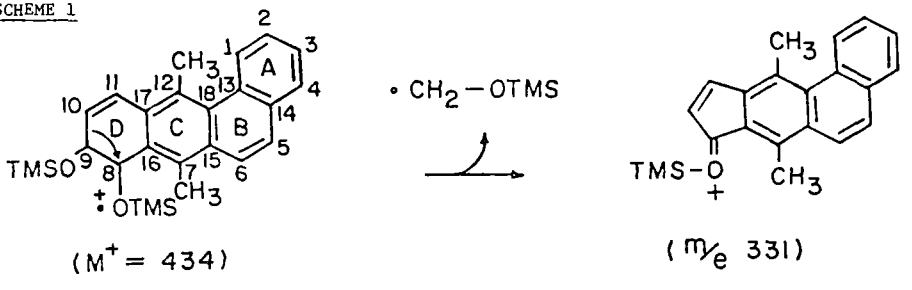
REGIOSELECTIVITY IN THE ENZYMATIC FORMATION OF DIHYDRODIOLS OF 7,12-DIMETHYLBENZ(a)ANTHRACENE

Chih-Lueh A. Wang, F. Bernard Daniel and Lan K. Wong*
Department of Pharmacology, Ohio State University, College of Medicine
Columbus, Ohio 43210

7,12-Dimethylbenz(a)anthracene (DMBA) is a carcinogenic polycyclic aromatic hydrocarbon. During biotransformation, it is metabolized to epoxides, dihydrodiols, phenols and conjugates. The carcinogenicity of this compound has been attributed to the interaction of its epoxide metabolites with biomacromolecules. Since the epoxides undergo hydrolysis to give rise to dihydrodiols, an examination of these dihydrodiol products will contribute to the understanding of the nature of the nucleophilic reactions on the epoxides. We have, therefore, studied the enzymatic incubation of the hydrocarbon in O^{18} labelled water in order to determine the orientation of hydrolysis for the 8,9- and 5,6-epoxides of DMBA by GC-MS. These two epoxides are commonly found in the metabolism of DMBA.

DMBA was incubated with rat liver microsomes in the presence of the necessary cofactors and 90% enriched O^{18} labelled water. After one hour, the reaction was quenched and the metabolites were extracted and analysed by GC-MS as the trimethylsilyl derivatives on a Hewlett Packard 5985 GC-MS system. The partial mass spectra of the resulting 8,9- and 5,6-dihydrodiols are shown in figures 1 and 2 respectively. The molecular ions of these compounds are found at m/e 436. This is consistent with the incorporation of one oxygen-18. A small fraction of unlabelled molecules were observed at m/e 434 since the incubation medium was only 90% enriched in the O^{18} isotope. Recently we have elucidated the mass spectral fragmentation patterns of unlabelled DMBA-8,9-dihydrodiol and DMBA-5,6-dihydrodiol (Biomedical Mass Spectrometry, in press). Some of the reported features are useful for assigning the position of the O^{18} label. Thus for the 8,9-dihydrodiol, the ion at m/e 331 involves the cleavage of C_9 and its accompanying trimethylsilyloxy group (scheme 1). If one examines the O^{18} labelled compound in figure 1, this ion remains at the same a.m.u. rather than shifting to m/e 333. Therefore the O^{18} label must be at C_9. Likewise for the 5,6-dihydrodiol, the ion at m/e 304 involves the loss of the C_5 fragment followed by a rearrangement. That the labelled compound retains the ion at the same a.m.u. (figure 2) suggests that the O^{18} label must be at C_5. On the basis of these mass spectral data, we conclude that hydrolytic openings of the 8,9-epoxide and the 5,6-epoxide occur at positions 9 and 5 respectively. This observation is in accord with steric considerations. (This work is supported by NCI grant CA24075).

SCHEME 1



SCHEME 2

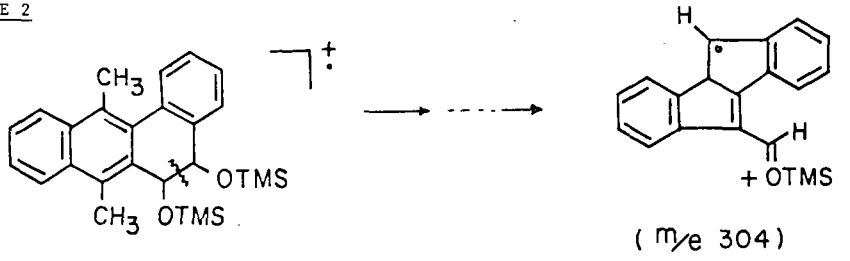


Figure 1: Partial mass spectrum of DMBA-8,9-dihydrodiol. The spectrum has been renormalized after subtraction of m/e 73 (base peak).

Figure 2: Partial mass spectrum of DMBA-5,6-dihydrodiol processed as above.

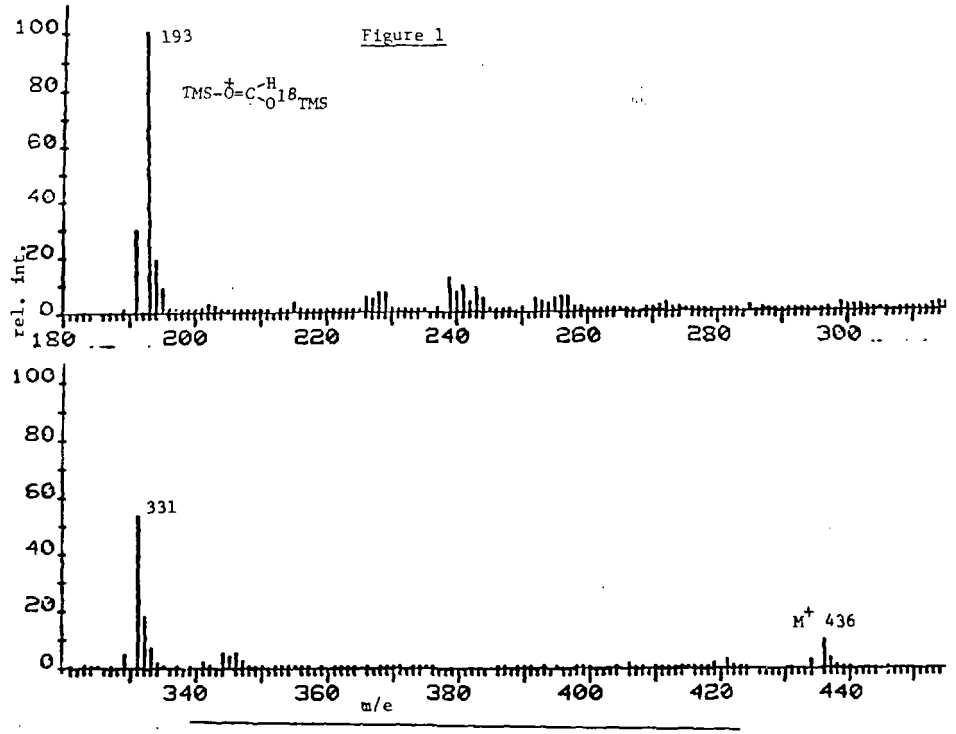


Figure 1

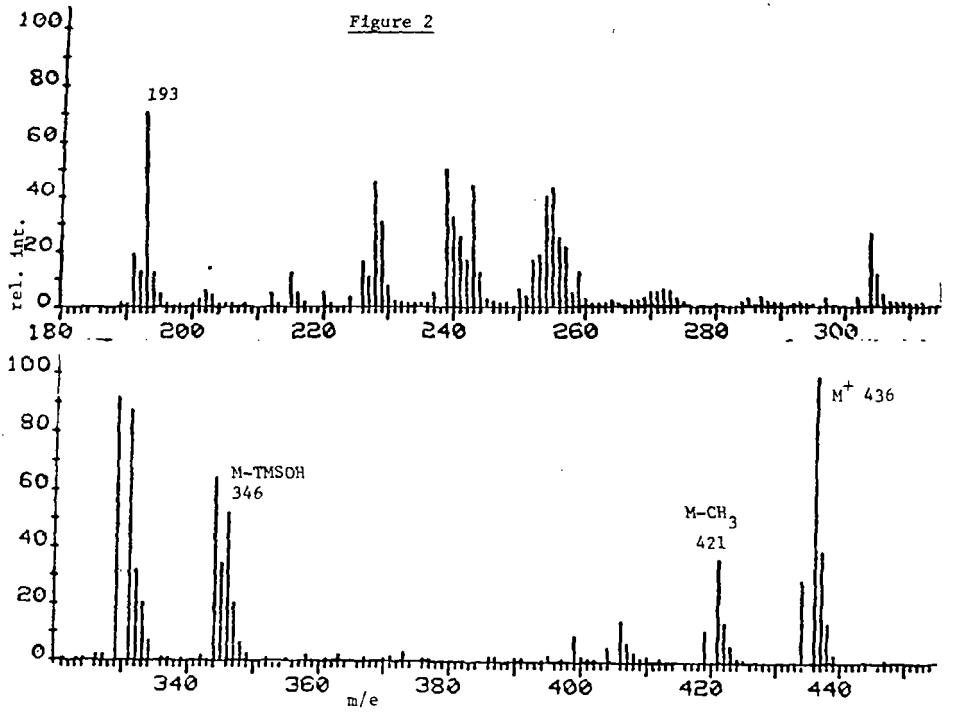


Figure 2

RPMP8 SELECTIVE METASTABLE PEAK MONITORING, D.S.MILLINGTON, J.A.SMITH VG-Organic Ltd., Altrincham and S.J.GASKELL, Tenovus Institute, Cardiff, U.K.

In conventional SID techniques, detection limits for specific components of biological samples are mainly determined by the extent of spurious signals due to interfering isobaric ions. These spurious signals can be minimised by increasing the specificity of the MS, e.g. using higher resolution or, with a double focussing MS, by monitoring characteristic fragmentation processes occurring in the first field-free region. This technique, referred to as metastable peak monitoring, was shown to be selective for detection of some endogenous steroids in human blood plasma[1]. An extension of the technique enables switching between product ions derived from different metastable precursors, thus allowing simultaneous detection of a component and an isotopically labelled internal standard.

1. S.J.Gaskell and D.S.Millington, Biomed. Mass Spectrom. 1978, 5, 557.

MASS SPECTROMETRY AND REACTIVITY OF CHLOROALKENE EPOXIDES.

JEROME J. SOLOMON, BENJAMIN L. VAN DUUREN, STANLEY A. KLINE AND SATISH C. AGARWAL, LAB. ORG. CHEM. AND CARCINOGENESIS, INST. ENV. MED., NEW YORK UNIV. MED. CENTER, NEW YORK, N.Y. 10016

HALOGENATED ALKENES ARE WIDELY USED AS SOLVENTS, INDUSTRIAL MONOMERS AND INSECTICIDES. VINYL CHLORIDE AND TRICHLOROETHYLENE HAVE BEEN SHOWN TO BE CARCINOGENIC TO ANIMALS. THESE HALOALKENES ARE BELIEVED TO EXHIBIT THEIR CARCINOGENIC RESPONSE AFTER METABOLISM. LIKELY CANDIDATES FOR THE ACTIVATED INTERMEDIATES ARE CHLOROALKENE EPOXIDES. SEVERAL CHLOROALKENE EPOXIDES WERE SYNTHESIZED AND CHARACTERIZED IN OUR LABORATORY. SEVERAL EPOXIDES WERE FOUND TO BE UNSTABLE. WE HAVE DEVELOPED A TECHNIQUE FOR TRAPPING ELECTROPHILIC SPECIES WITH REACTIVE NUCLEOPHILES. THE ADDUCTS FORMED ARE THEN CHARACTERIZED BY ISOBUTANE CHEMICAL IONIZATION MASS SEPCTROMETRY. DATA WILL BE PRESENTED ON THE MASS SPECTROMETRY, STABILITY, MUTAGENICITY AND BIOLOGICAL ACTIVITY OF THE VARIOUS SYNTHESIZED EPOXIDES.

(SUPPORTED BY NSF ENV-76-10656 AND CENTER GRANTS ES00260 AND CA13343).

MEASUREMENT OF PLASMA FFA TURNOVER AND OXIDATION USING 1-^{13}C-PALMITIC ACID.

Robert R. Wolfe, James E. Evans, Charles J. Mullany and John F. Burke, Department of Surgery, Harvard Medical School, Shriners Burns Institute and Massachusetts General Hospital, Boston, MA; and the Eunice Kennedy Shriver Center, Waltham, MA.

The measurement of plasma free fatty acid (FFA) turnover and oxidation by means of the isotopic dilution technique using a radiolabeled FFA has proven useful for the in vivo study of fat metabolism in animals. However, because of the ethical considerations regarding the administration of radioisotopes to humans, there is almost no information regarding the in vivo regulation of FFA turnover and oxidation in humans, particularly children. Consequently we have developed a technique using the stable, non-radioactive 1-^{13}C-palmitic acid molecule as an FFA tracer to measure plasma FFA metabolism in vivo. We have analyzed the isotopic enrichment of plasma palmitate by selected ion monitoring on a gas-chromatograph mass spectrometer (GC-MS), and we have used an isotope-ratio MS (IRMS) to determine the much lower isotopic enrichment of the expired CO_2. We have found this technique to be safe to administer, to have a high degree of analytical reproducibility, and to yield values in dogs comparable to those obtained using 1-^{14}C-palmitic acid as the tracer.

RPMP10 A SEARCH FOR NEW NEUROACTIVE COMPOUNDS IN THE CENTRAL NERVOUS SYSTEM OF MOLLUSCS, MARILYN W. McCAMAN, Division of Neurosciences, City of Hope National Medical Center, Duarte, CA 91010

Most of the known neurotransmitters (acetylcholine, serotonin, dopamine, etc.) are found in the ganglia of the marine mollusc, Aplysia californica. Some of these have been found in high concentrations in individual cell bodies isolated from these ganglia. The cell specificity of compounds such as acetylcholine and serotonin has supplemented other data supporting their functions as neurotransmitters. However, these neurons only account for a few of the total number, and the nature of the transmitter mediating the responses of many of the other neurons is unknown. We are attempting to determine whether or not these other cells contain new, previously uncharacterized "neurotransmitter" substances. Using a combination of column chromatography, GCMS and a sensitive bioassay system, partially purified tissue extracts were analyzed for amino acids and biogenic amines, and tested for physiological activity. Several compounds similar to, but not identical with, glutamate have been found, and some have biological activity. Positive identification of these compounds is in progress.

PERFORMANCE OF A WIDE DYNAMIC RANGE MASS SPECTROMETER DESIGNED FOR RESPIRATORY STUDIES, D.J. MARSHALL, Nuclide Corp., Acton, MA and J.LEHR, Harvard School of Public Health, Boston, MA - Performance results are presented for a small magnetic sector instrument which fulfills many needs in respiratory research. Combined peak stepping-sampling time under 10 ms. permits monitoring several components at least once every 100 ms., essential in respiratory studies. Relative sensitivities for O_2, N_2, and A, remain constant ($\pm$ 1-2%) for 8 hrs., even though absolute sensitivities may vary by several percents. Sensitivity is nearly constant over a dynamic range of 10^4 to 10^5, permitting low PPM level tracer investigations.

INSTRUMENTATION - Nuclide Model 3-60-G Magnetic Sector Mass Spectrometer with: 3-inch radius, 60° deflection analyzer. Programmed Ion accelerating voltage and/or magnetic field. Electron multiplier detector and/or Faraday Cup. Continuous sampling inlet from atmospheric pressure.

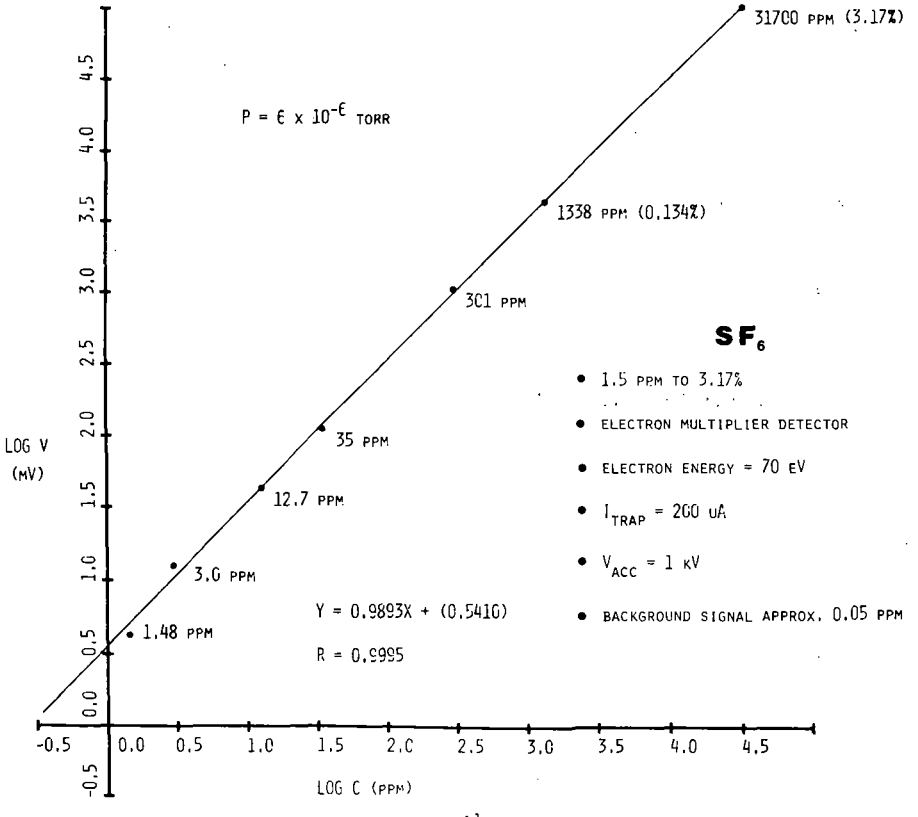
APPLICATIONS -

Respiration Studies: Time constants of 75 millisecond or less at sample consumption of 2 ml/minute permit following some details of respiration in small animals, e.g. white mice.

Trace Detectability: Good detectability of trace constituents, continuously sampled from air at atmosphere pressure. Example of 144 ppb $Fe(CO)_5$ shown.

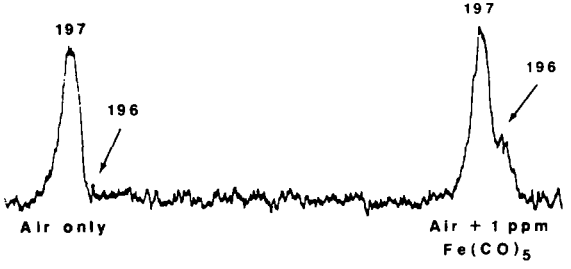
Wide Dynamic Range: Figure shows SF_6 signal level linearity over dynamic range of 31,700 ppm to 1.4 ppm.

Dynamic Range And Linearity



High-Mass Detectability

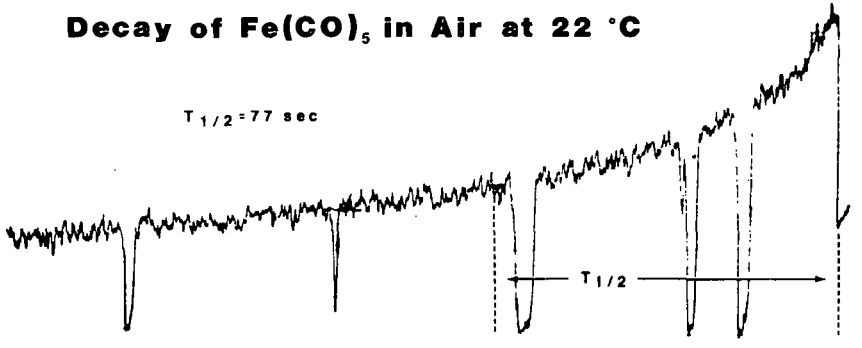
Example: trace $Fe(CO)_5$ in air



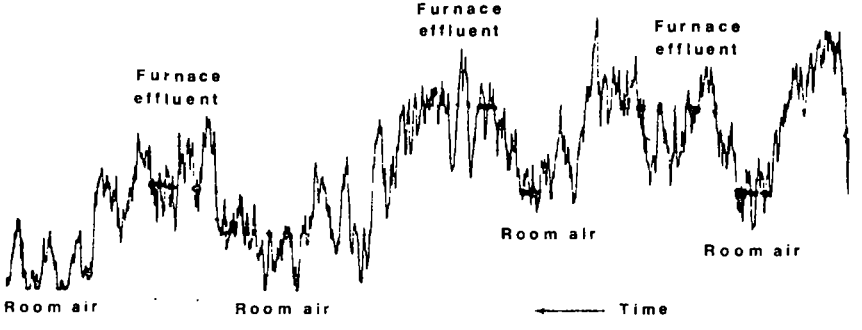
CONDITIONS:

- V_{ACC} = 1 kV
- I_{TRAP} = 200 uA
- ELECTRON ENERGY = 30 eV
- ELECTRON MULTIPLIER DETECTOR

Decay of $Fe(CO)_5$ in Air at 22 °C



$Fe(CO)_5$ in Furnace Effluent



Extrapolated Concentration at T=0 approx. 144 ppb.

APPLICATIONS OF ISOTOPE RATIO MASS SPECTROSCOPY TO METABOLIC STUDIES IN BURNED CHILDREN

D. K. Rohrbaugh, R. R. Wolfe, C. J. Mullany, J. F. Burke and V. R. Young

Shriners Burns Institute, Boston, Mass. 02114

Following severe burn injury marked changes in the metabolic processes occur. During the last 4 years we have been using the stable isotopes N-15 and C-13 to monitor changes in whole body protein synthesis and the turnover and oxidation rates of leucine, glucose and palmitic acid in burned children and healthy volunteers. Discussed here are two aspects of these studies; 1) the methodology and problems involved in the measurement of ^{15}N labelled urea as a measure of whole body N turnover and 2) methods for measuring glucose production and oxidation rates using isotope ratio mass spectroscopy.

Instrumentation ^{13}C and ^{15}N isotope enrichments were measured on a Nuclide model 3-60-RMS dual inlet double collector isotope ratio mass spectrometer(Nuclide Corporation, State College, Pa.). Frequent analysis of an ammonium sulfate standard over a one year period gave an ^{15}N enrichment and standard deviation of .0512 ± .0006 atom % excess N15. All ^{15}N enrichments were measured against a tank N_2 of known ^{15}N content (.367 % N15). Similar analysis of a ^{13}C enriched bicarbonate standard gave .0552 ± .0007 atom % excess C13. ^{13}C measurements were made in comparison to a K_2CO_3 standard of known C13 content(1.069% C13). Short term machine variation was assessed by repeated analysis of the same CO_2 gas sample over a one hour period and gave a standard deviation of ±.00007 atom % C13(n=10). Addition of a small inlet modification consisting of a charcoal trap for trapping N_2 in a small volume has reduced sample requirements to about 2 μmoles of CO_2 or N_2 gas.

Urea methodology Urinary and plasma urea were converted to ammonia for ^{15}N analysis by the Conway diffusion technique. After treatment with permutit to remove traces of ammonia, urea N was converted to ammonia by addition of urease at pH7 to either 5cc of urine or 5cc of deproteinized plasma. After trapping in 1% H_2SO_4 the ammonium sulfate was converted to N_2 for mass spec analysis by oxidation with NaOBr in a vacuum. Replicate preparation of samples gave a coefficient of variation of 3.9% for plasma and 1.0% for urinary urea.

We have shown that by priming the urea pool during a primed constant infusion of α-^{15}N-lysine in dogs that the time required to reach urea-^{15}N plateau enrichment can be reduced from several days to hours. However, even after 24 hours of continuous infusion of ^{15}N-urea, ^{15}N enrichment in urinary urea exceeds that in plasma by as much as 20%. Furthermore, simultaneous determination of rates of urea production in 7 dogs using ^{15}N and ^{14}C as tracers gave 10.9 ± 0.9 and 9.1 ± 0.6 μmoles/kg·min, respectively. A possible source of error could be the introduction of non-urea nitrogen during the plasma urea-^{15}N isolation procedures thus leading to an underestimate of ^{15}N enrichment and overestimate of urea production.

Glucose Methodology Glucose production and oxidation rates were obtained from measurements of ^{13}C enrichments of plasma glucose and expired air $^{13}CO_2$ at plateau during a primed-constant infusion of tracer amounts of U-^{13}C-glucose(approximately .0018 mg/kg·min). The bicarbonate pool was primed with a priming dose:infusion rate ratio of 85:1 in order to achieve rapid isotopic equilibrium, where the infusion rate of $^{13}CO_2$ was considered to be the rate of production of $^{13}CO_2$ from glucose oxidation.

Glucose was isolated for mass spec analysis by passing 1-2cc of deproteinized plasma through anion(Dowex AG1-X8) and cation(Dowex AG50W-X8) exchange columns. Combustion to CO_2 was done by heating to 1000° C in the presence of O_2 and a cupric oxide catalyst. A Toepler pump recycled gases to ensure complete combustion. Triplicate analysis gave a coefficient of variation of 1.0%.

The acceptability of our method was tested in two ways. First, specific isolation of glucose from an enriched plasma sample as the potassium gluconate derivative by Iodine oxidation and recrystallization from methanol/ether gave a ^{13}C enrichment of .432 ± .012 atom % excess C13 compared to .431 ± .002 atom % excess C13 for the chromatographic separa-

tion. Also, simultaneous infusion of U-^{13}C and U-^{14}C-glucose in four dogs and measurement of glucose production rates for both isotopes gave average values of 4.28 ± 0.48 and 4.18 ± 0.41 mg/kg.min, respectively. Thus significant contamination by non-glucose sources of carbon seems unlikely.

Measurement of $^{13}CO_2$ enrichment in expired air at plateau gives a direct measure of glucose oxidation. Expired air CO_2 was prepared for isotopic analysis by collection in 3 liter anesthesia bags and bubbling through 0.1N NaOH to trap CO_2. The CO_2 gas was released for mass spec analysis by addition of concentrated phosphoric acid in an evacuated Rittenberg tube. The standard deviation of breath analysis was ±.0005 atom % C13 and the coefficient of variation about the mean at plateau was always less than 4%.

By priming the bicarbonate pool as well as the glucose pool the time to reach equilibrium enrichment of expired $^{13}CO_2$ during a primed constant infusion of U-^{13}C-glucose has been reduced from 8 hours to 1 or less, thus making the measurement of glucose oxidation much more feasible in the burned patient. The goal of the application of this model is a better understanding of the metabolic response to glucose infusions and thus better clinical treatment of the burned patient.

RPMP15 AMPHETAMINE METABOLISM: IS PHENYLACETONE OXIME A NECESSARY INTERMEDIATE IN DEAMINATION REACTIONS? A STUDY BY STABLE ISOTOPE GC/MS. JEREMY WRIGHT, PATRICK S. CALLERY AND JOSEPH GAL, Univ. of MD., School of Pharmacy, Dept. of Medicinal Chemistry, Baltimore, MD 21201

Metabolic deamination of amphetamines could proceed by α C or N-hydroxylation routes. Inconsistant reports concerning the role of phenylacetone oxime as an intermediate in the deamination process prompted us to study the metabolism of amphetamine in presence of the postulated intermediate oxime. Racemic amphetamine-d_5 (ring labelled) was incubated in the presence of phenylacetone oxime d_0 with 9000 g supernatant of rabbit liver. Extracts (CH_2Cl_2) were estimated derivatized (as trifluoroacetyl deriv.), and underivatized. Estimation of the deamination metabolite 1-phenyl-2-propanol (P_2P) by GC/MS using selective ion monitoring at masses 118, 123 and 91, 96 revealed that P_2P derived mainly from amphetamine-d_5 in the incubation mixture indicating that phenylacetone oxime is not an obligatory intermediate in the deamination process.

A MASS SPECTRAL STUDY OF THE PERBENZOYL AND BO-PERBENZOYL DERIVATIVES OF VARIOUS POLYOLS, RICHARD M. THOMPSON* AND DAVID A CORY, I.U. SCH. MED., INDIANAPOLIS, IN 46223 AND BATTELLE COLUMBUS LABORATORIES, COLUMBUS, OHIO 43201.

In order to more efficiently detect disorders of carbohydrate metabolism, a sensitive HPLC procedure was developed for the determination of some UV-absorbing sugar derivatives in biologic fluids [J. Chromatogr. 166, 201 (1978)]. Each of the derivatives of 26 standards was purified by HPLC and its EI mass spectrum obtained by direct introduction. In general, the benzyloximes yield molecular ions and characteristic fragments due to m/e 77, 91, 105, and 122; losses of 30, 121, and 122 amu, chain cleavages (not between C-1 and C-2); and unique ions due to the combined loss of C_7H_7. and C_6H_5COO. from the molecular ions. The alditol benzoates fragment by chain cleavages and by losses of 121 and 122 amu, but do not give molecular ions. Except for isomeric aldoses and ketoses, the mass spectra of isomers do not differ significantly. Therefore, retention time data must be used along with the mass spectra for the identification of polyols in body fluids by this procedure.
This work is being published in extenso in Biomedical Mass Spectrometry.

ION PLASMA DESORPTION MASS SPECTROMETRY OF SULFHYDRYL DRUG CONJUGATES

R. N. Stillwell, J. R. Mitchell, W. G. Stillwell,
B. H. Lauterburg, E. C. Horning and J. G. Nowlin

Institute for Lipid Research
Baylor College of Medicine
Houston, Texas 77030

Metabolic pathways exist for many drugs and other compounds leading to reactive and potentially toxic species including epoxides, quinones, and quinonimines. Conjugation with the thiol group of glutathione (γ-glutamyl cysteinyl glycine) is an important route of detoxication of these intermediates; the glutathione conjugate is metabolically converted to the N-acetyl cysteine conjugate for excretion. Other metabolites of importance include glucuronides, sulfates, epoxides, hydroperoxides, and N-oxides. Many of these compounds are not amenable to GC-MS analysis, even after derivatization, but can usually be separated by high pressure liquid chromatography. Ion plasma desorption mass spectrometry promises to provide a general method of ionization for characterization and quantification of these and other highly polar compounds of biological importance. The technique is based on the reaction of gas-phase reagent ions with a solid or liquid substrate at the surface of probe inserted into the chemical ionization source. Copper or gold wire is used to allow control of both heating and the electrical potential of the probe. Under these conditions the mass spectra are stable and reproducible and apparently suitable for quantitative analysis by stable isotope dilution.

IN VITRO FORMATION OF METHYLTHIO METABOLITES OF NAPHTHALENE FROM MERCAPTURIC ACID DERIVATIVES

W. G. STILLWELL

Institute for Lipid Research
Baylor College of Medicine
Houston, Texas 77030

The mercapturic and premercapturic acids of naphthalene isolated from rat urine have been studied by GC and electron ionization mass spectrometry. The mercapturic acid conjugate of naphthalene (methyl ester derivative) exhibited ions of high abundance for M and M-59 (NH_2COCH_3), while the premercapturic acid conjugate (methyl ester-trimethylsilyl derivative) was detected by an ion of low abundance at M-15 and ions of higher abundance at M-90 (TMSOH) and M-90-59. After incubation of the mercapturic acid and premercapturic acid conjugates with a rat liver preparation (9000 g supernatant) two methylthio metabolites of naphthalene were formed and were characterized by GC and GC-MS. Incubation of the premercapturic acid conjugate with S-adenosyl-[methyl-^{14}C]-methionine indicated that the donor of the methyl group of the methylthio metabolites is S-adenosyl methionine.

Analysis of Peptides

L. A. Smith, R. M. Caprioli, S-H. Lin
University of Texas Medical School at Houston

During the past few years, a new technique for analyzing protein primary structure has been developed utilizing Dipeptidyl Aminopeptidases I & IV (DAP I & IV) and combined gas chromatography/mass spectrometry (GC/MS). This technique involves the digestion of the substrate to sequential dipeptides from the N-terminal residue, lyophilization followed by derivatization of the whole hydrolysate, and identification by GC/MS of the pentafluoro proprionyl-dipeptide-methyl ester derivatives.

In developing this system for use at 1-5 nanomolar levels, it is necessary to remove the proteases as well as other low-molecular weight constituents which would otherwise interfere in a GC/MS dipeptide analysis. We report here on a procedure which includes High Performance Liquid Chromatography (HPLC) as a preparatory step for a GC/MS analysis of enzyme released dipeptides. The dipeptides are separated into acidic and basic fractions by HPLC and these fractions collected and identified by GC/MS. In addition, analysis of histidine and arginine containing dipeptides are accomplished more easily by correlation with known HPLC retention times of basic dipeptides and collection of these individual HPLC peaks for Mass Spectral solid probe analysis.

GC-MS ANALYSIS OF METHYLMALONIC ACID FROM BIOLOGICAL FLUIDS AS THE DICYCLOHEXYL ESTER

E. J. Norman, H. K. Berry and M. D. Denton
Departments of Medicine and Pediatrics
University of Cincinnati College of Medicine
Cincinnati, Ohio 45267

Last year we reported a method for the rapid identification and quantitation of urinary dicarboxylic acids using cyclohexanol as an estification reagent. In particular, we applied this method to the quantitation of methylmalonic acid (MMA) elevated in patients with pernicious anemia and methylmalonic aciduria. We have developed this test into a routine clinical assay which has proven to be very beneficial in diagnosing patients and providing money for laboratory operating expenses.

The method consists of first pipetting 50 µl of unpurified urine into a small bottle. An internal standard, ethylmalonic acid (EMA), 50 µg, is added followed by evaporation to dryness with nitrogen at 80°C. To the residue, 200 µl of 1.5 NHCl in cyclohexanol is added, the bottle is capped with a Teflon cap, and placed in a module block heater for 15 minutes at 115°C. The cyclohexanol is evaporated to near dryness at 115°C with a stream of nitrogen and the residue is dissolved in 200 ml of methanol.

Quantitation is performed using a Finnigan 3200 GC-MS with multiple ion monitoring capability and a 4 pen Rikadenki KA recorder. A 3% OV-17 column programmed from 100°C to 275°C at 15°C/min. gave improved separation over 3% OV-1 previously used for quantitation of normal levels of MMA. The ion at m/e 119 is monitored for MMA and m/e 133 for EMA. A confirming ion for MMA at m/e 101 is also monitored insuring the ratio m/e 119/m/e 101 is consistent with a standard. A linear relationship has been shown for a plot of the intensity ratios m/e 119 (MMA)/m/e 133 (EMA) versus the µg's of MMA. Therefore, quantitation is accomplished by comparing the sample's MMA/EMA ratio to the standard containing 50 µg of both MMA and EMA.

A recent report indicates that urinary MMA may be a better indicator of Vitamin B_{12} deficiency than the serum concentration of the vitamin. The excretion of MMA may be the first indication of Vitamin B_{12} deficiency since MMA levels reflect tissue stores of B_{12} (1). A second article states that a number of patients with apparent pernicious anemia falsely showed a normal serum Vitamin B_{12} level through the established radiodilution assay[2]. In addition, pernicious anemia, thought to be predominate in elderly people of northern European origin may be also prevalent in other racial groups, particularly among young black women[3].

Using this method this past year we have successfully detected several pernicious anemia patients and our data substantiate the above mentioned papers. Two young black girls in their twenties were detected. One revealed a MMA level of 105 µg/ml urine with a corresponding serum Vitamin B_{12} level of 80 pg/ml serum. The normal range of urinary MMA in adults was 0.5 to 5.0 µg MMA/ml and normal serum Vitamin B_{12} levels were 225-1000 pg/ml. The other black girl showed 100 µg MMA/ml urine but gave a normal value of 385 pg/ml serum by radiodilution assay. She was confirmed to have pernicious anemia through the Shilling test. In addition, we detected a patient with pernicious anemia who had exhibited neurologic manifestations for 14 years prior to diagnosis (461 µg MMA/ml urine; 50 pg/ml serum). The patient is presently paralyzed. Other reports have appeared of patients with severe subacute combined degeneration of the spinal cord with normal serum cobalamin levels on radiodilution assay[2]. One died of the disease. One child was diagnosed with methylmalonic aciduria with 2000 µg MMA/ml urine and 195 µg MMA/ml serum. Four days after Vitamin B_{12} administration was begun he gave a level of 147 µg MMA/ml urine showing he was responding to therapy.

Mass spectrometry using multiple ion monitoring provides the capability of quantitating MMA within one hour using only 50 µl of urine. The measurement of MMA may be a more diagnostic tool than current radiodilution methods of measuring serum Vitamin B_{12}. The test is specific, rapid, and may prevent severe disability through the timely diagnosis of pernicious anemia or methylmalonic aciduria.

1. Higginbottom MC, Sweetman L and Nyhan WL. The New England Journal of Medicine 299(7):317, 1978.
2. Cooper BA, Whitehead VM. The New England Journal of Medicine 299(15):816, 1978.
3. Carmel R and Johnson CC. The New England Journal of Medicine 298(12):647, 1978

IDENTIFICATION OF A NOVEL TYPE OF GLUCURONIDE CONJUGATE IN THE METABOLISM OF CARAZOLOL

M. Senn, H. Hindermayr and K. Koch
Chemical Research Division,Analytical Department,BOEHRINGER MANNHEIM GMBH

C A R A Z O L O L
(4-(Hydroxy-3-isopropyl-amino-propyl)-Carbazole) is a beta-blocking drug.

The metabolic fate of C^{14} labelled Carazolol given as a single dose to a Beagle dog, will be discussed. A total of 160 mg was administered by a quick intravenous injection.

Carazolol is quickly metabolized to give extensively glucuronides. During the structure elucidation carried out by electron impact and chemical ionization mass spectrometry using different derivatives, a competely new type of metabolite was discovered which has not been described before in the exogenous metabolism of any drug substance.

The unconjugated metabolites M-1 and M-2 were recovered by extraction procedures and tlc. The conjugates (M-3 and M-4) were separated by ion exchange chromatography.

For the mass spectrometric analysis the following derivatives were prepared by standard methods:

Per-O-trimethylsilyl-derivatives
Per-O-trimethyl-d_9-silyl-derivatives
Trimethylsilyl-methylesters
Permethylated-derivatives

Unconjugated metabolites

M-1 was identified by mass spectrometry as 2-hydroxy-3-(carbazolyl-4-oxy)-propionic acid, M-2 was found to be the parent drug with a molecular ion at m/e 298. Identity was confirmed with authentic material.

Conjugated metabolites

Chromatography of M-3 and M-4 metabolites resolved each fraction into two portions containing radioactivity, (M3-1, M3-2 and M4-1, M4-2). Upon incubation with beta-glucuronidase hydrolysis to carazolol occured. The mass spectra of M3-1 and M3-2 are almost identical and show a molecular ion of 762 in the per-TMS derivative. The typical fragments of glucuronides are observed (1). The point of conjugation is clearly elucidated by the aminefragment (m/e 72) and by the 4-hydroxy-carbazole ion (m/e 183). These ions are shifted by 14 mass-units to higher mass in the per-methylated derivatives. The mass spectra indicate two isomeric O-glucuronides suggesting diastereomers. Only a few examples are known (2,3).

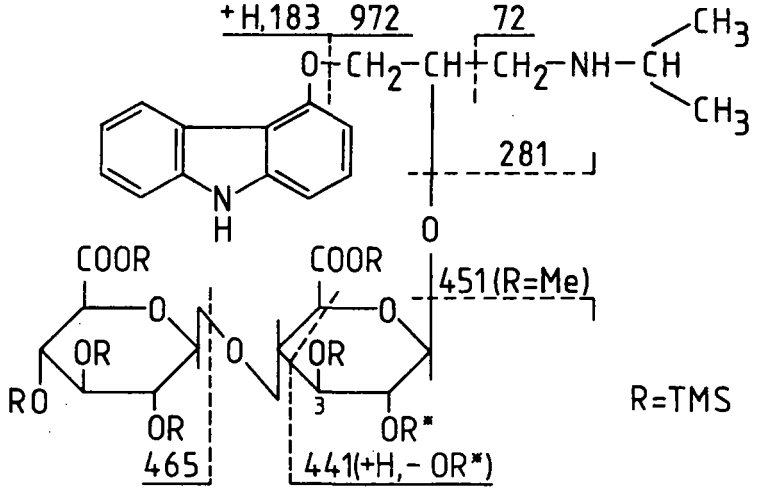
The mass spectra of M4-1 and M4-2 are again almost identical. The molecular weight was determined by the M-15 ion of the different TMS derivatives. Only in the e. i. and c. i. mass spectra of the per-methylated metabolites is a molecular ion present at m/e 776 and 777. The glucuronide fragments are observed (1). In the permethyl derivative the ion at m/e 451 provides significant information about the structure of the sugar moiety of the conjugate. Elimination of methanol from the 451 ion leads to m/e 419. This ion-type is observed in the spectra of the different derivatives:

TMS: m/e 767, d_9TMS: m/e 821, TMS-Me-ester: m/e 651.

These findings suggested a di-uronic nature of the conjugate. The terminal uronic acid residue is postulated to be the C-1 substituted glucuronic acid since, glucuronide fragments are present and upon incubation with beta-glucuronidase hydrolysis to carazolol occurs. The highly selective enzyme reaction cleaves the acetal linkage of glucuronic acid conjugates only. A monoglucuronide as an intermediate is assumed.

A series of aglucone fragments, mainly the amine and carbazole fragments, permit the characterization of the site of conjugation as occurring at the secondary hydroxyl group. M4-1 and M4-2 are considered diastereomers. A C-1→C-4 linkage of the glucuronide moities is postulated. C-1→C-2 is very unlikely. A C-1→C-3 linkage is excluded due to the explanation of mass 441 (TMS) where the 3-position is substituted.

Mass spectrometric analysis and enzymic hydrolysis enabled the elucidation of the structure of this novel type of metabolite:



Literature

1. St. Billet et. al. J. Med. Chem. 16, 30 (1973)
2. H. Ehresson J. Pharm. Pharmac. 27, 972 (1975)
3. H. W. Ruelius et. al. Drug Metab. Disp. 7, 40 (1979)

MEASUREMENT OF 6-KETO $PGF_{1\alpha}$ IN BIOLOGICAL FLUID BY SELECTED ION MONITORING.

M. Claeys, A. Duchateau, C. Van Hove and A.G. Herman, Laboratory for Experimental Phärmacology, University of Antwerp, Universiteitsplein 1, B-2610 Wilrijk, Belgium.

6-keto $PGF_{1\alpha}$ is of interest because it is the stable end-product of the physiologically active prostacyclin, an unstable metabolite af arachidonic acid with potent vasodilating properties and inhibiting effects on blood platelet aggregation. So far, little physico-chemical information is available as to how to determine this metabolite succesfully and precisely in biological fluids (1). To complement radioimmunoassay and bioassay determinations, which are performed in our laboratory on a routine basis, a GC/MS method has been worked out.

The GC/MS method includes the following sequential steps :

1. isolation of 6-keto $PGF_{1\alpha}$ from the biological matrix by solvent extraction.
2. purification by TLC.
3. derivative formation into the methyl ester, methoxime, trimethylsilyl ethers.
4. measurement by selected ion monitoring (SIM).

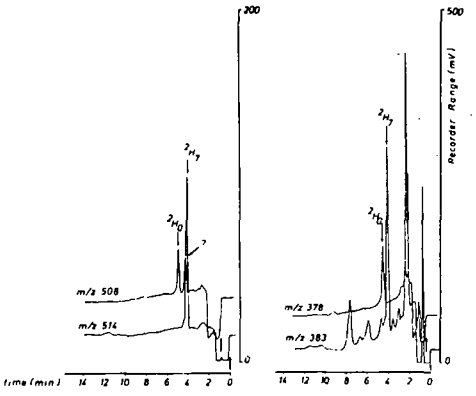
The applicability of a GC/MS method for the determination of small quantities of prostaglandins depends to a large extent onthe optimalisation of all the steps involved in the analytical procedure. Difficulties have been reported for the derivatisation of 6-keto $PGF_{1\alpha}$ and related compounds (2). In the present work, a significant improvement over the commonly employed method for sub-microgram derivatisation, in which the sequence of reactions is methyl ester formation, methoximation followed by trimethylsilylation, was obtained by carrying out the methoximation first. This procedure resulted in a 5-fold increase in derivative yield at the 100 ng level.

Quantitation was achieved by isotope dilution with $^2H_7$-analog, which was prepared biosynthetically in a two step procedure starting from $^2H_8$-arachidonic acid (20:4). Analysis were performed on a Finnigan 4000 GC/MS instrument, operated in the EI mode, and using a 1% Dexsil 300 column at 250°C with helium as carrier gas. SIM was carried out with a programmable multiple ion monitor by monitoring two abundant ions at m/z 378 and m/z 508, respectively corresponding

with the $[M^{+\cdot} - (C_5H_{11}^{\cdot} + 2\ TMSOH)]^-$ and $[M^{+\cdot} - (CH_3O^{\cdot} + TMSOH)]^-$ fragment ions, and their labeled species at m/z 383 and 514. Optimal sensitivity was obtained in the 25-30 eV range; lowering the electron energy from 70 eV to values below 30 eV resulted in a 2 à 3 fold increase in sensitivity without alteration of the [m/z 378] / [m/z 508] ratio ($\approx$3), employed for confirming the identity of the compound measured.

The method was applied to the analysis of pericardial, peritoneal and pleural fluid and to incubates of pericardium and peritoneum of the rabbit, for which a high prostacyclin synthetase activity has been demonstrated (3). The selected ion current profiles, corresponding with m/z 508 and m/z 514 obtained on standards and on the biological samples, show clean traces and well-shaped peaks and are therefore suitable for quantitation purposes; the resulting standard curves in the 10-100 ng/ml range gave correlation coefficients > 0.999 (N=5). A typical analysis, obtained on peritoneal fluid, is given in fig. 1. The measurements in the biological fluids

Fig. 1. Typical analysis of 6-keto $PGF_{1\alpha}$ in peritoneal fluid (1 ml) of the rabbit.



(table 1) show high 6-keto $PGF_{1\alpha}$ levels, indicating a substantial in vivo release of prostacyclin and pointing to a physiological role for it in the pericardial, peritoneal and pleural cavities.

Table 1. 6-keto $PGF_{1\alpha}$ levels in biological fluid.

Animal	Biological fluid	level (ng/ml)[a]
rabbit	pericardial fluid	12.9
	peritoneal fluid	22.7
	pleural fluid	10.9
	pericardium incubate[b]	30.6
	peritoneum incubate	56.4
dog	pericardial fluid	68.8

[a] S.E. = 0.3

[b] incubation conditions : 100 mg tissue/ml Tris HCl buffer (pH8, 0.05M); 20 min at 37°C.

Further work will include application of the same basic methodology to quantification of lower 6-keto $PGF_{1\alpha}$ levels in blood (range 1-10 ng/ml) and to verification of results obtained by radioimmunoassay measurements.

References.

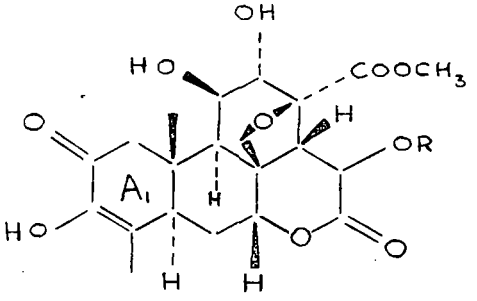
1. C.R. Pace-Asciak, Anal. Biochem., 81, 251-255 (1977).
2. F.F. Sun and B.M. Taylor, Biochemistry, 17, 4096-4101 (1978).
3. A.G. Herman, M. Claeys, S. Moncada and J.R.Vane, Arch Int. Pharmacodyn., 236, 303-304 (1978).

THE MASS SPECTRA OF BRUCEOLIDES: A PRELIMINARY INVESTIGATION

Michael Baldwin, David Carter and Fikria Darwish

The School of Pharmacy, University of London, England.

A series of bruceolides have been isolated from a Fijian sample of the Simaroubaceous tree Brucea javanica. Earlier work on Brucea antidysenterica showed these quassinoids to have significant anti-tumour activity (ref.1), marginal in the parent alcohol bruceolide (1) but of much greater activity in the unsaturated esters.

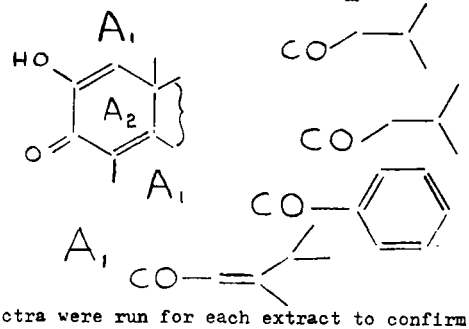


1.
bruceolide
R = H

The compounds were separated by column and preparative tlc and were identified using a ZAB 1F mass spectrometer. Four bruceolides were characterised (table 1), including the new compound dehydrobruceine A. Brucein A has been shown to inhibit lymphoid leukemia (ref. 2) and confirmation of identity of this compound was obtained by column chromatography and tlc with an authentic sample of bruceine A.

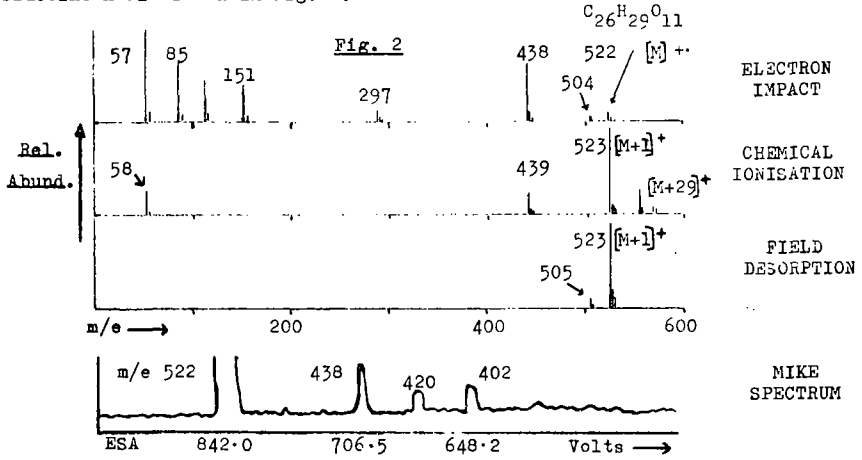
Table 1

Compound	R
2. bruceine A	
3. dehydrobruceine A	
4. bruceantarin	
5. bruceantin	



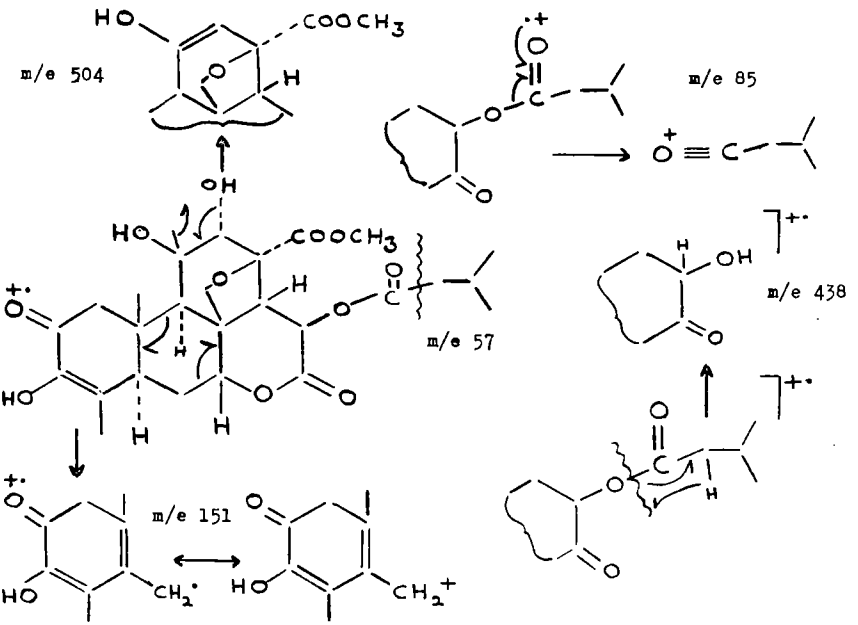
Field desorption mass spectra were run for each extract to confirm the integral molecular weights of the bruceolides and to determine those present as minor components. A MIKE spectrum on the molecular ions showed that m/e 438

(m/e 436 for 3) was a genuine fragment and not residual parent alcohol. This spectrum plus electron impact and methane chemical ionisation runs for bruceine A are shown in fig. 2.



Some fragmentation pathways are suggested for bruceine A.

Scheme 1



References:

1.) S. M. Kupchan et al. J. Org. Chem., Vol. 40, No. 5, 1975.

2.) J. D. Phillipson, F. A. Darwish. Planta Medica, Vol. 35, No. 5, 1979.

++++++++++

PULSED MOLECULAR BEAM STUDIES OF PHOTODISSOCIATION DYNAMICS*

W. Ronald Gentry
Chemical Dynamics Laboratory
Department of Chemistry
University of Minnesota
Minneapolis, Minnesota 55455

From a fundamental point of view, van der Waals molecules have several properties which make them especially appealing as model systems in which to study unimolecular fragmentation. First, the van der Waals bond in many dimer systems is so weak that even a single quantum of vibrational energy in one of the monomer modes is sufficient to dissociate the dimer. Thus, not only can the dissociation be induced at a well-defined internal energy level, but the density of states in the fragmentation products will necessarily be very low. Also, in van der Waals molecules there is an extreme disparity between the vibrational frequencies within the monomer, and those of the van der Waals coordinates into which energy must be transferred in order to cause dissociation. One might expect this feature to lead to unusual dynamical effects.

We have recently investigated the infrared photodissociation of several van der Waals dimer species, using our pulsed molecular beam apparatus[1], in combination with a pulsed, line-tuneable CO_2 laser. Fig. 1 shows a schematic diagram of the experiment. The pulsed source is operated with a pressure of several atmospheres of He, seeded with a small amount (typically 0.1-1%) of the desired monomer species. The conditions are chosen so that the dimer concentration in the expanded beam is small, and the concentration of trimer and higher-order clusters is negligible. The fwhm dimer pulse duration is typically about 6 microseconds, corresponding to a pulse length of about 1 cm. After collimation to an angular divergence of about 1° fwhm, the molecular beam pulse is intercepted transversely by the laser beam. We perform two types of experiments: (a) measurement of the fractional attenuation of the primary dimer beam, and (b) measurement of the speed and angle distribution of the monomer fragments. Fig. 2 shows an example of the first type of measurement. In this case, 90% of an ethylene dimer beam pulse is dissociated by the 1.5 cm-wide laser beam.

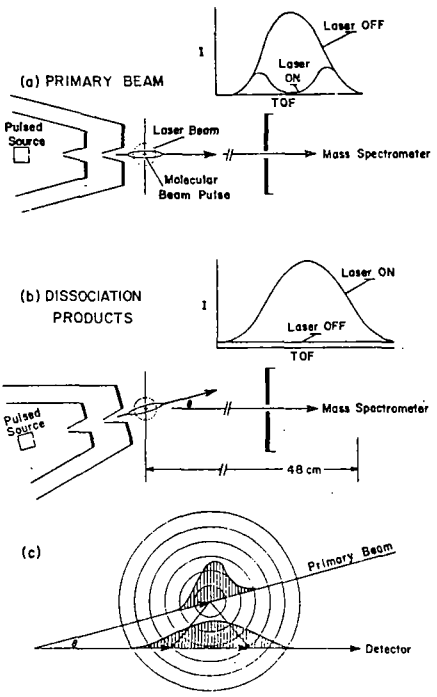


Fig. 1. Schematic diagram of experiments. (a) attenuation of primary beam pulse by photodissociation. (b) measurement of fragment TOF distribution at a laboratory scattering angle θ. (c) velocity vector diagram for an experiment of type (b), showing the relationship between the velocity distributions in the laboratory and center-of-mass frames.

Because the monomer units in a van der Waals complex are only weakly coupled, one generally expects the dimer to absorb photons of frequencies only near that one of the monomer modes. Also, because of the discrepancy between the frequency of the monomer mode which is excited and those of vibrations in the van der Waals coordinates, one expects a relatively long predissociation lifetime, and therefore a narrow absorption linewidth. Some systems which we have examined, such as benzene and cyclopropane dimers, are consistent with this

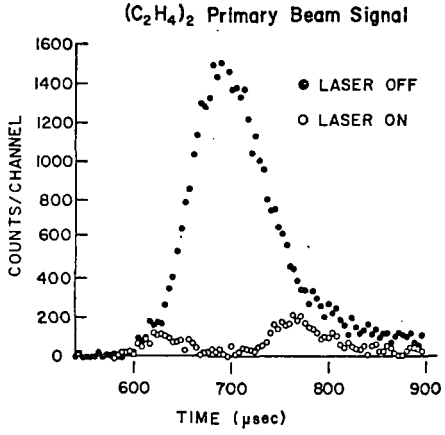


Fig. 2. TOF distributions measured for the ethylene dimer primary beam signal with and without laser radiation at 10.551 microns.

expectation, displaying dissociation linewidths only slightly broader than one estimates from power-broadening alone. One system, however, has proven to be very surprising. Fig. 3 shows the attenuation of the ethylene dimer, $(C_2H_4)_2$, signal in the primary beam, as a function of the laser wavelength and intensity. The dissociation probability is peaked, as expected, near the monomer absorption frequency. However, measurable attenuation is also observed for every other line in the CO_2 laser emission spectrum, even at frequencies more than 100 cm^{-1} away from the absorption maximum. The power broadening of the linewidth would only account at most for a few cm^{-1}, and the beam temperature (5 K in some experiments) is so low that rotational structure could also not contribute much to the observed linewidth.

Further information on the dissociation process is provided by our measurements of the speed and angle distribution of the monomer products. Fig. 4a shows the monomer product TOF spectrum at a 10° laboratory angle, and Fig. 4b shows the results of deconvoluting the measured speed and angle distributions to extract the product translational energy distributions in the center-of-mass coordinate system. The average product translational energy is 8 meV for λ = 9.271μ (20% dissociation). *If the dissociation process involved two or more photons, one would expect to see a* higher product translational energy for the laser line which more nearly saturates the dissociation. Instead, an increase of 16 meV in the energy of a single photon yields a 7 meV increase in the translational energy, with the remainder going into

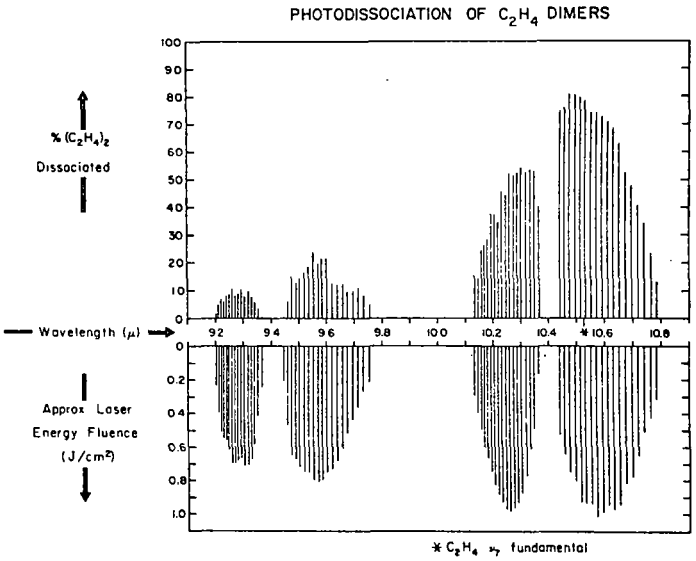


Fig. 3. Fractional attenuation of the C_2H_4 dimer signal, as a function of laser frequency and intensity.

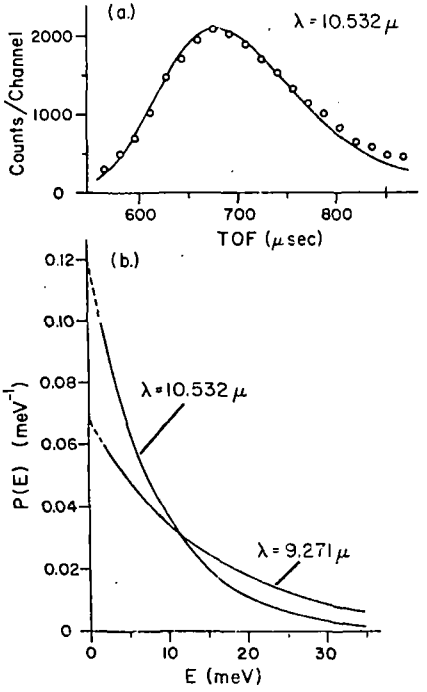


Fig. 4. Data on the C_2H_4 monomer energy distribution from photodissociation of $(C_2H_4)_2$. (a) Monomer TOF spectrum at $\theta_{lab}=10°$ and λ = 10.532μ. The solid line is the spectrum predicted for the distribution shown in part (b), taking into account the experimental resolution function. (b) Energy distributions from the deconvolution procedure at λ = 10.532μ and λ = 9.271μ. The assumed functional form in these cases was P(E) = A exp(-E/<E>).

additional product internal energy. At either wavelength, the translational energy is only a small fraction of the total energy available from the photon energy (110-140 meV) minus the estimated van der Waals bond energy of 17 meV [2]. Since the only lower-lying vibrational mode of C_2H_4 is inaccessible to most of the dissociation products, the excess energy must go mostly into rotational excitation of the monomers.

Although the experimental data seem clear enough, the interpretation is perhaps not. The simplest explanation for the large dissociation linewidth (about 35 cm^{-1}) is that it is determined by the uncertainty-principle lifetime of the upper state. However, the lifetime which follows from this interpretation is only one or a few vibrational periods of the monomer -- about 10^{-13} sec! This implies very strong coupling between the monomer and van der Waals modes, despite the great disparity in frequencies. This interpretation certainly falls outside the pale of theoretical treatments of vibrational predissociation in simpler van der Waals complexes [3], and is about two orders of magnitude faster than the fastest linewidth-deduced rates of dissociation which have been determined for complexes of rare gas atoms with vibronically excited diatomic and triatomic molecules [4].

Another model by which the broad dissociation spectrum might be explained is that absorption occurs in combination bands of the monomer mode with the various low-frequency van der Waals vibrations. However, this explanation requires that a large number of overlapping combination bands all be intense enough to produce dissociation at every CO_2 laser line. This explanation therefore also requires very strong coupling between the monomer and the van der Waals vibrations. In the presence of such strong coupling, it may be an arbitrary distinction whether we choose to describe motion in the van der Waals coordinates as highly excited vibration and rotation, or as translation. It may require more theoretical and experimental study before we can unambiguously define what we mean by the dissociation lifetime under such circumstances.

The dissociation spectrum for $(C_2D_4)_2$, shown in Fig. 5, is markedly narrower than that for $(C_2H_4)_2$. The mode which we excite in C_2H_4 is the ν_7 out-of-plane vibration, whereas in C_2D_4 we excite the ν_{12} in-plane mode. Clearly, the broad dissociation spectrum of C_2H_4 dimers is not due to some general property such as a loose, fluxional structure, but rather to a specific interaction involving the out-of-plane vibration. This mode-specific dynamical behavior is even more striking in the case of the mixed dimer $C_2H_4 \cdot C_2D_4$, for which the dissociation spectrum resembles the superposition of Figs. 3 and 5. Within the same molecule, the linewidth associated with the C_2H_4 out-of-plane vibration is very much greater than that associated with the C_2D_4 in-plane vibration.

Unfortunately, there is little definite information available about the structure of the ethylene dimer. Electric resonance experiments indicate that the dimer has no dipole moment [5]. This is consistent with the crystal structure [6], in which the planes of nearest-neighbor monomers are parallel. A line joining the centers of mass

of two adjacent monomers is perpendicular to the C-C axes of both molecules, and makes an angle with each monomer plane estimated to be 27°. Evidence that the crystal structure is similar to that of the gas phase dimer is provided by the fact that the absorption frequency of the C_2D_4 dimer is shifted from that of the monomer to almost the extent that the crystal absorption frequency is shifted. The crystal structure does appear to be consistent with stronger coupling of the van der Waals coordinates to out-of-plane vibration of the monomer than to in-plane vibration, and also with the high rotational excitation which is observed in the monomer products.

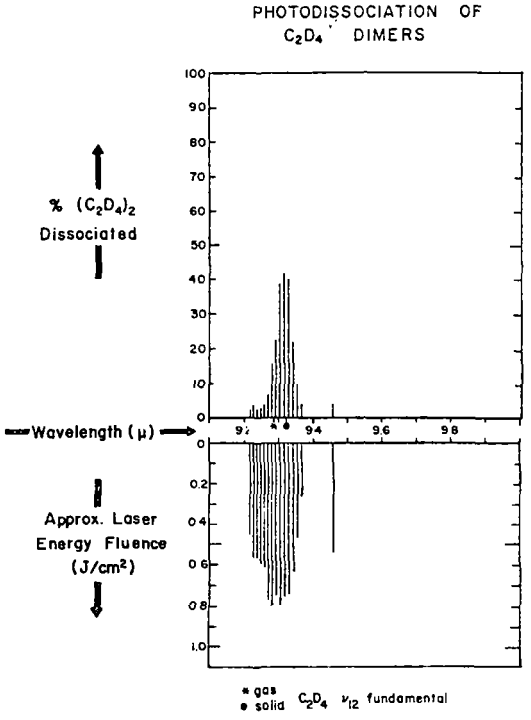


Fig. 5. Fractional attenuation of the C_2D_4 dimer signal, as a function of laser frequency and intensity.

*Research supported by the National Science Foundation. This work was done in collaboration with Mark A. Hoffbauer and Clayton F. Giese.

1. W.R. Gentry and C.F. Giese, J. Chem. Phys. 67, 5389 (1977); Phys. Rev. Lett. 39, 1259 (1977); Rev. Sci. Instrum. 49, 595 (1978).

2. J.O. Hirschfelder, C.F. Curtiss, and R.B. Bird, Molecular Theory of Gases and Liquids, p. 1112, 1213 (Wiley, New York, 1954).

3. J.A. Beswick and J. Jortner, J. Chem. Phys. 68, 2525 (1978), and refs. therein.

4. K.E. Johnson, L. Wharton and D.H. Levy, J. Chem. Phys. 69, 2719 (1978); and refs. therein.

5. S.E. Novick, P.B. Davies, T.R. Dyke and W. Klemperer, J. Amer Chem. Soc. 95, 8547 (1973).

6. C. Brecher and R.S. Halford, J. Chem. Phys 35, 1109 (1961).

FAM0A2 UNIMOLECULAR REACTIONS AND ENERGY TRANSFER IN IONIC SYSTEMS, M. T. BOWERS, Dept. of Chem., Univ. of Calif., Santa Barbara, Calif. 93106

The literature on unimolecular reactions in ionic systems is massive, primarily due to the large number of metastable ion studies reported and to the development of quasi equilibrium theory to explain mass spectral cracking patterns and their dependence on energy. In this talk, the emphasis will be on recent work, particularly work where angular momentum is important. Comparison between theory and experiment will be made whenever possible. The literature on energy transfer in neutral systems is very extensive, but energy transfer in ionic systems has been less extensively studied. The recent work will be summarized and compared to relevant neutral systems whenever possible. In both cases work from our laboratory will be emphasized.

Transients in Vibrational Relaxation of Polyatomic Molecules at High Temperatures by the Variable Encounter Method

M. C. Flowers,* D. F. Kelley, F. C. Wolters, and B. S. Rabinovitch

Department of Chemistry, University of Washington, Seattle, WA 98195

The study over the past two decades of the collisional de-excitation of highly vibrationally excited reacting neutrals has led to some general findings.[1] They are summarized as follows; obviously, details vary with circumstances from system to system:

1. Relatively strong collider bath gases (M) remove average amounts of energy, $\langle\Delta E\rangle$, of the order of 5-15 kcal mole^{-1} on each collision.
2. Relatively weak collider bath gases remove lesser amount of energy, say, 0.5-5 kcal mole^{-1} on each collision.
3. The cross sections for collisional deactivation are closely the same as ordinary gas kinetic cross sections.
4. Energy transfer is primarily V-T,R in nature. Collision complexes are formed, as governed by the attractive forces. Energy in the internal modes of the hot molecule relaxes into the transitional stretching and bending modes that correlate with translations and rotations of the collision partners. Participation of the internal modes of M occurs only if the interaction is strong and the mode spacings of M are intrinsically small.
5. The accommodation between internal modes and transitional modes is restricted by conservation of angular momentum.
6. Monatomic bath gases are less efficient colliders than are diatomic-linear molecules, which are less efficient than polyatomic-nonlinear molecules, in general.

The above generalizations are described by a model given by Lin and Rabinovitch.[1] More recently, a modified, more quantitative version has been given by Battacharjee and Forst.[2]

Several restrictions should be noted. The first is that the above summary refers to lower temperatures – below 600K-700K where most energy transfer studies of this sort have been made. Very little information is available about the temperature dependence of $\langle\Delta E\rangle$. Two studies have been published at higher temperatures with substrates cyclopropane and cyclopropane-d_2.[3,4] They reveal that a significant decline in $\langle\Delta E\rangle$ occurs (Table 1).

The second restriction is that measurements have hitherto been restricted to steady state conditions. It is obviously desirable to obtain information in the transient region prior to the establishment of the steady state. Such measurements in a low pressure unimolecular reaction system correspond to the measurement of the mean first passage time.[5]

Finally, there is an intermediate energy region, around 10-30 kcal mole^{-1}, where the energy transfer phenomenon is not well delineated.

We have developed a new technique for the study of neutrals in the transient region. The Variable Encounter Method[6] (VEM) permits the sequential study of the vibrational relaxation that occurs upon successive collisions of a substrate molecule with a surface. We have reported some preliminary measurements with cyclopropane-d_2.[7] Besides probing the transient behavior, other information may be gained: the efficiency of the wall has never been explicitly studied; the evidence suggests that it should be more efficient than gas molecules which are of lesser complexity;[3] the variation of $\langle\Delta E\rangle$ with temperature can also be probed; finally, whereas previous information has concerned the transition

probabilities in the region around E_0, the critical threshold energy, VEM is sensitive to the transitions over the whole energy spectrum, including $0 < E < E_0$.

VEM is a very simple technique for studying the dynamics of energy transfer at a surface. Several cylindrical quartz reactor fingers of varying dimensions are blown on to the surface of a large, fused quartz bulb. The fingers may be heated by a stainless block furnace. Entrance area to a reactor finger is $\lesssim$ 1/50 of the bulb area. The dimensions of the reactor used may be varied so as to provide mean wall collision numbers, m, from 2 to 100, per encounter. For a given m, the distribution of wall collisions may be found by Monte Carlo calculation.[7] Molecules that return to the bulb are cooled by collisions with the bulb wall before another encounter with the reactor occurs.

For the substrates chosen, brief pre-exposure of the heated reactor wall to substrate provided adequate seasoning and reproducible results. To perform a run, one reactor was heated, the bulb (at $\sim$ 375 K) was pumped to a stable residual pressure of $< 10^{-6}$ torr, and substrate was admitted at $1\text{-}2\times10^{-4}$ torr and left for a suitable time. Analysis was by gas chromatography; percent reaction varied from $\sim$ 1 - 50%.

Experimental energy transfer results are summarized in Table 2. Figure 1a illustrates the variation of $\overline{P}_c$, the average reaction probability per collision, with m at constant temperature for c-C_4H_8; the reactor m values were 2.6, 8.5 and 27.2. Figure 1b shows the sequential variation of P_c vs collision number n. The data were fitted by trial with various forms of the collisional probability distribution function, including gaussian and exponential forms having varying detail as a function of E.

We find, in elaboration of our previous results,[6] that accommodation to a proximate steady state with the wall takes place in a small number of collisions, $\sim$ 8-30 for both the cyclopropane and cylobutane systems (Fig. 1b), the number increasing with increase of temperature and decrease of $\langle\Delta E\rangle$. Wall collisions on a surface seasoned with a hydrocarbon film are more efficient than are binary gas phase collisions, as may be seen by comparison of Tables 1 and 2. The present data also support our previous findings[3,4] that energy transfer collision efficiency continues to decline at higher temperatures for these polyatomic unimolecular systems; a turning point at very high temperatures is plausible.

This work was supported by the Office of Naval Research and by the National Science Foundation.

References

*Permanent address: Department of Chemistry, University of Southampton.

1. Y. N. Lin and B. S. Rabinovitch, J. Phys. Chem. 74, 3151 (1970). S. C. Chan, et al., J. Phys. Chem. 74, 3160 (1970).
2. W. Forst and R. C. Bhattacharjee, Chem. Phys. 30, 217 (1978).
3. I. Klein and B. S. Rabinovitch, Chem. Phys. 35, 439 (1978).
4. E. Kamaratos, J. F. Burkhalter, D. G. Keil and B. S. Rabinovitch, J. Phys. Chem. 83, 984 (1979).
5. S. K. Kim, J. Chem. Phys., 28, 1057 (1958). B. Widom, J. Chem. Phys. 31, 1387 (1959); 34, 2050 (1961).
6. D. F. Kelley, B. Barton, L. Zalotai and B. S. Rabinovitch, J. Chem. Phys. in press.
7. B. D. Barton, Ph.D. Thesis, University of Washington, 1979.

Table 1. Measurement of $\langle\Delta E\rangle_d$ at Higher Temperatures by Steady State Methods

Method	Substrate	Bath Gas	T,K	$\langle\Delta E\rangle$cm^{-1}	ref
CCRS[a]	c-1,1-$C_3H_4D_2$	c-1,1-$C_3H_6D_2$	775	$\geq$ 3000G[b]	3
			975	1900G	
Diffusion Cloud	c-C_3H_6	CO_2	975	1100G	4
			1175	450G	
		N_2	975	400E	
			1175	350E	
		H_2	975	150E	
			1175	90E	
		He	975	190E	
			1175	160E	

a) Competitive collisional reaction "spectroscopy";

b) G, gaussian; E, exponential distribution

Table 2. Measurements of $\langle\Delta E\rangle$ at Various Surface Temperatures by VEM

Substrate	T,K	$\langle\Delta E\rangle$cm^{-1}	ref
c-1,1-$C_3H_4D_2$	800	4100G	7
	975	3400G	
	1175	2500G	
c-C_3H_6	800	4500G	present work
	950	3300G	
	1075	2300G	
c-C_4H_8	800	2400E	present work
	900	1900E	
	1125	1500E	

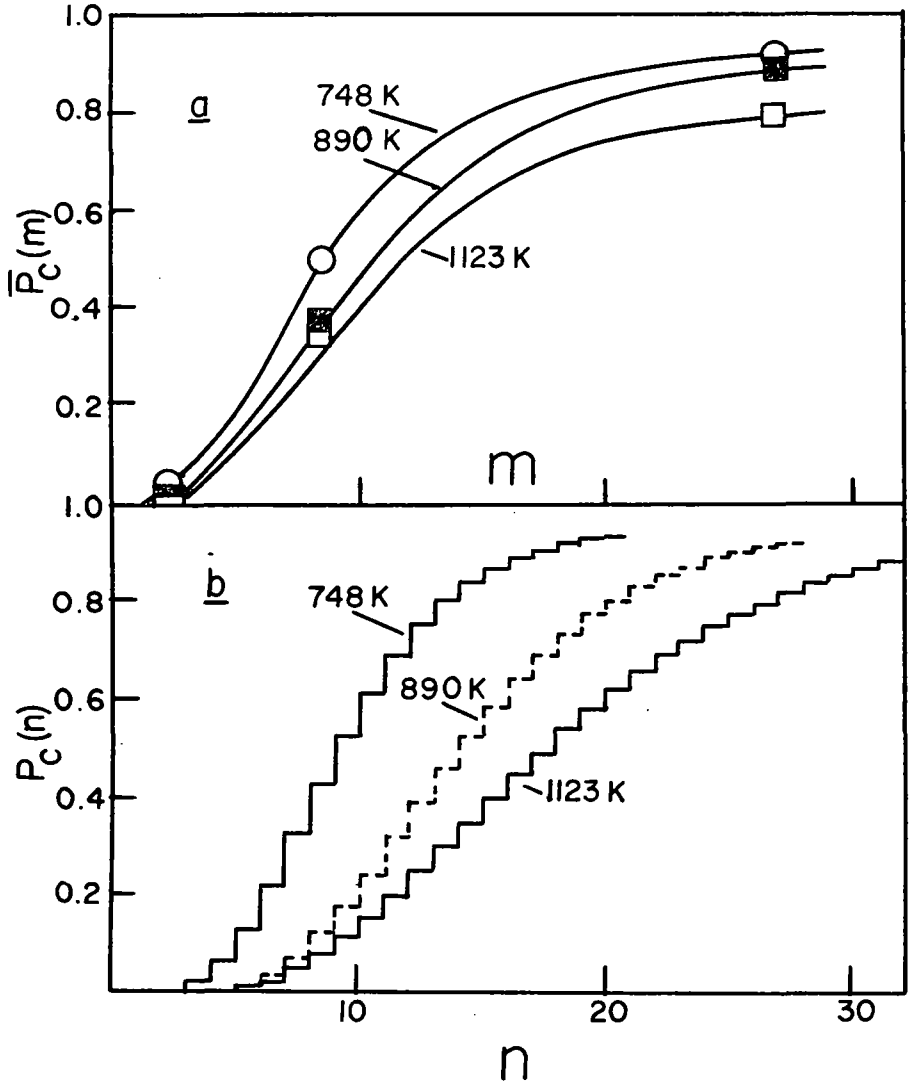


Figure 1a. Plots of experimental average probability of reaction per collision, $\bar{P}_c$, as a function of mean collision number per encounter, m , at the temperatures indicated. Solid curves are based on trial fit <ΔE> values at various temperatures (Table 2). The ordinate scale is normalized to $\bar{P}_c(\infty) = 1$.

Figure 1b. Plots of $P_c(n)$, the calculated sequential probability of reaction per collision, as a function of the consecutive number of collisions, for the temperatures shown and for the <ΔE> values of Table 2. The ordinate scale is normalized to $P_c(\infty) = 1$.

CHARGE TRANSFER REACTIONS OF MOLECULAR IONS

T.F. Moran
Department of Chemistry
Georgia Institute of Technology
Atlanta, Georgia 30332

In many ion-molecule interactions, charge transfer processes strongly compete with other reaction product channels. It is not unusual for charge transfer channels to dominate the reaction especially if the recombination energy of the reactant ion matches the energy required to form an ionic state of the target molecule. These and other factors that exert control over molecular charge transfer processes have been examined within the framework of a multistate impact parameter model. At high reactant ion velocities it has been shown that products emerging from collision may possess a significant amount of energy in vibrational modes; however, the question of vibrational deactivation of ions in charge transfer reactions is not well documented. These deactivation processes are examined in the first part of this paper. Recent drift tube experiments have shown that:

a) the rate constants for the reactions

$$O_2^+ + CH_4 \rightarrow CH_3O_2^+ + H \qquad (1a)$$

$$O_2^+ + CH_4 \rightarrow CH_3^+ + HO_2 \qquad (2a)$$

are very sensitive to O_2^+ vibrational energy;

b) the collision of ground state $O_2^+(X^2\Pi_g, v=0)$ with Ar buffer gas produces $O_2^+(X^2\Pi_g, v=1)$ ions (a fact in agreement with ion beam-neutral beam studies);

c) a small amount of O_2 added to this drift tube system acts as a surprisingly effective vibrational energy sink which inhibits $O_2^+(X^2\Pi_g, v=1)$ ions produced in (b) from reacting with CH_4 in reactions (1a) and (2a).

In order to gain a quantitative measure of vibrational deactivation, a multistate impact parameter treatment has been used to examine transitions occurring in the symmetric ion-molecule system

$$O_2^+(X^2\Pi_g, v_o=1) + O_2(X^3\Sigma_g^-, v_o=0) \rightarrow O_2(X^3\Sigma_g^-, v'') + O_2^+(X^2\Pi_g, v') \qquad (3)$$

$$O_2^+(X^2\Pi_g, v_o=1) + O_2(X^3\Sigma_g^-, v_o=0) \rightarrow O_2^+(X^2\Pi_g, v') + O_2(X^3\Sigma_g^-, v'') \qquad (4)$$

where charge transfer reactions predominate. Each of the charge transfer channels (3) is degenerate in energy with a corresponding direct channel (4) which leads to strong coupling between the charge transfer and direct processes in this symmetric ion-molecule system. The wavefunction which represents the time-dependent response of the internal motions of the system under the influence of the mutual interaction V(R,r) is

$$\Psi_i(r,R) = \sum_{\alpha=D,X} \sum_n C_n^\alpha(\rho,Z)\psi_n^\alpha(r)\exp - (iE_n^\alpha t) \qquad (5)$$

where $\psi_n^\alpha(r)$ are a complete set of molecular eigenfunctions describing the unperturbed Hamiltonian for the isolated system at infinite center-of-mass separation R with eigenenergies E_n^α. The index α denotes whether the labeled quantities refer to direct channels D or to charge exchange channels X. Substitution of the wavefunction (5) into the time-dependent Schrödinger equation results in the following set of coupled equations for the transition amplitudes $C_m^\alpha(t)$,

$$i\partial C_f^\alpha(\rho,t)/\partial t = \sum_m V(R)P_{fm}C_m^{\bar\alpha}(\rho,t)\exp(i\varepsilon_{fm}t) \ , \quad f = 1,2,\ldots,N \ , \qquad (6)$$

which are solved numerically subject to the boundary condition that the direct channel i is initially populated, i.e., $C_m^D(\rho,-\infty) = \delta_{mi}$, $C_m^X(\rho,-\infty) = 0$. Matrix elements P_{fm} are equal to $F(\upsilon_f',\upsilon_m'')F(\upsilon_m',\upsilon_f'')$, where $F(\upsilon_i',\upsilon_n'')$ is the vibrational overlap for the $O_2^+(X^2\Pi_g,\upsilon_o=1) \rightarrow O_2(X^3\Sigma_g^-,\upsilon'')$ transition. When α denotes X in (6), $\bar\alpha$ refers to D and vice versa. Transition probabilities, $|C_m^\alpha(\rho,\infty)|^2$, have been computed for the exchange and direct scattering channels. It is necessary to explicitly consider 14 product channels to obtain fully converged cross sections at several eV collision energy. At large distances the resonant charge transfer channel predominates but at smaller distances the inelastic charge transfer channels become important. For example at 8 eV and 4.15 a.u. distance, the relative X probabilities for forming product (ion,neutral) states υ',υ'' = 1,0; 0,1; 0,0; 0,2; 1,1; 2,0; 0,3 are 0.6483, 0.1307, 0.0669, 0.0104, 0.1136, 0.0300 respectively. At 1.6 a.u. the probabilities for these same channels are 0.4802, 0.02881, 0.0529, 0.03717, 0.2884, 0.1125. With the aid of transition probabilities computed over all impact parameters, integral cross sections have been determined from the relation

$$Q_{if}^\alpha(\upsilon_i) = 2\pi \int_o^\infty |C_f(\rho,\infty) - \delta_{if}|^2 \rho d\rho \ . \qquad (7)$$

At 8.0 eV the charge exchange cross sections for the 1,0; 0,1; 0,2; 1,1; 2,0 and 0,0 channels are 26.3, 2.45, 0.21, 1.55, 0.86 and 0.396 Å^2 respectively. At 1 eV the vibrational deexcitation channels predominate over the other inelastic channels. A measure of this fact is given by the ratio of the ionic deexcitation to excitation cross sections (summed over both X and D channels). At 8 eV this ratio is 1.56, but as the ion kinetic energy is lowered to 1 eV, the ratio increases to 124. At 0.5 eV this ratio is 193 which indicates symmetric charge transfer reactions provide an effective vibrational relaxation mechanism for $O_2^+(X^2\Pi_g,\upsilon_o=1)$ ions.

Information gained in the study of "normal" charge transfer reactions has been used to gain insight into the reactivities of doubly charged molecular ions. Comparatively little quantitative information exists for charge transfer reactions of the type

$$AB^{2+} + AB \rightarrow AB^{+} + AB^{+} \qquad (8)$$

where $AB^{2+} = N_2$, O_2, CO, NO and CO_2. Semiempirical approaches have been used to estimate the energies required to form AB^{2+} ions as well as the shape of the isolated AB^{2+} potential energy curves. Thresholds for formation of the doubly charged ions and the shapes of the ionization efficiency curves are consistent with Franck-Condon factors computed for $AB \rightarrow AB^{2+}$ ionizing transitions. Charge transfer reactions (8) are typically large and occur in both symmetric and nonsymmetric systems. For example, the single electron transfer cross sections for 2.0 keV N_2^{2+} ions interacting with N_2, O_2, CO, CO_2, NO and H_2 are 89, 22, 10, 34, 21 and 14 $\mathring{A}^2$ respectively. The reactivities of the doubly charged ions are in part due to the wide range of recombination energies possible in the single electron transfer processes. The combination of favorable vibrational overlaps, $F(v_i', v_n'')$, and small energy defects, ϵ_{fm}, contribute to large charge transfer cross sections for these doubly charged ions.

BEAM STUDIES OF ORGANIC CHEMIIONIZATION REACTIONS

R.J. Cross, A. Auerbach*, L. Lee, and M. Saunders

Department of Chemistry, Yale University, New Haven, Conn. 06520

Molecular-beam studies of the reactions of small molecules have provided a wealth of data unattainable using more traditional kinetic techniques.[1] We are extending this method to the study of organic chemistry such as the chemiionization reaction,

$$SbF_5 + RX \longrightarrow SbF_5X^- + R^+, \qquad (1)$$

where RX is an organic or inorganic halide. Our studies focus on three aspects of the reaction: the basic chemistry (what reactions go and what products are formed), the energy requirements (how much activation energy is needed and where in the reactants does it have to go), and what are the angular and energy distributions of the products.

The apparatus has two supersonic nozzle beams which cross at right angles.[2] The detector is mounted on the rotatable lid of the vaccum chamber to allow scanning of the angular distribution. The nozzle beams are formed by passing a gas mixture at a pressure of ~1 atm. through a small hole (0.003-0.010 in.) into a vacuum. As the gas expands, it undergoes an adiabatic cooling which converts the enthalpy of the original, stagnant gas into kinetic energy of the beam. All of the beam molecules end up traveling at very nearly the same velocity. By using a mixture of rare gas and reactants one can vary the beam energy from thermal energies up to a few eV for heavy species. The expansion typically takes place in only a few dozen collisions; this is not enough to relax the vibrational energy completely. Thus by varying the composition and temperature of the stagnant gas, one can separately and independently vary the translational energy of the beam and its vibrational temperature

The two beams intersect in a grid "cage" around the center of the apparatus. The detector forms one side of the cage and can be operated in two modes. For measurement of the total cross section all of the ions are drawn into the detector and focused with an ion lens system. They are then mass selected in a quadrupole filter and detected by a Daly detector. For measurements of the angular distribution the front of the detector is kept at the same potential as the cage so that only ions traveling in the direction of the opening are detected. Ions which pass through the entrance encounter a grid which serves as a retarding-potential energy analyser, after which they are focused and detected as before. Thus we can either measure relative total cross sections or the differential angular and energy distributions of the product ions.

Reaction (1) is well-known in solution[3] where it has been used to prepare carbonium ions for structural and kinetic studies, but it was not seen in the gas-phase prior to our work.[4] Because of the large energies of solvation of the products, one would expect large changes in the thermochemistry in going from solution to gas phase. We have found reaction with a few dozen halides; t-butyl chloride, bromide, and iodide, s-butyl iodide, and isopropyl iodide all react to form known, stable tertiary and secondary carbonium ions. Probably, all tertiary and secondary halides react. We saw reaction with C_2H_5I but not with CH_3I so that, at least some primary halides react. Reaction occurs with several acyl halides to form the very stable acylium cation. Several other reactions, producing known, very stable cations were seen. Benzyl chloride reacts readily to produce either the resonance-stabilized benzyl cation or the aromatic tropilium ion. Allyl bromide produces the resonance-stabilized allyl cation. Neopentyl chloride reacts to give $C_5H_9^+$ (probably t-amyl). We have also seen reaction with SF_6 and UF_6. The latter case has possible implications for isotope separation. With few exceptions only the parant R^+ ion is observed. The exceptions occur when R^+ can very easily decompose. For example, pivaloyl chloride $(CH_3)_3CCOCl$ gives 90% pivaloyl cation and only 10% t-butyl cation. In contrast, electron bombardment ionization of pivalic acid gives almost exclusively t-butyl and smaller fragments. Similarly, phenyl acetyl chloride gives roughly equal amounts of the parent acylium ion and $C_7H_7^+$ (benzyl or tropilium). We are not now able to detect the negative ion, but expect to be able to do so shortly.

The relative cross section Q for the reaction of SbF_5 with benzyl chloride was measured in the relative energy range of 2.8-5.4 eV and a range in vibrational temperatures of 300°-730°K for the benzyl chloride beam. In this region Q is almost independent of translational energy but depends very strongly on vibrational temperature. Therefore, vibrational energy in the halide is specifically required as activation energy. The reaction may also require translational energy below the lower limit of 2.8 eV. This is in marked contrast to our results on the chemiluminescent dioxetane reaction[5] where Q is insensitive to the vibrational temperature but depends strongly on the translational energy, rising rapidly above a threshold at the experimental activation energy. The dependence of Q on the vibrational temperature of SbF_5 is more complicated: it rises up to 50°C then decreases by an order of magnitude up to 100°C after which it remains roughly constant. A likely explaination is that the beam of SbF_5 also contains dimer which reacts with a higher cross section. As the temperature is raised, the dimer concentration decreases. Auerbach[6] has set up a flow system to meas-

ure the thermal rate constant and reports a preliminary activation energy of 17±3 kcal/mole. Although our $Q(T_{vib})$ data could not be fit to an Arhenius plot, Auerbach's activation energy is much higher than any reasonable fit to our data. This strongly suggests that additional activation energy is required in either translation or vibration of SbF_5.

A convenient way to plot the angular and energy distributions is in the form of a set of contours $P(\underset{\sim}{v})$ as a function of the vector velocity of one of the products.[7] Because there is no preferred direction in the reactants, $P(\underset{\sim}{v})$ must have axial symmetry about the initial relative velocity vector $\underset{\sim}{v}_{rel}$. If the reaction proceeds via a complex with a lifetime long compared to its rotational period, $P(\underset{\sim}{v})$ will also have reflection symmetry about the center of mass. Our measurements are complicated by the low energy of the product ions (~1 eV LAB) which makes them sensitive to contact potentials and surface charges built up on the detector. Our contours for SbF_5 and benzyl chloride are roughly symmetric about the center of mass but do not have the required symmetry about $\underset{\sim}{v}_{rel}$ (the LAB energy is low by ~0.2 eV). Our tentative conclusion is that the reaction probably goes by way of a long-lived complex.

Unfortunately, the basic thermochemistry of (1) is unknown. However, we now know some of the features of the potential-energy surface. On the product side there must be a Coulomb well 2-3 eV deep. This almost certainly leads to a long-lived complex, at least at low energies, in agreement with our data. The reaction is probably quite exoergic to the bottom of the well but may be endoergic to the separated products. Since there is an activation energy, there must be a barrier in the entrance channel or in the exit channel, and/or the reaction is endoergic. A barrier in the exit channel is unlikely in the present case due to the strength and long range of the Coulomb attraction. Because the reaction specifically requires vibrational energy in RX, there must be a barrier in the entrance channel before the energy has a chance to scramble among the normal modes. It is possible that there is a small barrier in the entrance channel but that most of the activation energy must be supplied to overcome the endothermicity of the reaction. In this case some of the initial energy would be required in in specific modes while the rest could be provided anywhere.

Reaction (1) has interesting dynamics, very different from most cases studied so far. Because of the ease of analysing and detecting ions we have greater sensitivity and flexibility than in comparable experiments involving either neutral or ion-molecule reactions. The reaction has possible uses as an analytic technique since one may be

able to detect halides with high sensitivity and specificity. It may also be useful as a way to prepare specific gas-phase ions without fragmentation.

Footnotes

* Present address: Naval Research Lab., Washington, DC 20904.

1) D. Herschbach, J. Chem. Faraday Disc. 55, 233 (1973). Z. Herman and R. Wolfgang, Ion-Molecule Reactions, ed. J. L. Franklin (Plenum Press, New York, 1971), vol. 2, p. 553.

2) J. B. Anderson, Gasdynamics 4, 1 (1974).

3) G. A. Olah, E. B. Baker, J. C. Evans, W. S. Tolgyesi, J. S. McIntyre, and I. J. Bastin, J. Am. Chem. Soc. 86, 1360 (1964). G. A. Olah, W. S. Tolgyesi, S. J. Kuhn, M. E. Moffatt, I. J. Bastien, and E. B. Baker, J. Am. Chem. Soc. 85,1328 (1963). M. Saunders, P. Vogel, E. L. Hagen, and J. Rosenfeld, Accts. Chem. Res. 6, 53 (1973).

4) A. Auerbach, R. J. Cross, and M. Saunders, J. Am. Chem. Soc. 100, 4908 (1978).

5) K. T. Alben, A. Auerbach, W. M. Ollison, J. Weiner, and R. J. Cross, J. Am. Chem. Soc. 100, 3274 (1978).

6) A. Auerbach, private communication.

7) R. J. Cross and R. Wolfgang, J. Phys. Chem. 73, 743 (1969).

SILYLATION-MEDIATED OXIDATION

J. A. Kelley
Drug Design and Chemistry Section
Laboratory of Medicinal Chemistry and Biology
NCI, NIH, Bethesda, MD 20205

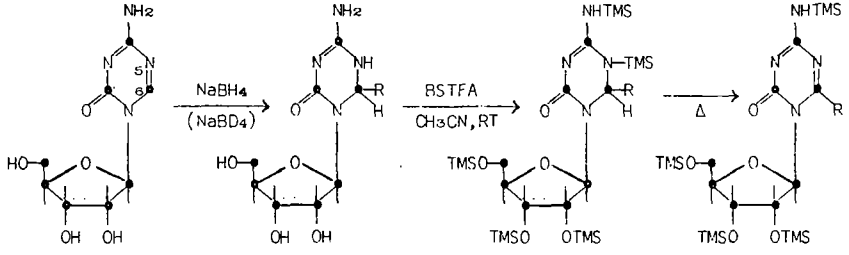
Trimethylsilylation is probably the most widely employed technique for the derivatization of polar compounds of biomedical interest for subsequent analysis by gas chromatography (GC) and combined gas chromatography-mass spectrometry (GC/MS) (1). The popularity of silylation rests with the simplicity of the procedure itself, its versatility and wide range of applicability, and the usually straightforward formation of derivatives. Out of all the compounds derivatized by silylation and reported in the literature, there have only been a few instances of the formation of what might be called abnormal silylation products (2-5). These examples all involved oxidation of the compounds being silylated. To this short list of anomalous reactions can be added the silylation-mediated oxidation of 5,6-dihydropyrimidine and 5,6-dihydro-s-triazine bases and nucleosides to the corresponding aromatic derivatives.

5,6-Dihydro-5-azacytidine (H_2-5-AC, 2a) was synthesized by sodium borohydride reduction of 5-azacytidine (5-AC, 1) in order to improve the latter's hydrolytic stability yet retain its antitumor activity (6) (See Scheme 1). Derivatization of 2a with N,O-bis(trimethylsilyl)-trifluoroacetamide (BSTFA) under conditions generally prescribed for nucleosides (7) did not produce the expected penta-silyl derivative 3a but only trimethylsilylated 5-AC (4a). When 2b was derivatized in the same way, dehydrogenation to 5-AC occurred with preferential retention of deuterium at the 6-position (4b). These initial observations prompted a more comprehensive examination of the apparent dehydrogenation that was occurring during trimethylsilylation.

The kinetics and mechanism of this reaction were investigated by quantitative GC analysis employing an internal standard. For conversion of 3a to 4a, the oxidation followed pseudo first order kinetics with a half-life of 2.02 hr at 76.5 ± 1° and required molecular oxygen as well as reagents capable of both N- and O-trimethylsilylation. Trace heavy metal impurities (Fe,Cu) which might catalyze the reaction were not present in the BSTFA, but the reaction was accelerated by heat or the free radical initiator dibenzoyl peroxide. Among free radical inhibitors diethyldithiocarbamate was somewhat more effective than galvinoxyl free radical in retarding the oxidation. Classical chemical dehydrogenating reagents such as 2,3-dichloro-5,6-dicyano-1,4-benzoquinone, chloranil and MnO_2 were unable to dehydrogenate 2a even under vigorous conditions. The rate of reaction was also dependent on the chemical identity of the base and the sugar moiety of the dihydronucleoside (Table 1). Dihydropyrimidines were dehydrogenated at substantially slower rates than dihydro-s-triazines. When either 3b or its arabinofuranosyl (Ara) analog was oxidized, deuterium was preferentially retained at the 6-position with an isotope effect of 2.8 ± 0.3. However, use of equimolar dibenzoyl peroxide as a radical initiator gave a product isotope d_1:d_o ratio of only 1.7 ± 0.3 upon oxidation of 3b.

Although there is insufficient data at present to formulate a detailed mechanism, the above results suggest that the reactive species in BSTFA might be a trimethylsiloxy radical (3,8). Thus current thinking postulates a three step mechanism for this reaction: 1) radical abstraction of H-6 in a rate-determining step, 2) combination with a trimethylsiloxy radical to give an oxygenated intermediate, and 3) elimination of trimethylsilanol to produce a new double bond or aromatic system.

The synthetic usefulness of silylation-mediated oxidation has already been demonstrated in the synthesis of the previously unattained nucleoside Ara-5-AC(9). This reaction provides a mild and simple method of obtaining an aromatic system from a suitable reduced precursor. The appreciable deuterium isotope effect also makes this reaction attractive for the microscale synthesis of non-exchangeable deuterated or tritiated derivatives in a simple one-pot procedure from an appropriately labelled precursor. Although the labelled molecule would not be 100% isotopically pure, one would not be faced with a total synthesis but simply a reduction and oxidation to obtain the target compound. Even in those cases where other labels are desired, aromatization through silylation-mediated oxidation has the potential to simplify the synthetic procedure (10).



Scheme 1

Table 1. Microscale Silylation-Mediated Oxidation of Various Substrates (T=70°)[a]

Substrate Product	No. TMS Groups	MW	I[b]	Complete Conversion (hr)
Dihydro-5-azacytidine	5	606	2530	22[c]
5-Azacytidine	4	532	2823	
1-β-D-Arabinofuranosyldihydro-5-azacytosine	5	606	2564	84
1-β-D-Arabinofuranosyl-5-azacytosine	4	532	2808	
Dihydrouridine	4	534	2539	>84
Uridine	4	532	2625	
Dihydro-5-azacytosine	3	330	1774	20
5-Azacytosine	2	256	1634	
5,6-Dihydrouracil	2	258	1636	45
Uracil	2	256	1453	
5,6-Dihydrothymine	2	272	1611	160
Thymine	2	270	1504	

a. Initial room temperature silylation of 1-2 mg of substrate.
b. Isothermal retention index (OV-17).
c. T=76°.

REFERENCES

1. C.F. Poole in "Handbook of Derivatives for Chromatography", K.Blau and G. King (Eds), Heyden and Son Ltd., London, 1977, pp. 152-200.

2. E.M. Chambaz, G. Maume, B. Maume and E.C. Horning, Anal. Letters, 1, 749 (1968).

3. G.M. Maume and E.C. Horning, Tetrahedron Letters, 343 (1969).

4. R.M. Thompson and E.C. Horning, Steroids Lipids Res., 4, 135 (1973).

5. D.L. von Minden, R.N. Stillwell, W.A. Koenig, K.J. Lyman and J.A. McCloskey, Anal. Biochem., 50, 110 (1972).

6. J.A. Beisler, M.M. Abbasi, J.A. Kelley and J. S. Driscoll, J. Med. Chem., 20, 806 (1977).

7. C.W. Gehrke and A. B. Patel, J. Chromatog., 123, 335 (1976).

8. P.G. Cookson, A.G. Davies, N.A. Fazal and B.P. Roberts, J. Amer. Chem. Soc., 98, 616 (1976).

9. J.A. Beisler, M.M. Abbasi and J.S. Driscoll, Biochem. Pharmacol., 26, 2469 (1977).

10. J.L. Roberts and C.D. Poulter, J. Org. Chem., 43, 1547 (1978).

IDENTIFICATION OF TMSi ETHER C_{26} BILE ALCOHOL ANALOGS VIA SIDE CHAIN FRAGMENTATION PATTERNS

G.S. Tint, B. Dayal, S. Shefer and G. Salen

East Orange VA Hospital, East Orange, N.J. 07019 and College of Medicine and Dentistry of New Jersey-New Jersey Medical School, Newark, N.J. 07103

Bile alcohols are C_{27} polyhydroxy sterols with a perhydrocyclopenteno phenanthrene nucleus and an iso-octyl side chain which are both the evolutionary and biochemical precursors of bile acids. In lower vertebrates which do not synthesize bile acids, bile alcohol sulfates serve, instead, as the major "digestive detergents". In the more evolved vertebrate species some of these bile alcohols become intermediates in the biosynthesis of bile acids from cholesterol. Synthetic C_{26} bile alcohol analogs have a side chain which has been shortened from eight to seven carbon atoms and are potentially useful as model compounds for studying bile acid and bile alcohol metabolism.

We have recently reported the synthesis of C_{26} bile alcohols (1) and have used the GC/MS of their trimethylsilyl (TMSi) ether derivatives as a means of identification. Although the fragmentation directing effects of side chain OTMSi substituents were found to be similar to those seen in the C_{27} compounds, several interesting differences were observed.

In the bile alcohols, a side chain OTMSi substituent has two major fragmentation effects (2). It will (a) induce the explusion of a neutral fragment consisting of that portion of the side chain more distant from the nucleus than the OTMSi substituted carbon and (b) induce the expulsion of a "charged terminal side chain fragment" consisting of the above fragment plus the attached OTMSi substituted carbon. Mechanism (a) leads to a series of mass peaks since the remaining charged nuclear fragment easily loses successive molecules of HOTMSi (90 amu) while mechanism (b) usually results in one or two intense ions.

The spectrum of TMSi 24-nor-3α,7α,12α,22ξ-tetrol was analogous to that obtained from other C-22 OTMSi sterols (2). The base peak appeared at m/e 159 and the series M-(N X 90 + 57) could be detected easily.

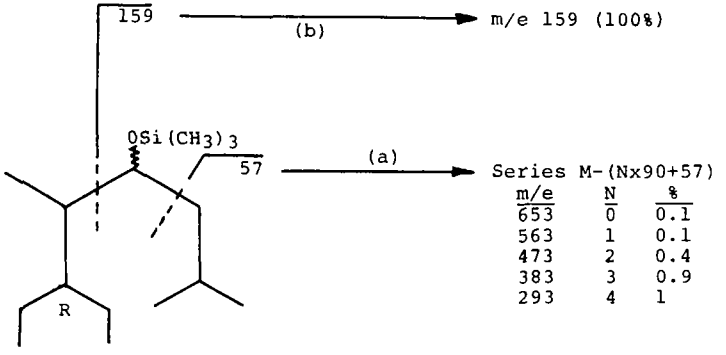


FIG.1: Fragmentation of the side chain of TMSi 24-nor-5β-cholestane-3α,7α, 12α,22ξ-tetrol illustrating mechanism (b) which yields the base peak at m/e 159 and mechanism (a) which produces the series M-(N X 90 + 57).

Similarly the spectra of TMSi (25R)-24-nor-3α,7α,12α,26-tetrol and TMSi (25S)-24-nor-3α,7α,12α,26-tetrol were identical to each other and were exact analogs of the corresponding C_{27} compounds. The base peak was observed at m/e 253, M-(3 X 90 + 187 side chain). No intense fragmentation due to the C-26 OTMSi substituent was seen.

The mass spectrum of TMSi 24-nor-3α,7α,23ξ-triol was comparable to that of its C_{27} analog. The base peak was seen at m/e 145 (C-23,25-27) and a fragmentation series M-(N X 90 + 43) was found at m/e 579, 489, 399, 309 as predicted (2). The mass spectrum of TMSi 24-nor-3α,7α,12α,23ξ-tetrol, in contrast, showed a base peak at m/e 143. This fragment requires the transfer of 2H atoms from the charged side fragment to the larger neutral one.

The base peak in the mass spectra of TMSi 24-nor-5β-cholestane-3α,7α,12α,25-tetrol and TMSi 24-nor-5β-cholestane-3α,7β,25-triol arises from process (b) and was found at m/e 131 (C-25-27) as expected (2). A weak fragmentation series was detectable in each spectrum at m/e 564, 494, 384, 294 and m/e 476, 386, 296 respectively. This arises from the loss of a 146 amu side chain fragment via mechanism (a), plus the loss of successive molecules of HOTMSi which was not seen in the spectra of the corresponding C_{27} bile alcohols (2). It probably arises from a McLafferty type rearrangement, possibly with the C-20 hydrogen being transferred to the OTMSi group.

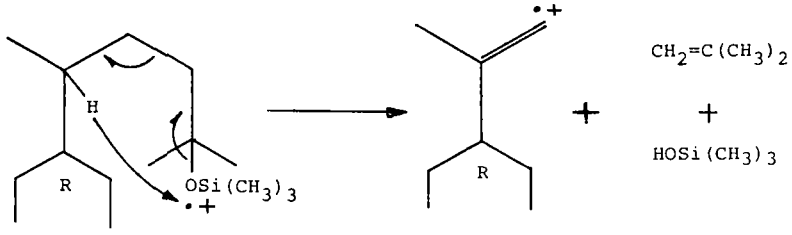


FIG.2: Suggested origin of M-146 ion in the mass spectrum of TMSi 24-nor-5β-cholestane-3α,7α,12α,25-tetrol and TMSi 24-nor-5β-cholestane-3α,7β,25-triol.

In general the mass spectra of the OTMSi ether derivatives of the C_{26} bile alcohol analogs were similar enough to those of the C_{27} compounds to use the general principles of side chain fragmentation of the latter (2) for purposes of identification. The shortened side chain did, however, induce fragmentations involving hydrogen transfers in four of the C_{26} compounds. This is similar to the effects we have described in the mass spectrum of TMSi 24-nor-5β-cholest-23-ene-3α,7α,12α-triol (1).

REFERENCES

1. B. Dayal, S. Shefer, G.S. Tint, G. Salen and E.H. Mosbach. J. Lipid Res. 17, 478 (1976).

2. G.S. Tint, B. Dayal, A.K. Batta, S. Shefer, F.W. Cheng, G. Salen and E.H. Mosbach. J. Lipid Res. 19, 956 (1978).

MASS SPECTROMETRY OF LABILE ORGANIC SOLIDS

by

D. L. Turner and D. C. Conway
Dept. of Chem. Texas A&M Univ.
College Station, Tex. 77843

In recent years a great deal of interest has been shown in the mass spectrometry of nonvolatile biologically important materials. Several methods have been used to vaporize and ionize these molecules including laser desorption; plasma desorption,[2] field desorption,[3] chemical ionization,[4] and rapid heating.[5] We have combined the simplest of these methods, chemical ionization and rapid heating to develop an ion source capable of vaporizing and ionizing several biologically important molecules. The compounds studied were the amino acids, glycine, arginine, creatine, cysteine, and cystine. Two tripeptides were also investigated, alanyl-leucyl-glycine and glycl-leucyl-alanine.

The ion source consists of a stainless steel plate with a thermocouple spot welded to the bottom and an electron filament for ionization of the carrier gas. The samples were vaporized in 30-90 sec from the plate. Chemical ionization is used to ionize the compounds in order to reduce their fragmentation. The carrier gas is Ar with a trace of isopentane. The major ionic component in this mixture is C_5H_{11} formed by the reaction of isopentane with Ar^+. The mass spectrometer that is used is a time-of-flight instrument which was originally developed to study ion-molecule reactions in the gas phase.[6] The ions enter the mass spectrometer through a 0.057 cm hole in a 0.1 cm thick stainless steel plate. Experimental conditions were optimized by varying the size of the sample and the rate of heating of the sample. The compound used for experimental optimization was arginine. The mass spectrum for arginine shows considerable fragmentation, however a parent-like ion is observed. Mass calibration using perfluorokerosene indicated that this was the $(M-H)^+$ ion, a rather suprising result. The remainder of the spectrum contains such ions as $(MH-H_2O)^+$, $(MH-2H_2O)^+$ and $(MH-COOH)^+$. The remaining amino acids and peptides studied contain the $(M+H)^+$ ion along with other fragments indicative of their structure. The only exception to this was cystine which contains a sulfur-sulfur bond linkage. The mass spectrum indicated that this linkage was ruptured either during the vaporization or ionization process leading to an ion with a mass half that of the molecule.

[1]M. A. Posthumus, P. G. Kistemaker, H. L. C. Meuzelaar, and M. C. Ten Noever de Brauw, Anal. Chem., 50, 985 (1978).

[2]R. D. Macfarlane and D. F. Torgerson, Int. J. Mass Spectrom. Ion Phys., 21, 81 (1976).

[3]H. M. Fales, G. W. A. Milne, H. U. Winkler, H. D. Beckey, J. N. Damico and R. Barron, Anal. Chem., 47, 207 (1975).

[4]B. Munson, Anal. Chem., 49, 772A (1977).

[5]R. J. Beuhler, E. Flanigan, L. J. Greene, and L. Friedman, J. Amer. Chem. Soc., 96, 3990 (1974).

[6]H. H. Teng and D. C. Conway, J. Chem. Phys., 59, 2316 (1973).

Mass Spectrometry of Chemically Derivatized Hypothalamic Oligopeptides

D.M. Desiderio, J.Z. Sabbatini and J.L. Stein, Department of Neurology and Stout Neuroscience Mass Spectrometry Laboratory, University of Tennessee Center for the Health Sciences, 800 Madison Avenue, Memphis, TN 38163

INTRODUCTION: Mass spectrometric techniques have been used to great advantage in the structural elucidation of biologically active oligopeptides. For example, the thyrotropic releasing factor(1), luteinizing hormone and other naturally occurring peptides extracted in very low amounts have been successfully elucidated by mass spectrometric techniques. Chemical derivatization of naturally occurring peptides is required for EI and a variety of derivatives (acetylation, permethylation and reduction) have been employed(2). Excellent reviews of mass spectrometry of peptides have been published by Biemann(3) and McLafferty(4). When sufficient material is isolated, random acid hydrolysis, followed by reduction and trimethylsilylation, has been successfully employed(5). Oligopeptides in a mixture have been sequenced.

The objective of this research program is to obtain the amino acid sequence of longer(6) biologic and synthetic oligopeptides (10-20 amino acids) at lower amounts (10-100 nmol), especially those containing blocked termini. Other goals include: 1) effect chromatographic separation of biologic oligopeptides in a fast, facile and sensitive manner with high resolving power; 2) chemical synthesis of appropriate derivatives of EI and CI MS; 3) for FD MS, obtain $(M+H)^+$ of underivatized oligopeptide at BAT, then increase e.h.c. to obtain sequence-determining ions; 4) whenever possible or required for corroborative evidence, obtain metastable ions and accurate masses and incorporate stable isotopes.

HIGH PERFORMANCE (PRESSURE) LIQUID CHROMATOGRAPHY (HPLC): We have successfully applied HPLC techniques using the triethylamine-phosphate (TEAP) buffer system described by Hancock, et al.(7) and Rivier(8). A linear solvent program was used to generate a gradient of 3%-60% solution B in 65 mins., where solution A is TEAP, pH 3.2, ionic strength = 0.08 M, solution B = TEAP (40%)-acetonitrile (60%). Peptides were detected with a variable wavelength UV detector set at 210 nm, 0.1 AUFS. Separation resulted with the following k' values: TRF-0.53; Met-Enkephalin-16.16; Bradykinin-16.56; Angiotensin II-17.93; Eledoisin-related peptide-19.37; Tyr^{11} SS-22.95; Substance P-22.97; Somatostatin (SS)-25.78; Tyr^{1} SS-22.95; β-Endorphin-28.69.

This chromatographic system quickly separates a complex mixture of oligopeptides within 70 mins. The UV sensitivity permits detection down to 5 ng of peptide. Current developments with fluorescence detection indicate even greater sensitivity. At the μg level of injected peptide, recovery is quantitative. High resolution of this system is demonstrated by the excellent separation between Tyr^{11} SS and Substance P.

All of these parameters are necessary to determine purity of oligopeptides (for example, pure standards are required for bioassays and RIA determinations) and to provide a "peptide profile" of hypothalamic and CNS tissues. The profile yields qualitative and quantitative estimates of hypothalamic releasing and inhibiting factors in a dependable, reproducible and rapid manner. Finally, the high resolving power of HPLC ensures pure peptide fractions for MS.

MASS SPECTROMETRY: For EI and CI MS it has been necessary to continue to develop acetylation and permethylation techniques and, in some cases to combine these two derivatives with chemical reduction of the peptide. For example, intact oligopeptides up to a nonapeptide are readily sequenced by a combination of these techniques with mass spectrometry(9). On the other hand, peptides containing more than 9-10 amino acids can be more readily analyzed, and in some cases sequences determined by field desorption mass spectrometry(10). Molecular weights have been determined for the following peptides: I) His-Ser-Gln-Gly-Thr-Phe, 675; II) Trp-Met-Gly-Asp-Phe-NH_2, 653; III) Trp-Met-Ser-Asp-Phe-NH_2, 683; IV) Trp-Met-Asp-Phe-NH_2, 596; V) Tyr-Gly-Gly-Phe-Leu, 555; VI) Tyr-Gly-Gly-Phe-Met, 573; VII) Lys-Glu-Thr-Tyr-Ser-Lys, 754.

Most FD mass spectra were obtained at 20 mA emitter heater current (e.h.c.), corresponding to approximately 200° C(10). Strong field-induced protonations of heteroatoms occurred in the FD spectra of these peptides; in some cases by elimination from $(M+H)^+$ of small, stable molecules such as

water and ammonia from $(M+H)^+$. In addition to such nonspecific eliminations, field-induced proton transfer reactions occur to various degrees on the underivatized peptide or, in some cases, from the solvent proton molecules. In either event, multiple signals arise in the $M^+\cdot$ region. Various amounts of cationization with Na and K occur in the FD mass spectra and most probably relate to the prior synthetic history of these oligopeptides, all of which were available from commercial sources.

DISCUSSION: We have found that $M^+\cdot$, $(M+H)^+$ or $(M+2H)^+\cdot$ is the base peak in every FD spectrum of an underivatized oligopeptide, data that greatly facilitates molecular weight determination. Cationization occurs in some cases (IV, V). In other cases, cationization and fragmentation occurs. For the one FD spectrum obtained for an acetylated, permethylated, reduced peptide (I), no $(M+H)^+$ was found, and more fragmentation occurred.

Our experience indicates derivatization of peptides is not required for FD MS. Indeed, the more the peptide is chemically derivatized, less information is retained in the molecular ion region. This finding is converse to our experience with EI and CI MS where peptides must of course be derivatized to confer stable gas phase properties to the molecule.

Methodology described herein furthers our knowledge of HPLC and mass spectrometric (in particular FD) analyses of oligopeptides. When working with biologic sources, for example hypothalamic releasing factors, it is imperative to have a combination of techniques such as HPLC and FD MS, to be able to isolate and identify isolated oligopeptides. When unknown oligopeptides are isolated, it is then necessary to have a very sensitive method to determine the sequence of the oligopeptide. Random acid hydrolysis and Edman degradation procedures usually apply to this situation, but in cases where either very little material has been isolated and/or blocked termini are present, sequence determination on the intact molecule is obviated with these methods.

Other areas of applicability of this methodology include detection, quantification and sequence determination of failure sequences in peptide synthesis and metabolism of naturally occurring hormones and enzymes. Quantification of endogenous levels of polar, long, intact oligopeptides is now feasible.

ACKNOWLEDGMENTS: The authors greatly appreciate the following colleagues sharing their FD MS instrumentation: Drs. White and Hertz, National Bureau of Standards, Washington, D.C. (731); Dr. Rapp and Mr. Hauptmann, Varian Applications Laboratory, Bremen, Germany (312); Dr. Mitchum and Mr. Rowland at the National Center for Toxicological Research, Jefferson, Arkansas (CH5).

REFERENCES:

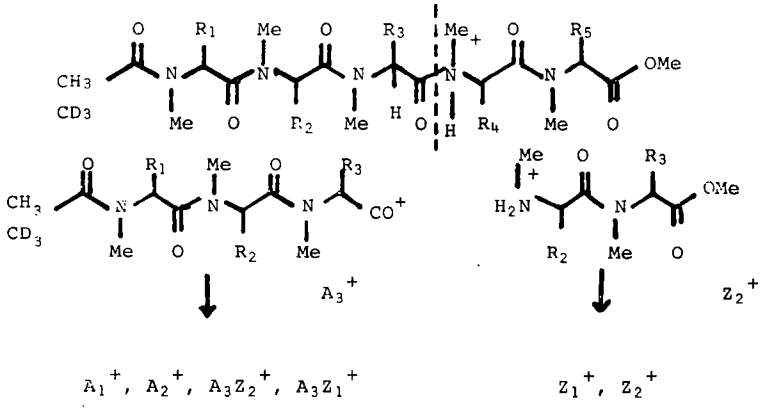
1. R. Burgus, T.F. Dunn, D.M. Desiderio, D.N. Ward, W. Vale and R. Guillemin, Nature 226, 321 (1970).
2. V.K. Mahajan and D.M. Desiderio, Biochem. Biophys. Res. Commun. 82, 1104 (1978).
3. K. Biemann, in "Biochemical Applications of Mass Spectrometry", G. Waller, Ed., Wiley, N.Y., 1972.
4. P.J. Arpino and F.W. McLafferty, in "Determination of Organic Structures", by Physical Methods, vol. 6, Nachod and Philips, Eds., Academic Press, N.Y., 1976.
5. R.J. Anderegg, K. Biemann, A. Manmade and A.C. Ghosh, Biomed. Mass Spectrom. 6, (1979).
6. K.D. Haegele, G. Holzer, W. Parr, S.H. Nakagawa and D.M. Desiderio, Biomed. Mass Spectrom. 1, 175 (1974).
7. W.S. Hancock, C.A. Bishop, L.J. Meyer, R.J. Harding and M.T.W. Hearn, J. Chromatography 161, 291 (1978).
8. J. Rivier, J. Liquid Chromatography 1, 343 (1978).
9. P.A. Leclercq, L.C. Smith and D.M. Desiderio, Biochem. Biophys. Res. Commun. 45, 937 (1971).
10. H.-R. Schulten, in "Methods of Biochemical Analysis", vol. 24, D. Glick, Ed., Wiley, 1977, p. 329.

POLYPEPTIDE SEQUENCING BY MASS SPECTROMETRY: NEW METHODOLOGY

Donald F. Hunt, Alexander M. Buko, John Ballard, and Jeffrey Shabanowitz

Department of Chemistry
University of Virginia
Charlottesville, Virginia 22901

We report new MS methodology for sequencing mixtures of polypeptides generated by enzmatic degradation of large polypeptide chains. Solids probe CI ($i\text{-}C_4H_{10}$) spectra of mixtures of d_3/d_0-N-acetyl-N,O-permethylated polypeptides afford abundant N-terminal sequence ions (An^+) as doublets separated by three mass units and C-terminal sequence ions (Zn^+) as singlets (Scheme 1).



SCHEME 1

Using a triple stage quadrupole mass spectrometer (TSQ)[1] a molecular ion or sequence ion of a peptide in a mixture can be selected and made to undergo collision induced dissociation (CID). Further sequence ions are thereby generated which enable sequencing of the unknown peptide. The CID of different molecular ions or sequence ions leads to sequencing of other peptides in the mixture.

The CID of a N-terminal sequence ion (An^+) produces the A^+ series sequence ions (A^+_{N-1}, A^+_{N-2}... A_1^+) (Scheme 1) and the rearrangement ions A_N Z^+_{n-1} (Figure 1). The CID of C-terminal sequence ions (Z^+) produces immonium ions (Figure 2) and the Z^+ series sequence ions (Z^+_{n-1}, Z^+_{n-2}...Z_1^+) (Scheme 1). The CID of N-terminal and C-terminal sequence ions leads to complementary sequencing of an unkown peptide.

We also report results of a study to find derivatives of polypeptides which take advantage of the potential 100-1000 fold increase in sensitivity afforded by electron capture negative ion CI[2]. N-Pentafluorobenzoyl peptide methyl esters and N-acetyl peptide pentafluorobenzyl esters show a 100-fold increase in ion current in the negative ion mode for ions characteristic of molecular weight.

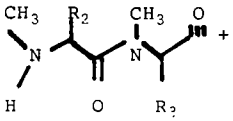


Figure 1

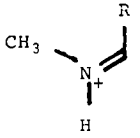


Figure 2

REFERENCES

1. D.F. Hunt, J. Shabanowitz, and A. Giordani, 27th Annual Conference on Mass Spectrometry and Allied Topics, Seattle, Washington, June 1979, paper FAMOC2.

2. D.F. Hunt, G.C. Stafford, Jr., F.W. Crow, and J.W. Russell, Anal. Chem., 48, 2098 (1976).

Structural Studies of the Non-host Specific and Host Specific Mycotoxins Associated with Southern Corn Leaf Blight.

David A. Hoisington and Virginia Walbot, Department of Biology, Washington University, and Michael K. Hoffman*, Department of Biological Chemistry, Washington University School of Medicine, St. Louis, Missouri 63110.

In 1970 an epidemic of fungal origin raged through the corn-growing regions of the United States, resulting in nearly a billion dollar loss in the corn crop.[1] Southern Corn Leaf Blight was caused by a previously unknown race of the fungus Helminthosporium Maydis, and affected corn varieties containing a specific type of cytoplasm, Texas Male Sterile (TMS) Cytoplasm. Early investigation of the Race T fungus showed that it produced pathotoxins which inhibited root growth of susceptible, but not normal (resistant) strains of corn seedlings.[2] A chemically similar toxic fraction was reported to be isolated from fungus infected corn leaves.[3] These chemically similar fractions, isolated from the fungus, were shown to be virulent on TMS corn, but not on other cytoplasmic variants. Numerous investigations dealing with the physiological effects of the toxin(s) have indicated that Helminthosporium Maydis, Race T, produce only host-specific toxins, but these studies have been hindered by the use of unpurified material. In an attempt to elucidate the site and mode of action of the mycotoxin(s) produced by Race T, as well as confirm the host specific nature of the toxin, we have begun to characterize the phytologically active fractions.

Experimental. The fungus was grown in a stationary culture on a modified Fries' media. After 14 days, the mycellium was removed by filtration and the culture filtrate was freeze-dried. The lyophilized material was stirred overnight with $CHCl_3$, filtered to remove particulate matter and rotovapped to produce a crude extract. The yellowish syrup was dissolved in a minimal mount of methanol and cooled to -25°C. The precipitated fraction was subjected to preparative TLC using $CHCl_3$/MeOH (92:8), while the methanol soluble fraction was further purified on an LH-20 column {$CHCl_3/CH_3OH$,(1:1)} before final separation on a neutral silica gel column {$CHCl_3/CH_3OH$,(95:5)}.

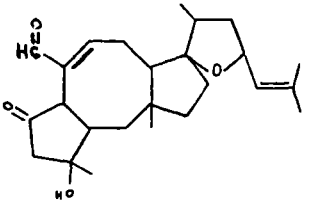
A protoplast bioassay using both Race T susceptible- and resistant-protoplasts has been developed to monitor biological activity. Low resolution electron impact and chemical ionization mass spectra were run on a Finnigan 3300 mass spectrometer using the direct insertion probe. High resolution mass spectra were run on AEI MS-50 double-focussing mass spectrometer. NMR spectra were obtained from 100ug samples, run on a JEOL FT 100 MHz NMR, using a $^{13}C/H$ dual microprobe.

Results and Discussions. Following the extraction and chromatographic procedures described in the experimental section, both host-specific (HST) and non-host-specific (NHST) phytotoxicity was found. These bioactivities were grossly separated by the -25°C methanol soluble and -25°C methanol insoluble fractionation step into the non-host-specific and host-specific toxins, respectively.

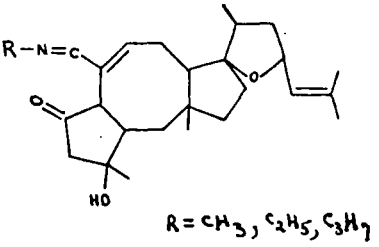
Because of their greater economic importance, initial attempts were made to identify the non-host-specific mycotoxins. Preparative TLC led to the isolation of at least eight non-host-specific toxins (listed in order of decreasing r_f) NHST-I and II (m.w. = 382, $C_{25}H_{34}O_3$), NHST-III (m.w. = 400, $C_{25}H_{36}O_4$), NHST-IV and V (m.w. = 384, $C_{25}H_{36}O_3$), and NHST-VIa,b,c...n. {NHST-VI consists of an homologous series of at least three components (a, m.w. = 413, $C_{26}H_{39}NO_3$; b, m.w. = 427, $C_{27}H_{41}NO_3$; and c, m.w. = 441, $C_{28}H_{43}NO_3$)}. NHST-III has been identified as ophiobolin A (ophiolbola-7, 18-dien-21-al-3α-ol-5-one-14α,17-oxide), the first identified member of a small and unusual group of sesterterpenes, consisting of the head to tail linkage of five isoprenoid units.[4] The other non-host-specific toxins

have been identified by NMR and mass spectrometry as new members of the ophiobolin family. The structures of these compounds are shown below. Because of the unusual structure of the Ophiobolins, their mass spectra are not particularly informative. Although many of the decomposition reactions are the result of cleavage adjacent to the ether oxygen, and indicate an unsaturated side chain, the presence and nature of the extensive ring system remains elusive to mass spectral analysis.

NMR and low resolution mass spectra have been obtained on one of at least eleven host-specific mycotoxins, and the compound, HST-4 appears to have a molecular weight of 520. Structure elucidation of HST-4 and the other host-specific toxins continues.



"Ophiobolin A"



"Alkylimine of Ophiobolin A"

Acknowledgments. We would like to thank Drs. M. L. Gross and P. A. Lyons of the Midwest Center for Mass Spectrometry at the University of Nebraska for running the high resolution mass spectra.

* Present address: USDA-FSQS, Chemistry Staff Laboratory, Bldg 318, Beltsville, Maryland 20705

1 L. A. Tatum, Science, 171, 1113 (1971).
2 A. L. Hooker, D. R. Smith, S. M. Lin, and J. B. Beckett, Plant Disease Reporter, 54, 708 (1970).
3 S. M. Lin and A. L. Hooker, Phytopathology, 62, 968 (1972).
4 L. Canonica and A. Fiecchi, Chapter 2 of Research Progress in Organic, Biological and Medicinal Chemistry, II, Ed. by U. Gallo and L. Santamaria, North Holland Publishing Co., 1970.

STUDIES ON MOLECULAR SPECIES OF GLYCEROPHOSPHOLIPIDS BY A GC-MS SYSTEM

Kunihiko Saito and Kiyoshi Satouchi, Department of Medical Chemistry, Kansai Medical School, Osaka, Japan 570

Naturally occurring glycerophospholipids are divided into four types, i.e., (A) 1,2-dialkyl-, (B) 1-alk-1-enyl-2-acyl-, (C) 1-alkyl-2-acyl- and (D) 1,2-diacyl-glycerophosphoryl bases. By the combination of constituent fatty acids or/and fatty alcohols, usually C_{16} - C_{24}, there are many molecular species in each type.

Glycerophospholipids are main component of biomembranes and we are interested in the identification of such molecular species in relation to some biomedical phenomena by a GC-MS system.

Derivatives to be analyzed were prepared as follows: glycerophospholipids were hydrolyzed with phospholipase C and the resulting 1-alkyl (or alk-1-enyl, acyl)-2-alkyl (or acyl) glycerols were converted to ter-butyldimethylsilyl (TBDMS) or trimethyl (TMS) derivatives.

TMS derivatives gave many informations on structural analyses of these four types particularly 1,2-diacyl types (Fig. 2). However, TBDMS derivatives showed stronger fragment ions than those of TMS derivatives concerning molecular weight determining ion ([M - 57]), alk-1-enyl residues ([RCH=CH + 56] and [RCH=CH + 130]), alkyl residues ([R + 130] and [R + 56]) and acyl residue ([R^{CO} + 74]). Particularly, ions at [M - 57] are very strong and useful for determining the molecular species as shown in Figs. 1 and 3. The fragment ions at [RCH=CH +130] and [R + 130] of TBDMS derivatives were not confused with ions at [RCO + 74] compared to TMS derivatives. The apparatus used was Shimadzu GC-MS PAC 300 and electron energy was 22.5 eV.

A mixture of TBDMS (or TMS) derivatives of model compounds of these four types, which have same carbon numbers as alk-1-enyl, alkyl and acyl residues, was separated by gas chromatography on OV-1 and eluted in the following order: (A) 1,2-dialkyl-, (B) 1-alk-1-enyl-2-acyl-, (C) 1-alkyl-2-acyl- and (D) 1,2-di-acyl-3-TBDMS (or TMS) glycerols (Fig. 4).

Ethanolamine glycerophospholipids of rat brain consisted of 1,2-diacyl (61 %), 1-alk-1-enyl-2-acyl (35 %) and alkyl (4 %) types. It was possible to determine the molecular species of 1-alk-1-enyl-2-acyl types by using TBDMS derivatives to be 34:1 (16/18:1), 36:1 (18/18:1), 36:2 (18/18:2), 38:4 (18/20:4), 38:6 (18/20:6), 40:4 (18/22:4), 40:5 (18/22:5) and 40:6 (18/22:6).

Fig. 1

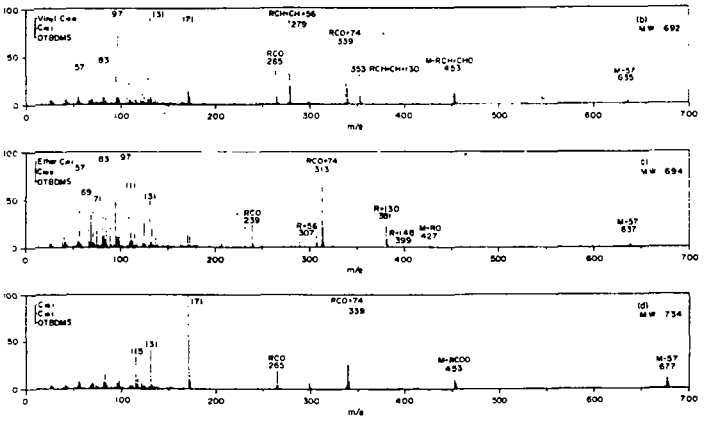


Fig.2

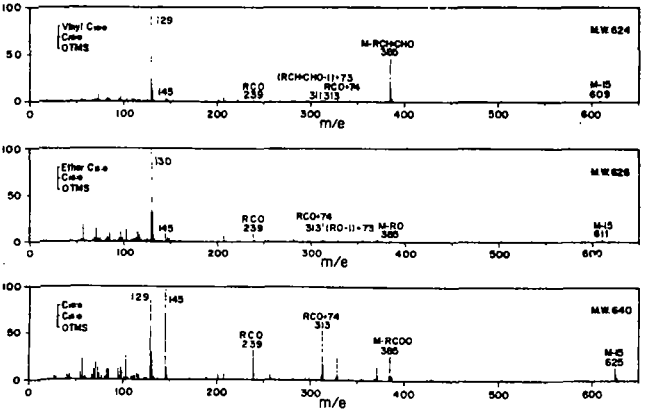
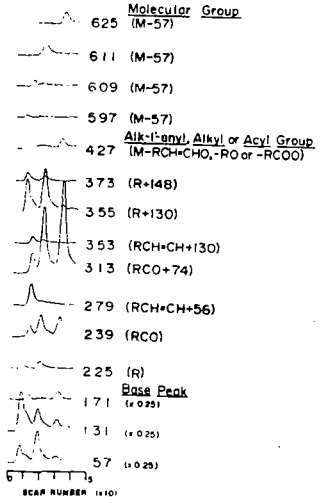


Fig. 3



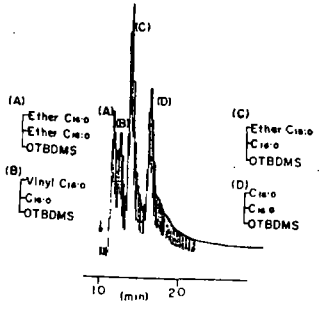


Fig. 4

ISOLATION AND IDENTIFICATION BY MASS SPECTROMETRY OF PHYTOTOXINS IN COFFEA ARABICA

George R. Waller and Chang-Hung Chou

Department of Biochemistry, Agricultural Experiment Station, Oklahoma State University, Stillwater, Oklahoma 74074, Institute of Botany, Academia Sinica, Taipei, Taiwan, Republic of China

Coffea arabica, one of the most important beverage plants for humans is also used for the production of caffeine, mainly from the fruit. In a recent conference on ecology, Anaya and co-workers reported that an allelopathic phenomenon occurs in coffee plantations, yet no responsible substances have been found (1). We have previously demonstrated that aqueous extracts of coffee plant tissues significantly inhibit seed germination and radicle growth of lettuce, rye grass, and fescue (2). Eleven phytotoxins including four alkaloids and seven phenolic compounds were reported in these extracts. These phytotoxins suppressed seed germination and radicle growth of lettuce at a concentration below 100 ppm. However, detailed information on the isolation and identification of these compounds was not reported. This paper presents such information including mass spectra.

From the rF values in paper and thin-layer chromatography (PC and TLC) in different solvent systems, response to UV light, and color reactions produced by spray reagents, phytotoxins present in C. arabica were identified. The PC and TLC data of each isolated compound agree with those of a known synthetic compound. The phytotoxins are caffeic, chlorogenic, ferulic, p-coumaric, p-hydroxybenzoic, vanillic acids, scopoletin, theobromine, theophylline, paraxanthine, and caffeine. Among these compounds, caffeine is the most abundant one. The caffeine content was significantly higher in young seedlings than in fallen leaves and roots. Threobromine, theophylline, and paraxanthine were found in the coffee seedlings but paraxanthine was absent in the fallen leaves. Paraxanthine is now reported to occur in C. arabica for the first time. On the other hand, more phenolics were present in the fallen leaves than in the young seedlings.

Each isolated compound (phytotoxin) was subjected to mass spectrometric (MS) analysis, and each spectrum was compared with that of known standards and a data bank-library through the Finnigan GC-MS-Computer Search System (courtesy of Continential Oil Company, Ponca City, Oklahoma, U.S.A.). The spectra of the isolated compounds agree with those of standards. Since the reference data bank lacks records for scopoletin, the mass spectra of this compound is shown in Fig. 1 and its partial fragmentation pattern in Scheme I.

In each mass spectrum, metastable peaks were seen. These peaks were formed as a result of the transitions denoted for the fragments of the compounds, however only the metastable peaks for scopoletin are shown (Fig. 1).

The purine alkaloids caffeine, theobromine, theophylline and paraxanthine contain methyl substituents on N-1, N-3, and N-7 and all four compounds show the molecular ion as the base peak, reflecting the stability of the aromatic heterocyclicring purine system toward fragmentation upon electron impact. Decomposition reactions account for at least some of the prominent spectral features. Metastable peaks occurring in the spectra of the phytotoxin phenolics were more variable. For example, chlorogenic acid exhibited only one metastable peak, while ferulic acid showed seven. The probably neutral products varied with compounds; they include COOH, H_2O, OH, CO, CH_3, C_2H_2, C_2H_3, and O. Scopoletin shows successive losses of radical ions CH_3 and CO forming m/z 177 and 164 respectively and each of these ions undergoes additional fragmentation giving radical losses of CO with the resulting ion being formed at m/z 149 and loss of radical CH_3 group from m/z 165 to give another ion at m/z 149. The loss of the ion (CO + CO) at -56 amu from m/z 177 and loss of -CO from each of the fragment ions of m/z 149 (although it was from a different portion of the fragment ions at m/z 149) gives rise to m/z 121 (Scheme I). The decomposition pathway involving metastable peaks serve to confirm the pathway for a given molecule and coincidence of the data for the known and the unknown permit the conclusive identification of plant phenolics and purine alkaloids.

From the ecological point, it is reasonable to extract phytotoxic compounds initially with water because most such compounds are water-soluble in nature. However, some such compounds may remain in the plant material after aqueous extractions, any such compound has been missed in this study. In addition, several unknown compounds found

by PC and TLC have not been identified even by MS analysis. Since the MS analysis was not conclusive, the compounds will be derivatized and reported later.

In MS analysis, enough eluate was placed in a vial for use in a direct probe by the method described by Waller and Lawrence (4) and analyzed with a prototype LKB 9000 GC/MS (5). The known compounds were run by the same techniques. High resolution mass spectra were obtained on an Du Pont CEC 21/110-B by Catherine B. Costello at the MIT Mass Spectrometer Facility (Support by N^{7}H).

Acknowledgement --- We are grateful to Drs. Otis C. Dermer, Tom J. Mabry, and A. Ulubelen for their critical comments on the manuscript, and to Mrs. Cheryl Cumberland for technical assistance. The senior author specially thanks the National Science Council, Taiwan, Republic of China for financial support of his Sabbatical Leave of Absence from the Institute of Botany, Academia Sinica, and National Taiwan University, Taiwan.

References:

1. Anaya, A.L., del Amo. S., Roy-Octla, G. and Ortiz, L.M. (1978) Abst. of Papers, 2nd Internat. Congress of Ecology, Jerusalem, Israel, Sept. 10-16.

2. Chou, C.H. and Waller, G.R. (1979) Manuscript submitted to Science.

3. Midha, K.K., Sved. S., Hossie, R.D. and McGilveray, I.J. (1977) Biomed. Mass Spectrum. 4, 172

4. Waller, G.R. and Lawrence, R.H. (1978) in Recent Development in Mass Spectrometry in Biochemistry and Medicine (Frigerio, A. ed.) Vol. 1, 429.

5. Waller, G.R. (1968) Proc. Okla. Acad. Sci. 47, 271.

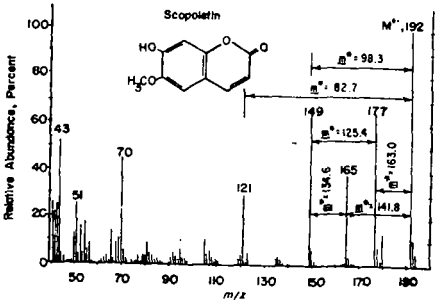
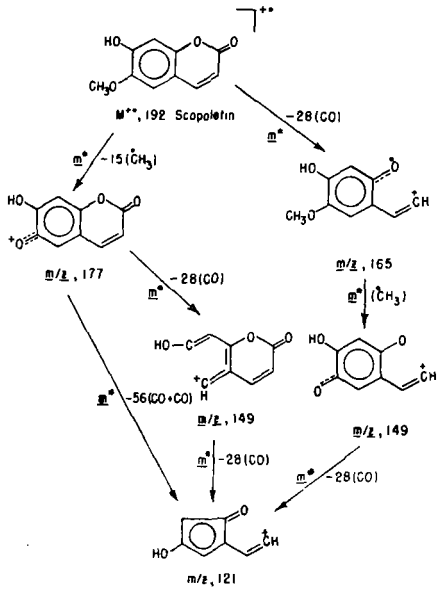


FIG 1 MASS SPECTRUM OF SCOPOLETIN (4). LKB-9000 PROTOTYPE (5). 70 eV. 250° ION SOURCE. 100° INLET, DIRECT INLET.



SCHEME 1. PARTIAL FRAGMENTATION PATTERN OF SCOPOLETIN

GLYCOCONJUGATE STRUCTURAL STUDIES BY FIELD DESORPTION MASS SPECTROMETRY

V. N. Reinhold
Department of Biological Chemistry
Harvard Medical School
Boston, MA 02115

Glycoconjugates are ubiquitous components of biological tissues, being found on cellular and extracellular structures, fluids and exudates. The specific involvement of glycoconjugates in molecular recognition and cellular adhesion unquestionably constitutes one of the more challenging frontiers of biomedical research. None of the chemical or structural bases of these biological specificities are known, but there is much evidence suggesting that these specificities may reside on a unique carbohydrate structure bound to either lipid or protein, analogous to the blood group specificities. The difficulties in carbohydrate and glycoconjugate related structural problems are immense and fundamental improvements must necessarily precede an understanding of these various biological phenomena.

The diversity of structural elements comprising glycoconjugate samples greatly limit the application of chemical approaches to component composition without severe loss of structural understanding. The biologically important isomeric structures, branched-chain entities, and acidic and basic constituents are examples of carbohydrate structural diversity which make chemical manipulation difficult and any method of direct analysis very attractive. We have used with considerable success field desorption mass spectrometry(FDMS) to analyze glycoconjugates of under one thousand daltons. The technique of desorbing samples from the surface of a specially prepared emitter with the aid of an intense electric field has provided a measurement of molecular weight for a number of these samples. It is clear, however, that the determination of molecular weight, as made possible by this method, by itself has limited value for structural analysis. Desorbing at higher emitter currents, however, imparts sufficient energy into the sample so that limited fragmentation can be expected and used to identify structure. Although this has in some cases provided sequence ions for certain lower molecular weight oligosaccharides,it is at the cost of an enhanced desorption rate. Maintaining the intensity of the molecular ion and structurally useful fragment ions while electrically scanning a large mass range offers considerable challenge in light of the fact that once desorption of carbohydrate sample has started it proceeds rapidly.

We have used field desorption mass spectrometry to study a lysomal enzyme deficiency disease in which mucopolysaccharides accumulate in the urine concomitant with severe neurological deficiencies. In this study, the primary lesion appears to be one of glycoprotein catabolism resulting in the accumulation of mannose-rich oligosaccharides. The structures below have been characterized after chromatographic purification by mass spectrometry. The first five of these structures gave adequate information by FDMS the remaining two did not. The increasing size of these oligomers corrolated with the difficulty in desorption both in ion yield and structurally useful ions.

	STRUCTURE	SOURCE	M. W.
1.)	GlcNAc$\xrightarrow{\beta(1-4)}$GlcNAc ol	synthetic	426
2.)	Man$\xrightarrow{\alpha(1-4)}$GlcNAc$\xrightarrow{\beta(1-4)}$GlcNAc ol	synthetic	588
3.)	Man$\xrightarrow{\alpha(1-3)}Man\xrightarrow{\beta(1-4)}$GlcNAc	urine	545
4.)	Man$\xrightarrow{\alpha(1-2)}Man\xrightarrow{\alpha(1-3)}Man\xrightarrow{\beta(1-4)}$GlcNAc	urine	707
5.)	Man$\xrightarrow{\alpha(1-2)}Man\xrightarrow{\alpha(1-2)}Man\xrightarrow{\alpha(1-3)}Man\xrightarrow{\beta(1-4)}$GlcNAc	urine	869
6.)	Man$\xrightarrow{\alpha(1-2)}Man\xrightarrow{\alpha(1-2)}$Man $\xrightarrow{\alpha(1-6)}$ Man$\xrightarrow{\beta(1-4)}$GlcNAc Man $\xrightarrow{\alpha(1-3)}$	urine	1031
7.)	Man$\xrightarrow{\alpha(1-2)}Man\xrightarrow{\alpha(1-2)}$Man $\xrightarrow{\alpha(1-6)}$ Man$\xrightarrow{\beta(1-4)}$GlcNAc Man$\xrightarrow{\alpha(1-2)}$Man $\xrightarrow{\alpha(1-3)}$	urine	1193

In related studies it has been observed that ions formed by field desorption of steroid carbohydrate conjugates, highly alkylated or derivatized materials and glycosphingolipids comparable in concentration and molecular weight (non-carbohydrate portion highly aliphatic) are much easier to focus and to sustain as a constant ion beam. This observation suggested that better desorption characteristics would be expected by depolarizing the sample by derivatization. A comparison of the desorption profile and total ion yield with equal amounts of the free and derivatized oligosaccharide material indicated, for the latter sample, a greater ion yield and sustained total ion profile when plotted against increasing emitter current. These preliminary studies suggest a finite range for analysis by FDMS of underivatized oligosaccharides--limited by poor desorption characteristics, not by mass analysis. Extension of this range can be brought about by sample depolarization which aids desorption but may be limited by analysis at the higher mass of derivatization. Greater ion yield and tailing total ion profiles may represent a process of sample migration to emitter tips, a rate limiting situation in which depolarized samples participate more effectively.

Acknowledgements:

Mass spectrometry studies were performed at the DRR Mass Spectrometry Facility M. I. T.; Professor K. Biemann, Principal Investigator.

FAM0B10 CI AND EI MASS SPECTRAL IDENTIFICATION OF THE URINARY METABOLITES OF ZOMEPIRAC, W. N. WU, L. E. WEANER, J. KALBRON, P. J. O'NEILL and J. M. GRINDEL, McNeil Laboratories, Ft. Washington, PA 19034

Zomepirac sodium, sodium 5-(4-chlorobenzoyl)-1,4-Dimethyl-1H-pyrrole-2-acetate dihydrate, is a novel analgesic agent currently undergoing clinical evaluation. The urinary metabolites of zomepirac from man, monkey, rat and mouse after oral administration of zomepirac sodium were isolated by solvent fractionation and chromatography (column, tlc, hplc and gc). Zomepirac acid (from man, monkey, rat and mouse), zomepirac glucuronide (from man, monkey, rat and mouse), hydroxyzomepirac acid (from man, rat and mouse), 4-chlorobenzoic acid (from man, monkey, rat and mouse) and 4-chlorohippuric acid (from monkey) were isolated and characterized mainly by CI and EI mass spectrometry and other spectroscopic (ir and nmr) data. The metabolism of zomepirac in man and monkey is characterized by glucuronide conjugation. The rat metabolizes zomepirac primarily by oxidative pathways to give hydroxyzomepirac and 4-chlorobenzoic acid. The mouse presents a balanced picture of conjugation and oxidative reactions.

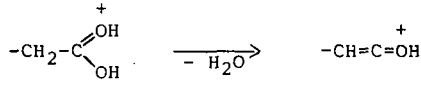
MASS SPECTROMETRY OF UNDERIVATIZED EPOXIDES, HYDROPEROXIDES, EPOXY- AND HYDROXY FATTY ACIDS

K. Halpaap-Wood, J. Nowlin, G. W. Griffin*,
M. G. Horning and E. C. Horning,

Institute for Lipid Research
Baylor College of Medicine
Houston, Texas 77030

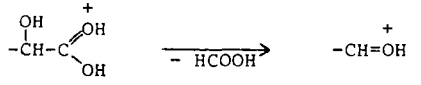
University of New Orleans*

Ion plasma desorption was used to study the CI spectra of non-derivatized epoxides, hydroperoxides, epoxy- and hydroxy fatty acids. A Finnigan 1015 quadrupole mass spectrometer, operated in a chemical ionization mode with isobutane as reagent gas was used. A single crystal or less than half a µl of sample was placed on the SE-30 coated metal probe tip, and introduced into the ion plasma. The fatty acids showed ions at MH^+ as the base peak and ions of low intensity for the loss of water from the protonated molecular ion.



Fatty Acid		MH^+	$[MH-18]^+$
Stearic Acid	18:0	100%	7%
Oleic Acid	18:1	100%	4%
Linoleic Acid	18:2	100%	16%
Linolenic Acid	18:3	100%	5%
Arachidonic Acid	20:4	100%	3%
Docosahexaenoic Acid	22:6	100%	2%

In the spectra of hydroxy- and epoxy- fatty acids ions of high intensity at MH^+ and at $[MH-H_2O]^+$ could be observed. When the hydroxy group is in the α-position there was also an ion at $[MH-46]^+$:



In addition the epoxy- fatty acids showed a loss of a second H_2O molecule.

	MH^+	$[MH-18]^+$	
2-Hydroxystearic Acid	301(100%)	283(12%)	255$[MH-HCOOH]^+$(11%)
3-Hydroxystearic Acid	301(100%)	283(18%)	
12-Hydroxystearic Acid	301(29%)	283(100%)	265$[MH-2H_2O]^+$(1%)
cis-9,10-Epoxystearic Acid	299(98%)	281(100%)	263$[MH-2H_2O]^+$(8%)
trans-9,10-Epoxystearic Acid	299(81%)	281(100%)	263$[MH-2H_2O]^+$(16%)

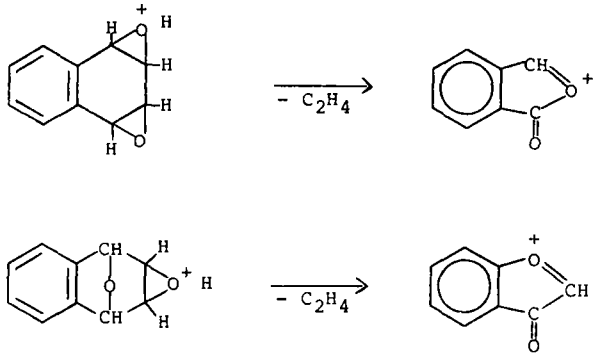
In the spectra of the fatty acid hydroperoxides only a very weak ion at MH^+ could be observed, but there were ions of high intensity at $[MH-H_2O]^+$ and $[MH-H_2O_2]^+$.

	MH^+	$[MH-18]^+$	$[MH-34]^+$
Linoleic Acid Hydroperoxide	1%	84%	100%
Linolenic Acid Hydroperoxide	5%	100%	85%
Arachidonic Acid Hydroperoxide	13%	100%	50%
Docosahexaenoic Acid Hydroperoxide	>1%	90%	100%

Protonated molecular ions [MH^+] were observed for the syn(1,2:3,4)- and anti(1,2:3,4)-dioxides of naphthalene and for the 1,4:2,3-dioxide of naphthalene, three derivatives that are difficult to analyze by GC-MS.

	MH^+	$[MH-28]^+$
Naphthalene anti-Dioxide	161 (100%)	133 (36%)
Naphthalene syn-Dioxide	161 (100%)	133 (25%)
Naphthalene Bridged Dioxide	161 (30%)	133 (100%)
1,4-Naphthoquinone Epoxide	175 (100%)	

The ions at [MH-28] probably represened the loss of C_2H_4, leading to the following structures:

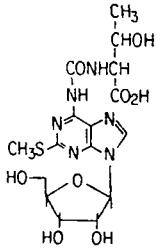


The protonated molecular ion of 1,4-naphthoquinone epoxide forms a very stable ion.

TECHNIQUES FOR THE STRUCTURE ELUCIDATION OF MODIFIED NUCLEOSIDES FROM tRNA BY HIGH RESOLUTION MASS SPECTROMETRY

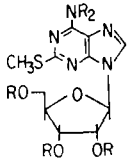
Z. Yamaizumi and S. Nishimura, National Cancer Center, Tokyo, Japan; H. J. Gross, Max Planck Inst. Biochem., Munich, Germany; H. Yamamoto, P. F. Crain and J. A. McCloskey, Univ. of Utah, Salt Lake City, Ut 84112

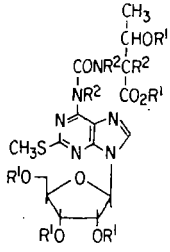
The chemical and conformational properties of modified nucleosides in tRNA, particularly those in the anticodon region, are thought to play a role in the biological functions of transfer RNA.[1,2] As interest in structure and function of eukaryotic tRNA grows, the structure elucidation of new nucleosides becomes more difficult due to the complexity of structures encountered[2] and limitations in sample quantity. We report here the structure of a new modified nucleoside (N) isolated from rabbit liver tRNA as N-[(9-β-D-ribofuranosyl-2-methylthiopurin-6-yl)carbamoyl]threonine (1)[3] based on mass spectrometry carried out on 35 μg of material.



1, 458.1203 (-1.7)

Complete low- and high-resolution (photographically recorded) mass spectra of various derivatives of N were obtained on a Varian MAT 731 instrument at 70 eV. Permethylation of the unknown nucleoside with CD_3I or CH_3I[4] each yields two products which are completely fractionated by vaporization from the mass spectrometer probe at 100° (2, 3) and 150° (4, 5), while trimethylsilylation[5] produces a single derivative ($Si(CH_3)_3$, 6; $Si(CD_3)_3$, 7).





2, R = CD_3, 398.2558 (0.1)
3, R = CH_3, 383.1611 (-1.6)
8, R = H, 313.0831 (-1.4)

4, $R^1 = R^2 = CD_3$
5, $R^1 = R^2 = CH_3$, 570.2448 (-2.4)
6, R^1 = TMS, R^2 = H, 818.3184 (-1.2)

Exact molecular masses were established by calculating mean values derived from experimentally measured molecular ion and base ion series,[6] in which the unknown parameter (exact mass of the base) is associated in each measurement with known mass differences (e.g., M - CH_3, base + H). Determination of the number of blocking groups introduced, by comparison of molecular weights (2 vs. 3; 6 vs. 7) then permits calculation of the masses of 1 and its degradation product 8, as shown.

Structure elucidation of nucleoside N followed from the characterization of 8 based on the premise that the identity of 8 permits selection of the basic skeleton from the four major bases. The exact mass of 2 yields 11 computer-generated molecular compositions, which can be narrowed by application of a set of restrictions, generally applicable to nucleosides: (1) total number of rings and double bonds between 4 and 12, (2) number of *oxygens* $\geq$ 4, (3) *number of nitrogens* $\geq$ 2, (4) *the nitrogen rule*. As a result, no candidates emerge which contain only C, H, D, N, and O; while inclusion of S produces a single possibility for 2: $C_{16}H_{10}D_{15}N_5O_4S$. The mass spectrum of 2 shows an unmodified sugar (m/e 149, 183),[4] an ion of m/e 120 ($C_6H_4D_5O_2$) generally characteristic of adenosine derivatives,[4] and loss of CD_2ND from the base + H species, thus revealing 8 to have a free exocyclic amino group.[4,7] The methylenethiol isomer would incorporate six and not five methyl groups and can be excluded; substitution at C-8 is excluded by incorporation of one deuterium (D_2O, 100° for one hour, then cold H_2O).

The mass difference between 1 and 8 (146.0467) permits three candidates for the side chain composition; the most likely corresponds to threonine plus CO, leading to structure 1.[8]

References

1. S. Nishimura, Prog. Nucleic Acid Res. Mol. Biol., 12, 49 (1972).
2. J. A. McCloskey and S. Nishimura, Accounts Chem. Res., 10, 403 (1977).
3. Exact masses shown are experimental values, followed by the found minus theoretical difference in millimass units.
4. D. L. von Minden and J. A. McCloskey, J. Am. Chem. Soc., 95, 7490 (1973).
5. S. E. Hattox and J. A. McCloskey, Anal. Chem., 46, 1378 (1974).
6. J. A. McCloskey, in "Basic Principles in Nucleic Acid Chemistry," Vol. I, P. O. P. Ts'o, ed., Academic Press, New York, 1976, chapter 3.
7. D. L. von Minden, J. G. Liehr, M. H. Wilson and J. A. McCloskey, J. Org. Chem., 39, 285 (1974).
8. Z. Yamaizumi, S. Nishimura, K. Limburg, M. Kaba, H. J. Gross, P. F. Crain and J. A. McCloskey, J. Am. Chem. Soc., 101, 2224 (1979).

FAM0B13 MASS SPECTRA OF PERMETHYLATED NUCLEOTIDES, Peter Brown, J. J. Finck and G. R. Pettit
Department of Chemistry, Arizona State University, Tempe, Arizona 85281

EI and FI mass spectra for a series of permethylated mononucleotides will be presented. Compounds examined include 5'-uridylic acid, 2'-, 3'- and 5'-adenylic acid and 5'-thymidylic acid. Implications of this work for oligonucleotide sequencing by mass spectrometry will be discussed also.

NEW GANGLIOSIDE STRUCTURE OF HUMAN ERYTHROCYTES AS ANALYZED BY MASS SPECTROMETRY COMBINED WITH ENZYMATIC DEGRADATION. FAM0B14

M. POWELL, K. WATANABE AND S. HAKOMORI, FRED HUTCHINSON CANCER RESEARCH CENTER, SEATTLE, WA 98104

Gangliosides are cell surface membrane components which may have several functions. They serve as important antigens (I, i; p; HD), receptors (cholera toxin, tetanus, interferon, hormones, virus), and cell growth mediators involving changes associated with cancer. The structure of gangliosides from brain have been well established by many studies. However, the chemical structures of extraneural gangliosides are fragmentary. Elucidation of these structures is significant in that correlations and conclusions could be drawn from the derived structure to its known biological activities. Our objective was to completely determine the structure of a series of gangliosides isolated from human red blood cell membranes.

We isolated nine monosialogangliosides (G_1-G_9) of human type O erythrocyte membranes by liquid chromatography and thin-layer separation techniques. We then employed several enzymatic and mass spectral analysis procedures that proved to be very convenient in the structural identification of this series of glycolipids. The following analysis of G_9, a fucoganglioside will exemplify the procedures utilized (Watanabe et al, J. Biol. Chem. 253, 8962-8967, 1978).

Compositional analysis was carried out by two different hydrolysis methods. Methanolysis, followed by N-acetylation, trimethylsilyl derivitization, and gas chromatography on 3% SE-30 determined the molar ratios of fucose:neuraminic acid:glucose:sphingosine (0.75/0.99/1.00/0.72). Acetolysis (90% acetic acid, 0.5 N H_2SO_4) and subsequent G.C. analysis on 3% OV-225 as alditol and hexosaminitol acetate derivatives, determined the molar ratio of fucose:galactose:glucose:glucosamine (0.84/3.95/1.00/3.01). GC/EI/MS confirmed identification of peaks. The fatty acids and sphingosines were analyzed as TMS derivatives on 3% SE-30 gas chromatography.

The glycolipid was hydrolyzed by α-L-fucosidase as well as by sialidase as evidenced by the change of mobility on TLC. The intact glycolipid was not hydrolyzed by any other exoglycosidases. The sialidase-cleaved glycolipid was hydrolyzed with β-galactosidase followed by β-N-acetylglucosaminidase. This product migrated on TLC similarly to H_2-glycolipid, a straight chain moiety. The product was then hydrolyzed by α-L-fucosidase, followed by β-galactosidase, followed by β-N-acetyl-glucosaminidase, which yielded a product with TLC migration similar to paragloboside, a tetraosylceramide. This was further degraded with β-galactosidase, followed by β-N-acetylglucosaminidase, which was

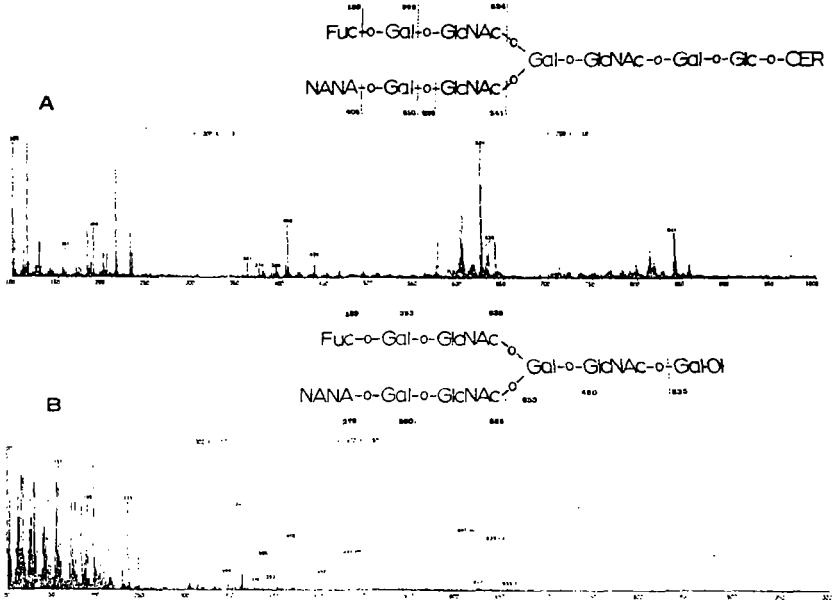


Fig. 1A. Intact fucoganglioside. B. Oligosaccharide liberated by endo-β-galactosidase.

in turn degraded by β-galactosidase, yielding a ceramide glucoside. This process yielded the sequence and anomeric structure of the fucoganglioside as indicated in Fig.1A. Susceptibility to hydrolysis with endo-β-galactosidase of Escherichia freundii (Fukuda, M. et al J. Biol. Chem. 253, 6814-6819, 1978), which has an enzymatic specificity requirement of GlcNAcβ1→3Galβ→X, further supports the data obtained from the degradation with exoglycosylhydrolases.

The intact and enzymatic degradation products were subjected to two methods involving gas chromatography/mass spectrometry. The first method was methylation analysis (Hakomori 1964; Björndal et al 1971; Jansson et al 1976). The moiety in question was permethylated, hydrolyzed, reduced, and acetylated. These permethylated alditol acetate derivatives of neutral and amino sugars were then identified by GC/EI/MS/data system analysis on 3% OV-225 or 3% ECNSS-M (Stellner et al 1973). This gives the linkage information, sugar identity (as compared to standard retention times), and quantitative molar ratios. When different samples gave similar sugar compositional results, methylation analysis allowed us to differentiate between their structures. As well, reduction with deuterated sodium borohydride significantly improved the ability to determine the methyl substitutions. The second method was the direct solid probe introduction of the total derivatized sample into the ion source. Careful application of heat to the capillary holder allowed the fractional microdistillation of the sample from any contaminating material and provided excellent spectra of oligosaccharide structures. In the case of G_9, the intact fucoganglioside was permethylated, aluminum hydride-reduced, and trimethylsilylated and the oligosaccharide liberated from the fucoganglioside by endo-β-galactosidase was reduced with sodium borohydride, permethylated, and purified on TLC. The mass assignments and deduced structures are indicated in Fig. 1.

Thus, methylation analysis on GC/MS and direct probe mass spectrometry before and after enzyme digestion, provided us with enough information to elucidate the structures of nine monosialogangliosides as shown in Table I. The information produced by one method was either confirmed or supported by the other methods. The structures of these gangliosides have the same basic core structure, Galβ1→4GlcNAcβ1→3Galβ1→4Glc→Cer (lacto-N-neotetraosylceramide), with the following new features: 1)ganglioside with NeuNAcα2→6 structure at the non-reducing terminal, 2)GM_{1b} structure (NeuNAcα2→3Galβ1→3GalNAcβ1→4 Galβ1→4Glc→Cer), 3)both GalNAc and GlcNAc present (sialyl pentaosylceramide), and 4) a branched structure of two different oligosaccharide chains with H and I activity (G_9).

TABLE I.

Proposed structures of monosialosylganglioside isolated from human erythrocyte membranes.

G_1 NeuNAcα2→3Galβ1→4Glc→Cer

G_2 NeuNAcα2→3Galβ1→4GlcNAcβ1→3Galβ1→4Glc→Cer

G_3 NeuNAcα2→3GalNacβ1→3Galβ1→4GlcNacβ1→3Galβ1→4Glc→Cer

G_4 NeuNAcα2→6Galβ1→4GlcNAcβ1→3Galβ1→4Glc→Cer

G_5 NeuNAcα2→3Gall→3GalNAcl→4Gall→4Glc→Cer

G_6 NeuNAcα2→3Galβ1→4GlcNAcβ1→3Galβ1→4GlcNAcβ1→3Galβ1→4Glc→Cer

G_7 NeuNAcα2→6Galβ1→4GlcNACβ1→3Galβ1→4GlcNAcβ1→3Galβ1→4Glc→Cer

G_8

Galβ1→4GlcNAcβ1 ↘ 6
NeuNAcα2→3Galβ1→4GlcNAcβ1 ↗ 3 Galβ1→4GlcNAcβ1→3Galβ1→4Glc→Cer

G_9

L-Fucα1→2Galβ1→4GlcNAcβ1 ↘ 6
NeuNAcα2→3Galβ1→4GlcNAcβ1 ↗ 3 Galβ1→4GlcNAcβ1→3Galβ1→4Glc→Cer

Sequence Analysis of Free Carbohydrates Using FD/CID Mass Spectrometry

H. Kambara* & A. L. Burlingame
Department of Pharmaceuitcal Chemistry,
University of California, San Francisco

While it has been recognized for some time that field desorption mass spectrometry could provide a way of measuring the molecular weight of free oligosaccharides by observation of M/M+1 (1) and/or (M+alkali metal)cations (2), little attention has been given to the "induction" of reproducible fragmentation patterns from field desorbed molecular species.

Reinhold and coworkers (3) have obtained fragments useful for glycoheteropolymer sequence investigation by using high emitter currents during field desorption of a tetrasaccharide.

We have reported the utility of field desorption/collision-induced desorption mass spectrometry (FD/CID MS) using a B/E linked scanning mode for the structural identification of free carcinogen/DNA covalent adducts (4), peptidyl alkaloids (5) and permethylated surcrose (5) either as the pure substances or in mixtures.

We wish to report the feasibility of determination of the glycosidic linkage using qualitative differences in the FD/CID spectra of the free disaccharides: Trehalose $\alpha,\alpha(1\text{-}1)G_2$; sophorose $\beta(1\text{-}2)G_2$; nigerose $\alpha(1\text{-}3)G_2$; celloboise $\beta(1\text{-}4)G_2$ and genitoboise $\beta(1\text{-}6)G_2$.

Experimental: The FD/CID spectra of the samples were determined as previously reported, except in the present studies short microneedle (~10μm) emitters were employed using heating current to the 10μW wire of 16-23 mA. At least 10 spectra of each substance was recorded - relative intensity reproducibility was approximately $\pm$ 20%. All spectra were recorded as the sodium cationized molecular species even as low as 12 m/A.

Results and Discussion: The FD/CID spectra for these free disaccharides are shown in Figure 1. In general, ions in the region m/z 300→365 are due to losses of two functional groups as CH_2OH, OH and H. Ions resulting from glycosidic bond rupture accompanied by H attachment or loss occur at m/z 203, 201 and 185.

Fragments occurring between m/z 230 and 310 are reproducible for each linkage isomer and are charateristic of the linkage type.

These isomers can be separated into two groups according to whether they have a strong CID peak at m/z 259. The disaccharides having (1-1), (1-2), or (1-3) linkages do not produce a strong ion of m/z=259. The key ions to distinquish (1-4) from (1-6) linkages are those of m/z=275 and 289, with very weak or no ions of m/z=273. On the other hand, cellobiose [(1-4) linkage] produces a strong ion of m/z=273, but only weak ions of m/z 275 and 289.

Nigerose [(1-3) linkage] can be distinguished from the remaining linkage types [trehalose (1-1) linkage], and sophorose [(1-2) linkage] by observing the ions of m/z=289. Among these three disaccharides, only nigerose produces a strong signal at m/z=289, with no or very weak ion current at m/z=259. The relative ion intensity difference of m/z=231 and 245 can be used to distinguish trehalose and sophorose. The ratios of m/z=245 to 231 were about 1:3 for trehalose and 1:1 to to 2:3 for sophorose. The ratio for trehalose never exceeded 1:2.5, while for sophorose it was always greater than this. Therefore, the species can be identified as trehalose in the case of $I_{245}I_{231}<0.4$ and as sophorose in the case of $I_{245}/I_{231}>0.4$.

Conclusion: This study has demonstrated that the FD/CID method employing a B/E linked scan is an excellent method to distinguish dissaccharides of different linkages. The daughter ions included species resulting from ring ruptures and

*Present Address: Hitachi, Central Research Lab., Kokubunji, Tokyo 185, Japan

thus provided information that can be directly related to the molecular structure. The ionization efficieny depends upon the emitter quality, and particularly upon the emitter microneedles. Long microneedles (~30μm or longer) did not produce high sensitivity, whereas shorter microneedles (approximately 10μm) provided a sensitivity high enough for the FD/CID study. This is probably because the major ionization pro- *in the case of shorter microneedles is a combination of field independent cationization* on the surface and only desorption of such ions from the surface by the strong electric field.

References

1. J. Moor & E. S. Waight, Org. Mass Spectrom., Vol. 9, 903 (1974).
2. G. Puzo and J. C. Prome, Adv. in Mass Spectrom., Vol. 7, 1596 (1978).
3. V. N. Reinhold, C. E. Costello, B. W. Wilson and K. Biemann in Proc. 25th Ann. Conf. on Mass Spectrom. and Allied Topics, Washington D.C., 1977, p. 485.
4. K. Straub, T. Meehan, H. Kambara, A. L. Burlingame and S. Evans, Proc. 26th Ann. Conf. on Mass Spectrom. and Allied Topics, St. Louis, Mo., 1978, p. 499.
5. A. L. Burlingame, H. Kambara and F. C. Walls, Proc. 26th Ann. Conf. on Mass Spectrom. and Allied Topics, St. Louis, Mo., 1978, p. 184.

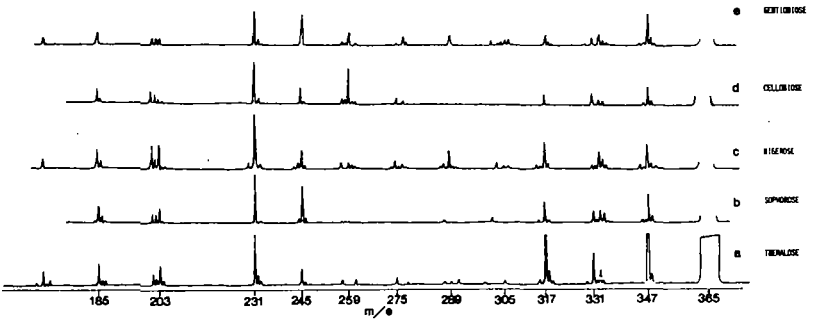


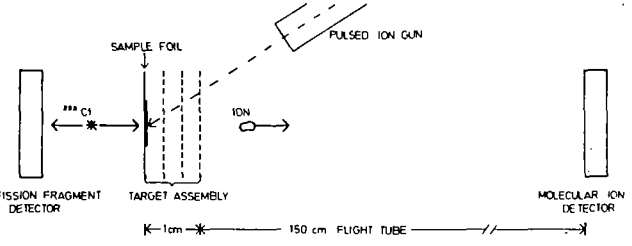
Figure 1. FD/CID Mass Spectra of Free Disaccharides

FAMOC1

A TIME-OF-FLIGHT MASS SPECTROMETER FOR MEASUREMENT OF SECONDARY ION MASS SPECTRA. B.T. CHAIT* and K.G. STANDING, Physics Dept., University of Manitoba, Winnipeg, Canada R3T 2N2.

During the past few years there has been a growing interest in the measurement of large molecules of low volatility. Several so-called soft-ionization techniques have been developed which enable these molecules to be observed with limited fragmentation. One method showing great promise is the desorption directly from the solid state and simultaneous ionization of the molecules of interest by energetic heavy ions. McFarlane and Torgerson[1,2] first demonstrated this technique using fast fission fragments from a spontaneously fissioning ^{252}Cf source in a time-of-flight spectrometer. Here typically the fragment ions have masses of around 100 and energies of 100 MeV. More recently Benninghoven et al.[3,4] have demonstrated that rather similar results (at least for the amino acids) could be obtained using 2 keV argon ions produced in a conventional ion gun in a single focussing magnetic spectrometer. In the present device we incorporate features of both these techniques.

The principle of the device is illustrated in figure 1.



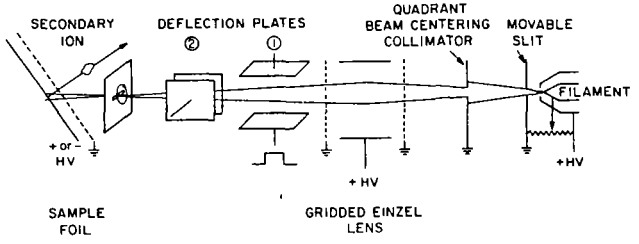
$$\frac{M}{q} \approx 2V(t_s)^2$$

Fig. 1

Here a thin layer of organic material is deposited on a target foil. When an organic ion is liberated from the foil, it is accelerated through a grid within the target assembly, then travels down the flight tube to a detector. The time-of-flight of the ion determines its ratio of mass to charge. The machine is designed so that organic molecules can be liberated either by a fission fragment emitted from an adjacent source of ^{252}Cf or by a heavy atomic ion (e.g. a few keV K^+) produced and accelerated in an ion gun. In the case of the californium fission fragment the start time marker is provided by the complementary fission fragment travelling in the opposite direction. The rate of arrival of the fragments at the target must be kept low enough so that the probability of a second fragment arriving during the time-of-flight of an organic ion is small, otherwise there is confusion as to which fission fragment is responsible for the ion detected. This arises because of the random nature of the fission process and severely limits the rate at which secondary ions can be produced. In the case of the ion gun the ion beam itself is pulsed at regular intervals with pulse lengths of the order of a few nanoseconds. The number of primary ions in each pulse may be increased without introducing any ambiguity in timing. We have concentrated our initial effort on this second technique since it is expected to offer a significant increase in sensitivity over the first (provided of course that this process gives comparable yields of molecular ions).

The system is metal sealed and uses a combination of sorption, sublimation and ion pumping to provide clean vacuum conditions with operating pressures in the low 10^{-8} torr range. Samples are introduced through a vacuum lock. Detection of single ions is performed with a chevron microchannel electron multiplier. The pulsed ion gun is illustrated in figure 2. Positive alkali metal ions (e.g. Na^+, K^+, Cs^+) are thermionically emitted from a small glassy pearl of alkali aluminosilicate mounted on a tungsten hairpin filament. This type of source was chosen for the initial configuration because of its simplicity, low cost and minimal

pumping requirements. The beam is focussed to a beam spot size of 100μ diameter by a gridded einzel lens and swept across a 100μ wide slit by a set of pulsed deflection plates. A second set of deflection plates oriented at right angles to the first set provides retrace elimination. The resulting beam pulses may be tuned to contain between 1-100 particles per pulse at pulse repetition rates up to 10 KHz. A beam pulse width of 6ns FWHM has been obtained thus far, limited by the small (100 volt) deflection pulses available at present. The system was designed so that the energy of the ions may be varied between 1 and 24 KV. Thus far ions have been accelerated up to 3 keV.



PULSED POSITIVE ION SOURCE

Fig. 2

The beam is fired through the secondary ion acceleration grid (90% transmission electroformed nickel) onto the sample foil which is coated with the organic material of interest. Either positive or negative secondary ion spectra may be taken by switching the polarity of the high voltage on the sample foil and changing the primary beam energy appropriately. Time spectra are recorded using a conventional time-to-amplitude converter and multichannel analyzer. Figure 3 shows the time spectra observed with the spectometer for a potassium iodide sample.

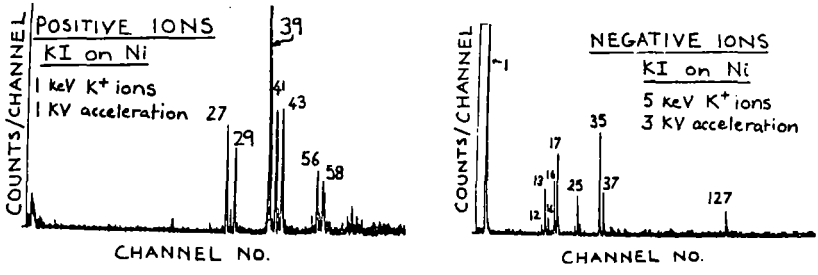


Fig. 3

References:

1. R.D. McFarlane & D.F. Torgerson, Science, March 1976.

2. R.D. Mcfarlane & D.F. Torgerson, Int. J. Mass Spectrom. Ion Phys., 21 (1976)81.

3. A. Benninghoven, D. Jaspers & W. Sichtermann, Appl. Phys. 11 (1976) 35.

4. A. Benninghoven & W. Sichtermann, Organic Mass Spectroscopy, 12 (1977) 595.

* Now at the Rockefeller University, New York, N.Y. 10021.

CID AND MIXTURE ANALYSIS STUDIES ON A FINNIGAN TRIPLE STAGE QUADRUPOLE MASS SPECTROMETER

Donald F. Hunt, Jeffrey Shabanowitz, and Anne Giordani FAMOC 2

Department of Chemistry, University of Virginia, Charlottesville, Virginia 22901

It has recently been shown that multistage mass spectrometers consisting of an ion source, mass analyzer, collision gas chamber, and second analyzer can be used in place of combined gas chromatography mass spectrometry for the analysis of complex mixtures of organic compounds.[1] In the latter technique neutral mixture components are separated chromatographically, and each molecule is then ionized separately and characterized by its molecular weight and fragmentation pattern. In the multistage mass spectrometry methodology ions characteristic of molecular weight are generated from all mixture components simultaneously. Each ionized mixture component is then separated in a mass analyzer, caused to fragment in a gas collision chamber, and identified from the mass spectrum of the resulting fragment ions. To investigate the collision induced dissociation of negative ions we have constructed a triple stage quadrupole instrument similar in design to that described by Enke and Yost.[2] The first and third quadrupole in this instrument function as conventional mass filters. The middle quadrupole operates with rf voltage only on the rods and serves both as a collision cell and an ion trap. The sensitivity of this new instrument is comparable to that obtained on conventional single quadrupole GC-MS equipment.

Construction and Operation of TSQMS for CID Studies: Construction of this unit was accomplished by adding two additional Finnigan quadrupole mass filters to a Finnigan Model 3200 quadrupole CI mass spectrometer. The resulting system (Figure 1) consists of a Model 3200 CI ion source, source lens, two Model 3200 mass filters (Q_1 and Q_2), a Model 4000 quadrupole mass filter (Q_3) and a conversion dynode electron multiplier detector for recording either positive and negative ions. Lenses 1-6 have aperture diameters of 3mm. Operation of this system does not require vacuum pumping capacity beyond that normally provided with a single stage Finnigan Model 3200 CI system.

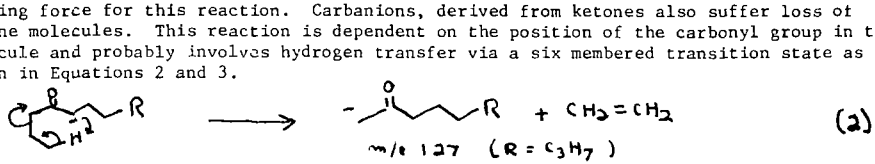
To utilize the TSQMS for CID studies of negative ions the ion source potential is set between -10 and -15V and all lens voltages are optimized at positive values. Q_1 is then set to pass the ion of interest into Q_2. Only rf voltage is placed on the rods in Q_2. In this mode Q_2 functions as an ion trap and transmits ions of all masses. Collision gas pressures between 1 and 6 x 10^{-3} torr in Q_2 are required to optimize formation and collection of fragment ions. A draw out potential of +10 to +30V is placed on Q_3 which in turn functions as a normal quadrupole mass filter and mass analyzes the fragment ions produced in Q_2. Both Argon and Neon were used as collision gases.

Results and Discussion: Production of $(M-1)^-$ ions from sample molecules was accomplished using OH^- as the CI reactant. This in turn was generated by the method of Field and Smith using a mixture of CH_4/N_2O as reagent gas under NICI conditions. Very little fragmentation accompanies production of sample $(M-1)^-$ ions when OH^- is employed as the CI reagent. One explanation of this result assumes that the lifetime of the ion/molecule complex is short and, therefore, the exothermicity of the reaction remains largely in the new bond that forms. As shown in Equation 1 the new bond is in the reagent gas molecule and not in the sample ion. Accordingly the $(M-1)^-$ ions are produced with little excess energy and, therefore, suffer little or no fragmentation.

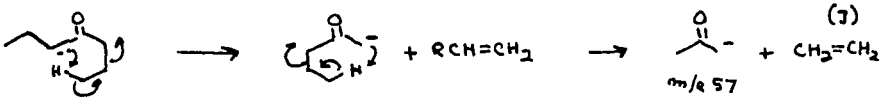
$$OH^{(-)} + CH_3COCH_3 \rightarrow H_2O + CH_3COCH_2^{(-)} \qquad (1)$$

After passage through the first mass filter, Q_1, the $(M-1)^-$ ion enters Q_2 where it becomes vibrationally excited during collisions with either argon or neon atoms. Carbanions can acquire 2 or 3eV of internal energy by this mechanism in the TSQ instrument. Accordingly dissociation pathways which are either endothermic or which involve considerable activation energy now become accessible and considerable fragmentation of the ion occurs.

A major fragmentation pathway observed for all ketones and aldehydes studied involves loss of H_2 from the $(M-1)^-$ ion. Formation of a conjugated anion presumably provides the driving force for this reaction. Carbanions, derived from ketones also suffer loss of alkene molecules. This reaction is dependent on the position of the carbonyl group in the molecule and probably involves hydrogen transfer via a six membered transition state as shown in Equations 2 and 3.



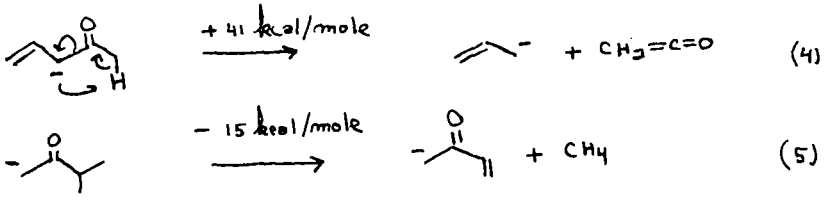
(2)



(3)

For R = C_3H_7, ΔH = 22.5, ΔH_{3a} = 20, ΔH_{3b} = 22.5 Kcal/mole.

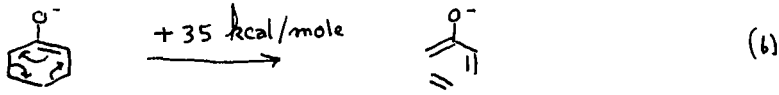
Compounds that lack a hydrogen six atoms away from the anionic site fail to eliminate alkene. Dissociation of $(M-1)^-$ ions from these compounds occurs by an alternate pathway involving loss of ketene and methane respectively as shown in Equations 4 and 5.



(4)

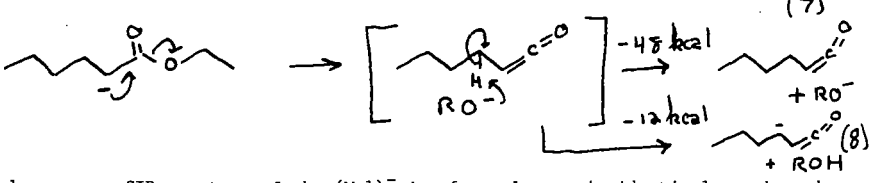
(5)

Elimination of olefin is also a major pathway in the CID of $(M-1)^-$ ions from cyclohexanones. This reaction appears to be an anionic retro Diels-Alder reaction (Equation (6)).



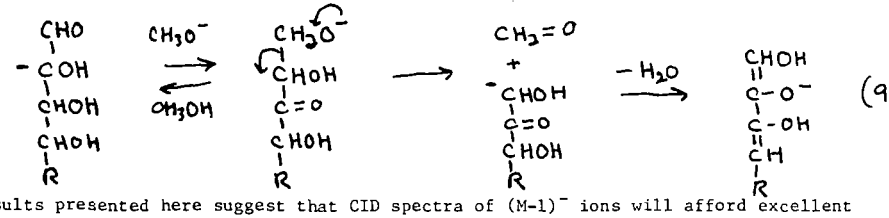
(6)

CID of $(M-1)^-$ ions from esters presumably occurs by a two step process involving dissociation into RO^- and ketene molecule, which then undergo a proton transfer reaction during the lifetime of the ion/molecule complex to produce neutral alcohol and a ketene anion (Equations 7 and 8).



(7) (8)

The TSQ low energy CID spectrum of the $(M-1)^-$ ion from glucose is identical to that obtained in the high energy MIKES experiment by Cooks et al.[1] The spectrum can be adequately explained by a combination of carbonyl group isomerization, anionic retro aldol condensation, and dehydration reactions, as shown in (Equation (9)).



(9)

Results presented here suggest that CID spectra of $(M-1)^-$ ions will afford excellent structural information from many molecules. Since $(M-1)^-$ ions can be generated under CI conditions without extensive fragmentation in the ion source, the above methodology should find considerable utility in the direct analyses of complex mixtures by multianalyser mass spectrometers.

REFERENCES

1. McClusky, G.A., Kondrat, R.W., and Cooks, R.G., Direct Mixture Analysis by Mass-Analyzed Ion kinetic Energy Spectrometry Using Negative Chemical Ionization. J. Amer. Chem. Soc., 100, 6045 (1978).
2. Enke, C. and Yost, R., Selected Ion Fragmentation with a Tandem Quadrupole Mass Spectrometer. J. Amer. Chem. Soc., 100, 2274 (1978).

A NEW MASS SPECTROMETER FOR THE STUDY OF FIELD-FREE REGION ION CHEMISTRY*

D. H. Russell, D. H. Smith, R. J. Warmack
Analytical Chemistry Division
Oak Ridge National Laboratory
Oak Ridge, Tennessee 37830

We have recently completed the design, construction, and performance evaluation of a three-sector mass spectrometer, viz. electric sector/magnet/electric sector. The three-sector configuration is ideally suited for both fundamental and analytical studies of metastable ions. Unimolecular or collision-induced dissociation reactions occurring in the first, second, or third field-free regions may be investigated by conventional defocused scan methods, i.e., accelerating voltage scans (HV), combined magnet/second electric sector (B/E or B^2/E) and second electric sector scans (MIKES), respectively.

The instrument is shown schematically in Fig. 1. The basic double focusing mass spectrometer, i.e., electric sector I and magnet, was designed and constructed at ORNL and has been described previously.[1] The instrument has partial second-order double focusing and has achieved a mass resolution of approximately 30,000. The second electric sector was added to the original instrument and is of the same design as electric sector I, with a 43.25 cm radius and a deflection angle of 90°. The image and object focal points (1_{i_2} and 1_{o_2}) for the second electric sector was calculated by the Hintenberger[2] method and give first-order direction focusing. Thus, the mass separation device, i.e., electric sector I and magnet, maintains the partial second-order double focusing characteristics which are necessary to achieve high mass resolution.

The large radii of the electric sector (43.25 cm) is important if one wishes to perform high energy resolution measurements. To date, the instrument has achieved ca. 5000 energy resolution with adequate sensitivity for single scan metastable data acquisition. In addition, the focusing characteristics of the instrument give good peak shapes for composite and dish-shaped metastable peaks. We have measured the kinetic energy release for a large number of unimolecular decompositions in the first and third field-free regions and find good agreement with published data.

The preliminary experimental data obtained with the three-sector mass spectrometer demonstrate the high potential of a three-sector configuration for the study of metastable reaction chemistry. The three-sector configuration is advantageous because of the wide range of metastable ion scan methods adaptable to a single instrument, i.e., HV, B/E, MIKES scans, as well as adaptability to other specialized techniques such as field-ionization kinetics (FIK). In addition, a relatively large range of average-ion lifetimes (~1-60 μs) may be sampled. Ions dissociating in each of the three field-free regions may be studied through suitable choice of scanning modes.

In many cases, the addition of a second electric sector to perform MIKES and collision-induced dissociation (CID) experiments may be preferred over conventional reversed-geometry configurations. It is not unusual to lose a factor of four in mass resolution when the geometry of a conventional modified Nier-Johnson instrument is reversed. However, this does not appear to be the case for commercially available reversed-geometry instruments where the ion optics are optimized for this configuration. A complete description of the instrument will be published in the *International Journal of Mass Spectrometry and Ion Physics*.

*Research sponsored by the U. S. Department of Energy under contract W-7405-eng-26 with the Union Carbide Corporation.

By acceptance of this article, the publisher or recipient acknowledges the U.S. Government's right to retain a non-exclusive, royalty-free license in and to any copyright covering the article.

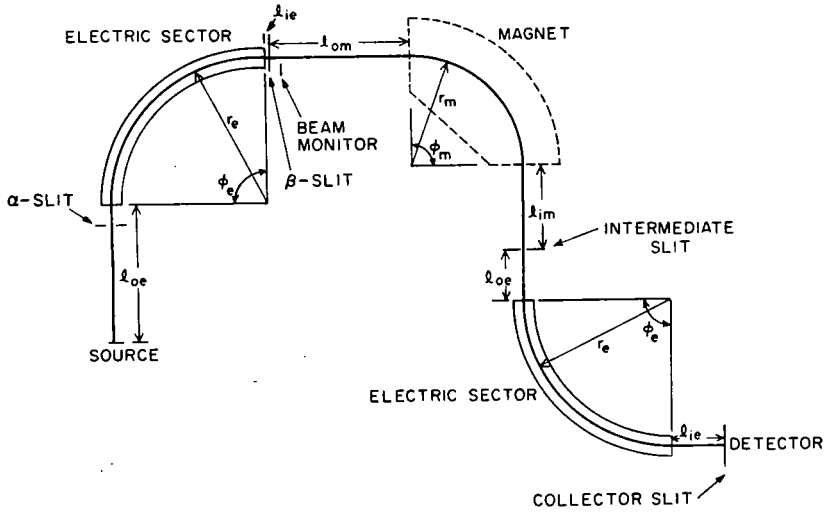
References

1. W. H. Christie, D. H. Smith, H. S. McKown, and G. R. Hertel, *Int. J. Mass Spectrom. Ion Phys.*, 8, 311 (1972).

2. H. Hintenberger and L. Konig, in J. D. Waldron (Ed.) *Adv. in Mass Spectrom.*, Pergamon Press, New York, 1959, pp. 16-35.

Figure 1

SCHEMATIC DRAWING OF THE THREE SECTOR INSTRUMENT



FAM0C4 A GENERAL METHOD FOR RECORDING B-E LINKED SCAN METASTABLE ION SPECTRA. W.F. HADDON, USDA, Western Regional Research Ctr., 800 Buchanan St., Albany, CA 94710

Linked magnetic field - electric sector scans are used to obtain defocused metastable ion spectra during rapid, repetitive scanning of a conventional geometry Nier-Johnson mass spectrometer. The electric sector voltage is set by a programmed power supply as the magnetic field cycles repetitively. Linked-scan (B-E) curves are calculated from mass-time calibration obtained separately. The metastable ion recording system is thus fully compatible with normal focused operation of the spectrometer.

The characteristics and uses of three linked scans will be described: the B/E scan (all daughter ions from a common precursor ion); the B^2/E scan (all precursors yielding the same daughter ion); and the $(B^2/E)(1-1/E)$ scan (constant neutral fragment).

THE MOVING-QUADRUPOLE IMPROVEMENT TO PHASE-SPECTROSCOPY

M. W. SIEGEL
Extranuclear Laboratories, Inc.
Pittsburgh, PA 15238

In elementary applications of modulated beam mass spectrometry, the purpose of beam modulation is to enable the use of narrow-band AC detection techniques, thus effectively providing automatic background subtraction and a substantial improvement in signal-to-noise ratio over non-beam techniques. A typical apparatus is illustrated in Figure 1, and typical DC and AC spectra for a weak air beam overwhelmed by an oil diffusion pumped background vacuum are shown in Figure 2.

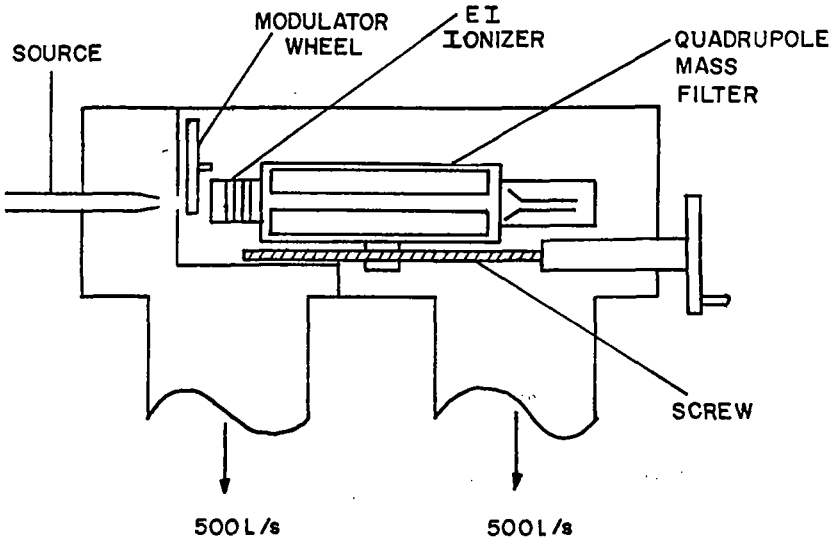


Figure 1

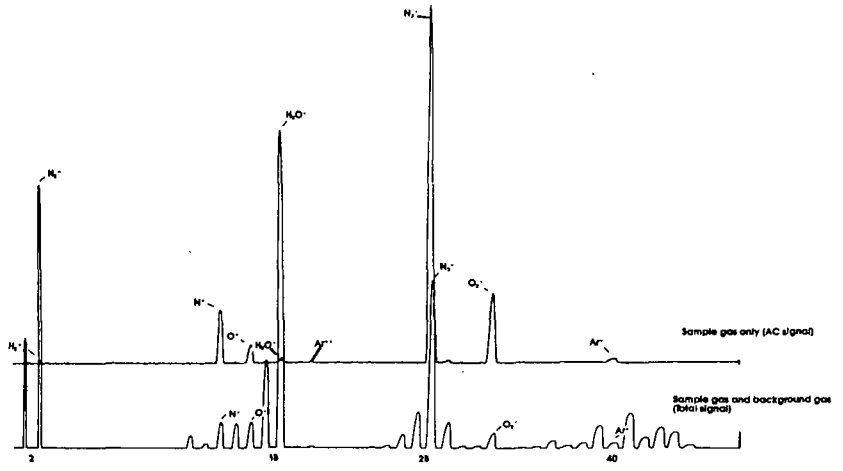


Figure 2

In somewhat more sophisticated applications, a lock-in amplifier is used not just for its narrow-banding capability, but also for its ability to measure the phase of an AC ion signal relative to a reference signal synchronous with the chopper. To first order (for a theoretically monoenergetic molecular beam), the phase shift between the modulator and an ionizer at distance ℓ downstream is

$$\frac{\phi}{360^{o}} = \frac{f\ell}{v} \approx (m/3kT)^{\frac{1}{2}}$$

where f is the modulation frequency, v is the thermal velocity, and ℓ/v is the time-of-flight from modulator to ionizer. Thus measurement of ϕ is equivalent to measurement of the time-of-flight of the neutral precursor of any ion in the mass spectrum, over a distance corresponding to the modulator-ionizer separation.

Exact treatment requires that ϕ be obtained by integration over the Maxwellian velocity distribution of molecular speeds, where $v = (\pi m/8kT)^{\frac{1}{2}}$. Numerical integrals as a function of the parameter $f\ell(\pi m/8kT)^{\frac{1}{2}}$ have been tabulated and graphed by Harrison, Hummer, and Fite(1), and in the range $0 \leq \phi \leq 100^{o}$ have been shown by Patterson(2) to be very well approximated by

$$\frac{f\ell}{v} = 2.22 \times 10^{-3}\ \phi + 3.69 \times 10^{-6}\ \phi^{2}$$

Naive consideration of these points leads to the conclusion that measurement of the phase shift, which is provided in calibrated form by the lock-in amplifier, is equivalent to measurement of m. That is, one is lead to believe that the mass of the neutral precursor of any observed ion may be measured by simply reading off the phase shift and the experimental parameters f, ℓ, and T.

In practice, such apparently straightforward measurements prove difficult. The actual phase measured includes unknown electrical phase shifts in the detector and amplifier, and phase shifts associated with the ion time-of-flight from ionizer to detector. Furthermore a large uncertainty must be attached to ℓ, since the ionizing volume has a finite spatial extent. Under conditions of fixed gain through the entire amplifier chain (from multiplier high voltage to current preamp input resistor to lock-in preamp voltage gain), all these effects are "end terms" independent of ℓ. Then measured differences in ϕ as ℓ is changed by well defined increments should be nearly linear in $\sqrt{m}$:

$$\frac{\Delta\phi}{\Delta\ell} \approx 0.031\ f\ \sqrt{m/T}$$

where f is in hertz, m in amu, T in kelvins, and $\Delta\phi/\Delta\ell$ in degrees/cm.

To make use of this technique, a modulated beam apparatus was constructed with a quadrupole mass filter movable under vacuum. The results are illustrated by Figure 3, which shows the measured phase shift per unit length obtained with samples of Xe, Kr, Ar, and Ne, in each case observing both the singly and doubly charged ions. It is important to note that while in the ion mass spectrum, sensitive to m/q, each doubly charged ion appears at apparently half the parent neutral mass, in the phase spectrum, sensitive to $\sqrt{m}$, all ions with the same neutral precursor have the same $\Delta\phi/\Delta\ell$. This conclusion is well confirmed by Figure 3; the only questionable datum, for Ne^{+}, is due to an argon impurity in the neon, resulting in some Ar^{++} in addition to Ne^{+} at m/e = 20.

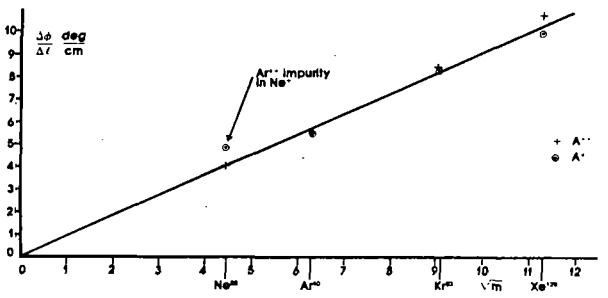


Figure 3

A useful application of the moving-quadrupole improvement to phase-spectrometry is the measurement of the electron impact ionization cross-sections for the production of O_3^+, O_2^+, and O^+ from ozone. In making these measurements, it is necessary to demonstrate that the ozone beam is free of O_2 and O contamination; in the absence of proof to the contrary, it might reasonably be assumed that the observed O_2^+ and O^+ was in part due to contamination and only in part due to dissociative ionization of O_3. Figure 4 shows phase shift data confirming the purity of the O_3 beam, i.e., it shows that O^+, O_2^+, and O_3^+ have identical values of $\Delta\phi/\Delta\ell$. The ozone was in a buffer gas consisting of a He-Ne-Ar mixture, and the He^+, Ne^+, and Ar^+ phase shifts are shown for comparison. From these data, it is possible to conclude that the separately measured electron impact cross sections for O^+, O_2^+, and O_3^+ from ozone are reliable. These cross section data will be published later.

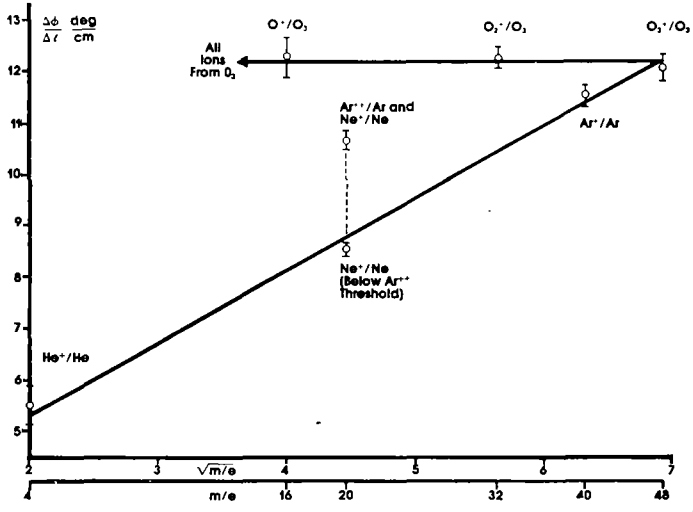


Figure 4

[1]H. Harrison, D. G. Hummer, and W. L. Fite, Boeing Scientific Research Laboratories, Flight Sciences Laboratory, Technical Memorandum No. 26, January 1964.

[2]T. A. Patterson, private communication.

FAM0C6 A NEW HIGH PERFORMANCE, MEDIUM RESOLUTION MASS SPECTROMETER - MS80

D. R. Denne, M. L. Aspinal, K. R. Compson, and W. Henderson, Kratos Ltd, Barton Dock Road, Urmston, Manchester M31 2LD, England.

The introduction of the MS25 marked a significant advance in the performance of low resolution mass spectrometers. This was achieved by the use of a sensitive source and classical sector geometry with the hexapole lens system. The MS80 has incorporated these proven high performance principles into a mid range instrument with a resolution of 20,000 (10% valley). Other factors include rapid switching between EI and CI modes without adjustment to the source configuration, this allows alternate CI/EI (ACE) spectra to be recorded routinely at the fastest scan speeds. Practical examples illustrating CI/EI switching, resolution and sensitivity will be presented.

FAMOC7

EXTENDING THE CAPABILITIES OF AN APCI-MS SYSTEM WITH A PRECONCENTRATOR FOR THE RAPID ULTRA-TRACE DETECTION OF POLYCHLORINATED BIPHENYLS AND HEXACHLOROBENZENE IN THE ATMOSPHERE

B.A. THOMSON, D.A.LANE, T. SAKUMA, N.M. REID, J.B. FRENCH, E. QUAN, S. NACSON, SCIEX INC., 55 Glencameron Road, # 202, Thornhill, Ontario, Canada,L3T 1P2.

1. PRINCIPLES OF ATMOSPHERIC PRESSURE CHEMICAL IONIZATION (APCI).

Atmospheric pressure chemical ionization is a novel but so far generally unappreciated analytical technique of great sensitivity and versatility. Chemical ionization at atmospheric pressure results in inherently higher sensitivity than 1 Torr CI due to the higher ion-molecule collision and reaction rates. Detection limits of below one part per trillion (v/v) have been demonstrated for many trace gases in air (1,2). The high pressure also results in faster collisional stabilization of product ions, so that less fragmentation occurs than in standard CI. The products are usually molecular or quasi-molecular in nature, with one peak per trace species; this makes interpretation of mass spectra particularly simple, and allows analysis of complex mixtures (such as ambient air) by direct sample injection. Techniques are available which supplement the molecular weight information in the mass spectrum, in order to aid in compound identification, and these are described in a companion paper.

Two types of ion source are in current use: 1) closed, in which the 760 Torr ionization region is isolated from the surrounding air; and 2) open, in which ambient air can be drawn directly into the source. The closed source design is similar in concept to a standard CI source. The sample to be analyzed must be collected and stored, often concentrated or separated from its matrix, chemically prepared for analysis and finally injected into the source. Each step is a source of possible sample loss or contamination, and the entire process can require considerable time and effort.

The open source design has been developed by SCIEX INC. for the TAGA™ 3000 (Trace Atmospheric Gas Analyzer) APCI-MS system. This type of design has a powerful advantage over the closed source for trace analysis of ambient air (and potentially for other types of complex gas mixtures) since the sample (air) is drawn directly and continuously into the ion region and analyzed in real time. The reagent ions generated from the air in the positive mode are $H_3O^+(H_2O)_n$, and in the negative mode, a mixture of $O_2^-(H_2O)_n$, $O_3^-(H_2O)_n$, $CO_3^-(H_2O)_n$, $HCO_3^-(H_2O)_n$ and $NO_3^-(H_2O)_n$. Essentially acid-base chemistry occurs between the reagents and the trace species, producing products of $MH^+(H_2O)_n$ in the positive mode and $(M-H)^-(H_2O)_n$ and $M^-(H_2O)_n$ in the negative mode. Air analysis performed in this way is real time, ultra trace (ppt detectabilities for many organics) and in-situ. No sample collection, storage or workup is required, and the results are obtained instantaneously. Many successful applications of the open ("ambient air") ion source combined with standard air ion chemistry have been noted (3,4), and its flexibility and simplicity make it the standard front end supplied with the TAGA™ 3000 system. Recent developments have expanded its utility with the demonstrated ability to alter the ion chemistry by adding various reagents to the incoming air, resulting in enhanced sensitivity or better specificity (4).

This paper reports on the development of a preconcentrator which collects (traps) trace species from the air, and transfers them into a source which is essentially closed. The integrating effect results in increased sensitivity to various trace gases, while the closed source allows better control over the ion chemistry than is presently possible with the open source. These advantages have been obtained while maintaining many of the virtues associated with the ambient air source, and described above.

2. PRECONCENTRATOR DESIGN AND CHARACTERISTICS.

The integrator (Figure 1) consists of a coil of Chromel wire (0.032" in diameter), coated with a thin layer of OV-17. The coil is suspended in the sample inlet line, and air is drawn past it at a flowrate of about 2 l/s. The ion source is isolated from the sample line by a nylon stopcock valve, and a flow of carrier ($\sim$ 80 cc/s) plus CI reagent (if desired) is maintained in the ionization region. After an absorption time of from one to a few minutes, the valve is opened and the integrator is pushed into the desorb position . It is supported on copper rods which are connected to a current source through the hollow handle. A current is passed through the coil to heat it resistively to about 300°C and the trapped species are desorbed in a pulse of several seconds duration. The response is measured by selected ion monitoring at the masses of interest. It can be shown that for trace concentrations (so that instrument response remains linear), and absence of probe saturation effects, the area under the signal vs time curve A is:

$A \alpha \varepsilon C_1 F_1 t_a / F_2$. Here ε is absorption efficiency, C_1 is trace concentration in the ambient air, F_1 is the sample flowrate, t_a is the absorption time and F_2 is the carrier flowrate. Thus the integrated signal is proportional to the trace concentration in the air.

The absorption efficiency of the integrator has been measured at between 20% and 40%, under the conditions described, depending upon the particular trace. Absorption times of 1 to 2 minutes are usually used, and the response is enhanced by a factor of 10

to 20 over real time measurement (again depending upon the species). Sixty second average measurements can be obtained routinely every three minutes. Up to eight compounds can in principle be monitored and quantitated during each absorption-desorption cycle by rapid peak jumping, taking full advantage of the software system which controls data acquisition and storage.(2) The potential is available for automating the entire process and placing it under the control of the computer.

Calibration is performed empirically by injecting a known flux of the trace into the sample line upstream of the integrator, and measuring the response at the mass of interest. Techniques are being developed and perfected which allow controlled concentrations down to the parts per trillion level to be produced. This "spiking" is the most direct method of calibration, and eliminates the necessity of knowing the trapping efficiency of the integrator.

3. APPLICATIONS: MONITORING PCB's AND HEXACHLOROBENZENE IN THE AIR.

The preconcentrator inlet system has been used with the TAGA™ 3000 in a mobile van to measure PCB's in the air at concentrations down to a few ng/m^3 (<1 ppt). The chemistry in the ion source is optimized for PCB detection by adding benzene to the carrier gas (zero air) in order to generate $C_6H_6^+$ reagent ions. The PCB reacts by charge transfer to produce M^+ product ions:

$$C_6H_6^+ + C_{12}H_nCl_{10-n} \longrightarrow C_6H_6 + C_{12}H_nCL_{10-n}^+$$

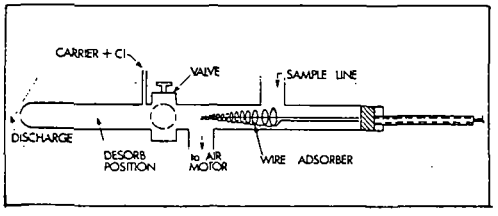
Software has been developed for the digitally controlled TAGA™ 3000 in order to allow the measurement of the concentrations of PCB homologues from the monochlorobiphenyl to the hexachlorobiphenyl in three successive collection and desorption cycles. An algorithm is being developed in order to provide positive identifiction of the PCB's based on their signature isotopic patterns. An example of the signal obtained at one mass during desorption is shown in Figure 2. The mass 222 is the first isotope of the dichlorobiphenyl. The signal rises and falls as the PCB is desorbed from the integrator, and the peak is quantitated by integrating between chosen limits as shown. In the absence of interfering peaks, PCB's can be measured in the air at levels down to 1 ng/m^3 for each homologue.

Hexachlorobenzene (HCB) has been monitored in the air with the same system. Carbon dioxide is used as a carrier, and the product ions from HCB in the negative mode are $(M-Cl+O)^-$. By monitoring one or more of the isotopes of this ion, HCB can be measured in the air at concentrations down to 30 ppb.

4. CONCLUSION. The wire integrator has demonstrated its application as a preconcentrator for enhancing sensitivity. It also functions as a preseparator, by preferentially absorbing certain compounds over others (water, for example, is not well absorbed), and it has the potential for being even more specific by appropriately tailoring the absorbent coating. It allows the use of a closed ion source in order to provide a high degree of control over the ion-molecule chemistry, while maintaining the advantages of rapid sample collection and transfer, no sample handling, and nearly real-time results. Although the wire integrator is inexpensive and is easy to manufacture and prepare, it has been proven that the unit is stable over hundreds of absorption-desorption cycles, requiring replacement or recoating only after several days of use.

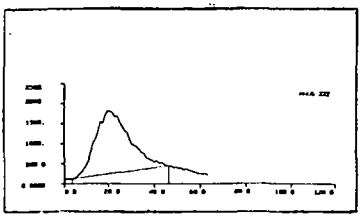
1. N.M. Reid, et al Proceedings of the 4th Joint Conference on Sensing of Environmental Pollution, New Orleans, 1978.
2. N.M. Reid, et al Proceedings of the 26th Annual Conference on Mass Spectrometry and Allied Topics". St. Louis, Missouri, May 28 - June 2, 1978.
3. F.W. Karasek, Industrial Research/Development, December 1978.
4. B.A. Thomson, et al Environmental Health Perspectives, 1979. In Press.

Figure 1



Schematic diagram of preconcentrator inlet System and ion source region

Figure 2



Example of the CRT display after a desorption from the wire. The ion current at m/z=222 (an isotope of dichlorobiphenyl is displayed as a function of time in seconds.

Transverse Ionization of a Seeded Molecular Beam: Effects of Space Charge on Mass Spectra and Velocity Measurements

M. J. Vasile and F. A. Stevie
Bell Laboratories
Murray Hill, New Jersey 07974

Optimization of the signal of the minor component of a seeded molecular beam resulted in ion source conditions that allowed space-charge trapping. Space-charge trapping of the ions from XeF_6 seeded into rare gases at or below a few mole percent had two deleterious effects: the relative intensities of the ionic species were inaccurately represented, and the translational temperature of the molecular beam could not be accurately determined. Ion residence times were sufficiently long to allow second or third ionization events, yielding large relative intensities of Xe^{+3}, and Xe^{+2}. When this situation was corrected, the relative intensities of these latter species was significantly reduced. Ionic species containing more than one xenon atom were found to be fragmentation products from the ionization of the van der Waal's dimer Xe_2F_{12}, and not a result of ion-molecule reactions. Accurate determination of the translational temperature of the molecular beam by the time of flight method requires elimination of space-charge trapping of the ions in the ionizer. The translational temperature of an argon molecular beam generated from a 0.0025 cm dia orifice with one atmosphere pressure was 6°K, in good agreement with other time of flight techniques.

ANALYTICAL PERFORMANCE OF A FOURIER TRANSFORM* MASS SPECTROMETER

E.B. Ledford, Jr., R. White, R.B. Spencer, P.S. Kulkarni, S. Ghaderi, C.L. Wilkins, M. L. Gross

Department of Chemistry
University of Nebraska
Lincoln, Nebraska 68588

Fourier Transform mass spectrometry (FT/MS) provides a method of acquiring high resolution mass spectra in times on the order of one second or less. This has stimulated interest in analytical applications of FT/MS. However, in order to be useful as an analytical instrument, the FT/MS must be capable of high sensitivity with respect to sample size, and mass measurement accuracy sufficient for determination of elemental compositions of ions. Here we report results of initial studies of mass measurement accuracy and sample size sensitivity in FT/MS.

The fundamental quantity measured in the FT/MS experiment is the resonance frequency of ions confined in a strong and uniform magnetic field. Exact mass measurement rests on the ability to measure ion resonance frequencies precisely, and to relate frequency to mass accurately. Thus, the mathematical relationship between mass and resonance frequency is of key importance; it must be accurate to the level of about a few parts-per-million for elemental composition assignments. The relationship between mass and resonance frequency depends upon the electric field configuration inside trapped ion cells, and this depends, in turn, upon the cell geometry. In our laboratory we have adopted a cubic analyzer cell design. Our theoretical treatment of ion motion in the cubic cell has led to a mass calibration equation of the form

$$m_i^2 f_i^2 = a_o m_i^2 - b_o m_i + c_o \qquad (1)$$

where m_i is the mass of the ith peak, and f_i the corresponding resonance frequency. The analytical form of the constants a_o, b_o, and c_o are too complicated to be presented here. However, they may be treated as arbitrary constants to be experimentally determined in relative mass measurement schemes. If the resonance frequencies of two more ions of known mass are measured, experimental values of the calibration constants a_o, b_o, and c_o can be computed. Once they are known, a third and unknown mass can be computed from a measurement of its resonance frequency.

We have found that the parabolic calibration procedure of equation (1) produces mass measurements of sufficient accuracy to permit unambiguous elemental composition assignments over a mass range of at least eighteen amu, centered at m/e 126. Resonance frequencies for the six major ions in the spectrum of 1,1,1,2-tetrachloroethane were measured over ten successive Fourier Transform mass spectra. Frequency measurement precision was typically $\pm$ 0.3 Hz and in no case exceeded $\pm$ 1.5 Hz (single standard deviation over ten trials). The quantity $m_i^2 f_i^2$ was fitted to the parabolic form in equation (1), and the masses then back-calculated (see Table I) using computed values of a_o, b_o, and c_o. Over an eighteen amu range, the parabolic calibration procedure gives mass errors of less than one millimass unit.

In practice we have found the mass accuracy shown in Table I is routinely obtained over a broad range of operating conditions. Computerized data reduction of successive mass spectra makes calculation of masses and standard deviations fast and reliable. At present, calibration studies over a wider mass range are in progress and will be reported in a full paper.

In the area of sample size sensitivity we have investigated the performance of a new analyzer cell which is constructed in an almost "gas tight" configuration. The strategy has been to route samples from a heated probe directly into the analyzer cell for low pressure chemical ionization. For polar compounds such as paracyanophenol, detection limits of about 50 ng (full range mass scan, 5:1 S/N ratio) are obtained. We have also examined sensitivity with respect to volatile materials by

desorbing them off Tenax packed into a glass capillary in the insertion probe tip. In this way 10 ng of cyclohexene is ample for full range mass scans under low pressure chemical ionization or electron impact conditions. Results suggest the construction of a completely gas tight analyzer cell which would retain small samples for long periods of time. Calculations indicate that sample sizes below 15 picograms should be sufficient for full range spectra up to 1000 amu.

TABLE I

m_i	Calculated Masses	Error amu	Error ppm
116.9066	116.9064 ± 0.0003	-0.0002	(1.7)
118.9036	118.9041 ± 0.0003	+0.0005	(4.2)
120.9007	120.8999 ± 0.0008	-0.0008	(6.6)
130.9222	130.9226 ± 0.0004	+0.0004	(3.1)
132.9192	132.9188 ± 0.0004	-0.0004	(3.0)
134.9163	134.9164 ± 0.0006	+0.0001	(0.7)

*This research was supported by Grant No. CHE-77-03964 and by a grant from the Gulf Research Foundation.

FAMOC10 FOURIER TRANSFORM ION CYCLOTRON RESONANCE SPECTROSCOPY, M. COMISAROW, Chemistry Department, University of British Columbia, Vancouver, B.C., Canada V6T 1W5

Fourier transform ion cyclotron resonance (FT-ICR) spectroscopy is a new method for conducting ion cyclotron resonance (ICR) experiments which was first demonstrated in our laboratories in 1974. The method involves the simultaneous excitation of the entire frequency domain ICR spectrum, sampling of the resultant transient response of the system, and numerical Fourier transformation to obtain the ICR frequency spectrum. The FT-ICR method combines the Fellgett advantage of multiplex techniques with the capability of conventional ICR spectroscopy. In addition, the FT-ICR method is capable of producing ultra-high resolution ICR mass spectra. Recent FT-ICR developments will be discussed.

ELECTRO-OPTICAL ION DETECTION USING SOLID STATE PHOTO DIODE ARRAY DETECTORS

C. GIFFIN, R. Britten, H. Boettger, J. Conley, D. Norris
Jet Propulsion Laboratory, Pasadena, California 91103

Over the past four years, under sponsorship by the National Institues of Health and NASA, a unique mass spectrometer ion detection scheme has been developed at the Caltech Jet Propulsion Laboratory. The detector represents a significant advancement in the state of the art in that it can integrate ion currents over a wide mass range as does a photoplate, but retains the ability to detect single ions, a capability featured only by electron multiplier detectors. The detection system can be termed an electronic photoplate in that the ions are converted to electrons and then to photons which are quantitatively measured using solid state imaging arrays.

Figure 1 is a schematic drawing of the layout of a Mattauch - Herzog mass spectrograph using electro-optical ion detection (EOID). Ions exiting the magnetic field impinge on the active surface of a two-dimensional micro-channel electron multiplier array. An electron cascading process is initiated ending typically with 10^4 electrons being produced for each impinging ion. These electrons are then accelerated to a phosphor coated fiber optic window, whereby photon images (typically >100 photons per electron) are generated and transmitted by the fiber conduits to the electronic imaging detectors for measurement of position (indicative of mass of the ion) and intensity (proportional to total number of ions collected). The imagers are self-scanned photodiode arrays having a dynamic range of $>1 \times 10^4$.

The wedge-shaped fiber optics shown in cross section - A of Figure 1 is in actuality a vacuum window composed of 6 μm, glass fibers, fused together. The angled front face is coated with 2-4 μm P-31 phosphor and aluminized to inhibit charging from the secondary electron currents. The micro-channel electron multiplier arrays contain 20 μm x 20 μm square channels. The active area of each channel-plate is 1mm high by 25.4 mm long. To accommodate the 356 mm long focal plane of the CEC 21-110B mass spectrograph, fourteen channel plates are used, butted end-to-end. The square channel geometry provides for little or no loss of active area along the entire focal plane.

The "ion" images conducted outside the vacuum by the fiber optic window are coupled to linear photo diode arrays (PDA's) via fiber optic couplers that have the ability to rotate the angled images, described in earlier publications (Ref. 1-3), into alignment with the individual photodiodes. The fiber optic rotators also provide for elimination of mechanical interference between adjacent PDAs as shown in Figure 1. Fourteen coupler/PDA assemblies are required to observe the 356 mm long focal plane: alternating seven above the horizontal and seven below the horizontal. Figure 2 depicts the geometry of the fiber optic rotators. They are made from forty-two square multifiber bundles of glass fibers epoxied together to form a warped plane. Each multifiber element is composed of a 320 x 320 matrix of 5.5 μm fibers.

The PDA detectors are received from the manufacturer with fiber optic windows. This feature allows the PDAs to be glued with optical cement directly to the back of the fiber optic couplers for maximum light transmission. The specifications of the PDAs are shown in Figure 3.

The mechanical details of the EOID are shown in Figures 4 and 5. Since significant reduction in PDA dark current can be achieved through cooling (x 10 current reduction per 20°C. temperature reduction) a cold gas cooling box is provided and coupled to the PDAs through copper cooling bars. The fiber optic vacuum window is O-ring sealed to the vacuum housing which is in turn O-ring sealed to the mass spectrometer in the same fashion as the original photoplate box.

As an example of instrument performance Figure 6 shows a computer average of 20 spectra from a solid probe run of 0.1 picogram 4,4' - dibromo-biphenyl. Total sample throughput over the twenty spectra was $\sim 8 \times 10^{-15}$ grams. Although not shown, each spectrum spanned the mass range from 98 - 328 amu. Integration time per spectrum was 1.05 seconds. Further details of performance can be obtained in paper RAMOA7 of these transactions.

This research is sponsored under a grant from the National Institute of General Medical Sciences, NIH (Grant No. GM20850).

References

1. Giffin, et. al, Int. Journ. of MS and Ion Phys 15 (1974)
2. Giffin, et. al, ASMS Transactions (1976)
3. Boettger, Giffin, et. al. Monograph on Image Detectors in Chemistry, Y. Talmi, Ed. (1978)

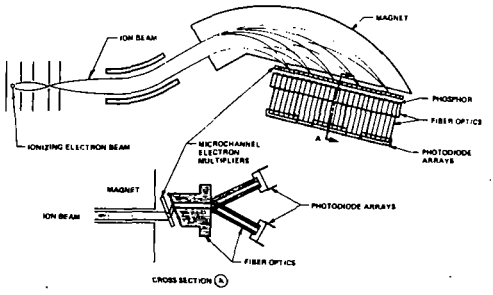


Fig. 1 - MS/EOID Schematic

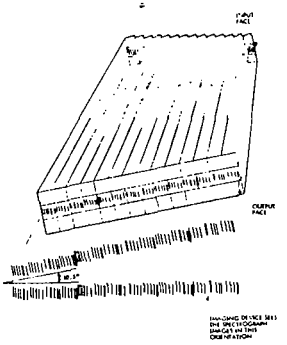


Fig. 2 - Fiber Optic Rotator

PHOTODIODE ARRAY SPECIFICATIONS

APERTURE WIDTH	2.54 cm
APERTURE HEIGHT	2.5 mm
DIODE WIDTH	25 μm
NUMBER OF DIODES	1024
SATURATION EXPOSURE	5.05×10^{-5} μ-WATT-SEC
QUANTUM EFFICIENCY	75% (@ 520 nm)
DYNAMIC RANGE	$\geq 1 \times 10^{4}$

Fig. 3 - Photodiode Array Specs

EOID MECHANICAL CONFIGURATION

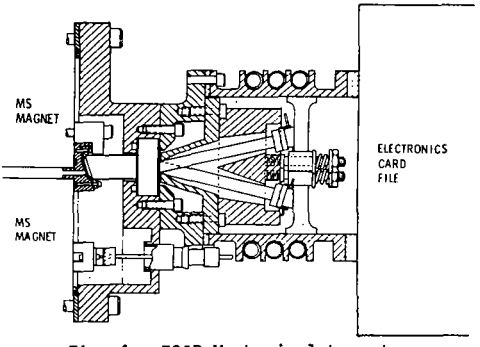


Fig. 4 - EOID Mechanical Layout

EOID MECHANICAL CONFIGURATION

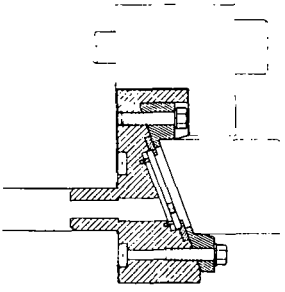


Fig. 5 - Microchannel Array Layout

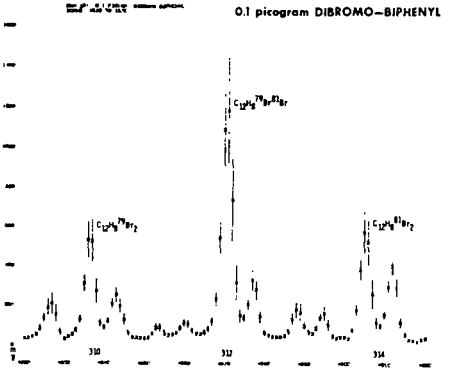


Fig. 6 - Twenty Spectrum Average

FAM0C12 MODIFICATION OF THE FINNIGAN 1015 M.S. FOR DIRECT CHEMICAL IONIZATION OF NON VOLATILE ORGANIC COMPOUNDS, D. I. CARROLL, J. G. NOWLIN, F. E. MONTGOMERY, R. N. STILLWELL and E. C. HORNING, Inst. for Lipid Research, Baylor College of Medicine, Houston, Texas 77030

Glass, teflon and vespel probe tips, inserted directly into the ion plasma in a CI source, or in the vicinity of the electron beam in an EI source have been used recently by several investigators to obtain mass spectral information using compounds which are normally considered non volatile. Our experience with such insulating probe tips in the Finnigan 1015 is that surface charging of the tip drastically alters the electric fields in the source, resulting in very erratic operation of the mass spectrometer. These problems have been overcome and reliable day to day operation achieved using a metal probe tip maintained at the ion source potential. The probe tip was used either bare, or coated with SE-30. Several illustrations of the type of mass spectra obtainable with these simple modifications from classic non volatile organic compounds will be presented.

A Modified Electron Bombardment Source for KRATOS/AEI MS9-MS50 Mass Spectrometer

FAMOC13

Guenter K. Eigendorf
University of British Columbia
Department of Chemistry
Vancouver, British Columbia
Canada V6T 1W5

Abstract

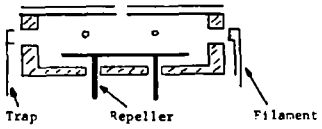
A previously described[1] EI/FI/FD combination source has been further modified to enable direct electron bombardment of solid materials prior to vapourization.

* * * * *

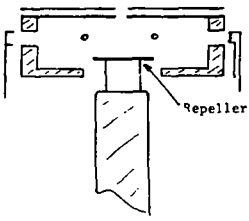
EIMS analysis of temperature labile molecules has for some years stimulated the interest of various research groups. Alternate methods such as CI and FI/FD were developed, however some of these, in particular the latter, have not reached wide spread application as yet. Instrumental costs and operational difficulties as well as sensitivity problems can be partly blamed.

Thus, attempts have been made to modify existing EIMS to make it more suitable for analysis of labile materials. Rapid sample heating[2,3], in beam techniques[4-7], the use of FD emitters as solid probes[8] and modified CI techniques[9-11] have been reported.

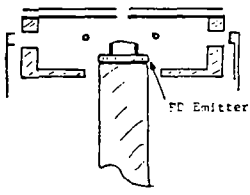
For several years this laboratory has utilized the "EI in beam" technique described by Sigmond[7] on MS9 and MS50 mass spectrometers. Subsequently a combined EI/FI/FD source was developed for these instruments.[1] However, the low sensitivity of the FI/FD technique has prompted further investigations towards modified EI techniques.



a



b



c

Fig. 1

The MS9-MS50 EI ion sources utilize an ion repeller and trap regulated filament (Fig. 1a). The previously described[1] combination source (Fig. 1b, EI mode; Fig. 1c, FI/FD mode) can now be utilized in the following manner. The FD emitter has been combined with a suitable repeller plate and this assembly is supported by a probe rod having four electrical contacts. This will permit utilization of the FD emitter as a solid probe as described by others.[8]

Furthermore an additional probe tip (Fig. 2) has been fashioned which consists of a stainless steel plate mounted at 45° on a heatable support socket. Mineral insulated heating wire serves as heat source for the latter. The EI filament and corresponding electron aperture have been lowered by 3.5mm. The original electron trap has been removed and its electrical connection transferred as to make contact to the new probe tip. Thus, the latter fulfills the functions of the electron trap and ion repeller.

Sample solutions are deposited on the angled plate and after evaporation of the solvent introduction of the probe is achieved via the previously described probe lock.[1] Micromanipulators located on the latter permit

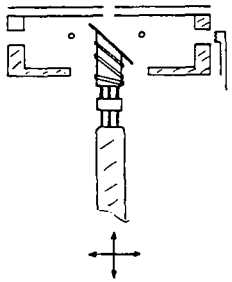


Fig. 2

movement of the probe tip in x, y and z directions. The source is presently operated at standard potentials. The new probe tip was constructed with the aim to bombard (sputter) the deposited sample with an electron beam to achieve ionization and vapourization (or vise versa).

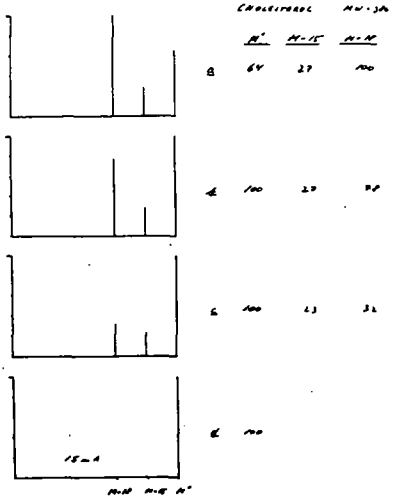


Fig. 3

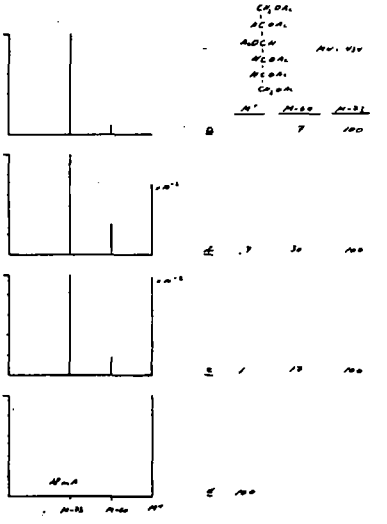


Fig. 4

Figures 3 and 4 illustrate results obtained at 70eV for cholesterol and glucitolhexaacetate (a=standard heatable probe, b=in beam technique, c=new angled trap plate, d=FD).

It is noteworthy that the M-18 fragment in cholesterol has significantly decreased in c as compared to b (32% vs. 78%). Glucitolhexaacetate does not provide a parent ion using the standard heatable probe (Fig. 4a). A very small M^+ (.7%) is observed with the in beam technique (b). The new angled plate provided only a slightly larger M^+ (1%).

Although improvements in these two examples are relatively small it is hoped that further investigations, i.e. development of a finely tunable electron gun, will make this a worthwhile effort. In addition, the source block opening originally occupied by the electron trap can now be utilized for the introduction of a Laser beam. Rotation of the new angled plate by 180° would permit analysis of samples under Laser beam inpact conditions, a development which is also of interest to this laborabory

Acknowledgement

The author would like to thank the Natural Sciences and Engineering Research Council of Canada (NSERC) for grants in aid of this development and Mr. M. Vagg for his valuable technical assistance.

References

1. G.K. Eigendorf and C.A. McDowell, Proceedings of the 24th Annual Conference on Mass Spectrometry and Allied Topics, May 1976, San Diego.
2. R.J. Beuhler, E. Flanigan, L.J. Greene, and L. Friedman, J. Amer. Chem. Soc., 96, 3990 (1974).
3. W.R. Anderson, W. Frick, and G.D. Daves, Jr., J. Amer. Chem. Soc., 100, 1974 (1978).
4. M. Ohashi, S. Yamada, H. Kudo, and N. Nakayama, Biomed. Mass Spectrom., 5, 578 (1978).
5. M. Ohashi, K. Tsujimoto, and A. Yasuda, Chem. Let., 439 (1976).
6. A. Dell, D.H. Williams, H.R. Morris, G.A. Smith, J. Feeney and G.C.K. Roberts, J. Amer. Chem. Soc., 97, 2497 (1975).
7. R. Sigmond and R.S. Sigmond, Proceedings AEI Users Meeting, 1969, Manchester, England.
8. D.F. Hunt, J. Shabanowitz, F.K. Botz, and D.A. Brent, Anal. Chem., 49, 1159 (1977).
9. G. Hansen and B. Munson, Anal. Chem., 50, 1130 (1978).
10. R.J. Cotter, Anal. Chem., 51, 317 (1979).
11. M.A. Baldwin and F.W. McLafferty, Org. Mass Spectrom., 7, 1353 (1973).

THE PERFORMANCE OF A SIMULTANEOUS ION DETECTOR USING SURFACE BARRIER DIODES

J. D. Stein and C. L. Peterson
General Electric Company, Vallecitos Nuclear Center, Pleasanton, CA 94566

At present two types of detectors are commonly used for high sensitivity mass spectrometry. The first of these is the photoplate which produces a latent image where a sufficient number of ions strike the emulsion. The second type detection system is based upon using a varying electric or magnetic field to sweep a mass resolved ion beam across an aperture. The detector, usually some form of electron multiplier, is located behind the slit and operates either in the pulsed or d.c. mode to detect ions with high sensitivity.

An ideal detector would be one that combines the high sensitivity of electrical detection together with the simultaniety of a photoplate. One possible system for achieving this result was first proposed by Dr. F. A. White of Rensselaer Polytechnic Institute (RPI) at the 1970 ASMS Conference.(1) This detector is made up of an ion to electron converter with the electrons produced then focused onto an array of individual surface barrier diode detectors. The reasons for the use of an ion to electron converter are, first, an individual ion striking the converter has a high probability of producing a number of electrons, second by properly biasing the converter the energy of particles striking the diode detectors can be significantly increased; also, diode detectors are much more sensitive to electrons than to ions of equivalent energy.

This type detector is used along the focal plane of a large energy and direction focusing mass spectrometer. This spectrometer consists of a 90° electric sector followed by a variably inhomogeneous field magnet. The magnet has an 80-inch linear focal plane covering the mass range of 20 to 305 amu. This focal plane is outside the magnet; however, there are some significant magnetic fringing fields in the detector region, particularly at the low mass end.

Positive ions leaving the magnet enter the detector from the left as shown in Figure 1. Ions initially pass through a set of grounded entrance slits and then are focused in the vertical direction by a pair of electrodes with asymmetrically applied voltages. The ions then strike a triangular aluminum ion-to-electron converter located at the magnet focal plane. Under typical operating conditions the converter is operated at a negative voltage of from 20 to 25 KV which means that the ions strike the converter with a total energy of 30 to 35 KeV. Each ion striking the converter produces from zero to twenty or more secondary electrons. These secondary electrons are accelerated through a slotted ground plane into individual p-n junction detectors located at each integral mass position producing a current pulse. The individual silicon surface barrier diodes have an active area of 0.10 x 0.50 inches and are located behind slots that are 0.09 x 0.45 inches. The charge collected by each diode is converted to a voltage pulse, shaped and amplified by a special high speed amplifier(2) whose output pulses are counted by an 18-bit CAMAC controlled discriminator and scaler. A set of these scalers is interfaced to a PDP-15 computer which controls the data collection.

We have developed a computer model of the detector geometry and the ion and electron focusing that occur within this geometry. Ion and electron trajectories are computed through the detector system in three dimensions and displayed on a video terminal two dimensions at a time. Initial ion trajectory input supplied to this program can be selected as either the final trajectories provided by the program that calculates ion trajectories through the mass spectrometer or as a set of parallel ion rays.

In the tantalum mass region resolution and abundance sensitivity were measured at 730 and 9,000:1 respectively by scanning the magnet. Resolution, however, varies as a function of location along the focal plane decreasing at lower masses. With a discriminator setting allowing 85% detection of the beam background was below 0.1 counts per second. With present electronics the amplifier output pulse width is 450 nanoseconds giving a useable count rate of over 200,000 counts per second or a dynamic range of approximately 10^6 to 1.

To date we have operated sets of 8 and 16 detectors simultaneously together with the data collection system.

While there are some problems in implementation, this type of detection system may offer substantial benefits for mass spectrometric applications. The advantage of having the high sensitivity of simultaneous detection of multiple masses as well as the ability to rapidly monitor complete spectra should prove useful in a number of applications.

References:

(1) F. A. White in The Proceedings of the 18th Annual Conference on Mass Spectrometry and Allied Topics, San Francisco, California, June 14th, 1970, Paper M6.

(2) G. Krycuk and J. D. Walling, IEEE Transactions on Nuclear Science, NS-20, 1, (1972), p. 228.

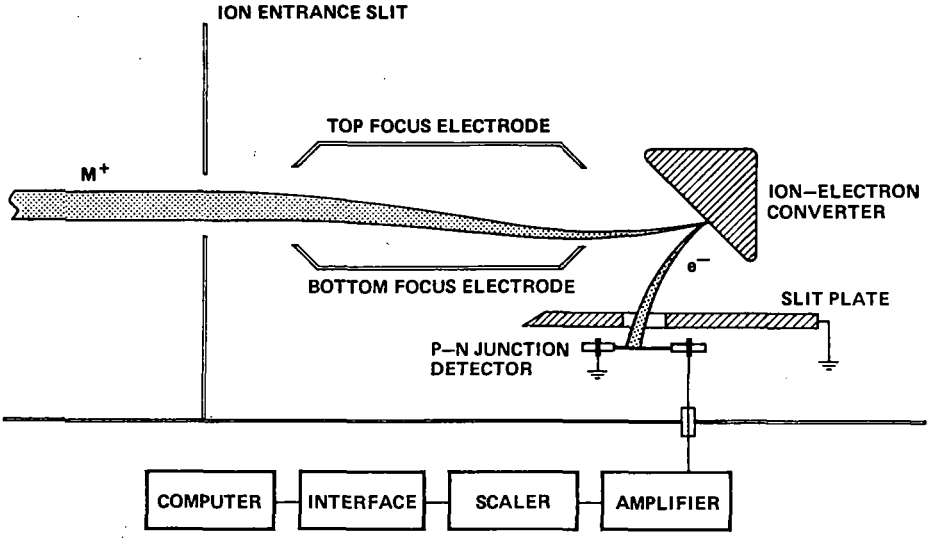


FIGURE 1

The NIH/EPA Chemical Ionization Mass Spectral Search System

D. P. Martinsen, Fein-Marquart Associates, Inc., Baltimore, MD 21212
S. R. Heller, Environmental Protection Agency, Washington, DC 20460
G. W. A. Milne, National Institutes of Health, Bethesda, MD 20205

The use of computers for searching large files of mass spectral data has been an aid in the interpretation of electron impact mass spectra for a number of years. Because of the growth in the use of chemical ionization mass spectrometry as an analytical tool, a new type of computerized search has been developed - a Chemical Ionization Mass Spectral search system (CIMS). CIMS is a subsystem of the NIH/EPA/MSDC Mass Spectral Search System (MSSS), one of the components of the NIH/EPA Chemical Information System(1). As such, CIMS is a complement to the MSSS and also allows access to the variety of data and information contained in the other CIS components.

The data base for this pilot version of the chemical ionization mass spectral search system contains 574 spectra. All compounds have been assigned a Registry Number by the Chemical Abstracts Service, which provides a unique identification of the compound as well as a link to the chemical literature. In addition to the mass spectral data, each spectrum contains information regarding the experimental conditions (source temperature and pressure, type of instrument, etc.) and the reactant gas. Since the CI spectrum of a compound may be obtained with several different reactant gases and also because the CI spectrum is very dependent upon operating conditions, all spectra for each compound are retained in the data base.

The search strategy in CIMS is very similar to that used in MSSS. The search options MW, PF, MF, and PEAK work in the same manner as their MSSS counterparts to retrieve the references with the given molecular weight, partial molecular formula, molecular formula, or peak/intensity range. The SET option may be used to set a search screen such that the search options will only consider spectra obtained with a specific reactant gas (or several reactant gases) or spectra of positive or negative ions. The results of each search are stored in temporary files which are erased at the end of the user's session. The files may be used with the Boolean operations MERGE, INTERSECT and NOT to create combination searches. They may also be used in the display options PLOT and SPEC to provide either a graphical or tabular presentation of the CI mass spectra in the data base.

Reference:

(1) S.R. Heller, G.W.A. Milne, and R.J. Feldmann, Science, 195, 253 (1977).

NEGATIVE ION CHEMICAL IONIZATION MASS SPECTROMETRY: REACTIONS OF F^- ION[≠]

C. C. Cheng, C. Chang, and T. O. Tiernan

The Brehm Laboratory and Department of Chemistry
Wright State University
Dayton, Ohio 45435

The recent development of mass spectrometry has seen a surge of interest in the use of negative ion chemical ionization as a complementary means for sample identification and quantification. Various chemical ionization reagent gases such as methylene chloride,[1] oxygen,[2,3] nitrous oxide,[4] and methyl nitrite,[5] have been reported and found to be successful for this application. In the present study NF_3 was explored in order to study its feasibility for acting as a new negative ion chemical ionization reagent gas. The possible reactions occurred in the mixtures of NF_3 with a broad range of organic compounds are also studied.

The basic instrument employed in this work is a Bendix Model 12-101 time-of-flight mass spectrometer equipped with a 100 cm drift tube. Except for some minor modifications to facilitate negative ion detection, the ion source is essentially the same one as described previously[6] which was designed primarily for positive ion-equilibrium studies. The ion source, which was constructed from a solid copper block, is actually an open cylinder (1.91 cm ID x 1 cm) with its open ends sealed with two identical cone-shaped plates serving as the electron entrance plate (EEP) and the ion exit plate (IEP). An orifice of 0.05 cm diameter is located at each cone apex of these plates. A DC voltage can be applied to either or both of these plates to form a favorable ion-focusing field to facilitate removal of ions from the source. However, experimental results have shown that an adequate number of ions can be extracted from the ion source even with both plates, as well as the ion source block, grounded. This arrangement was adopted for all the results reported here.

A coiled tungsten wire filament is located about 1 cm from the electron entrance plate. In order to collimate the electron beam, a beam focusing cylinder, which was constructed from 90% transparent rhenium mesh screen, is used to surround the filament. Use of the transparent wire mesh permits efficient pumping of neutral gas from the filament region, while focusing the electron beam into the entrance aperture of the electron entrance plate. This focusing cylinder and one end of the filament are maintained at a negative potential, ranging from -40 volts to -320 volts.

The filament is mounted in such a way that the electron beam path (largely) coincides with the ion axis. With this arrangement, all primary ions as well as secondary ions are formed along the electron beam path within the region directly adjacent to the ion exit aperture. This arrangement greatly enhances the population of ions (especially thermal ions) which can be extracted through the ion exit aperture and detected.

The negative ion CI spectrum of pure NF_3 at a total pressure of 100 μ shows that the m/e 19 (F^-) ion is the major peak, constituting more than 90% of the total ion current. Other ions present in trace quantities include m/e 39 (HF_2^-) and m/e 46. Presumably the ion HF_2^- is formed from the clustering reaction between the F^- ion and the HF molecules which may be present as an impurity in the NF_3 gas. However, it was found that, in many cases, the intensity of the HF_2 ion was enhanced when a small amount of hydrogen-containing compounds was separately added to the NF_3 in the ion source. In a mixture of 100 μ of NF_3 and 1 μ of n-butane, the $(HF)nF^-$ (n = 1-5) ion series actually became the major ions in the observed spectrum. The detailed mechanism for the formation of these ions is not clear. It is interesting to note that the ions $(HF)nF^-$(n = 1-3) have also been reported in the spectra of other fluorine-containing compounds.[7]

≠ A more detailed account of this work will be submitted for publication in the Journal of the American Chemical Society.

A major ion observed in many of the NICI spectra are the $(M-1)^-$ ions which are the base peaks for the carboxylic acids, ketones, aldehydes, and nitriles. These ions are formed by the abstraction of a proton from the sample, with the F^- ion acting as a base. The intensity of the $(M-1)^-$ ion produced should therefore reflect the acidity of the compound in question. In the case of carboxylic acids, the abstracted protons clearly come from the COOH groups, while for ketones, aldehydes, and nitriles, the active hydrogens, alpha to the hetero groups (i.e. c = O,C-CN), are believed to be abstracted by the F^- ion. Further clustering of the $(M-1)^-$ ion with a neutral M is also possible, as seen in the spectra of some acids and aldehydes.

All aliphatic alcohols examined in the present work exhibit significant $(M+F)^-$ ions. This peak is obviously formed by attachment of F^- to the molecule, probably through a strong hydrogen bond $(ROH---F)^-$. In addition, $(M+F)^-$ ions, in varying relative abundance, are also observed in the spectra of ketones and aldehydes. These probably are formed by way of tetrahedral intermediates resulting from the attack of the F^- ion at the carbonyl carbon, with the resulting negative charge residing on the oxygen group.[8] Other compounds including carboxylic acids, nitriles, and aliphatic hydrocarbons, also reveal small yet detectable amounts of $(M+F)^-$ ions in their spectra.

The third major reaction of the F^- ion, observed in the various NICI spectra, is nucleophilic displacement (S_N2) reaction, which has been studied extensively in solution chemistry. It can be expressed as

$$F^- + RX \rightarrow [F--R--X]^- \rightarrow FR + X^-$$

in which X = Cl, Br, CH_3COO, CN, C_2H_5O, and NO_2 for 1-chlorobutane, bromobenzene, esters, nitriles, ether, and nitrobenzene, respectively. This reaction is bimolecular and the rate can be closely correlated with the nucleophilicities of attacking ion (F^-) and the leaving group (X^-).[9]

In conclusion, NF_3 is shown to be a good reagent gas for negative ion chemical ionization applications. The system is simple since F^- is the only major ion formed under typical CI operating conditions. The F^- ion is reactive with nearly all the organic compounds examined in the present study, which encompass various functional groups. The reactions are highly specific, and closely correlated with the chemical nature of the samples. The resultant ions (especially $(M-1)^-$ and $(M+F)^-$ ions) are readily applicable for molecular identification. The proton affinity of the F^- ion is not as strong as that of the OH^- or CH_3O^- ion and it can be advantageously utilized to differentiate many chemically similar compounds (isomers, for example) simply based on their $(M-1)^-/(M+F)^-$ intensity ratios. On the other hand, F^- NICI mass spectrometry is considerably more sensitive than Cl^- NICI mass spectrometry for some organic compounds, such as aldehydes and ketones, although this is not well demonstrated in the present work.

References:

1. H. P. Tannenbaum, J. D. Roberts and R. C. Dougherty, Anal. Chem. 47, 49 (1975).
2. E. C. Horning, M. G. Horning, D. I. Carroll, I. Dzidic, and R. N. Stillwell, Anal. Chem. 45, 936 (1973).
3. D. F. Hunt, C. M. McEwen, T. M. Harvey, Anal, Chem. 47, 1730 (1975).
4. A. P. Bruins, A. J. Ferrer-Correia, A. G. Harrison, K. P. Jennings, and R. K. Mitchum, "Adv. in Mass Spectrometry," Vol. 7A, Ed. N. R. Daly, Published by Heyden, and Son, Ltd., London (1978), pp. 355-358.
5. D. F. Hunt, T. M. Harvey, and J. W. Russell, Anal. Chem. 48, 2098 (1976).
6. C. Chang and T. O. Tiernan, 22nd Annual Conference on Mass Spectrometry and Allied Topics, May 19-24, 1974, Philadelphia, PA, pp. 154-160.
7. R. Large and H. Knof, Org. Mass Spectrum. 11, 582 (1976).
8. O. I. Asubiojo, L. K. Blair and J. I. Brauman, J.A.C.S. 97, 6685 (1975).
9. W. N. Olmstead and J. I. Brauman, J.A.C.S. 99, 4219 (1977).

APPLICATION OF NEGATIVE CHEMICAL IONIZATION TO GC/MS AND LC/MS

David P. Beggs, and Attilio Melera,
Hewlett Packard Company, 1601 California Ave.
Palo Alto, CA 94304

Negative chemical ionization techniques have added new dimensions in sensitivity and selectivity to mass spectrometric analysis. The use of negative chemical ionization can be further enhanced by combining this technique with GC/MS or LC/MS.

Using methane as a carrier gas, one can analyze the GC effluent directly in the NCI mode. The methane carrier gas is used as the reagent gas in NCI and provides electron attachment ionization. The electron attachment mode is particularly useful for analyzing compounds which contain one or more fluorine atoms. If a compound does not contain fluorine, it is usually possible to derivatize it with a fluorinated derivitization reagent. These fluorinated compounds usually provide a strong molecular ion. They also provide enhanced sensitivity over other ionization techniques. Identification of these compounds at or below the 1 picogram level is possible.

Examples of this are octafluoronaphthalene (OFN), decafluorotriphenlyphosphine (DFTPP) and the TFA derivative of muramic acid. Each of these provide the molecular ion as the base peak. As an example of the sensitivity of this method, a full spectrum scan of octafluoronaphthalene could be detected a a concentration of one picogram injected on column. At these low levels, the chromatographic conditions become very important. Great care must be taken in the selection and conditioning of the column; and the design of the GC/MS interface. Any active sites in these areas will have the potential of adsorbing all of the sample (at low levels) and producing undesireable effects.

Compounds which do not contain fluorine (or fluorinated derivatives) do not generally respond nearly as well as those that do contain fluorine. Several general groups of compounds were tested using this NCI electron attachment technique to determine its sensitivity and selectivity for these compounds.

A mixture of aromatic hydrocarbons containing the following compounds was analyzed using both positive chemical ionization (PCI) and NCI.

TOLUENE
BROMOBENZENE
CHLOROTOLUENE
DIETHYLBENZENE
BIPHENYL
BIBENZYL
CHLORONAPHTHALENE

With the exception of chloronaphthalene, each of these compounds gave a more sensitive response to the PCI than the NCI. In the case of chloronaphthalene, the spectrum consisted almost entirely of the Cl^- ion. This is consistent with the previous observations this laboratory that mono, di and tri-chlorinated aromatic compounds give mostly Cl^- in the NCI mode. Thus, little qualitative information can be obtained for these compounds via NCI.

An amine mixture containing the following compounds was analyzed in the same manner.

2,6 DIMETHYL PIPERIDINE
ANILINE
CHLOROANILINE
N,N-DIETHYLANILINE
NITROANILINE
AZOBENZENE
DINITROANILINE

The nitroanilines gave a better response to NCI. Azobenzene gave an equivalent response in both PCI and NCI. The remaining compounds gave a better response in PCI. Similarly, a drug mixture containing caffeine, lidocaine, procaine, cocoaine, heroin and chlordiazepoxide showed that only the chlordiazepoxide gave a better response in NCI.

Thus, if the compounds tested, only those which contained fluorine, nitro or poly-chlorine substituents, reacted favorably to NCI via electron attachment.

The NCI technique was also applied to effluents from a liquid chromatograph. The LC/MS interface and techniques have been described earlier.[1] The acetonitrile/water LC solvent was introduced directly into the ion source. The hydroxyl ions are the dominant ionizing species under these conditions. Ionization is carried out via negative ion-molecule reactions. A mixture of indomethacine and benzanilide was analyzed via this technique.

Both positive ion and negative ion LC-MS-CI traces were obtained. The PCI trace gave a response for only benzanilide while the NCI trace gave a response for both compounds. This result points the way towards a new sophisticaed analytical technique, using the power of the liquid chromatograph combined with the selectivity and sensitivity of NCI.

1. Serum, J. W. and Melera, A., Paper. No. RP-8, 26th ASMS Meeting, St. Louis, May 28, 1978

FAMP4 MASS MEASUREMENT OF NEGATIVE ION CHEMICAL IONIZATION SPECTRY BY DOUBLE BEAM MASS SPECTROMETRY, M. L. Aspinal, D. R. Denne, K. R. Compson, and S. Evans, Kratos Ltd., Barton Dock Road, Urmston, Manchester M31 2LD, England.

The use of the MS30 double beam mass spectrometer for the quantitative determination of the insecticide malathion by negative ion chemical ionization has already been described [1]. The double beam technique has unique advantages because the sample is separated from the reference compound. Different methods of ionization may be used in the two sources providing a simple method of obtaining mass measurements of CI spectra. This principle has now been extended to mass measurements of negative ion chemical ionization spectra.

A number of examples from a variety of compounds of biological and environmental interest will be given.

1 M.L. Aspinal; J.R. Chapman; D. Done; D.R. Denne, ASMS no. 26 paper RF4 (1978)

INSTRUMENTAL ASPECTS OF POSITIVE AND NEGATIVE ION CHEMICAL IONIZATION MASS SPECTROMETRY

George C. Stafford, Finnigan Corporation, 845 W. Maude Avenue, Sunnyvale, California 94086

We have been involved in developing methodology to facilitate acquisition of positive and negative ion chemical ionization (CI) mass spectra on a quadrupole mass spectrometer. Operation of the ionizer under CI conditions provides a mixture of positive reagent ions and near thermal energy electrons. Accordingly, both positive and negative sample ions are produced simultaneously in large abundance in a CI ionizer.

With a quadrupole instrument, it is only necessary to reverse the ion accelerating potential and ionizer lens potentials to transmit ions of opposite charge to the mass analyzer. Detection of negative ions with an electron multiplier is the only inherant problem of a quadrupole instrument operated in the negative ion mode. Ions exiting a quadrupole mass filter will generally have less than 20eV of kinetic energy, and it is obvious that negative ions will not strike the cathode of a conventional positive ion electron multiplier.

The conventional approach for the detection of low energy negative ions produced on a quadrupole instrument is to electrically isolate the entire electron multiplier at a high positive potential so that the cathode is also at a sufficiently positive potential for efficient collection of the negative ions . This methodology has the disadvantage that the anode (signal) of the discrete or continuous dynode electron multiplier (CDEM) and the preamplifier must also be isolated at this high positive potential. Therefore, complex preamplifier circuitry is required to reference the signal to ground potential. A special high voltage floating coaxial signal feedthru is required on the vacuum envelope to prevent microphonic noise and charge leakage. The floated electron multiplier approach also has the problem that stray electrons in the vacuum system are efficiently detected, causing an increase in the baseline noise by approximately a factor of 30.

Our approach to negative ion detection is to convert the negative ions to secondary positive ions which are subsequently detected by a standard electron multiplier[1]. Negative to positive ion conversion can be accomplished by impacting the primary negative ions on a conversion dynode maintained at a high positive potential. This approach eliminates the problems associated with floating the anode of an electron multiplier at a high positive potential. A further advantage of this negative ion detector is that stray electrons in the vacuum system do not efficiently produce positive ions when they impact the conversion dynode and the baseline noise is significantly reduced.

Figures 1 and 2 exhibit the gain as a function of m/e for a positive ion CDEM and a conversion dynode negative ion detector on a quadrupole mass spectrometer. Positive ion detection shows a reduction in gain for the high mass ions. Presumably this is due to poor secondary electron emission from impact of high mass ions on the cathode of the CDEM[2]. On the other hand, negative ion detection using a conversion dynode shows an increase in gain for high mass ions. These data suggest that the larger organic negative ions are much more efficient in producing secondary positive ions upon impacting the conversion dynode.

If two conversion dynodes of opposite polarity are properly positioned at the cathode of a CDEM, both positive and negative ions can be simultaneously attracted and detected without any change in the operating voltages (Figure 3). Thus, selection of positive or negative ion spectra on a CI quadrupole instrument is accomplished by simply reversing the polarity of the lens and ion volume voltages.

The use of a positive ion conversion dynode improves the gain and signal to noise ratio for high mass positive ions. Figure 4 shows an improvement in the signal to noise ratio by a factor of 4 for m/e 866 when the positive ion conversion dynode voltage is increased from -1.8 KV to -3.0 KV. The higher voltage on the dynode improves the conversion of positive ions to secondary electrons thereby increasing the overall gain of positive ion detection.

REFERENCES

1. G. C. Stafford, J. R. Reeher, M. S. Story, 26th Annual Conference on Mass Spectrometry and Allied Topics, St. Louis, Mo., 1978, p. 459
2. R. J. Beuhler and L. Friedman, Int. J. Mass Spectrom. Ion Physics, 23, 81 (1977)

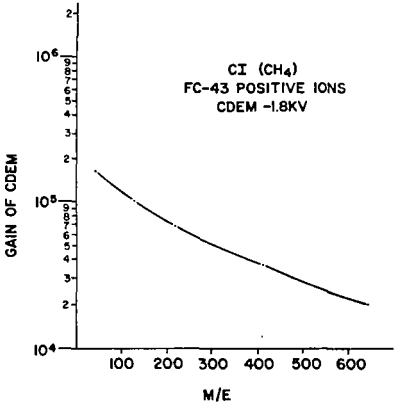


FIGURE 1 POSITIVE ION GAIN VERSUS m/e FOR A CDEM

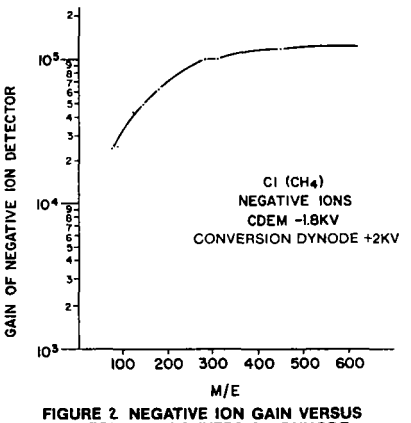


FIGURE 2 NEGATIVE ION GAIN VERSUS m/e FOR THE CONVERSION DYNODE NEGATIVE ION DETECTOR

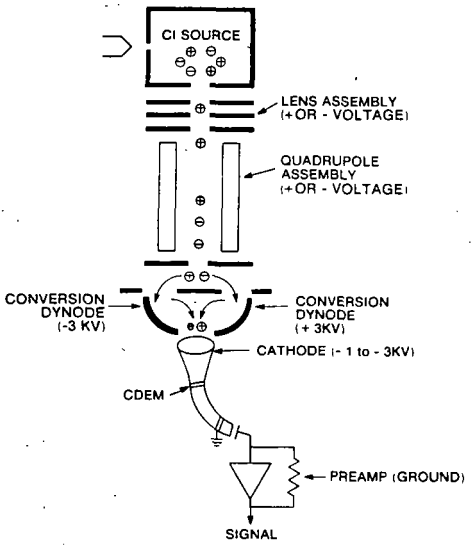


FIGURE 3 SIMULTANEOUS POSITIVE NEGATIVE ION DETECTOR

TRIS (PERFLUOROHEPTYL)—S—TRIAZINE
POSITIVE ION MODE M/E 866

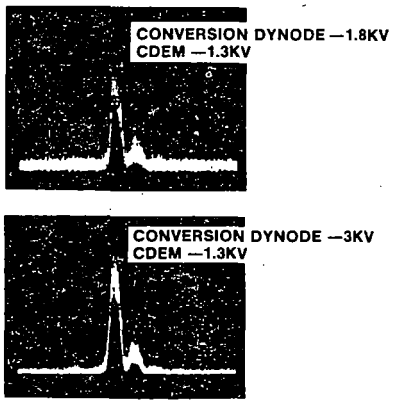


FIGURE 4 POSITIVE ION SIGNAL/NOISE IMPROVEMENT AT HIGH MASS DUE TO CONVERSION DYNODE VOLTAGE

NEGATIVE EC-CI ASSAYS FOR NOREPINEPHRINE METABOLITES. USE OF HEXAFLUOROACETONE TO PRODUCE CYCLIC DERIVATIVES.

P.A. BLOMBERY, S.P. MARKEY and I.J. KOPIN. Laboratory of Clinical Science, NIMH, Bethesda, MD. 20205

Assay of catecholamine metabolites in tissue, blood and urine provides information about neurotransmitter release and pathways of metabolism in different tissues. GC-MS methods of assay, in combination with stable isotope labelling of precursors and their metabolites extends the versatility of this technique by providing assessment of rates of metabolism and clearance. Currently available electron impact (EI) GC-MS methods of assay for norepinephrine (NE) metabolites (Table I) are limited in sensitivity, and with more sensitive assays, the above techniques could be extended to study NE metabolism in discrete parts of brain and other tissues, as well as allowing assay in very small volumes of plasma.

In this study, suitable derivatives of NE metabolites were investigated for assay by negative ion electron capture chemical ionization GC-MS (EC/CI GC-MS), as a result of the dramatic increase in sensitivity seen when this method was applied to assay of melatonin in human plasma. The utilization of EC/CI GC-MS depends upon the formation of stable electron-capturing derivatives which provide a high yield of compound-specific anions under CI conditions. When the pentafluoropropionyl derivatives of alcohol and amine NE metabolites, routinely used in EI GC-MS assay, were studied by EC/CI GC-MS, the only significant fragment was of the pentafluoropropionyl anion, and no compound-specific anion was available. Since the metabolites of interest have functional groups on adjacent carbons of the side chain, the formation of cyclic derivatives to increase stability was investigated. The

Table I

Derivatives of Norepinephrine Metabolites for GC-MS Assay

Metabolite	Derivative	Minimum Detectable Level*		Sensitivity Desired
		EI	Neg EC-CI	
MHPG	PFP & TFA	2 ng	–	Plasma – 5 ng/ml
	Ac-TFA	1 ng	–	
	HFA-TFA	5 ng	20 pg	Brain – 80 pg/mg
DHPG	PFP & TFA	5 ng	–	Plasma – 1 ng/ml
	Ac-PFP	1 ng	–	
	HFA-BuBor	5 ng	20 pg	Brain – 65 pg/mg
Normetanephrine	PFP	2 ng	–	Plasma – 500 pg/ml
	HFA-TFA	5 ng	50 pg	
Metanephrine	PFP	2 ng	–	Plasma – 300 pg/ml
	HFA-TFA	5 ng	100 pg	

*Minimum Detectable Level = Least amount detectable in biological sample or standard

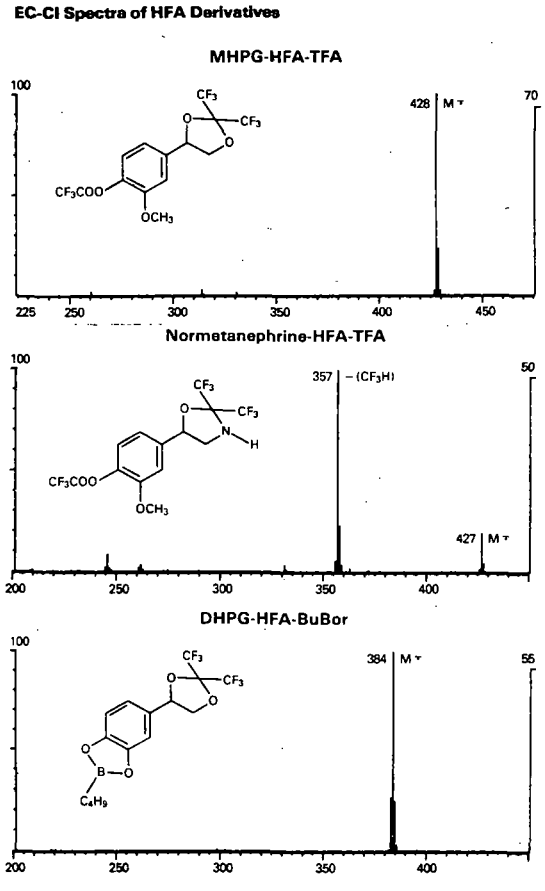
MHPG: 3-methoxy-4-hydroxyphenylethyleneglycol
DHPG: 3,4 dihydroxyphenylethyleneglycol
PFP: pentafluoropropionate
TFA: trifluoroacetate
Ac. acetate
HFA: hexafluoroacetone ketal
BuBor: butyl boronate

hexafluoroacetone (HFA) ketal was chosen for this purpose because of its potential electron-capturing properties in the EC/CI mode. Reaction of the different metabolites with HFA sesquihydrate for 30-60 minutes at 100°C produced a high yield of the cyclic derivatives, and phenolic hydroxyls were derivatized with trifluoroacetic anhydride (TFA).

EC-CI mass spectra for the HFA-TFA derivatives of MHPG and normetanephrine are in Fig. I. These spectra demonstrate high intensity compound-specific anions indicating stability of these derivatives under CI conditions. The HFA-TFA derivative of DHPG had a low yield of compound-specific anions, and butylboronic acid was used to derivatize the catechol groups, resulting in the mass spectrum in Fig. I.

In the selected ion monitoring (SIM) mode, as little as 5 pg of the above metabolites injected could readily be detected. When biological material was assayed, similar sensitivity was obtained, although there were some losses during the extraction and purification procedures. With MHPG-HFA-TFA, an interfering peak co-eluted with MHPG and this was avoided by using HFA gas as the derivatizing reagent.

Figure I



The use of HFA as a derivatizing reagent for NE metabolites produces cyclic ketals which are stable under EC/CI GC-MS conditions and provide a high yield of compound-specific anions. These derivatives in EC/CI mode increase the sensitivity of the GC-MS assay for the metabolites 50-100 fold over available EI methods, permitting studies of NE metabolism in much smaller amounts of biological material than is now possible.

Alternate Scan CI/EI GC-MS on the MS25

K T Taylor, J R Chapman, C J Wakefield and K R Compson
Kratos Limited, Barton Dock Road, Urmston, Manchester M31 2LD

The advent of high sensitivity, double-focusing mass spectrometers, such as the Kratos MS25, has enabled dual CI/EI sources to be designed that can switch between ionization modes without mechanical change to the ion source. A number of parameters have to be altered to effect the changeover, which include: the filament and ion repeller operating conditions and the flow of gas into the ion source. Since these changes can be made electronically they can be effected rapidly and simply.

The MS25 and its dual CI/EI source have been designed with these requirements in mind. Using the matrix facility on the instrument, optimized CI and EI operating conditions can be preset. Then to change between ionization modes it is necessary merely to select the appropriate matrix programme. A recent development of the MS25 has been to automate the programme change so that an ionization mode changeover occurs at the end of each scan. It has been found that the MS25 is capable of CI/EI switchover (and vice versa) between each scan in the magnet reset period. Typical operating conditions are 1s decade^{-1} scans with a 1s reset and under these operating conditions alternate scanning CI/EI (ACE) can be applied to capillary gc-ms.

In order to interpret the data produced by this technique additional software has been developed and incorporated in DS55. Among this software is included: a new version of XSCAN that can separate and process the CI or the EI scans only from an ACE run, and a new background subtraction algorithm that selects and subtracts background scans automatically as it separates the CI and EI spectra into dedicated files. Ionization mode headers have been included on all relevant reports and mass spectra are plotted with the major ions mass marked for improved clarity.

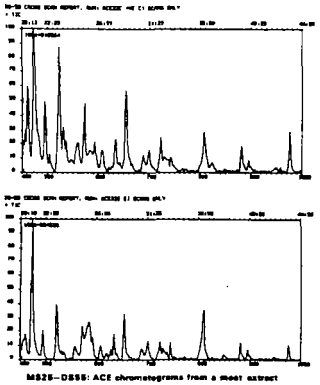
Some results from the application of the ACE technique in capillary column gc-ms analysis using ammonia as CI reagent gas are presented. Figure 1 shows a partial ACE chromatogram of a meat extract. Data have been background subtracted and separated into CI (ACE22C) and EI (ACE22E) versions. Total ion chromatograms for each mode are shown in this comparison plot, which indicates clearly that the relative intensities of the components are different in the two ionization modes. Although it is possible to run a sample twice to obtain CI and EI data on the components, trying to correlate the two chromatograms can present both obvious and subtle difficulties. In a complex mixture the ACE technique offers definite advantages with its unambiguous correlation between the scan sequences.

One such possible interpretative problem is illustrated by Figure 2. An apparent molecular ion in the EI spectrum at m/e 222 is clearly shown to be a water loss fragment by the strong quasi molecular ion at m/e 258 in the CI part of the 'ACE pair'. Only the complete correlation of ACE operation gives full confidence in such interpretations.

Figure 3 shows a similar ACE comparison plot of the CI and EI chromatograms from a further complex material analysis, that of thyme oil (Thymus Vulgaris sp.). Figures 4 and 5 show typical ACE spectra from this analysis (components A and B) which together with the EI library search results give positive identifications.

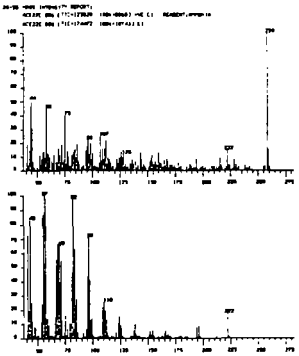
Conclusion

It can be seen that it is possible to operate the MS25 in the ACE mode with a switchover time between CI and EI of less than 1 second. With these fast cycle times the technique has been shown to produce reliable and valuable data from capillary gc-ms experiments.



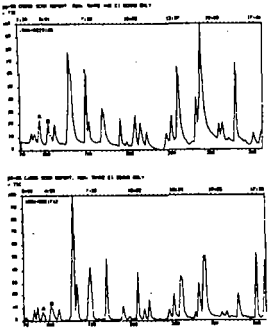
MS25—DS55: ACE chromatograms from a meat extract
1s decade⁻¹ scans

Figure
(1)



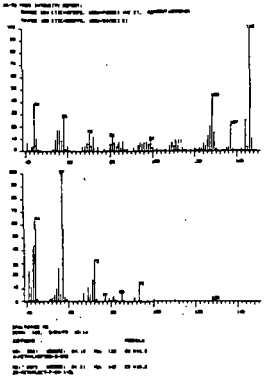
MS25—DS55: ACE spectra from a meat extract analysis
hexadecenol

Figure
(2)



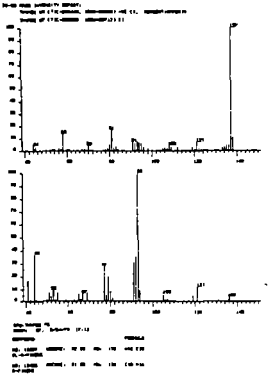
MS25 - DS55:
Comparison of ACE chromatograms from analysis
of Thyme oil. 1 sec. decade⁻¹. Ammonia ci.

Figure
(3)



MS25 DS55:
ACE spectra and ei library search of unresolved
doublet in Thyme oil 1 sec. decade⁻¹

Figure
(4)



MS25 - DS55:
ACE spectra and ei library search of minor
component from Thyme oil. 1 sec. decade⁻¹.

Figure
(5)

Ion-Molecule Reactions in N_2O/CH_4 Mixtures

C. W. Polley and G. G. Meisels
Department of Chemistry
University of Nebraska
Lincoln, Nebraska 68588

Ion-molecule reactions in N_2O/CH_4 mixtures were studied using a pulsed high-pressure source. Rate constants for the reactions of CH_5^+ with N_2O and N_2O^+ with CH_4 at 150°C were obtained from measured ion residence time distributions (1). For the reaction of CH_5^+ with N_2O, the measured rate constant is $1.11 \pm 0.07 \times 10^{-9}$ $cm^3 sec^{-1}$. This is in good agreement with the Langevin rate constant of 1.17×10^{-9} $cm^3 sec^{-1}$. The value of $1.03 \pm 0.12 \times 10^{-9}$ $cm^3 sec^{-1}$ determined for the reaction of N_2O^+ with CH_4 is also in good agreement with the Langevin value of 1.10×10^{-9} $cm^3 sec^{-1}$.

For these experiments, high energy ionizing elections (100 to 400 eV), and low source pressures (0.2 to 0.3 torr) were employed so that most of the ionizing events detected occurred close to the ion exit. These conditions were required to force the ions to have short residence times (5 to 50 μsec), and thus avoid complications due to the reverse reaction of the equilibrium

$$CH_5^+ + N_2O \rightleftharpoons N_2OH^+ + CH_4 \qquad (1)$$

Long ion residence times (200 to 400 μsec) can be obtained with low energy electrons (20 eV) and at high source pressures (1.0 torr), and ion equilibrium measurements can be performed. The CH_5^+/N_2OH^+ equilibrium just mentioned was studied from 25 to 230°C. Least squares analysis of the van't Hoff data yielded -6.6 ± 0.5 kcal/mole and -2.6 ± 1.0 eu for ΔH° and ΔS° respectively. The value for ΔH° is in good agreement with the value of -7.4 kcal/mole reported earlier by Bohme (2). From the measured entropy change, one obtains a value for S°_{298} (N_2OH^+) of 55.9 ± 1.0 eu, which is also in good agreement with the value of 54.9 ± 1.1 eu obtained from flowing afterglow studies of the N_2OH^+/HCO^+ equilibrium in CO/N_2O mixtures (3).

As part of these studies a 1:1 N_2O/CH_4 mixture was evaluated as a CI reagent gas. With a source pressure of 0.6 torr ($T_s \cong 150$°C; E/P = 10 V/cm-torr; Ion pathlength = 2.29 cm), the major reactant ions were N_2OH^+ (41%), $C_2H_5^+$ (18%), H_3O^+ (14%), NO^+ (12%) and $H(N_2O)_2^+$ (9%). With these experimental conditions the ions have average residence times on the order of 100 sec and undergo roughly 1400 collisions (assuming a collision rate of 1×10^{-11} $cm^3 sec^{-1}$).

The CI spectra of a variety of C_6H_{12} and C_6H_{14} isomers are presented in Table I. These spectra exhibit abundant ions in the molecular weight region as well as moderate fragmentation. Although the ion types are the same for all of the compounds listed, the ionic abundances exhibit enough variation to allow the compound types to be distinguished. The acyclic paraffins are characterized by abundant ions at m/e 85 and 71, $(M-H)^+$ and $(M-CH_3)^+$ respectively, and the absence of alkinyl ions. The cycloparaffins have abundant ions at m/e 83 and 85, $(M-H)^+$ and $(M+H)^+$. The olefins show the most extensive fragmentation patterns. The most abundant ions produced from these compounds are m/e 85 and 43, $(M+H)^+$ and $C_3H_7^+$. Olefins with internal double bonds have more abundant M^+ ions (m/e 84) than terminal olefins. The $(M+NO)^+$ ion at m/e 114, which is an abundant ion in the nitric oxide CI spectra of olefins (4), is a minor ion in these spectra. Nevertheless, its presence does help to distinguish C_6H_{12} from C_6H_{14} hydrocarbons.

N_2O/CH_4 CI spectra were also obtained for a number of simple alkylbenzenes (Benzene, Toluene, Ethylbenzene, and the isomeric Xylenes). The six compounds produce spectra containing primarily 4 peaks: $(M-H)^+$, $(M+H)^+$, $(M+NO)^+$, and $(M+43)^+$. The $(M+H)^+$ ion is the basepeak and accounts for about 80% of the sample ionization in all of the spectra. The $(M+NO)^+$ ion is about 10% of the total ionization. $(M+43)^+$ is a minor ion in all spectra, accounting for only about 1% of the sample ionization. Since $(M+C_2H_5)^+$ and $(M+C_3H_5)^+$ ions, which are normally present in the CH_4 CI spectra of aromatic compounds (5), were not observed, it is unlikely that this ion results from the addition of C_3H_7. We speculate that it is formed by addition of N_2OH^+ to the sample followed by loss of H_2.

The only trend with increasing molecular weight involves the $(M-H)^+$ ion. This ion is not observed in the spectrum of benzene, and rises to about 6% of the ionization in the spectra of the xylenes. This may be partly a result of the sensitivity of the abundance of

this ion to sample concentration as evidenced by the data for p-xylene given in Table II. We assume that sample concentrations, which were not measured directly, are related to the fraction of the total ion current assigned to sample ions. For the two highest p-xylene concentrations, $(M-H)^+$ ions were not observed. At sample ionizations below 12% the ion is observed and the spectra, although not very reproducible, become essentially invariant with sample concentration.

ACKNOWLEDGEMENT. We are grateful for the support of The Department of Energy under contract EY-76-S-02-2567.

Table I. CI Spectra of C_6 Hydrocarbons[a]

	% Sample Ionization[b]								
	43	55	57	69	71	83	84	85	114
1-Hexene	29.9	3.3	8.0	6.1	4.4	10.6	1.8	22.3	1.9
2-methyl-1-pentene	20.1	3.9	2.5	5.0	3.7	7.5	--	30.2	--
Cis-4-methyl-2-pentene	18.6	--	8.2	8.4	4.3	8.2	8.9	21.0	3.8
trans-4-methyl-2-pentene	12.0	1.2	6.6	6.7	4.5	9.4	7.8	17.4	1.9
cyclohexane	4.2	--	3.7	--	2.2	54.7	4.7	14.6	1.6
methylcyclopentene	11.3	--	5.9	10.0	1.9	32.6	3.3	22.5	1.8
n-Hexane	8.0	--	11.2	--	18.6	4.1	--	39.9	--
2-methylpentene	4.6	--	8.0	--	17.4	3.0	--	37.0	--
3-methylpentene	1.4	--	11.1	--	27.0	2.2	--	37.2	--

a. All spectra were recorded with an equimolar mixture of N_2O and CH_4 as reagent gas at a total pressure of 0.6 torr; Source Temperature: 150°C; E/P = 10 V/cm-torr; 100 eV ionizing electrons.
b. Includes only ions contributing ≥1% of total sample ionization.

Table II. Variation of Ion Intensities with p-Xylene Concentration

Sample Ion Current / Total Ion Current	% Sample Ionization		
	$(M-H)^+$	$(M+H)^+$	$(M+NO)^+$
0.18	--	84.7	11.1
0.13	--	85.9	9.8
0.11	8.2	75.8	8.9
0.05	8.9	78.1	7.4
0.03	6.2	81.7	6.3
0.02	6.1	73.3	9.8

References

1. G. Sroka, C. Chang, and G. G Meisels, J. Am. Chem. Soc., **95**, 1052 (1972).
2. D. K. Bohme, in "Interaction Between Ions and Molecule," Pierre Ausloos, Ed., Plenum, New York, 1975, p. 489.
3. R. S. Hensworth et al., J. Chem. Phys., **59**, 61 (1973).
4. D. F. Hunt and T. M. Harvey, Anal. Chem., **47**, 2136 (1975).
5. M. S. B. Munson and F. H. Field, J. Am. Chem. Soc., **89**, 1047 (1967).

Negative Chemical Ionization Analysis of Xenobiotic Chemicals from Milligram Quantities of Human Samples

Douglas W. Kuehl, ERL-D, U.S.E.P.A., Duluth, Mn. 55804
Michael J. Whitaker and Ralph C. Dougherty
Department of Chemistry, Florida State University
Tallahassee, Florida 32306

The isolation and identification of xenobiotic chemicals in human samples often requires techniques to perform part-per-billion level analysis on milligram quantities of tissue or milliliter quantities of fluids. Analytical procedures required to perform the isolation must be as simple as possible to avoid losses of compounds of interest and sample contamination, and the identification must be as sensitive and selective as possible to accurately characterize the residue chemicals.

The isolation methodologies we have used in this study have been either continuous extraction, steam distillation or gel permeation chromatography. We have generally attempted to avoid the use of adsorption chromatography because of low recoveries of polar xenobiotic molecules such as pentachlorophenol. The steam distillation apparatus we used is a modification of that described by Veith and Kiwus[1]. Most pesticide and industrial chemicals have vapor pressures over water that are greater than those of high molecular weight triglyceride lipids found in biofluids which makes this technique very simple but very efficient. The gel permeation chromatographic system is a scaled-down model of that described by Kuehl and Leonard[2], using a 10mm x 500mm column of BIO-RAD SX-8 beads and a 1:1 mixture of cyclohexane and methylene chloride flowing at 2.0ml/min..

The technique used for detection was negative chemical ionization mass spectrometry.[3] In general, commonly occuring xenobiotic chemicals have high electron affinities compared to biomolecules, and therefore will more readily capture thermal electrons or thermalized gas phase nucleophiles to form anionic complexes in the gas phase. This results in high selectivity for xenobiotic chemicals in a biological matrix[4,5]. The two reagent gases used were isobutane and methylenechloride, each with a trace of oxygen. The ionization processes observed were (a) resonance capture of an electron, (b) disassociative capture of an electron, (c) anion association, (d) deprotonation and (e) chloride/oxygen exchange. In addition, all samples are screened prior to mass spectrometry by electron capture gas chromatography.

The two sample types used in this study were human semen and human adipose tissue. 250mg aliquotes of adipose tissue were found to contain p,p'-DDE as the major contaminants and quantities of pentachlorophenol, hexachlorobenzene, chlordane, nonachlor, heptachlor epoxide, oxychlordane and tetra-octachlorobiphenyls. Sample sizes as low as 50mg gave good qualitative data on the major contaminants. Also 2.0ml samples of semen were found to contain p,p'-DDE, pentachlorophenol, tetra-octachlorobiphenyls and various occasionally occuring unidentified compounds. Both the aidpose tissue and semen spectra contained a seven-chloro ion cluster at m/z463; however, this contaminant has not yet been identified.

1. G.D. Veith and L.M. Kiwus, Bull. Envir. Contam. Tox., 17, 631 (1977).
2. D.W. Kuehl and E.N. Leonard, Anal. Chem., 50, 182 (1978).
3. R.C. Dougherty, J. Dalton and F.J. Biros, Org. Mass. Spec., 6, 1171 (1972).
4. R.C. Dougherty and K. Piotrowska, J.A.O.A.C., 59, 1023 (1976).
5. R.C. Dougherty and K. Piotrowska, Proc. Natl. Acad. Sci., 73, 1777 (1976).

FAMP10 EI TYPE MASS SPECTRA RECORDED UNDER CI CONDITIONS, DONALD F. HUNT AND P. JANE GALE, Department of Chemistry, University of Virginia Charlottesville, VA 22901

Earlier we reported that CI with Ar and N_2 as the reagent gases afford spectra which strongly resemble those obtained under EI conditions. In the CI mode sensitivity was found to be enhanced over that obtained in the EI mode. Problems encountered by other laboratories attempting to use this methodology have stimulated us to reexamine the advantages of the CI technique. We will discuss the effect of several instrumental parameters on the CI technique, the relative sensitivity of EI and CI modes of operation, and the use of EI libraries for the identification of spectra recorded under CI Ar and CI N_2 conditions. Several analytical applications of the CI (N_2) method will be presented.

ION-MOLECULE ISOTOPE EXCHANGE REACTION: METHODOLOGY FOR LOCATING PROTONS IN SAMPLE MOLECULES BY CIMS

Donald F. Hunt and Satinder K. Sethi

Department of Chemistry, University of Virginia, Charlottesville, Virginia 22901

FAMP 11

A scheme of hydrogen-deuterium isotope exchange ion-molecule reactions which can be utilized to locate and count protons in different chemical environments, using CIMS, was reported by us previously.[1] This paper represents an extension of that work.

Different reagent gas (ND_3, EtOD, D_2O) generate reagent cations and anions of varying acidities and basicities under CI conditions. These reagent ions on reaction with the sample molecule produce $(M+D)^+$ and $(M-1)^-$ ions under PICI and NICI conditions respectively. These sample ions on further collisions with the neutral reagent gas molecules undergo selective isotope exchange at certain sites on the sample. The results indicate that the extent of exchange increases with decreasing exothermicity of the proton transfer reaction between the reagent ion and the sample.

Two isomeric molecules, phenanthrene and anthracene can be distinguished under PICI conditions, using these ion-molecule reactions. Phenanthrene incorporates ten deuterium atoms on reaction with EtOD reagent gas, while anthracene exchanges only one hydrogen. Anthracene has a much higher proton affinity than phenanthrene. Use of more basic reagent gas, ND_3, leads to exchange of two hydrogens on anthracene (shown to be at sites 9 and 10) while phenanthrene affords only a molecular cation.

Thiophene exchanges all four hydrogens on reaction with CH_3OD reagent gas. The exchange of hydrogens at sites 2 and 5 is, however, faster than at other sites. 2,5-Dimethyl thiophene slowly exchanges its' two hydrogens. This result is in agreement with solution isotope exchange studies, which reported that deuterium incorporation at sites 2 and 5, of thiophene is 1000 times faster than at position 3 and 4 in the presence of solvent.[2]

Ferrocene and nickelocene both incorporate five deuteriums with ND_3. The reason why all the ten hydrogens of these metallocenes are not exchanged is not clear. Vinyl ferrocene, protonates on the side chain and undergoes exchange of two vinylic hydrogens.

Many of the samples studied under PICI conditions generate molecular cations. The general observations are (a) the relative intensity of $M^{+\cdot}$ ions increases with decreasing exothermicity of proton transfer from the reagent ion to the sample, and (b) more $M^{+\cdot}$ ions are formed at lower ion source temperatures. We believe that when the proton transfer rate is decreased (due to smaller exothermicity of the reaction or lower reaction temp.), the rate of molecular ion formation by interaction of sample with secondary electrons (~10eV) present in the ion source, competes effectively with sample ionization by proton transfer. The mechanism involving charge transfer from reagent ion RH_2^+ to the sample molecule to produce $M^{+\cdot}$ ion is not reasonable, since such reactions are generally very endothermic.

Reagent ion ND_2^- is the most basic species (PA = 403 Kcal/mole) we have generated under NICI conditions. With this reagent proton abstraction from benzene and polyaromatic hydrocarbons is exothermic, and the resulting $(M-1)^-$ ions undergo extensive incorporation of deuterium on subsequent reactions with neutral ND_3 molecules. Ferrocene and toluene chromium tricarbonyl also react with ND_2^-/ND_3 to incorporate nine and seven deuteriums respectively.

The exchange of benzylic hydrogens can be accomplished by using OD^- in D_2O as the reagent ion. The base strength of OD^- is such that it can abstract benzylic proton, but not aromatic protons. Accordingly selective exchange of benzylic protons is observed with this reagent.

Ketones, esters, diesters and aldehydes produce $(M-1)^-$ ions on reaction with OD^-, but fail to undergo isotope exchange. Incorporation of deuterium into these anions is observed if a weaker base, $C_2H_5O^-$ in C_2H_5OD, is employed. The $(M-1)^-$ ions undergo exchange at all positions alpha to the carbonyl group in these molecules. Hydrogen atoms on a methylene group adjacent to two carbonyl groups, as in diethyl malonate, are too acidic to suffer exchange with C_2H_5OD, but do undergo the isotope exchange reaction when the weaker base $CF_3CD_2O^-$ is employed as reagent.

For a sample molecule R'H and reagent ion ROD_2^+ the following sequence of events leads to hydrogen-deuterium exchange.

$$R'H + ROD_2^+ \rightarrow \underset{(1)}{[HR'\text{--}\overset{D}{\overset{|}{D}}OR]^+} \rightarrow \underset{(11a)}{[R'HD\text{--}\overset{D}{\overset{|}{O}}R]^+} \rightleftarrows \underset{(11b)}{[R'D\text{--}\overset{D}{\overset{|}{H}}OR]^+} \rightleftarrows \underset{(11c)}{[R'D_2\text{--}\overset{H}{\overset{|}{O}}R]^+} \rightarrow R'D_2 + ROH$$

We believe that when the exothermicity of the reaction acceeds approx. 20 - 25 Kcal/mole, the energy of the intermediate state (1) is greater than that of the products. During the reverse reaction this state is no longer accessible to the system and exchange is, therefore, not observed.

In conclusion, ion-molecule reactions reported here can be utilized to locate and count hydrogen atoms in different chemical environments. The information obtained is similar to that available from NMR chemical shift and integration measurements. Only nanogram samples are required for the mass spectrometry experiments.

REFERENCES:

1. D.F. Hunt, S.K. Sethi and J. Shabanowitz, paper presented at the 26th Annual Conference of Mass Spectrometry and Allied Topics, St. Louis, 1978. Paper #MF-1.

2. A.F. Thomas, "Deuterium Labeling in Organic Chemistry", Appleton-Century-Crofts Educational Division/Meredith Corporation, New York, 1971, Page 149.

A FLOWING DISCHARGE ION SOURCE FOR POSITIVE AND NEGATIVE ION MASS SPECTROMETRY OF COMPOUNDS IN AIR

S. E. Buttrill, Jr., SRI International, Menlo Park, CA 94025

Irreversible adsorption of trace substances on walls is one of the more difficult problems encountered in developing detectors for sub part-per-billion (ppb) levels of organics in air. Because of the inherent sensitivity of mass spectrometry, a direct sampling ion source is an attractive candidate for the detection of ppt levels of a variety of materials in air. A flowing discharge ion source recently developed at SRI runs with ambient air as the reagent and carrier gas without the need of a separator.

The flowing discharge mass spectrometer can operate over a range of source conditions that includes those normally associated with both atmospheric pressure ionization (API) and chemical ionization (CI) mass spectrometers. This instrument is based on the novel ion source shown in Figure 1. Gas samples enter the mass spectrometer at a pressure of up to one atmosphere and flow through a variable conductance restrictor (not shown) into the ion source. The sample passes through a heating coil and past a thermocouple (not shown), and then passes through a discharge region where it is ionized. The discharge electrode structure may be operated to inject either positive ions or electrons into the gas flow. The ionized gas then flows down to the end of the inner stainless-steel tube where the ion extraction orifice allows a controlled fraction of the gas and ions from the center of the flow to enter the high vacuum region. The excess gas molecules are pumped away while the ions (either positive or negative) are focused and steered into the mass spectrometer.

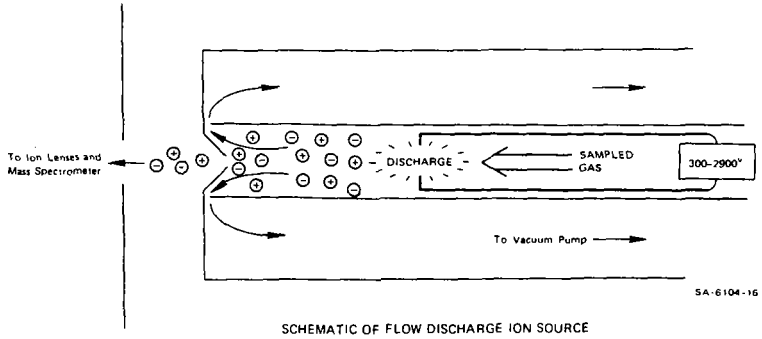
The flow-discharge ion source has several unique features that facilitate the optimization of sensitivity for any particular class of compounds:

- The pressure in the ion source may be varied from less than one torr up to one atmosphere.
- The position of the discharge region and the nature of the discharge may be changed.
- The velocity of the gas flow through the source may be varied by over two orders of magnitude by throttling the vacuum pump used to exhaust sample gas from the outer tube.

In addition, the source may be operated at any temperature from ambient up to 350°C, and various reagent gases may be added to the sample stream.

The principal advantage of this source in the development of new detection methods for specific compounds lies in the ability to independently vary and control all factors that may affect the formation of ions from the sample and their efficient extraction from the source. These factors are the reagent gas pressure, reagent gas temperature, reagent and sample ion residence time, and positive or negative ion mode. No other mass spectrometer source design allows this degree of flexibility and control over conditions. It thus gives us a unique ability to develop new methods of detecting and identifying trace amounts of substances in air.

Figure 1



SCHEMATIC OF FLOW DISCHARGE ION SOURCE

The sensitivity data presented here were obtained by injecting a known volume of headspace vapor of the test substance into 1-liter exponential dilution flask. The air flow through the flask was approximately 1 liter/min and a portion of this was sampled at one atmosphere into the flowing discharge ion source.

The negative ion air spectrum is fairly complex. The major ions are O^-, OH^-, O_2^-, NO_2^-, m/z 48 ($H_2O{\cdot}NO^-$), CO_3^-, HCO_3^-, and m/z 62 (NO_3^-). The air spectrum and the relative sensitivity both vary with source pressure and the position of the discharge. Figure 2 shows the sensitivity and dynamic range of detection for perfluorodimethylcyclohexane (PDCH). The molecular negative ion, $C_8F_{16}^-$ (m/z 400), was monitored while operating the source at 6 torr and 140°C. The detection limit is about 200 ppt.

The major ions in the positive ion spectrum of air are H_3O^+, O_2^+, NO_2^+, $H_5O_2^+$, and $H_7O_3^+$. The last two ions are simply hydrogen bonded clusters of one or two water molecules with H_3O^+. It is the reactions of these ions with trace organics that produce the characteristic MH^+ and $MH^+ \cdot H_2O$ ions. Figures 3 and 4 show data on the detection of methylsalicylate and nitrobenzene in air with the flow-discharge source operating at 20 torr and 190°C. Detection limits in both cases are about 100 ppt.

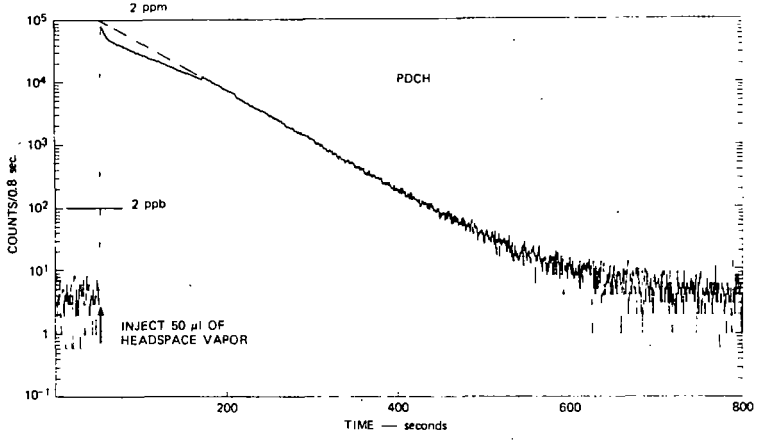


Figure 2

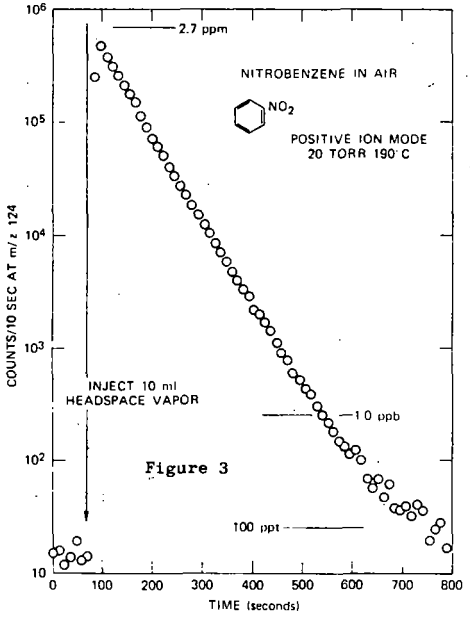


Figure 3

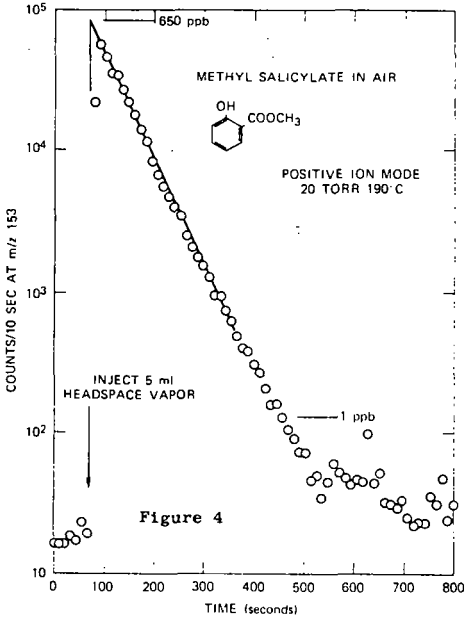


Figure 4

FAMP13 CHARACTERIZATION OF FOSSIL FUELS BY CHEMICAL IONIZATION MASS SPECTROMETRY,
L. WAYNE SIECK, National Bureau of Standards, Washington, D.C.,20234

Both positive and negative ion CI techniques have been utilized from screening of petroleum products. The positive CI measurements involved selective photoionization of various solvents for the fuel samples in order to produce specific reagent ions. Negative ion CI spectra of aromatic derivatives were obtained by OH^- reactions, where OH^- was generated by the reactions of O^- from N_2O with aliphatic fuel solvents. Both methods provided two minute turn-around times between samples and batch introduction, with no prior separation or fractionation. Extensions of the techniques to partial quantitation are also discussed.

CHARACTERIZATION OF UNDERIVATIZED PHENOLS IN HUMAN URINE BY HPLC/MS. 121
L. H. Wright and T. R. Edgerton, Health Effects Research Laboratory, U.S. EPA, MD-69, Research Triangle Park, NC 27711

Studies were undertaken to characterize free phenols in human urine extracts by combined high pressure liquid chromatography/mass spectrometry (HPLC/MS). Free phenols were utilized because appropriate derivatizing reagents are either toxic or there is a lack of quantifiable conversion to a chromatographical species. Gas chromatography/mass spectrometry was not feasible due to the unavailability of packed columns which allow for chromatography of underivatized phenols without excessive column bleed.

Chlorinated phenols in human urine were isolated by sorption on a small column of macroreticular resin, XAD-4. Sample preparation consisted of acid hydrolysis of 4 ml of human urine to free possible phenol conjugates and elution of chlorinated phenols and other acidic compounds from the resin column with organic solvent. Neutral and basic compounds were removed from the sample by elution of the resin column with acid and water. Low ng per ml (ppb) levels of 2,6- 2,4 or 2,5- and 3,5- dichlorophenol, 2,4,6 and 2,4,5-trichlorophenol, 2,3,4,6-tetrachlorophenol and pentachlorophenol were identified as the free phenols using gas chromatography employing electron-capture (EC) detection and support-bonded Diethylene Glycol Succinate (DEGS) as the chromatographic moiety.

Individual samples were concentrated to 200 µl for LCMS studies. Pooled samples of 16 to 48 ml of urine equivalent were concentrated to 100-200 µl for LCMS.

LC/MS studies were performed on a Finnigan 3200 MS equipped with a data system and LC/MS interface. MS data was collected in both scanning and select ion monitoring (SIM) modes. Methane chemical ionization was used exclusively.

Three different liquid chromatography systems were tested; A) 2-propanol/hexane on a Nucleosil-NO_2 column, B) acetonitrile/acetic acid/water on a DuPont-CN column, and C) water/2-propanol/hexane on a Whatman PAC column. Although all three systems were capable of separating most of the polychlorophenols, only C was suitable for LC/MS. System C could be adjusted so that the total LC effluent was delivered to the interface with sufficiently short peak elution times (i.e. 30-60 sec.).

Experimentation with the reverse phase system did, however, lead to the discovery that the addition of a second, water miscible solvent to the interface belt prior to the aqueous phase LC effluent could eliminate the tendency of such effluents to form droplets on the transport belt. Preliminary investigations indicated that ca. 0.3 ml/min of 2-propanol was sufficient to control up to 0.2 ml/min of aqueous phase.

Liquid chromatography using system C was optimized using a mixture of di-, tri-, tetra- and penta-chlorophenols. A concave gradient was employed starting with 1%(1% H_2O/2-PrOH)/n-hexane and finishing with 25%(1% H_2O/2-PrOH)/n-hexane.[2] Dual detection was employed with a 210 nm UV detector in series with the MS.

In tests on the standards mixture, it was possible to obtain scanning spectra (125-325 amu) on 150 ng quantities for all but pentachlorophenol (PCP). In SIM operation 10-30 ng of all but PCP were detectable at a signal/noise ratio $\geq$ 3:1.

Differences between the standards mixture and actual samples were enormous. Large variability in chlorophenol content and in interferences was encountered in both the pooled and individual urine samples. In general, individual samples proved easier to work with due to the reduced concentration of interfering compounds. The urine extracts contain the acid fraction so the number of components was high. Furthermore, the elution range of the non-chlorophenol components extended over the chlorophenol range. It soon became obvious that due to the large number of co-eluting compounds, scanning MS would be of little use for the quantification or identification of chlorophenols. Furthermore, in order to be reasonably sure of identification, several ions in the relevant isotope clusters would have to be monitored.

In individual samples, using SIM 2,5-, 3,5- and 2,3- and/or 2,4-dichlorophenols, 2,3,6- and/or 3,4,5-trichlorophenol, and pentachlorophenol were confirmed by LC retention times and by proper isotope ratios for the two major ions in the appropriate quasi-molecular ion clusters. The 2,3,6-trichlorophenol was ruled out on the basis of electron capture GC results.

QUANTITATIVE MASS SPECTROMETRY OF MIREX AND ITS DEGRADATION PRODUCTS BY MEANS OF HIGH PERFORMANCE WCOT COLUMN GAS CHROMATOGRAPHY/MASS SPECTROMETRY

F.I. Onuska, M.E. Comba, J.A. Coburn
National Water Research Institute, Burlington, Ontario

Presently, only mirex may be separated from the PCB matrix on certain conventionally packed columns. Glass capillary WCOT columns can provide additional separation for some of the related degradation products but in order to obtain an overall quantitative measurement, chemical pretreatment of the sample is required. In addition, the reliability of mirex levels in Lake Ontario fish were questioned by Laseter, et al. (1) on the basis of quantitative mass spectrometry results. It is the purpose of this paper to provide a rapid, quantitative procedure for the determination of mirex and the major environmental degradation products and to establish whether quantitative mass spectrometry does yield significantly different values.

Ten trout samples from eastern Lake Ontario, five lamprey samples from central Lake Ontario and two Niagara River sediment samples were analyzed. The tissues were homogenized and fractionated on Florisil and quantitative measurements were conducted using four separate techniques. Each fraction was analyzed on three different packed columns employing electron capture detection. Our experience with the analysis of mirex in tissue samples has indicated that only 3 percent OV-101 on Chromosorb W is capable of resolving mirex from the PCB matrix to permit accurate quantitation.

Three separate measurements were made using a Varian Mat 311-A mass spectrometer, interfaced to a 20m x 0.25mm, OV-101 glass capillary column via "open split" coupling. Single ion measurements were taken on the m/z 272 and m/z 546 signals of mirex at respective resolutions of 1800 and 1400 (10% valley) while a third set of data was acquired utilizing the computer controlled accelerating voltage alternation scan (MID) on the preselected ions at m/z's 203, 237, 238 and 272 at a resolution of $m/\Delta m = 800$.

Quantitative results for each determination are presented in Table I, with the total experimental error expressed as relative standard deviation (RSD). All the calibration curves were linear within the tested ranges.

TABLE I

MIREX LEVELS (pg/μL)

Sample No.		EC	m/z 546	m/z 272	MID
Trout	1	316	330	305	301
	2	138	83	110	136
	3	168	117	160	138
	4	106	75	93	94
	5	79	121	122	105
	6	103	93	118	97
	7	112	121	122	115
	8	77	101	93	113
	9	86	90	91	102
	9d	124	90	103	103
	10	111	78	77	78
Mean		129	118	127	126
RSD (%)		±12.8	±16.7	±10.5	±16.5
Sensitivity (pg Injected) S/N = 3)		10	100	0.5	50
Lamprey	11	18.7	23.2	19.5	17.4
	12	17.5	14.3	17.7	13.0
	13	11.3	10.0	10.0	10.2
	14	21.9	25.0	20.0	18.1
	15	16.4	13.7	15.5	13.4
Sediment	16	280[b]	273[b]	258[b]	262[b]
	17	782	692	837	710

d = duplicate

Linear regressions analyses performed on the trout results are listed in Table 2 and showed a high degree of correlation between all methods. The standard deviations of the respective methods were tested by paired analysis and were within the same population at a C.I. of 95 percent.

TABLE 2

REGRESSION ANALYSIS (TROUT SAMPLES)

Parameter	EC vs m/z 546	EC vs m/z 272	EC vs MID
m	0.961	0.882	0.851
b	-5.915	12.854	15.766
δn	64.291	64.291	64.291
δy	68.834	60.209	57.897
ρ	0.90	0.94	0.95

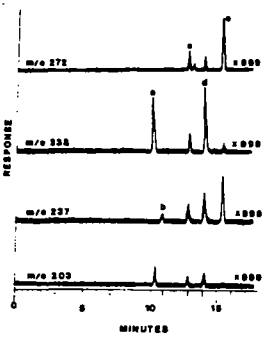
The single ion monitoring procedure at m/z 272 is a rapid procedure for screening and quantitating mirex. The two most prominent monohydro degradation products can also be detected in the same run.

Figure 1 shows the trace obtained for a mixed standard of 1 pg of each injected. The detection limits were essentially the same as the sensitivity values for all the samples examined, with no interferences encountered for any of the mass spectrometry procedures.

Figures 2 and 3 are traces of a standard and sample run obtained by the MID procedure. Only one small peak (2.8%) in the vicinity of mirex gives a signal at m/z 272 although it is well separated by capillary column.

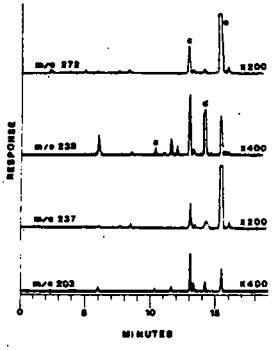
The ion ratios were constant for all the samples examined indicating no major coeluting species with similar fragmentation. The mean values obtained for the degradation products in the trout samples expressed as a percentage of mirex (8-monohydro, 28.7; 10-monohydro, 10.1; and 2,8-dihydro, 1.6%) were in good agreement with data reported earlier.

FIGURE 1



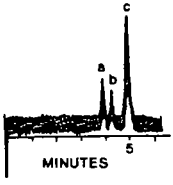
MID-trace of standard (100 pg injected)
(a) 2,8-dihydro-, (b) 10,10-dihydro-, (c) 8-monohydro-, (d) hydromirex

FIGURE 2



MID-trace Trout Sample

FIGURE 3



Single Ion Monitoring, m/z 272 of Mirex Standard (1 pg injected)
(a) 8-hydro-, (b) 10-hydromirex (c) mirex

References:
(1) Laseter, J.L., I.R. DeLeon, P.C. Remele, Anal. Chem., 50 (8): 1169 (1978).
(2) Hallett, D.J., Norstrom, R.J., Onuska, F.I., Comba, M.E. and Sampson, R.S. J. Agric. Food Chem., Vol. 24, No. 6 (1976).
(3) Millard, B.J., Quantitative Mass Spectrometry, Heyden, London, pp. 161-165 (1978).

A DIRECT SAMPLING FIELD IONIZATION MASS SPECTROMETER SYSTEM FOR DETECTING ORGANIC COMPOUNDS IN AIR AT SUB-PPB LEVELS

S. E. Buttrill, Jr. and G. A. St.John
SRI International, Menlo Park, CA 94025

The two most important requirements for a useful atmospheric monitor are sensitivity and specificity. Nonfragmenting field ionization mass spectrometry is well suited for this application because it forms only molecular ions from most substances. The concentration of all of the signals for a particular compound into a single ion peak maximizes sensitivity, and at the same time minimizes the possibility of interferences from ions formed from different compounds.

The development of SRI's highly efficient volcano-style source has made it possible to construct a sensitive laboratory prototype of a practical air monitor based on field ionization mass spectrometry. The interface between the ambient atmosphere and the ion source is shown schematically in Figure 1. Air is pulled into the interface through a heated 0.4 mm ID glass tube. The jet of air thus formed impinges on a 0.16 cm^2 dimethyl silicon rubber membrane. Typical flow rates are 100 to 500 atm cm^3/min, and the pressure at the membrane is approximately 200 torr. The use of a minimum surface area, all glass, heated air inlet is essential to avoid losses of polar compounds present in ppb concentrations. Typical operating temperatures are as follows: inlet 120°C, membrane 150°C, ion source 160°C.

The mass spectrometer used is a 60° magnetic sector instrument built at SRI. When the mass spectrometer is repetitively scanned over a range of 300 mass units and the spectra integrated using a multichannel analyzer, most compounds can be detected at concentrations below 10 ppb after about 5 minutes. When the magnetic sector is tuned to monitor molecular ions of a single compound, detection limits are usually less than 1 ppb. Figure 2 shows the dynamic range and sensitivity of detection of octafluoronaphthalene (OFN). 10 cm^3 of air saturated with OFN were injected into a 1-liter exponential dilution flask. The 1-liter/min of air flowing through the flask bathed the air inlet to the mass spectrometer. The detection limit of about 200 ppt would have been about 5-10 times lower in the absence of the large background signal at the molecular ion mass of m/z = 272.

Further examples of the linearity of response, dynamic range, and sensitivity of the FIMS air monitor are shown in Figures 3 and 4. The use of field ionization mass spectrometry for air monitoring appears to be extremely promising. The development of a versatile and portable instrument is both practical and desirable.

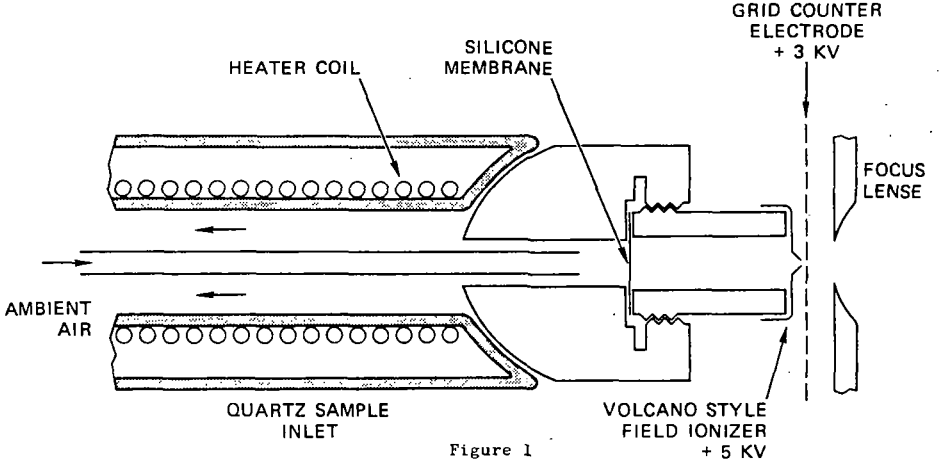
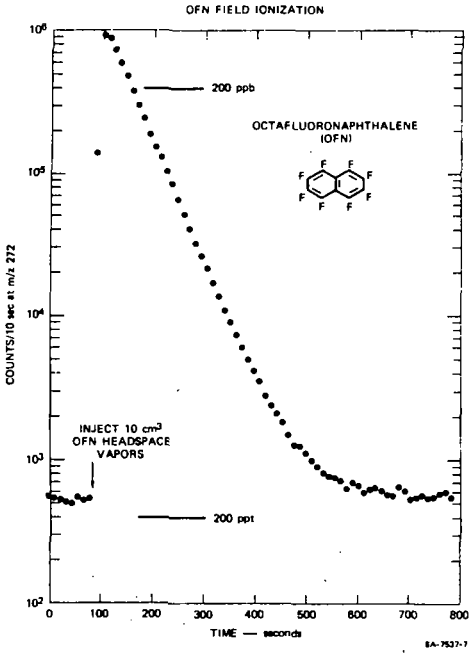


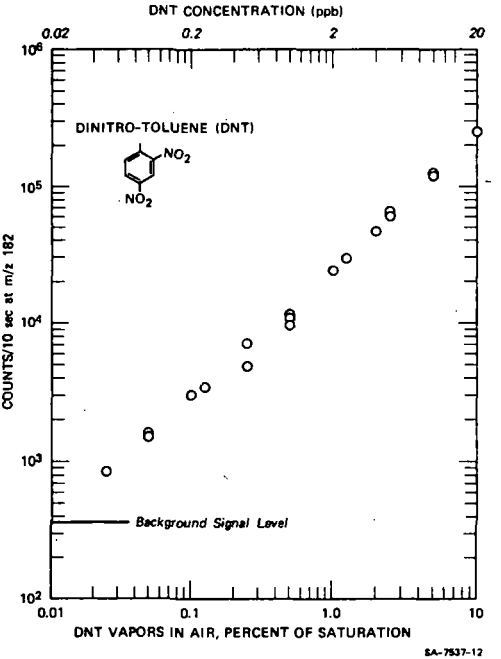
Figure 1

Figure 2



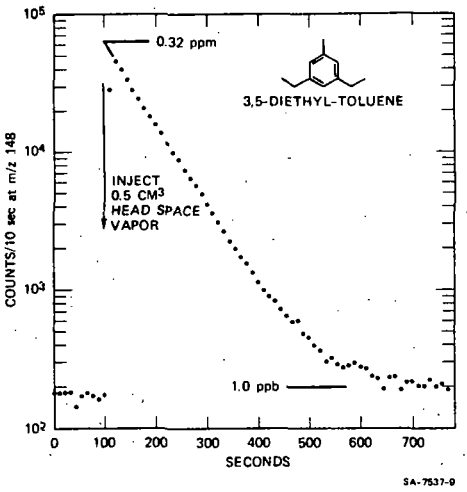
FIELD IONIZATION OF OFN IN AIR USING THE EXPONENTIAL DILUTION FLASK

Figure 3

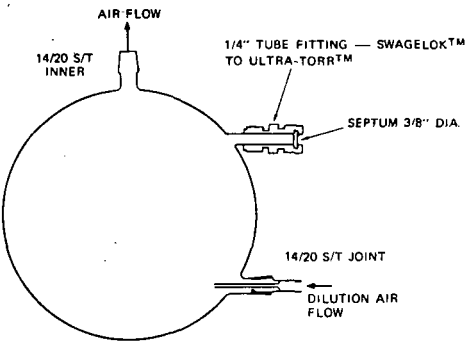


SENSITIVITY OF VOLCANO SOURCE FIMS FOR DETECTION OF DNT IN AIR AT 23°C

Figure 4



DETECTION OF 3,5 DIETHYL-TOLUENE VAPOR IN AIR USING FIMS



EXPONENTIAL DILUTION FLASK

FAMP19 METASTABLE SPECTRA OF POLY-NUCLEAR AROMATIC HYDROCARBONS BY LINKED SCAN TECHNIQUES. B. SHUSHAN and R.K. BOYD, Dept. of Chem., Univ. of Guelph, Guelph, Ont., CANADA, N1G 2W1.

The B/E linked scan technique permits acquisition of daughter-ion spectra, of metastable parent ions of preselected mass, using double-focussing instruments of conventional geometry. Analytical applications of the technique to identification of isomeric polycyclic aromatic hydrocarbons has been described (1); this work has been extended to all the major fragmentation reactions observed, and correlation of observed trends with known properties of the isomers has been attempted. A basic limitation of the B/E technique, involving interferences from broad metastable peaks arising from parent ions of mass close to that preselected, was explored via correlations between B/E and B^2/E linked scans of appropriate transitions.

(1) B. Shushan, S.H. Safe and R.K. Boyd, Anal. Chem. (in press).

APPLICATION OF MASS SPECTROMETRY TO THE QUANTIFICATION OF HYDROCARBONS IN AVIAN TISSUE

M. L. Gay and A. A. Belisle

Patuxent Wildlife Research Center, Fish and Wildlife Service,
U. S. Department of the Interior, Laurel, Maryland 20811

Residues of hydrocarbons were determined in liver, kidney, fat, and brain tissue of mallard ducks which had been fed a hydrocarbon mixture. Following extraction and cleanup on a Florisil column, aromatic and aliphatic fractions were separated on a Silicar column and quantified by GC/MS using mass fragmentography. Perdeuterohexadecane was used as an internal standard for the aliphatic fraction; perdeuterodimethylnaphthalene was the aromatic internal standard. Relative responses of compounds and standards were reproducible (% standard deviation 3-6%). Highest residues were found in the fat; lowest were in the brain. Branched aliphatic compounds accumulated in higher concentrations than did straight-chain aliphatic compounds. Computer programs to facilitate the quantification of several compounds by mass fragmentography using a single internal standard were written in Finnigan BASIC. One program calculates relative sensitivities, based upon the parameters of each peak and the amounts injected. The other calculates the amount of each compound present based upon peak parameters, the amount of internal standard injected, and the relative sensitivities calculated previously.

GC/MS Investigations of the Heterocyclic Aromatic Hydrocarbons Found in the Environment

R. C. Burk, R. S. Thomas and R. C. Lao, Chemistry Division, Air Pollution Control Directorate, Environment Canada, Ottawa, Canada K1A 1C8

Increasing concern about the concentration of organic constituents in the polluted environment has focussed attention on polycyclic organic matter (POM) because of the carcinogenic potential of many of these compounds. A steadily increasing incidence of lung cancer in industrial and polluted areas has provoked a deep concern about the control of encironmental pollution and the identification of the sources which emit these hazardous contaminants.

In terms of compositional complexity, POM mixtures cover the spectrum of simple to extremely complex. The increasing utilization of fossil fuels, the pyrolysis by-products rich in POM, will raise many environmental and public health questions.

Environmental samples may contain POM from many sources. Important constituents of POM are various polycyclic aromatic hydrocarbons (PAH) which include known carcinogenic members such as benzo(a)pyrene and dibenzanthracene. Out of some 600-odd carcinogens now given in the NIOSH toxic substance listings, scant attention is given to the GC/MS investigations of a few selected compounds. Heterocyclic aromatic hydrocarbons (HAH) are found throughout the biospheres as trace pollutants. Although they are often present only in trace concentrations, these compounds are the source of much concern to environmentalists and medical authorities because of their carcinogenic potential. Since there are practically no existing analytical procedures for HAH, sensitive and accurate GC/MS investigations must be considered a necessary part of the overall scheme for POM analysis.

The instrumentation used in this study was a combination of the Finnigan 9500 GC - modified 1015 D MS and 6000 Data system. The instrument was properly calibrated using FC-43 and DFTPP as reported in our earlier work. The additional GC used was a Perkin-Elmer 900. Its operation parameters were:

Detector:	FID
Detector Temperature:	300^0C
Liquid sample volume:	0.5 to 4 µl
Sample injection Temp:	325^0C
Carrier gas:	N_2 60 ml/min
Column Temperature:	295^0C
Columns:	12 ft long, 0.125 in in diameter, stainless steel packed with 6% Dexsil 300 on 80/100 mesh Chromosorb WCHP

Several aromatic nitrogen and oxygen compounds available from our stock were investigated. Their GC retention times (RT) and response factors (RF) were as follows:

Compound	RT(min)	RF(area/µg)
2,3 fluoroquinone	4.11	0.05
Pyrenequinone	7.06	3.75
5,6 benzoquinoline	21.50	5.41
2,3,5,6 and 3,4,5,6 dibenzocarbazole	41.4	unavailable
Pentacene quinone	62.41	unavailable

For comparison, the RT of six PAH standards are listed below:

Compound	RT (min)
Fluoranthene	3.26
Pyrene	3.76
Chrysene	7.66
BKF	15.42
BaP	18.87
Perylene	19.83

The mass spectra of heterocyclic quinones and quinolines all have the same fragmentation patterns as those of other aromatics. The molecular ion is the most intense peak in the spectrum, followed by the base peak of $(M-CO)^+$ for quinones and $(M-CN)^+$ or $(M-HCN)^+$ for quinolines and carbazoles. The $(M-H)^+$ ion almost certainly results from the loss of a hydrogen atom situated beta to the nitrogen or oxygen atoms. In dibenzcarbazoles, the loss of HCN and H_2CN furnish the only abundant ions and their intensities are low. This fact reflects the great stability of the aromatic rings.

Further work is in progress to attain better GC resolution using glass capillary columns and different GC operation conditions. Environmental samples will be investigated for possible contaminants of this class of compounds.

OPERATOR INTERACTIVE SEMIAUTOMATIC PROCESSING OF PRIORITY POLLUTANTS AND OTHER SPECIFIC COMPOUND ANALYSIS. Arthur D. Little, Inc. Cambridge, MA 02140. Carl E. Rechsteiner, James L. Stauffer, James E. Oberholtzer and Philip L. Levins.

To increase the efficiency of a Finnigan 4010 GC/MS/DS to allow rapid, repetitive analysis of samples for selected sets of compounds, a data link has been developed to allow transfer of complete data files to an off-line general purpose minicomputer (Data General ECLIPSE S/200) and procedures have been developed for semiautomatic processing of the transferred data. The procedures developed include provision for archival storage of GC-MS data files on 9-track magnetic tape in a variety of formats.

The data link physically consists of two IO boards, one for each minicomputer and two optically isolated line driver-receiver modules. Once initiated, the data transfer software, included in the 6110 - Rev I operating system, reads sequentially 3200 words of data (1/2 track of 6110 disk for one of the read-write heads). Each block of data is presented to a 16 bit parallel IO module in the 6110 data system and is transmitted through optically isolated lines to an IO module in the general purpose Data General minicomputer. Following transmission of each block of data, a checksum word is transmitted for error detection. The transmitted checksum word is compared to a checksum computed by the Data General system for the received block of data. If the checksums are different, the block of data will be retransmitted up to four times until the checksums agree. When the checksums agree, the transmitted block of data is written into a temporary disk file in the Data General minicomputer. The transfer of blocks of data between systems continues until all of the tracks used for data storage have been transmitted. The transfer procedure is performed in duplicate to allow further error checking.

The pair of temporary disk files are compared bitwise and then decoded to produce a GC-MS data file. The GC-MS data file is automatically searched for a selected set of compounds, for example priority pollutants, PAHs, PCBs, etc., using four ions diagnostic for each of the selected compounds and windows of 200 scans centered about its expected retention time. The results of each search are stored for evaluation at the operator's convenience.

During the evaluation, the data is presented to the operator as a set of four ion chromatograms for each compound selected with a marker indicating the expected retention time relative to an internal standard. The operator has several options for interaction with the display. To confirm the presence of a compound indicated by the diagnostic ions, the operator can examine mass spectra with or without background subtraction as well as listing the spectrum or plotting it. The operator interacts with the display to obtain retention times, peak areas and intensities by setting baselines, integrating peaks with setable regions, measuring retention times or intensities, and by 2-dimensional expansion of the chromatograms.

Following operator interaction, quantitative reports are automatically printed for the selected set of compounds. This report includes concentrations if a file of calibration data is available. The GC-MS data files are stored on 9-track magnetic tape primarily in two formats. The first format writes the data onto the magnetic tape in blocks of 6400 words, the other format writes the data in an easily readable "EPA" format. Of these the former is more convervative in terms of disk space, tape space and time required for transfers between tape and disk.

An important feature of the system is shown in Table 1. Using the conventional 6110 data system to obtain GC-MS data and process it prior to a subsequent run, the time between samples for a set of 47 compounds is 155 min; for the presented system the time is only 75 min. Since one is not tied to the data acquiring computer for processing, a second sample may be running while the first is processing, which emulates current practice with foreground-background GC-MS data systems.

TABLE 1

COMPARISON OF GC-MS RUN AND PROCESSING

TIME FOR 6110 ALONE AND 6110 + OFF-LINE PROCESSING

	6110 Only	Off-Line Processing
Data Acquisition	65 min.	65 min.
Saving GC-MS File on 4 Track Tape	10 min.	
Data Transfer from 6110 to Data General ECLIPSE		5 min.(X2 transfers)
GC-MS Processing for 47 Compounds in Complex Sample	70 min.	(35 min.)[1]
Minimum Time Between Acquisitions By 6110	155 min.	75 min.

[1] Processing independent of 6110 data acquisition.

ELECTRON TRANSFER IONIZATION MASS SPECTROMETRY FOR HYDRAZINE

P. BREISACHER, P. MAHADEVAN, AND W. A. HICKS,
AEROPHYSICS LABORATORY, THE IVAN A. GETTING LABORATORIES,
THE AEROSPACE CORPORATION, P. O. BOX 92957, LOS ANGELES, CA 90009

ABSTRACT

THE TECHNIQUE OF ELECTRON TRANSFER IONIZATION MASS SPECTROMETRY (ETIMS) IS ADOPTED TO MONITOR HYDRAZINE (N_2H_4) IN AIR. IN THIS "SOFT" COLLISION APPROACH, A LOW ENERGY PROJECTILE ION, POSITIVE OR NEGATIVE, COLLIDES UNDER CONTROLLED CONDITIONS WITH A SAMPLE SPECIES UNDER INVESTIGATION. SIMPLE MASS SPECTRA, CONSISTING IN MOST CASES OF THE PARENT MOLECULAR ION ONLY HAVE BEEN OBTAINED[1] FOR MOLECULES SUCH AS CH_4, C_2H_6, NO, NO_2, CO_2, AND SO_2 USING THE ETI TECHNIQUE. PROTONS FROM MOIST AIR AT A KINETIC ENERGY OF ABOUT 50 eV, COLLIDE WITH N_2H_4 AT A PRESSURE OF ABOUT 5×10^{-5} TORR IN A COLLISION CHAMBER RESULTING IN THE PRODUCTION OF A MASS PEAK AT 31 AMU ($N_2H_3^+$) ACCOMPANIED BY A WEAKER PARENT ION PEAK AT MASS 32 AMU. AT LOWER TARGET GAS PRESSURES, UNEQUIVOCAL IDENTIFICATION OF HYDRAZINE IS POSSIBLE SINCE THE MASS SPECTRUM REDUCES TO A SINGLE ION PEAK AT 31 AMU, INDEPENDENT OF POSSIBLE INTERFERENCE FROM ATMOSPHERIC OXYGEN.

INTRODUCTION

ALTERNATIVE METHODS FOR THE ANALYSIS OF N_2H_4 IN AIR ARE NEEDED BECAUSE OF THE INCREASED USE OF THIS COMPOUND IN SPACE AND MILITARY APPLICATIONS. PRESENT METHODS SUCH AS CHEMILUMINESCENCE, COLORIMETRY, AND ELECTROCHEMISTRY DO NOT MEET ALL THE REQUIREMENTS OF ACCURACY AND PORTABILITY. ETI MASS SPECTROMETRY IS PROPOSED AS A POTENTIAL SIMPLER METHOD FOR EVENTUAL FIELD MONITORING.

APPARATUS

THE ETI APPARATUS CONFIGURATION IS DESCRIBED IN DETAIL ELSEWHERE.[1] THE BEAM-GAS TYPE ARRANGEMENT CONSISTS OF: A CONVENTIONAL ION SOURCE FROM WHICH POSITIVE OR NEGATIVE IONS CAN BE EXTRACTED, A MAGNETIC SECTOR MASS SELECTOR, FOR THE PROJECTILE IONS, A SMALL COLLISION CHAMBER, AWAY FROM THE QUADRUPOLE ION SOURCE THROUGH WHICH THE PRIMARY ION BEAM PASSES, AND A QUADRUPOLE MASS SPECTROMETER WITH ITS AXIS NORMAL TO THE PROJECTILE ION BEAM AXIS. BACKGROUND PRESSURE IS 5×10^{-7} TORR. THE OPERATING PRESSURE OF SAMPLE GAS IN THE COLLISION CHAMBER RANGES FROM 5×10^{-5} TO 1×10^{-4} TORR.

RESULTS AND DISCUSSION

THE PRINCIPAL MASS PEAK OF HYDRAZINE IS EITHER 32 OR 31 DEPENDING UPON THE SOURCE OF H^+ PROJECTILE IONS. WHEN H_2 IS USED AS THE H^+ SOURCE (FIG. 1A) AMU 32 IS THE MAIN PEAK. WHEN H_2O IN AIR IS USED, AMU 31 IS THE PRINCIPAL PEAK (FIG. 1B). IT IS ALSO NOTED THAT THE SECONDARY SMALLER PEAKS (AMU 31 IN FIG. 1A, AMU 32 IN FIG. 1B) DECREASE DISPROPORTIONATELY FASTER THAN THE RESPECTIVE PRINCIPAL PEAKS AS THE PRESSURE IS LOWERED. SOURCE PRESSURE CAN, THEREFORE, BE CONTROLLED IN AN ANALYZER TO YIELD ONLY SINGLE ION PEAK SPECTRA.

A POSSIBLE EXPLANATION FOR THE DIFFERENCES NOTED USING H_2 AND H_2O AS H^+ SOURCES IS THE FORM OF N_2H_4 THAT IS ACTUALLY SUBJECTED TO CHARGE TRANSFER. USING H_2 AS THE SOURCE OF H^+, THE REACTIONS OCCURRING ARE

$$N_2H_4 + H^+ \longrightarrow N_2H_4^+ + H \qquad (1)$$

$$N_2H_4 + N_2H_4^+ \longrightarrow N_2H_3^+ + H + N_2H_4 \qquad (2)$$

AS THE PRESSURE IS LOWERED, REACTION (2) BECOMES MINIMAL. USING H_2O AS THE H^+ SOURCE, THE N_2H_4 CAN FORM THE MONOHYDRATE AT THE BACKGROUND H_2O CONCENTRATIONS. THE PRINCIPAL MOLECULE ACTUALLY SUBJECTED TO CHARGE TRANSFER IS, THEREFORE, N_2H_4, H_2O

$$2N_2H_4 \cdot H_2O + H^+ \longrightarrow 2N_2H_3^+ + H + 2H_2O + H_2 \qquad (3)$$

THE CONVENTIONAL ELECTRON IMPACT (EI) SPECTRUM OF N_2H_4 IS SHOWN IN FIG. 1C.

INTERFERENCES AND SENSITIVITY

SINCE THE IDENTIFYING ETI MASS PEAK IS 31 AMU FOR HYDRAZINE, ATMOSPHERIC OXYGEN DOES NOT INTERFERE WITH THIS MONITORING TECHNIQUE. THIS IS OBVIOUSLY A UNIQUE AND VALUABLE FEATURE OF THIS APPROACH. LOWER LIMIT OF DETECTABILITY SO FAR ACHIEVED IS ABOUT 0.1%. EFFORTS ARE BEING MADE TO MEASURE LOWER CONCENTRATIONS.

ALKYLATED DERIVATIVES

PRELIMINARY MEASUREMENTS WITH MMH AND UDMH INDICATE THAT PARENT ION IDENTIFICATION IS POSSIBLE USING ETIMS TECHNIQUE.

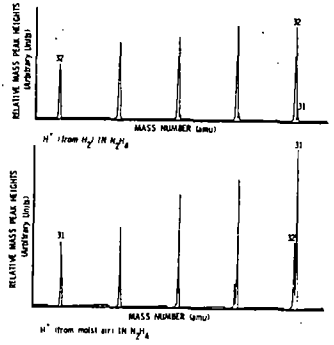
---

(1) AEROSPACE REPORT ATR-78(8112)-1, P. MAHADEVAN AND P. BREISACHER.

FIG. 1A

Electron Transfer Ionization (ETI) Positive Ion Mass Spectrum of Hydrazine

FIG. 1B



Electron Impact (EI) Positive Ion Mass Spectrum of Hydrazine

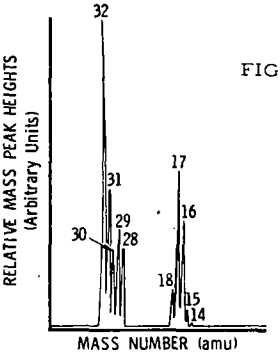


FIG. 1C

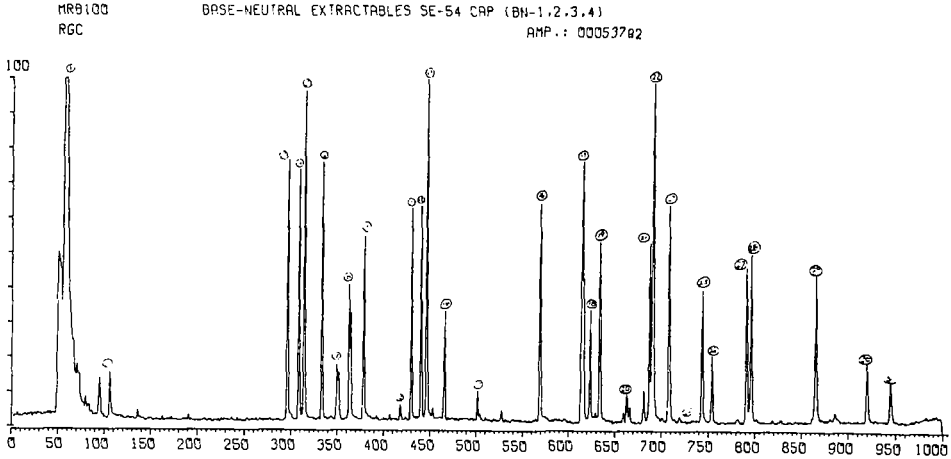
FAMP 1 : ANALYSIS OF BASE-NEUTRAL EXTRACTABLES BY GLASS CAPILLARY GAS CHROMATOGRAPHY-MASS SPECTROMETRY ON THE FINNIGAN 3200 MASS SPECTROMETER, R.D. Minard, Dept. of Chemistry, Pennsylvania State University, University Park, Pa. 16801, and M.R. Bogdan, Supelco Inc., Supelco Park, Bellefonte, Pa. 16823.

Since the advent of high efficiency capillary column gas chromatography many difficult to resolve compounds can now be routinely separated. The increased inertness of capillary columns makes them attractive for many applications now being conducted with packed columns. Such a specific application is the analysis of the EPA priority pollutant base-neutral extractables. For this analysis a 30-meter SE-54 WCOT capillary column was coupled to a Finnigan 3200 mass spectrometer operating in the electron-impact mode. A simple, direct link of the capillary column to the mass spectrometer was performed and is herein described.

A Conflat^{R} flange was modified to accept a section of .3mm ID x 1/16" OD glass lined stainless steel tubing. This section then replaced the jet separator assembly with the GLT being bent directly into the GC oven. A 30m SE-54 WCOT capillary column (manufactured by J & W) was installed and coupled to the GLT by two overlapping sleeves of heat-shrink Teflon. This connection was then bathed in helium. A low flow of He permeated through and around the Teflon coupling and allowed a linear velocity of He through the column to be 24cm/sec with the head pressure at 20 psig. The source of the mass spectrometer maintained a pressure of 2 x 10^{-5} torr using the original 2" diffusion pump. This arrangement allowed the chromatograph to be operated up to 260^{o} but is not recommended to maintain this temperature for an extended period.

FILE : MRB100
TITLE : BASE-NEUTRAL EXTRACTABLES SE-54 CAP (BN-1,2,3,4)
MASS RANGE : 50-300, 301-450
INTEG. TIME : 2,4
SECONDS PER SCAN : 0
THRESHOLD : 0
MAX RUN TIME : 999
Preamp : 10^{-8}
Mult : 2000

4µℓ of 50ng/µℓ base-neutral extractable standard
100:1 split injection
4 min. @ 50^{o}C, programmed to 260^{o} @ 8^{o}/min. and hold



Peak #	Identity
1	Solvent
2	Unknown
3	bis-(2-Chloroethyl)ether
4	1,3-Dichlorobenzene
5	1,4-Dichlorobenzene
6	1,2-Dichlorobenzene
7	bis-(2-Chloroisopropyl)ether
8	Hexachlorocyclopentadiene & N-nitroso-di-n-propylamine
9	Nitrobenzene
10	Unknown
11	bis-(2-Chloroethoxy)methane
12	1,2,4-Trichlorobenzene
13	Naphthalene
14	Hexachlorobutadiene
15	Unknown
16	2-Chloronaphthalene
17	Acenaphthylene & Dimethylphthalate
18	2,6-Dinitrotoluene
19	Acenaphthene
20	2,4-Dinitrotoluene
21	Fluorene
22	Diethylphthalate
23	1,2-Diphenyl hydrazine
24	Background
25	4-Bromophenyl phenyl ether
26	Hexachlorobenzene
27	Phenanthracene
28	Anthracene
29	Di-n-butylphthalate
30	Fluoranthene
31	Pyrene

AUTHOR INDEX

AUTHOR	PAPER NO.
ABBOTT, F. S.	TAMOB10
ABE, H.	RAMOA2
ABERHART, D. J.	RAMOA11
ABERTH, W.	MPMP10
	WAMP10
ABRAMSON, F.P.	TAMOB4
ADAMS, N.G.	WAMOC6
ADDISON, J. B.	RAMOC1
AGARWAL, S. C.	RPMP9
AHMED,A. E.	RPMOC3
ALBRITTON, D. L.	MPMOC7
ALEMAN, R.	MPMOB5
ALLEN, W. N.	MPMOC11
ALLISON, J.	TPMOC5
ALLMAN, D. D. J.	MPMP11
AMPULSKI, R. S.	TAMOB3
AMSTER, I. J.	RAMOA11
ANDERS, M. W.	TPMP2
ANDERSON, S.	RPMOA6
ANDRZEJEWSKI, D.	MAMOC13
ANICICH, V. G.	WAMP8
	TPMOC12
APPLER, M.	MAMP7
ARGHESTANI, S. M.	TAMP23
ARIJS, E.	WAMP19
ARMITAGE, M. A.	WAMP3
ARNETT, E. M.	TPMOA4
ARPINO, P. J.	TPMP20
ASHE, T. R.	MAMOA8
ASPINAL, M. L.	FAMP4
	FAMOC6
ATWATER, B. L.	TAMP5
AUE, D. H.	WAMOC14
	MPMOB11
AUERBACH, A.	FAMOA5
AULD, J. W.	TPMP9
AUSLOOS, P.	RAMP18
AUSTIN, E. R.	MPMOC5
AXENROD, T.	TAMP17
AZARNOFF, D. L.	MAMP10
BACZYNSKYJ, L.	RPMP5
BAER, T.	RPMOA4
	WAMOC1
	TPMOC13
BAILLIE, T. A.	WAMOA1
BALDWIN, M.	RPMP23
BALDWIN, M. A.	WAMP2
BALLARD, J.	FAMOB5
BAR-SHAI, R.	MPMOB13
BARDEN, L. K.	TAMP1
BARIL, M.	TPMOB8
BARTMESS, J. E.	RAMP22
BASTIAN, F. O.	TAMOB7
BATSON, C. H.	MAMOB13
BATY, J. D.	TPMP22
BAYKUT, G.	MPMOC2
	MPMOC1
BEDFORD, R. G.	RPMOB7
BEGGS, D. P.	FAMP3
BEIMER, R. G.	MAMOA10
BELASCO, I. J.	RPMOC4
BELISLE, A.	FAMP20
BENNETT, M. L.	MAMOA7
BENOIT, F. M.	RAMP4

AUTHOR	PAPER NO.
BENSON, P. A.	MAMOA2
BENZ, R. C.	MAMP17
BERKOWITZ, J.	MPMP1
	MAMP15
	MAMOB13
BERRY, E. K.	RPMP20
BERTRAM, L. K.	TPMOB11
BETOWSKI, L. D.	WAMOC14
	MPMOB11
BEYNON, J. H.	MPMOB1
BIELLING, K.	RAMP1
BIEMANN, K.	MAMOB8
	MAMOB6
BIER, D. M.	WAMOA14
BIERBAUM, V. M.	WAMOC7
BIERRE, K. J.	TAMP5
BILL, J. C.	RPMOB1
	TAMP18
BINIAKEWITZ, R.	TAMOC10
BJORSETH, A.	MPMOA4
BLAIS, J. C.	WAMOA15
BLAISDELL, B. E.	MPMP10
BLAKLEY, C. R.	RPMOC10
	RAMP11
BLAZER, T. A.	TPMP18
	TAMOA8
	TAMOA3
BLOMBERY, P. A.	FAMP6
BLUETT, L.	MAMP11
BLUM, W.	MPMOA6
BOBENRIETH, M. J.	RAMP12
BOCKHOFF, F. M.	RAMOA9
BOETTGER, H. G.	FAMOC11
	RAMOA9
	RAMOA7
BOGDAN, M. R.	MAMP4
	FAMP24
BOHME, D. K.	RAMP20
BOSTICK, JR.,J. K.	WAMOB7
	MPMP7
BOULDIN, J.	RAMOC5
BOWERS, M. T.	FAMOA2
	RAMP17
	WAMOC14
	MPMOC9
	MPMOB11
	MPMOC8
BOYD, R. K.	FAMP19
BRADICICH, R. B.	RPMOC2
BRADWAY, D. E.	RPMP1
BRAND, H. R.	RPMOB7
BRANDT, W.	MAMOB9
BRANFMAN, A. R.	MAMP9
BRASH, A. R.	TAMOB11
BRAUMAN, J. I.	TPMOA1
BREISACHER, P.	FAMP23
BRENTON, A. G.	MPMOB1
BRIDEN, F.	WAMOB8
BRITTEN, R. A.	RAMOA7
BRLETIC, K. A.	TPMOB9
BROWN, J. M.	RAMP2
BROWN, P.	FAMOB13
BRUMLEY, W. C.	MAMOC13
BRUNDRETT, R.	MAMP7

AUTHOR	PAPER NO.
BRUNER, T.	MPMOA3
BRUNI, R. J.	MAMP9
BRUNNEE, C.	WAMP20
	MPMP6
BRYANT, P. J.	MPMP11
BRYANT, W.	RPMOB10
	TPMP21
BUCHANAN, B. G.	TAMP7
BUCKLEY, J. A.	TAMOC3
BUCKLEY, T. J.	WAMP14
BUDDE, W. L.	RAMP8
	TAMOA6
BUDZIKIEWICZ, H.	MPMOB4
BUKO, A.	FAMOB5
BULUSU, S.	TAMP17
BURKE, J. F.	RPMP14
	WAMOA14
	RPMP11
BURLINGAME, A. L.	FAMOB15
	RAMOA6
	WAMOA16
	MPMP13
BURNS, P.	RPMOC11
BURSEY, J.	RAMOC3
BURSEY, M. M.	MPMP14
	RAMP15
	RAMP14
BURTON, R. R.	TAMOB10
BUSCH, K. L.	RAMP15
	RAMP14
	RAMOC10
BUSER, H. R.	WAMOB11
BUSH, E. D.	MAMP6
BUTLER, C.	RAMOA3
BUTLER, J. J.	WAMOC1
BUTTRILL, JR., S. E.	MPMP12
	FAMP18
	FAMP12
	TPMP10
	MAMOB3
CALKINS, C. A.	TPMOC10
CALLERY, P. S.	RPMP15
CAMERON, D.	WAMOC12
CAMPANA, J. E.	RPMOB4
CAMPBELL, I. M.	RAMOA5
CANADA, D. C.	MPMOB12
CAPRIOLI, R. M.	RPMP19
	TAMOB6
	MPMOB1
CARR, S. A.	MAMOB8
	MAMOB6
CARROL, D.I.	FAMOC12
CARTER, D.	RPMP23
CARTER, J. A.	WAMOB3
	TPMOB11
CARVER, R.	MAMOB14
CASTILLO, G. D.	RPMOC2
CELLI, F.	MPMOC10
CEYER, S.	RPMOA6
CHAIT, B. T.	EAMOC1
CHAIT, E. M.	TAMOA8
	TAMOA3
CHAKEL, J. A.	MPMOC4
CHANG, C.	FAMP2
CHAPMAN, J. R.	FAMP7
CHEN, C. Y.	TAMOB6
CHEN, G.	MAMP2
CHEN, R.	MPMOB10
CHENG, C. C.	FAMP2
CHESLER, S. N.	RAMP2
CHESNOVICH, W. J.	MPMOC9
CHIANG, T. C.	TAMOB9
CHOU, C.-H.	FAMOB8
CHRISTENSEN, R. G.	RPMOC9
CHRISTIE, W. H.	TPMOB3
CHRISTMAN, R. F.	RAMP12
CHUANG, C. C.	RPMOC8
CHUNG, K. M.	MPMOC2
	MPMOC1
CLAEYS, M.	RPMP22
CLARK, C. R.	RAMP6
CLARK, H. A.	RPMOB6
CLEM, T.	TAMP3
COBURN, J. A.	FAMP16
COHEN, A.	WAMOA10
COHEN, S.	RAMP1
COLBY, B. N.	TPMP13
	TAMP10
COLTON, R. J.	MPMP3
COLVIN, O. M.	MAMP7
COMBA, M. E.	FAMP16
COMISAROW, M.	FAMOC10
	RAMOB11
COMPSON, K. R.	FAMP7
	FAMP4
	FAMOC6
	WAMP17
	WAMP16
	MPMOB7
COMSTOCK, W.	TAMP3
CONLEY, J.	FAMOC11
CONRAD, R. L.	RPMOB13
	TAMOA5
CONWAY, D.C.	FAMOB3
	RAMOB1
COOK, K. D.	MAMOB5
COOKS, R. G.	WAMOC12
	WAMOB10
	TPMP6
CORY, D. A.	RPMP16
CORY, H. T.	TAMOB2
COSBY, P. C.	RPMOA5
COSTELLO, C. E.	MAMOB8
	MAMOB6
COTTER, M. L.	MPMOB10
COTTER, R. J.	RPMOB2
CRAIN, P. F.	FAMOB12
CRAMERS, C. A.	MPMOA1
CRANDALL, R. K.	MAMP11
CRAWFORD, R. W.	RPMOB7
CRETNEY, W. J.	TAMOC1
CROSS, R. J.	FAMOA5
CROW, F. W.	TPMP14
	MPMOA4
CUTIE, S. S.	WAMOB9

AUTHOR	PAPER NO.
DALEY, S. K.	WAMOA4
DANIEL, F. B.	RPMP7
DARLAND, E. J.	MPMOC4
DARWISH, F.	RPMP23
DAS, K. G.	MPMOB4
DAUBACH, R. O.	MAMOC3
DAUGHTREY, JR., E. H.	WAMOB7
	MPMP7
DAVES, G. D.	TAMOB2
DAVIDSON, W. R.	TAMOC3
	MPMOB11
DAVIS, T. S.	TAMP18
DAVISON, A.	MAMOB6
DAWSON, P. H.	WAMP6
DAY, R. A.	TAMP2
DAY. R. J.	WAMOB10
DAYAL, B.	FAMOB2
DECORPO, J. J.	MPMP3
	MPMOC11
	MAMP23
DELINE, V. R.	WAMOB2
DENNE, D. R.	FAMP4
	FAMOC6
DENTON, M. D.	RPMP20
	MAMP1
DEPUY, C. H.	WAMOC7
DERAI, R.	RAMOB9
DEROOS, F. L.	TPMP15
DESAGHER, R.	TAMOB8
DESIDERIO, D. M.	FAMOB4
DESILVA, J.A.F.	MAMP3
DESTEFANO, A. J.	TAMOA9
	MAMOB10
DEVANT, G.	TPMP20
DIELMANN, G.	TAMOA1
	TPMOC11
DOERFLER, D. L.	RAMOA5
DOIRON, C. E.	WAMOC9
DONOHUE, D. L.	WAMOB3
DORSEY, J.	WAMOB8
DOUGHERTY, R. C.	FAMP9
	WAMOB11
DOWTY, B. J.	TPMP3
DOYLE, JR., R. J.	WAMP14
DREIFUSS, P. A.	MAMOC13
DUBAY, G. R.	MAMOC11
DUCHATEAU, A.	RPMP22
DUDDING, G. F.	TAMOA7
DUNBAR, R. C.	TPMOC9
	MAMP17
	MAMP18
DUPUY, H. P.	TAMOA2
DURDEN, D. A.	WAMP5
DURKEE, S.	RAMP1
DYE, J.	MPMP8
DYER, E. W.	TAMP4
DYMERSKI, P. P.	RPMOC12
	WAMP1
EBY, R. E.	TPMOB3
ECKERS, C.	RPMOC13
EDGERTON, T. R.	FAMP15
EICHELBERGER, J.	RAMP8
	TAMOA6
EIGENDORF, G. K.	FAMOC13
EINCK, J. J.	FAMOB13
ELAND, J.H.D.	MAMP12
ELDER, F. A.	MAMP11
	MAMP12
ELKINS, C.	MPMP21
ELLIOTT, J. R.	RPMOB7
ELLIS, C. K.	WAMOA6
ELSOHLY, M. A.	MAMP5
EMKEN, E. A.	WAMOA8
ENGEL, T. M.	MPMOA4
ENGELS, J. C.	MPMP10
ENKE, C. G.	MPMOB6
	WAMP12
	MPMOC4
ERICKSON, M. D.	RAMOC7
ERK, S. D.	MAMP4
ERROCK, G. A.	WAMP17
ERVIN, T. J.	MAMP19
EVANS, J.	RPMP11
EVANS, J. V.	WAMOA4
EVANS, S.	FAMP4
	MPMOB7
EVANS, JR., C. A.	WAMOB2
	TPMOB1
EYLER, J. R.	WAMP14
	TPMOC7
	MAMOC3
FALES, H. M.	TAMP3
FALKNER, F. C.	TAMP20
FARQUHAR, D.	MAMP8
FARR, W. A.	TAMOA10
FEHSENFELD, F. C.	MPMOC7
	MAMOC7
FEIGE, L. E.	RPMP1
FENISTEIN, S.	RAMOB9
FENNESSEY, P. V.	RAMOA3
	RAMOA1
FENSELAU, C.	MAMP7
FERREIRA, L. F.	MAMP19
FIELD, F. H.	RAMOB6
	WAMOC13
FINLEY, B.	MAMP1
FISCHER, H. P.	MPMP16
FISHER, I.P.	MPMP16
FLOWERS, M. C.	FAMOA3
FOLTZ, R. L.	RAMOC6
	MPMP14
	RPMOC6
	TPMP14
	TPMP16
	MPMOA4
FRANCHETTI, V. M.	MAMOA11
FRANKLIN, J. C.	WAMOB3
FRANKLIN, J. L.	MAMOC4
FREAS, R.	WAMOC8
FREISER, B. S.	WAMOC10
FRENCH, J. B.	FAMOC7
	TAMOC3
FRIEDEL, R. O.	WAMOA2
FRIEDMAN, L.	MAMOB11
FRISCH, M. A.	MPMP4
FULFORD, J. E.	WAMP3
FUTRELL, J. H.	WAMP7
	MPMOC6

AUTHOR	PAPER NO.
GAL, J.	RPMP15
GALE, P. J.	FAMP10
GALLEGOS, E. J.	MAMOA12
GAMES, D. E.	RPMOC13
	TPMP8
	TPMOC11
GANJEI, J. F.	MPMP3
GARLAND, W. A.	MAMP2
	MAMP3
GARNER, E. L.	TPMOB9
GASKELL, S. J.	RPMP8
GAUMANN, T.	MPMOB2
GAVRILOVIC, J.	WAMOA1
GAY, M. L.	FAMP20
GEFEN, S.	RAMP23
GENTRY, W.R.	FAMOA1
GHADERI, S.	WAMP13
	FAMOC9
	RAMP16
	TAMOC2
GIFFIN, C. E.	FAMOC11
	RAMOA7
GIORDANI, A.	FAMOC2
GLEITMAN, Y.	RAMP23
GODSE, D. D.	WAMOA11
GOLDAN, P. D.	MAMOC7
GOODLOE, G. W.	MPMOC5
GORSE, R.	RAMP1
GOWER, J. L.	TPMOC11
GRABOWSKI, J. J.	WAMOC7
GRADE, H.	TAMOC8
GRAY, N.A.B.	TAMP7
GRAYSON, M. A.	MPMP19
GREEN, B. N.	TPMP22
GREEN, D. R.	RAMOC1
GREEN, J. P.	TAMOB1
GREEN, M. M.	WAMOC15
	MPMOB4
GRIGSBY, R. D.	MAMOA1
	MAMOA3
GRIMSRUD, E. P.	RAMOB4
GRINDEL, J. M.	FAMOB10
GRINDSTAFF, Q.	MAMOA2
	MAMOA3
GROSS, H. J.	FAMOB12
GROSS, M. L.	FAMOC9
	RAMP16
	RAMP5
	WAMP13
	WAMOC4
	WAMOC5
	TAMP23
	TAMP22
	TAMOC2
GUENTHER, F. R.	RAMP2
GUICHON, G.	TPMP20
GUTSHALL, P. L.	MPMP11
GUYON, P. M.	MAMP19
HACHEY, D. L.	WAMOA15
HADDON, W. F.	FAMOC4
HAHTO, M. P.	MPMP17
HAINES, R. C.	TPMOB10
HAKOMORI, S.	FAMOB14
HALPAAP-WOOD, K.	FAMOB11
HALPERN, B.	TAMOC11
HAMILL, R. L.	MAMOB7
HANEY, M. A.	TPMP5
HANKS, A. R.	MAMOA1
HANSEN, L. B.	RAMOC4
HANSON, R. L.	RAMP6
HARADA, K. I.	TAMOC9
HARAGUCHI, S.	RPMP3
HARAKI, K. S.	TAMP5
HARGROVE, W. F.	TAMP13
HARLESS, R. L.	RPMP1
HARMON, D. J.	MAMOB4
HARRINGTON, W. L.	TPMOB2
HARRIS, III, B.	RAMOC7
HARRISON, A. G.	WAMOC2
HARTMANN, H.	MPMOC2
	MPMOC1
HARVAN, D. J.	TAMP16
	RAMP15
	RAMOC10
HARVEY, D. J.	MPMOB8
HARVEY, T. M.	MPMOA5
HASE, W. L.	RPMOA2
HASS, J. R.	TAMP16
	RAMP15
	RAMP12
	RAMP14
	RAMOC10
HATTOX, S. E.	WAMOA9
HAYS, J. D.	TPMOC9
HAYS, R.	RAMP22
HAZELBY, D.	MPMOB7
HEIKES, D. L.	RPMOC1
HELLER, R. S.	TAMP12
HELLER, S. R.	FAMP1
HELM, H.	MAMP22
HENCHMAN, M. J.	WAMOC6
HENDERSON, T. R.	RAMP6
HENDERSON, W.	FAMOC6
HENIS, N.B.H.	MPMP14
	RAMP14
HERMAN, A. G.	RPMP22
HEROD, A. A.	MAMOA7
HERSCHBACH, D. R.	PL2
HERTZ, H.	WAMOA10
	RPMOC9
	RAMP2
HIDY, B.	RPMOC6
HIDY, B. J.	TPMP16
	MPMOA4
HIERL, P. M.	RAMOB8
HIGNITE, C. E.	MAMP10
HILEMAN, F. D.	MPMP20
HILKER, D. R.	TAMP22
HILKER, D.	RPMOC12
HILL, R. M.	MAMOC1
HILLER, J.	TPMOC6
HILPERT, L. R.	RAMP2
HINCHMAN, B.	RPMOB10
	TPMP21
HINDERMAYR, H.	RPMP21
HINES, H. B.	TAMOB7
HIROAKA,K.	MAMP13
HIROOKA, T.	RPMOA6
HIRTER, P.	RPMOC13
HISANAGA, N.	RPMP3

AUTHOR	PAPER NO.
HOBBS, C. H.	RAMP6
HODSHON, B. J.	MAMP2
HOFFMAN, M. K.	FAMOB6
HOGG, A. M.	MAMOA13
HOHN, M.	TAMOA4
	TAMOA1
HOISINGTON, D. A.	FAMOB6
HOLLAND, J. F.	MPMP9
	MPMP8
HOLMES, J. L.	WAMOC3
HONOVITCH, J. P.	MAMP18
HOPPER, D. G.	MAMOC2
HOPPESCH, J. P.	MPMP22
HORNING, E. C.	FAMOC12
	FAMOB11
	RPMP17
HORNING, M. G.	FAMOB11
HOSOKAWA, K.	TAMP5
HOUGH, A.	TAMOB11
HOWALD, W. N.	MAMP6
HOWARD, R. W.	TAMOA5
HOWORKA, F.	MPMOC7
HOY, D. J.	WAMP17
HOYLAND, J. R.	TAMP11
HSIEH, T.-C.	RAMOB2
	MAMOC5
HUBBARD, W.	TAMOB11
HUDGENS, J. W.	MAMP23
HUDSON, C. E.	WAMOC16
	MPMOB5
HUFF, J. R.	TAMP21
HUFF, S. B.	TAMOB5
HUFFMAN, D. H.	MAMP10
HUGHES, R. J.	WAMP3
HULL, C. W.	TAMOA5
HUNG, A.	TAMOB8
HUNT, D. F.	FAMP11
	FAMP10
	FAMOC2
	FAMOB5
HUNT, J. E.	RAMOA10
HUNTER, E. P.	RAMOB6
	WAMOC13
HUNTER, R. L.	WAMOC11
	RPMOB8
HUNTRESS, JR., W. T.	TPMOC12
	WAMP8
HUTCHINSON, F.	FAMOB14
HWANG, C. S.	MAMOA2
HYDE, W.	TPMP23
ILLIES, A. J.	TAMOC4
INANAGA,K.	RAMOA4
INFANTE, R.	TAMOC4
INGELS, J.	WAMP19
ITAGAKI, Y.	RPMP3
ITO,K.	MAMP19
JACKSON, K.	TPMOC5
JACKSON, M. E.	TAMP2
JACOBS, M. L.	WAMOB5
JAMIESON, W. D.	RAMOC1
	TAMP4
JASON, A. J.	TPMOC1
JENNINGS, K. R.	RAMP20
JOHNSON, R.	TAMOB11
JONES, E. G.	MPMOC3

AUTHOR	PAPER NO.
JUGOVITCH, J.	TAMP14
	TAMP15
JUNGCLAUS, G. A.	MPMOA4
JURS, P. C.	RPMOB4
	RPMOB6
JUSTICE, J.	RPMOB12
	TAMP8
KABASHIMA, K.	RAMOA2
KALBRON, J.	FAMOB10
KALMBACH, K.	WAMOC8
KAMBARA, H.	FAMOB15
	WAMOA1
	MPMP13
KAN, M. N.	TAMP14
	TAMP15
KANG, G. I.	TAMOB10
KANOJA, R.	MPMOB10
KARGER, B. L.	RPMOC6
KARNOFSKY, J.	TAMP16
KARPAS, Z.	TPMOC12
KATO, T.	RAMOA2
KAUFMANN, H.	TAMOA4
KAYSER, S. G.	MPMP9
KEBARLE, P.	TPMOA5
	MPMOC12
KEHOE, D. B.	TPMP9
KELLEY, D. F.	FAMOA3
KELLEY, J. A.	FAMOB1
KEOUGH, T.	MAMOB10
KHANDELWAL, J. K.	TPMP17
	TAMOB1
KIBLER, S.	RAMOA3
KIM, S. H.	RAMOB4
KINARD, G.	TPMP8
KING, G. K.	WAMOC7
KIRBY, D. P.	RPMOC6
KIREMIRE, B.	MPMOB3
KISER, R. W.	MAMP16
KLEIN, P. D.	WAMOA15
KLINE, S. A.	RPMP9
KLOTS, C. E.	RAMOB10
KNIGHT, J.	WAMP1
KNIGHT, M. E.	TPMP8
KOCH, K.	RPMP21
KOLLIE, T. G.	TPMOB3
KOLLMANN, K.	MAMP19
KOPIN, I. J.	FAMP6
KOSLIN, M. E.	TPMOB12
KRAY, W. D.	TAMOA7
KRIEN, P.	TPMP20
KRUGER, T. L.	WAMOC12
	TPMP6
KUEHL, D. W.	FAMP9
KUHARA, T.	RPMP3
	RPMP4
	RAMOC4
	RAMOA2
KULKARNI, P. S.	FAMOC9
	RAMP16
	TAMOC2
KURAMOTO, S.	RPMP4
KURZ, E. A.	WAMP21
	WAMP22

AUTHOR	PAPER NO.
LAI, S.T.F.	MAMOB5
LAKE, J. L.	RAMOC2
	TPMP7
LAMPARSKI, L. L.	WAMOB9
LAMPE, F. W.	MPMOC5
	MAMOC14
LANDIS, D. H.	WAMOA9
LANE, D. A.	FAMOC7
LAO, R. C.	FAMP21
LARES, N. E.	TPMOB7
LASER, B.	MPMP6
LASETER, J. L.	MAMOA9
LATTIMER, R. P.	MAMOB4
LATVEN, R. K.	MPMOB6
LAUTERBURG, B. H.	RPMP17
LAVANCHY, A.	TAMP7
LAY, J. O.	RAMP5
LEBEL, G. L.	RAMP4
LECLERCQ, P. A.	MPMOA1
LEDFORD, E.	RAMP16
	TAMOC2
LEDFORD, JR., E. B.	FAMOC9
	WAMP13
LEE, L.	FAMOA5
LEE, Y. T.	RPMOA6
LEEDY, D. W.	TAMOA9
LEGENDRE, M. G.	TAMOA2
LEHR, J.	RPMP13
LEMONS, S.	MAMP10
LEONARD, E. N.	RAMP3
LERNER, R. D.	MPMOB5
LEVINS, P. L.	FAMP22
LEWIS, E.	RPMOC13
	TPMP8
	TPMOC11
LEWIS, S.	RAMOA6
LI, Y.-H.	WAMOC2
LIAO, W. T.	RAMP12
LIAS, S. G.	RAMP18
LIEHR, G. G.	MPMOB1
LIEHR, J.	MPMOA6
LIFSHITZ, C.	RAMP23
LIGON, JR., W. V.	TAMOC8
	WAMP24
	TPMP12
	MAMOB2
LIN, D.C.K.	RAMOC6
	MPMOA4
LIN, M. S.	MPMOC14
LIN, S.-N.	RPMP19
	TAMOB6
LIN, Y. Y.	RPMOC3
LINCOLN, K. A.	WAMP18
LOCKE, M. J.	WAMOC11
LOO, T. L.	MAMP8
LORES, E. M.	RPMP1
LORY, E. R.	TPMOC8
LUCAS, S.	RAMOC6
LUCAS, S. V.	MPMOA4
LYON, P. A.	RAMP5
MAAS, J. W.	WAMOA9
MACDONALD, A.	MAMP2
MACFARLANE, R. D.	RAMOA10
	RAMOA8
MACGUIRE, S.	MPMP10
MACHINIST, J.	WAMOA5
MACKINNON, M. D.	RAMOC1
MADDEN, R.J.G.	TAMP2
MAGEE, C. W.	TPMOB2
MAGNERA, T. F.	MPMOC12
MAHADEVAN, P.	FAMP23
MAHAN, B. H.	RPMOA6
MALLOY, J. M.	RAMOA5
MALONEY, K. M.	MAMP11
	MAMP12
MANCUSO, N. R.	MAMOB8
MANDELBAUM, A.	MPMOB13
MARCH, R. E.	WAMP3
MARCUS, R. A.	RPMOA1
MARK, T. D.	MAMP22
MARKEL, E. L.	WAMP11
MARKEY, S. P.	FAMP6
	TAMP1
MARRIOTT, T. D.	MAMOA2
MARSH, P. G.	RAMOA1
	RAMOA3
MARSHALL, D. J.	RPMP13
MARSHALL, T. C.	RAMP6
MARTINSEN, D. P.	FAMP1
	TAMP12
MARUYAMA, I.	RAMOC4
	RAMOA2
MARX, R.	RAMOB9
MASCARELLA, S. W.	MAMOA9
MASON, F. G.	TAMP4
MASON, R. S.	RAMP20
MASUOKA, T.	RAMOB3
MATEJCEK, P.R.J.	RPMOB9
MATSUMOTO, I.	RPMP4
	RPMP3
	RAMOA4
	RAMOA2
MATTHEWS, D. E.	WAMOA14
MAUCLAIRE, G.	RAMOB9
MAY, R. J.	TPMP12
MAY, W. E.	RAMP2
MAYOTTE, G.	WAMOC15
MCADAMS, M. J.	RPMOC10
	RAMP11
	RAMOC5
MCADOO, D. J.	WAMOC16
	MPMOB5
MCBAY, E. H.	MPMOB12
MCCAMAN, M. W.	RPMP10
MCCLOSKEY, J. A.	FAMOB12
	TPMP4
MCCLUSKY, G. M.	WAMOC12
MCCRONE, W. C.	WAMOA1
MCCULLOH, K. E.	TPMOC4
MCDOWELL, R.	WAMP16
	MPMOB7
MCEWEN, C. N.	TAMOC5
	TAMOC6
MCGILVERY, D. C.	WAMP2
	TPMOA3
MCIVER, JR., R. T.	RPMOB8
	WAMOC11
MCLAFFERTY, F. W.	WAMP2
	TPMOC8
	TAMP5
	TPMOA3
MCMAHON, T. B.	WAMOC9

AUTHOR	PAPER NO.
MCMAHON, W. A.	RAMOC9
MCMANUS, I. T.	RAMOA5
MCNAY, J. L.	TAMOB5
MCNEAL, C. J.	RAMOA8
MCNULTY, W. P.	TAMOB2
MCPHERRON, R.	MPMP13
MEE, J.M.L.	TAMOC11
MEISELMAN, S.	RPMOC9
MEISELS, G. G.	FAMP8
	RAMOB2
	TAMOC4
	MAMP21
MEITES, L.	WAMOC15
MELERA, A.	FAMP3
	TPMP19
MENELL, R.	MAMP7
MEOT-NER, M.	WAMOC13
	RAMOB6
MERREN. T. O.	TPMOB10
MERRILL, G. L.	TPMOC10
MERRILL, Y.	MAMP9
MERRITT, C.	MPMP9
MERSKSAMMER, I.	MPMOB13
MESCHER, J. A.	RAMP10
MEUNIER, M.	WAMP6
MEUZELAAR, H.L.C.	MPMP20
MIDDLEDITCH, D. R.	TAMOB7
MIDDLEDITCH, B. S.	TAMOB7
MIDDLEMISS, N. E.	WAMOC2
MILLER, C. D.	RAMP9
MILLER, D. L.	RAMP5
MILLINGTON, D. S.	RPMP8
	RPMOC11
MILNE, G.W.A.	FAMP1
MIN, B. H.	MAMP3
MINARD, R. D.	FAMP24
	TPMP1
	MAMOC14
MITACHEK, P.	TPMP21
	RPMOB10
MITCHELL, J. R.	RPMP17
MITCHUM, R. K.	MAMOC8
MIZUNO, T.	RPMP3
MOLER, G. F.	MAMOC8
MONCUR, J. G.	MPMP15
MONTGOMERY, F. E.	FAMOC12
MORAN, T. F.	FAMOA4
MORDEN, W. E.	RPMOB1
MORGENTHALER, L. N.	TPMOC7
MORIN, L. M.	TAMP9
MORIN, P.	MAMP19
MOSELEY, J. T.	RPMOA5
MOTELL, E.	MPMOB11
MOTIL, K. J.	WAMOA14
MOTLEY, K.	MAMP6
MUELLER, S.	WAMOA5
MULLANY, C.	RPMP11
MULLANEY, C. J.	RPMP14
MUN, I. K.	TAMP5
MUNSON, B.	RAMP21
MURDAY, J. S.	MPMP3
MURPHY, S. D.	TAMOB6
MURRAY, P. T.	TPMOC13

AUTHOR	PAPER NO.
NACSON, S.	FAMOC7
NARANG, R.	WAMP1
NARASIMHACHARI, N.	WAMOA7
	WAMOA2
NAWAR, W. W.	MPMP9
NAWORAL, J. D.	RAMOA5
NELSON, S. D.	WAMOA1
NENNER, I.	MAMP19
NESTRICK, T. J.	WAMOB9
NEVEJANS, D.	WAMP19
NEWBURY, R.	MAMOB14
NEWTON, J. C.	RPMOB7
NGUYEN, M. T.	TPMP11
NIBBERING, N.M.M.	WAMOC5
NIELSEN, C. J.	WAMOA4
NISHIMURA, S.	FAMOB12
NISHIMURA, Y.	MPMOC6
NORMAN, E. J.	RPMP20
	MAMP1
NORRIS, D.	RAMOC11
NORWOOD, C. B.	RAMOC2
	TPMP7
NOVAK, R. A.	TPMP3
	TAMOA10
NOWLIN, J. G.	FAMOC12
	RPMP17
NOWLIN, J.	FAMOB11
NULTON, C. P.	RAMOC9
O'HARE, M.	TAMOC10
O'NEILL, P. J.	FAMOB10
OATES, J. A.	WAMOA6
	TAMOB11
OBERHOLTZER, J. E.	FAMP22
OCCOLOWITZ, J. L.	MAMOB7
ODOM, R. W.	MPMP12
	MAMOC1
OHNUMA, T.	WAMOA3
OLINGER, M. R.	MPMP9
OLINGER, R.	MPMP8
OLIVER, J. A.	TAMP1
ONUSKA, F. I.	FAMP16
OREILLY, R. A.	MAMP6
ORTH, R.	MPMOC6
ORVIG, C.	MAMOB6
OUCHI, G. I.	RPMOB3
OURDUE, P. A.	MAMP16
OVERTON, E. B.	MAMOA9
PALLANTE, S.	MAMP7
PANCIROV, R. J.	MAMOA8
PAO, J.	MAMP3
PARENT, D.	RAMP17
PARISOD, G.	RAMOB11
PARKER, C.E.	RAMP15
PARR, A. C.	TPMOC1
PARRIS, R. M.	RAMP2
PATEL, J. R.	MAMOA9
PAULSEN, P. J.	WAMOB4
PAYZANT, J. D.	MAMOA13
PEGUES, J. C.	MAMP8
PELINO, M.	MAMOB15
PELLIZZARI, E. D.	RAMOC7
	RAMOC3
PELROY, R. A.	MAMOA5
PERRY, D. L.	TPMP16

AUTHOR	PAPER NO.
PETAJAN, J. H.	MPMP20
PETERSEN, B. A.	RPMOC8
	RAMOC6
	MPMOA4
PETERSON, C. L.	FAMOC14
	TPMOC10
PETTIT, G. R.	FAMOB13
PETTY, J. D.	MAMOC11
PFAENDER, F. K.	RAMP12
PFAFFENBERGER, C. D.	RAMOC11
PHILLIPS, B. F.	TPMOB7
PHILLIPS, M. P.	MAMOC7
PIENTA, N. J.	TPMOA4
PINSON, C. J.	MPMP22
POLLEY, C. L.	FAMP8
POLLEY, C.	TAMOC4
POWELL, M.	FAMOB14
POWERS, P.	RPMOB1
	TAMP18
PRZYBYLSKI, Z.	MAMOA6
PURDUE, P. A.	MAMP16
QUAN, E.	FAMOC7
RABINOVITCH, B. S.	FAMOA3
RACHE, H.	WAMP20
	MPMP6
RADUS, T.	MAMOB11
RANDALL, L. G.	WAMP4
	TAMOA11
RAO, K.R.N.	RPMOC13
RAPP, U.	TPMOC11
	TAMOA4
	TAMOA1
RAPPE, C.	WAMOB11
RAVENS, H.	WAMP20
	MPMP6
RAY, M.	RAMOC7
RECHSTEINER, C. E.	FAMP22
REDDY, G. S.	MPMOB4
REENTS, JR., W. D.	WAMOC10
REGO, J.	MAMOB14
REICHERT, C.	MPMP2
REID, N. M.	FAMOC7
	TAMOC3
REINHOLD, V. N.	FAMOB9
REISER, R. W.	RPMOC4
RETCOFSKY, H. L.	MAMOA6
RHODES, R. C.	RPMOC4
RHODES, R. E.	TAMP21
RICHTER, W. J.	MPMOA6
RIDGE, D. P.	WAMOC8
	TPMP11
	MPMOC10
RIGGIN, R. M.	RPMOC8
RITZER, A.	TAMOA7
ROACH, J.A.G.	MAMOC13
ROBBIANI, R.	MAMOC4
ROBESON, J.	TPMOC6
ROBOZ, J.	WAMOA3
RODEN, H.	TAMOA8
	RPMOB13
RODRIGUEZ, C. F.	RAMOC9
ROHRBAUGH, D.	RPMP14
ROHRBAUGH, D. K.	WAMOA14
ROHWEDDER, W. K.	WAMOA8
ROSE, E.	WAMOA3
ROSE, M. E.	TPMP13
	TAMP10
ROSECRANCE, A. E.	TPMP13
	TAMP10
ROSENBLUM, E. R.	RAMOA5
ROSENSTOCK, H. M.	RPMOA3
	RAMOC5
ROSENTHAL, D.	TAMP13
ROY, R. L.	WAMP22
RUBEY, W. A.	RAMP10
RUBINSTEIN, I.	MAMOA13
RUDAT, M. A.	TAMOC5
	TAMOC6
RUO, T. I.	TAMOB8
RUSSELL, D. H.	FAMOC3
	WAMOC4
	WAMOC5
	MPMOB12
RYAN, J. F.	TPMP3
	TAMOA10
SAALFELD, F. E.	MPMOC11
SAARI, W. S.	TAMP21
SABBATINI, J. Z.	FAMOB4
SACHS, E. S.	MAMOC2
SAITO, K.	FAMOB7
SAKUMA, T.	FAMOC7
SALEN, G.	FAMOB2
SAMSON, J.	RAMOB3
SANDERS, R. A.	TAMOA9
SAPOROSCHENKO, M.	RAMP19
SATKIEWICZ, F. G.	TPMOB4
SATOUCHI,K.	FAMOB7
SAUNDERS, M.	FAMOA5
SAYYID, S.	TPMOB10
SCAMUFFA, M. D.	WAMOA5
SCHAEFFER, D.	RAMP7
SCHAFFER, R.	WAMOA10
SCHEPPELE, S. E.	MAMOA2
	MAMOA3
SCHLOSBERG, R. H.	MAMOA8
SCHLUMPF, E.	MPMOA6
SCHMIDT, C. E.	MAMOA6
SCHMITT, R. J.	WAMOC7
SCHNEIDER, V.	MPMP22
SCHOEN, A. E.	TPMP6
SCHOENGOLD, D. M.	MPMP18
SCHRONK, L. R.	MAMOA1
	MAMOA3
SCHULLER, W. H.	TAMOA2
SCHULTE, E.	TAMOA1
SCHULTZ, A. R.	TAMP1
SEAVER, M.	MAMP23
SEGESTA, R. M.	TPMP3
SENN, M.	RPMP21
SETHI, S.	FAMP11
SHABANOWITZ, J.	FAMOB5
	FAMOC2
SHADDOCK, V. M.	TPMP6
SHAINOK, U.	RAMP23
SHARP, T. R.	TPMP1
SHARVIT, J.	MPMOB13
SHAW, C. J.	MPMOB10
SHEETS, A.	MPMP10
SHEFER, S.	FAMOB2
SHELDON, L.	RAMOC3
SHEWBART, K.	RAMOC5

AUTHOR	PAPER NO.
SHINKA, T.	RPMP3
	RPMP4
	RAMOA2
SHROFF, J.	TAMOC10
SHUSHAN, B.	FAMP19
SIECK, L. W.	FAMP13
SIGSBY, M. L.	TPMP6
SIEGEL, M. W.	FAMOC5
	TAMOC1
SIEVERS, R.	MAMOC7
SIGSBY, M. L.	TPMP6
SLAYBACK, J.	TAMP14
	TAMP15
SLIVON, L.	RAMOC6
SMITH, D.	WAMOC6
SMITH, D. H.	TAMP7
SMITH, D. S.	RAMOC7
SMITH, DAVID H.	FAMOC3
	TPMOB11
SMITH, D. E.	RPMOB5
SMITH, D. L.	TPMP4
SMITH, J. A.	RPMP8
SMITH, L. A.	RPMP19
SMITH, L. M.	MAMOC11
SMITH, R. D.	MAMOA14
SMITH, R. G.	TAMOB2
	MAMP8
SNIEGOSKI, L.	WAMOA10
SOFRANKO, S.	RPMOB10
	TPMP21
SOLCH, J. D.	RAMP9
SOLOMON, J. J.	RPMP9
	TAMP9
SOLTMANN, B.	MPMP8
SOMANI, S. M.	RAMP7
SOVOCOOL, G. W.	RPMP1
SPARACINO, C.	RAMOC3
SPARROW, G. R.	TPMOB6
SPENCER, R. B.	FAMOC9
	WAMP13
SPENCER, R.	TAMOC2
SPHON, J. A.	MAMOC13
SPINDT, C. A.	MAMOB1
	MAMOB3
SPRATLEY, A. W.	RPMOC7
ST. JOHN, G. A.	FAMP18
	TPMP10
	MAMOB3
STAFFORD, G. C.	FAMP5
STAHL, D.	MPMOB2
STALEY, R. H.	MPMOC13
STALLING, D. L.	MAMOC11
STANDING, K. G.	FAMOC1
STANLEY, J. B.	TAMOA2
STAUFFER, J. L.	FAMP22
STEIN, J. D.	FAMOC14
STEIN, J. L.	FAMOB4
STEPHAN, K.	MAMP22
STEVENS, C. M.	RAMP1
STILLWELL, R. N.	FAMOC12
	RPMP17
STILLWELL, W. G.	RPMP17
	RPMP18
STOCKBAUER, R.	RAMOC5
	MAMP20
STONE, J. A.	RAMP20
	MPMOC14
STORY, M. S.	WAMP11
STOWE, R. N.	RAMOC5
STRADLING, R. S.	RAMP20
STRAUB, K.	WAMOA16
	MPMP13
STRAUSZ, O. P.	MAMOA13
SU, T.	MPMOC9
	MPMOC8
SULUSU, S.	TAMP17
SUNNER, J.	MPMOC12
SUZUKI, M.	TAMOC9
SUZUKI, R.	WAMOA3
SWANSON, A.	TPMP2
SWEELEY, C. C.	PL1
SWEENEY, S. L.	WAMOB5
SWEETMAN, B. J.	WAMOA6
SZILAGYI, P.	TAMOB1
TABCHE-FOUHAILE, A.	MAMP19
TAFT, R. W.	TPMOA2
TAIRA, T.	TPMOC2
	MAMP13
TAKEDA, N.	TAMOC9
TALBERT, D.	RPMOC7
TAM, W.-C.	WAMP6
TANAKA, K.	RAMOA11
TARRANT, J. D.	MAMP16
TATE, R. L.	TAMP1
TATEMATSU, A.	TAMOC9
TAYLOR, K. T.	FAMP7
	WAMP17
TAYLOR, M. L.	RAMP9
	MAMP4
	MAMOA11
TECON, P.	MPMOB2
TEECE, R. G.	RAMP7
TEETER, R. M.	MPMP15
TERLOUW, J. K.	MPMOB9
TERWILLIGER, D. T.	RPMOB11
THENOT, J. P.	TAMOB8
THOMAS, R. S.	FAMP21
THOMPSON, R. M.	RPMP16
THOMSON, B. A.	FAMOC7
	TAMOC3
TIEDEMANN, P.	RPMOA6
TIERNAN, T. O.	FAMP2
	RAMP9
	MAMOC6
	MAMOC2
	MAMOA11
TINT, G. S.	FAMOB2
TJOA, S.	RAMOA3
TODD, P. J.	WAMP2
	TPMOA3
TOMER, K.	RAMOC3
	RAMOC7
TONDUER, Y.	WAMOB11
TRAGER, W. F.	MAMP6
TRAN, V. T.	RAMP21
TRISCHAN, G. M.	WAMOB6
TRIVEDI, M.	RPMOB10
	TPMP21
TROGLER, W. C.	MPMP1
TSAO, C. S.	MPMP10
TSCHANZ, C.	MAMP10
TSUCHIYA, M.	TPMOC2
	MAMP13

AUTHOR	PAPER NO.
TURNER, C. E.	MAMP5
TURNER, D. L.	FAMOB3
TURNER, P. J.	TPMOB10
	MAMOB12
UDSETH, H. R.	MAMOB11
UNGER, S. E.	WAMOB10
	TPMP6
UNSWORTH, W. D.	MAMOB12
UPPAL, J. S.	MPMOC13
VAIRAMANI, M.	MPMOB4
VAISHNAV, Y.	WAMOA1
VAN DER GREFF, J.	WAMOC5
VAN HOVE, C.	RPMP22
VANDUUREN, B.	RPMP9
VASILE, M. J.	FAMOC8
	TPMOB5
VENKATARAGHAVAN, R.	TAMP5
VERZELE, M.	MPMOA2
VESTAL, M. L.	RPMOC10
	RAMP11
	TPMOC6
VIGGIANO, A. V.	MPMOC7
VOORHEES, K. J.	WAMP7
VOUROS, P.	RPMOC6
	MPMOB8
VU, V. T.	TAMOB4
WACHTER, M.	MPMOB10
WAHRHAFTIG, A. L.	WAMP4
	TAMOA11
WAKEFIELD, C. J.	FAMP7
	MAMOC9
WALBOT, V.	FAMOB6
WALKER, R. L.	WAMOB3
	TPMOB11
WALLER, G. R.	FAMOB8
WALLINGTON, M. J.	RPMOB1
	TAMP18
WALLS, F. C.	MPMP13
WANCZEK, K. P.	MPMOC2
	MPMOC1
WANG, C.-L. A.	RPMP7
WANG, J.	WAMOA5
WANG, Y.-M.	MAMP8
WARBURTON, G. A.	WAMP16
	MPMOB7
WARMACK, R. J.	FAMOC3
WARREN, P. L.	RPMOB5
WARREN, V. L.	RAMOC8
WARSH, J. J.	WAMOA11
WATANABE, K.	FAMOB14
WEANER, L. E.	FAMOB10
WEBB, H. M.	WAMOC14
WEDDLE, G.	MPMOC10
WEERASINGHE, N. C.	TPMP8
WEINSTEIN, H.	TPMP17
WEISS, G.	MAMP2
WEISS, M.	TAMP4
	TAMP16
WEISS, M. J.	RAMOB2
	MAMP21
WELCH, K. R.	MAMOB4
WELCH, M.	WAMOA10
WELLS, G.	WAMP7

AUTHOR	PAPER NO.
WENDEL, G. J.	WAMP2
WESTMORE, J. B.	MPMP2
WHITAKER, M. J.	FAMP9
WHITE, C. M.	MAMOA6
WHITE, E.	RPMOC9
	WAMOA10
WHITE, F. A.	TPMOB12
WHITE, R.	FAMOC9
WILKINS, C. L.	FAMOC9
	RAMP16
	WAMP13
	TAMOC2
WILLET, G. D.	WAMOC1
WILLIAMS, D. T.	RAMP4
WILLIAMS, R. L.	WAMP15
WILLIAMS, R. N.	RAMOC7
WILSON, B. W.	MAMOB6
WILSON, BARY W.	MAMOA5
WILSON, J. C.	MAMP11
	MAMP12
WINDEL, B.	WAMP20
WINMILL, D. L.	WAMP15
WISE, S. A.	RAMP2
WITIAK, D. N.	WAMOC16
WIXOM, M. R.	WAMP2
WOJCIK, L. H.	MPMP20
WOLFE, R. R.	RPMP14
	RPMP11
WOLKOFF, P.	WAMOC3
WOLSTENHOLME, W. A.	RPMOB9
WOLTERS, F. C.	FAMOA3
WONG, LAN K.	RPMP7
WOOD, G. W.	MPMOB3
WRIGHT, J.	RPMP15
WRIGHT, L.H.	RPMP1
	FAMP15
WRONKA, J.	WAMOC8
	TPMP11
WU, R.L.C.	MAMOC2
	MAMOC6
WU, W.N.	FAMOB10
WYATT, J. R.	MPMP3
	MPMOC11
	MAMP23
YAMADA, S.	RAMOC4
YAMAIZUMI, Z.	FAMOB12
YAMAMOTO, H.	FAMOB12
YELTON, R. O.	RAMP9
	MAMP4
	MAMOA11
YERGEY, A.L.	MPMP5
YINON, J.	TAMOC7
YORKE, D. A.	RPMOC11
	TPMP22
YOSHIDA, M.	RPMP4
YOST, R. A.	MPMOB6
	WAMP12
YOUNG, S. E.	TPMP10
YOUNG, V.R.	RPMP14
	WAMOA14
YOUNGLESS, T. L.	MPMP14
ZACCHEI, A. G.	TAMP21
ZAKETT, D.	TPMP6
ZARE, R. N.	TPMOC5
ZARETSKII, Z.V.I.	TAMP19
ZWEIDINGER, R. A.	RAMOC7

ASTM COMMITTEE E-14 AND

THE AMERICAN SOCIETY FOR MASS SPECTROMETRY

Year	President	Vice President Programs	Vice President Arrangements	Vice President Data & Stds.
1961-2	V. H. Dibeler	R. E. Fox	R. A. Brown	-
1963-4	R. E. Fox	N. D. Coggeshall	A. G. Sharkey	-
1965-6	N. D. Coggeshall	H. M. Rosenstock	M. K. Testerman	-
1967-8	H. M. Rosenstock	J. L. Franklin	D. B. Harrington	-
1968-9	J. L. Franklin	R. E. Honig	C. E. Johannsen	-
		ASMS		
1970	J. L. Franklin	R. E. Honig	C. E. Johannsen	H. R. Harless
1971-2	R. E. Honig	F. H. Field	G. L. Kearns	H. R. Harless
1972-4	F. H. Field	H. J. Svec	A. H. Struck	E. Lumpkin
1974-6	H. J. Svec	J. H. Futtrell	W. H. Brubaker	*Position was deleted in 1973-74
1976-8	J. H. Futtrell	J. A. McCloskey	E. J. Bonelli	
1978-9	J. A. McCloskey	B. Munson	E. J. Bonelli	

Year	Secretary	Treasurer	Directors at Large	
		ASTM E-14		
1961-2	C. F. Crable	-	J. H. Beynon	C. F. Robinson
1963-4	H. E. Lumpkin	-	S. Meyerson	A. L. Wahrhaftig
1965-6	G. L. Cook	-	H. I. Schiff	W. M. Hickam
1967-8	A. B. King	-	E. E. Muschlitz	R. M. Teeter
1969	J. M. McCrea	-	R. F. Porter	J. T. Herron
		ASMS		
1970	J. M. McCrea	H. D. Cook	R. F. Porter	J. T. Herron
1971-2	F. E. Saalfeld	H. D. Cook	A. G. Sharkey	A. L. Wahrhaftig
1972-4	F. E. Saalfeld	M. T. Laug	J. Berkowitz	E. B. Owens
1974-6	J. A. McCloskey	M. T. Laug	P. Kebarle ‡ E. M. Emery	J. L. Margrave
1976-8	K. E. McCulloh	M. T. Laug	H. M. Fales ‡ E. G. Carlson	A. G. Harrison
1978-79	H. M. Fales	M. A. Frisch	C. C. Fenselau M. C. Hamming‡	A. G. Harrison

*ASTM E-14 Chairman was dropped as a Vice President and made a Director at Large in 1974.

‡ ASTM E-14 Chairman

Minutes of Annual Business Meeting

June 5, 1979 Seattle, Washington, D. C.

The meeting was called to order by President James A. McCloskey. Secretary Henry M. Fales presented slides (Appendix 5) showing the membership, 1504 to date, and its composition followed by the election results (Tally Chairman H. A. Lloyd).

Vice-President for Arrangements:	
W. A. Wolstenholme	247 votes
E. M. Chait	228 votes
Director-at-Large:	
W. L. Fite	268 votes
W. V. Ligon, Jr.	214 votes

President McCloskey introduced the winning candidates.

Treasurer Margaret Frisch presented slides showing the current financial status of the Society (Appendix 4) and stated that Conference expenses and income were about balanced. It was pointed out that expenses associated with the production of the Proceedings are now split between the operating and Conference budget to reflect the fact that the Proceedings are paid for both by members' dues and non-members' registration.

Vice-President for Programs Burnaby Munson presented several slides (Appendix 2) showing that 1) there appears to be little correlation between meeting date (Memorial Day) and attendance, 2) the total number of papers is rising more rapidly than membership, 3) most submitted papers arrive at his desk on the deadline date, 4) number of papers presented by a given author. Slides were also presented showing geographical distribution of papers as well as subject matter over the years. Some subjects are disappearing (high resolution) and others increasing (environmental, etc.). He showed that the number of oral sessions was very near the limit at this meeting and announced that he would probably have to limit the number presented per laboratory next year. He further pointed out that plenary lectures each equated to 12 oral papers, symposia 6, etc., and said that the universal desire for more of everything was not realistic. Hard decisions will have to be made and he welcomed the membership's input on the matter.

Vice-President for Arrangements, Ernest Bonelli announced selection of the 1983 meeting site, the Boston-Sheraton Hotel, where conference facilities are excellent. He mentioned that the Olympic Hotel had made an error in not referring overbookings to the nearby hotel selected by ASMS and apologized on behalf of the Olympic.

McCloskey asked the Secretary to read the proposed Constitutional Amendments and revised by-laws to the assembly. The Amendments were discussed on the floor and the words "of the date of mailing" inserted after "...received within six weeks..." in Article XI, Sections 1 and 4 by unanimous vote. The Amendments are to be referred to the membership for a mail vote.

McCloskey then introduced Parliamentarian for the meeting, Milt Levenberg and the members of the new Nominating Committee. He thanked leaving Board of Directors members E. Bonelli and A. Harrison for their services to the Society. McCloskey next mentioned the desire by certain local mass spectrometry discussion groups for more formal affiliation with ASMS and asked for input by the membership on this matter also.

McCloskey announced that ten $300 conference fellowships are to be awarded to mass spectrometrists in early stages of their careers for attendance at the New York meeting, and asked for discussion. Various suggestions for modification of the announcement were made but no consensus appeared. McCloskey emphasized that the fellowships were an

experiment and asked for a straw vote on whether the matter proceed as outlined in the announcement. The vote was overwhelming in favor with five opposing.

McCloskey then read the letter from member Floie Vane requesting a letter from McCloskey stating that "...ASMS support the aims of ERA...". He reviewed the events leading to this request and announced that although the Board of Directors itself had gone on record in support of ERA, they were unwilling to speak for the membership as a whole on this matter. He stated his intention shortly to poll the membership by mail and communicate the results to Dr. Vane. Little discussion ensued, but a request that the poll include an exact statement of any commitment was favorably received by the President.

Under new business, Dr. Don Hunt requested that consideration be given to including a weekend in the meeting dates (i.e., Wednesday to Wednesday, etc.). This was not entirely supported by the assembly, and Bonelli pointed out that the hotels vary considerably in their attitude toward such scheduling. McCloskey promised that the Board of Directors would at least consider this idea and adjourned the meeting at 7:15 p.m.

ASMS COMMITTEES AND ASTM E-14 SUBCOMMITTEES

Nominating Committee: T. T. ACZEL, Exxon Research and Engineering Company, Box 4255, Baytown, Texas 77520

Fundamentals: G. G. MEISELS, Department of Chemistry, University of Nebraska, Lincoln, Nebraska 68588

Computer Applications: D. V. BOWEN, Union Carbide, Tarrytown, N.Y. 10591

Isotope Ratio Measurements: E. L. GARNER, Analytical Chemistry Center, National Bureau of Standards, Washington, D. C. 20234
D. J. ROKOP, Los Alamos Scientific Laboratory Los Alamos, New Mexico, 87545

Quantitative Organic Analysis: S. P. MARKEY, Building 10, Room N321, National Institute of Health, Bethesda, Maryland 20014

Biomedical Applications: K. BIEMANN, Department of Chemistry, Massachusetts Institute of Technology, Cambridge, Mass. 02139

Solids and Surface Analysis: W. HARRINGTON, RCA Laboratories, Princeton, New Jersey 08540

Qualitative Organic Techniques: M. L. GROSS, Department of Chemistry, University of Nebraska, Lincoln, Nebraska 68588

Education: L. I. BONE, Dow Chemical Company, Freeport, Texas 77541

Environmental Applications: J. T. BURSEY, Chemistry and Life Sciences Division, Research Triangle Institute, Research Triangle Park, North Carolina 27709

Forensic Applications: R. SAFERSTEIN, New Jersey State Police Laboratory, P. O. Box 7068, West Trenton, New Jersey 08625

Definition and Terms (ASTM-E14): (Chairmanship vacant)

ASMS COMMITTEE ON FUNDAMENTALS

Symposium on Fundamental Aspects. June 7 and 8

A one-day symosium on fundamental aspects of mass spectrometry with particular emphasis on reaction dynamics was held at Seattle. The symposium was preceded by a Plenary Lectury by Prof. Dudley Herschbach, and a series of contributed papers on Fundamentals. The eleven symposium speakers represented equally investigators concerned with ions and those dealing mostly with neutrals and not normally participants in this conference. About 130 individuals attended the Thursday afternoon session, while attendance at the Friday morning session trailed off throughout the morning as participants left the Conference. The symposium included some lively discussion, and was generally very well received.

Business meeting Thursday, June 7.

Approximately 40 participants attended the business meeting at the end of the first half-day session of the symposium. A statement of Committee function was accepted and follows this report. The chairman reported that the scheduled luncheon has been cancelled because of cost. Various ways of encouraging informal discussions among those interested in Fundamentals were explored. The one received most favorably was an evening social function in a separate hotel meeting room with blackboard and chalk and liquid refreshments.

The committee chairman was instructed to request approval for a full day symposium from the Board; if that should not be approved, a half-day symposium and a workshop should be sought. The attendees recommend Dr. Bernstein as plenary lecturer, with Prof. Zare as an alternate choice. Topics for symposia and possible workshops were discussed. These included Structure and Spectroscopy, with Dr. Dunbar a possible symposium chairperson. However, Dr. Berkowitz indicated that there might be a NATO workshop in 1980 arranged by him on a very similar topic. An alternate topic, if the NATO meeting should be held, would be on formation and energetics with Dr. McIver potential chairperson.

The chairman takes this opportunity to express his appreciation to all speakers and discussion participants in the symposium for their contributions which made this symposium such a rewarding one, and to those who stayed for the business meeting for their patience, their helpful comments, and their constructive discussion.

Minutes respectfully submitted by

Gerry Meisels
Chairman, ASMS Committee on Fundamentals
Department of Chemistry
University of Nebraska, Lincoln, NE 68588

FUNCTION OF THE ASMS COMMITTEE ON FUNDAMENTALS.

Adopted at the Committee meeting in Seattle, June 1979

Mass Spectrometry is both a scientific discipline in its own right and a technique used by other disciplines. This leads to the diversity of the topics covered at conferences, and is both an asset and a liability: the Conference must have appeal to those whose major concern is with fundamental aspects, and those whose problem statement comes from entirely different areas but who find mass spectrometry a valuable or optimal tool to obtain the needed solutions. The connective tissue, the common thread, which brings nearly a thousand people together annually is the fact that everyone deals with gaseous ions and electrons, and those whose interests are in these species for themselves therefore provide the steady base and the core around which those who use the technique congregate. The viability of the meeting, the improvement of methodology, the introduction of new techniques, the betterment of practice, all seek the support of this central core. Those concerned with fundamental aspects represent, of all groups, the one whose interests intersect most those of other groups. Vitality of the basic aspects of ASMS programs is essential to future continuity, health, and growth of the Annual meeting and of all practitioners of the field, basic and applied.

The principal mission of Committee II must therefore be to assure the quality and quantity of the fundamental parts of the program, to encourage participation of the highest caliber scientists in mass spectrometry and allied topics, and to foster an environment which will induce those individuals, as well as the high quality young investigators who have recently entered the field or are currently becoming part of the mass spectrometry community, to select the Annual Conference as their "home base". A secondary mission is the establishment of the Conference as a bridge to other branches of chemistry. This would assure that the practitioners of our field do not speak out only with each other. Committee II should take the initiative to integrate Mass Spectrometry more fully into other areas to which it relates and contributes insight.

Report of the Committee on Computer Applications

Program Exchange

The dedicated computer program exchange is still maintained by Fred Falkner. This committee will continue to accept programs for distribution. The exchange of high level language programs through the Quantum Chemistry Program Exchange is also continuing, subject to review by the ASMS Board.

New Activities

During the business meeting, interest was expressed in several new endeavors. Groups are being formed to follow each of them. If any ASMS member is interested, please contact David Bowen for further details.

Poll of ASMS Members. Some members felt it would help to learn how many labs have computers, what equipment they use, what special techniques they may have developed (which could perhaps be made available via the program exchange), and who might be willing to advise novices in the uses of computers for mass spectrometry. A draft questionnaire will be prepared.

Dedicated Microprocessors. Members were interested in discussing the application of microprocessors to mass spectrometry, and in asking how to balance the loss of operator initiative and flexibility which microprocessors may imply against their utility in freeing the operator from routine control chores. If interest remains high a workshop may be arranged.

Collection of Spectra. This is an area where ASMS should make a larger contribution. Large time-sharing libraries need many more spectra. How can we promote the gift of additional spectra to ASMS, or directly to the libraries themselves?

Intercomputer Communications. Is it possible to propose and achieve acceptance for a standard so that mass spectrometry data systems (and other dedicated or general lab management systems) can talk to one another? Would it also be possible to standardize the output from mass spectrometers with dedicated microprocessors so that larger data systems could be used to manipulate their data?

Workshop on New Developments in Computer Hardware.

The panel for this workshop included Philip Berger, Teknivent Corp.; Douglas Vincent, Finnegan Corp.; Dennis Smith, Stanford University; Jeff Justice. Hewlett-Packard Co.; and Patrick Powers, VG Data Systems. About 75 persons attended the workshop and the Committee business meeting which followed it.

The discussion began with a brief history of computers in mass spectrometry leading to the present when large computer systems (MSSS in CIS at NIH/EPA, PBM/STIRS at Cornell, and the DENDRAL system at Stanford) and small dedicated computers are both used in mass spectrometry. The panel felt that the cost of computing power is dropping so fast that mass spectrometers will soon have dedicated host/pre-processor systems. The hosts in these systems will be able to run large programs such as the package developed at Stanford.

The application of microcomputers was also discussed. There is some danger in the no-knobs approach to microcomputer/mass spectrometer design. Many people felt that there should be some provision for operator intervention during an experiment.

Other aspects of computer hardware, including very large scale integration of components into 'intelligent black boxes', were discussed. Exchanges between the audience and the panel continued until just before time to leave for the Society Banquet.

Committee V. Quantitative Organic Analysis

* Activities

A symposium entitled "Advances in GC and GC/MS" and a workshop "Quantitative GC/MS: Techniques and Problems" successfully initiated the new Committee V. The symposium was attended by 300-400 ASMS members, at times outnumbering the available seats. The workshop was organized and moderated by Dr. Rodger Foltz, and it similarly drew an interested crowd of approximately 200. A summary of the workshop appears below.

* Workshop: "Quantitative GC/MS: Techniques and Problems"

Summarized by Dr. Fred Falkner

Brief introductory remarks concerning general parameters used to evaluate quantitative assays were made by Fred Abramson. Accuracy (agreement between assay values and known standard values) and precision (reproducibility usually expressed as relative standard deviation) were discussed and noted to be a function of sample size. Sensitivity (limit of detection) was defined as the smallest amount of analyte which can be measured with acceptable accuracy and precision from a representative matrix. Although limit of detection may be defined quantitatively as a definite signal-to-noise ratio (e.g., 3/1), it was suggested that such preset limits may be too rigid, and detection limits should be defined for each individual application. Linearity was addressed by noting that although GC/MS assays are intrinsically linear, extrapolation of a standard curve to uncalibrated concentrations is not acceptable. Other important considerations mentioned were: 1) establishing accuracy as well as precision, a task ideally accomplished by comparing analyses of identical samples among several laboratories, 2) optimizing assay procedures to effectively utilize time and resources in the light of assay objectives, and 3) verifying the stability of samples as a function of time.

In the ensuing discussion the following comments were made. No written standards, definitions, or procedures like those encoded in ASTM proceedings have been written for quantitative GC/MS. That an effort in this direction might be useful was emphasized by the comment that inaccurate selected ion monitoring (SIM) assays have been reported in the literature. A suggestion was also made to establish some type of validation index for quantitative GC/MS assays.

Rodger Foltz led a discussion of general problems and techniques. An informal poll revealed that about 90% of the attendees polled used an internal standard (IS) rather than an external standard in their assays. Approximately two-thirds used an isotopically labeled IS as opposed to a homolog or analog IS. About 75% employed SIM rather than repetitive scanning for quantification.

The mode of addition of IS to samples was discussed, and the importance of equilibration of IS with the sample was noted. Very few workers arranged to collect samples in vials containing IS as described by Susan Hattox. Problems were mentioned in the determination of conjugates.

Use of peak areas *vs* peak heights for quantification prompted considerable discussion. One difficulty commonly experienced was the difficulty of calculating peak areas because of non-ideal peak shape. Peak heights or "central areas" were suggested by Throck Watson and Bill Sherman to cope with this difficulty. Calculation of parameters from smoothed data was discussed. Possible problems introduced by computer-assisted calculations permeated the discussion as the algorithms for data acquisition and calculation are not always known to the operator. Finally, in response to a question it was noted that quantification from total ion currents might not be advisable.

* Business Meeting

A short business meeting was convened following the workshop for the purpose of identifying members willing to plan next year's program. Volunteers included:

Dr. Magda Claeys
Dr. Fred C. Falkner
Dr. Rodger Foltz
Dr. Susan Hattox
Dr. W. D. Jamieson
Dr. R. C. Murphy

Dr. Lou Shadoff
Dr. William Sherman
Dr. H. Sullivan

Topics for program consideration include non-chromatographic mass spectral analysis of mixtures, synthesis of stable isotope compounds, quantitative analysis by negative or positive c.i.--special problems, sampling statistics, quality control, and guidelines for analytical methods.

Sanford P. Markey
Chairman, Committee V
Quantitative Organic Analysis

ASMS COMMITTEE ON BIOMEDICAL APPLICATIONS (Formerly ASMS Committee VI).

A workshop was held Wednesday, June 6, 1979 with 124 persons attending.

The subject "New Methods in Mass Spectrometry and their Contributions to the Solution of Real-life Problems" attracted an unexpectedly large number of people, much too large to engage in the intimate free-for-all discussion hoped for. However, there was good audience participation and response to the presentations (relatively spontaneous and without slides, etc.) of R.D. McFarland on ^{252}Cf-plasma desorption, R.C. Cooks and D.F. Hunt on "metastable" spectra, M. Gross and E. Ledford on FT-ICR spectrometry and F.W. McLafferty on Interpretive computer algorithm.

The high level of attendance and participation of the audience demonstrated the keen interest of those working in Biomedical mass spectrometry in finding out - in an informal environment - what the state of affairs is with respect to the practical utility of the more recently proposed mass spectrometric techniques.

Unfortunately, time was much too short to go into the nitty-gritty details of each of the subjects and one could have easily devoted an entire hour of workshop-time to each of them.

It is planned to have one particular subject for the 1980 ASMS meeting for detailed discussion of the present state of the art. Suggestions regarding the subject are welcomed by the chairman.

Klaus Biemann
Chairman

ASMS COMMITTEE ON SOLIDS AND SURFACE ANALYSIS

Summary of Activities at 27th Annual Conference

- A topical session on the Use of Combined Techniques for Solids Analysis was held on Tuesday afternoon, June 5, 1979. Dr. Charles Evans gave an invited 30-minute lecture introducing and comparing various techniques including AES, SIMS, ISS, and RBS. The session was well attended with a high of 85 and an average of 52 throughout the afternoon.

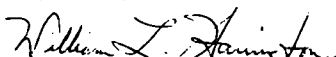
  In order to solicit participation in this session, a letter was sent to about 300 ASMS members and non-members who are associated with solids and surface analysis. I feel that this is an attractive alternate to the symposium format of totally invited speakers. Enough advance planning to include announcement of a topical session in the regular ASMS mailing would be a preferred method to the separate mailing.

- This committee in cooperation with Joan Bursey and the Committee on Environmental Applications co-sponsored a Symposium on the Analysis of Solid Environmental Samples held on Wednesday morning, June 6, 1979. Although details of the symposium will be given in Dr. Bursey's report, this session contained an excellent series of papers and strongly pointed out the need for both organic and solids inorganic mass spectrometry inputs to environmental problems.

- A business meeting and short workshop was held on Wednesday afternoon. The main purpose of the workshop was to provide time for a detailed exchange relating to the topical session on combined techniques. Considering the large amount of solids-related papers at this year's meeting, the workshop was poorly attended with only 15 people. Informal discussions included the following topics:

  (1) energy distributions of sputtered species.
  (2) evaluation of the Cameca IMS 3-F performance,
  (3) the status of laser probe mass spectrometry for solids analysis.

Respectfully submitted,



William L. Harrington
Chairman

ASMS COMMITTEE REPORT

"Qualitative Organic Techniques"
Activities for 1979

This committee sponsored two activities during the 1979 ASMS meeting in Seattle. First, with the considerable efforts of Professors Ralph Dougherty (Florida State) and Mark Green (Clarkson), a symposium entitled "The Chemistry of Ions: Gas Phase and Solution" was organized. The format included a full day of activities divided into an afternoon session on Tuesday devoted to five invited plenary lectures and a morning session on Wednesday consisting of sixteen invited contributions. Presenting the plenary lectures were Professors Brauman (Stanford), Taft (Irvine), McLafferty (Cornell), Arnett (Pittsburgh), and Kebarle (Alberta). Professor L. L. Miller (Minnesota) cancelled at the last minute.

Many favorable remarks were heard concerning the symposium. Particularly successful was the Wednesday morning session which gathered together a number of physical and physical organic chemists who presented papers on the chemistry of ions. A number of diverse techniques, including ICR, Metastable Methods, Flowing Afterglow, Field Ionization Kinetics, MIKES, Collisional Activation, and Electrochemistry, and their application to studies of the properties of gas-phase ions were discussed. The committee chairman recommends that future meetings incorporate a session of this nature devoted to studies of ion chemistry, a theme unifying the efforts of a number of diverse workers in mass spectrometry.

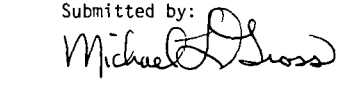
The second activity of this committee was a workshop entitled "Fundamental and Analytical Applications of Metastable Analysis: Where are We?" The program consisted of six short presentations:

SPEAKER	TOPIC
R. G. Cooks Purdue University	"Scope of Applications of MIKES"
F. W. McLafferty Cornell University	"How to Convert Present Spectrometers in Multianalyzer Instruments"
C. G. Enke Michigan State University	"Applications of a Triple Quadrupole Mass Spectrometer"
J. L. Holmes University of Ottawa	"Ion Structure Investigations: The Need for a Combined Approach"
C. N. McEwen E. I. duPont	"Abscissic and Indole Acetic Acid Analysis by MIKES vs. HPLC"
R. Hass NIEHS	"Some Experiences Using MIKES in Environmental Analyses"

Approximately 75 persons attended the workshop which was scheduled from 6 to 7:30 p.m. on Thursday evening.

The chairman is soliciting ideas for committee activities for the 1980 New York meeting. Your suggestions are invited and should be transmitted directly to him.

Submitted by:



Michael L. Gross
Professor
Dept. of Chemistry
University of Nebraska
Lincoln, NE 68588
(402) 472-4792

EDUCATION COMMITTEE

The Education Committee has been involved in three activities during the recent year. A short course was presented at the annual conference, a program for matching organizations wishing to donate a surplus instrument with an academic institution willing to accept such an instrument was readvertised, and the annual committee business meeting was held.

The Education Committee sponsored a short course entitled "Interpretation of Mass Spectra" on June 2 - June 3, 1979 at the Olympic Hotel in Seattle preceeding the 27th Annual Conference. The instructional staff was coordinated by Dr. William Trager and included Dr. Guenther Eigendorf, Dr. William Garland, Dr. David Bowen, Mike Peat and Dr. Larry Bone. The paid enrollment for the course was 33 including 2 participants at a reduced, full-time student rate. Participants were drawn from a wide area including Alaska, Hawaii and England with 27% coming from the Pacific Northwest. In contrast to recent years the majority stayed for the annual conference.

Evaluation of applications for this year's short course revealed that an increasing portion of new people entering the field of mass spectrometry are heavily involved in quantitative work. As a result the curriculum of this year's course was modified to include more quantitative techniques.

This year's instructional staff and the Education Committee recommend that separate courses be offered in Interpretation and Quantitative Techniques at the 28th Annual Meeting. The Northern New Jersey Discussion Group has volunteered to help with the Quantitative course in New York.

Respectfully submitted,

Larry Bone

Larry I. Bone, Chairman

ASMS Committee on Environmental Applications

(XI)

Business Meeting and Workshop

Chairman: Joan T. Bursey
Analytical Sciences Division
Chemistry and Life Sciences Group
Research Triangle Institute
Research Triangle Park, NC 27709

The meeting was opened by Dr. Joan Bursey who called for suggestions for ongoing activities for the Environmental Committee. Dr. Lew Shadoff (Dow) suggested that a directory of laboratories and/or workers in the field of environmental analysis be compiled. No further suggestions were elicited from the floor, and Dr. Bursey suggested that any other ideas be submitted on the questionnaire distributed to those attending the workshop.

The first presentation was made by Dr. D. Lin of Battelle on "Sampling". Each type of sample (gaseous, aqueous, solid) requires separate guidelines. A brisk discussion ensued concerning the problem of certain sampling situations not being amenable to existing guidelines. Although some guidelines exist for certain types of samples (e. g., industrial effluent), there may be difficulty locating them. Dr. D. Jamieson of the NRC (Canada) mentioned guidelines for sampling sea water which should be applicable to some other types of samples.

It was suggested that any attendees who had or know of guidelines for sampling should send the information to:

Lewis Shadoff
Dow Chemical Company
574 Building
Midland, MI 48640

Another area of discussion concerned those aspects of sampling not under the control of the analyst. These often include the sampling site and statistical design of the sampling experiment.

A second presentation was made by Dr. L. Wright of EPA on LC-MS. This concerned the use of the Finnigan moving band apparatus, and some solutions to problems encountered in transporting the effluent on the band. Examples were presented in its use for pesticide analysis.

The last presentation by Dr. K. Tomer of the Research Triangle Institute was on the use of Capillary GC/MS. Comparisions of the performance between packed and capillary columns were made. Some problems encountered in the use of capillary columns were discussed. Discussion following the presentation centered around the interface between the column and the MS, whether via a separator and make-up gas or direct coupling. The injector systems (both split and splitless) were also discussed.

MINUTES OF ASTM COMMITTEE E-14 ON MASS SPECTROMETRY

The annual meeting of ASTM Committee E-14 was held in conjunction with the ASMS meeting on June 5, 1979 at the Olympic Hotel, Seattle, Washington. Prior to the meeting a Board meeting was held which included Chairman, M. C. Hamming, Vice Chairman, Thomas Aczel, Secretary-Treasurer, E. M. Chait and ASTM Staff Manager, Janet Schroeder as well as the Chairman of Sub-Committee E-14.13, T. R. Ashe. The key topic for discussion at the Board meeting was the desire of the board to involve more ASMS members in E-14 activities and to make E-14 more responsive to the current practices of mass spectrometry. At the Board meeting a nominating committee was selected to choose a slate of officers to serve a term from January 1, 1980 to December 31, 1981. Chairman, M. C. Hamming presided over Committee E-14 meeting.

The Secretary-Treasurer report presented by E. M. Chait was approved with correction by T. R. Ashe to approve the fact that Kratos AEI had provided data on both the gas and liquid samples for quantitative analysis.

D-2 COMMITTEE REPORT

The report of ASTM Committee D-2 was presented by T. Aczel. The D-2 Committee decided to reactivate the shale oil analysis task group. Ten samples have been prepared and distributed for the analysis of the separation of coal liquid acids and bases. The Committee also decided to devote attention to heavy hydrocarbon analysis.

NEW BUSINESS ASTM E-14

E. M. Chait discussed the need for long range planning of Committee E-14 activities to provide for a more relevant response for the current needs for the mass spectrometer community since the two standards now in effect have been in existence for some years. It was the feeling of several in the Committee that additional standards were needed. The work of T. R. Ashe and his sub-committee on GC/MS will result in the first of these new standards once the approval cycle and balloting is complete. E. M. Chait suggested additional standards on quantitative mass spectrometry and library searching of mass spectra. M. Storey of Finnigan raised the question of influence of government regulations by ASTM standards. J. Schoeder of ASTM confirmed that, in general, the Government will try to follow established standards from ASTM if they exist and therefore it was within our interest to promote standards for mass spectrometry which could become part of government regulations and avoid arbitrary standards being imposed by government agencies on mass spectrometer analyses. As a result of this discussion it was moved and seconded that a committee on long range planning be formed. M. C. Hamming has chosen E. M. Chait as chairman of this sub-committee which will be designated E-14.91 Committee for Long Range Planning.

It was further suggested during the meeting that a mode of communication should be established with ASMS members to interest them in the activities of E-14 Committee considering that the committee wishes to update its activities in areas that have a broader interest among the ASMS membership.

EVALUATION OF EXISTING STANDARDS

The two standards which exist under ASTM E-14,Practice for Evaluation of Mass Spectrometers for Chemical Analysis and Practice for the Evaluation of Mass Spectrometers for Chemical Analysis of the Solids are being reviewed by W. E. Henderson of Kratos. He will suggest revision of existing standards and any revisions will be submitted by letter ballot for approval of the membership.

REPORT ON THE JOINT SYMPOSIUM ON GC/MS AND SUB-COMMITTEE E-14.13 ON COMBINED GC/MS

T. R. Ashe reported that the joint ASMS E-14 Symposium on GC/MS was very successful, receiving great interest from a large portion of the ASMS membership. Furthermore the meeting Monday, June 4 of the ASTM Committee

E-14.13 was attended by a large number of ASMS and ASTM members alike. A report of this meeting is attached to these minutes.

NOMINATIONS OF OFFICERS

The Nominating Committee made the recommendation that the present slate of officers be renominated for the term January 1, 1980 to December 31, 1981. A letter ballot will be sent from ASTM headquarters for the election of the nominated slate of officers. Due to the recent change of ASTM rules it was necessary to convene the Nominating Committee since the terms of the present officers would have ended July 1, 1979 after they had only served 18 months in their present capacity. Provision is made in the balloting for write-in candidates.

Respectfully submitted,

Edward M. Chait
Secretary-Treasurer

ATTACHMENT I

Minutes of the Meeting of
ASTM Subcommittee E-14.13 on Combined GC/MS

ASTM Subcommittee E-14.13 met Monday, June 4, at 8:00 p.m. in the Georgian Room of the Olympic Hotel, Seattle, Washington. The meeting was chaired by Terry Ashe of Exxon Research and Engineering Company and was attended by approximately 150 people.

The purposes of the subcommittee were summarized by the chairman and encompass standardization, evaluation and general educational activities in the areas of GC/MS instrumentation and methodology.

Thomas Aczel of Exxon Research and Engineering Company briefly explained the activities of Committee E-14 and D-2 and the various levels of participation available within them.

Terry Ashe introduced a "Draft for Standard Recommended Practice for the Evaluation of Combined Gas Chromatography and Mass Spectrometry for Chemical Analysis" for comments. Additional copies of the draft are available from Terry Ashe.

Jacon Shen from SOHIO, Cleveland, volunteered to head a task force to write a terminology and definition recommended practice. This work will possibly extend the excellent work of Sy Meyerson and John Beynon.

The remainder of the subcommittee meeting was arranged with the aid of the Finnigan Institute which we gratefully acknowledge.

Frank Crow of Battelle Columbus gave a presentation on injection modes for capillary GC/MS which covered split, splitless, and on-column injections.

Bill McFadden of Finnigan Instruments gave a presentation on GC/MS interfaces, concentrating on separators for use with packed columns.

The meeting was also attended by all six speakers from the very successful GC/MS symposium, cosponsored by Committee V of ASMS and ASTM E-14, held earlier in the afternoon. They answered several questions from the audience.

The meeting was adjourned by Terry Ashe at 9:53 p.m.

Respectfully submitted,

Thomas Aczel, "ad hoc" recorder

Appendage to the Minutes by T. R. Ashe

ASTM E-14.13 consists of 4 task force groups. These, their scope and chairman are listed below:

- Evaluation of Instrumentation - T. R. Ashe, Exxon Research and Engineering Co., Linden, N.J. 07036. The task force has submitted a draft proposal for an ASTM Standard Recommended Practice.

- Terminology and Definitions - J. Shen, SOHIO, Cleveland, Ohio 44128. The task force will develop a standard set of terms and definitions for GC/MS.

- Alternate Modes of Ionization - M. Storey, Finnigan Instruments, Sunnyvale, Ca. The task force will begin to develop a standard covering chemical ionization.

- Quantitative Analysis - E. Chait, Du Pont Instruments, Wilmington, Delaware 19898. The task force will begin to develop a standard for quantitative analysis by GC/MS.

WORKSHOP

"MS and GCMS Components and Accessories"

Discussions dealing with the availability of components for modification and repair of MS and GCMS equipment took place at a workshop held on Thursday June 7th at 18:00.

During the course of the meeting the number of attendees remained relatively constant at approximately 30 to 35.

There was a noticeable absence of representatives from major instrument manufacturers although some had been invited to attend.

A list of general registers of suppliers was distributed and the following points brought to discussion,

(i) What sources/suppliers does one have for obtaining materials to construct, modify and repair MS and GCMS components.

(ii) How should a newcomer to the field of MS and GCMS go about obtaining information concerning suitable manufacturers and suppliers.

(iii) How does a manufacturer contact new MS users.

(iv) Should an effort be made within ASMS to compose a "masterlist" of manufacturers and suppliers of MS and GCMS components and accessories.

The general feeling among attendees seemed to be that an effort should be made to inform MS users of various services and sources for materials and components utilised in MS instrumentation. The question remained how to go about this and the following suggestions were made,

a) Literature from suppliers could be displayed during manufacturers clinic.

b) Members of ASMS should provide their lists of suppliers during regular poster sessions.

c) Major equipment manufacturers should aid MS users in finding alternate sources for spare parts since it would allow the former to cut down on their long term inventory of spares.

d) ASMS should advertise in suitable journals to encourage more companies to attend the annual meetings or to provide literature for distribution during the meeting.

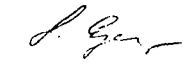
e) Stimulate exchange of information among ASMS members during workshop sessions.

f) Regional discussion groups should be encouraged to participate in above efforts.

Some of the attendees indicated that they would send a list of their suppliers to the workshop chairman.

The Chairman would like to thank the ASMS executive for providing facilities for this workshop.

Respectfully submitted



G.K. Eigendorf
Workshop Chairman

Department of Chemistry
University of British Columbia
Vancouver, B.C. Canada

H B	ABAJIAN	HOFFMANN LA ROCHE	BLDG 71, RM 108	340 KINGSLAND RD	NUTLEY	NJ 07110
L E	ABBEY	CHEMISTRY DEPT	GEORGIA TECH		ATLANTA	GA 30332
R H	ABEL	10337 MILLER AVE			CUPERTINO	CA 95014
R M	ABERNATHEY	120 MONTE REY DR N			LOS ALAMOS	NM 87544
W	ABERTH	2700 SAND HILL RD			MENLO PARK	CA 94025
F P	ABRAMSON	PHARMACOLOGY DEPT	GEORGE WASHINGTON UN		WASHINGTON	DC 20037
T	ACZEL	ER/E	PO BOX 4255		BAYTOWN	TX 77520
D M	ADAMS	20031 N 17 LAN			PHOENIX	AZ 85027
R A	ADAMS	SUITE 100	6650 POWERS FERRY RD		ATLANTA	GA 30331
R	ALBERTI	VARIAN MAT	25 HANOVER RD		FLORHAM PARK	NJ 07932
E D	ALFORD	B/W RES	PO BOX 35090		LOUISVILLE	KY 40232
D	ALKALAY	27 REVERE RD			ARDSLEY	NY 10502
B A	ALLEN,JR	ROUTE 2	PO BOX 268C		BRAZORIA	TX 77422
R H	ALLEN	R H ALLEN CO	PO BOX 27		BOULDER	CO 80306
W N	ALLEN	NRL, CODE 6110			WASHINGTON	DC 20375
J	ALLISON	CHEMISTRY DEPT	STANFORD UNIVERSITY		STANFORD	CA 94305
D L	ALLMAN	11103 COLLEGE			KANSAS CITY	MO 64137
V O	ALTEMOSE	CORNING GLASS WORKS			CORNING	NY 14830
J R	ALTHAUS	NCTR/FDA/DHEW			JEFFERSON	AR 72118
M M	AMES	ONC DEPT	MAYO CLINIC		ROCHESTER	MN 55901
R S	AMPULSKI	PROCTOR & GAMBLE CO	MIAMI VALLEY LAB	PO BOX 39175	CINCINNATI	OH 45239
M	ANBAR	181 HALWILL DR			SNYDER	NY 14226
R	ANDERSON	PCR CHEMICALS	PO BOX 1778		GAINESVILLE	FL 32602
W R	ANDERSON,JR	GRAD CT	19600 NW WALKER RD		BEAVERTON	OR 97005
V G	ANICICH	8036 GRAYSTONE			SUNLAND	CA 91040
E M	ARNETT	211 LYTTON AVE			PITTSBURGH	PA 15213
S	ASANTE-POKU	CHEMISTRY DEPT	CAL STATE UNIV		LOS ANGELES	CA 90032
T R	ASHE	EXXON RES & ENG	PO BOX 121		LINDEN	NJ 07036
D H	AUE	CHEMISTRY DEPT	UNIV OF CALIFORNIA		SANTA BARBARA	CA 93111
J W	AULD	37748 SUNNYDALE			LIVONIA	MI 48154
T	AXENROD	101 CHESTNUT STREET			ENGLEWOOD CLIFFS	NJ 07632
R J	AYERS	1560 E JEFFERSON			DETROIT	MI 48207
L	BACZYNSKYJ	THE UPJOHN CO	301 HENRIETTA		KALAMAZOO	MI 49001
T	BAER	CHEMISTRY DEPT	UNIV NO CAROLINA		CHAPEL HILL	NC 27514
D A	BAFUS	4114 CLOVERNOOK LANE			SEABROOK	TX 77586
T A	BAILLIE	DEPT PHARM CHEMISTRY	UNIV OF CALIFORNIA		SAN FRANCISCO	CA 94143
G L	BALL	109 SO OBSERVATORY	ROOM 1530		ANN ARBOR	MI 48109
J M	BALLARD	CHEMISTRY DEPT	UNIV OF VIRGINIA		CHARLOTTESVILLE	VA 22901
B M	BANSAL	LOCKHEED ELECT CO	1830 NASA RD 1	MAIL CODE C-23	HOUSTON	TX 77058
T L	BARRY	FDA	850 3RD AVE		BROOKLYN	NY 11232
D R	BARTHOLOMEW	G-24 URIS HALL	CORNELL UNIVERSITY		ITHACA	NY 14853
J E	BARTMESS	CHEMISTRY DEPT	INDIANA UNIV		BLOOMINGTON	IN 47405
P J	BARTNER	SCHERING CORP			BLOOMFIELD	NJ 07003
L M	BASS	CHEMISTRY DEPT	UNIV OF CALIFORNIA		SANTA BARBARA	CA 93017
M L	BAZINET	43 CYPRESS RD			NATICK	MA 01760
A J	BEATTIE	E I DUPONT	EXPER STA B256		WILMINGTON	DE 19898
M J	BEATTY	BOX 2226			BATON ROUGE	LA 70821
M D	BECK	360 N CIVIC	APT 508		WALNUT CREEK	CA 94596
D P	BEGGS	HP SCIENTIFIC INSTR	1601 CALIFORNIA AVE		PALO ALTO	CA 94304
R G	BEIMER	TRW SYSTEMS 01/2020	ONE SPACE PARK		REDONDO BEACH	CA 90278
J G	BENDORAITIS	RESEARCH & DEV	MOBIL CORP		PAULSBORO	NJ 08066
D J	BENNETT	FIRESTONE TIRE &	RUBBER CO	S MAIN & WILBETH RD	AKRON	OH 44317
C H	BENNEY	1 STRAWBERRY HILL AV			STAMFORD	CT 06902
R C	BENZ	CHEMISTRY DEPT	CASE WESTERN RESERVE		CLEVELAND	OH 44118
P S	BERGER	TEKNIVENT CORP	9261 OLD BONHOMME RD		ST LOUIS	MO 63132
J	BERKOWITZ	PHYSICS DIV	ARGONNE NATIONAL LAB	9700 S CASS AVE	ARGONNE	IL 60439
L D	BETOWSKI,JR	U S EPA	COLLEGE STATION RD		ATHENS	GA 30605
K	BIEMANN	CHEMISTRY, 56-010	M I T		CAMBRIDGE	MA 02139
M J	BIGLEY	205 W TAUHEY RD			PARK RIDGE	IL 60068
R C	BINIAKEWITZ	65 PROSPECT STREET			STAMFORD	CT 06902

B	N	PRAMANIK	ONE BRADFORD RD			MT VERNON	NY 10553
B	E	BLAISDELL	LINUS PAULING INST			MENLO PARK	CA 94025
C	R	BLAKLEY	CHEMISTRY DEPT	UNIVERSITY HOUSTON		HOUSTON	TX 77004
T	A	BLAZER	E I DUPONT			WILMINGTON	DE 19898
P	A	BLOMBERY	RM 3N 316/BLDG 10	NIH		BETHESDA	MD 20205
G	D	BLUE	PO BOX 183			MARYSVILLE	OH 43040
R	D	BOARD	HP SCIENTIFIC INSTR	1601 CALIFORNIA AVE		PALO ALTO	CA 94304
M	J	BOBENREITHE	NIEHS	PO BOX I2233		RTP	NC 27709
F	M	BOCKHOFF	JET PROPULSION LAB	183-901	4800 OAK GROVE DR	PASADENA	CA 91104
H	G	BOETTGER	5346 N STARDUST RD			LA CANADA	CA 91011
M	R	BOGDAN	320 TOFTREES AV	APT 243		STATE COLLEGE	PA 16801
P	A	BOLAND	SRI INTERNATIONAL	333 RAVENSWOOD AVE		MENLO PARK	CA 94025
L	I	BONE	DOW CHEMICAL CORP	B-1226		FREEPORT	TX 77541
E	J	BONELLI	HP SCIENTIFIC INSTR	1601 CALIFORNIA AVE		PALO ALTO	CA 94304
M	L	BONIN	4115 WINDSOR SP RD			HEPHZIBAH	GA 30815
J	K	BOSTICK	NORTHROP SERVICES			RESEARCH TRIANGLE PK	NC 27709
D	V	BOWEN	CENTRAL SCIENCE LAB	UNION CARBIDE		TARRYTOWN	NY 10591
M	T	BOWERS	CHEMISTRY DEPT	UNIV OF CALIFORNIA		SANTA BARBARA	CA 93106
D	C	BRADFORD	FINNIGAN CORP	845 W MAUDE AVE		SUNNYVALE	CA 94086
J	I	BRAUMAN	CHEMISTRY DEPT	STANFORD UNIVERSITY		STANFORD	CA 94305
P		BREISACHER	AEROSPACE CORP			EL SEGUNDO	CA 90245
F	E	BRIDEN	1305 KNIGHTS WAY			RALEIGH	NC 27609
P	R	BRIGGS	29 AUSTIN LANE			HOLLISTON	MA 01746
R	A	BRITTEN	JET PROPULSION LAB	5143 WHITE OAK AVE		ENCINO	CA 91316
C	L	BROWN	CHEMISTRY DPT	CAL STATE		LOS ANGELES	CA 90032
H	L	BROWN, JR	UTI	325 N MATHILDA		SUNNYVALE	CA 94086
H	W	BROWN	HP SCIENTIFIC INSTR	1601 CALIFORNIA AVE		PALO ALTO	CA 94304
P		BROWN	CHEMISTRY DEPT	ARIZONA STATE UNIV		TEMPE	AZ 85281
W	M	BRUBAKER	1954 HIGHLAND OAKS			ARCADIA	CA 91006
L	E	BRUGGEMAN	ARCO CHEM CO	PO BOX 85		GLENOLDEN	PA 19036
R	J	BRUNI	A D LITTLE INC			CAMBRIDGE	MA 02140
W	F	BRYANT	PO BOX 1710			ROCHESTER	NY 14603
W	L	BUDDE	EPA	26 W ST, CLAIR ST		CINCINNATI	OH 45268
A	M	BUKO	CHEMISTRY DEPT	MCCORMICK RD		CHARLOTTESVILLE	VA 22901
S	N	BULUSU	22 SKYVIEW TERRACE			MORRIS PLAINS	NJ 07950
A	L	BURLINGAME	PHARMCEUTICAL CHEM	UNIV OF CALIFORNIA		SAN FRANCISCO	CA 94143
P	H	BURR	286 S ROOSEVELT AVE			PASADENA	CA 91107
D	G	BURROWS	NORTHWEST & ALASKA	FISHERIES CENTER	2725 MONTLAKE BLVD E	SEATTLE	WA 98112
J	T	BURSEY	RES TRIANGLE INST	CLSD	PO BOX 12194	RESEARCH TRIANGLE PK	NC 27709
M	M	BURSEY	CHEMISTRY DEPT 045A	UNIV NORTH CAROLINA		CHAPEL HILL	NC 27514
K	L	BUSCH	CHEMISTRY DEPT	UNIV NO CAROLINA		CHAPEL HILL	NC 27514
E	D	BUSH	3645 WHITMAN AVE N	#204		SEATTLE	WA 98103
G	F	BUTLER,JR	PPG INDUSTRIES	PO BOX 4026		CORPUS CHRISTI	TX 78408
S	E	BUTTRILL,JR	STANFORD RES INST	RM 204A		MENLO PARK	CA 94025
P	C	CALA-TWAY	MERCK & CO	PO BOX 2000		RAHWAY	NJ 07065
V	J	CALDECOURT	DOW	1603 BLDG		MIDLAND	MI 48640
P	S	CALLERY	UNIV MARYLAND	636 W LOMBARD		BALTIMORE	MD 21201
E	L	CALLIS	ARGONNE NATL LAB	BLDG 200	9700 S CASS AVE	ARGONNE	IL 60439
D		CAMERON	CHEMISTRY DEPT	PURDUE UNIV		WEST LAFAYETTE	IN 47907
J	E	CAMPANA	152 DAVEY LAB			UNIVERSITY PARK	PA 16802
I	M	CAMPBELL	BIOCHEMISTRY DEPT	GSPH, ROOM 605	UNIV OF PITTSBURGH	PITTSBURGH	PA 15261
J	H	CAPPIS	LASL	MS 514		LOS ALAMOS	NM 87544
R	M	CAPRIOLI	MEDICAL SCHOOL	UNIV TEXAS	PO BOX 20708	HOUSTON	TX 77030
E	G	CARLSON	2203 DOROTHY ST			PASADENA	TX 77502
S	A	CARR	ROOM 56-012	MIT		CAMBRIDGE	MA 02139
D	I	CARROLL	21 DEWALT RD			NEWARK	DE 19711
D	I	CARROLL	INST LIPID RESEARCH	BAYLOR COLL MEDICINE	TEXAS MEDICAL CENTER	HOUSTON	TX 77025
G	T	CARTER	8 PRAIRIE AVE			SUFFERN	NY 10901
J	A	CARTER	109 EUCLID CIR			OAK RIDGE	TN 37830
S	J	CARTER	MIT	CHEMISTRY DEPT	ROOM 56-035	CAMBRIDGE	MA 02139

G D CASTILLO	FOOD & DRUG ADM	3032 BRYAN ST		DALLAS	TX	75204
R D CATES	776 MADRONA	APT A		GOLETA	CA	93017
S T CEYER	BLDG 62	U CAL LAWRENCE	BERKELEY LAB	BERKELEY	CA	19720
B CHAIT	500 EAST 63ST #20D			NEW YORK	NY	10021
E M CHAIT	QUILLEN BLDG	CONCORD PLAZA		WILMINGTON	DE	19898
J A CHAKEL	CHEMISTRY DEPT	MICHIGAN STATE UNIV		E LANSING	MI	48824
W S CHAMBERLIN	2183 B 36TH ST			LOS ALAMOS	NM	87544
K Y CHAN	DRUG METABOLISM DEPT	MERRELL LABORATORY		CINCINNATI	OH	45215
P CHANDRASURIN	BURROUGHS WELLCOME			RESEARCH TRIANGLE PK	NC	27709
C CHANG	WRIGHT STATE UNIV	BREHM LAB		DAYTON	OH	45431
Y H CHANG	1830B KING PLACE	FT DETRICK		FREDERICK	MD	21701
L M CHAPMAN	800 N LINDBERGH			ST LOUIS	MO	63166
P CHASTAGNER	SAV RIV LAB	DUPONT		AIKEN	SC	29801
T H CHEN	ARRADCOM, EMD	BLDG 407		DOVER	NJ	07801
E K CHESS	CHEMISTRY DEPT	UNIV OF NEBRASKA	PO BOX 715	LINCOLN	NE	68588
T C CHIANG	JOHNSON & JOHNSON	RESEARCH CENTER	RT 1	NORTH BRUNSWICK	NJ	08903
D M CHINN	HUMAN TOXICOLOGY	UNIV OF UTAH	SKAGGS HALL 38	SALT LAKE CITY	UT	84112
D K CHO	SYNTEX RESEARCH	3401 HILLVIEW AVE		PALO ALTO	CA	94304
N M CHOPRA	N C A&T STATE UNIV			GREENSBORO	NC	27411
F E CHOU	334 OVERBROOK RD			BALTIMORE	MD	21212
R G CHRISTENSEN	9 TULIP DR			GAITHERSBURG	MD	20760
W H CHRISTIE	952 W OUTER DRIVE			OAK RIDGE	TN	37830
M D CHU	JEROME AVE POST OFFC	PO BOX 481		BRONX	NY	10468
L B CHURCHILL	UOP INC	TEN UOP PLAZA	ALGONQUIN/MT PRSPECT	DES PLAINES	IL	60016
H A CLARK	126 E NITTANY AV #13			STATE COLLEGE	PA	16801
K L CLAY	MEDICAL CENTER	4200 E 9TH AVE	UNIV COLORADO	DENVER	CO	80262
A I COHEN	PO BOX 4000	SQUIBB INST MED RES		PRINCETON	NJ	08540
B N COLBY	BOX 1260	SYSTEMS, SCIENCE AND	SOFTWARE	LA JOLLA	CA	92038
K R COMPSON	KRATOS INC	24 BOOKER ST		WESTWOOD	NJ	07675
R L CONRAD	DUPONT	1500 S SHAMROCK		MONROVIA	CA	91012
D C CONWAY	CHEMISTRY DEPT	TEXAS A&M UNIV		COLLEGE STATION	TX	77843
R J CONZEMIUS	1211 GARFIELD AVE			AMES	IA	50010
J C COOK	31 NOYES LAB # 51			URBANA	IL	61801
K D COOK	CHEMICAL SCIENCES	UNIV OF ILLINOIS	44 ROGER ADAMS LAB	MADISON	IL	61801
R G COOKS	CHEMISTRY DEPT	PURDUE UNIVERSITY		WEST LAFAYETTE	IN	47906
R A COOMBS	BLDG 403	SANDOZ INC		E HANOVER	NJ	07936
H T CORY	OREGON GRAD CENTER	19600 NW WALKER RD		BEAVERTON	OR	97005
C E COSTELLO	MIT, 56-029	77 MASS AVE		CAMBRIDGE	MA	02139
R J COTTER	7 AMS			JOHNS HOPKINS UNIV	MD	21205
J E COTTON	2512-102 AVE NE			BELLEVUE	WA	98004
D W CRAWFORD	7725 S WOODWARD AVE	#3-B		WOODRIDGE	IL	60515
A L CRITTENDEN	CHEMISTRY DEPT	BLDG 10	UNIV OF WASHINGTON	SEATTLE	WA	98195
R J CROSS	DEPT OF CHEMISTRY	YALE UNIVERSITY		NEW HAVEN	CT	06520
F W CROW	BATTELLE LABS	505 KING AVE		COLUMBUS	OH	43201
P M CURTIS	BROOKHAVEN NATL LAB			UPTON	NY	11973
R DALSEG	METRO	821 SECOND AVE		SEATTLE	WA	98104
H S DANACEAU	7 BROOKES AVE			GAITHERSBURG	MD	20760
E H DAUGHTREY,JR	NORTHRUP SERVICES	PO BOX 12313		RESEARCH TRIANGLE PK	NC	27709
G D DAVES	OREGON GRAD CENTER	1900 NW WALKER ROAD		BEAVERTON	OR	97005
R DAWE	65 N BROOK LANE			LINDENHURST	IL	60046
J J DECORPO	NAVAL RESEARCH LAB	CODE 6110		WASHINGTON	DC	20375
J A DEFEVER	14469 ELLEN DR			LIVONIA	MI	48154
M L DEINZER	AGRICULTURAL CHEM	OREGON STATE UNIV		CORVALLIS	OR	97331
D C DEJONGH	FINNIGAN INSTITUTE	ATKINSON SQ, BLDG 5	11750 CHESTERDALE	CINCINNATI	OH	45246
J E DELMORE	ANAL DIV, ACC	550 2ND STREET		IDAHO FALLS	ID	83401
B R DEMARK	403 NORTH AVE			NAPERVILLE	IL	60540
C H DEPUY	CHEMISTRY DEPT	UNIV OF COLORADO		BOULDER	CO	80302
F L DEROOS	BATTELLE LABS	505 KING AVE		COLUMBUS	OH	43201
D M DESIDERIO	STOUT NEUROSCIENCE	UNIV TENNESSEE	800 MADISON AVE	MEMPHIS	TN	38163
A J DESTEFANO	PROCTER & GAMBLE CO	PO BOX 39175		CINCINNATI	OH	45247

J	A	DIAZ	1918 SW 155 PL			SEATTLE	WA 98166
D	R	DIFEO	ANAL CHEMISTRY CTR	UNIV TEXAS MED SCH	PO BOX 20708	HOUSTON	TX 77025
C	J	DOOLEY	600 E MERMAID LA			WYNDMOOR	PA 19118
R	J	DOUCET	VACUMETRICS INC	2261-#1 PALMA DR		VENTURA	CA 93003
R	C	DOUGHERTY	CHEMISTRY DEPT	FLORIDA STATE UNIV		TALLAHASSEE	FL 32306
G	R	DUBAY	COLUMBIA NATIONAL	FISHERIES LABORATORY		COLUMBIA	MO 65201
G	F	DUDDING	12-07 G E SILICONES			WATERFORD	NY 12188
W	K	DUHOLKE	THE UPJOHN CO	LOC 7831-233-2		KALAMAZOO	MI 49001
R	C	DUNBAR	CHEMISTRY DEPT	CASE WEST RES UNIV		CLEVELAND	OH 44106
L	P	DUNSTAN	NAT BUREAU STANDARDS	A-355 CHEMISTRY		WASHINGTON	DC 20234
M	N	DURLAND	HP SCIENTIFIC INSTR	1601 CALIFORNIA AVE		PALO ALTO	CA 94304
P	P	DYMERSKI	NY STATE HEALTH DEPT	D250, SOUTH MALL	EMPIRE STATE PLAZA	ALBANY	NY 12201
D	W	EFURD	5424 RAMBLER WAY			SACRAMENTO	CA 95841
J	H	ELAND	PHYSICS DIV, D203	ARGONNE NATIONAL LAB	9700 S CASS AVE	ARGONNE	IL 60439
F	A	ELDER,FRED	237 JUDSON ST			WEBSTER	NY 14580
C	H	ELKINS	STAUFFER CHEMICAL	EAST RESEARCH CENTER		DOBBS FERRY	NY 10522
R	E	ELLEFSON	MRC-MOUND LAB R171			MIAMISBURG	OH 45342
B		ELLIS	HEWLETT PACKARD	ROUTE 41 & STARR RD		AVONDALE	PA 19311
E	M	EMERY	PULLMAN KELLOGG	16200 PARK ROW		HOUSTON	TX 77084
J		ENGELS	348 WAVERLEY #2			MENLO PARK	CA 94025
W	T	ENGELSKIRCHEN	NALCO CHEMICAL CO	6216 W 66TH PLACE		CHICAGO	IL 60638
C	G	ENKE	CHEMISTRY DEPT	MICHIGAN STATE UNIV		E LANSING	MI 48824
T	J	ESKEW	NUCLIDE CORP	642 E COLLEGE AVE		STATE COLLEGE	PA 16801
C	A	EVANS	1670 S AMPHLETT BLVD	SUITE 120		SAN MATEO	CA 94402
J	E	EVANS	E KENNEDY SHRIVER	CTR MENTAL RETARDATN	200 TRAPELO ROAD	WALTHAM	MA 02154
J	V	EVANS	FREDERICK CANCER RES	PO BOX B		FREDERICK	MD 21701
S	L	EVANS	4052 BOYD DR			NASHVILLE	TN 37218
J	R	EYLER	CHEMISTRY DEPT	UNIV OF FLORIDA		GAINESVILLE	FL 32611
H	M	FALES	6502 STONEHAM RD			BETHESDA	MD 20034
F	C	FALKNER	METAB	PFIZER INC		GROTON	CT 06340
F	C	FEHSENFELD	NOAA	ENV RES LABS	RADIO BLDG, 3521	BOULDER	CO 80302
V	J	FEIL	1438 3RD ST N			FARGO	ND 58102
W	D	FELIX	BATTELLE-NW	BLDG 329, AREA 300		RICHLAND	WA 99352
J		FELSHER	KRATOS-AEI	24 BOOKER ST		WESTWOOD	NJ 07675
P	V	FENNESSEY	PEDIATTRICS, MED CTR	UNIV OF COLORADO	4200 E 9TH	DENVER	CO 80220
C	C	FENSELAU	MEDICAL SCHOOL	JOHNS HOPKINS UNIV		BALTIMORE	MD 21205
G	J	FERGUSSON	PERKIN-ELMER CORP	AEROSPACE DIVISION	PO BOX 2801	POMONA	CA 91766
W	J	FIES,JR	155 CHEROKEE WAY			PORTOLA VALLEY	CA 94025
R	E	FINNIGAN	FINNIGAN CORP	845 W MAUDE AVE		SUNNYVALE	CA 94086
W	L	FITE	EXTRANUCLEAR LAB	250 ALPHA DRIVE	PO BOX 11512	PITTSBURGH	PA 15238
R	L	FOLTZ	1736 BERKSHIRE RD			COLUMBUS	OH 43221
H	T	FORD	CONTINENTAL OIL CO	RESEARCH & DEVELOP	PO DRAW 1267	PONCA CITY	OK 74601
J	B	FOREHAND	A H ROBINS CO	1211 SHERWOOD AVE		RICHMOND	VA 23220
G	O	FOSS	980 KIELY BLVD	APT 203		SANTA CLARA	CA 95051
N	G	FOSTER	2719 ROBINWOOD LANE			DENTON	TX 76201
L	E	FOX	THE UPJOHN CO	DEPT 7831-233-2		KALAMAZOO	MI 49001
V	M	FRANCHETTI	1341 BERWIN AVE			KETTERING	OH 45429
T	J	FRANCL	DEPT OF CHEMISTRY	U C IRVINE		IRVINE	CA 92717
D	J	FRANK	LOS ALAMOS SCI LAB	PO BOX 1663, CNC-11	103 CARLSBAD	LOS ALAMOS	NM 87545
J	C	FRANKLIN	141 CUMBERLAND VIEW			OAK RIDGE	TN 37830
J	L	FRANKLIN	CHEMISTRY DEPT	RICE UNIV	PO BOX 1892	HOUSTON	TX 77001
B	A	FRASER	FDA-BOB/DBP	8800 ROCKVILLE PIKE		BETHESDA	MO 20205
W		FRASURE	MEDICAL SCHOOL	ST LOUIS UNIVERSITY	1402 SO GRAND	ST LOUIS	MO 63104
B	S	FREISER	CHEMISTRY DEPT	PURDUE UNIV		WEST LAFAYETTE	IN 47907
N	M	FREW	387 TURTLEBACK RD			MARSTONS MILLS	MA 02648
R	D	FRIESEN	LLL	BOX 808 L-230		LIVERMORE	CA 94550
R		FRISBEE	7159 DEL NORTE DR			GOLETA	CA 93017
M	A	FRISCH	IBM RESEARCH CENTER	PO BOX 218		YORKTOWN HEIGHTS	NY 10598
G	J	FRISONE	GEN TIRE & RUBBER CO	RESEARCH DIV	2990 GILCHRIST RD	AKRON	OH 44305
E	W	FU	CLAIROL INC	2 BLACHLEY		STAMFORD	CT 06902

H	FUJIWARA	MONSANTO CO	800 N LINDBERGH BLVD		ST LOUIS	MO 63166
E K	FUKUDA	DEPT OF CHEMISTRY	U C IRVINE		IRVINE	CA 92717
W	FULLER	1500 SHAMROCK			MONROVIA	CA 91016
P T	FUNKE	E R SQUIBB	PO BOX 4000		PRINCETON	NJ 08540
J H	FUTRELL	CHEMISTRY DEPT	UNIVERSITY OF UTAH		SALT LAKE CITY	UT 84112
P J	GALE	CHEMISTRY DEPT	UNIVERSITY VIRGINIA		CHARLOTTESVILLE	VA 22901
E J	GALLEGOS	CHEVRON	PO BOX 1627		RICHMOND	CA 94804
W A	GARLAND	BIOCHEMISTRY DEPT	HOFFMAN - LA ROCHE		NUTLEY	NJ 07110
E L	GARNER	A25 PHYSICS BLDG	ANALYTICAL CHEMISTRY	NAT BUREAU STANDARDS	WASHINGTON	DC 20234
D A	GARTEIZ	8797 STURBRIDGE			CINCINNATI	OH 45236
M D	GAUL	312 HAYWARD	APT 3		AMES	IA 50010
J	GAVRILOVIC	WALTER C MCCRONE	ASSOC INC	2820 S MICHIGAN	CHICAGO	IL 60616
M L	GAY	328 EAGLE HARBOR SQ			LAUREL	MD 20810
D L	GEIGER	31 S PHILADELPHIA ST			DAYTON	OH 45403
W R	GENTRY	DEPT OF CHEMISTRY	UNIV OF MINNESOTA		MINNEAPOLIS	MN 55455
J N	GERBER	HEWLETT PACKARD	1021 EIGHTH AVE		KING OF PRUSSIA	PA 19406
T E	GESELLE	158 BEACHFIELD DR			BATTLE CREEK	MI 49015
S	GHADERI	BOX 721, HAH	UNIV OF NEBRASKA		LINCOLN	NE 68588
D E	GIBLIN	4526 PRESCOTT			LINCOLN	NE 68506
C E	GIFFIN	JPL 233-202	4800 OAK GROVE DR		PASADENA	CA 91103
L	GILBERT	CVC PRODUCTS	525 LEE RD		ROCHESTER	NY 14603
A B	GIORDANI	240 MONTE VISTA AVE			CHARLOTTESVILLE	VA 22903
G L	GLISH	216-5 NIMITZ DR			WEST LAFAYETTE	IN 47906
M W	GOHEEN	1211 KNOLLWOOD CT			RICHLAND	WA 99352
P C	GOODLEY	MASS SPECTOMETRY CNT	MURRAY STATE UNIV		MURRAY	KY 42071
G W	GOODLOE	034 BROWN LAB			U OF DELAWARE	NEWARK D
R L	GORDON	1014 MARSHALL AVE			RICHLAND	WA 99352
S M	GORDON	CHEM DIV, IITRI	10 W 35 ST		CHICAGO	IL 60616
L A	GORMAN	VARIAN	134 JUNEDALE DR		CINCINNATI	OH 45218
H	GRADE	K-1	GENERAL ELECTRIC		SCHENECTADY	NY 12309
M M	GRADE	GENERAL ELECTRIC	K-1		SCHENECTADY	NY 12345
C S	GRANT	MARTIN MARIETTA CROP	PO BOX 179	MAIL NO T-0483	DENVER	CO 80201
P W	GRAVES	LAKE RD			BROOKFIELD	MA 01506
M A	GRAYSON	427 GLENMEADOW DR			BALLWIN	MO 63011
L A	GREEN	MOBIL RES & DEV CORP	708 UNION RD		MICKLETON	NJ 08056
M M	GREEN	CHEMISTRY DEPT	CLARKSON COLLEGE		POTSDAM	NY 13676
F T	GREENE	MRI	425 VOLKER BLVD		KANSAS CITY	MO 64110
S H	GREENHOUSE	21 OAK TERRACE	APT 1A		SOMERVILLE	NJ 08876
G J	GREENWOOD	224 RESEARCH, BLDG 1	PHILLIPS PETROLEUM		BARTLESVILLE	OK 74003
D A	GRIFFIN	AGRICULTURAL CHEM	OREGON STATE UNIV		CORVALLIS	OR 97331
R D	GRIGSBY	BIOPHYSICS DEPT	TEXAS A&M		COLLEGE STATION	TX 77843
E P	GRIMSRUD	CHEMISTRY DEPT	MONTANA STATE UNIV		BOZEMAN	MT 59715
Q G	GRINDSTAFF	CHEMISTRY DEPT	OKLAHOMA STATE UNIV		STILLWATER	OK 74074
R J	GRITTER	IBM RESEARCH	K42/282		SAN JOSE	CA 95193
G S	GROENEWOLD	720 HAMILTON HALL	U NEB LINCOLN		LINCOLN	NE 68588
J O	GROOMS	450 GOLDEN GATE	PO BOX 36075		SAN FRANCISCO	CA 94102
M L	GROSS	CHEMISTRY DEPT	UNIV OF NEBRASKA		LINCOLN	NE 68588
M F	GROSTIC	THE UPJOHN CO	DEPT 7820		KALAMAZOO	MI 49001
R J	GUIDOBONI	KENNECOTT COPPER			LEXINGTON	MA 02173
J W	GUTHRIE	SANDIA CORP	ORG 2553		ALBUQUERQUE	NM 87185
P L	GUTSHALL	UNIVERSITY OF MO	1110 E 48TH		KANSAS CITY	MO 64110
D L	HACHEY	ARGONNE NATIONAL LAB	9700 S CASS AVE		ARGONNE	IL 60439
W F	HADDON	WESTERN REG LAB	USDA		ALBANY	CA 94710
K	HALPAAP	6535 FANNIN	F-503		HOUSTON	TX 77030
C G	HAMMAR	PHARMACOLOGY DEPT	OHIO STATE UNIV		COLUMBUS	OH 43210
M C	HAMMING	CONOCO, INC			PONCA CITY	OK 74601
M A	HANEY	1030 RUSSELL DRIVE			PORTER	TX 77365
G E	HANSEN	PHARMACOLOGY DEPT	JOHN HOPKINS MED SCH	725 N WOLFE ST	BALTIMORE	MD 21205
L B	HANSEN	2409 NOTTINGHAM DR			GARLAND	TX 75041
W D	HARMAN	UCNC			OAK RIDGE	TN 37830

W L HARRINGTON	RCA LABORATORIES			PRINCETON	NJ 08540
D J HARVAN	NIEHS	PO BOX 12233		RESEARCH TRIANGLE PK	NC 27709
T M HARVEY	PO BOX 2053	FORD RES LAB, 3061		DEARBORN	MI 48121
W HASE	CHEMISTRY DEPT	RM 35	WAYNE STATE UNIV	DETROIT	MI 48202
J R HASS	NIEHS	PO BOX 12233		RESEARCH TRIANGLE PK	NC 27709
F W HATCH	PHILIP MORRIS USA	RESEARCH CENTER	PO BOX 26583	RICHMOND	VA 23261
S E HATTOX	PHARMACOLOGY DEPT	YALE MED SCHOOL		NEW HAVEN	CT 06510
J D HAYS	CHEMISTRY DEPT	CASE WESTERN RESERVE		CLEVELAND	OH 44106
E C HEATH	SCHERING CORP	60 ORANGE		BLOOMFIELD	NJ 07003
D L HEIKES	FDA	1009 CHERRY		KANSAS CITY	MO 64106
R E HEIN	NICOLET INSTRUMENTS	5225 VERONA RD		MADISON	WI 53711
H R HELBIG	MEDICAL SCHOOL	UNIV COLORADO		DENVER	CO 80262
R S HELLER	2413 LILLIAN DR			SILVER SPRING	MD 20902
S R HELLER	EPA, PM218	401 M ST SW, RM 3614		WASHINGTON	DC 20460
R J HELLMANN	PO BOX 39158			CINCINNATI	OH 45239
S T HELLRUNG	MEDICAL SCHOOL	ST LOUIS UNIV	1402 S GRAND	ST LOUIS	MO 63104
H HELM	SRI INTERNATIONAL	106B	333 RAVENSWOOD AVE	MENLO PARK	CA 94025
M J HENCHMAN	CHEMISTRY DEPT	BRANDEIS UNIV		WALTHAM	MA 02154
T R HENDERSON	5609 DON FELIPE CT S			ALBUQUERQUE	NM 87105
R A HEPPNER	LARAMIE ENERGY TECH	UNIVERSITY STATION	PO BOX 3395	LARAMIE	WY 82071
E J HERON	HP SCIENTIFIC INSTR	1601 CALIFORNIA AVE		PALO ALTO	CA 94304
C B HERRIN	1702 QUEENS			PONCA CITY	OK 74601
D HERSCHBACH	DEPT OF CHEMISTRY	HARVARD UNIVERSITY	12 OXFORD ST	CAMBRIDGE	MA 02138
H S HERTZ	NAT BUREAU STANDARDS	A113 CHEMISTRY		WASHINGTON	DC 20234
L F HERZOG	NUCLIDE CORP	642 E COLLEGE AVE		STATE COLLEGE	PA 16801
W B HESS	DUPONT	SAVANNAH RIVER LAB	BLDG 232-H	AIKEN	SC 29801
R J HESSLER	CAMECA	37 BROWNHOUSE RD		STAMFORD	CT 06902
B J HIDY	BATTELLE LABS	505 KING AVE		COLUMBUS	OH 43201
P M HIERL	CHEMISTRY DEPT	KANSAS UNIV		LAWRENCE	KS 66044
M C HIGGINS	MASS SPECTROMETRY LA	UNIV OF WASHINGTON		SEATTLE	WA 98195
C E HIGNITE	VETERANS ADMIN HOSP	4801 LINWOOD BLVD		KANSAS CITY	MO 64128
F D HILEMAN	MONSANTO RES CORP	STATION B BOX 8		DAYTON	OH 45407
D R HILKER	HIGHLAND HILLS	APT 2601		EAST GREENBUSH	NY 12061
J F HILLER	FLEMING BLDG	UNIV OF HOUSTON		HOUSTON	TX 77004
L R HILPERT	NAT BUREAU STANDARDS	RM B-124, BLDG 222		WASHINGTON	DC 20234
H B HINES	1370 AFTON ST	APT 806		HOUSTON	TX 77055
L D HINSHAW	US INDUSTRIAL CHEM	1275 SECTION RD		CINCINATI	OH 45237
B J HODSHON	HOFFMANN-LA ROCHE			NUTLEY	NJ 07110
H T HOFFMAN	AMERICAN CAN CO	PO BOX 50		PRINCETON	NJ 08540
M K HOFFMAN	USDA-FSQS			BELTSVILLE	MD 20705
D H HOLKEBOER	231 WINDCREST DR			CAMILLUS	NY 13031
J F HOLLAND	BIOCHEMISTRY DEPT	MICHIGAN STATE UNIV		EAST LANSING	MI 48824
J S HOLLER	TOXICOLOGY BRANCH	CENTER DISEASE CNTRL		ATLANTA	GA 30333
W F HOLMES	BIOCHEMISTRY DEPT	WASHINGTON UNIV	660 S EUCLID	ST LOUIS	MO 63110
J P HONOVICH	2193 GRANDVIEW #6			CLEVELAND HTS	OH 44106
J J HOPPE	VACUMETRICS INC	2261-#1 PALMA DR		VENTURA	CA 93003
D G HOPPER	SCIENCE APPLICATIONS	4124 LINDEN AVE	SUITE 202	DAYTON	OH 45432
J P HOPPESCH	BORG-WARNER RESEARCH	WOLF & ALGONQUIN RDS		DES PLAINES	IL 60018
E C HORNING	11610 STARWOOD DR			HOUSTON	TX 77024
M G HORNING	INST LIPID RESEARCH	BAYLOR COLL MEDICINE	TEXAS MEDICAL CENTER	HOUSTON	TX 77030
E P HORWITZ	1401 BURR OAK RD			HINSDALE	IL 60521
W N HOWALD	PHARMACEUTICAL SCI	BLDG 20	UNIV OF WASHINGTON	SEATTLE	WA 98195
H E HOWARD	PO BOX 76	UNION OIL		BREA	CA 92621
C R HSIEH	DEPT OF CHEMISTRY	UNIV OF HOUSTON		HOUSTON	TX 77004
C S HSU	EXXON RES & ENGR	P O BOX 121		LINDEN	NJ 07076
W C HUBBARD	SCHOOL OF MEDICINE	VANDERBILT UNIV		NASHVILLE	TN 37232
C E HUDSON	MARINE BIOMEDICAL	200 UNIVERSITY BLVD		GALVESTON	TX 77550
J E HUDSON	CHEMISTRY DEPT	103W WELCH HALL	UNIV OF TEXAS	AUSTIN	TX 78712
B M HUGHES	GULF SOUTH RES INST			NEW ORLEANS	LA
D A HUGHES	VARIAN MAT	26 EAST ST		ANNAPOLIS	MD 21401

C W HULL	1500 S SHAMROCK AVE			MONROVIA	CA 91016
D F HUNT	CHEMISTRY DEPT	UNIV OF VIRGINIA		CHARLOTTESVILLE	VA 22901
J E HUNT	CHEMISTRY DEPT	TEXAS A&M UNIV		COLLEGE STATION	TX 77843
M H HUNT	DOMINION TERRACE 18A	RFD 1	PO BOX 1000	SEQUIM	WA 98382
R L HUNTER	CHEMISTRY DEPT	UNIV CALIFORNIA		IRVINE	CA 92717
T W HUNTER	MONSANTO	T2B	800 N LINDBERG BLVD	ST LOUIS	MO 63166
W T HUNTRESS,JR	SSD	JET PROPULSION LAB		PASADENA	CA 91103
W N HUSE	1500 S SHAMROCK AVE			MONROVIA	CA 91016
C S HWANG	36-10 S UNIV PLACE			STILLWATER	OK 74074
F D HWANG	2927 WINWOOD WAY			SAN JOSE	CA 95122
P HYDE	DEPT BIOCHEMISTRY	L S U SC OF MEDICINE	1542 TULANE AVE	NEW ORLEANS	LA 70112
W G HYDE	VET DIAG LAB	IOWA STATE UNIV		AMES	IA 50011
C R IDLE	CHEMISTRY DEPT	STATE UNIV NEW YORK		STONY BROOK	NY 11794
A J ILLIES	CHEMISTRY DEPT	UNIV OF NEBRASKA		LINCOLN	NE 68588
P IRVING	BALZERS HIGH VACUUM	8 SAGAMORE PARK ROAD		HUDSON	NH 03051
P ISSENBERG	EPPLEY INST	MEDICAL CENTER	UNIV NEBRASKA	OMAHA	NE 68105
R T ITEN	E I DUPONT DENEMOURS	EXPERIMENTAL STATION	E336	WILMINGTON	DE 19898
R H IWAMOTO	940 HENSLEY ST			RICHMOND	CA 94084
T J JACKSON	2122 RICHBROOK			GARLAND	TX 75042
M L JACOBS	490 ORCHARD ST			GOLDEN	CO 80401
I JARDINE	SCHOOL OF PHARMACY	MEDICINAL CHEMISTRY	PURDUE UNIV	WEST LAFAYETTE	IN 47907
B L JELUS	AVON PRODUCTS			SUFFERN	NY 10901
E JENKINS	1617 MAPLE AVE			SALT LAKE CITY	UT 84106
D JEROLAMON	ALLIED CHEMICAL CORP	PO BOX 1021-R		MORRISTOWN	NJ 07960
J V JOHNSON	SCM ORGANICS	PO BOX 389		JACKSONVILLE	FL 3220
R H JOHNSEN	CHEMISTRY DEPT	FLORIDA STATE UNIV		TALLAHASSEE	FL 32306
B M JOHNSON	PFIZER CENTRAL RES			GROTON	CT 06340
R L JOHNSON	5933 FARNGATE RD			RALEIGH	NC 27606
E G JONES	CHEMISTRY DEPT	WRIGHT STATE UNIV		DAYTON	OH 45431
G G JONES	STANDARD OIL INDIANA	PO BOX 400		NAPERVILLE	IL 60540
H C JONES	UNION CARBIDE NUCLR	MS 461	PO BOX P	OAK RIDGE	TN 37830
C M JUDSON	7000 N ROSEMEAD BLVD	APT #12		SAN GABRIEL	CA 91775
G A JUNK	USDOE	AMES LAB	IOWA STATE UNIV	AMES	IA 50010
J D JUSTICE	HP SCIENTIFIC INSTR	1601 CALIFORNIA AVE		PALO ALTO	CA 94304
J R KALASKY	1053 GREENFIELD CIR			STATE COLLEGE	PA 16801
J J KALBRON	MCNEIL LABORATORIES	RD 3	ACORN DRIVE	VINCENTOWN	NJ 08088
R G KALEY,II	800 N LINDBERGH	APT T2F		ST LOUIS	MO 63166
D KALMAN	15233 11TH NE			SEATTLE	WA 98155
L A KAMINSKI	1 TROTTERS TURN			NEWARK	DE 19711
N M KAN	FINNIGAN CORP	6110 EXECUTIVE BLVD		ROCKVILLE	MD 20852
T KAY	419 BOLYSTON AVE E			SEATTLE	WA 98102
S G KAYSER	22 LONGMEADOW RD			WESTBORO	MA 01581
G L KEARNS	58 BUCKINGHAM DR			STAMFORD	CT 06902
G W KEEN	CONOCO	1000 S PINE		PONCA CITY	OK 74601
J A KELLEY	DRUG DESIGN-CHEMICAL	NIH, NCI	BLDG 37, RM 6D-23	BETHESDA	MD 20014
P E KELLEY	FINNIGAN CORP	845 W MAUDE AVE		SUNNYVALE	CA 94086
D L KEMP	UNION CARBIDE CORP			BOUND BROOK	NJ 08805
P R KEMPER	CHEMISTRY DEPT	UNIV OF CALIFORNIA		SANTA BARBARA	CA 93106
C N KENYON	HEWLETT PACKARD	1601 CALIFORNIA AVE		PALO ALTO	CA 94304
T W KEOUGH	1416 LONGACRE DRIVE			CINCINNATI	OH 45240
E G KERFOOT	13483 W OREGON CT			LAKEWOOD	CO 80228
J K KHANDELWAL	MT SINAI MED SCHOOL	PHARMACOLOGY DEPT	100 ST AND 5TH AVE	NEW YORK	NY 10029
E KILBERG	PILLSBURY CORP	311 2ND ST SE		MINNEAPOLIS	MN 55414
M S KIM	CHT	38 SKAGGS HALL	UNIV OF UTAH	SALT LAKE CITY	UT 84112
B J KIMBLE	RADIOBIOLOGY LAB	UNIV OF CALIF-DAVIS		DAVIS	CA 95616
G KING	956 MARINE ST			BOULDER	CO 80302
J D KING	PO BOX 25046	MS977 DFC		DENVER	CO 80225
J W KING	NATL CENTER TOX RES			JEFFERSON	AR 72079
R W KING	CHEMISTRY DEPT	UNIV OF FLORIDA		GAINESVILLE	FL 32611
R D KINSER	PHILIP MORRIS USA	RESEARCH CENTER	PO BOX 26583	RICHMOND	VA 23261

J A KINSINGER	RALTECH SCIENTIFIC	PO BOX 7545		MADISON	WI	53719
M C KIRK	K-MEYER LAB	2000 NINTH AV S	SRI	BIRMINGHAM	AL	35205
R W KISER	781 GLENDOVER ROAD			LEXINGTON	KY	40502
F G KITSON	3 HARTFORD PLACE			NEWARK	DE	19711
D R KNAPP	PHARMACOLOGY DEPT	MED UNIV SO CAROLINA		CHARLESTON	SC	29403
M M KNIGHT	WEYERHAEUSER CO			TACOMA	WA	98401
R L KNIGHTS	CHEMISTRY DEPT	UNIV OF WASHINGTON		SEATTLE	WA	98195
J M KNOX	1011 FETTERMAN			LARAMIE	WY	82070
T P KNUDSEN	FINNIGAN CORP	845 W MAUDE AVE		SUNNYVALE	CA	94086
G L KOCHANNY,JR	705 E ST ANDREWS			MIDLAND	MI	48640
M G KOLOR	GENERAL FOODS	555 BROADWAY		TARRYTOWN	NY	10591
R A KORNFELD	PMRC	PO BOX 26583		RICHMOND	VA	23261
M E KOSLIN	450 W FOOTHILL	APT 66		POMONA	CA	91767
T KRICK	BIOCHEMISTRY DEPT	UNIV MINNESOTA		ST PAUL	MN	55108
T KRISHNAMURTHY	JTC ENVIRONMENTAL	CONSULTANTS, INC	7979 OLD GEORGETOWN	BETHESDA	MD	20014
D W KUEHL	6201 CONGDON BLVD			DULUTH	MN	55804
P S KULKARNI	CHEMISTRY DEPT	HAMILTON HALL	UNIV OF NEBRASKA	LINCOLN	NE	68588
E A KURZ	GALILEO	ELECTRO-OPTICS	GALILEO PK	STURBRIDGE	MA	01518
L KURZWEG	EXTRANUCLEAR LAB	250 ALPHA DR		PITTSBURGH	PA	15238
L E LAFLEUR	ENG EXPT STN	OREGON STATE UNIV		CORVALLIS	OR	97331
C R LAGERGREN	2110 HOWELL AVE			RICHLAND	WA	99352
S T LAI	PO BOX 2832	STATION A		CHAMPAIGN	IL	61820
J LAKE	E P A			NARRAGANSETT	RI	02882
L LAMPARSKI	755 E OLSON			MIDLAND	MI	48640
F W LAMPE	150 DAVEY	PENNSYLVANIA STATE U		UNIVERSITY PARK	PA	16802
D W LATER	333 W 400 N			PROVO	UT	84601
R P LATTIMER	B F GOODRICH R & D	9921 BRECKSVILLE RD		BRECKSVILLE	OH	44141
R K LATVEN	DEPT OF CHEMISTRY	MICHIGAN STATE U		E LANSING	MI	48823
P Y LAU	CHEMISTRY DEPT	LITTON BIONETICS INC	5516 NICHOLSON LANE	KENSINGTON	MD	20795
M T LAUG	ARGONNE NATIONAL LAB	PO BOX 2528		IDAHO FALLS	ID	83401
A LAVANCHY	77E ESCONDIDO VLLG			STANFORD	CA	9430
D L LAWRENCE	10826 WEST RD			HARRISON	OH	45030
J O LAY,JR	CHEMISTRY DEPT	UNIV OF NEBRASKA		LINCOLN	NE	68502
J LAZAR	1006 N MONROE ST			WILMINGTON	DE	19801
E B LEDFORD	CHEMISTRY DEPT	HAMILTON HALL, B-30	UNIV OF NEBRASKA	LINCOLN	NE	68510
A M LEGRAND,JR	886 TRAILMORE CIRCLE			SUMTER	SC	29150
T J LEIKER	UNIV COLORADO	MEDICAL CENTER	4200 E 7TH AVE	DENVER	CO	80220
F D LEIPZIGER	KENNECOTT COPPER LAB			LEXINGTON	MA	02173
F LEMUNYON	4414 NW 79TH TERRACE			KANSAS CITY	MO	64151
N B LEV	DEPT OF CHEMISTRY	CWRU		CLEVELAND	OH	44118
M I LEVENBERG	ABBOTT LABS	DEPT 417		NORTH CHICAGO	IL	60064
S LEWIS	SPACE SCIENCES LAB	UNIV OF CALIFORNIA		BERKELEY	CA	94720
W T LEWIS	MOBIL CHEMICAL CO	PO BOX 240		EDISON	NJ	08817
S G LIAS	NAT BUREAU STANDARDS			WASHINGTON	DC	20234
J G LIEHR	ANAL CHEMISTRY	UTHSC	PO BOX 20708	HOUSTON	TX	77005
W V LIGON	PO BOX 8	K1-2A-40		SCHENECTADY	NY	12309
D C LIN	BATTELLE LABS	505 KING AVE		COLUMBUS	OH	43201
K C LIN	325 N MATHILDA AVE			SUNNYVALE	CA	94086
P H LIN	RADIAN CORP	PO BOX 9948		AUSTIN	TX	78766
S N LIN	UNIV OF TEXAS	MED AT HOUSTON	ANAL CHEM CTR	HOUSTON	TX	77025
Y Y LIN	BIOCHEMISTRY DEPT	MEDICAL BRANCH	UNIV TEXAS	GALVESTON	TX	77550
K A LINCOLN	2016 STOCKBRIDGE AVE			REDWOOD CITY	CA	94061
J F LITTON	OCC RES	PO BOX 19601		IRVINE	CA	92713
N LIU	2545 THE MALL			HONOLULU	HI	96822
H A LLOYD	NIH	BLDG 10, RM 7N-312		BETHESDA	MD	20014
M J LOCKE	CHEMISTRY DEPT	UNIV OF CALIFORNIA		IRVINE	CA	92717
V LOPEZ-AVILA	CHEM ENG 66-525	MIT		CAMBRIDGE	MA	02139
E R LORY	CHEMISTRY DEPT	CORNELL UNIVERSITY		ITHACA	NY	14853
E D LOUGHRAN	MS 920	LASL	PO BOX 1663	LOS ALAMOS	NM	87544
P R LOY	PO BOX 105005			ATLANTA	GA	30348

H E	LUMPKIN	PO BOX 4255	EXXON R/E		BAYTOWN	TX 77520
P A	LYON	CHEMISTRY DEPT	UNIV OF NEBRASKA		LINCOLN	NE 68588
J L	MACDONALD	3RS RALSTON PURINA			ST LOUIS	MO 63188
R D	MACFARLANE	CHEMISTRY DEPT	TEXAS A&M		COLLEGE STATION	TX 77843
M H	MACH	AEROSPACE CORP			LOS ANGELES	CA 90009
R J	MADDEN	DEPT MEDICINAL CHEM	ROOM 311A	UNIV OF UTAH	SALT LAKE CITY	UT 84112
P	MAHADEVAN	AEROSPACE CORP			EL SEGUNDO	CA 90245
V K	MAHAJAN	1218 TICONDEROGA			CHESTERFIELD	MO 63017
N H	MAHLE	574 BLDG	DOW CHEMICAL CO		MIDLAND	MI 48640
K	MAHLER	2800 LONGHORN BLVD	#104		AUSTIN	TX 78759
J J	MANNION	PO BOX 348	DIAMOND SHAMROCK CO		PAINESVILLE	OH 44077
R	MARCUS	CAL INST TECH	331 S HILL		PASADENA	CA 91106
S P	MARKEY	NIMH	NIH	BLDG 10, RM 2D-46	BETHESDA	MD 20014
T D	MARRIOTT	CHEMISTRY DEPT	RICE UNIV		HOUSTON	TX 77001
P G	MARSH	B F STOLINSKY RES LB	UNIV OF COLORADO	4200 E NINTH AVE	DENVER	CO 80262
D J	MARSHALL	PO BOX 315			ACTON	MA 01720
D P	MARTINSEN	5 SUGARLOAF CT	APT T-1		BALTIMORE	MD 21209
F C	MASELES	103 WELCH	UNIV OF TEXAS		AUSTIN	TX 78712
I J	MASSEY	SYNTEX RESEARCH	3401 HILLVIEW AVE		PALO ALTO	CA 94304
T	MASUOKA	5801 TANGERMAN TERR	#20		LINCOLN	NE 68505
W R	MATHEWS	1685 GARFIELD #10			DENVER	CO 80206
S M	MATSUSHITA	AMERICAN CYANAMID	PO BOX 400		PRINCETON	NJ 08540
D E	MATTHEWS	METABOLIC DIV	SCHOOL OF MEDICINE	WASHINGTON UNIV	ST LOUIS	MO 63110
M	MAUTNER	ROCKEFELLER UNIV			NEW YORK	NY 10021
R J	MAY	1048 WAVERLY PL			SCHENECTADY	NY 12308
D R	MCADAMS	EXXON CORP	RESEARCH & DEVELOP	PO BOX 2226	BATON ROUGE	LA 70821
M J	MCADAMS	203 OAK DRIVE			LAKE JACKSON	TX 77566
D J	MCADOO	62 LE BRUN COURT W			GALVESTON	TX 77551
M W	MCCAMAN	CITY OF HOPE MED CEN			DUARTE	CA 91010
E R	MCCARTHY	ALLIED CHEMICAL CORP	PO BOX 1021-R		MORRISTOWN	NJ 07950
J A	MCCLOSKEY	BIOPHARMACEUTICAL	SCIENCES DEPT	UNIV UTAH	SALT LAKE CITY	UT 84112
C R	MCCLURE	845 W MAUDE			SUNNYVALE	CA 94086
G A	MCCLUSKY	FREDERICK CANCER RES	BLDG 538	PO BOX B	FREDERICK	MD 21701
J M	MCCREA	PO BOX 172			MONROEVILLE	PA 15146
K E	MCCULLOH	NAT BUREAU STANDARDS			WASHINGTON	DC 20234
C N	MCEWEN	24 COACHLIGHT CT			NEW CASTLE	DE 19720
M J	MCEWAN	J P L	4800 OAK GROVE DR		PASADENA	CA 91103
W H	MCFADDEN	FINNIGAN CORP	845 W MAUDE AVE		SUNNYVALE	CA 94086
D C	MCGILVERY	CORNELL UNIVERSITY	BAKER LAB	PO BOX 241	ITHACA	NY 14850
J H	MCGLOTTEN	SCHERING CORP			BLOOMFIELD	NJ 07003
D J	MCINTOSH	INST MARINE SCI	UNIV OF ALASKA		FAIRBANKS	AK 99701
R T	MCIVER	CHEMISTRY DEPT	UNIV OF CALIFORNIA		IRVINE	CA 92717
L W	MCKEEN	3500 GRAYS FERRY AVE			PHILADELPHIA	PA 19146
M C	MCKEOWN	EXTRANUCLEAR LAB	250 ALPHA DRIVE	PO BOX 11512	PITTSBURGH	PA 15238
C R	MCKINNEY	303 WOODACRE LN			MONROVIA	CA 91016
F W	MCLAFFERTY	CHEMISTRY DEPT	CORNELL UNIV		ITHACA	NY 14853
C J	MCNEAL	CHEMISTRY DEPT	TEXAS A & M UNIV		COLLEGE STATION	TX 77843
J H	MCREYNOLDS	DEPT BIOPHYS SCIENCE	SCHOOL OF MEDICINE	118 CARY HALL	BUFFALO	NY 14214
R D	MEAD	JILA	UNIV OF COLORADO		BOULDER	CO 80309
T E	MEAD	1937 W MAIN ST			STAMFORD	CT 06904
K A	MEDE	UNION CARBIDE CORP	PO BOX 8361		SOUTH CHARLESTON	WV 25303
J M	MEE	HENKE HALL	UNIV OF HAWAII		HONOLULU	HI 96822
H H	MEHNERT	ISOT GLG	US GEOLOGICAL SURVEY		DENVER	CO 80225
G G	MEISELS	CHEMISTRY DEPT	HAMILTON HALL	UNIV NEBRASKA	LINCOLN	NE 68588
A	MELERA	HP SCIENTIFIC INSTR	1601 CALIFORNIA AVE		PALO ALTO	CA 94304
G L	MERRILL,JR	4228 CHURCHILL DR			PLEASANTON	CA 94566
C	MERRITT,JR	CHEMISTRY, FSL	US ARMY NATICK LABS		NATICK	MA 01760
J A	MESCHER	UNIV DAYTON RES INST			DAYTON	OH 45469
J A	MICHNOWICZ	HP SCIENTIFIC INSTR	1601 CALIFORNIA AVE		PALO ALTO	CA 94304
B S	MIDDLEDITCH	DEPT BIOPHYS SCIENCE	UNIV HOUSTON		HOUSTON	TX 77004

R M MILBERG	CHEMISTRY DEPT	31NL	UNIV ILLINOIS	URBANA	IL	61801
D MILLER	MONTANA STATE UNIV			BOZEMAN	MT	59715
D J MILLER	D O E GFETC			GRAND FORKS	ND	58201
D L MILLER	DEPT OF CHEMISTRY	U OF NEBRASKA		LINCOLN	NE	68588
G W MILNE	LC-NHLBI	10-7N318	NAT INSTS OF HEALTH	BETHESDA	MD	20014
B H MIN	HOFFMANN LA ROCHE			NUTLEY	NJ	07450
R D MINARD	152 DAVEY LAB			UNIVERSITY PARK	PA	16802
R F MINER	1500 S SHAMROCK			MONROVIA	CA	91016
D M MINTZ	FINNIGAN CORP	845 W MAUDE AVE		SUNNYVALE	CA	94086
S R MISSLER	BIOPHYSICAL SCI DEPT	UNIV OF HOUSTON	3423 CAMPBELL	HOUSTON	TX	77080
R K MITCHUM	NATIONAL CENTER FOR	TOXICOLOGICAL RESRCH	BIOANALYTICAL	JEFFERSON	AR	72079
K MIYASHITA	LINUS PAULING INST	SCI & MED	2700 SAND HILL RD	MENLO PARK	CA	94025
G J MOL	IBM	1662 PUERTO VALLARTA		SAN JOSE	CA	95120
J G MONCUR	FINNIGAN CORP	845 W MAUDE AVE		SUNNYVALE	CA	94086
K R MONSON	BIOMEDICAL RES LAB	ICI AMERICAS INC		WILMINGTON	DE	19897
F E MONTGOMERY,JR	INST LIPID RESEARCH	BAYLOR COLL MEDICINE	TEXAS MEDICAL CENTER	HOUSTON	TX	77030
A MOORE	PO BOX 269	MARATHON OIL CO		LITTLETON	CO	80210
T F MORAN	CHEMISTRY DEPT	GEORGIA TECH		ATLANTA	GA	30332
W R MORGAN	EXTRANUCLEAR LABS	PO BOX 11512		PITTSBURGH	PA	15238
W J MORRIS	RM 500 US CUSTOMS	19TH ST STOUT ST		DENVER	CO	80016
J MOSELEY	SRI - 106B			MENLO PARK	CA	94025
S L MUELLER	ABBOTT LABS	D-417		NORTH CHICAGO	IL	60064
I K MUN	BAKER LAB	PO BOX 231	CORNELL UNIV	ITHACA	NY	14853
D J MUNCH	US EPA	RM 116	5555 RIDGE AV	CINCINNATI	OH	45268
B MUNSON	CHEMISTRY DEPT	UNIV DELAWARE		NEWARK	DE	19711
T O MUNSON	US EPA	ANNAPOLIS SCI CTR		ANNAPOLIS	MD	21401
D L MUSGRAVE	INST OF MAN SCIENCE	UNIV OF ALASKA		I FAIRBANKS	AK	99701
B D MUSSELMAN	1120 COMMERCE AVE			UNION	NJ	07083
Y NAITO	JEOL CORP	(A1) 235 BIRCHWOOD		CRANFORD	NJ	07016
K NAKAMURA	ARGONNE NATIONAL LAB	BIOMEDICAL DIV	9700 S CASS AVE	ARGONNE	IL	60439
N NARASIMHACHARI	PSYCHIATRY AND	PHARMACOLOGY DEPT	MEDICAL COLL OF VA	RICHMOND	VA	23298
B NAYAR	USC PSC	1985 ZONAL AVE		LOS ANGELES	CA	90033
S D NELSON	PHARMACEUT SCIENCES	BLDG 20	UNIV OF WASHINGTON	SEATTLE	WA	98195
R S NEWBURY	LLL	BOX 808, L-232		LIVERMORE	CA	94550
A S NEWTON	1665 THOUSAND OAKS			BERKELEY	CA	94707
J C NEWTON	LLL	BOX 808, L-325		LIVERMORE	CA	94550
K T NG	CIBA-GEIGY CORP			ARDSLEY	NY	10502
M L NGUYEN	141-4 THORN LA			NEWARK	DE	19711
M G NISHIOKA	411 DENSON AVE SW			CULLMAN	AL	35055
D R NORDLUND	MAGIE 7S			PRINCETON	NJ	08540
E J NORMAN	1044 SUNWOOD CT			CINCINNATI	OH	45231
J G NOWLIN	BAYLOR COL OF MED	9626 JUDALON		HOUSTON	TX	77063
J L OCCOLOWITZ	CHEMISTRY RESEARCH	ELI LILLY	PO BOX 618	INDIANAPOLIS	IN	46206
R W ODOM	2535 CLAIRE CT			MOUNTAIN VIEW	CA	94043
A D ODONNELL	9216 S HOYNE AVE			CHICAGO	IL	60620
M J OHARE	USV PHARMACEUTICAL			TUCKAHOE	NY	10707
R G OLDHAM	RADIAN CORPORATION	PO BOX 9948		AUSTIN	TX	78766
G I OUCHI	FINNIGAN CORP	845 W MAUDE AVE		SUNNYVALE	CA	94086
R P PAGE	400 E SIBLEY BLVD			HARVEY	IL	60426
S L PALLANTE	PHARMACOLOGY DEPT	JOHNS HOPKINS MED	725 N WOLFE ST	BALTIMORE	MD	21205
C A PALMER	7 EMBARCADEN WEST	APT 317		OAKLAND	CA	94607
R J PANCIROV	10 SHADY LAWN DR			MADISON	NJ	07940
J PAO	HOFFMANN-LAROCHE INC			NUTLEY	NJ	07110
D PARENT	DEPT OF CHEMISTRY	UNIV OF CALIFORNIA		SANTA BARBARA	CA	93106
C E PARKER	PO BOX 232	ROUTE 3		APEX	NC	27502
A C PARR	PHYSICS DEPT	PO BOX 1921		UNIVERSITY	AL	35486
N H PARSONS	GENERAL ELECTRIC CO	PO BOX 11508	N D DEPT	ST PETERSBURG	FL	33733
J R PATEL	CENTER FOR	BIO-ORGANIC STUDIES	UNO LAKESHORE	NEW ORLEANS	LA	70122
T A PATTERSON	EXTRANUCLEAR LAB	250 ALPHA DRIVE	PO BOX 11512	PITTSBURGH	PA	15238
P J PAULSEN	NAT BUREAU STANDARDS	ROOM A25, BLDG 221		WASHINGTON	DC	20234

M D PEDLEY	6521 CORDOBA #17			GOLETA	CA	93017
G L PEELE	VACUMETRICS INC	2261-#1 PALMA DRIVE		VENTURA	CA	93003
R E PERRIN	LASL	UNIV OF CALIFORNIA	MAILSTOP 514	LOS ALAMOS	NM	87545
D L PERRY	GULF SOUTH RES INST			NEW ORLEANS	LA	70126
B A PETERSEN	BATTELLE LABS	505 KING AVE		COLUMBUS	OH	43214
C D PFAFFENBERGER	3301 N E 5TH AVE	#1107		MIAMI	FL	33137
B F PHILLIPS	PHYSICAL ELECTRONICS	INDUSTRIES	6509 FLYING CLOUD DR	EDEN PRAIRIE	MN	55344
C R PHILLIPS	FINNIGAN CORP	845 W MAUDE AVE		SUNNYVALE	CA	94086
M P PHILLIPS	1300 30TH ST	#B4-23		BOULDER	CO	80010
A J PIRONE	10 KENLEIGH CT			WILMINGTON	DE	19808
M O POEPPEL	AMERICAN CYANAMIDE	PO BOX 400		PRINCETON	NJ	08540
S K POLLACK	CHEMISTRY DEPT	UNIV OF CALIFORNIA		IRVINE	CA	92717
C W POLLEY,JR	CHEMISTRY DEPT	UNIV NEBRASKA		LINCOLN	NE	68588
B T POON	WALTER REED ARMY	INST OF RESEARCH	EXPTL THERAPEUTICS	WASHINGTON	DC	20012
M E POWELL	1124 COLUMBIA ST			SEATTLE	WA	98104
M L POWELL	PHARMACEUTICAL SCI	UNIV OF WASHINGTON		SEATTLE	WA	98195
P C PRICE	TECHNICAL CENTER	UNION CARBIDE	PO BOX 8361	SO CHARLESTON	WV	25303
J F PRINCE	8231 HOLLY OAK ST			CITRUS HEIGHTS	CA	95610
D G PRITCHARD	MICROBIOLOGY DEPT	UNIV OF ALABAMA		BIRMINGHAM	AL	35294
S RABINOVITCH	12530 42 AVE NE			SEATTLE	WA	98195
G RADOLOVICH	7611 TERRACE ST			KANSAS CITY	MO	64110
T P RADUS	BROOKHAVEN NATL LAB			UPTON, LI	NY	11973
L RAFTOGIANIS	FINNIGAN CORP	845 W MAUDE AVE		SUNNYVALE	CA	94086
L G RANDALL-FRANK	B-537 UNIV VILLAGE			SALT LAKE CITY	UT	84108
C E RECHSTEINER,JR	2906 STEARNS HILL RD			WALTHAM	MA	02154
J R REEHER	FINNIGAN CORP	845 W MAUDE AVE		SUNNYVALE	CA	94086
V N REINHOLD	HARVARD MEDICAL SCH	LHRRB	45 SHATTUCK ST	BOSTON	MA	02115
R W REISER	DUPONT EXPERTL STN	BIOCHEMISTRY DEPT	BLDG 324	WILMINGTON	DE	19898
D K REMLING	8111 LONGMEADOW			WEST CHESTER	OH	45069
M E RENNEKAMP	MS LAB	ASHLAND OIL INC	PO BOX 2458	COLUMBUS	OH	43216
T P REYNOLDS	PO BOX 314			BETHEL	CT	06801
H L RHODES	US BUREAU OF MINES	HELIUM OPERATION	PO H4375 HERRING PLZ	AMARILLO	TX	79101
R C RHODES	818 FOREST LAKE DR			SEABROOK	TX	77586
R E RHODES	RESEARCH LABS	MERCK SHARP & DOHME		WEST POINT	PA	19486
D P RIDGE	CHEMISTRY DEPT	UNIV OF DELAWARE		NEWARK	DE	19711
A RITZER	GENERAL ELECTRIC	SILICONE PROD DEPT		WATERFORD	NY	12188
D J RIZZO	GENERAL FOODS CORP	555 SO BROADWAY		TARRYTOWN	NY	10591
J A ROACH	FDA. HFF-144	200 C ST SW		WASHINGTON	DC	20204
J ROBOZ	123 PHELPS AVE			CRESSKILL	NJ	07626
H J RODEN	DUPONT	1500 SO SHAMROCK		MONROVIA	CA	91016
A M RODRIGUES	FINNIGAN CORP	10347 VISTA KNOLL BL		CUPERTINO	CA	95014
C F RODRIGUEZ	PO DRAWER 28510			SAN ANTONIO	TX	78284
D K ROHRBAUGH	125 ST PAUL ST			BROOKLINE	MA	02146
W K ROHWEDDER	205 CHATEAU TOURAINE	3900 N STABLE COURT		PEORIA	IL	61614
D J ROKOP	208 DOS BRAZOS			LOS ALAMOS	NM	87544
A E ROSECRANCE	PO BOX 1620			LA JOLLA	CA	92101
H ROSELIUS	35 BROOKLYN MT RD			HOPATCONG	NJ	07843
R T ROSEN	FMC CORP	PO BOX 8		PRINCETON	NJ	08540
H M ROSENSTOCK	CHEMICAL THERMO DIV	NAT BUREAU STANDARDS		WASHINGTON	DC	20234
D ROSENTHAL	RTI	PO BOX 12194		RESEARCH TRIANGLE PK	NC	27709
S M ROTHSTEIN	CVC	525 LEE		ROCHESTER	NY	14603
S ROTTSCHAEFER	1195 HART LANE			HARTSVILLE	PA	18974
K L ROWLAND	NCTR			JEFFERSON	AR	72079
T A ROY	ANAL ENVIRON CHEM	BATTELLE LABS	505 KING AVE	COLUMBUS	OH	43201
M A RUDAT	CENTRAL RES DEPT	EXPERIMENTAL STA	228/101	WILMINGTON	DE	19898
D H RUSSELL	UNION CARBIDE CORP	NUCLEAR DIVISION	PO BOX X	OAK RIDGE	TN	37830
J F RYAN	GSRI	PO BOX 26518		NEW ORLEANS	LA	70186
P W RYAN	CHEMISTRY DEPT	COLORADO STATE UNIV		FORT COLLINS	CO	80523
R J RYBA	STANDARD OIL CO(IND)			NAPERVILLE	IL	60540
F E SAALFELD	CODE 6100	NAVAL RESEARCH		WASHINGTON	DC	20375

R N	SAMDAHL	4130 BEEBE CIR			SAN JOSE	CA 95121
P C	SAMSON	112 E BARRETT LANE			SCHAUMBURG	IL 60193
R A	SANDERS	1900 WILTSHIRE BLVD			*FAIRFIELD*	*OH 45014*
G L	SANTEE	150 BELMEADE RD			ROCHESTER	NY 14617
M	SAPOROSCHENKO	PHYSICS DEPT	SOUTHERN ILLINOIS U		CARBONDALE	IL 62901
F G	SATKIEWICZ	JOHN HOPKINS UNIV	APL	JOHNS HOPKINS RD	LAUREL	MD 20810
M D	SCAMUFFA	ABBOTT LABS	ABBOTT PARK	D-417 AP-9	NO CHICAGO	IL 60064
R F	SCARR	UNION CARBIDE	PO BOX 6056		CLEVELAND	OH 44101
J	SCBBATINI	STOUT NEUROSCIENCE	324 BOWLD HOSPITAL		MEMPHIS	TN 38163
T A	SCHEHL	4400 LONGBOW DR			TITUSVILLE	FL 32780
S E	SCHEPPELE	US DEPT OF ENERGY	PO BOX 1398		BARTLESVILLE	OK 74003
C E	SCHMIDT	*PITT ENERGY RESEARCH*	*4800 FORBES AVE*		PITTSBURGH	PA 15213
W C	SCHNUTE	IMMUNOLOGY DEV	CITY OF HOPE MED CTR		DUARTE	CA 91010
D A	SCHOELLER	UNIV CHICAGO	BH-BOX 243		CHICAGO	IL 60637
A E	SCHOEN	CHEMISTRY DEPT	PO BOX 737	PURDUE UNIV	WEST LAFAYETTE	IN 47907
D M	SCHOENGOLD	2305 EASTON			RICHLAND	WA 99352
J R	SCHROEDER	ASTM	1916 RACE ST		*PHILADELPHIA*	*PA 19103*
J N	SCHROEPFER	3M COMPANY	3M CENTER	BLDG 201-1W	ST PAUL	MN 55101
L R	SCHRONK	BIOCHEMISTRY DEPT	TEXAS A & M		COLLEGE STATION	TX 77843
D	SCHUETZLE	SCIENTIFIC RES S3061	FORD MOTORS	PO BOX 2053	DEARBORN	MI 48033
K E	SCHWARZ	HP SCIENTIFIC INSTR	1601 CALIFORNIA AVE		PALO ALTO	CA 94304
M E	SEAVER	CODE 6110	NAVAL RESEARCH LAB		WASHINGTON	DC 20375
C F	SEHNERT	KRATOS INC	3344 N TORREY PINES		LA JOLLA	CA 92037
W E	SEIFERT,JR	*UTHSC*	*PO BOX 20708*		*HOUSTON*	*TX 77030*
J H	SELLSTEDT	WNETH LABS INC	BOX 8299		PHILADELPHIA	PA 19101
S K	SETHI	CHEMISTRY DEPT	UNIVERSITY VIRGINIA		CHARLOTTESVILLE	VA 22903
R L	SETTINE	GCMS CENTER	UNIV ALABAMA		BIRMINGHAM	AL 35294
J	SHABANOWITZ	CHEMISTRY DEPT	UNIV VIRGINIA		CHARLOTTESVILLE	VA 22901
L A	SHADOFF	574 BLDG	DOW CHEMICAL COMPANY		MIDLAND	MI 48640
T E	SHARP	LOCKHEED RES LAB	3251 HANOVER	D52-35 B204	PALO ALTO	CA 94304
C J	SHAW	12 RUTGERS DRIVE			DELRAN	NJ 08075
J	SHEN	SOHIO R3D	4440 WARRENSV CEN RD		CLEVELAND	OH 44128
W R	SHERMAN	PSYCHIATRY DEPT	SCHOOL OF MEDICINE	WASHINGTON UNIV	ST LOUIS	MO 63110
N D	SHERRILL	US GEOLOGICAL SURVEY	MS-18	345 MIDDLEFIELD RD	MENLO PARK	CA 94025
D C	SHEW	EPA	PO BOX 1198		ADA	OK 74820
S R	SHRADER	SHRADER ANAL LAB	*VINEWOOD*		DETROIT	MI 48210
G D	SIDES	1732 TAHITI LANE			ALABASTER	AL 35007
L W	SIECK	NAT BUREAU STANDARDS	A256 CHEMISTRY		WASHINGTON	DC 20234
M W	SIEGEL	EXTRANUCLEAR LAB	250 ALPHA DRIVE	PO BOX 11512	PITTSBURGH	PA 15238
E G	SIEGMUND	6437 CHAFFEE ST			TUJUNGA	CA 91042
R E	SIEVERS	DEPT OF CHEMISTRY	*UNIV OF COLORADO*		*BOULDER*	*CO 80309*
E J	SILVEIRA,JR	PO BOX 4248	SHELL BSRC		MODESTO	CA 95352
R W	SILVERMAN	PHARMACOLOGY DEPT	CENTER HEALTH SCI	UNIV OF CALIFORNIA	LOS ANGELES	CA 90024
B R	SIMONEIT	INST GEOPHYSICS AND	PLANETARY PHYSICS	UNIV OF CALIFORNIA	LOS ANGELES	CA 90024
M P	SINHA	J.P.L.	M.S.233-202	4800 OAK GROVE ST	PASADENA	CA 91103
M E	SISAK	CHEMISTRY DEPT	UNIV OF VIRGINIA		CHARLOTTESVILLE	VA 22901
P A	SKOTNICKI	HOOKER CHEMICALS	PO BOX 344		NIAGARA FALLS	NY 14302
J R	SLAYBACK	FINNIGAN CORP	6110 EXECUTIVE BLVD		ROCKVILLE	MD 20852
L E	SLIVON	BATTELLE LABS	505 KING AVE		COLUMBUS	OH 43201
D E	SMITH,DANNE	44 CENTER GROVE RD	APT T 12		DOVER	NJ 07801
D E	SMITH,DAVID	960 JUNESONG WAY			SAN JOSE	CA 95133
D H	SMITH	OAK RIDGE NAT LAB	BLDG 9735	PO BOX Y	OAK RIDGE	TN 37830
D H	SMITH	CHEMISTRY DEPT	STANFORD UNIV		STANFORD	CA 94305
D L	SMITH	311 SKAGGS HALL	UNIVERSITY UTAH		SALT LAKE CITY	UT 84112
L A	SMITH,LAURENCE	UNIV OF TEXAS	MEDICAL SCHOOL	PO BOX 20708	HOUSTON	TX 77035
L L	SMITH	MEDICAL BRANCH	UNIV TEXAS		GALVESTON	TX 77550
R D	SMITH	BATTELLE-NW	BLDG 329, 300 AREA		RICHLAND	WA 99352
R G	SMITH	DEV THER DEPT	M D ANDERSON HOSP		HOUSTON	TX 77030
R G	SNOOK	6 CHENANGO ST			CAZENOVIA	NY 13035
J G	SOLCH	WRIGHT STATE UNIV	*BREHM LABORATORY*		*DAYTON*	*OH 45424*

J J SOLOMON	ENVIRONMENTAL MED	NY UNIV MED CENTER		TUXEDO	NY 10987
G W SOVOCOOL	112 CARMEL LANE			DURHAM	NC 27713
O D SPARKMAN	1657 LUIKA PLACE			CAMPBELL	CA 95008
G R SPARROW	ANAL SYSTEMS	3M CENTER		ST PAUL	MN 55101
R B SPENCER	5225 VERONN RD			MADISON	WI 53711
J A SPHON	FDA, HFF-144	200 C ST SW		WASHINGTON	DC 20204
C A SPINDT	SRI INTERNATIONAL	333 RAVENSWOOD AVE		MENLO PARK	CA 94025
R L SPRAGGINS	10610 HARD ROCK RD			AUSTIN	TX 78750
A W SPRATLEY,JR	UNION CARBIDE	PO BOX 50		HAHNVILLE	LA 70057
B STACKLER	BOX 572			DAVIS	CA 95616
R STADNICKI	P O BOX 313			POWAY	CA 92064
G C STAFFORD,JR	1463 ILIKAI AVE			SAN JOSE	CA 95118
H M STAHR	VET DIAG LAB	IOWA STATE UNIV		AMES	IA 50011
R H STALEY	CHEMISTRY DEPT	MIT, 6-128A		CAMBRIDGE	MA 02139
J B STANLEY	SRRL-USDA	PO BOX 19687		NEW ORLEANS	LA 70179
J L STAUFFER	A D LITTLE	ACORN PK		CAMBRIDGE	MA 02140
J F STEARNS	PO BOX 972			DALY CITY	CA 94017
J D STEIN	GENERAL ELECTRIC	1334 KATHY CT		LIVERMORE	CA 94550
F STELLAARD	ARGONNE NATIONAL LAB	9700 S CASS AVE		ARGONNE	IL 06043
C M STEVENS	ARGONNE NATL LAB			ARGONNE	IL 60439
T E STEWART	THOMPSON-HAYWARD CHM	5200 SPEAKER RD		KANSAS CITY	KS 66106
R N STILLWELL	INST LIPID RESEARCH	BAYLOR COLL MEDICINE	TEXAS MEDICAL CENTER	HOUSTON	TX 77025
W G STILLWELL	INST LIPID RESEARCH	BAYLOR COLL MEDICINE	TEXAS MEDICAL CENTER	HOUSTON	TX 77025
D STIVERS	333 RAVENSWOOD AVE			MENLO PARK	CA 94025
R L STOCKBAUER	NAT BUREAU STANDARDS	RM A-145, BLDG 222		WASHINGTON	DC 20234
J J STOFFELS	BATTELLE-NW	BLDG 320, AREA 300		RICHLAND	WA 99352
M S STORY	15745 WOODACRES RD			LOS GATOS	CA 95030
S J STOUT	AMERICAN CYANIMID	AGRICULTURE DIV	PO BOX 400	PRINCETON	NJ 08540
R N STOWE	TEXAS DIVISION	DOW CHEMICAL	B1226	FREEPORT	TX 77541
K M STRAUB	SPACE SCIENCE LAB	UNIV OF CALIFORNIA		BERKELEY	CA 94720
P A STRAUSS	DUPONT INST PROD DIV	MCKEAN BLDG	CONCORD PLA	WILMINGTON	DE 19898
A H STRUCK	PERKIN-ELMER CORP	MAIN AVE		NORWALK	CT 06856
T SU	CHEMISTRY DEPT	SMU		NORTH DARTMOUTH	MA 02747
D D SUITER	KRATOS	701 E IRVING PARK		ROSELLE	IL 60172
H R SULLIVAN,JR	ELI LILLY CO	PO BOX 618		INDIANAPOLIS	IN 46206
R L SUMMERS	1002 FALLING LEAF			FRIENDS WOOD	TX 77546
H J SVEC	CHEMISTRY DEPT	IOWA STATE UNIV		AMES	IA 50011
J T SWANSIGER	GULF RES & DEV	PO DRAWER 2038		PITTSBURGH	PA 15230
A R SWANSON	UNIV MINNESOTA	105 MILLARD		MINNEAPOLIS	MN 55455
C C SWEELEY	BIOCHEMISTRY DEPT	MICHIGAN STATE UNIV		E LANSING	MI 48824
B J SWEETMAN	PHARMACOLOGY DEPT	VANDERBILT UNIV		NASHVILLE	TN 37232
R W TAFT	CHEMISTRY DEPT	UNIV OF CALIFORNIA		IRVINE	CA 92717
C R TALLEY	E I DUPONT EXP STA	PETRO CHEMICALS	336 BLDG	WILMINGTON	DE 19898
Y L TAN	DOE	ENVIRON MEAS LAB	376 HUDSON ST	NEW YORK	NY 10014
K TANAKA	HUMAN GENETICS	YALE MEDICAL SCHOOL	333 CEDAR ST	NEW HAVEN	CT 06510
O P TANNER	12664 MARKAIRE			ST LOUIS	MO 63141
M L TAYLOR	CHEMISTRY DEPT	BREHM LABORATORY	WRIGHT STATE UNIV	DAYTON	OH 45435
P A TAYLOR	2503 BUENO DR			DAVIS	CA 95616
R G TEECE	SCHOOL OF MEDICINE	ILLINOIS STATE UNIV	PO BOX 3926	SPRINGFIELD	IL 62708
R M TEETER	CHEVRON RESEARCH			RICHMOND	CA 94802
D T TERWILLIGER	29 CHETWYND RD			PAOLI	PA 19301
M TETSUO	LAB OF CLINICAL SCI	NIMH, NIH		BETHESDA	MD 20205
J P THENOT	CLIN PHARMACOLOGY	NORTHWEST MEM HOSP	303 E SUPERIOR ST	CHICAGO	IL 60611
F THOMAS	NIH	BLDG 10, RM 7N-115		BETHESDA	MD 20014
Q V THOMAS	1383 PARK WAY COURT			FAIRFIELD	OH 45014
R M THOMPSON	BATTELLE LABS	505 KING AVE		COLUMBUS	OH 43201
M L THOMSON	AMERICAN CYANIMID	AGRICULTURAL DIV	PO BOX 400	PRINCETON	NJ 08540
J R THORP	3111 WINDMILL			SUGAR LAND	TX 77478
T O TIERNAN	BREHM LAB	WRIGHT STATE UNIV		DAYTON	OH 45435
S J TILLIN	USDA-WRRC	800 BUCHANAN		ALBANY	CA 94710

G	S	TINT	EAST ORANGE VA HOSP			EAST ORANGE	NJ 07019
P	J	TODD	BAKER LAB	CORNELL UNIV	PO BOX 380	ITHACA	NY 14853
K	B	TOMER	RES TRIANGLE INST	CL5D	PO BOX 12194	RESEARCH TRIANGLE PK	NC 27709
J	C	TOU	ANALYTICAL LAB	B-574	DOW CHEMICAL CO	MIDLAND	MI 48640
W	F	TRAGER	PHARMACEUTICAL SCI	BLDG 20	UNIV OF WASH	SEATTLE	WA 98195
V	T	TRAN	CHEMISTRY DEPT	UNIV OF DELAWARE		NEWARK	DE 19711
G	M	TRISCHAN	MIDWEST RES INST	425 VOLKER BLVD		KANSAS CITY	MO 64110
B	P	TSAI	CHEMISTRY DEPT	UNIV MINN		DULUTH	MN 55812
K	Y	TSERNG	20 W 463 BELLER DR			DOWNERS GROVE	IL 60515
J	R	TURBETT	JAMESTOWN STAR ROUTE			BOULDER	CO 80302
D	L	TURNER	CHEMISTRY DEPT	TEXAS A & M UNIV		COLLEGE STATION	TX 77843
B	J	TYSON	HEWLETT PACKARD	1003 SCOTT BLVD		SANTA CLARA	CA 95050
W	H	ULDRICHT,JR	NEW BRUNSWICK LAB	DEPT OF ENERGY, D350	9800 S CASS AVE	ARGONNE	IL 60439
R	A	UPHAM	CHEMISTRY DEPT	UNIV MINNESOTA		MINNEAPOLIS	MN 55455
R	W	VANDER HAAR	STANDARD OIL CO	PO BOX 400		NAPERVILLE	IL 60540
G		VANDER VELDE	5326 TALLTREE WAY			WEST CHESTER	OH 45069
P	A	M VAN KOPPEN	4174 MODOE RD			SANTA BARBARA	CA 93110
M	J	VASILE	1A 259	BELL TELEPHONE LABS		MURRAY HILL	NJ 07974
D		VASSILAROS	B 7494 UNIV STATION			PROVO	UT 84602
G	W	VAUGHN	MRI	425 VOLKER BVD		KANSAS CITY	MO 64110
M	A	VAZQUEZ	ITT RAYONIER INC	409 E HARVARD		SHELTON	WA 98584
M	L	VESTAL	CHEMISTRY DEPT	UNIVERSITY HOUSTON	4800 CALHOUN	HOUSTON	TX 77004
M	M	VESTLING	CHEMISTRY DEPT	SUNY		BROCKPORT	NY 14420
B	A	VIEUX	329 BLDG/300 AREA	BATTELLE PNL		RICHLAND	WA 99352
A		VIGGIANO	1350 20TH ST J22			BOULDER	CO 80011
P		VOUROS	INST CHEMICAL ANAL	NORTHEASTERN UNIV		BOSTON	MA 02115
P	A	WADSWORTH,JR	SHELL DEVELOPMENT	W HOLLOW RES CTR	PO BOX 1380	HOUSTON	TX 77001
A	L	WAHRHAFTIG	CHEMISTRY DEPT	UNIV OF UTAH		SALT LAKE CITY	UT 84112
R	W	WALKER	MERCK SHARP & DOHME	PO BOX 2000		RAHWAY	NJ 07065
G	R	WALLER	BIOCHEMISTRY DEPT	OKLAHOMA STATE UNIV		STILLWATER	OK 74074
F	C	WALLS	SPACE SCIENCES LAB	UNIV OF CALIFORNIA		BERKELEY	CA 94720
S		WARDEN	MONTANA STATE UNIV			BOZEMAN	MT 59715
B	A	WARREN	H109	CIBA-GEIGY		SUMMIT	NJ 07901
P	L	WARREN	FINNIGAN CORP	845 W MAUDE AVE		SUNNYVALE	CA 94086
V	L	WARREN	BIOLOGICAL ORGANIC	UNIV NEW ORLEANS	LAKEFRONT	NEW ORLEANS	LA 70122
J	T	WATSON	PHARMACOLOGY DEPT	SCHOOL OF MEDICINE	VANDERBILT UNIV	NASHVILLE	TN 37232
J	G	WATT	FINNIGAN CORP	845 W MAUDE		SUNNYVALE	CA 94086
H	M	WEBB	519 W ALAMAR			SANTA BARBARA	CA 93105
G	H	WEDDLE	PO BOX 722			NEWARK	DE 19711
M		WEISS	1901 VALPARAISO			MENLO PARK	CA 94025
M	J	WEISS	PERKIN-ELMER CORP	AEROSPACE DIVISION	PO BOX 2801	POMONA	CA 91766
M	J	WELCH	1774 STONEHAVEN			FREDERICK	MD 21701
G	J	WELLS	VARIAN INC	2700 MITCHELL		WALNUT CREEK	CA 94598
W	A	WELSH	WR GRACE & CO	7379 ROUTE 32		COLUMBIA	MD 21044
B	E	WENZEL	ASHLAND PETROLEUM CO	PO BOX 391		ASHLAND	KY 41101
D	L	WEST	BIOPHYSICAL SCIENCES	UNIV OF HOUSTON		HOUSTON	TX 77004
D	G	WESTMORELAND	ROHM & HAAS CO			SPRING HOUSE	PA 19477
A	F	WESTON	HOOKER CHEMICALS	GRAND ISLAND COMPLEX	LONG ROAD	GRAND ISLAND	NY 14072
E		WHITE	CHEMISTRY A 113	NAT BUREAU STANDARDS		WASHINGTON	DC 20234
R	R	WHITNEY	CARBORUNDUM CO	3401 LA GRANDE BLVD		SACRAMENTO	CA 95823
R	A	WIELESEK	1452 EAST 19TH			EUGENE	OR 97403
J	T	WILDER	UNIV OF CALIFORNIA	1474 FIELDCREST CIR		PLEASANT HILL	CA 94523
B	E	WILKES	BLDG 770-318	UNION CARBIDE	PO BOX 8361	SOUTH CHARLESTON	WV 25303
P	S	WILKES	FDA	60 8TH STREET NE		ATLANTA	GA 30309
C	L	WILKINS	CHEMISTRY DEPT	UNIVERSITY NEBRASKA		LINCOLN	NE 68588
G	D	WILLETT	CHEMISTRY DEPT	UNIV NO CAROLINA		CHAPEL HILL	NC 27514
C		WILLEY	272 NORTH 800 EAST			PROVO	UT 84601
B	W	WILSON	56-035	CHEMISTRY DEPT	MIT	CAMBRIDGE	MA 01887
J	M	WILSON	6201 LAKE WASH BLVD			KIRKLAND	WN 98033
M		WILSON	E I DUPONT	INSTRUMENT PROD DIV	QUILLEN BLDG	WILMINGTON	DE 19898

J G WINDSOR,JR	NORTHROP	PO BOX 12313		RESEARCH TRIANGLE PK	NC	27709
D L WINMILL	RESEARCH CENTER	HERCULES INC		WILMINGTON	DE	19899
L H WOJCIK,JR	FLAM RES	391 CHIPETA WAY		SALT LAKE CITY	UT	84108
S F WOJINSKI	1235 POND			CARY	NC	27511
R J WOLF	35 CHEMISTRY BLDG	WAYNE STATE UNIV		DETROIT	MI	48202
W A WOLSTENHOLME	VARIAN MAT	25 HANOVER RD		FLORHAM PARK	NJ	07932
L K WONG	PHARMACOLOGY DEPT	SCHOOL OF MEDICINE	OHIO STATE UNIV	COLUMBUS	OH	43210
P W WOODWARD	DOE	BERC	PO BOX 1398	BARTLESVILLE	OK	74003
A J WRIGHT	MONSANTO RESEARCH	STA B BOX 8		DAYTON	OH	45407
J WRIGHT	SCHOOL OF PHARMACY	UNIVERSITY MARYLAND	636 W LOMBARD ST	BALTIMORE	MD	21201
L H WRIGHT	EPA	HERL (MD-69)		RESEARCH TRIANGLE PK	NC	27711
J WRONKA	5011 CARFIELD AVE			PENNSAUKEN	NJ	08110
R L WU	BREHM LABORATORY	WRIGHT STATE UNIV		DAYTON	OH	45435
W N WU	BIOCHEMISTRY DEPT	MCNEIL LABORATORIES		FT WASHINGTON	PA	19038
J R WYATT	NRL	CODE 6110		WASHINGTON	DC	20375
R D YELTON	116 WALDEN FARM CIR			UNION	OH	45322
A L YERGEY	NIH	BLDG 6, RM 408		BETHESDA	MD	20014
L W YERT	RMS TOXICOLOGY	BLDG 31, ROOM 5	CDC	ATLANTA	GA	30333
R A YOST	CHEMISTRY DEPT	MICHIGAN STATE UNIV		E LANSING	MI	48824
G W YOUNG	RESEARCH	R J REYNOLDS TOBACCO		WINSTON-SALEM	NC	27101
S E YOUNG	2455 THADDEUS			MOUNTAIN VIEW	CA	94043
A G ZACCHEI	MERCK SHARP & DOHME			WEST POINT	PA	19486
M S ZADIG	1020 CORPORATION WAY			PALO ALTO	CA	94303
P J ZIELINSKI	8600 JOLIET RD			MCCOOK	IL	60525
J A ZIRROLLI	AFESC/RDVC			TYNDALL AFB	FL	32403
R ZUBYK	19 ATTERBURY DR			MALVERN	PA	19355

F S ABBOTT	U BRITISH COLUMBIA	PHARMACEUTICAL SCI		VANCOUVER, BC	V6T	1W5
G P ARSENAULT	PO BOX 2210, R R 1			KINGSTON, ONTARIO	K7L	4V1
C M BANIC	DEPT OF PHYSICS	RM 707	UNIV OF TORONTO	TORONTO, ONTARIO		
M BARIL	PHYSICS DEPT	UNIVERSITE LAVAL		QUEBEC 10, QUEBEC	G1K	7P4
F M BENOIT	HEALTH-WELFARE DEPT	ENVIRONMENTAL HEALTH	TUNNEYS PASTURE	OTTAWA, ONTARIO	K1A	0L9
M BERTRAND	INRS UNIV OF QUEBEC	7401 HOCHELAGA		MONTREAL, QUEBEC	H1N	3M5
R F BONNER	MINISTRY OF ENVIRON	PO BOX 213		REXDALE, ONTARIO	M9W	5L1
R W BURTON	FACULTY OF PHARMACY	UNIVERSITY OF	BRITISH COLUMBIA	VANCOUVER BC	V6T	1W5
M B COMISAROW	CHEMISTRY DEPT	UNIV BRIT COLUMBIA		VANCOUVER, BC	V6T	1W5
A L DA COSTA	ESSO CHEMICAL CANADA	PO BOX 3004		SARNIA, ONTARIO	N7T	7M5
W R DAVIDSON	SCIEX INC	55 GLENCAMERON RD	SUITE 202	THORNHILL, ONTARIO	L3T	1P2
D A DURDEN	PSYCHIATRIC RESEARCH	508 UNIV RES HOSP		SASKATOON	S7N	0W8
G K EIGENDORF	CHEMISTRY DEPT	UN BRITISH COLUMBIA		VANCOUVER, BC	V6T	1W5
I P FISHER	GULF CANADA	RESEARCH & DEVELOP	2489 N SHERIDAN WAY	SHERIDAN PARK, ONT	L5K	1A8
W FORST	DEPT OF CHEMISTRY	LAVAL UNIVERSITY		QUEBEC	1K	7P4
M G FOSTER	OTC	MINISTRY ENVIRONMENT	PO BOX 213	REXDALE. ONTARIO	M9W	5L1
D D GODSE	CLARKE INST PSYCHIAT	250 COLLEGE STREET		TORONTO, ONTARIO	M5T	1R8
M GORDON	MERCK-ISOTOPES	606-1209 RICHMOND ST		LONDON ONTARIO	N6A	3L7
G A GUDAUSKAS	CANCER CONTROL AGNCY	OF BRITISH COLUMBIA	2656 HEATHER ST	VANCOUVER, BC	V5Z	3J3

M P	HAHTO	GULF R&D	2489 N SHERIDAN WAY		MISSISSAUGA, ONT	L5K 1A8
A G	HARRISON	CHEMISTRY DEPT	UNIV OF TORONTO		TORONTO, ONTARIO	M5S 1A1
J A	HERMAN	DEPT CHIMIE	UNIVERSITE LAVAL		QUEBEC, QUEBEC	G1K 7P4
A M	HOGG	CHEMISTRY DEPT	UNIVERSITY ALBERTA		EDMONTON, ALBERTA	T6G 2G2
L	HOGGE	PRARIE REGIONAL LAB			SASKATOON SASK	S7N 0W8
J L	HOLMES	CHEMISTRY DEPT	UNIV OTTAWA		OTTAWA, ONTARIO	K1N 9B4
W D	JAMIESON	NRC	1411 OXFORD ST		HALIFAX, NOVA SCOTIA	B3H 3Z1
P	KEBARLE	CHEMISTRY DEPT	UNIV ALBERTA		EDMONTON, ALBERTA	T6G 2G2
R C	LAO	CHEMISTRY DIV	APCD	ENVIRONMENT CANADA	OTTAWA, ONTARIO	K1A 1C8
T	MAGHERA	DEPT OF CHEMISTRY	UNIV OF ALBERTA		EDMUNTON	
R E	MARCH	TRENT UNIVERSITY			PETERBOROUGH, ONT	K9J 7B8
D L	MCGILLIVRAY	CHEMISTRY DEPT	UNIVERSITY VICTORIA		VICTORIA, BC	V8W 2Y2
T B	MCMAHON	CHEMISTRY DEPT	UNIV NEW BRUNSWICK		FREDERICTON, NB	E3B 5A3
J B	OLTHETEN	2710BRABANT MARINEAU			MONTREAL, QUEBEC	H4S 1L1
F I	ONUSKA	CCIW-AMRS	PO BOX 5050		BURLINGTON	L7R 4A6
J D	PAYZANT	CHEMISTRY DEPT	UNIV OF ALBERTA		EDMONTON ALBERTA	
O	PELLETIER	HEALTH PROTECTION BR	ROOM 277, HPB BLDG	TUNNEYS PASTURE	OTTAWA, ONTARIO	K1A 0L2
M A	QUILLIAM	3238 LANSDOWN DRIVE			BURLINGTON, ONTARIO	L7M 1K3
D A	REA	12620 CANNINGTON WAY	SW		CALGARY, ALBERTA	
N M	REID	SCIEX INC	55 GLENCAMERON RD	SUITE 202	THORNHILL, ONTARIO	L3T 1P2
G S	RITCHIE	345 3223 83 ST NW			CALGARY, ALBERTA	
R W	SADLIER	10 WOODMAN DR, 402			HAMILTON, ONTARIO	L8K 4E1
G	SANCHEZ	INRS	UNIV OF QUEBEC	7401 HOCHELAGA	MONTREAL, QUEBEC	1N 3M5
B I	SHUSHAN	CHEMISTRY DEPT	UNIVERSITY GUELPH		GUELPH, ONTARIO	N1G 2W1
K	STANDING	PHYSICS DEPT	UNIV OF MANITOBA		WINNIPEG	R3T 2N2
J A	STONE	CHEMISTRY DEPT	QUEEN'S UNIVERSITY		KINGSTON, ONTARIO	K7L 3N6
J	SUNNER	DEPT OF CHEMISTRY	U OF ALBERTA		EDMONTON	
W C	TAM	DIV OF PHYSICS	NATIONAL RES COUNCIL		OTTAWA, ONTARIO	K1A 0R6
B	THOMSON	SCIEX INC	55 GLENCAMERON RD		THORNHILL, ONTARIO	
H M	TOSINE	PESTICIDES SECTION	MINISTRY ENVIRONMENT	PO BOX 213	REXDALE, ONTARIO	M9W 5L1
J B	WESTMORE	CHEMISTRY DEPT	UNIV OF MANITOBA		WINNIPEG, MANITOBA	
G W	WOOD	CHEMISTRY DEPT	UNIV WINDSOR		WINDSOR, ONTARIO	N9B 3P4
R	YAMDAGNI	CHEMISTRY DEPT	UNIV CALGARY		CALGARY, ALBERTA	T2N 1N4

P J	ARPINO	LAB CHIM ANAL PHYS	ECOLE POLYTECHNIQUE		91128 PALAISEAU	FRANCE
R	BATEMAN	VG MICROMASS	ALTRINCHAM		CHESHIRE	ENGLAND
J D	BATY	BIOCHEMICAL MED	NINEWELLS HOSP		DUNDEE	SCOTLAND
G	BAYKUT	6000 FRANKFURT/M 50			HOHERODSKOPFSTR 7	F.R.G.
M L	BENNETT	BHP CENTRAL RES LABS	PO BOX 188		WALLSEND, NSW 2287	AUSTRALIA
J H	BEYNON	CHEMISTRY DEPT	UNIV COLLEGE		SWANSEA, SA2 8PP	WALES
J C	BILL	VG DATA SYSTEMS LTD	4 TAYMERE CLOSE	SANDBACH	CHESHIRE	ENGLAND
F	BRUNER	LIA-CNR	VIA MONTORIO ROMANO	36	00131 ROMA	ITALY
C	BRUNNEE	VARIAN MAT GMBH	BARKHAUSENSTR 2	POSTFACH 14 4062	D-2800 BREMEN 10	WEST GERMANY
A	CARRICK	KRATOS LTD	BARTON DOCK ROAD		URMSTON MANCHESTER	ENGLAND
D M	CARTER	SCHOOL OF PHARMACY	BRUNSWICK SQUARE		LONDON, WC1	ENGLAND
M M	CLAEYS	UNIV OF ANWERP	DEPT PHARMACY	UNIVERSITEITS PLEIN	B-2610 WILRUK	BELGIUM
D	COVENEY	BARTON DOCK ROAD			MANCHESTER	ENGLAND
C A	CRAMERS	10 EUROPALAAN			5691 EN SON	THE NETHERLA
P H	D'ARCY	7 HAMBLETON ROAD	HEALD GREEN	CHEADLE	CHESHIRE, SK8 3DW	ENGLAND
G L	DEVANT	7 NICOLAS RORET			PARIS, 75013	FRANCE
I	DOTAN	ISOTOPE DEPT	WEIZMANN INS SCIENCE		REHOVOT	ISRAEL
S	EVANS	KRATOS-AEI LTD	BARTON DOCK ROAD	URMSTON	MANCHESTER	ENGLAND
D E	GAMES	CHEMISTRY DEPT	UNIV COLLEGE	PO BOX 78	CARDIFF, CF1 1XL	WALES
T	GAUMANN	FED SCHOOL OF TECH			1015 LAUSANNE	SWITZERLAND

K E HABFAST	VARIAN MAT GMBH	BARKHAUSENSTR 2	POSTFACH 14 4062	D-2800 BREMEN 10	WEST GERMANY
R C HAINES	VG ISOTOPES	ROAD 3, WINSFORD		CHESHIRE	G BRITAIN
W H HENDERSON	KRATOS LTD	BARTON DOCK ROAD		MANCHESTER	ENGLAND
T HICKSON	BROADSTONE COTTAGE	COMMON LANE	LACH DENNIS	NORTHWICH	UNITED KINGD
J INGELS	BELIGIAN INST FOR	SPACE AERONOMY	RINGLAAN 3	B-1180 BRUSSELS	BELGIUM
S ISHII	1418 NAKAGAMI			AKISHIMA TOKYO	JAPAN
Y I ITAGAKI	JEOL LTD, 1418	NAKAGAMI AKISHIMA		TOKYO 196	JAPAN
D JOHNSON	65 UNDERWOOD ROAD			READING	ENGLAND
J D JOLY	NERMAG	49 QUAI DE HALAGE	92500 RUEIL-	MODMAISOR	FRANCE
C LIFSHITZ	PHYS CHEM DEPT	HEBREW UNIVERSITY		JERUSALEM	ISRAEL
R S MASON	DEPT OF CHEMISTRY	UNIV OF WARWICK		COVENTRY	ENGLAND CV4
I M MATSUMOTO	RES LAB OF GC-MS	SCHOOL OF MEDICINE	KURUME UNIVERSITY	FUKUOKA, 830	JAPAN
G J MAUCLAIRE	UNIV OF PARIS-SUD			91405 ORSAY	FRANCE
T MERREN	VG ISOTOPES	RODE 3		WINSFORD, CHESHIRE	ENGLAND
D S MILLINGTON	VG ORGANIC LTD	TUDOR ROAD		ALTRINCHAM, WA14 5RZ	ENGLAND
L E MOORE	KRATOS LTD	BARTON DOCK ROAD		URMSTON, MANCHESTER	ENGLAND
I J NENNER	CEN SACLAY	BP 2		91190 GIF SUR YVET	FRANCE
T NODA	TOYOHASHI UNIV OFS	TECHNOLOGY	TEMPAKU-CHO	TOYOHASHI	JAPAN 440
P POWERS	296 BRAMHALL LANE	SO BRAMHALL		CHESHIRE, SK7 3DJ	ENGLAND
U RAPP	VARIAN GMBH	DARKHAUSENSTR 2		D-2800 BREMEN	W GERMANY
S V RENSBURG	143 HAAK-EN-STEEK AV			WONDERBOOM 0182	REP OF S AFR
B K ROBINSON	6 CORONATION CRESCEN			WEYMOUTH	ENGLAND
P A RYAN	KRATOS LTD	BARTON DOCK RD		URMSTON, MANCHESTER	ENGLAND
K SAITO	DEPT MED CHEMISTRY	KANSAI MEDICAL SCH		MORIGUCHI, OSAKA 570	JAPAN
K SAKATA	RES INST OF MEDICAL	MASS SPECTROMETRY	KURUME UNIV SCH MED	KURUME FUKUOKA 830	JAPAN
M SENN	BOEHRINGER MANNHEIM			6800 MANNHEIM	W GERMANY
T SHINKA	67 ASAHIMACHI KURUME			FUKUOKA	JAPAN
M SUZUKI	PHARMACY FACULTY	MEIJO UNIVERSITY	TEMPAKU	NAGOYA, 468	JAPAN
E TAJIMA	871-1 TSUDA	KATSTA-SMI		IBARAKI-KEN	JAPAN
J K TERLOUW	LAB ANAL CHEM	CROESESTRAAT 77A		3522AD UTRECHT	NETHERLANDS
M TSUCHIYA	4 37 27 KUGAYAMA	SUGINIMI KU		TOKYO, 168	JAPAN
W UNSWORTH	IOM PATH			WINSFORD	UNITED KINGD
M E VERZELE	KRIJGSLAAN 49			B-9000 GENT	BELGIUM
I WAHLBERG	SWEDISH TOBACCO CO	PO BOX 17007		S-10462 STOCKHOLM	SWEDEN
K P WANCZEK	PARKALLEE 197			D-2800 BREMEN	WEST GERMANY
S A WIKSTROM	KAROLINSKA INST	RESEARCH CENTER	HUDDINGE UNIV HOSP	S-141 86 HUDDINGE	SWEDEN
D WOOD	12 STYAL AVE	SOUTH REDDISH		STOCKPORT	ENGLAND
S YAMADA	RES LAB OF GC-MS	SCHOOL OF MEDICINE	KURUME UNIVERSITY	FUKUOKA, 830	JAPAN
J YINON	WEIZMANN INS SCIENCE			REHOVOT	ISRAEL
M YOSHIDA	DEPT NEUROSURG	KUNME UNIV HOSPITAL	67 ASAHI-MACHI	KURUME 830	JAPAN
Z V ZARETSKII	WEIZMANN INS SCIENCE	PO BOX 26		REHOVOT	ISRAEL